

**A Multiphase Continuum Mechanics Model for Shock
Loading of Soft Porous Materials**

by

Z. T. Irwin

B.A., Cornell University, 2017

M.S., University of Colorado Boulder, 2023

A thesis submitted to the
Faculty of the Graduate School of the
University of Colorado in partial fulfillment
of the requirements for the degree of
Doctor of Philosophy
Department of Mechanical Engineering
2024

Committee Members:

Richard A. Regueiro, Chair

John D. Clayton

Rong Long

Debanjan Mukherjee

Franck J. Vernerey

Yida Zhang

Irwin, Z. T. (Ph.D., Mechanical Engineering)

A Multiphase Continuum Mechanics Model for Shock Loading of Soft Porous Materials

Thesis directed by Prof. Richard A. Regueiro

A large deformation, coupled finite-element (FE) model is developed to simulate the multiphase response of soft porous materials subjected to high strain-rate (shock) loading, with particular application for lung parenchyma. The approach is based on the theory of porous media (TPM) at large deformations. The theoretical model developed herein is general and thermodynamically consistent to allow for a range of applications. An overview of several different time integration schemes is presented for the purpose of solving the nonlinear dynamic coupled balance of momentum (mixture and fluid), balance of mass of the mixture, and balance of energy (solid and fluid) equations. Simplifications to the one-dimensional regime studied in the numerical simulations follow.

Numerical examples are presented for (i) verification against closed-form analytical solutions assuming small loads, (ii) demonstrating large deformation effects at high strain-rate, and (iii) showing differences in deformations between a single-phase elastodynamics model with occluded compressible pore fluid and a multiphase poroelastodynamics model at high strain-rate. The multiphase model shows that the relative motion of the pore fluid significantly dampens the deformation response of the solid skeleton as compared to the single-phase model, and makes it possible to extract quantitative values for the stresses of the different constituents, thereby allowing one to form preliminary conclusions about the onset of damage in the solid skeleton. The novelty of the current work is developing a multiphase, large deformation, mixture theory numerical model for high strain-rate loading of soft porous materials. Therein, it was discovered that (i) explicit, adaptive time-stepping Runge–Kutta schemes offer high accuracy at relatively low cost when compared to traditional implicit (or explicit central difference) schemes, (ii) shock viscosity is necessary to regularize the shock front, and (iii) additional stabilization parameters and non-standard mixed-element types improve both computational cost and accuracy compared to traditional implementations.

Dedication

To those that inspire us to push the boundaries of the impossible to discover something new,
without and within.

Acknowledgements

First and foremost, I would like to extend my sincere gratitude to my advisor, Prof. Richard A. Regueiro for his continual devotion to my success. Without his guidance, mentorship, and support, I would not be the researcher I am today. Much of this work presented herein resulted from materials he developed and taught, on top of the many fruitful discussions we have had over the years. Thank you for believing in me and always pushing me to do more.

I would also like to thank my informal co-advisor, Dr. John D. Clayton, for his mentorship over the past three years. His expertise on constitutive modeling and thermodynamics provided me with a better understanding of these physics and endowed me with a greater appreciation thereof. I look forward to starting my career alongside him and the other dedicated civil servants at Army Research Laboratory (ARL). Thank you also to ARL and the DoD SMART program for partially funding this work.

To my other committee members, I have greatly valued your feedback on this work. Thank you to Prof. Rong Long, Prof. Franck Vernerey, and Prof. Yida Zhang for your excellent questions that helped to shape the motivation, applicability, and theory behind the present work. Thank you to Prof. Debanjan Mukherjee for starting me down the path of finite-element modeling in the fluid-structure interaction application space all those years ago. Thank you also to my numerous teachers throughout my education, particularly Prof. Peter Hamlington, Dr. Jeffrey Knutsen, and Dr. Scott Runnels for showing me the juice is (almost always) worth the squeeze.

Lastly, I owe my sincerest gratitude to my friends and family. Completion of this thesis would not have been possible without your support, encouragement, patience, and love. I am grateful beyond words for the climbs, hikes, meals, and laughs that we have shared together on this beautiful planet we call home.

Contents

Chapter	
1	Introduction 1
1.1	Motivation 1
1.1.1	Lung injury pathology 1
1.1.2	Numerical challenges in TPM 3
1.1.3	Temperature and damage modeling 5
1.1.4	Limitations of the current work 7
1.2	Viscoelasticity vs. poroelasticity 7
1.2.1	Linear viscoelasticity in one dimension at small strain 8
1.2.2	Linear poroelasticity in one dimension at small strain 10
1.2.3	Comparison of linear viscoelasticity and poroelasticity in 1-D at small strain 13
1.3	Objectives 17
2	Theory of Porous Media 19
2.1	Concept of volume fractions 19
2.2	Kinematics 20
2.3	Balance of Mass 22
2.4	Balance of Momentum 25
2.5	Balance of Energy 29
2.6	Balance of Entropy 32
2.7	Dissipation Inequality 34

3	Constitutive Theory	36
3.1	Locally inhomogeneous temperature model	36
3.1.1	Determination of the Helmholtz free energies	39
3.1.2	Evaluation of the Clausius-Duhem inequality	41
3.1.3	Identifying constitutive relations	43
3.1.4	Defining proportionality parameters	47
3.2	Locally homogeneous temperature model	51
3.2.1	Determination of the Helmholtz free energies	52
3.2.2	Evaluation of the Clausius-Duhem inequality	53
3.2.3	Identifying constitutive relations	55
3.2.4	Defining proportionality parameters	56
3.3	Constituent modeling	56
3.3.1	Hyperelastic solid skeleton	57
3.3.2	Compressible pore fluid	63
4	Numerical Implementation	67
4.1	Strong and variational forms of the governing equations	68
4.1.1	(\mathbf{u}) formulation	68
4.1.2	$(\mathbf{u}-\theta)$ formulation	72
4.1.3	$(\mathbf{u}-p_f)$ formulation	78
4.1.4	$(\mathbf{u}-\mathbf{u}_f-p_f)$ formulation	88
4.1.5	$(\mathbf{u}-p_f-\theta^s-\theta^f)$ formulation	108
4.1.6	$(\mathbf{u}-\mathbf{u}_f-p_f-\theta^s-\theta^f)$ formulation	132
4.2	Finite element implementation	155
4.2.1	Interpolation	156
4.3	Time integration	168
4.3.1	Runge-Kutta integration	169

4.3.2	Implicit integration	221
4.3.3	Central-difference integration	250
4.4	Stabilization techniques	260
4.4.1	Shock viscosity	261
4.4.2	Pressure stabilization	267
4.4.3	Streamline upwind Petrov-Galerkin	269
5	Numerical Examples	274
5.1	Differences between LS-DYNA and SPONGE-1D models	274
5.2	Verification	276
5.2.1	Method of manufactured solutions	277
5.2.2	Elastodynamics	291
5.2.3	Poroelasticity	296
5.2.4	Poroelastodynamics	299
5.3	High strain-rate loading	307
5.3.1	Effects of shock viscosity for single-phase models	307
5.3.2	Effects of pore fluid pressure stabilization	315
5.3.3	Shock loading of lung parenchyma	321
6	Conclusion	403
6.1	Recapitulation of present work	403
6.2	Ongoing and future work	406
	Bibliography	408
	Appendix	
A	Derivation of the Gateaux derivatives	424

B	Derivation of linearized equations	430
B.1	(\mathbf{u}) formulation	430
B.2	$(\mathbf{u}-\theta)$ formulation	432
B.3	$(\mathbf{u}-p_f)$ formulation	434
B.4	$(\mathbf{u}-\mathbf{u}_f-p_f)$ formulation	438
B.5	$(\mathbf{u}-p_f-\theta^s-\theta^f)$ formulation	444
C	Derivation of the FE equations	472
C.1	Implicit integration	472
C.1.1	(\mathbf{u}) formulation	472
C.1.2	$(\mathbf{u}-p_f)$ formulation	476
C.1.3	$(\mathbf{u}-\mathbf{u}_f-p_f)$ formulation	484
C.2	Explicit integration	494
C.2.1	CD scheme	494

Tables

Table

4.1	Acronyms for different element types.	159
5.1	Material parameters for the $(\mathbf{u}-p_f)$ and $(\mathbf{u}-\mathbf{u}_f-p_f)$ MMS convergence studies.	284
5.2	Material parameters for elastodynamics verification example.	294
5.3	Geometrical and loading parameters for elastodynamics verification example.	294
5.4	Material parameters for the poroelasticity verification example.	296
5.5	Geometrical and loading parameters for the poroelasticity verification example.	297
5.6	Material parameters for the poroelastodynamics verification example.	300
5.7	Geometrical and loading parameters for the poroelastodynamics verification example.	300
5.8	Material parameters for an example on shock viscosity for a column of single-phase, elastodynamic lung parenchyma. Values taken from Clayton et al. [2021].	308
5.9	Geometrical and loading parameters for an example on shock viscosity for a column of single-phase, elastodynamic lung parenchyma.	308
5.10	Material parameters for multiphase lung parenchyma simulations. Values taken from Clayton et al. [2021], Lande and Mitzner [2006].	315
5.11	Geometrical and loading parameters for pressure stabilization study.	315
5.12	Geometrical and loading parameters for multiphase porous material simulations demonstrating Taylor-Hood mixed elements.	322
5.13	Geometrical and loading aprameters for the no-flux boundary condition study. Values taken from Clayton et al. [2021], Lande and Mitzner [2006].	335

5.14 Geometrical and loading parameters for the no-flux boundary condition study. . . .	335
5.15 Material parameters for sensitivity study of \varkappa . Known values taken from Clayton et al. [2021]. $\varkappa \in [1.89 \times 10^{-8}, 1.89 \times 10^{-12}] \text{ m}^2$	339
5.16 Geometrical and loading parameters for sensitivity study on \varkappa	339
5.17 Material parameters for sensitivity study of κ . Known values taken from Clayton et al. [2021]. $\kappa \in [1.0, 5.0]$	350
5.18 Geometrical and loading parameters for sensitivity study on κ	350
5.19 Material parameters for pore fluid viscous stress tensor simulations. Values taken from Clayton et al. [2021], Lande and Mitzner [2006], Holmes et al. [2011], Rand et al. [1964], Shang et al. [2019]. Viscosity values for air are interpolated for resting body temperature 37° C ; bulk modulus, density and bulk viscosity for blood are estimated using values for water at resting body temperature 37° C , while shear viscosity is estimated from Rand et al. [1964]. A value of $\kappa = 2.5$ was chosen for the hyperbolic hydraulic conductivity.	363
5.20 Geometrical and loading parameters for pore fluid viscous stress tensor simulations.	364
5.21 Material parameters for single-phase vs. multiphase simulations. Values taken from Clayton et al. [2021], Lande and Mitzner [2006].	383
5.22 Geometrical and loading parameters for single-phase vs. multiphase simulations. . .	383
5.23 Material parameters for thermoporoelastodynamic simulations at low-to-moderate strain rate. Values taken from Clayton et al. [2021], Lande and Mitzner [2006], Yang and Cao [2020]. Initial temperatures are $\theta_0^s = \theta_0^f = 310 \text{ K}$. The hyperbolic hydraulic conductivity model is assumed with $\kappa = 2.5$	389
5.24 Geometrical and loading parameters for thermoporoelastodynamics simulations at low-to-moderate strain-rate.	389

5.25	Material parameters for thermoporoelastodynamics simulations at high strain rates. Values taken from Clayton et al. [2021], Lande and Mitzner [2006], Yang and Cao [2020]. (·)* indicates values used for single-phase formulation (some of which are also the initial mixture values).	393
5.26	Geometrical and loading parameters for thermoporoelastodynamics simulations at high strain-rate.	394

Figures

Figure

1.1	Scanning electron microscope image of intact alveolar air sacs, adapted from Tsokos et al. [2003]	2
1.2	The standard linear solid model, adapted from Simo and Hughes [1998].	8
1.3	The applied Heaviside step function that is applied to the top of the column.	14
1.4	Schematic of the columns used for this thought experiment. The cross-sectional areas are identical between both, but the second column is double the height of the first.	15
1.5	Comparison for lung parenchyma with initial applied stress $t^\sigma = 10$ Pa.	16
2.1	(a) Concept of volume fraction for biphasic (solid(s)-fluid(f)) mixture theory, showing solid skeleton composed of alveolar tissue. Note that in the theory of porous media, it is assumed that the control space is that of the solid phase $\mathcal{B} := \mathcal{B}^s$, also known as “solid skeleton.” (b) Kinematics of a biphasic (solid-fluid) mixture theory.	21
3.1	A comparison, adapted from Markert [2005], of different deformation-dependent hydraulic conductivities for $\kappa = 3.0$ (a) showing the instability of the Kozeny-Carman relation for high compression of the solid skeleton and (b) a zoomed-in version of (a) showing the inadequacy of the Eipper [1998] model for high expansion of the solid skeleton.	50

4.1	The Q3H-Q3H-P1 line element used for C^1 continuity of the field variables u and u_f . Shown in red are the gradient DOFs which are allowed to “float”, i.e., no boundary conditions are prescribed for these DOFs.	106
4.2	Schematic for different element types: (a) left to right: Q3H, Q3, Q2, Q1; (b) left to right: Q3H-T1, Q3-T1, Q2-T1, Q1-T1.	160
4.2	Schematic for different element types (cont.): (c) left to right: Q3H-P1, Q3-P1, Q2-P1, Q1-P1; (d) left to right, top to bottom: Q3H-Q3H-P1, Q3H-Q2-P1, Q3H-Q1-P1, Q3-Q3-P1, Q2-Q2-P1, Q2-Q1-P1, Q1-Q1-P1.	161
4.2	Schematics of different element types (cont.): (e) Q3H-P1-T1-T1; (f) left to right: Q3H-Q3H-P1-T1-T1, Q3H-Q1-P1-T1-T1.	162
4.3	Illustration of Newton-Raphson method for solution of d , where we show iteration $k = 0, 1, 2$, and convergence likely at iteration $k = 3$. The black curve is a plot of $F^{\text{INT}}(d)$	225
5.1	Temporal convergence of the elastodynamics MMS, using (a) quadratic elements with $u(X, t) := X^2 t^3$, and (b) Hermite cubic elements with $u(X, t) := X^3 t^3$, plotted at $t = 0.01$ s. A single element was used to minimize spatial discretization error.	281
5.2	Spatial convergence of the elastodynamics MMS, using (a) quadratic elements with $u(X, t) := X^3 t^3$, and (b) Hermite cubic elements with $u(X, t) := X^4 t^3$, plotted at $t = 0.01$ s. The time step $\Delta t = 10^{-6}$ s was fixed to minimize temporal discretization error.	281
5.3	Temporal convergence of the poroelastodynamics (\mathbf{u} - p_f) formulation MMS, using (a) quadratic-linear displacement-pressure elements with $u(X, t) := X^2 t^3$, $p_f(X, t) := (H - X)t^2$, and (b) Hermite cubic-linear displacement-pressure elements with $u(X, t) := X^3 t^3$, $p_f(X, t) := (H - X)t^2$, plotted at $t = 0.01$ s. A single mixed-element was used to minimize spatial discretization error.	286

- 5.4 Spatial convergence of the poroelastodynamics (\mathbf{u} - p_f) formulation MMS, using (a) quadratic-linear displacement-pressure elements with $u(X, t) := X^3 t^3$, $p_f(X, t) := (H - X)t^2$, and (b) Hermite cubic-linear displacement-pressure elements with $u(X, t) := X^4 t^3$, $p_f(X, t) := (H - X)t^2$, plotted at $t = 0.01$ s. Time step is held fixed at $\Delta t = 10^{-6}$ s to minimize temporal discretization error. 286
- 5.5 Temporal convergence of the poroelastodynamics (\mathbf{u} - p_f) formulation MMS, using (a) quadratic-quadratic-linear solid displacement-fluid displacement-pressure elements with $u(X, t) := X^2 t^3$, $u_f(X, t) := \frac{1}{2} X^2 t^3$, $p_f(X, t) := (H - X)t^2$, and (b) Hermite cubic-Hermite cubic-linear solid displacement-fluid displacement-pressure elements with $u(X, t) := X^3 t^3$, $u_f(X, t) := \frac{1}{2} X^3 t^3$, $p_f(X, t) := (H - X)t^2$, plotted at $t = 0.01$ s. A single element was used to minimize spatial discretization error. 290
- 5.6 Spatial convergence of the poroelastodynamics (\mathbf{u} - p_f) formulation MMS, using (a) quadratic-quadratic-linear solid displacement-fluid displacement-pressure elements with $u(X, t) := X^3 t^3$, $u_f(X, t) := \frac{1}{2} X^3 t^3$, $p_f(X, t) := (H - X)t^2$, and (b) Hermite cubic-Hermite cubic-linear solid displacement-fluid displacement-pressure elements with $u(X, t) := X^4 t^3$, $u_f(X, t) := \frac{1}{2} X^4 t^3$, $p_f(X, t) := (H - X)t^2$, plotted at $t = 0.01$ s. The time step $\Delta t = 10^{-6}$ s was fixed to minimize temporal discretization error. . . . 290
- 5.8 Results for the displacements for the elastodynamics verification. Here, Q1 elements were used in SPONGE-1D with mesh size $h_0^e = 1$ m. 295
- 5.10 Porous layer with uniform step load: vertical displacement-time history at topmost node for load $t_0^\sigma = 40$ kPa. 297
- 5.11 Porous layer with uniform step load: vertical displacement-time histories at topmost node for loads $t_0^\sigma = 2, 4$ and 8 MPa. 298
- 5.12 (a) Traction application and (b) schematic of column mesh for the poroelastodynamics verification example. 300

5.13	Verification results for the numerical approximation to the de Boer analytical solution, using $h_0^e = 1$ m. All element types used in SPONGE-1D are stable, i.e., Q2-P1 or Q2-Q2-P1 depending on the formulation.	302
5.14	Comparison between two different mesh resolutions for multiple integrators demonstrating the importance of finer meshes in resolving the pore fluid displacement (using SPONGE-1D).	303
5.15	Relative solid skeleton displacement error (logarithmic scale) at $t = 0.2$ s for fixed $\Delta t = 10^{-6}$ s.	304
5.16	Verification results for the numerical approximation to the de Boer analytical solution, comparing the nearly inviscid (Darcy) to viscous (Darcy-Brinkman) formulations, using $h_0^e = 0.1$ m.	305
5.17	Viscous pore fluid stress for the de Boer verification problem.	306
5.18	(a) Yen impulse traction application (b) Friedlander impulse traction application (c) schematic of column mesh for an example on shock viscosity for a column of single-phase/elastodynamic lung parenchyma, highlighting the Q1 element.	310
5.19	Comparison of elastodynamical response to Yen impulse loading for peak overpressure of 50 kPa with element size $h_0^e = 1$ cm for (a) simulations without shock viscosity enabled (b) shock viscosity set to default values.	311
5.20	Comparison of elastodynamical response to Yen impulse loading for peak overpressure of 50kPa with element size $h_0^e = 0.1$ cm for (a) simulations without shock viscosity enabled (b) shock viscosity set to default values.	311
5.21	Comparison of elastodynamical response to Friedlander impulse loading for peak overpressure of 25kPa with element size $h_0^e = 1$ cm for (a) simulations without shock viscosity enabled (b) shock viscosity set to default values.	312
5.22	Comparison of elastodynamical response to Friedlander impulse loading for peak overpressure of 25kPa with element size $h_0^e = 0.1$ cm for (a) simulations without shock viscosity enabled (b) shock viscosity set to default values.	312

- 5.23 The effect of changing the shock viscosity coefficients C_0 and C_1 for the Yen impulse at peak overpressure of 50 kPa; here, all simulations were conducted using a neo-Hookean hyperelastic material (UMAT 45) in LS-DYNA with $h_0^e = 0.1$ cm. 313
- 5.24 The effect of changing the shock viscosity coefficients C_0 and C_1 for the Friedlander impulse at peak overpressure of 25 kPa; here, all simulations were conducted using a neo-Hookean hyperelastic material (UMAT 45) in LS-DYNA with $h_0^e = 0.1$ cm 314
- 5.25 (a) Yen impulse traction application (b) Friedlander impulse traction application (c) schematic of multiphase column mesh for examples of lung parenchyma deformations, highlighting the Q1-P1 element type. 316
- 5.26 Comparison of lung parenchyma displacements undergoing overpressure loading from the Yen impulse at 15 kPa, using RKFNC numerical time integration with consistent mass matrices, tracking the nodes at the top of the column for varying values of α^{stab} . Here, we invoke a Q1-P1 element with $h_0^e = 1$ cm. 317
- 5.27 Comparison of lung parenchyma displacements undergoing overpressure loading from the Friedlander impulse at 15 kPa, using RKFNC numerical time integration with consistent mass matrices, tracking the nodes at the top of the column for varying values of α^{stab} . Here, we invoke a Q1-P1 element with $h_0^e = 1$ cm. 318
- 5.28 Comparison of lung parenchyma pressure p_E^s and pore fluid pressure p_f after overpressure loading from the Yen impulse at 15 kPa, using RKFNC numerical time integration with consistent mass matrices, tracking the Gauss point closest to $X = H$ for varying values of α^{stab} . Here, we invoke a Q1-P1 element with $h_0^e = 1$ cm, and $K = 7.5$ kPa is the bulk modulus of the solid skeleton. 319
- 5.29 Comparison of lung parenchyma pressure p_E^s and pore fluid pressure p_f after overpressure loading from the Friedlander impulse at 15 kPa, using RKFNC numerical time integration with consistent mass matrices, tracking the Gauss points closest to $X = H$ for varying values of α^{stab} . Here, we invoke a Q1-P1 element with $h_0^e = 1$ cm, and $K = 7.5$ kPa is the bulk modulus of the solid skeleton. 320

5.30 Schematic of multiphase column mesh for examples of lung parenchyma deformations, highlighting the Q2-Q2-P1 Taylor-Hood mixed-element type.	322
5.31 Comparison of solid skeleton displacements undergoing overpressure loading from the Yen impulse at 15 kPa between (a) the single-phase (Clayton & Freed) and multiphase models tracking the nodes at the top of the column, and (b) the multiphase models from SPONGE-1D tracking the nodes at the middle of the column with and without stabilization methods. Without shock viscosity Q and pressure stabilization α^{stab} , we invoke a Q2-P1 or Q2-Q2-P1 element; with shock viscosity Q (where $C_0 = 1.5, C_1 = 0.06$) and pressure stabilization (where $\alpha^{\text{stab}} = 10^{-10}$), we invoke a Q1-Q1-P1 element.	323
5.32 Comparison of solid skeleton displacements undergoing overpressure loading from the Friedlander impulse at 15 kPa between (a) the single-phase (Clayton & Freed) and multiphase models tracking the nodes at the top of the column, and (b) the multiphase models from SPONGE-1D tracking the nodes at the middle of the column with and without stabilization methods. Without shock viscosity Q and pressure stabilization α^{stab} , we invoke a Q2-P1 or Q2-Q2-P1 element; with shock viscosity Q (where $C_0 = 1.5, C_1 = 0.06$) and pressure stabilization (where $\alpha^{\text{stab}} = 10^{-10}$), we invoke a Q1-Q1-P1 element.	324

5.33 A demonstration of the instability of the neo-Hookean/Kozeny-Carman (NHKC) model versus the neo-Hookean-Eipper/hyperbolic (NHEH) model for (a) $(\mathbf{u}-\mathbf{u}_f-p_f)$ in response to Friedlander impulse loading at 50 kPa overpressure, and (b) $(\mathbf{u}-p_f)$ in response to Friedlander impulse loading at 100 kPa overpressure, both simulated using linear elements, with pressure and shock stabilization, for lung parenchyma with material parameters repeated from Table 5.10. The dashed black line is the initial solid volume fraction, n_0^s , relative to the secondary y -ordinate. In (a), the NHKC model J approaches its lower limit, n_0^s , and the NHKC model relative hydraulic conductivity approaches zero before simulation termination. In (b), the NHKC model values of J and relative hydraulic conductivity are non-physical well before simulation termination, demonstrating the issue with relying on results from the NHKC model combination at higher strain. In both (a) and (b), values for the NHEH model remain physical ($J > n_0^s$ and $\hat{k}/\hat{k}_0 > 0$), demonstrating its robustness at adhering to the incompressibility constraint on the solid phase. A value of $\kappa = 2.5$ was chosen for the NHEH simulations. 326

- 5.34 A demonstration of the instability of the neo-Hookean/Kozeny-Carman (NHKC) model versus the neo-Hookean-Eipper/hyperbolic (NHEH) model for (a) $(\mathbf{u}-\mathbf{u}_f-p_f)$ and (b) $(\mathbf{u}-p_f)$, both in response to Yen impulse loading at 100 kPa overpressure and simulated using linear elements, with pressure and shock stabilization, for lung parenchyma with material parameters repeated from Table 5.10. The dashed black line is the initial solid volume fraction, n_0^s , relative to the secondary y -ordinate. In (a), the NHKC model J approaches its lower limit, n_0^s , and the NHKC model relative hydraulic conductivity approaches zero before simulation termination. In (b), the NHKC model values of J and relative hydraulic conductivity are non-physical well before simulation termination, demonstrating the issue with relying on results from the NHKC model combination at higher strain. In both (a) and (b), values for the NHEH model remain physical ($J > n_0^s$ and $\hat{k}/\hat{k}_0 > 0$), demonstrating its robustness at adhering to the incompressibility constraint on the solid phase. A value of $\kappa = 2.5$ was chosen for the NHEH simulations. 327
- 5.35 An example of the *ad-hoc* “strong” enforcement of the no-flux boundary condition applied to a 5-element Q2-Q2-P1 mesh. The leftmost element represents the “unperturbed” global DOFs where the pore fluid displacement global DOF, d_{12f} , is free, as it would be for a “weak” enforcement of the no-flux boundary condition alone. The rightmost element represents the assignment of the pore fluid displacement global DOF at the boundary to take on the value of the solid skeleton displacement global DOF at the boundary. 328
- 5.36 Solid and fluid displacements at $X = H$ of the various no-flux methods following application of the Friedlander impulse. Black, red, and green curves overlap throughout. 336
- 5.37 Solid and fluid displacements contours of the various no-flux methods following application of the Friedlander impulse at 25 kPa overpressure. Black and red curves, and green and blue curves overlap at this scale. 337

5.38	Pore fluid pressure at $X = H$ of the various no-flux methods following application of the Friedlander impulse at 25 kPa overpressure.	338
5.39	Absolute difference in relative velocities for (a) the weak and Lagrange method with element size $h_0^e = 1$ mm, and (b) the weak method for varying element sizes.	338
5.40	Displacements at $X = H$ for varying values of \varkappa in response to the Yen impulse at 50 kPa overpressure for (a) the solid skeleton and (b) the pore fluid. Note the lower bound on the y -ordinate in (b) to account for irrecoverable pore fluid displacement when $\varkappa = 1.89 \times 10^{-8}$ m ² as compared to the lower permeabilities.	341
5.41	Comparing displacements at $X = H$ between $(\mathbf{u}-p_f)$ and $(\mathbf{u}-\mathbf{u}_f-p_f)$ formulations in response to the Yen impulse at 50 kPa overpressure for (a) lower permeabilities and (b) higher permeabilities.	341
5.42	Comparing total stress at the Gauss point closest to $X = H$ between $(\mathbf{u}-p_f)$ and $(\mathbf{u}-\mathbf{u}_f-p_f)$ formulations in response to the Yen impulse at 50 kPa overpressure for (a) lower permeabilities and (b) higher permeabilities.	342
5.43	Comparing solid extra stress at $X = H$ between $(\mathbf{u}-p_f)$ and $(\mathbf{u}-\mathbf{u}_f-p_f)$ formulations in response to the Yen impulse at 50 kPa overpressure for (a) lower permeabilities and (b) higher permeabilities.	342
5.44	Comparing total pore fluid stress at the Gauss point closest to $X = H$ between $(\mathbf{u}-p_f)$ and $(\mathbf{u}-\mathbf{u}_f-p_f)$ formulations in response to the Yen impulse at 50 kPa overpressure for (a) lower permeabilities and (b) higher permeabilities.	343
5.45	Contours along the length of the mesh for Darcy velocity $(n^f \tilde{v}_f)$ for various permeabilities in response to the Yen impulse at 50 kPa overpressure. Note the change in y -ordinate for the bottom row.	344
5.46	Displacements at $X = H$ for varying values of \varkappa in response to the Friedlander impulse at 50 kPa overpressure for (a) the solid skeleton and (b) the pore fluid.	345

5.47	Comparing displacements at $X = H$ between $(\mathbf{u}-p_f)$ and $(\mathbf{u}-\mathbf{u}_f-p_f)$ formulations in response to the Friedlander impulse at 50 kPa overpressure for (a) lower permeabilities and (b) higher permeabilities.	346
5.48	Comparing total stress at the Gauss point closest to $X = H$ between $(\mathbf{u}-p_f)$ and $(\mathbf{u}-\mathbf{u}_f-p_f)$ formulations in response to the Friedlander impulse at 50 kPa overpressure for (a) lower permeabilities and (b) higher permeabilities.	347
5.49	Comparing solid extra stress at the Gauss point closest to $X = H$ between $(\mathbf{u}-p_f)$ and $(\mathbf{u}-\mathbf{u}_f-p_f)$ formulations in response to the Friedlander impulse at 50 kPa overpressure for (a) lower permeabilities and (b) higher permeabilities.	347
5.50	Comparing total pore fluid stress at $X = H$ between $(\mathbf{u}-p_f)$ and $(\mathbf{u}-\mathbf{u}_f-p_f)$ formulations in response to the Friedlander impulse at 50 kPa overpressure for (a) lower permeabilities and (b) higher permeabilities.	348
5.51	Contours along the length of the mesh for Darcy velocity $(n^f \tilde{v}_f)$ for various permeabilities in response to the Friedlander impulse at 50 kPa overpressure. Note the change in y -ordinate for the bottom row. Time samples are shown in Figure 5.83.	349
5.52	Solid skeleton displacements in response to the Yen impulse at 50 kPa overpressure at $X = H$ for (a) a moderate range of κ and (b) a greater range of κ	351
5.53	Solid skeleton displacements in response to the Yen impulse at 50 kPa overpressure at $X = H/2$ for (a) a moderate range of κ and (b) a greater range of κ	352
5.54	Pore fluid displacements in response to the Yen impulse at 50 kPa overpressure at $X = H$ for (a) a moderate range of κ and (b) a greater range of κ	352
5.55	Pore fluid displacements in response to the Yen impulse at 50 kPa overpressure at $X = H/2$ for (a) a moderate range of κ and (b) a greater range of κ	353
5.56	Total Cauchy stress in response to the Yen impulse at 50 kPa overpressure at the Gauss point closest to $X = H$ for (a) a moderate range of κ and (b) a greater range of κ	353

5.57	Solid extra stress in response to the Yen impulse at 50 kPa overpressure at the Gauss point closest to $X = H$ for (a) a moderate range of κ and (b) a greater range of κ	354
5.58	Total pore fluid stress in response to the Yen impulse at 50 kPa overpressure at the Gauss point closest to $X = H$ for (a) a moderate range of κ and (b) a greater range of κ	354
5.59	Darcy velocity contours in response to the Yen impulse at 50 kPa overpressure for (a)–(c) a moderate range of κ and (d)–(f) a greater range of κ	355
5.60	Relative hydraulic conductivity contours in response to the Yen impulse at 50 kPa overpressure for (a)–(c) a moderate range of κ and (d)–(f) a greater range of κ . Note that (a), (b), (d), and (e) all zoom in at the top of the mesh (where loading is applied) so as to better observe differences in relative hydraulic conductivity, differences which are non-existent futher down the mesh for earlier simulation times.	356
5.61	Solid skeleton displacements in response to the Friedlander impulse at $X = H$ for (a) 25 kPa overpressure and a moderate range of κ and (b) 50 kPa overpressure and a greater range of κ	358
5.62	Solid skeleton displacements in response to the Friedlander impulse at $X = H/2$ for (a) 25 kPa overpressure and a moderate range of κ and (b) 50 kPa overpressure and a greater range of κ	358
5.63	Pore fluid displacements in response to the Friedlander impulse at $X = H$ for (a) 25 kPa overpressure and a moderate range of κ and (b) 50 kPa overpressure and a greater range of κ	359
5.64	Pore fluid displacements in response to the Friedlander impulse at $X = H$ for (a) 25 kPa overpressure and a moderate range of κ and (b) 50 kPa overpressure and a greater range of κ	359
5.65	Total Cauchy stress in response to the Friedlander impulse at the Gauss point closest to $X = H$ for (a) 25 kPa overpressure and a moderate range of κ and (b) 50 kPa overpressure and a greater range of κ	360

- 5.66 Solid extra stress in response to the Friedlander impulse at the Gauss point closest to $X = H$ for (a) 25 kPa overpressure and a moderate range of κ and (b) 50 kPa overpressure and a greater range of κ 360
- 5.67 Total pore fluid stress in response to the Friedlander impulse at the Gauss point closest to $X = H$ for (a) 25 kPa overpressure and a moderate range of κ and (b) 50 kPa overpressure and a greater range of κ 361
- 5.68 Darcy velocity contours in response to the Friedlander impulse (a)–(c) at 25 kPa overpressure for a moderate range of κ and (d)–(f) at 50 kPa overpressure for a greater range of κ . Time samples are shown in Figure 5.83. 361
- 5.69 Relative hydraulic conductivity contours in response to the Friedlander impulse (a)–(c) at 25 kPa overpressure for a moderate range of κ and (d)–(f) at 50 kPa overpressure for a greater range of κ . Note that (a), (b), (d), and (e) all zoom in at the top of the mesh (where loading is applied) so as to better observe differences in relative hydraulic conductivity, differences which are non-existent further down the mesh for earlier simulation times. Time samples are shown in Figure 5.83. 362
- 5.70 Displacement results from applying the Yen impulse (50 kPa) to the impermeable lung parenchyma for (a) solid skeleton displacement $u(X = H, t)$ and pore fluid displacement $u_f(X = H, t)$, and (b) solid skeleton displacement $u(X = H/2, t)$ and pore fluid displacement $u_f(X = H/2, t)$. Initial porosity is $n_0^f = 0.664$ 364
- 5.71 Pore fluid stress results from applying the Yen impulse (50 kPa) to the impermeable lung parenchyma for (a) pore fluid extra stress at the Gauss point closest to $X = H$, and (b) total pore fluid stress $\sigma_{11}^f := \sigma_{11(E)}^f - n^f p_f$ at the Gauss point closest to $X = H$. Initial porosity is $n_0^f = 0.664$ 365
- 5.72 Displacement results from applying the Yen impulse (50 kPa) to the permeable lung parenchyma for (a) solid skeleton displacement $u(X = H, t)$ and pore fluid displacement $u_f(X = H, t)$, and (b) solid skeleton displacement $u(X = H/2, t)$ and pore fluid displacement $u_f(X = H/2, t)$. Initial porosity is $n_0^f = 0.664$ 366

- 5.73 Pore fluid stress results from applying the Yen impulse (50 kPa) to the permeable lung parenchyma for (a) pore fluid extra stress at the Gauss point closest to $X = H$, and (b) total pore fluid stress $\sigma_{11}^f := \sigma_{11(E)}^f - n^f p_f$ at the Gauss point closest to $X = H$. Initial porosity is $n_0^f = 0.664$ 367
- 5.74 Contours along the length of the mesh for pore fluid extra stress $\sigma_{11(E)}^f$, pore fluid velocity v_f and porosity n^f for permeable lung parenchyma after applying the Yen impulse with 50 kPa maximum overpressure. Initial porosity is $n_0^f = 0.664$ 369
- 5.75 Displacement results from applying the Yen impulse (50 kPa) to the permeable, blood-saturated lung parenchyma for (a) solid skeleton displacement $u(X = H, t)$ and pore fluid displacement $u_f(X = H, t)$, and (b) solid skeleton displacement $u(X = H/2, t)$ and pore fluid displacement $u_f(X = H/2, t)$. Initial porosity is $n_0^f = 0.99$. . . 370
- 5.76 Pore fluid stress results from applying the Yen impulse (50 kPa) to the permeable, blood-saturated lung parenchyma for the Gauss point closest to $X = H$. Initial porosity is $n_0^f = 0.99$ 370
- 5.77 Solid extra stress results from applying the Yen impulse (50 kPa) to the permeable, blood-saturated lung parenchyma for the Gauss point closest to $X = H$. Initial porosity is $n_0^f = 0.99$ 371
- 5.78 Contours along the length of the mesh for pore fluid extra stress $\sigma_{11(E)}^f$, pore fluid velocity v_f and porosity n^f for permeable, blood-saturated lung parenchyma after applying the Yen impulse with 50 kPa maximum overpressure. 372
- 5.79 Displacement results from applying the Friedlander impulse (50 kPa) to the impermeable lung parenchyma for (a) solid skeleton displacement $u(X = H, t)$ and pore fluid displacement $u_f(X = H, t)$, and (b) solid skeleton displacement $u(X = H/2, t)$ and pore fluid displacement $u_f(X = H/2, t)$. Initial porosity is $n_0^f = 0.664$ 373

- 5.80 Pore fluid stress results from applying the Friedlander impulse (50 kPa) to the impermeable lung parenchyma for (a) pore fluid extra stress at the Gauss point closest to $X = H$, and (b) total pore fluid stress $\sigma_{11}^f := \sigma_{11(E)}^f - n^f p_f$ at the Gauss point closest to $X = H$. Initial porosity is $n_0^f = 0.664$ 374
- 5.81 Displacement results from applying the Friedlander impulse (50 kPa) to the permeable lung parenchyma for (a) solid skeleton displacement $u(X = H, t)$ and pore fluid displacement $u_f(X = H, t)$, and (b) solid skeleton displacement $u(X = H/2, t)$ and pore fluid displacement $u_f(X = H/2, t)$. Initial porosity is $n_0^f = 0.664$ 375
- 5.82 Pore fluid stress results from applying the Friedlander impulse (50 kPa) to the permeable lung parenchyma for (a) pore fluid extra stress at the Gauss point closest to $X = H$, and (b) total pore fluid stress $\sigma_{11}^f := \sigma_{11(E)}^f - n^f p_f$ at the Gauss point closest to $X = H$. Initial porosity is $n_0^f = 0.664$ 376
- 5.83 Sampling locations along the Friedlander impulse for 50 kPa maximum overpressure used in the contour plots 377
- 5.84 Contours along the length of the mesh for pore fluid extra stress $\sigma_{11(E)}^f$, pore fluid velocity v_f and porosity n^f for permeable lung parenchyma after applying the Friedlander impulse with 50 kPa maximum overpressure. Initial porosity is $n_0^f = 0.664$. . . 378
- 5.85 Displacement results from applying the Friedlander impulse (50 kPa) to the permeable, blood-saturated lung parenchyma for (a) solid skeleton displacement $u(X = H, t)$ and pore fluid displacement $u_f(X = H, t)$, and (b) solid skeleton displacement $u(X = H/2, t)$ and pore fluid displacement $u_f(X = H/2, t)$. Initial porosity is $n_0^f = 0.99$ 379
- 5.86 Pore fluid stress results from applying the Friedlander impulse (50 kPa) to the permeable, blood-saturated lung parenchyma for the Gauss point closest to $X = H$. Initial porosity is $n_0^f = 0.99$ 379

5.87	Solid extra stress results from applying the Friedlander impulse (50 kPa) to the permeable, blood-saturated lung parenchyma for the Gauss point closest to $X = H$. Slightly greater amplitude in the zoomed-in figure is due to higher time resolution for a second, shorter simulation. Initial porosity is $n_0^f = 0.99$	380
5.88	Contours along the length of the mesh for pore fluid extra stress $\sigma_{11(E)}^f$, pore fluid velocity v_f and porosity n^f for permeable, blood-saturated lung parenchyma after applying the Friedlander impulse with 50 kPa maximum overpressure.	381
5.89	Overpressure loading from the Yen impulse at 50 kPa showing a comparison of (a) solid displacements between the single-phase LS-DYNA model developed by Clayton and Freed [2019a], Clayton et al. [2021] and the multiphase model developed in SPONGE-1D at $X = H$ and (b) solid and pore fluid displacements between aforementioned models at $X = H/2$	384
5.90	Overpressure loading from the Yen impulse at 50 kPa showing a comparison of accelerations at $X = H/2$ between the single-phase LS-DYNA model developed by Clayton and Freed [2019a], Clayton et al. [2021] and the multiphase model developed in SPONGE-1D.	384
5.91	Overpressure loading from the Yen impulse at 50 kPa showing a comparison of (a) total pressures between the single-phase LS-DYNA model developed by Clayton and Freed [2019a], Clayton et al. [2021] and the multiphase model developed in SPONGE-1D at the Gauss point closest to $X = H$, as well as distinct solid skeleton extra pressure and pore air pressures, and (b) the total axial Cauchy stress between the single-phase and multiphase model, as well as the solid skeleton axial Cauchy stress for the multiphase model.	385

5.92	Overpressure loading from the Friedlander impulse at 50 kPa showing a comparison of (a) solid displacements between the single-phase LS-DYNA model developed by Clayton and Freed [2019a], Clayton et al. [2021] and the multiphase model developed in SPONGE-1D at $X = H$ and (b) solid and pore fluid displacements between aforementioned models at $X = H/2$	386
5.93	Overpressure loading from the Friedlander impulse at 50 kPa showing a comparison of accelerations at $X = H/2$ between the single-phase LS-DYNA model developed by Clayton and Freed [2019a], Clayton et al. [2021] and the multiphase model developed in SPONGE-1D.	387
5.94	Overpressure loading from the Friedlander impulse at 50 kPa showing a comparison of (a) total pressures between the single-phase LS-DYNA model developed by Clayton and Freed [2019a], Clayton et al. [2021] and the multiphase model developed in SPONGE-1D at the Gauss point closest to $X = H$, as well as distinct solid skeleton extra pressure and pore air pressures, and (b) the total axial Cauchy stress between the single-phase and multiphase model, as well as the solid skeleton axial Cauchy stress for the multiphase model.	387
5.95	(a) Triangular impulse traction application (b) schematic of column mesh for the thermoporoelastodynamic simulations of lung parenchyma at low-to-moderate strain-rate, highlighting the Q3H-P1-T1-T1 element.	390
5.96	Solid skeleton displacements following slower, dynamic impulse loading at 10 kPa overpressure comparing the isothermal $(\mathbf{u}-p_f)$ formulation to the non-isothermal $(\mathbf{u}-p_f-\theta^s-\theta^f)$, $(\mathbf{u}-\mathbf{u}_f-p_f-\theta^s-\theta^f)$ formulations at (a) $X = H$ and (b) $X = H/2$	390
5.97	Slower, dynamic impulse loading at 10 kPa overpressure comparing the isothermal $(\mathbf{u}-p_f)$ formulation to the non-isothermal $(\mathbf{u}-p_f-\theta^s-\theta^f)$, $(\mathbf{u}-\mathbf{u}_f-p_f-\theta^s-\theta^f)$ formulations at the Gauss point closest to $X = H$ for (a) total axial Cauchy stress and (b) solid axial Cauchy stress (solid extra [effective] stress).	391

5.98	Slower, dynamic impulse loading at 10 kPa overpressure comparing the isothermal $(\mathbf{u}-p_f)$ formulation to the non-isothermal $(\mathbf{u}-p_f-\theta^s-\theta^f)$, $(\mathbf{u}-\mathbf{u}_f-p_f-\theta^s-\theta^f)$ formulations for (a) pore fluid pressure p_f and (b) comparing the pore fluid temperature θ^f for $(\mathbf{u}-p_f-\theta^s-\theta^f)$ and $(\mathbf{u}-\mathbf{u}_f-p_f-\theta^s-\theta^f)$ formulations.	391
5.99	Slower, dynamic impulse loading at 10 kPa overpressure comparing the temperatures near the (a) bottom of the mesh and (b) top of the mesh.	392
5.100	Overpressure loading from the Yen impulse at 50 kPa showing a comparison of (a) solid displacements between the single-phase LS-DYNA model developed by Clayton and Freed [2019a], Clayton et al. [2021] and the multiphase model developed in SPONGE-1D at $X = H$ and (b) solid displacements between aforementioned models at $X = H/2$	394
5.101	Overpressure loading from the Yen impulse at 50 kPa showing a comparison of (a) total pressures between the single-phase LS-DYNA model developed by Clayton and Freed [2019a], Clayton et al. [2021] and the multiphase model developed in SPONGE-1D at the Gauss point closest to $X = H$, as well as distinct solid skeleton extra pressure, and (b) the total axial Cauchy stress between the single-phase and multiphase model, as well as the solid skeleton axial Cauchy stress for the multiphase model.	395
5.102	Overpressure loading from the Yen impulse at 50 kPa showing a comparison of $(\mathbf{u}-p_f)$ (barotropic exponential model) and $(\mathbf{u}-p_f-\theta^s-\theta^f)$ (baroclinic ideal gas model) formulations.	396
5.103	Overpressure loading from the Yen impulse at 50 kPa showing (a) pore fluid temperature θ^f and (b) solid lung tissue temperature θ^s for $(\mathbf{u}-p_f-\theta^s-\theta^f)$ plotted at the $X = H$ and $X = H/2$ nodes.	396

5.104	Overpressure loading at 50 kPa showing contour plots of pore fluid velocity v_f against pore fluid temperature θ^f for the $(\mathbf{u}-p_f-\theta^s-\theta^f)$ and $(\mathbf{u}-\mathbf{u}_f-p_f-\theta^s-\theta^f)$ formulations for (a)–(c) the Yen impulse and (d)–(f) the Friedlander impulse. Note the increasing range of y -ordinates as the simulation progresses.	397
5.105	Overpressure loading from the Yen impulse at 50 kPa showing (a)–(c) contour plots of mixture temperature θ between the single-phase and multiphase models, and (d)–(f) contour plots of solid lung tissue temperature θ^s	398
5.106	Overpressure loading from the Friedlander impulse at 50 kPa showing a comparison of (a) solid displacements between the single-phase LS-DYNA model developed by Clayton and Freed [2019a], Clayton et al. [2021] and the multiphase model developed in SPONGE-1D at $X = H$ and (b) solid displacements between aforementioned models at $X = H/2$	399
5.107	Overpressure loading from the Friedlander impulse at 50 kPa showing a comparison of (a) total pressures between the single-phase LS-DYNA model developed by Clayton and Freed [2019a], Clayton et al. [2021] and the multiphase model developed in SPONGE-1D at the Gauss point closest to $X = H$, as well as distinct solid skeleton extra pressure, and (b) the total axial Cauchy stress between the single-phase and multiphase model, as well as the solid skeleton axial Cauchy stress for the multiphase model.	400
5.108	Overpressure loading from the Friedlander impulse at 50 kPa showing a comparison of $(\mathbf{u}-p_f)$ (barotropic exponential model) and $(\mathbf{u}-p_f-\theta^s-\theta^f)$ (baroclinic ideal gas model) formulations.	401
5.109	Overpressure loading from the Friedlander impulse at 50 kPa showing (a) pore fluid temperature θ^f and (b) solid lung tissue temperature θ^s for $(\mathbf{u}-p_f-\theta^s-\theta^f)$ plotted at the $X = H$ and $X = H/2$ nodes.	401

5.110	Overpressure loading from the Friedlander impulse at 50 kPa showing (a)–(c) contour plots of mixture temperature θ between the single-phase and multiphase models, and (d)–(f) contour plots of solid lung tissue temperature θ^s	402
-------	---	-----

Nomenclature

Nomenclature in this thesis follows de Boer [2005] and Holzapfel [2000] as much as possible, with some minor exceptions which are also noted below. Notation of the nomenclature listed herein is adapted from Markert [2005].

Conventions

Index and suffix conventions

i, j, k, l, m, \dots	indices as sub- or superscripts range from 1 to N ; usually $N = 3$ in the 3-D physical space
$(\cdot)^s, (\cdot)^f$	capital superscripts indicate the belonging of non-kinematical quantities to a constituent within mixture theories
$(\cdot)_s, (\cdot)_f$	capital superscripts indicate the belonging of kinematical quantities to a constituent within mixture theories

Kernel conventions

(\cdot)	placeholder for kernel quantity
$s, t, \dots, \sigma, \tau, \dots$	scalars (0^{th} -order tensors)
$\mathbf{s}, \mathbf{t}, \dots$	vectors (1^{st} -order tensors)
$\mathbf{S}, \mathbf{T}, \dots$	2^{nd} -order tensors
$\overset{n}{\mathbf{S}}, \overset{n}{\mathbf{T}}, \dots$	n^{th} -order tensors, e.g., $\overset{4}{\mathbf{D}}, \overset{3}{\mathbf{E}}, \overset{2}{\mathbf{F}} = \mathbf{F}, \overset{1}{\mathbf{G}} = \mathbf{g}$

Tensor operations

$(\cdot)^T$	transpose of vectors, tensors, or matrices
$(\cdot)^{\overset{nm}{T}}$	special transposition of higher-order tensors by an exchange of the n^{th} and the m^{th} basis system of the tensorial basis
$\overset{n}{\mathbf{S}} \otimes \overset{n}{\mathbf{T}} = \overset{n+m}{\mathbf{R}}$	dyadic tensor product
$\overset{n}{\mathbf{S}} : \overset{m}{\mathbf{T}} = \overset{n-m}{\mathbf{R}}$ with $n \geq m$	inner tensor product
$\overset{n}{\mathbf{S}} \cdot \overset{n}{\mathbf{T}} = r$	dot product

Symbols

Symbol	Units	Description
α	[-]	constituent identifier (herein, $\alpha = \{s, f\}$)
α^α	[1/K]	linear coefficient of thermal expansion of φ^α ; $3\alpha^\alpha := \alpha_V^\alpha$ for thermally isotropic materials
$\alpha_V, \alpha_V^\alpha$	[1/K]	volumetric coefficient of thermal expansion of φ, φ^α
α^{stab}	[m ³ -s ² /kg]	pore fluid pressure stabilization parameter
β	[-]	Newmark-beta numerical time integration parameter
\mathcal{B}^α	[-]	volumetric control space of φ^α in the current (Eulerian) configuration
\mathcal{B}_0^α	[-]	volumetric control space of φ^α in the reference (Lagrangian) configuration
\mathcal{D}	[-]	reduced dissipation inequality
\mathcal{D}	[-]	internal state variable for solid phase damage
$\Delta(\cdot)$	[-]	change of (\cdot) with respect to a reference value, e.g., $\Delta t = t_{n+1} - t_n$
η, η^α	[J/kg-K]	specific entropy of φ, φ^α
γ	[-]	Newmark-beta numerical time integration parameter
γ^α	[-]	Grüneisen parameter for φ^α
Γ, Γ_0^x	[-]	boundary in current (Eulerian) configuration, boundary in reference (Lagrangian) configuration for arbitrary variable x^1
$\lambda, \lambda^{\text{skel}}$	[Pa]	second Lamé constant of φ, φ^s
Λ	[Pa]	Lagrange multiplier representing temperature-scaled pore fluid pressure
κ	[-]	exponent governing the deformation dependency of hydraulic conductivity \hat{k}
κ_f	[Pa-s]	real bulk viscosity of φ^f
μ, μ^{skel}	[Pa]	1 st Lamé parameter (shear modulus) of φ, φ^s
μ_f	[Pa-s]	real shear viscosity of φ^f

¹ With Γ_0^x , this usually implies the boundary on which to enforce a Dirichlet or Neumann boundary condition related to x .

\mathcal{P}	[Pa]	Lagrange multiplier representing pore fluid pressure
φ, φ^α	[-]	entire mixture ² and constituent α
ψ^α	[J/kg]	specific constituent Helmholtz free energy
ρ	[kg/m ³]	mass density of mixture
$\rho^\alpha, \rho^{\alpha R}$	[kg/m ³]	partial and real mass density of φ^α
$\hat{\rho}, \hat{\rho}^\alpha$	[kg/m ³ -s]	volume-specific mass supply of φ^α
\mathfrak{R}	[J/kg-K]	gas constant for the ideal gas pore fluid (air)
θ, θ^α	[K]	absolute temperature of φ, φ^α
$\hat{\varepsilon}^\alpha$	[J/kg-s]	local interaction for energy supply to (or specific interal energy production of) φ^α
\varkappa	[m ²]	intrinsic permeability ³ of φ^s
ν	[-]	Poisson's ratio of φ, φ^s
ν_0	[s]	viscous damping parameter applied to solid skeleton extra stress
ξ	[m]	length scale in finite-element space
$\pi, \dot{\pi}, \ddot{\pi}$	[-]	finite-element trial function for $p_f, \dot{p}_f, \ddot{p}_f$
σ, σ^α	[Pa]	total and partial Cauchy stress of φ, φ^α , respectively
σ_E^α	[Pa]	extra (effective) Cauchy stress of φ^α
$\vartheta, \dot{\vartheta}$	[-]	finite-element trial function for $\theta, \dot{\theta}$
$\vartheta^s, \dot{\vartheta}^s$	[-]	finite-element trial function for $\theta^s, \dot{\theta}^s$
$\vartheta^f, \dot{\vartheta}^f$	[-]	finite-element trial function for $\theta^f, \dot{\theta}^f$
χ_α	[-]	mapping vector from \mathbf{x} to \mathbf{X}_α
a_{ij}	[-]	Runge-Kutta Butcher table coefficients
A	[m ²]	area in reference (Lagrangian) configuration
b_i^m	[-]	Runge-Kutta Butcher table weights of order m
B^s	[-]	tortuosity of φ^s
c_i	[-]	Runge-Kutta Butcher table nodes

² Or a single-phase material, depending on context.

³ This value is held constant. Deformation-dependent permeability occurs through manipulation of $\hat{k}(n^f)$.

c, c^α	[m/s]	P-wave speed of φ, φ^α
c_V, c_V^α	[J/kg-K]	specific heat of φ, φ^α
$\text{div}, \text{DIV}_\alpha$	[1/m]	divergence operator in current (Eulerian) configuration, reference (Lagrangian) configuration w.r.t. φ^α
$dx, dX, d\xi$	[m]	infinitesimal length scale in current (Eulerian) configuration, reference (Lagrangian) configuration, local finite-element space
da, dA	[m ²]	infinitesimal area scale in current (Eulerian) configuration, reference (Lagrangian) configuration
dv, dV	[m ³]	infinitesimal volume scale in current (Eulerian) configuration, reference (Lagrangian) configuration
$D_t^\alpha(\cdot)$	[-]	material time derivative operating on (\cdot) with respect to α of φ^α
e, e^α	[J/kg]	specific internal energy of φ, φ^α
\hat{e}^α	[J/m ³]	total power density supply to phase φ^α
$(\cdot)^e$	[-]	element-wise quantity
E	[Pa]	Young's modulus of φ, φ^s
E^α	[J/kg]	total specific internal energy of φ^α
g^p	[Pa]	Dirichlet condition for the balance of mass of the mixture
g^{θ^α}	[K]	Dirichlet condition for the balance of energy of φ^α
$\text{grad}, \text{GRAD}_\alpha$	[1/m]	gradient operator in current (Eulerian) configuration, reference (Lagrangian) configuration w.r.t. φ^α
h^e, h_0^e	[m]	finite-element length in current (Eulerian) configuration, reference (Lagrangian) configuration
j^e	[-]	element jacobian of transformation from physical space to element space
J_α	[-]	Jacobian of deformation of φ^α
\hat{k}	[m ² /Pa-s]	hydraulic conductivity
k, k^α	[W/m-K]	thermal conductivity of φ, φ^α
k_θ^ε	[W/m ³ -K]	convective heat transfer coefficient
K^α	[J/kg]	specific total kinetic energy of φ^α
K, K^{skel}	[Pa]	bulk modulus of φ, φ^s

K_α^η	[Pa]	isentropic bulk modulus of φ^α
K_α^θ	[Pa]	isothermal bulk modulus of φ^α
n^α	[-]	volume fraction of φ^α
n^e	[-]	number of finite-elements
n_{dof}^y	[-]	number of finite-element degrees of freedom for arbitrary variable y
p	[Pa]	pressure of φ
p^α, p_α	[Pa]	partial and real pressure of φ^α
p_E^α	[Pa]	extra (effective) partial pressure of φ^α
P_{ext}^α	[J/kg]	external work on φ^α
q	[Pa]	shock viscosity applied to φ, φ^s in current (Eulerian) configuration
Q	[Pa]	shock viscosity applied to φ, φ^s in reference (Lagrangian) configuration
Q_f	[m/s]	pore fluid flux per unit area
$Q^\theta, Q^{\theta^\alpha}$	[W/m ²]	heat flux applied to φ, φ^α
r, r^α	[J/kg-s]	heat input rate of φ, φ^α
t	[s]	current time
Δt	[s]	numerical time-step
T	[s]	total time
v, v^α	[m ³ /kg]	volume, partial volume ⁴ of φ, φ^α in the current (Eulerian) configuration
v_α	[m/s]	velocity of φ^α in 1-D uniaxial strain w.r.t. φ^α
V, V^α	[m ³ /kg]	volume, partial volume of φ, φ^α in the reference (Lagrangian) configuration
W^s	[J-kg/m ³]	strain energy density of φ^s
$w^{pf}, w^\theta, w^{\theta^s}, w^{\theta^f}$	[-]	finite-element test functions for pore fluid pressure, single-phase temperature, solid phase temperature, fluid phase temperature
\mathbf{a}_α	[m/s ²]	acceleration of φ^α w.r.t. φ^α

⁴ For the 1-D uniaxial strain numerical implementation herein, we may also denote this as a velocity $v = v_s$ (or the velocity of a single-phase material depending on the context).

A	[−]	finite-element assembly operator
$\mathbf{b}, \mathbf{b}^\alpha$	[N/kg]	body force acting on φ, φ^α
$\mathbf{B}^{e,y}$	[−]	finite-element shape function gradient for arbitrary variable y
$\mathbf{c}^{y,e}$	[−]	finite-element weighting function for arbitrary variable y
\mathbf{C}_α	[−]	right Cauchy-Green tensor of φ^α
$\mathbf{d}, \dot{\mathbf{d}}, \ddot{\mathbf{d}}$	[−]	finite-element trial functions for $\mathbf{u}_s, \mathbf{v}_s, \mathbf{a}_s$
$\mathbf{d}_f, \dot{\mathbf{d}}_f, \ddot{\mathbf{d}}_f$	[−]	finite-element trial functions for $\mathbf{u}_f, \mathbf{v}_f, \mathbf{a}_f$
\mathbf{d}_α	[1/s]	symmetric velocity gradient of φ^α
\mathbf{f}, \mathbf{F}	[−]	finite-element local, global vector of applied forces (internal and external)
\mathbf{F}_α	[−]	deformation gradient of φ^α
\mathbf{g}	[m/s ²]	gravitational body force
\mathbf{h}^α	[N/kg]	interaction body force from other constituents acting on φ^α
\mathbf{h}_E^f	[N/kg]	extra interaction body force (momentum production force) from φ^s acting on φ^f
$\mathbf{H}^{e,y}$	[−]	finite-element Hermite cubic shape function second-order gradient for arbitrary variable y
\mathbf{k}_i	[−]	vector of Runge-Kutta stage i variables
$\mathbf{k}^{\theta^{mix}}, \mathbf{k}^{\theta^\alpha}$	[W/m-K]	heat conduction tensor of φ, φ^α
$\mathbf{k}_{x,y}, \mathbf{K}_{x,y}$	[−]	finite-element local, global stiffness matrix for coupling between arbitrary variables x and y
$\mathbf{l}, \mathbf{l}_\alpha$	[1/s]	velocity gradient of φ, φ^α
$\mathbf{m}_{x,x}, \mathbf{M}_{x,x}$	[−]	finite-element local, global mass matrix for arbitrary variable x
\mathbf{n}	[−]	unit normal vector
$\mathbf{N}^{e,y}$	[−]	finite-element shape function for arbitrary variable y
$\mathbf{P}, \mathbf{P}_s^\alpha$	[Pa]	first Piola-Kirchhoff stress of φ, φ^α
$\mathbf{q}, \mathbf{q}^\alpha$	[W/m ²]	heat flux of φ, φ^α
\mathbf{R}_x	[−]	finite-element global residual for arbitrary variable x
$\mathbf{S}, \mathbf{S}_s^\alpha$	[Pa]	second Piola-Kirchhoff stress of φ, φ^α

\mathbf{S}_w	[Pa-s/m ²]	permeability tensor
$\mathbf{t}, \mathbf{t}^\alpha$	[Pa]	external traction applied to φ, φ^α
\mathbf{t}^σ	[Pa]	external traction <i>load</i> applied to φ
\mathbf{u}_α	[m]	displacement of φ^α w.r.t. φ^α
$\mathbf{v}, \mathbf{v}_\alpha$	[m/s]	velocity of φ, φ^α
$\tilde{\mathbf{v}}_f$	[m/s]	relative velocity of φ^f w.r.t. φ^s
$(n^f \tilde{\mathbf{v}}_f)$	[m/s]	Darcy (seepage) velocity ⁵
$\mathbf{w}^u, \mathbf{w}^{u_f}$	[-]	finite-element test functions for \mathbf{u}, \mathbf{u}_f
\mathbf{x}	[m]	position in the current (Eulerian) configuration
\mathbf{X}_α	[m]	position in the reference (Lagrangian) configuration w.r.t. φ^α
\mathbf{z}^m	[-]	Runge-Kutta solution of order m

⁵ Typically, when the relative velocity of the pore fluid is multiplied by the porosity and both are enclosed in parentheses, the constitutive relationship for the Darcy velocity is used. See Chapter 3.1.4 for details.

Chapter 1

Introduction

1.1 Motivation

1.1.1 Lung injury pathology

Behind Armor Blunt Trauma (BABT) refers to injuries from non-penetrating impacts that a soldier experiences despite wearing personal protective equipment (PPE), wherein the buildup of kinetic energy is absorbed by the soft tissue and bone behind the body armor. Shock wave induced pulmonary injuries, i.e., Blast Lung Injury (BLI), account for upwards of 47% of the injuries experienced by survivors and up to 86% of fatalities when compared to secondary and tertiary injuries, resulting from direct impact of shrapnel and tissue impact on nearby surroundings, respectively [Mayorga, 1997]. Shock waves induce large pressure gradients which are assumed to be the direct cause of hemorrhaging caused by the microstructural tearing of the lung parenchyma [Cooper et al., 1991, Cooper, 1996, Tsokos et al., 2003]. In civilian populations, injury to the lung tissue can also occur from other high-impact events, such as falls, motor vehicle accidents, or sports injury [Dehghan et al., 2014, Pauzé and Pauzé, 2013, Idriz et al., 2013].

Broadly speaking, injury pathology and progression is well understood [Cohn and DuBose, 2010], however the details of how injury propagates through the lung parenchyma at the ultrastructural (tissue fibers) and microstructural (air sac) level are not well understood and is an active area of research [Clayton, 2020, Freed et al., 2021]. The approach undertaken by Freed et al. [2021] to model the microstructural level necessitates a multiscale model of the whole lung tissue, which

includes the highly heterogeneous structure of the lung parenchyma. The associated mesoscale model (with the macroscale referring to a 3-D model of the two lobes of lung themselves) is being developed as part of this work.

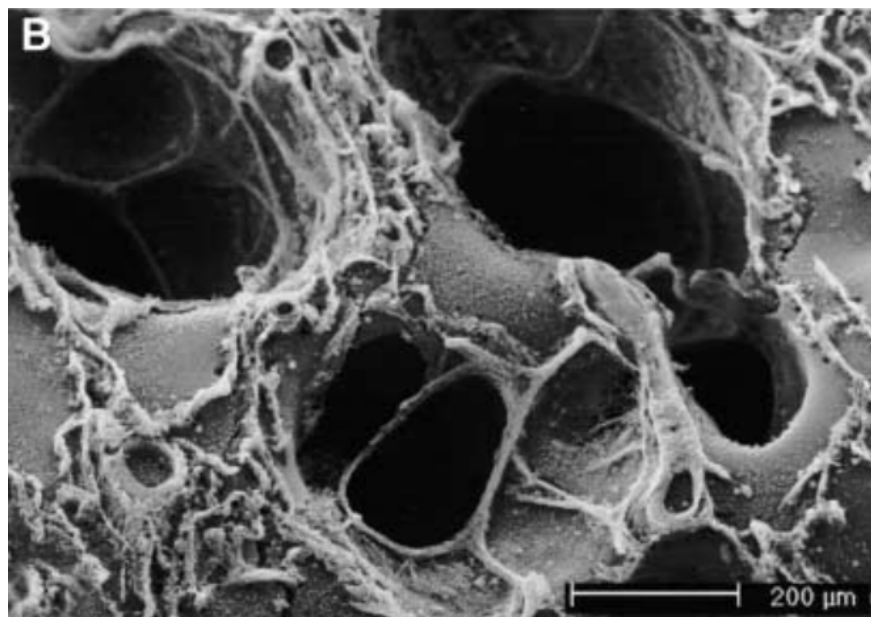


Figure 1.1: Scanning electron microscope image of intact alveolar air sacs, adapted from Tsokos et al. [2003]

The lung parenchyma accounts for roughly 90% of the volume in the lung, with the remaining 10% due to the bronchi and bronchioles, the tube-like structures made of connective tissue that are dedicated to moving large volumes of air [Sanborn et al., 2013]. The parenchyma facilitates gas exchange between the blood and the lungs. It is comprised of alveolar air sacs (ranging from 100-330 μm in diameter [Sobin et al., 1988]) and connective tissues, made up of a complex network of collagen and elastin fibers [Suki et al., 2005]. Collagen fibers in the parenchyma organize to form both an axial fiber network that connects the central airways to the alveolar ducts, and a network that extends from the visceral pleura of the lung to the alveolar ducts. The elastin fibers are connected to the collagen fibers via microfibrils and proteoglycans, the latter of which have chemical interactions (in addition to topological interactions) with the collagen fibrils. The composition and physical dimensions of these unique collagen fibers play a great role in determining the stiffness of

these networks. Furthermore, mechanical forces that act upon the extra-cellular matrix (ECM), in which the collagen and elastin fibers reside, can induce the secretion of growth factors which accelerate ECM remodeling and alter the microstructural composition of the collagen and elastin networks [Suki et al., 2005]. At low strain, the stress response of fibril network appears to be heterogeneous as the elastin fibers bear much of the stress. However, at higher rates of strain, such as those induced by a shock wave, elastin fibers are prone to rupture [Freed et al., 2021] and the remaining stress response percolates through the collagen fibril networks as the collagen fibers start to extend to their uncoiled lengths, which increases the stress response of the entire lung parenchyma [Suki and Bates, 2011]. The complex role that collagen and elastin fibers play in the dynamics of the lung parenchyma is beyond the scope of this thesis and is discussed in detail by Freed et al. [2021]; here we focus on the role that poro-elasto-dynamics plays at the mesoscale level.

Lung parenchyma has generally been modeled as a viscoelastic material [Brannen et al., 2022, Naumann et al., 2022, Cronin, 2011, Clayton et al., 2020, Clayton and Freed, 2019a, 2020a, Clayton, 2020, Clayton et al., 2021, Gayzik et al., 2010, Pydi et al., 2023] within the finite-strain regime. However, as we aim to show in Section 1.2.3, such an approach may not be physically realistic when compared to assuming poroelastic models. In recent years, efforts to model lung parenchyma as a poroelastic material have become more popular [Lande and Mitzner, 2006, Patte et al., 2022, Concha et al., 2018, Concha and Hurtado, 2020], but still focus on quasi-static or low strain-rate loading. Given the susceptibility of lung to blast injury, it behooves us to develop a numerical model that can capture the kinematics of lung parenchyma within this dynamic regime.

1.1.2 Numerical challenges in TPM

Mixture theory was established at finite strain by Truesdell and Toupin [1960], with later works for mixture theory applied to porous media by Bowen [1971, 1980, 1982] and others Coussy [2004], de Boer [2005], Clayton [2022], to name a few. The Theory of Porous Media (TPM) is an appropriate approximation to a more robust, but much more computationally expensive, Fluid-Structure Interaction (FSI) model at the pore length-scale. In TPM, these interactions are smeared

across a continuum material point, thereby simplifying not just the discretization of the governing mathematical equations (namely, mass balance, momentum balance, energy balance and entropy inequality), but also the discretization of the geometry itself. The advantages to using TPM over a FSI model are simplicity of implementation and computational cost. Here we incorporate TPM to take into account the different response times of the two constituents (phases) in a soft porous material subjected to shock loading: solid skeleton (s) and the pore fluid (f) that occupies the pore space. Generally speaking, we will assume material properties for lung parenchyma (Figure 1.1) for the solid skeleton, and air for the pore fluid, unless noted otherwise.

Past numerical models involving TPM have typically addressed geological and geotechnical engineering applications, e.g., soil consolidation problems, wherein inertia terms are typically ignored, the solid and pore fluid phases are nearly incompressible, and strains are small [Lewis and Schrefler, 1987, Schanz, 2009]. In other works [Markert et al., 2009, Heider, 2012, Zienkiewicz et al., 1993, Li et al., 2019], inertia terms are retained, but small-strain theory is still assumed. In Li et al. [2004], Regueiro et al. [2014], inertia terms are retained, constituents are compressible, nonlinear constitutive theory is present, and deformation is finite. However, it was assumed that dynamic loading frequencies were relatively small ($\mathcal{O}(10^1\text{-}10^2)$ rad/s), and therefore the acceleration of the fluid phase was approximately the same as that of the solid phase, i.e., $\mathbf{a}_f \approx \mathbf{a}_s = \mathbf{a}$. In this work, we continue from Regueiro et al. [2014] but with the assumption that for higher strain-rate loadings, $\mathbf{a}_f \neq \mathbf{a}_s$, necessitating a “three-field” formulation [Regueiro et al., 2014], and comparison to “two-field” formulation results. The three-field formulation is not new, see, e.g., Zienkiewicz and Shiomi [1984] for the initial theory and Gajo et al. [1994], Levenston et al. [1998], Yang [2006], Lotfian and Sivaselvan [2018], Wu et al. [2019], Zhang et al. [2019] for various numerical implementations. However, to the best of our knowledge, no authors consider the following novel contributions **simultaneously**:

- large deformations [Berger, 2015, Cao et al., 2016, Chapelle and Moireau, 2014, Burtschell et al., 2017, Patte et al., 2022, Concha and Hurtado, 2020, Diebels and Ehlers, 1996,

Zinatbakhsh et al., 2016, Gajo and Denzer, 2011, Ghorbani et al., 2016, Klahr et al., 2022, Li et al., 2004, Navas et al., 2017, Obaid et al., 2017, Regueiro et al., 2014, Rohan and Lukeš, 2017, Vuong et al., 2015, Yang, 2006, Yuan et al., 2022],

- inertial effects [Cao et al., 2016, Chapelle and Moireau, 2014, Burtschell et al., 2017, Diebels and Ehlers, 1996, Zinatbakhsh et al., 2016, Gajo et al., 1994, Gajo and Denzer, 2011, Ghorbani et al., 2016, Heider, 2012, Hosseinejad et al., 2019, Li et al., 2004, 2019, Markert et al., 2009, Navas et al., 2017, Obaid et al., 2017, Pedroso, 2015, Regueiro et al., 2014, Rohan and Lukeš, 2017, Salomoni and Schrefler, 2005, Vuong et al., 2015, Yang, 2006, Yuan et al., 2022, Zhang et al., 2019],
- non-linear constitutive theory [Berger, 2015, Chapelle and Moireau, 2014, Burtschell et al., 2017, Patte et al., 2022, Concha and Hurtado, 2020, Diebels and Ehlers, 1996, Ghorbani et al., 2016, Hosseinejad et al., 2019, Levenston et al., 1998, Markert et al., 2009, Navas et al., 2017, Obaid et al., 2017, Regueiro et al., 2014, Rohan and Lukeš, 2017, Vuong et al., 2015],
- compressible constituents [Cao et al., 2016, Gajo and Denzer, 2011, Ghorbani et al., 2016, Heider, 2012, Markert et al., 2009, Pedroso, 2015, Regueiro et al., 2014, Rohan and Lukeš, 2017, Yoon and Kim, 2018, Zhang et al., 2019],

and high strain-rate loading with nonlinear geometric effects. Accommodating high strain-rate loading within the context of TPM at large deformations, with inertia terms, nonlinear constitutive models, compressible constituents, within the framework of locally inhomogeneous phase temperatures is the primary contribution of this work.

Furthermore, many applications of TPM use implicit time-stepping methods, e.g., the well known Newmark-beta schemes, or semi-implicit time-stepping methods, see, e.g., Zienkiewicz et al. [1993], Markert et al. [2009], Heider [2012], Zhang et al. [2019], which, even for dynamic loadings, are not always suitable computationally speaking for shock-like loadings wherein small time steps are required to resolve the shock physics. Those that do present explicit time integration schemes

generally stick to the well-known central-difference scheme or variations thereof [Navas et al., 2017, Yuan et al., 2022]. Herein, we have developed two explicit integration schemes—central-differencing and a 3(2) and 5(4) Runge-Kutta scheme—as well as two implicit integration schemes—a Newmark-beta scheme and the standard trapezoidal rule.

1.1.3 Temperature and damage modeling

In order to address the challenge of quantifying “damage” to the lung tissue (in general, the solid constituent), one must first quantify lung tissue (solid constituent) temperature. For lung tissue specifically, the Grüneisen parameter is quite low¹ [Clayton and Freed, 2019a, 2020a], and any rate-effect from damage in an energy balance (refer to Section 3.3.1) is likely to have a negligible effect on solid temperature change. However, if one wishes to be thermodynamically consistent, one must pursue a temperature model and it is partially for this reason that we have done so in Chapters 3 and 4.

It would not be inaccurate to mention that the other reason for pursuing a locally inhomogeneous temperature model is for academic interest as well as physical realism when using an ideal gas model for the pore fluid wherein it may be inappropriate to neglect thermo-mechanical coupling. Many formulations in TPM assume the mixture is isothermal. Those that do assume temperature evolves [Wang, 2014, Fankell, 2017] also assume locally homogeneous constituent temperatures $\theta^s = \theta^f = \theta$. For an ideal gas pore fluid constituent circulating within a water-like solid constituent, this is a poor approximation, particularly past 50% compression of the pore fluid [Clayton, 2022] which we are liable to see for high strain-rate loading applications. Few TPM models for locally inhomogeneous temperatures exist. Ghadiani [2005] uses an ideal gas model for the pore fluid, but neglects finite strain and dynamic processes. Koch [2016], Sweidan et al. [2020] focus on geological applications of TPM, but also assume small strains as well as *mechanically* incompressible

¹ There is some uncertainty regarding the thermodynamic parameters for lung tissue used in this work, specifically their relation to the deformations of the solid skeleton. Thermodynamic parameters for lung tissue used in Clayton and Freed [2019a, 2020a] were based on experimental data which measured the thermodynamics of the *solid* lung tissue. To the best of our knowledge, no such data exists for the *solid skeleton* “matrix” of lung tissue. It is expected that the Grüneisen parameter for the solid skeleton would be higher than that of the solid constituent when considering lung tissue, given that the latter has thermodynamic properties similar to water, which is nearly incompressible.

constituents (refer to discussion of this in Section 2.3).

There has also been a considerable amount of experimental work to characterize thermodynamic properties for soft, porous materials which may then be used to parameterize numerical models. Unfortunately, experimental data for lung tissue thermal properties is limited, if not non-existent altogether. For brain tissue, Liu et al. [2017] performed shear-wave elastography to show that brain tissue shear modulus is inversely related to brain tissue temperature. A study by Mohammadi et al. [2021] measured the thermal conductivity, thermal diffusivity, and heat capacity of (calf) brain and (porcine) liver and pancreatic tissues, wherein, for all tissues, those properties remained constant up to around 60° C and increased thereafter. Multiple experiments have been conducted on various cartilage samples showing that elastic stiffness degrades as internal tissue temperature increases [Chae et al., 2008, Liu et al., 2015, Marshall et al., 2019, Marshall, 2019, Protsenko et al., 2008, Zemek et al., 2012]. If these same behaviors—a degradation of elastic stiffness and an increase in internal heating—were to be observed in lung tissue, then unique parameterization of the convective heat transfer coefficient between phases k_{θ}^{ε} would be necessary to accurately capture the degree to which the lung parenchyma would heat up from the shock-compressed air in its pores. An extensive literature review for elastic and thermomechanical properties of biological tissues subjected to thermal loading is provided by Bianchi et al. [2022].

In addition, there exists an abundant amount of experimental data for another soft porous material of interest, polyurethane (PUR) foams. PUR foams have wide applicability, from the automotive industry [Chen et al., 2023, Ates et al., 2022, Sebaey et al., 2021, Markert, 2008, 2005, Rossio et al., 1993] to PPE [Decker and Kedziora, 2024, Rodriguez-Millan et al., 2023, Naderi et al., 2022, Bhinder et al., 2021]. Experiments have been conducted to characterize the material properties of PUR foam when applying thermal loads [Constantinescu and Apostol, 2020, Kim et al., 2017, Song et al., 2009]² where again there is consensus that thermal degradation (of the elastic stiffness) is proportional to increases in temperature. Modeling of PUR foam using

² Stiffer foams are also popular for this area of research, see, e.g., [Rostami-Tapeh-Esmaeil et al., 2022, Bhagavathula et al., 2021, Jain et al., 2021, Liang et al., 2019, Wang et al., 2014, Arezoo et al., 2013, Tan et al., 2013, Vedula et al., 1998].

TPM is limited, and constituents are assumed isothermal [Markert, 2008, Ehlers et al., 2003]. Most numerical approaches assume simplified poroelastic models [Shrestha et al., 2023, Zhang et al., 2022, Lutsenko and Levin, 2017, Brun and Dumitrescu, 1995] or viscoelastic/visco-thermoelastic models [Decker and Kedziora, 2024, Naderi et al., 2022, Kim et al., 2017, Zhao et al., 2007]. Therefore, there is a need for a numerical model than capture the complete thermo-poro-elastodynamic effects at high rates of strain to address industry needs, such as the model pursued in this work.

1.1.4 Limitations of the current work

It should be noted, however, that there are physiological limitations of the current framework. To start, Brannen et al. [2022] showed that the tertiary bronchial tubes had a significant effect on lung tissue deformations, an anatomical interaction which we ignore in the present work, despite the lung parenchyma itself behaving as an isotropic [Weed et al., 2015] and homogeneous [Tai and Lee, 1981] material. Other anatomical interactions such as those between the lung and the surrounding organs and ribcage are also ignored (refer to Clayton et al. [2021], Clayton [2020], Cronin [2011]), as well as any complex reflective waves induced by the initial shock wave after impacting said anatomy and the surrounding environment [Stuhmiller, 2010]. Such interactions would necessitate, at a minimum, a three-dimensional (3-D) model, which was not pursued in this work.

Furthermore, we neglect microstructural interactions (as previously stated) at the solid-fluid interface when using TPM to smear the FSI at the pore scale. Most lung parenchyma modeling approaches [Stuhmiller et al., 1988, Bush and Challener, 1988, Clayton et al., 2021] will approximate the wave speed through the lung tissue an air as an average of the wave speed through both mediums so as not to resolve the (computationally prohibitive) fine-scale interactions. As Grimal et al. [2002] notes, this may not be appropriate in the high-frequency domain such as occurs after shock loading. In their approach, Grimal et al. [2002] assumed a closed-cell model, such that the pore air is contained within the walls of the alveoli. For sufficiently long rise times of the incident pressure wave (e.g., those occurring from a motor vehicle accident), lung parenchyma can be regarded as a homogeneous material; however, for shorter rise times (such as those from blast), distortion of

the incident pressure wave is dependent upon the microstructure, i.e., the diameter of the alveoli Grimal et al. [2002]. Therefore, an important part of future work will be utilizing upscaling from the microstructural model, with, e.g., a machine-learning approach, to account for variations in the microstructure to more accurately capture the underlying shock physics.

1.2 Viscoelasticity vs. poroelasticity

To help argue for the necessity of poromechanics models in this area of research (soft porous materials), we will briefly compare the stress relaxation times between a purely viscoelastic model and a poroelastic model, of lung parenchyma fully-saturated with air, at small strain.

1.2.1 Linear viscoelasticity in one dimension at small strain

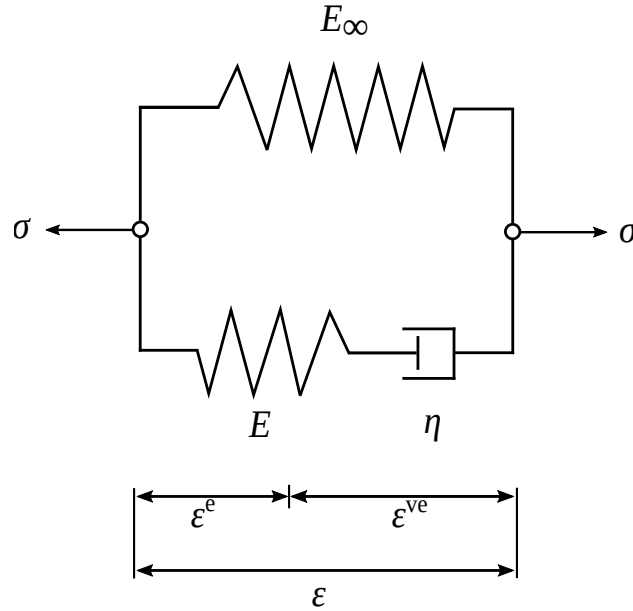


Figure 1.2: The standard linear solid model, adapted from Simo and Hughes [1998].

Consider the following viscoelastic standard linear solid model (refer to Simo and Hughes [1998]) in Figure 1.2 with axial strain ϵ that can be decomposed into its elastic strain ϵ^e and viscoelastic strain ϵ^{ve} components. Then the total stress contributed by the two parallel elements

of the model can be expressed as

$$\sigma = E_{\infty}\epsilon + \sigma^v, \quad (1.1)$$

where E_{∞} is the steady-state elastic modulus and

$$\sigma^v = \eta\dot{\epsilon}^{ve} = E\epsilon^e = E(\epsilon - \epsilon^{ve}), \quad (1.2)$$

where η is the viscosity of the dashpot. Rearranging Equation (1.2) leads to the following ODE:

$$\dot{\epsilon}^{ve} + \frac{1}{\tau}\epsilon^{ve} = \frac{1}{\tau}\epsilon, \quad (1.3)$$

where $\tau = \eta/E$ is the time relaxation constant. We will solve for $\epsilon^{ve}(t)$ using the integration factor $\exp[t/\tau]$ and convolution integral as follows:

$$\begin{aligned} & \exp[t/\tau]\dot{\epsilon}^{ve} + \frac{1}{\tau}\exp[t/\tau]\epsilon^{ve} = \frac{1}{\tau}\exp[t/\tau]\epsilon, \\ & \Rightarrow \int_{-\infty}^t \frac{d}{ds} (\exp[s/\tau]\epsilon^{ve}(s)) ds = \int_{-\infty}^t \frac{1}{\tau}\exp[s/\tau]\epsilon(s) ds, \\ & \Rightarrow \exp[t/\tau]\epsilon^{ve}(t) = \frac{1}{\tau} \int_{-\infty}^t \exp[s/\tau]\epsilon(s) ds, \\ & \Rightarrow \epsilon^{ve}(t) = \int_{-\infty}^t \frac{1}{\tau} \exp[(s-t)/\tau] \epsilon(s) ds; \\ & \frac{d}{ds} (\exp[(s-t)/\tau] \epsilon(s)) = \frac{1}{\tau} \exp[(s-t)/\tau] \epsilon(s) + \exp[(s-t)/\tau] \dot{\epsilon}(s), \\ & \Rightarrow \epsilon^{ve}(t) = \underbrace{\int_{-\infty}^t \frac{d}{ds} (\exp[(s-t)/\tau] \epsilon(s)) ds}_{:=\epsilon(t)} - \int_{-\infty}^t \exp[(s-t)/\tau] \dot{\epsilon}(s) ds. \end{aligned} \quad (1.4)$$

Thus the total stress may be written as follows:

$$\sigma(t) = E_{\infty}\epsilon(t) + E \int_{-\infty}^t \exp[(s-t)/\tau] \dot{\epsilon}(s) ds = \int_{-\infty}^t G(t-s)\dot{\epsilon}(s) ds, \quad (1.5)$$

where the relaxation function is

$$G(t-s) := E_{\infty} + E \exp[-(t-s)/\tau]. \quad (1.6)$$

Suppose, now, that we write the strain $\epsilon(t)$ in terms of the creep function $J(t)$ as follows:

$$\epsilon(t) = \int_{-\infty}^t J(t-s)\dot{\sigma}(s) ds; \quad J(t) = \frac{1}{E_\infty} \left(1 - \frac{E}{E_\infty} \exp \left[\frac{-E_\infty t}{E_0 t} \right] \right), \quad (1.7)$$

where we apply a step function for the total stress such that

$$\sigma(t) = \sigma_0 H(t); \quad \dot{\sigma}(t) = \sigma_0 \delta(t). \quad (1.8)$$

Substitution of the above into Equation (1.7)₁ gives

$$\epsilon(t) = \int_{-\infty}^t J(t-s)\sigma_0\delta(s) ds = \sigma_0 J(t). \quad (1.9)$$

We will compare the effects of this creeping viscoelastic model to that of a poroelastic model, the latter equations of which we will derive in the following section.

1.2.2 Linear poroelasticity in one dimension at small strain

Terzaghi's 1-D consolidation theory [Taylor, 1948] makes the following assumptions:

1. The solid constituent is homogeneous.
2. The porous medium is fully saturated, i.e., there are only two constituents in the porous medium (solid skeleton, and pore fluid).
3. The solid constituent and pore fluid constituent are incompressible. (Note that the porous solid skeleton "matrix" remains compressible so that deformation may occur.)
4. The applied compression is purely vertical in the z direction (uniaxial strain), and the motion of the pore fluid is purely vertical as well (unidirectional flow).
5. Darcy's law (sans inertia terms), i.e., $v_{z(f)} = -\hat{k}\gamma_f \frac{dh}{dz}$, is valid (where $v_{z(f)}$ is the pore fluid seepage velocity in the z direction, \hat{k} is the hydraulic conductivity, γ_f is the unit weight of the pore fluid, and h is the pressure head).
6. The results are valid for small strain:

- (a) \hat{k} is independent of the void ratio change Δe , and is assumed constant during the consolidation process. Note that porosity $n^f := e/(1 + e)$.
- (b) m_v (compressibility factor under uniaxial strain) is assumed constant during the consolidation process (i.e., linear isotropic elasticity will hold).

7. There are no sources or sinks of pore fluid.

From Assumptions 3, 4 and 7, the continuity equation reduces to

$$\frac{dv_{z(f)}}{dz} dx dy dz = 0, \quad (1.10)$$

which we may also write as

$$\frac{dv_{z(f)}}{dz} dx dy dz = \frac{dV}{dt}. \quad (1.11)$$

Substitution of Darcy's law into Equation (1.10) gives us

$$\frac{dv_{z(f)}}{dz} = -\hat{k}\gamma_f \frac{d^2 h}{dz^2}, \quad (1.12)$$

where the pressure head is defined as,

$$h := \frac{p_f}{\gamma_f} + z, \quad (1.13)$$

and the pore fluid pressure p_f may be written as the summation of the fluid unit weight γ_f times the position z and an excess pore fluid pressure $p_{f,e}$. Thus, we can rewrite Equation (1.12) as

$$\frac{dv_{z(f)}}{dz} = -\hat{k} \frac{d^2 p_{f,e}}{dz^2}. \quad (1.14)$$

Now, assuming a linear isotropic elastic constitutive relation for the volumetric strain for uniaxial strain under vertical stress, we may write

$$\frac{\Delta V}{V} = m_v \Delta \sigma_{E^s}^r. \quad (1.15)$$

Rearranging, dividing both sides by Δt and taking the limit as $\Delta t \rightarrow 0$ gives us

$$\frac{dV}{dt} = m_v \frac{d\sigma_{E^s}^s}{dt} dx dy dz. \quad (1.16)$$

Recall the effective stress principle, $\sigma = \sigma_E^s + p_f$, for compressible solid skeleton, and nearly incompressible solid constituent (see Chapters 2 & 3). Here, we assume soil mechanics convention for which the normal components of stress are positive in compression, along with the pore fluid pressure p_f . Decomposing the pore fluid pressure in terms of the hydrostatic and excess pore fluid pressure, $p_f = \gamma_f z + p_{f,e}$, and then taking the time derivative of all four terms above provides the useful relation

$$\frac{d\sigma_E^s}{dt} = -\frac{dp_{f,e}}{dt}. \quad (1.17)$$

Substitution of this result back into Equation (1.16), equating with Equations (1.11) & (1.14), and rearranging, gives us the following partial differential equation (PDE) for $p_{f,e}$:

$$\frac{\partial p_{f,e}}{\partial t} = c_v \frac{\partial^2 p_{f,e}}{\partial z^2}, \quad (1.18)$$

where the coefficient of consolidation $c_v = \hat{k}/(m_v \gamma_f)$. We further assume the following “drained” (atmospheric) boundary conditions:

$$p_{f,e}(0, t) = 0, \quad p_{f,e}(2H, t) = 0, \quad (1.19)$$

where H is defined as the longest flow path to “drained” (atmospheric) boundary for a given pore fluid molecule, and an initial pressure along the domain is defined as

$$p_{f,e}(z, 0) = p_{f,e,0}(z). \quad (1.20)$$

Note that a “drained” boundary condition implies atmospheric pressure, which we assume is reference at 0 atm. This PDE may be solved using the method of separation of variables where

$$p_{f,e}(z, t) = F(z)\Phi(t), \quad (1.21)$$

and thus Equation (1.18) becomes

$$\frac{1}{F(z)} \frac{\partial^2 F}{\partial z^2} = \frac{1}{c_v \Phi(t)} \frac{\partial \Phi}{\partial t}. \quad (1.22)$$

Since the left and right hand sides of Equation (1.22) are independent of t and z , respectively, they must both be equal to some constant, e.g., $-A^2$. Solving for $F(z)$ yields

$$F(z) = c_1 \cos(Az) + c_2 \sin(Az), \quad (1.23)$$

and likewise solving for $\Phi(t)$ yields

$$\Phi(t) = c_3 \exp[-A^2 c_v t]. \quad (1.24)$$

Then, Equation (1.21) may be rewritten as the product of these solutions:

$$p_{f,e} = (c_4 \cos(Az) + c_5 \sin(Az)) \exp[-A^2 c_v t], \quad (1.25)$$

where $c_4 = c_1 c_3$ and $c_5 = c_2 c_3$. Using the boundary condition given by Equation (1.19)₁ gives $c_4 = 0$. Likewise, using the boundary condition given by Equation (1.19)₂ gives

$$p_{f,e}(2H, t) = 0 = c_5 \sin\left(\frac{n\pi}{2H} z\right) \exp\left[-\left(\frac{n\pi}{2H}\right)^2 c_v t\right]. \quad (1.26)$$

Since c_5 is arbitrary, we may write the solution for the excess pore fluid pressure as a summation over all n as

$$p_{f,e}(z, t) = \sum_{n=1}^{\infty} B_n \sin\left(\frac{n\pi}{2H} z\right) \exp\left[-\left(\frac{n\pi}{2H}\right)^2 c_v t\right], \quad (1.27)$$

where B_n is a yet to be determined constant. Using our initial condition defined by Equation (1.20) allows us to write

$$p_{f,e,0}(z) = \sum_{n=1}^{\infty} B_n \sin\left(\frac{n\pi}{2H} z\right). \quad (1.28)$$

This is a Fourier sine series, which when multiplied by $\sin(n\pi z/2H)$ allows us to solve for B_n using the orthogonality relation of two sinusoidal waves over the period $2H$ as

$$B_n = \frac{1}{H} \int_0^{2H} p_{f,e,0}(z) \sin\left(\frac{n\pi}{2H} z\right) dz. \quad (1.29)$$

Substitution of this result back into Equation (1.27) gives

$$p_{f,e}(z, t) = \sum_{n=1}^{\infty} \left(\frac{1}{H} \int_0^{2H} p_{f,e,0}(z) \sin\left(\frac{n\pi}{2H} z\right) dz \right) \sin\left(\frac{n\pi}{2H} z\right) \exp\left[-\frac{(n\pi)^2}{4} T\right], \quad (1.30)$$

where $T = c_v t/H$ is the dimensionless time factor. Consider now the case where the initial excess pore fluid pressure is constant, i.e. $p_{f,e,0}(z) = t^\sigma$. Then we may solve for B_n by integrating Equation (1.29) directly as

$$B_n = \frac{1}{H} \int_0^{2H} t^\sigma \sin\left(\frac{n\pi}{2H}z\right) dz = \frac{2t^\sigma}{n\pi} (1 - \cos(n\pi)), \quad (1.31)$$

which gives

$$p_{f,e}(z, t) = \sum_{n=1}^{\infty} \frac{2t^\sigma}{M} \sin\left(\frac{M}{H}z\right) \exp[-M^2 T], \quad (1.32)$$

where $M = n\pi/2$.

1.2.3 Comparison of linear viscoelasticity and poroelasticity in 1-D at small strain

We now compare the one-dimensional, uniaxial strain, unidirectional flow poroelastic response to the creep viscoelastic response, where both models are subject to a Heaviside step function application of boundary traction, which results in a constant initial stress with distance if we ignore gravitational effects. Figure 1.5 shows that for the shorter column, the relaxation times between the viscoelastic and poroelastic models are identical. For the taller column, the relaxation time for the viscoelastic model is identical to that of the shorter column. However, the relaxation time is significantly increased for the poroelastic model. This is because the direct consideration of the pore fluid means that the solid skeleton must displace said fluid before reaching steady-state displacement.

In the context of lung deformations, this is an important distinction to make because a simple difference in geometry leads to drastically different deformation processes. One might consider designing a lung deformation model to quantify injury metrics and parameterize design of PPE based on the results of the numerical model in an effort to better protect the soldier in the field. However, if a viscoelastic model is assumed outright, then, depending on size of lungs (e.g., between biological male and biological female soldiers) assumed in the model, the ensuing PPE design may prove to be inadequate as lung injury is coupled to (violent) deformations Fung [1990].

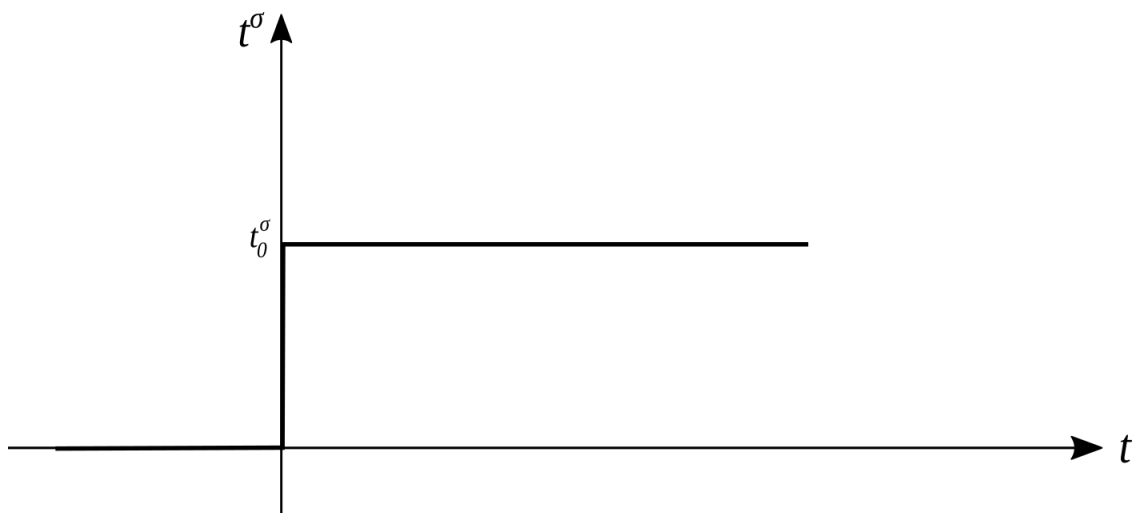


Figure 1.3: The applied Heaviside step function that is applied to the top of the column.

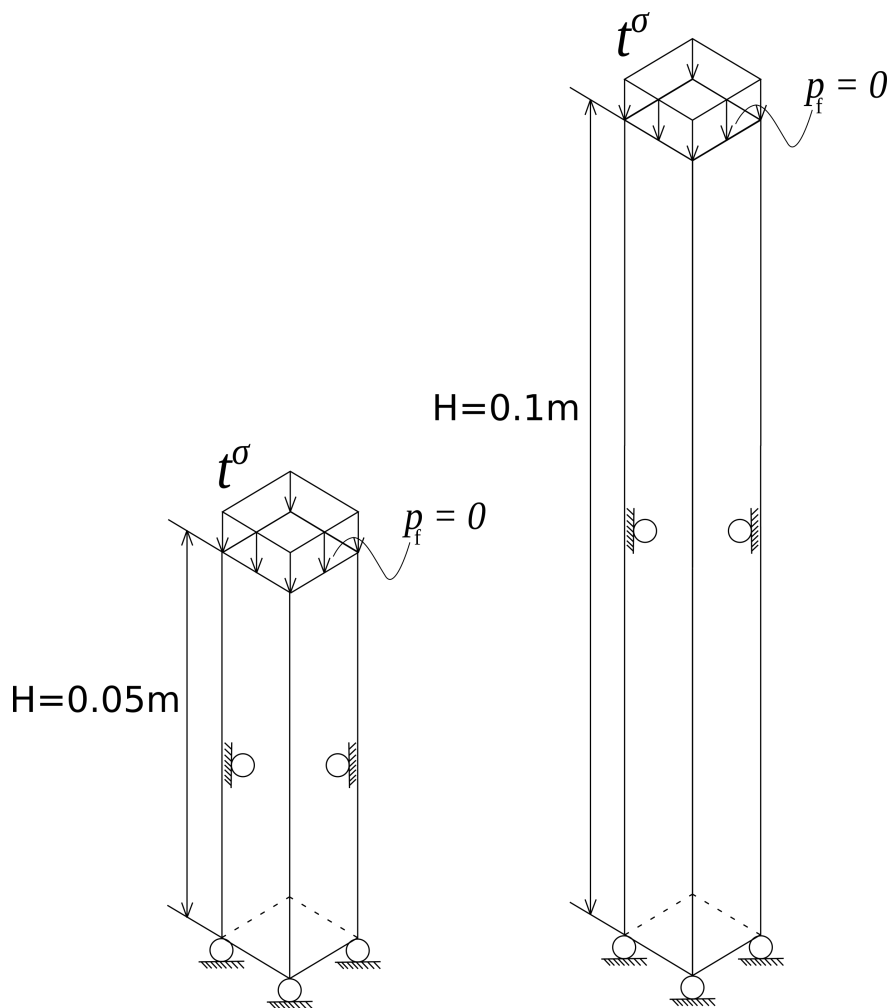


Figure 1.4: Schematic of the columns used for this thought experiment. The cross-sectional areas are identical between both, but the second column is double the height of the first.

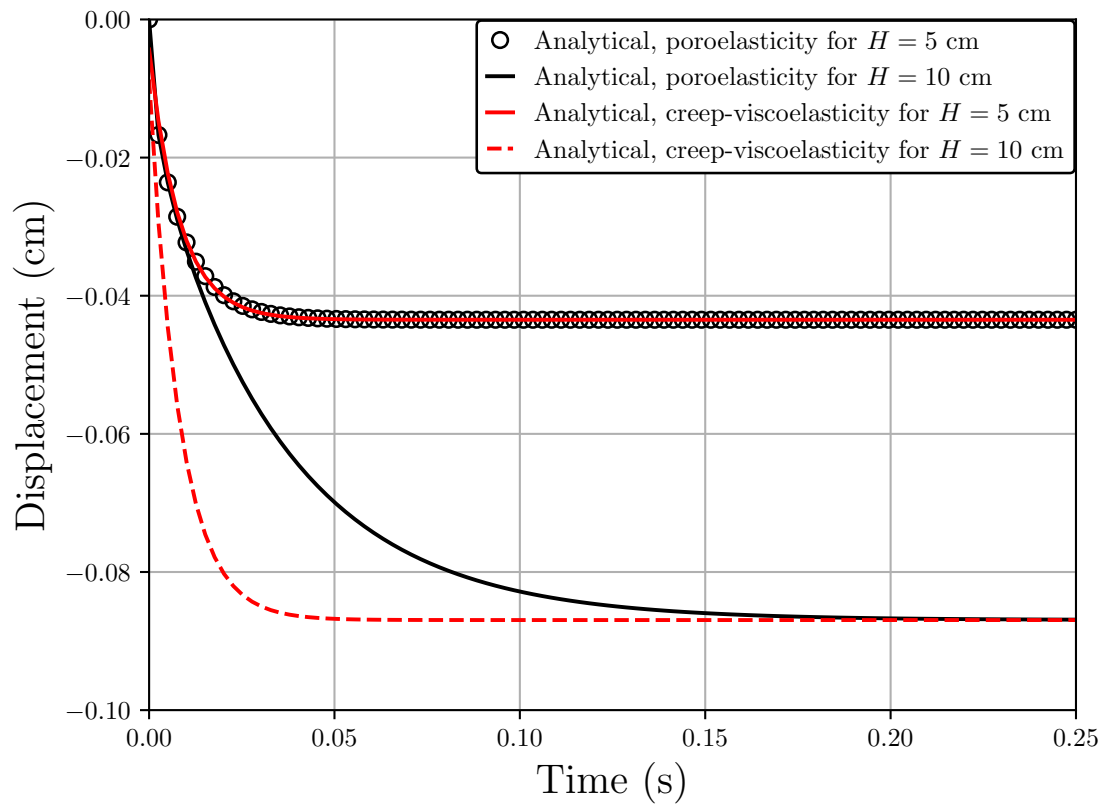


Figure 1.5: Comparison for lung parenchyma with initial applied stress $t^\sigma = 10$ Pa.

1.3 Objectives

The goal of the present work is to demonstrate the efficacy of a poro-elasto-dynamic model where the subsequent geometry is subjected high strain-rate loadings that mimic shock waves occurring from blast, or shock-tube testing in a lab. This model will be contrasted against a single-phase model to demonstrate how the latter cannot simulate the realistic physics that occur for a porous medium. The work is outlined as follows.

In Chapter 2 we introduce TPM and provide definitions for important concepts, such as volume fraction. Following this, the balance laws are either stated, or derived, for each phase and, when appropriate, the mixture as a whole. Chapter 3 continues with the development of a complete, thermodynamically consistent model from which all subsequent numerical modeling approaches then follow. We discuss different assumptions to the physical model, and how said assumptions impact the physics. Chapter 3 concludes with a brief discussion of a damage model for the solid constituent, which was not implemented in the present work and will be developed as part of future work.

Chapter 4 then follows with a presentation of the variational and weakened forms of the different physics models implemented into the numerical code, SPONGE-1D. For each physical formulation, we present the time-discretized forms of the spatially-discretized governing equations in great detail, with associated derivations covered in the Appendix. The chapter concludes with a brief discussion of various numerical stabilization approaches that were pursued in this thesis and which are implemented into SPONGE-1D.

Chapter 5 presents the results of all numerical simulations, beginning with verification examples to demonstrate the robustness of the code and the numerical approach discussed in Chapter 4. Then, we provide examples pertaining to the numerical stabilization techniques, and how different parameters thereof may alter the resulting kinematics. The bulk of the chapter is dedicated to the numerical results from simulating lung parenchyma undergoing high strain-rate loadings. Therein, we showcase different finite element types, constitutive limitations, sensitivity studies for the pore

fluid & porous material parameters, and the comparison between the single-phase model developed by Clayton and Freed [2019a], Clayton et al. [2021] and the multiphase model developed for this thesis. We finish with a brief discussion of preliminary results pertaining to thermo-mechanical coupling for the multiphase model.

Chapter 2

Theory of Porous Media

An extensive background of mixture theory for porous media is provided by Bowen [1971, 1976, 1980, 1982], Coussy [2004], de Boer [2005] and Ehlers [2002]. We will follow the notation of Holzapfel [2000] (for solid mechanics) and de Boer [2005] in our presentation of the governing equations and constitutive relations.

2.1 Concept of volume fractions

We assume that the porous solid continuum body constitutes a control space \mathcal{B} (current configuration of the solid skeleton) and that only liquids or gases in the pores can leave this control space. Rather than modeling the exact microstructure of the porous solid, we assume that the pores are modeled in a statistical sense such that their specific locations are arbitrary. This concept of volume fraction is illustrated in Figure 2.1(a). The volume fractions n^α are defined such that they relate the “real” differential volumes dv_α of each constituent φ^α (or phase, α) to the smeared (homogenized), total differential volume dv , i.e.,

$$n^\alpha(\mathbf{x}, t) = \frac{dv_\alpha(\mathbf{x}, t)}{dv(\mathbf{x}, t)}, \quad (2.1)$$

where \mathbf{x} is the position vector in the current configuration \mathcal{B} (see Figure 2.1(b)), and t is current time. Thus, for any mixture, the constituents φ^α occupying some control volume dv in the control space \mathcal{B} must satisfy

$$\sum_{\alpha} n^\alpha(\mathbf{x}, t) = 1, \quad \sum_{\alpha} dv_\alpha(\mathbf{x}, t) = dv(\mathbf{x}, t). \quad (2.2)$$

We furthermore assume that the constituents are immiscible (following the *principle of phase separation* [Ehlers, 2002], see also Section 3.1.1) such that we can relate the partial mass density ρ^α , that is, the mass density of φ^α occupying the total differential volume dv containing multiple constituents, to the real mass density $\rho^{\alpha R}$, the mass density of φ^α occupying the differential volume dv_α containing only φ^α , as follows:

$$m_\alpha(\mathbf{x}, t) = \int_{\mathcal{B}^\alpha} \rho^{\alpha R}(\mathbf{x}, t) dv_\alpha(\mathbf{x}, t) = \int_{\mathcal{B}} \rho^{\alpha R}(\mathbf{x}, t) n^\alpha(\mathbf{x}, t) dv(\mathbf{x}, t) = \int_{\mathcal{B}} \rho^\alpha(\mathbf{x}, t) dv(\mathbf{x}, t), \quad (2.3)$$

where m_α is the mass of φ^α in the control space \mathcal{B} . Hereafter we assume that variables written in the current configuration \mathcal{B} are dependent on position \mathbf{x} at time t so as to simplify the notation. Similarly, variables written in the reference configuration \mathcal{B}_0 are dependent on position \mathbf{X} at time t .

2.2 Kinematics

The kinematics of a biphasic solid-fluid mixture theory ($\alpha = s, f$, and f is *either* a liquid or a gas, and cannot be decomposed into both as is common in triphasic solid-liquid-gas mixture theory, see, e.g., de Boer [2005]), are shown in Figure 2.1. The vector \mathbf{x} is the spatial position vector which is occupied by both constituent material points X_s and X_f of the mixture such that $\mathbf{x} = \chi_f(\mathbf{X}_f, t) = \chi_s(\mathbf{X}_s, t)$, where the material point of the solid constituent is mapped from the reference position \mathbf{X}_s to the current position \mathbf{x} through mapping χ_s . The inverse map is defined as $\mathbf{X}_\alpha = \chi_\alpha^{-1}(\mathbf{x}, t)$, assuming smoothly differentiable fields. The deformation gradient and its inverse are defined as follows (assuming Cartesian coordinates):

$$\begin{aligned} \mathbf{F}_\alpha &= \frac{\partial \chi_\alpha}{\partial \mathbf{X}_\alpha}, & \mathbf{F}_\alpha^{-1} &= \frac{\partial \mathbf{X}_\alpha}{\partial \mathbf{x}}, \\ F_{iI(\alpha)} &= \frac{\partial \chi_{i(\alpha)}}{\partial X_{I(\alpha)}}, & F_{Ii(\alpha)}^{-1} &= \frac{\partial X_{I(\alpha)}}{\partial x_i}. \end{aligned} \quad (2.4)$$

The differential volumes dV_f and dV_s in their respective reference configurations \mathcal{B}_0^f and \mathcal{B}_0^s both map to the same differential volume dv in the current configuration \mathcal{B}_t through their

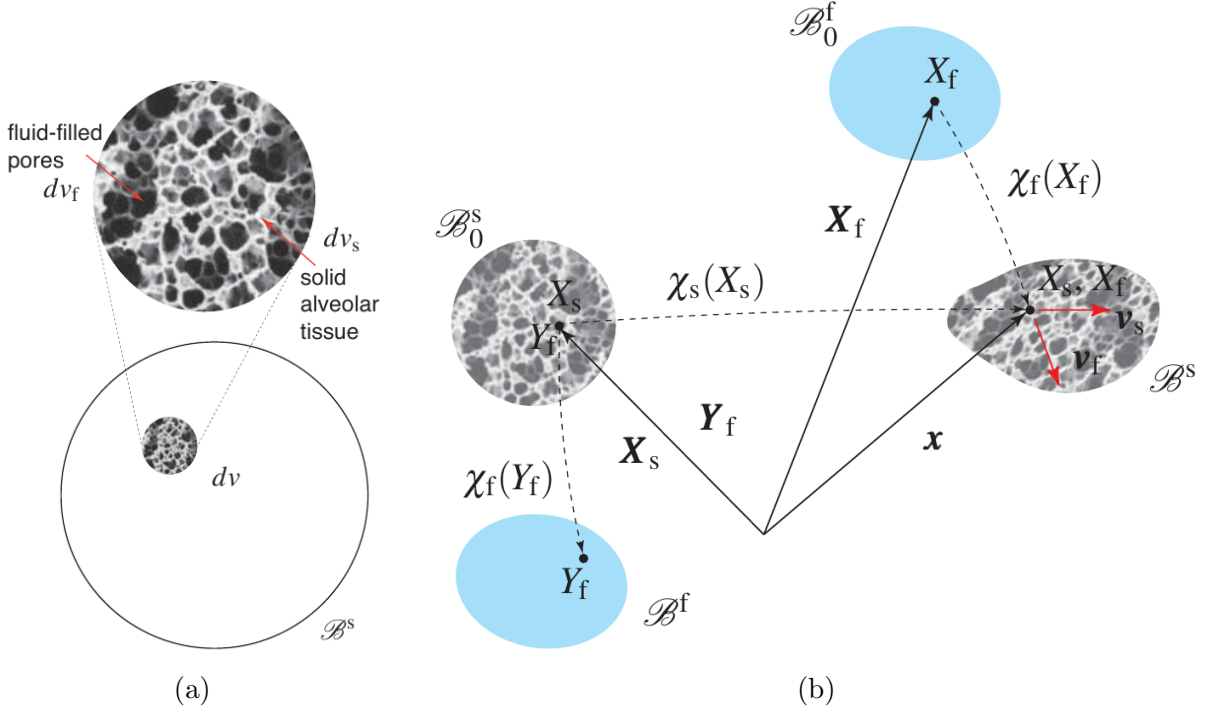


Figure 2.1: (a) Concept of volume fraction for biphasic (solid(s)-fluid(f)) mixture theory, showing solid skeleton composed of alveolar tissue. Note that in the theory of porous media, it is assumed that the control space is that of the solid phase $\mathcal{B} := \mathcal{B}^s$, also known as “solid skeleton.” (b) Kinematics of a biphasic (solid-fluid) mixture theory.

deformation gradients \mathbf{F}_f and \mathbf{F}_s . The Jacobian of deformation for both constituents is defined as follows:

$$\begin{aligned}
 J_s &= \det \mathbf{F}_s > 0; & J_f &= \det \mathbf{F}_f > 0, \\
 dv &= J_s dV_s = J_f dV_f, \\
 dv_\alpha &= n^\alpha dv = n^\alpha J_\alpha dV_\alpha, \\
 dV_f &\subset \mathcal{B}_0^f, & dV_s &\subset \mathcal{B}_0^s.
 \end{aligned} \tag{2.5}$$

We will convert all material time derivatives with respect to the solid (s) constituent motion (equivalently, the solid skeleton motion; see note in Figure 2.1(a) for details) such that for φ^α the material

time derivative is

$$\begin{aligned}
D_t^\alpha(\square) &= \frac{D^\alpha(\square)}{Dt} = \frac{D^s(\square)}{Dt} + \frac{\partial(\square)}{\partial \mathbf{x}} \cdot \tilde{\mathbf{v}}_\alpha, \\
\tilde{\mathbf{v}}_\alpha &= \mathbf{v}_\alpha - \mathbf{v}_s, \\
D_t^s(\square) &= \frac{D^s(\square)}{Dt} = \frac{\partial(\square)}{\partial t} + \frac{\partial(\square)}{\partial \mathbf{x}} \cdot \mathbf{v}_s,
\end{aligned} \tag{2.6}$$

where $\tilde{\mathbf{v}}_\alpha$ is the relative velocity vector of φ^α with respect to the solid (s) constituent motion.

2.3 Balance of Mass

The total mass of a φ^α in the current configuration \mathcal{B} can be written as

$$m_\alpha = \int_{\mathcal{B}} \rho^\alpha dv = \int_{\mathcal{B}_0} \rho^\alpha J_\alpha dV_\alpha. \tag{2.7}$$

After taking the material time derivative of m_α with respect to the motion of φ^α , the balance of mass of φ^α can be written as

$$D_t^\alpha m_\alpha = \int_{\mathcal{B}} (D_t^\alpha \rho^\alpha + \rho^\alpha \operatorname{div} \mathbf{v}_\alpha) dv = \int_{\mathcal{B}} \hat{\rho}^\alpha dv, \tag{2.8}$$

where $\hat{\rho}^\alpha$ is the mass supply of φ^α per unit total current volume. The local form of Equation (2.8) is, upon dividing by $\rho^{\alpha R}$,

$$D_t^\alpha n^\alpha + \frac{n^\alpha}{\rho^{\alpha R}} D_t^\alpha \rho^{\alpha R} + n^\alpha \operatorname{div} \mathbf{v}_\alpha = \frac{\hat{\rho}^\alpha}{\rho^{\alpha R}}. \tag{2.9}$$

We assume that there is no supply of solid mass to the solid (s) constituent such that $\hat{\rho}^s \rightarrow 0$, and that the solid (s) constituent of the soft porous material (solid skeleton wall material) is incompressible. If we allowed *thermal* compressibility under the assumption of locally inhomogeneous temperatures ($\theta^s \neq \theta^f$), i.e.,

$$\rho^{\text{sR}} = \rho^{\text{sR}}(\theta^s) \quad \Rightarrow \quad D_t^s \rho^{\text{sR}} = \frac{\partial \rho^{\text{sR}}}{\partial \theta^s} D_t^s \theta^s, \tag{2.10}$$

wherein we might use the constitutive relation developed by Lu and Pister [1975]:

$$\rho^{\text{sR}}(\theta^s) = \rho_0^{\text{sR}} \exp[-\alpha_V^s \Delta \theta^s], \tag{2.11}$$

where α_V^s is the volumetric CTE of the solid (s) constituent and $\Delta\theta^s := \theta^s - \theta_0^s$, with θ_0^s being the prescribed initial temperature of the solid (s) constituent. This would potentially be inconsistent with the *mechanically* incompressible assumption: at the microscopic level, heat is the movement of individual atoms, and thus a paradox is formed. For the small Grüneisen parameter of the solid lung tissue used in this thesis, only large changes in temperature of the solid lung tissue, beyond what one would expect resulting from a shock loading, would affect volume change of the solid lung tissue. For further reading on a *mechanically* incompressible and *thermally* compressible constituent, refer to Ghadiani [2005], Koch [2016], Ehlers and Häberle [2016], Sweidan et al. [2020], Vujosevic and Lubarda [2002].

Following this, we may proceed with constitutive assumptions for the internal energy function of the fluid phase: either it produces a pressure that depends only on its real mass density, i.e., $p_f = p_f(\rho^{\text{fR}})$ (barotropic), or it produces a pressure that depends on both its real mass density and entropy per unit mass η^f , i.e., $p_f = p_f(\rho^{\text{fR}}, \eta^f)$ (baroclinic) in the case of adiabatic conditions, or it produces a pressure that depends on both its real mass density and temperature θ^f , i.e., $p_f = p_f(\rho^{\text{fR}}, \theta^f)$, which is the preferred form for non-adiabatic conditions. Denoting the isentropic bulk modulus of the pore fluid K_f^η , isothermal bulk modulus of the pore fluid K_f^θ , the Grüneisen parameter of the pore fluid γ^f and specific heat of the pore fluid c_V^f ,

$$K_f^\eta := \rho^{\text{fR}} \left. \frac{\partial p_f}{\partial \rho^{\text{fR}}} \right|_{\eta^f}, \quad K_f^\theta := \rho^{\text{fR}} \left. \frac{\partial p_f}{\partial \rho^{\text{fR}}} \right|_{\theta^f}, \quad \gamma^f := \frac{1}{\rho^{\text{fR}} \theta^f} \left. \frac{\partial p_f}{\partial \eta^f} \right|_{\rho^{\text{fR}}}, \quad c_V^f := \frac{1}{\rho^{\text{fR}} \gamma^f} \left. \frac{\partial p_f}{\partial \theta^f} \right|_{\rho^{\text{fR}}}. \quad (2.12)$$

The barotropic pore fluid. Suppose that pore fluid pressure is defined as $p_f(v^f)$ where v^f is the specific volume of the pore fluid, then,

$$D_t^f p_f = \left. \frac{\partial p_f}{\partial v^f} \right|_{\eta^f} D_t^f v^f. \quad (2.13)$$

Then, using the definition given by Equation (2.12)₁,

$$D_t^f p_f = \frac{K_f^\eta}{\rho^{\text{fR}}} D_t^f \rho^{\text{fR}}. \quad (2.14)$$

Next, as we express the balance of mass for both constituents (solid and fluid) individually, the incompressibility assumption ($D_t^\alpha \rho^{\alpha\text{R}} \rightarrow 0$) is used for the solid phase in Equation (2.9) for $\alpha =$

s and Equation (2.14) is used in Equation (2.9) for $\alpha = f$. Adding these two equations together using the relationship between volume fractions $n^f = 1 - n^s$, the combined balance of mass of the mixture becomes

$$\frac{n^f}{K_f^\eta} D_t^s p_f + \operatorname{div} \mathbf{v}_s + \frac{1}{K_f^\eta} \operatorname{grad}(p_f) \cdot (n^f \tilde{\mathbf{v}}_f) + \operatorname{div}(n^f \tilde{\mathbf{v}}_f) = \frac{\hat{\rho}^f}{\rho^{\text{fR}}}. \quad (2.15)$$

We can map (2.15) back to the reference configuration of the solid skeleton $\mathcal{B}_0 = \mathcal{B}_0^s$, i.e.,

$$\frac{J_s n^f}{K_f^\eta} D_t^s p_f + D_t^s J_s + \frac{J_s}{K_f^\eta} \operatorname{GRAD}_s(p_f) \cdot \mathbf{F}_s^{-1} \cdot (n^f \tilde{\mathbf{v}}_f) + J_s \operatorname{GRAD}_s(n^f \tilde{\mathbf{v}}_f) : \mathbf{F}_s^{-T} = \frac{J_s \hat{\rho}^f}{\rho^{\text{fR}}}, \quad (2.16)$$

where subscript or superscript s implies with respect to the motion of the solid skeleton.

The baroclinic pore fluid: locally inhomogeneous temperature regime. Suppose instead $p_f(v^f, \eta^f)$, then

$$D_t^f p_f = \left. \frac{\partial p_f}{\partial v^f} \right|_{\eta^f} D_t^f v^f + \left. \frac{\partial p_f}{\partial \eta^f} \right|_{v^f} D_t^f \eta^f. \quad (2.17)$$

Then, using the definitions given by Equation (2.12)_{1,3}, we may write

$$D_t^f p_f = \frac{K_f^\eta}{\rho^{\text{fR}}} D_t^f \rho^{\text{fR}} + \rho^{\text{fR}} \gamma^f \theta^f D_t^f \eta^f. \quad (2.18)$$

If instead $p_f(v^f, \theta^f)$, then

$$D_t^f p_f = \left. \frac{\partial p_f}{\partial v^f} \right|_{\theta^f} D_t^f v^f + \left. \frac{\partial p_f}{\partial \theta^f} \right|_{v^f} D_t^f \theta^f. \quad (2.19)$$

Then, using the definitions given by Equation (2.12)_{2,4}, we may write

$$D_t^f p_f = \frac{K_f^\theta}{\rho^{\text{fR}}} D_t^f \rho^{\text{fR}} + \rho^{\text{fR}} \gamma^f c_V^f D_t^f \theta^f. \quad (2.20)$$

Given the prevalence of θ^f in the balance and constitutive equations when locally inhomogeneous temperatures are considered, it is more convenient to work with Equation (2.20) than Equation (2.14), where the former follows from *free energy* formulations and the latter follows from *internal energy* formulations.

Next, as we express the balance of mass for both constituents (solid and fluid) individually, the incompressibility assumption is used for the solid phase in Equation (2.9) for $\alpha = s$ and

Equation (2.20) is used in Equation (2.9) for $\alpha = f$. Adding these two equations together using the relationship between volume fractions $n^f = 1 - n^s$, the combined balance of mass of the mixture becomes

$$\begin{aligned} & -\frac{\gamma^f \rho^{\text{fR}} c_V^f}{K_f^\theta} [n^f D_t^s \theta^f + \text{grad}(\theta^f) \cdot (n^f \tilde{\mathbf{v}}_f)] + \frac{n^f}{K_f^\theta} D_t^s p_f + \text{div} \mathbf{v}_s \\ & + \frac{1}{K_f^\theta} \text{grad}(p_f) \cdot (n^f \tilde{\mathbf{v}}_f) + \text{div}(n^f \tilde{\mathbf{v}}_f) = \frac{\hat{\rho}^f}{\rho^{\text{fR}}}. \end{aligned} \quad (2.21)$$

Using the definition of the volumetric coefficient of thermal expansion (CTE) of the pore fluid

$$\alpha_V^f := \frac{\gamma^f \rho^{\text{fR}} c_V^f}{K_f^\theta}; \alpha_V^f = 3\alpha^f, \quad (2.22)$$

where α^f is the linear CTE of the pore fluid, taken to be constant, we may write the balance of mass of the mixture as

$$\begin{aligned} & -\alpha_V^f [n^f D_t^s \theta^f + \text{grad}(\theta^f) \cdot (n^f \tilde{\mathbf{v}}_f)] + \frac{n^f}{K_f^\theta} D_t^s p_f + \text{div} \mathbf{v}_s \\ & + \frac{1}{K_f^\theta} \text{grad}(p_f) \cdot (n^f \tilde{\mathbf{v}}_f) + \text{div}(n^f \tilde{\mathbf{v}}_f) = \frac{\hat{\rho}^f}{\rho^{\text{fR}}}. \end{aligned} \quad (2.23)$$

We can map (2.23) back to the reference configuration of the solid skeleton $\mathcal{B}_0 = \mathcal{B}_0^s$, which gives

$$\begin{aligned} & -J_s \alpha_V^f [n^f D_t^s \theta^f + \text{GRAD}_s(\theta^f) \cdot \mathbf{F}_s^{-1} \cdot (n^f \tilde{\mathbf{v}}_f)] + \frac{J_s n^f}{K_f^\theta} D_t^s p_f + D_t^s J_s \\ & + \frac{J_s}{K_f^\theta} \text{GRAD}_s(p_f) \cdot \mathbf{F}_s^{-1} \cdot (n^f \tilde{\mathbf{v}}_f) + J_s \text{GRAD}_s(n^f \tilde{\mathbf{v}}_f) : \mathbf{F}_s^{-T} = \frac{J_s \hat{\rho}^f}{\rho^{\text{fR}}}, \end{aligned} \quad (2.24)$$

where subscript or superscript s implies with respect to the motion of the solid skeleton. For the constitutive assumption of an ideal gas made later (refer to Section 3.3.2, paragraph *The ideal gas model*), $\alpha_V^f := 1/\theta^f$ and $K_f^\theta := p_f$, thus Equation (2.24) may also be written as

$$\begin{aligned} & -\frac{J_s}{\theta^f} [n^f D_t^s \theta^f + \text{GRAD}_s(\theta^f) \cdot \mathbf{F}_s^{-1} \cdot (n^f \tilde{\mathbf{v}}_f)] + \frac{J_s n^f}{p_f} D_t^s p_f + D_t^s J_s \\ & + \frac{J_s}{p_f} \text{GRAD}_s(p_f) \cdot \mathbf{F}_s^{-1} \cdot (n^f \tilde{\mathbf{v}}_f) + J_s \text{GRAD}_s(n^f \tilde{\mathbf{v}}_f) : \mathbf{F}_s^{-T} = \frac{J_s \hat{\rho}^f}{\rho^{\text{fR}}}. \end{aligned} \quad (2.25)$$

2.4 Balance of Momentum

The balance of linear momentum for φ^α is written as

$$D_t^\alpha \left(\int_{\mathcal{B}} \rho^\alpha \mathbf{v}_\alpha dv \right) = \int_{\mathcal{B}} \rho^\alpha \mathbf{b}^\alpha dv + \int_{\Gamma} \mathbf{t}^\alpha da + \int_{\mathcal{B}} \mathbf{h}^\alpha dv, \quad (2.26)$$

where $\Gamma := \partial\mathcal{B}$. After carrying through the material time derivative (and applying the balance of mass given by Equation (2.8)), applying the divergence theorem to the traction term \mathbf{t}^α , and localizing the integral, we may write

$$\operatorname{div} \boldsymbol{\sigma}^\alpha + \rho^\alpha \mathbf{b}^\alpha + \mathbf{h}^\alpha = \rho^\alpha \mathbf{a}_\alpha + \hat{\rho}^\alpha \mathbf{v}_\alpha, \quad (2.27)$$

where $\boldsymbol{\sigma}^\alpha$ is the partial Cauchy stress, such that the total Cauchy stress $\boldsymbol{\sigma} = \boldsymbol{\sigma}^s + \boldsymbol{\sigma}^f$, ρ^α is the partial mass density (total mass density $\rho = \rho^s + \rho^f$), \mathbf{b}^α is the body force per unit mass on φ^α (e.g., acceleration due to gravity such that $\mathbf{b}^\alpha = \mathbf{g}$), \mathbf{h}^α is the interaction body force from all other constituents on φ^α , \mathbf{a}_α is the acceleration vector, and $\hat{\rho}^\alpha \mathbf{v}_\alpha$ is the mass supply momentum (which we typically assume is negligible). Usually, the interaction body forces between constituents are due to drag and will sum to zero because they are equal and opposite. Thus, these forces do not affect the mixture as a whole such that $\mathbf{h}^s + \mathbf{h}^f = \mathbf{0}$. Via the balance of angular momentum it can be shown that the partial Cauchy stresses for each φ^α are symmetric, i.e., $\boldsymbol{\sigma}^\alpha = (\boldsymbol{\sigma}^\alpha)^T$. Equation (2.27) can be mapped back to the reference configuration of the solid skeleton for φ^α as

$$\operatorname{DIV}_s \mathbf{P}_s^\alpha + \rho_{0(s)}^\alpha \mathbf{b}^\alpha + J_s \mathbf{h}^\alpha = \rho_{0(s)}^\alpha \mathbf{a}_\alpha + \hat{\rho}_{0(s)}^\alpha \mathbf{v}_\alpha, \quad (2.28)$$

where again, subscript s or (s) implies with respect to solid skeleton reference configuration, such that $\rho_{0(s)}^\alpha = J_s \rho^\alpha$. From Equation (2.28) we can derive the balance of linear momentum equation for the biphasic mixture in the reference configuration \mathcal{B}_0^s using the following equations and assumptions:

- (1) Total Cauchy stress, and first Piola stress with respect to \mathcal{B}_0^s :

$$\boldsymbol{\sigma} = \boldsymbol{\sigma}^s + \boldsymbol{\sigma}^f, \quad \mathbf{P}_s = \mathbf{P}_s^s + \mathbf{P}_s^f \quad (2.29)$$

- (2) Decomposition of the solid partial Cauchy stress into an extra stress, hereafter referred to as the solid skeleton extra stress (or solid extra stress), and temperature-scaled pore fluid pressure (justified in Chapter 3, see also Ehlers [2002])¹, and shock viscosity q (refer to

¹ Note that the $\frac{\theta^s}{\theta^f} p_f n^s$ term that appears in Equation (2.30) necessitates an initial spatial homogeneity of both

Section 4.4.1):

$$\boldsymbol{\sigma}^s = \boldsymbol{\sigma}_E^s - \left(\frac{\theta^s}{\theta^f} p_f n^s + q \right) \mathbf{1} \quad (2.30)$$

(3) Assume all mass supplies are negligible: $\hat{\rho}^\alpha = 0$

(4) Assume body forces per unit mass are only due to gravity: $\mathbf{b}^\alpha = \mathbf{g}$, where \mathbf{g} is the acceleration vector of gravity.

We may then write the balance of linear momentum equation for the biphasic mixture in the reference configuration \mathcal{B}_0^s as

$$\begin{aligned} \text{DIV}_s \mathbf{P}_s + \rho_{0(s)} \mathbf{g} &= \rho_{0(s)}^s \mathbf{a}_s + \rho_{0(s)}^f \mathbf{a}_f, \\ \mathbf{P}_s &= \mathbf{P}_{E(s)}^s + \mathbf{P}_{E(s)}^f - J_s p_f \mathbf{F}_s^{-T} \left(\frac{\theta^f}{\theta^s} n^s + n^f \right) - J_s Q \mathbf{F}_s^{-T}. \end{aligned} \quad (2.31)$$

For the $(\mathbf{u}-p_f)$ formulation, we will further assume that $\mathbf{a}_f \approx \mathbf{a}_s = \mathbf{a}$, which should be valid only for slower dynamic loadings. With that assumption in mind, the pore fluid viscous stress tensor $\mathbf{P}_{E(s)}^f$ drops from Equation (2.31)₂ because the constitutive law that defines it in Chapter 3 includes spatial dependence on pore fluid velocity, which cannot be determined without a third governing equation for the pore fluid displacement. Note that under the assumption of a nearly-inviscid pore fluid ($\boldsymbol{\sigma}_E^f \rightarrow \mathbf{0}$) and locally homogeneous temperatures ($\theta^s = \theta^f = \theta$), Equation (2.31)₂ may be rewritten as

$$\mathbf{P}_s = \mathbf{P}_{E(s)}^s - J_s p_f \mathbf{F}_s^{-T} - J_s Q \mathbf{F}_s^{-T}. \quad (2.32)$$

For brevity, the balance relations hereafter do not make explicit use of the shock viscosity Q , except for the derivation of the balance of energy of a single phase material (or solid phase in biphasic mixture theory) in Sections 4.1.2, 4.1.5, & 4.1.6, where it is included to account for dissipation of energy.

constituent temperatures, θ_0^s and θ_0^f , as well as initial spatial homogeneity of porosity n_0^f . Otherwise, taking $\text{div}(\boldsymbol{\sigma}^s)$ to evaluate the linear momentum balance of the solid phase results in $\text{grad}(\theta^s)$, $\text{grad}(\theta^f)$, $\text{grad}(n^f)$ terms, indicating that the solid skeleton has an initial acceleration prior to any applied load. For the mixture linear momentum balance, only initial spatial homogeneity of the constituent temperatures is required.

Balance of Linear Momentum of Pore Fluid. Equation (2.31)₁ allows us to solve for the displacement of the solid skeleton (the connective tissue network of the soft porous material), but not for the displacement (or velocity) of the pore fluid (f) phase. Thus, we require an additional governing equation, namely, the balance of linear momentum of the pore fluid (f) phase:

$$\operatorname{div} \boldsymbol{\sigma}^f + \rho^f \mathbf{b}^f + \mathbf{h}^f = \rho^f \mathbf{a}_f + \hat{\rho}^f \mathbf{v}_f. \quad (2.33)$$

As motivated by satisfying the second law of thermodynamics in Clausius-Duhem form [Coussy, 2004, de Boer, 2005] (see also Chapter 3), the pore fluid interaction force can be decomposed as follows:²

$$\mathbf{h}^f = \mathbf{h}_E^f + \frac{\theta^s}{\theta^f} p_f \operatorname{grad} n^f, \quad (2.34)$$

where it may also be shown that (refer to Section 3.1.3)

$$\mathbf{h}_E^f = \frac{(n^f)^2}{\hat{k}} \tilde{\mathbf{v}}_f, \quad (2.35)$$

where \hat{k} is the hydraulic conductivity (a proportionality parameter in the Clausius-Duhem inequality, that may be a function of fluid volume fraction n^f) and where it has been assumed that the solid skeleton's permeability is isotropic (refer to Equation (3.61)). Direct substitution of Equation (2.35) into Equation (2.34), and Equation (2.34) into Equation (2.33) with

$$\boldsymbol{\sigma}^f := \boldsymbol{\sigma}_E^f - n^f p_f \mathbf{1}; \operatorname{div} \boldsymbol{\sigma}^f = \operatorname{div} \boldsymbol{\sigma}_E^f - n^f \operatorname{grad} p_f - p_f \operatorname{grad} n^f, \quad (2.36)$$

and assuming $\mathbf{b}^f = \mathbf{b}^s = \mathbf{b} = \mathbf{g}$ and $\hat{\rho}^f = 0$, yields

$$\rho^f \mathbf{a}_f - \operatorname{div} \boldsymbol{\sigma}_E^f + n^f \operatorname{grad} p_f + p_f \operatorname{grad}(n^f) \left(1 - \frac{\theta^s}{\theta^f}\right) + \frac{(n^f)^2}{\hat{k}} (\mathbf{v}_f - \mathbf{v}_s) - \rho^f \mathbf{g} = \mathbf{0}. \quad (2.37)$$

For a nearly-inviscid pore fluid and locally homogeneous temperatures, the balance of linear momentum of the pore fluid is written as

$$\rho^f \mathbf{a}_f + n^f \operatorname{grad} p_f + \frac{(n^f)^2}{\hat{k}} (\mathbf{v}_f - \mathbf{v}_s) - \rho^f \mathbf{g} = \mathbf{0}. \quad (2.38)$$

² Note that this form of \mathbf{h}^f necessitates initial phase temperatures that are in equilibrium with one another. Otherwise, Equation (2.37) does not hold for an initial heterogeneous porosity.

We can map both equations to the reference configuration \mathcal{B}_0^s and write them as

$$\begin{aligned} \rho_{0(s)}^f \mathbf{a}_f - \text{DIV}_s \mathbf{P}_{E(s)}^f + J_s n^f \text{GRAD}_s p_f \cdot \mathbf{F}_s^{-1} + J_s p_f \text{GRAD}_s(n^f) \left(1 - \frac{\theta^s}{\theta^f}\right) \cdot \mathbf{F}_s^{-1} \\ + \frac{J_s (n^f)^2}{\hat{k}} (\mathbf{v}_f - \mathbf{v}_s) - \rho_{0(s)}^f \mathbf{g} = \mathbf{0} \end{aligned} \quad (2.39)$$

for the case of viscous pore fluid and locally inhomogeneous temperatures and

$$\rho_{0(s)}^f \mathbf{a}_f + J_s n^f \text{GRAD}_s p_f \cdot \mathbf{F}_s^{-1} + \frac{J_s (n^f)^2}{\hat{k}} (\mathbf{v}_f - \mathbf{v}_s) - \rho_{0(s)}^f \mathbf{g} = \mathbf{0} \quad (2.40)$$

for the case of nearly-inviscid pore fluid and locally homogeneous temperatures.

Now we have three coupled governing equations that describe the kinematics of the biphasic mixture which we can use to solve for three unknown “fields” (solution variables): Cauchy pore fluid pressure p_f , solid skeleton displacement \mathbf{u} (dropping subscript s), and pore fluid displacement \mathbf{u}_f , respectively. For locally homogeneous temperatures, these three coupled governing equations are commonly referred to as the $(\mathbf{u}-\mathbf{u}_f-p_f)$ formulation. In the $(\mathbf{u}-p_f)$ formulation, we assume that the acceleration of the pore fluid (f) constituent is approximately equal to the acceleration of the solid skeleton, i.e. $\mathbf{a}_f \approx \mathbf{a}_s = \mathbf{a}$; thus, we do not need to solve Equation (2.40). We employ variational forms of these equations in the total Lagrangian finite element formulation in Chapter 4.

To describe the evolution of phase entropies and temperature(s), additional governing equations are required, irrespective of whether or not thermo-mechanical coupling and/or locally homogeneous temperatures are assumed. The governing equations that describe the thermodynamics will end up being the balance of energy of each phase. However, constitutive relations must be determined prior. The process for determining constitutive equations is outlined in the next three sections, and in more detail in Chapter 3.

2.5 Balance of Energy

The first law of thermodynamics provides the balance of energy for the mixture as a whole, and can be written in the current configuration \mathcal{B} for φ^α as

$$D_t^\alpha [K^\alpha(t) + E^\alpha(t)] = P_{\text{ext}}^\alpha(t) + Q^\alpha(t) + \bar{E}^\alpha(t), \quad (2.41)$$

where the kinetic energy is defined as

$$K^\alpha(t) = \int_{\mathcal{B}} \frac{1}{2} \rho^\alpha \mathbf{v}_\alpha \cdot \mathbf{v}_\alpha dv, \quad (2.42)$$

the internal energy is defined as

$$P_{\text{int}}^\alpha(t) = D_t^\alpha E^\alpha(t) = D_t^\alpha \int_{\mathcal{B}} \rho^\alpha e^\alpha(\mathbf{x}, t) dv, \quad (2.43)$$

and where the e^α is the internal energy per unit mass (referred to as ε^α in Bowen [1976], de Boer [2005]). The external work on φ^α is defined as

$$P_{\text{ext}}^\alpha(t) = \int_{\Gamma} \mathbf{t}^\alpha \cdot \mathbf{v}_\alpha da + \int_{\mathcal{B}} \rho^\alpha \mathbf{b}^\alpha \cdot \mathbf{v}_\alpha dv, \quad (2.44)$$

where $\mathbf{t}^\alpha = \mathbf{n} \cdot \boldsymbol{\sigma}^\alpha$. The rate of thermal work (thermal power) acting on an individual constituent as

$$Q^\alpha(t) = - \int_{\Gamma} \mathbf{q}^\alpha \cdot \mathbf{n} da + \int_{\mathcal{B}} \rho^\alpha r^\alpha dv, \quad (2.45)$$

where for φ^α , \mathbf{q}^α is the heat flux vector, r^α is the heat input rate per unit mass. Lastly, the power supply to φ^α by other phases is defined as

$$\bar{E}^\alpha(t) = \int_{\mathcal{B}} \hat{e}^\alpha dv = \int_{\mathcal{B}} \left(\hat{\varepsilon}^\alpha + \mathbf{h}^\alpha \cdot \mathbf{v}_\alpha + \hat{\rho}^\alpha \left[e^\alpha + \frac{1}{2} \mathbf{v}_\alpha \cdot \mathbf{v}_\alpha \right] \right) dv, \quad (2.46)$$

where $\hat{\varepsilon}^\alpha$ is “local interaction” [Bowen, 1976] for energy supply to φ^α from other phases and \hat{e}^α is the total power density (per unit volume) supply to φ^α by other phases. Combining the above energy terms, Equations (2.42)–(2.46), the first law of thermodynamics may be written as follows:

$$\begin{aligned} D_t^\alpha \int_{\mathcal{B}} \left(\frac{1}{2} \rho^\alpha \mathbf{v}_\alpha \cdot \mathbf{v}_\alpha + \rho^\alpha e^\alpha \right) dv &= \int_{\Gamma} \mathbf{t}^\alpha \cdot \mathbf{v}_\alpha da + \int_{\mathcal{B}} \rho^\alpha \mathbf{b}^\alpha \cdot \mathbf{v}_\alpha dv \\ &\quad - \int_{\Gamma} \mathbf{q}^\alpha \cdot \mathbf{n} da + \int_{\mathcal{B}} (\rho^\alpha r^\alpha + \hat{e}^\alpha) dv. \end{aligned} \quad (2.47)$$

Start by applying the material time derivative: switch to reference configuration \mathcal{B}_0^α .

$$D_t^\alpha \int_{\mathcal{B}} \left(\frac{1}{2} \rho^\alpha \mathbf{v}_\alpha \cdot \mathbf{v}_\alpha + \rho^\alpha e^\alpha \right) dv = D_t^\alpha \int_{\mathcal{B}_0^\alpha} \left(\frac{1}{2} \rho^\alpha \mathbf{v}_\alpha \cdot \mathbf{v}_\alpha + \rho^\alpha e^\alpha \right) J_\alpha dV_\alpha \quad (2.48)$$

Carry out material time derivative in reference configuration \mathcal{B}_0^α .

$$\begin{aligned} D_t^\alpha \int_{\mathcal{B}_0^\alpha} \left(\frac{1}{2} \rho^\alpha \mathbf{v}_\alpha \cdot \mathbf{v}_\alpha + \rho^\alpha e^\alpha \right) J_\alpha dV_\alpha &= \int_{\mathcal{B}_0^\alpha} \left(\left[D_t^\alpha \mathbf{v}_\alpha \cdot \mathbf{v}_\alpha + D_t^\alpha e^\alpha \right] (\rho^\alpha J_\alpha) \right. \\ &\quad \left. + \left[\frac{1}{2} \mathbf{v}_\alpha \cdot \mathbf{v}_\alpha + e^\alpha \right] \left[D_t^\alpha \rho^\alpha J_\alpha + \rho^\alpha D_t^\alpha J_\alpha \right] \right) dV_\alpha \end{aligned} \quad (2.49)$$

The first term in first set of brackets [] on r.h.s. of Equation (2.49) is acceleration of φ^α , i.e.,

$$D_t^\alpha \mathbf{v}_\alpha := \mathbf{a}_\alpha. \quad (2.50)$$

Thus the first set of brackets [] on r.h.s. Equation (2.49) of may be written as

$$\left[D_t^\alpha \mathbf{v}_\alpha \cdot \mathbf{v}_\alpha + D_t^\alpha e^\alpha \right] (\rho^\alpha J_\alpha) = \left[\mathbf{a}_\alpha \cdot \mathbf{v}_\alpha + D_t^\alpha e^\alpha \right] (\rho^\alpha J_\alpha). \quad (2.51)$$

The first term in the third set of brackets [] on r.h.s. of Equation (2.49) is evaluated from balance of mass, i.e.,

$$D_t^\alpha \rho^\alpha = \hat{\rho}^\alpha - \rho^\alpha \operatorname{div} \mathbf{v}_\alpha. \quad (2.52)$$

The second term in third set of brackets [] on r.h.s. of Equation (2.49) is evaluated from the continuity equation, i.e.,

$$D_t^\alpha J_\alpha = J_\alpha \operatorname{div} \mathbf{v}_\alpha. \quad (2.53)$$

Thus the third set of brackets [] on r.h.s. of Equation (2.49) may be written as

$$\left[\frac{1}{2} \mathbf{v}_\alpha \cdot \mathbf{v}_\alpha + e^\alpha \right] \left[D_t^\alpha \rho^\alpha J_\alpha + \rho^\alpha D_t^\alpha J_\alpha \right] = \hat{\rho}^\alpha \left[\frac{1}{2} \mathbf{v}_\alpha \cdot \mathbf{v}_\alpha + e^\alpha \right] J_\alpha. \quad (2.54)$$

Rewriting the material time derivative of total internal energy in current configuration, such that

$J_\alpha dV_\alpha \rightarrow dv$,

$$D_t^\alpha \int_{\mathcal{B}} \left(\frac{1}{2} \rho^\alpha \mathbf{v}_\alpha \cdot \mathbf{v}_\alpha + \rho^\alpha e^\alpha \right) dv = \int_{\mathcal{B}} \left(\rho^\alpha \mathbf{a}_\alpha \cdot \mathbf{v}_\alpha + \rho^\alpha D_t^\alpha e^\alpha + \hat{\rho}^\alpha \left[e^\alpha + \frac{1}{2} \mathbf{v}_\alpha \cdot \mathbf{v}_\alpha \right] \right) dv. \quad (2.55)$$

Next, apply divergence theorem to the boundary terms (external work via traction, rate of thermal work via heat flux):

$$\begin{aligned} \int_{\Gamma} \mathbf{t}^\alpha \cdot \mathbf{v}_\alpha da &= \int_{\mathcal{B}} \operatorname{div}(\boldsymbol{\sigma}^\alpha \cdot \mathbf{v}_\alpha) dv, \\ \int_{\Gamma} \mathbf{q}^\alpha \cdot \mathbf{n} da &= \int_{\mathcal{B}} \operatorname{div} \mathbf{q}^\alpha dv. \end{aligned} \quad (2.56)$$

Expand divergence on Cauchy stress & velocity:

$$\operatorname{div}(\boldsymbol{\sigma}^\alpha \cdot \mathbf{v}_\alpha) = \operatorname{div}(\boldsymbol{\sigma}^\alpha) \cdot \mathbf{v}_\alpha + \boldsymbol{\sigma}^\alpha : \mathbf{l}_\alpha, \quad (2.57)$$

where \mathbf{l}_α is the velocity gradient. Next, apply localization theorem such that the energy balance for φ^α is written as

$$\begin{aligned} \rho^\alpha \mathbf{a}_\alpha \cdot \mathbf{v}_\alpha + \rho^\alpha D_t^\alpha e^\alpha + \hat{\rho}^\alpha \left(e^\alpha + \frac{1}{2} \mathbf{v}_\alpha \cdot \mathbf{v}_\alpha \right) &= \operatorname{div}(\boldsymbol{\sigma}^\alpha) \cdot \mathbf{v}_\alpha + \boldsymbol{\sigma}^\alpha : \mathbf{l}_\alpha + \rho^\alpha \mathbf{b}^\alpha \cdot \mathbf{v}_\alpha \\ &\quad - \operatorname{div} \mathbf{q}^\alpha + \rho^\alpha r^\alpha + \hat{e}^\alpha. \end{aligned} \quad (2.58)$$

Third term on r.h.s. of Equation (2.58) can be rewritten by substituting balance of momentum, i.e.,

$$\rho^\alpha \mathbf{b}^\alpha = \rho^\alpha \mathbf{a}_\alpha + \hat{\rho}^\alpha \mathbf{v}_\alpha - \operatorname{div} \boldsymbol{\sigma}^\alpha - \mathbf{h}^\alpha. \quad (2.59)$$

Substitute into Equation (2.58):

$$\begin{aligned} \rho^\alpha \mathbf{a}_\alpha \cdot \mathbf{v}_\alpha + \rho^\alpha D_t^\alpha e^\alpha + \hat{\rho}^\alpha \left(e^\alpha + \frac{1}{2} \mathbf{v}_\alpha \cdot \mathbf{v}_\alpha \right) &= \operatorname{div}(\boldsymbol{\sigma}^\alpha) \cdot \mathbf{v}_\alpha + \boldsymbol{\sigma}^\alpha : \mathbf{l}_\alpha \\ + (\rho^\alpha \mathbf{a}_\alpha + \hat{\rho}^\alpha \mathbf{v}_\alpha - \operatorname{div} \boldsymbol{\sigma}^\alpha - \mathbf{h}^\alpha) \cdot \mathbf{v}_\alpha - \operatorname{div} \mathbf{q}^\alpha + \rho^\alpha r^\alpha + \hat{e}^\alpha. \end{aligned} \quad (2.60)$$

The acceleration terms, divergence on partial Cauchy stress terms cancel, leaving

$$\rho^\alpha D_t^\alpha e^\alpha = \boldsymbol{\sigma}^\alpha : \mathbf{l}_\alpha - \operatorname{div} \mathbf{q}^\alpha + \rho^\alpha r^\alpha + \hat{e}^\alpha + \hat{\rho}^\alpha \left(\frac{1}{2} \mathbf{v}_\alpha \cdot \mathbf{v}_\alpha - e^\alpha \right) - \mathbf{h}^\alpha \cdot \mathbf{v}_\alpha. \quad (2.61)$$

Note that this is equivalent to the derivation provided by Bowen [1976] if one substitutes the definition of the total power density supply given by Equation (2.46), such that

$$\rho^\alpha D_t^\alpha e^\alpha = \boldsymbol{\sigma}^\alpha : \mathbf{l}_\alpha - \operatorname{div} \mathbf{q}^\alpha + \rho^\alpha r^\alpha + \hat{e}^\alpha. \quad (2.62)$$

2.6 Balance of Entropy

Deriving an entropy balance for the mixture as a whole is preferred to deriving one for individual constituents given that the latter can lead to incomplete constitutive relations [de Boer, 2005], i.e.,

$$\sum_\alpha \Gamma^\alpha(t) \geq 0, \quad (2.63)$$

wherein,

$$\Gamma^\alpha(t) = D_t^\alpha H^\alpha(t) - \tilde{Q}^\alpha(t). \quad (2.64)$$

Thus, the balance of entropy can be written in the current configuration \mathcal{B} as

$$\sum_\alpha D_t^\alpha H^\alpha(t) \geq \sum_\alpha \tilde{Q}^\alpha(t), \quad (2.65)$$

where the total internal entropy of φ^α is

$$H^\alpha(t) = \int_{\mathcal{B}} \rho^\alpha \eta^\alpha dv, \quad (2.66)$$

and the rate of total entropy input for φ^α is

$$\tilde{Q}^\alpha(t) = \int_{\mathcal{B}} \frac{1}{\theta^\alpha} \rho^\alpha r^\alpha dv - \int_{\Gamma} \frac{1}{\theta^\alpha} \mathbf{q}^\alpha \cdot \mathbf{n} da. \quad (2.67)$$

Start by applying the material time derivative: switch to reference configuration \mathcal{B}_0^α :

$$D_t^\alpha \int_{\mathcal{B}} \rho^\alpha \eta^\alpha dv = D_t^\alpha \int_{\mathcal{B}_0^\alpha} \rho^\alpha \eta^\alpha J_\alpha dV_\alpha. \quad (2.68)$$

Carry out material time derivative in reference configuration \mathcal{B}_0^α :

$$D_t^\alpha \int_{\mathcal{B}_0^\alpha} \rho^\alpha \eta^\alpha J_\alpha dV_\alpha = \int_{\mathcal{B}_0^\alpha} \left((\eta^\alpha J_\alpha) D_t^\alpha \rho^\alpha + (\rho^\alpha J_\alpha) D_t^\alpha \eta^\alpha + (\rho^\alpha \eta^\alpha) D_t^\alpha J_\alpha \right) dV_\alpha. \quad (2.69)$$

The first and last terms are simplified using mass balance and continuity equation, per Equations (2.52) and (2.53), respectively, such that

$$D_t^\alpha \int_{\mathcal{B}_0^\alpha} \rho^\alpha \eta^\alpha J_\alpha dV_\alpha = \int_{\mathcal{B}_0^\alpha} \left(\eta^\alpha J_\alpha \hat{\rho}^\alpha + (\rho^\alpha J_\alpha) D_t^\alpha \eta^\alpha \right) dV_\alpha. \quad (2.70)$$

Rewrite the material time derivative of total internal entropy in current configuration, such that $J_\alpha dV_\alpha \rightarrow dv$:

$$D_t^\alpha \int_{\mathcal{B}} \rho^\alpha \eta^\alpha dv = \int_{\mathcal{B}} \left(\eta^\alpha \hat{\rho}^\alpha + \rho^\alpha D_t^\alpha \eta^\alpha \right) dv. \quad (2.71)$$

Apply divergence theorem to the heat flux term in rate of entropy input, Equation (2.67):

$$\int_{\Gamma} \frac{1}{\theta^\alpha} \mathbf{q}^\alpha \cdot \mathbf{n} da = \int_{\mathcal{B}} \operatorname{div} \left(\frac{1}{\theta^\alpha} \mathbf{q}^\alpha \right) dv. \quad (2.72)$$

Next, apply localization theorem, such that entropy balance is written as

$$\sum_{\alpha} \left(\hat{\rho}^\alpha \eta^\alpha + \rho^\alpha D_t^\alpha \eta^\alpha - \frac{1}{\theta^\alpha} \rho^\alpha r^\alpha + \operatorname{div} \left[\frac{1}{\theta^\alpha} \mathbf{q}^\alpha \right] \right) \geq 0. \quad (2.73)$$

2.7 Dissipation Inequality

In order to produce constitutive relations that adhere to the thermodynamic principles laid out by Truesdell and Toupin [1960] and Coleman and Noll [1963], the second and first laws will be combined to form the dissipation inequality, i.e., the Clausius-Duhem inequality. Introduce the Helmholtz free energy potential

$$\psi^\alpha = e^\alpha - \theta^\alpha \eta^\alpha, \quad (2.74)$$

and substitute it into the first law, Equation (2.61), such that

$$\rho^\alpha D_t^\alpha (\psi^\alpha + \theta^\alpha \eta^\alpha) = \boldsymbol{\sigma}^\alpha : \mathbf{l}_\alpha - \operatorname{div} \mathbf{q}^\alpha + \rho^\alpha r^\alpha + \hat{e}^\alpha + \hat{\rho}^\alpha \left(\frac{1}{2} \mathbf{v}_\alpha \cdot \mathbf{v}_\alpha - e^\alpha \right) - \mathbf{h}^\alpha \cdot \mathbf{v}_\alpha. \quad (2.75)$$

Next, isolate the material time derivative on the phase entropy:

$$\begin{aligned} \rho^\alpha D_t^\alpha \eta^\alpha = \frac{1}{\theta^\alpha} \left(-\rho^\alpha [D_t^\alpha \psi^\alpha + \eta^\alpha D_t^\alpha \theta^\alpha] + \boldsymbol{\sigma}^\alpha : \mathbf{l}_\alpha - \operatorname{div} \mathbf{q}^\alpha + \rho^\alpha r^\alpha + \hat{e}^\alpha \right. \\ \left. + \hat{\rho}^\alpha \left[\frac{1}{2} \mathbf{v}_\alpha \cdot \mathbf{v}_\alpha - e^\alpha \right] - \mathbf{h}^\alpha \cdot \mathbf{v}_\alpha \right). \end{aligned} \quad (2.76)$$

Substitute this into the entropy balance, Equation (2.73), such that

$$\begin{aligned} \sum_{\alpha} \frac{1}{\theta^\alpha} \left(\hat{\rho}^\alpha \theta^\alpha \eta^\alpha - \rho^\alpha [D_t^\alpha \psi^\alpha + \eta^\alpha D_t^\alpha \theta^\alpha] + \boldsymbol{\sigma}^\alpha : \mathbf{l}_\alpha - \operatorname{div} \mathbf{q}^\alpha + \rho^\alpha r^\alpha + \hat{e}^\alpha \right. \\ \left. + \hat{\rho}^\alpha \left[\frac{1}{2} \mathbf{v}_\alpha \cdot \mathbf{v}_\alpha - e^\alpha \right] - \mathbf{h}^\alpha \cdot \mathbf{v}_\alpha - \rho^\alpha r^\alpha + \theta^\alpha \operatorname{div} \left[\frac{1}{\theta^\alpha} \mathbf{q}^\alpha \right] \right) \geq 0. \end{aligned} \quad (2.77)$$

Recognize that heat source/sink terms cancel, such that the total dissipation inequality may be written as

$$\begin{aligned} \sum_{\alpha} \frac{1}{\theta^\alpha} \left(\rho^\alpha [D_t^\alpha \psi^\alpha + \eta^\alpha D_t^\alpha \theta^\alpha] - \boldsymbol{\sigma}^\alpha : \mathbf{l}_\alpha - \hat{e}^\alpha + \hat{\rho}^\alpha \left[\psi^\alpha - \frac{1}{2} \mathbf{v}_\alpha \cdot \mathbf{v}_\alpha \right] + \mathbf{h}^\alpha \cdot \mathbf{v}_\alpha \right. \\ \left. + \frac{1}{\theta^\alpha} \operatorname{grad}(\theta^\alpha) \cdot \mathbf{q}^\alpha \right) \geq 0. \end{aligned} \quad (2.78)$$

Given the summation over the mixture, iff $\theta^\alpha = \theta$, i.e., locally homogeneous temperatures, could we write

$$\sum_{\alpha} \left(\rho^{\alpha} [D_t^{\alpha} \psi^{\alpha} + \eta^{\alpha} D_t^{\alpha} \theta^{\alpha}] - \boldsymbol{\sigma}^{\alpha} : \mathbf{l}_{\alpha} + \hat{\rho}^{\alpha} \left[\psi^{\alpha} - \frac{1}{2} \mathbf{v}_{\alpha} \cdot \mathbf{v}_{\alpha} \right] + \mathbf{h}^{\alpha} \cdot \mathbf{v}_{\alpha} + \frac{1}{\theta} \text{grad}(\theta) \cdot \mathbf{q}^{\alpha} \right) \geq 0, \quad (2.79)$$

where by definition the power density supply terms have cancelled with one another, and a constitutive relation for the local energy interaction term $\hat{\varepsilon}^{\alpha}$ is not needed.

If we naïvely multiply both sides of Equation (2.78) by phase temperature under the (admittedly reasonable) assumption that temperature, being a positive quantity, would not change the sign of the dissipation inequality, then, when carrying out the summation of the dissipation inequality over constituents $\alpha = s, f$, the power density supply terms would cancel. The issue with such a scenario is that if we were to solve the energy balance later, Equation (2.62), for any one phase, the local energy interaction term would not have been able to be defined constitutively via the dissipation inequality. This is also the difficulty that arises when supposing that the second law need only be satisfied for an individual constituent, i.e., we might have written the dissipation inequality as

$$\rho^{\alpha} [D_t^{\alpha} \psi^{\alpha} + \eta^{\alpha} D_t^{\alpha} \theta^{\alpha}] - \boldsymbol{\sigma}^{\alpha} : \mathbf{l}_{\alpha} - \hat{\varepsilon}^{\alpha} + \hat{\rho}^{\alpha} \left[\psi^{\alpha} - \frac{1}{2} \mathbf{v}_{\alpha} \cdot \mathbf{v}_{\alpha} \right] + \mathbf{h}^{\alpha} \cdot \mathbf{v}_{\alpha} + \frac{1}{\theta^{\alpha}} \text{grad}(\theta)^{\alpha} \cdot \mathbf{q}^{\alpha} \geq 0, \quad (2.80)$$

where the power density supply terms $\hat{\varepsilon}^{\alpha}$ (including its expanded form above, given by the two terms following $\hat{\varepsilon}^{\alpha}$ in Equation (2.80)) would cancel with one another when summing Equation (2.80) because they are not temperature-scaled as in Equation (2.78).

Chapter 3

Constitutive Theory

This chapter provides the foundational basis for the constitutive models used in Chapters 4 and 5. Said models are derived in a *thermodynamically consistent* manner, i.e., they do not violate the second law of thermodynamics. As such, we proceed directly from the second law to derive the constitutive models relating stresses to deformations, pressures to densities, etc.

3.1 Locally inhomogeneous temperature model

Herein we assume that constituent temperatures may vary, i.e., $\theta^s \neq \theta^f$. It is convenient not to assume anything about the form of an effective stress principle *a priori* (see, e.g., Biot and Wills [1957] for background on an effective stress principle), as this makes the determination of constitutive relations of the unknown variables difficult. We may begin by assuming that

$$\hat{\rho}^s = \hat{\rho}^f = 0. \quad (3.1)$$

Using this, we may write the Clausius-Duhem inequality for the mixture as

$$\begin{aligned} & \frac{1}{\theta^s} \left(\rho^s [D_t^s \psi^s + \eta^s D_t^s \theta^s] - \boldsymbol{\sigma}^s : \mathbf{l}_s - \hat{e}^s + \mathbf{h}^s \cdot \mathbf{v}_s + \frac{1}{\theta^s} \text{grad}(\theta^s) \cdot \mathbf{q}^s \right) \\ & + \frac{1}{\theta^f} \left(\rho^f [D_t^f \psi^f + \eta^f D_t^f \theta^f] - \boldsymbol{\sigma}^f : \mathbf{l}_f - \hat{e}^f + \mathbf{h}^f \cdot \mathbf{v}_f + \frac{1}{\theta^f} \text{grad}(\theta^f) \cdot \mathbf{q}^f \right) \geq 0. \end{aligned} \quad (3.2)$$

Next, multiply through by solid (s) phase temperature, i.e.,

$$\begin{aligned} & \left(\rho^s D_t^s \psi^s + \frac{\theta^s}{\theta^f} \rho^f D_t^f \psi^f \right) + \left(\rho^s \eta^s D_t^s \theta^s + \frac{\theta^s}{\theta^f} \rho^f \eta^f D_t^f \theta^f \right) - \left(\boldsymbol{\sigma}^s : \mathbf{l}_s + \frac{\theta^s}{\theta^f} \boldsymbol{\sigma}^f : \mathbf{l}_f \right) \\ & - \left(\hat{e}^s + \frac{\theta^s}{\theta^f} \hat{e}^f \right) + \left(\mathbf{h}^s \cdot \mathbf{v}_s + \frac{\theta^s}{\theta^f} \mathbf{h}^f \cdot \mathbf{v}_f \right) + \left(\frac{1}{\theta^s} \text{grad}(\theta^s) \cdot \mathbf{q}^s + \frac{\theta^s}{(\theta^f)^2} \text{grad}(\theta^f) \cdot \mathbf{q}^f \right) \geq 0. \end{aligned} \quad (3.3)$$

From Equation (3.1), the power density supply terms simplify to

$$\begin{aligned}\hat{e}^s &= \hat{\varepsilon}^s + \mathbf{h}^s \cdot \mathbf{v}_s, \\ \hat{e}^f &= \hat{\varepsilon}^f + \mathbf{h}^f \cdot \mathbf{v}_f.\end{aligned}\tag{3.4}$$

By definition, for a closed system, i.e., without supply from an external source,

$$\sum_{\alpha} \hat{\gamma}^{\alpha} = 0, \quad \sum_{\alpha} \mathbf{h}^{\alpha} = 0, \quad \sum_{\alpha} \hat{e}^{\alpha} = 0,\tag{3.5}$$

and thus the solid power density supply, Equation (3.4)₁, may be written as

$$\hat{e}^s = -\hat{e}^f = -(\hat{\varepsilon}^f + \mathbf{h}^f \cdot \mathbf{v}_f),\tag{3.6}$$

such that the power density supply terms in Equation (3.3) sum to

$$\hat{e}^s + \frac{\theta^s}{\theta^f} \hat{e}^f = \hat{\varepsilon}^f \left(\frac{\theta^s}{\theta^f} - 1 \right) + \mathbf{h}^f \cdot \mathbf{v}_f \left(\frac{\theta^s}{\theta^f} - 1 \right).\tag{3.7}$$

From Equation (3.5)₂, the interphase power terms in Equation (3.3) simplify to

$$\mathbf{h}^s \cdot \mathbf{v}_s + \frac{\theta^s}{\theta^f} \mathbf{h}^f \cdot \mathbf{v}_f = -\mathbf{h}^f \cdot \mathbf{v}_s + \frac{\theta^s}{\theta^f} \mathbf{h}^f \cdot \mathbf{v}_f = \mathbf{h}^f \cdot \tilde{\mathbf{v}}_f + \mathbf{h}^f \cdot \mathbf{v}_f \left(\frac{\theta^s}{\theta^f} - 1 \right).\tag{3.8}$$

Substitution of Equations (3.7) & (3.8) into Equation (3.3) gives

$$\begin{aligned}& \left(\rho^s D_t^s \psi^s + \frac{\theta^s}{\theta^f} \rho^f D_t^f \psi^f \right) + \left(\rho^s \eta^s D_t^s \theta^s + \frac{\theta^s}{\theta^f} \rho^f \eta^f D_t^f \theta^f \right) - \left(\boldsymbol{\sigma}^s : \mathbf{l}_s + \frac{\theta^s}{\theta^f} \boldsymbol{\sigma}^f : \mathbf{l}_f \right) \\ & - \left(\hat{\varepsilon}^f \left[\frac{\theta^s}{\theta^f} - 1 \right] + \mathbf{h}^f \cdot \mathbf{v}_f \left[\frac{\theta^s}{\theta^f} - 1 \right] \right) + \left(\mathbf{h}^f \cdot \tilde{\mathbf{v}}_f + \mathbf{h}^f \cdot \mathbf{v}_f \left[\frac{\theta^s}{\theta^f} - 1 \right] \right) \\ & + \left(\frac{1}{\theta^s} \text{grad}(\theta^s) \cdot \mathbf{q}^s + \frac{\theta^s}{(\theta^f)^2} \text{grad}(\theta^f) \cdot \mathbf{q}^f \right) \geq 0,\end{aligned}\tag{3.9}$$

or, noting cancellation of the fluid interphase power terms,

$$\begin{aligned}& \left(\rho^s D_t^s \psi^s + \frac{\theta^s}{\theta^f} \rho^f D_t^f \psi^f \right) + \left(\rho^s \eta^s D_t^s \theta^s + \frac{\theta^s}{\theta^f} \rho^f \eta^f D_t^f \theta^f \right) - \left(\boldsymbol{\sigma}^s : \mathbf{l}_s + \frac{\theta^s}{\theta^f} \boldsymbol{\sigma}^f : \mathbf{l}_f \right) \\ & - \hat{\varepsilon}^f \left(\frac{\theta^s}{\theta^f} - 1 \right) + \mathbf{h}^f \cdot \tilde{\mathbf{v}}_f + \left(\frac{1}{\theta^s} \text{grad}(\theta^s) \cdot \mathbf{q}^s + \frac{\theta^s}{(\theta^f)^2} \text{grad}(\theta^f) \cdot \mathbf{q}^f \right) \geq 0.\end{aligned}\tag{3.10}$$

Following the approach of de Boer [2005], Ehlers [2002], we introduce the saturation constraint to the Clausius-Duhem inequality given by Equation (3.10), namely,

$$n^s + n^f = 1, \quad D_t^s n^s + D_t^f n^f = 0,\tag{3.11}$$

which we can also express as

$$D_t^s n^s + D_t^f n^f - \text{grad}(n^f) \cdot \tilde{\mathbf{v}}_f = 0. \quad (3.12)$$

Utilization of the balance of mass,

$$\frac{n^\alpha}{\rho^{\alpha R}} D_t^\alpha \rho^{\alpha R} + D_t^\alpha n^\alpha + n^\alpha \text{div} \mathbf{v}_\alpha = \frac{\hat{\rho}^\alpha}{\rho^{\alpha R}}, \quad (3.13)$$

of each constituent (s) and (f) with assumption of negligible mass supplies and incompressible solid constituent, allows us to write the saturation constraint as

$$n^s \text{div} \mathbf{v}_s + \frac{n^f}{\rho^{\text{fR}}} D_t^f \rho^{\text{fR}} + n^f \text{div} \mathbf{v}_f + \text{grad}(n^f) \cdot \tilde{\mathbf{v}}_f = 0. \quad (3.14)$$

The saturation constraint may be added to the Clausius-Duhem inequality, Equation (3.10), with the introduction of a Lagrange multiplier Λ (which we will soon identify as temperature-scaled excess pore fluid pressure):

$$\Lambda \left(n^s \mathbf{d}_s : \mathbf{1} + \frac{n^f}{\rho^{\text{fR}}} D_t^f \rho^{\text{fR}} + n^f \mathbf{d}_f : \mathbf{1} + \text{grad}(n^f) \cdot \tilde{\mathbf{v}}_f \right) = 0. \quad (3.15)$$

Noting symmetry of the partial Cauchy stress tensors, i.e., $\boldsymbol{\sigma}^\alpha = (\boldsymbol{\sigma}^\alpha)^T$, we may rewrite the Clausius-Duhem inequality as

$$\begin{aligned} & \left(\rho^s D_t^s \psi^s + \frac{\theta^s}{\theta^f} \rho^f D_t^f \psi^f \right) + \left(\rho^s \eta^s D_t^s \theta^s + \frac{\theta^s}{\theta^f} \rho^f \eta^f D_t^f \theta^f \right) - \left(\boldsymbol{\sigma}^s : \mathbf{d}_s + \frac{\theta^s}{\theta^f} \boldsymbol{\sigma}^f : \mathbf{d}_f \right) \\ & - \hat{\varepsilon}^f \left(\frac{\theta^s}{\theta^f} - 1 \right) + \mathbf{h}^f \cdot \tilde{\mathbf{v}}_f + \left(\frac{1}{\theta^s} \text{grad}(\theta^s) \cdot \mathbf{q}^s + \frac{\theta^s}{(\theta^f)^2} \text{grad}(\theta^f) \cdot \mathbf{q}^f \right) \\ & - \Lambda \left(n^s \mathbf{d}_s : \mathbf{1} + \frac{n^f}{\rho^{\text{fR}}} D_t^f \rho^{\text{fR}} + n^f \mathbf{d}_f : \mathbf{1} + \text{grad}(n^f) \cdot \tilde{\mathbf{v}}_f \right) \geq 0. \end{aligned} \quad (3.16)$$

Next, combine like terms, such that

$$\begin{aligned} & \left(\rho^s D_t^s \psi^s + \frac{\theta^s}{\theta^f} \rho^f D_t^f \psi^f \right) + \left(\rho^s \eta^s D_t^s \theta^s + \frac{\theta^s}{\theta^f} \rho^f \eta^f D_t^f \theta^f \right) \\ & - \left([\boldsymbol{\sigma}^s + \Lambda n^s \mathbf{1}] : \mathbf{d}_s + \left[\frac{\theta^s}{\theta^f} \boldsymbol{\sigma}^f + \Lambda n^f \mathbf{1} \right] : \mathbf{d}_f \right) \\ & + (\mathbf{h}^f - \Lambda \text{grad} n^f) \cdot \tilde{\mathbf{v}}_f - \Lambda \frac{n^f}{\rho^{\text{fR}}} D_t^f \rho^{\text{fR}} \\ & - \hat{\varepsilon}^f \left(\frac{\theta^s}{\theta^f} - 1 \right) + \left(\frac{1}{\theta^s} \text{grad}(\theta^s) \cdot \mathbf{q}^s + \frac{\theta^s}{(\theta^f)^2} \text{grad}(\theta^f) \cdot \mathbf{q}^f \right) \geq 0. \end{aligned} \quad (3.17)$$

Introduce the so-called ‘‘extra’’ terms (which we can define constitutive models for later):

$$\begin{aligned}
\boldsymbol{\sigma}_E^s &= \boldsymbol{\sigma}^s + (\Lambda n^s + q)\mathbf{1}, \\
\boldsymbol{\sigma}_E^f &= \boldsymbol{\sigma}^f + \Lambda \frac{\theta^f}{\theta^s} n^f \mathbf{1}, \\
\mathbf{h}_E^f &= \mathbf{h}^f - \Lambda \text{grad} n^f,
\end{aligned} \tag{3.18}$$

where q is the shock viscosity (refer to Section 4.4.1) acting on the solid constituent, and substitute the extra terms back into Equation (3.17):

$$\begin{aligned}
&\left(\rho^s D_t^s \psi^s + \frac{\theta^s}{\theta^f} \rho^f D_t^f \psi^f \right) + \left(\rho^s \eta_s D_t^s \theta^s + \frac{\theta^s}{\theta^f} \rho^f \eta^f D_t^f \theta^f \right) - \boldsymbol{\sigma}_E^s : \mathbf{d}_s + q \text{div} \mathbf{v}_s - \frac{\theta^s}{\theta^f} \boldsymbol{\sigma}_E^f : \mathbf{d}_f \\
&+ \mathbf{h}_E^f \cdot \tilde{\mathbf{v}}_f - \Lambda \frac{n^f}{\rho^{\text{fR}}} D_t^f \rho^{\text{fR}} - \hat{\varepsilon}^f \left(\frac{\theta^s}{\theta^f} - 1 \right) + \left(\frac{1}{\theta^s} \text{grad}(\theta^s) \cdot \mathbf{q}^s + \frac{\theta^s}{(\theta^f)^2} \text{grad}(\theta^f) \cdot \mathbf{q}^f \right) \geq 0.
\end{aligned} \tag{3.19}$$

3.1.1 Determination of the Helmholtz free energies

Discussion of how to formulate constitutive equations is discussed in detail in Coleman and Noll [1963], Marsden and Hughes [1983], Truesdell [1984], and specifically for TPM in Truesdell and Toupin [1960], Ehlers [2002], de Boer [2005]. Following the approach of Ghadiani [2005] (see also de Boer [2005]), the following response functions \mathcal{R} must be determined:

$$\mathcal{R} := \left\{ \psi^s, \psi^f, \boldsymbol{\sigma}_E^s, q, \boldsymbol{\sigma}_E^f, \mathbf{h}_E^f, \hat{\varepsilon}^f, \mathbf{q}^s, \mathbf{q}^f \right\} \tag{3.20}$$

which depend on a set \mathcal{S} of variables, i.e.,

$$\mathcal{R} := \mathcal{R}(\mathcal{S}), \tag{3.21}$$

where \mathcal{S} is a subset of the fundamental constitutive variables \mathcal{V} for a biphasic continuum with an elastic solid constituent, i.e.,

$$\mathcal{V} := \left\{ \theta^\alpha, \text{grad} \theta^\alpha, n^f, \text{grad} n^f, \rho^{\alpha\text{R}}, \text{grad} \rho^{\alpha\text{R}}, \mathbf{F}_\alpha, \text{GRAD}_\alpha \mathbf{F}_\alpha, \text{div} \mathbf{v}_s, \mathbf{v}_f, \text{GRAD}_f \mathbf{v}_f, \mathbf{X}_\alpha \right\}. \tag{3.22}$$

For an isotropic pore fluid, it can be shown [Cross, 1973] that the deformation gradient \mathbf{F}_f is a function of $\det(\mathbf{F}_f)$, which can in turn be determined through porosity n^f and real fluid mass density ρ^{fR} in the absence of fluid mass supply $\hat{\rho}^f$. Using the principle of frame indifference, we may

also substitute the pore fluid velocity \mathbf{v}_f by the seepage velocity $\tilde{\mathbf{v}}_f$. The solid pore fluid velocity gradient $\text{GRAD}_f \mathbf{v}_f$ may also be substituted by the deformation rate tensor \mathbf{d}_f .

From the balance of mass for the incompressible solid constituent with no mass supply,

$$D_t^s n^s + n^s \text{div} \mathbf{v}_s = 0. \quad (3.23)$$

Using continuity equation

$$D_t^s J_s = J_s \text{div} \mathbf{v}_s, \quad (3.24)$$

we may write Equation (3.23) as

$$D_t^s n^s = -\frac{n^s}{J_s} D_t^s J_s \rightarrow \frac{1}{n^s} D_t^s n^s = -\frac{1}{J_s} D_t^s J_s. \quad (3.25)$$

Integration of Equation (3.25) yields the useful relation

$$n^s = \frac{n_{0(s)}^s}{J_s} = \frac{n_{0(s)}^s}{\det(\mathbf{F}_s)}, \quad (3.26)$$

and thus the real mass density of the solid constituent and its gradient, and porosity and its gradient, may be eliminated from the set of the response functions. Thus, the set of constitutive variables pertaining to the problem at hand is

$$\mathcal{S} = \left\{ \theta^\alpha, \text{grad} \theta^\alpha, \rho^{\text{fR}}, \text{grad} \rho^{\text{fR}}, \mathbf{F}_s, \text{GRAD}_s \mathbf{F}_s, \text{div} \mathbf{v}_s, \tilde{\mathbf{v}}_f, \mathbf{d}_f \right\}. \quad (3.27)$$

Combining Equations (3.20), (3.21) and (3.27) gives

$$\left\{ \psi^s, \psi^f, \boldsymbol{\sigma}_E^s, q, \boldsymbol{\sigma}_E^f, \mathbf{h}_E^f, \hat{\boldsymbol{\varepsilon}}^f, \mathbf{q}^s, \mathbf{q}^f \right\} = \mathcal{R}(\theta^\alpha, \text{grad} \theta^\alpha, \rho^{\text{fR}}, \text{grad} \rho^{\text{fR}}, \mathbf{F}_s, \text{GRAD}_s \mathbf{F}_s, \text{div} \mathbf{v}_s, \tilde{\mathbf{v}}_f, \mathbf{d}_f). \quad (3.28)$$

Based on the principle of phase separation, that the Helmholtz free energy of φ^α should depend only on the φ^α variables, we may write

$$\begin{aligned} \psi^s &:= \psi^s(\theta^s, \text{grad} \theta^s, \mathbf{C}_s, \text{GRAD}_s \mathbf{C}_s, \text{div} \mathbf{v}_s), \\ \psi^f &:= \psi^f(\theta^f, \text{grad} \theta^f, \rho^{\text{fR}}, \text{grad} \rho^{\text{fR}}, \tilde{\mathbf{v}}_f, \mathbf{d}_f), \end{aligned} \quad (3.29)$$

where we have used the right Cauchy-Green tensor $\mathbf{C}_s = \mathbf{F}_s^T \mathbf{F}_s$ in place of \mathbf{F}_s . The material time derivatives of the Helmholtz free energy functions are

$$D_t^s \psi^s = \frac{\partial \psi^s}{\partial \theta^s} D_t^s \theta^s + \frac{\partial \psi^s}{\partial (\text{grad} \theta^s)} D_t^s (\text{grad} \theta^s) + \frac{\partial \psi^s}{\partial \mathbf{C}_s} D_t^s \mathbf{C}_s + \frac{\partial \psi^s}{\partial (\text{GRAD}_s \mathbf{C}_s)} D_t^s (\text{GRAD}_s \mathbf{C}_s) + \frac{\partial \psi^s}{\partial (\text{div} \mathbf{v}_s)} D_t^s (\text{div} \mathbf{v}_s), \quad (3.30)$$

$$D_t^f \psi^f = \frac{\partial \psi^f}{\partial \theta^f} D_t^f \theta^f + \frac{\partial \psi^f}{\partial (\text{grad} \theta^f)} D_t^f (\text{grad} \theta^f) + \frac{\partial \psi^f}{\partial \rho^{\text{fR}}} D_t^f \rho^{\text{fR}} + \frac{\partial \psi^f}{\partial (\text{grad} \rho^{\text{fR}})} D_t^f (\text{grad} \rho^{\text{fR}}) + \frac{\partial \psi^f}{\partial \tilde{\mathbf{v}}_f} D_t^f \tilde{\mathbf{v}}_f + \frac{\partial \psi^f}{\partial \mathbf{d}_f} D_t^f \mathbf{d}_f. \quad (3.31)$$

3.1.2 Evaluation of the Clausius-Duhem inequality

Returning our attention to Equation (3.19), we may substitute the material time derivatives of the Helmholtz free energy functions, such that

$$\begin{aligned} & \left(\rho^s \frac{\partial \psi^s}{\partial \theta^s} + \rho^s \eta^s \right) D_t^s \theta^s + \rho^s \frac{\partial \psi^s}{\partial (\text{grad} \theta^s)} D_t^s (\text{grad} \theta^s) + \left(\rho^s \frac{\partial \psi^s}{\partial \mathbf{C}_s} \mathbf{C}_s - \frac{1}{2J_s} \mathbf{S}_{E(s)}^s \right) : D_t^s \mathbf{C}_s \\ & + \rho^s \frac{\partial \psi^s}{\partial (\text{GRAD}_s \mathbf{C}_s)} D_t^s (\text{GRAD}_s \mathbf{C}_s) + \frac{\partial \psi^s}{\partial (\text{div} \mathbf{v}_s)} D_t^s (\text{div} \mathbf{v}_s) + \left(\frac{\theta^s}{\theta^f} \rho^f \frac{\partial \psi^f}{\partial \theta^f} + \frac{\theta^s}{\theta^f} \rho^f \eta^f \right) D_t^f \theta^f \\ & \quad + \frac{\theta^s}{\theta^f} \rho^f \frac{\partial \psi^f}{\partial (\text{grad} \theta^f)} D_t^f (\text{grad} \theta^f) + \left(\frac{\theta^s}{\theta^f} \rho^f \frac{\partial \psi^f}{\partial \rho^{\text{fR}}} - \Lambda \frac{n^f}{\rho^{\text{fR}}} \right) D_t^f \rho^{\text{fR}} \\ & \quad + \frac{\theta^s}{\theta^f} \rho^f \frac{\partial \psi^f}{\partial (\text{grad} \rho^{\text{fR}})} D_t^f (\text{grad} \rho^{\text{fR}}) + \frac{\theta^s}{\theta^f} \rho^f \frac{\partial \psi^f}{\partial \tilde{\mathbf{v}}_f} D_t^f \tilde{\mathbf{v}}_f + \frac{\partial \psi^f}{\partial \mathbf{d}_f} D_t^f \mathbf{d}_f + q \mathbf{1} : \mathbf{d}_s \\ & - \frac{\theta^s}{\theta^f} \boldsymbol{\sigma}_E^f : \mathbf{d}_f - \hat{\varepsilon}^f \left(\frac{\theta^s}{\theta^f} - 1 \right) + \mathbf{h}_E^f \cdot \tilde{\mathbf{v}}_f + \left(\frac{1}{\theta^s} \text{grad}(\theta^s) \cdot \mathbf{q}^s + \frac{\theta^s}{(\theta^f)^2} \text{grad}(\theta^f) \cdot \mathbf{q}^f \right) \geq 0, \end{aligned} \quad (3.32)$$

where we have used the identities

$$D_t^s \mathbf{C}_s = 2 \mathbf{F}_s^T \mathbf{d}_s \mathbf{F}_s, \quad \boldsymbol{\sigma}_E^s = \frac{1}{J_s} \mathbf{F}_s \mathbf{S}_{E(s)}^s \mathbf{F}_s^T, \quad (3.33)$$

to transform the solid extra stress to the reference configuration of the solid skeleton.

Using the Coleman and Noll [1963] argument, i.e., that the free parameters $D_t^s \theta^s$, $D_t^s (\text{grad} \theta^s)$, \mathbf{l}_s , $D_t^s (\text{GRAD}_s \mathbf{C}_s)$, $D_t^f \theta^f$, $D_t^f (\text{grad} \theta^f)$, $D_t^f \rho^{\text{fR}}$, $D_t^f (\text{grad} \rho^{\text{fR}})$, $\text{div} \mathbf{v}_s$, $\tilde{\mathbf{v}}_f$ and \mathbf{d}_f maintain arbitrary

values, the following constitutive relations must hold:

$$\begin{aligned}
\left(\rho^s \frac{\partial \psi^s}{\partial \theta^s} + \rho^s \eta^s\right) &= 0 \Rightarrow \rho_{0(s)}^s \eta^s = -\frac{\partial(\rho_{0(s)}^s \psi^s)}{\partial \theta^s}, \\
\frac{\partial \psi^s}{\partial(\text{grad} \theta^s)} &= 0, \\
\left(\rho^s \frac{\partial \psi^s}{\partial \mathbf{C}_s} \mathbf{C}_s - \frac{1}{2J_s} \mathbf{S}_{E(s)}^s\right) &= \mathbf{0} \Rightarrow \mathbf{S}_{E(s)}^s = 2 \frac{\partial(\rho_{0(s)}^s \psi^s)}{\partial \mathbf{C}_s}, \\
\frac{\partial \psi^s}{\partial(\text{GRAD}_s \mathbf{C}_s)} &= \mathbf{0}, \\
\left(\frac{\theta^s}{\theta^f} \rho^f \frac{\partial \psi^f}{\partial \theta^f} + \frac{\theta^s}{\theta^f} \rho^f \eta^f\right) &= 0 \Rightarrow \eta^f = -\frac{\partial \psi^f}{\partial \theta^f}, \\
\frac{\partial \psi^f}{\partial(\text{grad} \theta^f)} &= 0, \\
\left(\frac{\theta^s}{\theta^f} \rho^f \frac{\partial \psi^f}{\partial \rho^{\text{fR}}} - \Lambda \frac{n^f}{\rho^{\text{fR}}}\right) &= 0 \Rightarrow \Lambda = \frac{\theta^s}{\theta^f} (\rho^{\text{fR}})^2 \frac{\partial \psi^f}{\partial \rho^{\text{fR}}}, \\
\frac{\partial \psi^f}{\partial(\text{grad} \rho^{\text{fR}})} &= 0, \\
\frac{\partial \psi^f}{\partial \tilde{\mathbf{v}}_f} &= \mathbf{0}, \\
\frac{\partial \psi^f}{\partial \mathbf{d}_f} &= \mathbf{0},
\end{aligned} \tag{3.34}$$

where the constitutive relations in Equations (3.34)_{1,3} have been transformed to the reference configuration of the solid skeleton making use of

$$\begin{aligned}
\int_{\mathcal{B}} \rho^s D_t^s \psi^s dv &= \int_{\mathcal{B}_0} \rho^s J_s D_t^s \psi^s dV_s = \int_{\mathcal{B}_0} \rho_{0(s)}^s D_t^s \psi^s dV_s, \\
\rho_{0(s)}^s D_t^s \psi^s &= D_t^s (\rho_{0(s)}^s \psi^s) - \psi^s D_t^s \rho_{0(s)}^s \\
&= D_t^s (\rho_{0(s)}^s \psi^s) - \psi^s (J_s D_t^s \rho^s + \rho^s D_t^s J_s) \\
&= D_t^s (\rho_{0(s)}^s \psi^s) - \psi^s \hat{\rho}^s J_s \Rightarrow \rho^s D_t^s \psi^s = \frac{1}{J_s} D_t^s (\rho_{0(s)}^s \psi^s).
\end{aligned} \tag{3.36}$$

We also define the *reduced dissipation inequality*:

$$\mathcal{D} := \frac{\theta^s}{\theta^f} \boldsymbol{\sigma}_E^f : \mathbf{d}_f - q \operatorname{div} \mathbf{v}_s + \frac{1}{\theta^f} \hat{\varepsilon}^f (\theta^s - \theta^f) - \mathbf{h}_E^f \cdot \tilde{\mathbf{v}}_f - \frac{1}{\theta^f} \left(\frac{\theta^f}{\theta^s} \operatorname{grad}(\theta^s) \cdot \mathbf{q}^s + \frac{\theta^s}{\theta^f} \operatorname{grad}(\theta^f) \cdot \mathbf{q}^f \right) \geq 0. \tag{3.37}$$

From Equation (3.34), we can deduce that the Helmholtz free energy functions simplify to:

$$\begin{aligned}\psi^s &:= \psi^s(\theta^s, \mathbf{C}_s), \\ \psi^f &:= \psi^f(\theta^f, \rho^{\text{fR}}).\end{aligned}\tag{3.38}$$

Given the dependence of solid stress on the solid Helmholtz free energy, we must have

$$\boldsymbol{\sigma}_E^s := \boldsymbol{\sigma}_E^s(\theta^s, \mathbf{C}_s),\tag{3.39}$$

and analogously for the pore fluid,

$$\begin{aligned}\Lambda &:= \Lambda(\theta^s, \theta^f, \rho^{\text{fR}}), \\ \eta^f &:= \eta^f(\theta^f, \rho^{\text{fR}}).\end{aligned}\tag{3.40}$$

Identification of the Lagrange multiplier. From thermodynamic principles (see, e.g., Davison [2008]) for a compressible fluid with free energy as a function of specific volume v^f and temperature θ^f , we know that

$$\frac{\partial \psi^f}{\partial v^f} = -p_f \Rightarrow \frac{\partial \psi^f}{\partial \rho^{\text{fR}}} \frac{\partial \rho^{\text{fR}}}{\partial v^f} = -p_f \Rightarrow (\rho^{\text{fR}})^2 \frac{\partial \psi^f}{\partial \rho^{\text{fR}}} = p_f,\tag{3.41}$$

and therefore by using Equation (3.34)₇, we see that

$$\Lambda = \frac{\theta^s}{\theta^f} p_f,\tag{3.42}$$

such that the partial Cauchy stresses for each constituent are defined as

$$\begin{aligned}\boldsymbol{\sigma}^s &= \boldsymbol{\sigma}_E^s - \frac{\theta^s}{\theta^f} p_f n^s \mathbf{1} - q \mathbf{1}, \\ \boldsymbol{\sigma}^f &= \boldsymbol{\sigma}_E^f - p_f n^f \mathbf{1},\end{aligned}\tag{3.43}$$

with

$$\mathbf{h}^f = \mathbf{h}_E^f + \frac{\theta^s}{\theta^f} p_f \text{grad} n^f.\tag{3.44}$$

3.1.3 Identifying constitutive relations

From Equation (3.37), we must find the following set of response functions for \mathcal{D} :

$$\left\{ \boldsymbol{\sigma}_E^f, q, \hat{\boldsymbol{\varepsilon}}^f, \mathbf{h}_E^f, \mathbf{q}^s, \mathbf{q}^f \right\} := \Upsilon(\mathcal{S}),\tag{3.45}$$

where

$$\mathcal{S} = \left\{ \theta^s, \text{grad}\theta^s, \theta^f, \text{grad}\theta^f, \rho^{\text{fR}}, \text{grad}\rho^{\text{fR}}, \mathbf{C}_s, \text{GRAD}_s \mathbf{C}_s, \text{div} \mathbf{v}_s, \tilde{\mathbf{v}}_f, \mathbf{d}_f \right\}. \quad (3.46)$$

In order to identify the form of the response functions as they relate to the set of constitutive variables, we will expand \mathcal{D} into equilibrium and non-equilibrium parts:

$$\mathcal{D} = \mathcal{D}_0(\mathcal{S}_0) + \mathcal{D}_n(\mathcal{S}), \quad (3.47)$$

where

$$\mathcal{D}_0(\mathcal{S}) = 0; \quad \mathcal{D}(\mathcal{S}_0) = 0, \quad (3.48)$$

and the initial state is at thermal and mechanical equilibrium, i.e.,

$$\begin{aligned} \mathcal{S}_0 = \{ \theta^s = \theta, \text{grad}\theta^s = \mathbf{0}, \theta^f = \theta, \text{grad}\theta^f = \mathbf{0}, \rho^{\text{fR}} = \rho_0^{\text{fR}}, \text{grad}\rho^{\text{fR}} = \mathbf{0}, \mathbf{C}_s = \mathbf{1}, \\ \text{GRAD}_s \mathbf{C}_s = \mathbf{0}, \text{div} \mathbf{v}_s = \mathbf{0}, \tilde{\mathbf{v}}_f = \mathbf{0}, \mathbf{d}_f = \mathbf{0} \}. \end{aligned} \quad (3.49)$$

Thus, it follows that the response functions satisfy

$$\begin{aligned} \boldsymbol{\sigma}_E^f(\mathcal{S}) &= \boldsymbol{\sigma}_{E_n}^f(\mathcal{S}), \\ q(\mathcal{S}) &= q_n(\mathcal{S}), \\ \hat{\boldsymbol{\varepsilon}}^f(\mathcal{S}) &= \hat{\boldsymbol{\varepsilon}}_n^f(\mathcal{S}), \\ \mathbf{h}_E^f(\mathcal{S}) &= \mathbf{h}_{E_n}^f(\mathcal{S}), \\ \mathbf{q}^s(\mathcal{S}) &= \mathbf{q}_n^s(\mathcal{S}), \\ \mathbf{q}^f(\mathcal{S}) &= \mathbf{q}_n^f(\mathcal{S}). \end{aligned} \quad (3.50)$$

Next, we make the following constitutive assumptions about the functional dependencies of the response functions. The pore fluid extra stress $\boldsymbol{\sigma}_E^f$ is identified as the fluid frictional stress for a single-phase fluid, and, assuming a Newtonian fluid law, it is directly related to the pore fluid deformation rate tensor \mathbf{d}_f . The strength of shock viscosity q is dependent upon the strength of the solid velocity gradient along the direction of compression, i.e., via $\text{div} \mathbf{v}_s$. The heat fluxes \mathbf{q}^s and \mathbf{q}^f are assumed to depend only on their own temperature gradients via Fourier's law. Lastly,

the interaction terms $\hat{\varepsilon}^f$ and \mathbf{h}_E^f depend on the interaction variables $(\theta^s - \theta^f)$ and $\tilde{\mathbf{v}}_f$, respectively. Herein we have made the assumption that the local energy interaction term is a caloric variable only, i.e., kinematical interaction is accounted for in the lumped interaction force term \mathbf{h}_E^f , and vice versa. In other words,

$$\begin{aligned}
\boldsymbol{\sigma}_E^f &:= \boldsymbol{\sigma}_E^f(\mathbf{d}_f), \\
q &:= q(\operatorname{div} \mathbf{v}_s), \\
\hat{\varepsilon}^f &:= \hat{\varepsilon}^f(\theta^s, \theta^f), \\
\mathbf{h}_E^f &:= \mathbf{h}_E^f(\tilde{\mathbf{v}}_f), \\
\mathbf{q}^s &:= \mathbf{q}^s(\theta^s), \\
\mathbf{q}^f &:= \mathbf{q}^f(\theta^f),
\end{aligned} \tag{3.51}$$

which leads to the following linearizations of the response functions using a Taylor series expansion around \mathcal{S}_0 and neglecting higher order terms:

$$\begin{aligned}
\boldsymbol{\sigma}_{E_n}^f(\mathcal{S}) &= \boldsymbol{\sigma}_{E_0}^f + \left. \frac{\partial \boldsymbol{\sigma}_{E_n}^f}{\partial \mathbf{d}_f} \right|_{\mathcal{S}_0} \mathbf{d}_f, \\
q_n(\mathcal{S}) &= q_0 + \left. \frac{\partial q_n}{\partial (\operatorname{div} \mathbf{v}_s)} \right|_{\mathcal{S}_0} \operatorname{div} \mathbf{v}_s, \\
\hat{\varepsilon}_n^f(\mathcal{S}) &= \hat{\varepsilon}_0^f + \left. \frac{\partial \hat{\varepsilon}_n^f}{\partial \theta^s} \right|_{\mathcal{S}_0} (\theta^s - \theta) + \left. \frac{\partial \hat{\varepsilon}_n^f}{\partial \theta^f} \right|_{\mathcal{S}_0} (\theta^f - \theta), \\
\mathbf{h}_{E_n}^f(\mathcal{S}) &= \mathbf{h}_{E_0}^f + \left. \frac{\partial \mathbf{h}_{E_n}^f}{\partial \tilde{\mathbf{v}}_f} \right|_{\mathcal{S}_0} \tilde{\mathbf{v}}_f, \\
\mathbf{q}_n^s(\mathcal{S}) &= \mathbf{q}_0^s + \left. \frac{\partial \mathbf{q}^s}{\partial (\operatorname{grad} \theta^s)} \right|_{\mathcal{S}_0} \operatorname{grad} \theta^s, \\
\mathbf{q}_n^f(\mathcal{S}) &= \mathbf{q}_0^f + \left. \frac{\partial \mathbf{q}^f}{\partial (\operatorname{grad} \theta^f)} \right|_{\mathcal{S}_0} \operatorname{grad} \theta^f.
\end{aligned} \tag{3.52}$$

It is assumed that the initial values of the response functions are zero based on Equation (3.49), such that the Taylor series expansion simplifies to

$$\begin{aligned}
\boldsymbol{\sigma}_{E_n}^f(\mathcal{S}) &= \overset{4}{\mathbf{Z}}_f \mathbf{d}_f, \\
q_n(\mathcal{S}) &= -C \operatorname{div} \mathbf{v}_s, \\
\hat{\varepsilon}_n^f(\mathcal{S}) &= k_{\theta^s}^\varepsilon (\theta^s - \theta) + k_{\theta^f}^\varepsilon (\theta^f - \theta), \\
\mathbf{h}_{E_n}^f(\mathcal{S}) &= -\mathbf{S}_w \tilde{\mathbf{v}}_f, \\
\mathbf{q}_n^s(\mathcal{S}) &= -\mathbf{k}^{\theta^s} \operatorname{grad} \theta^s, \\
\mathbf{q}_n^f(\mathcal{S}) &= -\mathbf{k}^{\theta^f} \operatorname{grad} \theta^f,
\end{aligned} \tag{3.53}$$

where we have defined

$$\begin{aligned}
\overset{4}{\mathbf{Z}}_f &:= \frac{\partial \boldsymbol{\sigma}_{E_n}^f}{\partial \mathbf{d}_f} \Big|_{\mathcal{S}_0}, \\
C &:= -\frac{\partial q_n}{\partial (\operatorname{div} \mathbf{v}_s)} \Big|_{\mathcal{S}_0}, \\
k_{\theta^s}^\varepsilon &:= \frac{\partial \hat{\varepsilon}_n^f}{\partial \theta^s} \Big|_{\mathcal{S}_0}, \\
k_{\theta^f}^\varepsilon &:= \frac{\partial \hat{\varepsilon}_n^f}{\partial \theta^f} \Big|_{\mathcal{S}_0}, \\
\mathbf{S}_w &:= -\frac{\partial \mathbf{h}_{E_n}^f}{\partial \tilde{\mathbf{v}}_f} \Big|_{\mathcal{S}_0}, \\
\mathbf{k}^{\theta^s} &:= -\frac{\partial \mathbf{q}^s}{\partial (\operatorname{grad} \theta^s)} \Big|_{\mathcal{S}_0}, \\
\mathbf{k}^{\theta^f} &:= -\frac{\partial \mathbf{q}^s}{\partial (\operatorname{grad} \theta^s)} \Big|_{\mathcal{S}_0}.
\end{aligned} \tag{3.54}$$

Given that the caloric interaction defined by $\hat{\varepsilon}^f$ is driven by a difference in temperature between θ^s and θ^f , we must have

$$\frac{\partial \hat{\varepsilon}_n^f}{\partial \theta^s} \Big|_{\mathcal{S}_0} = -\frac{\partial \hat{\varepsilon}_n^f}{\partial \theta^f} \Big|_{\mathcal{S}_0} \Rightarrow k_{\theta^s}^\varepsilon = -k_{\theta^f}^\varepsilon, \tag{3.55}$$

and thus the reduced dissipation inequality, Equation (3.37), becomes

$$\begin{aligned}
\mathcal{D} &= \frac{\theta^s}{\theta^f} (\overset{4}{\mathbf{Z}}_f \mathbf{d}_f) : \mathbf{d}_f - (-C \operatorname{div} \mathbf{v}_s) \operatorname{div} \mathbf{v}_s + \frac{1}{\theta^f} k_{\theta^s}^\varepsilon (\theta^s - \theta^f)^2 - (-\mathbf{S}_w \tilde{\mathbf{v}}_f) \cdot \tilde{\mathbf{v}}_f \\
&\quad - \frac{1}{\theta^f} \left(\frac{\theta^f}{\theta^s} \operatorname{grad}(\theta^s) \cdot (-\mathbf{k}^{\theta^s} \operatorname{grad} \theta^s) + \frac{\theta^s}{\theta^f} \operatorname{grad}(\theta^f) \cdot (-\mathbf{k}^{\theta^f} \operatorname{grad} \theta^f) \right) \geq 0.
\end{aligned} \tag{3.56}$$

In order to satisfy the inequality, each term must be non-negative by itself, and thus the following restrictions must hold:

$$\begin{aligned}
\mathbf{Z}_f^4 &\rightarrow \text{positive definite,} \\
C &> 0, \\
\mathbf{S}_w &\rightarrow \text{positive definite,} \\
\mathbf{k}^{\theta^s} &\rightarrow \text{positive definite,} \\
\mathbf{k}^{\theta^f} &\rightarrow \text{positive definite,} \\
k_{\theta^s}^\varepsilon &> 0.
\end{aligned} \tag{3.57}$$

Substitution of Equation (3.57) back into Equation (3.53) gives

$$\begin{aligned}
\boldsymbol{\sigma}_E^f &= \mathbf{Z}_f^4 \mathbf{d}_f, \\
q &= -C \operatorname{div} \mathbf{v}_s, \\
\varepsilon^f &= k_{\theta}^\varepsilon (\theta^s - \theta^f), \\
\mathbf{h}_E^f &= -\mathbf{S}_w \tilde{\mathbf{v}}_f, \\
\mathbf{q}^s &= -\mathbf{k}^{\theta^s} \operatorname{grad} \theta^s, \\
\mathbf{q}^f &= -\mathbf{k}^{\theta^f} \operatorname{grad} \theta^f,
\end{aligned} \tag{3.58}$$

where we have replaced $k_{\theta^s}^\varepsilon := k_{\theta}^\varepsilon$.

3.1.4 Defining proportionality parameters

Definition of the shock viscosity q , and choices for the constant C , is provided in greater detail in Section 4.4.1. A common choice for the fourth-order tensor \mathbf{Z}_f is a simple Newtonian fluid law (see Holzapfel [2000] p. 203), i.e.,

$$\mathbf{Z}_f^4 := n^f \kappa_f (\mathbf{1} \otimes \mathbf{1})^T + 2n^f \mu_f (\mathbf{1} \otimes \mathbf{1}), \tag{3.59}$$

where κ_f and μ_f are the bulk and shear viscosity of the pore fluid, respectively.

When determining the form of $\mathbf{k}^{\theta\alpha}$, we may assume isotropic heat conduction for simplicity, such that

$$\mathbf{k}^{\theta\alpha} = \begin{bmatrix} k^{\theta\alpha} & 0 & 0 \\ 0 & k^{\theta\alpha} & 0 \\ 0 & 0 & k^{\theta\alpha} \end{bmatrix} (\mathbf{e}_i \otimes \mathbf{e}_j). \quad (3.60)$$

The permeability tensor \mathbf{S}_w may be defined as

$$\mathbf{S}_w := (n^f)^2 (\mathbf{K}^s)^{-1} = \frac{(n^f)^2}{\hat{k}} \mathbf{1}, \quad (3.61)$$

where \mathbf{K}^s is the intrinsic permeability *tensor* of the solid skeleton, which we have also taken to be isotropic for sake of simplicity, and \hat{k} is the hydraulic conductivity,

$$\hat{k} := \frac{\varkappa}{\mu_f} \frac{\mathcal{F}(n^f)}{\mathcal{F}(n_{0(s)}^f)}, \quad (3.62)$$

where \varkappa is the intrinsic permeability *value* (units m^2) of the solid skeleton. \mathcal{F} is a nonlinear function of porosity n^f accounting for change in hydraulic permeability due to change in porosity, e.g., the Kozeny-Carman relation

$$\mathcal{F}(n^f) := \frac{(n^f)^3}{1 - (n^f)^2}. \quad (3.63)$$

Another form motivated by work with soft biological tissues was presented by Lai et al. [1981]:

$$\mathcal{F}(n^f) = \exp[\kappa(J_s - 1)]. \quad (3.64)$$

However, under extreme volumetric compression, which one may encounter in the finite strain regime, both the Kozeny-Carman and exponential functional forms of hydraulic conductivity do not respect the restrictions that a materially incompressible solid constituent demands (refer to Equation (3.26)), as was noted by Markert [2005]:

$$\hat{k} \rightarrow \begin{Bmatrix} 0 \\ \infty \end{Bmatrix} \quad \text{if} \quad \begin{cases} n^f \rightarrow 0 \Leftrightarrow n^s \rightarrow 1 \Leftrightarrow J_s \rightarrow n_{0(s)}^s \\ n^f \rightarrow 1 \Leftrightarrow n^s \rightarrow 0 \Leftrightarrow J_s \rightarrow \infty \end{cases}. \quad (3.65)$$

As such, Eipper [1998] proposed a deformation dependent permeability that respects the restriction of materially incompressible solid constituent:

$$\mathcal{F}(n^f) := (n^f)^\kappa \quad (3.66)$$

for $\kappa > 0$, however, such a function is ill-suited for rapidly expanding materials, as shown in Figure 3.1(b). In light of this, Markert [2005] proposed

$$\mathcal{F}(n^f) := \left(\frac{n^f}{1 - n^f} \right)^\kappa, \quad (3.67)$$

such that

$$\hat{k} = \frac{\varkappa}{\mu_f} \left(\frac{J_s - n_{0(s)}^s}{1 - n_{0(s)}^s} \right)^\kappa. \quad (3.68)$$

Irwin et al. [2023a,b,c,d, 2024] erroneously used the Kozeny-Carman relation (as well as not enforcing the incompressibility restriction in the solid skeleton strain energy function—refer to Section 3.3.1); however, compressive strains did not exceed the lower limit of solid volume fraction, and thus, the results are still valid. A comparison between Markert’s hyperbolic model and the Kozeny-Carman model regarding the instability of the latter at higher strain is made in Section 5.3.3.1, paragraph *Necessary constitutive adjustments for higher strain*.

Returning our attention to the formulation of Darcy’s law, note that

$$\mathbf{h}_E^f := \mathbf{h}^f - \frac{\theta^s}{\theta^f} p_f \text{grad} n^f = \mathbf{h}^f - p_f \text{grad} n^f + p_f \text{grad}(n^f) \left[1 - \frac{\theta^s}{\theta^f} \right]. \quad (3.69)$$

Following this, we may use the balance of momentum, Equation (2.27), for $\alpha = f$ and taking $\hat{\rho}^f = 0$ and $\mathbf{b}^f = \mathbf{b}^s = \mathbf{b}$, and Equation (3.43)₂ to substitute the term $\mathbf{h}^f - p_f \text{grad} n^f$ in Equation (3.69), such that

$$\mathbf{h}_E^f = \rho^f (\mathbf{a}_f - \mathbf{b}) - \text{div} \boldsymbol{\sigma}_E^f + n^f \text{grad} p_f + p_f \text{grad}(n^f) \left[1 - \frac{\theta^s}{\theta^f} \right]. \quad (3.70)$$

Then we may establish a generalized Darcy’s law for locally inhomogeneous temperature flow by substitution of Equation (3.70) into Equation (3.58)₃ using the definition for \mathbf{S}_w in Equation (3.61):

$$n^f \tilde{\mathbf{v}}_f = -\hat{k} \left(\rho^{\text{fR}} (\mathbf{a}_f - \mathbf{b}) + \text{grad} p_f - \frac{1}{n^f} \text{div} \boldsymbol{\sigma}_E^f + \frac{1}{n^f} p_f \text{grad}(n^f) \left[1 - \frac{\theta^s}{\theta^f} \right] \right). \quad (3.71)$$

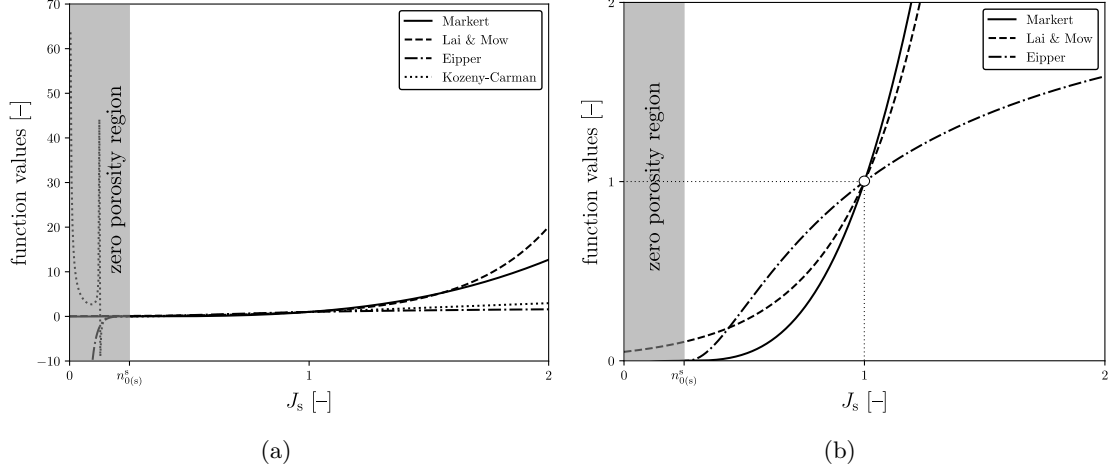


Figure 3.1: A comparison, adapted from Markert [2005], of different deformation-dependent hydraulic conductivities for $\kappa = 3.0$ (a) showing the instability of the Kozeny-Carman relation for high compression of the solid skeleton and (b) a zoomed-in version of (a) showing the inadequacy of the Eipper [1998] model for high expansion of the solid skeleton.

Lastly, the physical meaning of the heat transfer coefficient k_θ^ε can be understood via direct substitution into the local interaction energy supply of the solid (s) phase (making use of Equation (3.5) and definition Equation (2.46)):

$$\hat{\varepsilon}^s = -\hat{\varepsilon}^f - \mathbf{h}^f \cdot \mathbf{v}_f - \mathbf{h}^s \cdot \mathbf{v}_s = -k_\theta^\varepsilon(\theta^s - \theta^f) - \mathbf{h}^f \cdot \tilde{\mathbf{v}}_f. \quad (3.72)$$

Using Equation (3.58)₃ and Equation (3.61), we may write the above as

$$\hat{\varepsilon}^s = -k_\theta^\varepsilon(\theta^s - \theta^f) - \frac{\theta^s}{\theta^f} p_f \text{grad}(n^f) \cdot \tilde{\mathbf{v}}_f + \frac{(n^f)^2}{\hat{k}} \tilde{\mathbf{v}}_f \cdot \tilde{\mathbf{v}}_f. \quad (3.73)$$

From this equation, it is apparent that the heat transfer coefficient is independent of frictional effects, described by the the viscosity of the pore fluid embedded within the hydraulic conductivity in the last term, and deformation effects, embedded within the porosity gradient in the second term. Therefore, we cannot *a priori* use a heat transfer coefficient determined from classical heat exchange equations as the frictional effects from the fluid viscosity are embedded within these parameters by corresponding Nusselt number, Prandtl number, Rayleigh number, etc. Instead, the heat transfer coefficient must be determined through coupled experimentation-simulation techniques, wherein the

value of the heat transfer coefficient is adjusted through an iterative process to minimize differences between experimental and numerical results.

3.2 Locally homogeneous temperature model

In the locally homogeneous temperature model, we may assume that there is no heat exchange between constituents in the mixture, i.e., $\theta^s = \theta^f = \theta$. Therefore, the dissipation inequality may be written as

$$\rho^s [D_t^s \psi^s + \eta^s D_t^s \theta] - \boldsymbol{\sigma}^s : \mathbf{l}_s + \frac{1}{\theta} \text{grad}(\theta) \cdot (\mathbf{q}^s + \mathbf{q}^f) + \rho^f [D_t^f \psi^f + \eta^f D_t^f \theta] - \boldsymbol{\sigma}^f : \mathbf{l}_f + \mathbf{h}^f \cdot \tilde{\mathbf{v}}_f \geq 0, \quad (3.74)$$

where use has been made of Equation (3.5)_{2,3} to group the interaction force terms and eliminate the phase power terms, respectively. As we did for the locally inhomogeneous temperatures model, we will introduce the saturation constraint multiplied by the Lagrange multiplier \mathcal{P} (which will be identified later as excess pore fluid pressure):

$$\mathcal{P} \left(n^s \mathbf{d}_s : \mathbf{1} + \frac{n^f}{\rho^{\text{fR}}} D_t^f \rho^{\text{fR}} + n^f \mathbf{d}_f : \mathbf{1} + \text{grad}(n^f) \cdot \tilde{\mathbf{v}}_f \right) = 0. \quad (3.75)$$

As before, we can add this to the Clausius-Duhem inequality, and, combining terms and exploiting the symmetry of the partial Cauchy stress tensors, we may re-write the Clausius-Duhem inequality for the locally homogeneous temperature model as

$$\begin{aligned} & \rho^s D_t^s \psi^s + \rho^f D_t^f \psi^f + \rho^s \eta^s D_t^s \theta + \rho^f \eta^f D_t^f \theta - \left([\boldsymbol{\sigma}^s + \mathcal{P} n^s \mathbf{1} - q \mathbf{1}] : \mathbf{d}_s + [\boldsymbol{\sigma}^f + \mathcal{P} n^f \mathbf{1}] : \mathbf{d}_f \right) \\ & + (\mathbf{h}^f - \mathcal{P} \text{grad} n^f) \cdot \tilde{\mathbf{v}}_f + \frac{1}{\theta} \text{grad}(\theta) \cdot (\mathbf{q}^s + \mathbf{q}^f) - \mathcal{P} \frac{n^f}{\rho^{\text{fR}}} D_t^f \rho^{\text{fR}} \geq 0. \end{aligned} \quad (3.76)$$

Introduce the so-called “extra” terms for the locally homogeneous temperature model:

$$\begin{aligned} \boldsymbol{\sigma}_E^s &= \boldsymbol{\sigma}^s + \mathcal{P} n^s \mathbf{1}, \\ \boldsymbol{\sigma}_E^f &= \boldsymbol{\sigma}^f + \mathcal{P} n^f \mathbf{1}, \\ \mathbf{h}_E^f &= \mathbf{h}^f - \mathcal{P} \text{grad} n^f, \end{aligned} \quad (3.77)$$

and substitute back into Equation (3.76):

$$\begin{aligned} & \rho^s D_t^s \psi^s + \rho^f D_t^f \psi^f + \rho^s \eta^s D_t^s \theta + \rho^f \eta^f D_t^f \theta - \left(\boldsymbol{\sigma}_E^s : \mathbf{d}_s + \boldsymbol{\sigma}_E^f : \mathbf{d}_f \right) \\ & + \mathbf{h}_E^f \cdot \tilde{\mathbf{v}}_f - q \operatorname{div} \mathbf{v}_s - \mathcal{P} \frac{n^f}{\rho^{\text{fR}}} D_t^f \rho^{\text{fR}} + \frac{1}{\theta} \operatorname{grad} \theta \cdot (\mathbf{q}^s + \mathbf{q}^f) \geq 0. \end{aligned} \quad (3.78)$$

3.2.1 Determination of the Helmholtz free energies

The response functions to be determined for the locally homogeneous temperature model are

$$\mathcal{Q} := \left\{ \psi^s, \psi^f, \boldsymbol{\sigma}_E^s, \boldsymbol{\sigma}_E^f, \mathbf{h}_E^f, q, \mathbf{q}^s, \mathbf{q}^f \right\}, \quad (3.79)$$

which depend on a set \mathcal{T} of variables, i.e.,

$$\mathcal{Q} := \mathcal{Q}(\mathcal{T}), \quad (3.80)$$

where \mathcal{T} is a subset of the fundamental constitutive variables \mathcal{V} for a biphasic continuum with an elastic solid constituent,

$$\mathcal{V} := \left\{ \theta^\alpha, \operatorname{grad} \theta^\alpha, n^f, \operatorname{grad} n^f, \rho^{\alpha\text{R}}, \operatorname{grad} \rho^{\alpha\text{R}}, \mathbf{F}_\alpha, \operatorname{GRAD}_\alpha \mathbf{F}_\alpha, \operatorname{div} \mathbf{v}_s, \mathbf{v}_f, \operatorname{GRAD}_f \mathbf{v}_f, \mathbf{X}_\alpha \right\}. \quad (3.81)$$

Using the same arguments outlined in Section 3.1.1, we may define

$$\mathcal{T} = \left\{ \theta, \operatorname{grad} \theta, \rho^{\text{fR}}, \operatorname{grad} \rho^{\text{fR}}, \mathbf{F}_s, \operatorname{GRAD}_s \mathbf{F}_s, \operatorname{div} \mathbf{v}_s, \tilde{\mathbf{v}}_f, \mathbf{d}_f \right\}, \quad (3.82)$$

where we have also made use of $\theta^\alpha = \theta$. Combining Equations (3.79), (3.80) and (3.82),

$$\left\{ \psi^s, \psi^f, \boldsymbol{\sigma}_E^s, \boldsymbol{\sigma}_E^f, \mathbf{h}_E^f, \mathbf{q}^s, \mathbf{q}^f \right\} = \mathcal{Q}(\theta, \operatorname{grad} \theta, \rho^{\text{fR}}, \operatorname{grad} \rho^{\text{fR}}, \mathbf{F}_s, \operatorname{GRAD}_s \mathbf{F}_s, \operatorname{div} \mathbf{v}_s, \tilde{\mathbf{v}}_f, \mathbf{d}_f). \quad (3.83)$$

Based on the principle of phase separation, we may write

$$\begin{aligned} \psi^s & := \psi^s(\theta, \operatorname{grad} \theta, \mathbf{C}_s, \operatorname{GRAD}_s \mathbf{C}_s, \operatorname{div} \mathbf{v}_s), \\ \psi^f & := \psi^f(\theta, \operatorname{grad} \theta, \rho^{\text{fR}}, \operatorname{grad} \rho^{\text{fR}}, \tilde{\mathbf{v}}_f, \mathbf{d}_f), \end{aligned} \quad (3.84)$$

where we have used the right Cauchy-Green tensor $\mathbf{C}_s = \mathbf{F}_s^T \mathbf{F}_s$ in place of \mathbf{F}_s . The material time derivatives of the Helmholtz free energy functions are

$$D_t^s \psi^s = \frac{\partial \psi^s}{\partial \theta} D_t^s \theta + \frac{\partial \psi^s}{\partial(\text{grad}\theta)} D_t^s(\text{grad}\theta) + \frac{\partial \psi^s}{\partial \mathbf{C}_s} D_t^s \mathbf{C}_s + \frac{\partial \psi^s}{\partial(\text{GRAD}_s \mathbf{C}_s)} D_t^s(\text{GRAD}_s \mathbf{C}_s) + \frac{\partial \psi^s}{\partial(\text{div } \mathbf{v}_s)} D_t^s(\text{div } \mathbf{v}_s), \quad (3.85)$$

$$D_t^f \psi^f = \frac{\partial \psi^f}{\partial \theta} D_t^f \theta + \frac{\partial \psi^f}{\partial(\text{grad}\theta)} D_t^f(\text{grad}\theta) + \frac{\partial \psi^f}{\partial \rho^{\text{fR}}} D_t^f \rho^{\text{fR}} + \frac{\partial \psi^f}{\partial(\text{grad}\rho^{\text{fR}})} D_t^f(\text{grad}\rho^{\text{fR}}) + \frac{\partial \psi^f}{\partial \tilde{\mathbf{v}}_f} D_t^f \tilde{\mathbf{v}}_f + \frac{\partial \psi^f}{\partial \mathbf{d}_f} D_t^f \mathbf{d}_f. \quad (3.86)$$

3.2.2 Evaluation of the Clausius-Duhem inequality

Returning our attention to Equation (3.78), we may substitute the material time derivatives of the Helmholtz free energy functions:

$$\begin{aligned} & \left(\rho^s \frac{\partial \psi^s}{\partial \theta} + \rho^s \eta^s \right) D_t^s \theta + \rho^s \frac{\partial \psi^s}{\partial(\text{grad}\theta)} D_t^s(\text{grad}\theta) + \left(\rho^s \frac{\partial \psi^s}{\partial \mathbf{C}_s} \mathbf{C}_s - \frac{1}{2J_s} \mathbf{S}_{E(s)}^s \right) : D_t^s \mathbf{C}_s \\ & + \rho^s \frac{\partial \psi^s}{\partial(\text{GRAD}_s \mathbf{F}_s)} D_t^s(\text{GRAD}_s \mathbf{F}_s) + \frac{\partial \psi^s}{\partial(\text{div } \mathbf{v}_s)} D_t^s(\text{div } \mathbf{v}_s) + \left(\rho^f \frac{\partial \psi^f}{\partial \theta} + \rho^f \eta^f \right) D_t^f \theta \\ & \quad + \rho^f \frac{\partial \psi^f}{\partial(\text{grad}\theta)} D_t^f(\text{grad}\theta) + \left(\rho^f \frac{\partial \psi^f}{\partial \rho^{\text{fR}}} - \mathcal{P} \frac{n^f}{\rho^{\text{fR}}} \right) D_t^f \rho^{\text{fR}} \\ & \quad + \rho^f \frac{\partial \psi^f}{\partial(\text{grad}\rho^{\text{fR}})} D_t^f(\text{grad}\rho^{\text{fR}}) + \rho^f \frac{\partial \psi^f}{\partial \tilde{\mathbf{v}}_f} D_t^f \tilde{\mathbf{v}}_f + \frac{\partial \psi^f}{\partial \mathbf{d}_f} D_t^f \mathbf{d}_f - \boldsymbol{\sigma}_E^f : \mathbf{d}_f \\ & \quad + q \mathbf{1} : \mathbf{d}_s + \mathbf{h}_E^f \cdot \tilde{\mathbf{v}}_f + \frac{1}{\theta} \text{grad}\theta \cdot (\mathbf{q}^s + \mathbf{q}^f) \geq 0, \end{aligned} \quad (3.87)$$

where the identities in Equation (3.33) have been used, here, too.

Using the Coleman and Noll [1963] argument, the following constitutive relations must hold:

$$\begin{aligned}
\left(\rho^s \frac{\partial \psi^s}{\partial \theta} + \rho^s \eta^s\right) &= 0 \Rightarrow \rho_{0(s)}^s \eta^s = -\frac{\partial(\rho_{0(s)}^s \psi^s)}{\partial \theta}, \\
\frac{\partial \psi^s}{\partial(\text{grad} \theta)} &= 0, \\
\left(\rho^s \frac{\partial \psi^s}{\partial \mathbf{C}_s} \mathbf{C}_s - \frac{1}{2J_s} \mathbf{S}_{E(s)}^s\right) &= \mathbf{0} \Rightarrow \mathbf{S}_{E(s)}^s = 2 \frac{\partial(\rho_{0(s)}^s \psi^s)}{\partial \mathbf{C}_s}, \\
\frac{\partial \psi^s}{\partial(\text{GRAD}_s \mathbf{C}_s)} &= \mathbf{0}, \\
\left(\rho^f \frac{\partial \psi^f}{\partial \theta} + \rho^f \eta^f\right) &= 0 \Rightarrow \eta^f = -\frac{\partial \psi^f}{\partial \theta}, \\
\frac{\partial \psi^f}{\partial(\text{grad} \theta)} &= 0, \\
\left(\rho^f \frac{\partial \psi^f}{\partial \rho^{\text{fR}}} - \mathcal{P} \frac{n^f}{\rho^{\text{fR}}}\right) &= 0 \Rightarrow \mathcal{P} = (\rho^{\text{fR}})^2 \frac{\partial \psi^f}{\partial \rho^{\text{fR}}}, \\
\frac{\partial \psi^f}{\partial(\text{grad} \rho^{\text{fR}})} &= 0, \\
\frac{\partial \psi^f}{\partial \tilde{\mathbf{v}}_f} &= \mathbf{0}, \\
\frac{\partial \psi^f}{\partial \mathbf{d}_f} &= \mathbf{0},
\end{aligned} \tag{3.88}$$

and

$$\mathcal{D} := \boldsymbol{\sigma}_E^f : \mathbf{d}_f - q \operatorname{div} \mathbf{v}_s - \mathbf{h}_E^f \cdot \tilde{\mathbf{v}}_f - \frac{1}{\theta} \operatorname{grad}(\theta) \cdot (\mathbf{q}^s + \mathbf{q}^f) \geq 0. \tag{3.89}$$

From Equation (3.88), we can deduce that the Helmholtz free energy functions simplify to:

$$\begin{aligned}
\psi^s &:= \psi^s(\theta, \mathbf{C}_s), \\
\psi^f &:= \psi^f(\theta, \rho^{\text{fR}}).
\end{aligned} \tag{3.90}$$

Given the dependence of solid entropy and stress on the solid Helmholtz free energy, we must have:

$$\begin{aligned}
\boldsymbol{\sigma}_E^s &:= \boldsymbol{\sigma}_E^s(\theta, \mathbf{C}_s), \\
\eta^s &:= \eta^s(\theta, \mathbf{C}_s),
\end{aligned} \tag{3.91}$$

and analogously for the pore fluid

$$\begin{aligned}
\mathcal{P} &:= \mathcal{P}(\rho^{\text{fR}}), \\
\eta^f &:= \eta^f(\theta, \rho^{\text{fR}}).
\end{aligned} \tag{3.92}$$

Identification of the Lagrange multiplier. Using Equation (3.41), the Lagrange multiplier \mathcal{P} is identified as excess pore fluid pressure such that the partial Cauchy stresses for each constituent are defined as

$$\begin{aligned}\boldsymbol{\sigma}^s &= \boldsymbol{\sigma}_E^s - p_f n^s \mathbf{1}, \\ \boldsymbol{\sigma}^f &= \boldsymbol{\sigma}_E^f - p_f n^f \mathbf{1},\end{aligned}\tag{3.93}$$

with

$$\mathbf{h}_E^f = \mathbf{h}^f - p_f \text{grad} n^f.\tag{3.94}$$

3.2.3 Identifying constitutive relations

The analysis for identifying constitutive relations for the locally homogeneous temperature model is analogous to that for the locally inhomogeneous temperature model. Thus we will skip the details for brevity and summarize. The set of response functions for \mathcal{D} :

$$\left\{ \boldsymbol{\sigma}_E^f, q, \mathbf{h}_E^f, \mathbf{q}^s, \mathbf{q}^f \right\} := \Phi(\mathcal{T}),\tag{3.95}$$

where

$$\mathcal{T} = \left\{ \theta, \text{grad}\theta, \rho^{\text{fR}}, \text{grad}\rho^{\text{fR}}, \mathbf{F}_s, \text{GRAD}_s \mathbf{F}_s, \text{div} \mathbf{v}_s, \tilde{\mathbf{v}}_f, \mathbf{d}_f \right\},\tag{3.96}$$

with similar assumptions as for the locally inhomogeneous temperature model, such that

$$\begin{aligned}\boldsymbol{\sigma}_E^f &:= \boldsymbol{\sigma}_E^f(\mathbf{d}_f), \\ q &:= q(\text{div} \mathbf{v}_s), \\ \mathbf{h}_E^f &:= \mathbf{h}_E^f(\tilde{\mathbf{v}}_f), \\ \mathbf{q}^s &:= \mathbf{q}^s(\theta), \\ \mathbf{q}^f &:= \mathbf{q}^f(\theta).\end{aligned}\tag{3.97}$$

Thus the reduced dissipation inequality, Equation (3.89), becomes, with use of Equation (3.54),

$$\mathcal{D} = (\overset{4}{\mathbf{Z}}_f \mathbf{d}_f) : \mathbf{d}_f - (C \text{div} \mathbf{v}_s) \text{div} \mathbf{v}_s - (\mathbf{S}_w \tilde{\mathbf{v}}_f) \cdot \tilde{\mathbf{v}}_f - \frac{1}{\theta} \text{grad}(\theta) \cdot (\mathbf{k}^{\theta^{mix}} \text{grad}\theta) \geq 0,\tag{3.98}$$

where we have introduced

$$\mathbf{k}^{\theta^{mix}} := n^s \mathbf{k}^{\theta^s} + n^f \mathbf{k}^{\theta^f} . \quad (3.99)$$

In order to satisfy the inequality, each term must be non-negative by itself, and thus the following restrictions must hold:

$$\begin{aligned} \mathbf{Z}_f &\rightarrow \text{positive definite} , \\ C &> 0 , \\ -\mathbf{S}_w &\rightarrow \text{positive definite} , \\ -\mathbf{k}^\theta &\rightarrow \text{positive definite} . \end{aligned} \quad (3.100)$$

3.2.4 Defining proportionality parameters

As before: details on shock viscosity q are covered in Section 4.4.1, and the fourth-order tensor \mathbf{Z}_f can be defined using a Newtonian fluid constitutive law, see, e.g. Equation (3.59). We might also assume isotropic heat conduction through the mixture to define $\mathbf{k}^{\theta^{mix}}$, see, e.g., Equation (3.60). Definition of the seepage tensor does not need to change from Equation (3.61), however, determination of the seepage velocity is simplified for the locally homogeneous temperatures model in that we do not need to perform algebraic tricks with Equation (3.69), and can substitute from the balance of linear momentum of the pore fluid directly. Thus, Darcy's law in the locally homogeneous temperatures model is written as

$$n^f \tilde{\mathbf{v}}_f = -\hat{k} \left(\rho^{\text{fR}} (\mathbf{a}_f - \mathbf{b}) + \text{grad} p_f - \frac{1}{n^f} \text{div} \boldsymbol{\sigma}_E^f \right) , \quad (3.101)$$

and for a nearly-inviscid pore fluid

$$n^f \tilde{\mathbf{v}}_f = -\hat{k} \left(\rho^{\text{fR}} (\mathbf{a}_f - \mathbf{b}) + \text{grad} p_f \right) . \quad (3.102)$$

3.3 Constituent modeling

In the event that adiabatic conditions are assumed, then, for high rate loading pertinent to stress waves, including shocks, it is more convenient to work with an internal energy formulation than a free energy formulation. Shock wave propagation is neither isentropic nor isothermal.

Legendre transformations can be used to replace Equation (3.34)_{1,3,5,7} with constitutive equations in terms of internal energy functionals e^α . First, assume a functional dependence of internal energy and temperature of each phase as

$$(\rho_{0(s)}^s e^s) = (\rho_{0(s)}^s e^s)(\mathbf{C}_s, \eta^s), \quad \theta^s = \theta^s(\mathbf{C}_s, \eta^s), \quad e^f = e^f(\rho^{\text{fR}}, \eta^f), \quad \theta^f = \theta^f(\rho^{\text{fR}}, \eta^f). \quad (3.103)$$

Then, chain-rule differentiation of Equation (3.103) in combination with Equations (3.34)_{1,3,5,7}, (3.41) and (3.42) leads to the following constitutive relations:

$$\begin{aligned} \theta^s &= \frac{1}{\rho_{0(s)}^s} \frac{\partial(\rho_{0(s)}^s e^s)}{\partial \eta^s}, \\ \mathbf{S}_{E(s)}^s &= 2 \frac{\partial(\rho_{0(s)}^s e^s)}{\partial \mathbf{C}_s}, \\ \theta^f &= \frac{\partial e^f}{\partial \eta^f}, \\ p_f &= (\rho^{\text{fR}})^2 \frac{\partial e^f}{\partial \rho^{\text{fR}}}. \end{aligned} \quad (3.104)$$

Of course, for the locally homogeneous temperatures model, θ^s and θ^f are interchangeable as both become θ . Thus, only one constituent's internal energy function is sufficient to describe the temperature of the mixture if that constituent's entropy can be determined from the corresponding energy balance.

3.3.1 Hyperelastic solid skeleton

Oftentimes it is easier to constitutively define the solid skeleton stress (the solid extra stress) in terms of the symmetric second Piola-Kirchhoff effective stress $\mathbf{S}_{E(s)}^s$ which is what follows herein. However, for the numerical implementation, we convert one reference leg to the current configuration and use the first Piola-Kirchhoff stress, i.e.,

$$\mathbf{P}_{E(s)}^s = \mathbf{F}_s \mathbf{S}_{E(s)}^s. \quad (3.105)$$

The neo-Hookean hyperelastic model. One of the most common strain-energy functions for modeling non-linear elastic materials in the finite strain regime is the neo-Hookean elastic strain-

energy function:

$$W^s(\mathbf{C}_s, J_s(\mathbf{C}_s)) = \frac{1}{2}\mu(\text{tr } \mathbf{C}_s - 3) - \mu \ln(J_s) + U^s(J_s), \quad (3.106)$$

where oftentimes

$$U^s(J_s) := \frac{1}{2}\lambda(\ln(J_s))^2, \quad (3.107)$$

and where the solid skeleton isentropic Lamé parameters are μ and $\lambda := K^{\text{skel}} - \frac{2}{3}\mu$. In Irwin et al. [2023a,b,c,d, 2024], we used the form for $U^s(J_s)$ given by Equation (3.107). However, for the incompressible solid constituent, it was noted by Ehlers and Eipper [1999] that the restriction from Equation (3.26),

$$n_{0(s)}^s < J_s < \infty, \quad (3.108)$$

must be encapsulated by the strain-energy function. Therefore, they proposed

$$U^s(J_s) := \lambda(1 - n_{0(s)}^s)^2 \left(\frac{J_s - 1}{1 - n_{0(s)}^s} - \ln \frac{J_s - n_{0(s)}^s}{1 - n_{0(s)}^s} \right), \quad (3.109)$$

which behaves like a penalty function to ensure J_s is appropriately bounded. Thus, the internal energy function for the solid skeleton may be written as

$$(\rho_{0(s)}^s e^s)(\mathbf{C}_s, \eta^s) := W^s(\mathbf{C}_s, J_s(\mathbf{C}_s)) + \rho_{0(s)}^s \theta_0^s (\eta^s - \eta_0^s) \left[1 - \gamma^s \ln J_s + \frac{\eta^s - \eta_0^s}{2c_V^s} \right], \quad (3.110)$$

where simple non-linear thermoelasticity is assumed via the inclusion of the Grüneisen parameter of the solid γ^s , and c_V^s is the specific heat of the solid at constant volume per unit mass. The temperature and second Piola effective stress are then, from Equation (3.104)_{1,2},

$$\begin{aligned} \theta^s &= \theta_0^s \left[1 - \gamma^s \ln J_s + \frac{\eta_E^s - \eta_0^s}{c_V^s} \right], \\ \mathbf{S}_{E(s)}^s &= \mu \mathbf{1} + \begin{cases} \left(\lambda \ln J_s - \mu - \rho_{0(s)}^s \theta_0^s \gamma^s [\eta_E^s - \eta_0^s] \right) \mathbf{C}_s^{-1} & \text{per (3.107)} \\ \left(\lambda(1 - n_{0(s)}^s)^2 \left[\frac{J_s}{1 - n_{0(s)}^s} - \frac{J_s}{J_s - n_{0(s)}^s} \right] - \mu - \rho_{0(s)}^s \theta_0^s \gamma^s [\eta^s - \eta_0^s] \right) \mathbf{C}_s^{-1} & \text{per (3.109)} \end{cases}. \end{aligned} \quad (3.111)$$

For the locally homogeneous temperatures regime, we would write

$$\begin{aligned} \theta &= \theta_0 \left[1 - \gamma^s \ln J_s + \frac{\eta_E^s - \eta_0^s}{c_V^s} \right], \\ \mathbf{S}_{E(s)}^s &= \mu \mathbf{1} + \begin{cases} \left(\lambda \ln J_s - \mu - \rho_{0(s)}^s \theta_0 \gamma^s [\eta_E^s - \eta_0^s] \right) \mathbf{C}_s^{-1} & \text{per (3.107)} \\ \left(\lambda(1 - n_{0(s)}^s)^2 \left[\frac{J_s}{1 - n_{0(s)}^s} - \frac{J_s}{J_s - n_{0(s)}^s} \right] - \mu - \rho_{0(s)}^s \theta_0 \gamma^s [\eta^s - \eta_0^s] \right) \mathbf{C}_s^{-1} & \text{per (3.109)} \end{cases}. \end{aligned} \quad (3.112)$$

In both Equations (3.111) and (3.112), thermo-mechanical coupling can be neglected by assuming $\gamma^s \rightarrow 0$.

However, as stated previously, it is more convenient in the locally inhomogeneous temperature model to work with a free energy formulation such that

$$(\rho_{0(s)}^s \psi^s)(\mathbf{C}_s, \theta^s) := W^s(\mathbf{C}_s, J_s(\mathbf{C}_s)) - K^{\text{skel}} \alpha_V^s \ln(J_s) \Delta \theta^s - \rho_{0(s)}^s c_V^s \left(\theta^s \ln \frac{\theta^s}{\theta_0^s} - \Delta \theta^s \right), \quad (3.113)$$

where $\Delta \theta^s := \theta^s - \theta_0^s$, and K^{skel} is the solid skeleton isothermal bulk modulus. The solid entropy and second Piola-Kirchhoff solid extra stress are then, from Equations (3.34)_{1,3},

$$\begin{aligned} \eta^s &= c_V^s \ln \frac{\theta^s}{\theta_0^s} + \frac{1}{\rho_{0(s)}^s} K^{\text{skel}} \alpha_V^s \ln J_s, \\ \mathbf{S}_{E(s)}^s &= \mu \mathbf{1} + \begin{cases} \left(\lambda \ln J_s - \mu - K^{\text{skel}} \alpha_V^s \Delta \theta^s \right) \mathbf{C}_s^{-1} & \text{per (3.107)} \\ \left(\lambda (1 - n_{0(s)}^s)^2 \left[\frac{J_s}{1 - n_{0(s)}^s} - \frac{J_s}{J_s - n_{0(s)}^s} \right] - \mu - K^{\text{skel}} \alpha_V^s \Delta \theta^s \right) \mathbf{C}_s^{-1} & \text{per (3.109)} \end{cases}. \end{aligned} \quad (3.114)$$

For the locally homogeneous temperatures regime, we would write

$$\begin{aligned} \eta^s &= c_V^s \ln \frac{\theta}{\theta_0} + \frac{1}{\rho_{0(s)}^s} K^{\text{skel}} \alpha_V^s \ln J_s, \\ \mathbf{S}_{E(s)}^s &= \mu \mathbf{1} + \begin{cases} \left(\lambda \ln J_s - \mu - K^{\text{skel}} \alpha_V^s \Delta \theta^s \right) \mathbf{C}_s^{-1} & \text{per (3.107)} \\ \left(\lambda (1 - n_{0(s)}^s)^2 \left[\frac{J_s}{1 - n_{0(s)}^s} - \frac{J_s}{J_s - n_{0(s)}^s} \right] - \mu - K^{\text{skel}} \alpha_V^s \Delta \theta \right) \mathbf{C}_s^{-1} & \text{per (3.109)} \end{cases}. \end{aligned} \quad (3.115)$$

In both Equations (3.114) and (3.115), thermo-mechanical coupling can be neglected by assuming $\alpha_V^s \rightarrow 0$. In such a case, using Equation (3.107), we may assume the existence of the viscous damping component of $\mathbf{S}_{E(s)}^s$ proposed by Li et al. [2004]:

$$\mathbf{S}_{E(s),\text{vis}}^s = \nu_0 \mathbf{C}_s : \left(\frac{1}{2} \dot{\mathbf{C}}_{(s)} \right), \quad (3.116)$$

where ν_0 is a viscous damping parameter with units of seconds, and the second tangential elasticity tensor is defined as

$$\begin{aligned} \mathbf{C}_{JIKL(s)} &= 4 \frac{\partial^2 (\rho_{0(s)}^s \psi^s)}{\partial C_{JI(s)} \partial C_{KL(s)}} \\ &= \lambda C_{JI(s)}^{-1} C_{KL(s)}^{-1} + (\mu - \ln J_s) (C_{IK(s)}^{-1} C_{JL(s)}^{-1} + C_{IL(s)}^{-1} C_{JK(s)}^{-1}), \end{aligned} \quad (3.117)$$

such that

$$\begin{aligned} S_{IJ(E)}^s &= S_{IJ(E),\text{inv}}^s + S_{IJ(E),\text{vis}}^s \\ &= (\lambda(\ln J_s) - \mu)C_{IJ(s)}^{-1} + \mu\delta_{IJ} + \frac{\nu_0}{2}C_{IJKL(s)}\dot{C}_{KL(s)}. \end{aligned} \quad (3.118)$$

Using Equation (3.33)₁, we may write the viscous component of second Piola-Kirchhoff stress as follows:

$$\begin{aligned} S_{IJ(E),\text{vis}}^s &= \nu_0 \left[\lambda C_{IJ(s)}^{-1} C_{KL(s)}^{-1} + (\mu - \ln J_s) \left(C_{IK(s)}^{-1} C_{JL(s)}^{-1} + C_{IL(s)}^{-1} C_{JK(s)}^{-1} \right) \right] \times \\ &\quad \left[F_{mK(s)} d_{mn(s)} F_{nL(s)} \right], \end{aligned} \quad (3.119)$$

which simplifies to

$$S_{IJ(E),\text{vis}}^s = \nu_0 \left[\lambda F_{Ji(s)}^{-1} F_{Ii(s)}^{-1} F_{Kk(s)}^{-1} \frac{\partial v_{k(s)}}{\partial X_K} + 2(\mu - \ln J_s) F_{Ji(s)}^{-1} F_{Ii(s)}^{-1} F_{Kj(s)}^{-1} \frac{\partial v_{j(s)}}{\partial X_K} \right]. \quad (3.120)$$

Note that the viscous component of the solid extra stress is not included in any of the numerical results shown in Chapter 5, and is only shown here for the interested reader.

A damage model for the solid constituent. Ultimately, this thesis is intended to provide a foundation for which to quantify damage of the solid constituent in the multiphase regime. While a numerical implementation of a damage model is outside the current scope, it behooves us to derive theory which will be used in future work.

We begin by introducing an internal state variable \mathcal{D} that exists in the solid phase but not the fluid:

$$\mathcal{D} = \mathcal{D}(\mathbf{X}_s, t) \in [0, 1]. \quad (3.121)$$

We then introduce a general kinetic law for damage—which will need to be validated by experimental data—which is an irreversible function $\mathcal{R}^{\mathcal{D}}$ of local state (i.e., its rate is non-negative):

$$D_t^s \mathcal{D} := \mathcal{R}^{\mathcal{D}}(\cdot, t) \geq 0. \quad (3.122)$$

Now, the free energy of the solid skeleton is defined as

$$(\rho_{0(s)}^s \psi^s) = (\rho_{0(s)}^s \psi^s)(\mathbf{F}_s, \theta^s, \mathcal{D}), \quad (3.123)$$

such that the set of response functions given in Equation (3.27) is now

$$\mathcal{S} = \left\{ \theta^\alpha, \text{grad} \theta^\alpha, \rho^{\text{fR}}, \text{grad} \rho^{\text{fR}}, \mathbf{F}_s, \text{GRAD}_s \mathbf{F}_s, \text{div} \mathbf{v}_s, \tilde{\mathbf{v}}_f, \mathbf{d}_f, \mathcal{D} \right\}. \quad (3.124)$$

Therefore (using again the principle of phase separation, and substituting \mathbf{C}_s for \mathbf{F}_s), the material time derivative of the solid skeleton free energy, Equation (3.30) becomes

$$\begin{aligned} D_t^s \psi^s &= \frac{\partial \psi^s}{\partial \theta^s} D_t^s \theta^s + \frac{\partial \psi^s}{\partial (\text{grad} \theta^s)} D_t^s (\text{grad} \theta^s) + \frac{\partial \psi^s}{\partial \mathbf{C}_s} D_t^s \mathbf{C}_s + \frac{\partial \psi^s}{\partial (\text{GRAD}_s \mathbf{C}_s)} D_t^s (\text{GRAD}_s \mathbf{C}_s) \\ &\quad + \frac{\partial \psi^s}{\partial (\text{div} \mathbf{v}_s)} D_t^s (\text{div} \mathbf{v}_s) + \frac{\partial \psi^s}{\partial \mathcal{D}} D_t^s \mathcal{D}. \end{aligned} \quad (3.125)$$

From arguments presented in Section 3.1.2, the Clausius-Duhem inequality for the mixture may be written as

$$\begin{aligned} &\left(\rho^s \frac{\partial \psi^s}{\partial \theta^s} + \rho^s \eta^s \right) D_t^s \theta^s + \rho^s \frac{\partial \psi^s}{\partial (\text{grad} \theta^s)} D_t^s (\text{grad} \theta^s) + \left(\rho^s \frac{\partial \psi^s}{\partial \mathbf{C}_s} \mathbf{C}_s - \frac{1}{2J_s} \mathbf{S}_{E(s)}^s \right) : D_t^s \mathbf{C}_s \\ &+ \rho^s \frac{\partial \psi^s}{\partial (\text{GRAD}_s \mathbf{C}_s)} D_t^s (\text{GRAD}_s \mathbf{C}_s) + \frac{\partial \psi^s}{\partial (\text{div} \mathbf{v}_s)} D_t^s (\text{div} \mathbf{v}_s) + \left(\frac{\theta^s}{\theta^f} \rho^f \frac{\partial \psi^f}{\partial \theta^f} + \frac{\theta^s}{\theta^f} \rho^f \eta^f \right) D_t^f \theta^f \\ &\quad + \frac{\theta^s}{\theta^f} \rho^f \frac{\partial \psi^f}{\partial (\text{grad} \theta^f)} D_t^f (\text{grad} \theta^f) + \left(\frac{\theta^s}{\theta^f} \rho^f \frac{\partial \psi^f}{\partial \rho^{\text{fR}}} - \Lambda \frac{n^f}{\rho^{\text{fR}}} \right) D_t^f \rho^{\text{fR}} \\ &\quad + \frac{\theta^s}{\theta^f} \rho^f \frac{\partial \psi^f}{\partial (\text{grad} \rho^{\text{fR}})} D_t^f (\text{grad} \rho^{\text{fR}}) + \frac{\theta^s}{\theta^f} \rho^f \frac{\partial \psi^f}{\partial \tilde{\mathbf{v}}_f} D_t^f \tilde{\mathbf{v}}_f + \frac{\partial \psi^f}{\partial \mathbf{d}_f} D_t^f \mathbf{d}_f + q \mathbf{1} : \mathbf{d}_s \\ &- \frac{\theta^s}{\theta^f} \boldsymbol{\sigma}_E^f : \mathbf{d}_f - \varepsilon^f \left(\frac{\theta^s}{\theta^f} - 1 \right) + \mathbf{h}_E^f \cdot \tilde{\mathbf{v}}_f + \left(\frac{1}{\theta^s} \text{grad}(\theta^s) \cdot \mathbf{q}^s + \frac{\theta^s}{(\theta^f)^2} \text{grad}(\theta^f) \cdot \mathbf{q}^f \right) \\ &\quad - \frac{1}{J_s} \frac{\partial (\rho_{0(s)}^s \psi^s)}{\partial \mathcal{D}} D_t^s \mathcal{D} \geq 0, \end{aligned} \quad (3.126)$$

such that, after applying the Coleman and Noll [1963] argument, an additional term appears in the reduced dissipation inequality \mathcal{D} :

$$\begin{aligned} \mathcal{D} &:= \frac{\theta^s}{\theta^f} \boldsymbol{\sigma}_E^f : \mathbf{d}_f - q \text{div} \mathbf{v}_s + \frac{1}{\theta^f} \varepsilon^f (\theta^s - \theta^f) - \mathbf{h}_E^f \cdot \tilde{\mathbf{v}}_f + \mathcal{F}^{\mathcal{D}} \mathcal{R}^{\mathcal{D}} \\ &\quad - \frac{1}{\theta^f} \left(\frac{\theta^f}{\theta^s} \text{grad}(\theta^s) \cdot \mathbf{q}^s + \frac{\theta^s}{\theta^f} \text{grad}(\theta^f) \cdot \mathbf{q}^f \right) \geq 0, \end{aligned} \quad (3.127)$$

wherein

$$\mathcal{F}^{\mathcal{D}} := - \frac{1}{J_s} \frac{\partial (\rho_{0(s)}^s \psi^s)}{\partial \mathcal{D}}. \quad (3.128)$$

Since $\mathcal{F}^{\mathcal{D}}$ is defined by, and dependent on the form of, the constitutive model for the solid skeleton free energy, we do not need to step through the same process in Section 3.1.3 so long as the constitutive model is written in such a way that $\mathcal{F}^{\mathcal{D}} \geq 0$. Suppose then that

$$(\rho_{0(s)}^s \psi^s)(\mathbf{C}_s, \theta^s, \mathcal{D}) := W^s(\mathbf{C}_s, J_s(\mathbf{C}_s)) \cdot f^{\mathcal{D}}(\mathcal{D}) - K^{\text{skel}} \alpha_V^s \ln(J_s) \Delta \theta^s - \rho_{0(s)}^s c_V^s \left(\theta^s \ln \frac{\theta^s}{\theta_0^s} - \Delta \theta^s \right), \quad (3.129)$$

where the degradation function is defined as

$$f^{\mathcal{D}} := \zeta_0 + (1 - \zeta_0)(1 - \mathcal{D}). \quad (3.130)$$

The constant $\zeta_0 \in [0, 1]$ allows the material to maintain remnant elastic stiffness when $\mathcal{D} \rightarrow 1$.

Thus, the conjugate force to damage rate is

$$\mathcal{F}^{\mathcal{D}} = -\frac{W^s}{J_s} \frac{\partial f^{\mathcal{D}}}{\partial \mathcal{D}} = \frac{1}{J_s} (1 - \zeta_0) W^s. \quad (3.131)$$

Therefore, $\mathcal{F}^{\mathcal{D}} \geq 0$ so long as strain energy W^s is non-negative. Thus with the inclusion of a damage parameter, the solid skeleton second Piola-Kirchhoff extra stress is written as

$$\mathbf{S}_{E(s)}^s = \begin{cases} [\mu \mathbf{1} + (\lambda \ln J_s - \mu - K^{\text{skel}} \alpha_V^s \Delta \theta^s) \mathbf{C}_s^{-1}] [\zeta_0 + (1 - \zeta_0)(1 - \mathcal{D})] & \text{per (3.107)} \\ \left[\mu \mathbf{1} + \left(\lambda (1 - n_{0(s)}^s)^2 \left[\frac{J_s}{1 - n_{0(s)}^s} - \frac{J_s}{J_s - n_{0(s)}^s} \right] - \mu - K^{\text{skel}} \alpha_V^s \Delta \theta^s \right) \mathbf{C}_s^{-1} \right] [\zeta_0 + (1 - \zeta_0)(1 - \mathcal{D})] & \text{per (3.109)} \end{cases} \quad (3.132)$$

Then, the energy balance of the solid constituent, with the inclusion of damage, may be written in the reference configuration of the solid skeleton as¹

$$\begin{aligned} \rho_{0(s)}^s c_V^s D_t^s \theta^s + \left(\frac{K^{\text{skel}} \alpha_V^s \theta^s}{J_s} + n^s p_f \frac{\theta^s}{\theta^f} + Q \right) D_t^s J_s + J_s \mathcal{F}^{\mathcal{D}} D_t^s \mathcal{D} + J_s \text{GRAD}_s(\mathbf{q}^s) : \mathbf{F}_s^{-T} \\ + J_s k_{\theta}^s (\theta^s - \theta^f) - \frac{J_s (n^f)^2}{\hat{k}} + J_s \frac{\theta^s}{\theta^f} \frac{p_f}{n^f} \text{GRAD}_s(n^f) \cdot \mathbf{F}_s^{-1} \cdot (n^f \tilde{\mathbf{v}}_f) = 0. \end{aligned} \quad (3.133)$$

With the inclusion of damage, it is apparent that free energy ψ^s is now conjugate, by Equation (3.131), to rate of damage growth. Thus, a damage model must include information about the solid temperature, which in TPM and for high strain-rate loading, is likely to be influenced by relative motion between solid and fluid as well as heat transfer via convection from an independent pore

¹ Refer to Section 4.1.5, paragraph *Derivation of the solid phase energy balance* for details on the derivation. We do not show the trivial derivation of adding the damage rate term herein.

fluid temperature. It is for this reason that in Chapter 4 we pursue a numerical implementation that includes *distinct* phase temperatures.

Note that in the form of Equation (3.129), we have made at least two gross simplifications with regards to the damage model. Physically speaking, damage is the degradation of the solid material. Thus, as degradation occurs, one might expect the intrinsic permeability of the solid to increase. For simplicity, one might assume that the intrinsic permeability remains constant and that as cracks and cavities form in the solid constituent, pore fluid leaks in, i.e., porosity increases. The second simplification we have made is assuming thermal conductivity is independent of a degradation process. In reality, as the solid material is degraded, we would expect its conductivity to equilibrate to that of the surrounding medium, in this case, the pore fluid. One such functional form for a degradation-dependent thermal conductivity is proposed in Miehe et al. [2015]. We note, however, that said form also includes convection to an equilibrium temperature (where the crack forms) and thus, in its current form, would be inappropriate in the current framework of this work for the thermal conductivity of the solid constituent given that convection is handled through the k_θ^ε term.

3.3.2 Compressible pore fluid

Recall from Section 2.3 that we consider two functional forms for the pore fluid pressure:

$$p_f = p_f(\rho^{\text{fR}}) \text{ (barotropic model)}; p_f = p_f(\rho^{\text{fR}}, \theta^f) \text{ (baroclinic model)}. \quad (3.134)$$

Herein we present the constitutive models for pore fluid internal energy, and pore fluid free energy, that produce constitutive relations used in the numerical formulation and resulting numerical simulations in Chapters 4 & 5, respectively.

The barotropic model. The following form for the internal energy of the pore fluid is assumed:

$$e^f(\rho^{\text{fR}}, \eta^f) := -\frac{1}{\rho^{\text{fR}}} \left[K_f^\eta \ln \left(\frac{\rho^{\text{fR}}}{\rho_0^{\text{fR}}} \right) + K_f^\eta + p_{f0} \right] + \theta_0 \left[(\eta^f - \eta_0^f) + \frac{(\eta^f - \eta_0^f)^2}{2c_V^f} \right], \quad (3.135)$$

where p_{f0} is the fluid pressure at reference density ρ_0^{fR} and recalling K_f^η is the isentropic bulk modulus of the fluid. The reference entropy per unit mass, and specific heat at constant volume per unit mass of the fluid are η_0^f , and c_V^f . Applying Equations (3.104)_{3,4} allows us to derive the pressure-density and temperature-entropy relations as

$$\begin{aligned} p_f &= K_f^\eta \ln(\rho^{\text{fR}}/\rho_0^{\text{fR}}) + p_{f0} \quad \Rightarrow \quad \rho^{\text{fR}} = \rho_0^{\text{fR}} \exp[(p_f - p_{f0})/K_f^\eta], \\ \theta &= \theta_0[1 + (\eta^f - \eta_0^f)/c_V^f]. \end{aligned} \quad (3.136)$$

Applying the D_t^f operation to Equation (3.136)₁ with $K_f^\eta = \text{constant}$ produces Equation (2.14).

Alternatively, we could write the free energy formulation, such that

$$\psi^f(\rho^{\text{fR}}, \theta) := -\frac{K_f^\theta}{\rho^{\text{fR}}}(1 + \ln \rho^{\text{fR}}) + c_V^f \left[\theta \left(\ln \left[\frac{\theta}{\theta_0} \right] - 1 \right) + \theta_0 \right]. \quad (3.137)$$

Applying Equations (3.88)_{5,7} allows us to derive the pressure-density and temperature-entropy constitutive equations as

$$\begin{aligned} p_f &= K_f^\theta \ln(\rho^{\text{fR}}/\rho_0^{\text{fR}}) + p_{f0} \quad \Rightarrow \quad \rho^{\text{fR}} = \rho_0^{\text{fR}} \exp[(p_f - p_{f0})/K_f^\theta], \\ \eta^f &= c_V^f \ln \frac{\theta}{\theta_0}. \end{aligned} \quad (3.138)$$

Applying the D_t^f operation to Equation (3.138)₁ with $K_f^\theta = \text{constant}$ produces Equation (2.14) with K_f^θ instead of K_f^η .

We have also implemented a linear form of Equation (3.137), which is used in Section 5.2.1,

$$\psi^f(\rho^{\text{fR}}, \theta) := K_f^\theta \ln \rho^{\text{fR}} + c_V^f \left[\theta \left(\ln \left[\frac{\theta}{\theta_0} \right] - 1 \right) + \theta_0 \right], \quad (3.139)$$

such that applying Equations (3.88)_{5,7} allows us to derive the pressure-density and temperature-entropy constitutive equations as

$$\begin{aligned} p_f &= K_f^\theta (\rho^{\text{fR}} - \rho_0^{\text{fR}}) + p_{f0} \quad \Rightarrow \quad \rho^{\text{fR}} = \rho_0^{\text{fR}} \left[(p_f - p_{f0})/K_f^\theta \right], \\ \eta^f &= c_V^f \ln \frac{\theta}{\theta_0}. \end{aligned} \quad (3.140)$$

The ideal gas model. Assume the ideal gas law as the constitutive form for pore fluid pressure, with \mathfrak{R} the specific gas constant,

$$p_f = \rho^{\text{fR}} \theta^f \mathfrak{R}. \quad (3.141)$$

The form for the internal energy function for the fluid phase for an ideal gas is [Clayton, 2022]

$$\begin{aligned} e^f(\rho^{\text{fR}}, \eta^f) &:= e_0^f \left(\frac{\rho^{\text{fR}}}{\rho_0^{\text{fR}}} \right)^{\Gamma-1} \exp\left(\frac{\eta^f - \eta_0^f}{c_V^f} \right), \\ \rho_0^{\text{fR}} e_0^f &= \frac{p_{f0}}{\Gamma - 1}, \quad \Gamma = 1 + \gamma^f, \quad K_f^\eta = \Gamma p_f, \quad c_V^f = \frac{e_0^f}{\theta_0^f}, \end{aligned} \quad (3.142)$$

where p_{f0} is the fluid pressure at reference density ρ_0^{fR} and recalling K_f^η is the isentropic bulk modulus of the fluid. The reference temperature, entropy per unit mass, and specific heat at constant volume per unit mass of the fluid are θ_0^f , η_0^f , and c_V^f . The datum entropy is arbitrary, so typically $\eta_0^f = 0$ for convenience. Applying Equation (3.104)_{3,4} allows us to derive the temperature-entropy and pressure-density constitutive relations as

$$\begin{aligned} p_f &= p_{f0} \left(\frac{\rho^{\text{fR}}}{\rho_0^{\text{fR}}} \right)^\Gamma \exp\left(\frac{\eta^f - \eta_0^f}{c_V^f} \right) \Rightarrow \rho^{\text{fR}} = \rho_0^{\text{fR}} \left(\frac{p_{f0}}{p_f} \right)^\Gamma \exp\left(\frac{\eta_0^f - \eta^f}{\Gamma c_V^f} \right), \\ \theta^f &= \theta_0^f \left(\frac{\rho^{\text{fR}}}{\rho_0^{\text{fR}}} \right)^{\Gamma-1} \exp\left(\frac{\eta^f - \eta_0^f}{c_V^f} \right). \end{aligned} \quad (3.143)$$

It is more convenient in the multiphase temperature scheme to work with a free energy formulation for the pore fluid; thus, the present objective is to determine the form of $\psi^f(\rho^{\text{fR}}, \theta^f)$. Insertion of Equation (3.141) into Equation (3.41) yields

$$\frac{\partial \psi^f}{\partial \rho^{\text{fR}}} = \frac{\theta^f \mathfrak{R}}{\rho^{\text{fR}}}. \quad (3.144)$$

Integration of the above gives

$$\begin{aligned} \psi^f &= \int \theta^f \mathfrak{R} \frac{1}{\rho^{\text{fR}}} d\rho^{\text{fR}} \\ &= \theta^f \mathfrak{R} \ln \frac{\rho^{\text{fR}}}{\rho_0^{\text{fR}}} + f_1(\theta^f). \end{aligned} \quad (3.145)$$

Taking the derivative with respect to pore fluid temperature θ^f ,

$$\frac{\partial \psi^f}{\partial \theta^f} = \mathfrak{R} \ln \frac{\rho^{\text{fR}}}{\rho_0^{\text{fR}}} + \frac{\partial(f_1(\theta^f))}{\partial \theta^f}. \quad (3.146)$$

Recall that

$$c_V^f := \frac{\partial e^f}{\partial \theta^f} \Rightarrow c_V^f = \frac{\partial(\psi^f + \theta^f \eta^f)}{\partial \theta^f}. \quad (3.147)$$

Utilization of Equation (3.34)₇ allows us to express the specific heat of the pore fluid at constant volume in terms of free energy and temperature *only*:

$$c_V^f = -\frac{\partial^2 \psi^f}{\partial(\theta^f)^2} \theta^f, \quad (3.148)$$

and thus

$$\begin{aligned} \frac{\partial \psi^f}{\partial \theta^f} &= -\int \frac{c_V^f}{\theta^f} d\theta^f \\ &= -c_V^f \ln \frac{\theta^f}{\theta_0^f} + f_2(\rho^{\text{fR}}). \end{aligned} \quad (3.149)$$

Comparing Equations (3.145) and (3.149) we may identify

$$\begin{aligned} \frac{\partial(f_1(\theta^f))}{\partial \theta^f} &= -c_V^f \ln \frac{\theta^f}{\theta_0^f}, \\ f_2(\rho^{\text{fR}}) &= \Re \ln \frac{\rho^{\text{fR}}}{\rho_0^{\text{fR}}}, \end{aligned} \quad (3.150)$$

such that after integrating Equation (3.150)₁

$$\psi^f := \theta^f \Re \ln \frac{\rho^{\text{fR}}}{\rho_0^{\text{fR}}} - c_V^f \theta^f \left(\ln \frac{\theta^f}{\theta_0^f} - 1 \right). \quad (3.151)$$

Applying Equation (3.34)₅ allows us to derive the temperature-entropy constitutive relation as

$$\eta^f = c_V^f \ln \frac{\theta^f}{\theta_0^f} - \Re \ln \frac{\rho^{\text{fR}}}{\rho_0^{\text{fR}}}. \quad (3.152)$$

Also, note that applying the D_t^f operation to Equation (3.141) produces Equation (2.20), making use of Equation (2.12)_{2,4}.

The compressible liquid model. In the case that the pore fluid is a liquid whose pressure $p_f(\rho^{\text{fR}}, \theta^f)$, we may use the pore fluid real mass density equation of state for water provided by Fernandez [1972],

$$\rho^{\text{fR}} = \rho_0^{\text{fR}} \exp \left[\frac{p_f - p_{f,0}}{K_f^\theta} - \alpha_V^f \theta^f \right], \quad (3.153)$$

recalling the isothermal bulk modulus K_f^θ and coefficient of volumetric thermal expansion α_V^f , both of which are taken to be constant. Then, the following form for the Helmholtz free energy must be

assumed, recalling also Equation (3.148):

$$\psi^f(\rho^{\text{fR}}, \theta^f) = -\frac{1}{\rho^{\text{fR}}} \left[K_f^\theta \ln \left(\frac{\rho^{\text{fR}}}{\rho_0^{\text{fR}}} \right) + K_f^\theta \alpha_V^f \theta^f + K_f^\theta + p_{f0} \right] - c_V^f \left[\theta^f \left(\ln \left[\frac{\theta^f}{\theta_0^f} \right] - 1 \right) + \theta_0^f \right] \quad (3.154)$$

Applying Equation (3.34)_{5,7} to Equation (3.154) allows us to derive the temperature-entropy and pressure-density relations as

$$\begin{aligned} \eta^f &= c_V^f \ln \left(\frac{\theta^f}{\theta_0^f} \right) + \frac{K_f^\theta \alpha_V^f}{\rho^{\text{fR}}}, \\ p_f &= K_f^\theta \left[\ln \left(\frac{\rho^{\text{fR}}}{\rho_0^{\text{fR}}} \right) + \alpha_V^f \theta^f \right] + p_{f0} \end{aligned} \quad (3.155)$$

Applying the D_t^f operation to Equation (3.155)₂ produces Equation (2.20) using the definition of α_V^f :

$$\alpha_V^f := \frac{\gamma^f c_V^f \rho^{\text{fR}}}{K_f^\theta}. \quad (3.156)$$

Chapter 4

Numerical Implementation

This chapter presents (1) a recapitulation of the strong forms of the governing equations, (2) the derivations of the variational equations for (a) balance of linear momentum of a single-phase material, (b) balance of linear momentum and balance of energy for a single-phase material, (c) balance of mass and balance of linear momentum for a biphasic mixture, (d) balance of mass and balance of linear momentum for a biphasic mixture and balance of linear momentum for a pore fluid within the biphasic mixture, (e) balance of mass and balance of linear momentum for a biphasic mixture and balance of energies of said constituents within that biphasic mixture, (f) balance of mass and balance of linear momentum for a biphasic mixture and balance of linear momentum for a pore fluid within the biphasic mixture and balance of energies of said constituents within that biphasic mixture, all at large deformations, and (3) the finite element (FE) implementation of the variational forms for various time integration schemes and any relevant stabilization parameters.

In this chapter, a total Lagrangian implementation is assumed, such that constituents move relative to the solid skeleton, that is, the reference configuration follows the motion of the solid skeleton (see Chapter 2 for details). For this reason, we choose to drop $(\cdot)^s$ and $(\cdot)_s$ designations for notational simplicity for operations, variables, and some parameters (where it makes sense to do so) associated with the solid phase and solid skeleton.

4.1 Strong and variational forms of the governing equations

4.1.1 (\mathbf{u}) formulation

The strong formulation for elasticity (i.e., neglecting the inertia term in the single-phase momentum balance) and elastodynamics (i.e., retaining the inertia term in the single-phase momentum balance) has the solution space

$$\mathcal{S}^u = (\mathbf{u} : \mathcal{B}_0 \times [0, T] \rightarrow \mathbb{R}^3, \mathbf{u} \in H^1, \mathbf{u}(t) = \mathbf{g}^u(t) \text{ on } \Gamma_0^u, \mathbf{u}(\mathbf{X}, t = 0) = \mathbf{u}_0(\mathbf{X})), \quad (4.1)$$

where \mathbf{g}^u is the prescribed displacement on Γ_0^u , either directly or via integration of a prescribed velocity.

The corresponding strong formulation for elasticity is thus:

$$(\mathcal{S}) = \left\{ \begin{array}{l} \text{Find } \mathbf{u}(\mathbf{X}, t) \in \mathcal{S}^u, \text{ with } t \in [0, T], \text{ such that:} \\ \\ \text{DIV } \mathbf{P} + \rho_0 \mathbf{g} = \mathbf{0} \in \mathcal{B}_0, \\ \\ \mathbf{u}(\mathbf{X}, t) = \mathbf{g}^u(\mathbf{X}, t) \text{ on } \Gamma_0^u, \\ \\ \mathbf{P}(\mathbf{X}, t) \cdot \mathbf{N}(\mathbf{X}) = \mathbf{t}^\sigma(\mathbf{X}, t) \text{ on } \Gamma_0^t, \\ \\ \mathbf{u}(\mathbf{X}, t = 0) = \mathbf{u}_0(\mathbf{X}) \in \mathcal{B}_0, \\ \\ \mathbf{v}(\mathbf{X}, t = 0) = \mathbf{v}_0(\mathbf{X}) \in \mathcal{B}_0, \end{array} \right. \quad (4.2)$$

where \mathbf{t}^σ is the prescribed traction *load* on Γ_0^t .

For elastodynamics, inertial forces are considered, such that Equation (4.2) is written as

$$(\mathcal{S}) = \left\{ \begin{array}{l} \text{Find } \mathbf{u}(\mathbf{X}, t) \in \mathcal{S}^u, \text{ with } t \in [0, T], \text{ such that:} \\ \\ \text{DIV } \mathbf{P} + \rho_0 \mathbf{g} - \rho_0 \mathbf{a} = \mathbf{0} \in \mathcal{B}_0, \\ \\ \mathbf{u}(\mathbf{X}, t) = \mathbf{g}^u(\mathbf{X}, t) \text{ on } \Gamma_0^u, \\ \\ \mathbf{P}(\mathbf{X}, t) \cdot \mathbf{N}(\mathbf{X}) = \mathbf{t}^\sigma(\mathbf{X}, t) \text{ on } \Gamma_0^t, \\ \\ \mathbf{u}(\mathbf{X}, t = 0) = \mathbf{u}_0(\mathbf{X}) \in \mathcal{B}_0, \\ \\ \mathbf{v}(\mathbf{X}, t = 0) = \mathbf{v}_0(\mathbf{X}) \in \mathcal{B}_0, \\ \\ \mathbf{a}(\mathbf{X}, t = 0) = \mathbf{a}_0(\mathbf{X}) \in \mathcal{B}_0. \end{array} \right. \quad (4.3)$$

To solve Equations (4.2) & Equation (4.3), we employ the variational form with the variational (weighting) space

$$\mathcal{V}^u = (\mathbf{w}^u : \mathcal{B}_0 \rightarrow \mathbb{R}^3, \mathbf{w}^u \in H^1, \mathbf{w}^u(t) = \mathbf{0} \forall \mathbf{X} \in \Gamma_0^u). \quad (4.4)$$

Let $\mathcal{G}(u_i, w_i^u)$ be the variational form of Equation (4.2) such that

$$\mathcal{G} : \mathcal{S}^u \times \mathcal{V}^u \rightarrow \mathbb{R}. \quad (4.5)$$

We may then rewrite Equation (4.2) as

$$\mathcal{G}(u_i, w_i^u) = \int_{\mathcal{B}_0} w_i^u \frac{\partial P_{iI}}{\partial X_I} dV + \int_{\mathcal{B}_0} w_i^u \rho_0 g_i dV = 0. \quad (4.6)$$

The first term in Equation (4.6) can be rewritten as follows:

$$\int_{\mathcal{B}_0} w_i^u \frac{\partial P_{iI}}{\partial X_I} dV = \int_{\mathcal{B}_0} \frac{\partial (w_i^u P_{iI})}{\partial X_I} dV - \int_{\mathcal{B}_0} \frac{\partial w_i^u}{\partial X_I} P_{iI} dV. \quad (4.7)$$

Substitution of Equation (4.7) into Equation (4.6) gives us

$$\mathcal{G}(u_i, w_i^u) = \int_{\mathcal{B}_0} \frac{\partial (w_i^u P_{iI})}{\partial X_I} dV - \int_{\mathcal{B}_0} \frac{\partial w_i^u}{\partial X_I} P_{iI} dV + \int_{\mathcal{B}_0} w_i^u \rho_0 g_i dV = 0. \quad (4.8)$$

Applying divergence theorem to the first term in Equation (4.8) and using the boundary conditions in Equations (4.2)₂ & Equation (4.2)₃, the variational form for the balance of linear momentum under quasi-static conditions becomes:

$$\mathcal{G}(u_i, w_i^u) = \int_{\mathcal{B}_0} \frac{\partial w_i^u}{\partial X_I} P_{iI} dV - \int_{\mathcal{B}_0} w_i^u \rho_0 g_i dV - \int_{\Gamma_0^t} w_i^u t_i^\sigma dA = 0. \quad (4.9)$$

This may be formally written as:

$$\mathcal{W} = \left\{ \begin{array}{l} \text{Find } u_i(X_I, t) \in \mathcal{S}^u, \text{ with } t \in [0, T], \text{ such that:} \\ \int_{\mathcal{B}_0} \frac{\partial w_i^u}{\partial X_I} P_{iI} dV - \int_{\mathcal{B}_0} w_i^u \rho_0 g_i dV - \int_{\Gamma_0^t} w_i^u t_i^\sigma dA = 0 \\ \text{holds } \forall w_i^u \in \mathcal{V}^u, \text{ with} \\ \mathcal{S}^u = (u_i : \mathcal{B}_0 \times [0, T] \rightarrow \mathbb{R}^3, u_i \in H^1, u_i(t) = g_i^u(t) \text{ on } \Gamma_0^u, \\ u_i(X_I, t = 0) = u_{i,0}(X_I), \\ \mathcal{V}^u = (w_i^u : \mathcal{B}_0 \rightarrow \mathbb{R}^3, w_i^u \in H^1, w_i^u(t) = 0 \text{ on } \Gamma_0^u). \end{array} \right. \quad (4.10)$$

Considering now inertia terms (elastodynamics), let $\mathcal{G}(u_i, w_i^u)$ be the variational form of Equation (4.3) such that

$$\mathcal{G} : \mathcal{S}^u \times \mathcal{V}^u \rightarrow \mathbb{R}. \quad (4.11)$$

We may then rewrite Equation (4.3) as

$$\mathcal{G}(u_i, w_i^u) = \int_{\mathcal{B}_0} w_i^u \frac{\partial P_{iI}}{\partial X_I} dV + \int_{\mathcal{B}_0} w_i^u \rho_0 g_i dV - \int_{\mathcal{B}_0} w_i^u \rho_0 a_i dV = 0. \quad (4.12)$$

Weakening of the first Piola-Kirchhoff stress, application of divergence theorem and boundary conditions then follows, such that the variational form for the balance of linear momentum with inertia terms becomes

$$\mathcal{G}(u_i, w_i^u) = \int_{\mathcal{B}_0} w_i^u \rho_0 a_i dV + \int_{\mathcal{B}_0} \frac{\partial w_i^u}{\partial X_I} P_{iI} dV - \int_{\mathcal{B}_0} w_i^u \rho_0 g_i dV - \int_{\Gamma_0^t} w_i^u t_i^\sigma dA = 0. \quad (4.13)$$

Though not written here, when the solid skeleton acceleration is considered, we often employ the canonical shock viscosity, Q , defined in Section 4.4.1. This in turn affects the form of the first Piola-Kirchhoff stress, and, technically speaking, introduces an additional term in the explicit formulation of the Neumann boundary condition. However, since the Neumann boundary condition is a consideration of the *total* traction acting on the boundary Γ_0^t , inclusion, or exclusion, of the shock viscosity term does not affect total traction. For brevity, the shock viscosity will not be included in the balance of linear momentum in other sections. However, since it is a dissipative mechanism, it is considered when deriving the single-phase energy balance and solid phase energy balance, as shown in Sections 4.1.2 and 4.1.5, respectively.

Equation (4.13) may be formally written as:

$$\mathcal{W} = \left\{ \begin{array}{l} \text{Find } u_i(X_I, t) \in \mathcal{S}^u, \text{ with } t \in [0, T], \text{ such that:} \\ \int_{\mathcal{B}_0} w_i^u \rho_0 a_i dV + \int_{\mathcal{B}_0} \frac{\partial w_i^u}{\partial X_I} P_{iI} dV - \int_{\mathcal{B}_0} w_i^u \rho_0 g_i dV - \int_{\Gamma_0^t} w_i^u t_i^\sigma dA = 0 \\ \text{holds } \forall w_i^u \in \mathcal{V}^u, \text{ with} \\ \mathcal{S}^u = (u_i : \mathcal{B}_0 \times [0, T] \rightarrow \mathbb{R}^3, u_i \in H^1, u_i(t) = g_i^u(t) \text{ on } \Gamma_0^u, \\ \quad u_i(X_I, t = 0) = u_{i,0}(X_I)), \\ \mathcal{V}^u = (w_i^u : \mathcal{B}_0 \rightarrow \mathbb{R}^3, w_i^u \in H^1, w_i^u(t) = 0 \text{ on } \Gamma_0^u). \end{array} \right. \quad (4.14)$$

In the FE implementation that follows, it behooves us to simplify the variational forms, such that for elasticity

$$\mathcal{G} = \mathcal{G}_2^{\text{INT}} + \mathcal{G}_4^{\text{INT}} + \mathcal{G}_1^{\text{EXT}} = 0, \quad (4.15)$$

and for elastodynamics

$$\mathcal{G} = \mathcal{G}_1^{\text{INT}} + \mathcal{G}_2^{\text{INT}} + \mathcal{G}_4^{\text{INT}} + \mathcal{G}_1^{\text{EXT}} = 0, \quad (4.16)$$

wherein

$$\begin{aligned}
\mathcal{G}_1^{\text{INT}} &= \int_{\mathcal{B}_0} w_i^u \rho_0 a_i dV, \\
\mathcal{G}_2^{\text{INT}} &= \int_{\mathcal{B}_0} \frac{\partial w_i^u}{\partial X_I} P_{iI} dV, \\
\mathcal{G}_4^{\text{INT}} &= - \int_{\mathcal{B}_0} w_i^u \rho_0 g_i dV, \\
\mathcal{G}_1^{\text{EXT}} &= \int_{\Gamma_0^t} w_i^u t_i^\sigma dA.
\end{aligned} \tag{4.17}$$

In the case of 1-D uniaxial strain, i.e., the underlying assumption for the proceeding FE model, the above terms simplify to the following:

$$\begin{aligned}
\mathcal{G}_1^{\text{INT}} &= \int_0^{X=H} w^u \rho_0 a A dX, \\
\mathcal{G}_2^{\text{INT}} &= \int_0^{X=H} \frac{\partial w^u}{\partial X} P_{11} A dX, \\
\mathcal{G}_4^{\text{INT}} &= \int_0^{X=H} w^u \rho_0 g A dX, \\
\mathcal{G}_1^{\text{EXT}} &= \int_{\Gamma_0^t} w^u t^\sigma dA = t^\sigma A.
\end{aligned} \tag{4.18}$$

4.1.2 (\mathbf{u} - θ) formulation

The energy balance for a single-phase thermoelastic material is written as

$$\rho D_t e = \boldsymbol{\sigma} : \mathbf{l} - \text{div } \mathbf{q} + \rho r. \tag{4.19}$$

Substitution of the Helmholtz free energy term ψ into e and neglection of the heat source r yields

$$\rho(D_t \psi + \eta D_t \theta + \theta D_t \eta) = \boldsymbol{\sigma} : \mathbf{l} - \text{div } \mathbf{q}. \tag{4.20}$$

Simultaneous mapping of Equation (4.20) to the reference configuration and expansion of the material time derivative on the Helmholtz free energy term allows us to rewrite Equation (4.20) as

$$\frac{\partial(\rho_0 \psi)}{\partial \theta} D_t \theta + \frac{\partial(\rho_0 \psi)}{\partial \mathbf{C}} : D_t \mathbf{C} + \rho_0 \eta D_t \theta + \rho_0 \theta D_t \eta = \frac{1}{2} \mathbf{S} : D_t \mathbf{C} - Q D_t J - J \text{GRAD } \mathbf{q} : \mathbf{F}^{-T}, \tag{4.21}$$

where Q is the shock viscosity (refer to Section 4.4.1 for details).

Recalling Equation (3.88)_{1,3} allows us to write Equation (4.21) as

$$\rho_0 \theta D_t \eta + Q D_t J + J \text{GRAD}(\mathbf{q}) : \mathbf{F}^{-T} = 0. \quad (4.22)$$

For a thermoelastic material, or an ideal gas, it may be shown that (refer to Section 3.3.1, Davison [2008], respectively)

$$\eta = c_V \ln \frac{\theta}{\theta_0} + \frac{1}{\rho_0} K \alpha_V \ln J, \quad (4.23)$$

such that

$$D_t \eta = \frac{c_V}{\theta} D_t \theta + \frac{1}{J \rho_0} K \alpha_V D_t J. \quad (4.24)$$

Thus, we may write Equation (4.22) as

$$\rho_0 c_V D_t \theta + \left(\frac{K \alpha_V \theta}{J} + Q \right) D_t J + J \text{GRAD}(\mathbf{q}) : \mathbf{F}^{-T} = 0. \quad (4.25)$$

The strong formulation for thermoelastodynamics has the solution space

$$\begin{aligned} \mathcal{S}^u &= (\mathbf{u} : \mathcal{B}_0 \times [0, T] \rightarrow \mathbb{R}^3, \mathbf{u} \in H^1, \mathbf{u}(t) = \mathbf{g}^u(t) \text{ on } \Gamma_0^u, \mathbf{u}(\mathbf{X}, t = 0) = \mathbf{u}_0(\mathbf{X})), \\ \mathcal{S}^\theta &= (\theta : \mathcal{B}_0 \times [0, T] \rightarrow \mathbb{R}, \theta \in H^1, \theta(t) = g^\theta(t) \text{ on } \Gamma_0^\theta, \theta(\mathbf{X}, t = 0) = \theta_0(\mathbf{X})), \end{aligned} \quad (4.26)$$

where g^θ is the prescribed temperature on Γ_0^θ .

The corresponding strong formulation for thermoelastodynamics is thus:

$$\begin{aligned}
 (\mathcal{S}) = \left\{ \begin{array}{l}
 \text{Find } \mathbf{u}(\mathbf{X}, t) \in \mathcal{S}^u \text{ and } \theta(\mathbf{X}, t) \in \mathcal{S}^\theta, \\
 \\
 \text{with } t \in [0, T], \text{ such that:} \\
 \\
 \text{DIV } \mathbf{P} + \rho_0 \mathbf{g} - \rho_0 \mathbf{a} = \mathbf{0} \in \mathcal{B}_0, \\
 \\
 \mathbf{u}(\mathbf{X}, t) = \mathbf{g}^u(\mathbf{X}, t) \text{ on } \Gamma_0^u, \\
 \\
 \mathbf{P}(\mathbf{X}, t) \cdot \mathbf{N}(\mathbf{X}) = \mathbf{t}^\sigma(\mathbf{X}, t) \text{ on } \Gamma_0^t, \\
 \\
 \mathbf{u}(\mathbf{X}, t = 0) = \mathbf{u}_0(\mathbf{X}) \in \mathcal{B}_0, \\
 \\
 \mathbf{v}(\mathbf{X}, t = 0) = \mathbf{v}_0(\mathbf{X}) \in \mathcal{B}_0, \\
 \\
 \mathbf{a}(\mathbf{X}, t = 0) = \mathbf{a}_0(\mathbf{X}) \in \mathcal{B}_0, \\
 \\
 \rho_0 c_V D_t \theta + \left(\frac{K \alpha_V \theta}{J} + Q \right) D_t J + J \text{GRAD}(\mathbf{q}) \cdot \mathbf{F}^{-T} = 0 \in \mathcal{B}_0, \\
 \\
 \theta(\mathbf{X}, t) = g^\theta \text{ on } \Gamma_0^\theta, \\
 \\
 -(J \mathbf{F}^{-1} \cdot \mathbf{q}) \cdot \mathbf{N} = Q^\theta(\mathbf{X}, t) \text{ on } \Gamma_0^{Q^\theta}, \\
 \\
 \theta(\mathbf{X}, t = 0) = \theta_0(\mathbf{X}) \in \mathcal{B}_0, \\
 \\
 \dot{\theta}(\mathbf{X}, t = 0) = \dot{\theta}_0(\mathbf{X}) \in \mathcal{B}_0.
 \end{array} \right. \quad (4.27)
 \end{aligned}$$

Let $\mathcal{G}(u_i, \theta, w_i^u)$ be the variational form of Equation (4.27)₁₋₆, such that

$$\mathcal{G} : \mathcal{S}^u \times \mathcal{S}^\theta \times \mathcal{V}^u \rightarrow \mathbb{R}. \quad (4.28)$$

We may then rewrite Equation (4.27)₁₋₆ as

$$\mathcal{G}(u_i, \theta, w_i^u) = \int_{\mathcal{B}_0} w_i^u \frac{\partial P_{iI}}{\partial X_I} dV + \int_{\mathcal{B}_0} w_i^u \rho_0 g_i dV - \int_{\mathcal{B}_0} w_i^u \rho_0 a_i dV = 0. \quad (4.29)$$

Weakening of the first Piola-Kirchhoff stress, application of divergence theorem and boundary conditions then follows, such that the variational form for the balance of linear momentum with inertia terms becomes

$$\mathcal{G}(u_i, \theta, w_i^u) = \int_{\mathcal{B}_0} w_i^u \rho_0 a_i dV + \int_{\mathcal{B}_0} \frac{\partial w_i^u}{\partial X_I} P_{iI} dV - \int_{\mathcal{B}_0} w_i^u \rho_0 g_i dV - \int_{\Gamma_0^t} w_i^u t_i^\sigma dA = 0, \quad (4.30)$$

where $P_{iI} = P_{iI}(J(u), \theta)$.

Let $\mathcal{J}(u_i, \theta, w^\theta)$ be the variational form of Equation (4.27)₇₋₁₂, such that

$$\mathcal{J} : \mathcal{S}^\theta \times \mathcal{S}^u \times \mathcal{V}^\theta \rightarrow \mathbb{R}. \quad (4.31)$$

We may then rewrite Equation (4.27)₇₋₁₂ as

$$\mathcal{J}(u_i, \theta, w^\theta) = \int_{\mathcal{B}_0} w^\theta \rho_0 c_V D_t \theta \, dV + \int_{\mathcal{B}_0} w^\theta \left(\frac{K \alpha_V \theta}{J} + Q \right) D_t J \, dV + \int_{\mathcal{B}_0} w^\theta J \frac{\partial q_i}{\partial X_I} F_{Ii}^1 \, dV = 0. \quad (4.32)$$

Recall Fourier's law:

$$q_i = -k \frac{\partial \theta}{\partial x_i}. \quad (4.33)$$

The final term in Equation (4.32) may be weakened using chain rule as follows:

$$\int_{\mathcal{B}_0} \frac{\partial(w^\theta J q_i F_{Ii}^{-1})}{\partial X_I} \, dV = \int_{\mathcal{B}_0} \frac{\partial w^\theta}{\partial X_I} J q_i F_{Ii}^{-1} \, dV + \int_{\mathcal{B}_0} w^\theta J \frac{\partial q_i}{\partial X_I} F_{Ii}^{-1} \, dV + \int_{\mathcal{B}_0} w^\theta q_i \frac{\partial(J F_{Ii}^{-1})}{\partial X_I} \, dV, \quad (4.34)$$

wherein the last term in Equation (4.34) goes to zero via the Piola identity. Thus, using divergence theorem and Equations (4.27)_{8,9} allows us to rewrite Equation (4.32) as

$$\begin{aligned} \mathcal{J}(u_i, \theta, w^\theta) &= \int_{\mathcal{B}_0} w^\theta \rho_0 c_V D_t \theta \, dV + \int_{\mathcal{B}_0} w^\theta \left(\frac{K \alpha_V \theta}{J} + Q \right) D_t J \, dV - \int_{\mathcal{B}_0} \frac{\partial w^\theta}{\partial X_I} J q_i F_{Ii}^1 \, dV \\ &\quad - \int_{\Gamma_0^{Q^\theta}} w^\theta Q^\theta \, dA = 0. \end{aligned} \quad (4.35)$$

Thus, the formal statement for the variational forms \mathcal{G} and \mathcal{J} may be written as follows:

$$\mathcal{W} = \left\{ \begin{array}{l} \text{Find } u_i(X_I, t) \in \mathcal{S}^u \text{ and } \theta(X_I, t) \in \mathcal{S}^\theta, \text{ with } t \in [0, T], \text{ such that:} \\ \int_{\mathcal{B}_0} w_i^u \rho_0 a_i dV + \int_{\mathcal{B}_0} \frac{\partial w_i^u}{\partial X_I} P_{iI} dV - \int_{\mathcal{B}_0} w_i^u \rho_0 g_i dV - \int_{\Gamma_0^t} w_i^u t_i^\sigma dA = 0, \\ \int_{\mathcal{B}_0} w^\theta \rho_0 c_V D_t \theta dV + \int_{\mathcal{B}_0} w^\theta \left(\frac{K \alpha_V \theta}{J} + Q \right) D_t J dV - \int_{\mathcal{B}_0} \frac{\partial w^\theta}{\partial X_I} J q_i F_{Ii}^1 dV \\ - \int_{\Gamma_0^{Q^\theta}} w^\theta Q^\theta dA = 0 \\ \text{holds } \forall w_i^u \in \mathcal{V}^u \text{ and } \forall w^\theta \in \mathcal{V}^\theta, \text{ with} \\ \mathcal{S}^u = (u_i : \mathcal{B}_0 \times [0, T] \rightarrow \mathbb{R}^3, u_i \in H^1, u_i(t) = g_i^u(t) \text{ on } \Gamma_0^u, \\ u_i(X_I, t = 0) = u_{i,0}(X_I)), \\ \mathcal{S}^\theta = (\theta : \mathcal{B}_0 \times [0, T] \rightarrow \mathbb{R}, \theta \in H^1, \theta(t) = g^\theta(t) \text{ on } \Gamma_0^\theta, \theta(X_I, t = 0) = \theta_0(X_I)), \\ \mathcal{V}^u = (w_i^u : \mathcal{B}_0 \rightarrow \mathbb{R}^3, w_i^u \in H^1, w_i^u(t) = 0 \text{ on } \Gamma_0^u), \\ \mathcal{V}^\theta = (w^\theta : \mathcal{B}_0 \rightarrow \mathbb{R}, w^\theta \in H^1, w^\theta(t) = 0 \text{ on } \Gamma_0^\theta). \end{array} \right. \quad (4.36)$$

In the FE implementation that follows, it behooves us to simplify the variational forms such that

$$\begin{aligned} \mathcal{G} &= \mathcal{G}_1^{\text{INT}} + \mathcal{G}_2^{\text{INT}} + \mathcal{G}_4^{\text{INT}} + \mathcal{G}_1^{\text{EXT}} = 0, \\ \mathcal{J} &= \mathcal{J}_1^{\text{INT}} + \mathcal{J}_2^{\text{INT}} + \mathcal{J}_3^{\text{INT}} + \mathcal{J}^{\text{EXT}} = 0, \end{aligned} \quad (4.37)$$

wherein

$$\begin{aligned} \mathcal{G}_1^{\text{INT}} &= \int_{\mathcal{B}_0} w_i^u \rho_0 a_i dV, \\ \mathcal{G}_2^{\text{INT}} &= \int_{\mathcal{B}_0} \frac{\partial w_i^u}{\partial X_I} P_{iI} dV, \\ \mathcal{G}_4^{\text{INT}} &= - \int_{\mathcal{B}_0} w_i^u \rho_0 g_i dV, \\ \mathcal{G}_1^{\text{EXT}} &= \int_{\Gamma_0^t} w_i^u t_i^\sigma dA, \end{aligned} \quad (4.38)$$

and

$$\begin{aligned}
\mathcal{J}_1^{\text{INT}} &= \int_{\mathcal{B}_0} w^\theta \rho_0 c_V D_t \theta dV, \\
\mathcal{J}_2^{\text{INT}} &= \int_{\mathcal{B}_0} w^\theta \left(\frac{K \alpha_V \theta}{J} + Q \right) D_t J dV, \\
\mathcal{J}_3^{\text{INT}} &= - \int_{\mathcal{B}_0} \frac{\partial w^\theta}{\partial X_I} J q_i F_{Ii}^{-1} dV, \\
\mathcal{J}^{\text{EXT}} &= - \int_{\Gamma_0^{Q^\theta}} w^\theta Q^\theta dA.
\end{aligned} \tag{4.39}$$

In the case of 1-D uniaxial strain, i.e., the underlying assumption for the proceeding FE model, the above terms simplify to the following:

$$\begin{aligned}
\mathcal{G}_1^{\text{INT}} &= \int_0^{X=H} w^u \rho_0 a A dX, \\
\mathcal{G}_2^{\text{INT}} &= \int_0^{X=H} \frac{\partial w^u}{\partial X} P_{11} A dX, \\
\mathcal{G}_4^{\text{INT}} &= \int_0^{X=H} w^u \rho_0 g A dX, \\
\mathcal{G}_1^{\text{EXT}} &= \int_{\Gamma_0^t} w^u t^\sigma dA = t^\sigma A,
\end{aligned} \tag{4.40}$$

and

$$\begin{aligned}
\mathcal{J}_1^{\text{INT}} &= \int_0^{X=H} w^\theta \rho_0 c_V D_t \theta A dX, \\
\mathcal{J}_2^{\text{INT}} &= \int_0^{X=H} w^\theta \left(\frac{K \alpha_V \theta}{J} + Q \right) D_t J A dX, \\
\mathcal{J}_3^{\text{INT}} &= - \int_0^{X=H} \frac{\partial w^\theta}{\partial X} q A dX, \\
\mathcal{J}^{\text{EXT}} &= - \int_{\Gamma_0^Q} w^\theta Q^\theta dA = Q^\theta A.
\end{aligned} \tag{4.41}$$

4.1.3 (\mathbf{u} - p_f) formulation

Herein, barotropic constituents are assumed, i.e., $\rho^{\text{sR}} = \text{const.}$ (from the mechanically incompressible solid assumption) and $\rho^{\text{fR}} = \rho^{\text{fR}}(p_f)$. Locally homogeneous temperatures are also assumed, i.e., $\theta^{\text{s}} = \theta^{\text{f}} = \theta$. The strong formulation for poroelasticity (i.e., neglecting the inertia terms in the multiphase linear momentum balance and mass balance) and poroelastodynamics (i.e., retaining the inertia terms in the multiphase momentum balance and mass balance) with the assumption $\mathbf{a}_f = \mathbf{a}_s = \mathbf{a}$ has the solution space

$$\begin{aligned} \mathcal{S}^u &= (\mathbf{u} : \mathcal{B}_0 \times [0, T] \rightarrow \mathbb{R}^3, \mathbf{u} \in H^1, \mathbf{u}(t) = \mathbf{g}^u(t) \text{ on } \Gamma_0^u, \mathbf{u}(\mathbf{X}, t = 0) = \mathbf{u}_0(\mathbf{X})), \\ \mathcal{S}^{p_f} &= (p_f : \mathcal{B}_0 \times [0, T] \rightarrow \mathbb{R}, p_f \in H^1, p_f(t) = g^p(t) \text{ on } \Gamma_0^p, p_f(\mathbf{X}, t = 0) = p_{f,0}(\mathbf{X})), \end{aligned} \quad (4.42)$$

where g^p is the prescribed pore fluid pressure on Γ_0^p (typically set for the “drained” boundary condition).

The corresponding strong formulation for poroelasticity is thus:

$$(\mathcal{S}) = \left\{ \begin{array}{l} \text{Find } \mathbf{u}(\mathbf{X}, t) \in \mathcal{S}^u \text{ and } p_f(\mathbf{X}, t) \in \mathcal{S}^{p_f}, \\ \\ \text{with } t \in [0, T], \text{ such that:} \\ \\ \text{DIV } \mathbf{P} + \rho_0 \mathbf{g} = \mathbf{0} \in \mathcal{B}_0, \\ \\ \mathbf{u}(\mathbf{X}, t) = \mathbf{g}^u(\mathbf{X}, t) \text{ on } \Gamma_0^u, \\ \\ \mathbf{P}(\mathbf{X}, t) \cdot \mathbf{N}(\mathbf{X}) = \mathbf{t}^\sigma(\mathbf{X}, t) \text{ on } \Gamma_0^t, \\ \\ \mathbf{u}(\mathbf{X}, t = 0) = \mathbf{u}_0(\mathbf{X}) \in \mathcal{B}_0, \\ \\ \mathbf{v}(\mathbf{X}, t = 0) = \mathbf{v}_0(\mathbf{X}) \in \mathcal{B}_0, \\ \\ \frac{J n^f}{K_f^\eta} D_t p_f + D_t J + \frac{J}{K_f^\eta} \text{GRAD}(p_f) \cdot \mathbf{F}^{-1} \cdot (n^f \tilde{\mathbf{v}}_f) \\ \\ + J \text{GRAD}(n^f \tilde{\mathbf{v}}_f) \cdot \mathbf{F}^{-T} = 0 \in \mathcal{B}_0, \\ \\ p_f(\mathbf{X}, t) = g^p(\mathbf{X}, t) \text{ on } \Gamma_0^p, \\ \\ -[J \mathbf{F}^{-1} \cdot (n^f \tilde{\mathbf{v}}_f)] \cdot \mathbf{N} = Q_f(\mathbf{X}, t) \text{ on } \Gamma_0^{Q_f}, \\ \\ p_f(\mathbf{X}, t = 0) = p_{f,0}(\mathbf{X}) \in \mathcal{B}_0, \\ \\ \dot{p}_f(\mathbf{X}, t = 0) = \dot{p}_{f,0}(\mathbf{X}) \in \mathcal{B}_0, \end{array} \right. \quad (4.43)$$

where Q_f is the prescribed fluid flux (positive inward) on $\Gamma_0^{Q_f}$, where we have assumed that the mass supply of the pore fluid (f) constituent is negligible.

For poroelastodynamics, inertial forces are considered, such that Equation (4.43) is written

as

$$(\mathcal{S}) = \left\{ \begin{array}{l} \text{Find } \mathbf{u}(\mathbf{X}, t) \in \mathcal{S}^u \text{ and } p_f(\mathbf{X}, t) \in \mathcal{S}^{p_f}, \\ \text{with } t \in [0, T], \text{ such that:} \\ \text{DIV } \mathbf{P} + \rho_0 \mathbf{g} - \rho_0 \mathbf{a} = \mathbf{0} \in \mathcal{B}_0, \\ \mathbf{u}(\mathbf{X}, t) = \mathbf{g}^u(\mathbf{X}, t) \text{ on } \Gamma_0^u, \\ \mathbf{P}(\mathbf{X}, t) \cdot \mathbf{N}(\mathbf{X}) = \mathbf{t}^\sigma(\mathbf{X}, t) \text{ on } \Gamma_0^t, \\ \mathbf{u}(\mathbf{X}, t = 0) = \mathbf{u}_0(\mathbf{X}) \in \mathcal{B}_0, \\ \mathbf{v}(\mathbf{X}, t = 0) = \mathbf{v}_0(\mathbf{X}) \in \mathcal{B}_0, \\ \mathbf{a}(\mathbf{X}, t = 0) = \mathbf{a}_0(\mathbf{X}) \in \mathcal{B}_0, \\ \frac{J n^f}{K_f^\eta} D_t p_f + D_t J + \frac{J}{K_f^\eta} \text{GRAD}(p_f) \cdot \mathbf{F}^{-1} \cdot (n^f \tilde{\mathbf{v}}_f) \\ + J \text{GRAD}(n^f \tilde{\mathbf{v}}_f) \cdot \mathbf{F}^{-T} = 0 \in \mathcal{B}_0, \\ p_f(\mathbf{X}, t) = g^p(\mathbf{X}, t) \text{ on } \Gamma_0^p, \\ -[J \mathbf{F}^{-1} \cdot (n^f \tilde{\mathbf{v}}_f)] \cdot \mathbf{N} = Q_f(\mathbf{X}, t) \text{ on } \Gamma_0^{Q_f}, \\ p_f(\mathbf{X}, t = 0) = p_{f,0}(\mathbf{X}) \in \mathcal{B}_0, \\ \dot{p}_f(\mathbf{X}, t = 0) = \dot{p}_{f,0}(\mathbf{X}) \in \mathcal{B}_0. \end{array} \right. \quad (4.44)$$

To solve Equations (4.43) & Equation (4.44), we employ the variational form with the variational (weighting) spaces

$$\begin{aligned} \mathcal{V}^u &= (\mathbf{w}^u : \mathcal{B}_0 \rightarrow \mathbb{R}^3, \mathbf{w}^u \in H^1, \mathbf{w}^u(t) = \mathbf{0} \text{ on } \Gamma_0^u), \\ \mathcal{V}^{p_f} &= (w^{p_f} : \mathcal{B}_0 \rightarrow \mathbb{R}, w^{p_f} \in H^1, w^{p_f}(t) = 0 \text{ on } \Gamma_0^p). \end{aligned} \quad (4.45)$$

Let $\mathcal{G}(u_i, p_f, w_i^u)$ be the variational form of Equations (4.43)₁₋₅ such that

$$\mathcal{G} : \mathcal{S}^u \times \mathcal{S}^{p_f} \times \mathcal{V}^u \rightarrow \mathbb{R}. \quad (4.46)$$

We may then rewrite Equations (4.43)_{1–5} as

$$\mathcal{G}(u_i, p_f, w_i^u) = \int_{\mathcal{B}_0} w_i^u \frac{\partial P_{iI}}{\partial X_I} dV + \int_{\mathcal{B}_0} w_i^u \rho_0 g_i dV = 0. \quad (4.47)$$

As before, weakening of the first Piola-Kirchhoff stress is made possible via chain rule, where use has been made of the Piola identity (as shown in Holzapfel [2000] p. 146) on the pore fluid pressure term, such that the resulting terms allow us to write Equation (4.47) as

$$\begin{aligned} \mathcal{G}(u_i, p_f, w_i^u) &= \int_{\mathcal{B}_0} \frac{\partial w_i^u}{\partial X_I} P_{iI(E)}^s dV - \int_{\mathcal{B}_0} \frac{\partial w_i^u}{\partial X_I} J p_f F_{Ii}^{-1} dV - \int_{\mathcal{B}_0} w_i^u \rho_0 g_i dV \\ &\quad - \left(\int_{\Gamma_0^t} w_i^u t_i^{\sigma_E^s} dA - \int_{\Gamma_0^t} w_i^u p_f J F_{Ii}^{-1} N_I dA \right) = 0, \end{aligned} \quad (4.48)$$

wherein use has been made of Equation (2.32) to split the mixture first Piola-Kirchhoff stress into the solid extra stress (solid skeleton effective stress) \mathbf{P}_E^s and the pore fluid pressure component.

Let $\mathcal{H}(u_i, p_f, w^{p_f})$ be the variational form of Equations (4.43)_{6–10} such that

$$\mathcal{H} : \mathcal{S}^u \times \mathcal{S}^{p_f} \times \mathcal{V}^{p_f} \rightarrow \mathbb{R}. \quad (4.49)$$

We may then rewrite Equations (4.43)_{6–10} as

$$\begin{aligned} \mathcal{H}(u_i, p_f, w^{p_f}) &= \int_{\mathcal{B}_0} w^{p_f} \left(\frac{J n^f}{K_f^\eta} \dot{p}_f + \dot{j} \right) dV + \int_{\mathcal{B}_0} w^{p_f} \frac{J}{K_f^\eta} \frac{\partial p_f}{\partial X_I} F_{Ii}^{-1} (n^f \tilde{v}_{i(f)}) dV \\ &\quad + \int_{\mathcal{B}_0} w^{p_f} J \frac{\partial (n^f \tilde{v}_{i(f)})}{\partial X_I} F_{Ii}^{-1} dV = 0. \end{aligned} \quad (4.50)$$

Using chain rule, the last term in Equation (4.50) can be rewritten as follows:

$$\begin{aligned} \int_{\mathcal{B}_0} w^{p_f} J \frac{\partial (n^f \tilde{v}_{i(f)})}{\partial X_I} F_{Ii}^{-1} dV &= \int_{\mathcal{B}_0} \frac{\partial (w^{p_f} J (n^f \tilde{v}_{i(f)}) F_{Ii}^{-1})}{\partial X_I} dV - \int_{\mathcal{B}_0} \frac{\partial w^{p_f}}{\partial X_I} J (n^f \tilde{v}_{i(f)}) F_{Ii}^{-1} dV \\ &\quad - \int_{\mathcal{B}_0} w^{p_f} (n^f \tilde{v}_{i(f)}) \frac{\partial (J F_{Ii}^{-1})}{\partial X_I} dV, \end{aligned} \quad (4.51)$$

wherein the last term goes to zero via the Piola identity. Substitution of Equation (4.51) into

Equation (4.50) gives us

$$\begin{aligned} \mathcal{H}(u_i, p_f, w^{p_f}) &= \int_{\mathcal{B}_0} w^{p_f} \left(\frac{J n^f}{K_f^\eta} \dot{p}_f + \dot{j} \right) dV + \int_{\mathcal{B}_0} w^{p_f} \frac{J}{K_f^\eta} \frac{\partial p_f}{\partial X_I} F_{Ii}^{-1} (n^f \tilde{v}_{i(f)}) dV \\ &\quad + \int_{\mathcal{B}_0} \frac{\partial (w^{p_f} J (n^f \tilde{v}_{i(f)}) F_{Ii}^{-1})}{\partial X_I} dV - \int_{\mathcal{B}_0} \frac{\partial w^{p_f}}{\partial X_I} J (n^f \tilde{v}_{i(f)}) F_{Ii}^{-1} dV = 0. \end{aligned} \quad (4.52)$$

Applying the divergence theorem to the third term in Equation (4.52), using the boundary conditions in Equation (4.43)₇₋₈, the variational form for the balance of mass of the biphasic mixture becomes

$$\begin{aligned} \mathcal{H}(u_i, p_f, w^{p_f}) &= \int_{\mathcal{B}_0} w^{p_f} \left(\frac{J n^f}{K_f^\eta} \dot{p}_f + \dot{j} \right) dV + \int_{\mathcal{B}_0} w^{p_f} \frac{J}{K_f^\eta} \frac{\partial p_f}{\partial X_I} F_{Ii}^{-1} (n^f \tilde{v}_{i(f)}) dV \\ &\quad - \int_{\mathcal{B}_0} \frac{\partial w^{p_f}}{\partial X_I} J (n^f \tilde{v}_{i(f)}) F_{Ii}^{-1} dV - \int_{\Gamma_0^{Q_f}} w^{p_f} Q_f dA = 0. \end{aligned} \quad (4.53)$$

Thus, the formal statement for the variational forms \mathcal{G} and \mathcal{H} may be written as follows:

$$\mathcal{W} = \left\{ \begin{array}{l} \text{Find } u_i(X_I, t) \in \mathcal{S}^u \text{ and } p_f(X_I, t) \in \mathcal{S}^{p_f}, \text{ with } t \in [0, T], \text{ such that:} \\ \int_{\mathcal{B}_0} \frac{\partial w_i^u}{\partial X_I} P_{iI}^s dV - \int_{\mathcal{B}_0} \frac{\partial w_i^u}{\partial X_I} J p_f F_{Ii}^{-1} dV - \int_{\mathcal{B}_0} w_i^u \rho_0 g_i dV \\ - \left(\int_{\Gamma_0^t} w_i^u t_i^{\sigma^s} dA - \int_{\Gamma_0^t} w_i^u p_f J F_{Ii}^{-1} N_I dA \right) = 0, \\ \int_{\mathcal{B}_0} w^{p_f} \left(\frac{J n^f}{K_f^\eta} \dot{p}_f + j \right) dV + \int_{\mathcal{B}_0} w^{p_f} \frac{J}{K_f^\eta} \frac{\partial p_f}{\partial X_I} F_{Ii}^{-1} (n^f \tilde{v}_{i(f)}) dV \\ - \int_{\mathcal{B}_0} \frac{\partial w^{p_f}}{\partial X_I} J (n^f \tilde{v}_{i(f)}) F_{Ii}^{-1} dV - \int_{\Gamma_0^{Q_f}} w^{p_f} Q_f dA = 0 \\ \text{holds } \forall w_i^u \in \mathcal{V}^u \text{ and } \forall w^{p_f} \in \mathcal{V}^{p_f}, \text{ with} \\ \mathcal{S}^u = (u_i : \mathcal{B}_0 \times [0, T] \rightarrow \mathbb{R}^3, u_i \in H^1, u_i(t) = g_i^u(t) \text{ on } \Gamma_0^u, \\ u_i(X_I, t = 0) = u_{i,0}(X_I)), \\ \mathcal{S}^{p_f} = (p_f : \mathcal{B}_0 \times [0, T] \rightarrow \mathbb{R}, p_f \in H^1, p_f(t) = g^p(t) \text{ on } \Gamma_0^p, \\ p_f(X_I, t = 0) = p_{f,0}(X_I)), \\ \mathcal{V}^u = (w_i^u : \mathcal{B}_0 \rightarrow \mathbb{R}^3, w_i^u \in H^1, w_i^u(t) = 0 \text{ on } \Gamma_0^u), \\ \mathcal{V}^{p_f} = (w^{p_f} : \mathcal{B}_0 \rightarrow \mathbb{R}, w^{p_f} \in H^1, w^{p_f}(t) = 0 \text{ on } \Gamma_0^p). \end{array} \right. \quad (4.54)$$

Turning our attention now to *poroelastodynamics* where $\mathbf{a} \neq \mathbf{0}$, let $\mathcal{G}(u_i, p_f, w_i^u)$ be the variational form of Equations (4.44)_{1–5} such that

$$\mathcal{G} : \mathcal{S}^u \times \mathcal{S}^{p_f} \times \mathcal{V}^u \rightarrow \mathbb{R}. \quad (4.55)$$

We may then rewrite Equations (4.44)_{1–5} as

$$\mathcal{G}(u_i, p_f, w_i^u) = \int_{\mathcal{B}_0} w_i^u \rho_0 a_i dV + \int_{\mathcal{B}_0} w_i^u \frac{\partial P_{iI}}{\partial X_I} dV + \int_{\mathcal{B}_0} w_i^u \rho_0 g_i dV = 0. \quad (4.56)$$

Weakening of the first Piola-Kirchhoff stress of the mixture and decomposition proceeds as before,

such that Equation (4.56) is written as

$$\begin{aligned} \mathcal{G}(u_i, p_f, w_i^u) &= \int_{\mathcal{B}_0} w_i^u \rho_0 a_i dV + \int_{\mathcal{B}_0} w_i^u \frac{\partial P_{iI}^s(E)}{\partial X_I} dV - \int_{\mathcal{B}_0} w_i^u J p_f F_{Ii}^{-1} dV + \int_{\mathcal{B}_0} w_i^u \rho_0 g_i dV \\ &\quad - \left(\int_{\Gamma_0^t} w_i^u t_i^{\sigma_s^E} dA - \int_{\Gamma_0^t} w_i^u p_f J F_{Ii}^{-1} N_I dA \right) = 0. \end{aligned} \quad (4.57)$$

The procedure for deriving the variational form of the balance of mass of the mixture, that is, the variational form of Equation (4.44)_{6–10} is identical that as above, the difference being that the inertia term is now included in the Darcy velocity (not shown in Equation (4.53)). Thus, one may refer to Equation (4.53) for the abstract form of the variational form for the balance of mass of the mixture.

The formal statement for the variational forms \mathcal{G} and \mathcal{H} may be written as follows:

$$\mathcal{W} = \left\{ \begin{array}{l} \text{Find } u_i(X_I, t) \in \mathcal{S}^u \text{ and } p_f(X_I, t) \in \mathcal{S}^{p_f}, \text{ with } t \in [0, T], \text{ such that:} \\ \int_{\mathcal{B}_0} w_i^u \rho_0 a_i dV + \int_{\mathcal{B}_0} \frac{\partial w_i^u}{\partial X_I} P_{iI(E)}^s dV - \int_{\mathcal{B}_0} \frac{\partial w_i^u}{\partial X_I} J p_f F_{Ii}^{-1} dV - \int_{\mathcal{B}_0} w_i^u \rho_0 g_i dV \\ - \left(\int_{\Gamma_0^t} w_i^u t_i^{\sigma_E^s} dA - \int_{\Gamma_0^t} w_i^u p_f J F_{Ii}^{-1} N_I dA \right) = 0, \\ \int_{\mathcal{B}_0} w^{p_f} \left(\frac{J n^f}{K_f^\eta} \dot{p}_f + \dot{J} \right) dV + \int_{\mathcal{B}_0} w^{p_f} \frac{J}{K_f^\eta} \frac{\partial p_f}{\partial X_I} F_{Ii}^{-1} (n^f \tilde{v}_{i(f)}) dV \\ - \int_{\mathcal{B}_0} \frac{\partial w^{p_f}}{\partial X_I} J (n^f \tilde{v}_{i(f)}) F_{Ii}^{-1} dV - \int_{\Gamma_0^{Q_f}} w^{p_f} Q_f dA = 0 \\ \text{holds } \forall w_i^u \in \mathcal{V}^u \text{ and } \forall w^{p_f} \in \mathcal{V}^{p_f}, \text{ with} \\ \mathcal{S}^u = (u_i : \mathcal{B}_0 \times [0, T] \rightarrow \mathbb{R}^3, u_i \in H^1, u_i(t) = g_i^u(t) \text{ on } \Gamma_0^u, \\ u_i(X_I, t = 0) = u_{i,0}(X_I)), \\ \mathcal{S}^{p_f} = (p_f : \mathcal{B}_0 \times [0, T] \rightarrow \mathbb{R}, p_f \in H^1, p_f(t) = g^p(t) \text{ on } \Gamma_0^p, \\ p_f(X_I, t = 0) = p_{f,0}(X_I)), \\ \mathcal{V}^u = (w_i^u : \mathcal{B}_0 \rightarrow \mathbb{R}^3, w_i^u \in H^1, w_i^u(t) = 0 \text{ on } \Gamma_0^u), \\ \mathcal{V}^{p_f} = (w^{p_f} : \mathcal{B}_0 \rightarrow \mathbb{R}, w^{p_f} \in H^1, w^{p_f}(t) = 0 \text{ on } \Gamma_0^p). \end{array} \right. \quad (4.58)$$

In the FE implementation that follows, it behooves us to simplify the variational forms, such that for poroelasticity

$$\begin{aligned} \mathcal{G} &= \mathcal{G}_2^{\text{INT}} + \mathcal{G}_3^{\text{INT}} + \mathcal{G}_4^{\text{INT}} + \mathcal{G}_1^{\text{EXT}} + \mathcal{G}_2^{\text{EXT}} = 0, \\ \mathcal{H} &= \mathcal{H}_1^{\text{INT}} + \mathcal{H}_2^{\text{INT}} + \mathcal{H}_3^{\text{INT}} + \mathcal{H}_4^{\text{INT}} + \mathcal{H}^{\text{EXT}} = 0, \end{aligned} \quad (4.59)$$

and for poroelastodynamics

$$\begin{aligned} \mathcal{G} &= \mathcal{G}_1^{\text{INT}} + \mathcal{G}_2^{\text{INT}} + \mathcal{G}_3^{\text{INT}} + \mathcal{G}_4^{\text{INT}} + \mathcal{G}_1^{\text{EXT}} + \mathcal{G}_2^{\text{EXT}} = 0, \\ \mathcal{H} &= \mathcal{H}_1^{\text{INT}} + \mathcal{H}_2^{\text{INT}} + \mathcal{H}_3^{\text{INT}} + \mathcal{H}_4^{\text{INT}} + \mathcal{H}^{\text{EXT}} = 0, \end{aligned} \quad (4.60)$$

wherein

$$\begin{aligned}
\mathcal{G}_1^{\text{INT}} &= \int_{\mathcal{B}_0} w_i^u \rho_0 a_i dV, \\
\mathcal{G}_2^{\text{INT}} &= \int_{\mathcal{B}_0} \frac{\partial w_i^u}{\partial X_I} P_{iI(E)}^s dV, \\
\mathcal{G}_3^{\text{INT}} &= - \int_{\mathcal{B}_0} \frac{\partial w_i^u}{\partial X_I} J p_f F_{Ii}^{-1} dV, \\
\mathcal{G}_4^{\text{INT}} &= - \int_{\mathcal{B}_0} w_i^u \rho_0 g_i dV, \\
\mathcal{G}_1^{\text{EXT}} &= \int_{\Gamma_0^t} w_i^u t_i^{\sigma^s} dA, \\
\mathcal{G}_2^{\text{EXT}} &= - \int_{\Gamma_0^t} w_i^u J p_f F_{Ii} N_I dA,
\end{aligned} \tag{4.61}$$

and

$$\begin{aligned}
\mathcal{H}_1^{\text{INT}} &= \int_{\mathcal{B}_0} w^{p_f} \left(\frac{J n^f}{K_f \eta} \dot{p}_f + j \right) dV, \\
\mathcal{H}_2^{\text{INT}} &= \int_{\mathcal{B}_0} w^{p_f} \frac{J}{K_f \eta} \frac{\partial p_f}{\partial X_I} F_{Ii}^{-1} (n^f \tilde{v}_{i(f)}) dV, \\
\mathcal{H}_3^{\text{INT}} &= \int_{\mathcal{B}_0} \frac{\partial w^{p_f}}{\partial X_I} J F_{Ii}^{-1} \hat{k} \frac{\partial p_f}{\partial X_K} F_{Ki}^{-1} dV, \\
\mathcal{H}_4^{\text{INT}} &= \int_{\mathcal{B}_0} \frac{\partial w^{p_f}}{\partial X_I} J F_{Ii}^{-1} \hat{k} \rho^{\text{fR}} (a_i - g_i) dV, \\
\mathcal{H}^{\text{EXT}} &= \int_{\Gamma_0^{Q_f}} w^{p_f} Q_f dA.
\end{aligned} \tag{4.62}$$

For poroelasticity,

$$\mathcal{H}_4^{\text{INT}} = - \int_{\mathcal{B}_0} \frac{\partial w^{p_f}}{\partial X_I} J F_{Ii}^{-1} \hat{k} \rho^{\text{fR}} g_i dV. \tag{4.63}$$

In the case of 1-D uniaxial strain, i.e., the underlying assumption for the proceeding FE model, the

above terms simplify to the following:

$$\begin{aligned}
\mathcal{G}_1^{\text{INT}} &= \int_0^{X=H} w^u \rho_0 a A dX, \\
\mathcal{G}_2^{\text{INT}} &= \int_0^{X=H} \frac{\partial w^u}{\partial X} P_{11(E)}^s A dX, \\
\mathcal{G}_3^{\text{INT}} &= - \int_0^{X=H} w^u p_f A dX, \\
\mathcal{G}_4^{\text{INT}} &= \int_0^{X=H} w^u \rho_0 g A dX, \\
\mathcal{G}_1^{\text{EXT}} &= \int_{\Gamma_0^t} w^u t^{\sigma_E^s} dA = t^{\sigma_E^s} A, \\
\mathcal{G}_2^{\text{EXT}} &= - \int_{\Gamma_0^t} w^u p_f dA = p_f A,
\end{aligned} \tag{4.64}$$

such that

$$\mathcal{G}_1^{\text{EXT}} + \mathcal{G}_2^{\text{EXT}} = t^\sigma A, \tag{4.65}$$

and

$$\begin{aligned}
\mathcal{H}_1^{\text{INT}} &= \int_0^{X=H} w^{p_f} \left(\frac{J n^f}{K_f^\eta} \dot{p}_f + \dot{J} \right) A dX, \\
\mathcal{H}_2^{\text{INT}} &= \int_0^{X=H} w^{p_f} \frac{1}{K_f^\eta} \frac{\partial p_f}{\partial X} (n^f \tilde{v}_f) A dX, \\
\mathcal{H}_3^{\text{INT}} &= \int_0^{X=H} \frac{\partial w^{p_f}}{\partial X} \hat{k} \frac{\partial p_f}{\partial X} F_{11}^{-1} A dX, \\
\mathcal{H}_4^{\text{INT}} &= \int_0^{X=H} \frac{\partial w^{p_f}}{\partial X} \hat{k} \rho^{\text{fR}} (a + g) A dX, \\
\mathcal{H}^{\text{EXT}} &= \int_{\Gamma_0^{Q_f}} w^{p_f} Q_f dA = Q_f|_{X=H} A,
\end{aligned} \tag{4.66}$$

where for poroelasticity,

$$\mathcal{H}_4^{\text{INT}} = \int_0^{X=H} \frac{\partial w^{p_f}}{\partial X} \hat{k} \rho^{\text{fR}} g A dX . \quad (4.67)$$

4.1.4 (\mathbf{u} - \mathbf{u}_f - p_f) formulation

Herein, barotropic constituents are assumed, i.e., $\rho^{\text{sR}} = \text{const.}$ (from the mechanically incompressible solid assumption) and $\rho^{\text{fR}} = \rho^{\text{fR}}(p_f)$. Locally homogeneous temperatures are also assumed, i.e., $\theta^{\text{s}} = \theta^{\text{f}} = \theta$. The strong formulation for poroelastodynamics with $\mathbf{a}_f \neq \mathbf{a}_s$ has the solution space

$$\begin{aligned} \mathcal{S}^u &= (\mathbf{u} : \mathcal{B}_0 \times [0, T] \rightarrow \mathbb{R}^3, \mathbf{u} \in H^1, \mathbf{u}(t) = \mathbf{g}^u(t) \text{ on } \Gamma_0^u, \mathbf{u}(\mathbf{X}, t = 0) = \mathbf{u}_0(\mathbf{X})), \\ \mathcal{S}^{u_f} &= (\mathbf{u}_f : \mathcal{B}_0 \times [0, T] \rightarrow \mathbb{R}^3, \mathbf{u}_f \in H^1, \mathbf{u}_f(t) = \mathbf{g}^{u_f}(t) \text{ on } \Gamma_0^{u_f}, \mathbf{u}_f(\mathbf{X}, t = 0) = \mathbf{u}_{f,0}(\mathbf{X})), \\ \mathcal{S}^{p_f} &= (p_f : \mathcal{B}_0 \times [0, T] \rightarrow \mathbb{R}, p_f \in H^1, p_f(t) = g^p(t) \text{ on } \Gamma_0^p, p_f(\mathbf{X}, t = 0) = p_{f,0}(\mathbf{X})), \end{aligned} \quad (4.68)$$

where \mathbf{g}^{u_f} is the prescribed pore fluid displacement on $\Gamma_0^{u_f}$, either directly or via integration of a prescribed velocity. A potential no-flux, or “no-slip”, boundary condition is imposed in a weak sense by setting the pore fluid flux to zero at the desired boundary (Equation (4.69)₁₄). Further discussion of this type of boundary condition as used in this work can be found in Section 5.3.3.1, paragraph *Remarks on the impermeable boundary condition*; for further reading on no-slip conditions in poromechanics, refer to Vuong et al. [2016].

The corresponding strong form for poroelastodynamics is

$$\begin{aligned}
 (\mathcal{S}) = \left\{ \begin{array}{l}
 \text{Find } \mathbf{u}(\mathbf{X}, t) \in \mathcal{S}^u, \mathbf{u}_f(\mathbf{X}, t) \in \mathcal{S}^{u_f}, \text{ and } p_f(\mathbf{X}, t) \in \mathcal{S}^{p_f}, \\
 \\
 \text{with } t \in [0, T], \text{ such that:} \\
 \\
 \text{DIV } \mathbf{P} + \rho_0 \mathbf{g} - (\rho_0^s \mathbf{a} + \rho_0^f \mathbf{a}_f) = \mathbf{0} \in \mathcal{B}_0, \\
 \\
 \mathbf{u}(\mathbf{X}, t) = \mathbf{g}^u(\mathbf{X}, t) \text{ on } \Gamma_0^u, \\
 \\
 \mathbf{P}(\mathbf{X}, t) \cdot \mathbf{N}(\mathbf{X}) = \mathbf{t}^\sigma(\mathbf{X}, t) \text{ on } \Gamma_0^t, \\
 \\
 \mathbf{u}(\mathbf{X}, t = 0) = \mathbf{u}_0(\mathbf{X}) \in \mathcal{B}_0, \\
 \\
 \mathbf{v}(\mathbf{X}, t = 0) = \mathbf{v}_0(\mathbf{X}) \in \mathcal{B}_0, \\
 \\
 \mathbf{a}(\mathbf{X}, t = 0) = \mathbf{a}_0(\mathbf{X}) \in \mathcal{B}_0, \\
 \\
 \rho_0^f \mathbf{a}_f + J n^f \text{GRAD}(p_f) \cdot \mathbf{F}^{-1} + J \frac{(n^f)^2}{\hat{k}} (\mathbf{v}_f - \mathbf{v}) - \rho_0^f \mathbf{g} = \mathbf{0} \in \mathcal{B}_0, \\
 \\
 \mathbf{u}_f(\mathbf{X}, t) = \mathbf{g}^{u_f}(\mathbf{X}, t) \text{ on } \Gamma_0^{u_f}, \quad (4.69) \\
 \\
 \mathbf{u}_f(\mathbf{X}, t = 0) = \mathbf{u}_{f,0}(\mathbf{X}) \in \mathcal{B}_0, \\
 \\
 \mathbf{v}_f(\mathbf{X}, t = 0) = \mathbf{v}_{f,0}(\mathbf{X}) \in \mathcal{B}_0, \\
 \\
 \mathbf{a}_f(\mathbf{X}, t = 0) = \mathbf{a}_{f,0}(\mathbf{X}) \in \mathcal{B}_0, \\
 \\
 \frac{J n^f}{K_f^\eta} D_t p_f + D_t J + \frac{J}{K_f^\eta} \text{GRAD}(p_f) \cdot \mathbf{F}^{-1} \cdot (n^f \tilde{\mathbf{v}}_f) \\
 \\
 + J \text{GRAD}(n^f \tilde{\mathbf{v}}_f) \cdot \mathbf{F}^{-T} = \mathbf{0} \in \mathcal{B}_0, \\
 \\
 p_f(\mathbf{X}, t) = g^p(\mathbf{X}, t) \text{ on } \Gamma_0^p, \\
 \\
 -[J \mathbf{F}^{-1} \cdot (n^f \tilde{\mathbf{v}}_f)] \cdot \mathbf{N} = Q_f(\mathbf{X}, t) \text{ on } \Gamma_0^{Q_f}, \\
 \\
 p_f(\mathbf{X}, t = 0) = p_{f,0}(\mathbf{X}) \in \mathcal{B}_0, \\
 \\
 \dot{p}_f(\mathbf{X}, t = 0) = \dot{p}_{f,0}(\mathbf{X}) \in \mathcal{B}_0.
 \end{array} \right.
 \end{aligned}$$

In Equation (4.69), it was assumed that the contribution of the pore fluid extra stress to dissipative

mechanisms was negligible. If such an assumption is not made, instead we would write

$$\begin{aligned}
 (\mathcal{S}) = \left\{ \begin{array}{l}
 \text{Find } \mathbf{u}(\mathbf{X}, t) \in \mathcal{S}^u, \mathbf{u}_f(\mathbf{X}, t) \in \mathcal{S}^{u_f}, \text{ and } p_f(\mathbf{X}, t) \in \mathcal{S}^{p_f}, \\
 \\
 \text{with } t \in [0, T], \text{ such that:} \\
 \\
 \text{DIV } \mathbf{P} + \rho_0 \mathbf{g} - (\rho_0^s \mathbf{a} + \rho_0^f \mathbf{a}_f) = \mathbf{0} \in \mathcal{B}_0, \\
 \\
 \mathbf{u}(\mathbf{X}, t) = \mathbf{g}^u(\mathbf{X}, t) \text{ on } \Gamma_0^u, \\
 \\
 \mathbf{P}(\mathbf{X}, t) \cdot \mathbf{N}(\mathbf{X}) = \mathbf{t}^\sigma(\mathbf{X}, t) \text{ on } \Gamma_0^t, \\
 \\
 \mathbf{u}(\mathbf{X}, t = 0) = \mathbf{u}_0(\mathbf{X}) \in \mathcal{B}_0, \\
 \\
 \mathbf{v}(\mathbf{X}, t = 0) = \mathbf{v}_0(\mathbf{X}) \in \mathcal{B}_0, \\
 \\
 \mathbf{a}(\mathbf{X}, t = 0) = \mathbf{a}_0(\mathbf{X}) \in \mathcal{B}_0, \\
 \\
 \rho_0^f \mathbf{a}_f - \text{DIV } \mathbf{P}_E^f + J n^f \text{GRAD}(p_f) \cdot \mathbf{F}^{-1} \\
 + J \frac{(n^f)^2}{\hat{k}} (\mathbf{v}_f - \mathbf{v}) - \rho_0^f \mathbf{g} = \mathbf{0} \in \mathcal{B}_0, \\
 \\
 \mathbf{u}_f(\mathbf{X}, t) = \mathbf{g}^{u_f}(\mathbf{X}, t) \text{ on } \Gamma_0^{u_f}, \\
 \\
 \mathbf{u}_f(\mathbf{X}, t = 0) = \mathbf{u}_{f,0}(\mathbf{X}) \in \mathcal{B}_0, \\
 \\
 \mathbf{v}_f(\mathbf{X}, t = 0) = \mathbf{v}_{f,0}(\mathbf{X}) \in \mathcal{B}_0, \\
 \\
 \mathbf{a}_f(\mathbf{X}, t = 0) = \mathbf{a}_{f,0}(\mathbf{X}) \in \mathcal{B}_0, \\
 \\
 \frac{J n^f}{K_f^\eta} D_t p_f + D_t J + \frac{J}{K_f^\eta} \text{GRAD}(p_f) \cdot \mathbf{F}^{-1} \cdot (n^f \tilde{\mathbf{v}}_f) \\
 + J \text{GRAD}(n^f \tilde{\mathbf{v}}_f) \cdot \mathbf{F}^{-T} = 0 \in \mathcal{B}_0, \\
 \\
 p_f(\mathbf{X}, t) = g^p(\mathbf{X}, t) \text{ on } \Gamma_0^p, \\
 \\
 -[J \mathbf{F}^{-1} \cdot (n^f \tilde{\mathbf{v}}_f)] \cdot \mathbf{N} = Q_f(\mathbf{X}, t) \text{ on } \Gamma_0^{Q_f}, \\
 \\
 p_f(\mathbf{X}, t = 0) = p_{f,0}(\mathbf{X}) \in \mathcal{B}_0, \\
 \\
 \dot{p}_f(\mathbf{X}, t = 0) = \dot{p}_{f,0}(\mathbf{X}) \in \mathcal{B}_0.
 \end{array} \right. \tag{4.70}
 \end{aligned}$$

Let $\mathcal{G}(u_i, u_{i(f)}, p_f, w_i^u)$ be the variational form of Equations (4.69)_{1–6} such that

$$\mathcal{G} : \mathcal{S}^u \times \mathcal{S}^{u_f} \times \mathcal{S}^{p_f} \times \mathcal{V}^u \rightarrow \mathbb{R}. \quad (4.71)$$

We may then rewrite Equations (4.69)_{1–6} as

$$\mathcal{G}(u_i, u_{i(f)}, p_f, w_i^u) = \int_{\mathcal{B}_0} w_i^u (\rho_0^s a_i + \rho_0^f a_{i(f)}) dV + \int_{\mathcal{B}_0} w_i^u \frac{\partial P_{iI}}{\partial X_I} dV + \int_{\mathcal{B}_0} w_i^u \rho_0 g_i dV = 0. \quad (4.72)$$

Weakening of the first Piola-Kirchhoff stress of the mixture and decomposition proceeds as before, such that Equation (4.72) is written as

$$\begin{aligned} \mathcal{G}(u_i, u_{i(f)}, p_f, w_i^u) &= \int_{\mathcal{B}_0} w_i^u (\rho_0^s a_i + \rho_0^f a_{i(f)}) dV + \int_{\mathcal{B}_0} w_i^u \frac{\partial P_{iI}^s}{\partial X_I} dV - \int_{\mathcal{B}_0} w_i^u J p_f F_{Ii}^{-1} dV \\ &\quad + \int_{\mathcal{B}_0} w_i^u \rho_0 g_i dV - \left(\int_{\Gamma_0^t} w_i^u t_i^{\sigma^s} dA - \int_{\Gamma_0^t} w_i^u p_f J F_{Ii}^{-1} N_I dA \right) = 0. \end{aligned} \quad (4.73)$$

When a viscous pore fluid is considered, an additional two terms appear in Equation (4.73), such that

$$\begin{aligned} \mathcal{G}(u_i, u_{i(f)}, p_f, w_i^u) &= \int_{\mathcal{B}_0} w_i^u (\rho_0^s a_i + \rho_0^f a_{i(f)}) dV + \int_{\mathcal{B}_0} \frac{\partial w_i^u}{\partial X_I} P_{iI}^s dV + \int_{\mathcal{B}_0} \frac{\partial w_i^u}{\partial X_I} P_{iI}^f dV \\ &\quad - \int_{\mathcal{B}_0} w_i^u J p_f F_{Ii}^{-1} dV + \int_{\mathcal{B}_0} w_i^u \rho_0 g_i dV \\ &\quad - \left(\int_{\Gamma_0^t} w_i^u t_i^{\sigma^s} dA + \int_{\Gamma_0^t} w_i^u t_i^{\sigma^f} dA - \int_{\Gamma_0^t} w_i^u p_f J F_{Ii}^{-1} N_I dA \right) = 0. \end{aligned} \quad (4.74)$$

Let $\mathcal{I}(u_i, u_{i(f)}, p_f, w_i^{u_f})$ be the variational form of Equations (4.69)_{7–11} such that

$$\mathcal{I} : \mathcal{S}^{u_f} \times \mathcal{S}^u \times \mathcal{S}^{p_f} \times \mathcal{V}^{u_f} \rightarrow \mathbb{R}. \quad (4.75)$$

We may then rewrite Equations (4.69)_{7–11} as:

$$\begin{aligned} \mathcal{I}(u_i, u_{i(f)}, p_f, w_i^{u_f}) &= \int_{\mathcal{B}_0} w_i^{u_f} \rho_0^f a_{i(f)} dV + \int_{\mathcal{B}_0} w_i^{u_f} J n^f \frac{\partial p_f}{\partial X_I} F_{Ii}^{-1} dV \\ &\quad + \int_{\mathcal{B}_0} w_i^{u_f} J \frac{(n^f)^2}{\hat{k}} (v_{i(f)} - v_i) dV - \int_{\mathcal{B}_0} w_i^{u_f} \rho_0^f g_i dV = 0, \end{aligned} \quad (4.76)$$

or, for a viscous pore fluid:

$$\begin{aligned}
\mathcal{I}(u_i, u_{i(f)}, p_f, w_i^{u_f}) &= \int_{\mathcal{B}_0} w_i^{u_f} \rho_0^f a_{i(f)} dV + \int_{\mathcal{B}_0} w_i^{u_f} J n^f \frac{\partial p_f}{\partial X_I} F_{Ii}^{-1} dV \\
&+ \int_{\mathcal{B}_0} w_i^{u_f} J \frac{(n^f)^2}{\hat{k}} (v_{i(f)} - v_i) dV \\
&- \int_{\mathcal{B}_0} w_i^{u_f} \frac{\partial P_{iI}^f(E)}{\partial X_I} dV - \int_{\mathcal{B}_0} w_i^{u_f} \rho_0^f g_i dV = 0, \tag{4.77}
\end{aligned}$$

wherein the second to last term in Equation (4.77) can be split into two terms, similar to the procedure in the balance of momentum of the mixture, as follows:

$$\begin{aligned}
\mathcal{I}(u_i, u_{i(f)}, p_f, w_i^{u_f}) &= \int_{\mathcal{B}_0} w_i^{u_f} \rho_0^f a_{i(f)} dV + \int_{\mathcal{B}_0} w_i^{u_f} J n^f \frac{\partial p_f}{\partial X_I} F_{Ii}^{-1} dV \\
&+ \int_{\mathcal{B}_0} w_i^{u_f} J \frac{(n^f)^2}{\hat{k}} (v_{i(f)} - v_i) dV \\
&+ \int_{\mathcal{B}_0} \frac{\partial w_i^{u_f}}{\partial X_I} P_{iI}^f(E) dV - \int_{\Gamma_0} w_i^{u_f} t_i^{\sigma_f^E} dA \\
&- \int_{\mathcal{B}_0} w_i^{u_f} \rho_0^f g_i dV = 0. \tag{4.78}
\end{aligned}$$

However, doing so creates an additional complexity, namely that now $t_i^{\sigma_f^E}$ must be determined. In Vuong et al. [2016], Vuong [2016], such a traction is merely a stress balance between solid and fluid phases, and does not take into account an external load as implied here. There are at least two ways in which one might approximate the viscous traction.

The first follows from analysis by Heider [2012] for a nearly-inviscid pore fluid. It involves applying traction to the solid and fluid phases *separately*, which thus necessitates an equation that solves balance of linear momentum of the solid phase, rather than an equation that solves the balance of linear momentum of the mixture. Supposing then that the total traction

$$\mathbf{t}^\sigma = \underbrace{\mathbf{t}^{\sigma^s}}_{\text{applied to solid mom. bal.}} + \underbrace{\mathbf{t}^{\sigma^f}}_{\text{applied to fluid mom. bal.}} \tag{4.79}$$

is specified (e.g., from known data), one may deduce the viscous traction component $\mathbf{t}^{\sigma_f^E}$ via an

implicit solve using the solutions \mathbf{u} and p_f , i.e.,

$$\mathbf{t}^{\sigma^f} = \mathbf{t}^\sigma - \mathbf{t}^{\sigma^s} \Rightarrow \mathbf{t}^{\sigma^f_E}(\mathbf{u}, p_f) = \mathbf{t}^\sigma - (\boldsymbol{\sigma}^s_E - n^s p_f \mathbf{1}) \cdot \mathbf{n} + n^f p_f \mathbf{n}, \quad (4.80)$$

where $\boldsymbol{\sigma}^s_E, n^s, n^f$ are functions of solid displacement \mathbf{u} . Heider [2012] observed inaccurate pore fluid pressure solutions with such a scheme for low permeabilities, small strain theory and low strain-rate loadings, unless additional stabilization parameters were provided. Given difficulties that we have had with respect to obtaining stable solutions at finite strain for high strain-rate loadings [Irwin et al., 2024, 2023c], it is outside the current scope of present work to pursue such a method.

The other approach would be to use the mixture linear momentum balance equation, and approximate the value of $\mathbf{t}^{\sigma^f_E}$ using the interpolated values of porosity and pore fluid velocity gradient at the Gauss point closest to the boundary where $\mathbf{t}^{\sigma^f_E}$ is applied. However, this would be inconsistent with how the total traction is applied to the mixture in the balance of linear momentum of the mixture; there, no such approximations are used for $\mathbf{t}^{\sigma^f_E}$, nor $\mathbf{t}^{\sigma^s_E}$ nor the pore fluid pressure component.

Most consistent is to not weaken the divergence of the pore fluid extra stress term, i.e., to use Equation (4.77). It will be shown that in the balance of mass of the mixture for viscous pore fluid flow that the pore fluid velocity cannot be weakened in the balance of mass of the mixture equations. Therefore, requiring C^1 continuity in the balance of linear momentum of the pore fluid raises no issues, and alleviates the problem of specifying the “viscous traction” term.

The procedure for deriving the variational form of the balance of mass of the mixture for a nearly-inviscid pore fluid, that is, the variational form of Equation (4.69)_{12–16} is identical to the procedure carried out in Section 4.1.3, with the difference herein being that the Darcy velocity depends upon pore fluid acceleration $a_{i(f)}$ rather than a_i .

The formal statement for the variational forms \mathcal{G} , \mathcal{I} , and \mathcal{H} , assuming a nearly-inviscid pore

fluid, may be written as follows:

$$\begin{aligned}
\mathcal{W} = & \left\{ \begin{aligned}
& \text{Find } u_i(X_I, t) \in \mathcal{S}^u, u_{i(f)}(X_I, t) \in \mathcal{S}^{u_f}, \text{ and } p_f(X_I, t) \in \mathcal{S}^{p_f}, \\
& \text{with } t \in [0, T], \text{ such that:} \\
& \int_{\mathcal{B}_0} w_i^u (\rho_0^s a_i + \rho_0^f a_{i(f)}) dV + \int_{\mathcal{B}_0} \frac{\partial w_i^u}{\partial X_I} P_{iI(E)}^s dV - \int_{\mathcal{B}_0} \frac{\partial w_i^u}{\partial X_I} J p_f F_{Ii}^{-1} dV - \int_{\mathcal{B}_0} w_i^u \rho_0 g_i dV \\
& - \left(\int_{\Gamma_0^t} w_i^u t_i^{\sigma^S} dA - \int_{\Gamma_0^t} w_i^u p_f J F_{Ii}^{-1} N_I dA \right) = 0, \\
& \int_{\mathcal{B}_0} w_i^{u_f} \rho_0^f a_{i(f)} dV + \int_{\mathcal{B}_0} w_i^{u_f} J n^f \frac{\partial p_f}{\partial X_I} F_{Ii}^{-1} dV \\
& + \int_{\mathcal{B}_0} w_i^{u_f} J \frac{(n^f)^2}{\hat{k}} (v_{i(f)} - v_i) dV - \int_{\mathcal{B}_0} w_i^{u_f} \rho_0^f g_i dV = 0, \\
& \int_{\mathcal{B}_0} w^{p_f} \left(\frac{J n^f}{K_f^\eta} \dot{p}_f + j \right) dV + \int_{\mathcal{B}_0} w^{p_f} \frac{J}{K_f^\eta} \frac{\partial p_f}{\partial X_I} F_{Ii}^{-1} (n^f \tilde{v}_{i(f)}) dV \\
& - \int_{\mathcal{B}_0} \frac{\partial w^{p_f}}{\partial X_I} J (n^f \tilde{v}_{i(f)}) F_{Ii}^{-1} dV - \int_{\Gamma_0^{Q_f}} w^{p_f} Q_f dA = 0 \\
& \text{holds } \forall w_i^u \in \mathcal{V}^u, w_i^{u_f} \in \mathcal{V}^{u_f}, \text{ and } \forall w^{p_f} \in \mathcal{V}^{p_f}, \text{ with} \\
& \mathcal{S}^u = (u_i : \mathcal{B}_0 \times [0, T] \rightarrow \mathbb{R}^3, u_i \in H^1, u_i(t) = g_i^u(t) \text{ on } \Gamma_0^u, \\
& \quad u_i(X_I, t = 0) = u_{i,0}(X_I)), \\
& \mathcal{S}^{u_f} = (u_{i(f)} : \mathcal{B}_0 \times [0, T] \rightarrow \mathbb{R}^3, u_{i(f)} \in H^1, u_{i(f)}(t) = g_i^{u_f}(t) \text{ on } \Gamma_0^{u_f}, \\
& \quad u_{i(f)}(X_I, t = 0) = u_{i(f),0}(X_I)), \\
& \mathcal{S}^{p_f} = (p_f : \mathcal{B}_0 \times [0, T] \rightarrow \mathbb{R}, p_f \in H^1, p_f(t) = g^p(t) \text{ on } \Gamma_0^p, \\
& \quad p_f(X_I, t = 0) = p_{f,0}(X_I)), \\
& \mathcal{V}^u = (w_i^u : \mathcal{B}_0 \rightarrow \mathbb{R}^3, w_i^u \in H^1, w_i^u(t) = 0 \text{ on } \Gamma_0^u), \\
& \mathcal{V}^{u_f} = (w_i^{u_f} : \mathcal{B}_0 \rightarrow \mathbb{R}^3, w_i^{u_f} \in H^1, w_i^{u_f}(t) = 0 \text{ on } \Gamma_0^{u_f}), \\
& \mathcal{V}^{p_f} = (w^{p_f} : \mathcal{B}_0 \rightarrow \mathbb{R}, w^{p_f} \in H^1, w^{p_f}(t) = 0 \text{ on } \Gamma_0^p).
\end{aligned} \right. \tag{4.81}
\end{aligned}$$

In the FE implementation that follows, it behooves us to simplify the variational forms, such that

$$\begin{aligned}
\mathcal{G} &= \mathcal{G}_1^{\text{INT}} + \mathcal{G}_2^{\text{INT}} + \mathcal{G}_3^{\text{INT}} + \mathcal{G}_4^{\text{INT}} + \mathcal{G}_1^{\text{EXT}} + \mathcal{G}_2^{\text{EXT}} = 0, \\
\mathcal{I} &= \mathcal{I}_1^{\text{INT}} + \mathcal{I}_2^{\text{INT}} + \mathcal{I}_3^{\text{INT}} + \mathcal{I}_4^{\text{INT}} = 0, \\
\mathcal{H} &= \mathcal{H}_1^{\text{INT}} + \mathcal{H}_2^{\text{INT}} + \mathcal{H}_3^{\text{INT}} + \mathcal{H}_4^{\text{INT}} + \mathcal{H}^{\text{EXT}} = 0,
\end{aligned} \tag{4.82}$$

wherein

$$\begin{aligned}
\mathcal{G}_1^{\text{INT}} &= \int_{\mathcal{B}_0} w_i^u (\rho_0^s a_i + \rho_0^f a_{i(f)}) dV, \\
\mathcal{G}_2^{\text{INT}} &= \int_{\mathcal{B}_0} \frac{\partial w_i^u}{\partial X_I} P_{iI}^s dV, \\
\mathcal{G}_3^{\text{INT}} &= - \int_{\mathcal{B}_0} \frac{\partial w_i^u}{\partial X_I} J p_f F_{Ii}^{-1} dV, \\
\mathcal{G}_4^{\text{INT}} &= - \int_{\mathcal{B}_0} w_i^u \rho_0 g_i dV, \\
\mathcal{G}_1^{\text{EXT}} &= \int_{\Gamma_0^t} w_i^u t_i^{\sigma_E^s} dA, \\
\mathcal{G}_2^{\text{EXT}} &= - \int_{\Gamma_0^t} w_i^u J p_f F_{Ii}^{-1} dA,
\end{aligned} \tag{4.83}$$

and

$$\begin{aligned}
\mathcal{I}_1^{\text{INT}} &= \int_{\mathcal{B}_0} w_i^{u_f} \rho_0^f a_{i(f)} dV, \\
\mathcal{I}_2^{\text{INT}} &= \int_{\mathcal{B}_0} w_i^{u_f} J n^f \frac{\partial p_f}{\partial X_I} F_{Ii}^{-1} dV, \\
\mathcal{I}_3^{\text{INT}} &= \int_{\mathcal{B}_0} w_i^{u_f} J \frac{(n^f)^2}{\hat{k}} (v_{i(f)} - v_i) dV, \\
\mathcal{I}_4^{\text{INT}} &= - \int_{\mathcal{B}_0} w_i^{u_f} \rho_0^f g_i dV,
\end{aligned} \tag{4.84}$$

and

$$\begin{aligned}
\mathcal{H}_1^{\text{INT}} &= \int_{\mathcal{B}_0} w^{p_f} \left(\frac{J n^f}{K_f^\eta} \dot{p}_f + j \right) dV, \\
\mathcal{H}_2^{\text{INT}} &= \int_{\mathcal{B}_0} w^{p_f} \frac{J}{K_f^\eta} \frac{\partial p_f}{\partial X_I} F_{Ii}^{-1} (n^f \tilde{v}_{i(f)}) dV, \\
\mathcal{H}_3^{\text{INT}} &= \int_{\mathcal{B}_0} \frac{\partial w^{p_f}}{\partial X_I} J F_{Ii}^{-1} \hat{k} \frac{\partial p_f}{\partial X_K} F_{Ki}^{-1} dV, \\
\mathcal{H}_4^{\text{INT}} &= \int_{\mathcal{B}_0} \frac{\partial w^{p_f}}{\partial X_I} J F_{Ii}^{-1} \hat{k} \rho^{\text{fR}} (a_{i(f)} - g_i) dV, \\
\mathcal{H}^{\text{EXT}} &= \int_{\Gamma_0^{Q_f}} w^{p_f} Q_f dA.
\end{aligned} \tag{4.85}$$

In the case of 1-D uniaxial strain, i.e., the underlying assumption for the proceeding FE model, the above terms simplify to the following:

$$\begin{aligned}
\mathcal{G}_1^{\text{INT}} &= \int_0^{X=H} w^u (\rho_0^s a + \rho^f a_f) A dX, \\
\mathcal{G}_2^{\text{INT}} &= \int_0^{X=H} \frac{\partial w^u}{\partial X} P_{11(E)}^s A dX, \\
\mathcal{G}_3^{\text{INT}} &= - \int_0^{X=H} w^u p_f A dX, \\
\mathcal{G}_4^{\text{INT}} &= \int_0^{X=H} w^u \rho_0 g A dX, \\
\mathcal{G}_1^{\text{EXT}} &= \int_{\Gamma_0^t} w^u t^{\sigma^s} dA = t^{\sigma^s} A, \\
\mathcal{G}_2^{\text{EXT}} &= - \int_{\Gamma_0^t} w^u p_f dA = -p_f A,
\end{aligned} \tag{4.86}$$

such that

$$\mathcal{G}_1^{\text{EXT}} + \mathcal{G}_2^{\text{EXT}} = t^{\sigma} A, \tag{4.87}$$

and

$$\begin{aligned}
\mathcal{I}_1^{\text{INT}} &= \int_0^{X=H} w^{u_f} \rho_0^f a_f A dX, \\
\mathcal{I}_2^{\text{INT}} &= \int_0^{X=H} w^{u_f} n^f \frac{\partial p_f}{\partial X} A dX, \\
\mathcal{I}_3^{\text{INT}} &= \int_0^{X=H} w^{u_f} J \frac{(n^f)^2}{\hat{k}} (v_f - v) A dX, \\
\mathcal{I}_4^{\text{INT}} &= \int_0^{X=H} w^{u_f} \rho_0^f g A dX,
\end{aligned} \tag{4.88}$$

and

$$\begin{aligned}
\mathcal{H}_1^{\text{INT}} &= \int_0^{X=H} w^{p_f} \left(\frac{J n^f}{K_f^\eta} \dot{p}_f + \dot{J} \right) A dX, \\
\mathcal{H}_2^{\text{INT}} &= \int_0^{X=H} w^{p_f} \frac{1}{K_f^\eta} \frac{\partial p_f}{\partial X} (n^f \tilde{v}_f) A dX, \\
\mathcal{H}_3^{\text{INT}} &= \int_0^{X=H} \frac{\partial w^{p_f}}{\partial X} \hat{k} \frac{\partial p_f}{\partial X} F_{11}^{-1} A dX, \\
\mathcal{H}_4^{\text{INT}} &= \int_0^{X=H} \frac{\partial w^{p_f}}{\partial X} \hat{k} \rho^{\text{fR}} (a_f + g) A dX, \\
\mathcal{H}^{\text{EXT}} &= \int_{\Gamma_0^{Q_f}} w^{p_f} Q_f dA = Q_f|_{X=H} A.
\end{aligned} \tag{4.89}$$

The formal statement for the variational forms \mathcal{G} , \mathcal{I} , and \mathcal{H} for a viscous pore fluid may be written

as follows:

$$\begin{aligned}
& \text{Find } u_i(X_I, t) \in \mathcal{S}^u, u_{i(f)}(X_I, t) \in \mathcal{S}^{u_f}, \text{ and } p_f(X_I, t) \in \mathcal{S}^{p_f}, \\
& \text{with } t \in [0, T], \text{ such that:} \\
& \int_{\mathcal{B}_0} w_i^u (\rho_0^s a_i + \rho_0^f a_{i(f)}) dV + \int_{\mathcal{B}_0} \frac{\partial w_i^u}{\partial X_I} P_{iI(E)}^s dV + \int_{\mathcal{B}_0} \frac{\partial w_i^u}{\partial X_I} P_{iI(E)}^f dV \\
& - \int_{\mathcal{B}_0} \frac{\partial w_i^u}{\partial X_I} J p_f F_{Ii}^{-1} dV - \int_{\mathcal{B}_0} w_i^u \rho_0 g_i dV \\
& - \left(\int_{\Gamma_0^t} w_i^u t_i^{\sigma_E^s} dA + \int_{\Gamma_0^t} w_i^u t_i^{\sigma_E^f} dA - \int_{\Gamma_0^t} w_i^u p_f J F_{Ii}^{-1} N_I dA \right) = 0, \\
& \int_{\mathcal{B}_0} w_i^{u_f} \rho_0^f a_{i(f)} dV - \int_{\mathcal{B}_0} w_i^{u_f} \frac{\partial P_{iI(E)}^f}{\partial X_I} dV + \int_{\mathcal{B}_0} w_i^{u_f} J n^f \frac{\partial p_f}{\partial X_I} F_{Ii}^{-1} dV \\
& + \int_{\mathcal{B}_0} w_i^{u_f} J \frac{(n^f)^2}{\hat{k}} (v_{i(f)} - v_i) dV - \int_{\mathcal{B}_0} w_i^{u_f} \rho_0^f g_i dV = 0, \\
& \int_{\mathcal{B}_0} w^{p_f} \left(\frac{J n^f}{K_f^\eta} \dot{p}_f + j \right) dV + \int_{\mathcal{B}_0} w^{p_f} \frac{J}{K_f^\eta} \frac{\partial p_f}{\partial X_I} F_{Ii}^{-1} (n^f \tilde{v}_{i(f)}) dV \\
& - \int_{\mathcal{B}_0} \frac{\partial w^{p_f}}{\partial X_I} J (n^f \tilde{v}_{i(f)}) F_{Ii}^{-1} dV - \int_{\Gamma_0^{Q_f}} w^{p_f} Q_f dA = 0 \tag{4.90} \\
& \text{holds } \forall w_i^u \in \mathcal{V}^u, w_i^{u_f} \in \mathcal{V}^{u_f}, \text{ and } \forall w^{p_f} \in \mathcal{V}^{p_f}, \text{ with} \\
& \mathcal{S}^u = (u_i : \mathcal{B}_0 \times [0, T] \rightarrow \mathbb{R}^3, u_i \in H^1, u_i(t) = g_i^u(t) \text{ on } \Gamma_0^u, \\
& \quad u_i(X_I, t = 0) = u_{i,0}(X_I)), \\
& \mathcal{S}^{u_f} = (u_{i(f)} : \mathcal{B}_0 \times [0, T] \rightarrow \mathbb{R}^3, u_{i(f)} \in H^1, u_{i(f)}(t) = g_i^{u_f}(t) \text{ on } \Gamma_0^{u_f}, \\
& \quad u_{i(f)}(X_I, t = 0) = u_{i(f),0}(X_I)), \\
& \mathcal{S}^{p_f} = (p_f : \mathcal{B}_0 \times [0, T] \rightarrow \mathbb{R}, p_f \in H^1, p_f(t) = g^p(t) \text{ on } \Gamma_0^p, \\
& \quad p_f(X_I, t = 0) = p_{f,0}(X_I)), \\
& \mathcal{V}^u = (w_i^u : \mathcal{B}_0 \rightarrow \mathbb{R}^3, w_i^u \in H^1, w_i^u(t) = 0 \text{ on } \Gamma_0^u), \\
& \mathcal{V}^{u_f} = (w_i^{u_f} : \mathcal{B}_0 \rightarrow \mathbb{R}^3, w_i^{u_f} \in H^1, w_i^{u_f}(t) = 0 \text{ on } \Gamma_0^{u_f}), \\
& \mathcal{V}^{p_f} = (w^{p_f} : \mathcal{B}_0 \rightarrow \mathbb{R}, w^{p_f} \in H^1, w^{p_f}(t) = 0 \text{ on } \Gamma_0^p).
\end{aligned}$$

There are now four additional terms which appear in \mathcal{G} , \mathcal{I} , and \mathcal{H} , namely,

$$\begin{aligned}
\mathcal{G}_5^{\text{INT}} &= \int_{\mathcal{B}_0} \frac{\partial w_i^u}{\partial X_I} P_{iI}^{\text{f}} dV, \\
\mathcal{G}_3^{\text{EXT}} &= \int_{\Gamma_0^t} w_i^u t_i^{\sigma_E^{\text{f}}} dA, \\
\mathcal{I}_5^{\text{INT}} &= \int_{\mathcal{B}_0} w_i^{u_{\text{f}}} \frac{\partial P_{iI}^{\text{f}}}{\partial X_I} dV, \\
\mathcal{H}_5^{\text{INT}} &= - \int_{\mathcal{B}_0} \frac{\partial w^{p_{\text{f}}}}{\partial X_I} \frac{\hat{k}}{n^{\text{f}}} J F_{Ii}^{-1} \frac{\partial \sigma_{ij}^{\text{f}}(E)}{\partial X_J} F_{Jj}^{-1} dV,
\end{aligned} \tag{4.91}$$

wherein $\mathcal{H}_5^{\text{INT}}$ arises from Darcy's law Equation (3.101). Thus we may write

$$\begin{aligned}
\mathcal{G} &= \mathcal{G}_1^{\text{INT}} + \mathcal{G}_2^{\text{INT}} + \mathcal{G}_3^{\text{INT}} + \mathcal{G}_4^{\text{INT}} + \mathcal{G}_1^{\text{EXT}} + \mathcal{G}_2^{\text{EXT}} + \mathcal{G}_3^{\text{EXT}} = 0, \\
\mathcal{I} &= \mathcal{I}_1^{\text{INT}} + \mathcal{I}_2^{\text{INT}} + \mathcal{I}_3^{\text{INT}} + \mathcal{I}_4^{\text{INT}} + \mathcal{I}_5^{\text{INT}} = 0, \\
\mathcal{H} &= \mathcal{H}_1^{\text{INT}} + \mathcal{H}_2^{\text{INT}} + \mathcal{H}_3^{\text{INT}} + \mathcal{H}_4^{\text{INT}} + \mathcal{H}_5^{\text{INT}} + \mathcal{H}^{\text{EXT}} = 0.
\end{aligned} \tag{4.92}$$

1-D counterparts to Equations (4.91) are

$$\begin{aligned}
\mathcal{G}_5^{\text{INT}} &= \int_0^{X=H} \frac{\partial w^u}{\partial X} P_{11}^{\text{f}}(E) A dX, \\
\mathcal{G}_3^{\text{EXT}} &= \int_{\Gamma_0^t} w^u t^{\sigma_E^{\text{f}}} dA = t^{\sigma_E^{\text{f}}} A \\
\mathcal{I}_5^{\text{INT}} &= \int_0^{X=H} w^{u_{\text{f}}} \frac{\partial P_{11}^{\text{f}}(E)}{\partial X} A dX, \\
\mathcal{H}_5^{\text{INT}} &= - \int_0^{X=H} \frac{\partial w^{p_{\text{f}}}}{\partial X} \frac{\hat{k}}{n^{\text{f}}} \frac{\partial \sigma_{11}^{\text{f}}(E)}{\partial X} F_{11}^{-1} A dX,
\end{aligned} \tag{4.93}$$

The need for higher-order elements in the case of viscous pore fluid flow. Consider the Darcy velocity term appearing in Equation (4.85)₂ and, more directly, the divergence on the pore fluid viscous stress tensor appearing in Equation (4.91)₄. Recall that the pore fluid viscous stress tensor σ_E^{f} appears in the Darcy-Brinkman equation as

$$n^{\text{f}} \tilde{\mathbf{v}}_{\text{f}} = -\hat{k} \left(\text{grad} p_{\text{f}} + \rho^{\text{fR}} (\mathbf{a}_{\text{f}} - \mathbf{g}) - \frac{1}{n^{\text{f}}} \text{div} \sigma_E^{\text{f}} \right). \tag{4.94}$$

For a general Newtonian fluid,

$$\boldsymbol{\sigma}_E^f := n^f \kappa_f \text{tr}(\mathbf{d}_f) \mathbf{1} + 2n^f \mu_f \mathbf{d}_f, \quad (4.95)$$

where

$$\mathbf{d}_f := \frac{1}{2}(\text{grad} \mathbf{v}_f + \text{grad}^T \mathbf{v}_f). \quad (4.96)$$

Thus, taking the divergence of Equation (4.95) introduces a porosity gradient as well as a Laplacian of the pore fluid velocity (dropping also (s) subscripts for derivatives with respect to the reference configuration, for notational convenience):

$$\begin{aligned} \frac{1}{n^f} \frac{\partial \sigma_{ij(E)}^f}{\partial X_J} F_{Jj}^{-1} &= \frac{1}{n^f} \left(\kappa_f \frac{\partial v_{k(f)}}{\partial X_K} F_{Kk}^{-1} F_{Jj}^{-1} + \mu_f \left[\frac{\partial v_{i(f)}}{\partial X_K} F_{Kj}^{-1} + \frac{\partial v_{j(f)}}{\partial X_K} F_{Ki}^{-1} \right] F_{Jj}^{-1} \right) \frac{\partial n^f}{\partial X_J} \\ &+ \kappa_f \frac{\partial^2 v_{k(f)}}{\partial X_J \partial X_K} F_{Kk}^{-1} F_{Jj}^{-1} + \mu_f \left(\frac{\partial^2 v_{i(f)}}{\partial X_J \partial X_K} F_{Kj}^{-1} F_{Jj}^{-1} + \frac{\partial^2 v_{j(f)}}{\partial X_J \partial X_K} F_{Ki}^{-1} F_{Jj}^{-1} \right), \end{aligned} \quad (4.97)$$

where the porosity gradient, under the assumption of mechanically incompressible solid (s) constituents, can be expressed as

$$\begin{aligned} \frac{\partial n^f}{\partial x_j} &= \frac{\partial n^f}{\partial X_J} F_{Jj}^{-1} = -\frac{\partial n^s}{\partial X_J} F_{Jj}^{-1} = -\frac{\partial}{\partial X_J} \left(\frac{n_0^s}{J} \right) F_{Jj}^{-1} = \frac{n_0^s}{J^2} \frac{\partial J_s}{\partial X_J} F_{Jj}^{-1} \\ &= \frac{n_0^s}{J^2} \frac{\partial \det(1 + \partial u_i / \partial X_I)}{\partial X_J} F_{Jj}^{-1} = \frac{n_0^s}{J} \frac{\partial^2 u_i}{\partial X_I \partial X_J} F_{Ii}^{-1} F_{Jj}^{-1}. \end{aligned} \quad (4.98)$$

The terms highlighted in red in Equations (4.97) & Equation (4.98) possess second derivatives and are thus problematic for standard finite element implementations if not weakened appropriately, i.e., they would require finite elements (for the respective fields) that possess C^1 continuity rather than the standard C^0 continuity (e.g., a typical Lagrange element). Returning our focus to the variational equation, for $\mathcal{H}_2^{\text{INT}}$ we have, upon expanding the Darcy-Brinkman term:

$$\begin{aligned} \mathcal{H}_2^{\text{INT}} &= - \int_{\mathcal{B}_0} w^{p_f} \frac{J \hat{k}}{K_f^\eta} \frac{\partial p_f}{\partial X_I} F_{Ii}^{-1} \frac{\partial p_f}{\partial X_K} F_{Kk}^{-1} dV - \int_{\mathcal{B}_0} w^{p_f} \frac{J \hat{k}}{K_f^\eta} \frac{\partial p_f}{\partial X_I} F_{Ii}^{-1} \rho^{\text{fR}} (a_{i(f)} - g_i) dV \\ &+ \int_{\mathcal{B}_0} w^{p_f} \frac{J \hat{k}}{K_f^\eta} \frac{\partial p_f}{\partial X_I} F_{Ii}^{-1} \left(\frac{1}{n^f} \left(\kappa_f \frac{\partial v_{k(f)}}{\partial X_K} F_{Kk}^{-1} F_{Ji}^{-1} + \eta_f \left[\frac{\partial v_{i(f)}}{\partial X_K} F_{Kj}^{-1} + \frac{\partial v_{j(f)}}{\partial X_K} F_{Ki}^{-1} \right] F_{Jj}^{-1} \right) \frac{\partial n^f}{\partial X_J} \right. \\ &\quad \left. + \kappa_f \frac{\partial^2 v_{k(f)}}{\partial X_J \partial X_K} F_{Kk}^{-1} F_{Ji}^{-1} + \mu_f \left(\frac{\partial^2 v_{i(f)}}{\partial X_J \partial X_K} F_{Kj}^{-1} F_{Jj}^{-1} + \frac{\partial^2 v_{j(f)}}{\partial X_J \partial X_K} F_{Ki}^{-1} F_{Jj}^{-1} \right) \right) dV. \end{aligned} \quad (4.99)$$

The first two terms can be integrated normally; however the last cannot be integrated by parts to reduce continuity requirements of the solid skeleton (s) displacement and pore fluid (f) displacement given that a gradient is also applied to pore fluid pressure p_f (i.e., weakening continuity requirements on the displacements in turn strengthens the continuity requirement on pore fluid pressure). This problem also arises in $\mathcal{H}_5^{\text{INT}}$, although there the gradient is applied to the weighting function w^{pf} :

$$\begin{aligned} \mathcal{H}_5^{\text{INT}} = & - \int_{\mathcal{B}_0} \frac{\partial w^{pf}}{\partial X_I} J F_{Ii}^{-1} \left(\frac{1}{n^f} \left(\kappa_f \frac{\partial v_{k(f)}}{\partial X_K} F_{Kk}^{-1} F_{Ji}^{-1} + \mu_f \left[\frac{\partial v_{i(f)}}{\partial X_K} F_{Kj}^{-1} + \frac{\partial v_{j(f)}}{\partial X_K} F_{Ki}^{-1} \right] F_{Jj}^{-1} \right) \frac{\partial n^f}{\partial X_J} \right. \\ & \left. + \kappa_f \frac{\partial^2 v_{k(f)}}{\partial X_J \partial X_K} F_{Kk}^{-1} F_{Ji}^{-1} + \mu_f \left(\frac{\partial^2 v_{i(f)}}{\partial X_J \partial X_K} F_{Kj}^{-1} F_{Jj}^{-1} + \frac{\partial^2 v_{j(f)}}{\partial X_J \partial X_K} F_{Ki}^{-1} F_{Jj}^{-1} \right) \right) dV. \end{aligned} \quad (4.100)$$

Furthermore, the ‘‘mixed approach’’ taken by Vuong et al. [2016], Vuong [2016] to treat porosity n^f as an independent field variable in the finite element implementation (with the assumption of incompressible pore fluid (f) constituent, i.e., $\nabla \cdot \mathbf{v}_f = 0$), thereby eliminating strict dependence on solid skeleton (s) displacement, does not in and of itself relieve us of the issue of higher order continuity requirements since second derivatives appear for pore fluid velocity when the pore fluid is assumed to be compressible ($\nabla \cdot \mathbf{v}_f \neq 0$), in both the balance of mass of the mixture and the balance of linear momentum of the pore fluid (assuming the divergence on the pore fluid extra stress is not weakened in the latter).

One potential remedy to this problem is to ignore the pore fluid extra stress tensor $\boldsymbol{\sigma}_E^f$ altogether. It was shown by Markert [2005] and Ehlers [2022] (originally in Ehlers et al. [1999]) that the fluid friction (viscous) forces are negligible when compared to the drag forces on the macroscale. The derivation from Ehlers [2022] proceeds as follows.

Begin by assuming an incompressible pore fluid constituent and a rigid, non-deforming solid constituent, i.e.,

$$D_t^f \rho^{\text{fR}} \rightarrow 0, \quad \mathbf{u} \rightarrow \mathbf{0}. \quad (4.101)$$

Then, the balance of mass of phase α reduces to (still under the assumption of negligible mass

supply to phase α)

$$D_t^\alpha n^\alpha + n^\alpha \operatorname{div} \mathbf{v}_\alpha = 0. \quad (4.102)$$

Given that

$$\sum_\alpha D_t^\alpha n^\alpha = \operatorname{grad}(n^f) \cdot \tilde{\mathbf{v}}_f = \operatorname{div}(n^f \tilde{\mathbf{v}}_f) - n^f \operatorname{div} \mathbf{v}_f + (1 - n^s) \operatorname{div} \mathbf{v}_s, \quad (4.103)$$

the balance of mass of the mixture for incompressible constituents reduces to

$$\operatorname{div}(n^f \tilde{\mathbf{v}}_f) = 0. \quad (4.104)$$

For non-deforming solid, n^s is constant ($\operatorname{grad}(n^f) \rightarrow \mathbf{0}$), and thus

$$\operatorname{div} \mathbf{v}_f = 0. \quad (4.105)$$

Pore fluid momentum balance is written as

$$\rho^f \mathbf{a}_f + \operatorname{div}(n^f p_f) - \operatorname{div} \boldsymbol{\sigma}_E^f - \mathbf{h}^f - \rho^f \mathbf{g} = \mathbf{0}. \quad (4.106)$$

Recall from Section 3.2 that

$$\mathbf{h}^f = \mathbf{h}_E^f + p_f \operatorname{grad} n^f, \quad (4.107)$$

with

$$\mathbf{h}_E^f = -\mathbf{S}_w \tilde{\mathbf{v}}_f = -\frac{(n^f)^2}{\hat{k}} \tilde{\mathbf{v}}_f, \quad \mathbf{S}_w := \frac{(n^f)^2}{\hat{k}} \mathbf{1}. \quad (4.108)$$

With this, and by inserting the Newtonian fluid law given by Equation (4.95) (using the identity $\operatorname{tr}(\mathbf{d}_f) = \operatorname{div} \mathbf{v}_f$, which is zero by Equation (4.105)) into Equation (4.106) gives the pore fluid momentum balance for incompressible constituents and non-deforming solid skeleton:

$$\rho^f \mathbf{a}_f + n^f \operatorname{grad} p_f - n^f \mu_f \operatorname{div} \operatorname{grad} \mathbf{v}_f + \frac{(n^f)^2}{\hat{k}} \mathbf{v}_f - \rho^f \mathbf{g} = \mathbf{0}. \quad (4.109)$$

Introducing the dimensionless quantities

$$\mathbf{x}^* := \frac{\mathbf{x}}{L}, \quad \mathbf{v}_f^* := \frac{\mathbf{v}_f}{V}, \quad (4.110)$$

with L as a characteristic length scale and V as a characteristic velocity allows us to write the dimensionless gradient and divergence operators as

$$\overset{*}{\text{grad}}(\cdot) = L\text{grad}(\cdot), \quad \overset{*}{\text{div}}(\cdot) = L\text{div}(\cdot). \quad (4.111)$$

Then we may recast the viscous and drag forces in Equation (4.109) as, respectively,

$$\begin{aligned} \text{div } \boldsymbol{\sigma}_E^f &= n^f \mu_f \frac{V}{L^2} \overset{*}{\text{div}}(\overset{*}{\text{grad}} \mathbf{v}_f^*), \\ \mathbf{h}_E^f &= -\frac{(n^f)^2}{\hat{k}} V \mathbf{v}_f^*. \end{aligned} \quad (4.112)$$

Taking the ratio of the viscous force to the drag force yields

$$\frac{\text{Viscous force}}{\text{Drag force}} \propto \frac{\mu_f \hat{k}}{n^f L^2} = \frac{\varkappa}{n^f L^2}. \quad (4.113)$$

For porous media applications, \varkappa is typically several orders of magnitude smaller than the length scale of interest L , e.g., in the current work $\varkappa \sim \mathcal{O}(10^{-10} \text{ m}^2)$ [Lande and Mitzner, 2006] and $L \sim \mathcal{O}(10^{-2} \text{ m})$. Thus, it may be appropriate to ignore the pore fluid extra stress (the viscous force) when solving the balance equations for the mesoscale/macroscale regime, but not necessarily for the microscale regime where the pore size $\sqrt{\varkappa}$ is on the order of L .

However, as Vuong points out (see Chapter 3.3.6 of Vuong [2016] and the figures therein), a nearly-inviscid fluid creates infinitesimally large velocity gradients at the porous channel walls to counteract an infinitesimally small boundary layer, which could lead to numerical instability for 3-D simulations, particularly for highly permeable materials, i.e., those with larger pore sizes (larger fluid domains). Whether or not it is necessary to account for the boundary layer in a numerical simulation where flow is modeled on the macroscale regime is an area of debate [Nield and Bejan, 2013]. This boundary layer has thickness of order $(\tilde{\eta}_f \varkappa / \mu_f)^{1/2}$, where $\tilde{\eta}_f$ is an effective viscosity of the pore fluid. For lung parenchyma, $\varkappa \sim 10^{-10}$ – 10^{-11} m^2 [Lande and Mitzner, 2006, Dai et al., 2014], thus these viscous effects are probably negligible at the mesoscale level of interest for lung parenchyma which is $\mathcal{O}(10^{-2}) \text{ m}$.

Generally speaking, it is believed that both the Darcy and Darcy-Brinkman (the inclusion of the pore fluid viscous stress tensor) equations only hold in the range of Reynolds numbers

$1 < \text{Re} < 10$ [Bear, 1972, Nield and Bejan, 2013, Vuong, 2016, Winter et al., 2022]—for reference, in prior work [Irwin et al., 2024, 2023c], the maximum Reynolds number resulting from numerical simulations was roughly $\text{Re} = 9.8$. Nevertheless, the Reynolds number limits are based upon experimental data wherein it is difficult to measure the inertia forces [Sobieski and Trykozko, 2014], and, with the exception of Vuong [2016], many authors do not include the inertia term in Darcy’s law and use the classical form which relates seepage velocity to pore fluid pressure gradient and (if applicable) body forces. Nield and Bejan [2013] notes that the inertia term is only consequential when the kinematic viscosity of the pore fluid ν_f is on the order of \varkappa/t_0 where t_0 is the characteristic time scale of interest. For lung parenchyma and air, this is satisfied when $t_0 \sim 10^{-5}$ s, i.e., for the shock-loading regime considered in this thesis.

An alternative representation of the seepage velocity which accounts for non-linear drag effects at higher Re (but not the turbulent regime, i.e., $10 < \text{Re} < 100$, [Bear, 1972]) is to use the Darcy-Forchheimer equation given by Equation (4.114) [Markert, 2005, Ehlers, 2002]:

$$-\text{grad}p_f = \left(\hat{k} + \frac{\rho^{\text{fR}}}{B^s} |(n^f \tilde{\mathbf{v}}_f)| \right) (n^f \tilde{\mathbf{v}}_f), \quad (4.114)$$

where B^s is a tortuosity parameter measuring the irregularity of the pore channels (with deviations from $B^s = 1$ indicating higher irregularity). Such a parameter is hard to determine for complex materials such as lung parenchyma, e.g., in Dai et al. [2014] the geometry of lung parenchyma—for the purpose of determining a value for the tortuosity—was approximated as parallel cylinders, such that $B^s = 1.33$. Note also in Equation (4.114), Markert [2005] has made the *a priori* assumption that inertia forces are negligible as well. A brief attempt to reformulate the Darcy-Forchheimer with inertia terms is presented as follows.

A thermodynamically consistent approach [Ehlers, 2022] starts by defining

$$\mathbf{h}_E^f := -\mathbf{S}_w(n^f \tilde{\mathbf{v}}_f) - \mathbf{S}_q |n^f \tilde{\mathbf{v}}_f| (n^f \tilde{\mathbf{v}}_f), \quad (4.115)$$

with \mathbf{S}_w defined as per Equation (3.61), and

$$\mathbf{S}_q := (n^f)^3 \frac{\rho^{\text{fR}}}{B^s} \mathbf{1}. \quad (4.116)$$

Per Section 3.1.4 and Equation (3.70), we may substitute the new form of \mathbf{h}_E^f given by Equation (4.115) into the momentum balance of the pore fluid (dropping the pore fluid extra stress on the assumption that at higher Re, pore fluid viscous effects are negligible), such that

$$\frac{1}{\hat{k}}(n^f \tilde{\mathbf{v}}_f) + (n^f)^2 \frac{\rho^{\text{fR}}}{B^s} |n^f \tilde{\mathbf{v}}_f| (n^f \tilde{\mathbf{v}}_f) = -\rho^{\text{fR}}(\mathbf{a}_f - \mathbf{b}^f) - \text{grad} p_f - \frac{1}{n^f} p_f \text{grad}(n^f) \left[1 - \frac{\theta^s}{\theta^f}\right]. \quad (4.117)$$

Following the approach of Markert [2005], taking the norm of both sides of Equation (4.117) allows us to solve for $|n^f \tilde{\mathbf{v}}_f|$ as

$$|n^f \tilde{\mathbf{v}}_f| = -\frac{B^s}{\hat{k} \rho^{\text{fR}}} \left(\frac{1}{2} \pm \sqrt{\frac{1}{4} + \frac{B^s (\hat{k})^2}{\rho^{\text{fR}}} \left(\rho^{\text{fR}} [|\mathbf{a}_f| - |\mathbf{b}|] + |\text{grad} p_f| + \frac{1}{(n^f)^2} |p_f \text{grad}(n^f)| \left(1 - \frac{\theta^s}{\theta^f}\right)^2 \right)} \right). \quad (4.118)$$

In the static conditions (e.g., no pressure gradients, inertia, etc.) Equation (4.118) recovers the natural condition where $|n^f \tilde{\mathbf{v}}_f| = 0$ if only the positive root is considered. Therefore, substitution into Equation (4.117) gives the following expression for the seepage velocity:

$$n^f \tilde{\mathbf{v}}_f = -\hat{k} \mathbf{K}_f^{-1} \left(\rho^{\text{fR}}(\mathbf{a}_f - \mathbf{b}^f) - \text{grad} p_f - \frac{1}{n^f} p_f \text{grad}(n^f) \left[1 - \frac{\theta^s}{\theta^f}\right] \right), \quad (4.119)$$

with

$$\mathbf{K}_f := 1 - (n^f)^2 \left[\frac{1}{2} + \sqrt{\frac{1}{4} + \frac{(\hat{k})^2 B^s}{\rho^{\text{fR}}} \left(\rho^{\text{fR}} [|\mathbf{a}_f| - |\mathbf{b}|] + |\text{grad} p_f| + \frac{1}{(n^f)^2} |p_f \text{grad} n^f| \left[1 - \frac{\theta^s}{\theta^f}\right]^2 \right)} \right]. \quad (4.120)$$

In any case, higher order element types that possess C^1 continuity are necessary to guarantee convergence of equations containing porosity gradients.

Using Hermite polynomials to satisfy C^1 continuity requirements. If the porosity gradient needs to be resolved, elements with continuous first derivatives along their boundaries must be used in order to guarantee convergence. The approach taken by Vuong et al. [2016], Vuong [2016] to guarantee C^1 continuity was to use Non-Uniform Rational Basis Splines (NURBS) (refer to work by Hughes et al. [2005] for a finite element application). However, for the simple 1-D geometry

considered herein, NURBS would introduce an additional layer of complexity given that the basis functions are not interpolatory.

A simpler solution would be to invoke the Hermite cubic polynomial element (which is C^1 continuous), which is typically employed in FE analysis of beams. Herein, the analogy to a rotational degree of freedom (DOF) in beam analysis is the gradient DOF. However, unlike beam analysis, the gradient DOFs of the field variables of interest (u and u_f) are allowed to “float”, i.e., no Dirichlet nor Neumann boundary conditions are prescribed on these DOFs; in essence, they go unused outside of their interpolatory functionality.

The element (refer to Fig. 4.1) will not be isoparametric, i.e.,

$$x^{h^e}(\xi) = \mathbf{N}^e(\xi) \cdot \mathbf{x}^e, \quad u^{h^e}(\xi) = \mathbf{N}_H^{e,u}(\xi) \cdot \mathbf{d}^e, \quad (4.121)$$

with

$$\begin{aligned} N_1^e &:= \frac{1}{2}(1 - \xi), \\ N_2^e &:= \frac{1}{2}(1 + \xi), \end{aligned} \quad (4.122)$$

and

$$\mathbf{d}^e = \begin{Bmatrix} d_1^e \\ d_2^e \\ d_3^e \\ d_4^e \end{Bmatrix} = \begin{Bmatrix} u^{h^e}(\xi = -1) \\ u_{,x}^{h^e}(-1) \\ u^{h^e}(1) \\ u_{,x}^{h^e}(1) \end{Bmatrix}, \quad (4.123)$$

such that

$$u^{h^e}(\xi) = \begin{bmatrix} N_{1(H)}^{e,u} & j^e N_{2(H)}^{e,u} & N_{3(H)}^{e,u} & j^e N_{4(H)}^{e,u} \end{bmatrix} \begin{bmatrix} d_1^e \\ d_2^e \\ d_3^e \\ d_4^e \end{bmatrix} = \mathbf{N}_H^{e,u}(\xi) \cdot \mathbf{d}^e, \quad (4.124)$$

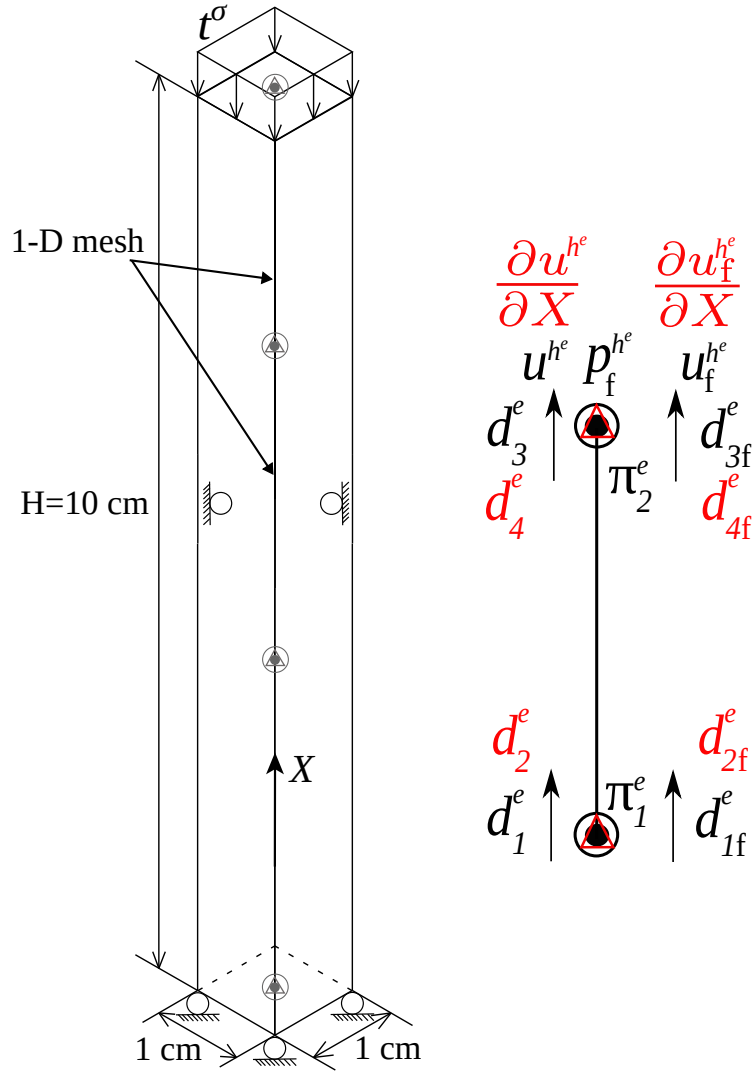


Figure 4.1: The Q3H-Q3H-P1 line element used for C^1 continuity of the field variables u and u_f . Shown in red are the gradient DOFs which are allowed to “float”, i.e., no boundary conditions are prescribed for these DOFs.

where $N_H^{e,u}(\xi)$ are the element Hermite cubic polynomials:

$$\begin{aligned}
 N_{1(H)}^{e,u} &:= \frac{1}{4}(1 - \xi)^2(2 + \xi), \\
 N_{2(H)}^{e,u} &:= \frac{1}{4}(1 - \xi)^2(1 + \xi), \\
 N_{3(H)}^{e,u} &:= \frac{1}{4}(1 + \xi)^2(2 - \xi), \\
 N_{4(H)}^{e,u} &:= \frac{1}{4}(1 + \xi)^2(-1 + \xi),
 \end{aligned} \tag{4.125}$$

and

$$\begin{aligned}
j^e &:= \frac{\partial x^{h^e}}{\partial \xi} = \frac{h^e}{2}, \\
\frac{\partial u^{h^e}}{\partial \xi} &= j^e \frac{\partial u^{h^e}}{\partial X}, \\
w^{u^{h^e}}(\xi) &= \mathbf{N}_H^{e,u} \cdot \mathbf{c}^{u,e} = (\mathbf{c}^{u,e})^T \cdot (\mathbf{N}_H^{e,u})^T.
\end{aligned} \tag{4.126}$$

Herein, the “strain-displacement” matrix $\mathbf{H}^{e,u}$ is defined as:

$$\frac{\partial^2 u^{h^e}(\xi)}{\partial X^2} = \frac{d^2 \mathbf{N}_H^{e,u}(\xi)}{dX^2} \cdot \mathbf{d}^e = \frac{1}{(j^e)^2} \frac{d^2 \mathbf{N}_H^{e,u}(\xi)}{d\xi^2} \cdot \mathbf{d}^e = \mathbf{H}^{e,u}(\xi) \cdot \mathbf{d}^e, \tag{4.127}$$

and

$$\frac{\partial u^{h^e}(\xi)}{\partial X} = \frac{d \mathbf{N}_H^{e,u}(\xi)}{dX} \cdot \mathbf{d}^e = \frac{1}{j^e} \frac{d \mathbf{N}_H^{e,u}(\xi)}{d\xi} \cdot \mathbf{d}^e = \mathbf{B}_H^{e,u}(\xi) \cdot \mathbf{d}^e. \tag{4.128}$$

For notational purposes, the $(\cdot)_H$ subscript will be dropped from $\mathbf{N}_H^{e,u}$ and $\mathbf{B}_H^{e,u}$. In the finite element equations where $\mathbf{H}^{e,u}$ is used, the reader should assume that the shape functions for the respective field, and its first derivative, are the Hermite shape functions as shown here (i.e., only one element type will be used to represent a field variable, not a mix of element types). Of course the same interpolation applies to the shape functions \mathbf{N}_H^{e,u_f} , \mathbf{B}_H^{e,u_f} and \mathbf{H}^{e,u_f} when the pore fluid displacement u_f requires a C^1 continuous element.

4.1.5 (\mathbf{u} - p_f - θ^s - θ^f) formulation

Herein, baroclinic fluid constituent is assumed, i.e., $\rho^{\text{fr}} = \rho^{\text{fr}}(p_f, \theta^f)$. Locally inhomogeneous temperatures are also assumed. Furthermore, we assume that $\mathbf{a}_f = \mathbf{a}_s = \mathbf{a}$. The strong formulation for thermoporoelastodynamics has the solution space

$$\begin{aligned}
\mathcal{S}^u &= (\mathbf{u} : \mathcal{B}_0 \times [0, T] \rightarrow \mathbb{R}^3, \mathbf{u} \in H^1, \mathbf{u}(t) = \mathbf{g}^u(t) \text{ on } \Gamma_0^u, \mathbf{u}(\mathbf{X}, t = 0) = \mathbf{u}_0(\mathbf{X})), \\
\mathcal{S}^{p_f} &= (p_f : \mathcal{B}_0 \times [0, T] \rightarrow \mathbb{R}, p_f \in H^1, p_f(t) = g^p(t) \text{ on } \Gamma_0^p, p_f(\mathbf{X}, t = 0) = p_{f,0}(\mathbf{X})), \\
\mathcal{S}^{\theta^s} &= (\theta^s : \mathcal{B}_0 \times [0, T] \rightarrow \mathbb{R}, \theta^s \in H^1, \theta^s(t) = g^{\theta^s} \text{ on } \Gamma_0^{\theta^s}, \theta^s(\mathbf{X}, t = 0) = \theta_0^s(\mathbf{X})), \\
\mathcal{S}^{\theta^f} &= (\theta^f : \mathcal{B}_0 \times [0, T] \rightarrow \mathbb{R}, \theta^f \in H^1, \theta^f(t) = g^{\theta^f} \text{ on } \Gamma_0^{\theta^f}, \theta^f(\mathbf{X}, t = 0) = \theta_0^f(\mathbf{X})),
\end{aligned} \tag{4.129}$$

where g^{θ^s} and g^{θ^f} are the prescribed temperatures on $\Gamma_0^{\theta^s}$ and $\Gamma_0^{\theta^f}$, respectively. Prior to writing the strong formulation, the energy balances of each phase must be derived.

Derivation of the solid phase energy balance. We may write Equation (2.62) for $\alpha = s$ as

$$\rho^s D_t^s e^s = \boldsymbol{\sigma}^s : \mathbf{l}_s - \operatorname{div} \mathbf{q}^s + \rho^s r^s + \hat{\varepsilon}^s. \quad (4.130)$$

Assuming no heat source r^s , and making use of Equations (3.43)₁, Equation (3.72), we may write

$$\rho^s (D_t^s \psi^s + \theta^s D_t^s \eta^s + \eta^s D_t^s \theta^s) = (\boldsymbol{\sigma}_E^s - \frac{\theta^s}{\theta^f} p_f n^s \mathbf{1} - q \mathbf{1}) : \mathbf{l}_s - \operatorname{div} \mathbf{q}^s - k_\theta^\varepsilon (\theta^s - \theta^f) - \mathbf{h}^f \cdot \tilde{\mathbf{v}}_f. \quad (4.131)$$

Since the momentum production term \mathbf{h}^f cannot be constitutively determined, a substitution may be made via use of Equation (3.44), such that we may write Equation (4.131) as¹

$$\begin{aligned} \rho^s (D_t^s \psi^s + \theta^s D_t^s \eta^s + \eta^s D_t^s \theta^s) &= \boldsymbol{\sigma}_E^s : \mathbf{d}_s - \left(\frac{\theta^s}{\theta^f} p_f n^s + q \right) \operatorname{div} \mathbf{v}_s - \operatorname{div} \mathbf{q}^s - k_\theta^\varepsilon (\theta^s - \theta^f) \\ &\quad - \mathbf{h}_E^f \cdot \tilde{\mathbf{v}}_f - \frac{\theta^s}{\theta^f} p_f \operatorname{grad}(n^f) \cdot \tilde{\mathbf{v}}_f. \end{aligned} \quad (4.132)$$

Prior to invoking the constitutive model(s), it is useful to transform Equation (4.132) to the reference configuration (dropping also $(\cdot)_s$ and $(\cdot)^s$ for convenience, where appropriate):

$$\begin{aligned} D_t(\rho_0^s \psi^s) + \rho_0^s \theta^s D_t \eta^s + \rho_0^s \eta^s D_t \theta^s &= \frac{1}{2} \mathbf{S}_E^s : D_t \mathbf{C} - \left(\frac{\theta^s}{\theta^f} p_f n^s + Q \right) D_t J \\ - J \operatorname{GRAD}(\mathbf{q}^s) : \mathbf{F}^{-T} - J k_\theta^\varepsilon (\theta^s - \theta^f) - J \mathbf{h}_E^f \cdot \tilde{\mathbf{v}}_f - J \frac{\theta^s}{\theta^f} p_f \operatorname{GRAD}(n^f) \cdot \mathbf{F}^{-1} \cdot \tilde{\mathbf{v}}_f. \end{aligned} \quad (4.133)$$

Expanding the material time derivative on the first term and using Equations (3.34)_{1,3}, we may write

$$\begin{aligned} \rho_0^s \theta^s D_t \eta^s &= - \left(\frac{\theta^s}{\theta^f} p_f n^s + Q \right) D_t J - J \operatorname{GRAD}(\mathbf{q}^s) : \mathbf{F}^{-T} - J k_\theta^\varepsilon (\theta^s - \theta^f) \\ &\quad - J \mathbf{h}_E^f \cdot \tilde{\mathbf{v}}_f - J \frac{\theta^s}{\theta^f} p_f \operatorname{GRAD}(n^f) \cdot \mathbf{F}^{-1} \cdot \tilde{\mathbf{v}}_f. \end{aligned} \quad (4.134)$$

At this point, the terms on the l.h.s. of Equation (4.132) require a constitutive form for the solid in order to be further simplified.

¹ Note that the last three terms are consistent with result given by Equation (3.73) if we use the constitutive relation for the seepage tensor, Equation (3.61), in the second to last term of Equation (4.132).

The linear isotropic thermoelastic model. For a material undergoing linear isotropic thermal expansion, recall, from Equations (2.11) & Equation (3.44),

$$\eta^s = c_V^s \ln \frac{\theta^s}{\theta_0^s} + \frac{1}{\rho_0^s} K^{\text{skel}} \alpha_V^s \ln J_s. \quad (4.135)$$

The first term of Equation (4.134) is thus (assuming constant volumetric CTE α_V^s and isothermal bulk modulus K^{skel}):

$$\rho_0^s \theta^s D_t \eta^s = \rho_0^s c_V^s D_t \theta^s + \frac{K^{\text{skel}} \alpha_V^s \theta^s}{J} D_t J. \quad (4.136)$$

Then, substitution of Equation (4.136) back into Equation (4.134) yields the governing equation for the balance of energy of the solid constituent:

$$\begin{aligned} \rho_0^s c_V^s D_t \theta^s + \left(\frac{K^{\text{skel}} \alpha_V^s \theta^s}{J} + n^s p_f \frac{\theta^s}{\theta^f} + Q \right) D_t J + J \text{GRAD}(\mathbf{q}^s) : \mathbf{F}^{-T} + J k_\theta^s (\theta^s - \theta^f) \\ + \frac{J (n^f \tilde{\mathbf{v}}_f)^2}{\hat{k}} + J \frac{\theta^s}{\theta^f} \frac{p_f}{n^f} \text{GRAD}(n^f) \cdot \mathbf{F}^{-1} \cdot (n^f \tilde{\mathbf{v}}_f) = 0, \end{aligned} \quad (4.137)$$

where on the last line of Equation (4.137) we have used the following identities to simplify the extra fluid interaction force term:

$$\mathbf{h}_E^f \cdot \tilde{\mathbf{v}}_f = (-\mathbf{S}_w \tilde{\mathbf{v}}_f) \cdot \tilde{\mathbf{v}}_f, \quad \mathbf{S}_w := \frac{(n^f)^2}{\hat{k}} \mathbf{1}. \quad (4.138)$$

Derivation of the fluid phase energy balance. Next, we may write the balance of energy for the fluid phase as

$$\rho^f D_t^f e^f = \boldsymbol{\sigma}^f : \mathbf{l}_f - \text{div} \mathbf{q}^f + \rho^f r^f + \hat{\varepsilon}^f. \quad (4.139)$$

Assuming no heat source r^f , and making use of Equations (3.43)₂, Equation (3.72), we may write

$$\rho^f (D_t^f \psi^f + \theta^f D_t^f \eta^f + \eta^f D_t^f \theta^f) = (\boldsymbol{\sigma}_E^f - p_f n^f \mathbf{1}) : \mathbf{l}_f - \text{div} \mathbf{q}^f + k_\theta^s (\theta^s - \theta^f). \quad (4.140)$$

Expansion of the fluid Helmholtz free energy term in Equation (4.140) yields

$$D_t^f \psi^f(\rho^{\text{fR}}, \theta^f) = \frac{\partial \psi^f}{\partial \rho^{\text{fR}}} D_t^f \rho^{\text{fR}} + \frac{\partial \psi^f}{\partial \theta^f} D_t^f \theta^f. \quad (4.141)$$

Making use of Equations (3.34)_{5,7} and Equation (3.41) allows us to write Equation (4.141) as

$$D_t^f \psi^f(\rho^{\text{fR}}, \theta^f) = \frac{p_f}{(\rho^{\text{fR}})^2} D_t^f \rho^{\text{fR}} - \eta^f D_t^f \theta^f. \quad (4.142)$$

Thus, with some simplification of the r.h.s. of Equation (4.140), we may write

$$\rho^f \left(\theta^f D_t^f \eta^f + \frac{p_f}{(\rho^{\text{fR}})^2} D_t^f \rho^{\text{fR}} \right) = \boldsymbol{\sigma}_E^f : \mathbf{d}_f - p_f n^f \operatorname{div} \mathbf{v}_f - \operatorname{div} \mathbf{q}^f + k_\theta^\varepsilon (\theta^s - \theta^f). \quad (4.143)$$

With the assumption that $\mathbf{a}_f = \mathbf{a}_s = \mathbf{a}$, the $\operatorname{div} \mathbf{v}_f$, $\boldsymbol{\sigma}_E^f$, and \mathbf{d}_f terms in Equation (4.143) cannot be explicitly determined, from, e.g., the balance of linear momentum of the pore fluid. For the latter two terms, we will assume the fluid is nearly-inviscid such that $\boldsymbol{\sigma}_E^f \approx \mathbf{0}$. Recall the balance of mass for $\alpha = f$ (Equation (2.9)) with negligible mass supply $\hat{\rho}^f$:

$$D_t^f n^f + \frac{n^f}{\rho^{\text{fR}}} D_t^f \rho^{\text{fR}} + n^f \operatorname{div} \mathbf{v}_f = 0 \rightarrow -n^f p_f \operatorname{div} \mathbf{v}_f = p_f D_t^f n^f + \frac{n^f p_f}{\rho^{\text{fR}}} D_t^f \rho^{\text{fR}}. \quad (4.144)$$

Thus the pore fluid velocity term can be determined given a constitutive model for the pore fluid real mass density. Additionally, the terms on the l.h.s. of Equation (4.143) require a constitutive form for the pore fluid in order to be further simplified.

The ideal gas model. For the ideal gas pore fluid, recall

$$\eta^f = c_V^f \ln \frac{\theta^f}{\theta_0^f} - \mathfrak{R} \ln \frac{\rho^{\text{fR}}}{\rho_0^{\text{fR}}}. \quad (4.145)$$

Then

$$\theta^f D_t^f \eta^f = c_V^f D_t^f \theta^f - \frac{\theta^f \mathfrak{R}}{\rho^{\text{fR}}} D_t^f \rho^{\text{fR}} = c_V^f D_t^f \theta^f - \frac{p_f}{(\rho^{\text{fR}})^2} D_t^f \rho^{\text{fR}}. \quad (4.146)$$

As for the $\operatorname{div} \mathbf{v}_f$ term, recall that for an ideal gas

$$D_t^f \rho^{\text{fR}} = D_t^f \left(\frac{p_f}{\mathfrak{R} \theta^f} \right) = \frac{1}{\mathfrak{R} \theta^f} D_t^f p_f - \frac{p_f}{\mathfrak{R} (\theta^f)^2} D_t^f \theta^f = \frac{\rho^{\text{fR}}}{p_f} D_t^f p_f - \frac{\rho^{\text{fR}}}{\theta^f} D_t^f \theta^f. \quad (4.147)$$

Substitution of Equation (4.147) into Equation (4.144) yields

$$\begin{aligned} -n^f p_f \operatorname{div} \mathbf{v}_f &= p_f D_t^f n^f + \frac{n^f p_f}{\rho^{\text{fR}}} \left(\frac{\rho^{\text{fR}}}{p_f} D_t^f p_f - \frac{\rho^{\text{fR}}}{\theta^f} D_t^f \theta^f \right) \\ &= p_f D_t^f n^f + n^f D_t^f p_f - \frac{n^f p_f}{\theta^f} D_t^f \theta^f. \end{aligned} \quad (4.148)$$

Recognizing

$$D_t^f n^f = -D_t^f n^s \rightarrow D_t^f n^f = -D_t^s n^s + \text{grad}(n^f) \cdot \tilde{\mathbf{v}}_f, \quad (4.149)$$

and utilizing Equation (3.26), we may write

$$D_t^f n^f = \frac{n^s}{J_s} D_t^s J + \text{grad}(n^f) \cdot \tilde{\mathbf{v}}_f. \quad (4.150)$$

Thus, we may write the $\text{div } \mathbf{v}_f$ term as

$$\begin{aligned} -n^f p_f \text{div } \mathbf{v}_f &= \frac{n^s p_f}{J_s} D_t^s J_s + p_f \text{grad}(n^f) \cdot \tilde{\mathbf{v}}_f + n^f (D_t^s p_f + \text{grad}(p_f) \cdot \tilde{\mathbf{v}}_f) \\ &\quad - \frac{n^f p_f}{\theta^f} (D_t^s \theta^f + \text{grad}(\theta^f) \cdot \tilde{\mathbf{v}}_f). \end{aligned} \quad (4.151)$$

Thus, the energy balance for the pore fluid may be written as

$$\begin{aligned} \rho^f (c_V^f + \mathfrak{R}) D_t^s \theta^f + \rho^{\text{fR}} (c_V^f + \mathfrak{R}) \text{grad}(\theta^f) \cdot (n^f \tilde{\mathbf{v}}_f) - \frac{n^s p_f}{J_s} D_t^s J_s - \frac{p_f}{n^f} \text{grad}(n^f) \cdot (n^f \tilde{\mathbf{v}}_f) \\ - n^f D_t^s p_f - \text{grad}(p_f) \cdot (n^f \tilde{\mathbf{v}}_f) + \text{div } \mathbf{q}^f - k_{\theta}^{\varepsilon} (\theta^s - \theta^f) = 0, \end{aligned} \quad (4.152)$$

which we may convert to the reference configuration of the solid skeleton \mathcal{B}_0 (dropping also $(\cdot)_s$ and $(\cdot)^s$ for convenience, where appropriate):

$$\begin{aligned} \rho_0^f (c_V^f + \mathfrak{R}) D_t \theta^f + \rho_0^{\text{fR}} (c_V^f + \mathfrak{R}) \text{GRAD}(\theta^f) \cdot \mathbf{F}^{-1} \cdot (n^f \tilde{\mathbf{v}}_f) - n^s p_f D_t J \\ - \frac{J p_f}{n^f} \text{GRAD}(n^f) \cdot \mathbf{F}^{-1} \cdot (n^f \tilde{\mathbf{v}}_f) - J n^f D_t p_f - J \text{GRAD}(p_f) \cdot \mathbf{F}^{-1} \cdot (n^f \tilde{\mathbf{v}}_f) \\ + J \text{GRAD}(\mathbf{q}^f) : \mathbf{F}^{-T} - J k_{\theta}^{\varepsilon} (\theta^s - \theta^f) = 0. \end{aligned} \quad (4.153)$$

As such, the strong formulation for the balances of linear momenta, mass, and energies, assuming a linear thermoelastic solid constituent and ideal gas pore fluid constituent, may be written as

follows:

$$\begin{aligned}
& \text{Find } \mathbf{u}(\mathbf{X}, t) \in \mathcal{S}^u, p_f(\mathbf{X}, t) \in \mathcal{S}^{p_f}, \\
& \theta^s(\mathbf{X}, t) \in \mathcal{S}^{\theta^s}, \text{ and } \theta^f(\mathbf{X}, t) \in \mathcal{S}^{\theta^f}, \\
& \text{with } t \in [0, T], \text{ such that:} \\
& \quad \text{DIV } \mathbf{P} + \rho_0 \mathbf{g} - \rho_0 \mathbf{a} = \mathbf{0} \in \mathcal{B}_0, \\
& \quad \mathbf{u}(\mathbf{X}, t) = \mathbf{g}^u(\mathbf{X}, t) \text{ on } \Gamma_0^u, \\
& \quad \mathbf{P}(\mathbf{X}, t) \cdot \mathbf{N}(\mathbf{X}) = \mathbf{t}^\sigma(\mathbf{X}, t) \text{ on } \Gamma_0^t, \\
& \quad \mathbf{u}(\mathbf{X}, t = 0) = \mathbf{u}_0(\mathbf{X}) \in \mathcal{B}_0, \\
& \quad \mathbf{v}(\mathbf{X}, t = 0) = \mathbf{v}_0(\mathbf{X}) \in \mathcal{B}_0, \\
& \quad \mathbf{a}(\mathbf{X}, t = 0) = \mathbf{a}_0(\mathbf{X}) \in \mathcal{B}_0, \\
& -\frac{J}{\theta^f} [n^f D_t \theta^f + \text{GRAD}(\theta^f) \cdot \mathbf{F}^{-1} \cdot (n^f \tilde{\mathbf{v}}_f)] + \frac{J n^f}{p_f} D_t p_f + D_t J \\
& \quad + \frac{J}{p_f} \text{GRAD}(p_f) \cdot \mathbf{F}^{-1} \cdot (n^f \tilde{\mathbf{v}}_f) + J \text{GRAD}(n^f \tilde{\mathbf{v}}_f) \cdot \mathbf{F}^{-T} = 0 \in \mathcal{B}_0, \\
& \quad p_f(\mathbf{X}, t) = g^p(\mathbf{X}, t) \text{ on } \Gamma_0^p, \\
& \quad -[J \mathbf{F}^{-1} \cdot (n^f \tilde{\mathbf{v}}_f)] \cdot \mathbf{N} = Q_f^Q(\mathbf{X}, t) \text{ on } \Gamma_0^{Q_f}, \\
& \quad p_f(\mathbf{X}, t = 0) = p_{f,0}(\mathbf{X}) \in \mathcal{B}_0, \\
& \quad \dot{p}_f(\mathbf{X}, t = 0) = \dot{p}_{f,0}(\mathbf{X}) \in \mathcal{B}_0, \\
& \quad \rho_0^s c_V^s D_t \theta^s + \left(\frac{K^{\text{skel}} \alpha_V^s \theta^s}{J} + n^s p_f \frac{\theta^s}{\theta^f} + Q \right) D_t J \\
& \quad \quad + J \text{GRAD}(q^s) \cdot \mathbf{F}^{-T} + J k_\theta^s (\theta^s - \theta^f) \\
& \quad - \frac{J (n^f \tilde{\mathbf{v}}_f)^2}{\dot{k}} + J \frac{\theta^s}{\theta^f} \frac{p_f}{n^f} \text{GRAD}(n^f) \cdot \mathbf{F}^{-1} \cdot (n^f \tilde{\mathbf{v}}_f) = 0 \in \mathcal{B}_0, \\
& \quad \theta^s(\mathbf{X}, t) = g^{\theta^s}(\mathbf{X}, t) \text{ on } \Gamma_0^{\theta^s}, \\
& \quad -(J q^s \cdot \mathbf{F}^{-T}) \cdot \mathbf{N} = Q_s^Q(\mathbf{X}, t) \text{ on } \Gamma_0^{Q_s}, \\
& \quad \theta^s(\mathbf{X}, t = 0) = \theta_0^s(\mathbf{X}) \in \mathcal{B}_0 \\
& \quad \dot{\theta}^s(\mathbf{X}, t = 0) = \dot{\theta}_0^s(\mathbf{X}) \in \mathcal{B}_0 \\
& \quad \rho_0^f (c_V^f + \mathfrak{R}) D_t \theta^f + \rho_0^{\text{FR}} (c_V^f + \mathfrak{R}) \text{GRAD}(\theta^f) \cdot \mathbf{F}^{-1} \cdot (n^f \tilde{\mathbf{v}}_f) \\
& \quad - n^s p_f D_t J - \frac{J p_f}{n^f} \text{GRAD}(n^f) \cdot \mathbf{F}^{-1} \cdot (n^f \tilde{\mathbf{v}}_f) \\
& \quad - J n^f D_t p_f - J \text{GRAD}(p_f) \cdot \mathbf{F}^{-1} \cdot (n^f \tilde{\mathbf{v}}_f) \\
& \quad + J \text{GRAD}(q^f) \cdot \mathbf{F}^{-T} - J k_\theta^s (\theta^s - \theta^f) = 0 \in \mathcal{B}_0 \\
& \quad \theta^f(\mathbf{X}, t) = g^{\theta^f}(\mathbf{X}, t) \text{ on } \Gamma_0^{\theta^f}, \\
& \quad -(J q^f \cdot \mathbf{F}^{-T}) \cdot \mathbf{N} = Q_f^Q(\mathbf{X}, t) \text{ on } \Gamma_0^{Q_f}, \\
& \quad \theta^f(\mathbf{X}, t = 0) = \theta_0^f(\mathbf{X}) \in \mathcal{B}_0 \\
& \quad \dot{\theta}^f(\mathbf{X}, t = 0) = \dot{\theta}_0^f(\mathbf{X}) \in \mathcal{B}_0.
\end{aligned} \tag{S) =} \tag{4.154}$$

Let $\mathcal{G}(u_i, p_f, \theta^s, \theta^f, w_i^u)$ be the variational form of Equations (4.154)₁₋₆ such that

$$\mathcal{G} : \mathcal{S}^u \times \mathcal{S}^{p_f} \times \mathcal{S}^{\theta^s} \times \mathcal{S}^{\theta^f} \times \mathcal{V}^u \rightarrow \mathbb{R}. \tag{4.155}$$

We may then rewrite Equations (4.154)₁₋₆ as

$$\mathcal{G}(u_i, p_f, \theta^s, \theta^f, w_i^u) = \int_{\mathcal{B}_0} w_i^u \rho_0 a_i dV + \int_{\mathcal{B}_0} w_i^u \frac{\partial P_i}{\partial X_I} dV + \int_{\mathcal{B}_0} w_i^u \rho_0 g_i dV = 0. \tag{4.156}$$

Weakening of the first Piola-Kirchhoff stress of the mixture and subsequent decomposition proceeds as before, such that Equation (4.156) is written as

$$\begin{aligned} \mathcal{G}(u_i, p_f, \theta^s, \theta^f, w_i^u) &= \int_{\mathcal{B}_0} w_i^u \rho_0 a_i dV + \int_{\mathcal{B}_0} \frac{\partial w_i^u}{\partial X_I} P_{iI(E)}^s dV \\ &\quad - \int_{\mathcal{B}_0} \frac{\partial w_i^u}{\partial X_I} J p_f F_{Ii}^{-1} \left(\frac{\theta^s}{\theta^f} n^s + n^f \right) dV + \int_{\mathcal{B}_0} w_i^u \rho_0 g_i dV \\ &\quad - \left(\int_{\Gamma_0^t} w_i^u t_i^{\sigma^s} dA - \int_{\Gamma_0^t} w_i^u p_f J F_{Ii}^{-1} \left(\frac{\theta^f}{\theta^s} n^s + n^f \right) N_I dA \right) = 0, \end{aligned} \quad (4.157)$$

where use has been made of the locally inhomogenous temperature first Piola-Kirchhoff stress of the mixture,

$$P_{iI} = P_{iI(E)}^s - J p_f F_{Ii}^{-1} \left(\frac{\theta^s}{\theta^f} n^s + n^f \right). \quad (4.158)$$

Let $\mathcal{H}(u_i, p_f, \theta^s, \theta^f, w^{p_f})$ be the variational form of Equations (4.154)₇₋₁₁ such that

$$\mathcal{H} : \mathcal{S}^{p_f} \times \mathcal{S}^u \times \mathcal{S}^{\theta^s} \times \mathcal{S}^{\theta^f} \times \mathcal{V}^{p_f} \rightarrow \mathbb{R}. \quad (4.159)$$

Since the additional (first) term in Equation (4.154)₇ does not require use of chain rule to weaken, weakening procedure follows from Section 4.1.3, such that we may then rewrite Equations (4.154)₇₋₁₁ as

$$\begin{aligned} \mathcal{H}(u_i, p_f, \theta^s, \theta^f, w^{p_f}) &= - \int_{\mathcal{B}_0} w^{p_f} \frac{J}{\theta^f} \left(n^f D_t \theta^f + \frac{\partial \theta^f}{\partial X_I} F_{Ii}^{-1} (n^f \tilde{v}_{i(f)}) \right) dV \\ &\quad + \int_{\mathcal{B}_0} w^{p_f} \left(\frac{J n^f}{p_f} \dot{p}_f + j \right) dV + \int_{\mathcal{B}_0} w^{p_f} \frac{J}{p_f} \frac{\partial p_f}{\partial X_I} F_{Ii}^{-1} (n^f \tilde{v}_{i(f)}) dV \\ &\quad - \int_{\mathcal{B}_0} \frac{\partial w^{p_f}}{\partial X_I} J (n^f \tilde{v}_{i(f)}) F_{Ii}^{-1} dV - \int_{\Gamma_0^Q} w^{p_f} Q_f dA = 0. \end{aligned} \quad (4.160)$$

Let $\mathcal{J}(u_i, p_f, \theta^s, \theta^f, w^{\theta^s})$ be the variational form of Equations (4.154)₁₂₋₁₆, such that

$$\mathcal{J} : \mathcal{S}^{\theta^s} \times \mathcal{S}^u \times \mathcal{S}^{p_f} \times \mathcal{S}^{\theta^f} \times \mathcal{V}^{\theta^s} \rightarrow \mathbb{R}. \quad (4.161)$$

Then, we may write the variational form of Equations (4.154)_{12–16} as

$$\begin{aligned}
\mathcal{J}(u_i, p_f, \theta^s, \theta^f, w^{\theta^s}) &= \int_{\mathcal{B}_0} w^{\theta^s} \rho_0^s c_V^s D_t \theta^s dV + \int_{\mathcal{B}_0} w^{\theta^s} \left(\frac{K^{\text{skel}} \alpha_V^s \theta^s}{J} + n^s p_f \frac{\theta^s}{\theta^f} + Q \right) D_t J dV \\
&+ \int_{\mathcal{B}_0} w^{\theta^s} J \frac{\partial q_i^s}{\partial X_I} F_{Ii}^{-1} dV + \int_{\mathcal{B}_0} w^{\theta^s} J k_\theta^\varepsilon (\theta^s - \theta^f) dV \\
&- \int_{\mathcal{B}_0} w^{\theta^s} \frac{J (n^f \tilde{v}_f)^2}{\hat{k}} dV + \int_{\mathcal{B}_0} w^{\theta^s} J \frac{\theta^s p_f}{\theta^f n^f} \frac{\partial n^f}{\partial X_I} F_{Ii}^{-1} (n^f \tilde{v}_{i(f)}) dV = 0. \quad (4.162)
\end{aligned}$$

As shown in Section 4.1.2, the gradient of the solid heat flux term may be weakened using chain rule and the Neumann boundary condition given by Equation (4.27)₁₄, such that Equation (4.162) is written as

$$\begin{aligned}
\mathcal{J}(u_i, p_f, \theta^s, \theta^f, w^{\theta^s}) &= \int_{\mathcal{B}_0} w^{\theta^s} \rho_0^s c_V^s D_t \theta^s dV + \int_{\mathcal{B}_0} w^{\theta^s} \left(\frac{K^{\text{skel}} \alpha_V^s \theta^s}{J} + n^s p_f \frac{\theta^s}{\theta^f} + Q \right) D_t J dV \\
&- \int_{\mathcal{B}_0} \frac{\partial w^{\theta^s}}{\partial X_I} J q_i F_{Ii}^{-1} dV + \int_{\mathcal{B}_0} w^{\theta^s} J k_\theta^\varepsilon (\theta^s - \theta^f) dV \\
&- \int_{\mathcal{B}_0} w^{\theta^s} \frac{J (n^f)^2}{\hat{k}} dV + \int_{\mathcal{B}_0} w^{\theta^s} J \frac{\theta^s p_f}{\theta^f n^f} \frac{\partial n^f}{\partial X_I} F_{Ii}^{-1} (n^f \tilde{v}_{i(f)}) dV \\
&- \int_{\Gamma_0^{Q_s^\theta}} w^{\theta^s} Q_s^\theta dA = 0. \quad (4.163)
\end{aligned}$$

Let $\mathcal{K}(u_i, p_f, \theta^s, \theta^f, w^{\theta^f})$ be the variational form of Equations (4.154)_{17–21}, such that

$$\mathcal{K} : \mathcal{S}^{\theta^f} \times \mathcal{S}^u \times \mathcal{S}^{p_f} \times \mathcal{S}^{\theta^s} \times \mathcal{V}^{\theta^f} \rightarrow \mathbb{R}. \quad (4.164)$$

Then, we may write the variational form of Equations (4.154)_{17–21} as

$$\begin{aligned}
\mathcal{K}(u_i, p_f, \theta^s, \theta^f, w^{\theta^f}) &= \int_{\mathcal{B}_0} w^{\theta^f} \rho_0^f (c_V^f + \mathfrak{R}) D_t \theta^f dV \\
&+ \int_{\mathcal{B}_0} w^{\theta^f} \rho_0^{\text{fR}} (c_V^f + \mathfrak{R}) \frac{\partial \theta^f}{\partial X_I} (n^f \tilde{v}_{i(f)}) F_{Ii}^{-1} dV \\
&- \int_{\mathcal{B}_0} w^{\theta^f} n^s p_f D_t J dV - \int_{\mathcal{B}_0} w^{\theta^f} \frac{J p_f}{n^f} \frac{\partial n^f}{\partial X_I} (n^f \tilde{v}_{i(f)}) F_{Ii}^{-1} dV \\
&- \int_{\mathcal{B}_0} w^{\theta^f} J n^f D_t p_f dV - \int_{\mathcal{B}_0} w^{\theta^f} J \frac{\partial p_f}{\partial X_I} (n^f \tilde{v}_{i(f)}) F_{Ii}^{-1} dV \\
&+ \int_{\mathcal{B}_0} w^{\theta^f} J \frac{\partial q_i^f}{\partial X_I} F_{Ii}^{-1} dV - \int_{\mathcal{B}_0} w^{\theta^f} J k_\theta^\varepsilon (\theta^s - \theta^f) dV = 0. \tag{4.165}
\end{aligned}$$

The gradient of the pore fluid heat flux is weakend using chain rule and Equation (4.154)₁₉, such that Equation (4.165) is written as

$$\begin{aligned}
\mathcal{K}(u_i, p_f, \theta^s, \theta^f, w^{\theta^f}) &= \int_{\mathcal{B}_0} w^{\theta^f} \rho_0^f (c_V^f + \mathfrak{R}) D_t \theta^f dV \\
&+ \int_{\mathcal{B}_0} w^{\theta^f} \rho_0^{\text{fR}} (c_V^f + \mathfrak{R}) \frac{\partial \theta^f}{\partial X_I} (n^f \tilde{v}_{i(f)}) F_{Ii}^{-1} dV \\
&- \int_{\mathcal{B}_0} w^{\theta^f} n^s p_f D_t J dV - \int_{\mathcal{B}_0} w^{\theta^f} \frac{J p_f}{n^f} \frac{\partial n^f}{\partial X_I} (n^f \tilde{v}_{i(f)}) F_{Ii}^{-1} dV \\
&- \int_{\mathcal{B}_0} w^{\theta^f} J n^f D_t p_f dV - \int_{\mathcal{B}_0} w^{\theta^f} J \frac{\partial p_f}{\partial X_I} (n^f \tilde{v}_{i(f)}) F_{Ii}^{-1} dV \\
&- \int_{\mathcal{B}_0} \frac{\partial w^{\theta^f}}{\partial X_I} J q_i^f F_{Ii}^{-1} dV - \int_{\mathcal{B}_0} w^{\theta^f} J k_\theta^\varepsilon (\theta^s - \theta^f) dV \\
&- \int_{\Gamma_0^{Q_f^\theta}} w^{\theta^f} Q_f^\theta dA = 0. \tag{4.166}
\end{aligned}$$

The formal statement for the variational forms \mathcal{G} , \mathcal{H} , \mathcal{J} , and \mathcal{K} —assuming nearly-inviscid pore fluid, $\mathbf{a}_f = \mathbf{a}_s = \mathbf{a}$, isotropic thermoelasticity of the solid, and an ideal gas model of the pore

fluid—may be written as follows:

$$\begin{aligned}
\mathcal{W} = & \left\{ \begin{aligned}
& \text{Find } u_i(X_I, t) \in \mathcal{S}^u, p_f(X_I, t) \in \mathcal{S}^{p_f}, \\
& \theta^s(X_I, t) \in \mathcal{S}^{\theta^s}, \text{ and } \theta^f(X_I, t) \in \mathcal{S}^{\theta^f}, \text{ with } t \in [0, T], \text{ such that:} \\
& \int_{\mathcal{B}_0} w_i^u \rho_0 a_i dV + \int_{\mathcal{B}_0} \frac{\partial w_i^u}{\partial X_I} P_{iI(E)}^s dV - \int_{\mathcal{B}_0} \frac{\partial w_i^u}{\partial X_I} J p_f F_{Ii}^{-1} \left(\frac{\theta^s}{\theta^f} n^s + n^f \right) dV \\
& - \int_{\mathcal{B}_0} w_i^u \rho_0 g_i dV - \left(\int_{\Gamma_0^t} w_i^u t_i^{\sigma^E} dA - \int_{\Gamma_0^t} w_i^u p_f J F_{Ii}^{-1} \left(\frac{\theta^s}{\theta^f} n^s + n^f \right) N_I dA \right) = 0, \\
& - \int_{\mathcal{B}_0} w^{p_f} \frac{J}{\theta^f} \left(n^f D_t \theta^f + \frac{\partial \theta^f}{\partial X_I} F_{Ii}^{-1} (n^f \tilde{v}_{i(f)}) \right) dV + \int_{\mathcal{B}_0} w^{p_f} \left(\frac{J n^f}{p_f} \dot{p}_f + \dot{J} \right) dV \\
& + \int_{\mathcal{B}_0} w^{p_f} \frac{J}{p_f} \frac{\partial p_f}{\partial X_I} F_{Ii}^{-1} (n^f \tilde{v}_{i(f)}) dV - \int_{\mathcal{B}_0} \frac{\partial w^{p_f}}{\partial X_I} J (n^f \tilde{v}_{i(f)}) F_{Ii}^{-1} dV - \int_{\Gamma_0^{Q_f}} w^{p_f} Q_f dA = 0, \\
& \int_{\mathcal{B}_0} w^{\theta^s} \rho_0^s c_V^s D_t \theta^s dV + \int_{\mathcal{B}_0} w^{\theta^s} \left(\frac{K^{\text{skel}} \alpha_V^s \theta^s}{J} + n^s p_f \frac{\theta^s}{\theta^f} + Q \right) D_t J dV \\
& - \int_{\mathcal{B}_0} \frac{\partial w^{\theta^s}}{\partial X_I} J q_i F_{Ii}^{-1} dV + \int_{\mathcal{B}_0} w^{\theta^s} J k_\theta^\varepsilon (\theta^s - \theta^f) dV \\
& - \int_{\mathcal{B}_0} w^{\theta^s} \frac{J (n^f \tilde{v}_f)^2}{\hat{k}} dV + \int_{\mathcal{B}_0} w^{\theta^s} J \frac{\theta^s}{\theta^f} \frac{p_f}{n^f} \frac{\partial n^f}{\partial X_I} F_{Ii}^{-1} (n^f \tilde{v}_{i(f)}) dV - \int_{\Gamma_0^{Q_s^\theta}} w^{\theta^s} Q_s^\theta dA = 0, \\
& \int_{\mathcal{B}_0} w^{\theta^f} \rho_0^f (c_V^f + \mathfrak{R}) D_t \theta^f dV + \int_{\mathcal{B}_0} w^{\theta^f} \rho_0^{fR} (c_V^f + \mathfrak{R}) \frac{\partial \theta^f}{\partial X_I} (n^f \tilde{v}_{i(f)}) F_{Ii}^{-1} dV \\
& - \int_{\mathcal{B}_0} w^{\theta^f} n^s p_f D_t J dV - \int_{\mathcal{B}_0} w^{\theta^f} \frac{J p_f}{n^f} \frac{\partial n^f}{\partial X_I} (n^f \tilde{v}_{i(f)}) F_{Ii}^{-1} dV - \int_{\mathcal{B}_0} w^{\theta^f} J n^f D_t p_f dV \\
& - \int_{\mathcal{B}_0} w^{\theta^f} J \frac{\partial p_f}{\partial X_I} (n^f \tilde{v}_{i(f)}) F_{Ii}^{-1} dV - \int_{\mathcal{B}_0} \frac{\partial w^{\theta^f}}{\partial X_I} J q_i^f F_{Ii}^{-1} dV - \int_{\mathcal{B}_0} w^{\theta^f} J k_\theta^\varepsilon (\theta^s - \theta^f) dV \\
& - \int_{\Gamma_0^{Q_f^\theta}} w^{\theta^f} Q_f^\theta dA = 0 \\
& \text{holds } \forall w_i^u \in \mathcal{V}^u, \forall w^{p_f} \in \mathcal{V}^{p_f}, w^{\theta^s} \in \mathcal{V}^{\theta^s}, \text{ and } w^{\theta^f} \in \mathcal{V}^{\theta^f} \text{ with} \\
& \mathcal{S}^u = (u_i : \mathcal{B}_0 \times [0, T] \rightarrow \mathbb{R}^3, u_i \in H^1, u_i(t) = g_i^u(t) \text{ on } \Gamma_0^u, u_i(X_I, t = 0) = u_{i,0}(X_I)), \\
& \mathcal{S}^{p_f} = (p_f : \mathcal{B}_0 \times [0, T] \rightarrow \mathbb{R}, p_f \in H^1, p_f(t) = g^p(t) \text{ on } \Gamma_0^p, p_f(X_I, t = 0) = p_{f,0}(X_I)), \\
& \mathcal{S}^{\theta^s} = (\theta^s : \mathcal{B}_0 \times [0, T] \rightarrow \mathbb{R}, \theta^s \in H^1, \theta^s(t) = g^{\theta^s} \text{ on } \Gamma_0^{\theta^s}, \theta^s(X_I, t = 0) = \theta_0^s(X_I)), \\
& \mathcal{S}^{\theta^f} = (\theta^f : \mathcal{B}_0 \times [0, T] \rightarrow \mathbb{R}, \theta^f \in H^1, \theta^f(t) = g^{\theta^f} \text{ on } \Gamma_0^{\theta^f}, \theta^f(X_I, t = 0) = \theta_0^f(X_I)), \\
& \mathcal{V}^u = (w_i^u : \mathcal{B}_0 \rightarrow \mathbb{R}^3, w_i^u \in H^1, w_i^u(t) = 0 \text{ on } \Gamma_0^u), \\
& \mathcal{V}^{p_f} = (w^{p_f} : \mathcal{B}_0 \rightarrow \mathbb{R}, w^{p_f} \in H^1, w^{p_f}(t) = 0 \text{ on } \Gamma_0^p), \\
& \mathcal{V}^{\theta^s} = (w^{\theta^s} : \mathcal{B}_0 \rightarrow \mathbb{R}, w^{\theta^s} \in H^1, w^{\theta^s}(t) = 0 \text{ on } \Gamma_0^{\theta^s}), \\
& \mathcal{V}^{\theta^f} = (w^{\theta^f} : \mathcal{B}_0 \rightarrow \mathbb{R}, w^{\theta^f} \in H^1, w^{\theta^f}(t) = 0 \text{ on } \Gamma_0^{\theta^f}).
\end{aligned} \right. \tag{4.167}
\end{aligned}$$

In the FE implementation that follows, it behooves us to simplify the variational forms, such that

$$\begin{aligned}
\mathcal{G} &= \mathcal{G}_1^{\text{INT}} + \mathcal{G}_2^{\text{INT}} + \mathcal{G}_3^{\text{INT}} + \mathcal{G}_4^{\text{INT}} + \mathcal{G}_1^{\text{EXT}} + \mathcal{G}_2^{\text{EXT}} = 0, \\
\mathcal{H} &= \mathcal{H}_1^{\text{INT}} + \mathcal{H}_2^{\text{INT}} + \mathcal{H}_3^{\text{INT}} + \mathcal{H}_4^{\text{INT}} + \mathcal{H}_6^{\text{INT}} + \mathcal{H}_7^{\text{INT}} + \mathcal{H}^{\text{EXT}} = 0, \\
\mathcal{J} &= \mathcal{J}_1^{\text{INT}} + \mathcal{J}_2^{\text{INT}} + \mathcal{J}_3^{\text{INT}} + \mathcal{J}_4^{\text{INT}} + \mathcal{J}_5^{\text{INT}} + \mathcal{J}_6^{\text{INT}} + \mathcal{J}^{\text{EXT}} = 0, \\
\mathcal{K} &= \mathcal{K}_1^{\text{INT}} + \mathcal{K}_2^{\text{INT}} + \mathcal{K}_3^{\text{INT}} + \mathcal{K}_4^{\text{INT}} + \mathcal{K}_5^{\text{INT}} + \mathcal{K}_6^{\text{INT}} + \mathcal{K}_7^{\text{INT}} + \mathcal{K}_8^{\text{INT}} + \mathcal{K}^{\text{EXT}} = 0,
\end{aligned} \tag{4.168}$$

wherein

$$\begin{aligned}
\mathcal{G}_1^{\text{INT}} &= \int_{\mathcal{B}_0} w_i^u \rho_0 a_i dV, \\
\mathcal{G}_2^{\text{INT}} &= \int_{\mathcal{B}_0} \frac{\partial w_i^u}{\partial X_I} P_{iI}^s(E) dV, \\
\mathcal{G}_3^{\text{INT}} &= - \int_{\mathcal{B}_0} \frac{\partial w_i^u}{\partial X_I} J p_f F_{Ii}^{-1} \left(\frac{\theta^s}{\theta^f} n^s + n^f \right) dV, \\
\mathcal{G}_4^{\text{INT}} &= - \int_{\mathcal{B}_0} w_i^u \rho_0 g_i dV, \\
\mathcal{G}_1^{\text{EXT}} &= \int_{\Gamma_0^t} w_i^u t_i^{\sigma^s} dA, \\
\mathcal{G}_2^{\text{EXT}} &= - \int_{\Gamma_0^t} w_i^u J p_f F_{Ii} \left(\frac{\theta^s}{\theta^f} n^s + n^f \right) N_I dA,
\end{aligned} \tag{4.169}$$

and

$$\begin{aligned}
\mathcal{H}_1^{\text{INT}} &= \int_{\mathcal{B}_0} w^{p_f} \left(\frac{J n^f}{p_f} \dot{p}_f + j \right) dV, \\
\mathcal{H}_2^{\text{INT}} &= \int_{\mathcal{B}_0} w^{p_f} \frac{J}{p_f} \frac{\partial p_f}{\partial X_I} F_{Ii}^{-1} (n^f \tilde{v}_{i(f)}) dV, \\
\mathcal{H}_3^{\text{INT}} &= \int_{\mathcal{B}_0} \frac{\partial w^{p_f}}{\partial X_I} J F_{Ii}^{-1} \hat{k} \frac{\partial p_f}{\partial X_K} F_{Ki}^{-1} dV, \\
\mathcal{H}_4^{\text{INT}} &= \int_{\mathcal{B}_0} \frac{\partial w^{p_f}}{\partial X_I} J F_{Ii}^{-1} \hat{k} \rho^{\text{fR}} (a_i - g_i) dV, \\
\mathcal{H}_6^{\text{INT}} &= \int_{\mathcal{B}_0} \frac{\partial w^{p_f}}{\partial X_I} J F_{Ii}^{-1} \frac{\hat{k}}{n^f p_f} \frac{\partial n^f}{\partial X_K} F_{Ki}^{-1} \left(1 - \frac{\theta^s}{\theta^f} \right) dV, \\
\mathcal{H}_7^{\text{INT}} &= - \int_{\mathcal{B}_0} w^{p_f} \frac{J}{\theta^f} \left(n^f D_t \theta^f + \frac{\partial \theta^f}{\partial X_I} F_{Ii}^{-1} (n^f \tilde{v}_{i(f)}) \right) dV, \\
\mathcal{H}^{\text{EXT}} &= \int_{\Gamma_0^{Q_f}} w^{p_f} Q_f dA,
\end{aligned} \tag{4.170}$$

and

$$\begin{aligned}
\mathcal{J}_1^{\text{INT}} &= \int_{\mathcal{B}_0} w^{\theta^s} \rho_0^s c_V^s D_t \theta^s dV, \\
\mathcal{J}_2^{\text{INT}} &= \int_{\mathcal{B}_0} w^{\theta^s} \left(\frac{K^{\text{skel}} \alpha_V^s \theta^s}{J} + n^s p_f \frac{\theta^s}{\theta^f} + Q \right) D_t J dV, \\
\mathcal{J}_3^{\text{INT}} &= - \int_{\mathcal{B}_0} \frac{\partial w^{\theta^s}}{\partial X_I} J q_i^s F_{Ii}^{-1} dV, \\
\mathcal{J}_4^{\text{INT}} &= \int_{\mathcal{B}_0} w^{\theta^s} J k_{\theta}^s (\theta^s - \theta^f) dV, \\
\mathcal{J}_5^{\text{INT}} &= - \int_{\mathcal{B}_0} w^{\theta^s} \frac{J (n^f \tilde{v}_f)^2}{\hat{k}} dV, \\
\mathcal{J}_6^{\text{INT}} &= \int_{\mathcal{B}_0} w^{\theta^s} J \frac{\theta^s}{\theta^f} \frac{p_f}{n^f} \frac{\partial n^f}{\partial X_I} F_{Ii}^{-1} (n^f \tilde{v}_{i(f)}) dV, \\
\mathcal{J}^{\text{EXT}} &= - \int_{\Gamma_0^{Q_s}} w^{\theta^s} Q_s^\theta dA,
\end{aligned} \tag{4.171}$$

and

$$\begin{aligned}
\mathcal{K}_1^{\text{INT}} &= \int_{\mathcal{B}_0} w^{\theta^f} \rho_0^f (c_V^f + \mathfrak{R}) D_t \theta^f dV \\
\mathcal{K}_2^{\text{INT}} &= \int_{\mathcal{B}_0} w^{\theta^f} \rho_0^{\text{fR}} (c_V^f + \mathfrak{R}) \frac{\partial \theta^f}{\partial X_I} (n^f \tilde{v}_{i(f)}) F_{Ii}^{-1} dV, \\
\mathcal{K}_3^{\text{INT}} &= - \int_{\mathcal{B}_0} w^{\theta^f} n^s p_f D_t J dV, \\
\mathcal{K}_4^{\text{INT}} &= - \int_{\mathcal{B}_0} w^{\theta^f} \frac{J p_f}{n^f} \frac{\partial n^f}{\partial X_I} (n^f \tilde{v}_{i(f)}) F_{Ii}^{-1} dV, \\
\mathcal{K}_5^{\text{INT}} &= - \int_{\mathcal{B}_0} w^{\theta^f} J n^f D_t p_f dV, \\
\mathcal{K}_6^{\text{INT}} &= - \int_{\mathcal{B}_0} w^{\theta^f} J \frac{\partial p_f}{\partial X_I} (n^f \tilde{v}_{i(f)}) F_{Ii}^{-1} dV, \\
\mathcal{K}_7^{\text{INT}} &= - \int_{\mathcal{B}_0} \frac{\partial w^{\theta^f}}{\partial X_I} J q_i^f F_{Ii}^{-1} dV, \\
\mathcal{K}_8^{\text{INT}} &= - \int_{\mathcal{B}_0} w^{\theta^f} J k_\theta^\varepsilon (\theta^s - \theta^f) dV, \\
\mathcal{K}^{\text{EXT}} &= - \int_{\Gamma_0^{Q_f^\theta}} w^{\theta^f} Q_f^\theta dA.
\end{aligned} \tag{4.172}$$

In the case of 1-D uniaxial strain, i.e., the underlying assumption for the proceeding FE model, the above terms simplify to the following:

$$\begin{aligned}
\mathcal{G}_1^{\text{INT}} &= \int_0^{X=H} w^u \rho_0 a A dX, \\
\mathcal{G}_2^{\text{INT}} &= \int_0^{X=H} \frac{\partial w^u}{\partial X} P_{11(E)}^s A dX, \\
\mathcal{G}_3^{\text{INT}} &= - \int_0^{X=H} \frac{\partial w^u}{\partial X} p_f \left(\frac{\theta^s}{\theta^f} n^s + n^f \right) A dX, \\
\mathcal{G}_4^{\text{INT}} &= \int_0^{X=H} w^u \rho_0 g A dX, \\
\mathcal{G}_1^{\text{EXT}} &= \int_{\Gamma_0^t} w^u t^{\sigma_E^s} dA = t^{\sigma_E^s} A, \\
\mathcal{G}_2^{\text{EXT}} &= - \int_{\Gamma_0^t} w^u p_f \left(\frac{\theta^s}{\theta^f} n^s + n^f \right) dA = p_f \left(\frac{\theta^s}{\theta^f} n^s + n^f \right) A,
\end{aligned} \tag{4.173}$$

and

$$\begin{aligned}
\mathcal{H}_1^{\text{INT}} &= \int_0^{X=H} w^{p_f} \left(\frac{J n^f}{p_f} \dot{p}_f + \dot{J} \right) A dX, \\
\mathcal{H}_2^{\text{INT}} &= \int_0^{X=H} w^{p_f} \frac{1}{p_f} \frac{\partial p_f}{\partial X} (n^f \tilde{v}_f) A dX, \\
\mathcal{H}_3^{\text{INT}} &= \int_0^{X=H} \frac{\partial w^{p_f}}{\partial X} \hat{k} \frac{\partial p_f}{\partial X} F_{11}^{-1} A dX, \\
\mathcal{H}_4^{\text{INT}} &= \int_0^{X=H} \frac{\partial w^{p_f}}{\partial X} \hat{k} \rho^{\text{fR}} (a + g) A dX, \\
\mathcal{H}_6^{\text{INT}} &= \int_0^{X=H} \frac{\partial w^{p_f}}{\partial X} \frac{\hat{k}}{n^f p_f} \frac{\partial n^f}{\partial X} F_{11}^{-1} \left(1 - \frac{\theta^s}{\theta^f} \right) A dX, \\
\mathcal{H}_7^{\text{INT}} &= - \int_0^{X=H} w^{p_f} \frac{J}{\theta^f} \left(n^f D_t \theta^f + \frac{\partial \theta^f}{\partial X} (n^f \tilde{v}_f) F_{11}^{-1} \right) A dX, \\
\mathcal{H}^{\text{EXT}} &= \int_{\Gamma_0^{Q_f}} w^{p_f} Q_f dA = Q_f A,
\end{aligned} \tag{4.174}$$

and

$$\begin{aligned}
\mathcal{J}_1^{\text{INT}} &= \int_0^{X=H} w^{\theta^s} \rho_0^s c_V^s D_t \theta^s A dX, \\
\mathcal{J}_2^{\text{INT}} &= \int_0^{X=H} w^{\theta^s} \left(\frac{K^{\text{skel}} \alpha_V^s \theta^s}{J} + n^s p_f \frac{\theta^s}{\theta^f} + Q \right) D_t J A dX, \\
\mathcal{J}_3^{\text{INT}} &= - \int_0^{X=H} \frac{\partial w^{\theta^s}}{\partial X} q^s A dX, \\
\mathcal{J}_4^{\text{INT}} &= \int_0^{X=H} w^{\theta^s} J k_\theta^s (\theta^s - \theta^f) A dX, \\
\mathcal{J}_5^{\text{INT}} &= - \int_0^{X=H} w^{\theta^s} \frac{J (n^f \tilde{v}_f)^2}{\hat{k}} A dX, \\
\mathcal{J}_6^{\text{INT}} &= \int_0^{X=H} w^{\theta^s} \frac{\theta^s p_f}{\theta^f n^f} \frac{\partial n^f}{\partial X} (n^f \tilde{v}_f) A dX, \\
\mathcal{J}^{\text{EXT}} &= - \int_{\Gamma_0^{Q_s^\theta}} w^{\theta^s} Q_s^\theta dA = Q_s^\theta A,
\end{aligned} \tag{4.175}$$

and

$$\begin{aligned}
\mathcal{K}_1^{\text{INT}} &= \int_0^{X=H} w^{\theta^f} \rho_0^f (c_V^f + \mathfrak{R}) D_t \theta^f A dX, \\
\mathcal{K}_2^{\text{INT}} &= \int_0^{X=H} w^{\theta^f} \rho^{\text{fR}} (c_V^f + \mathfrak{R}) \frac{\partial \theta^f}{\partial X} (n^f \tilde{v}_f) A dX, \\
\mathcal{K}_3^{\text{INT}} &= - \int_0^{X=H} w^{\theta^f} n^s p_f D_t J A dX, \\
\mathcal{K}_4^{\text{INT}} &= - \int_0^{X=H} w^{\theta^f} \frac{p_f}{n^f} \frac{\partial n^f}{\partial X} (n^f \tilde{v}_f) A dX, \\
\mathcal{K}_5^{\text{INT}} &= - \int_0^{X=H} w^{\theta^f} J n^f D_t p_f A dX, \\
\mathcal{K}_6^{\text{INT}} &= - \int_0^{X=H} w^{\theta^f} \frac{\partial p_f}{\partial X} (n^f \tilde{v}_f) A dX, \\
\mathcal{K}_7^{\text{INT}} &= - \int_0^{X=H} \frac{\partial w^{\theta^f}}{\partial X} q^f A dX, \\
\mathcal{K}_8^{\text{INT}} &= - \int_0^{X=H} w^{\theta^f} J k_\theta^\varepsilon (\theta^s - \theta^f) A dX, \\
\mathcal{K}^{\text{EXT}} &= - \int_{\Gamma_0^{Q_f^\theta}} w^{\theta^f} Q_f^\theta dA = Q_f^\theta A.
\end{aligned} \tag{4.176}$$

The compressible liquid model. For the compressible liquid pore fluid, recall

$$\eta^f = c_V^f \ln \left(\frac{\theta^f}{\theta_0^f} \right) + \frac{K_f^\theta \alpha_V^f}{\rho^{\text{fR}}}. \tag{4.177}$$

Then,

$$\rho^f \theta^f D_t^f \eta^f = \rho^f c_V^f D_t^f \theta^f - \frac{n^f \theta^f K_f^\theta \alpha_V^f}{\rho^{\text{fR}}} D_t^f \rho^{\text{fR}}, \tag{4.178}$$

where

$$D_t^f \rho^{\text{fR}} = \rho^{\text{fR}} \left(\frac{1}{K_f^\theta} D_t^f p_f - \alpha_V^f D_t^f \theta^f \right), \tag{4.179}$$

such that

$$\rho^f \theta^f D_t^f \eta^f = (\rho^f c_V^f + n^f \theta^f K_f^\theta [\alpha_V^f]^2) D_t^f \theta^f - n^f \theta^f \alpha_V^f D_t^f p_f. \quad (4.180)$$

From Equation (4.144)₂, we know that

$$-n^f p_f \operatorname{div} \mathbf{v}_f = p_f D_t^f n^f + \frac{n^f p_f}{\rho^{\text{fR}}} D_t^f \rho^{\text{fR}}, \quad (4.181)$$

and from the second term in Equation (4.143),

$$\rho^f \frac{p_f}{(\rho^{\text{fR}})^2} D_t^f \rho^{\text{fR}} = \frac{n^f p_f}{\rho^{\text{fR}}} D_t^f \rho^{\text{fR}}, \quad (4.182)$$

such that when the fluid stress power term (Equation (4.181)) is added to the l.h.s. of Equation (4.143), the terms containing the material time derivative of the pore fluid real mass densities will cancel, such that the pore fluid energy balance for the compressible liquid may be written as (making use of Equations (4.150) and Equation (4.151)):

$$\begin{aligned} & (\rho^f c_V^f + n^f \theta^f K_f^\theta [\alpha_V^f]^2) (D_t^s \theta^f + \operatorname{grad}(\theta^f) \cdot \tilde{\mathbf{v}}_f) - n^f \theta^f \alpha_V^f (D_t^s p_f + \operatorname{grad}(p_f) \cdot \tilde{\mathbf{v}}_f) - \frac{n^s p_f}{J_s} D_t^s J_s \\ & - \frac{p_f}{n^f} \operatorname{grad}(n^f) \cdot (n^f \tilde{\mathbf{v}}_f) + \operatorname{div} \mathbf{q}^f - k_\theta^\varepsilon (\theta^s - \theta^f) = 0, \end{aligned} \quad (4.183)$$

which equates to

$$\begin{aligned} & (\rho^f c_V^f + n^f \theta^f K_f^\theta [\alpha_V^f]^2) D_t^s \theta^f + (\rho^{\text{fR}} c_V^f + \theta^f K_f^\theta [\alpha_V^f]^2) \operatorname{grad}(\theta^f) \cdot (n^f \tilde{\mathbf{v}}_f) - n^f \theta^f \alpha_V^f D_t^s p_f \\ & - \theta^f \alpha_V^f \operatorname{grad}(p_f) \cdot (n^f \tilde{\mathbf{v}}_f) - \frac{n^s p_f}{J_s} D_t^s J_s - \frac{p_f}{n^f} \operatorname{grad}(n^f) \cdot (n^f \tilde{\mathbf{v}}_f) + \operatorname{div} \mathbf{q}^f - k_\theta^\varepsilon (\theta^s - \theta^f) = 0. \end{aligned} \quad (4.184)$$

Upon inspection of Equation (4.184), substitution of $\alpha_V^f := 1/\theta^f$ and $K_f^\theta := p_f$ for an ideal gas allows us to recover Equation (4.152).² Conversion of Equation (4.184) to the reference configuration \mathcal{B}_0 (dropping also $(\cdot)_s$ and $(\cdot)^s$ for convenience, where appropriate) yields:

$$\begin{aligned} & (\rho_0^f c_V^f + J n^f \theta^f K_f^\theta [\alpha_V^f]^2) D_t \theta^f + (\rho_0^{\text{fR}} c_V^f + J \theta^f K_f^\theta [\alpha_V^f]^2) \operatorname{GRAD}(\theta^f) \cdot \mathbf{F}^{-1} \cdot (n^f \tilde{\mathbf{v}}_f) \\ & - J n^f \theta^f \alpha_V^f D_t p_f - J \theta^f \alpha_V^f \operatorname{GRAD}(p_f) \cdot \mathbf{F}^{-1} \cdot (n^f \tilde{\mathbf{v}}_f) - n^s p_f D_t J \\ & - \frac{J p_f}{n^f} \operatorname{GRAD}(n^f) \cdot \mathbf{F}^{-1} \cdot (n^f \tilde{\mathbf{v}}_f) + J \operatorname{GRAD}(\mathbf{q}^f) : \mathbf{F}^{-T} - J k_\theta^\varepsilon (\theta^s - \theta^f) = 0. \end{aligned} \quad (4.185)$$

² Recall that $\rho^{\text{fR}} \mathfrak{R} = \frac{p_f}{\theta^f}$, such that $n^f \rho^{\text{fR}} \mathfrak{R} = \rho^f \mathfrak{R} = \frac{n^f p_f}{\theta^f}$, the last of which is equivalent to $n^f \theta^f K_f^\theta (\alpha_V^f)^2$ when the definitions $\alpha_V^f := 1/\theta^f$ and $K_f^\theta := p_f$ are used.

As such, the strong formulation for the balances of linear momenta, mass, and energies, assuming a linear thermoelastic solid constituent and a compressible liquid pore fluid constituent, may be written as follows:

$$\begin{aligned}
 (\mathcal{S}) = \left\{ \begin{array}{l}
 \text{Find } \mathbf{u}(\mathbf{X}, t) \in \mathcal{S}^u, p_f(\mathbf{X}, t) \in \mathcal{S}^{p_f}, \\
 \theta^s(\mathbf{X}, t) \in \mathcal{S}^{\theta^s}, \text{ and } \theta^f(\mathbf{X}, t) \in \mathcal{S}^{\theta^f}, \\
 \text{with } t \in [0, T], \text{ such that:} \\
 \text{DIV } \mathbf{P} + \rho_0 \mathbf{g} - \rho_0 \mathbf{a} = \mathbf{0} \in \mathcal{B}_0, \\
 \mathbf{u}(\mathbf{X}, t) = \mathbf{g}^u(\mathbf{X}, t) \text{ on } \Gamma_0^u, \\
 \mathbf{P}(\mathbf{X}, t) \cdot \mathbf{N}(\mathbf{X}) = \mathbf{t}^\sigma(\mathbf{X}, t) \text{ on } \Gamma_0^\sigma, \\
 \mathbf{u}(\mathbf{X}, t = 0) = \mathbf{u}_0(\mathbf{X}) \in \mathcal{B}_0, \\
 \mathbf{v}(\mathbf{X}, t = 0) = \mathbf{v}_0(\mathbf{X}) \in \mathcal{B}_0, \\
 \mathbf{a}(\mathbf{X}, t = 0) = \mathbf{a}_0(\mathbf{X}) \in \mathcal{B}_0, \\
 -J\alpha_V^f [n^f D_t \theta^f + \text{GRAD}(\theta^f) \cdot \mathbf{F}^{-1} \cdot (n^f \tilde{\mathbf{v}}_f)] + \frac{Jn^f}{K_f^\theta} D_t p_f + D_t J \\
 + \frac{J}{K_f^\theta} \text{GRAD}(p_f) \cdot \mathbf{F}^{-1} \cdot (n^f \tilde{\mathbf{v}}_f) + J \text{GRAD}(n^f \tilde{\mathbf{v}}_f) \cdot \mathbf{F}^{-T} = 0 \in \mathcal{B}_0, \\
 p_f(\mathbf{X}, t) = g^p(\mathbf{X}, t) \text{ on } \Gamma_0^p, \\
 -[J\mathbf{F}^{-1} \cdot (n^f \tilde{\mathbf{v}}_f)] \cdot \mathbf{N} = Q_f^Q(\mathbf{X}, t) \text{ on } \Gamma_0^{Q_f}, \\
 p_f(\mathbf{X}, t = 0) = p_{f,0}(\mathbf{X}) \in \mathcal{B}_0, \\
 \dot{p}_f(\mathbf{X}, t = 0) = \dot{p}_{f,0}(\mathbf{X}) \in \mathcal{B}_0, \\
 \rho_0^s c_V^s D_t \theta^s + \left(\frac{K^{\text{ske1}} \alpha_V^s \theta^s}{J} + n^s p_f \frac{\theta^s}{\theta^f} + Q \right) D_t J \\
 + J \text{GRAD}(q^s) \cdot \mathbf{F}^{-T} + J k_\theta^s (\theta^s - \theta^f) \\
 + \frac{J(n^f \tilde{\mathbf{v}}_f)^2}{\hat{k}} + J \frac{\theta^s p_f}{\theta^f n^f} \text{GRAD}(n^f) \cdot \mathbf{F}^{-1} \cdot (n^f \tilde{\mathbf{v}}_f) = 0 \in \mathcal{B}_0, \\
 \theta^s(\mathbf{X}, t) = g^{\theta^s}(\mathbf{X}, t) \text{ on } \Gamma_0^{\theta^s}, \\
 -(Jq^s \cdot \mathbf{F}^{-T}) \cdot \mathbf{N} = Q_0^\theta(\mathbf{X}, t) \text{ on } \Gamma_0^{Q_0^\theta}, \\
 \theta^s(\mathbf{X}, t = 0) = \theta_0^s(\mathbf{X}) \in \mathcal{B}_0 \\
 \dot{\theta}^s(\mathbf{X}, t = 0) = \dot{\theta}_0^s(\mathbf{X}) \in \mathcal{B}_0 \\
 (\rho_0^f c_V^f + Jn^f \theta^f K_f^\theta [\alpha_V^f]^2) D_t \theta^f + (\rho_0^{\text{fR}} c_V^f + J\theta^f K_f^\theta [\alpha_V^f]^2) \text{GRAD}(\theta^f) \cdot \mathbf{F}^{-1} \cdot (n^f \tilde{\mathbf{v}}_f) \\
 - n^s p_f D_t J - \frac{J p_f}{n^f} \text{GRAD}(n^f) \cdot \mathbf{F}^{-1} \cdot (n^f \tilde{\mathbf{v}}_f) \\
 - J n^f D_t p_f - J \text{GRAD}(p_f) \cdot \mathbf{F}^{-1} \cdot (n^f \tilde{\mathbf{v}}_f) \\
 + J \text{GRAD}(q^f) \cdot \mathbf{F}^{-T} - J k_\theta^s (\theta^s - \theta^f) = 0 \in \mathcal{B}_0 \\
 \theta^f(\mathbf{X}, t) = g^{\theta^f}(\mathbf{X}, t) \text{ on } \Gamma_0^{\theta^f}, \\
 -(Jq^f \cdot \mathbf{F}^{-T}) \cdot \mathbf{N} = Q_f^\theta(\mathbf{X}, t) \text{ on } \Gamma_0^{Q_f^\theta}, \\
 \theta^f(\mathbf{X}, t = 0) = \theta_0^f(\mathbf{X}) \in \mathcal{B}_0 \\
 \dot{\theta}^f(\mathbf{X}, t = 0) = \dot{\theta}_0^f(\mathbf{X}) \in \mathcal{B}_0.
 \end{array} \right. \tag{4.186}
 \end{aligned}$$

Let $\mathcal{G}(u_i, p_f, \theta^s, \theta^f, w_i^u)$ be the variational form of Equations (4.186)_{1–6} such that

$$\mathcal{G} : \mathcal{S}^u \times \mathcal{S}^{p_f} \times \mathcal{S}^{\theta^s} \times \mathcal{S}^{\theta^f} \times \mathcal{V}^u \rightarrow \mathbb{R}, \tag{4.187}$$

and let $\mathcal{J}(u_i, p_f, \theta^s, \theta^f, w^{\theta^s})$ be the variational form of Equations (4.186)_{12–16}, such that

$$\mathcal{J} : \mathcal{S}^{\theta^s} \times \mathcal{S}^u \times \mathcal{S}^{p_f} \times \mathcal{S}^{\theta^f} \times \mathcal{V}^{\theta^s} \rightarrow \mathbb{R}. \tag{4.188}$$

The variational forms for the mixture momentum balance and the solid energy balance remain unchanged from the ideal gas pore fluid model—refer to the previous section for details. Let $\mathcal{H}(u_i, p_f, \theta^s, \theta^f, w^{p_f})$ be the variational form of Equations (4.186)_{7–11} such that

$$\mathcal{H} : \mathcal{S}^{p_f} \times \mathcal{S}^u \times \mathcal{S}^{\theta^s} \times \mathcal{S}^{\theta^f} \times \mathcal{V}^{p_f} \rightarrow \mathbb{R}. \quad (4.189)$$

This variational form changes slightly from the previous section in that the pore fluid volumetric CTE and pore fluid isothermal bulk modulus may not be replaced by the inverse pore fluid temperature or pore fluid pressure, respectively. Therefore,

$$\begin{aligned} \mathcal{H}(u_i, p_f, \theta^s, \theta^f, w^{p_f}) = & - \int_{\mathcal{B}_0} w^{p_f} J \alpha_V^f \left(n^f D_t \theta^f + \frac{\partial \theta^f}{\partial X_I} F_{Ii}^{-1} (n^f \tilde{v}_{i(f)}) \right) dV \\ & + \int_{\mathcal{B}_0} w^{p_f} \left(\frac{J n^f}{K_f^\theta} \dot{p}_f + j \right) dV + \int_{\mathcal{B}_0} w^{p_f} \frac{J}{K_f^\theta} \frac{\partial p_f}{\partial X_I} F_{Ii}^{-1} (n^f \tilde{v}_{i(f)}) dV \\ & - \int_{\mathcal{B}_0} \frac{\partial w^{p_f}}{\partial X_I} J (n^f \tilde{v}_{i(f)}) F_{Ii}^{-1} dV - \int_{\Gamma_0^Q} w^{p_f} Q_f dA = 0. \end{aligned} \quad (4.190)$$

Let $\mathcal{K}(u_i, p_f, \theta^s, \theta^f, w^{\theta^f})$ be the variational form of Equations (4.186)_{17–21}, such that

$$\mathcal{K} : \mathcal{S}^{\theta^f} \times \mathcal{S}^u \times \mathcal{S}^{p_f} \times \mathcal{S}^{\theta^s} \times \mathcal{V}^{\theta^f} \rightarrow \mathbb{R}. \quad (4.191)$$

Then, we may write the variational form of Equations (4.186)_{17–21} as

$$\begin{aligned} \mathcal{K}(u_i, p_f, \theta^s, \theta^f, w^{\theta^f}) = & \int_{\mathcal{B}_0} w^{\theta^f} (\rho_0^f c_V^f + J n^f \theta^f K_f^\theta [\alpha_V^f]^2) D_t \theta^f dV \\ & + \int_{\mathcal{B}_0} w^{\theta^f} (\rho_0^{\text{fR}} c_V^f + J \theta^f K_f^\theta [\alpha_V^f]^2) \frac{\partial \theta^f}{\partial X_I} (n^f \tilde{v}_{i(f)}) F_{Ii}^{-1} dV \\ & - \int_{\mathcal{B}_0} w^{\theta^f} n^s p_f D_t J dV - \int_{\mathcal{B}_0} w^{\theta^f} \frac{J p_f}{n^f} \frac{\partial n^f}{\partial X_I} (n^f \tilde{v}_{i(f)}) F_{Ii}^{-1} dV \\ & - \int_{\mathcal{B}_0} w^{\theta^f} J n^f D_t p_f dV - \int_{\mathcal{B}_0} w^{\theta^f} J \frac{\partial p_f}{\partial X_I} (n^f \tilde{v}_{i(f)}) F_{Ii}^{-1} dV \\ & + \int_{\mathcal{B}_0} w^{\theta^f} J \frac{\partial q_i^f}{\partial X_I} F_{Ii}^{-1} dV - \int_{\mathcal{B}_0} w^{\theta^f} J k_\theta^\varepsilon (\theta^s - \theta^f) dV = 0. \end{aligned} \quad (4.192)$$

The gradient of the pore fluid heat flux is weakend using chain rule and Equation (4.186)₁₉, such that Equation (4.192) is written as

$$\begin{aligned}
\mathcal{K}(u_i, p_f, \theta^s, \theta^f, w^{\theta^f}) &= \int_{\mathcal{B}_0} w^{\theta^f} (\rho_0^f c_V^f + J n^f \theta^f K_f^\theta [\alpha_V^f]^2) D_t \theta^f dV \\
&+ \int_{\mathcal{B}_0} w^{\theta^f} (\rho_0^{\text{fR}} c_V^f + J \theta^f K_f^\theta [\alpha_V^f]^2) \frac{\partial \theta^f}{\partial X_I} (n^f \tilde{v}_{i(t)}) F_{Ii}^{-1} dV \\
&- \int_{\mathcal{B}_0} w^{\theta^f} n^s p_f D_t J dV - \int_{\mathcal{B}_0} w^{\theta^f} \frac{J p_f}{n^f} \frac{\partial n^f}{\partial X_I} (n^f \tilde{v}_{i(t)}) F_{Ii}^{-1} dV \\
&- \int_{\mathcal{B}_0} w^{\theta^f} J n^f D_t p_f dV - \int_{\mathcal{B}_0} w^{\theta^f} J \frac{\partial p_f}{\partial X_I} (n^f \tilde{v}_{i(t)}) F_{Ii}^{-1} dV \\
&- \int_{\mathcal{B}_0} \frac{\partial w^{\theta^f}}{\partial X_I} J q_i^f F_{Ii}^{-1} dV - \int_{\mathcal{B}_0} w^{\theta^f} J k_\theta^\varepsilon (\theta^s - \theta^f) dV \\
&- \int_{\Gamma_0^{Q_f^\theta}} w^{\theta^f} Q_f^\theta dA = 0. \tag{4.193}
\end{aligned}$$

The formal statement for the variational forms \mathcal{G} , \mathcal{H} , \mathcal{J} , and \mathcal{K} —assuming nearly-inviscid pore fluid, $\mathbf{a}_f = \mathbf{a}_s = \mathbf{a}$, isotropic thermoelasticity of the solid, and a compressible liquid model of the

pore fluid—may be written as follows:

$$\begin{aligned}
& \text{Find } u_i(X_I, t) \in \mathcal{S}^u, p_f(X_I, t) \in \mathcal{S}^{p_f}, \\
& \theta^s(X_I, t) \in \mathcal{S}^{\theta^s}, \text{ and } \theta^f(X_I, t) \in \mathcal{S}^{\theta^f}, \text{ with } t \in [0, T], \text{ such that:} \\
& \int_{\mathcal{B}_0} w_i^u \rho_0 a_i dV + \int_{\mathcal{B}_0} \frac{\partial w_i^u}{\partial X_I} P_{iI(E)}^s dV - \int_{\mathcal{B}_0} \frac{\partial w_i^u}{\partial X_I} J p_f F_{Ii}^{-1} \left(\frac{\theta^s}{\theta^f} n^s + n^f \right) dV \\
& - \int_{\mathcal{B}_0} w_i^u \rho_0 g_i dV - \left(\int_{\Gamma_0^t} w_i^u t_i^{\sigma^E} dA - \int_{\Gamma_0^t} w_i^u p_f J F_{Ii}^{-1} \left(\frac{\theta^s}{\theta^f} n^s + n^f \right) N_I dA \right) = 0, \\
& - \int_{\mathcal{B}_0} w^{p_f} J \alpha_V^f \left(n^f D_t \theta^f + \frac{\partial \theta^f}{\partial X_I} F_{Ii}^{-1} (n^f \tilde{v}_{i(t)}) \right) dV + \int_{\mathcal{B}_0} w^{p_f} \left(\frac{J n^f}{K_f^\theta} \dot{p}_f + j \right) dV \\
& + \int_{\mathcal{B}_0} w^{p_f} \frac{J}{K_f^\theta} \frac{\partial p_f}{\partial X_I} F_{Ii}^{-1} (n^f \tilde{v}_{i(t)}) dV - \int_{\mathcal{B}_0} \frac{\partial w^{p_f}}{\partial X_I} J (n^f \tilde{v}_{i(t)}) F_{Ii}^{-1} dV - \int_{\Gamma_0^{Q_f}} w^{p_f} Q_f dA = 0, \\
& \int_{\mathcal{B}_0} w^{\theta^s} \rho_0^s c_V^s D_t \theta^s dV + \int_{\mathcal{B}_0} w^{\theta^s} \left(\frac{K^{\text{skel}} \alpha_V^s \theta^s}{J} + n^s p_f \frac{\theta^s}{\theta^f} + Q \right) D_t J dV \\
& - \int_{\mathcal{B}_0} \frac{\partial w^{\theta^s}}{\partial X_I} J q_i F_{Ii}^{-1} dV + \int_{\mathcal{B}_0} w^{\theta^s} J k_\theta^s (\theta^s - \theta^f) dV \\
& + \int_{\mathcal{B}_0} w^{\theta^s} \frac{J (n^f \tilde{v}_f)^2}{\hat{k}} dV + \int_{\mathcal{B}_0} w^{\theta^s} J \frac{\theta^s}{\theta^f} \frac{p_f}{n^f} \frac{\partial n^f}{\partial X_I} F_{Ii}^{-1} (n^f \tilde{v}_{i(t)}) dV - \int_{\Gamma_0^{Q_s}} w^{\theta^s} Q_s^\theta dA = 0, \\
& \int_{\mathcal{B}_0} w^{\theta^f} (\rho_0^f c_V^f + J n^f \theta^f K_f^\theta [\alpha_V^f]^2) D_t \theta^f dV + \int_{\mathcal{B}_0} w^{\theta^f} (\rho_0^{\text{fr}} c_V^f + J \theta^f K_f^\theta [\alpha_V^f]^2) \frac{\partial \theta^f}{\partial X_I} (n^f \tilde{v}_{i(t)}) F_{Ii}^{-1} dV \\
& - \int_{\mathcal{B}_0} w^{\theta^f} n^s p_f D_t J dV - \int_{\mathcal{B}_0} w^{\theta^f} \frac{J p_f}{n^f} \frac{\partial n^f}{\partial X_I} (n^f \tilde{v}_{i(t)}) F_{Ii}^{-1} dV - \int_{\mathcal{B}_0} w^{\theta^f} J n^f D_t p_f dV \\
& - \int_{\mathcal{B}_0} w^{\theta^f} J \frac{\partial p_f}{\partial X_I} (n^f \tilde{v}_{i(t)}) F_{Ii}^{-1} dV - \int_{\mathcal{B}_0} \frac{\partial w^{\theta^f}}{\partial X_I} J q_i^f F_{Ii}^{-1} dV - \int_{\mathcal{B}_0} w^{\theta^f} J k_\theta^s (\theta^s - \theta^f) dV \\
& - \int_{\Gamma_0^{Q_f}} w^{\theta^f} Q_f^\theta dA = 0 \\
& \text{holds } \forall w_i^u \in \mathcal{V}^u, \forall w^{p_f} \in \mathcal{V}^{p_f}, w^{\theta^s} \in \mathcal{V}^{\theta^s}, \text{ and } w^{\theta^f} \in \mathcal{V}^{\theta^f} \text{ with} \\
& \mathcal{S}^u = (u_i : \mathcal{B}_0 \times [0, T] \rightarrow \mathbb{R}^3, u_i \in H^1, u_i(t) = g_i^u(t) \text{ on } \Gamma_0^u, u_i(X_I, t = 0) = u_{i,0}(X_I)), \\
& \mathcal{S}^{p_f} = (p_f : \mathcal{B}_0 \times [0, T] \rightarrow \mathbb{R}, p_f \in H^1, p_f(t) = g^p(t) \text{ on } \Gamma_0^p, p_f(X_I, t = 0) = p_{f,0}(X_I)), \\
& \mathcal{S}^{\theta^s} = (\theta^s : \mathcal{B}_0 \times [0, T] \rightarrow \mathbb{R}, \theta^s \in H^1, \theta^s(t) = g^{\theta^s} \text{ on } \Gamma_0^{\theta^s}, \theta^s(X_I, t = 0) = \theta_0^s(X_I)), \\
& \mathcal{S}^{\theta^f} = (\theta^f : \mathcal{B}_0 \times [0, T] \rightarrow \mathbb{R}, \theta^f \in H^1, \theta^f(t) = g^{\theta^f} \text{ on } \Gamma_0^{\theta^f}, \theta^f(X_I, t = 0) = \theta_0^f(X_I)), \\
& \mathcal{V}^u = (w_i^u : \mathcal{B}_0 \rightarrow \mathbb{R}^3, w_i^u \in H^1, w_i^u(t) = 0 \text{ on } \Gamma_0^u), \\
& \mathcal{V}^{p_f} = (w^{p_f} : \mathcal{B}_0 \rightarrow \mathbb{R}, w^{p_f} \in H^1, w^{p_f}(t) = 0 \text{ on } \Gamma_0^p), \\
& \mathcal{V}^{\theta^s} = (w^{\theta^s} : \mathcal{B}_0 \rightarrow \mathbb{R}, w^{\theta^s} \in H^1, w^{\theta^s}(t) = 0 \text{ on } \Gamma_0^{\theta^s}), \\
& \mathcal{V}^{\theta^f} = (w^{\theta^f} : \mathcal{B}_0 \rightarrow \mathbb{R}, w^{\theta^f} \in H^1, w^{\theta^f}(t) = 0 \text{ on } \Gamma_0^{\theta^f}).
\end{aligned} \tag{4.194}$$

In the FE implementation that follows, it behooves us to simplify the variational forms, such that

$$\begin{aligned}
\mathcal{G} &= \mathcal{G}_1^{\text{INT}} + \mathcal{G}_2^{\text{INT}} + \mathcal{G}_3^{\text{INT}} + \mathcal{G}_4^{\text{INT}} + \mathcal{G}_1^{\text{EXT}} + \mathcal{G}_2^{\text{EXT}} = 0, \\
\mathcal{H} &= \mathcal{H}_1^{\text{INT}} + \mathcal{H}_2^{\text{INT}} + \mathcal{H}_3^{\text{INT}} + \mathcal{H}_4^{\text{INT}} + \mathcal{H}_6^{\text{INT}} + \mathcal{H}_7^{\text{INT}} + \mathcal{H}^{\text{EXT}} = 0, \\
\mathcal{J} &= \mathcal{J}_1^{\text{INT}} + \mathcal{J}_2^{\text{INT}} + \mathcal{J}_3^{\text{INT}} + \mathcal{J}_4^{\text{INT}} + \mathcal{J}_5^{\text{INT}} + \mathcal{J}_6^{\text{INT}} + \mathcal{J}^{\text{EXT}} = 0, \\
\mathcal{K} &= \mathcal{K}_1^{\text{INT}} + \mathcal{K}_2^{\text{INT}} + \mathcal{K}_3^{\text{INT}} + \mathcal{K}_4^{\text{INT}} + \mathcal{K}_5^{\text{INT}} + \mathcal{K}_6^{\text{INT}} + \mathcal{K}_7^{\text{INT}} + \mathcal{K}_8^{\text{INT}} + \mathcal{K}^{\text{EXT}} = 0,
\end{aligned} \tag{4.195}$$

wherein \mathcal{G}, \mathcal{J} remain unchanged from the previous section, and

$$\begin{aligned}
\mathcal{H}_1^{\text{INT}} &= \int_{\mathcal{B}_0} w^{p_f} \left(\frac{J n^f}{K_f^\theta} \dot{p}_f + \dot{j} \right) dV, \\
\mathcal{H}_2^{\text{INT}} &= \int_{\mathcal{B}_0} w^{p_f} \frac{J}{K_f^\theta} \frac{\partial p_f}{\partial X_I} F_{Ii}^{-1} (n^f \tilde{v}_{i(f)}) dV, \\
\mathcal{H}_3^{\text{INT}} &= \int_{\mathcal{B}_0} \frac{\partial w^{p_f}}{\partial X_I} J F_{Ii}^{-1} \hat{k} \frac{\partial p_f}{\partial X_K} F_{Ki}^{-1} dV, \\
\mathcal{H}_4^{\text{INT}} &= \int_{\mathcal{B}_0} \frac{\partial w^{p_f}}{\partial X_I} J F_{Ii}^{-1} \hat{k} \rho^{\text{fR}} (a_i - g_i) dV, \\
\mathcal{H}_6^{\text{INT}} &= \int_{\mathcal{B}_0} \frac{\partial w^{p_f}}{\partial X_I} J F_{Ii}^{-1} \frac{\hat{k}}{n^f p_f} \frac{\partial n^f}{\partial X_K} F_{Ki}^{-1} \left(1 - \frac{\theta^s}{\theta^f} \right) dV, \\
\mathcal{H}_7^{\text{INT}} &= - \int_{\mathcal{B}_0} w^{p_f} J \alpha_V^f \left(n^f D_t \theta^f + \frac{\partial \theta^f}{\partial X_I} F_{Ii}^{-1} (n^f \tilde{v}_{i(f)}) \right) dV, \\
\mathcal{H}^{\text{EXT}} &= \int_{\Gamma_0^{\text{Q}_f}} w^{p_f} Q_f dA,
\end{aligned} \tag{4.196}$$

and

$$\begin{aligned}
\mathcal{K}_1^{\text{INT}} &= \int_{\mathcal{B}_0} w^{\theta^f} (\rho_0^f c_V^f + J n^f \theta^f K_f^\theta [\alpha_V^f]^2) D_t \theta^f dV \\
\mathcal{K}_2^{\text{INT}} &= \int_{\mathcal{B}_0} w^{\theta^f} (\rho_0^{\text{fR}} c_V^f + J \theta^f K_f^\theta [\alpha_V^f]^2) \frac{\partial \theta^f}{\partial X_I} (n^f \tilde{v}_{i(f)}) F_{Ii}^{-1} dV, \\
\mathcal{K}_3^{\text{INT}} &= - \int_{\mathcal{B}_0} w^{\theta^f} n^s p_f D_t J dV, \\
\mathcal{K}_4^{\text{INT}} &= - \int_{\mathcal{B}_0} w^{\theta^f} \frac{J p_f}{n^f} \frac{\partial n^f}{\partial X_I} (n^f \tilde{v}_{i(f)}) F_{Ii}^{-1} dV, \\
\mathcal{K}_5^{\text{INT}} &= - \int_{\mathcal{B}_0} w^{\theta^f} J n^f D_t p_f dV, \\
\mathcal{K}_6^{\text{INT}} &= - \int_{\mathcal{B}_0} w^{\theta^f} J \frac{\partial p_f}{\partial X_I} (n^f \tilde{v}_{i(f)}) F_{Ii}^{-1} dV, \\
\mathcal{K}_7^{\text{INT}} &= - \int_{\mathcal{B}_0} \frac{\partial w^{\theta^f}}{\partial X_I} J q_i^f F_{Ii}^{-1} dV, \\
\mathcal{K}_8^{\text{INT}} &= - \int_{\mathcal{B}_0} w^{\theta^f} J k_\theta^\varepsilon (\theta^s - \theta^f) dV, \\
\mathcal{K}^{\text{EXT}} &= - \int_{\Gamma_0^{Q_f^\theta}} w^{\theta^f} Q_f^\theta dA.
\end{aligned} \tag{4.197}$$

In the case of 1-D uniaxial strain, i.e., the underlying assumption for the proceeding FE model, the above terms simplify to the following:

$$\begin{aligned}
\mathcal{H}_1^{\text{INT}} &= \int_0^{X=H} w^{p_f} \left(\frac{J n^f}{K_f^\theta} \dot{p}_f + \dot{J} \right) A dX, \\
\mathcal{H}_2^{\text{INT}} &= \int_0^{X=H} w^{p_f} \frac{1}{K_f^\theta} \frac{\partial p_f}{\partial X} (n^f \tilde{v}_f) A dX, \\
\mathcal{H}_3^{\text{INT}} &= \int_0^{X=H} \frac{\partial w^{p_f}}{\partial X} \hat{k} \frac{\partial p_f}{\partial X} F_{11}^{-1} A dX, \\
\mathcal{H}_4^{\text{INT}} &= \int_0^{X=H} \frac{\partial w^{p_f}}{\partial X} \hat{k} \rho^{\text{fR}} (a + g) A dX, \\
\mathcal{H}_6^{\text{INT}} &= \int_0^{X=H} \frac{\partial w^{p_f}}{\partial X} \frac{\hat{k}}{n^f p_f} \frac{\partial n^f}{\partial X} F_{11}^{-1} \left(1 - \frac{\theta^s}{\theta^f} \right) A dX, \\
\mathcal{H}_7^{\text{INT}} &= - \int_0^{X=H} w^{p_f} J \alpha_V^f \left(n^f D_t \theta^f + \frac{\partial \theta^f}{\partial X} (n^f \tilde{v}_f) F_{11}^{-1} \right) A dX, \\
\mathcal{H}^{\text{EXT}} &= \int_{\Gamma_0^{Q_f}} w^{p_f} Q_f dA = Q_f A,
\end{aligned} \tag{4.198}$$

and

$$\begin{aligned}
\mathcal{K}_1^{\text{INT}} &= \int_0^{X=H} w^{\theta^f} (\rho_0^f c_V^f + J n^f \theta^f K_f^\theta [\alpha_V^f]^2) D_t \theta^f A dX, \\
\mathcal{K}_2^{\text{INT}} &= \int_0^{X=H} w^{\theta^f} (\rho^{\text{fR}} c_V^f + n^f \theta^f K_f^\theta [\alpha_V^f]^2) \frac{\partial \theta^f}{\partial X} (n^f \tilde{v}_f) A dX, \\
\mathcal{K}_3^{\text{INT}} &= - \int_0^{X=H} w^{\theta^f} n^s p_f D_t J A dX, \\
\mathcal{K}_4^{\text{INT}} &= - \int_0^{X=H} w^{\theta^f} \frac{p_f}{n^f} \frac{\partial n^f}{\partial X} (n^f \tilde{v}_f) A dX, \\
\mathcal{K}_5^{\text{INT}} &= - \int_0^{X=H} w^{\theta^f} J n^f D_t p_f A dX, \\
\mathcal{K}_6^{\text{INT}} &= - \int_0^{X=H} w^{\theta^f} \frac{\partial p_f}{\partial X} (n^f \tilde{v}_f) A dX, \\
\mathcal{K}_7^{\text{INT}} &= - \int_0^{X=H} \frac{\partial w^{\theta^f}}{\partial X} q^f A dX, \\
\mathcal{K}_8^{\text{INT}} &= - \int_0^{X=H} w^{\theta^f} J k_\theta^\varepsilon (\theta^s - \theta^f) A dX, \\
\mathcal{K}^{\text{EXT}} &= - \int_{\Gamma_0^{Q_f^\theta}} w^{\theta^f} Q_f^\theta dA = Q_f^\theta A.
\end{aligned} \tag{4.199}$$

4.1.6 ($\mathbf{u}-\mathbf{u}_f-p_f-\theta^s-\theta^f$) formulation

Herein, baroclinic pore fluid constituent is assumed, i.e., $\rho^{\text{fR}} = \rho^{\text{fR}}(p_f, \theta^f)$. Locally inhomogeneous temperatures are also assumed. The strong formulation for thermoporoelastodynamics has

the solution space

$$\begin{aligned}
\mathcal{S}^u &= (\mathbf{u} : \mathcal{B}_0 \times [0, T] \rightarrow \mathbb{R}^3, \mathbf{u} \in H^1, \mathbf{u}(t) = \mathbf{g}^u(t) \text{ on } \Gamma_0^u, \mathbf{u}(\mathbf{X}, t = 0) = \mathbf{u}_0(\mathbf{X})), \\
\mathcal{S}^{u_f} &= (\mathbf{u}_f : \mathcal{B}_0 \times [0, T] \rightarrow \mathbb{R}^3, \mathbf{u}_f \in H^1, \mathbf{u}_f(t) = \mathbf{g}^{u_f}(t) \text{ on } \Gamma_0^{u_f}, \mathbf{u}_f(\mathbf{X}, t = 0) = \mathbf{u}_{f,0}(\mathbf{X})), \\
\mathcal{S}^{p_f} &= (p_f : \mathcal{B}_0 \times [0, T] \rightarrow \mathbb{R}, p_f \in H^1, p_f(t) = g^p(t) \text{ on } \Gamma_0^p, p_f(\mathbf{X}, t = 0) = p_{f,0}(\mathbf{X})), \\
\mathcal{S}^{\theta^s} &= (\theta^s : \mathcal{B}_0 \times [0, T] \rightarrow \mathbb{R}, \theta^s \in H^1, \theta^s(t) = g^{\theta^s} \text{ on } \Gamma_0^{\theta^s}, \theta^s(\mathbf{X}, t = 0) = \theta_0^s(\mathbf{X})), \\
\mathcal{S}^{\theta^f} &= (\theta^f : \mathcal{B}_0 \times [0, T] \rightarrow \mathbb{R}, \theta^f \in H^1, \theta^f(t) = g^{\theta^f} \text{ on } \Gamma_0^{\theta^f}, \theta^f(\mathbf{X}, t = 0) = \theta_0^f(\mathbf{X})).
\end{aligned} \tag{4.200}$$

Derivations of constituent energy balances were carried out in Section 4.1.5; the difference in this formulation lies in the pore fluid energy balance. With the inclusion of a governing equation for \mathbf{u}_f , we have chosen in this formulation to include pore fluid extra stress $\boldsymbol{\sigma}_E^f$ and not to substitute the balance of mass of the pore fluid for the $\text{div } \mathbf{v}_f$ term.

Derivation of the fluid phase energy balance. We may write the balance of energy for the fluid phase as

$$\rho^f D_t^f e^f = \boldsymbol{\sigma}^f : \mathbf{l}_f - \text{div } \mathbf{q}^f + \rho^f r^f + \hat{\varepsilon}^f. \tag{4.201}$$

Assuming no heat source r^f , and making use of Equations (3.43)₂, Equation (3.72), we may write

$$\rho^f (D_t^f \psi^f + \theta^f D_t^f \eta^f + \eta^f D_t^f \theta^f) = (\boldsymbol{\sigma}_E^f - p_f n^f \mathbf{1}) : \mathbf{l}_f - \text{div } \mathbf{q}^f + k_\theta^\varepsilon (\theta^s - \theta^f). \tag{4.202}$$

Expansion of the fluid Helmholtz free energy term in Equation (4.202) yields

$$D_t^f \psi^f(\rho^{\text{fR}}, \theta^f) = \frac{\partial \psi^f}{\partial \rho^{\text{fR}}} D_t^f \rho^{\text{fR}} + \frac{\partial \psi^f}{\partial \theta^f} D_t^f \theta^f. \tag{4.203}$$

Making use of Equations (3.34)_{5,7} and Equation (3.41) allows us to write Equation (4.203) as

$$D_t^f \psi^f(\rho^{\text{fR}}, \theta^f) = \frac{p_f}{(\rho^{\text{fR}})^2} D_t^f \rho^{\text{fR}} - \eta^f D_t^f \theta^f. \tag{4.204}$$

Thus, with some simplification of the r.h.s. of Equation (4.202), we may write

$$\rho^f \left(\theta^f D_t^f \eta^f + \frac{p_f}{(\rho^{\text{fR}})^2} D_t^f \rho^{\text{fR}} \right) = \boldsymbol{\sigma}_E^f : \mathbf{d}_f - p_f n^f \text{div } \mathbf{v}_f - \text{div } \mathbf{q}^f + k_\theta^\varepsilon (\theta^s - \theta^f). \tag{4.205}$$

At this point, the terms on the l.h.s. of Equation (4.143) require a constitutive form for the pore fluid in order to be further simplified.

The ideal gas model. For the ideal gas pore fluid, recall

$$\eta^f = c_V^f \ln \frac{\theta^f}{\theta_0^f} - \mathfrak{R} \ln \frac{\rho^{fR}}{\rho_0^{fR}}. \quad (4.206)$$

Then

$$\theta^f D_t^f \eta^f = c_V^f D_t^f \theta^f - \frac{\theta^f \mathfrak{R}}{\rho^{fR}} D_t^f \rho^{fR} = c_V^f D_t^f \theta^f - \frac{p_f}{(\rho^{fR})^2} D_t^f \rho^{fR}. \quad (4.207)$$

Thus, the energy balance for the pore fluid may be written as

$$\rho^f c_V^f \left(D_t^s \theta^f + \text{grad}(\theta^f) \cdot \tilde{\mathbf{v}}_f \right) - \boldsymbol{\sigma}_E^f : \mathbf{d}_f + p_f n^f \text{div} \mathbf{v}_f + \text{div} \mathbf{q}^f - k_\theta^\varepsilon (\theta^s - \theta^f) = 0, \quad (4.208)$$

which we may convert to the reference configuration of the solid skeleton \mathcal{B}_0 (dropping also $(\cdot)_s$ and $(\cdot)^s$ for convenience, where appropriate):

$$\begin{aligned} \rho_0^f c_V^f \left(D_t \theta^f + \text{GRAD}(\theta^f) \cdot \mathbf{F}^{-1} \cdot \tilde{\mathbf{v}}_f \right) - J \boldsymbol{\sigma}_E^f : \mathbf{d}_f + J p_f n^f \text{GRAD}(\mathbf{v}_f) : \mathbf{F}^{-T} \\ - J k_\theta^\varepsilon (\theta^s - \theta^f) + J \text{GRAD}(\mathbf{q}^f) : \mathbf{F}^{-T} = 0. \end{aligned} \quad (4.209)$$

As such, the strong formulation for the balances of linear momenta, mass, and energies, under the assumption of a linear thermoelastic solid constituent and ideal gas pore fluid constituent, may be

written as follows:

$$\begin{aligned}
& \text{Find } \mathbf{u}(\mathbf{X}, t) \in \mathcal{S}^u, \mathbf{u}_f(\mathbf{X}, t) \in \mathcal{S}^{u_f}, p_f(\mathbf{X}, t) \in \mathcal{S}^{p_f}, \\
& \theta^s(\mathbf{X}, t) \in \mathcal{S}^{\theta^s}, \text{ and } \theta^f(\mathbf{X}, t) \in \mathcal{S}^{\theta^f}, \\
& \text{with } t \in [0, T], \text{ such that:} \\
& \text{DIV } \mathbf{P} + \rho_0 \mathbf{g} - (\rho_0^s \mathbf{a} + \rho_0^f \mathbf{a}_f) = \mathbf{0} \in \mathcal{B}_0, \\
& \mathbf{u}(\mathbf{X}, t) = \mathbf{g}^u(\mathbf{X}, t) \text{ on } \Gamma_0^u, \\
& \mathbf{P}(\mathbf{X}, t) \cdot \mathbf{N}(\mathbf{X}) = \mathbf{t}^\sigma(\mathbf{X}, t) \text{ on } \Gamma_0^t, \\
& \mathbf{u}(\mathbf{X}, t = 0) = \mathbf{u}_0(\mathbf{X}) \in \mathcal{B}_0, \\
& \mathbf{v}(\mathbf{X}, t = 0) = \mathbf{v}_0(\mathbf{X}) \in \mathcal{B}_0, \\
& \mathbf{a}(\mathbf{X}, t = 0) = \mathbf{a}_0(\mathbf{X}) \in \mathcal{B}_0, \\
& \rho_0^f \mathbf{a}_f - \text{DIV } \mathbf{P}_E^f + J n^f \text{GRAD}(p_f) \cdot \mathbf{F}^{-1} \\
& + J p_f \text{GRAD } n^f \left(1 - \frac{\theta^s}{\theta^f}\right) \cdot \mathbf{F}^{-1} + J \frac{(n^f)^2}{k} (\mathbf{v}_f - \mathbf{v}) - \rho_0^f \mathbf{g} = \mathbf{0} \in \mathcal{B}_0, \\
& \mathbf{u}_f(\mathbf{X}, t) = \mathbf{g}_{u_f}(\mathbf{X}, t) \text{ on } \Gamma_0^{u_f}, \\
& \mathbf{u}_f(\mathbf{X}, t = 0) = \mathbf{u}_{f,0}(\mathbf{X}) \in \mathcal{B}_0, \\
& \mathbf{v}_f(\mathbf{X}, t = 0) = \mathbf{v}_{f,0}(\mathbf{X}) \in \mathcal{B}_0, \\
& \mathbf{a}_f(\mathbf{X}, t = 0) = \mathbf{a}_{f,0}(\mathbf{X}) \in \mathcal{B}_0, \\
& -\frac{J}{\theta^f} [n^f D_t \theta^f + \text{GRAD}(\theta^f) \cdot \mathbf{F}^{-1} \cdot (n^f \tilde{\mathbf{v}}_f)] + \frac{J n^f}{p_f} D_t p_f + D_t J \\
& + \frac{J}{p_f} \text{GRAD}(p_f) \cdot \mathbf{F}^{-1} \cdot (n^f \tilde{\mathbf{v}}_f) + J \text{GRAD}(n^f \tilde{\mathbf{v}}_f) \cdot \mathbf{F}^{-T} = 0 \in \mathcal{B}_0, \\
& p_f(\mathbf{X}, t) = g^p(\mathbf{X}, t) \text{ on } \Gamma_0^p, \\
& -[J \mathbf{F}^{-1} \cdot (n^f \tilde{\mathbf{v}}_f)] \cdot \mathbf{N} = Q_f^Q(\mathbf{X}, t) \text{ on } \Gamma_0^{Q_f}, \\
& p_f(\mathbf{X}, t = 0) = p_{f,0}(\mathbf{X}) \in \mathcal{B}_0, \\
& \dot{p}_f(\mathbf{X}, t = 0) = \dot{p}_{f,0}(\mathbf{X}) \in \mathcal{B}_0, \\
& \rho_0^s c_V^s D_t \theta^s + \left(\frac{K^{\text{skel}} \alpha_V^s \theta^s}{J} + n^s p_f \frac{\theta^s}{\theta^f} + Q\right) D_t J \\
& + J \text{GRAD}(q^s) \cdot \mathbf{F}^{-T} + J k_\theta^s (\theta^s - \theta^f) \\
& - \frac{J (n^f)^2}{k} (\mathbf{v}_f - \mathbf{v})^2 + J \frac{\theta^s}{\theta^f} \frac{p_f}{n^f} \text{GRAD}(n^f) \cdot \mathbf{F}^{-1} \cdot (n^f \tilde{\mathbf{v}}_f) = 0 \in \mathcal{B}_0, \\
& \theta^s(\mathbf{X}, t) = g^{\theta^s}(\mathbf{X}, t) \text{ on } \Gamma_0^{\theta^s}, \\
& -(J q^s \cdot \mathbf{F}^{-T}) \cdot \mathbf{N} = Q_s^Q(\mathbf{X}, t) \text{ on } \Gamma_0^{Q_s}, \\
& \theta^s(\mathbf{X}, t = 0) = \theta_0^s(\mathbf{X}) \in \mathcal{B}_0 \\
& \dot{\theta}^s(\mathbf{X}, t = 0) = \dot{\theta}_0^s(\mathbf{X}) \in \mathcal{B}_0 \\
& \rho_0^f c_V^f (D_t \theta^f + \text{GRAD}(\theta^f) \cdot \mathbf{F}^{-1} \cdot \tilde{\mathbf{v}}_f) - J \sigma_E^f \cdot \mathbf{d}_f + J p_f n^f \text{GRAD}(v_f) \cdot \mathbf{F}^{-T} \\
& - J k_\theta^f (\theta^s - \theta^f) + J \text{GRAD}(q^f) \cdot \mathbf{F}^{-T} = 0 \in \mathcal{B}_0 \\
& \theta^f(\mathbf{X}, t) = g^{\theta^f}(\mathbf{X}, t) \text{ on } \Gamma_0^{\theta^f}, \\
& -(J q^f \cdot \mathbf{F}^{-T}) \cdot \mathbf{N} = Q_f^Q(\mathbf{X}, t) \text{ on } \Gamma_0^{Q_f}, \\
& \theta^f(\mathbf{X}, t = 0) = \theta_0^f(\mathbf{X}) \in \mathcal{B}_0 \\
& \dot{\theta}^f(\mathbf{X}, t = 0) = \dot{\theta}_0^f(\mathbf{X}) \in \mathcal{B}_0.
\end{aligned} \tag{4.210}$$

Let $\mathcal{G}(u_i, u_{i(f)}, p_f, \theta^s, \theta^f, w_i^u)$ be the variational form of Equations (4.210)₁₋₆ such that

$$\mathcal{G} : \mathcal{S}^u \times \mathcal{S}^{u_f} \times \mathcal{S}^{p_f} \times \mathcal{S}^{\theta^s} \times \mathcal{S}^{\theta^f} \times \mathcal{V}^u \rightarrow \mathbb{R}. \tag{4.211}$$

We may then rewrite Equations (4.210)_{1–6} as

$$\mathcal{G}(u_i, u_{i(f)}, p_f, \theta^s, \theta^f, w_i^u) = \int_{\mathcal{B}_0} w_i^u (\rho_0^s a_i + \rho_0^f a_{i(f)}) dV + \int_{\mathcal{B}_0} w_i^u \frac{\partial P_{iI}}{\partial X_I} dV + \int_{\mathcal{B}_0} w_i^u \rho_0 g_i dV = 0. \quad (4.212)$$

Weakening of the first Piola-Kirchhoff stress of the mixture and subsequent decomposition proceeds as before, such that Equation (4.212) is written as

$$\begin{aligned} \mathcal{G}(u_i, u_{i(f)}, p_f, \theta^s, \theta^f, w_i^u) &= \int_{\mathcal{B}_0} w_i^u (\rho_0^s a_i + \rho_0^f a_{i(f)}) dV + \int_{\mathcal{B}_0} \frac{\partial w_i^u}{\partial X_I} P_{iI}^s dV + \int_{\mathcal{B}_0} \frac{\partial w_i^u}{\partial X_I} P_{iI}^f dV \\ &\quad - \int_{\mathcal{B}_0} w_i^u J p_f F_{Ii}^{-1} \left(\frac{\theta^f}{\theta^s} n^s + n^f \right) dV + \int_{\mathcal{B}_0} w_i^u \rho_0 g_i dV \\ &\quad - \left(\int_{\Gamma_0^t} w_i^u t_i^{\sigma^s} dA + \int_{\Gamma_0^t} w_i^u t_i^{\sigma^f} dA - \int_{\Gamma_0^t} w_i^u p_f J F_{Ii}^{-1} \left(\frac{\theta^f}{\theta^s} n^s + n^f \right) N_I dA \right) = 0, \end{aligned} \quad (4.213)$$

where use has been made of the locally inhomogenous temperature first Piola-Kirchhoff stress of the mixture,

$$P_{iI} = P_{iI}^s + P_{iI}^f - J p_f F_{Ii}^{-1} \left(\frac{\theta^f}{\theta^s} n^s + n^f \right). \quad (4.214)$$

Let $\mathcal{I}(u_i, u_{i(f)}, p_f, \theta^s, \theta^f, w^{u_f})$ be the variational form of Equations (4.210)_{7–11} such that

$$\mathcal{I} : \mathcal{S}^{u_f} \times \mathcal{S}^u \times \mathcal{S}^{p_f} \times \mathcal{S}^{\theta^s} \times \mathcal{S}^{\theta^f} \times \mathcal{V}^{u_f} \rightarrow \mathbb{R}. \quad (4.215)$$

We may then rewrite Equations (4.210)_{7–11} as

$$\begin{aligned} \mathcal{I}(u_i, u_{i(f)}, p_f, \theta^s, \theta^f, w_i^{u_f}) &= \int_{\mathcal{B}_0} w_i^{u_f} \rho_0^f a_{i(f)} dV - \int_{\mathcal{B}_0} w_i^{u_f} \frac{\partial P_{iI}^f}{\partial X_I} dV + \int_{\mathcal{B}_0} w_i^{u_f} J n^f \frac{\partial p_f}{\partial X_I} F_{Ii}^{-1} dV \\ &\quad + \int_{\mathcal{B}_0} w_i^{u_f} J p_f \frac{\partial n^f}{\partial X_I} \left(1 - \frac{\theta^s}{\theta^f} \right) F_{Ii}^{-1} + \int_{\mathcal{B}_0} w_i^{u_f} J \frac{(n^f)^2}{\hat{k}} (\mathbf{v}_f - \mathbf{v}) \\ &\quad - \int_{\mathcal{B}_0} w_i^u \rho_0^f g_i dV = 0. \end{aligned} \quad (4.216)$$

Let $\mathcal{H}(u_i, u_{i(f)}, p_f, \theta^s, \theta^f, w^{p_f})$ be the variational form of Equations (4.210)_{12–16}, such that

$$\mathcal{H} : \mathcal{S}^{p_f} \times \mathcal{S}^u \times \mathcal{S}^{u_f} \times \mathcal{S}^{\theta^f} \times \mathcal{V}^{p_f} \rightarrow \mathbb{R}. \quad (4.217)$$

The variational form only changes from the one in Section 4.1.5 in an implicit manner (Darcy's law is now a function of pore fluid acceleration \mathbf{a}_f , rather than mixture acceleration $\mathbf{a} = \mathbf{a}_s = \mathbf{a}_f$, and also includes the pore fluid viscous stress contribution). Thus we may write Equation (4.210)_{12–16} as

$$\begin{aligned} \mathcal{H}(u_i, u_{i(f)}, p_f, \theta^s, \theta^f, w^{p_f}) = & - \int_{\mathcal{B}_0} w^{p_f} \frac{J}{\theta^f} \left(n^f D_t \theta^f + \frac{\partial \theta^f}{\partial X_I} F_{Ii}^{-1} (n^f \tilde{v}_{i(f)}) \right) dV \\ & + \int_{\mathcal{B}_0} w^{p_f} \left(\frac{J n^f}{p_f} \dot{p}_f + j \right) dV + \int_{\mathcal{B}_0} w^{p_f} \frac{J}{p_f} \frac{\partial p_f}{\partial X_I} F_{Ii}^{-1} (n^f \tilde{v}_{i(f)}) dV \\ & - \int_{\mathcal{B}_0} \frac{\partial w^{p_f}}{\partial X_I} J (n^f \tilde{v}_{i(f)}) F_{Ii}^{-1} dV - \int_{\Gamma_0^Q} w^{p_f} Q_f dA = 0. \end{aligned} \quad (4.218)$$

Let $\mathcal{J}(u_i, u_{i(f)}, p_f, \theta^s, \theta^f, w^{\theta^s})$ be the variational form of Equations (4.210)_{17–21}, such that

$$\mathcal{J} : \mathcal{S}^{\theta^s} \times \mathcal{S}^u \times \mathcal{S}^{p_f} \times \mathcal{S}^{\theta^f} \times \mathcal{V}^{\theta^s} \rightarrow \mathbb{R}. \quad (4.219)$$

The variational form for the balance of the energy of the solid constituent only changes from Section 4.1.5 in that the porosity gradient term need not use the Darcy velocity, such that

$$\begin{aligned} \mathcal{J}(u_i, u_{i(f)}, p_f, \theta^s, \theta^f, w^{\theta^s}) = & \int_{\mathcal{B}_0} w^{\theta^s} \rho_0^s c_V^s D_t \theta^s dV + \int_{\mathcal{B}_0} w^{\theta^s} \left(\frac{K^{\text{skel}} \alpha_V^s \theta^s}{J} + n^s p_f \frac{\theta^s}{\theta^f} + Q \right) D_t J dV \\ & - \int_{\mathcal{B}_0} \frac{\partial w^{\theta^s}}{\partial X_I} J q_i F_{Ii}^{-1} dV + \int_{\mathcal{B}_0} w^{\theta^s} J k_\theta^\varepsilon (\theta^s - \theta^f) dV \\ & - \int_{\mathcal{B}_0} w^{\theta^s} \frac{J (n^f)^2}{\hat{k}} (v_{i(f)} - v_i)^2 dV + \int_{\mathcal{B}_0} w^{\theta^s} J \frac{\theta^s}{\theta^f} p_f \frac{\partial n^f}{\partial X_I} F_{Ii}^{-1} (v_{i(f)} - v_i) dV \\ & - \int_{\Gamma_0^{Q_s^\theta}} w^{\theta^s} Q_s^\theta dA = 0. \end{aligned} \quad (4.220)$$

Let $\mathcal{K}(u_i, u_{i(f)}, p_f, \theta^s, \theta^f, w^{\theta^f})$ be the variational form of Equations (4.210)_{22–26}, such that

$$\mathcal{K} : \mathcal{S}^{\theta^f} \times \mathcal{S}^u \times \mathcal{S}^{p_f} \times \mathcal{S}^{\theta^s} \times \mathcal{V}^{\theta^f} \rightarrow \mathbb{R}. \quad (4.221)$$

We may then rewrite Equations (4.210)_{22–26} as

$$\begin{aligned}
\mathcal{K}(u_i, u_{i(\mathfrak{f})}, p_{\mathfrak{f}}, \theta^{\mathfrak{s}}, \theta^{\mathfrak{f}}, w^{\theta^{\mathfrak{f}}}) &= \int_{\mathfrak{B}_0} w^{\theta^{\mathfrak{f}}} \rho_0^{\mathfrak{f}} c_V^{\mathfrak{f}} D_t \theta^{\mathfrak{f}} dV + \int_{\mathfrak{B}_0} w^{\theta^{\mathfrak{f}}} \rho_0^{\mathfrak{f}} c_V^{\mathfrak{f}} \frac{\partial \theta^{\mathfrak{f}}}{\partial X_I} F_{Ii}^{-1} (v_{i(\mathfrak{f})} - v_i) dV \\
&\quad - \int_{\mathfrak{B}_0} J \sigma_{ij(E)}^{\mathfrak{f}} d_{ij(\mathfrak{f})} dV + \int_{\mathfrak{B}_0} w^{\theta^{\mathfrak{f}}} J n^{\mathfrak{f}} p_{\mathfrak{f}} \frac{\partial v_{i(\mathfrak{f})}}{\partial X_I} F_{Ii}^{-1} dV - \int_{\mathfrak{B}_0} \frac{\partial w^{\theta^{\mathfrak{f}}}}{\partial X_I} J q_i^{\mathfrak{f}} F_{Ii}^{-1} dV \\
&\quad - \int_{\mathfrak{B}_0} w^{\theta^{\mathfrak{f}}} J k_{\theta}^{\varepsilon} (\theta^{\mathfrak{s}} - \theta^{\mathfrak{f}}) dV - \int_{\Gamma_0^{Q_{\mathfrak{f}}^{\theta}}} w^{\theta^{\mathfrak{f}}} Q_{\mathfrak{f}}^{\theta} dA = 0,
\end{aligned} \tag{4.222}$$

where a repeated derivation of the weakening of the pore fluid heat flux term has been omitted (refer to Section 4.1.5 for details).

The formal statement for the variational forms \mathcal{G} , \mathcal{I} , \mathcal{H} , \mathcal{J} , and \mathcal{K} —assuming isotropic

thermoelasticity of the solid and an ideal gas model of the pore fluid—may be written as follows:

$$\begin{aligned}
& \text{Find } u_i(X_I, t) \in \mathcal{S}^u, u_{i(f)}(X_I, t) \in \mathcal{S}^{u_f}, p_f(X_I, t) \in \mathcal{S}^{p_f}, \\
& \theta^s(X_I, t) \in \mathcal{S}^{\theta^s}, \text{ and } \theta^f(X_I, t) \in \mathcal{S}^{\theta^f}, \text{ with } t \in [0, T], \text{ such that:} \\
& \int_{\mathcal{B}_0} w_i^u (\rho_0^s a_i + \rho_0^f a_{i(f)}) dV + \int_{\mathcal{B}_0} \frac{\partial w_i^u}{\partial X_I} P_{iI}^s dV + \int_{\mathcal{B}_0} \frac{\partial w_i^u}{\partial X_I} P_{iI}^f dV \\
& - \int_{\mathcal{B}_0} \frac{\partial w_i^u}{\partial X_I} J p_f F_{Ii}^{-1} \left(\frac{\theta^s}{\theta^f} n^s + n^f \right) dV - \int_{\mathcal{B}_0} w_i^u \rho_0 g_i dV \\
& - \left(\int_{\Gamma_0^t} w_i^u t_i^{\sigma E} dA + \int_{\Gamma_0^t} w_i^u t_i^{\sigma f} dA - \int_{\Gamma_0^t} w_i^u p_f J F_{Ii}^{-1} \left(\frac{\theta^s}{\theta^f} n^s + n^f \right) N_I dA \right) = 0, \\
& \int_{\mathcal{B}_0} w_i^{uf} \rho_0^f a_{i(f)} dV - \int_{\mathcal{B}_0} w_i^{uf} \frac{\partial P_{iI}^f(E)}{\partial X_I} dV + \int_{\mathcal{B}_0} w_i^{uf} J n^f \frac{\partial p_f}{\partial X_I} F_{Ii}^{-1} dV \\
& + \int_{\mathcal{B}_0} w_i^{uf} J p_f \frac{\partial n^f}{\partial X_I} \left(1 - \frac{\theta^s}{\theta^f} \right) F_{Ii}^{-1} dV + \int_{\mathcal{B}_0} w_i^{uf} J \frac{(n^f)^2}{\bar{k}} (v_{i(f)} - v_i) dV - \int_{\mathcal{B}_0} w_i^{uf} \rho_0^f g_i dV = 0, \\
& - \int_{\mathcal{B}_0} w^{pf} \frac{J}{\theta^f} \left(n^f D_t \theta^f + \frac{\partial \theta^f}{\partial X_I} F_{Ii}^{-1} (n^f \tilde{v}_{i(f)}) \right) dV + \int_{\mathcal{B}_0} w^{pf} \left(\frac{J n^f}{p_f} \dot{p}_f + j \right) dV \\
& + \int_{\mathcal{B}_0} w^{pf} \frac{J}{p_f} \frac{\partial p_f}{\partial X_I} F_{Ii}^{-1} (n^f \tilde{v}_{i(f)}) dV - \int_{\mathcal{B}_0} \frac{\partial w^{pf}}{\partial X_I} J (n^f \tilde{v}_{i(f)}) F_{Ii}^{-1} dV - \int_{\Gamma_0^{Q_f}} w^{pf} Q_f dA = 0, \\
& \int_{\mathcal{B}_0} w^{\theta^s} \rho_0^s c_V^s D_t \theta^s dV + \int_{\mathcal{B}_0} w^{\theta^s} \left(\frac{K^{\text{skel}} \alpha_V^s \theta^s}{J} + n^s p_f \frac{\theta^s}{\theta^f} + Q \right) D_t J dV \\
& - \int_{\mathcal{B}_0} \frac{\partial w^{\theta^s}}{\partial X_I} J q_i F_{Ii}^{-1} dV + \int_{\mathcal{B}_0} w^{\theta^s} J k_\theta^s (\theta^s - \theta^f) dV \\
& - \int_{\mathcal{B}_0} w^{\theta^s} \frac{J (n^f)^2}{\bar{k}} (v_{i(f)} - v_i)^2 dV + \int_{\mathcal{B}_0} w^{\theta^s} J \frac{\theta^s}{\theta^f} p_f \frac{\partial n^f}{\partial X_I} F_{Ii}^{-1} (v_{i(f)} - v_i) dV - \int_{\Gamma_0^{Q_s}} w^{\theta^s} Q_s^\theta dA = 0, \\
& \int_{\mathcal{B}_0} w^{\theta^f} \rho_0^f c_V^f D_t \theta^f dV + \int_{\mathcal{B}_0} w^{\theta^f} \rho_0^f c_V^f \frac{\partial \theta^f}{\partial X_I} (v_{i(f)} - v_i) F_{Ii}^{-1} dV \\
& - \int_{\mathcal{B}_0} w^{\theta^f} J \sigma_{ij}^f d_{ij(f)} dV + \int_{\mathcal{B}_0} w^{\theta^f} J n^f p_f \frac{\partial v_{i(f)}}{\partial X_I} F_{Ii}^{-1} dV - \int_{\mathcal{B}_0} \frac{\partial w^{\theta^f}}{\partial X_I} J q_i^f F_{Ii}^{-1} dV \\
& - \int_{\mathcal{B}_0} w^{\theta^f} J k_\theta^f (\theta^s - \theta^f) dV - \int_{\Gamma_0^{Q_f}} w^{\theta^f} Q_f^\theta dA = 0 \\
& \text{holds } \forall w_i^u \in \mathcal{V}^u, \forall w_i^{uf} \in \mathcal{V}^{uf}, \forall w^{pf} \in \mathcal{V}^{pf}, w^{\theta^s} \in \mathcal{V}^{\theta^s}, \text{ and } w^{\theta^f} \in \mathcal{V}^{\theta^f} \text{ with} \\
& \mathcal{S}^u = (u_i : \mathcal{B}_0 \times [0, T] \rightarrow \mathbb{R}^3, u_i \in H^1, u_i(t) = g_i^u(t) \text{ on } \Gamma_0^u, u_i(X_I, t = 0) = u_{i,0}(X_I)), \\
& \mathcal{S}^{u_f} = (u_{i(f)} : \mathcal{B}_0 \times [0, T] \rightarrow \mathbb{R}^3, u_{i(f)} \in H^1, u_{i(f)}(t) = g_{i(f)}^{u_f}(t) \text{ on } \Gamma_0^{u_f}, u_{i(f)}(X_I, t = 0) = u_{i(f),0}(X_I)), \\
& \mathcal{S}^{p_f} = (p_f : \mathcal{B}_0 \times [0, T] \rightarrow \mathbb{R}, p_f \in H^1, p_f(t) = g^p(t) \text{ on } \Gamma_0^p, p_f(X_I, t = 0) = p_{f,0}(X_I)), \\
& \mathcal{S}^{\theta^s} = (\theta^s : \mathcal{B}_0 \times [0, T] \rightarrow \mathbb{R}, \theta^s \in H^1, \theta^s(t) = g^{\theta^s} \text{ on } \Gamma_0^{\theta^s}, \theta^s(X_I, t = 0) = \theta_0^s(X_I)), \\
& \mathcal{S}^{\theta^f} = (\theta^f : \mathcal{B}_0 \times [0, T] \rightarrow \mathbb{R}, \theta^f \in H^1, \theta^f(t) = g^{\theta^f} \text{ on } \Gamma_0^{\theta^f}, \theta^f(X_I, t = 0) = \theta_0^f(X_I)), \\
& \mathcal{V}^u = (w_i^u : \mathcal{B}_0 \rightarrow \mathbb{R}^3, w_i^u \in H^1, w_i^u(t) = 0 \text{ on } \Gamma_0^u), \\
& \mathcal{V}^{u_f} = (w_i^{u_f} : \mathcal{B}_0 \rightarrow \mathbb{R}^3, w_i^{u_f} \in H^1, w_i^{u_f}(t) = 0 \text{ on } \Gamma_0^{u_f}), \\
& \mathcal{V}^{p_f} = (w^{p_f} : \mathcal{B}_0 \rightarrow \mathbb{R}, w^{p_f} \in H^1, w^{p_f}(t) = 0 \text{ on } \Gamma_0^p), \\
& \mathcal{V}^{\theta^s} = (w^{\theta^s} : \mathcal{B}_0 \rightarrow \mathbb{R}, w^{\theta^s} \in H^1, w^{\theta^s}(t) = 0 \text{ on } \Gamma_0^{\theta^s}), \\
& \mathcal{V}^{\theta^f} = (w^{\theta^f} : \mathcal{B}_0 \rightarrow \mathbb{R}, w^{\theta^f} \in H^1, w^{\theta^f}(t) = 0 \text{ on } \Gamma_0^{\theta^f}).
\end{aligned} \tag{4.223}$$

In the FE implementation that follows, it behooves us to simplify the variational forms, such that

$$\begin{aligned}
\mathcal{G} &= \mathcal{G}_1^{\text{INT}} + \mathcal{G}_2^{\text{INT}} + \mathcal{G}_3^{\text{INT}} + \mathcal{G}_4^{\text{INT}} + \mathcal{G}_5^{\text{INT}} + \mathcal{G}_1^{\text{EXT}} + \mathcal{G}_2^{\text{EXT}} + \mathcal{G}_3^{\text{EXT}} = 0, \\
\mathcal{I} &= \mathcal{I}_1^{\text{INT}} + \mathcal{I}_2^{\text{INT}} + \mathcal{I}_3^{\text{INT}} + \mathcal{I}_4^{\text{INT}} + \mathcal{I}_5^{\text{INT}} + \mathcal{I}_6^{\text{EXT}} = 0, \\
\mathcal{H} &= \mathcal{H}_1^{\text{INT}} + \mathcal{H}_2^{\text{INT}} + \mathcal{H}_3^{\text{INT}} + \mathcal{H}_4^{\text{INT}} + \mathcal{H}_5^{\text{INT}} + \mathcal{H}_6^{\text{INT}} + \mathcal{H}_7^{\text{INT}} + \mathcal{H}^{\text{EXT}} = 0, \\
\mathcal{J} &= \mathcal{J}_1^{\text{INT}} + \mathcal{J}_2^{\text{INT}} + \mathcal{J}_3^{\text{INT}} + \mathcal{J}_4^{\text{INT}} + \mathcal{J}_5^{\text{INT}} + \mathcal{J}_6^{\text{INT}} + \mathcal{J}^{\text{EXT}} = 0, \\
\mathcal{K} &= \mathcal{K}_1^{\text{INT}} + \mathcal{K}_2^{\text{INT}} + \mathcal{K}_3^{\text{INT}} + \mathcal{K}_4^{\text{INT}} + \mathcal{K}_7^{\text{INT}} + \mathcal{K}_8^{\text{INT}} + \mathcal{K}^{\text{EXT}} = 0,
\end{aligned} \tag{4.224}$$

wherein

$$\begin{aligned}
\mathcal{G}_1^{\text{INT}} &= \int_{\mathcal{B}_0} w_i^u (\rho_0^s a_i + \rho^f a_{i(f)}) dV, \\
\mathcal{G}_2^{\text{INT}} &= \int_{\mathcal{B}_0} \frac{\partial w_i^u}{\partial X_I} P_{iI(E)}^s dV, \\
\mathcal{G}_3^{\text{INT}} &= - \int_{\mathcal{B}_0} \frac{\partial w_i^u}{\partial X_I} J p_f F_{Ii}^{-1} \left(\frac{\theta^s}{\theta^f} n^s + n^f \right) dV, \\
\mathcal{G}_4^{\text{INT}} &= - \int_{\mathcal{B}_0} w_i^u \rho_0 g_i dV, \\
\mathcal{G}_5^{\text{INT}} &= \int_{\mathcal{B}_0} \frac{\partial w_i^u}{\partial X_I} P_{iI(E)}^f dV, \\
\mathcal{G}_1^{\text{EXT}} &= \int_{\Gamma_0^t} w_i^u t_i^{\sigma_E^s} dA, \\
\mathcal{G}_2^{\text{EXT}} &= - \int_{\Gamma_0^t} w_i^u J p_f F_{Ii} \left(\frac{\theta^s}{\theta^f} n^s + n^f \right) N_I dA, \\
\mathcal{G}_3^{\text{EXT}} &= \int_{\Gamma_0^t} w_i^u t_i^{\sigma_E^f} dA,
\end{aligned} \tag{4.225}$$

and

$$\begin{aligned}
\mathcal{I}_1^{\text{INT}} &= \int_{\mathcal{B}_0} w_i^{u_f} \rho_0^f a_{i(f)} dV, \\
\mathcal{I}_2^{\text{INT}} &= \int_{\mathcal{B}_0} w_i^{u_f} J n^f \frac{\partial p_f}{\partial X_I} F_{Ii}^{-1} dV, \\
\mathcal{I}_3^{\text{INT}} &= \int_{\mathcal{B}_0} w_i^{u_f} J \frac{(n^f)^2}{\hat{k}} (v_{i(f)} - v_i) dV, \\
\mathcal{I}_4^{\text{INT}} &= - \int_{\mathcal{B}_0} w_i^{u_f} \rho_0^f g_i dV, \\
\mathcal{I}_5^{\text{INT}} &= \int_{\mathcal{B}_0} w_i^{u_f} \frac{\partial P_{iI}^f(E)}{\partial X_I} dV, \\
\mathcal{I}_6^{\text{INT}} &= \int_{\mathcal{B}_0} w_i^{u_f} J p_f \frac{\partial n^f}{\partial X_I} \left(1 - \frac{\theta^s}{\theta^f}\right) F_{Ii}^{-1} dV,
\end{aligned} \tag{4.226}$$

and

$$\begin{aligned}
\mathcal{H}_1^{\text{INT}} &= \int_{\mathcal{B}_0} w^{p_f} \left(\frac{J n^f}{p_f} \dot{p}_f + \dot{J} \right) dV, \\
\mathcal{H}_2^{\text{INT}} &= \int_{\mathcal{B}_0} w^{p_f} \frac{J}{p_f} \frac{\partial p_f}{\partial X_I} F_{Ii}^{-1} (n^f \tilde{v}_{i(f)}) dV, \\
\mathcal{H}_3^{\text{INT}} &= \int_{\mathcal{B}_0} \frac{\partial w^{p_f}}{\partial X_I} J F_{Ii}^{-1} \hat{k} \frac{\partial p_f}{\partial X_K} F_{Ki}^{-1} dV, \\
\mathcal{H}_4^{\text{INT}} &= \int_{\mathcal{B}_0} \frac{\partial w^{p_f}}{\partial X_I} J F_{Ii}^{-1} \hat{k} \rho^{fR} (a_{i(f)} - g_i) dV, \\
\mathcal{H}_5^{\text{INT}} &= - \int_{\mathcal{B}_0} \frac{\partial w^{p_f}}{\partial X_I} \frac{\hat{k}}{n^f} J F_{Ii}^{-1} \frac{\partial \sigma_{ij}^f(E)}{\partial X_J} F_{Ji}^{-1} dV, \\
\mathcal{H}_6^{\text{INT}} &= \int_{\mathcal{B}_0} \frac{\partial w^{p_f}}{\partial X_I} J F_{Ii}^{-1} \frac{\hat{k}}{n^f p_f} \frac{\partial n^f}{\partial X_K} F_{Ki}^{-1} \left(1 - \frac{\theta^s}{\theta^f}\right) dV, \\
\mathcal{H}_7^{\text{INT}} &= - \int_{\mathcal{B}_0} w^{p_f} \frac{J}{\theta^f} \left(n^f D_t \theta^f + \frac{\partial \theta^f}{\partial X_I} F_{Ii}^{-1} (n^f \tilde{v}_{i(f)}) \right) dV, \\
\mathcal{H}^{\text{EXT}} &= \int_{\Gamma_0^{Q_f}} w^{p_f} Q_f dA,
\end{aligned} \tag{4.227}$$

and

$$\begin{aligned}
\mathcal{J}_1^{\text{INT}} &= \int_{\mathcal{B}_0} w^{\theta^s} \rho_0^s c_V D_t \theta \, dV, \\
\mathcal{J}_2^{\text{INT}} &= \int_{\mathcal{B}_0} w^{\theta^s} \left(\frac{K^{\text{skel}} \alpha_V^s \theta^s}{J} + n^s p_f \frac{\theta^s}{\theta^f} + Q \right) D_t J \, dV, \\
\mathcal{J}_3^{\text{INT}} &= - \int_{\mathcal{B}_0} \frac{\partial w^{\theta^s}}{\partial X_I} J q_i^s F_{Ii}^{-1} \, dV, \\
\mathcal{J}_4^{\text{INT}} &= \int_{\mathcal{B}_0} w^{\theta^s} J k_\theta^\varepsilon (\theta^s - \theta^f) \, dV, \\
\mathcal{J}_5^{\text{INT}} &= - \int_{\mathcal{B}_0} w^{\theta^s} \frac{J (n^f)^2}{\hat{k}} (v_{i(f)} - v_i)^2 \, dV, \\
\mathcal{J}_6^{\text{INT}} &= \int_{\mathcal{B}_0} w^{\theta^s} J \frac{\theta^s}{\theta^f} p_f \frac{\partial n^f}{\partial X_I} F_{Ii}^{-1} (v_{i(f)} - v_i) \, dV, \\
\mathcal{J}^{\text{EXT}} &= - \int_{\Gamma_0^{Q_s^\theta}} w^{\theta^s} Q_s^\theta \, dA,
\end{aligned} \tag{4.228}$$

and

$$\begin{aligned}
\mathcal{K}_1^{\text{INT}} &= \int_{\mathcal{B}_0} w^{\theta^f} \rho_0^f c_V^f D_t \theta^f \, dV \\
\mathcal{K}_2^{\text{INT}} &= \int_{\mathcal{B}_0} w^{\theta^f} \rho_0^f c_V^f \frac{\partial \theta^f}{\partial X_I} (v_{i(f)} - v_i) F_{Ii}^{-1} \, dV, \\
\mathcal{K}_3^{\text{INT}} &= \int_{\mathcal{B}_0} w^{\theta^f} J n^f p_f \frac{\partial v_{i(f)}}{\partial X_I} F_{Ii}^{-1} \, dV, \\
\mathcal{K}_4^{\text{INT}} &= - \int_{\mathcal{B}_0} w^{\theta^f} J \sigma_{ij(E)}^f d_{ij(f)} \, dV, \\
\mathcal{K}_7^{\text{INT}} &= - \int_{\mathcal{B}_0} \frac{\partial w^{\theta^f}}{\partial X_I} J q_i^f F_{Ii}^{-1} \, dV, \\
\mathcal{K}_8^{\text{INT}} &= - \int_{\mathcal{B}_0} w^{\theta^f} J k_\theta^\varepsilon (\theta^s - \theta^f) \, dV, \\
\mathcal{K}^{\text{EXT}} &= - \int_{\Gamma_0^{Q_f^\theta}} w^{\theta^f} Q_f^\theta \, dA.
\end{aligned} \tag{4.229}$$

In the case of 1-D uniaxial strain, i.e., the underlying assumption for the proceeding FE model, the

above terms simplify to the following:

$$\begin{aligned}
\mathcal{G}_1^{\text{INT}} &= \int_0^{X=H} w^u \rho_0 a A dX, \\
\mathcal{G}_2^{\text{INT}} &= \int_0^{X=H} \frac{\partial w^u}{\partial X} P_{11(E)}^s A dX, \\
\mathcal{G}_3^{\text{INT}} &= - \int_0^{X=H} \frac{\partial w^u}{\partial X} p_f \left(\frac{\theta^s}{\theta^f} n^s + n^f \right) A dX, \\
\mathcal{G}_4^{\text{INT}} &= \int_0^{X=H} w^u \rho_0 g A dX, \\
\mathcal{G}_5^{\text{INT}} &= \int_0^{X=H} \frac{\partial w^u}{\partial X} P_{11(E)}^f A dX, \\
\mathcal{G}_1^{\text{EXT}} &= \int_{\Gamma_0^t} w^u t^{\sigma_E^s} dA = t^{\sigma_E^s} A, \\
\mathcal{G}_2^{\text{EXT}} &= - \int_{\Gamma_0^t} w^u p_f \left(\frac{\theta^s}{\theta^f} n^s + n^f \right) dA = p_f \left(\frac{\theta^s}{\theta^f} n^s + n^f \right) A, \quad \mathcal{G}_3^{\text{EXT}} = \int_{\Gamma_0^t} w^u t^{\sigma_E^f} dA = t^{\sigma_E^f} A,
\end{aligned} \tag{4.230}$$

such that

$$\mathcal{G}_1^{\text{EXT}} + \mathcal{G}_2^{\text{EXT}} + \mathcal{G}_3^{\text{EXT}} = t^\sigma A, \tag{4.231}$$

and

$$\begin{aligned}
 \mathcal{I}_1^{\text{INT}} &= \int_0^{X=H} w^{u_f} \rho_0^f a_f A dX, \\
 \mathcal{I}_2^{\text{INT}} &= \int_0^{X=H} w^{u_f} n^f \frac{\partial p_f}{\partial X} A dX, \\
 \mathcal{I}_3^{\text{INT}} &= \int_0^{X=H} w^{u_f} J \frac{(n^f)^2}{\hat{k}} (v_f - v) A dX, \\
 \mathcal{I}_4^{\text{INT}} &= \int_0^{X=H} w^{u_f} \rho_0^f g A dX, \\
 \mathcal{I}_5^{\text{INT}} &= \int_0^{X=H} w^{u_f} \frac{\partial P_{11}^f(E)}{\partial X} A dX, \\
 \mathcal{I}_6^{\text{INT}} &= \int_0^{X=H} w^{u_f} p_f \frac{\partial n^f}{\partial X} \left(1 - \frac{\theta^s}{\theta^f}\right) A dX,
 \end{aligned} \tag{4.232}$$

and

$$\begin{aligned}
\mathcal{H}_1^{\text{INT}} &= \int_0^{X=H} w^{p_f} \left(\frac{J n^f}{p_f} \dot{p}_f + j \right) A dX, \\
\mathcal{H}_2^{\text{INT}} &= \int_0^{X=H} w^{p_f} \frac{1}{p_f} \frac{\partial p_f}{\partial X} (n^f \tilde{v}_f) A dX, \\
\mathcal{H}_3^{\text{INT}} &= \int_0^{X=H} \frac{\partial w^{p_f}}{\partial X} \hat{k} \frac{\partial p_f}{\partial X} F_{11}^{-1} A dX, \\
\mathcal{H}_4^{\text{INT}} &= \int_0^{X=H} \frac{\partial w^{p_f}}{\partial X} \hat{k} \rho^{\text{fR}} (a_f + g) A dX, \\
\mathcal{H}_5^{\text{INT}} &= - \int_0^{X=H} \frac{\partial w^{p_f}}{\partial X} \frac{\hat{k}}{n^f} \frac{\partial \sigma_{11}^f(E)}{\partial X} F_{11}^{-1} A dX, \\
\mathcal{H}_6^{\text{INT}} &= \int_0^{X=H} \frac{\partial w^{p_f}}{\partial X} \frac{\hat{k}}{n^f p_f} \frac{\partial n^f}{\partial X} F_{11}^{-1} \left(1 - \frac{\theta^s}{\theta^f} \right) A dX, \\
\mathcal{H}_7^{\text{INT}} &= - \int_0^{X=H} w^{p_f} \frac{J}{\theta^f} \left(n^f D_t \theta^f + \frac{\partial \theta^f}{\partial X} (n^f \tilde{v}_f) \right) A dX, \\
\mathcal{H}^{\text{EXT}} &= \int_{\Gamma_0^{Q_f}} w^{p_f} Q_f dA = Q_f A,
\end{aligned} \tag{4.233}$$

and

$$\begin{aligned}
\mathcal{J}_1^{\text{INT}} &= \int_0^{X=H} w^{\theta^s} \rho_0^s c_V D_t \theta A dX, \\
\mathcal{J}_2^{\text{INT}} &= \int_0^{X=H} w^{\theta^s} \left(\frac{K^{\text{skel}} \alpha_V^s \theta^s}{J} + n^s p_f \frac{\theta^s}{\theta^f} + Q \right) D_t J A dX, \\
\mathcal{J}_3^{\text{INT}} &= - \int_0^{X=H} \frac{\partial w^{\theta^s}}{\partial X} q^s A dX, \\
\mathcal{J}_4^{\text{INT}} &= \int_0^{X=H} w^{\theta^s} J k_\theta^s (\theta^s - \theta^f) A dX, \\
\mathcal{J}_5^{\text{INT}} &= - \int_0^{X=H} w^{\theta^s} \frac{J (n^f)^2}{\hat{k}} (v_f - v)^2 A dX, \\
\mathcal{J}_6^{\text{INT}} &= \int_0^{X=H} w^{\theta^s} \frac{\theta^s}{\theta^f} p_f \frac{\partial n^f}{\partial X} (v_f - v) A dX, \\
\mathcal{J}^{\text{EXT}} &= - \int_{\Gamma_0^{Q_s^\theta}} w^{\theta^s} Q_s^\theta dA = Q_s^\theta A,
\end{aligned} \tag{4.234}$$

and

$$\begin{aligned}
\mathcal{K}_1^{\text{INT}} &= \int_0^{X=H} w^{\theta^f} \rho_0^f c_V^f D_t \theta^f A dX \\
\mathcal{K}_2^{\text{INT}} &= \int_0^{X=H} w^{\theta^f} \rho_0^f c_V^f \frac{\partial \theta^f}{\partial X} (v_f - v) F_{11}^{-1} A dX, \\
\mathcal{K}_3^{\text{INT}} &= \int_0^{X=H} w^{\theta^f} n^f p_f \frac{\partial v_f}{\partial X} A dX, \\
\mathcal{K}_4^{\text{INT}} &= - \int_0^{X=H} w^{\theta^f} \frac{n^f}{J} \left(\frac{\partial v_f}{\partial X} \right)^2 (\kappa_f + 2\mu_f) A dX, \\
\mathcal{K}_7^{\text{INT}} &= - \int_0^{X=H} \frac{\partial w^{\theta^f}}{\partial X} q^f A dX, \\
\mathcal{K}_8^{\text{INT}} &= - \int_0^{X=H} w^{\theta^f} J k_\theta^\varepsilon (\theta^s - \theta^f) A dX, \\
\mathcal{K}^{\text{EXT}} &= - \int_{\Gamma_0^{Q_f^\theta}} w^{\theta^f} Q_f^\theta dA = Q_f^\theta A.
\end{aligned} \tag{4.235}$$

The compressible liquid model. For the compressible liquid pore fluid model, recall that

$$\begin{aligned}
\eta^f &= c_V^f \ln \left(\frac{\theta^f}{\theta_0^f} \right) + \frac{K_f^\theta \alpha_V^f}{\rho^{\text{fR}}}, \\
\rho^{\text{fR}} &= \rho_0^{\text{fR}} \exp \left[\frac{p_f - p_{f,0}}{K_f^\theta} - \alpha_V^f \theta^f \right],
\end{aligned} \tag{4.236}$$

such that

$$\begin{aligned}
D_t^f \rho^{\text{fR}} &= \rho^{\text{fR}} \left(\frac{1}{K_f^\theta} D_t^f p_f - \alpha_V^f D_t^f \theta^f \right), \\
\theta^f D_t^f \eta^f &= c_V^f D_t^f \theta^f - \frac{\alpha_V^f K_f^\theta \theta^f}{\rho^{\text{fR}}} \left(\frac{1}{K_f^\theta} D_t^f p_f - \alpha_V^f D_t^f \theta^f \right).
\end{aligned} \tag{4.237}$$

Then the left hand side of Equation (4.143) simplifies to³

$$(\rho^f c_V^f + n^f \alpha_V^f [\alpha_V^f K_f^\theta \theta^f - p_f]) D_t^f \theta^f + n^f \left(\frac{p_f}{K_f^\theta} - \alpha_V^f \theta^f \right) D_t^f p_f. \tag{4.238}$$

³ As with the $(\mathbf{u}-p_f-\theta^s-\theta^f)$ formulation compressible liquid model, note again that when $\alpha_V^f := 1/\theta^f$ and $K_f^\theta := p_f$, the term in brackets evaluates to zero and the second parenthetical term evaluates to zero, such that we recover the ideal gas model.

Thus, the energy balance for the compressible pore liquid may be written as

$$\begin{aligned}
& (\rho^f c_V^f + n^f \alpha_V^f [\alpha_V^f K_f^\theta \theta^f - p_f]) (D_t^s \theta^f + \text{grad}(\theta^f) \cdot \tilde{\mathbf{v}}_f) \\
& \quad + n^f \left(\frac{p_f}{K_f^\theta} - \alpha_V^f \theta^f \right) (D_t^s p_f + \text{grad}(p_f) \cdot \tilde{\mathbf{v}}_f) \\
& - \boldsymbol{\sigma}_E^f : \mathbf{d}_f + p_f n^f \text{div } \mathbf{v}_f + \text{div } \mathbf{q}^f - k_\theta^\varepsilon (\theta^s - \theta^f) = 0, \tag{4.239}
\end{aligned}$$

which we may convert to the reference configuration of the solid skeleton \mathcal{B}_0 , dropping the appropriate $(\cdot)^s$ and $(\cdot)_s$ designations, as follows:

$$\begin{aligned}
& (\rho_0^f c_V^f + J n^f \alpha_V^f [\alpha_V^f K_f^\theta \theta^f - p_f]) (D_t \theta^f + \text{GRAD}(\theta^f) \cdot \tilde{\mathbf{v}}_f) \cdot \mathbf{F}^{-1} \\
& \quad + J n^f \left(\frac{p_f}{K_f^\theta} - \alpha_V^f \theta^f \right) (D_t p_f + \text{grad}(p_f) \cdot \tilde{\mathbf{v}}_f \cdot \mathbf{F}^{-1}) \\
& - J \boldsymbol{\sigma}_E^f : \mathbf{d}_f + J p_f n^f \text{GRAD}(\mathbf{v}_f) : \mathbf{F}^{-T} - J k_\theta^\varepsilon (\theta^s - \theta^f) + J \text{GRAD}(\mathbf{q}^f) : \mathbf{F}^{-T} = 0. \tag{4.240}
\end{aligned}$$

As such, the strong formulation for the balances of linear momenta, mass, and energies—under the assumption of a linear thermoelastic solid constituent and compressible liquid pore fluid constituent—

may be written as follows:

$$\begin{aligned}
& \text{Find } \mathbf{u}(\mathbf{X}, t) \in \mathcal{S}^u, \mathbf{u}_f(\mathbf{X}, t) \in \mathcal{S}^{u_f}, p_f(\mathbf{X}, t) \in \mathcal{S}^{p_f}, \\
& \theta^s(\mathbf{X}, t) \in \mathcal{S}^{\theta^s}, \text{ and } \theta^f(\mathbf{X}, t) \in \mathcal{S}^{\theta^f}, \\
& \text{with } t \in [0, T], \text{ such that:} \\
& \text{DIV } \mathbf{P} + \rho_0 \mathbf{g} - (\rho_0^s \mathbf{a} + \rho_0^f \mathbf{a}_f) = \mathbf{0} \in \mathcal{B}_0, \\
& \mathbf{u}(\mathbf{X}, t) = \mathbf{g}^u(\mathbf{X}, t) \text{ on } \Gamma_0^u, \\
& \mathbf{P}(\mathbf{X}, t) \cdot \mathbf{N}(\mathbf{X}) = \mathbf{t}^\sigma(\mathbf{X}, t) \text{ on } \Gamma_0^t, \\
& \mathbf{u}(\mathbf{X}, t = 0) = \mathbf{u}_0(\mathbf{X}) \in \mathcal{B}_0, \\
& \mathbf{v}(\mathbf{X}, t = 0) = \mathbf{v}_0(\mathbf{X}) \in \mathcal{B}_0, \\
& \mathbf{a}(\mathbf{X}, t = 0) = \mathbf{a}_0(\mathbf{X}) \in \mathcal{B}_0, \\
& \rho_0^f \mathbf{a}_f - \text{DIV } \mathbf{P}_E^f + J n^f \text{GRAD}(p_f) \cdot \mathbf{F}^{-1} \\
& + J p_f \text{GRAD } n^f \left(1 - \frac{\theta^s}{\theta^f}\right) \cdot \mathbf{F}^{-1} + J \frac{(n^f)^2}{k} (\mathbf{v}_f - \mathbf{v}) - \rho_0^f \mathbf{g} = \mathbf{0} \in \mathcal{B}_0, \\
& \mathbf{u}_f(\mathbf{X}, t) = \mathbf{g}_{u_f}(\mathbf{X}, t) \text{ on } \Gamma_0^{u_f}, \\
& \mathbf{u}_f(\mathbf{X}, t = 0) = \mathbf{u}_{f,0}(\mathbf{X}) \in \mathcal{B}_0, \\
& \mathbf{v}_f(\mathbf{X}, t = 0) = \mathbf{v}_{f,0}(\mathbf{X}) \in \mathcal{B}_0, \\
& \mathbf{a}_f(\mathbf{X}, t = 0) = \mathbf{a}_{f,0}(\mathbf{X}) \in \mathcal{B}_0, \\
& -J \alpha_V^f [n^f D_t \theta^f + \text{GRAD}(\theta^f) \cdot \mathbf{F}^{-1} \cdot (n^f \tilde{\mathbf{v}}_f)] + \frac{J n^f}{K_f^\theta} D_t p_f + D_t J \\
& + \frac{J}{K_f^\theta} \text{GRAD}(p_f) \cdot \mathbf{F}^{-1} \cdot (n^f \tilde{\mathbf{v}}_f) + J \text{GRAD}(n^f \tilde{\mathbf{v}}_f) \cdot \mathbf{F}^{-T} = 0 \in \mathcal{B}_0, \\
& p_f(\mathbf{X}, t) = g^p(\mathbf{X}, t) \text{ on } \Gamma_0^p, \\
& -[J \mathbf{F}^{-1} \cdot (n^f \tilde{\mathbf{v}}_f)] \cdot \mathbf{N} = Q_f(\mathbf{X}, t) \text{ on } \Gamma_0^{Q_f}, \\
& p_f(\mathbf{X}, t = 0) = p_{f,0}(\mathbf{X}) \in \mathcal{B}_0, \\
& \dot{p}_f(\mathbf{X}, t = 0) = \dot{p}_{f,0}(\mathbf{X}) \in \mathcal{B}_0, \\
& \rho_0^s c_V^s D_t \theta^s + \left(\frac{K^{\text{skel}} \alpha_V^s \theta^s}{J} + n^s p_f \frac{\theta^s}{\theta^f} + Q \right) D_t J \\
& + J \text{GRAD}(q^s) \cdot \mathbf{F}^{-T} + J k_\theta^s (\theta^s - \theta^f) \\
& - \frac{J (n^f)^2}{k} (\mathbf{v}_f - \mathbf{v})^2 + J \frac{\theta^s}{\theta^f} \frac{p_f}{n^f} \text{GRAD}(n^f) \cdot \mathbf{F}^{-1} \cdot (n^f \tilde{\mathbf{v}}_f) = 0 \in \mathcal{B}_0, \\
& \theta^s(\mathbf{X}, t) = g^{\theta^s}(\mathbf{X}, t) \text{ on } \Gamma_0^{\theta^s}, \\
& -(J q^s \cdot \mathbf{F}^{-T}) \cdot \mathbf{N} = Q_s^\theta(\mathbf{X}, t) \text{ on } \Gamma_0^{Q_s^\theta}, \\
& \theta^s(\mathbf{X}, t = 0) = \theta_0^s(\mathbf{X}) \in \mathcal{B}_0 \\
& \dot{\theta}^s(\mathbf{X}, t = 0) = \dot{\theta}_0^s(\mathbf{X}) \in \mathcal{B}_0 \\
& (\rho_0^f c_V^f + J n^f \alpha_V^f [\alpha_V^f K_f^\theta \theta^f - p_f]) (D_t \theta^f + \text{GRAD}(\theta^f) \cdot \tilde{\mathbf{v}}_f) \cdot \mathbf{F}^{-1} \\
& + J n^f \left(\frac{p_f}{K_f^\theta} - \alpha_V^f \theta^f \right) (D_t p_f + \text{grad}(p_f) \cdot \tilde{\mathbf{v}}_f \cdot \mathbf{F}^{-1}) \\
& - J \boldsymbol{\sigma}_E^f \cdot \mathbf{d}_f + J p_f n^f \text{GRAD}(\mathbf{v}_f) \cdot \mathbf{F}^{-T} - J k_\theta^s (\theta^s - \theta^f) + J \text{GRAD}(q^f) \cdot \mathbf{F}^{-T} = 0 \in \mathcal{B}_0, \\
& \theta^f(\mathbf{X}, t) = g^{\theta^f}(\mathbf{X}, t) \text{ on } \Gamma_0^{\theta^f}, \\
& -(J q^f \cdot \mathbf{F}^{-T}) \cdot \mathbf{N} = Q_s^{\theta^f}(\mathbf{X}, t) \text{ on } \Gamma_0^{Q_s^{\theta^f}}, \\
& \theta^f(\mathbf{X}, t = 0) = \theta_0^f(\mathbf{X}) \in \mathcal{B}_0 \\
& \dot{\theta}^f(\mathbf{X}, t = 0) = \dot{\theta}_0^f(\mathbf{X}) \in \mathcal{B}_0.
\end{aligned} \tag{S) =} \tag{4.241}$$

The variational forms for $\mathcal{G}, \mathcal{I}, \mathcal{J}$ remain unchanged from the ideal gas formulation. Let

$\mathcal{H}(u_i, u_{i(f)}, p_f, \theta^s, \theta^f, w^{p_i})$ be the variational form of Equations (4.241)_{12–16}, such that

$$\mathcal{H} : \mathcal{S}^{p_f} \times \mathcal{S}^u \times \mathcal{S}^{u_f} \times \mathcal{S}^{\theta^f} \times \mathcal{V}^{p_f} \rightarrow \mathbb{R}. \tag{4.242}$$

Thus we may write Equation (4.241)_{12–16} as

$$\begin{aligned}
\mathcal{H}(u_i, u_{i(f)}, p_f, \theta^s, \theta^f, w^{p_f}) &= - \int_{\mathcal{B}_0} w^{p_f} J \alpha_V^f \left(n^f D_t \theta^f + \frac{\partial \theta^f}{\partial X_I} F_{Ii}^{-1} (n^f \tilde{v}_{i(f)}) \right) dV \\
&+ \int_{\mathcal{B}_0} w^{p_f} \left(\frac{J n^f}{K_f^\theta} \dot{p}_f + j \right) dV + \int_{\mathcal{B}_0} w^{p_f} \frac{J}{K_f^\theta} \frac{\partial p_f}{\partial X_I} F_{Ii}^{-1} (n^f \tilde{v}_{i(f)}) dV \\
&- \int_{\mathcal{B}_0} \frac{\partial w^{p_f}}{\partial X_I} J (n^f \tilde{v}_{i(f)}) F_{Ii}^{-1} dV - \int_{\Gamma_0^Q} w^{p_f} Q_f dA = 0.
\end{aligned} \tag{4.243}$$

Let $\mathcal{K}(u_i, u_{i(f)}, p_f, \theta^s, \theta^f, w^{\theta^f})$ be the variational form of Equations (4.241)_{22–26}, such that

$$\mathcal{K} : \mathcal{S}^{\theta^f} \times \mathcal{S}^u \times \mathcal{S}^{p_f} \times \mathcal{S}^{\theta^s} \times \mathcal{V}^{\theta^f} \rightarrow \mathbb{R}. \tag{4.244}$$

We may then rewrite Equations (4.241)_{22–26} as

$$\begin{aligned}
\mathcal{K}(u_i, u_{i(f)}, p_f, \theta^s, \theta^f, w^{\theta^f}) &= \int_{\mathcal{B}_0} w^{\theta^f} (\rho_0^f c_V^f + J n^f \alpha_V^f [\alpha_V^f K_f^\theta \theta^f - p_f]) D_t \theta^f dV \\
&+ \int_{\mathcal{B}_0} w^{\theta^f} (\rho_0^f c_V^f + J n^f \alpha_V^f [\alpha_V^f K_f^\theta \theta^f - p_f]) \frac{\partial \theta^f}{\partial X_I} F_{Ii}^{-1} (v_{i(f)} - v_i) dV \\
&- \int_{\mathcal{B}_0} J \sigma_{ij(E)}^f d_{ij(f)} dV + \int_{\mathcal{B}_0} w^{\theta^f} J n^f p_f \frac{\partial v_{i(f)}}{\partial X_I} F_{Ii}^{-1} dV - \int_{\mathcal{B}_0} \frac{\partial w^{\theta^f}}{\partial X_I} J q_i^f F_{Ii}^{-1} dV \\
&- \int_{\mathcal{B}_0} w^{\theta^f} J k_\theta^\varepsilon (\theta^s - \theta^f) dV - \int_{\Gamma_0^{Q_f^\theta}} w^{\theta^f} Q_f^\theta dA = 0.
\end{aligned} \tag{4.245}$$

The formal statement for the variational forms \mathcal{G} , \mathcal{I} , \mathcal{H} , \mathcal{J} , and \mathcal{K} —assuming isotropic thermoelasticity of the solid and a compressible liquid model of the pore fluid—may be written as follows:

$$\begin{aligned}
 \mathcal{W} = & \left\{ \begin{aligned}
 & \text{Find } u_i(X_I, t) \in \mathcal{S}^u, u_{i(f)}(X_I, t) \in \mathcal{S}^{u_f}, p_f(X_I, t) \in \mathcal{S}^{p_f}, \\
 & \theta^s(X_I, t) \in \mathcal{S}^{\theta^s}, \text{ and } \theta^f(X_I, t) \in \mathcal{S}^{\theta^f}, \text{ with } t \in [0, T], \text{ such that:} \\
 & \int_{\mathcal{B}_0} w_i^u (\rho_0^s a_i + \rho_0^f a_{i(f)}) dV + \int_{\mathcal{B}_0} \frac{\partial w_i^u}{\partial X_I} P_{iI}^s dV + \int_{\mathcal{B}_0} \frac{\partial w_i^u}{\partial X_I} P_{iI}^f dV \\
 & - \int_{\mathcal{B}_0} \frac{\partial w_i^u}{\partial X_I} J p_f F_{Ii}^{-1} \left(\frac{\theta^s}{\theta^f} n^s + n^f \right) dV - \int_{\mathcal{B}_0} w_i^u \rho_0 g_i dV \\
 & - \left(\int_{\Gamma_0^t} w_i^u t_i^{\sigma^s} dA + \int_{\Gamma_0^t} w_i^u t_i^{\sigma^f} dA - \int_{\Gamma_0^t} w_i^u p_f J F_{Ii}^{-1} \left(\frac{\theta^s}{\theta^f} n^s + n^f \right) N_I dA \right) = 0, \\
 & \int_{\mathcal{B}_0} w_i^{u_f} \rho_0^f a_{i(f)} dV - \int_{\mathcal{B}_0} w_i^{u_f} \frac{\partial P_{iI}^f(E)}{\partial X_I} dV + \int_{\mathcal{B}_0} w_i^{u_f} J n^f \frac{\partial p_f}{\partial X_I} F_{Ii}^{-1} dV \\
 & + \int_{\mathcal{B}_0} w_i^{u_f} J p_f \frac{\partial n^f}{\partial X_I} \left(1 - \frac{\theta^s}{\theta^f} \right) F_{Ii}^{-1} dV + \int_{\mathcal{B}_0} w_i^{u_f} J \frac{(n^f)^2}{k} (v_{i(f)} - v_i) dV - \int_{\mathcal{B}_0} w_i^{u_f} \rho_0^f g_i dV = 0, \\
 & - \int_{\mathcal{B}_0} w^{p_f} J \alpha_V^f \left(n^f D_t \theta^f + \frac{\partial \theta^f}{\partial X_I} F_{Ii}^{-1} (n^f \tilde{v}_{i(f)}) \right) dV + \int_{\mathcal{B}_0} w^{p_f} \left(\frac{J n^f}{K_f^\theta} \dot{p}_f + j \right) dV \\
 & + \int_{\mathcal{B}_0} w^{p_f} \frac{J}{K_f^\theta} \frac{\partial p_f}{\partial X_I} F_{Ii}^{-1} (n^f \tilde{v}_{i(f)}) dV - \int_{\mathcal{B}_0} \frac{\partial w^{p_f}}{\partial X_I} J (n^f \tilde{v}_{i(f)}) F_{Ii}^{-1} dV - \int_{\Gamma_0^{Q_f}} w^{p_f} Q_f dA = 0, \\
 & \int_{\mathcal{B}_0} w^{\theta^s} \rho_0^s c_V^s D_t \theta^s dV + \int_{\mathcal{B}_0} w^{\theta^s} \left(\frac{K^{\text{skel}} \alpha_V^s \theta^s}{J} + n^s p_f \frac{\theta^s}{\theta^f} + Q \right) D_t J dV \\
 & - \int_{\mathcal{B}_0} \frac{\partial w^{\theta^s}}{\partial X_I} J q_i F_{Ii}^{-1} dV + \int_{\mathcal{B}_0} w^{\theta^s} J k_\theta^s (\theta^s - \theta^f) dV \\
 & - \int_{\mathcal{B}_0} w^{\theta^s} \frac{J (n^f)^2}{k} (v_{i(f)} - v_i)^2 dV + \int_{\mathcal{B}_0} w^{\theta^s} J \frac{\theta^s}{\theta^f} p_f \frac{\partial n^f}{\partial X_I} F_{Ii}^{-1} (v_{i(f)} - v_i) dV - \int_{\Gamma_0^{Q_s}} w^{\theta^s} Q_s^\theta dA = 0, \\
 & \int_{\mathcal{B}_0} w^{\theta^f} (\rho_0^f c_V^f + J n^f \alpha_V^f [\alpha_V^f K_f^\theta \theta^f - p_f]) D_t \theta^f dV \\
 & + \int_{\mathcal{B}_0} w^{\theta^f} (\rho_0^f c_V^f + J n^f \alpha_V^f [\alpha_V^f K_f^\theta \theta^f - p_f]) \frac{\partial \theta^f}{\partial X_I} F_{Ii}^{-1} (v_{i(f)} - v_i) dV \\
 & - \int_{\mathcal{B}_0} J \sigma_{ij}^f(E) d_{ij(f)} dV + \int_{\mathcal{B}_0} w^{\theta^f} J n^f p_f \frac{\partial v_{i(f)}}{\partial X_I} F_{Ii}^{-1} dV - \int_{\mathcal{B}_0} \frac{\partial w^{\theta^f}}{\partial X_I} J q_i^f F_{Ii}^{-1} dV \\
 & - \int_{\mathcal{B}_0} w^{\theta^f} J k_\theta^f (\theta^s - \theta^f) dV - \int_{\Gamma_0^{Q_f}} w^{\theta^f} Q_f^\theta dA = 0 \\
 & \text{holds } \forall w_i^u \in \mathcal{V}^u, \forall w_i^{u_f} \in \mathcal{V}^{u_f}, \forall w^{p_f} \in \mathcal{V}^{p_f}, w^{\theta^s} \in \mathcal{V}^{\theta^s}, \text{ and } w^{\theta^f} \in \mathcal{V}^{\theta^f} \text{ with} \\
 & \mathcal{S}^u = (u_i : \mathcal{B}_0 \times [0, T] \rightarrow \mathbb{R}^3, u_i \in H^1, u_i(t) = g_i^u(t) \text{ on } \Gamma_0^u, u_i(X_I, t = 0) = u_{i,0}(X_I)), \\
 & \mathcal{S}^{u_f} = (u_{i(f)} : \mathcal{B}_0 \times [0, T] \rightarrow \mathbb{R}^3, u_{i(f)} \in H^1, u_{i(f)}(t) = g_{i(f)}^{u_f}(t) \text{ on } \Gamma_0^{u_f}, u_{i(f)}(X_I, t = 0) = u_{i(f),0}(X_I)), \\
 & \mathcal{S}^{p_f} = (p_f : \mathcal{B}_0 \times [0, T] \rightarrow \mathbb{R}, p_f \in H^1, p_f(t) = g^{p_f}(t) \text{ on } \Gamma_0^{p_f}, p_f(X_I, t = 0) = p_{f,0}(X_I)), \\
 & \mathcal{S}^{\theta^s} = (\theta^s : \mathcal{B}_0 \times [0, T] \rightarrow \mathbb{R}, \theta^s \in H^1, \theta^s(t) = g^{\theta^s} \text{ on } \Gamma_0^{\theta^s}, \theta^s(X_I, t = 0) = \theta_0^s(X_I)), \\
 & \mathcal{S}^{\theta^f} = (\theta^f : \mathcal{B}_0 \times [0, T] \rightarrow \mathbb{R}, \theta^f \in H^1, \theta^f(t) = g^{\theta^f} \text{ on } \Gamma_0^{\theta^f}, \theta^f(X_I, t = 0) = \theta_0^f(X_I)), \\
 & \mathcal{V}^u = (w_i^u : \mathcal{B}_0 \rightarrow \mathbb{R}^3, w_i^u \in H^1, w_i^u(t) = 0 \text{ on } \Gamma_0^u), \\
 & \mathcal{V}^{u_f} = (w_i^{u_f} : \mathcal{B}_0 \rightarrow \mathbb{R}^3, w_i^{u_f} \in H^1, w_i^{u_f}(t) = 0 \text{ on } \Gamma_0^{u_f}), \\
 & \mathcal{V}^{p_f} = (w^{p_f} : \mathcal{B}_0 \rightarrow \mathbb{R}, w^{p_f} \in H^1, w^{p_f}(t) = 0 \text{ on } \Gamma_0^{p_f}), \\
 & \mathcal{V}^{\theta^s} = (w^{\theta^s} : \mathcal{B}_0 \rightarrow \mathbb{R}, w^{\theta^s} \in H^1, w^{\theta^s}(t) = 0 \text{ on } \Gamma_0^{\theta^s}), \\
 & \mathcal{V}^{\theta^f} = (w^{\theta^f} : \mathcal{B}_0 \rightarrow \mathbb{R}, w^{\theta^f} \in H^1, w^{\theta^f}(t) = 0 \text{ on } \Gamma_0^{\theta^f}).
 \end{aligned} \right. \tag{4.246}
 \end{aligned}$$

In the FE implementation that follows, it behooves us to simplify the variational forms, such that

$$\begin{aligned}
\mathcal{G} &= \mathcal{G}_1^{\text{INT}} + \mathcal{G}_2^{\text{INT}} + \mathcal{G}_3^{\text{INT}} + \mathcal{G}_4^{\text{INT}} + \mathcal{G}_5^{\text{INT}} + \mathcal{G}_1^{\text{EXT}} + \mathcal{G}_2^{\text{EXT}} + \mathcal{G}_3^{\text{EXT}} = 0, \\
\mathcal{I} &= \mathcal{I}_1^{\text{INT}} + \mathcal{I}_2^{\text{INT}} + \mathcal{I}_3^{\text{INT}} + \mathcal{I}_4^{\text{INT}} + \mathcal{I}_5^{\text{INT}} + \mathcal{I}_6^{\text{EXT}} = 0, \\
\mathcal{H} &= \mathcal{H}_1^{\text{INT}} + \mathcal{H}_2^{\text{INT}} + \mathcal{H}_3^{\text{INT}} + \mathcal{H}_4^{\text{INT}} + \mathcal{H}_5^{\text{INT}} + \mathcal{H}_6^{\text{INT}} + \mathcal{H}_7^{\text{INT}} + \mathcal{H}^{\text{EXT}} = 0, \\
\mathcal{J} &= \mathcal{J}_1^{\text{INT}} + \mathcal{J}_2^{\text{INT}} + \mathcal{J}_3^{\text{INT}} + \mathcal{J}_4^{\text{INT}} + \mathcal{J}_5^{\text{INT}} + \mathcal{J}_6^{\text{INT}} + \mathcal{J}^{\text{EXT}} = 0, \\
\mathcal{K} &= \mathcal{K}_1^{\text{INT}} + \mathcal{K}_2^{\text{INT}} + \mathcal{K}_3^{\text{INT}} + \mathcal{K}_4^{\text{INT}} + \mathcal{K}_7^{\text{INT}} + \mathcal{K}_8^{\text{INT}} + \mathcal{K}^{\text{EXT}} = 0,
\end{aligned} \tag{4.247}$$

wherein \mathcal{G} terms are defined in Equation (4.225), \mathcal{I} terms are defined in Equation (4.226), \mathcal{J} terms are defined in Equation (4.228), and

$$\begin{aligned}
\mathcal{H}_1^{\text{INT}} &= \int_{\mathcal{B}_0} w^{p_f} \left(\frac{J n^f}{K_f^\theta} \dot{p}_f + j \right) dV, \\
\mathcal{H}_2^{\text{INT}} &= \int_{\mathcal{B}_0} w^{p_f} \frac{J}{K_f^\theta} \frac{\partial p_f}{\partial X_I} F_{Ii}^{-1} (n^f \tilde{v}_{i(f)}) dV, \\
\mathcal{H}_3^{\text{INT}} &= \int_{\mathcal{B}_0} \frac{\partial w^{p_f}}{\partial X_I} J F_{Ii}^{-1} \hat{k} \frac{\partial p_f}{\partial X_K} F_{Ki}^{-1} dV, \\
\mathcal{H}_4^{\text{INT}} &= \int_{\mathcal{B}_0} \frac{\partial w^{p_f}}{\partial X_I} J F_{Ii}^{-1} \hat{k} \rho^{\text{fR}} (a_{i(f)} - g_i) dV, \\
\mathcal{H}_5^{\text{INT}} &= - \int_{\mathcal{B}_0} \frac{\partial w^{p_f}}{\partial X_I} \frac{\hat{k}}{n^f} J F_{Ii}^{-1} \frac{\partial \sigma_{ij(E)}^f}{\partial X_J} F_{Jj}^{-1} dV, \\
\mathcal{H}_6^{\text{INT}} &= \int_{\mathcal{B}_0} \frac{\partial w^{p_f}}{\partial X_I} J F_{Ii}^{-1} \frac{\hat{k}}{n^f} p_f \frac{\partial n^f}{\partial X_K} F_{Ki}^{-1} \left(1 - \frac{\theta^s}{\theta^f} \right) dV, \\
\mathcal{H}_7^{\text{INT}} &= - \int_{\mathcal{B}_0} w^{p_f} J \alpha_V^f \left(n^f D_t \theta^f + \frac{\partial \theta^f}{\partial X_I} F_{Ii}^{-1} (n^f \tilde{v}_{i(f)}) \right) dV, \\
\mathcal{H}^{\text{EXT}} &= \int_{\Gamma_0^{Q_f}} w^{p_f} Q_f dA,
\end{aligned} \tag{4.248}$$

and

$$\begin{aligned}
\mathcal{K}_1^{\text{INT}} &= \int_{\mathcal{B}_0} w^{\theta^f} (\rho_0^f c_V^f + J n^f \alpha_V^f [\alpha_V^f K_f^\theta \theta^f - p_f]) D_t \theta^f dV \\
\mathcal{K}_2^{\text{INT}} &= \int_{\mathcal{B}_0} w^{\theta^f} (\rho_0^f c_V^f + J n^f \alpha_V^f [\alpha_V^f K_f^\theta \theta^f - p_f]) \frac{\partial \theta^f}{\partial X_I} (v_{i(f)} - v_i) F_{Ii}^{-1} dV, \\
\mathcal{K}_3^{\text{INT}} &= \int_{\mathcal{B}_0} w^{\theta^f} J n^f p_f \frac{\partial v_{i(f)}}{\partial X_I} F_{Ii}^{-1} dV, \\
\mathcal{K}_4^{\text{INT}} &= - \int_{\mathcal{B}_0} w^{\theta^f} J \sigma_{ij(E)}^f d_{ij(f)} dV, \\
\mathcal{K}_7^{\text{INT}} &= - \int_{\mathcal{B}_0} \frac{\partial w^{\theta^f}}{\partial X_I} J q_i^f F_{Ii}^{-1} dV, \\
\mathcal{K}_8^{\text{INT}} &= - \int_{\mathcal{B}_0} w^{\theta^f} J k_\theta^\varepsilon (\theta^s - \theta^f) dV, \\
\mathcal{K}^{\text{EXT}} &= - \int_{\Gamma_0^{Q_f^\theta}} w^{\theta^f} Q_f^\theta dA.
\end{aligned} \tag{4.249}$$

In the case of 1-D uniaxial strain, i.e., the underlying assumption for the proceeding FE model, the above terms simplify to the following:

$$\begin{aligned}
\mathcal{H}_1^{\text{INT}} &= \int_0^{X=H} w^{p_f} \left(\frac{J n^f}{K_f^\theta} \dot{p}_f + j \right) A dX, \\
\mathcal{H}_2^{\text{INT}} &= \int_0^{X=H} w^{p_f} \frac{1}{K_f^\theta} \frac{\partial p_f}{\partial X} (n^f \tilde{v}_f) A dX, \\
\mathcal{H}_3^{\text{INT}} &= \int_0^{X=H} \frac{\partial w^{p_f}}{\partial X} \hat{k} \frac{\partial p_f}{\partial X} F_{11}^{-1} A dX, \\
\mathcal{H}_4^{\text{INT}} &= \int_0^{X=H} \frac{\partial w^{p_f}}{\partial X} \hat{k} \rho^{\text{fR}} (a_f + g) A dX, \\
\mathcal{H}_5^{\text{INT}} &= - \int_0^{X=H} \frac{\partial w^{p_f}}{\partial X} \frac{\hat{k}}{n^f} \frac{\partial \sigma_{11}^f(E)}{\partial X} F_{11}^{-1} A dX, \\
\mathcal{H}_6^{\text{INT}} &= \int_0^{X=H} \frac{\partial w^{p_f}}{\partial X} \frac{\hat{k}}{n^f p_f} \frac{\partial n^f}{\partial X} F_{11}^{-1} \left(1 - \frac{\theta^s}{\theta^f} \right) A dX, \\
\mathcal{H}_7^{\text{INT}} &= - \int_0^{X=H} w^{p_f} J \alpha_V^f \left(n^f D_t \theta^f + \frac{\partial \theta^f}{\partial X} (n^f \tilde{v}_f) \right) A dX, \\
\mathcal{H}^{\text{EXT}} &= \int_{\Gamma_0^{Q_f}} w^{p_f} Q_f dA = Q_f A,
\end{aligned} \tag{4.250}$$

and

$$\begin{aligned}
\mathcal{K}_1^{\text{INT}} &= \int_0^{X=H} w^{\theta^f} (\rho_0^f c_V^f + J n^f \alpha_V^f [\alpha_V^f K_f^\theta \theta^f - p_f]) D_t \theta^f A dX \\
\mathcal{K}_2^{\text{INT}} &= \int_0^{X=H} w^{\theta^f} (\rho^f c_V^f + n^f \alpha_V^f [\alpha_V^f K_f^\theta \theta^f - p_f]) \frac{\partial \theta^f}{\partial X} (v_f - v) A dX, \\
\mathcal{K}_3^{\text{INT}} &= \int_0^{X=H} w^{\theta^f} n^f p_f \frac{\partial v_f}{\partial X} A dX, \\
\mathcal{K}_4^{\text{INT}} &= - \int_0^{X=H} w^{\theta^f} \frac{n^f}{J} \left(\frac{\partial v_f}{\partial X} \right)^2 (\kappa_f + 2\mu_f) A dX, \\
\mathcal{K}_7^{\text{INT}} &= - \int_0^{X=H} \frac{\partial w^{\theta^f}}{\partial X} q^f A dX, \\
\mathcal{K}_8^{\text{INT}} &= - \int_0^{X=H} w^{\theta^f} J k_\theta^\varepsilon (\theta^s - \theta^f) A dX, \\
\mathcal{K}^{\text{EXT}} &= - \int_{\Gamma_0^{Q_f^\theta}} w^{\theta^f} Q_f^\theta dA = Q_f^\theta A.
\end{aligned} \tag{4.251}$$

4.2 Finite element implementation

An extensive overview of the finite element method (FEM) is given by Hughes [2000], Zienkiewicz et al. [2005], Belytschko et al. [2014], Donea and Huerta [2003], to name a few. We will use Bubnov-Galerkin to approximate the solutions to the weak formulations given in Section 4.1, such that

$$\begin{aligned}
\mathbf{y}^h &\in (\mathcal{S}^y)^h; \quad (\mathcal{S}^y)^h \subset \mathcal{S}^y, \\
\mathbf{w}^{y^h} &\in (\mathcal{V}^y)^h; \quad (\mathcal{V}^y)^h \subset \mathcal{V}^y,
\end{aligned} \tag{4.252}$$

for general solution variable of interest y , where the superscript h denotes the FE approximation (of some finite length scale) of said variable within the discretization (the mesh) of the domain \mathcal{B}_0 .

It is also assumed that

$$w_i^{y^h} = 0 \text{ on } \Gamma^y, \quad \forall w_i^{y^h}(x_i) \in (\mathcal{V}^y)^h. \tag{4.253}$$

4.2.1 Interpolation

As stated in previous sections, for uniaxial strain and unidirectional flow with axial symmetry, our geometry of a column of porous lung parenchyma is reduced to one-dimension. Therefore, we employ a one-dimensional finite element mesh to solve the variational equations above. For interpolating our solution variables, we use standard Lagrange polynomials up to cubic order, and Hermite cubic polynomials when appropriate (i.e., when C^1 continuity is required). Displacements (of both solid and fluid) can either be interpolated using cubic, quadratic, or linear Lagrange polynomials, or cubic Hermite polynomials. Often we choose linear Lagrange polynomials for improved performance and stability, at the cost of reduced accuracy compared to quadratic Lagrange polynomials, unless C^1 continuity is required, in which case the cubic Hermite polynomials are employed. For pore fluid pressure and phase temperatures, we stick to linear Lagrange polynomials since pressure and temperature variables remain C^0 continuous for all forms of the variational equations.

Consider then a generic solution variable $y(X(\xi))$ interpolated across the local element coordinate system ξ . For cubic interpolation, we have

$$y^h(\xi, t) = \sum_{a=1}^4 N_a^y(\xi) y_a^e(t) = \underbrace{\left\{ \mathbf{N}^{e,y} \right\}}_{1 \times 4} \cdot \underbrace{\left\{ \mathbf{y}^e \right\}}_{4 \times 1}, \quad (4.254)$$

where the shape function matrix

$$\mathbf{N}^{e,y} := \left\{ \begin{array}{cc} -\frac{9}{16}(\xi + \frac{1}{3})(\xi - \frac{1}{3})(\xi - 1), & \frac{27}{16}(\xi + 1)(\xi - \frac{1}{3})(\xi - 1), \\ -\frac{27}{16}(\xi + 1)(\xi + \frac{1}{3})(\xi - 1), & \frac{9}{16}(\xi + \frac{1}{3})(\xi - \frac{1}{3})(\xi + 1) \end{array} \right\}, \quad (4.255)$$

where “ a ” refers to local finite element “ e ” node number, h^e is the element length and \mathbf{y}^e are the nodal values of y . For quadratic interpolation, we have

$$y^h(\xi, t) = \sum_{a=1}^3 N_a^y(\xi) y_a^e(t) = \underbrace{\left\{ \mathbf{N}^{e,y} \right\}}_{1 \times 3} \cdot \underbrace{\left\{ \mathbf{y}^e \right\}}_{3 \times 1}, \quad (4.256)$$

where

$$\mathbf{N}^{e,y} := \left\{ \frac{1}{2}\xi(\xi - 1), \frac{1}{2}\xi(\xi + 1), 1 - \xi^2 \right\}, \quad (4.257)$$

For linear interpolation, we have

$$y^h(\xi, t) = \sum_{a=1}^2 N_a^y(\xi) y_a^e(t) = \underbrace{\left\{ \mathbf{N}^{e,y} \right\}}_{1 \times 2} \cdot \underbrace{\left\{ \mathbf{y}^e \right\}}_{2 \times 1}, \quad (4.258)$$

where

$$\mathbf{N}^{e,y} := \left\{ \frac{1 - \xi}{2}, \frac{1 + \xi}{2} \right\}. \quad (4.259)$$

For the Hermite cubic interpolation, we have

$$y^h(\xi, t) = \sum_{a=1}^4 N_a^y(\xi) y_a^e(t) = \underbrace{\left\{ \mathbf{N}^{e,y} \right\}}_{1 \times 4} \cdot \underbrace{\left\{ \mathbf{y}^e \right\}}_{4 \times 1}, \quad (4.260)$$

where

$$\mathbf{N}^{e,y} := \left\{ \frac{1}{4}(1 - \xi)^2(2 + \xi), \frac{j^e}{4}(1 - \xi)^2(1 + \xi), \frac{1}{4}(1 + \xi)^2(2 - \xi), \frac{j^e}{4}(1 + \xi)^2(-1 + \xi) \right\}, \quad (4.261)$$

where the jacobian of coordinate transformation $j^e = \partial X^{h^e} / \partial \xi = h_0^e / 2$ for the initial finite element length h_0^e . Next, consider the gradient of the generic solution variable $y(X)$, such that $\partial y(X(\xi)) / \partial X = (\partial y(\xi) / \partial \xi)(\partial \xi / \partial X)$, interpolated across the local coordinate system ξ . For cubic interpolation, we have

$$\frac{\partial y^h(\xi, t)}{\partial X} = \sum_{a=1}^4 B_a^y(\xi) y_a^e(t) = \underbrace{\left\{ \mathbf{B}^{e,y} \right\}}_{1 \times 4} \cdot \underbrace{\left\{ \mathbf{y}^e \right\}}_{4 \times 1}, \quad (4.262)$$

where

$$\mathbf{B}^{e,y} := \frac{1}{j^e} \left\{ -\frac{27}{16}\xi^2 + \frac{9}{8}\xi + \frac{1}{16}, \frac{9}{16}(9\xi^2 - 2\xi + 3), -\frac{9}{16}(9\xi^2 + 2\xi + 3), \frac{27}{16}\xi^2 + \frac{9}{8}\xi - \frac{1}{16} \right\}. \quad (4.263)$$

For quadratic interpolation, we have

$$\frac{\partial y^h(\xi, t)}{\partial X} = \sum_{a=1}^3 B_a^y(\xi) y_a^e(t) = \underbrace{\left\{ \mathbf{B}^{e,y} \right\}}_{1 \times 3} \cdot \underbrace{\left\{ \mathbf{y}^e \right\}}_{3 \times 1}, \quad (4.264)$$

where

$$\mathbf{B}^{e,y} := \frac{1}{j^e} \left\{ \xi - \frac{1}{2}, \xi + \frac{1}{2}, -2\xi \right\}. \quad (4.265)$$

For linear interpolation, we have

$$\frac{\partial y^h(\xi, t)}{\partial X} = \sum_{a=1}^2 B_a^y(\xi) y_a^e(t) = \underbrace{\left\{ \mathbf{B}^{e,y} \right\}}_{1 \times 2} \cdot \underbrace{\left\{ \mathbf{y}^e \right\}}_{2 \times 1}, \quad (4.266)$$

where

$$\mathbf{B}^{e,y} := \frac{1}{j^e} \left\{ -\frac{1}{2}, \frac{1}{2} \right\}. \quad (4.267)$$

For the Hermite cubic interpolation, we have

$$y^h(\xi, t) = \sum_{a=1}^4 B_a^y(\xi) y_a^e(t) = \underbrace{\left\{ \mathbf{B}^{e,y} \right\}}_{1 \times 4} \cdot \underbrace{\left\{ \mathbf{y}^e \right\}}_{4 \times 1}, \quad (4.268)$$

where

$$\mathbf{B}^{e,y} := \frac{1}{j^e} \left\{ \frac{3}{4}(\xi^2 - 1), \frac{j^e}{4}(3\xi^2 - 2\xi - 1), -\frac{3}{4}(\xi^2 - 1), \frac{j^e}{4}(3\xi^2 + 2\xi - 1) \right\}. \quad (4.269)$$

Consider the second order gradient of the generic solution variable $y(X)$, such that $\partial^2 y(X(\xi))/\partial X^2 = (\partial^2 y(\xi)/\partial \xi^2)(\partial^2 \xi/\partial X^2)$, interpolated across local coordinate system ξ . Since this is typically only included for equations that require C^1 continuity, we will only consider the Hermite cubic interpolation⁴

$$\frac{\partial^2 y^h(\xi, t)}{\partial X^2} = \sum_{a=1}^3 H_a^y(\xi) y_a^e(t) = \underbrace{\left\{ \mathbf{H}^{e,y} \right\}}_{1 \times 4} \cdot \underbrace{\left\{ \mathbf{y}^e \right\}}_{4 \times 1}, \quad (4.270)$$

where

$$\mathbf{H}^{e,y} := \frac{1}{(j^e)^2} \left\{ \frac{3\xi}{2}, \frac{j^e}{2}(3\xi - 1), -\frac{3\xi}{2}, \frac{j^e}{2}(3\xi + 1) \right\}. \quad (4.271)$$

Hereafter, the length of the vectors $\mathbf{N}^{e,y}$ and $\mathbf{B}^{e,y}$ will be determined by the number of degrees of freedom, or $n_{\text{dof}}^{y,e}$, of the solution variable of interest. Where the vector $\mathbf{H}^{e,y}$ is present, the reader

⁴ SPONGE-1D has implemented second derivatives for Lagrange cubic elements, for the interested reader.

should assume it corresponds to the Hermite cubic polynomial interpolation, and thus the length is always 4. Pore fluid pressure and constituent temperatures are assumed to be evaluated at the endpoints of the element, i.e., $n_{\text{dof}}^{pf,e} = n_{\text{dof}}^{\theta,e} = n_{\text{dof}}^{\theta^s,e} = n_{\text{dof}}^{\theta^f,e} = 2$. However, we allow degrees of freedom (of the solid skeleton and pore fluid displacements) to vary, e.g., we may have $n_{\text{dof}}^{s,e} = 3$ and $n_{\text{dof}}^{f,e} = 2$, i.e., three degrees of freedom (which will be interpolated using quadratic shape functions) for the solid skeleton displacement and two degrees of freedom (which will be interpolated using linear shape functions) for the pore fluid displacement. A list of element types with their corresponding degrees of freedom can be found in Table 4.1 (note that not all element types are used in Chapter 5) with illustrations given in Figure 4.2.

Table 4.1: Acronyms for different element types.

Element type	$n_{\text{dof}}^{s,e}$	$n_{\text{dof}}^{f,e}$	$n_{\text{dof}}^{pf,e}$	$n_{\text{dof}}^{\theta,e}$	$n_{\text{dof}}^{\theta^s,e}$	$n_{\text{dof}}^{\theta^f,e}$
Q3H	4	N/A	N/A	N/A	N/A	N/A
Q3	4	N/A	N/A	N/A	N/A	N/A
Q2	3	N/A	N/A	N/A	N/A	N/A
Q1	4	N/A	N/A	N/A	N/A	N/A
Q3H-T1	4	N/A	N/A	2	N/A	N/A
Q3-T1	4	N/A	N/A	2	N/A	N/A
Q2-T1	3	N/A	N/A	2	N/A	N/A
Q1-T1	2	N/A	N/A	2	N/A	N/A
Q3H-P1	4	N/A	2	N/A	N/A	N/A
Q3-P1	4	N/A	2	N/A	N/A	N/A
Q2-P1	3	N/A	2	N/A	N/A	N/A
Q1-P1	2	N/A	2	N/A	N/A	N/A
Q3H-Q3H-P1	4	4	2	N/A	N/A	N/A
Q3-Q3-P1	4	4	2	N/A	N/A	N/A
Q3H-Q2-P1	4	3	2	N/A	N/A	N/A
Q3H-Q1-P1	4	2	2	N/A	N/A	N/A
Q2-Q2-P1	3	3	2	N/A	N/A	N/A
Q2-Q1-P1	3	2	2	N/A	N/A	N/A
Q1-Q1-P1	2	2	2	N/A	N/A	N/A
Q3H-P1-T1-T1	4	N/A	2	N/A	2	2
Q3H-Q3H-P1-T1-T1	4	4	2	N/A	2	2
Q3H-Q1-P1-T1-T1	4	2	2	N/A	2	2

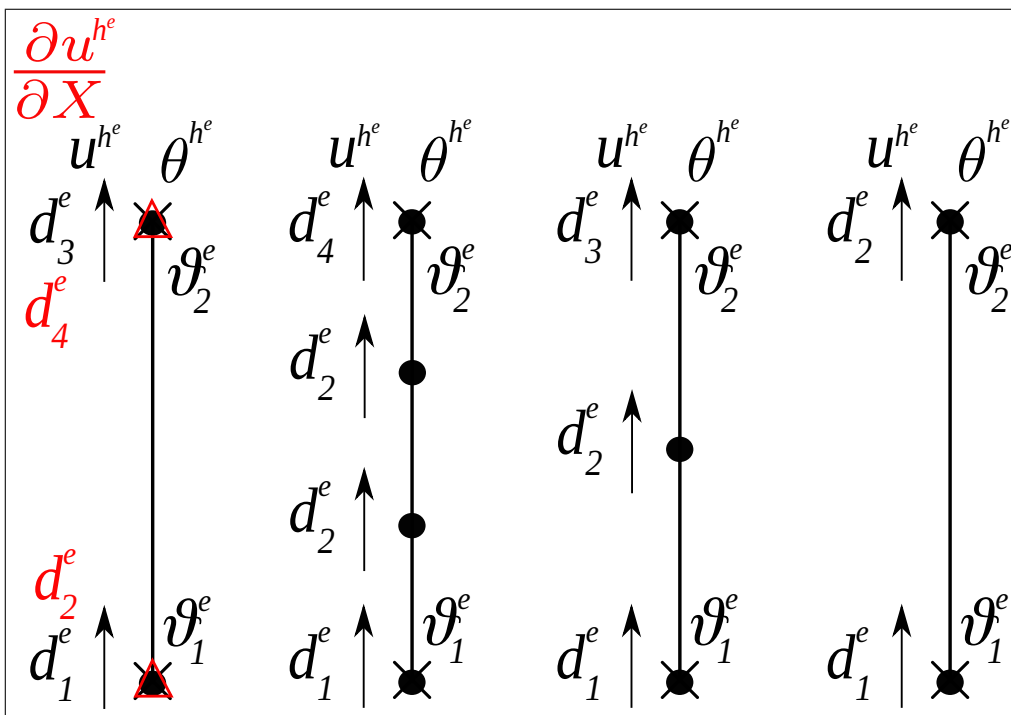
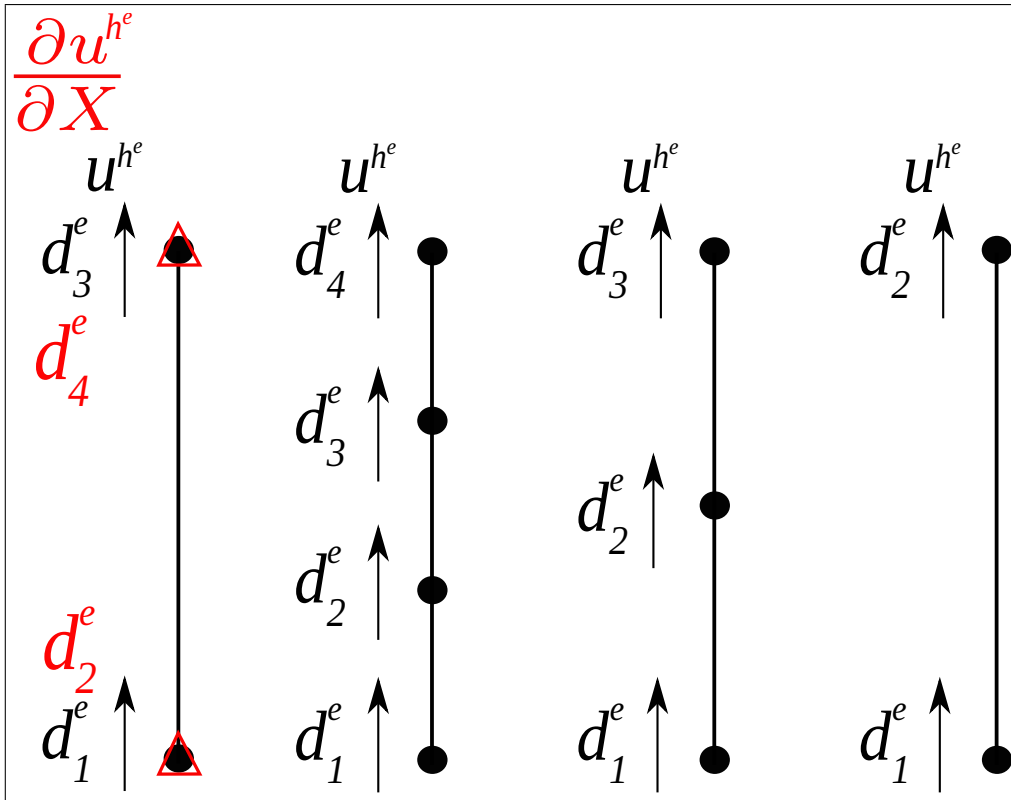
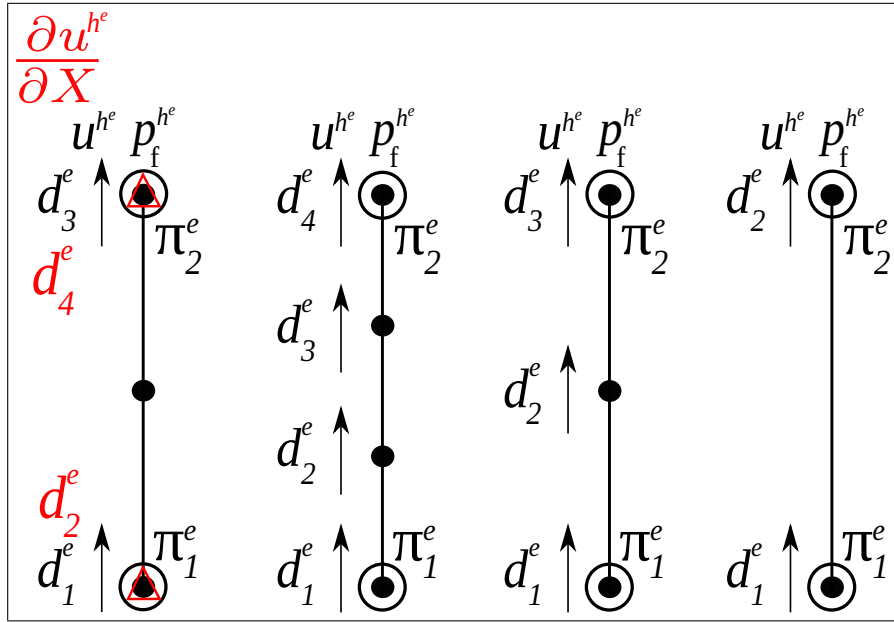
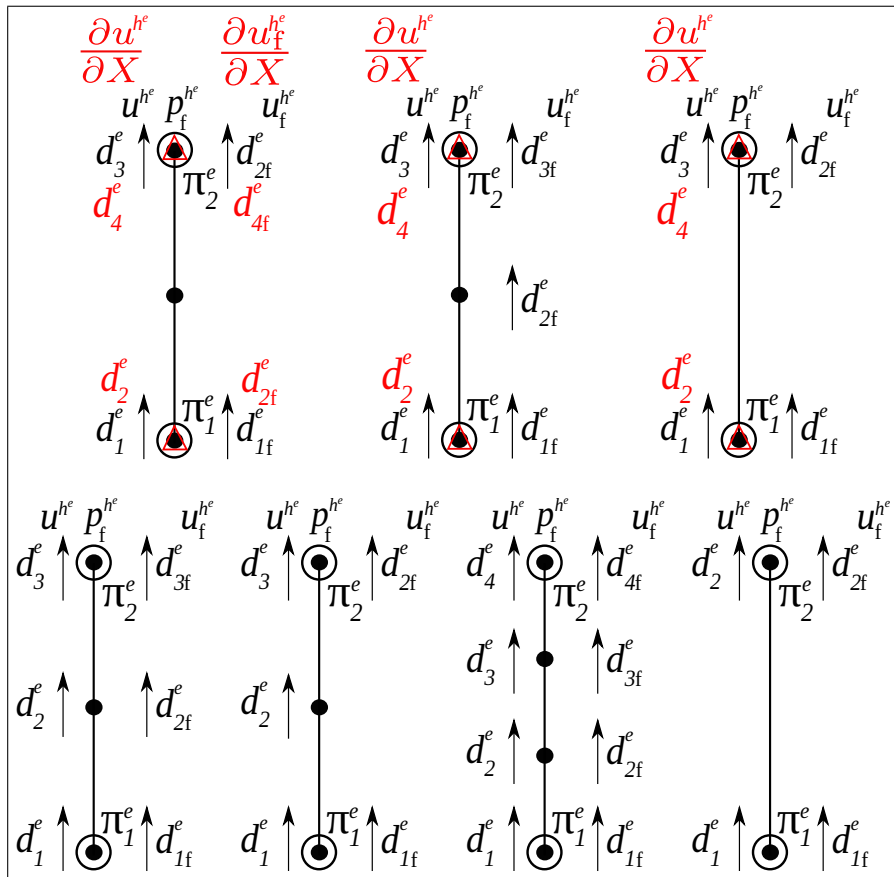


Figure 4.2: Schematic for different element types: (a) left to right: Q3H, Q3, Q2, Q1; (b) left to right: Q3H-T1, Q3-T1, Q2-T1, Q1-T1.



(c) $(\mathbf{u}-p_f)$ formulation element types



(d) $(\mathbf{u}-\mathbf{u}_f-p_f)$ formulation element types

Figure 4.2: Schematic for different element types (cont.): (c) left to right: Q3H-P1, Q3-P1, Q2-P1, Q1-P1; (d) left to right, top to bottom: Q3H-Q3H-P1, Q3H-Q2-P1, Q3H-Q1-P1, Q3-Q3-P1, Q2-Q2-P1, Q2-Q1-P1, Q1-Q1-P1.

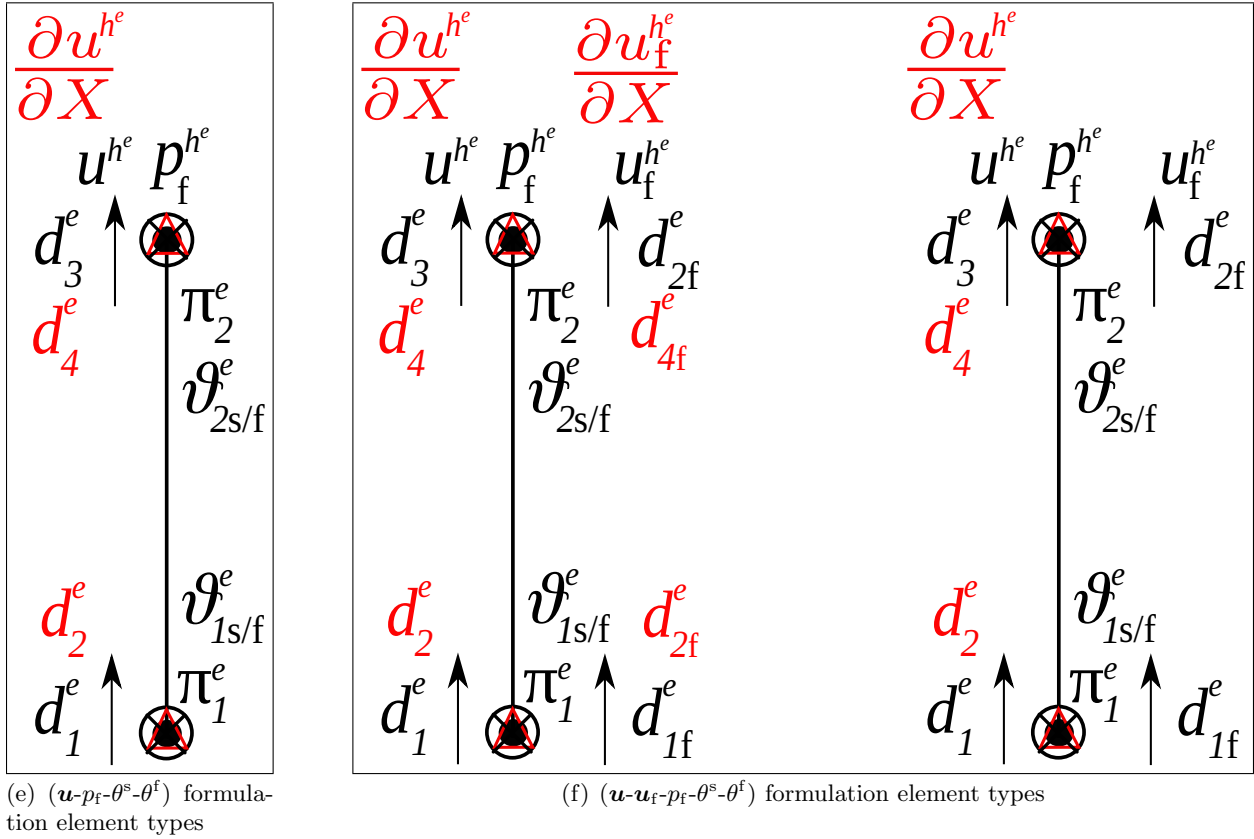


Figure 4.2: Schematics of different element types (cont.): (e) Q3H-P1-T1-T1; (f) left to right: Q3H-Q3H-P1-T1-T1, Q3H-Q1-P1-T1-T1.

For our solution variables of interest, i.e., u , θ , p_f , u_f , θ^s and θ^f , we introduce the corresponding discretizations \mathbf{d} , $\boldsymbol{\vartheta}$, $\boldsymbol{\pi}$, \mathbf{d}_f , $\boldsymbol{\vartheta}^s$ and $\boldsymbol{\vartheta}^f$, respectively. For solid skeleton displacement \mathbf{d} , we have

$$u^{h^e}(\xi, t) = \sum_{a=1}^{n_{\text{dof}}^{s,e}} N_a^u(\xi) d_a^e(t) = \underbrace{\left\{ \mathbf{N}^{e,u} \right\}}_{1 \times n_{\text{dof}}^{s,e}} \cdot \underbrace{\left\{ \mathbf{d}^e \right\}}_{n_{\text{dof}}^{s,e} \times 1}. \quad (4.272)$$

The solid skeleton velocity and acceleration are defined similarly:

$$\begin{aligned} v^{h^e}(\xi, t) &= \sum_{a=1}^{n_{\text{dof}}^{s,e}} N_a^u(\xi) \dot{d}_a^e(t) = \underbrace{\left\{ \mathbf{N}^{e,u} \right\}}_{1 \times n_{\text{dof}}^{s,e}} \cdot \underbrace{\left\{ \dot{\mathbf{d}}^e \right\}}_{n_{\text{dof}}^{s,e} \times 1}, \\ a^{h^e}(\xi, t) &= \sum_{a=1}^{n_{\text{dof}}^{s,e}} N_a^u(\xi) \ddot{d}_a^e(t) = \underbrace{\left\{ \mathbf{N}^{e,u} \right\}}_{1 \times n_{\text{dof}}^{s,e}} \cdot \underbrace{\left\{ \ddot{\mathbf{d}}^e \right\}}_{n_{\text{dof}}^{s,e} \times 1}. \end{aligned} \quad (4.273)$$

Solid skeleton displacement gradient, velocity gradient and acceleration gradient are defined as follows, respectively:

$$\begin{aligned} \frac{\partial u^{h^e}(\xi, t)}{\partial X} &= \sum_{a=1}^{n_{\text{dof}}^{s,e}} B_a^u(\xi) d_a^e(t) = \underbrace{\left\{ \mathbf{B}^{e,u} \right\}}_{1 \times n_{\text{dof}}^{s,e}} \cdot \underbrace{\left\{ \mathbf{d}^e \right\}}_{n_{\text{dof}}^{s,e} \times 1}, \\ \frac{\partial v^{h^e}(\xi, t)}{\partial X} &= \sum_{a=1}^{n_{\text{dof}}^{s,e}} B_a^u(\xi) \dot{d}_a^e(t) = \underbrace{\left\{ \mathbf{B}^{e,u} \right\}}_{1 \times n_{\text{dof}}^{s,e}} \cdot \underbrace{\left\{ \dot{\mathbf{d}}^e \right\}}_{n_{\text{dof}}^{s,e} \times 1}, \\ \frac{\partial a^{h^e}(\xi, t)}{\partial X} &= \sum_{a=1}^{n_{\text{dof}}^{s,e}} B_a^u(\xi) \ddot{d}_a^e(t) = \underbrace{\left\{ \mathbf{B}^{e,u} \right\}}_{1 \times n_{\text{dof}}^{s,e}} \cdot \underbrace{\left\{ \ddot{\mathbf{d}}^e \right\}}_{n_{\text{dof}}^{s,e} \times 1}. \end{aligned} \quad (4.274)$$

Second order gradients are defined as follows:

$$\begin{aligned} \frac{\partial^2 u^{h^e}(\xi, t)}{\partial X^2} &= \sum_{a=1}^{n_{\text{dof}}^{s,e}} H_a^u(\xi) d_a^e(t) = \underbrace{\left\{ \mathbf{H}^{e,u} \right\}}_{1 \times n_{\text{dof}}^{s,e}} \cdot \underbrace{\left\{ \mathbf{d}^e \right\}}_{n_{\text{dof}}^{s,e} \times 1}, \\ \frac{\partial^2 v^{h^e}(\xi, t)}{\partial X^2} &= \sum_{a=1}^{n_{\text{dof}}^{s,e}} H_a^u(\xi) \dot{d}_a^e(t) = \underbrace{\left\{ \mathbf{H}^{e,u} \right\}}_{1 \times n_{\text{dof}}^{s,e}} \cdot \underbrace{\left\{ \dot{\mathbf{d}}^e \right\}}_{n_{\text{dof}}^{s,e} \times 1}, \\ \frac{\partial^2 a^{h^e}(\xi, t)}{\partial X^2} &= \sum_{a=1}^{n_{\text{dof}}^{s,e}} H_a^u(\xi) \ddot{d}_a^e(t) = \underbrace{\left\{ \mathbf{H}^{e,u} \right\}}_{1 \times n_{\text{dof}}^{s,e}} \cdot \underbrace{\left\{ \ddot{\mathbf{d}}^e \right\}}_{n_{\text{dof}}^{s,e} \times 1}. \end{aligned} \quad (4.275)$$

Single-phase temperature discretizations ϑ are given as follows:

$$\begin{aligned}
\theta^{h^e}(\xi, t) &= \sum_{a=1}^{n_{\text{dof}}^{\theta, e}} N_a^\theta(\xi) \vartheta_a^e(t) = \underbrace{\left\{ \mathbf{N}^{e, \theta} \right\}}_{1 \times n_{\text{dof}}^{\theta, e}} \cdot \underbrace{\left\{ \vartheta^e \right\}}_{n_{\text{dof}}^{\theta, e} \times 1}, \\
\dot{\theta}^{h^e}(\xi, t) &= \sum_{a=1}^{n_{\text{dof}}^{\theta, e}} N_a^\theta(\xi) \dot{\vartheta}_a^e(t) = \underbrace{\left\{ \mathbf{N}^{e, \theta} \right\}}_{1 \times n_{\text{dof}}^{\theta, e}} \cdot \underbrace{\left\{ \dot{\vartheta}^e \right\}}_{n_{\text{dof}}^{\theta, e} \times 1}, \\
\frac{\partial \theta^{h^e}(\xi, t)}{\partial X} &= \sum_{a=1}^{n_{\text{dof}}^{\theta, e}} B_a^\theta(\xi) \vartheta_a^e(t) = \underbrace{\left\{ \mathbf{B}^{e, \theta} \right\}}_{1 \times n_{\text{dof}}^{\theta, e}} \cdot \underbrace{\left\{ \vartheta^e \right\}}_{n_{\text{dof}}^{\theta, e} \times 1}, \\
\frac{\partial \dot{\theta}^{h^e}(\xi, t)}{\partial X} &= \sum_{a=1}^{n_{\text{dof}}^{\theta, e}} B_a^\theta(\xi) \dot{\vartheta}_a^e(t) = \underbrace{\left\{ \mathbf{B}^{e, \theta} \right\}}_{1 \times n_{\text{dof}}^{\theta, e}} \cdot \underbrace{\left\{ \dot{\vartheta}^e \right\}}_{n_{\text{dof}}^{\theta, e} \times 1}.
\end{aligned} \tag{4.276}$$

Pore fluid pressure discretizations π are given as follows:

$$\begin{aligned}
p_f^{h^e}(\xi, t) &= \sum_{a=1}^{n_{\text{dof}}^{p_f, e}} N_a^{p_f}(\xi) \pi_a^e(t) = \underbrace{\left\{ \mathbf{N}^{e, p_f} \right\}}_{1 \times n_{\text{dof}}^{p_f, e}} \cdot \underbrace{\left\{ \pi^e \right\}}_{n_{\text{dof}}^{p_f, e} \times 1}, \\
\dot{p}_f^{h^e}(\xi, t) &= \sum_{a=1}^{n_{\text{dof}}^{p_f, e}} N_a^{p_f}(\xi) \dot{\pi}_a^e(t) = \underbrace{\left\{ \mathbf{N}^{e, p_f} \right\}}_{1 \times n_{\text{dof}}^{p_f, e}} \cdot \underbrace{\left\{ \dot{\pi}^e \right\}}_{n_{\text{dof}}^{p_f, e} \times 1}, \\
\ddot{p}_f^{h^e}(\xi, t) &= \sum_{a=1}^{n_{\text{dof}}^{p_f, e}} N_a^{p_f}(\xi) \ddot{\pi}_a^e(t) = \underbrace{\left\{ \mathbf{N}^{e, p_f} \right\}}_{1 \times n_{\text{dof}}^{p_f, e}} \cdot \underbrace{\left\{ \ddot{\pi}^e \right\}}_{n_{\text{dof}}^{p_f, e} \times 1}, \\
\frac{\partial p_f^{h^e}(\xi, t)}{\partial X} &= \sum_{a=1}^{n_{\text{dof}}^{p_f, e}} B_a^{p_f}(\xi) \pi_a^e(t) = \underbrace{\left\{ \mathbf{B}^{e, p_f} \right\}}_{1 \times n_{\text{dof}}^{p_f, e}} \cdot \underbrace{\left\{ \pi^e \right\}}_{n_{\text{dof}}^{p_f, e} \times 1}, \\
\frac{\partial \dot{p}_f^{h^e}(\xi, t)}{\partial X} &= \sum_{a=1}^{n_{\text{dof}}^{p_f, e}} B_a^{p_f}(\xi) \dot{\pi}_a^e(t) = \underbrace{\left\{ \mathbf{B}^{e, p_f} \right\}}_{1 \times n_{\text{dof}}^{p_f, e}} \cdot \underbrace{\left\{ \dot{\pi}^e \right\}}_{n_{\text{dof}}^{p_f, e} \times 1}, \\
\frac{\partial \ddot{p}_f^{h^e}(\xi, t)}{\partial X} &= \sum_{a=1}^{n_{\text{dof}}^{p_f, e}} B_a^{p_f}(\xi) \ddot{\pi}_a^e(t) = \underbrace{\left\{ \mathbf{B}^{e, p_f} \right\}}_{1 \times n_{\text{dof}}^{p_f, e}} \cdot \underbrace{\left\{ \ddot{\pi}^e \right\}}_{n_{\text{dof}}^{p_f, e} \times 1}.
\end{aligned} \tag{4.277}$$

Discretizations of the pore fluid displacement \mathbf{d}_f are given as follows:

$$\begin{aligned}
u_f^{h^e}(\xi, t) &= \sum_{a=1}^{n_{\text{dof}}^{f,e}} N_a^{u_f}(\xi) d_{a,f}^e(t) = \underbrace{\left\{ \mathbf{N}^{e,u_f} \right\}}_{1 \times n_{\text{dof}}^{f,e}} \cdot \underbrace{\left\{ \mathbf{d}_f^e \right\}}_{n_{\text{dof}}^{f,e} \times 1}, \\
v_f^{h^e}(\xi, t) &= \sum_{a=1}^{n_{\text{dof}}^{f,e}} N_a^{u_f}(\xi) \dot{d}_{a,f}^e(t) = \underbrace{\left\{ \mathbf{N}^{e,u_f} \right\}}_{1 \times n_{\text{dof}}^{f,e}} \cdot \underbrace{\left\{ \dot{\mathbf{d}}_f^e \right\}}_{n_{\text{dof}}^{f,e} \times 1}, \\
a_f^{h^e}(\xi, t) &= \sum_{a=1}^{n_{\text{dof}}^{f,e}} N_a^{u_f}(\xi) \ddot{d}_{a,f}^e(t) = \underbrace{\left\{ \mathbf{N}^{e,u_f} \right\}}_{1 \times n_{\text{dof}}^{f,e}} \cdot \underbrace{\left\{ \ddot{\mathbf{d}}_f^e \right\}}_{n_{\text{dof}}^{f,e} \times 1}, \\
\frac{\partial u_f^{h^e}(\xi, t)}{\partial X} &= \sum_{a=1}^{n_{\text{dof}}^{f,e}} B_a^{u_f}(\xi) d_{a,f}^e(t) = \underbrace{\left\{ \mathbf{B}^{e,u_f} \right\}}_{1 \times n_{\text{dof}}^{f,e}} \cdot \underbrace{\left\{ \mathbf{d}_f^e \right\}}_{n_{\text{dof}}^{f,e} \times 1}, \\
\frac{\partial v_f^{h^e}(\xi, t)}{\partial X} &= \sum_{a=1}^{n_{\text{dof}}^{f,e}} B_a^{u_f}(\xi) \dot{d}_{a,f}^e(t) = \underbrace{\left\{ \mathbf{B}^{e,u_f} \right\}}_{1 \times n_{\text{dof}}^{f,e}} \cdot \underbrace{\left\{ \dot{\mathbf{d}}_f^e \right\}}_{n_{\text{dof}}^{f,e} \times 1}, \\
\frac{\partial a_f^{h^e}(\xi, t)}{\partial X} &= \sum_{a=1}^{n_{\text{dof}}^{f,e}} B_a^{u_f}(\xi) \ddot{d}_{a,f}^e(t) = \underbrace{\left\{ \mathbf{B}^{e,u_f} \right\}}_{1 \times n_{\text{dof}}^{f,e}} \cdot \underbrace{\left\{ \ddot{\mathbf{d}}_f^e \right\}}_{n_{\text{dof}}^{f,e} \times 1}, \\
\frac{\partial^2 u_f^{h^e}(\xi, t)}{\partial X^2} &= \sum_{a=1}^{n_{\text{dof}}^{f,e}} H_a^{u_f}(\xi) d_{a,f}^e(t) = \underbrace{\left\{ \mathbf{H}^{e,u_f} \right\}}_{1 \times n_{\text{dof}}^{f,e}} \cdot \underbrace{\left\{ \mathbf{d}_f^e \right\}}_{n_{\text{dof}}^{f,e} \times 1}, \\
\frac{\partial^2 v_f^{h^e}(\xi, t)}{\partial X^2} &= \sum_{a=1}^{n_{\text{dof}}^{f,e}} H_a^{u_f}(\xi) \dot{d}_{a,f}^e(t) = \underbrace{\left\{ \mathbf{H}^{e,u_f} \right\}}_{1 \times n_{\text{dof}}^{f,e}} \cdot \underbrace{\left\{ \dot{\mathbf{d}}_f^e \right\}}_{n_{\text{dof}}^{f,e} \times 1}, \\
\frac{\partial^2 a_f^{h^e}(\xi, t)}{\partial X^2} &= \sum_{a=1}^{n_{\text{dof}}^{f,e}} H_a^{u_f}(\xi) \ddot{d}_{a,f}^e(t) = \underbrace{\left\{ \mathbf{H}^{e,u_f} \right\}}_{1 \times n_{\text{dof}}^{f,e}} \cdot \underbrace{\left\{ \ddot{\mathbf{d}}_f^e \right\}}_{n_{\text{dof}}^{f,e} \times 1}.
\end{aligned} \tag{4.278}$$

Solid phase temperature discretizations $\boldsymbol{\vartheta}^s$ are given as follows:

$$\begin{aligned}
\theta^{s,h^e}(\xi, t) &= \sum_{a=1}^{n_{\text{dof}}^{\theta^s,e}} N_a^{\theta^s}(\xi) \vartheta_a^{s,e}(t) = \underbrace{\left\{ \mathbf{N}^{e,\theta^s} \right\}}_{1 \times n_{\text{dof}}^{\theta^s,e}} \cdot \underbrace{\left\{ \boldsymbol{\vartheta}^{s,e} \right\}}_{n_{\text{dof}}^{\theta^s,e} \times 1}, \\
\dot{\theta}^{s,h^e}(\xi, t) &= \sum_{a=1}^{n_{\text{dof}}^{\theta^s,e}} N_a^{\theta^s}(\xi) \dot{\vartheta}_a^{s,e}(t) = \underbrace{\left\{ \mathbf{N}^{e,\theta^s} \right\}}_{1 \times n_{\text{dof}}^{\theta^s,e}} \cdot \underbrace{\left\{ \dot{\boldsymbol{\vartheta}}^{s,e} \right\}}_{n_{\text{dof}}^{\theta^s,e} \times 1}, \\
\frac{\partial \theta^{s,h^e}(\xi, t)}{\partial X} &= \sum_{a=1}^{n_{\text{dof}}^{\theta^s,e}} B_a^{\theta^s}(\xi) \vartheta_a^{s,e}(t) = \underbrace{\left\{ \mathbf{B}^{e,\theta^s} \right\}}_{1 \times n_{\text{dof}}^{\theta^s,e}} \cdot \underbrace{\left\{ \boldsymbol{\vartheta}^{s,e} \right\}}_{n_{\text{dof}}^{\theta^s,e} \times 1}, \\
\frac{\partial \dot{\theta}^{s,h^e}(\xi, t)}{\partial X} &= \sum_{a=1}^{n_{\text{dof}}^{\theta^s,e}} B_a^{\theta^s}(\xi) \dot{\vartheta}_a^{s,e}(t) = \underbrace{\left\{ \mathbf{B}^{e,\theta^s} \right\}}_{1 \times n_{\text{dof}}^{\theta^s,e}} \cdot \underbrace{\left\{ \dot{\boldsymbol{\vartheta}}^{s,e} \right\}}_{n_{\text{dof}}^{\theta^s,e} \times 1}.
\end{aligned} \tag{4.279}$$

Fluid phase temperature discretizations $\boldsymbol{\vartheta}^f$ are given as follows:

$$\begin{aligned}
\theta^{f,h^e}(\xi, t) &= \sum_{a=1}^{n_{\text{dof}}^{\theta^f,e}} N_a^{\theta^f}(\xi) \vartheta_a^{f,e}(t) = \underbrace{\left\{ \mathbf{N}^{e,\theta^f} \right\}}_{1 \times n_{\text{dof}}^{\theta^f,e}} \cdot \underbrace{\left\{ \boldsymbol{\vartheta}^{f,e} \right\}}_{n_{\text{dof}}^{\theta^f,e} \times 1}, \\
\dot{\theta}^{f,h^e}(\xi, t) &= \sum_{a=1}^{n_{\text{dof}}^{\theta^f,e}} N_a^{\theta^f}(\xi) \dot{\vartheta}_a^{f,e}(t) = \underbrace{\left\{ \mathbf{N}^{e,\theta^f} \right\}}_{1 \times n_{\text{dof}}^{\theta^f,e}} \cdot \underbrace{\left\{ \dot{\boldsymbol{\vartheta}}^{f,e} \right\}}_{n_{\text{dof}}^{\theta^f,e} \times 1}, \\
\frac{\partial \theta^{f,h^e}(\xi, t)}{\partial X} &= \sum_{a=1}^{n_{\text{dof}}^{\theta^f,e}} B_a^{\theta^f}(\xi) \vartheta_a^{f,e}(t) = \underbrace{\left\{ \mathbf{B}^{e,\theta^f} \right\}}_{1 \times n_{\text{dof}}^{\theta^f,e}} \cdot \underbrace{\left\{ \boldsymbol{\vartheta}^{f,e} \right\}}_{n_{\text{dof}}^{\theta^f,e} \times 1}, \\
\frac{\partial \dot{\theta}^{f,h^e}(\xi, t)}{\partial X} &= \sum_{a=1}^{n_{\text{dof}}^{\theta^f,e}} B_a^{\theta^f}(\xi) \dot{\vartheta}_a^{f,e}(t) = \underbrace{\left\{ \mathbf{B}^{e,\theta^f} \right\}}_{1 \times n_{\text{dof}}^{\theta^f,e}} \cdot \underbrace{\left\{ \dot{\boldsymbol{\vartheta}}^{f,e} \right\}}_{n_{\text{dof}}^{\theta^f,e} \times 1}.
\end{aligned} \tag{4.280}$$

The weighting functions for solid skeleton displacement \mathbf{d} and their interpolations (including gra-

dients) are given as follows:

$$\begin{aligned}
w^{u^{h^e}}(\xi) &= \underbrace{\left\{ \mathbf{N}^{e,u} \right\}}_{1 \times n_{\text{dof}}^{s,e}} \cdot \underbrace{\left\{ \mathbf{c}^{u,e} \right\}}_{n_{\text{dof}}^{s,e} \times 1} = \underbrace{\left\{ \mathbf{c}^{u,e} \right\}^T}_{1 \times n_{\text{dof}}^{s,e}} \cdot \underbrace{\left\{ \mathbf{N}^{e,u} \right\}^T}_{n_{\text{dof}}^{s,e} \times 1}, \\
\frac{\partial w^{u^{h^e}}(\xi, t)}{\partial X} &= \underbrace{\left\{ \mathbf{B}^{e,u} \right\}}_{1 \times n_{\text{dof}}^{s,e}} \cdot \underbrace{\left\{ \mathbf{c}^{u,e} \right\}}_{n_{\text{dof}}^{s,e} \times 1} = \underbrace{\left\{ \mathbf{c}^{u,e} \right\}^T}_{1 \times n_{\text{dof}}^{s,e}} \cdot \underbrace{\left\{ \mathbf{B}^{e,u} \right\}^T}_{n_{\text{dof}}^{s,e} \times 1}, \\
\frac{\partial^2 w^{u^{h^e}}(\xi, t)}{\partial X^2} &= \underbrace{\left\{ \mathbf{H}^{e,u} \right\}}_{1 \times n_{\text{dof}}^{s,e}} \cdot \underbrace{\left\{ \mathbf{c}^{u,e} \right\}}_{n_{\text{dof}}^{s,e} \times 1} = \underbrace{\left\{ \mathbf{c}^{u,e} \right\}^T}_{1 \times n_{\text{dof}}^{s,e}} \cdot \underbrace{\left\{ \mathbf{H}^{e,u} \right\}^T}_{n_{\text{dof}}^{s,e} \times 1}.
\end{aligned} \tag{4.281}$$

The weighting functions for single-phase temperature ϑ and their interpolations (including gradients) are given as follows:

$$\begin{aligned}
w^{\vartheta^{h^e}}(\xi) &= \underbrace{\left\{ \mathbf{N}^{e,\vartheta} \right\}}_{1 \times n_{\text{dof}}^{\vartheta,e}} \cdot \underbrace{\left\{ \mathbf{c}^{\vartheta,e} \right\}}_{n_{\text{dof}}^{\vartheta,e} \times 1} = \underbrace{\left\{ \mathbf{c}^{\vartheta,e} \right\}^T}_{1 \times n_{\text{dof}}^{\vartheta,e}} \cdot \underbrace{\left\{ \mathbf{N}^{e,\vartheta} \right\}^T}_{n_{\text{dof}}^{\vartheta,e} \times 1}, \\
\frac{\partial w^{\vartheta^{h^e}}(\xi, t)}{\partial X} &= \underbrace{\left\{ \mathbf{B}^{e,\vartheta} \right\}}_{1 \times n_{\text{dof}}^{\vartheta,e}} \cdot \underbrace{\left\{ \mathbf{c}^{\vartheta,e} \right\}}_{n_{\text{dof}}^{\vartheta,e} \times 1} = \underbrace{\left\{ \mathbf{c}^{\vartheta,e} \right\}^T}_{1 \times n_{\text{dof}}^{\vartheta,e}} \cdot \underbrace{\left\{ \mathbf{B}^{e,\vartheta} \right\}^T}_{n_{\text{dof}}^{\vartheta,e} \times 1}.
\end{aligned} \tag{4.282}$$

The weighting functions for pore fluid pressure π and their interpolations (including gradients) are given as follows:

$$\begin{aligned}
w^{\pi^{h^e}}(\xi) &= \underbrace{\left\{ \mathbf{N}^{e,p_f} \right\}}_{1 \times n_{\text{dof}}^{p_f,e}} \cdot \underbrace{\left\{ \mathbf{c}^{p_f,e} \right\}}_{n_{\text{dof}}^{p_f,e} \times 1} = \underbrace{\left\{ \mathbf{c}^{p_f,e} \right\}^T}_{1 \times n_{\text{dof}}^{p_f,e}} \cdot \underbrace{\left\{ \mathbf{N}^{e,p_f} \right\}^T}_{n_{\text{dof}}^{p_f,e} \times 1}, \\
\frac{\partial w^{\pi^{h^e}}(\xi, t)}{\partial X} &= \underbrace{\left\{ \mathbf{B}^{e,p_f} \right\}}_{1 \times n_{\text{dof}}^{p_f,e}} \cdot \underbrace{\left\{ \mathbf{c}^{p_f,e} \right\}}_{n_{\text{dof}}^{p_f,e} \times 1} = \underbrace{\left\{ \mathbf{c}^{p_f,e} \right\}^T}_{1 \times n_{\text{dof}}^{p_f,e}} \cdot \underbrace{\left\{ \mathbf{B}^{e,p_f} \right\}^T}_{n_{\text{dof}}^{p_f,e} \times 1}.
\end{aligned} \tag{4.283}$$

The weighting functions for pore fluid displacement \mathbf{d}_f and their interpolations (including gradients)

are given as follows:

$$\begin{aligned}
w^{u_f^{h^e}}(\xi) &= \underbrace{\left\{ \mathbf{N}^{e,u_f} \right\}}_{1 \times n_{\text{dof}}^{f,e}} \cdot \underbrace{\left\{ \mathbf{c}^{u_f,e} \right\}}_{n_{\text{dof}}^{f,e} \times 1} = \underbrace{\left\{ \mathbf{c}^{u_f,e} \right\}^T}_{1 \times n_{\text{dof}}^{f,e}} \cdot \underbrace{\left\{ \mathbf{N}^{e,u_f} \right\}^T}_{n_{\text{dof}}^{f,e} \times 1}, \\
\frac{\partial w^{u_f^{h^e}}(\xi, t)}{\partial X} &= \underbrace{\left\{ \mathbf{B}^{e,u_f} \right\}}_{1 \times n_{\text{dof}}^{f,e}} \cdot \underbrace{\left\{ \mathbf{c}^{u_f,e} \right\}}_{n_{\text{dof}}^{f,e} \times 1} = \underbrace{\left\{ \mathbf{c}^{u_f,e} \right\}^T}_{1 \times n_{\text{dof}}^{f,e}} \cdot \underbrace{\left\{ \mathbf{B}^{e,u_f} \right\}^T}_{n_{\text{dof}}^{f,e} \times 1}, \\
\frac{\partial^2 w^{u_f^{h^e}}(\xi, t)}{\partial X^2} &= \underbrace{\left\{ \mathbf{H}^{e,u_f} \right\}}_{1 \times n_{\text{dof}}^{f,e}} \cdot \underbrace{\left\{ \mathbf{c}^{u_f,e} \right\}}_{n_{\text{dof}}^{f,e} \times 1} = \underbrace{\left\{ \mathbf{c}^{u_f,e} \right\}^T}_{1 \times n_{\text{dof}}^{f,e}} \cdot \underbrace{\left\{ \mathbf{H}^{e,u_f} \right\}^T}_{n_{\text{dof}}^{f,e} \times 1}.
\end{aligned} \tag{4.284}$$

The weighting functions for solid phase temperature ϑ^s and their interpolations (including gradients) are given as follows:

$$\begin{aligned}
w^{\vartheta^{s,h^e}}(\xi) &= \underbrace{\left\{ \mathbf{N}^{e,\vartheta^s} \right\}}_{1 \times n_{\text{dof}}^{\vartheta^s,e}} \cdot \underbrace{\left\{ \mathbf{c}^{\vartheta^s,e} \right\}}_{n_{\text{dof}}^{\vartheta^s,e} \times 1} = \underbrace{\left\{ \mathbf{c}^{\vartheta^s,e} \right\}^T}_{1 \times n_{\text{dof}}^{\vartheta^s,e}} \cdot \underbrace{\left\{ \mathbf{N}^{e,\vartheta^s} \right\}^T}_{n_{\text{dof}}^{\vartheta^s,e} \times 1}, \\
\frac{\partial w^{\vartheta^{s,h^e}}(\xi, t)}{\partial X} &= \underbrace{\left\{ \mathbf{B}^{e,\vartheta^s} \right\}}_{1 \times n_{\text{dof}}^{\vartheta^s,e}} \cdot \underbrace{\left\{ \mathbf{c}^{\vartheta^s,e} \right\}}_{n_{\text{dof}}^{\vartheta^s,e} \times 1} = \underbrace{\left\{ \mathbf{c}^{\vartheta^s,e} \right\}^T}_{1 \times n_{\text{dof}}^{\vartheta^s,e}} \cdot \underbrace{\left\{ \mathbf{B}^{e,\vartheta^s} \right\}^T}_{n_{\text{dof}}^{\vartheta^s,e} \times 1}.
\end{aligned} \tag{4.285}$$

The weighting functions for fluid phase temperature ϑ^f and their interpolations (including gradients) are given as follows:

$$\begin{aligned}
w^{\vartheta^{f,h^e}}(\xi) &= \underbrace{\left\{ \mathbf{N}^{e,\vartheta^f} \right\}}_{1 \times n_{\text{dof}}^{\vartheta^f,e}} \cdot \underbrace{\left\{ \mathbf{c}^{\vartheta^f,e} \right\}}_{n_{\text{dof}}^{\vartheta^f,e} \times 1} = \underbrace{\left\{ \mathbf{c}^{\vartheta^f,e} \right\}^T}_{1 \times n_{\text{dof}}^{\vartheta^f,e}} \cdot \underbrace{\left\{ \mathbf{N}^{e,\vartheta^f} \right\}^T}_{n_{\text{dof}}^{\vartheta^f,e} \times 1}, \\
\frac{\partial w^{\vartheta^{f,h^e}}(\xi, t)}{\partial X} &= \underbrace{\left\{ \mathbf{B}^{e,\vartheta^f} \right\}}_{1 \times n_{\text{dof}}^{\vartheta^f,e}} \cdot \underbrace{\left\{ \mathbf{c}^{\vartheta^f,e} \right\}}_{n_{\text{dof}}^{\vartheta^f,e} \times 1} = \underbrace{\left\{ \mathbf{c}^{\vartheta^f,e} \right\}^T}_{1 \times n_{\text{dof}}^{\vartheta^f,e}} \cdot \underbrace{\left\{ \mathbf{B}^{e,\vartheta^f} \right\}^T}_{n_{\text{dof}}^{\vartheta^f,e} \times 1}.
\end{aligned} \tag{4.286}$$

4.3 Time integration

In the proceeding subsections, the numerical time discretization of the weak forms of the governing equations is presented. Our general system of equations when inertia terms are included resembles the following form:

$$\mathbf{M}\ddot{\mathbf{x}} + \mathbf{C}\dot{\mathbf{x}} + \mathbf{K}\mathbf{x} = \mathbf{F}, \tag{4.287}$$

where \mathbf{M} is a mass matrix, \mathbf{C} is a viscous damping matrix, \mathbf{K} is a stiffness matrix and \mathbf{F} is a vector of applied forces (internal and external) for each variational equation, i.e., each matrix in Equation (4.287) is a collection of submatrices for each variational equation. Similarly, the accelerations, velocities, and displacements of solid skeleton, pore fluid pressure, pore fluid displacement, solid temperature, and pore fluid temperature are given by the vectors $\ddot{\mathbf{x}}$, $\dot{\mathbf{x}}$ and \mathbf{x} , respectively, i.e.,⁵

$$\mathbf{x} = \begin{pmatrix} \mathbf{u} \\ \mathbf{u}_f \\ p_f \\ \theta^s \\ \theta^f \end{pmatrix}, \quad \dot{\mathbf{x}} = \begin{pmatrix} \mathbf{v} \\ \mathbf{v}_f \\ \dot{p}_f \\ \dot{\theta}^s \\ \dot{\theta}^f \end{pmatrix}, \quad \ddot{\mathbf{x}} = \begin{pmatrix} \mathbf{a} \\ \mathbf{a}_f \\ \ddot{p}_f \\ \ddot{\theta}^s \\ \ddot{\theta}^f \end{pmatrix}. \quad (4.288)$$

In the proceeding subsections, we briefly introduce the general forms of the different time-integration schemes that we have employed. The exact ordinary differential equations for the variational forms are provided in the subsequent sections.

4.3.1 Runge-Kutta integration

For explicit time integration of the matrix-vector equations, we apply a generalized adaptive time-stepping Runge-Kutta method for solving Equation (4.287), which involves transforming the second-order ordinary differential equations (ODEs) into first-order ODEs by variable substitution:

$$\mathbf{z} := \begin{pmatrix} \mathbf{z}_x \\ \mathbf{z}_{\dot{x}} \end{pmatrix} = \begin{pmatrix} \mathbf{x} \\ \dot{\mathbf{x}} \end{pmatrix}, \quad (4.289)$$

such that

$$\dot{\mathbf{z}} = \begin{pmatrix} \dot{\mathbf{z}}_x \\ \dot{\mathbf{z}}_{\dot{x}} \end{pmatrix} = \begin{pmatrix} \dot{\mathbf{x}} \\ \ddot{\mathbf{x}} \end{pmatrix}. \quad (4.290)$$

⁵ Strictly speaking, the second time derivatives on pore fluid pressure and constituent temperatures are not actually computed since they do not appear in the variational equations. For the implicit schemes, the variation of the second derivative in time of the pore fluid pressure and constituent temperatures are computed.

For a general nonlinear multi-degree-of-freedom ODE,

$$\dot{\mathbf{z}} = \mathbf{f}(t, \mathbf{z}), \quad (4.291)$$

where $\mathbf{f}(t, \mathbf{z})$ is in general a nonlinear equation in terms of time t and unknown variable \mathbf{z} . For a general Runge-Kutta method of m^{th} order, the intermediate stages \mathbf{k}_i are defined as follows using standard notation for a Butcher table:

$$\mathbf{k}_i = \mathbf{f} \left(t_n + c_i \Delta t, \mathbf{z}(t_n) + \Delta t \sum_{j=1}^{i-1} a_{ij} \mathbf{k}_j \right), \quad (4.292)$$

where c_i are the “nodes” and a_{ij} are the coefficients of the Butcher table. The higher order solution is given by

$$\mathbf{z}^m(t_{n+1}) = \mathbf{z}(t_n) + \Delta t \sum_{i=1}^{m+1} b_i^m \mathbf{k}_i, \quad (4.293)$$

and the lower order solution is given by

$$\mathbf{z}^{m-1}(t_{n+1}) = \mathbf{z}(t_n) + \Delta t \sum_{i=1}^m b_i^{m-1} \mathbf{k}_i, \quad (4.294)$$

where the b_i^m weights are different from the b_i^{m-1} weights (refer to Bogacki and Shampine [1989], Cash and Karp [1990] for specific values). The difference between the higher and lower order solutions allows us to define a truncation error⁶

$$\epsilon_{TE} := \left\| \mathbf{z}^m(t_{n+1}) - \mathbf{z}^{m-1}(t_{n+1}) \right\|_{\infty, 2}. \quad (4.295)$$

The adapted time step Δt^* is typically adjusted as follows:

$$\Delta t^* = \text{SF} \times \left(\frac{\epsilon_a}{\epsilon_{TE}} \right)^{1/(m-1)} \Delta t, \quad (4.296)$$

where SF is a safety factor, typically set to 0.9, and ϵ_a is a user-defined absolute tolerance, typically set to $\epsilon_a \in [10^{-8}, 10^{-2}]$. If the absolute error

$$\left(\frac{\epsilon_{TE}}{\epsilon_a} \right)^{1/(m-1)} < 1, \quad (4.297)$$

⁶ In practice, estimation of truncation error using the L^2 -norm (the Euclidean norm) is often preferred for accuracy over cost, particularly for simulations using higher-order elements where the ∞ -norm trends towards unstable solutions for high strain-rate loadings.

then the solution \mathbf{z}^m is accepted with $\Delta t_{n+1} \leftarrow \Delta t^*$. Otherwise, the stages \mathbf{k}_i are recomputed at time t_n with $\Delta t_n \leftarrow \Delta t^*$, new solutions are computed, and a new absolute error is computed until the condition defined by Equation (4.297) is met. In the event that the time step starts to approach zero, the simulation is terminated with an error message.

For further reading on Runge-Kutta integrators with adaptive time-stepping schemes based on truncation errors, refer to Cash and Karp [1990], Bogacki and Shampine [1989], Press et al. [1992]. In numerical simulations described in Chapter 5, we typically employ the fixed-order, 5(4) Runge-Kutta Cash-Karp (RKFNC) scheme [Cash and Karp, 1990].

4.3.1.1 (\mathbf{u}) formulation

For the (\mathbf{u}) formulation, the Runge-Kutta integrators transform the general solution variables given by Equation (4.291) to

$$\left\{ \dot{\mathbf{z}} \right\} := \left\{ \begin{array}{c} \dot{\mathbf{z}}_u \\ \dot{\mathbf{z}}_v \end{array} \right\} = \left\{ \mathbf{f}(t, \mathbf{z}) \right\} = \left\{ \begin{array}{c} \mathbf{f}_v(t, \mathbf{z}) \\ \mathbf{f}_a(t, \mathbf{z}) \end{array} \right\}, \quad (4.298)$$

such that

$$\left\{ \mathbf{z} \right\} = \left\{ \begin{array}{c} \mathbf{d} \\ \dot{\mathbf{d}} \end{array} \right\}, \quad \dot{\mathbf{z}} = \left\{ \begin{array}{c} \dot{\mathbf{d}} \\ \ddot{\mathbf{d}} \end{array} \right\}. \quad (4.299)$$

The FE formulation for the balance of momentum of the single-phase, with variational equation given by Equation (4.18), is written in block-matrix form as

$$\underbrace{\left\{ \mathbf{R}_u \right\}}_{n_{\text{dof}}^s \times 1} = \mathbf{0}, \quad (4.300)$$

where the global residual for the single-phase displacement is given as

$$\mathbf{c}^{u,T} \cdot \mathbf{R}_u = \mathcal{G}^h = \mathcal{G}_1^{\text{INT},h} + \mathcal{G}_2^{\text{INT},h} + \mathcal{G}_4^{\text{INT},h} - \mathcal{G}^{\text{EXT},h} = 0. \quad (4.301)$$

Therein,

$$\begin{aligned}
\mathcal{G}_1^{\text{INT},h} &= \mathbf{A}_e^{n_e} \underbrace{\left\{ \mathbf{c}^{u,e} \right\}^T}_{1 \times n_{\text{dof}}^{s,e}} \cdot \underbrace{\left[\mathbf{m}_{u,u}^{\mathcal{G}_1^{\text{INT},e}} \right]}_{n_{\text{dof}}^{s,e} \times n_{\text{dof}}^{s,e}} \cdot \underbrace{\left\{ \dot{\mathbf{d}}^e \right\}}_{n_{\text{dof}}^{s,e} \times 1}, & \mathcal{G}_2^{\text{INT},h} &= \mathbf{A}_e^{n_e} \underbrace{\left\{ \mathbf{c}^{u,e} \right\}^T}_{1 \times n_{\text{dof}}^{s,e}} \cdot \underbrace{\left\{ \mathbf{f}^{\mathcal{G}_2^{\text{INT},e}} \right\}}_{n_{\text{dof}}^{s,e} \times 1}, \\
\mathcal{G}_4^{\text{INT},h} &= \mathbf{A}_e^{n_e} \underbrace{\left\{ \mathbf{c}^{u,e} \right\}^T}_{1 \times n_{\text{dof}}^{s,e}} \cdot \underbrace{\left\{ \mathbf{f}^{\mathcal{G}_4^{\text{INT},e}} \right\}}_{n_{\text{dof}}^{s,e} \times 1}, & \mathcal{G}^{\text{EXT},h} &= \mathbf{A}_e^{n_e} \underbrace{\left\{ \mathbf{c}^{u,e} \right\}^T}_{1 \times n_{\text{dof}}^{s,e}} \cdot \underbrace{\left\{ \mathbf{f}^{\mathcal{G}^{\text{EXT},e}} \right\}}_{n_{\text{dof}}^{s,e} \times 1},
\end{aligned} \tag{4.302}$$

where

$$\begin{aligned}
\underbrace{\left\{ \mathbf{f}^{\mathcal{G}_2^{\text{INT},e}} \right\}}_{n_{\text{dof}}^{s,e} \times 1} &= \int_{-1}^1 \underbrace{\left\{ \mathbf{B}^{e,u} \right\}^T}_{n_{\text{dof}}^{s,e} \times 1} P_{11}^{h^e} A_j^e d\xi, & \underbrace{\left\{ \mathbf{f}^{\mathcal{G}_4^{\text{INT},e}} \right\}}_{n_{\text{dof}}^{s,e} \times 1} &= \int_{-1}^1 \underbrace{\left\{ \mathbf{N}^{e,u} \right\}^T}_{n_{\text{dof}}^{s,e} \times 1} \rho_0^{h^e} g A_j^e d\xi, \\
\underbrace{\left\{ \mathbf{f}^{\mathcal{G}^{\text{EXT},e}} \right\}}_{n_{\text{dof}}^{s,e} \times 1} &= \begin{cases} \underbrace{\left\{ \mathbf{N}^{e,u}(X=0, H) \right\}^T}_{n_{\text{dof}}^{s,e} \times 1} t^\sigma A & X=0, H \\ \mathbf{0} & 0 < X < H. \end{cases}
\end{aligned} \tag{4.303}$$

The mass matrix associated with the single-phase acceleration is given by⁷

$$\underbrace{\left[\mathbf{m}_{u,u}^{\mathcal{G}_1^{\text{INT},e}} \right]}_{n_{\text{dof}}^{s,e} \times n_{\text{dof}}^{s,e}} = \int_{-1}^1 \rho_0^{h^e} \underbrace{\left\{ \mathbf{N}^{e,u} \right\}^T}_{n_{\text{dof}}^{s,e} \times 1} \underbrace{\left\{ \mathbf{N}^{e,u} \right\}}_{1 \times n_{\text{dof}}^{s,e}} A_j^e d\xi. \tag{4.304}$$

Thus,

$$\underbrace{\left\{ \dot{\mathbf{z}} \right\}}_{(2 \times n_{\text{dof}}^s) \times 1} = \underbrace{\left[\mathbf{M}_{u,u}^{\mathcal{G}_1^{\text{INT}}} \right]^{-1}}_{n_{\text{dof}}^s \times n_{\text{dof}}^s} \cdot \left(- \underbrace{\left\{ \mathbf{F}^{\mathcal{G}_2^{\text{INT}}} \right\}}_{n_{\text{dof}}^s \times 1} - \underbrace{\left\{ \mathbf{F}^{\mathcal{G}_4^{\text{INT}}} \right\}}_{n_{\text{dof}}^s \times 1} + \underbrace{\left\{ \mathbf{F}^{\mathcal{G}^{\text{EXT}}} \right\}}_{n_{\text{dof}}^s \times 1} \right) \cdot \underbrace{\left\{ \dot{\mathbf{d}} \right\}}_{n_{\text{dof}}^{s,e} \times 1}, \tag{4.305}$$

where

$$\begin{aligned}
\underbrace{\left[\mathbf{M}_{u,u}^{\mathcal{G}_1^{\text{INT}}} \right]}_{n_{\text{dof}}^s \times n_{\text{dof}}^s} &= \mathbf{A}_e^{n_e} \underbrace{\left[\mathbf{m}_{u,u}^{\mathcal{G}_1^{\text{INT},e}} \right]}_{n_{\text{dof}}^{s,e} \times n_{\text{dof}}^{s,e}}, & \underbrace{\left\{ \mathbf{F}^{\mathcal{G}_2^{\text{INT}}} \right\}}_{n_{\text{dof}}^s \times 1} &= \mathbf{A}_e^{n_e} \underbrace{\left\{ \mathbf{f}^{\mathcal{G}_2^{\text{INT},e}} \right\}}_{n_{\text{dof}}^{s,e} \times 1}, \\
\underbrace{\left\{ \mathbf{F}^{\mathcal{G}_4^{\text{INT}}} \right\}}_{n_{\text{dof}}^s \times 1} &= \mathbf{A}_e^{n_e} \underbrace{\left\{ \mathbf{f}^{\mathcal{G}_4^{\text{INT},e}} \right\}}_{n_{\text{dof}}^{s,e} \times 1}, & \underbrace{\left\{ \mathbf{F}^{\mathcal{G}^{\text{EXT}}} \right\}}_{n_{\text{dof}}^s \times 1} &= \mathbf{A}_e^{n_e} \underbrace{\left\{ \mathbf{f}^{\mathcal{G}^{\text{EXT},e}} \right\}}_{n_{\text{dof}}^{s,e} \times 1}.
\end{aligned} \tag{4.306}$$

⁷ Note that for single-phase materials, the quantity $\rho_0^{h^e}$ is constant over the element, i.e., $\rho_0^{h^e} = \rho_0$.

As described in Section 4.3.1, Equation (4.305) is solved for each stage increment i at time $t_n + \Delta t c_i$ (i.e., any variables that are *explicit* functions of time, such as a time-dependent external traction, are to be evaluated at time $t_n + \Delta t c_i$), with stage solution \mathbf{k}_i given by

$$\underbrace{\left\{ \mathbf{k}_i \right\}}_{(2 \times n_{\text{dof}}^s) \times 1} := \underbrace{\left\{ \begin{array}{c} \underbrace{\left\{ \mathbf{k}_{i(v)} \right\}}_{n_{\text{dof}}^s \times 1} \\ \underbrace{\left\{ \mathbf{k}_{i(a)} \right\}}_{n_{\text{dof}}^s \times 1} \end{array} \right\}} = \underbrace{\left\{ \begin{array}{c} \underbrace{\left\{ \mathbf{z}_v(t_n) \right\}}_{n_{\text{dof}}^s \times 1} + \Delta t \sum_{j=1}^{i-1} a_{ij} \underbrace{\left\{ \mathbf{k}_{j(v)} \right\}}_{n_{\text{dof}}^s \times 1} \\ \underbrace{\left\{ \mathbf{z}_a(t_n) \right\}}_{n_{\text{dof}}^s \times 1} + \Delta t \sum_{j=1}^{i-1} a_{ij} \underbrace{\left\{ \mathbf{k}_{j(a)} \right\}}_{n_{\text{dof}}^s \times 1} \end{array} \right\}}. \quad (4.307)$$

Then, according to Equation (4.293), the higher order solution to be accepted or rejected at time t_{n+1} is given by

$$\underbrace{\left\{ \mathbf{z}^m(t_{n+1}) \right\}}_{(2 \times n_{\text{dof}}^s) \times 1} := \underbrace{\left\{ \begin{array}{c} \underbrace{\left\{ \mathbf{z}_u^m(t_{n+1}) \right\}}_{n_{\text{dof}}^s \times 1} \\ \underbrace{\left\{ \mathbf{z}_v^m(t_{n+1}) \right\}}_{n_{\text{dof}}^s \times 1} \end{array} \right\}} = \underbrace{\left\{ \begin{array}{c} \underbrace{\left\{ \mathbf{z}_u(t_n) \right\}}_{n_{\text{dof}}^s \times 1} + \Delta t \sum_{i=1}^{m+1} b_i^m \underbrace{\left\{ \mathbf{k}_{i(v)} \right\}}_{n_{\text{dof}}^s \times 1} \\ \underbrace{\left\{ \mathbf{z}_v(t_n) \right\}}_{n_{\text{dof}}^s \times 1} + \Delta t \sum_{i=1}^{m+1} b_i^m \underbrace{\left\{ \mathbf{k}_{i(a)} \right\}}_{n_{\text{dof}}^s \times 1} \end{array} \right\}}. \quad (4.308)$$

According to Equation (4.294), the lower order solution at time t_{n+1} is given by

$$\underbrace{\left\{ \mathbf{z}^{m-1}(t_{n+1}) \right\}}_{(2 \times n_{\text{dof}}^s) \times 1} := \underbrace{\left\{ \begin{array}{c} \underbrace{\left\{ \mathbf{z}_u^{m-1}(t_{n+1}) \right\}}_{n_{\text{dof}}^s \times 1} \\ \underbrace{\left\{ \mathbf{z}_v^{m-1}(t_{n+1}) \right\}}_{n_{\text{dof}}^s \times 1} \end{array} \right\}} = \underbrace{\left\{ \begin{array}{c} \underbrace{\left\{ \mathbf{z}_u(t_n) \right\}}_{n_{\text{dof}}^s \times 1} + \Delta t \sum_{i=1}^m b_i^{m-1} \underbrace{\left\{ \mathbf{k}_{i(v)} \right\}}_{n_{\text{dof}}^s \times 1} \\ \underbrace{\left\{ \mathbf{z}_v(t_n) \right\}}_{n_{\text{dof}}^s \times 1} + \Delta t \sum_{i=1}^m b_i^{m-1} \underbrace{\left\{ \mathbf{k}_{i(a)} \right\}}_{n_{\text{dof}}^s \times 1} \end{array} \right\}}. \quad (4.309)$$

Then, a truncation error is calculated for all values of the solutions $\mathbf{z}(t_{n+1})$ according to Equation (4.295), and the new time step Δt^* is adjusted according to Equation (4.296). If the absolute error does not meet the condition defined by Equation (4.297), the solutions given by Equation (4.308) and Equation (4.309) are recomputed at time t_{n+1} using the smaller time step Δt^* in place of Δt in Equation (4.307)–Equation (4.309). This process of computing the truncation error and substituting the adapted time step is repeated for the $(\mathbf{u}-\theta)$, $(\mathbf{u}-p_f)$, $(\mathbf{u}-\mathbf{u}_f-p_f)$, $(\mathbf{u}-p_f-\theta^s-\theta^f)$, and $(\mathbf{u}-\mathbf{u}_f-p_f-\theta^s-\theta^f)$ formulations, and is thus not repeated for brevity in the corresponding sections 4.3.1.2–4.3.1.6.

4.3.1.2 (\mathbf{u} - θ) formulation

For the (\mathbf{u} - θ) formulation, the Runge-Kutta integrators transform the general solution variables given by Equation (4.291) to

$$\left\{ \dot{\mathbf{z}} \right\} := \begin{Bmatrix} \dot{z}_u \\ \dot{z}_v \\ \dot{z}_\theta \end{Bmatrix} = \left\{ \mathbf{f}(t, \mathbf{z}) \right\} = \begin{Bmatrix} \mathbf{f}_v(t, \mathbf{z}) \\ \mathbf{f}_a(t, \mathbf{z}) \\ \mathbf{f}_\theta(t, \mathbf{z}) \end{Bmatrix}, \quad (4.310)$$

such that

$$\left\{ \mathbf{z} \right\} = \begin{Bmatrix} \mathbf{d} \\ \dot{\mathbf{d}} \\ \vartheta \end{Bmatrix}, \quad \dot{\mathbf{z}} = \begin{Bmatrix} \dot{\mathbf{d}} \\ \ddot{\mathbf{d}} \\ \dot{\vartheta} \end{Bmatrix}. \quad (4.311)$$

Thus, we require at least one governing equation to solve for the primary unknown $\ddot{\mathbf{d}}$, which when integrated once gives us $\dot{\mathbf{d}}$, and when integrated twice gives us \mathbf{d} ; and at least one governing equation to solve for the primary unknown $\dot{\vartheta}$, which when integrated once gives us ϑ .

The FE formulation for the balance of momentum of the single-phase, with variational equation given by Equation (4.40), is written in block-matrix form as

$$\underbrace{\left\{ \mathbf{R}_u \right\}}_{n_{\text{dof}}^s \times 1} = \mathbf{0}, \quad (4.312)$$

where the global residual for the single-phase displacement is given as

$$\mathbf{c}^{u,T} \cdot \mathbf{R}_u = \mathcal{G}^h = \mathcal{G}_1^{\text{INT},h} + \mathcal{G}_2^{\text{INT},h} + \mathcal{G}_4^{\text{INT},h} - \mathcal{G}^{\text{EXT},h} = 0. \quad (4.313)$$

Therein,

$$\begin{aligned} \mathcal{G}_1^{\text{INT},h} &= \mathbf{A}_e^{n_e} \underbrace{\left\{ \mathbf{c}^{u,e} \right\}^T}_{1 \times n_{\text{dof}}^{s,e}} \cdot \underbrace{\left[\mathbf{m}_{u,u}^{\mathcal{G}_1^{\text{INT},e}} \right]}_{n_{\text{dof}}^{s,e} \times n_{\text{dof}}^{s,e}} \cdot \underbrace{\left\{ \ddot{\mathbf{d}} \right\}}_{n_{\text{dof}}^{s,e} \times 1}, & \mathcal{G}_2^{\text{INT},h} &= \mathbf{A}_e^{n_e} \underbrace{\left\{ \mathbf{c}^{u,e} \right\}^T}_{1 \times n_{\text{dof}}^{s,e}} \cdot \underbrace{\left\{ \mathbf{f}^{\mathcal{G}_2^{\text{INT},e}} \right\}}_{n_{\text{dof}}^{s,e} \times 1}, \\ \mathcal{G}_4^{\text{INT},h} &= \mathbf{A}_e^{n_e} \underbrace{\left\{ \mathbf{c}^{u,e} \right\}^T}_{1 \times n_{\text{dof}}^{s,e}} \cdot \underbrace{\left\{ \mathbf{f}^{\mathcal{G}_4^{\text{INT},e}} \right\}}_{n_{\text{dof}}^{s,e} \times 1}, & \mathcal{G}^{\text{EXT},h} &= \mathbf{A}_e^{n_e} \underbrace{\left\{ \mathbf{c}^{u,e} \right\}^T}_{1 \times n_{\text{dof}}^{s,e}} \cdot \underbrace{\left\{ \mathbf{f}^{\mathcal{G}^{\text{EXT},e}} \right\}}_{n_{\text{dof}}^{s,e} \times 1}, \end{aligned} \quad (4.314)$$

where

$$\begin{aligned}
\underbrace{\left\{ \mathbf{f}^{\mathcal{G}_2^{\text{INT},e}} \right\}}_{n_{\text{dof}}^{s,e} \times 1} &= \int_{-1}^1 \underbrace{\left\{ \mathbf{B}^{e,u} \right\}^T}_{n_{\text{dof}}^{s,e} \times 1} P_{11}^{h^e} A j^e d\xi, \quad \underbrace{\left\{ \mathbf{f}^{\mathcal{G}_4^{\text{INT},e}} \right\}}_{n_{\text{dof}}^{s,e} \times 1} = \int_{-1}^1 \underbrace{\left\{ \mathbf{N}^{e,u} \right\}^T}_{n_{\text{dof}}^{s,e} \times 1} \rho_0^{h^e} g A j^e d\xi, \\
\underbrace{\left\{ \mathbf{f}^{\mathcal{G}^{\text{EXT},e}} \right\}}_{n_{\text{dof}}^{s,e} \times 1} &= \begin{cases} \underbrace{\left\{ \mathbf{N}^{e,u}(X=0, H) \right\}^T}_{n_{\text{dof}}^{s,e} \times 1} t^\sigma A & X=0, H \\ \mathbf{0} & 0 < X < H. \end{cases} \quad (4.315)
\end{aligned}$$

The mass matrix associated with the single-phase acceleration is given by

$$\underbrace{\left[\mathbf{m}_{u,u}^{\mathcal{G}_1^{\text{INT},e}} \right]}_{n_{\text{dof}}^{s,e} \times n_{\text{dof}}^{s,e}} = \int_{-1}^1 \rho_0^{h^e} \underbrace{\left\{ \mathbf{N}^{e,u} \right\}^T}_{n_{\text{dof}}^{s,e} \times 1} \underbrace{\left\{ \mathbf{N}^{e,u} \right\}}_{1 \times n_{\text{dof}}^{s,e}} A j^e d\xi. \quad (4.316)$$

The FE formulation for the balance of energy of the single-phase, with variational equation given by Equation (4.41), is written in block-matrix form as

$$\underbrace{\left\{ \mathbf{R}_\theta \right\}}_{n_{\text{dof}}^\theta \times 1} = \mathbf{0}, \quad (4.317)$$

where the global residual for the single-phase temperature is given as

$$\mathbf{c}^{\theta,T} \cdot \mathbf{R}_\theta = \mathcal{J}^h = \mathcal{J}_1^{\text{INT},h} + \mathcal{J}_2^{\text{INT},h} + \mathcal{J}_3^{\text{INT},h} - \mathcal{J}^{\text{EXT},h} = 0. \quad (4.318)$$

Therein,

$$\begin{aligned}
\mathcal{J}_1^{\text{INT},h} &= \mathbf{A}_e^{n_e} \underbrace{\left\{ \mathbf{c}^{\theta,e} \right\}^T}_{1 \times n_{\text{dof}}^{\theta,e}} \cdot \underbrace{\left[\mathbf{m}_{\theta,\theta}^{\mathcal{J}_1^{\text{INT},e}} \right]}_{n_{\text{dof}}^{\theta,e} \times n_{\text{dof}}^{\theta,e}} \cdot \underbrace{\left\{ \dot{\vartheta}^e \right\}}_{n_{\text{dof}}^{\theta,e} \times 1}, & \mathcal{J}_2^{\text{INT},h} &= \mathbf{A}_e^{n_e} \underbrace{\left\{ \mathbf{c}^{\theta,e} \right\}^T}_{1 \times n_{\text{dof}}^{\theta,e}} \cdot \underbrace{\left\{ \mathbf{f}^{\mathcal{J}_2^{\text{INT},e}} \right\}}_{n_{\text{dof}}^{\theta,e} \times 1}, \\
\mathcal{J}_3^{\text{INT},h} &= \mathbf{A}_e^{n_e} \underbrace{\left\{ \mathbf{c}^{\theta,e} \right\}^T}_{1 \times n_{\text{dof}}^{\theta,e}} \cdot \underbrace{\left\{ \mathbf{f}^{\mathcal{J}_3^{\text{INT},e}} \right\}}_{n_{\text{dof}}^{\theta,e} \times 1}, & \mathcal{J}^{\text{EXT},h} &= \mathbf{A}_e^{n_e} \underbrace{\left\{ \mathbf{c}^{\theta,e} \right\}^T}_{1 \times n_{\text{dof}}^{\theta,e}} \cdot \underbrace{\left\{ \mathbf{f}^{\mathcal{J}^{\text{EXT},e}} \right\}}_{n_{\text{dof}}^{\theta,e} \times 1}, \quad (4.319)
\end{aligned}$$

where

$$\begin{aligned}
\underbrace{\left\{ \mathbf{f}_{\mathcal{J}_2^{\text{INT}},e} \right\}}_{n_{\text{dof}}^{\theta,e} \times 1} &= \int_{-1}^1 \underbrace{\left\{ \mathbf{N}^{e,\theta} \right\}}_{n_{\text{dof}}^{\theta,e} \times 1}^T \left(\frac{K \alpha_V \theta^{h^e}}{J^{h^e}} + Q^{h^e} \right) j^{h^e} A_j^e d\xi, \\
\underbrace{\left\{ \mathbf{f}_{\mathcal{J}_3^{\text{INT}},e} \right\}}_{n_{\text{dof}}^{\theta,e} \times 1} &= - \int_{-1}^1 \underbrace{\left\{ \mathbf{B}^{e,\theta} \right\}}_{n_{\text{dof}}^{\theta,e} \times 1}^T q^{h^e} A_j^e d\xi, \\
\underbrace{\left\{ \mathbf{f}_{\mathcal{J}^{\text{EXT}},e} \right\}}_{n_{\text{dof}}^{\theta,e} \times 1} &= \begin{cases} \underbrace{\left\{ \mathbf{N}^{e,\theta}(X=0, H) \right\}}_{n_{\text{dof}}^{\theta,e} \times 1}^T Q^\theta A & X=0, H \\ \mathbf{0} & 0 < X < H. \end{cases}
\end{aligned} \tag{4.320}$$

The mass matrix associated with the temperature is given by

$$\underbrace{\left[\mathbf{m}_{\theta,\theta}^{\mathcal{J}_1^{\text{INT}},e} \right]}_{n_{\text{dof}}^{\theta,e} \times n_{\text{dof}}^{\theta,e}} = \int_{-1}^1 \rho_0^{h^e} c_V \underbrace{\left\{ \mathbf{N}^{e,\theta} \right\}}_{n_{\text{dof}}^{\theta,e} \times 1}^T \underbrace{\left\{ \mathbf{N}^{e,\theta} \right\}}_{1 \times n_{\text{dof}}^{\theta,e}} A_j^e d\xi. \tag{4.321}$$

Then, returning our attention to Equation (4.310), we have

$$\underbrace{\left\{ \dot{\mathbf{z}} \right\}}_{(2 \times n_{\text{dof}}^s + n_{\text{dof}}^\theta) \times 1} = \left[\begin{array}{c} \underbrace{\left\{ \dot{\mathbf{d}} \right\}}_{n_{\text{dof}}^s \times 1} \\ \underbrace{\left[\mathbf{M}_{u,u}^{\mathcal{G}_1^{\text{INT}}} \right]^{-1}}_{n_{\text{dof}}^s \times n_{\text{dof}}^s} \cdot \left(- \underbrace{\left\{ \mathbf{F}^{\mathcal{G}_2^{\text{INT}}} \right\}}_{n_{\text{dof}}^s \times 1} - \underbrace{\left\{ \mathbf{F}^{\mathcal{G}_4^{\text{INT}}} \right\}}_{n_{\text{dof}}^s \times 1} + \underbrace{\left\{ \mathbf{F}^{\mathcal{G}^{\text{EXT}}} \right\}}_{n_{\text{dof}}^s \times 1} \right) \\ \underbrace{\left[\mathbf{M}_{p_f,p_f}^{\mathcal{J}_1^{\text{INT}}} \right]^{-1}}_{n_{\text{dof}}^\theta \times n_{\text{dof}}^\theta} \cdot \left(- \underbrace{\left\{ \mathbf{F}^{\mathcal{J}_2^{\text{INT}}} \right\}}_{n_{\text{dof}}^\theta \times 1} - \underbrace{\left\{ \mathbf{F}^{\mathcal{J}_3^{\text{INT}}} \right\}}_{n_{\text{dof}}^\theta \times 1} + \underbrace{\left\{ \mathbf{F}^{\mathcal{J}^{\text{EXT}}} \right\}}_{n_{\text{dof}}^\theta \times 1} \right) \end{array} \right], \tag{4.322}$$

where

$$\begin{aligned}
\underbrace{\left[M_{u,u}^{\mathcal{G}_1^{\text{INT}}} \right]}_{n_{\text{dof}}^s \times n_{\text{dof}}^s} &= \mathbf{A}_e^{n_e} \underbrace{\left[\mathbf{m}_{u,u}^{\mathcal{G}_1^{\text{INT},e}} \right]}_{n_{\text{dof}}^{s,e} \times n_{\text{dof}}^{s,e}}, & \underbrace{\left\{ \mathbf{F}^{\mathcal{G}_2^{\text{INT}}} \right\}}_{n_{\text{dof}}^s \times 1} &= \mathbf{A}_e^{n_e} \underbrace{\left\{ \mathbf{f}^{\mathcal{G}_2^{\text{INT},e}} \right\}}_{n_{\text{dof}}^{s,e} \times 1}, \\
\underbrace{\left\{ \mathbf{F}^{\mathcal{G}_4^{\text{INT}}} \right\}}_{n_{\text{dof}}^s \times 1} &= \mathbf{A}_e^{n_e} \underbrace{\left\{ \mathbf{f}^{\mathcal{G}_4^{\text{INT},e}} \right\}}_{n_{\text{dof}}^{s,e} \times 1}, & \underbrace{\left\{ \mathbf{F}^{\mathcal{G}^{\text{EXT}}} \right\}}_{n_{\text{dof}}^s \times 1} &= \mathbf{A}_e^{n_e} \underbrace{\left\{ \mathbf{f}^{\mathcal{G}^{\text{EXT},e}} \right\}}_{n_{\text{dof}}^{s,e} \times 1}, \\
\underbrace{\left[M_{\theta,\theta}^{\mathcal{J}_1^{\text{INT}}} \right]}_{n_{\text{dof}}^\theta \times n_{\text{dof}}^\theta} &= \mathbf{A}_e^{n_e} \underbrace{\left[\mathbf{m}_{\theta,\theta}^{\mathcal{J}_1^{\text{INT},e}} \right]}_{n_{\text{dof}}^{\theta,e} \times n_{\text{dof}}^{\theta,e}}, & \underbrace{\left\{ \mathbf{F}^{\mathcal{J}_2^{\text{INT}}} \right\}}_{n_{\text{dof}}^\theta \times 1} &= \mathbf{A}_e^{n_e} \underbrace{\left\{ \mathbf{f}^{\mathcal{J}_2^{\text{INT},e}} \right\}}_{n_{\text{dof}}^{\theta,e} \times 1}, \\
\underbrace{\left\{ \mathbf{F}^{\mathcal{J}_3^{\text{INT}}} \right\}}_{n_{\text{dof}}^\theta \times 1} &= \mathbf{A}_e^{n_e} \underbrace{\left\{ \mathbf{f}^{\mathcal{J}_3^{\text{INT},e}} \right\}}_{n_{\text{dof}}^{\theta,e} \times 1}, & \underbrace{\left\{ \mathbf{F}^{\mathcal{J}^{\text{EXT}}} \right\}}_{n_{\text{dof}}^\theta \times 1} &= \mathbf{A}_e^{n_e} \underbrace{\left\{ \mathbf{f}^{\mathcal{J}^{\text{EXT},e}} \right\}}_{n_{\text{dof}}^{\theta,e} \times 1}.
\end{aligned} \tag{4.323}$$

As described in Section 4.3.1, Equation (4.322) is solved for each stage increment i at time $t_n + \Delta t c_i$ (i.e., any variables that are *explicit* functions of time, such as a time-dependent external traction, are to be evaluated at time $t_n + \Delta t c_i$), with stage solution \mathbf{k}_i given by

$$\underbrace{\left\{ \mathbf{k}_i \right\}}_{(2 \times n_{\text{dof}}^s + n_{\text{dof}}^\theta) \times 1} := \underbrace{\left\{ \mathbf{k}_{i(v)} \right\}}_{n_{\text{dof}}^s \times 1} = \underbrace{\left\{ \mathbf{k}_{i(a)} \right\}}_{n_{\text{dof}}^s \times 1} = \underbrace{\left\{ \mathbf{k}_{i(\dot{\theta})} \right\}}_{n_{\text{dof}}^\theta \times 1} = \underbrace{\left\{ \underbrace{\mathbf{z}_v(t_n)}_{n_{\text{dof}}^s \times 1} + \Delta t \sum_{j=1}^{i-1} a_{ij} \underbrace{\mathbf{k}_{j(v)}}_{n_{\text{dof}}^s \times 1} \right\}}_{n_{\text{dof}}^s \times 1} = \underbrace{\left\{ \underbrace{\mathbf{z}_a(t_n)}_{n_{\text{dof}}^s \times 1} + \Delta t \sum_{j=1}^{i-1} a_{ij} \underbrace{\mathbf{k}_{j(a)}}_{n_{\text{dof}}^s \times 1} \right\}}_{n_{\text{dof}}^s \times 1} = \underbrace{\left\{ \underbrace{\mathbf{z}_{\dot{\theta}}(t_n)}_{n_{\text{dof}}^\theta \times 1} + \Delta t \sum_{j=1}^{i-1} a_{ij} \underbrace{\mathbf{k}_{j(\dot{\theta})}}_{n_{\text{dof}}^\theta \times 1} \right\}}_{n_{\text{dof}}^\theta \times 1}. \tag{4.324}$$

Then, according to Equation (4.293), the higher order solution to be accepted or rejected at time

t_{n+1} is given by

$$\underbrace{\left\{ \mathbf{z}^m(t_{n+1}) \right\}}_{(2 \times n_{\text{dof}}^s + n_{\text{dof}}^\theta) \times 1} := \left\{ \begin{array}{c} \underbrace{\left\{ \mathbf{z}_u^m(t_{n+1}) \right\}}_{n_{\text{dof}}^s \times 1} \\ \underbrace{\left\{ \mathbf{z}_v^m(t_{n+1}) \right\}}_{n_{\text{dof}}^s \times 1} \\ \underbrace{\left\{ \mathbf{z}_\theta^m(t_{n+1}) \right\}}_{n_{\text{dof}}^\theta \times 1} \end{array} \right\} = \left\{ \begin{array}{c} \underbrace{\left\{ \mathbf{z}_u(t_n) \right\}}_{n_{\text{dof}}^s \times 1} + \Delta t \sum_{i=1}^{m+1} b_i^m \underbrace{\left\{ \mathbf{k}_{i(v)} \right\}}_{n_{\text{dof}}^s \times 1} \\ \underbrace{\left\{ \mathbf{z}_v(t_n) \right\}}_{n_{\text{dof}}^s \times 1} + \Delta t \sum_{i=1}^{m+1} b_i^m \underbrace{\left\{ \mathbf{k}_{i(a)} \right\}}_{n_{\text{dof}}^s \times 1} \\ \underbrace{\left\{ \mathbf{z}_\theta(t_n) \right\}}_{n_{\text{dof}}^\theta \times 1} + \Delta t \sum_{i=1}^{m+1} b_i^m \underbrace{\left\{ \mathbf{k}_{i(\dot{\theta})} \right\}}_{n_{\text{dof}}^\theta \times 1} \end{array} \right\}, \quad (4.325)$$

and, according to Equation (4.294), the lower order solution at time t_{n+1} is given by

$$\underbrace{\left\{ \mathbf{z}^{m-1}(t_{n+1}) \right\}}_{(2 \times n_{\text{dof}}^s + n_{\text{dof}}^\theta) \times 1} := \left\{ \begin{array}{c} \underbrace{\left\{ \mathbf{z}_u^{m-1}(t_{n+1}) \right\}}_{n_{\text{dof}}^s \times 1} \\ \underbrace{\left\{ \mathbf{z}_v^{m-1}(t_{n+1}) \right\}}_{n_{\text{dof}}^s \times 1} \\ \underbrace{\left\{ \mathbf{z}_\theta^{m-1}(t_{n+1}) \right\}}_{n_{\text{dof}}^\theta \times 1} \end{array} \right\} = \left\{ \begin{array}{c} \underbrace{\left\{ \mathbf{z}_u(t_n) \right\}}_{n_{\text{dof}}^s \times 1} + \Delta t \sum_{i=1}^m b_i^{m-1} \underbrace{\left\{ \mathbf{k}_{i(v)} \right\}}_{n_{\text{dof}}^s \times 1} \\ \underbrace{\left\{ \mathbf{z}_v(t_n) \right\}}_{n_{\text{dof}}^s \times 1} + \Delta t \sum_{i=1}^m b_i^{m-1} \underbrace{\left\{ \mathbf{k}_{i(a)} \right\}}_{n_{\text{dof}}^s \times 1} \\ \underbrace{\left\{ \mathbf{z}_\theta(t_n) \right\}}_{n_{\text{dof}}^\theta \times 1} + \Delta t \sum_{i=1}^m b_i^{m-1} \underbrace{\left\{ \mathbf{k}_{i(\dot{\theta})} \right\}}_{n_{\text{dof}}^\theta \times 1} \end{array} \right\}. \quad (4.326)$$

4.3.1.3 (\mathbf{u} - p_f) formulation

For the (\mathbf{u} - p_f) formulation, the Runge-Kutta integrators transform the general solution variables given by Equation (4.291) to

$$\left\{ \dot{\mathbf{z}} \right\} := \left\{ \begin{array}{c} \dot{\mathbf{z}}_u \\ \dot{\mathbf{z}}_v \\ \dot{\mathbf{z}}_{p_f} \end{array} \right\} = \left\{ \mathbf{f}(t, \mathbf{z}) \right\} = \left\{ \begin{array}{c} \mathbf{f}_v(t, \mathbf{z}) \\ \mathbf{f}_a(t, \mathbf{z}) \\ \mathbf{f}_{\dot{p}_f}(t, \mathbf{z}) \end{array} \right\}, \quad (4.327)$$

such that

$$\left\{ \mathbf{z} \right\} = \left\{ \begin{array}{c} \mathbf{d} \\ \dot{\mathbf{d}} \\ \boldsymbol{\pi} \end{array} \right\}, \quad \dot{\mathbf{z}} = \left\{ \begin{array}{c} \dot{\mathbf{d}} \\ \ddot{\mathbf{d}} \\ \dot{\boldsymbol{\pi}} \end{array} \right\}. \quad (4.328)$$

Thus, we require at least one governing equation to solve for the primary unknown $\ddot{\mathbf{d}}$, which when integrated once gives us $\dot{\mathbf{d}}$, and when integrated twice gives us \mathbf{d} ; and at least one governing equation to solve for the primary unknown $\dot{\boldsymbol{\pi}}$, which when integrated once gives us $\boldsymbol{\pi}$. Contrary to the central-difference scheme, these equations are solved separately (i.e., not in a staggered manner, refer to Section 4.3.3.2 and Algorithm 1 therein).

The FE formulation for the balance of momentum of the mixture, with variational equation given by Equation (4.64), is written in block-matrix form as

$$\underbrace{\left\{ \mathbf{R}_u \right\}}_{n_{\text{dof}}^s \times 1} = \mathbf{0}, \quad (4.329)$$

where the global residual for the solid skeleton displacement is given as

$$\mathbf{c}^{u,T} \cdot \mathbf{R}_u = \mathcal{G}^h = \mathcal{G}_1^{\text{INT},h} + \mathcal{G}_2^{\text{INT},h} + \mathcal{G}_3^{\text{INT},h} + \mathcal{G}_4^{\text{INT},h} - \mathcal{G}^{\text{EXT},h} = 0. \quad (4.330)$$

Therein,

$$\begin{aligned} \mathcal{G}_1^{\text{INT},h} &= \mathbf{A}_e^{n_e} \underbrace{\left\{ \mathbf{c}^{u,e} \right\}^T}_{1 \times n_{\text{dof}}^{s,e}} \cdot \underbrace{\left[\mathbf{m}_{u,u}^{\mathcal{G}_1^{\text{INT},e}} \right]}_{n_{\text{dof}}^{s,e} \times n_{\text{dof}}^{s,e}} \cdot \underbrace{\left\{ \ddot{\mathbf{d}}^e \right\}}_{n_{\text{dof}}^{s,e} \times 1}, & \mathcal{G}_2^{\text{INT},h} &= \mathbf{A}_e^{n_e} \underbrace{\left\{ \mathbf{c}^{u,e} \right\}^T}_{1 \times n_{\text{dof}}^{s,e}} \cdot \underbrace{\left\{ \mathbf{f}^{\mathcal{G}_2^{\text{INT},e}} \right\}}_{n_{\text{dof}}^{s,e} \times 1}, \\ \mathcal{G}_3^{\text{INT},h} &= \mathbf{A}_e^{n_e} \underbrace{\left\{ \mathbf{c}^{u,e} \right\}^T}_{1 \times n_{\text{dof}}^{s,e}} \cdot \underbrace{\left\{ \mathbf{f}^{\mathcal{G}_3^{\text{INT},e}} \right\}}_{n_{\text{dof}}^{s,e} \times 1}, & \mathcal{G}_4^{\text{INT},h} &= \mathbf{A}_e^{n_e} \underbrace{\left\{ \mathbf{c}^{u,e} \right\}^T}_{1 \times n_{\text{dof}}^{s,e}} \cdot \underbrace{\left\{ \mathbf{f}^{\mathcal{G}_4^{\text{INT},e}} \right\}}_{n_{\text{dof}}^{s,e} \times 1}, \\ \mathcal{G}^{\text{EXT},h} &= \mathbf{A}_e^{n_e} \underbrace{\left\{ \mathbf{c}^{u,e} \right\}^T}_{1 \times n_{\text{dof}}^{s,e}} \cdot \underbrace{\left\{ \mathbf{f}^{\mathcal{G}^{\text{EXT},e}} \right\}}_{n_{\text{dof}}^{s,e} \times 1}, \end{aligned} \quad (4.331)$$

where

$$\begin{aligned}
\underbrace{\left\{ \mathbf{f}^{\mathcal{G}_2^{\text{INT},e}} \right\}}_{n_{\text{dof}}^{s,e} \times 1} &= \int_{-1}^1 \underbrace{\left\{ \mathbf{B}^{e,u} \right\}}_{n_{\text{dof}}^{s,e} \times 1}^T P_{11(E)}^{s,h^e} A j^e d\xi, \quad \underbrace{\left\{ \mathbf{f}^{\mathcal{G}_3^{\text{INT},e}} \right\}}_{n_{\text{dof}}^{s,e} \times 1} = - \int_{-1}^1 \underbrace{\left\{ \mathbf{B}^{e,u} \right\}}_{n_{\text{dof}}^{s,e} \times 1}^T p_f^{h^e} A j^e d\xi, \\
\underbrace{\left\{ \mathbf{f}^{\mathcal{G}_4^{\text{INT},e}} \right\}}_{n_{\text{dof}}^{s,e} \times 1} &= \int_{-1}^1 \underbrace{\left\{ \mathbf{N}^{e,u} \right\}}_{n_{\text{dof}}^{s,e} \times 1}^T \rho_0^{h^e} g A j^e d\xi, \\
\underbrace{\left\{ \mathbf{f}^{\mathcal{G}^{\text{EXT},e}} \right\}}_{n_{\text{dof}}^{s,e} \times 1} &= \begin{cases} \underbrace{\left\{ \mathbf{N}^{e,u}(X=0, H) \right\}}_{n_{\text{dof}}^{s,e} \times 1}^T t^\sigma A & X=0, H \\ \mathbf{0} & 0 < X < H. \end{cases}
\end{aligned} \tag{4.332}$$

The mass matrix associated with the solid skeleton acceleration is given by

$$\underbrace{\left[\mathbf{m}_{u,u}^{\mathcal{G}_1^{\text{INT},e}} \right]}_{n_{\text{dof}}^{s,e} \times n_{\text{dof}}^{s,e}} = \int_{-1}^1 \rho_0^{h^e} \underbrace{\left\{ \mathbf{N}^{e,u} \right\}}_{n_{\text{dof}}^{s,e} \times 1}^T \underbrace{\left\{ \mathbf{N}^{e,u} \right\}}_{1 \times n_{\text{dof}}^{s,e}} A j^e d\xi. \tag{4.333}$$

The FE formulation for the balance of mass of the mixture, with variational equation given by Equation (4.66), is written in block-matrix form as

$$\underbrace{\left\{ \mathbf{R}_{p_f} \right\}}_{n_{\text{dof}}^{p_f,e} \times 1} = \mathbf{0}, \tag{4.334}$$

where the global residual for the pore fluid pressure is given as

$$\mathbf{c}^{p_f,T} \cdot \mathbf{R}_{p_f} = \mathcal{H}^h = \mathcal{H}_1^{\text{INT},h} + \mathcal{H}_2^{\text{INT},h} + \mathcal{H}_3^{\text{INT},h} + \mathcal{H}_4^{\text{INT},h} - \mathcal{H}^{\text{EXT},h} = 0. \tag{4.335}$$

Therein,

$$\begin{aligned}
\mathcal{H}_1^{\text{INT},h} &= \mathbf{A}_e^{n_e} \underbrace{\left\{ \mathbf{c}^{p_f,e} \right\}}_{1 \times n_{\text{dof}}^{p_f,e}}^T \cdot \left(\underbrace{\left[\mathbf{m}_{p_f,p_f}^{\mathcal{H}_1^{\text{INT},e}} \right]}_{n_{\text{dof}}^{p_f,e} \times n_{\text{dof}}^{p_f,e}} \cdot \underbrace{\left\{ \dot{\boldsymbol{\pi}}^e \right\}}_{n_{\text{dof}}^{p_f,e} \times 1} + \underbrace{\left\{ \mathbf{f}^{\mathcal{H}_1^{\text{INT},e}} \right\}}_{n_{\text{dof}}^{p_f,e} \times 1} \right), \\
\mathcal{H}_2^{\text{INT},h} &= \mathbf{A}_e^{n_e} \underbrace{\left\{ \mathbf{c}^{p_f,e} \right\}}_{1 \times n_{\text{dof}}^{p_f,e}}^T \cdot \underbrace{\left\{ \mathbf{f}^{\mathcal{H}_2^{\text{INT},e}} \right\}}_{n_{\text{dof}}^{p_f,e} \times 1}, \quad \mathcal{H}_3^{\text{INT},h} = \mathbf{A}_e^{n_e} \underbrace{\left\{ \mathbf{c}^{p_f,e} \right\}}_{1 \times n_{\text{dof}}^{p_f,e}}^T \cdot \underbrace{\left\{ \mathbf{f}^{\mathcal{H}_3^{\text{INT},e}} \right\}}_{n_{\text{dof}}^{p_f,e} \times 1}, \\
\mathcal{H}_4^{\text{INT},h} &= \mathbf{A}_e^{n_e} \underbrace{\left\{ \mathbf{c}^{p_f,e} \right\}}_{1 \times n_{\text{dof}}^{p_f,e}}^T \cdot \underbrace{\left\{ \mathbf{f}^{\mathcal{H}_4^{\text{INT},e}} \right\}}_{n_{\text{dof}}^{p_f,e} \times 1}, \quad \mathcal{H}^{\text{EXT},h} = \mathbf{A}_e^{n_e} \underbrace{\left\{ \mathbf{c}^{p_f,e} \right\}}_{1 \times n_{\text{dof}}^{p_f,e}}^T \cdot \underbrace{\left\{ \mathbf{f}^{\mathcal{H}^{\text{EXT},e}} \right\}}_{n_{\text{dof}}^{p_f,e} \times 1},
\end{aligned} \tag{4.336}$$

where

$$\begin{aligned}
\underbrace{\left\{ \mathbf{f}^{\mathcal{H}_1^{\text{INT}},e} \right\}}_{n_{\text{dof}}^{p_f,e} \times 1} &= \int_{-1}^1 \underbrace{\left\{ \mathbf{N}^{e,p_f} \right\}}_{n_{\text{dof}}^{p_f,e} \times 1}^T j^{h^e} A_j^e d\xi, \\
\underbrace{\left\{ \mathbf{f}^{\mathcal{H}_2^{\text{INT}},e} \right\}}_{n_{\text{dof}}^{p_f,e} \times 1} &= \int_{-1}^1 \underbrace{\left\{ \mathbf{N}^{e,p_f} \right\}}_{n_{\text{dof}}^{p_f,e} \times 1}^T \frac{1}{K_f^\eta} \frac{\partial p_f^{h^e}}{\partial X} (n^f \tilde{v}_f)^{h^e} A_j^e d\xi, \\
\underbrace{\left\{ \mathbf{f}^{\mathcal{H}_3^{\text{INT}},e} \right\}}_{n_{\text{dof}}^{p_f,e} \times 1} &= \int_{-1}^1 \underbrace{\left\{ \mathbf{B}^{e,p_f} \right\}}_{n_{\text{dof}}^{p_f,e} \times 1}^T \hat{k}^{h^e} \frac{\partial p_f^{h^e}}{\partial X} (F_{11}^{h^e})^{-1} A_j^e d\xi, \\
\underbrace{\left\{ \mathbf{f}^{\mathcal{H}_4^{\text{INT}},e} \right\}}_{n_{\text{dof}}^{p_f,e} \times 1} &= \int_{-1}^1 \underbrace{\left\{ \mathbf{B}^{e,p_f} \right\}}_{n_{\text{dof}}^{p_f,e} \times 1}^T \hat{k}^{h^e} \rho^{\text{fR},h^e} (a^{h^e} + g) A_j^e d\xi, \\
\underbrace{\left\{ \mathbf{f}^{\mathcal{H}^{\text{EXT}},e} \right\}}_{n_{\text{dof}}^{p_f,e} \times 1} &= \begin{cases} \underbrace{\left\{ \mathbf{N}^{e,p_f}(X=0, H) \right\}}_{n_{\text{dof}}^{p_f,e} \times 1}^T Q_f A & X=0, H \\ \mathbf{0} & 0 < X < H. \end{cases}
\end{aligned} \tag{4.337}$$

The mass matrix associated with the pore fluid pressure is given by

$$\underbrace{\left[\mathbf{m}_{p_f,p_f}^{\mathcal{H}_1^{\text{INT}},e} \right]}_{n_{\text{dof}}^{p_f,e} \times n_{\text{dof}}^{p_f,e}} = \int_{-1}^1 \frac{J^{h^e} n^{f,h^e}}{K_f^\eta} \underbrace{\left\{ \mathbf{N}^{e,p_f} \right\}}_{n_{\text{dof}}^{p_f,e} \times 1}^T \underbrace{\left\{ \mathbf{N}^{e,p_f} \right\}}_{1 \times n_{\text{dof}}^{p_f,e}} A_j^e d\xi. \tag{4.338}$$

When pressure stabilization is enabled, an additional term $\mathcal{H}^{\text{stab}}$ is added to the l.h.s. of Equation (4.335) and is defined as

$$\mathcal{H}^{\text{stab}} = \mathbf{A}_e^{n_e} \mathbf{c}^{p_f e, T} \cdot \underbrace{\left[\mathbf{m}_{p_f,p_f}^{\mathcal{H}^{\text{stab},e}} \right]}_{n_{\text{dof}}^{p_f,e} \times n_{\text{dof}}^{p_f,e}} \cdot \underbrace{\left\{ \dot{\boldsymbol{\pi}}^e \right\}}_{n_{\text{dof}}^{p_f,e} \times 1}, \tag{4.339}$$

where

$$\underbrace{\left[\mathbf{m}_{p_f,p_f}^{\mathcal{H}^{\text{stab},e}} \right]}_{n_{\text{dof}}^{p_f,e} \times n_{\text{dof}}^{p_f,e}} = \int_{-1}^1 \alpha^{\text{stab}} (F_{11}^{h^e})^{-1} \underbrace{\left\{ \mathbf{B}^{e,p_f} \right\}}_{n_{\text{dof}}^{p_f,e} \times 1}^T \underbrace{\left\{ \mathbf{B}^{e,p_f} \right\}}_{1 \times n_{\text{dof}}^{p_f,e}} A_j^e d\xi. \tag{4.340}$$

Then, returning our attention to Equation (4.327), we have

$$\underbrace{\left\{ \mathbf{z} \right\}}_{(2 \times n_{\text{dof}}^s + n_{\text{dof}}^{p_f}) \times 1} = \left\{ \begin{array}{c} \underbrace{\left\{ \mathbf{d} \right\}}_{n_{\text{dof}}^s \times 1} \\ \underbrace{\left[\mathbf{M}_{u,u}^{\mathcal{G}^{\text{INT}}} \right]^{-1}}_{n_{\text{dof}}^s \times n_{\text{dof}}^s} \cdot \left(- \underbrace{\left\{ \mathbf{F}^{\mathcal{G}_2^{\text{INT}}} \right\}}_{n_{\text{dof}}^s \times 1} - \underbrace{\left\{ \mathbf{F}^{\mathcal{G}_3^{\text{INT}}} \right\}}_{n_{\text{dof}}^s \times 1} - \underbrace{\left\{ \mathbf{F}^{\mathcal{G}_4^{\text{INT}}} \right\}}_{n_{\text{dof}}^s \times 1} + \underbrace{\left\{ \mathbf{F}^{\mathcal{G}^{\text{EXT}}} \right\}}_{n_{\text{dof}}^s \times 1} \right) \\ \underbrace{\left[\mathbf{M}_{p_f,p_f}^{\mathcal{H}^{\text{INT}}} \right]^{-1}}_{n_{\text{dof}}^{p_f} \times n_{\text{dof}}^{p_f}} \cdot \left(- \underbrace{\left\{ \mathbf{F}^{\mathcal{H}_1^{\text{INT}}} \right\}}_{n_{\text{dof}}^{p_f} \times 1} - \underbrace{\left\{ \mathbf{F}^{\mathcal{H}_2^{\text{INT}}} \right\}}_{n_{\text{dof}}^{p_f} \times 1} - \underbrace{\left\{ \mathbf{F}^{\mathcal{H}_3^{\text{INT}}} \right\}}_{n_{\text{dof}}^{p_f} \times 1} - \underbrace{\left\{ \mathbf{F}^{\mathcal{H}_4^{\text{INT}}} \right\}}_{n_{\text{dof}}^{p_f} \times 1} + \underbrace{\left\{ \mathbf{F}^{\mathcal{H}^{\text{EXT}}} \right\}}_{n_{\text{dof}}^{p_f} \times 1} \right) \end{array} \right\}, \quad (4.341)$$

where

$$\begin{aligned} \underbrace{\left[\mathbf{M}_{u,u}^{\mathcal{G}^{\text{INT}}} \right]}_{n_{\text{dof}}^s \times n_{\text{dof}}^s} &= \mathbf{A}_e \underbrace{\left[\mathbf{m}_{u,u}^{\mathcal{G}^{\text{INT},e}} \right]}_{n_{\text{dof}}^{s,e} \times n_{\text{dof}}^{s,e}}, & \underbrace{\left\{ \mathbf{F}^{\mathcal{G}_2^{\text{INT}}} \right\}}_{n_{\text{dof}}^s \times 1} &= \mathbf{A}_e \underbrace{\left\{ \mathbf{f}^{\mathcal{G}_2^{\text{INT},e}} \right\}}_{n_{\text{dof}}^{s,e} \times 1}, \\ \underbrace{\left\{ \mathbf{F}^{\mathcal{G}_3^{\text{INT}}} \right\}}_{n_{\text{dof}}^s \times 1} &= \mathbf{A}_e \underbrace{\left\{ \mathbf{f}^{\mathcal{G}_3^{\text{INT},e}} \right\}}_{n_{\text{dof}}^{s,e} \times 1}, & \underbrace{\left\{ \mathbf{F}^{\mathcal{G}_4^{\text{INT}}} \right\}}_{n_{\text{dof}}^s \times 1} &= \mathbf{A}_e \underbrace{\left\{ \mathbf{f}^{\mathcal{G}_4^{\text{INT},e}} \right\}}_{n_{\text{dof}}^{s,e} \times 1}, \\ \underbrace{\left\{ \mathbf{F}^{\mathcal{G}^{\text{EXT}}} \right\}}_{n_{\text{dof}}^s \times 1} &= \mathbf{A}_e \underbrace{\left\{ \mathbf{f}^{\mathcal{G}^{\text{EXT},e}} \right\}}_{n_{\text{dof}}^{s,e} \times 1}, & \underbrace{\left[\mathbf{M}_{p_f,p_f}^{\mathcal{H}^{\text{INT}}} \right]}_{n_{\text{dof}}^{p_f} \times n_{\text{dof}}^{p_f}} &= \mathbf{A}_e \underbrace{\left[\mathbf{m}_{p_f,p_f}^{\mathcal{H}^{\text{INT},e}} \right]}_{n_{\text{dof}}^{p_f,e} \times n_{\text{dof}}^{p_f,e}}, \\ \underbrace{\left\{ \mathbf{F}^{\mathcal{H}_1^{\text{INT}}} \right\}}_{n_{\text{dof}}^{p_f} \times 1} &= \mathbf{A}_e \underbrace{\left\{ \mathbf{f}^{\mathcal{H}_1^{\text{INT},e}} \right\}}_{n_{\text{dof}}^{p_f,e} \times 1}, & \underbrace{\left\{ \mathbf{F}^{\mathcal{H}_2^{\text{INT}}} \right\}}_{n_{\text{dof}}^{p_f} \times 1} &= \mathbf{A}_e \underbrace{\left\{ \mathbf{f}^{\mathcal{H}_2^{\text{INT},e}} \right\}}_{n_{\text{dof}}^{p_f,e} \times 1}, \\ \underbrace{\left\{ \mathbf{F}^{\mathcal{H}_3^{\text{INT}}} \right\}}_{n_{\text{dof}}^{p_f} \times 1} &= \mathbf{A}_e \underbrace{\left\{ \mathbf{f}^{\mathcal{H}_3^{\text{INT},e}} \right\}}_{n_{\text{dof}}^{p_f,e} \times 1}, & \underbrace{\left\{ \mathbf{F}^{\mathcal{H}_4^{\text{INT}}} \right\}}_{n_{\text{dof}}^{p_f} \times 1} &= \mathbf{A}_e \underbrace{\left\{ \mathbf{f}^{\mathcal{H}_4^{\text{INT},e}} \right\}}_{n_{\text{dof}}^{p_f,e} \times 1}, \\ \underbrace{\left\{ \mathbf{F}^{\mathcal{H}^{\text{EXT}}} \right\}}_{n_{\text{dof}}^{p_f} \times 1} &= \mathbf{A}_e \underbrace{\left\{ \mathbf{f}^{\mathcal{H}^{\text{EXT},e}} \right\}}_{n_{\text{dof}}^{p_f,e} \times 1}. \end{aligned} \quad (4.342)$$

If pressure stabilization is enabled, then we must invert a summation of matrices in Equation (4.341):

$$\underbrace{\left\{ \mathbf{z} \right\}}_{(2 \times n_{\text{dof}}^s + n_{\text{dof}}^{p_f}) \times 1} = \left\{ \begin{array}{c} \underbrace{\left\{ \mathbf{d} \right\}}_{n_{\text{dof}}^s \times 1} \\ \underbrace{\left[\mathbf{M}_{u,u}^{\mathcal{G}^{\text{INT}}} \right]^{-1}}_{n_{\text{dof}}^s \times n_{\text{dof}}^s} \cdot \left(- \underbrace{\left\{ \mathbf{F}^{\mathcal{G}_2^{\text{INT}}} \right\}}_{n_{\text{dof}}^s \times 1} - \underbrace{\left\{ \mathbf{F}^{\mathcal{G}_3^{\text{INT}}} \right\}}_{n_{\text{dof}}^s \times 1} - \underbrace{\left\{ \mathbf{F}^{\mathcal{G}_4^{\text{INT}}} \right\}}_{n_{\text{dof}}^s \times 1} + \underbrace{\left\{ \mathbf{F}^{\mathcal{G}^{\text{EXT}}} \right\}}_{n_{\text{dof}}^s \times 1} \right) \\ \left(\underbrace{\left[\mathbf{M}_{p_f,p_f}^{\mathcal{H}^{\text{INT}}} \right]}_{n_{\text{dof}}^{p_f} \times n_{\text{dof}}^{p_f}} + \underbrace{\left[\mathbf{M}_{p_f,p_f}^{\mathcal{H}^{\text{stab}}} \right]}_{n_{\text{dof}}^{p_f} \times n_{\text{dof}}^{p_f}} \right)^{-1} \cdot \left(- \underbrace{\left\{ \mathbf{F}^{\mathcal{H}_1^{\text{INT}}} \right\}}_{n_{\text{dof}}^{p_f} \times 1} - \underbrace{\left\{ \mathbf{F}^{\mathcal{H}_2^{\text{INT}}} \right\}}_{n_{\text{dof}}^{p_f} \times 1} - \underbrace{\left\{ \mathbf{F}^{\mathcal{H}_3^{\text{INT}}} \right\}}_{n_{\text{dof}}^{p_f} \times 1} - \underbrace{\left\{ \mathbf{F}^{\mathcal{H}_4^{\text{INT}}} \right\}}_{n_{\text{dof}}^{p_f} \times 1} + \underbrace{\left\{ \mathbf{F}^{\mathcal{H}^{\text{EXT}}} \right\}}_{n_{\text{dof}}^{p_f} \times 1} \right) \end{array} \right\}, \quad (4.343)$$

where

$$\underbrace{\left[M_{p_f, p_f}^{\mathcal{H}^{\text{stab}}} \right]}_{n_{\text{dof}}^{p_f} \times n_{\text{dof}}^{p_f}} = \mathbf{A}_e^{n_e} \underbrace{\left[m_{p_f, p_f}^{\mathcal{H}^{\text{stab}, e}} \right]}_{n_{\text{dof}}^{p_f, e} \times n_{\text{dof}}^{p_f, e}}. \quad (4.344)$$

As described in Section 4.3.1, Equation (4.341) or Equation (4.343) is solved for each stage increment i at time $t_n + \Delta t c_i$ (i.e., any variables that are *explicit* functions of time, such as a time-dependent external traction, are to be evaluated at time $t_n + \Delta t c_i$), with stage solution \mathbf{k}_i given by

$$\underbrace{\left\{ \mathbf{k}_i \right\}}_{(2 \times n_{\text{dof}}^s + n_{\text{dof}}^{p_f}) \times 1} := \underbrace{\left\{ \begin{array}{c} \left\{ \mathbf{k}_{i(v)} \right\} \\ n_{\text{dof}}^s \times 1 \\ \left\{ \mathbf{k}_{i(a)} \right\} \\ n_{\text{dof}}^s \times 1 \\ \left\{ \mathbf{k}_{i(p_f)} \right\} \\ n_{\text{dof}}^{p_f} \times 1 \end{array} \right\}} = \underbrace{\left\{ \begin{array}{c} \left\{ \mathbf{z}_v(t_n) \right\} + \Delta t \sum_{j=1}^{i-1} a_{ij} \left\{ \mathbf{k}_{j(v)} \right\} \\ n_{\text{dof}}^s \times 1 \\ \left\{ \mathbf{z}_a(t_n) \right\} + \Delta t \sum_{j=1}^{i-1} a_{ij} \left\{ \mathbf{k}_{j(a)} \right\} \\ n_{\text{dof}}^s \times 1 \\ \left\{ \mathbf{z}_{p_f}(t_n) \right\} + \Delta t \sum_{j=1}^{i-1} a_{ij} \left\{ \mathbf{k}_{j(p_f)} \right\} \\ n_{\text{dof}}^{p_f} \times 1 \end{array} \right\}}. \quad (4.345)$$

Then, according to Equation (4.293), the higher order solution to be accepted or rejected at time t_{n+1} is given by

$$\underbrace{\left\{ \mathbf{z}^m(t_{n+1}) \right\}}_{(2 \times n_{\text{dof}}^s + n_{\text{dof}}^{p_f}) \times 1} := \underbrace{\left\{ \begin{array}{c} \left\{ \mathbf{z}_u^m(t_{n+1}) \right\} \\ n_{\text{dof}}^s \times 1 \\ \left\{ \mathbf{z}_v^m(t_{n+1}) \right\} \\ n_{\text{dof}}^s \times 1 \\ \left\{ \mathbf{z}_{p_f}^m(t_{n+1}) \right\} \\ n_{\text{dof}}^{p_f} \times 1 \end{array} \right\}} = \underbrace{\left\{ \begin{array}{c} \left\{ \mathbf{z}_u(t_n) \right\} + \Delta t \sum_{i=1}^{m+1} b_i^m \left\{ \mathbf{k}_{i(v)} \right\} \\ n_{\text{dof}}^s \times 1 \\ \left\{ \mathbf{z}_v(t_n) \right\} + \Delta t \sum_{i=1}^{m+1} b_i^m \left\{ \mathbf{k}_{i(a)} \right\} \\ n_{\text{dof}}^s \times 1 \\ \left\{ \mathbf{z}_{p_f}(t_n) \right\} + \Delta t \sum_{i=1}^{m+1} b_i^m \left\{ \mathbf{k}_{i(p_f)} \right\} \\ n_{\text{dof}}^{p_f} \times 1 \end{array} \right\}}, \quad (4.346)$$

and, according to Equation (4.294), the lower order solution at time t_{n+1} is given by

$$\underbrace{\left\{ \mathbf{z}^{m-1}(t_{n+1}) \right\}}_{(2 \times n_{\text{dof}}^s + n_{\text{dof}}^{p_f}) \times 1} := \left\{ \begin{array}{c} \underbrace{\left\{ \mathbf{z}_u^{m-1}(t_{n+1}) \right\}}_{n_{\text{dof}}^s \times 1} \\ \underbrace{\left\{ \mathbf{z}_v^{m-1}(t_{n+1}) \right\}}_{n_{\text{dof}}^s \times 1} \\ \underbrace{\left\{ \mathbf{z}_{p_f}^{m-1}(t_{n+1}) \right\}}_{n_{\text{dof}}^{p_f} \times 1} \end{array} \right\} = \left\{ \begin{array}{c} \underbrace{\left\{ \mathbf{z}_u(t_n) \right\}}_{n_{\text{dof}}^s \times 1} + \Delta t \sum_{i=1}^m b_i^{m-1} \underbrace{\left\{ \mathbf{k}_{i(v)} \right\}}_{n_{\text{dof}}^s \times 1} \\ \underbrace{\left\{ \mathbf{z}_v(t_n) \right\}}_{n_{\text{dof}}^s \times 1} + \Delta t \sum_{i=1}^m b_i^{m-1} \underbrace{\left\{ \mathbf{k}_{i(a)} \right\}}_{n_{\text{dof}}^s \times 1} \\ \underbrace{\left\{ \mathbf{z}_{p_f}(t_n) \right\}}_{n_{\text{dof}}^{p_f} \times 1} + \Delta t \sum_{i=1}^m b_i^{m-1} \underbrace{\left\{ \mathbf{k}_{i(p_f)} \right\}}_{n_{\text{dof}}^{p_f} \times 1} \end{array} \right\}. \quad (4.347)$$

4.3.1.4 ($\mathbf{u}-\mathbf{u}_f-p_f$) formulation

For the ($\mathbf{u}-\mathbf{u}_f-p_f$) formulation, the Runge-Kutta integrators transform the general solution variables given by Equation (4.291) to

$$\left\{ \dot{\mathbf{z}} \right\} := \left\{ \begin{array}{c} \dot{\mathbf{z}}_u \\ \dot{\mathbf{z}}_v \\ \dot{\mathbf{z}}_{u_f} \\ \dot{\mathbf{z}}_{v_f} \\ \dot{\mathbf{z}}_{p_f} \end{array} \right\} = \left\{ \mathbf{f}(t, \mathbf{z}) \right\} = \left\{ \begin{array}{c} \mathbf{f}_v(t, \mathbf{z}) \\ \mathbf{f}_a(t, \mathbf{z}) \\ \mathbf{f}_{v_f}(t, \mathbf{z}) \\ \mathbf{f}_{a_f}(t, \mathbf{z}) \\ \mathbf{f}_{p_f}(t, \mathbf{z}) \end{array} \right\}, \quad (4.348)$$

such that

$$\left\{ \mathbf{z} \right\} = \left\{ \begin{array}{c} \mathbf{d} \\ \dot{\mathbf{d}} \\ \mathbf{d}_f \\ \dot{\mathbf{d}}_f \\ \boldsymbol{\pi} \end{array} \right\}, \quad \dot{\mathbf{z}} = \left\{ \begin{array}{c} \dot{\mathbf{d}} \\ \ddot{\mathbf{d}} \\ \dot{\mathbf{d}}_f \\ \ddot{\mathbf{d}}_f \\ \dot{\boldsymbol{\pi}} \end{array} \right\}. \quad (4.349)$$

Thus, we require at least one governing equation to solve for the primary unknown $\ddot{\mathbf{d}}$, which when integrated once gives us $\dot{\mathbf{d}}$, and when integrated twice gives us \mathbf{d} ; at least one governing equation to solve for the primary unknown $\ddot{\mathbf{d}}_f$, which when integrated once gives us $\dot{\mathbf{d}}_f$, and when integrated

twice gives us \mathbf{d}_f ; and at least one governing equation to solve for the primary unknown $\dot{\boldsymbol{\pi}}$, which when integrated once gives us $\boldsymbol{\pi}$.

The FE formulation for the balance of momentum of the mixture, with variational equations given by Equation (4.86) & Equation (4.93)₁, is written in block-matrix form as

$$\underbrace{\left\{ \mathbf{R}_u \right\}}_{n_{\text{dof}}^s \times 1} = \mathbf{0}, \quad (4.350)$$

where the global residual for the solid skeleton displacement is given as

$$\mathbf{c}^{u,T} \cdot \mathbf{R}_u = \mathcal{G}^h = \mathcal{G}_1^{\text{INT},h} + \mathcal{G}_2^{\text{INT},h} + \mathcal{G}_3^{\text{INT},h} + \mathcal{G}_4^{\text{INT},h} + \mathcal{G}_5^{\text{INT},h} - \mathcal{G}^{\text{EXT},h} = 0. \quad (4.351)$$

Therein,

$$\begin{aligned} \mathcal{G}_1^{\text{INT},h} &= \underbrace{\mathbf{A}_e}_{1 \times n_{\text{dof}}^{s,e}} \left\{ \mathbf{c}^{u,e} \right\}^T \cdot \left(\underbrace{\left[\mathbf{m}_{u,u}^{\mathcal{G}_1^{\text{INT},e}} \right]}_{n_{\text{dof}}^{s,e} \times n_{\text{dof}}^{s,e}} \cdot \underbrace{\left\{ \ddot{\mathbf{d}}^e \right\}}_{n_{\text{dof}}^{s,e} \times 1} + \underbrace{\left\{ \mathbf{f}^{\mathcal{G}_1^{\text{INT},e}} \right\}}_{n_{\text{dof}}^{s,e} \times 1} \right), \\ \mathcal{G}_2^{\text{INT},h} &= \underbrace{\mathbf{A}_e}_{1 \times n_{\text{dof}}^{s,e}} \left\{ \mathbf{c}^{u,e} \right\}^T \cdot \underbrace{\left\{ \mathbf{f}^{\mathcal{G}_2^{\text{INT},e}} \right\}}_{n_{\text{dof}}^{s,e} \times 1}, \quad \mathcal{G}_3^{\text{INT},h} = \underbrace{\mathbf{A}_e}_{1 \times n_{\text{dof}}^{s,e}} \left\{ \mathbf{c}^{u,e} \right\}^T \cdot \underbrace{\left\{ \mathbf{f}^{\mathcal{G}_3^{\text{INT},e}} \right\}}_{n_{\text{dof}}^{s,e} \times 1}, \\ \mathcal{G}_4^{\text{INT},h} &= \underbrace{\mathbf{A}_e}_{1 \times n_{\text{dof}}^{s,e}} \left\{ \mathbf{c}^{u,e} \right\}^T \cdot \underbrace{\left\{ \mathbf{f}^{\mathcal{G}_4^{\text{INT},e}} \right\}}_{n_{\text{dof}}^{s,e} \times 1}, \quad \mathcal{G}_5^{\text{INT},h} = \underbrace{\mathbf{A}_e}_{1 \times n_{\text{dof}}^{s,e}} \left\{ \mathbf{c}^{u,e} \right\}^T \cdot \underbrace{\left\{ \mathbf{f}^{\mathcal{G}_5^{\text{INT},e}} \right\}}_{n_{\text{dof}}^{s,e} \times 1}, \\ \mathcal{G}^{\text{EXT},h} &= \underbrace{\mathbf{A}_e}_{1 \times n_{\text{dof}}^{s,e}} \left\{ \mathbf{c}^{u,e} \right\}^T \cdot \underbrace{\left\{ \mathbf{f}^{\mathcal{G}^{\text{EXT},e}} \right\}}_{n_{\text{dof}}^{s,e} \times 1}, \end{aligned} \quad (4.352)$$

with

$$\begin{aligned}
\underbrace{\left\{ \mathbf{f}^{\mathcal{G}_1^{\text{INT}},e} \right\}}_{n_{\text{dof}}^{s,e} \times 1} &= \int_{-1}^1 \underbrace{\left\{ \mathbf{N}^{e,u} \right\}^T}_{n_{\text{dof}}^{s,e} \times 1} \rho_0^{f,h^e} a_f^{h^e} A j^e d\xi, \quad \underbrace{\left\{ \mathbf{f}^{\mathcal{G}_2^{\text{INT}},e} \right\}}_{n_{\text{dof}}^{s,e} \times 1} = \int_{-1}^1 \underbrace{\left\{ \mathbf{B}^{e,u} \right\}^T}_{n_{\text{dof}}^{s,e} \times 1} P_{11(E)}^{s,h^e} A j^e d\xi, \\
\underbrace{\left\{ \mathbf{f}^{\mathcal{G}_3^{\text{INT}},e} \right\}}_{n_{\text{dof}}^{s,e} \times 1} &= - \int_{-1}^1 \underbrace{\left\{ \mathbf{B}^{e,u} \right\}^T}_{n_{\text{dof}}^{s,e} \times 1} p_f^{h^e} A j^e d\xi, \quad \underbrace{\left\{ \mathbf{f}^{\mathcal{G}_4^{\text{INT}},e} \right\}}_{n_{\text{dof}}^{s,e} \times 1} = \int_{-1}^1 \underbrace{\left\{ \mathbf{N}^{e,u} \right\}^T}_{n_{\text{dof}}^{s,e} \times 1} \rho_0^{h^e} g A j^e d\xi, \\
\underbrace{\left\{ \mathbf{f}^{\mathcal{G}_5^{\text{INT}},e} \right\}}_{n_{\text{dof}}^{s,e} \times 1} &= \int_{-1}^1 \underbrace{\left\{ \mathbf{B}^{e,u} \right\}^T}_{n_{\text{dof}}^{s,e} \times 1} P_{11(E)}^{f,h^e} A j^e d\xi, \\
\underbrace{\left\{ \mathbf{f}^{\mathcal{G}^{\text{EXT}},e} \right\}}_{n_{\text{dof}}^{s,e} \times 1} &= \begin{cases} \underbrace{\left\{ \mathbf{N}^{e,u}(X=0, H) \right\}^T}_{n_{\text{dof}}^{s,e} \times 1} t^\sigma A & X=0, H \\ \mathbf{0} & 0 < X < H. \end{cases}
\end{aligned} \tag{4.353}$$

For a nearly-inviscid pore fluid, Equation (4.353)₅ is zero. The mass matrix associated with the solid skeleton acceleration is given by

$$\underbrace{\left[\mathbf{m}_{u,u}^{\mathcal{G}_1^{\text{INT}},e} \right]}_{n_{\text{dof}}^{s,e} \times n_{\text{dof}}^{s,e}} = \int_{-1}^1 \rho_0^{s,h^e} \underbrace{\left\{ \mathbf{N}^{e,u} \right\}^T}_{n_{\text{dof}}^{s,e} \times 1} \underbrace{\left\{ \mathbf{N}^{e,u} \right\}}_{1 \times n_{\text{dof}}^{s,e}} A j^e d\xi. \tag{4.354}$$

The FE formulation for the balance of momentum of the fluid, with variational equations given by Equation (4.88) & Equation (4.93)₃, is written in block-matrix form as

$$\underbrace{\left\{ \mathbf{R}_{u_f} \right\}}_{n_{\text{dof}}^f \times 1} = \mathbf{0}, \tag{4.355}$$

where the global residual for the pore fluid displacement is given as

$$\mathbf{c}^{u_f,T} \cdot \mathbf{R}_{u_f} = \mathcal{I}^h = \mathcal{I}_1^{\text{INT},h} + \mathcal{I}_2^{\text{INT},h} + \mathcal{I}_3^{\text{INT},h} + \mathcal{I}_4^{\text{INT},h} + \mathcal{I}_5^{\text{INT},h} = 0. \tag{4.356}$$

Therein,

$$\begin{aligned}
\mathcal{I}_1^{\text{INT},h} &= \mathbf{A}_e^{n_e} \underbrace{\left\{ \mathbf{c}^{u_f,e} \right\}^T}_{1 \times n_{\text{dof}}^{f,e}} \cdot \underbrace{\left[\mathbf{m}_{u_f,u_f}^{\mathcal{I}_1^{\text{INT},e}} \right]}_{n_{\text{dof}}^{f,e} \times n_{\text{dof}}^{f,e}} \cdot \underbrace{\left\{ \ddot{\mathbf{d}}_f^e \right\}}_{n_{\text{dof}}^{f,e} \times 1}, & \mathcal{I}_2^{\text{INT},h} &= \mathbf{A}_e^{n_e} \underbrace{\left\{ \mathbf{c}^{u_f,e} \right\}^T}_{1 \times n_{\text{dof}}^{f,e}} \cdot \underbrace{\left\{ \mathbf{f}^{\mathcal{I}_2^{\text{INT},e}} \right\}}_{n_{\text{dof}}^{f,e} \times 1}, \\
\mathcal{I}_3^{\text{INT},h} &= \mathbf{A}_e^{n_e} \underbrace{\left\{ \mathbf{c}^{u_f,e} \right\}^T}_{1 \times n_{\text{dof}}^{f,e}} \cdot \underbrace{\left\{ \mathbf{f}^{\mathcal{I}_3^{\text{INT},e}} \right\}}_{n_{\text{dof}}^{f,e} \times 1}, & \mathcal{I}_4^{\text{INT},h} &= \mathbf{A}_e^{n_e} \underbrace{\left\{ \mathbf{c}^{u_f,e} \right\}^T}_{1 \times n_{\text{dof}}^{f,e}} \cdot \underbrace{\left\{ \mathbf{f}^{\mathcal{I}_4^{\text{INT},e}} \right\}}_{n_{\text{dof}}^{f,e} \times 1}, \\
\mathcal{I}_5^{\text{INT},h} &= \mathbf{A}_e^{n_e} \underbrace{\left\{ \mathbf{c}^{u_f,e} \right\}^T}_{1 \times n_{\text{dof}}^{f,e}} \cdot \underbrace{\left\{ \mathbf{f}^{\mathcal{I}_5^{\text{INT},e}} \right\}}_{n_{\text{dof}}^{f,e} \times 1},
\end{aligned} \tag{4.357}$$

with

$$\begin{aligned}
\underbrace{\left\{ \mathbf{f}^{\mathcal{I}_2^{\text{INT},e}} \right\}}_{n_{\text{dof}}^{f,e} \times 1} &= \int_{-1}^1 \underbrace{\left\{ \mathbf{N}^{e,u_f} \right\}^T}_{n_{\text{dof}}^{f,e} \times 1} n^{f,h^e} \frac{\partial p_f^{h^e}}{\partial X} A j^e d\xi, \\
\underbrace{\left\{ \mathbf{f}^{\mathcal{I}_3^{\text{INT},e}} \right\}}_{n_{\text{dof}}^{f,e} \times 1} &= \int_{-1}^1 \underbrace{\left\{ \mathbf{N}^{e,u_f} \right\}^T}_{n_{\text{dof}}^{f,e} \times 1} \frac{J^{h^e} (n^{f,h^e})^2}{\hat{k}} (v_f^{h^e} - v^{h^e}) A j^e d\xi, \\
\underbrace{\left\{ \mathbf{f}^{\mathcal{I}_4^{\text{INT},e}} \right\}}_{n_{\text{dof}}^{f,e} \times 1} &= \int_{-1}^1 \underbrace{\left\{ \mathbf{N}^{e,u_f} \right\}^T}_{n_{\text{dof}}^{f,e} \times 1} \rho_0^{f,h^e} g A j^e d\xi, \\
\underbrace{\left\{ \mathbf{f}^{\mathcal{I}_5^{\text{INT},e}} \right\}}_{n_{\text{dof}}^{f,e} \times 1} &= - \int_{-1}^1 \underbrace{\left\{ \mathbf{N}^{e,u_f} \right\}^T}_{n_{\text{dof}}^{f,e} \times 1} \frac{\partial P_{11(E)}^{f,h^e}}{\partial X} A j^e d\xi.
\end{aligned} \tag{4.358}$$

For a nearly-inviscid pore fluid, Equation (4.358)₅ is zero. The mass matrix associated with the pore fluid acceleration is given by

$$\underbrace{\left[\mathbf{m}_{u_f,u_f}^{\mathcal{I}_1^{\text{INT},e}} \right]}_{n_{\text{dof}}^{f,e} \times n_{\text{dof}}^{f,e}} = \int_{-1}^1 \rho_0^{f,h^e} \underbrace{\left\{ \mathbf{N}^{e,u_f} \right\}^T}_{n_{\text{dof}}^{f,e} \times 1} \underbrace{\left\{ \mathbf{N}^{e,u_f} \right\}}_{1 \times n_{\text{dof}}^{f,e}} A j^e d\xi. \tag{4.359}$$

The FE formulation for the balance of mass, with variational equations given by Equation (4.89) & Equation (4.93)₄, is written in block-matrix form as

$$\underbrace{\left\{ \mathbf{R}_{pf} \right\}}_{n_{\text{dof}}^{pf} \times 1} = \mathbf{0}, \tag{4.360}$$

where the global residual for the pore fluid pressure is given as

$$\mathbf{c}^{p_f, T} \cdot \mathbf{R}_{p_f} = \mathcal{H}^h = \mathcal{H}_1^{\text{INT}, h} + \mathcal{H}_2^{\text{INT}, h} + \mathcal{H}_3^{\text{INT}, h} + \mathcal{H}_4^{\text{INT}, h} + \mathcal{H}_5^{\text{INT}, h} - \mathcal{H}_1^{\text{EXT}, h} = 0. \quad (4.361)$$

Therein,

$$\begin{aligned} \mathcal{H}_1^{\text{INT}, h} &= \mathbf{A}_e^{n_e} \underbrace{\left\{ \mathbf{c}^{p_f, e} \right\}^T}_{1 \times n_{\text{dof}}^{p_f, e}} \cdot \left(\underbrace{\left[\mathbf{m}_{p_f, p_f}^{\mathcal{H}_1^{\text{INT}, e}} \right]}_{n_{\text{dof}}^{p_f, e} \times n_{\text{dof}}^{p_f, e}} \cdot \underbrace{\left\{ \bar{\boldsymbol{\pi}}^e \right\}}_{n_{\text{dof}}^{p_f, e} \times 1} + \underbrace{\left\{ \mathbf{f}^{\mathcal{H}_1^{\text{INT}, e}} \right\}}_{n_{\text{dof}}^{p_f, e} \times 1} \right), \\ \mathcal{H}_2^{\text{INT}, h} &= \mathbf{A}_e^{n_e} \underbrace{\left\{ \mathbf{c}^{p_f, e} \right\}^T}_{1 \times n_{\text{dof}}^{p_f, e}} \cdot \underbrace{\left\{ \mathbf{f}^{\mathcal{H}_2^{\text{INT}, e}} \right\}}_{n_{\text{dof}}^{p_f, e} \times 1}, \quad \mathcal{H}_3^{\text{INT}, h} = \mathbf{A}_e^{n_e} \underbrace{\left\{ \mathbf{c}^{p_f, e} \right\}^T}_{1 \times n_{\text{dof}}^{p_f, e}} \cdot \underbrace{\left\{ \mathbf{f}^{\mathcal{H}_3^{\text{INT}, e}} \right\}}_{n_{\text{dof}}^{p_f, e} \times 1}, \\ \mathcal{H}_4^{\text{INT}, h} &= \mathbf{A}_e^{n_e} \underbrace{\left\{ \mathbf{c}^{p_f, e} \right\}^T}_{1 \times n_{\text{dof}}^{p_f, e}} \cdot \underbrace{\left\{ \mathbf{f}^{\mathcal{H}_4^{\text{INT}, e}} \right\}}_{n_{\text{dof}}^{p_f, e} \times 1}, \quad \mathcal{H}_5^{\text{INT}, h} = \mathbf{A}_e^{n_e} \underbrace{\left\{ \mathbf{c}^{p_f, e} \right\}^T}_{1 \times n_{\text{dof}}^{p_f, e}} \cdot \underbrace{\left\{ \mathbf{f}^{\mathcal{H}_5^{\text{INT}, e}} \right\}}_{n_{\text{dof}}^{p_f, e} \times 1}, \\ \mathcal{H}^{\text{EXT}, h} &= \mathbf{A}_e^{n_e} \underbrace{\left\{ \mathbf{c}^{p_f, e} \right\}^T}_{1 \times n_{\text{dof}}^{p_f, e}} \cdot \underbrace{\left\{ \mathbf{f}^{\mathcal{H}^{\text{EXT}, e}} \right\}}_{n_{\text{dof}}^{p_f, e} \times 1}, \end{aligned} \quad (4.362)$$

with

$$\begin{aligned}
\underbrace{\left\{ \mathbf{f}^{\mathcal{H}_1^{\text{INT},e}} \right\}}_{n_{\text{dof}}^{p_f,e} \times 1} &= \int_{-1}^1 \underbrace{\left\{ \mathbf{N}^{e,p_f} \right\}^T}_{n_{\text{dof}}^{p_f,e} \times 1} j^{h^e} A_j^e d\xi, \\
\underbrace{\left\{ \mathbf{f}^{\mathcal{H}_2^{\text{INT},e}} \right\}}_{n_{\text{dof}}^{p_f,e} \times 1} &= \int_{-1}^1 \underbrace{\left\{ \mathbf{N}^{e,p_f} \right\}^T}_{n_{\text{dof}}^{p_f,e} \times 1} \frac{1}{K_f^\eta} \frac{\partial p_f^{h^e}}{\partial X} (n^f \tilde{v}_f)^{h^e} A_j^e d\xi, \\
\underbrace{\left\{ \mathbf{f}^{\mathcal{H}_3^{\text{INT},e}} \right\}}_{n_{\text{dof}}^{p_f,e} \times 1} &= \int_{-1}^1 \underbrace{\left\{ \mathbf{B}^{e,p_f} \right\}^T}_{n_{\text{dof}}^{p_f,e} \times 1} \hat{k}^{h^e} \frac{\partial p_f^{h^e}}{\partial X} (F_{11}^{h^e})^{-1} A_j^e d\xi, \\
\underbrace{\left\{ \mathbf{f}^{\mathcal{H}_4^{\text{INT},e}} \right\}}_{n_{\text{dof}}^{p_f,e} \times 1} &= \int_{-1}^1 \underbrace{\left\{ \mathbf{B}^{e,p_f} \right\}^T}_{n_{\text{dof}}^{p_f,e} \times 1} \hat{k}^{h^e} \rho^{\text{fR},h^e} (a_f^{h^e} + g) A_j^e d\xi, \\
\underbrace{\left\{ \mathbf{f}^{\mathcal{H}_5^{\text{INT},e}} \right\}}_{n_{\text{dof}}^{p_f,e} \times 1} &= - \int_{-1}^1 \underbrace{\left\{ \mathbf{B}^{e,p_f} \right\}^T}_{n_{\text{dof}}^{p_f,e} \times 1} \frac{\hat{k}}{n^f} \frac{\partial \sigma_{11(E)}^{f,h^e}}{\partial X} (F_{11}^{h^e})^{-1} \frac{1}{K_f^\eta} A_j^e d\xi, \\
\underbrace{\left\{ \mathbf{f}^{\mathcal{H}^{\text{EXT},e}} \right\}}_{n_{\text{dof}}^{p_f,e} \times 1} &= \begin{cases} \underbrace{\left\{ \mathbf{N}^{e,p_f}(X=0, H) \right\}^T}_{n_{\text{dof}}^{p_f,e} \times 1} Q_f A & X=0, H \\ \mathbf{0} & 0 < X < H. \end{cases}
\end{aligned} \tag{4.363}$$

For a nearly-inviscid pore fluid, Equation (4.363)₅ is zero. The mass matrix associated with the pore fluid pressure is given by

$$\underbrace{\left[\mathbf{m}_{p_f,p_f}^{\mathcal{H}_1^{\text{INT},e}} \right]}_{n_{\text{dof}}^{p_f,e} \times n_{\text{dof}}^{p_f,e}} = \int_{-1}^1 \frac{J^{h^e} n^{f,h^e}}{K_f^\eta} \underbrace{\left\{ \mathbf{N}^{e,p_f} \right\}^T}_{n_{\text{dof}}^{p_f,e} \times 1} \underbrace{\left\{ \mathbf{N}^{e,p_f} \right\}}_{1 \times n_{\text{dof}}^{p_f,e}} A_j^e d\xi. \tag{4.364}$$

When pressure stabilization is enabled, an additional term $\mathcal{H}^{\text{stab}}$ is added to the l.h.s. of Equation (4.361) and is defined as

$$\mathcal{H}^{\text{stab}} = \mathbf{A}_e^{n_e} \mathbf{c}^{p_f e, T} \cdot \underbrace{\left[\mathbf{m}_{p_f,p_f}^{\mathcal{H}^{\text{stab},e}} \right]}_{n_{\text{dof}}^{p_f,e} \times n_{\text{dof}}^{p_f,e}} \cdot \underbrace{\left\{ \dot{\boldsymbol{\pi}}^e \right\}}_{n_{\text{dof}}^{p_f,e} \times 1}, \tag{4.365}$$

where

$$\underbrace{\begin{bmatrix} \mathbf{m}_{p_f, p_f}^{\mathcal{H}^{\text{stab}, e}} \end{bmatrix}}_{n_{\text{dof}}^{p_f, e} \times n_{\text{dof}}^{p_f, e}} = \int_{-1}^1 \alpha^{\text{stab}} (F_{11}^{h^e})^{-1} \underbrace{\left\{ \mathbf{B}^{e, p_f} \right\}^T}_{n_{\text{dof}}^{p_f, e} \times 1} \underbrace{\left\{ \mathbf{B}^{e, p_f} \right\}}_{1 \times n_{\text{dof}}^{p_f, e}} A_j^e d\xi. \quad (4.366)$$

Then, returning our attention to Equation (4.348), we have

$$\underbrace{\begin{Bmatrix} \mathbf{z} \end{Bmatrix}}_{\substack{(2 \times n_{\text{dof}}^s \\ + 2 \times n_{\text{dof}}^f \\ + n_{\text{dof}}^{p_f}) \times 1}} = \left\{ \begin{array}{l} \underbrace{\begin{Bmatrix} \mathbf{d} \end{Bmatrix}}_{n_{\text{dof}}^s \times 1} \\ \underbrace{\left[\mathbf{M}_{u, u}^{\mathcal{G}^{\text{INT}}} \right]^{-1}}_{n_{\text{dof}}^s \times n_{\text{dof}}^s} \cdot \left(- \underbrace{\left\{ \mathbf{F}^{\mathcal{G}_1^{\text{INT}}} \right\}}_{n_{\text{dof}}^s \times 1} - \underbrace{\left\{ \mathbf{F}^{\mathcal{G}_2^{\text{INT}}} \right\}}_{n_{\text{dof}}^s \times 1} - \underbrace{\left\{ \mathbf{F}^{\mathcal{G}_3^{\text{INT}}} \right\}}_{n_{\text{dof}}^s \times 1} - \underbrace{\left\{ \mathbf{F}^{\mathcal{G}_4^{\text{INT}}} \right\}}_{n_{\text{dof}}^s \times 1} - \underbrace{\left\{ \mathbf{F}^{\mathcal{G}_5^{\text{INT}}} \right\}}_{n_{\text{dof}}^s \times 1} + \underbrace{\left\{ \mathbf{F}^{\mathcal{G}^{\text{EXT}}} \right\}}_{n_{\text{dof}}^s \times 1} \right) \\ \underbrace{\begin{Bmatrix} \mathbf{d}_f \end{Bmatrix}}_{n_{\text{dof}}^f \times 1} \\ \underbrace{\left[\mathbf{M}_{u_f, u_f}^{\mathcal{I}^{\text{INT}}} \right]^{-1}}_{n_{\text{dof}}^f \times n_{\text{dof}}^f} \cdot \left(- \underbrace{\left\{ \mathbf{F}^{\mathcal{I}_2^{\text{INT}}} \right\}}_{n_{\text{dof}}^f \times 1} - \underbrace{\left\{ \mathbf{F}^{\mathcal{I}_3^{\text{INT}}} \right\}}_{n_{\text{dof}}^f \times 1} - \underbrace{\left\{ \mathbf{F}^{\mathcal{I}_4^{\text{INT}}} \right\}}_{n_{\text{dof}}^f \times 1} - \underbrace{\left\{ \mathbf{F}^{\mathcal{I}_5^{\text{INT}}} \right\}}_{n_{\text{dof}}^f \times 1} \right) \\ \underbrace{\left[\mathbf{M}_{p_f, p_f}^{\mathcal{H}^{\text{INT}}} \right]^{-1}}_{n_{\text{dof}}^{p_f} \times n_{\text{dof}}^{p_f}} \cdot \left(- \underbrace{\left\{ \mathbf{F}^{\mathcal{H}_1^{\text{INT}}} \right\}}_{n_{\text{dof}}^{p_f} \times 1} - \underbrace{\left\{ \mathbf{F}^{\mathcal{H}_2^{\text{INT}}} \right\}}_{n_{\text{dof}}^{p_f} \times 1} - \underbrace{\left\{ \mathbf{F}^{\mathcal{H}_3^{\text{INT}}} \right\}}_{n_{\text{dof}}^{p_f} \times 1} - \underbrace{\left\{ \mathbf{F}^{\mathcal{H}_4^{\text{INT}}} \right\}}_{n_{\text{dof}}^{p_f} \times 1} - \underbrace{\left\{ \mathbf{F}^{\mathcal{H}_5^{\text{INT}}} \right\}}_{n_{\text{dof}}^{p_f} \times 1} + \underbrace{\left\{ \mathbf{F}^{\mathcal{H}^{\text{EXT}}} \right\}}_{n_{\text{dof}}^{p_f} \times 1} \right) \end{array} \right\} \quad (4.367)$$

where

$$\begin{aligned}
\underbrace{\begin{bmatrix} M_{u,u}^{\mathcal{G}^{\text{INT}}} \end{bmatrix}}_{n_{\text{dof}}^s \times n_{\text{dof}}^s} &= \mathbf{A}_e^{n_e} \underbrace{\begin{bmatrix} \mathbf{m}_{u,u}^{\mathcal{G}^{\text{INT}},e} \end{bmatrix}}_{n_{\text{dof}}^{s,e} \times n_{\text{dof}}^{s,e}}, & \underbrace{\{ \mathbf{F}^{\mathcal{G}^{\text{INT}}} \}}_{n_{\text{dof}}^s \times 1} &= \mathbf{A}_e^{n_e} \underbrace{\{ \mathbf{f}^{\mathcal{G}^{\text{INT}},e} \}}_{n_{\text{dof}}^{s,e} \times 1}, \\
\underbrace{\{ \mathbf{F}^{\mathcal{G}_2^{\text{INT}}} \}}_{n_{\text{dof}}^s \times 1} &= \mathbf{A}_e^{n_e} \underbrace{\{ \mathbf{f}^{\mathcal{G}_2^{\text{INT}},e} \}}_{n_{\text{dof}}^{s,e} \times 1}, & \underbrace{\{ \mathbf{F}^{\mathcal{G}_3^{\text{INT}}} \}}_{n_{\text{dof}}^s \times 1} &= \mathbf{A}_e^{n_e} \underbrace{\{ \mathbf{f}^{\mathcal{G}_3^{\text{INT}},e} \}}_{n_{\text{dof}}^{s,e} \times 1}, \\
\underbrace{\{ \mathbf{F}^{\mathcal{G}_4^{\text{INT}}} \}}_{n_{\text{dof}}^s \times 1} &= \mathbf{A}_e^{n_e} \underbrace{\{ \mathbf{f}^{\mathcal{G}_4^{\text{INT}},e} \}}_{n_{\text{dof}}^{s,e} \times 1}, & \underbrace{\{ \mathbf{F}^{\mathcal{G}_5^{\text{INT}}} \}}_{n_{\text{dof}}^s \times 1} &= \mathbf{A}_e^{n_e} \underbrace{\{ \mathbf{f}^{\mathcal{G}_5^{\text{INT}},e} \}}_{n_{\text{dof}}^{s,e} \times 1}, \\
\underbrace{\{ \mathbf{F}^{\mathcal{G}^{\text{EXT}}} \}}_{n_{\text{dof}}^s \times 1} &= \mathbf{A}_e^{n_e} \underbrace{\{ \mathbf{f}^{\mathcal{G}^{\text{EXT}},e} \}}_{n_{\text{dof}}^{s,e} \times 1}, & \underbrace{\begin{bmatrix} M_{u_f, u_f}^{\mathcal{I}^{\text{INT}}} \end{bmatrix}}_{n_{\text{dof}}^f \times n_{\text{dof}}^f} &= \mathbf{A}_e^{n_e} \underbrace{\begin{bmatrix} \mathbf{m}_{u_f, u_f}^{\mathcal{I}^{\text{INT}},e} \end{bmatrix}}_{n_{\text{dof}}^{f,e} \times n_{\text{dof}}^{f,e}}, \\
\underbrace{\{ \mathbf{F}^{\mathcal{I}_2^{\text{INT}}} \}}_{n_{\text{dof}}^f \times 1} &= \mathbf{A}_e^{n_e} \underbrace{\{ \mathbf{f}^{\mathcal{I}_2^{\text{INT}},e} \}}_{n_{\text{dof}}^{f,e} \times 1}, & \underbrace{\{ \mathbf{F}^{\mathcal{I}_3^{\text{INT}}} \}}_{n_{\text{dof}}^f \times 1} &= \mathbf{A}_e^{n_e} \underbrace{\{ \mathbf{f}^{\mathcal{I}_3^{\text{INT}},e} \}}_{n_{\text{dof}}^{f,e} \times 1}, \\
\underbrace{\{ \mathbf{F}^{\mathcal{I}_4^{\text{INT}}} \}}_{n_{\text{dof}}^f \times 1} &= \mathbf{A}_e^{n_e} \underbrace{\{ \mathbf{f}^{\mathcal{I}_4^{\text{INT}},e} \}}_{n_{\text{dof}}^{f,e} \times 1}, & \underbrace{\{ \mathbf{F}^{\mathcal{I}_5^{\text{INT}}} \}}_{n_{\text{dof}}^f \times 1} &= \mathbf{A}_e^{n_e} \underbrace{\{ \mathbf{f}^{\mathcal{I}_5^{\text{INT}},e} \}}_{n_{\text{dof}}^{f,e} \times 1}, \\
\underbrace{\begin{bmatrix} M_{p_f, p_f}^{\mathcal{H}^{\text{INT}}} \end{bmatrix}}_{n_{\text{dof}}^{p_f} \times n_{\text{dof}}^{p_f}} &= \mathbf{A}_e^{n_e} \underbrace{\begin{bmatrix} \mathbf{m}_{p_f, p_f}^{\mathcal{H}^{\text{INT}},e} \end{bmatrix}}_{n_{\text{dof}}^{p_f,e} \times n_{\text{dof}}^{p_f,e}}, & \underbrace{\{ \mathbf{F}^{\mathcal{H}_1^{\text{INT}}} \}}_{n_{\text{dof}}^{p_f} \times 1} &= \mathbf{A}_e^{n_e} \underbrace{\{ \mathbf{f}^{\mathcal{H}_1^{\text{INT}},e} \}}_{n_{\text{dof}}^{p_f,e} \times 1}, \\
\underbrace{\{ \mathbf{F}^{\mathcal{H}_2^{\text{INT}}} \}}_{n_{\text{dof}}^{p_f} \times 1} &= \mathbf{A}_e^{n_e} \underbrace{\{ \mathbf{f}^{\mathcal{H}_2^{\text{INT}},e} \}}_{n_{\text{dof}}^{p_f,e} \times 1}, & \underbrace{\{ \mathbf{F}^{\mathcal{H}_3^{\text{INT}}} \}}_{n_{\text{dof}}^{p_f} \times 1} &= \mathbf{A}_e^{n_e} \underbrace{\{ \mathbf{f}^{\mathcal{H}_3^{\text{INT}},e} \}}_{n_{\text{dof}}^{p_f,e} \times 1}, \\
\underbrace{\{ \mathbf{F}^{\mathcal{H}_4^{\text{INT}}} \}}_{n_{\text{dof}}^{p_f} \times 1} &= \mathbf{A}_e^{n_e} \underbrace{\{ \mathbf{f}^{\mathcal{H}_4^{\text{INT}},e} \}}_{n_{\text{dof}}^{p_f,e} \times 1}, & \underbrace{\{ \mathbf{F}^{\mathcal{H}_5^{\text{INT}}} \}}_{n_{\text{dof}}^{p_f} \times 1} &= \mathbf{A}_e^{n_e} \underbrace{\{ \mathbf{f}^{\mathcal{H}_5^{\text{INT}},e} \}}_{n_{\text{dof}}^{p_f,e} \times 1}, \\
\underbrace{\{ \mathbf{F}^{\mathcal{H}^{\text{EXT}}} \}}_{n_{\text{dof}}^{p_f} \times 1} &= \mathbf{A}_e^{n_e} \underbrace{\{ \mathbf{f}^{\mathcal{H}^{\text{EXT}},e} \}}_{n_{\text{dof}}^{p_f,e} \times 1}.
\end{aligned} \tag{4.368}$$

If pressure stabilization is enabled, refer to the addition given by Equation (4.344) and insert into Equation (4.367) as necessary. This was done in Equation (4.343).

As described in Section 4.3.1, Equation (4.367) is solved for each stage increment i at time $t_n + \Delta t c_i$ (i.e., any variables that are *explicit* functions of time, such as a time-dependent external

traction, are to be evaluated at time $t_n + \Delta t c_i$, with stage solution \mathbf{k}_i given by

$$\underbrace{\left\{ \mathbf{k}_i \right\}}_{(2 \times n_{\text{dof}}^s + 2 \times n_{\text{dof}}^f + n_{\text{dof}}^{p_f}) \times 1} := \underbrace{\left\{ \begin{array}{l} \underbrace{\left\{ \mathbf{k}_{i(v)} \right\}}_{n_{\text{dof}}^s \times 1} \\ \underbrace{\left\{ \mathbf{k}_{i(a)} \right\}}_{n_{\text{dof}}^s \times 1} \\ \underbrace{\left\{ \mathbf{k}_{i(v_f)} \right\}}_{n_{\text{dof}}^f \times 1} \\ \underbrace{\left\{ \mathbf{k}_{i(a_f)} \right\}}_{n_{\text{dof}}^f \times 1} \\ \underbrace{\left\{ \mathbf{k}_{i(p_f)} \right\}}_{n_{\text{dof}}^{p_f} \times 1} \end{array} \right\}} = \underbrace{\left\{ \begin{array}{l} \underbrace{\left\{ \mathbf{z}_v(t_n) \right\}}_{n_{\text{dof}}^s \times 1} + \Delta t \sum_{j=1}^{i-1} a_{ij} \underbrace{\left\{ \mathbf{k}_{j(v)} \right\}}_{n_{\text{dof}}^s \times 1} \\ \underbrace{\left\{ \mathbf{z}_a(t_n) \right\}}_{n_{\text{dof}}^s \times 1} + \Delta t \sum_{j=1}^{i-1} a_{ij} \underbrace{\left\{ \mathbf{k}_{j(a)} \right\}}_{n_{\text{dof}}^s \times 1} \\ \underbrace{\left\{ \mathbf{z}_{v_f}(t_n) \right\}}_{n_{\text{dof}}^f \times 1} + \Delta t \sum_{j=1}^{i-1} a_{ij} \underbrace{\left\{ \mathbf{k}_{j(v_f)} \right\}}_{n_{\text{dof}}^f \times 1} \\ \underbrace{\left\{ \mathbf{z}_{a_f}(t_n) \right\}}_{n_{\text{dof}}^f \times 1} + \Delta t \sum_{j=1}^{i-1} a_{ij} \underbrace{\left\{ \mathbf{k}_{j(a_f)} \right\}}_{n_{\text{dof}}^f \times 1} \\ \underbrace{\left\{ \mathbf{z}_{p_f}(t_n) \right\}}_{n_{\text{dof}}^{p_f} \times 1} + \Delta t \sum_{j=1}^{i-1} a_{ij} \underbrace{\left\{ \mathbf{k}_{j(p_f)} \right\}}_{n_{\text{dof}}^{p_f} \times 1} \end{array} \right\}} \quad (4.369)$$

Then, according to Equation (4.293), the higher order solution to be accepted or rejected at time t_{n+1} is given by

$$\underbrace{\left\{ \mathbf{z}^m(t_{n+1}) \right\}}_{(2 \times n_{\text{dof}}^s + 2 \times n_{\text{dof}}^f + n_{\text{dof}}^{p_f}) \times 1} := \underbrace{\left\{ \begin{array}{l} \underbrace{\left\{ \mathbf{z}_u^m(t_{n+1}) \right\}}_{n_{\text{dof}}^s \times 1} \\ \underbrace{\left\{ \mathbf{z}_v^m(t_{n+1}) \right\}}_{n_{\text{dof}}^s \times 1} \\ \underbrace{\left\{ \mathbf{z}_{u_f}^m(t_{n+1}) \right\}}_{n_{\text{dof}}^f \times 1} \\ \underbrace{\left\{ \mathbf{z}_{v_f}^m(t_{n+1}) \right\}}_{n_{\text{dof}}^f \times 1} \\ \underbrace{\left\{ \mathbf{z}_{p_f}^m(t_{n+1}) \right\}}_{n_{\text{dof}}^{p_f} \times 1} \end{array} \right\}} = \underbrace{\left\{ \begin{array}{l} \underbrace{\left\{ \mathbf{z}_u(t_n) \right\}}_{n_{\text{dof}}^s \times 1} + \Delta t \sum_{i=1}^{m+1} b_i^m \underbrace{\left\{ \mathbf{k}_{i(v)} \right\}}_{n_{\text{dof}}^s \times 1} \\ \underbrace{\left\{ \mathbf{z}_v(t_n) \right\}}_{n_{\text{dof}}^s \times 1} + \Delta t \sum_{i=1}^{m+1} b_i^m \underbrace{\left\{ \mathbf{k}_{i(a)} \right\}}_{n_{\text{dof}}^s \times 1} \\ \underbrace{\left\{ \mathbf{z}_{u_f}(t_n) \right\}}_{n_{\text{dof}}^f \times 1} + \Delta t \sum_{i=1}^{m+1} b_i^m \underbrace{\left\{ \mathbf{k}_{i(v_f)} \right\}}_{n_{\text{dof}}^f \times 1} \\ \underbrace{\left\{ \mathbf{z}_{v_f}(t_n) \right\}}_{n_{\text{dof}}^f \times 1} + \Delta t \sum_{i=1}^{m+1} b_i^m \underbrace{\left\{ \mathbf{k}_{i(a_f)} \right\}}_{n_{\text{dof}}^f \times 1} \\ \underbrace{\left\{ \mathbf{z}_{p_f}(t_n) \right\}}_{n_{\text{dof}}^{p_f} \times 1} + \Delta t \sum_{i=1}^{m+1} b_i^m \underbrace{\left\{ \mathbf{k}_{i(p_f)} \right\}}_{n_{\text{dof}}^{p_f} \times 1} \end{array} \right\}} \quad (4.370)$$

and, according to Equation (4.294), the lower order solution at time t_{n+1} is given by

$$\underbrace{\left\{ \mathbf{z}^{m-1}(t_{n+1}) \right\}}_{(2 \times n_{\text{dof}}^s + 2 \times n_{\text{dof}}^f + n_{\text{dof}}^{p_f}) \times 1} := \left\{ \begin{array}{c} \underbrace{\left\{ \mathbf{z}_u^{m-1}(t_{n+1}) \right\}}_{n_{\text{dof}}^s \times 1} \\ \underbrace{\left\{ \mathbf{z}_v^{m-1}(t_{n+1}) \right\}}_{n_{\text{dof}}^s \times 1} \\ \underbrace{\left\{ \mathbf{z}_{u_f}^{m-1}(t_{n+1}) \right\}}_{n_{\text{dof}}^f \times 1} \\ \underbrace{\left\{ \mathbf{z}_{v_f}^{m-1}(t_{n+1}) \right\}}_{n_{\text{dof}}^f \times 1} \\ \underbrace{\left\{ \mathbf{z}_{p_f}^{m-1}(t_{n+1}) \right\}}_{n_{\text{dof}}^{p_f} \times 1} \end{array} \right\} = \left\{ \begin{array}{c} \underbrace{\left\{ \mathbf{z}_u(t_n) \right\}}_{n_{\text{dof}}^s \times 1} + \Delta t \sum_{i=1}^m b_i^{m-1} \underbrace{\left\{ \mathbf{k}_{i(v)} \right\}}_{n_{\text{dof}}^s \times 1} \\ \underbrace{\left\{ \mathbf{z}_v(t_n) \right\}}_{n_{\text{dof}}^s \times 1} + \Delta t \sum_{i=1}^m b_i^{m-1} \underbrace{\left\{ \mathbf{k}_{i(a)} \right\}}_{n_{\text{dof}}^s \times 1} \\ \underbrace{\left\{ \mathbf{z}_{u_f}(t_n) \right\}}_{n_{\text{dof}}^f \times 1} + \Delta t \sum_{i=1}^m b_i^{m-1} \underbrace{\left\{ \mathbf{k}_{i(v_f)} \right\}}_{n_{\text{dof}}^f \times 1} \\ \underbrace{\left\{ \mathbf{z}_{v_f}(t_n) \right\}}_{n_{\text{dof}}^f \times 1} + \Delta t \sum_{i=1}^m b_i^{m-1} \underbrace{\left\{ \mathbf{k}_{i(a_f)} \right\}}_{n_{\text{dof}}^f \times 1} \\ \underbrace{\left\{ \mathbf{z}_{p_f}(t_n) \right\}}_{n_{\text{dof}}^{p_f} \times 1} + \Delta t \sum_{i=1}^m b_i^{m-1} \underbrace{\left\{ \mathbf{k}_{i(p_f)} \right\}}_{n_{\text{dof}}^{p_f} \times 1} \end{array} \right\} \quad (4.371)$$

4.3.1.5 $(\mathbf{u}-p_f-\theta^s-\theta^f)$ formulation

For the $(\mathbf{u}-p_f-\theta^s-\theta^f)$ formulation, the Runge-Kutta integrators transform the general solution variables given by Equation (4.291) to

$$\left\{ \dot{\mathbf{z}} \right\} := \left\{ \begin{array}{c} \dot{\mathbf{z}}_u \\ \dot{\mathbf{z}}_v \\ \dot{\mathbf{z}}_{p_f} \\ \dot{\mathbf{z}}_{\theta^s} \\ \dot{\mathbf{z}}_{\theta^f} \end{array} \right\} = \left\{ \mathbf{f}(t, \mathbf{z}) \right\} = \left\{ \begin{array}{c} \mathbf{f}_v(t, \mathbf{z}) \\ \mathbf{f}_a(t, \mathbf{z}) \\ \mathbf{f}_{p_f}(t, \mathbf{z}) \\ \mathbf{f}_{\theta^s}(t, \mathbf{z}) \\ \mathbf{f}_{\theta^f}(t, \mathbf{z}) \end{array} \right\}, \quad (4.372)$$

such that

$$\left\{ \mathbf{z} \right\} = \left\{ \begin{array}{c} \mathbf{d} \\ \dot{\mathbf{d}} \\ \boldsymbol{\pi} \\ \boldsymbol{\vartheta}^s \\ \boldsymbol{\vartheta}^f \end{array} \right\}, \quad \dot{\mathbf{z}} = \left\{ \begin{array}{c} \dot{\mathbf{d}} \\ \ddot{\mathbf{d}} \\ \dot{\boldsymbol{\pi}} \\ \dot{\boldsymbol{\vartheta}}^s \\ \dot{\boldsymbol{\vartheta}}^f \end{array} \right\}. \quad (4.373)$$

Thus, we require at least one governing equation to solve for the primary unknown $\ddot{\mathbf{d}}$, which when integrated once gives us $\dot{\mathbf{d}}$, and when integrated twice gives us \mathbf{d} ; and at least one governing equation to solve for the primary unknown $\dot{\boldsymbol{\pi}}$, which when integrated once gives us $\boldsymbol{\pi}$; at least one governing equation to solve for the primary unknown $\dot{\boldsymbol{\vartheta}}^s$, which when integrated once gives us $\boldsymbol{\vartheta}^s$; and at least one governing equation to solve for the primary unknown $\dot{\boldsymbol{\vartheta}}^f$, which when integrated gives us $\boldsymbol{\vartheta}^f$.

The FE formulation for the balance of momentum of the mixture, with variational equation given by Equation (4.173), is written in block-matrix form as

$$\underbrace{\{\mathbf{R}_u\}}_{n_{\text{dof}}^s \times 1} = \mathbf{0}, \quad (4.374)$$

where the global residual for the solid skeleton displacement is given as

$$\mathbf{c}^{u,T} \cdot \mathbf{R}_u = \mathcal{G}^h = \mathcal{G}_1^{\text{INT},h} + \mathcal{G}_2^{\text{INT},h} + \mathcal{G}_3^{\text{INT},h} + \mathcal{G}_4^{\text{INT},h} - \mathcal{G}^{\text{EXT},h} = 0. \quad (4.375)$$

Therein,

$$\begin{aligned} \mathcal{G}_1^{\text{INT},h} &= \mathbf{A}_e^{n_e} \underbrace{\{\mathbf{c}^{u,e}\}^T}_{1 \times n_{\text{dof}}^{s,e}} \cdot \underbrace{\left[\mathbf{m}_{u,u}^{\mathcal{G}_1^{\text{INT},e}} \right]}_{n_{\text{dof}}^{s,e} \times n_{\text{dof}}^{s,e}} \cdot \underbrace{\{\ddot{\mathbf{d}}^e\}}_{n_{\text{dof}}^{s,e} \times 1}, & \mathcal{G}_2^{\text{INT},h} &= \mathbf{A}_e^{n_e} \underbrace{\{\mathbf{c}^{u,e}\}^T}_{1 \times n_{\text{dof}}^{s,e}} \cdot \underbrace{\{\mathbf{f}^{\mathcal{G}_2^{\text{INT},e}}\}}_{n_{\text{dof}}^{s,e} \times 1}, \\ \mathcal{G}_3^{\text{INT},h} &= \mathbf{A}_e^{n_e} \underbrace{\{\mathbf{c}^{u,e}\}^T}_{1 \times n_{\text{dof}}^{s,e}} \cdot \underbrace{\{\mathbf{f}^{\mathcal{G}_3^{\text{INT},e}}\}}_{n_{\text{dof}}^{s,e} \times 1}, & \mathcal{G}_4^{\text{INT},h} &= \mathbf{A}_e^{n_e} \underbrace{\{\mathbf{c}^{u,e}\}^T}_{1 \times n_{\text{dof}}^{s,e}} \cdot \underbrace{\{\mathbf{f}^{\mathcal{G}_4^{\text{INT},e}}\}}_{n_{\text{dof}}^{s,e} \times 1}, \\ \mathcal{G}^{\text{EXT},h} &= \mathbf{A}_e^{n_e} \underbrace{\{\mathbf{c}^{u,e}\}^T}_{1 \times n_{\text{dof}}^{s,e}} \cdot \underbrace{\{\mathbf{f}^{\mathcal{G}^{\text{EXT},e}}\}}_{n_{\text{dof}}^{s,e} \times 1}, \end{aligned} \quad (4.376)$$

where

$$\begin{aligned}
\underbrace{\left\{ \mathbf{f}^{\mathcal{G}_2^{\text{INT},e}} \right\}}_{n_{\text{dof}}^{s,e} \times 1} &= \int_{-1}^1 \underbrace{\left\{ \mathbf{B}^{e,u} \right\}}_{n_{\text{dof}}^{s,e} \times 1}^T P_{11(E)}^{s,h^e} A_j^e d\xi, \\
\underbrace{\left\{ \mathbf{f}^{\mathcal{G}_3^{\text{INT},e}} \right\}}_{n_{\text{dof}}^{s,e} \times 1} &= - \int_{-1}^1 \underbrace{\left\{ \mathbf{B}^{e,u} \right\}}_{n_{\text{dof}}^{s,e} \times 1}^T p_f^{h^e} \left(\frac{\theta^{s,h^e}}{\theta^{f,h^e}} n^{s,h^e} + n^{f,h^e} \right) A_j^e d\xi, \\
\underbrace{\left\{ \mathbf{f}^{\mathcal{G}_4^{\text{INT},e}} \right\}}_{n_{\text{dof}}^{s,e} \times 1} &= \int_{-1}^1 \underbrace{\left\{ \mathbf{N}^{e,u} \right\}}_{n_{\text{dof}}^{s,e} \times 1}^T \rho_0^{h^e} g A_j^e d\xi, \\
\underbrace{\left\{ \mathbf{f}^{\mathcal{G}^{\text{EXT},e}} \right\}}_{n_{\text{dof}}^{s,e} \times 1} &= \begin{cases} \underbrace{\left\{ \mathbf{N}^{e,u}(X=0, H) \right\}}_{n_{\text{dof}}^{s,e} \times 1}^T t^\sigma A & X=0, H \\ \mathbf{0} & 0 < X < H. \end{cases}
\end{aligned} \tag{4.377}$$

The mass matrix associated with the solid skeleton acceleration is given by

$$\underbrace{\left[\mathbf{m}_{u,u}^{\mathcal{G}_1^{\text{INT},e}} \right]}_{n_{\text{dof}}^{s,e} \times n_{\text{dof}}^{s,e}} = \int_{-1}^1 \rho_0^{h^e} \underbrace{\left\{ \mathbf{N}^{e,u} \right\}}_{n_{\text{dof}}^{s,e} \times 1}^T \underbrace{\left\{ \mathbf{N}^{e,u} \right\}}_{1 \times n_{\text{dof}}^{s,e}} A_j^e d\xi. \tag{4.378}$$

The FE formulation for the balance of mass of the mixture, with variational equation given by Equation (4.174), is written in block-matrix form as

$$\underbrace{\left\{ \mathbf{R}_{p_f} \right\}}_{n_{\text{dof}}^{p_f} \times 1} = \mathbf{0}, \tag{4.379}$$

where the global residual for the pore fluid pressure is given as

$$\mathbf{c}^{p_f, T} \cdot \mathbf{R}_{p_f} = \mathcal{H}^h = \mathcal{H}_1^{\text{INT},h} + \mathcal{H}_2^{\text{INT},h} + \mathcal{H}_3^{\text{INT},h} + \mathcal{H}_4^{\text{INT},h} + \mathcal{H}_6^{\text{INT},h} + \mathcal{H}_7^{\text{INT},h} - \mathcal{H}^{\text{EXT},h} = 0. \tag{4.380}$$

Therein,

$$\begin{aligned}
\mathcal{H}_1^{\text{INT},h} &= \mathbf{A}_e \underbrace{\left\{ \mathbf{c}^{p_f,e} \right\}^T}_{1 \times n_{\text{dof}}^{p_f,e}} \cdot \left(\underbrace{\left[\mathbf{m}_{p_f,p_f}^{\mathcal{H}_1^{\text{INT},e}} \right]}_{n_{\text{dof}}^{p_f,e} \times n_{\text{dof}}^{p_f,e}} \cdot \underbrace{\left\{ \dot{\boldsymbol{\pi}}^e \right\}}_{n_{\text{dof}}^{p_f,e} \times 1} + \underbrace{\left\{ \mathbf{f}^{\mathcal{H}_1^{\text{INT},e}} \right\}}_{n_{\text{dof}}^{p_f,e} \times 1} \right), \\
\mathcal{H}_2^{\text{INT},h} &= \mathbf{A}_e \underbrace{\left\{ \mathbf{c}^{p_f,e} \right\}^T}_{1 \times n_{\text{dof}}^{p_f,e}} \cdot \underbrace{\left\{ \mathbf{f}^{\mathcal{H}_2^{\text{INT},e}} \right\}}_{n_{\text{dof}}^{p_f,e} \times 1}, \quad \mathcal{H}_3^{\text{INT},h} = \mathbf{A}_e \underbrace{\left\{ \mathbf{c}^{p_f,e} \right\}^T}_{1 \times n_{\text{dof}}^{p_f,e}} \cdot \underbrace{\left\{ \mathbf{f}^{\mathcal{H}_3^{\text{INT},e}} \right\}}_{n_{\text{dof}}^{p_f,e} \times 1}, \\
\mathcal{H}_4^{\text{INT},h} &= \mathbf{A}_e \underbrace{\left\{ \mathbf{c}^{p_f,e} \right\}^T}_{1 \times n_{\text{dof}}^{p_f,e}} \cdot \underbrace{\left\{ \mathbf{f}^{\mathcal{H}_4^{\text{INT},e}} \right\}}_{n_{\text{dof}}^{p_f,e} \times 1}, \quad \mathcal{H}_6^{\text{INT},h} = \mathbf{A}_e \underbrace{\left\{ \mathbf{c}^{p_f,e} \right\}^T}_{1 \times n_{\text{dof}}^{p_f,e}} \cdot \underbrace{\left\{ \mathbf{f}^{\mathcal{H}_6^{\text{INT},e}} \right\}}_{n_{\text{dof}}^{p_f,e} \times 1}, \\
\mathcal{H}_7^{\text{INT},h} &= \mathbf{A}_e \underbrace{\left\{ \mathbf{c}^{p_f,e} \right\}^T}_{1 \times n_{\text{dof}}^{p_f,e}} \cdot \underbrace{\left\{ \mathbf{f}^{\mathcal{H}_7^{\text{INT},e}} \right\}}_{n_{\text{dof}}^{p_f,e} \times 1}, \quad \mathcal{H}^{\text{EXT},h} = \mathbf{A}_e \underbrace{\left\{ \mathbf{c}^{p_f,e} \right\}^T}_{1 \times n_{\text{dof}}^{p_f,e}} \cdot \underbrace{\left\{ \mathbf{f}^{\mathcal{H}^{\text{EXT},e}} \right\}}_{n_{\text{dof}}^{p_f,e} \times 1},
\end{aligned} \tag{4.381}$$

where

$$\begin{aligned}
\underbrace{\left\{ \mathbf{f}^{\mathcal{H}_1^{\text{INT},e}} \right\}}_{n_{\text{dof}}^{p_f,e} \times 1} &= \int_{-1}^1 \underbrace{\left\{ \mathbf{N}^{e,p_f} \right\}^T}_{n_{\text{dof}}^{p_f,e} \times 1} \mathbf{j}^{h^e} A_j^e d\xi, \\
\underbrace{\left\{ \mathbf{f}^{\mathcal{H}_2^{\text{INT},e}} \right\}}_{n_{\text{dof}}^{p_f,e} \times 1} &= \int_{-1}^1 \underbrace{\left\{ \mathbf{N}^{e,p_f} \right\}^T}_{n_{\text{dof}}^{p_f,e} \times 1} \frac{1}{p_f} \frac{\partial p_f^{h^e}}{\partial X} (n^f \tilde{v}_f)^{h^e} A_j^e d\xi, \\
\underbrace{\left\{ \mathbf{f}^{\mathcal{H}_3^{\text{INT},e}} \right\}}_{n_{\text{dof}}^{p_f,e} \times 1} &= \int_{-1}^1 \underbrace{\left\{ \mathbf{B}^{e,p_f} \right\}^T}_{n_{\text{dof}}^{p_f,e} \times 1} \hat{k}^{h^e} \frac{\partial p_f^{h^e}}{\partial X} (F_{11}^{h^e})^{-1} A_j^e d\xi, \\
\underbrace{\left\{ \mathbf{f}^{\mathcal{H}_4^{\text{INT},e}} \right\}}_{n_{\text{dof}}^{p_f,e} \times 1} &= \int_{-1}^1 \underbrace{\left\{ \mathbf{B}^{e,p_f} \right\}^T}_{n_{\text{dof}}^{p_f,e} \times 1} \hat{k}^{h^e} \rho^{\text{fR},h^e} (a^{h^e} + g) A_j^e d\xi, \\
\underbrace{\left\{ \mathbf{f}^{\mathcal{H}_6^{\text{INT},e}} \right\}}_{n_{\text{dof}}^{p_f,e} \times 1} &= \int_{-1}^1 \underbrace{\left\{ \mathbf{B}^{e,p_f} \right\}^T}_{n_{\text{dof}}^{p_f,e} \times 1} \frac{\hat{k}^{h^e}}{n^{f,h^e} p_f^{h^e}} \frac{\partial n^{f,h^e}}{\partial X} (F_{11}^{h^e})^{-1} \left(1 - \frac{\theta^{s,h^e}}{\theta^{f,h^e}} \right) A_j^e d\xi, \\
\underbrace{\left\{ \mathbf{f}^{\mathcal{H}_7^{\text{INT},e}} \right\}}_{n_{\text{dof}}^{p_f,e} \times 1} &= - \int_{-1}^1 \underbrace{\left\{ \mathbf{B}^{e,p_f} \right\}^T}_{n_{\text{dof}}^{p_f,e} \times 1} \frac{1}{\theta^{f,h^e}} \left(J^{h^e} n^{f,h^e} \dot{\theta}^{f,h^e} + \frac{\partial \theta^{f,h^e}}{\partial X} (n^f \tilde{v}_f)^{h^e} \right) A_j^e d\xi, \\
\underbrace{\left\{ \mathbf{f}^{\mathcal{H}^{\text{EXT},e}} \right\}}_{n_{\text{dof}}^{p_f,e} \times 1} &= \begin{cases} \underbrace{\left\{ \mathbf{N}^{e,p_f}(X=0, H) \right\}^T}_{n_{\text{dof}}^{p_f,e} \times 1} Q_f A & X=0, H \\ \mathbf{0} & 0 < X < H. \end{cases}
\end{aligned} \tag{4.382}$$

The mass matrix associated with the pore fluid pressure is given by

$$\underbrace{\left[\mathbf{m}_{p_f,p_f}^{\mathcal{H}_1^{\text{INT},e}} \right]}_{n_{\text{dof}}^{p_f,e} \times n_{\text{dof}}^{p_f,e}} = \int_{-1}^1 \frac{J^{h^e} n^{f,h^e}}{p_f^{h^e}} \underbrace{\left\{ \mathbf{N}^{e,p_f} \right\}^T}_{n_{\text{dof}}^{p_f,e} \times 1} \underbrace{\left\{ \mathbf{N}^{e,p_f} \right\}}_{1 \times n_{\text{dof}}^{p_f,e}} A_j^e d\xi. \tag{4.383}$$

For the compressible liquid pore fluid model (Equation (3.153), Equation (4.198)),

$$\begin{aligned} \underbrace{\left\{ \mathbf{f}^{\mathcal{H}_7^{\text{INT},e}} \right\}}_{n_{\text{dof}}^{p_f,e} \times 1} &= - \int_{-1}^1 \underbrace{\left\{ \mathbf{B}^{e,p_f} \right\}}_{n_{\text{dof}}^{p_f,e} \times 1}^T \alpha_V^f \left(J^{h^e} n^{f,h^e} \dot{\theta}^{f,h^e} + \frac{\partial \theta^{f,h^e}}{\partial X} (n^f \tilde{v}_f)^{h^e} \right) A_j^e d\xi, \\ \underbrace{\left[\mathbf{m}_{p_f,p_f}^{\mathcal{H}_1^{\text{INT},e}} \right]}_{n_{\text{dof}}^{p_f,e} \times n_{\text{dof}}^{p_f,e}} &= \int_{-1}^1 \frac{J^{h^e} n^{f,h^e}}{K_f^\theta} \underbrace{\left\{ \mathbf{N}^{e,p_f} \right\}}_{n_{\text{dof}}^{p_f,e} \times 1}^T \underbrace{\left\{ \mathbf{N}^{e,p_f} \right\}}_{1 \times n_{\text{dof}}^{p_f,e}} A_j^e d\xi. \end{aligned} \quad (4.384)$$

When pressure stabilization is enabled, an additional term $\mathcal{H}^{\text{stab}}$ is added to the l.h.s. of Equation (4.380) and is defined as

$$\mathcal{H}^{\text{stab}} = \mathbf{A}_e^{n_e} \mathbf{c}^{p_f e, T} \cdot \underbrace{\left[\mathbf{m}_{p_f,p_f}^{\mathcal{H}^{\text{stab},e}} \right]}_{n_{\text{dof}}^{p_f,e} \times n_{\text{dof}}^{p_f,e}} \cdot \underbrace{\left\{ \dot{\boldsymbol{\pi}}^e \right\}}_{n_{\text{dof}}^{p_f,e} \times 1}, \quad (4.385)$$

where

$$\underbrace{\left[\mathbf{m}_{p_f,p_f}^{\mathcal{H}^{\text{stab},e}} \right]}_{n_{\text{dof}}^{p_f,e} \times n_{\text{dof}}^{p_f,e}} = \int_{-1}^1 \alpha^{\text{stab}} (F_{11}^{h^e})^{-1} \underbrace{\left\{ \mathbf{B}^{e,p_f} \right\}}_{n_{\text{dof}}^{p_f,e} \times 1}^T \underbrace{\left\{ \mathbf{B}^{e,p_f} \right\}}_{1 \times n_{\text{dof}}^{p_f,e}} A_j^e d\xi. \quad (4.386)$$

The FE formulation for the balance of energy of the solid, with variational equation given by Equation (4.175), is written in block-matrix form as

$$\underbrace{\left\{ \mathbf{R}_{\theta^s} \right\}}_{n_{\text{dof}}^{\theta^s} \times 1} = \mathbf{0}, \quad (4.387)$$

where the global residual for the solid phase temperature is given as

$$\mathbf{c}^{\theta^s, T} \cdot \mathbf{R}_{\theta^f} = \mathcal{J}^h = \mathcal{J}_1^{\text{INT},h} + \mathcal{J}_2^{\text{INT},h} + \mathcal{J}_3^{\text{INT},h} + \mathcal{J}_4^{\text{INT},h} + \mathcal{J}_5^{\text{INT},h} + \mathcal{J}_6^{\text{INT},h} - \mathcal{J}^{\text{EXT},h} = 0. \quad (4.388)$$

Therein,

$$\begin{aligned}
\mathcal{J}_1^{\text{INT},h} &= \mathbf{A}_e^{n_e} \underbrace{\left\{ \mathbf{c}^{\theta^s,e} \right\}^T}_{1 \times n_{\text{dof}}^{\theta^s,e}} \cdot \underbrace{\left[\mathbf{m}_{\theta^s,\theta^s}^{\mathcal{J}_1^{\text{INT},e}} \right]}_{n_{\text{dof}}^{\theta^s,e} \times n_{\text{dof}}^{\theta^s,e}} \cdot \underbrace{\left\{ \dot{\boldsymbol{\vartheta}}^{s,e} \right\}}_{n_{\text{dof}}^{\theta^s,e} \times 1}, & \mathcal{J}_2^{\text{INT},h} &= \mathbf{A}_e^{n_e} \underbrace{\left\{ \mathbf{c}^{\theta^s,e} \right\}^T}_{1 \times n_{\text{dof}}^{\theta^s,e}} \cdot \underbrace{\left\{ \mathbf{f}_{\mathcal{J}_2^{\text{INT},e}}^{\mathcal{J}_2^{\text{INT},e}} \right\}}_{n_{\text{dof}}^{\theta^s,e} \times 1}, \\
\mathcal{J}_3^{\text{INT},h} &= \mathbf{A}_e^{n_e} \underbrace{\left\{ \mathbf{c}^{\theta^s,e} \right\}^T}_{1 \times n_{\text{dof}}^{\theta^s,e}} \cdot \underbrace{\left\{ \mathbf{f}_{\mathcal{J}_3^{\text{INT},e}}^{\mathcal{J}_3^{\text{INT},e}} \right\}}_{n_{\text{dof}}^{\theta^s,e} \times 1}, & \mathcal{J}_4^{\text{INT},h} &= \mathbf{A}_e^{n_e} \underbrace{\left\{ \mathbf{c}^{\theta^s,e} \right\}^T}_{1 \times n_{\text{dof}}^{\theta^s,e}} \cdot \underbrace{\left\{ \mathbf{f}_{\mathcal{J}_4^{\text{INT},e}}^{\mathcal{J}_4^{\text{INT},e}} \right\}}_{n_{\text{dof}}^{\theta^s,e} \times 1}, \\
\mathcal{J}_5^{\text{INT},h} &= \mathbf{A}_e^{n_e} \underbrace{\left\{ \mathbf{c}^{\theta^s,e} \right\}^T}_{1 \times n_{\text{dof}}^{\theta^s,e}} \cdot \underbrace{\left\{ \mathbf{f}_{\mathcal{J}_5^{\text{INT},e}}^{\mathcal{J}_5^{\text{INT},e}} \right\}}_{n_{\text{dof}}^{\theta^s,e} \times 1}, & \mathcal{J}_6^{\text{INT},h} &= \mathbf{A}_e^{n_e} \underbrace{\left\{ \mathbf{c}^{\theta^s,e} \right\}^T}_{1 \times n_{\text{dof}}^{\theta^s,e}} \cdot \underbrace{\left\{ \mathbf{f}_{\mathcal{J}_6^{\text{INT},e}}^{\mathcal{J}_6^{\text{INT},e}} \right\}}_{n_{\text{dof}}^{\theta^s,e} \times 1}, \\
\mathcal{J}^{\text{EXT},h} &= \mathbf{A}_e^{n_e} \underbrace{\left\{ \mathbf{c}^{\theta^s,e} \right\}^T}_{1 \times n_{\text{dof}}^{\theta^s,e}} \cdot \underbrace{\left\{ \mathbf{f}^{\mathcal{J}^{\text{EXT},e}} \right\}}_{n_{\text{dof}}^{\theta^s,e} \times 1},
\end{aligned} \tag{4.389}$$

where

$$\begin{aligned}
\underbrace{\left\{ \mathbf{f}_{\mathcal{J}_2^{\text{INT},e}}^{\mathcal{J}_2^{\text{INT},e}} \right\}}_{n_{\text{dof}}^{\theta^s,e} \times 1} &= \int_{-1}^1 \underbrace{\left\{ \mathbf{N}^{e,\theta^s} \right\}^T}_{n_{\text{dof}}^{\theta^s,e} \times 1} \left(\frac{K^{\text{skel}} \alpha_V^s \theta^{s,h^e}}{J^{h^e}} + n^{s,h^e} p_f^{h^e} \frac{\theta^{s,h^e}}{\theta^{f,h^e}} + Q^{h^e} \right) j^{h^e} A_j^e d\xi, \\
\underbrace{\left\{ \mathbf{f}_{\mathcal{J}_3^{\text{INT},e}}^{\mathcal{J}_3^{\text{INT},e}} \right\}}_{n_{\text{dof}}^{\theta^s,e} \times 1} &= - \int_{-1}^1 \underbrace{\left\{ \mathbf{B}^{e,\theta^s} \right\}^T}_{n_{\text{dof}}^{\theta^s,e} \times 1} q^{s,h^e} A_j^e d\xi, \\
\underbrace{\left\{ \mathbf{f}_{\mathcal{J}_4^{\text{INT},e}}^{\mathcal{J}_4^{\text{INT},e}} \right\}}_{n_{\text{dof}}^{\theta^s,e} \times 1} &= \int_{-1}^1 \underbrace{\left\{ \mathbf{N}^{e,\theta^s} \right\}^T}_{n_{\text{dof}}^{\theta^s,e} \times 1} J^{h^e} k_{\tilde{\theta}}^{\varepsilon} (\theta^{s,h^e} - \theta^{f,h^e}) A_j^e d\xi, \\
\underbrace{\left\{ \mathbf{f}_{\mathcal{J}_5^{\text{INT},e}}^{\mathcal{J}_5^{\text{INT},e}} \right\}}_{n_{\text{dof}}^{\theta^s,e} \times 1} &= - \int_{-1}^1 \underbrace{\left\{ \mathbf{N}^{e,\theta^s} \right\}^T}_{n_{\text{dof}}^{\theta^s,e} \times 1} \frac{J^{h^e} \left((n^f \tilde{v}_f)^{h^e} \right)^2}{\hat{k}^{h^e}} A_j^e d\xi, \\
\underbrace{\left\{ \mathbf{f}_{\mathcal{J}_6^{\text{INT},e}}^{\mathcal{J}_6^{\text{INT},e}} \right\}}_{n_{\text{dof}}^{\theta^s,e} \times 1} &= \int_{-1}^1 \underbrace{\left\{ \mathbf{N}^{e,\theta^s} \right\}^T}_{n_{\text{dof}}^{\theta^s,e} \times 1} \frac{\theta^{s,h^e}}{\theta^{f,h^e}} \frac{p_f^{h^e}}{n^{f,h^e}} \frac{\partial n^{f,h^e}}{\partial X} (n^f \tilde{v}_f)^{h^e} A_j^e d\xi, \\
\underbrace{\left\{ \mathbf{f}^{\mathcal{J}^{\text{EXT},e}} \right\}}_{n_{\text{dof}}^{\theta^s,e} \times 1} &= \begin{cases} \underbrace{\left\{ \mathbf{N}^{e,\theta^s}(X=0, H) \right\}^T}_{n_{\text{dof}}^{\theta^s,e} \times 1} Q_s^\theta A & X=0, H \\ \mathbf{0} & 0 < X < H. \end{cases}
\end{aligned} \tag{4.390}$$

The mass matrix associated with the solid phase temperature is given by

$$\underbrace{\left[\mathbf{m}_{\theta^s, \theta^s}^{\mathcal{J}_1^{\text{INT}, e}} \right]}_{n_{\text{dof}}^{\theta^s, e} \times n_{\text{dof}}^{\theta^s, e}} = \int_{-1}^1 \rho_0^{s, h^e} c_V^s \underbrace{\left\{ \mathbf{N}^{e, \theta^s} \right\}^T}_{n_{\text{dof}}^{\theta^s, e} \times 1} \underbrace{\left\{ \mathbf{N}^{e, \theta^s} \right\}}_{1 \times n_{\text{dof}}^{\theta^s, e}} A_j^e d\xi. \quad (4.391)$$

The FE formulation for the balance of energy of the pore fluid (assuming an ideal gas), with variational equation given by Equation (4.176), is written in block-matrix form as

$$\underbrace{\left\{ \mathbf{R}_{\theta^f} \right\}}_{n_{\text{dof}}^{\theta^f} \times 1} = \mathbf{0}, \quad (4.392)$$

where the global residual for the fluid phase temperature is given as

$$\mathbf{c}^{\theta^f, T} \cdot \mathbf{R}_{\theta^f} = \mathcal{K}^h = \mathcal{K}_1^{\text{INT}, h} + \mathcal{K}_2^{\text{INT}, h} + \mathcal{K}_3^{\text{INT}, h} + \mathcal{K}_4^{\text{INT}, h} + \mathcal{K}_5^{\text{INT}, h} + \mathcal{K}_6^{\text{INT}, h} + \mathcal{K}_7^{\text{INT}, h} + \mathcal{K}_8^{\text{INT}, h} - \mathcal{K}^{\text{EXT}, h} = 0. \quad (4.393)$$

Therein,

$$\begin{aligned} \mathcal{K}_1^{\text{INT}, h} &= \mathbf{A}_e^{n_e} \underbrace{\left\{ \mathbf{c}^{\theta^f, e} \right\}^T}_{1 \times n_{\text{dof}}^{\theta^f, e}} \cdot \underbrace{\left[\mathbf{m}_{\theta^f, \theta^f}^{\mathcal{K}_1^{\text{INT}, e}} \right]}_{n_{\text{dof}}^{\theta^f, e} \times n_{\text{dof}}^{\theta^f, e}} \cdot \underbrace{\left\{ \dot{\vartheta}^{f, e} \right\}}_{n_{\text{dof}}^{\theta^f, e} \times 1}, & \mathcal{K}_2^{\text{INT}, h} &= \mathbf{A}_e^{n_e} \underbrace{\left\{ \mathbf{c}^{\theta^f, e} \right\}^T}_{1 \times n_{\text{dof}}^{\theta^f, e}} \cdot \underbrace{\left\{ \mathbf{f}^{\mathcal{K}_2^{\text{INT}, e}} \right\}}_{n_{\text{dof}}^{\theta^f, e} \times 1}, \\ \mathcal{K}_3^{\text{INT}, h} &= \mathbf{A}_e^{n_e} \underbrace{\left\{ \mathbf{c}^{\theta^f, e} \right\}^T}_{1 \times n_{\text{dof}}^{\theta^f, e}} \cdot \underbrace{\left\{ \mathbf{f}^{\mathcal{K}_3^{\text{INT}, e}} \right\}}_{n_{\text{dof}}^{\theta^f, e} \times 1}, & \mathcal{K}_4^{\text{INT}, h} &= \mathbf{A}_e^{n_e} \underbrace{\left\{ \mathbf{c}^{\theta^f, e} \right\}^T}_{1 \times n_{\text{dof}}^{\theta^f, e}} \cdot \underbrace{\left\{ \mathbf{f}^{\mathcal{K}_4^{\text{INT}, e}} \right\}}_{n_{\text{dof}}^{\theta^f, e} \times 1}, \\ \mathcal{K}_5^{\text{INT}, h} &= \mathbf{A}_e^{n_e} \underbrace{\left\{ \mathbf{c}^{\theta^f, e} \right\}^T}_{1 \times n_{\text{dof}}^{\theta^f, e}} \cdot \underbrace{\left\{ \mathbf{f}^{\mathcal{K}_5^{\text{INT}, e}} \right\}}_{n_{\text{dof}}^{\theta^f, e} \times 1}, & \mathcal{K}_6^{\text{INT}, h} &= \mathbf{A}_e^{n_e} \underbrace{\left\{ \mathbf{c}^{\theta^f, e} \right\}^T}_{1 \times n_{\text{dof}}^{\theta^f, e}} \cdot \underbrace{\left\{ \mathbf{f}^{\mathcal{K}_6^{\text{INT}, e}} \right\}}_{n_{\text{dof}}^{\theta^f, e} \times 1}, \\ \mathcal{K}_7^{\text{INT}, h} &= \mathbf{A}_e^{n_e} \underbrace{\left\{ \mathbf{c}^{\theta^f, e} \right\}^T}_{1 \times n_{\text{dof}}^{\theta^f, e}} \cdot \underbrace{\left\{ \mathbf{f}^{\mathcal{K}_7^{\text{INT}, e}} \right\}}_{n_{\text{dof}}^{\theta^f, e} \times 1}, & \mathcal{K}_8^{\text{INT}, h} &= \mathbf{A}_e^{n_e} \underbrace{\left\{ \mathbf{c}^{\theta^f, e} \right\}^T}_{1 \times n_{\text{dof}}^{\theta^f, e}} \cdot \underbrace{\left\{ \mathbf{f}^{\mathcal{K}_8^{\text{INT}, e}} \right\}}_{n_{\text{dof}}^{\theta^f, e} \times 1}, \\ \mathcal{K}^{\text{EXT}, h} &= \mathbf{A}_e^{n_e} \underbrace{\left\{ \mathbf{c}^{\theta^f, e} \right\}^T}_{1 \times n_{\text{dof}}^{\theta^f, e}} \cdot \underbrace{\left\{ \mathbf{f}^{\mathcal{K}^{\text{EXT}, e}} \right\}}_{n_{\text{dof}}^{\theta^f, e} \times 1}, \end{aligned} \quad (4.394)$$

where

$$\begin{aligned}
\underbrace{\left\{ \mathbf{f}^{\mathcal{K}_2^{\text{INT},e}} \right\}}_{n_{\text{dof}}^{\theta^f,e} \times 1} &= \int_{-1}^1 \underbrace{\left\{ \mathbf{N}^{e,\theta^f} \right\}}_{n_{\text{dof}}^{\theta^f,e} \times 1}^T \rho^{\text{fR},h^e} (c_V^f + \mathfrak{R}) \frac{\partial \theta^{f,h^e}}{\partial X} (n^f \tilde{v}_f)^{h^e} A_j^e d\xi, \\
\underbrace{\left\{ \mathbf{f}^{\mathcal{K}_3^{\text{INT},e}} \right\}}_{n_{\text{dof}}^{\theta^f,e} \times 1} &= - \int_{-1}^1 \underbrace{\left\{ \mathbf{N}^{e,\theta^f} \right\}}_{n_{\text{dof}}^{\theta^f,e} \times 1}^T n^{s,h^e} p_f^{h^e} j^{h^e} A_j^e d\xi, \\
\underbrace{\left\{ \mathbf{f}^{\mathcal{K}_4^{\text{INT},e}} \right\}}_{n_{\text{dof}}^{\theta^f,e} \times 1} &= - \int_{-1}^1 \underbrace{\left\{ \mathbf{N}^{e,\theta^f} \right\}}_{n_{\text{dof}}^{\theta^f,e} \times 1}^T \frac{p_f^{h^e}}{n^{f,h^e}} \frac{\partial n^{f,h^e}}{\partial X} (n^f \tilde{v}_f)^{h^e} A_j^e d\xi, \\
\underbrace{\left\{ \mathbf{f}^{\mathcal{K}_5^{\text{INT},e}} \right\}}_{n_{\text{dof}}^{\theta^f,e} \times 1} &= - \int_{-1}^1 \underbrace{\left\{ \mathbf{N}^{e,\theta^f} \right\}}_{n_{\text{dof}}^{\theta^f,e} \times 1}^T n_0^{f,h^e} \dot{p}_f^{h^e} A_j^e d\xi, \\
\underbrace{\left\{ \mathbf{f}^{\mathcal{K}_6^{\text{INT},e}} \right\}}_{n_{\text{dof}}^{\theta^f,e} \times 1} &= - \int_{-1}^1 \underbrace{\left\{ \mathbf{N}^{e,\theta^f} \right\}}_{n_{\text{dof}}^{\theta^f,e} \times 1}^T \frac{\partial p_f^{h^e}}{\partial X} (n^f \tilde{v}_f)^{h^e} A_j^e d\xi, \\
\underbrace{\left\{ \mathbf{f}^{\mathcal{K}_7^{\text{INT},e}} \right\}}_{n_{\text{dof}}^{\theta^f,e} \times 1} &= - \int_{-1}^1 \underbrace{\left\{ \mathbf{B}^{e,\theta^f} \right\}}_{n_{\text{dof}}^{\theta^f,e} \times 1}^T q^{f,h^e} A_j^e d\xi, \\
\underbrace{\left\{ \mathbf{f}^{\mathcal{K}_8^{\text{INT},e}} \right\}}_{n_{\text{dof}}^{\theta^f,e} \times 1} &= - \int_{-1}^1 \underbrace{\left\{ \mathbf{N}^{e,\theta^f} \right\}}_{n_{\text{dof}}^{\theta^f,e} \times 1}^T Jk_{\theta}^{\varepsilon} (\theta^{s,h^e} - \theta^{f,h^e}) A_j^e d\xi, \\
\underbrace{\left\{ \mathbf{f}^{\mathcal{K}^{\text{EXT},e}} \right\}}_{n_{\text{dof}}^{\theta^f,e} \times 1} &= \begin{cases} \underbrace{\left\{ \mathbf{N}^{e,\theta^f}(X=0, H) \right\}}_{n_{\text{dof}}^{\theta^f,e} \times 1}^T Q_f^{\theta} A & X=0, H \\ \mathbf{0} & 0 < X < H. \end{cases}
\end{aligned} \tag{4.395}$$

The mass matrix associated with the pore fluid phase temperature is given by

$$\underbrace{\left[\mathbf{m}_{\theta^f}^{\mathcal{K}_1^{\text{INT},e}} \right]}_{n_{\text{dof}}^{\theta^f,e} \times n_{\text{dof}}^{\theta^f,e}} = \int_{-1}^1 \rho_0^{f,h^e} (c_V^f + \mathfrak{R}) \underbrace{\left\{ \mathbf{N}^{e,\theta^f} \right\}}_{n_{\text{dof}}^{\theta^f,e} \times 1}^T \underbrace{\left\{ \mathbf{N}^{e,\theta^f} \right\}}_{1 \times n_{\text{dof}}^{\theta^f,e}} A_j^e d\xi. \tag{4.396}$$

For the compressible liquid pore fluid (Equation (3.153), Equation (4.199)),

$$\underbrace{\left\{ \mathbf{f}^{\mathcal{K}_2^{\text{INT}},e} \right\}}_{n_{\text{dof}}^{\theta^f,e} \times 1} = \int_{-1}^1 \underbrace{\left\{ \mathbf{N}^{e,\theta^f} \right\}^T}_{n_{\text{dof}}^{\theta^f,e} \times 1} \left(\rho^{\text{fR},h^e} c_V^f + n^{f,h^e} \theta^{f,h^e} K_f^\theta [\alpha_V^f]^2 \right) \frac{\partial \theta^{f,h^e}}{\partial X} (n^f \tilde{v}_f)^{h^e} A_j^e d\xi, \quad (4.397)$$

$$\underbrace{\left[\mathbf{m}_{\theta^f,\theta^f}^{\mathcal{K}_1^{\text{INT}},e} \right]}_{n_{\text{dof}}^{\theta^f,e} \times n_{\text{dof}}^{\theta^f,e}} = \int_{-1}^1 \left(\rho_0^{f,h^e} c_V^f + J^{h^e} n^{f,h^e} \theta^{f,h^e} K_f^\theta [\alpha_V^f]^2 \right) \underbrace{\left\{ \mathbf{N}^{e,\theta^f} \right\}^T}_{n_{\text{dof}}^{\theta^f,e} \times 1} \underbrace{\left\{ \mathbf{N}^{e,\theta^f} \right\}}_{1 \times n_{\text{dof}}^{\theta^f,e}} A_j^e d\xi.$$

Then, returning our attention to Equation (4.372), we have

$$\underbrace{\left\{ \mathbf{z} \right\}}_{\substack{(2 \times n_{\text{dof}}^s \\ + n_{\text{dof}}^{\text{PF}} \\ + n_{\text{dof}}^{\theta^s} \\ + n_{\text{dof}}^{\theta^f}) \times 1}} = \left[\begin{array}{c} \underbrace{\left\{ \mathbf{d} \right\}}_{n_{\text{dof}}^s \times 1} \\ \underbrace{\left[\mathbf{M}_{u,u}^{\text{GINT}} \right]^{-1}}_{n_{\text{dof}}^s \times n_{\text{dof}}^s} \cdot \left(- \underbrace{\left\{ \mathbf{F}^{\mathcal{G}_2^{\text{INT}}} \right\}}_{n_{\text{dof}}^s \times 1} - \underbrace{\left\{ \mathbf{F}^{\mathcal{G}_3^{\text{INT}}} \right\}}_{n_{\text{dof}}^s \times 1} - \underbrace{\left\{ \mathbf{F}^{\mathcal{G}_4^{\text{INT}}} \right\}}_{n_{\text{dof}}^s \times 1} + \underbrace{\left\{ \mathbf{F}^{\mathcal{G}^{\text{EXT}}} \right\}}_{n_{\text{dof}}^s \times 1} \right) \\ \underbrace{\left[\mathbf{M}_{p_f,p_f}^{\mathcal{H}_1^{\text{INT}}} \right]^{-1}}_{n_{\text{dof}}^{\text{PF}} \times n_{\text{dof}}^{\text{PF}}} \cdot \left(- \underbrace{\left\{ \mathbf{F}^{\mathcal{H}_1^{\text{INT}}} \right\}}_{n_{\text{dof}}^{\text{PF}} \times 1} - \underbrace{\left\{ \mathbf{F}^{\mathcal{H}_2^{\text{INT}}} \right\}}_{n_{\text{dof}}^{\text{PF}} \times 1} - \underbrace{\left\{ \mathbf{F}^{\mathcal{H}_3^{\text{INT}}} \right\}}_{n_{\text{dof}}^{\text{PF}} \times 1} - \underbrace{\left\{ \mathbf{F}^{\mathcal{H}_4^{\text{INT}}} \right\}}_{n_{\text{dof}}^{\text{PF}} \times 1} - \underbrace{\left\{ \mathbf{F}^{\mathcal{H}_6^{\text{INT}}} \right\}}_{n_{\text{dof}}^{\text{PF}} \times 1} - \underbrace{\left\{ \mathbf{F}^{\mathcal{H}_7^{\text{INT}}} \right\}}_{n_{\text{dof}}^{\text{PF}} \times 1} + \underbrace{\left\{ \mathbf{F}^{\mathcal{H}^{\text{EXT}}} \right\}}_{n_{\text{dof}}^{\text{PF}} \times 1} \right) \\ \underbrace{\left[\mathbf{M}_{\theta^s,\theta^s}^{\mathcal{J}_1^{\text{INT}}} \right]^{-1}}_{n_{\text{dof}}^{\theta^s} \times n_{\text{dof}}^{\theta^s}} \cdot \left(- \underbrace{\left\{ \mathbf{F}^{\mathcal{J}_2^{\text{INT}}} \right\}}_{n_{\text{dof}}^{\theta^s} \times 1} - \underbrace{\left\{ \mathbf{F}^{\mathcal{J}_3^{\text{INT}}} \right\}}_{n_{\text{dof}}^{\theta^s} \times 1} - \underbrace{\left\{ \mathbf{F}^{\mathcal{J}_4^{\text{INT}}} \right\}}_{n_{\text{dof}}^{\theta^s} \times 1} - \underbrace{\left\{ \mathbf{F}^{\mathcal{J}_5^{\text{INT}}} \right\}}_{n_{\text{dof}}^{\theta^s} \times 1} - \underbrace{\left\{ \mathbf{F}^{\mathcal{J}_6^{\text{INT}}} \right\}}_{n_{\text{dof}}^{\theta^s} \times 1} + \underbrace{\left\{ \mathbf{F}^{\mathcal{J}^{\text{EXT}}} \right\}}_{n_{\text{dof}}^{\theta^s} \times 1} \right) \\ \underbrace{\left[\mathbf{M}_{\theta^f,\theta^f}^{\mathcal{K}_1^{\text{INT}}} \right]^{-1}}_{n_{\text{dof}}^{\theta^f} \times n_{\text{dof}}^{\theta^f}} \cdot \left(- \underbrace{\left\{ \mathbf{F}^{\mathcal{K}_2^{\text{INT}}} \right\}}_{n_{\text{dof}}^{\theta^f} \times 1} - \underbrace{\left\{ \mathbf{F}^{\mathcal{K}_3^{\text{INT}}} \right\}}_{n_{\text{dof}}^{\theta^f} \times 1} - \underbrace{\left\{ \mathbf{F}^{\mathcal{K}_4^{\text{INT}}} \right\}}_{n_{\text{dof}}^{\theta^f} \times 1} - \underbrace{\left\{ \mathbf{F}^{\mathcal{K}_5^{\text{INT}}} \right\}}_{n_{\text{dof}}^{\theta^f} \times 1} - \underbrace{\left\{ \mathbf{F}^{\mathcal{K}_6^{\text{INT}}} \right\}}_{n_{\text{dof}}^{\theta^f} \times 1} - \underbrace{\left\{ \mathbf{F}^{\mathcal{K}_7^{\text{INT}}} \right\}}_{n_{\text{dof}}^{\theta^f} \times 1} - \underbrace{\left\{ \mathbf{F}^{\mathcal{K}_8^{\text{INT}}} \right\}}_{n_{\text{dof}}^{\theta^f} \times 1} + \underbrace{\left\{ \mathbf{F}^{\mathcal{K}^{\text{EXT}}} \right\}}_{n_{\text{dof}}^{\theta^f} \times 1} \right) \end{array} \right], \quad (4.398)$$

where

$$\begin{aligned}
\underbrace{\left[M_{u,u}^{\mathcal{G}^{\text{INT}}} \right]}_{n_{\text{dof}}^s \times n_{\text{dof}}^s} &= \mathbf{A}_e \underbrace{\left[\mathbf{m}_{u,u}^{\mathcal{G}^{\text{INT},e}} \right]}_{n_{\text{dof}}^{s,e} \times n_{\text{dof}}^{s,e}}, & \underbrace{\left\{ \mathbf{F}^{\mathcal{G}_2^{\text{INT}}} \right\}}_{n_{\text{dof}}^s \times 1} &= \mathbf{A}_e \underbrace{\left\{ \mathbf{f}^{\mathcal{G}_2^{\text{INT},e}} \right\}}_{n_{\text{dof}}^{s,e} \times 1}, \\
\underbrace{\left\{ \mathbf{F}^{\mathcal{G}_3^{\text{INT}}} \right\}}_{n_{\text{dof}}^s \times 1} &= \mathbf{A}_e \underbrace{\left\{ \mathbf{f}^{\mathcal{G}_3^{\text{INT},e}} \right\}}_{n_{\text{dof}}^{s,e} \times 1}, & \underbrace{\left\{ \mathbf{F}^{\mathcal{G}_4^{\text{INT}}} \right\}}_{n_{\text{dof}}^s \times 1} &= \mathbf{A}_e \underbrace{\left\{ \mathbf{f}^{\mathcal{G}_4^{\text{INT},e}} \right\}}_{n_{\text{dof}}^{s,e} \times 1}, \\
\underbrace{\left\{ \mathbf{F}^{\mathcal{G}^{\text{EXT}}} \right\}}_{n_{\text{dof}}^s \times 1} &= \mathbf{A}_e \underbrace{\left\{ \mathbf{f}^{\mathcal{G}^{\text{EXT},e}} \right\}}_{n_{\text{dof}}^{s,e} \times 1}, & \underbrace{\left[M_{p_f,p_f}^{\mathcal{H}_1^{\text{INT}}} \right]}_{n_{\text{dof}}^{p_f} \times n_{\text{dof}}^{p_f}} &= \mathbf{A}_e \underbrace{\left[\mathbf{m}_{p_f,p_f}^{\mathcal{H}_1^{\text{INT},e}} \right]}_{n_{\text{dof}}^{p_f,e} \times n_{\text{dof}}^{p_f,e}}, \\
\underbrace{\left\{ \mathbf{F}^{\mathcal{H}_1^{\text{INT}}} \right\}}_{n_{\text{dof}}^{p_f} \times 1} &= \mathbf{A}_e \underbrace{\left\{ \mathbf{f}^{\mathcal{H}_1^{\text{INT},e}} \right\}}_{n_{\text{dof}}^{p_f,e} \times 1}, & \underbrace{\left\{ \mathbf{F}^{\mathcal{H}_2^{\text{INT}}} \right\}}_{n_{\text{dof}}^{p_f} \times 1} &= \mathbf{A}_e \underbrace{\left\{ \mathbf{f}^{\mathcal{H}_2^{\text{INT},e}} \right\}}_{n_{\text{dof}}^{p_f,e} \times 1}, \\
\underbrace{\left\{ \mathbf{F}^{\mathcal{H}_3^{\text{INT}}} \right\}}_{n_{\text{dof}}^{p_f} \times 1} &= \mathbf{A}_e \underbrace{\left\{ \mathbf{f}^{\mathcal{H}_3^{\text{INT},e}} \right\}}_{n_{\text{dof}}^{p_f,e} \times 1}, & \underbrace{\left\{ \mathbf{F}^{\mathcal{H}_4^{\text{INT}}} \right\}}_{n_{\text{dof}}^{p_f} \times 1} &= \mathbf{A}_e \underbrace{\left\{ \mathbf{f}^{\mathcal{H}_4^{\text{INT},e}} \right\}}_{n_{\text{dof}}^{p_f,e} \times 1}, \\
\underbrace{\left\{ \mathbf{F}^{\mathcal{H}_6^{\text{INT}}} \right\}}_{n_{\text{dof}}^{p_f} \times 1} &= \mathbf{A}_e \underbrace{\left\{ \mathbf{f}^{\mathcal{H}_6^{\text{INT},e}} \right\}}_{n_{\text{dof}}^{p_f,e} \times 1}, & \underbrace{\left\{ \mathbf{F}^{\mathcal{H}_7^{\text{INT}}} \right\}}_{n_{\text{dof}}^{p_f} \times 1} &= \mathbf{A}_e \underbrace{\left\{ \mathbf{f}^{\mathcal{H}_7^{\text{INT},e}} \right\}}_{n_{\text{dof}}^{p_f,e} \times 1}, \\
\underbrace{\left\{ \mathbf{F}^{\mathcal{H}^{\text{EXT}}} \right\}}_{n_{\text{dof}}^{p_f} \times 1} &= \mathbf{A}_e \underbrace{\left\{ \mathbf{f}^{\mathcal{H}^{\text{EXT},e}} \right\}}_{n_{\text{dof}}^{p_f,e} \times 1}, & &
\end{aligned} \tag{4.399}$$

$$\begin{aligned}
\underbrace{\begin{bmatrix} M_{\theta^s, \theta^s}^{\mathcal{J}^{\text{INT}}} \end{bmatrix}}_{n_{\text{dof}}^{\theta^s} \times n_{\text{dof}}^{\theta^s}} &= \mathbf{A}_e \underbrace{\begin{bmatrix} m_{\theta^s, \theta^s}^{\mathcal{J}^{\text{INT}}, e} \end{bmatrix}}_{n_{\text{dof}}^{\theta^s, e} \times n_{\text{dof}}^{\theta^s, e}}, & \underbrace{\{ F_{\mathcal{J}_2^{\text{INT}}} \}}_{n_{\text{dof}}^{\theta^s} \times 1} &= \mathbf{A}_e \underbrace{\{ f_{\mathcal{J}_2^{\text{INT}}, e} \}}_{n_{\text{dof}}^{\theta^s, e} \times 1}, \\
\underbrace{\{ F_{\mathcal{J}_3^{\text{INT}}} \}}_{n_{\text{dof}}^{\theta^s} \times 1} &= \mathbf{A}_e \underbrace{\{ f_{\mathcal{J}_3^{\text{INT}}, e} \}}_{n_{\text{dof}}^{\theta^s, e} \times 1}, & \underbrace{\{ F_{\mathcal{J}_4^{\text{INT}}} \}}_{n_{\text{dof}}^{\theta^s} \times 1} &= \mathbf{A}_e \underbrace{\{ f_{\mathcal{J}_4^{\text{INT}}, e} \}}_{n_{\text{dof}}^{\theta^s, e} \times 1}, \\
\underbrace{\{ F_{\mathcal{J}_5^{\text{INT}}} \}}_{n_{\text{dof}}^{\theta^s} \times 1} &= \mathbf{A}_e \underbrace{\{ f_{\mathcal{J}_5^{\text{INT}}, e} \}}_{n_{\text{dof}}^{\theta^s, e} \times 1}, & \underbrace{\{ F_{\mathcal{J}_6^{\text{INT}}} \}}_{n_{\text{dof}}^{\theta^s} \times 1} &= \mathbf{A}_e \underbrace{\{ f_{\mathcal{J}_4^{\text{INT}}, e} \}}_{n_{\text{dof}}^{\theta^s, e} \times 1}, \\
\underbrace{\{ F_{\mathcal{J}^{\text{EXT}}} \}}_{n_{\text{dof}}^{\theta^s} \times 1} &= \mathbf{A}_e \underbrace{\{ f_{\mathcal{J}^{\text{EXT}}, e} \}}_{n_{\text{dof}}^{\theta^s, e} \times 1}, & \underbrace{\begin{bmatrix} M_{\theta^f, \theta^f}^{\mathcal{K}^{\text{INT}}} \end{bmatrix}}_{n_{\text{dof}}^{\theta^f} \times n_{\text{dof}}^{\theta^f}} &= \mathbf{A}_e \underbrace{\begin{bmatrix} m_{\theta^f, \theta^f}^{\mathcal{K}^{\text{INT}}, e} \end{bmatrix}}_{n_{\text{dof}}^{\theta^f, e} \times n_{\text{dof}}^{\theta^f, e}}, \\
\underbrace{\{ F_{\mathcal{K}_2^{\text{INT}}} \}}_{n_{\text{dof}}^{\theta^f} \times 1} &= \mathbf{A}_e \underbrace{\{ f_{\mathcal{K}_2^{\text{INT}}, e} \}}_{n_{\text{dof}}^{\theta^f, e} \times 1}, & \underbrace{\{ F_{\mathcal{K}_3^{\text{INT}}} \}}_{n_{\text{dof}}^{\theta^f} \times 1} &= \mathbf{A}_e \underbrace{\{ f_{\mathcal{K}_3^{\text{INT}}, e} \}}_{n_{\text{dof}}^{\theta^f, e} \times 1}, \\
\underbrace{\{ F_{\mathcal{K}_4^{\text{INT}}} \}}_{n_{\text{dof}}^{\theta^f} \times 1} &= \mathbf{A}_e \underbrace{\{ f_{\mathcal{K}_4^{\text{INT}}, e} \}}_{n_{\text{dof}}^{\theta^f, e} \times 1}, & \underbrace{\{ F_{\mathcal{K}_5^{\text{INT}}} \}}_{n_{\text{dof}}^{\theta^f} \times 1} &= \mathbf{A}_e \underbrace{\{ f_{\mathcal{K}_5^{\text{INT}}, e} \}}_{n_{\text{dof}}^{\theta^f, e} \times 1}, \\
\underbrace{\{ F_{\mathcal{K}_6^{\text{INT}}} \}}_{n_{\text{dof}}^{\theta^f} \times 1} &= \mathbf{A}_e \underbrace{\{ f_{\mathcal{K}_6^{\text{INT}}, e} \}}_{n_{\text{dof}}^{\theta^f, e} \times 1}, & \underbrace{\{ F_{\mathcal{K}_7^{\text{INT}}} \}}_{n_{\text{dof}}^{\theta^f} \times 1} &= \mathbf{A}_e \underbrace{\{ f_{\mathcal{K}_7^{\text{INT}}, e} \}}_{n_{\text{dof}}^{\theta^f, e} \times 1}, \\
\underbrace{\{ F_{\mathcal{K}_8^{\text{INT}}} \}}_{n_{\text{dof}}^{\theta^f} \times 1} &= \mathbf{A}_e \underbrace{\{ f_{\mathcal{K}_8^{\text{INT}}, e} \}}_{n_{\text{dof}}^{\theta^f, e} \times 1}, & \underbrace{\{ F_{\mathcal{K}^{\text{EXT}}} \}}_{n_{\text{dof}}^{\theta^f} \times 1} &= \mathbf{A}_e \underbrace{\{ f_{\mathcal{K}^{\text{EXT}}, e} \}}_{n_{\text{dof}}^{\theta^f, e} \times 1}.
\end{aligned} \tag{4.400}$$

As described in Section 4.3.1, Equation (4.398) is solved for each stage increment i at time $t_n + \Delta t c_i$ (i.e., any variables that are *explicit* functions of time, such as a time-dependent external traction,

are to be evaluated at time $t_n + \Delta t c_i$, with stage solution \mathbf{k}_i given by

$$\underbrace{\left\{ \mathbf{k}_i \right\}}_{(2 \times n_{\text{dof}}^s + n_{\text{dof}}^{p_f} + n_{\text{dof}}^{\theta^s} + n_{\text{dof}}^{\theta^f}) \times 1} := \left\{ \begin{array}{l} \left\{ \mathbf{k}_{i(v)} \right\} \\ n_{\text{dof}}^s \times 1 \\ \left\{ \mathbf{k}_{i(a)} \right\} \\ n_{\text{dof}}^s \times 1 \\ \left\{ \mathbf{k}_{i(\dot{p}_f)} \right\} \\ n_{\text{dof}}^{p_f} \times 1 \\ \left\{ \mathbf{k}_{i(\dot{\theta}^s)} \right\} \\ n_{\text{dof}}^{\theta^s} \times 1 \\ \left\{ \mathbf{k}_{i(\dot{\theta}^f)} \right\} \\ n_{\text{dof}}^{\theta^f} \times 1 \end{array} \right\} = \left\{ \begin{array}{l} \left\{ \mathbf{z}_v(t_n) \right\} + \Delta t \sum_{j=1}^{i-1} a_{ij} \left\{ \mathbf{k}_{j(v)} \right\} \\ n_{\text{dof}}^s \times 1 \quad n_{\text{dof}}^s \times 1 \\ \left\{ \mathbf{z}_a(t_n) \right\} + \Delta t \sum_{j=1}^{i-1} a_{ij} \left\{ \mathbf{k}_{j(a)} \right\} \\ n_{\text{dof}}^s \times 1 \quad n_{\text{dof}}^s \times 1 \\ \left\{ \mathbf{z}_{\dot{p}_f}(t_n) \right\} + \Delta t \sum_{j=1}^{i-1} a_{ij} \left\{ \mathbf{k}_{j(\dot{p}_f)} \right\} \\ n_{\text{dof}}^{p_f} \times 1 \quad n_{\text{dof}}^{p_f} \times 1 \\ \left\{ \mathbf{z}_{\dot{\theta}^s}(t_n) \right\} + \Delta t \sum_{j=1}^{i-1} a_{ij} \left\{ \mathbf{k}_{j(\dot{\theta}^s)} \right\} \\ n_{\text{dof}}^{\theta^s} \times 1 \quad n_{\text{dof}}^{\theta^s} \times 1 \\ \left\{ \mathbf{z}_{\dot{\theta}^f}(t_n) \right\} + \Delta t \sum_{j=1}^{i-1} a_{ij} \left\{ \mathbf{k}_{j(\dot{\theta}^f)} \right\} \\ n_{\text{dof}}^{\theta^f} \times 1 \quad n_{\text{dof}}^{\theta^f} \times 1 \end{array} \right\}. \quad (4.401)$$

Then, according to Equation (4.293), the higher order solution to be accepted or rejected at time t_{n+1} is given by

$$\underbrace{\left\{ \mathbf{z}^m(t_{n+1}) \right\}}_{(2 \times n_{\text{dof}}^s + n_{\text{dof}}^{p_f} + n_{\text{dof}}^{\theta^s} + n_{\text{dof}}^{\theta^f}) \times 1} := \left\{ \begin{array}{l} \left\{ \mathbf{z}_u^m(t_{n+1}) \right\} \\ n_{\text{dof}}^s \times 1 \\ \left\{ \mathbf{z}_v^m(t_{n+1}) \right\} \\ n_{\text{dof}}^s \times 1 \\ \left\{ \mathbf{z}_{p_f}^m(t_{n+1}) \right\} \\ n_{\text{dof}}^{p_f} \times 1 \\ \left\{ \mathbf{z}_{\theta^s}^m(t_{n+1}) \right\} \\ n_{\text{dof}}^{\theta^s} \times 1 \\ \left\{ \mathbf{z}_{\theta^f}^m(t_{n+1}) \right\} \\ n_{\text{dof}}^{\theta^f} \times 1 \end{array} \right\} = \left\{ \begin{array}{l} \left\{ \mathbf{z}_u(t_n) \right\} + \Delta t \sum_{i=1}^{m+1} b_i^m \left\{ \mathbf{k}_{i(v)} \right\} \\ n_{\text{dof}}^s \times 1 \quad n_{\text{dof}}^s \times 1 \\ \left\{ \mathbf{z}_v(t_n) \right\} + \Delta t \sum_{i=1}^{m+1} b_i^m \left\{ \mathbf{k}_{i(a)} \right\} \\ n_{\text{dof}}^s \times 1 \quad n_{\text{dof}}^s \times 1 \\ \left\{ \mathbf{z}_{p_f}(t_n) \right\} + \Delta t \sum_{i=1}^{m+1} b_i^m \left\{ \mathbf{k}_{i(\dot{p}_f)} \right\} \\ n_{\text{dof}}^{p_f} \times 1 \quad n_{\text{dof}}^{p_f} \times 1 \\ \left\{ \mathbf{z}_{\theta^s}(t_n) \right\} + \Delta t \sum_{i=1}^{m+1} b_i^m \left\{ \mathbf{k}_{i(\dot{\theta}^s)} \right\} \\ n_{\text{dof}}^{\theta^s} \times 1 \quad n_{\text{dof}}^{\theta^s} \times 1 \\ \left\{ \mathbf{z}_{\theta^f}(t_n) \right\} + \Delta t \sum_{i=1}^{m+1} b_i^m \left\{ \mathbf{k}_{i(\dot{\theta}^f)} \right\} \\ n_{\text{dof}}^{\theta^f} \times 1 \quad n_{\text{dof}}^{\theta^f} \times 1 \end{array} \right\}, \quad (4.402)$$

and, according to Equation (4.294), the lower order solution at time t_{n+1} is given by

$$\underbrace{\left\{ \mathbf{z}^{m-1}(t_{n+1}) \right\}}_{(2 \times n_{\text{dof}}^s + n_{\text{dof}}^{p_f} + n_{\text{dof}}^{\theta^s} + n_{\text{dof}}^{\theta^f}) \times 1} := \left\{ \begin{array}{l} \underbrace{\left\{ \mathbf{z}_u^{m-1}(t_{n+1}) \right\}}_{n_{\text{dof}}^s \times 1} \\ \underbrace{\left\{ \mathbf{z}_v^{m-1}(t_{n+1}) \right\}}_{n_{\text{dof}}^s \times 1} \\ \underbrace{\left\{ \mathbf{z}_{p_f}^{m-1}(t_{n+1}) \right\}}_{n_{\text{dof}}^{p_f} \times 1} \\ \underbrace{\left\{ \mathbf{z}_{\theta^s}^{m-1}(t_{n+1}) \right\}}_{n_{\text{dof}}^{\theta^s} \times 1} \\ \underbrace{\left\{ \mathbf{z}_{\theta^f}^{m-1}(t_{n+1}) \right\}}_{n_{\text{dof}}^{\theta^f} \times 1} \end{array} \right\} = \left\{ \begin{array}{l} \underbrace{\left\{ \mathbf{z}_u(t_n) \right\}}_{n_{\text{dof}}^s \times 1} + \Delta t \sum_{i=1}^m b_i^{m-1} \underbrace{\left\{ \mathbf{k}_{i(v)} \right\}}_{n_{\text{dof}}^s \times 1} \\ \underbrace{\left\{ \mathbf{z}_v(t_n) \right\}}_{n_{\text{dof}}^s \times 1} + \Delta t \sum_{i=1}^m b_i^{m-1} \underbrace{\left\{ \mathbf{k}_{i(a)} \right\}}_{n_{\text{dof}}^s \times 1} \\ \underbrace{\left\{ \mathbf{z}_{p_f}(t_n) \right\}}_{n_{\text{dof}}^{p_f} \times 1} + \Delta t \sum_{i=1}^m b_i^{m-1} \underbrace{\left\{ \mathbf{k}_{i(p_f)} \right\}}_{n_{\text{dof}}^{p_f} \times 1} \\ \underbrace{\left\{ \mathbf{z}_{\theta^s}(t_n) \right\}}_{n_{\text{dof}}^{\theta^s} \times 1} + \Delta t \sum_{i=1}^m b_i^{m-1} \underbrace{\left\{ \mathbf{k}_{i(\theta^s)} \right\}}_{n_{\text{dof}}^{\theta^s} \times 1} \\ \underbrace{\left\{ \mathbf{z}_{\theta^f}(t_n) \right\}}_{n_{\text{dof}}^{\theta^f} \times 1} + \Delta t \sum_{i=1}^m b_i^{m-1} \underbrace{\left\{ \mathbf{k}_{i(\theta^f)} \right\}}_{n_{\text{dof}}^{\theta^f} \times 1} \end{array} \right\}. \quad (4.403)$$

4.3.1.6 $(\mathbf{u}-\mathbf{u}_f-p_f-\theta^s-\theta^f)$ formulation

For the $(\mathbf{u}-\mathbf{u}_f-p_f-\theta^s-\theta^f)$ formulation, the Runge-Kutta integrators transform the general solution variables given by Equation (4.291) to

$$\left\{ \dot{\mathbf{z}} \right\} := \left\{ \begin{array}{l} \dot{z}_u \\ \dot{z}_v \\ \dot{z}_{u_f} \\ \dot{z}_{v_f} \\ \dot{z}_{p_f} \\ \dot{z}_{\theta^s} \\ \dot{z}_{\theta^f} \end{array} \right\} = \left\{ \mathbf{f}(t, \mathbf{z}) \right\} = \left\{ \begin{array}{l} \mathbf{f}_v(t, \mathbf{z}) \\ \mathbf{f}_a(t, \mathbf{z}) \\ \mathbf{f}_{v_f}(t, \mathbf{z}) \\ \mathbf{f}_{a_f}(t, \mathbf{z}) \\ \mathbf{f}_{\dot{p}_f}(t, \mathbf{z}) \\ \mathbf{f}_{\dot{\theta}^s}(t, \mathbf{z}) \\ \mathbf{f}_{\dot{\theta}^f}(t, \mathbf{z}) \end{array} \right\}, \quad (4.404)$$

such that

$$\left\{ z \right\} = \begin{pmatrix} \mathbf{d} \\ \dot{\mathbf{d}} \\ \mathbf{d}_f \\ \dot{\mathbf{d}}_f \\ \boldsymbol{\pi} \\ \boldsymbol{\vartheta}^s \\ \boldsymbol{\vartheta}^f \end{pmatrix}, \quad \dot{z} = \begin{pmatrix} \dot{\mathbf{d}} \\ \ddot{\mathbf{d}} \\ \dot{\mathbf{d}}_f \\ \ddot{\mathbf{d}}_f \\ \dot{\boldsymbol{\pi}} \\ \dot{\boldsymbol{\vartheta}}^s \\ \dot{\boldsymbol{\vartheta}}^f \end{pmatrix}. \quad (4.405)$$

Thus, we require at least one governing equation to solve for the primary unknown $\ddot{\mathbf{d}}$, which when integrated once gives us $\dot{\mathbf{d}}$, and when integrated twice gives us \mathbf{d} ; and at least one governing equation to solve for the primary unknown $\ddot{\mathbf{d}}_f$, which when integrated once gives us $\dot{\mathbf{d}}_f$, and when integrated twice gives us \mathbf{d}_f ; and at least one governing equation to solve for the primary unknown $\dot{\boldsymbol{\pi}}$, which when integrated once gives us $\boldsymbol{\pi}$; at least one governing equation to solve for the primary unknown $\dot{\boldsymbol{\vartheta}}^s$, which when integrated once gives us $\boldsymbol{\vartheta}^s$; and at least one governing equation to solve for the primary unknown $\dot{\boldsymbol{\vartheta}}^f$, which when integrated gives us $\boldsymbol{\vartheta}^f$.

The FE formulation for the balance of momentum of the mixture, with variational equation given by Equation (4.230), is written in block-matrix form as

$$\underbrace{\left\{ \mathbf{R}_u \right\}}_{n_{\text{dof}}^s \times 1} = \mathbf{0}, \quad (4.406)$$

where the global residual for the solid skeleton displacement is given as

$$\mathbf{c}^{u,T} \cdot \mathbf{R}_u = \mathcal{G}^h = \mathcal{G}_1^{\text{INT},h} + \mathcal{G}_2^{\text{INT},h} + \mathcal{G}_3^{\text{INT},h} + \mathcal{G}_4^{\text{INT},h} + \mathcal{G}_5^{\text{INT},h} - \mathcal{G}^{\text{EXT},h} = 0. \quad (4.407)$$

Therein,

$$\begin{aligned}
\mathcal{G}_1^{\text{INT},h} &= \mathbf{A}_e^{n_e} \underbrace{\left\{ \mathbf{c}^{u,e} \right\}^T}_{1 \times n_{\text{dof}}^{s,e}} \cdot \left(\underbrace{\left[\mathbf{m}_{u,u}^{\text{GINT},e} \right]}_{n_{\text{dof}}^{s,e} \times n_{\text{dof}}^{s,e}} \cdot \underbrace{\left\{ \ddot{\mathbf{d}}^e \right\}}_{n_{\text{dof}}^{s,e} \times 1} + \underbrace{\left\{ \mathbf{f}^{\mathcal{G}_1^{\text{INT},e}} \right\}}_{n_{\text{dof}}^{s,e} \times 1} \right), \\
\mathcal{G}_2^{\text{INT},h} &= \mathbf{A}_e^{n_e} \underbrace{\left\{ \mathbf{c}^{u,e} \right\}^T}_{1 \times n_{\text{dof}}^{s,e}} \cdot \underbrace{\left\{ \mathbf{f}^{\mathcal{G}_2^{\text{INT},e}} \right\}}_{n_{\text{dof}}^{s,e} \times 1}, & \mathcal{G}_3^{\text{INT},h} &= \mathbf{A}_e^{n_e} \underbrace{\left\{ \mathbf{c}^{u,e} \right\}^T}_{1 \times n_{\text{dof}}^{s,e}} \cdot \underbrace{\left\{ \mathbf{f}^{\mathcal{G}_3^{\text{INT},e}} \right\}}_{n_{\text{dof}}^{s,e} \times 1}, \\
\mathcal{G}_4^{\text{INT},h} &= \mathbf{A}_e^{n_e} \underbrace{\left\{ \mathbf{c}^{u,e} \right\}^T}_{1 \times n_{\text{dof}}^{s,e}} \cdot \underbrace{\left\{ \mathbf{f}^{\mathcal{G}_4^{\text{INT},e}} \right\}}_{n_{\text{dof}}^{s,e} \times 1}, & \mathcal{G}_5^{\text{INT},h} &= \mathbf{A}_e^{n_e} \underbrace{\left\{ \mathbf{c}^{u,e} \right\}^T}_{1 \times n_{\text{dof}}^{s,e}} \cdot \underbrace{\left\{ \mathbf{f}^{\mathcal{G}_5^{\text{INT},e}} \right\}}_{n_{\text{dof}}^{s,e} \times 1}, \\
\mathcal{G}^{\text{EXT},h} &= \mathbf{A}_e^{n_e} \underbrace{\left\{ \mathbf{c}^{u,e} \right\}^T}_{1 \times n_{\text{dof}}^{s,e}} \cdot \underbrace{\left\{ \mathbf{f}^{\mathcal{G}^{\text{EXT},e}} \right\}}_{n_{\text{dof}}^{s,e} \times 1},
\end{aligned} \tag{4.408}$$

where

$$\begin{aligned}
\underbrace{\left\{ \mathbf{f}^{\mathcal{G}_1^{\text{INT},e}} \right\}}_{n_{\text{dof}}^{s,e} \times 1} &= \int_{-1}^1 \underbrace{\left\{ \mathbf{N}^{e,u} \right\}^T}_{n_{\text{dof}}^{s,e} \times 1} \rho_0^{f,h^e} a_f^{h^e} A j^e d\xi, & \underbrace{\left\{ \mathbf{f}^{\mathcal{G}_2^{\text{INT},e}} \right\}}_{n_{\text{dof}}^{s,e} \times 1} &= \int_{-1}^1 \underbrace{\left\{ \mathbf{B}^{e,u} \right\}^T}_{n_{\text{dof}}^{s,e} \times 1} P_{11(E)}^{s,h^e} A j^e d\xi, \\
\underbrace{\left\{ \mathbf{f}^{\mathcal{G}_3^{\text{INT},e}} \right\}}_{n_{\text{dof}}^{s,e} \times 1} &= - \int_{-1}^1 \underbrace{\left\{ \mathbf{B}^{e,u} \right\}^T}_{n_{\text{dof}}^{s,e} \times 1} p_f^{h^e} \left(\frac{\theta^{s,h^e}}{\theta^{f,h^e}} n^{s,h^e} + n^{f,h^e} \right) A j^e d\xi, \\
\underbrace{\left\{ \mathbf{f}^{\mathcal{G}_4^{\text{INT},e}} \right\}}_{n_{\text{dof}}^{s,e} \times 1} &= \int_{-1}^1 \underbrace{\left\{ \mathbf{N}^{e,u} \right\}^T}_{n_{\text{dof}}^{s,e} \times 1} \rho_0^{h^e} g A j^e d\xi, \\
\underbrace{\left\{ \mathbf{f}^{\mathcal{G}^{\text{EXT},e}} \right\}}_{n_{\text{dof}}^{s,e} \times 1} &= \begin{cases} \underbrace{\left\{ \mathbf{N}^{e,u}(X=0, H) \right\}^T}_{n_{\text{dof}}^{s,e} \times 1} t^\sigma A & X=0, H \\ \mathbf{0} & 0 < X < H. \end{cases}
\end{aligned} \tag{4.409}$$

The mass matrix associated with the solid skeleton acceleration is given by

$$\underbrace{\left[\mathbf{m}_{u,u}^{\text{GINT},e} \right]}_{n_{\text{dof}}^{s,e} \times n_{\text{dof}}^{s,e}} = \int_{-1}^1 \rho_0^{h^e} \underbrace{\left\{ \mathbf{N}^{e,u} \right\}^T}_{n_{\text{dof}}^{s,e} \times 1} \underbrace{\left\{ \mathbf{N}^{e,u} \right\}}_{1 \times n_{\text{dof}}^{s,e}} A j^e d\xi. \tag{4.410}$$

The FE formulation for the balance of momentum of the fluid, with variational equations given by

Equation (4.232), is written in block-matrix form as

$$\underbrace{\left\{ \mathbf{R}_{u_f} \right\}}_{n_{\text{dof}}^f \times 1} = \mathbf{0}, \quad (4.411)$$

where the global residual for the pore fluid displacement is given as

$$\mathbf{c}^{u_f, T} \cdot \mathbf{R}_{u_f} = \mathcal{I}^h = \mathcal{I}_1^{\text{INT}, h} + \mathcal{I}_2^{\text{INT}, h} + \mathcal{I}_3^{\text{INT}, h} + \mathcal{I}_4^{\text{INT}, h} + \mathcal{I}_5^{\text{INT}, h} + \mathcal{I}_6^{\text{INT}, h} = 0. \quad (4.412)$$

Therein,

$$\begin{aligned} \mathcal{I}_1^{\text{INT}, h} &= \mathbf{A}_e^{n_e} \underbrace{\left\{ \mathbf{c}^{u_f, e} \right\}^T}_{1 \times n_{\text{dof}}^{f, e}} \cdot \underbrace{\left[\mathbf{m}_{u_f, u_f}^{\mathcal{I}_1^{\text{INT}, e}} \right]}_{n_{\text{dof}}^{f, e} \times n_{\text{dof}}^{f, e}} \cdot \underbrace{\left\{ \ddot{\mathbf{d}}_f^e \right\}}_{n_{\text{dof}}^{f, e} \times 1}, & \mathcal{I}_2^{\text{INT}, h} &= \mathbf{A}_e^{n_e} \underbrace{\left\{ \mathbf{c}^{u_f, e} \right\}^T}_{1 \times n_{\text{dof}}^{f, e}} \cdot \underbrace{\left\{ \mathbf{f}^{\mathcal{I}_2^{\text{INT}, e}} \right\}}_{n_{\text{dof}}^{f, e} \times 1}, \\ \mathcal{I}_3^{\text{INT}, h} &= \mathbf{A}_e^{n_e} \underbrace{\left\{ \mathbf{c}^{u_f, e} \right\}^T}_{1 \times n_{\text{dof}}^{f, e}} \cdot \underbrace{\left\{ \mathbf{f}^{\mathcal{I}_3^{\text{INT}, e}} \right\}}_{n_{\text{dof}}^{f, e} \times 1}, & \mathcal{I}_4^{\text{INT}, h} &= \mathbf{A}_e^{n_e} \underbrace{\left\{ \mathbf{c}^{u_f, e} \right\}^T}_{1 \times n_{\text{dof}}^{f, e}} \cdot \underbrace{\left\{ \mathbf{f}^{\mathcal{I}_4^{\text{INT}, e}} \right\}}_{n_{\text{dof}}^{f, e} \times 1}, \\ \mathcal{I}_5^{\text{INT}, h} &= \mathbf{A}_e^{n_e} \underbrace{\left\{ \mathbf{c}^{u_f, e} \right\}^T}_{1 \times n_{\text{dof}}^{f, e}} \cdot \underbrace{\left\{ \mathbf{f}^{\mathcal{I}_5^{\text{INT}, e}} \right\}}_{n_{\text{dof}}^{f, e} \times 1}, & \mathcal{I}_6^{\text{INT}, h} &= \mathbf{A}_e^{n_e} \underbrace{\left\{ \mathbf{c}^{u_f, e} \right\}^T}_{1 \times n_{\text{dof}}^{f, e}} \cdot \underbrace{\left\{ \mathbf{f}^{\mathcal{I}_6^{\text{INT}, e}} \right\}}_{n_{\text{dof}}^{f, e} \times 1}, \end{aligned} \quad (4.413)$$

with

$$\begin{aligned} \underbrace{\left\{ \mathbf{f}^{\mathcal{I}_2^{\text{INT}, e}} \right\}}_{n_{\text{dof}}^{f, e} \times 1} &= \int_{-1}^1 \underbrace{\left\{ \mathbf{N}^{e, u_f} \right\}^T}_{n_{\text{dof}}^{f, e} \times 1} n^{f, h^e} \frac{\partial p_f^{h^e}}{\partial X} A j^e d\xi, \\ \underbrace{\left\{ \mathbf{f}^{\mathcal{I}_3^{\text{INT}, e}} \right\}}_{n_{\text{dof}}^{f, e} \times 1} &= \int_{-1}^1 \underbrace{\left\{ \mathbf{N}^{e, u_f} \right\}^T}_{n_{\text{dof}}^{f, e} \times 1} \frac{J^{h^e} (n^{f, h^e})^2}{\hat{k}} (v_f^{h^e} - v^{h^e}) A j^e d\xi, \\ \underbrace{\left\{ \mathbf{f}^{\mathcal{I}_4^{\text{INT}, e}} \right\}}_{n_{\text{dof}}^{f, e} \times 1} &= \int_{-1}^1 \underbrace{\left\{ \mathbf{N}^{e, u_f} \right\}^T}_{n_{\text{dof}}^{f, e} \times 1} \rho_0^{f, h^e} g A j^e d\xi, & \underbrace{\left\{ \mathbf{f}^{\mathcal{I}_5^{\text{INT}, e}} \right\}}_{n_{\text{dof}}^{f, e} \times 1} &= - \int_{-1}^1 \underbrace{\left\{ \mathbf{N}^{e, u_f} \right\}^T}_{n_{\text{dof}}^{f, e} \times 1} \frac{\partial P_{11(E)}^{f, h^e}}{\partial X} A j^e d\xi, \\ \underbrace{\left\{ \mathbf{f}^{\mathcal{I}_6^{\text{INT}, e}} \right\}}_{n_{\text{dof}}^{f, e} \times 1} &= - \int_{-1}^1 \underbrace{\left\{ \mathbf{N}^{e, u_f} \right\}^T}_{n_{\text{dof}}^{f, e} \times 1} p_f^{h^e} \frac{\partial n^{f, h^e}}{\partial X} \left(1 - \frac{\theta^{s, h^e}}{\theta^{f, h^e}} \right) A j^e d\xi. \end{aligned} \quad (4.414)$$

For a nearly-inviscid pore fluid, Equation (4.414)₅ is zero. The mass matrix associated with the

pore fluid acceleration is given by

$$\underbrace{\left[\mathbf{m}_{u_f, u_f}^{\mathcal{I}^{\text{INT}, e}} \right]}_{n_{\text{dof}}^{f, e} \times n_{\text{dof}}^{f, e}} = \int_{-1}^1 \rho_0^{f, h^e} \underbrace{\left\{ \mathbf{N}^{e, u_f} \right\}^T}_{n_{\text{dof}}^{f, e} \times 1} \underbrace{\left\{ \mathbf{N}^{e, u_f} \right\}}_{1 \times n_{\text{dof}}^{f, e}} A_j^e d\xi. \quad (4.415)$$

The FE formulation for the balance of mass of the mixture, with variational equation given by Equation (4.233), is written in block-matrix form as

$$\underbrace{\left\{ \mathbf{R}_{p_f} \right\}}_{n_{\text{dof}}^{p_f} \times 1} = \mathbf{0}, \quad (4.416)$$

where the global residual for the pore fluid pressure is given as

$$\mathbf{c}^{p_f, T} \cdot \mathbf{R}_{p_f} = \mathcal{H}^h = \mathcal{H}_1^{\text{INT}, h} + \mathcal{H}_2^{\text{INT}, h} + \mathcal{H}_3^{\text{INT}, h} + \mathcal{H}_4^{\text{INT}, h} + \mathcal{H}_6^{\text{INT}, h} + \mathcal{H}_7^{\text{INT}, h} - \mathcal{H}^{\text{EXT}, h} = 0. \quad (4.417)$$

Therein,

$$\begin{aligned} \mathcal{H}_1^{\text{INT}, h} &= \underbrace{\mathbf{A}_e}_{1 \times n_{\text{dof}}^{p_f, e}} \left\{ \mathbf{c}^{p_f, e} \right\}^T \cdot \left(\underbrace{\left[\mathbf{m}_{p_f, p_f}^{\mathcal{H}_1^{\text{INT}, e}} \right]}_{n_{\text{dof}}^{p_f, e} \times n_{\text{dof}}^{p_f, e}} \cdot \underbrace{\left\{ \dot{\boldsymbol{\pi}}^e \right\}}_{n_{\text{dof}}^{p_f, e} \times 1} + \underbrace{\left\{ \mathbf{f}^{\mathcal{H}_1^{\text{INT}, e}} \right\}}_{n_{\text{dof}}^{p_f, e} \times 1} \right), \\ \mathcal{H}_2^{\text{INT}, h} &= \underbrace{\mathbf{A}_e}_{1 \times n_{\text{dof}}^{p_f, e}} \left\{ \mathbf{c}^{p_f, e} \right\}^T \cdot \underbrace{\left\{ \mathbf{f}^{\mathcal{H}_2^{\text{INT}, e}} \right\}}_{n_{\text{dof}}^{p_f, e} \times 1}, \quad \mathcal{H}_3^{\text{INT}, h} = \underbrace{\mathbf{A}_e}_{1 \times n_{\text{dof}}^{p_f, e}} \left\{ \mathbf{c}^{p_f, e} \right\}^T \cdot \underbrace{\left\{ \mathbf{f}^{\mathcal{H}_3^{\text{INT}, e}} \right\}}_{n_{\text{dof}}^{p_f, e} \times 1}, \\ \mathcal{H}_4^{\text{INT}, h} &= \underbrace{\mathbf{A}_e}_{1 \times n_{\text{dof}}^{p_f, e}} \left\{ \mathbf{c}^{p_f, e} \right\}^T \cdot \underbrace{\left\{ \mathbf{f}^{\mathcal{H}_4^{\text{INT}, e}} \right\}}_{n_{\text{dof}}^{p_f, e} \times 1}, \quad \mathcal{H}_6^{\text{INT}, h} = \underbrace{\mathbf{A}_e}_{1 \times n_{\text{dof}}^{p_f, e}} \left\{ \mathbf{c}^{p_f, e} \right\}^T \cdot \underbrace{\left\{ \mathbf{f}^{\mathcal{H}_6^{\text{INT}, e}} \right\}}_{n_{\text{dof}}^{p_f, e} \times 1}, \\ \mathcal{H}_7^{\text{INT}, h} &= \underbrace{\mathbf{A}_e}_{1 \times n_{\text{dof}}^{p_f, e}} \left\{ \mathbf{c}^{p_f, e} \right\}^T \cdot \underbrace{\left\{ \mathbf{f}^{\mathcal{H}_7^{\text{INT}, e}} \right\}}_{n_{\text{dof}}^{p_f, e} \times 1}, \quad \mathcal{H}^{\text{EXT}, h} = \underbrace{\mathbf{A}_e}_{1 \times n_{\text{dof}}^{p_f, e}} \left\{ \mathbf{c}^{p_f, e} \right\}^T \cdot \underbrace{\left\{ \mathbf{f}^{\mathcal{H}^{\text{EXT}, e}} \right\}}_{n_{\text{dof}}^{p_f, e} \times 1}, \end{aligned} \quad (4.418)$$

where

$$\begin{aligned}
\underbrace{\left\{ \mathbf{f}^{\mathcal{H}_1^{\text{INT},e}} \right\}}_{n_{\text{dof}}^{p_f,e} \times 1} &= \int_{-1}^1 \underbrace{\left\{ \mathbf{N}^{e,p_f} \right\}^T}_{n_{\text{dof}}^{p_f,e} \times 1} \mathbf{j}^{h^e} A_j^e d\xi, \\
\underbrace{\left\{ \mathbf{f}^{\mathcal{H}_2^{\text{INT},e}} \right\}}_{n_{\text{dof}}^{p_f,e} \times 1} &= \int_{-1}^1 \underbrace{\left\{ \mathbf{N}^{e,p_f} \right\}^T}_{n_{\text{dof}}^{p_f,e} \times 1} \frac{1}{p_f} \frac{\partial p_f^{h^e}}{\partial X} (n^f \tilde{v}_f)^{h^e} A_j^e d\xi, \\
\underbrace{\left\{ \mathbf{f}^{\mathcal{H}_3^{\text{INT},e}} \right\}}_{n_{\text{dof}}^{p_f,e} \times 1} &= \int_{-1}^1 \underbrace{\left\{ \mathbf{B}^{e,p_f} \right\}^T}_{n_{\text{dof}}^{p_f,e} \times 1} \hat{k}^{h^e} \frac{\partial p_f^{h^e}}{\partial X} (F_{11}^{h^e})^{-1} A_j^e d\xi, \\
\underbrace{\left\{ \mathbf{f}^{\mathcal{H}_4^{\text{INT},e}} \right\}}_{n_{\text{dof}}^{p_f,e} \times 1} &= \int_{-1}^1 \underbrace{\left\{ \mathbf{B}^{e,p_f} \right\}^T}_{n_{\text{dof}}^{p_f,e} \times 1} \hat{k}^{h^e} \rho^{\text{fR},h^e} (a_f^{h^e} + g) A_j^e d\xi, \\
\underbrace{\left\{ \mathbf{f}^{\mathcal{H}_6^{\text{INT},e}} \right\}}_{n_{\text{dof}}^{p_f,e} \times 1} &= \int_{-1}^1 \underbrace{\left\{ \mathbf{B}^{e,p_f} \right\}^T}_{n_{\text{dof}}^{p_f,e} \times 1} \frac{\hat{k}^{h^e}}{n^{f,h^e} p_f^{h^e}} \frac{\partial n^{f,h^e}}{\partial X} (F_{11}^{h^e})^{-1} \left(1 - \frac{\theta^{s,h^e}}{\theta^{f,h^e}} \right) A_j^e d\xi, \\
\underbrace{\left\{ \mathbf{f}^{\mathcal{H}_7^{\text{INT},e}} \right\}}_{n_{\text{dof}}^{p_f,e} \times 1} &= - \int_{-1}^1 \underbrace{\left\{ \mathbf{B}^{e,p_f} \right\}^T}_{n_{\text{dof}}^{p_f,e} \times 1} \frac{1}{\theta^{f,h^e}} \left(J^{h^e} n^{f,h^e} \dot{\theta}^{f,h^e} + \frac{\partial \theta^{f,h^e}}{\partial X} (n^f \tilde{v}_f)^{h^e} \right) A_j^e d\xi, \\
\underbrace{\left\{ \mathbf{f}^{\mathcal{H}^{\text{EXT},e}} \right\}}_{n_{\text{dof}}^{p_f,e} \times 1} &= \begin{cases} \underbrace{\left\{ \mathbf{N}^{e,p_f}(X=0, H) \right\}^T}_{n_{\text{dof}}^{p_f,e} \times 1} Q_f A & X=0, H \\ \mathbf{0} & 0 < X < H. \end{cases}
\end{aligned} \tag{4.419}$$

The mass matrix associated with the pore fluid pressure is given by

$$\underbrace{\left[\mathbf{m}_{p_f,p_f}^{\mathcal{H}_1^{\text{INT},e}} \right]}_{n_{\text{dof}}^{p_f,e} \times n_{\text{dof}}^{p_f,e}} = \int_{-1}^1 \frac{J^{h^e} n^{f,h^e}}{p_f^{h^e}} \underbrace{\left\{ \mathbf{N}^{e,p_f} \right\}^T}_{n_{\text{dof}}^{p_f,e} \times 1} \underbrace{\left\{ \mathbf{N}^{e,p_f} \right\}}_{1 \times n_{\text{dof}}^{p_f,e}} A_j^e d\xi. \tag{4.420}$$

For the compressible liquid pore fluid model (Equation (3.153), Equation (4.250)),

$$\begin{aligned} \underbrace{\left\{ \mathbf{f} \mathcal{H}_7^{\text{INT},e} \right\}}_{n_{\text{dof}}^{p_f,e} \times 1} &= - \int_{-1}^1 \underbrace{\left\{ \mathbf{B}^{e,p_f} \right\}}_{n_{\text{dof}}^{p_f,e} \times 1}^T \alpha_V^f \left(J^{h^e} n^{f,h^e} \dot{\theta}^{f,h^e} + \frac{\partial \theta^{f,h^e}}{\partial X} (n^f \tilde{v}_f)^{h^e} \right) A_j^e d\xi, \\ \underbrace{\left[\mathbf{m}_{p_f,p_f}^{\mathcal{H}_1^{\text{INT},e}} \right]}_{n_{\text{dof}}^{p_f,e} \times n_{\text{dof}}^{p_f,e}} &= \int_{-1}^1 \frac{J^{h^e} n^{f,h^e}}{K_f^\theta} \underbrace{\left\{ \mathbf{N}^{e,p_f} \right\}}_{n_{\text{dof}}^{p_f,e} \times 1}^T \underbrace{\left\{ \mathbf{N}^{e,p_f} \right\}}_{1 \times n_{\text{dof}}^{p_f,e}} A_j^e d\xi. \end{aligned} \quad (4.421)$$

When pressure stabilization is enabled, an additional term $\mathcal{H}^{\text{stab}}$ is added to the l.h.s. of Equation (4.417) and is defined as

$$\mathcal{H}^{\text{stab}} = \mathbf{A}_e^{n_e} \mathbf{c}^{p_f e, T} \cdot \underbrace{\left[\mathbf{m}_{p_f,p_f}^{\mathcal{H}^{\text{stab},e}} \right]}_{n_{\text{dof}}^{p_f,e} \times n_{\text{dof}}^{p_f,e}} \cdot \underbrace{\left\{ \dot{\boldsymbol{\pi}}^e \right\}}_{n_{\text{dof}}^{p_f,e} \times 1}, \quad (4.422)$$

where

$$\underbrace{\left[\mathbf{m}_{p_f,p_f}^{\mathcal{H}^{\text{stab},e}} \right]}_{n_{\text{dof}}^{p_f,e} \times n_{\text{dof}}^{p_f,e}} = \int_{-1}^1 \alpha^{\text{stab}} (F_{11}^{h^e})^{-1} \underbrace{\left\{ \mathbf{B}^{e,p_f} \right\}}_{n_{\text{dof}}^{p_f,e} \times 1}^T \underbrace{\left\{ \mathbf{B}^{e,p_f} \right\}}_{1 \times n_{\text{dof}}^{p_f,e}} A_j^e d\xi. \quad (4.423)$$

The FE formulation for the balance of energy of the solid, with variational equation given by Equation (4.234), is written in block-matrix form as

$$\underbrace{\left\{ \mathbf{R}_{\theta^s} \right\}}_{n_{\text{dof}}^{\theta^s} \times 1} = \mathbf{0}, \quad (4.424)$$

where the global residual for the solid phase temperature is given as

$$\mathbf{c}^{\theta^s, T} \cdot \mathbf{R}_{\theta^f} = \mathcal{J}^h = \mathcal{J}_1^{\text{INT},h} + \mathcal{J}_2^{\text{INT},h} + \mathcal{J}_3^{\text{INT},h} + \mathcal{J}_4^{\text{INT},h} + \mathcal{J}_5^{\text{INT},h} + \mathcal{J}_6^{\text{INT},h} - \mathcal{J}^{\text{EXT},h} = 0. \quad (4.425)$$

Therein,

$$\begin{aligned}
\mathcal{J}_1^{\text{INT},h} &= \mathbf{A}_e^{n_e} \underbrace{\left\{ \mathbf{c}^{\theta^s,e} \right\}^T}_{1 \times n_{\text{dof}}^{\theta^s,e}} \cdot \underbrace{\left[\mathbf{m}_{\theta^s,\theta^s}^{\mathcal{J}_1^{\text{INT},e}} \right]}_{n_{\text{dof}}^{\theta^s,e} \times n_{\text{dof}}^{\theta^s,e}} \cdot \underbrace{\left\{ \dot{\boldsymbol{\vartheta}}^{s,e} \right\}}_{n_{\text{dof}}^{\theta^s,e} \times 1}, & \mathcal{J}_2^{\text{INT},h} &= \mathbf{A}_e^{n_e} \underbrace{\left\{ \mathbf{c}^{\theta^s,e} \right\}^T}_{1 \times n_{\text{dof}}^{\theta^s,e}} \cdot \underbrace{\left\{ \mathbf{f}_{\mathcal{J}_2^{\text{INT},e}} \right\}}_{n_{\text{dof}}^{\theta^s,e} \times 1}, \\
\mathcal{J}_3^{\text{INT},h} &= \mathbf{A}_e^{n_e} \underbrace{\left\{ \mathbf{c}^{\theta^s,e} \right\}^T}_{1 \times n_{\text{dof}}^{\theta^s,e}} \cdot \underbrace{\left\{ \mathbf{f}_{\mathcal{J}_3^{\text{INT},e}} \right\}}_{n_{\text{dof}}^{\theta^s,e} \times 1}, & \mathcal{J}_4^{\text{INT},h} &= \mathbf{A}_e^{n_e} \underbrace{\left\{ \mathbf{c}^{\theta^s,e} \right\}^T}_{1 \times n_{\text{dof}}^{\theta^s,e}} \cdot \underbrace{\left\{ \mathbf{f}_{\mathcal{J}_4^{\text{INT},e}} \right\}}_{n_{\text{dof}}^{\theta^s,e} \times 1}, \\
\mathcal{J}_5^{\text{INT},h} &= \mathbf{A}_e^{n_e} \underbrace{\left\{ \mathbf{c}^{\theta^s,e} \right\}^T}_{1 \times n_{\text{dof}}^{\theta^s,e}} \cdot \underbrace{\left\{ \mathbf{f}_{\mathcal{J}_5^{\text{INT},e}} \right\}}_{n_{\text{dof}}^{\theta^s,e} \times 1}, & \mathcal{J}_6^{\text{INT},h} &= \mathbf{A}_e^{n_e} \underbrace{\left\{ \mathbf{c}^{\theta^s,e} \right\}^T}_{1 \times n_{\text{dof}}^{\theta^s,e}} \cdot \underbrace{\left\{ \mathbf{f}_{\mathcal{J}_6^{\text{INT},e}} \right\}}_{n_{\text{dof}}^{\theta^s,e} \times 1}, \\
\mathcal{J}^{\text{EXT},h} &= \mathbf{A}_e^{n_e} \underbrace{\left\{ \mathbf{c}^{\theta^s,e} \right\}^T}_{1 \times n_{\text{dof}}^{\theta^s,e}} \cdot \underbrace{\left\{ \mathbf{f}^{\mathcal{J}^{\text{EXT},e}} \right\}}_{n_{\text{dof}}^{\theta^s,e} \times 1},
\end{aligned} \tag{4.426}$$

where

$$\begin{aligned}
\underbrace{\left\{ \mathbf{f}_{\mathcal{J}_2^{\text{INT},e}} \right\}}_{n_{\text{dof}}^{\theta^s,e} \times 1} &= \int_{-1}^1 \underbrace{\left\{ \mathbf{N}^{e,\theta^s} \right\}^T}_{n_{\text{dof}}^{\theta^s,e} \times 1} \left(\frac{K^{\text{skel}} \alpha_V^s \theta^{s,h^e}}{J^{h^e}} + n^{s,h^e} p_f^{h^e} \frac{\theta^{s,h^e}}{\theta^{f,h^e}} + Q^{h^e} \right) j^{h^e} A_j^e d\xi, \\
\underbrace{\left\{ \mathbf{f}_{\mathcal{J}_3^{\text{INT},e}} \right\}}_{n_{\text{dof}}^{\theta^s,e} \times 1} &= - \int_{-1}^1 \underbrace{\left\{ \mathbf{B}^{e,\theta^s} \right\}^T}_{n_{\text{dof}}^{\theta^s,e} \times 1} q^{s,h^e} A_j^e d\xi, \\
\underbrace{\left\{ \mathbf{f}_{\mathcal{J}_4^{\text{INT},e}} \right\}}_{n_{\text{dof}}^{\theta^s,e} \times 1} &= \int_{-1}^1 \underbrace{\left\{ \mathbf{N}^{e,\theta^s} \right\}^T}_{n_{\text{dof}}^{\theta^s,e} \times 1} J^{h^e} k_{\bar{\theta}}^e (\theta^{s,h^e} - \theta^{f,h^e}) A_j^e d\xi, \\
\underbrace{\left\{ \mathbf{f}_{\mathcal{J}_5^{\text{INT},e}} \right\}}_{n_{\text{dof}}^{\theta^s,e} \times 1} &= - \int_{-1}^1 \underbrace{\left\{ \mathbf{N}^{e,\theta^s} \right\}^T}_{n_{\text{dof}}^{\theta^s,e} \times 1} \frac{J^{h^e} (n^{f,h^e})^2}{\hat{k}^{h^e}} (v_f^{h^e} - v^{h^e}) A_j^e d\xi, \\
\underbrace{\left\{ \mathbf{f}_{\mathcal{J}_6^{\text{INT},e}} \right\}}_{n_{\text{dof}}^{\theta^s,e} \times 1} &= \int_{-1}^1 \underbrace{\left\{ \mathbf{N}^{e,\theta^s} \right\}^T}_{n_{\text{dof}}^{\theta^s,e} \times 1} \frac{\theta^{s,h^e}}{\theta^{f,h^e}} p_f^{h^e} \frac{\partial n^{f,h^e}}{\partial X} (v_f^{h^e} - v^{h^e}) A_j^e d\xi, \\
\underbrace{\left\{ \mathbf{f}^{\mathcal{J}^{\text{EXT},e}} \right\}}_{n_{\text{dof}}^{\theta^s,e} \times 1} &= \begin{cases} \underbrace{\left\{ \mathbf{N}^{e,\theta^s}(X=0, H) \right\}^T}_{n_{\text{dof}}^{\theta^s,e} \times 1} Q_s^\theta A & X=0, H \\ \mathbf{0} & 0 < X < H. \end{cases}
\end{aligned} \tag{4.427}$$

The mass matrix associated with the solid phase temperature is given by

$$\underbrace{\left[\mathbf{m}_{\theta^s, \theta^s}^{\mathcal{J}_1^{\text{INT}, e}} \right]}_{n_{\text{dof}}^{\theta^s, e} \times n_{\text{dof}}^{\theta^s, e}} = \int_{-1}^1 \rho_0^{s, h^e} c_V^s \underbrace{\left\{ \mathbf{N}^{e, \theta^s} \right\}^T}_{n_{\text{dof}}^{\theta^s, e} \times 1} \underbrace{\left\{ \mathbf{N}^{e, \theta^s} \right\}}_{1 \times n_{\text{dof}}^{\theta^s, e}} A_j^e d\xi. \quad (4.428)$$

The FE formulation for the balance of energy of the pore fluid, with variational equation given by Equation (4.235), is written in block-matrix form as

$$\underbrace{\left\{ \mathbf{R}_{\theta^f} \right\}}_{n_{\text{dof}}^{\theta^f} \times 1} = \mathbf{0}, \quad (4.429)$$

where the global residual for the fluid phase temperature is given as

$$\mathbf{c}^{\theta^f, T} \cdot \mathbf{R}_{\theta^f} = \mathcal{K}^h = \mathcal{K}_1^{\text{INT}, h} + \mathcal{K}_2^{\text{INT}, h} + \mathcal{K}_3^{\text{INT}, h} + \mathcal{K}_4^{\text{INT}, h} + \mathcal{K}_7^{\text{INT}, h} + \mathcal{K}_8^{\text{INT}, h} - \mathcal{K}^{\text{EXT}, h} = 0. \quad (4.430)$$

Therein,

$$\begin{aligned} \mathcal{K}_1^{\text{INT}, h} &= \mathbf{A}_e^{n_e} \underbrace{\left\{ \mathbf{c}^{\theta^f, e} \right\}^T}_{1 \times n_{\text{dof}}^{\theta^f, e}} \cdot \underbrace{\left[\mathbf{m}_{\theta^f, \theta^f}^{\mathcal{K}_1^{\text{INT}, e}} \right]}_{n_{\text{dof}}^{\theta^f, e} \times n_{\text{dof}}^{\theta^f, e}} \cdot \underbrace{\left\{ \boldsymbol{\vartheta}^{\text{f}, e} \right\}}_{n_{\text{dof}}^{\theta^f, e} \times 1}, & \mathcal{K}_2^{\text{INT}, h} &= \mathbf{A}_e^{n_e} \underbrace{\left\{ \mathbf{c}^{\theta^f, e} \right\}^T}_{1 \times n_{\text{dof}}^{\theta^f, e}} \cdot \underbrace{\left\{ \mathbf{f}^{\mathcal{K}_2^{\text{INT}, e}} \right\}}_{n_{\text{dof}}^{\theta^f, e} \times 1}, \\ \mathcal{K}_3^{\text{INT}, h} &= \mathbf{A}_e^{n_e} \underbrace{\left\{ \mathbf{c}^{\theta^f, e} \right\}^T}_{1 \times n_{\text{dof}}^{\theta^f, e}} \cdot \underbrace{\left\{ \mathbf{f}^{\mathcal{K}_3^{\text{INT}, e}} \right\}}_{n_{\text{dof}}^{\theta^f, e} \times 1}, & \mathcal{K}_4^{\text{INT}, h} &= \mathbf{A}_e^{n_e} \underbrace{\left\{ \mathbf{c}^{\theta^f, e} \right\}^T}_{1 \times n_{\text{dof}}^{\theta^f, e}} \cdot \underbrace{\left\{ \mathbf{f}^{\mathcal{K}_4^{\text{INT}, e}} \right\}}_{n_{\text{dof}}^{\theta^f, e} \times 1}, \\ \mathcal{K}_7^{\text{INT}, h} &= \mathbf{A}_e^{n_e} \underbrace{\left\{ \mathbf{c}^{\theta^f, e} \right\}^T}_{1 \times n_{\text{dof}}^{\theta^f, e}} \cdot \underbrace{\left\{ \mathbf{f}^{\mathcal{K}_7^{\text{INT}, e}} \right\}}_{n_{\text{dof}}^{\theta^f, e} \times 1}, & \mathcal{K}_8^{\text{INT}, h} &= \mathbf{A}_e^{n_e} \underbrace{\left\{ \mathbf{c}^{\theta^f, e} \right\}^T}_{1 \times n_{\text{dof}}^{\theta^f, e}} \cdot \underbrace{\left\{ \mathbf{f}^{\mathcal{K}_8^{\text{INT}, e}} \right\}}_{n_{\text{dof}}^{\theta^f, e} \times 1}, \\ \mathcal{K}^{\text{EXT}, h} &= \mathbf{A}_e^{n_e} \underbrace{\left\{ \mathbf{c}^{\theta^f, e} \right\}^T}_{1 \times n_{\text{dof}}^{\theta^f, e}} \cdot \underbrace{\left\{ \mathbf{f}^{\mathcal{K}^{\text{EXT}, e}} \right\}}_{n_{\text{dof}}^{\theta^f, e} \times 1}, \end{aligned} \quad (4.431)$$

where

$$\begin{aligned}
\underbrace{\left\{ \mathbf{f}^{\mathcal{K}_2^{\text{INT}},e} \right\}}_{n_{\text{dof}}^{\theta^f,e} \times 1} &= \int_{-1}^1 \underbrace{\left\{ \mathbf{N}^{e,\theta^f} \right\}}_{n_{\text{dof}}^{\theta^f,e} \times 1}^T \rho^{f,h^e} (c_V^f + \mathfrak{R}) \frac{\partial \theta^{f,h^e}}{\partial X} (v_f^{h^e} - v^{h^e}) A j^e d\xi, \\
\underbrace{\left\{ \mathbf{f}^{\mathcal{K}_3^{\text{INT}},e} \right\}}_{n_{\text{dof}}^{\theta^f,e} \times 1} &= \int_{-1}^1 \underbrace{\left\{ \mathbf{N}^{e,\theta^f} \right\}}_{n_{\text{dof}}^{\theta^f,e} \times 1}^T n^{f,h^e} p_f^{h^e} \frac{\partial v_f^{h^e}}{\partial X} A j^e d\xi, \\
\underbrace{\left\{ \mathbf{f}^{\mathcal{K}_4^{\text{INT}},e} \right\}}_{n_{\text{dof}}^{\theta^f,e} \times 1} &= - \int_{-1}^1 \underbrace{\left\{ \mathbf{N}^{e,\theta^f} \right\}}_{n_{\text{dof}}^{\theta^f,e} \times 1}^T \frac{n^f h^e}{J^{h^e}} \left(\frac{\partial v_f^{h^e}}{\partial X} \right)^2 (\kappa_f + 2\mu_f) A j^e d\xi, \\
\underbrace{\left\{ \mathbf{f}^{\mathcal{K}_7^{\text{INT}},e} \right\}}_{n_{\text{dof}}^{\theta^f,e} \times 1} &= - \int_{-1}^1 \underbrace{\left\{ \mathbf{B}^{e,\theta^f} \right\}}_{n_{\text{dof}}^{\theta^f,e} \times 1}^T q^{f,h^e} A j^e d\xi, \\
\underbrace{\left\{ \mathbf{f}^{\mathcal{K}_8^{\text{INT}},e} \right\}}_{n_{\text{dof}}^{\theta^f,e} \times 1} &= - \int_{-1}^1 \underbrace{\left\{ \mathbf{N}^{e,\theta^f} \right\}}_{n_{\text{dof}}^{\theta^f,e} \times 1}^T J k_\theta^\varepsilon (\theta^{s,h^e} - \theta^{f,h^e}) A j^e d\xi, \\
\underbrace{\left\{ \mathbf{f}^{\mathcal{K}^{\text{EXT}},e} \right\}}_{n_{\text{dof}}^{\theta^f,e} \times 1} &= \begin{cases} \underbrace{\left\{ \mathbf{N}^{e,\theta^f}(X=0, H) \right\}}_{n_{\text{dof}}^{\theta^f,e} \times 1}^T Q_f^\theta A & X=0, H \\ \mathbf{0} & 0 < X < H. \end{cases}
\end{aligned} \tag{4.432}$$

The mass matrix associated with the pore fluid phase temperature is given by

$$\underbrace{\left[\mathbf{m}_{\theta^f, \theta^f}^{\mathcal{K}_1^{\text{INT}},e} \right]}_{n_{\text{dof}}^{\theta^f,e} \times n_{\text{dof}}^{\theta^f,e}} = \int_{-1}^1 \rho_0^{f,h^e} (c_V^f + \mathfrak{R}) \underbrace{\left\{ \mathbf{N}^{e,\theta^f} \right\}}_{n_{\text{dof}}^{\theta^f,e} \times 1}^T \underbrace{\left\{ \mathbf{N}^{e,\theta^f} \right\}}_{1 \times n_{\text{dof}}^{\theta^f,e}} A j^e d\xi. \tag{4.433}$$

For the compressible liquid pore fluid (Equation (3.153), Equation (4.251)),

$$\begin{aligned}
\underbrace{\left\{ \mathbf{f}^{\mathcal{K}_2^{\text{INT}},e} \right\}}_{n_{\text{dof}}^{\theta^f,e} \times 1} &= \int_{-1}^1 \underbrace{\left\{ \mathbf{N}^{e,\theta^f} \right\}}_{n_{\text{dof}}^{\theta^f,e} \times 1}^T (\rho^{f,h^e} c_V^f + (n^{f,h^e})^2 \theta^{f,h^e} K_f^\theta [\alpha_V^f]^2) \frac{\partial \theta^{f,h^e}}{\partial X} (v_f^{h^e} - v^{h^e}) A j^e d\xi, \\
\underbrace{\left[\mathbf{m}_{\theta^f, \theta^f}^{\mathcal{K}_1^{\text{INT}},e} \right]}_{n_{\text{dof}}^{\theta^f,e} \times n_{\text{dof}}^{\theta^f,e}} &= \int_{-1}^1 (\rho_0^{f,h^e} c_V^f + J^{h^e} n^{f,h^e} \theta^{f,h^e} K_f^\theta [\alpha_V^f]^2) \underbrace{\left\{ \mathbf{N}^{e,\theta^f} \right\}}_{n_{\text{dof}}^{\theta^f,e} \times 1}^T \underbrace{\left\{ \mathbf{N}^{e,\theta^f} \right\}}_{1 \times n_{\text{dof}}^{\theta^f,e}} A j^e d\xi,
\end{aligned} \tag{4.434}$$

and we must add $\mathcal{K}_5^{\text{INT},h}$ to Equation (4.431), wherein

$$\underbrace{\left\{ \mathbf{f}^{\mathcal{K}_5^{\text{INT},e}} \right\}}_{n_{\text{dof}}^{\theta^f,e} \times 1} = \int_{-1}^1 \underbrace{\left\{ \mathbf{N}^{e,\theta^f} \right\}^T}_{n_{\text{dof}}^{\theta^f,e} \times 1} J^{he} n^{f,h^e} \left(\frac{p_f^{h^e}}{K_f^\theta} - \alpha_{V,\theta^f,h^e} \right) \left(\dot{p}_f^{h^e} + \frac{\partial p_f^{h^e}}{\partial X} (v_f^{h^e} - v^{h^e}) (F_{11}^{h^e})^{-1} \right) A_j^e d\xi. \quad (4.435)$$

Then, returning our attention to Equation (4.404), we have

$$\underbrace{\left\{ \dot{\mathbf{z}} \right\}}_{\substack{(2 \times n_{\text{dof}}^s \\ + 2 \times n_{\text{dof}}^f \\ + n_{\text{dof}}^{p_f} \\ + n_{\text{dof}}^{\theta^s} \\ + n_{\text{dof}}^{\theta^f}) \times 1}} = \left[\begin{array}{c} \underbrace{\left\{ \dot{\mathbf{d}} \right\}}_{n_{\text{dof}}^s \times 1} \\ \underbrace{\left[\mathbf{M}_{u,u}^{\mathcal{G}_1^{\text{INT}}} \right]^{-1}}_{n_{\text{dof}}^s \times n_{\text{dof}}^s} \cdot \left(- \underbrace{\left\{ \mathbf{F}^{\mathcal{G}_1^{\text{INT}}} \right\}}_{n_{\text{dof}}^s \times 1} - \underbrace{\left\{ \mathbf{F}^{\mathcal{G}_2^{\text{INT}}} \right\}}_{n_{\text{dof}}^s \times 1} - \underbrace{\left\{ \mathbf{F}^{\mathcal{G}_3^{\text{INT}}} \right\}}_{n_{\text{dof}}^s \times 1} - \underbrace{\left\{ \mathbf{F}^{\mathcal{G}_4^{\text{INT}}} \right\}}_{n_{\text{dof}}^s \times 1} + \underbrace{\left\{ \mathbf{F}^{\mathcal{G}^{\text{EXT}}} \right\}}_{n_{\text{dof}}^s \times 1} \right) \\ \underbrace{\left\{ \dot{\mathbf{d}}_f \right\}}_{n_{\text{dof}}^f \times 1} \\ \underbrace{\left[\mathbf{M}_{u_f,u_f}^{\mathcal{I}_1^{\text{INT}}} \right]^{-1}}_{n_{\text{dof}}^f \times n_{\text{dof}}^f} \cdot \left(- \underbrace{\left\{ \mathbf{F}^{\mathcal{I}_2^{\text{INT}}} \right\}}_{n_{\text{dof}}^f \times 1} - \underbrace{\left\{ \mathbf{F}^{\mathcal{I}_3^{\text{INT}}} \right\}}_{n_{\text{dof}}^f \times 1} - \underbrace{\left\{ \mathbf{F}^{\mathcal{I}_4^{\text{INT}}} \right\}}_{n_{\text{dof}}^f \times 1} - \underbrace{\left\{ \mathbf{F}^{\mathcal{I}_5^{\text{INT}}} \right\}}_{n_{\text{dof}}^f \times 1} - \underbrace{\left\{ \mathbf{F}^{\mathcal{I}_6^{\text{INT}}} \right\}}_{n_{\text{dof}}^f \times 1} \right) \\ \underbrace{\left[\mathbf{M}_{p_f,p_f}^{\mathcal{H}_1^{\text{INT}}} \right]^{-1}}_{n_{\text{dof}}^{p_f} \times n_{\text{dof}}^{p_f}} \cdot \left(- \underbrace{\left\{ \mathbf{F}^{\mathcal{H}_1^{\text{INT}}} \right\}}_{n_{\text{dof}}^{p_f} \times 1} - \underbrace{\left\{ \mathbf{F}^{\mathcal{H}_2^{\text{INT}}} \right\}}_{n_{\text{dof}}^{p_f} \times 1} - \underbrace{\left\{ \mathbf{F}^{\mathcal{H}_3^{\text{INT}}} \right\}}_{n_{\text{dof}}^{p_f} \times 1} - \underbrace{\left\{ \mathbf{F}^{\mathcal{H}_4^{\text{INT}}} \right\}}_{n_{\text{dof}}^{p_f} \times 1} - \underbrace{\left\{ \mathbf{F}^{\mathcal{H}_5^{\text{INT}}} \right\}}_{n_{\text{dof}}^{p_f} \times 1} - \underbrace{\left\{ \mathbf{F}^{\mathcal{H}_6^{\text{INT}}} \right\}}_{n_{\text{dof}}^{p_f} \times 1} - \underbrace{\left\{ \mathbf{F}^{\mathcal{H}_7^{\text{INT}}} \right\}}_{n_{\text{dof}}^{p_f} \times 1} + \underbrace{\left\{ \mathbf{F}^{\mathcal{H}^{\text{EXT}}} \right\}}_{n_{\text{dof}}^{p_f} \times 1} \right) \\ \underbrace{\left[\mathbf{M}_{\theta^s,\theta^s}^{\mathcal{J}_1^{\text{INT}}} \right]^{-1}}_{n_{\text{dof}}^{\theta^s} \times n_{\text{dof}}^{\theta^s}} \cdot \left(- \underbrace{\left\{ \mathbf{F}^{\mathcal{J}_2^{\text{INT}}} \right\}}_{n_{\text{dof}}^{\theta^s} \times 1} - \underbrace{\left\{ \mathbf{F}^{\mathcal{J}_3^{\text{INT}}} \right\}}_{n_{\text{dof}}^{\theta^s} \times 1} - \underbrace{\left\{ \mathbf{F}^{\mathcal{J}_4^{\text{INT}}} \right\}}_{n_{\text{dof}}^{\theta^s} \times 1} - \underbrace{\left\{ \mathbf{F}^{\mathcal{J}_5^{\text{INT}}} \right\}}_{n_{\text{dof}}^{\theta^s} \times 1} - \underbrace{\left\{ \mathbf{F}^{\mathcal{J}_6^{\text{INT}}} \right\}}_{n_{\text{dof}}^{\theta^s} \times 1} + \underbrace{\left\{ \mathbf{F}^{\mathcal{J}^{\text{EXT}}} \right\}}_{n_{\text{dof}}^{\theta^s} \times 1} \right) \\ \underbrace{\left[\mathbf{M}_{\theta^f,\theta^f}^{\mathcal{K}_1^{\text{INT}}} \right]^{-1}}_{n_{\text{dof}}^{\theta^f} \times n_{\text{dof}}^{\theta^f}} \cdot \left(- \underbrace{\left\{ \mathbf{F}^{\mathcal{K}_2^{\text{INT}}} \right\}}_{n_{\text{dof}}^{\theta^f} \times 1} - \underbrace{\left\{ \mathbf{F}^{\mathcal{K}_3^{\text{INT}}} \right\}}_{n_{\text{dof}}^{\theta^f} \times 1} - \underbrace{\left\{ \mathbf{F}^{\mathcal{K}_4^{\text{INT}}} \right\}}_{n_{\text{dof}}^{\theta^f} \times 1} - \underbrace{\left\{ \mathbf{F}^{\mathcal{K}_7^{\text{INT}}} \right\}}_{n_{\text{dof}}^{\theta^f} \times 1} - \underbrace{\left\{ \mathbf{F}^{\mathcal{K}_8^{\text{INT}}} \right\}}_{n_{\text{dof}}^{\theta^f} \times 1} + \underbrace{\left\{ \mathbf{F}^{\mathcal{K}^{\text{EXT}}} \right\}}_{n_{\text{dof}}^{\theta^f} \times 1} \right) \end{array} \right], \quad (4.436)$$

where

$$\begin{aligned}
\underbrace{\left[M_{u,u}^{\mathcal{G}_1^{\text{INT}}} \right]}_{n_{\text{dof}}^s \times n_{\text{dof}}^s} &= \mathbf{A}_e \underbrace{\left[m_{u,u}^{\mathcal{G}_1^{\text{INT},e}} \right]}_{n_{\text{dof}}^{s,e} \times n_{\text{dof}}^{s,e}}, & \underbrace{\left\{ \mathbf{F}^{\mathcal{G}_1^{\text{INT}}} \right\}}_{n_{\text{dof}}^s \times 1} &= \mathbf{A}_e \underbrace{\left\{ f^{\mathcal{G}_1^{\text{INT},e}} \right\}}_{n_{\text{dof}}^{s,e} \times 1}, \\
\underbrace{\left\{ \mathbf{F}^{\mathcal{G}_2^{\text{INT}}} \right\}}_{n_{\text{dof}}^s \times 1} &= \mathbf{A}_e \underbrace{\left\{ f^{\mathcal{G}_2^{\text{INT},e}} \right\}}_{n_{\text{dof}}^{s,e} \times 1}, & \underbrace{\left\{ \mathbf{F}^{\mathcal{G}_3^{\text{INT}}} \right\}}_{n_{\text{dof}}^s \times 1} &= \mathbf{A}_e \underbrace{\left\{ f^{\mathcal{G}_3^{\text{INT},e}} \right\}}_{n_{\text{dof}}^{s,e} \times 1}, \\
\underbrace{\left\{ \mathbf{F}^{\mathcal{G}_4^{\text{INT}}} \right\}}_{n_{\text{dof}}^s \times 1} &= \mathbf{A}_e \underbrace{\left\{ f^{\mathcal{G}_4^{\text{INT},e}} \right\}}_{n_{\text{dof}}^{s,e} \times 1}, & \underbrace{\left[M_{u_f, u_f}^{\mathcal{I}_1^{\text{INT}}} \right]}_{n_{\text{dof}}^f \times n_{\text{dof}}^f} &= \mathbf{A}_e \underbrace{\left[m_{u_f, u_f}^{\mathcal{I}_1^{\text{INT},e}} \right]}_{n_{\text{dof}}^{f,e} \times n_{\text{dof}}^{f,e}}, \\
\underbrace{\left\{ \mathbf{F}^{\mathcal{I}_2^{\text{INT}}} \right\}}_{n_{\text{dof}}^f \times 1} &= \mathbf{A}_e \underbrace{\left\{ f^{\mathcal{I}_2^{\text{INT},e}} \right\}}_{n_{\text{dof}}^{f,e} \times 1}, & \underbrace{\left\{ \mathbf{F}^{\mathcal{I}_3^{\text{INT}}} \right\}}_{n_{\text{dof}}^f \times 1} &= \mathbf{A}_e \underbrace{\left\{ f^{\mathcal{I}_3^{\text{INT},e}} \right\}}_{n_{\text{dof}}^{f,e} \times 1}, \\
\underbrace{\left\{ \mathbf{F}^{\mathcal{I}_4^{\text{INT}}} \right\}}_{n_{\text{dof}}^f \times 1} &= \mathbf{A}_e \underbrace{\left\{ f^{\mathcal{I}_4^{\text{INT},e}} \right\}}_{n_{\text{dof}}^{f,e} \times 1}, & \underbrace{\left\{ \mathbf{F}^{\mathcal{I}_5^{\text{INT}}} \right\}}_{n_{\text{dof}}^f \times 1} &= \mathbf{A}_e \underbrace{\left\{ f^{\mathcal{I}_5^{\text{INT},e}} \right\}}_{n_{\text{dof}}^{f,e} \times 1}, \\
\underbrace{\left\{ \mathbf{F}^{\mathcal{I}_6^{\text{INT}}} \right\}}_{n_{\text{dof}}^f \times 1} &= \mathbf{A}_e \underbrace{\left\{ f^{\mathcal{I}_6^{\text{INT},e}} \right\}}_{n_{\text{dof}}^{f,e} \times 1}, & \underbrace{\left[M_{p_f, p_f}^{\mathcal{H}_1^{\text{INT}}} \right]}_{n_{\text{dof}}^{p_f} \times n_{\text{dof}}^{p_f}} &= \mathbf{A}_e \underbrace{\left[m_{p_f, p_f}^{\mathcal{H}_1^{\text{INT},e}} \right]}_{n_{\text{dof}}^{p_f,e} \times n_{\text{dof}}^{p_f,e}}, \\
\underbrace{\left\{ \mathbf{F}^{\mathcal{H}_1^{\text{INT}}} \right\}}_{n_{\text{dof}}^{p_f} \times 1} &= \mathbf{A}_e \underbrace{\left\{ f^{\mathcal{H}_1^{\text{INT},e}} \right\}}_{n_{\text{dof}}^{p_f,e} \times 1}, & \underbrace{\left\{ \mathbf{F}^{\mathcal{H}_2^{\text{INT}}} \right\}}_{n_{\text{dof}}^{p_f} \times 1} &= \mathbf{A}_e \underbrace{\left\{ f^{\mathcal{H}_2^{\text{INT},e}} \right\}}_{n_{\text{dof}}^{p_f,e} \times 1}, \\
\underbrace{\left\{ \mathbf{F}^{\mathcal{H}_3^{\text{INT}}} \right\}}_{n_{\text{dof}}^{p_f} \times 1} &= \mathbf{A}_e \underbrace{\left\{ f^{\mathcal{H}_3^{\text{INT},e}} \right\}}_{n_{\text{dof}}^{p_f,e} \times 1}, & \underbrace{\left\{ \mathbf{F}^{\mathcal{H}_4^{\text{INT}}} \right\}}_{n_{\text{dof}}^{p_f} \times 1} &= \mathbf{A}_e \underbrace{\left\{ f^{\mathcal{H}_4^{\text{INT},e}} \right\}}_{n_{\text{dof}}^{p_f,e} \times 1}, \\
\underbrace{\left\{ \mathbf{F}^{\mathcal{H}_6^{\text{INT}}} \right\}}_{n_{\text{dof}}^{p_f} \times 1} &= \mathbf{A}_e \underbrace{\left\{ f^{\mathcal{H}_6^{\text{INT},e}} \right\}}_{n_{\text{dof}}^{p_f,e} \times 1}, & \underbrace{\left\{ \mathbf{F}^{\mathcal{H}_7^{\text{INT}}} \right\}}_{n_{\text{dof}}^{p_f} \times 1} &= \mathbf{A}_e \underbrace{\left\{ f^{\mathcal{H}_7^{\text{INT},e}} \right\}}_{n_{\text{dof}}^{p_f,e} \times 1}, \\
\underbrace{\left\{ \mathbf{F}^{\mathcal{H}^{\text{EXT}}} \right\}}_{n_{\text{dof}}^{p_f} \times 1} &= \mathbf{A}_e \underbrace{\left\{ f^{\mathcal{H}^{\text{EXT},e}} \right\}}_{n_{\text{dof}}^{p_f,e} \times 1}, & &
\end{aligned} \tag{4.437}$$

$$\begin{aligned}
\underbrace{\left[M_{\theta^s, \theta^s}^{\mathcal{J}_1^{\text{INT}}} \right]}_{n_{\text{dof}}^{\theta^s} \times n_{\text{dof}}^{\theta^s}} &= \mathbf{A}_e^{n_e} \underbrace{\left[m_{\theta^s, \theta^s}^{\mathcal{J}_1^{\text{INT}}, e} \right]}_{n_{\text{dof}}^{\theta^s, e} \times n_{\text{dof}}^{\theta^s, e}}, & \underbrace{\left\{ F^{\mathcal{J}_2^{\text{INT}}} \right\}}_{n_{\text{dof}}^{\theta^s} \times 1} &= \mathbf{A}_e^{n_e} \underbrace{\left\{ f^{\mathcal{J}_2^{\text{INT}}, e} \right\}}_{n_{\text{dof}}^{\theta^s, e} \times 1}, \\
\underbrace{\left\{ F^{\mathcal{J}_3^{\text{INT}}} \right\}}_{n_{\text{dof}}^{\theta^s} \times 1} &= \mathbf{A}_e^{n_e} \underbrace{\left\{ f^{\mathcal{J}_3^{\text{INT}}, e} \right\}}_{n_{\text{dof}}^{\theta^s, e} \times 1}, & \underbrace{\left\{ F^{\mathcal{J}_4^{\text{INT}}} \right\}}_{n_{\text{dof}}^{\theta^s} \times 1} &= \mathbf{A}_e^{n_e} \underbrace{\left\{ f^{\mathcal{J}_4^{\text{INT}}, e} \right\}}_{n_{\text{dof}}^{\theta^s, e} \times 1}, \\
\underbrace{\left\{ F^{\mathcal{J}_5^{\text{INT}}} \right\}}_{n_{\text{dof}}^{\theta^s} \times 1} &= \mathbf{A}_e^{n_e} \underbrace{\left\{ f^{\mathcal{J}_4^{\text{INT}}, e} \right\}}_{n_{\text{dof}}^{\theta^s, e} \times 1}, & \underbrace{\left\{ F^{\mathcal{J}_6^{\text{INT}}} \right\}}_{n_{\text{dof}}^{\theta^s} \times 1} &= \mathbf{A}_e^{n_e} \underbrace{\left\{ f^{\mathcal{J}_4^{\text{INT}}, e} \right\}}_{n_{\text{dof}}^{\theta^s, e} \times 1}, \\
\underbrace{\left\{ F^{\mathcal{J}^{\text{EXT}}} \right\}}_{n_{\text{dof}}^{\theta^s} \times 1} &= \mathbf{A}_e^{n_e} \underbrace{\left\{ f^{\mathcal{J}^{\text{EXT}}, e} \right\}}_{n_{\text{dof}}^{\theta^s, e} \times 1}, & \underbrace{\left[M_{\theta^f, \theta^f}^{\mathcal{K}_1^{\text{INT}}} \right]}_{n_{\text{dof}}^{\theta^f} \times n_{\text{dof}}^{\theta^f}} &= \mathbf{A}_e^{n_e} \underbrace{\left[m_{\theta^f, \theta^f}^{\mathcal{K}_1^{\text{INT}}, e} \right]}_{n_{\text{dof}}^{\theta^f, e} \times n_{\text{dof}}^{\theta^f, e}}, \\
\underbrace{\left\{ F^{\mathcal{K}_2^{\text{INT}}} \right\}}_{n_{\text{dof}}^{\theta^f} \times 1} &= \mathbf{A}_e^{n_e} \underbrace{\left\{ f^{\mathcal{K}_2^{\text{INT}}, e} \right\}}_{n_{\text{dof}}^{\theta^f, e} \times 1}, & \underbrace{\left\{ F^{\mathcal{K}_3^{\text{INT}}} \right\}}_{n_{\text{dof}}^{\theta^f} \times 1} &= \mathbf{A}_e^{n_e} \underbrace{\left\{ f^{\mathcal{K}_3^{\text{INT}}, e} \right\}}_{n_{\text{dof}}^{\theta^f, e} \times 1}, \\
\underbrace{\left\{ F^{\mathcal{K}_4^{\text{INT}}} \right\}}_{n_{\text{dof}}^{\theta^f} \times 1} &= \mathbf{A}_e^{n_e} \underbrace{\left\{ f^{\mathcal{K}_4^{\text{INT}}, e} \right\}}_{n_{\text{dof}}^{\theta^f, e} \times 1}, & \underbrace{\left\{ F^{\mathcal{K}_7^{\text{INT}}} \right\}}_{n_{\text{dof}}^{\theta^f} \times 1} &= \mathbf{A}_e^{n_e} \underbrace{\left\{ f^{\mathcal{K}_7^{\text{INT}}, e} \right\}}_{n_{\text{dof}}^{\theta^f, e} \times 1}, \\
\underbrace{\left\{ F^{\mathcal{K}_8^{\text{INT}}} \right\}}_{n_{\text{dof}}^{\theta^f} \times 1} &= \mathbf{A}_e^{n_e} \underbrace{\left\{ f^{\mathcal{K}_8^{\text{INT}}, e} \right\}}_{n_{\text{dof}}^{\theta^f, e} \times 1}, & \underbrace{\left\{ F^{\mathcal{K}^{\text{EXT}}} \right\}}_{n_{\text{dof}}^{\theta^f} \times 1} &= \mathbf{A}_e^{n_e} \underbrace{\left\{ f^{\mathcal{K}^{\text{EXT}}, e} \right\}}_{n_{\text{dof}}^{\theta^f, e} \times 1}.
\end{aligned} \tag{4.438}$$

For the compressible liquid pore fluid, we must add $F^{\mathcal{K}_5^{\text{INT}}}$ on the last line of Equation (4.438), such that

$$\underbrace{\left\{ F^{\mathcal{K}_5^{\text{INT}}} \right\}}_{n_{\text{dof}}^{\theta^f} \times 1} = \mathbf{A}_e^{n_e} \underbrace{\left\{ f^{\mathcal{K}_5^{\text{INT}}, e} \right\}}_{n_{\text{dof}}^{\theta^f, e} \times 1}. \tag{4.439}$$

As described in Section 4.3.1, Equation (4.436) is solved for each stage increment i at time $t_n + \Delta t c_i$ (i.e., any variables that are *explicit* functions of time, such as a time-dependent external traction,

are to be evaluated at time $t_n + \Delta t c_i$), with stage solution \mathbf{k}_i given by

$$\underbrace{\left\{ \mathbf{k}_i \right\}}_{(2 \times n_{\text{dof}}^s + 2 \times n_{\text{dof}}^f + n_{\text{dof}}^{p_f} + n_{\text{dof}}^{\theta^s} + n_{\text{dof}}^{\theta^f}) \times 1} := \left(\begin{array}{c} \underbrace{\left\{ \mathbf{k}_{i(v)} \right\}}_{n_{\text{dof}}^s \times 1} \\ \underbrace{\left\{ \mathbf{k}_{i(a)} \right\}}_{n_{\text{dof}}^s \times 1} \\ \underbrace{\left\{ \mathbf{k}_{i(v_f)} \right\}}_{n_{\text{dof}}^f \times 1} \\ \underbrace{\left\{ \mathbf{k}_{i(a_f)} \right\}}_{n_{\text{dof}}^f \times 1} \\ \underbrace{\left\{ \mathbf{k}_{i(\hat{p}_f)} \right\}}_{n_{\text{dof}}^{p_f} \times 1} \\ \underbrace{\left\{ \mathbf{k}_{i(\hat{\theta}^s)} \right\}}_{n_{\text{dof}}^{\theta^s} \times 1} \\ \underbrace{\left\{ \mathbf{k}_{i(\hat{\theta}^f)} \right\}}_{n_{\text{dof}}^{\theta^f} \times 1} \end{array} \right) = \left(\begin{array}{c} \underbrace{\left\{ \mathbf{z}_v(t_n) \right\}}_{n_{\text{dof}}^s \times 1} + \Delta t \sum_{j=1}^{i-1} a_{ij} \underbrace{\left\{ \mathbf{k}_{j(v)} \right\}}_{n_{\text{dof}}^s \times 1} \\ \underbrace{\left\{ \mathbf{z}_a(t_n) \right\}}_{n_{\text{dof}}^s \times 1} + \Delta t \sum_{j=1}^{i-1} a_{ij} \underbrace{\left\{ \mathbf{k}_{j(a)} \right\}}_{n_{\text{dof}}^s \times 1} \\ \underbrace{\left\{ \mathbf{z}_{v_f}(t_n) \right\}}_{n_{\text{dof}}^f \times 1} + \Delta t \sum_{j=1}^{i-1} a_{ij} \underbrace{\left\{ \mathbf{k}_{j(v_f)} \right\}}_{n_{\text{dof}}^f \times 1} \\ \underbrace{\left\{ \mathbf{z}_{a_f}(t_n) \right\}}_{n_{\text{dof}}^f \times 1} + \Delta t \sum_{j=1}^{i-1} a_{ij} \underbrace{\left\{ \mathbf{k}_{j(a_f)} \right\}}_{n_{\text{dof}}^f \times 1} \\ \underbrace{\left\{ \mathbf{z}_{\hat{p}_f}(t_n) \right\}}_{n_{\text{dof}}^{p_f} \times 1} + \Delta t \sum_{j=1}^{i-1} a_{ij} \underbrace{\left\{ \mathbf{k}_{j(\hat{p}_f)} \right\}}_{n_{\text{dof}}^{p_f} \times 1} \\ \underbrace{\left\{ \mathbf{z}_{\hat{\theta}^s}(t_n) \right\}}_{n_{\text{dof}}^{\theta^s} \times 1} + \Delta t \sum_{j=1}^{i-1} a_{ij} \underbrace{\left\{ \mathbf{k}_{j(\hat{\theta}^s)} \right\}}_{n_{\text{dof}}^{\theta^s} \times 1} \\ \underbrace{\left\{ \mathbf{z}_{\hat{\theta}^f}(t_n) \right\}}_{n_{\text{dof}}^{\theta^f} \times 1} + \Delta t \sum_{j=1}^{i-1} a_{ij} \underbrace{\left\{ \mathbf{k}_{j(\hat{\theta}^f)} \right\}}_{n_{\text{dof}}^{\theta^f} \times 1} \end{array} \right). \quad (4.44)$$

Then, according to Equation (4.293), the higher order solution to be accepted or rejected at time

t_{n+1} is given by

$$\underbrace{\left\{ \mathbf{z}^m(t_{n+1}) \right\}}_{(2 \times n_{\text{dof}}^s + n_{\text{dof}}^{p_f} + n_{\text{dof}}^{\theta^s} + n_{\text{dof}}^{\theta^f}) \times 1} := \left\{ \begin{array}{l} \underbrace{\left\{ \mathbf{z}_u^m(t_{n+1}) \right\}}_{n_{\text{dof}}^s \times 1} \\ \underbrace{\left\{ \mathbf{z}_v^m(t_{n+1}) \right\}}_{n_{\text{dof}}^s \times 1} \\ \underbrace{\left\{ \mathbf{z}_{u_f}^m(t_{n+1}) \right\}}_{n_{\text{dof}}^f \times 1} \\ \underbrace{\left\{ \mathbf{z}_{v_f}^m(t_{n+1}) \right\}}_{n_{\text{dof}}^f \times 1} \\ \underbrace{\left\{ \mathbf{z}_{p_f}^m(t_{n+1}) \right\}}_{n_{\text{dof}}^{p_f} \times 1} \\ \underbrace{\left\{ \mathbf{z}_{\theta^s}^m(t_{n+1}) \right\}}_{n_{\text{dof}}^{\theta^s} \times 1} \\ \underbrace{\left\{ \mathbf{z}_{\theta^f}^m(t_{n+1}) \right\}}_{n_{\text{dof}}^{\theta^f} \times 1} \end{array} \right\} = \left\{ \begin{array}{l} \underbrace{\left\{ \mathbf{z}_u(t_n) \right\}}_{n_{\text{dof}}^s \times 1} + \Delta t \sum_{i=1}^{m+1} b_i^m \underbrace{\left\{ \mathbf{k}_{i(v)} \right\}}_{n_{\text{dof}}^s \times 1} \\ \underbrace{\left\{ \mathbf{z}_v(t_n) \right\}}_{n_{\text{dof}}^s \times 1} + \Delta t \sum_{i=1}^{m+1} b_i^m \underbrace{\left\{ \mathbf{k}_{i(a)} \right\}}_{n_{\text{dof}}^s \times 1} \\ \underbrace{\left\{ \mathbf{z}_{u_f}(t_n) \right\}}_{n_{\text{dof}}^f \times 1} + \Delta t \sum_{i=1}^{m+1} b_i^m \underbrace{\left\{ \mathbf{k}_{i(v_f)} \right\}}_{n_{\text{dof}}^f \times 1} \\ \underbrace{\left\{ \mathbf{z}_{v_f}(t_n) \right\}}_{n_{\text{dof}}^f \times 1} + \Delta t \sum_{i=1}^{m+1} b_i^m \underbrace{\left\{ \mathbf{k}_{i(a_f)} \right\}}_{n_{\text{dof}}^f \times 1} \\ \underbrace{\left\{ \mathbf{z}_{p_f}(t_n) \right\}}_{n_{\text{dof}}^{p_f} \times 1} + \Delta t \sum_{i=1}^{m+1} b_i^m \underbrace{\left\{ \mathbf{k}_{i(p_f)} \right\}}_{n_{\text{dof}}^{p_f} \times 1} \\ \underbrace{\left\{ \mathbf{z}_{\theta^s}(t_n) \right\}}_{n_{\text{dof}}^{\theta^s} \times 1} + \Delta t \sum_{i=1}^{m+1} b_i^m \underbrace{\left\{ \mathbf{k}_{i(\dot{\theta}^s)} \right\}}_{n_{\text{dof}}^{\theta^s} \times 1} \\ \underbrace{\left\{ \mathbf{z}_{\theta^f}(t_n) \right\}}_{n_{\text{dof}}^{\theta^f} \times 1} + \Delta t \sum_{i=1}^{m+1} b_i^m \underbrace{\left\{ \mathbf{k}_{i(\dot{\theta}^f)} \right\}}_{n_{\text{dof}}^f \times 1} \end{array} \right\}, \quad (4.441)$$

and, according to Equation (4.294), the lower order solution at time t_{n+1} is given by

$$\underbrace{\left\{ \mathbf{z}^{m-1}(t_{n+1}) \right\}}_{(2 \times n_{\text{dof}}^s + n_{\text{dof}}^{pf} + n_{\text{dof}}^{\theta s} + n_{\text{dof}}^{\theta f}) \times 1} := \left[\begin{array}{c} \underbrace{\left\{ \mathbf{z}_u^{m-1}(t_{n+1}) \right\}}_{n_{\text{dof}}^s \times 1} \\ \underbrace{\left\{ \mathbf{z}_v^{m-1}(t_{n+1}) \right\}}_{n_{\text{dof}}^s \times 1} \\ \underbrace{\left\{ \mathbf{z}_{u_f}^{m-1}(t_{n+1}) \right\}}_{n_{\text{dof}}^f \times 1} \\ \underbrace{\left\{ \mathbf{z}_{v_f}^{m-1}(t_{n+1}) \right\}}_{n_{\text{dof}}^f \times 1} \\ \underbrace{\left\{ \mathbf{z}_{p_f}^{m-1}(t_{n+1}) \right\}}_{n_{\text{dof}}^{pf} \times 1} \\ \underbrace{\left\{ \mathbf{z}_{\theta^s}^{m-1}(t_{n+1}) \right\}}_{n_{\text{dof}}^{\theta s} \times 1} \\ \underbrace{\left\{ \mathbf{z}_{\theta^f}^{m-1}(t_{n+1}) \right\}}_{n_{\text{dof}}^{\theta f} \times 1} \end{array} \right] = \left[\begin{array}{c} \underbrace{\left\{ \mathbf{z}_u(t_n) \right\}}_{n_{\text{dof}}^s \times 1} + \Delta t \sum_{i=1}^m b_i^{m-1} \underbrace{\left\{ \mathbf{k}_{i(v)} \right\}}_{n_{\text{dof}}^s \times 1} \\ \underbrace{\left\{ \mathbf{z}_v(t_n) \right\}}_{n_{\text{dof}}^s \times 1} + \Delta t \sum_{i=1}^m b_i^{m-1} \underbrace{\left\{ \mathbf{k}_{i(a)} \right\}}_{n_{\text{dof}}^s \times 1} \\ \underbrace{\left\{ \mathbf{z}_{u_f}(t_n) \right\}}_{n_{\text{dof}}^f \times 1} + \Delta t \sum_{i=1}^m b_i^{m-1} \underbrace{\left\{ \mathbf{k}_{i(v_f)} \right\}}_{n_{\text{dof}}^f \times 1} \\ \underbrace{\left\{ \mathbf{z}_{v_f}(t_n) \right\}}_{n_{\text{dof}}^f \times 1} + \Delta t \sum_{i=1}^m b_i^{m-1} \underbrace{\left\{ \mathbf{k}_{i(a_f)} \right\}}_{n_{\text{dof}}^f \times 1} \\ \underbrace{\left\{ \mathbf{z}_{p_f}(t_n) \right\}}_{n_{\text{dof}}^{pf} \times 1} + \Delta t \sum_{i=1}^m b_i^{m-1} \underbrace{\left\{ \mathbf{k}_{i(p_f)} \right\}}_{n_{\text{dof}}^{pf} \times 1} \\ \underbrace{\left\{ \mathbf{z}_{\theta^s}(t_n) \right\}}_{n_{\text{dof}}^{\theta s} \times 1} + \Delta t \sum_{i=1}^m b_i^{m-1} \underbrace{\left\{ \mathbf{k}_{i(\dot{\theta}^s)} \right\}}_{n_{\text{dof}}^{\theta s} \times 1} \\ \underbrace{\left\{ \mathbf{z}_{\theta^f}(t_n) \right\}}_{n_{\text{dof}}^{\theta f} \times 1} + \Delta t \sum_{i=1}^m b_i^{m-1} \underbrace{\left\{ \mathbf{k}_{i(\dot{\theta}^f)} \right\}}_{n_{\text{dof}}^{\theta f} \times 1} \end{array} \right]. \quad (4.442)$$

4.3.2 Implicit integration

For the poroelastodynamic equations that retain inertial terms, we apply the Newmark-beta method [Newmark, 1959] for solving Equation (4.287) wherein

$$\begin{aligned}
 \mathbf{M} \ddot{\mathbf{x}}_{n+1} + \mathbf{C} \dot{\mathbf{x}}_{n+1} + \mathbf{K} \mathbf{x}_{n+1} &= \mathbf{F}_{n+1}, \\
 \mathbf{x}_{n+1} &= \mathbf{x}_n + \Delta t \dot{\mathbf{x}}_n + \frac{\Delta t^2}{2} [(1 - 2\beta) \ddot{\mathbf{x}}_n + 2\beta \ddot{\mathbf{x}}_{n+1}], \\
 \dot{\mathbf{x}}_{n+1} &= \dot{\mathbf{x}}_n + \Delta t [(1 - \gamma) \ddot{\mathbf{x}}_n + \gamma \ddot{\mathbf{x}}_{n+1}],
 \end{aligned} \quad (4.443)$$

where

$$\mathbf{x} = \begin{Bmatrix} \mathbf{u} \\ \mathbf{u}_f \\ p_f \end{Bmatrix}, \quad \dot{\mathbf{x}} = \begin{Bmatrix} \mathbf{v} \\ \mathbf{v}_f \\ \dot{p}_f \end{Bmatrix}, \quad \ddot{\mathbf{x}} = \begin{Bmatrix} \mathbf{a} \\ \mathbf{a}_f \\ \ddot{p}_f \end{Bmatrix}. \quad (4.444)$$

The predictors are

$$\begin{aligned} \tilde{\mathbf{x}}_{n+1} &= \mathbf{x}_n + \Delta t \dot{\mathbf{x}}_n + \frac{\Delta t^2}{2} (1 - 2\beta) \ddot{\mathbf{x}}_n, \\ \dot{\tilde{\mathbf{x}}}_{n+1} &= \dot{\mathbf{x}}_n + \Delta t (1 - \gamma) \ddot{\mathbf{x}}_n, \end{aligned} \quad (4.445)$$

such that

$$\begin{aligned} \mathbf{x}_{n+1} &= \tilde{\mathbf{x}}_{n+1} + \beta \Delta t^2 \ddot{\mathbf{x}}_{n+1}, \\ \dot{\mathbf{x}}_{n+1} &= \dot{\tilde{\mathbf{x}}}_{n+1} + \gamma \Delta t \ddot{\mathbf{x}}_{n+1}. \end{aligned} \quad (4.446)$$

This allows us to solve for the accelerations at the next time step as follows:

$$\begin{aligned} (\mathbf{M} + \gamma \Delta t \mathbf{C} + \beta \Delta t^2 \mathbf{K}) \ddot{\mathbf{x}}_{n+1} &= \mathbf{F}_{n+1} - \mathbf{C} \dot{\tilde{\mathbf{x}}}_{n+1} - \mathbf{K} \tilde{\mathbf{x}}_{n+1} \\ \rightarrow \ddot{\mathbf{x}}_{n+1} &= (\mathbf{M} + \gamma \Delta t \mathbf{C} + \beta \Delta t^2 \mathbf{K})^{-1} \cdot (\mathbf{F}_{n+1} - \mathbf{C} \dot{\tilde{\mathbf{x}}}_{n+1} - \mathbf{K} \tilde{\mathbf{x}}_{n+1}). \end{aligned} \quad (4.447)$$

When inertia terms are ignored, the system of equations becomes

$$\mathbf{C} \dot{\mathbf{x}} + \mathbf{K} \mathbf{x} = \mathbf{F}. \quad (4.448)$$

Note that in this formulation

$$\mathbf{x} = \begin{Bmatrix} \mathbf{u} \\ p_f \end{Bmatrix}, \quad \dot{\mathbf{x}} = \begin{Bmatrix} \mathbf{v} \\ \dot{p}_f \end{Bmatrix}, \quad (4.449)$$

because pore fluid displacement does not have a balance equation associated with it.

For these equations (those that do not retain inertial terms), we apply a general trapezoidal rule for solving Equation (4.287) wherein

$$\begin{aligned} \mathbf{C} \dot{\mathbf{x}}_{n+1} + \mathbf{K} \mathbf{x}_{n+1} &= \mathbf{F}_{n+1}, \\ \mathbf{x}_{n+1} &= \mathbf{x}_n + \gamma \Delta t \dot{\mathbf{x}}_n, \end{aligned} \quad (4.450)$$

with predictor

$$\tilde{\mathbf{x}}_{n+1} = \mathbf{x}_n + (1 - \gamma)\Delta t \dot{\mathbf{x}}_n, \quad (4.451)$$

such that

$$\mathbf{x}_{n+1} = \tilde{\mathbf{x}}_{n+1} + \gamma\Delta t \dot{\mathbf{x}}_{n+1}. \quad (4.452)$$

This allows us to solve for the velocities at the next time step as follows:

$$\begin{aligned} (\mathbf{C} + \gamma\Delta t \mathbf{K}) \dot{\mathbf{x}}_{n+1} &= \mathbf{F}_{n+1} - \mathbf{K} \tilde{\mathbf{x}}_{n+1} \\ \rightarrow \dot{\mathbf{x}}_{n+1} &= (\mathbf{C} + \gamma\Delta t \mathbf{K})^{-1} \cdot (\mathbf{F}_{n+1} - \mathbf{K} \tilde{\mathbf{x}}_{n+1}). \end{aligned} \quad (4.453)$$

In addition to a fixed time-stepping scheme, we have also implemented an ad-hoc adaptive time-stepping scheme. However, most of the applications of non-inertial problems in the context of this work are for verification examples only, and we find that fixed time-step is suitable for this purpose. The method is most useful for dynamic problems where higher order of accuracy is pertinent, and is described as follows: in the event that the local number of Newton-Raphson iterations (see details in Section 4.3.2.1) exceeds a user-defined threshold (usually 6 iterations, which is typically beyond the criteria for quadratic convergence), the time step is reduced by a user-defined factor (e.g., $\Delta t^* \rightarrow 0.25\Delta t$). Conversely, if the solution converges before the user-defined threshold, the time-step is increased by a user-defined factor (e.g., $\Delta t^* \rightarrow 1.1\Delta t$). For further details, refer to Laadhari and Székely [2017].

4.3.2.1 Newton-Raphson method

Generally speaking, Equation (4.443)₁ can be reduced to a force residual r as a function of displacement d for static force equilibrium,

$$r(d) = F^{\text{EXT}} - F^{\text{INT}}(d) = 0 \quad (4.454)$$

where F^{EXT} is our external force (typically a pressure wave in the form of an applied traction force) and F^{INT} are the internal forces that work to oppose F^{EXT} . In this particular research

application, the internal forces are non-linear, therefore requiring us to employ a non-linear solver for Equation (4.454). For simplicity, we use the Newton-Raphson method to find the “exact” solution d^* such that $r(d^*) = 0$ given the applied external force F^{EXT} . Consider the Taylor-series expansion about the past iterate d^k :

$$\begin{aligned} d^* &= d^k + \delta d^k, \\ r(d^*) &= r(d^k) + \frac{\partial r(d^k)}{\partial d} \delta d^k + \frac{1}{2} \frac{\partial^2 r(d^k)}{\partial d^2} (\delta d^k)^2 + \text{h.o.t.} = 0. \end{aligned} \quad (4.455)$$

Then we “linearize”: let $\frac{\partial r(d^k)}{\partial d}$ be the consistent tangent at iteration k , drop the quadratic and higher order terms (h.o.t.s), and thus $d^* \approx d^{k+1}$.

$$r(d^k) + \frac{\partial r(d^k)}{\partial d} \delta d^k \approx 0 \quad ; \quad d^* \approx d^{k+1} = d^k + \delta d^k \quad (4.456)$$

Then, to find the solution to Equation (4.454), set

$$\begin{aligned} r(d^k) &= F^{\text{EXT}} - F^{\text{INT}}(d^k), \\ \delta d^k &= \left(\frac{\partial r(d^k)}{\partial d} \right)^{-1} [-r(d^k)] = \left(\frac{\partial F^{\text{INT}}(d^k)}{\partial d} \right)^{-1} r(d^k), \\ d^{k+1} &= d^k + \delta d^k, \\ r(d^{k+1}) &= F^{\text{EXT}} - F^{\text{INT}}(d^{k+1}), \end{aligned} \quad (4.457)$$

and check for convergence:

$$\begin{aligned} \text{IF } \frac{|r(d^{k+1})|}{|r(d^0)|} < \text{tol THEN } d^* = d^{k+1} \\ \text{ELSE iterate} \end{aligned}$$

where **tol** is a relative residual tolerance, relative to the initial residual $r(d^0)$. The proceeding section is concerned with how to find δd^k given by Eq. Equation (4.457)₂.

4.3.2.2 Gateaux derivatives for implicit integration methods

In order to properly linearize the matrix forms of the governing equations listed above, we will need to find the directional (Gateaux) derivatives of all the terms that have a dependence on

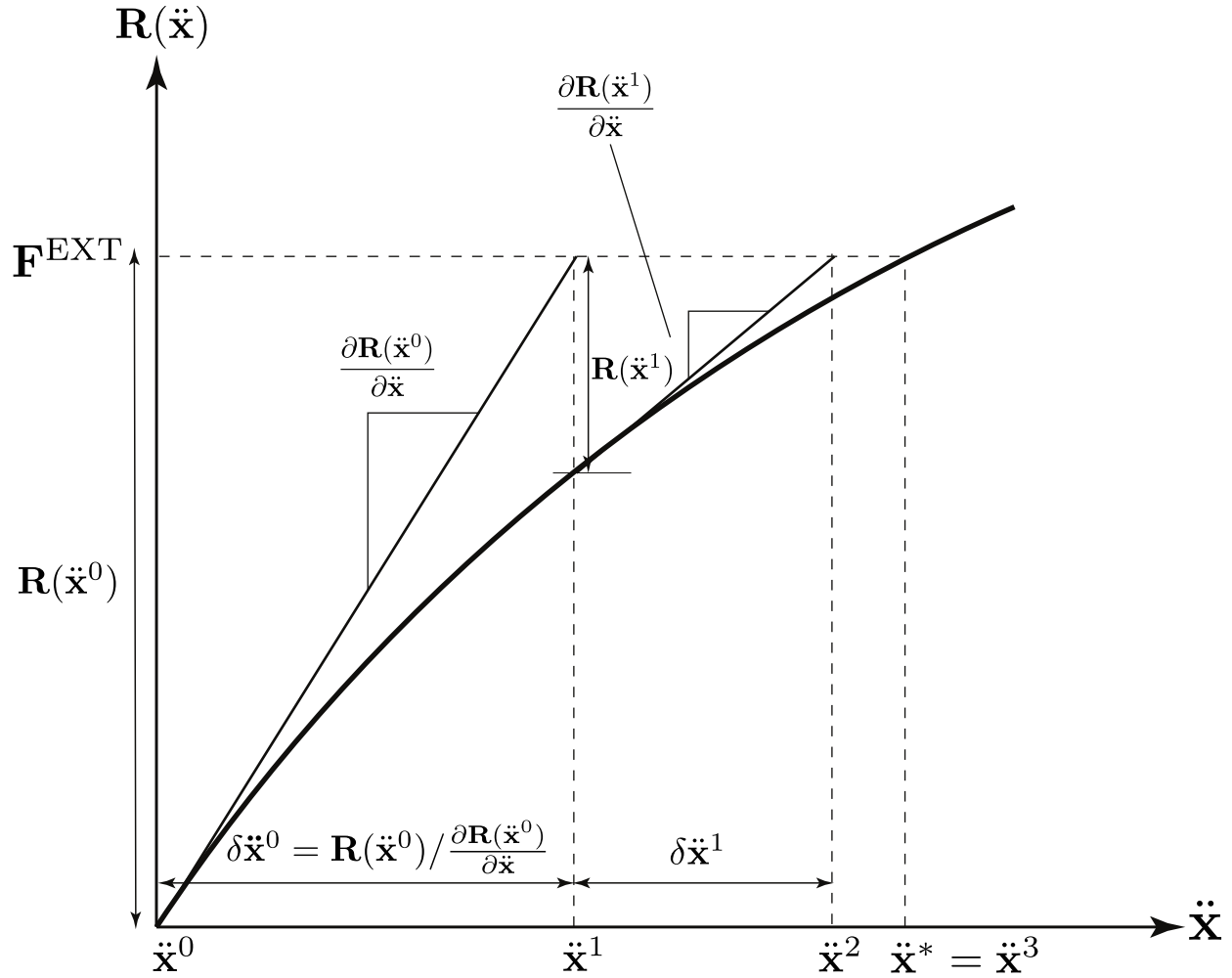


Figure 4.3: Illustration of Newton-Raphson method for solution of d , where we show iteration $k = 0, 1, 2$, and convergence likely at iteration $k = 3$. The black curve is a plot of $F^{\text{INT}}(d)$.

any one of the three solutions variables $(u_i, u_{i(f)}, p_f)$. In the following section we will substitute the results obtained here into the linearized forms of each term of our variational equations defined in Section 4.1. Again, we have assumed a 1-D uniaxial strain approximation to the deformation of lung parenchyma and the pore air within. All displacement and pressure vectors (i.e., solution vectors whose components are degrees of freedom) can be written in terms of their second time derivatives (or first time derivatives for the non-inertial equations) and subsequently integrated using an appropriate integration scheme to find the nodal solutions for displacement and pressure.

The variations are given by⁸

$$\begin{pmatrix} \delta \mathbf{u} \\ \delta \mathbf{u}_f \\ \delta p_f \end{pmatrix} = \beta \Delta t^2 \begin{pmatrix} \delta \mathbf{a} \\ \delta \mathbf{a}_f \\ \delta \ddot{p}_f \end{pmatrix}, \quad \begin{pmatrix} \delta \mathbf{v} \\ \delta \mathbf{v}_f \\ \delta \dot{p}_f \end{pmatrix} = \gamma \Delta t \begin{pmatrix} \delta \mathbf{a} \\ \delta \mathbf{a}_f \\ \delta \ddot{p}_f \end{pmatrix}. \quad (4.458)$$

In the following equations, we assume localized one-dimensional solution variables and drop the boldface notation. Detailed derivations are provided in Appendix A.

Starting with the Gateaux derivative of the deformation gradient, we have

$$\delta(F_{11}) = \beta \Delta t^2 \frac{\partial(\delta a)}{\partial X} = \gamma \Delta t \frac{\partial(\delta v)}{\partial X}. \quad (4.459)$$

For the deformation gradient raised to any power n , Equation (4.459) becomes

$$\delta(F_{11}^n) = n F_{11}^{n-1} \beta \Delta t^2 \frac{\partial(\delta a)}{\partial X} = n F_{11}^{n-1} \gamma \Delta t \frac{\partial(\delta v)}{\partial X}. \quad (4.460)$$

In the 1-D approximation, the Jacobian J is equivalent to F_{11} and thus

$$\begin{aligned} \delta(J) &= \delta(F_{11}) = \beta \Delta t^2 \frac{\partial(\delta a)}{\partial X} = \gamma \Delta t \frac{\partial(\delta v)}{\partial X}, \\ \delta(J^n) &= \delta(F_{11}^n) = n J^{n-1} \beta \Delta t^2 \frac{\partial(\delta a)}{\partial X} = n J^{n-1} \gamma \Delta t \frac{\partial(\delta v)}{\partial X}. \end{aligned} \quad (4.461)$$

Given the constitutive relation for the solid second Piola-Kirchoff extra stress shown in Section 3.3.1, we will also require the Gateaux derivative on the $\ln(J)$ terms, namely,

$$\delta(\ln(J)) = \frac{1}{J} \beta \Delta t^2 \frac{\partial(\delta a)}{\partial X} = \frac{1}{J} \gamma \Delta t \frac{\partial(\delta v)}{\partial X}, \quad (4.462)$$

as well as the Gateaux derivative on the inverse Cauchy green tensor component C_{11}^{-1} :

$$\delta(C_{11}^{-1}) = -2 F_{11}^{-3} \beta \Delta t^2 \frac{\partial(\delta a)}{\partial X} = -2 F_{11}^{-3} \gamma \Delta t \frac{\partial(\delta v)}{\partial X}. \quad (4.463)$$

⁸ Users of **SPONGE-1D** (refer to Chapter 5) will note that an implicit integration scheme has been developed for thermoporoelasticity and thermoporoelastodynamics, specifically for the $(\mathbf{u}-p_f-\theta^s-\theta^f)$ formulation. However, in testing we found that the results between the explicit and implicit thermoporoelastodynamic formulations do match well with the results between the poroelastodynamic formulations for the examples given in Section 5.3.3.2 (more than might be accounted for by numerical error). For this reason, the FE equations for the implicit $(\mathbf{u}-p_f-\theta^s-\theta^f)$ formulation are not presented anywhere in this work. The interested reader may find the linearizations (and derivations therein) for implicit $(\mathbf{u}-p_f-\theta^s-\theta^f)$ listed in Appendix B.5.

Now that we have both Equations (4.462) & Equation (4.463), we can apply the Gateaux derivative to the solid second Piola-Kirchoff extra stress component $\delta(S_{11(E)}^s)$ (assuming a neo-Hookean hyperelastic material model⁹) as follows:

$$\begin{aligned}\delta(S_{11(E)}^s) &= (\lambda - 2[\lambda \ln(J) - \mu]) F_{11}^{-3} \beta \Delta t^2 \frac{\partial(\delta a)}{\partial X} \\ &= (\lambda - 2[\lambda \ln(J) - \mu]) F_{11}^{-3} \gamma \Delta t \frac{\partial(\delta v)}{\partial X}.\end{aligned}\quad (4.464)$$

Then the Gateaux derivative applied to the solid first Piola-Kirchoff extra stress component $\delta(P_{11(E)}^s)$ is

$$\begin{aligned}\delta(P_{11(E)}^s) &= (\mu + [\lambda - \lambda \ln(J) + \mu] F_{11}^{-2}) \beta \Delta t^2 \frac{\partial(\delta a)}{\partial X} \\ &= (\mu + [\lambda - \lambda \ln(J) + \mu] F_{11}^{-2}) \gamma \Delta t \frac{\partial(\delta v)}{\partial X}.\end{aligned}\quad (4.465)$$

As an aside, consider the case where viscous damping is introduced (refer to Equation (3.118)):

$$\begin{aligned}\delta(P_{11(E)}^s) &= F_{11}^{-2} \left([\lambda + 2\mu] \left(\nu_0 \gamma \Delta t - 2\nu_0 F_{11}^{-1} \frac{\partial v}{\partial X} \beta \Delta t^2 \right) \right. \\ &\quad \left. - \ln F_{11} \left(2\nu_0 \gamma \Delta t - \left[4\nu_0 F_{11}^{-1} \frac{\partial v}{\partial X} - \lambda \right] \beta \Delta t^2 \right) \right. \\ &\quad \left. + \left([\lambda + \mu + \mu F_{11}^2] - 2\nu_0 F_{11}^{-1} \frac{\partial v}{\partial X} \right) \beta \Delta t^2 \right) \frac{\partial(\delta a)}{\partial X} \\ &= F_{11}^{-2} \left([\lambda + 2\mu] \left(\nu_0 - 2\nu_0 F_{11}^{-1} \frac{\partial v}{\partial X} \gamma \Delta t \right) \right. \\ &\quad \left. - \ln F_{11} \left(2\nu_0 - \left[4\nu_0 F_{11}^{-1} \frac{\partial v}{\partial X} - \lambda \right] \gamma \Delta t \right) \right. \\ &\quad \left. + \left([\lambda + \mu + \mu F_{11}^2] - 2\nu_0 F_{11}^{-1} \frac{\partial v}{\partial X} \right) \gamma \Delta t \right) \frac{\partial(\delta v)}{\partial X}.\end{aligned}\quad (4.466)$$

The real mass density of the barotropic pore fluid ρ^{fR} is dependent on the pore fluid pressure as defined in Section 3.3.2, therefore

$$\delta(\rho^{\text{fR}}) = \frac{\rho^{\text{fR}}}{K_f^{\eta}} \beta \Delta t^2 \delta \ddot{p}_f = \frac{\rho^{\text{fR}}}{K_f^{\eta}} \gamma \Delta t \delta \dot{p}_f, \quad (4.467)$$

and for a linear relationship given by Equation (3.140)₁

$$\delta(\rho^{\text{fR}}) = \frac{\rho_0^{\text{fR}}}{K_f^{\eta}} \beta \Delta t^2 \delta \ddot{p}_f = \frac{\rho_0^{\text{fR}}}{K_f^{\eta}} \gamma \Delta t \delta \dot{p}_f. \quad (4.468)$$

⁹ The neo-Hookean model with the extension from Ehlers and Eipper [1999] has been implemented in SPONGE-1D but is not presented here for brevity.

The volume fraction of pore fluid is dependent on the volume fraction of the solid skeleton which is dependent on the deformation of the solid skeleton, therefore

$$\delta(n^f) = \frac{n^s}{J} \beta \Delta t^2 \frac{\partial(\delta a)}{\partial X} = \frac{n^s}{J} \gamma \Delta t \frac{\partial(\delta v)}{\partial X}. \quad (4.469)$$

The mass density of the pore fluid is likewise dependent on both the volume fraction of the pore fluid as well as the real mass density of the pore fluid, therefore

$$\begin{aligned} \delta(\rho_0^f) &= \beta \Delta t^2 \left(\rho^{\text{fR}} \frac{\partial(\delta a)}{\partial X} + \frac{J n^f \rho^{\text{fR}}}{K_f} \delta \ddot{p}_f \right) \\ &= \gamma \Delta t \left(\rho^{\text{fR}} \frac{\partial(\delta v)}{\partial X} + \frac{J n^f \rho^{\text{fR}}}{K_f} \delta \dot{p}_f \right). \end{aligned} \quad (4.470)$$

As discussed in Section 3.1.4, to express the hydraulic conductivity as a function of the porosity we employ the either the Kozeny-Carman relation as shown in Equation (3.63) such that

$$\begin{aligned} \delta(\hat{k}) &= \underbrace{\frac{\hat{k} n^s}{J} \left[\frac{3}{n^f} + \frac{2n^f}{1 - (n^f)^2} \right]}_{\delta_{\hat{k}}} \beta \Delta t^2 \frac{\partial(\delta a)}{\partial X} \\ &= \delta_{\hat{k}} \gamma \Delta t \frac{\partial(\delta v)}{\partial X}, \end{aligned} \quad (4.471)$$

or the hyperbolic form given by Markert [2005], as shown in Equation (3.68), such that

$$\begin{aligned} \delta(\hat{k}) &= \underbrace{\frac{\varkappa}{\mu_f} \frac{\kappa}{1 - n_{0(s)}^s} \left(\frac{J_s - n_{0(s)}^s}{1 - n_{0(s)}^s} \right)^{\kappa-1}}_{\delta_{\hat{k}}} \beta \Delta t^2 \frac{\partial(\delta a)}{\partial X} \\ &= \delta_{\hat{k}} \gamma \Delta t \frac{\partial(\delta v)}{\partial X}. \end{aligned} \quad (4.472)$$

Later, for simplicity, we will reference $\delta_{\hat{k}}$ alone. The interested reader should refer to Equations (4.471) and Equation (4.472) for the individual forms.

4.3.2.3 (u) formulation

Linearization of the variational equations. Detailed derivations of the following linearizations are provided in Appendix B.1. The linearization of Equation (4.18)₁ is given by:

$$\delta \mathcal{G}_1^{\text{INT}} = \int_0^{X=H} w^u \rho_0 \delta a A dX. \quad (4.473)$$

For elasticity, Equation (4.473) is zero.

The linearization of Equation (4.18)₂ is given by:

$$\delta \mathcal{G}_2^{\text{INT}} = \int_0^{X=H} \frac{\partial w^u}{\partial X} (\mu + [\lambda - \lambda \ln(J) + \mu] F_{11}^{-2}) (\beta \Delta t^2) \frac{\partial(\delta a)}{\partial X} A dX . \quad (4.474)$$

For linearizations of $\mathcal{G}_2^{\text{INT}}$ with elasticity and viscous damping, refer to Equations (B.3)-Equation (B.5).

For linearization of $\mathcal{G}_2^{\text{INT}}$ when shock viscosity is enabled, refer to Equation (B.10).

The linearization of Equation (4.18)₃ is zero under the assumption that the variation of the reference mass density of the material is constant. In addition, the variation of the external force vector given by Equation (4.18)₄ is of course unnecessary as this term is simply subtracted from the residual at every Newton-Raphson iteration.

Finite element formulation. The finite element formulation for the (\mathbf{u}) formulation is presented as follows, with additional details being covered in Appendix C.1.1.

The finite element formulation for the elastodynamics variational equation is written in block-matrix formation as

$$\underbrace{\begin{bmatrix} \mathbf{K}_{u,u} \end{bmatrix}}_{n_{\text{dof}}^s \times n_{\text{dof}}^s} \cdot \underbrace{\left\{ \delta \dot{\mathbf{d}} \right\}}_{n_{\text{dof}}^s \times 1} = \underbrace{\left\{ -\mathbf{R}_u \right\}}_{n_{\text{dof}}^s \times 1} . \quad (4.475)$$

The finite element formulation for the elasticity variational equation is written in block-matrix formation as

$$\underbrace{\begin{bmatrix} \mathbf{K}_{u,u} \end{bmatrix}}_{n_{\text{dof}}^s \times n_{\text{dof}}^s} \cdot \underbrace{\left\{ \delta \dot{\mathbf{d}} \right\}}_{n_{\text{dof}}^s \times 1} = \underbrace{\left\{ -\mathbf{R}_u \right\}}_{n_{\text{dof}}^s \times 1} . \quad (4.476)$$

The global residual for the solid displacement is given as

$$\mathbf{e}^{u,T} \cdot \mathbf{R}_u = \mathcal{G}^h = \mathcal{G}_1^{\text{INT},h} + \mathcal{G}_2^{\text{INT},h} + \mathcal{G}_4^{\text{INT},h} - \mathcal{G}^{\text{EXT},h} = 0 \quad (4.477)$$

where

$$\begin{aligned}
\mathcal{G}_1^{\text{INT},h} &= \mathbf{A}_e^{n_e} \underbrace{\left\{ \mathbf{c}^{u,e} \right\}^T}_{1 \times n_{\text{dof}}^{s,e}} \cdot \left(\int_{-1}^1 \underbrace{\left\{ \mathbf{N}^{e,u} \right\}^T}_{n_{\text{dof}}^{s,e} \times 1} \rho_0^{h^e} a^{h^e} A j^e d\xi \right), \\
\mathcal{G}_2^{\text{INT},h} &= \mathbf{A}_e^{n_e} \underbrace{\left\{ \mathbf{c}^{u,e} \right\}^T}_{1 \times n_{\text{dof}}^{s,e}} \cdot \left(\int_{-1}^1 \underbrace{\left\{ \mathbf{B}^{e,u} \right\}^T}_{n_{\text{dof}}^{s,e} \times 1} P_{11}^{h^e} A j^e d\xi \right), \\
\mathcal{G}_4^{\text{INT},h} &= \mathbf{A}_e^{n_e} \underbrace{\left\{ \mathbf{c}^{u,e} \right\}^T}_{1 \times n_{\text{dof}}^{s,e}} \cdot \left(\int_{-1}^1 \underbrace{\left\{ \mathbf{N}^{e,u} \right\}^T}_{n_{\text{dof}}^{s,e} \times 1} \rho_0^{h^e} g A j^e d\xi \right), \\
\mathcal{G}^{\text{EXT},h} &= \mathbf{A}_e^{n_e} \underbrace{\left\{ \mathbf{c}^{u,e} \right\}^T}_{1 \times n_{\text{dof}}^{s,e}} \cdot \begin{cases} \underbrace{\left\{ \mathbf{N}^{e,u}(X=0, H) \right\}^T}_{n_{\text{dof}}^{s,e} \times 1} t^\sigma A & X=0, H \\ \mathbf{0} & 0 < X < H. \end{cases}
\end{aligned} \tag{4.478}$$

For elasticity, Equation (4.478)₁ is zero.

Recall that the tangent matrix for each Newton-Raphson iteration must be of the form

$$\mathbf{0} = \mathbf{R}_u^k = \left(\frac{\partial \mathbf{R}_u}{\partial \mathbf{a}} \right) \delta \mathbf{a} = \underbrace{\left[\mathbf{K}_{u,u} \right]}_{n_{\text{dof}}^s \times n_{\text{dof}}^s} \cdot \underbrace{\left\{ \delta \ddot{\mathbf{d}} \right\}}_{n_{\text{dof}}^s \times 1}, \tag{4.479}$$

or

$$\mathbf{0} = \mathbf{R}_u^k = \left(\frac{\partial \mathbf{R}_u}{\partial \mathbf{v}} \right) \delta \mathbf{v} = \underbrace{\left[\mathbf{K}_{u,u} \right]}_{n_{\text{dof}}^s \times n_{\text{dof}}^s} \cdot \underbrace{\left\{ \delta \dot{\mathbf{d}} \right\}}_{n_{\text{dof}}^s \times 1}, \tag{4.480}$$

where

$$\underbrace{\left[\mathbf{K}_{u,u} \right]}_{n_{\text{dof}}^s \times n_{\text{dof}}^s} = \mathbf{A}_e^{n_e} \underbrace{\left\{ \mathbf{c}^{u,e} \right\}^T}_{1 \times n_{\text{dof}}^{s,e}} \cdot \sum_{i=1}^2 \underbrace{\left[\mathbf{k}_{u,u}^{\mathcal{G}_i^{\text{INT},e}} \right]}_{n_{\text{dof}}^{s,e} \times n_{\text{dof}}^{s,e}}, \tag{4.481}$$

and where

$$\begin{aligned}
\underbrace{\left[\mathbf{k}_{u,u}^{\mathcal{G}_1^{\text{INT},e}} \right]}_{n_{\text{dof}}^{s,e} \times n_{\text{dof}}^{s,e}} &= \int_{-1}^1 \rho_0^{h^e} \underbrace{\left\{ \mathbf{N}^{e,u} \right\}^T}_{n_{\text{dof}}^{s,e} \times 1} \underbrace{\left\{ \mathbf{N}^{e,u} \right\}}_{1 \times n_{\text{dof}}^{s,e}} A j^e d\xi, \\
\underbrace{\left[\mathbf{k}_{u,u}^{\mathcal{G}_2^{\text{INT},e}} \right]}_{n_{\text{dof}}^{s,e} \times n_{\text{dof}}^{s,e}} &= \int_{-1}^1 (\mu + [\lambda - \lambda \ln(J^{h^e}) + \mu] (F_{11}^{h^e})^{-2} (\beta \Delta t^2)) \underbrace{\left\{ \mathbf{B}^{e,u} \right\}^T}_{n_{\text{dof}}^{s,e} \times 1} \underbrace{\left\{ \mathbf{B}^{e,u} \right\}}_{1 \times n_{\text{dof}}^{s,e}} A j^e d\xi.
\end{aligned} \tag{4.482}$$

For elasticity, Equation (4.482)₁ is zero. For the formulations of $\mathbf{k}_{u,u}^{\mathcal{G}_2^{\text{INT},e}}$ with elasticity and viscous damping, refer to Equations (C.9), Equation (C.12) and Equation (C.15). For the formulation of $\mathbf{k}_{u,u}^{\mathcal{G}_2^{\text{INT},e}}$ when shock viscosity is enabled, refer to Equation (C.18).

4.3.2.4 (\mathbf{u} - p_f) formulation

Linearization of the variational equations. Detailed derivations of the following linearized equations are provided in Appendix B.3. The linearizations of Equations (4.64)_{1,2} remain unchanged from the (\mathbf{u}) formulation (the former under the assumption that the Gateaux derivative of the mass density of the biphasic mixture is negligible); refer to Equations (4.473) & Equation (4.474) for $\delta\mathcal{G}_1^{\text{INT}}$ & $\delta\mathcal{G}_2^{\text{INT}}$, respectively.

The linearization of Equation (4.64)₃ is given by (for poroelasticity, refer to Equation (B.24)):

$$\delta\mathcal{G}_3^{\text{INT}} = - \int_0^{X=H} \frac{\partial w^u}{\partial X} B(\beta\Delta t^2) \delta\ddot{p}_f A dX . \quad (4.483)$$

The linearization of Equation (4.64)₄ is zero under the assumption the Gateaux derivative of the mass density of the biphasic mixture is very small. In addition, the external force vector given by Equations (4.61)_{5,6} is of course unnecessary as this term is simply subtracted from the residual at every Newton-Raphson iteration.

The linearization of Equation (4.66)₁ is given by (for poroelasticity, refer to Equation (B.26)):

$$\delta\mathcal{H}_1^{\text{INT}} = \int_0^{X=H} w^{p_f} \left(\left[\frac{\dot{p}_f}{K_f^\eta} (\beta\Delta t^2) + (\gamma\Delta t) \right] \frac{\partial(\delta a)}{\partial X} + \frac{Jn^f}{K_f^\eta} (\gamma\Delta t) \delta\ddot{p}_f \right) A dX . \quad (4.484)$$

The linearization of Equation (4.66)₂ is given by (for poroelasticity, refer to Equation (B.30)):

$$\begin{aligned} \delta\mathcal{H}_2^{\text{INT}} = \int_0^{X=H} w^{p_f} \left(\left[(n^f \tilde{v}_f) - \hat{k} \frac{\partial p_f}{\partial X} (F_{11})^{-1} \right] (\beta\Delta t^2) \frac{\partial(\delta\ddot{p}_f)}{\partial X} - \hat{k} \frac{\partial p_f}{\partial X} (a + g) \frac{\rho^{\text{fR}}}{K_f^\eta} (\beta\Delta t^2) \delta\ddot{p}_f \right. \\ \left. + \frac{\partial p_f}{\partial X} \left[\frac{\delta \hat{k}}{\hat{k}} (n^f \tilde{v}_f) + \frac{\partial p_f}{\partial X} \hat{k} F_{11}^{-2} \right] (\beta\Delta t^2) \frac{\partial(\delta a)}{\partial X} - \frac{\partial p_f}{\partial X} \hat{k} \rho^{\text{fR}} \delta a \right) \frac{A}{K_f^\eta} dX . \quad (4.485) \end{aligned}$$

The linearization of Equation (4.66)₃ is given by (for poroelasticity, refer to Equation (B.33)):

$$\begin{aligned} \delta\mathcal{H}_3^{\text{INT}} = \int_0^{X=H} \frac{\partial w^{p_f}}{\partial X} \left([\delta_{\hat{k}} - \hat{k}F_{11}^{-1}] \frac{\partial p_f}{\partial X} F_{11}^{-1} (\beta\Delta t^2) \frac{\partial(\delta a)}{\partial X} \right. \\ \left. + \hat{k}F_{11}^{-1} (\beta\Delta t^2) \frac{\partial(\delta\ddot{p}_f)}{\partial X} \right) A dX . \end{aligned} \quad (4.486)$$

The linearization of Equation (4.66)₄ is given by (for poroelasticity, refer to Equation (B.35)):

$$\begin{aligned} \delta\mathcal{H}_4^{\text{INT}} = \int_0^{X=H} \frac{\partial w^{p_f}}{\partial X} \rho^{\text{fR}} \left(\delta_{\hat{k}} (a + g) (\beta\Delta t^2) \frac{\partial(\delta a)}{\partial X} \right. \\ \left. + \hat{k}(a + g) \frac{1}{K_f} (\beta\Delta t^2) \delta\ddot{p}_f + \hat{k}\delta a \right) A dX . \end{aligned} \quad (4.487)$$

The linearization of the external force vector given by Equation (4.66)₅ is of course unnecessary as this term is simply subtracted from the residual at every Newton-Raphson iteration. For pressure stabilization, the linearization of Equation (4.600) is given by (for poroelasticity, which often does not require the employment of pressure stabilization, refer to Equation (B.37)):

$$\delta\mathcal{H}^{\text{stab}} = \int_0^{X=H} \frac{\partial w^{p_f}}{\partial X} \alpha^{\text{stab}} F_{11}^{-1} \left((\gamma\Delta t) \frac{\partial(\delta\ddot{p}_f)}{\partial X} - \frac{\partial\dot{p}_f}{\partial X} F_{11}^{-1} (\beta\Delta t^2) \frac{\partial(\delta a)}{\partial X} \right) A dX . \quad (4.488)$$

Finite element formulation. The finite element formulation for the $(\mathbf{u}-p_f)$ formulation is presented as follows, with additional details being covered in Appendix C.1.2.

The FE formulation for the $(\mathbf{u}-p_f)$ poroelastodynamics variational equations is written in block-matrix form as

$$\underbrace{\begin{bmatrix} \mathbf{K}_{u,u} & \mathbf{K}_{p_f,u} \\ \mathbf{K}_{u,p_f} & \mathbf{K}_{p_f,p_f} \end{bmatrix}}_{(n_{\text{dof}}^s + n_{\text{dof}}^{p_f}) \times (n_{\text{dof}}^s + n_{\text{dof}}^{p_f})} \cdot \underbrace{\begin{Bmatrix} \delta\mathbf{d} \\ \delta\dot{\pi} \end{Bmatrix}}_{(n_{\text{dof}}^s + n_{\text{dof}}^{p_f}) \times 1} = \underbrace{\begin{Bmatrix} -\mathbf{R}_u \\ -\mathbf{R}_{p_f} \end{Bmatrix}}_{(n_{\text{dof}}^s + n_{\text{dof}}^{p_f}) \times 1} . \quad (4.489)$$

The finite element formulation for the poroelasticity variational equations is written in block-matrix formation as

$$\underbrace{\begin{bmatrix} \mathbf{K}_{u,u} & \mathbf{K}_{p_f,u} \\ \mathbf{K}_{u,p_f} & \mathbf{K}_{p_f,p_f} \end{bmatrix}}_{(n_{\text{dof}}^s + n_{\text{dof}}^{p_f}) \times (n_{\text{dof}}^s + n_{\text{dof}}^{p_f})} \cdot \underbrace{\begin{Bmatrix} \delta\mathbf{d} \\ \delta\dot{\pi} \end{Bmatrix}}_{(n_{\text{dof}}^s + n_{\text{dof}}^{p_f}) \times 1} = \underbrace{\begin{Bmatrix} -\mathbf{R}_u \\ -\mathbf{R}_{p_f} \end{Bmatrix}}_{(n_{\text{dof}}^s + n_{\text{dof}}^{p_f}) \times 1} . \quad (4.490)$$

The global residual for the solid skeleton displacement is given as

$$\mathbf{c}^{u,T} \cdot \mathbf{R}_u = \mathcal{G}^h = \mathcal{G}_1^{\text{INT},h} + \mathcal{G}_2^{\text{INT},h} + \mathcal{G}_3^{\text{INT},h} + \mathcal{G}_4^{\text{INT},h} - \mathcal{G}^{\text{EXT},h} = 0, \quad (4.491)$$

where

$$\begin{aligned} \mathcal{G}_1^{\text{INT},h} &= \mathbf{A}_e^{n_e} \underbrace{\left\{ \mathbf{c}^{u,e} \right\}^T}_{1 \times n_{\text{dof}}^{s,e}} \cdot \left(\int_{-1}^1 \underbrace{\left\{ \mathbf{N}^{e,u} \right\}^T}_{n_{\text{dof}}^{s,e} \times 1} \rho_0^{h^e} a^{h^e} A j^e d\xi \right), \\ \mathcal{G}_2^{\text{INT},h} &= \mathbf{A}_e^{n_e} \underbrace{\left\{ \mathbf{c}^{u,e} \right\}^T}_{1 \times n_{\text{dof}}^{s,e}} \cdot \left(\int_{-1}^1 \underbrace{\left\{ \mathbf{B}^{e,u} \right\}^T}_{n_{\text{dof}}^{s,e} \times 1} P_{11(E)}^{s,h^e} A j^e d\xi \right), \\ \mathcal{G}_3^{\text{INT},h} &= \mathbf{A}_e^{n_e} \underbrace{\left\{ \mathbf{c}^{u,e} \right\}^T}_{1 \times n_{\text{dof}}^{s,e}} \cdot \left(- \int_{-1}^1 \underbrace{\left\{ \mathbf{B}^{e,u} \right\}^T}_{n_{\text{dof}}^{s,e} \times 1} p_f^{h^e} A j^e d\xi \right) \\ \mathcal{G}_4^{\text{INT},h} &= \mathbf{A}_e^{n_e} \underbrace{\left\{ \mathbf{c}^{u,e} \right\}^T}_{1 \times n_{\text{dof}}^{s,e}} \cdot \left(\int_{-1}^1 \underbrace{\left\{ \mathbf{N}^{e,u} \right\}^T}_{n_{\text{dof}}^{s,e} \times 1} \rho_0^{h^e} g A j^e d\xi \right), \\ \mathcal{G}^{\text{EXT},h} &= \mathbf{A}_e^{n_e} \underbrace{\left\{ \mathbf{c}^{u,e} \right\}^T}_{1 \times n_{\text{dof}}^{s,e}} \cdot \begin{cases} \underbrace{\left\{ \mathbf{N}^{e,u}(X=0, H) \right\}^T}_{n_{\text{dof}}^{s,e} \times 1} t^\sigma A & X=0, H \\ \mathbf{0} & 0 < X < H. \end{cases} \end{aligned} \quad (4.492)$$

For poroelasticity, Equation (4.492)₁ is zero.

The global residual for the pore fluid pressure is given as

$$\mathbf{c}^{p_f,T} \cdot \mathbf{R}_{p_f} = \mathcal{H}^h = \mathcal{H}_1^{\text{INT},h} + \mathcal{H}_2^{\text{INT},h} + \mathcal{H}_3^{\text{INT},h} + \mathcal{H}_4^{\text{INT},h} - \mathcal{H}^{\text{EXT},h} = 0, \quad (4.493)$$

where

$$\begin{aligned}
\mathcal{H}_1^{\text{INT},h} &= \mathbf{A}_e \underbrace{\left\{ \mathbf{c}^{p_f,e} \right\}^T}_{1 \times n_{\text{dof}}^{p_f,e}} \cdot \left(\int_{-1}^1 \underbrace{\left\{ \mathbf{N}^{e,p_f} \right\}^T}_{n_{\text{dof}}^{p_f,e} \times 1} \left[\frac{J^{h^e} n^{f,h^e}}{K_f^\eta} \dot{p}_f^{h^e} + j^{h^e} \right] A_j^e d\xi \right), \\
\mathcal{H}_2^{\text{INT},h} &= \mathbf{A}_e \underbrace{\left\{ \mathbf{c}^{p_f,e} \right\}^T}_{1 \times n_{\text{dof}}^{p_f,e}} \cdot \left(\int_{-1}^1 \underbrace{\left\{ \mathbf{N}^{e,p_f} \right\}^T}_{n_{\text{dof}}^{p_f,e} \times 1} \frac{1}{K_f^\eta} \frac{\partial p_f^{h^e}}{\partial X} (n^f \tilde{v}_f)^{h^e} A_j^e d\xi \right), \\
\mathcal{H}_3^{\text{INT},h} &= \mathbf{A}_e \underbrace{\left\{ \mathbf{c}^{p_f,e} \right\}^T}_{1 \times n_{\text{dof}}^{p_f,e}} \cdot \left(\int_{-1}^1 \underbrace{\left\{ \mathbf{B}^{e,p_f} \right\}^T}_{n_{\text{dof}}^{p_f,e} \times 1} \hat{k}^{h^e} \frac{\partial p_f^{h^e}}{\partial X} (F_{11}^{h^e})^{-1} A_j^e d\xi \right), \\
\mathcal{H}_4^{\text{INT},h} &= \mathbf{A}_e \underbrace{\left\{ \mathbf{c}^{p_f,e} \right\}^T}_{1 \times n_{\text{dof}}^{p_f,e}} \cdot \left(\int_{-1}^1 \underbrace{\left\{ \mathbf{B}^{e,p_f} \right\}^T}_{n_{\text{dof}}^{p_f,e} \times 1} \hat{k}^{h^e} \rho^{\text{fR},h^e} (a^{h^e} + g) A_j^e d\xi \right), \\
\mathcal{H}^{\text{EXT},h} &= \mathbf{A}_e \underbrace{\left\{ \mathbf{c}^{p_f,e} \right\}^T}_{1 \times n_{\text{dof}}^{p_f,e}} \cdot \begin{cases} \underbrace{\left\{ \mathbf{N}^{e,p_f}(X=0, H) \right\}^T}_{n_{\text{dof}}^{p_f,e} \times 1} Q_f A & X=0, H \\ \mathbf{0} & 0 < X < H. \end{cases}
\end{aligned} \tag{4.494}$$

For poroelasticity, Equation (4.494)₄ becomes

$$\mathcal{H}_4^{\text{INT},h} = \mathbf{A}_e \underbrace{\left\{ \mathbf{c}^{p_f,e} \right\}^T}_{1 \times n_{\text{dof}}^{p_f,e}} \cdot \left(\int_{-1}^1 \underbrace{\left\{ \mathbf{B}^{e,p_f} \right\}^T}_{n_{\text{dof}}^{p_f,e} \times 1} \hat{k}^{h^e} \rho^{\text{fR},h^e} g A_j^e d\xi \right). \tag{4.495}$$

When pressure stabilization is enabled, an additional term $\mathcal{H}^{\text{stab}}$ is added to the l.h.s. of Equation (4.493) and is defined as

$$\mathcal{H}^{\text{stab}} = \mathbf{A}_e \underbrace{\left\{ \mathbf{c}^{p_f,e} \right\}^T}_{1 \times n_{\text{dof}}^{p_f,e}} \cdot \left(\int_{-1}^1 \underbrace{\left\{ \mathbf{B}^{e,p_f} \right\}^T}_{n_{\text{dof}}^{p_f,e} \times 1} \alpha^{\text{stab}} \frac{\partial p_f^{h^e}}{\partial X} (F_{11}^{h^e})^{-1} A_j^e d\xi \right). \tag{4.496}$$

The tangent matrix for the (\mathbf{u} - p_f) formulation for each iteration must be of the form

$$\begin{aligned} \mathbf{0} = \mathbf{R}^k &= \left(\frac{\partial \mathbf{R}}{\partial \mathbf{A}} \right) \delta \mathbf{A} = \begin{bmatrix} \frac{\partial \mathbf{R}_u}{\partial \mathbf{a}} & \frac{\partial \mathbf{R}_u}{\partial \ddot{p}_f} \\ \frac{\partial \mathbf{R}_{p_f}}{\partial \mathbf{a}} & \frac{\partial \mathbf{R}_{p_f}}{\partial \ddot{p}_f} \end{bmatrix} \cdot \begin{Bmatrix} \delta \mathbf{a} \\ \delta \ddot{p}_f \end{Bmatrix} \\ &= \underbrace{\begin{bmatrix} \mathbf{K}_{u,u} & \mathbf{K}_{u,p_f} \\ \mathbf{K}_{p_f,u} & \mathbf{K}_{p_f,p_f} \end{bmatrix}}_{(n_{\text{dof}}^s + n_{\text{dof}}^{p_f}) \times (n_{\text{dof}}^s + n_{\text{dof}}^{p_f})} \cdot \underbrace{\begin{Bmatrix} \delta \ddot{\mathbf{d}} \\ \delta \ddot{\boldsymbol{\pi}} \end{Bmatrix}}_{(n_{\text{dof}}^s + n_{\text{dof}}^{p_f}) \times 1}, \end{aligned} \quad (4.497)$$

or, for poroelasticity,

$$\begin{aligned} \mathbf{0} = \mathbf{R}^k &= \left(\frac{\partial \mathbf{R}}{\partial \mathbf{V}} \right) \delta \mathbf{V} = \begin{bmatrix} \frac{\partial \mathbf{R}_u}{\partial \mathbf{v}} & \frac{\partial \mathbf{R}_u}{\partial \dot{p}_f} \\ \frac{\partial \mathbf{R}_{p_f}}{\partial \mathbf{v}} & \frac{\partial \mathbf{R}_{p_f}}{\partial \dot{p}_f} \end{bmatrix} \cdot \begin{Bmatrix} \delta \mathbf{v} \\ \delta \dot{p}_f \end{Bmatrix} \\ &= \underbrace{\begin{bmatrix} \mathbf{K}_{u,u} & \mathbf{K}_{u,p_f} \\ \mathbf{K}_{p_f,u} & \mathbf{K}_{p_f,p_f} \end{bmatrix}}_{(n_{\text{dof}}^s + n_{\text{dof}}^{p_f}) \times (n_{\text{dof}}^s + n_{\text{dof}}^{p_f})} \cdot \underbrace{\begin{Bmatrix} \delta \dot{\mathbf{d}} \\ \delta \dot{\boldsymbol{\pi}} \end{Bmatrix}}_{(n_{\text{dof}}^s + n_{\text{dof}}^{p_f}) \times 1}, \end{aligned} \quad (4.498)$$

where

$$\begin{aligned} \underbrace{\begin{bmatrix} \mathbf{K}_{u,u} \end{bmatrix}}_{n_{\text{dof}}^s \times n_{\text{dof}}^s} &= \underbrace{\mathbf{A}_e}_{1 \times n_{\text{dof}}^{s,e}} \underbrace{\left\{ \mathbf{c}^{u,e} \right\}^T}_{1 \times n_{\text{dof}}^{s,e}} \cdot \sum_{i=1}^2 \underbrace{\left[\mathbf{k}_{u,u}^{\mathcal{G}_i^{\text{INT},e}} \right]}_{n_{\text{dof}}^{s,e} \times n_{\text{dof}}^{s,e}}, \\ \underbrace{\begin{bmatrix} \mathbf{K}_{u,p_f} \end{bmatrix}}_{n_{\text{dof}}^s \times n_{\text{dof}}^{p_f}} &= \underbrace{\mathbf{A}_e}_{1 \times n_{\text{dof}}^{s,e}} \underbrace{\left\{ \mathbf{c}^{u,e} \right\}^T}_{1 \times n_{\text{dof}}^{s,e}} \cdot \underbrace{\left[\mathbf{k}_{u,p_f}^{\mathcal{G}_3^{\text{INT},e}} \right]}_{n_{\text{dof}}^{s,e} \times n_{\text{dof}}^{p_f,e}}, \\ \underbrace{\begin{bmatrix} \mathbf{K}_{p_f,u} \end{bmatrix}}_{n_{\text{dof}}^{p_f} \times n_{\text{dof}}^s} &= \underbrace{\mathbf{A}_e}_{1 \times n_{\text{dof}}^{p_f,e}} \underbrace{\left\{ \mathbf{c}^{p_f,e} \right\}^T}_{1 \times n_{\text{dof}}^{p_f,e}} \cdot \sum_{i=1}^4 \underbrace{\left[\mathbf{k}_{p_f,u}^{\mathcal{H}_i^{\text{INT},e}} \right]}_{n_{\text{dof}}^{p_f,e} \times n_{\text{dof}}^{s,e}}, \\ \underbrace{\begin{bmatrix} \mathbf{K}_{p_f,p_f} \end{bmatrix}}_{n_{\text{dof}}^{p_f} \times n_{\text{dof}}^{p_f}} &= \underbrace{\mathbf{A}_e}_{1 \times n_{\text{dof}}^{p_f,e}} \underbrace{\left\{ \mathbf{c}^{p_f,e} \right\}^T}_{1 \times n_{\text{dof}}^{p_f,e}} \cdot \sum_{i=1}^4 \underbrace{\left[\mathbf{k}_{p_f,p_f}^{\mathcal{H}_i^{\text{INT},e}} \right]}_{n_{\text{dof}}^{p_f,e} \times n_{\text{dof}}^{p_f,e}}, \end{aligned} \quad (4.499)$$

where the definitions for $\mathbf{K}_{u,u}$ remain unchanged from Section 4.3.2.3 (refer to Equations (4.482)_{1,2}).

The skeleton displacement and pore fluid pressure coupling tangent is given as follows:

$$\underbrace{\left[\mathbf{k}_{u,p_f}^{\mathcal{G}_3^{\text{INT},e}} \right]}_{n_{\text{dof}}^{s,e} \times n_{\text{dof}}^{p_f,e}} = - \int_{-1}^1 (\beta \Delta t^2) \underbrace{\left\{ \mathbf{B}^{e,u} \right\}^T}_{n_{\text{dof}}^{s,e} \times 1} \underbrace{\left\{ \mathbf{N}^{e,p_f} \right\}}_{1 \times n_{\text{dof}}^{p_f,e}} A_j^e d\xi \quad (4.500)$$

The pore fluid pressure and solid skeleton coupling tangents are given as follows:

$$\begin{aligned} \underbrace{\left[\mathbf{k}_{p_f,u}^{\mathcal{H}_1^{\text{INT},e}} \right]}_{n_{\text{dof}}^{p_f,e} \times n_{\text{dof}}^{s,e}} &= \int_{-1}^1 \left(\frac{\dot{p}_f^{h^e}}{K_f^\eta} (\beta \Delta t^2) + (\gamma \Delta t) \right) \underbrace{\left\{ \mathbf{N}^{e,p_f} \right\}^T}_{n_{\text{dof}}^{p_f,e} \times 1} \underbrace{\left\{ \mathbf{B}^{e,u} \right\}}_{1 \times n_{\text{dof}}^{s,e}} A_j^e d\xi, \\ \underbrace{\left[\mathbf{k}_{p_f,u}^{\mathcal{H}_2^{\text{INT},e}} \right]}_{n_{\text{dof}}^{p_f,e} \times n_{\text{dof}}^{s,e}} &= \int_{-1}^1 \underbrace{\left\{ \mathbf{N}^{e,p_f} \right\}^T}_{n_{\text{dof}}^{p_f,e} \times 1} \left(\frac{\delta_k^{h^e}}{\hat{k}^{h^e}} (n^f \tilde{v}_f)^{h^e} + \hat{k}^{h^e} \frac{\partial p_f^{h^e}}{\partial X} (F_{11}^{h^e})^{-2} \right) (\beta \Delta t^2) \underbrace{\left\{ \mathbf{B}^{e,u} \right\}}_{1 \times n_{\text{dof}}^{s,e}} \\ &\quad - \hat{k}^{h^e} \rho^{\text{fR},h^e} \underbrace{\left\{ \mathbf{N}^{e,u} \right\}}_{1 \times n_{\text{dof}}^{s,e}} \frac{\partial p_f^{h^e}}{\partial X} \frac{1}{K_f^\eta} A_j^e d\xi, \end{aligned} \quad (4.501)$$

$$\begin{aligned} \underbrace{\left[\mathbf{k}_{p_f,u}^{\mathcal{H}_3^{\text{INT},e}} \right]}_{n_{\text{dof}}^{p_f,e} \times n_{\text{dof}}^{s,e}} &= \int_{-1}^1 \frac{\partial p_f^{h^e}}{\partial X} (F_{11}^{h^e})^{-1} (\delta_k^{h^e} - \hat{k}^{h^e} [F_{11}^{h^e}]^{-1}) (\beta \Delta t^2) \underbrace{\left\{ \mathbf{B}^{e,p_f} \right\}^T}_{n_{\text{dof}}^{p_f,e} \times 1} \underbrace{\left\{ \mathbf{B}^{e,u} \right\}}_{1 \times n_{\text{dof}}^{s,e}} A_j^e d\xi, \\ \underbrace{\left[\mathbf{k}_{p_f,u}^{\mathcal{H}_4^{\text{INT},e}} \right]}_{n_{\text{dof}}^{p_f,e} \times n_{\text{dof}}^{s,e}} &= \int_{-1}^1 \underbrace{\left\{ \mathbf{B}^{e,p_f} \right\}^T}_{n_{\text{dof}}^{p_f,e} \times 1} \left(\delta_k^{h^e} (a^{h^e} + g) (\beta \Delta t^2) \underbrace{\left\{ \mathbf{B}^{e,u} \right\}}_{1 \times n_{\text{dof}}^{s,e}} + \hat{k}^{h^e} \underbrace{\left\{ \mathbf{N}^{e,u} \right\}}_{1 \times n_{\text{dof}}^{s,e}} \right) \rho^{\text{fR},h^e} A_j^e d\xi. \end{aligned}$$

For poroelasticity, Equations (4.501)₁₋₄ are given by Equations (C.31), Equation (C.39), Equation (C.47) and Equation (C.55). When pressure stabilization is enabled, we must add one more pore fluid pressure and solid skeleton coupling tangent to Equation (4.499)₃:

$$\underbrace{\left[\mathbf{k}_{p_f,u}^{\mathcal{H}^{\text{stab},e}} \right]}_{n_{\text{dof}}^{p_f,e} \times n_{\text{dof}}^{s,e}} = - \int_{-1}^1 \alpha^{\text{stab}} (F_{11}^{h^e})^{-2} \frac{\partial p_f^{h^e}}{\partial X} (\beta \Delta t^2) \underbrace{\left\{ \mathbf{B}^{e,p_f} \right\}^T}_{n_{\text{dof}}^{p_f,e} \times 1} \underbrace{\left\{ \mathbf{B}^{e,u} \right\}}_{1 \times n_{\text{dof}}^{s,e}} A_j^e d\xi. \quad (4.502)$$

For poroelasticity, Equation (4.502) is given by Equation (C.63). Lastly, the pore fluid pressure

tangents are given as follows:

$$\begin{aligned}
\underbrace{\left[\mathbf{k}_{p_f, p_f}^{\mathcal{H}_1^{\text{INT}, e}} \right]}_{n_{\text{dof}}^{p_f, e} \times n_{\text{dof}}^{p_f, e}} &= \int_{-1}^1 \frac{J^{h^e} n^{f, h^e}}{K_f^\eta} (\gamma \Delta t) \underbrace{\left\{ \mathbf{N}^{e, p_f} \right\}^T}_{n_{\text{dof}}^{p_f, e} \times 1} \underbrace{\left\{ \mathbf{N}^{e, p_f} \right\}}_{1 \times n_{\text{dof}}^{p_f, e}} A_j^e d\xi, \\
\underbrace{\left[\mathbf{k}_{p_f, p_f}^{\mathcal{H}_2^{\text{INT}, e}} \right]}_{n_{\text{dof}}^{p_f, e} \times n_{\text{dof}}^{p_f, e}} &= \int_{-1}^1 \underbrace{\left\{ \mathbf{N}^{e, p_f} \right\}^T}_{n_{\text{dof}}^{p_f, e} \times 1} \left(\left[(n^f \tilde{v}_f)^{h^e} - \hat{k}^{h^e} \frac{\partial p_f^{h^e}}{\partial X} (F_{11}^{h^e})^{-1} \right] \underbrace{\left\{ \mathbf{B}^{e, p_f} \right\}}_{1 \times n_{\text{dof}}^{p_f, e}} \right. \\
&\quad \left. - \hat{k}^{h^e} \frac{\partial p_f^{h^e}}{\partial X} (a^{h^e} + g) \frac{\rho^{\text{fR}, h^e}}{K_f^\eta} \underbrace{\left\{ \mathbf{N}^{e, p_f} \right\}}_{1 \times n_{\text{dof}}^{p_f, e}} \right) \frac{1}{K_f^\eta} (\beta \Delta t^2) A_j^e d\xi, \tag{4.503}
\end{aligned}$$

$$\begin{aligned}
\underbrace{\left[\mathbf{k}_{p_f, p_f}^{\mathcal{H}_3^{\text{INT}, e}} \right]}_{n_{\text{dof}}^{p_f, e} \times n_{\text{dof}}^{p_f, e}} &= \int_{-1}^1 \hat{k}^{h^e} (F_{11}^{h^e})^{-1} (\beta \Delta t^2) \underbrace{\left\{ \mathbf{B}^{e, p_f} \right\}^T}_{n_{\text{dof}}^{p_f, e} \times 1} \underbrace{\left\{ \mathbf{B}^{e, p_f} \right\}}_{1 \times n_{\text{dof}}^{p_f, e}} A_j^e d\xi, \\
\underbrace{\left[\mathbf{k}_{p_f, p_f}^{\mathcal{H}_4^{\text{INT}, e}} \right]}_{n_{\text{dof}}^{p_f, e} \times n_{\text{dof}}^{p_f, e}} &= \int_{-1}^1 \hat{k}^{h^e} (a^{h^e} + g) \frac{\rho^{\text{fR}, h^e}}{K_f^\eta} (\beta \Delta t^2) \underbrace{\left\{ \mathbf{B}^{e, p_f} \right\}^T}_{n_{\text{dof}}^{p_f, e} \times 1} \underbrace{\left\{ \mathbf{N}^{e, p_f} \right\}}_{1 \times n_{\text{dof}}^{p_f, e}} A_j^e d\xi.
\end{aligned}$$

For poroelasticity, Equations (4.503)_{1–4} are given by Equations (C.32), Equation (C.40), Equation (C.48) and Equation (C.56). When pressure stabilization is enabled, we must add one more pore fluid pressure tangent to Equation (4.499)₄:

$$\underbrace{\left[\mathbf{k}_{p_f, p_f}^{\mathcal{H}^{\text{stab}, e}} \right]}_{n_{\text{dof}}^{p_f, e} \times n_{\text{dof}}^{p_f, e}} = \int_{-1}^1 \alpha^{\text{stab}} (F_{11}^{h^e})^{-1} (\gamma \Delta t) \underbrace{\left\{ \mathbf{B}^{e, p_f} \right\}^T}_{n_{\text{dof}}^{p_f, e} \times 1} \underbrace{\left\{ \mathbf{B}^{e, p_f} \right\}}_{1 \times n_{\text{dof}}^{p_f, e}} A_j^e d\xi. \tag{4.504}$$

For poroelasticity, Equation (4.504) is given by Equation (C.64).

4.3.2.5 ($\mathbf{u}-\mathbf{u}_f-p_f$) formulation

Linearization of the variational equations. Detailed derivations of the following linearized equations are provided in Appendix B.4. The linearization of Equation (4.86)₁ is given as follows under the assumption that the Gateaux derivative of the real mass density of the solid phase is negligible owing to the incompressibility assumption:

$$\delta \mathcal{G}_1^{\text{INT}} = \int_0^{X=H} w^u \left(\rho_0^s \delta a + a_f (\beta \Delta t^2) \left[\rho^{\text{fR}} \frac{\partial (\delta a)}{\partial X} + \frac{J n^f \rho^{\text{fR}}}{K_f^\eta} \delta \ddot{p}_f \right] + \rho_0^f \delta a_f \right) A dX. \tag{4.505}$$

The linearizations of Equations (4.86)_{2,3} remain unchanged from the $(\mathbf{u}-p_f)$ formulation; refer to Equations (4.474), Equation (4.483) for $\delta\mathcal{G}_2^{\text{INT}}$ and $\delta\mathcal{G}_3^{\text{INT}}$, respectively. As before, $\delta\mathcal{G}_4^{\text{INT}} \approx 0$ under the assumption that the variation of mass density of the mixture is negligible.

The derivation of the Gateaux derivative of the pore fluid extra stress tensor, which contributes to block matrices $\mathbf{K}_{u,u}$, \mathbf{K}_{u,u_f} , proceeds as follows:

$$\delta(\sigma_{11(E)}^f) = \delta\left(n^f \frac{\partial v_f}{\partial X}\right) (\kappa_f + 2\mu_f) = \left(\frac{n^s}{J} (\beta\Delta t^2) \frac{\partial(\delta a)}{\partial X} + n^f (\gamma\Delta t) \frac{\partial(\delta a_f)}{\partial X}\right) (\kappa_f + 2\eta_f), \quad (4.506)$$

where we assume pore fluid bulk viscosity κ_f and pore fluid shear viscosity μ_f are not functions of the independent variables u, u_f, p_f . Thus, the linearization of Equation (4.93)₁, $\delta\mathcal{G}_5^{\text{INT}}$, is

$$\delta\mathcal{G}_5^{\text{INT}} = \int_0^{X=H} \frac{\partial w^u}{\partial X} \left(\frac{n^s}{J} (\beta\Delta t^2) \frac{\partial(\delta a)}{\partial X} + n^f (\gamma\Delta t) \frac{\partial(\delta a_f)}{\partial X}\right) (\kappa_f + 2\mu_f) A dX. \quad (4.507)$$

The linearization of Equation (4.88)₁ is given as

$$\delta\mathcal{I}_1^{\text{INT}} = \int_0^{X=H} w^{u_f} \left(a_f (\beta\Delta t^2) \left[\rho^{\text{fR}} \frac{\partial(\delta a)}{\partial X} + \frac{J n^f \rho^{\text{fR}}}{K_f^\eta} \delta \ddot{p}_f\right] + \rho_0^f \delta a_f\right) A dX. \quad (4.508)$$

The linearization of Equation (4.88)₂ is given as

$$\delta\mathcal{I}_2^{\text{INT}} = \int_0^{X=H} w^{u_f} \left(\frac{n^s}{J} \frac{\partial p_f}{\partial X} \frac{\partial(\delta a)}{\partial X} + n^f \frac{\partial(\delta \ddot{p}_f)}{\partial X}\right) (\beta\Delta t^2) A dX. \quad (4.509)$$

The linearization of Equation (4.88)₃ is given as

$$\delta\mathcal{I}_3^{\text{INT}} = \int_0^{X=H} w^{u_f} \left(\left[1 + \frac{2n^s}{n^f} - \frac{J\delta_{\hat{k}}}{\hat{k}}\right] \frac{(n^f)^2 \tilde{v}_f}{\hat{k}} (\beta\Delta t^2) \frac{\partial \delta a}{\partial X} + \frac{J(n^f)^2}{\hat{k}} (\gamma\Delta t) (\delta a_f - \delta a)\right) A dX. \quad (4.510)$$

The linearization of Equation (4.88)₄ is given as

$$\delta\mathcal{I}_4^{\text{INT}} = \int_0^{X=H} w^{u_f} \left(\left[\rho^{\text{fR}} \frac{\partial(\delta a)}{\partial X} + \frac{J n^f \rho^{\text{fR}}}{K_f^\eta} \delta \ddot{p}_f\right] (\beta\Delta t^2)\right) g A dX. \quad (4.511)$$

The variation of Equation (4.93)₃, $\delta\mathcal{I}_5^{\text{INT}}$, is

$$\begin{aligned} \delta\mathcal{I}_5^{\text{INT}} = \int_0^{X=H} w^{u_f} (\kappa_f + 2\mu_f) & \left(\left[(n^s - n^f) \frac{\partial^2 v_f}{\partial X^2} - 4 \frac{\partial n^f}{\partial X} \frac{\partial v_f}{\partial X}\right] F_{11}^{-2} (\beta\Delta t^2) \frac{\partial(\delta a)}{\partial X} \right. \\ & \left. + (\gamma\Delta t) F_{11}^{-1} \left[\frac{\partial n^f}{\partial X} \frac{\partial(\delta a_f)}{\partial X} + n^f \frac{\partial^2(\delta a_f)}{\partial X^2}\right]\right) A dX. \end{aligned} \quad (4.512)$$

The linearizations of Equations (4.89)_{1,3} and 4.600 remain unchanged from the $(\mathbf{u}-p_f)$ formulation; refer to Eqs. 4.484, 4.486 and 4.488, respectively.

The linearizations of Eqs. 4.89_{2,4} are different from the $(\mathbf{u}-p_f)$ formulation given that the pore fluid acceleration is used in place of the mixture's acceleration (i.e., the solid skeleton acceleration in the $(\mathbf{u}-\mathbf{u}_f-p_f)$ formulation) in the constitutive model for Darcy's law. Furthermore, the pore fluid viscous stress appears in these terms when considered. The Gateaux derivative of the divergence of the pore fluid extra stress term that is scaled by porosity and inverse deformation gradient, is used in variation of $\mathcal{H}_2^{\text{INT}}$, $\mathcal{H}_5^{\text{INT}}$, and is given by

$$\begin{aligned} \delta \left(\frac{1}{n^f} \frac{\partial \sigma_{11}^f(E)}{\partial X} F_{11}^{-1} \right) = & - \left(\frac{\partial n^f}{\partial X} \frac{\partial v_f}{\partial X} \frac{n^s}{(n^f)^2} + 5 \frac{1}{n^f} \frac{\partial n^f}{\partial X} \frac{\partial v_f}{\partial X} + 2 \frac{\partial^2 v_f}{\partial X^2} \right) F_{11}^{-3} (\kappa_f + 2\mu_f) \beta \Delta t^2 \frac{\partial(\delta a)}{\partial X} \\ & + \frac{n_0^s}{F_{11}^5} \frac{1}{n^f} \frac{\partial v_f}{\partial X} (\kappa_f + 2\mu_f) \beta \Delta t^2 \frac{\partial^2(\delta a)}{\partial X^2} + \frac{1}{n^f} \frac{\partial n^f}{\partial X} (\kappa_f + 2\mu_f) F_{11}^{-2} \gamma \Delta t \frac{\partial(\delta a_f)}{\partial X} \\ & + (\kappa_f + 2\mu_f) F_{11}^{-2} \gamma \Delta t \frac{\partial^2(\delta a_f)}{\partial X^2}. \end{aligned} \quad (4.513)$$

Thus, variation of Equation (4.89)₂, δH_2^{INT} , becomes

$$\begin{aligned} \delta \mathcal{H}_2^{\text{INT}} = & \int_0^{X=H} w^{p_f} \left(\left[(n^f \tilde{v}_f) - \hat{k} \frac{\partial p_f}{\partial X} \right] (\beta \Delta t^2) \frac{\partial(\delta \ddot{p}_f)}{\partial X} - \hat{k} \frac{\partial p_f}{\partial X} (a_f + g) \frac{\rho^{\text{fR}}}{K_f^\eta} \right. \\ & \times (\beta \Delta t^2) \delta \ddot{p}_f + \frac{\partial p_f}{\partial X} \left[\frac{\delta \hat{k}}{\hat{k}} (n^f \tilde{v}_f) + \hat{k} \frac{\partial p_f}{\partial X} F_{11}^{-2} \right. \\ & + \hat{k} \left(\left[\frac{n^s}{(n^f)^2} + \frac{5}{n^f} \right] \frac{\partial n^f}{\partial X} \frac{\partial v_f}{\partial X} + 2 \frac{\partial^2 v_f}{\partial X^2} \right) F_{11}^{-3} (\kappa_f + 2\mu_f) \left. \right] (\beta \Delta t^2) \frac{\partial(\delta a)}{\partial X} \\ & - \frac{\partial p_f}{\partial X} \hat{k} \frac{n_0^s}{n^f} F_{11}^{-5} \frac{\partial v_f}{\partial X} (\kappa_f + 2\mu_f) \beta \Delta t^2 \frac{\partial^2(\delta a)}{\partial X^2} - \frac{\partial p_f}{\partial X} \hat{k} \rho^{\text{fR}} \delta a_f \\ & \left. - \frac{\partial p_f}{\partial X} \hat{k} F_{11}^{-2} (\gamma \Delta t) \left[\frac{1}{n^f} \frac{\partial n^f}{\partial X} \frac{\partial(\delta a_f)}{\partial X} + \frac{\partial^2(\delta a_f)}{\partial X^2} \right] \right) \frac{A}{K_f^\eta} dX. \end{aligned} \quad (4.514)$$

The terms highlighted in red in Equation (4.514) correspond to the pore fluid viscous stress tensor; when a nearly-inviscid pore fluid is assumed, these terms are zero.

Next, variation of Equation (4.93)₄, $\delta\mathcal{H}_5^{\text{INT}}$, is given as

$$\begin{aligned} \delta\mathcal{H}_5^{\text{INT}} = & - \int_0^{X=H} \frac{\partial w^{p_f}}{\partial X} \hat{k} \left(\left[\left(\frac{\delta_{\hat{k}}}{n^f \hat{k}} \frac{\partial \sigma_{11}^f(E)}{\partial X} F_{11}^2 - \left[\frac{\partial n^f}{\partial X} \frac{\partial v_f}{\partial X} \left(\frac{n^s}{(n^f)^2} + \frac{5}{n^f} \right) + 2 \frac{\partial^2 v_f}{\partial X^2} \right] (\kappa_f + 2\mu_f) \right) \times \right. \right. \\ & F_{11}^{-3} \beta \Delta t^2 \frac{\partial(\delta a)}{\partial X} + \frac{n_0^s}{F_{11}^5} \frac{1}{n^f} \frac{\partial v_f}{\partial X} (\kappa_f + 2\mu_f) \beta \Delta t^2 \frac{\partial^2(\delta a)}{\partial X^2} \\ & \left. \left. + \frac{1}{n^f} \frac{\partial n^f}{\partial X} (\kappa_f + 2\mu_f) F_{11}^{-2} \gamma \Delta t \frac{\partial(\delta a_f)}{\partial X} + (\kappa_f + 2\mu_f) F_{11}^{-2} \gamma \Delta t \frac{\partial^2(\delta a_f)}{\partial X^2} \right) A dX . \end{aligned} \quad (4.515)$$

Finite element formulation. The FE formulation for the $(\mathbf{u}-\mathbf{u}_f-p_f)$ formulation is written in block-matrix form as

$$\underbrace{\begin{bmatrix} \mathbf{K}_{u,u} & \mathbf{K}_{u,u_f} & \mathbf{K}_{u,p_f} \\ \mathbf{K}_{u_f,u} & \mathbf{K}_{u_f,u_f} & \mathbf{K}_{u_f,p_f} \\ \mathbf{K}_{p_f,u} & \mathbf{K}_{p_f,u_f} & \mathbf{K}_{p_f,p_f} \end{bmatrix}}_{(n_{\text{dof}}^s+n_{\text{dof}}^f+n_{\text{dof}}^{p_f}) \times (n_{\text{dof}}^s+n_{\text{dof}}^f+n_{\text{dof}}^{p_f})} \cdot \underbrace{\begin{Bmatrix} \delta \ddot{\mathbf{d}} \\ \delta \ddot{\mathbf{d}}_f \\ \delta \ddot{\pi} \end{Bmatrix}}_{(n_{\text{dof}}^s+n_{\text{dof}}^f+n_{\text{dof}}^{p_f}) \times 1} = \underbrace{\begin{Bmatrix} -\mathbf{R}_u \\ -\mathbf{R}_{u_f} \\ -\mathbf{R}_{p_f} \end{Bmatrix}}_{(n_{\text{dof}}^s+n_{\text{dof}}^f+n_{\text{dof}}^{p_f}) \times 1} \quad (4.516)$$

The global residual for the solid skeleton displacement is given as

$$\mathbf{c}^{u,T} \cdot \mathbf{R}_u = \mathcal{G}^h = \mathcal{G}_1^{\text{INT},h} + \mathcal{G}_2^{\text{INT},h} + \mathcal{G}_3^{\text{INT},h} + \mathcal{G}_4^{\text{INT},h} + \mathcal{G}_5^{\text{INT},h} - \mathcal{G}^{\text{EXT},h} = 0, \quad (4.517)$$

where

$$\begin{aligned}
\mathcal{G}_1^{\text{INT},h} &= \mathbf{A}_e^{n_e} \underbrace{\left\{ \mathbf{c}^{u,e} \right\}^T}_{1 \times n_{\text{dof}}^{s,e}} \cdot \left(\int_{-1}^1 \underbrace{\left\{ \mathbf{N}^{e,u} \right\}^T}_{n_{\text{dof}}^{s,e} \times 1} (\rho_0^{s,h^e} a^{h^e} + \rho_0^{f,h^e} a_f^{h^e}) A j^e d\xi \right), \\
\mathcal{G}_2^{\text{INT},h} &= \mathbf{A}_e^{n_e} \underbrace{\left\{ \mathbf{c}^{u,e} \right\}^T}_{1 \times n_{\text{dof}}^{s,e}} \cdot \left(\int_{-1}^1 \underbrace{\left\{ \mathbf{B}^{e,u} \right\}^T}_{n_{\text{dof}}^{s,e} \times 1} P_{11(E)}^{s,h^e} A j^e d\xi \right), \\
\mathcal{G}_3^{\text{INT},h} &= \mathbf{A}_e^{n_e} \underbrace{\left\{ \mathbf{c}^{u,e} \right\}^T}_{1 \times n_{\text{dof}}^{s,e}} \cdot \left(- \int_{-1}^1 \underbrace{\left\{ \mathbf{B}^{e,u} \right\}^T}_{n_{\text{dof}}^{s,e} \times 1} p_f^{h^e} A j^e d\xi \right), \\
\mathcal{G}_4^{\text{INT},h} &= \mathbf{A}_e^{n_e} \underbrace{\left\{ \mathbf{c}^{u,e} \right\}^T}_{1 \times n_{\text{dof}}^{s,e}} \cdot \left(\int_{-1}^1 \underbrace{\left\{ \mathbf{N}^{e,u} \right\}^T}_{n_{\text{dof}}^{s,e} \times 1} \rho_0^{h^e} g A j^e d\xi \right), \\
\mathcal{G}_5^{\text{INT},h} &= \mathbf{A}_e^{n_e} \underbrace{\left\{ \mathbf{c}^{u,e} \right\}^T}_{1 \times n_{\text{dof}}^{s,e}} \cdot \left(\int_{-1}^1 \underbrace{\left\{ \mathbf{B}^{e,u} \right\}^T}_{n_{\text{dof}}^{s,e} \times 1} P_{11(E)}^{f,h^e} A j^e d\xi \right), \\
\mathcal{G}^{\text{EXT},h} &= \mathbf{A}_e^{n_e} \underbrace{\left\{ \mathbf{c}^{u,e} \right\}^T}_{1 \times n_{\text{dof}}^{s,e}} \cdot \begin{cases} \underbrace{\left\{ \mathbf{N}^{e,u}(X=0, H) \right\}^T}_{n_{\text{dof}}^{s,e} \times 1} t^\sigma A & X=0, H \\ \mathbf{0} & 0 < X < H. \end{cases}
\end{aligned} \tag{4.518}$$

When the pore fluid viscous stress tensor is not considered, $\mathcal{G}_5^{\text{INT},h}$ drops from Equation (4.517).

The global residual for the pore fluid displacement is given as

$$\mathbf{c}^{u_f, T} \cdot \mathbf{R}_{u_f} = \mathcal{I}^h = \mathcal{I}_1^{\text{INT},h} + \mathcal{I}_2^{\text{INT},h} + \mathcal{I}_3^{\text{INT},h} + \mathcal{I}_4^{\text{INT},h} + \mathcal{I}_5^{\text{INT},h} = 0 \tag{4.519}$$

where

$$\begin{aligned}
\mathcal{I}_1^{\text{INT},h} &= \mathbf{A}_e^{n_e} \underbrace{\left\{ \mathbf{c}^{u_f,e} \right\}^T}_{1 \times n_{\text{dof}}^{f,e}} \cdot \left(\int_{-1}^1 \underbrace{\left\{ \mathbf{N}^{e,u_f} \right\}^T}_{n_{\text{dof}}^{f,e} \times 1} \rho_0^{f,h^e} a_f^{h^e} A_j^e d\xi \right), \\
\mathcal{I}_2^{\text{INT},h} &= \mathbf{A}_e^{n_e} \underbrace{\left\{ \mathbf{c}^{u_f,e} \right\}^T}_{1 \times n_{\text{dof}}^{f,e}} \cdot \left(\int_{-1}^1 \underbrace{\left\{ \mathbf{N}^{e,u_f} \right\}^T}_{n_{\text{dof}}^{f,e} \times 1} n^{f,h^e} \frac{\partial p_f^{h^e}}{\partial X} A_j^e d\xi \right), \\
\mathcal{I}_3^{\text{INT},h} &= \mathbf{A}_e^{n_e} \underbrace{\left\{ \mathbf{c}^{u_f,e} \right\}^T}_{1 \times n_{\text{dof}}^{f,e}} \cdot \left(\int_{-1}^1 \underbrace{\left\{ \mathbf{N}^{e,u_f} \right\}^T}_{n_{\text{dof}}^{f,e} \times 1} \frac{J^{h^e} (n^{f,h^e})^2 \tilde{v}_f^{h^e}}{\hat{k}^{h^e}} A_j^e d\xi \right), \\
\mathcal{I}_4^{\text{INT},h} &= \mathbf{A}_e^{n_e} \underbrace{\left\{ \mathbf{c}^{u_f,e} \right\}^T}_{1 \times n_{\text{dof}}^{f,e}} \cdot \left(\int_{-1}^1 \underbrace{\left\{ \mathbf{N}^{e,u_f} \right\}^T}_{n_{\text{dof}}^{f,e} \times 1} \rho_0^{f,h^e} g A_j^e d\xi \right), \\
\mathcal{I}_5^{\text{INT},h} &= \mathbf{A}_e^{n_e} \underbrace{\left\{ \mathbf{c}^{u_f,e} \right\}^T}_{1 \times n_{\text{dof}}^{f,e}} \cdot \left(- \int_{-1}^1 \underbrace{\left\{ \mathbf{N}^{e,u_f} \right\}^T}_{n_{\text{dof}}^{f,e} \times 1} \frac{\partial P_{11}^{f,h^e(E)}}{\partial X} A_j^e d\xi \right).
\end{aligned} \tag{4.520}$$

When the pore fluid viscous stress tensor is not considered, $\mathcal{I}_5^{\text{INT},h}$ drops from Equation (4.519).

The global residual for the pore fluid pressure is given as

$$\mathbf{c}^{p_f,T} \cdot \mathbf{R}_{p_f} = \mathcal{H}^h = \mathcal{H}_1^{\text{INT},h} + \mathcal{H}_2^{\text{INT},h} + \mathcal{H}_3^{\text{INT},h} + \mathcal{H}_4^{\text{INT},h} + \mathcal{H}_5^{\text{INT}} - \mathcal{H}^{\text{EXT},h} = 0, \tag{4.521}$$

where

$$\begin{aligned}
\mathcal{H}_1^{\text{INT},h} &= \mathbf{A}_e^{n_e} \underbrace{\left\{ \mathbf{c}^{p_f,e} \right\}^T}_{1 \times n_{\text{dof}}^{p_f,e}} \cdot \left(\int_{-1}^1 \underbrace{\left\{ \mathbf{N}^{e,p_f} \right\}^T}_{n_{\text{dof}}^{p_f,e} \times 1} \left[\frac{J^{h^e} n^{f,h^e}}{K_f^\eta} \dot{p}_f^{h^e} + j^{h^e} \right] A_j^e d\xi \right), \\
\mathcal{H}_2^{\text{INT},h} &= \mathbf{A}_e^{n_e} \underbrace{\left\{ \mathbf{c}^{p_f,e} \right\}^T}_{1 \times n_{\text{dof}}^{p_f,e}} \cdot \left(\int_{-1}^1 \underbrace{\left\{ \mathbf{N}^{e,p_f} \right\}^T}_{n_{\text{dof}}^{p_f,e} \times 1} \frac{1}{K_f^\eta} \frac{\partial p_f^{h^e}}{\partial X} (n^f \tilde{v}_f)^{h^e} A_j^e d\xi \right), \\
\mathcal{H}_3^{\text{INT},h} &= \mathbf{A}_e^{n_e} \underbrace{\left\{ \mathbf{c}^{p_f,e} \right\}^T}_{1 \times n_{\text{dof}}^{p_f,e}} \cdot \left(\int_{-1}^1 \underbrace{\left\{ \mathbf{B}^{e,p_f} \right\}^T}_{n_{\text{dof}}^{p_f,e} \times 1} \hat{k}^{h^e} \frac{\partial p_f^{h^e}}{\partial X} (F_{11}^{h^e})^{-1} A_j^e d\xi \right), \\
\mathcal{H}_4^{\text{INT},h} &= \mathbf{A}_e^{n_e} \underbrace{\left\{ \mathbf{c}^{p_f,e} \right\}^T}_{1 \times n_{\text{dof}}^{p_f,e}} \cdot \left(\int_{-1}^1 \underbrace{\left\{ \mathbf{B}^{e,p_f} \right\}^T}_{n_{\text{dof}}^{p_f,e} \times 1} \hat{k}^{h^e} \rho^{\text{fR},h^e} (a_f^{h^e} + g) A_j^e d\xi \right), \\
\mathcal{H}_5^{\text{INT},h} &= \mathbf{A}_e^{n_e} \underbrace{\left\{ \mathbf{c}^{p_f,e} \right\}^T}_{1 \times n_{\text{dof}}^{p_f,e}} \cdot \left(- \int_{-1}^1 \underbrace{\left\{ \mathbf{B}^{e,p_f} \right\}^T}_{n_{\text{dof}}^{p_f,e} \times 1} \frac{\hat{k}^{h^e}}{n^{f,h^e}} \frac{\partial \sigma_{11}^{f,h^e}}{\partial X} (F_{11}^{h^e})^{-1} A_j^e d\xi \right), \\
\mathcal{H}^{\text{EXT},h} &= \mathbf{A}_e^{n_e} \underbrace{\left\{ \mathbf{c}^{p_f,e} \right\}^T}_{1 \times n_{\text{dof}}^{p_f,e}} \cdot \begin{cases} \underbrace{\left\{ \mathbf{N}^{e,p_f}(X=0, H) \right\}^T}_{n_{\text{dof}}^{p_f,e} \times 1} Q_f A & X=0, H \\ \mathbf{0} & 0 < X < H. \end{cases}
\end{aligned} \tag{4.522}$$

When pressure stabilization is enabled, an additional term $\mathcal{H}^{\text{stab}}$ is added to the l.h.s. of Equation (4.521) and is defined as

$$\mathcal{H}^{\text{stab}} = \mathbf{A}_e^{n_e} \underbrace{\left\{ \mathbf{c}^{p_f,e} \right\}^T}_{1 \times n_{\text{dof}}^{p_f,e}} \cdot \left(\int_{-1}^1 \underbrace{\left\{ \mathbf{B}^{e,p_f} \right\}^T}_{n_{\text{dof}}^{p_f,e} \times 1} \alpha^{\text{stab}} \frac{\partial p_f^{h^e}}{\partial X} (F_{11}^{h^e})^{-1} A_j^e d\xi \right). \tag{4.523}$$

The tangent matrix for each iteration must be of the form

$$\mathbf{0} = -\mathbf{R}^k = \underbrace{\begin{bmatrix} \mathbf{K}_{u,u} & \mathbf{K}_{u,u_f} & \mathbf{K}_{u,p_f} \\ \mathbf{K}_{u_f,u} & \mathbf{K}_{p u_f,u_f} & \mathbf{K}_{u_f,p_f} \\ \mathbf{K}_{p_f,u} & \mathbf{K}_{p_f,u_f} & \mathbf{K}_{p_f,p_f} \end{bmatrix}}_{(n_{\text{dof}}^s + n_{\text{dof}}^f + n_{\text{dof}}^{p_f}) \times (n_{\text{dof}}^s + n_{\text{dof}}^f + n_{\text{dof}}^{p_f})} \cdot \underbrace{\begin{Bmatrix} \delta \ddot{\mathbf{d}} \\ \delta \ddot{\mathbf{d}}_f \\ \delta \ddot{\boldsymbol{\pi}} \end{Bmatrix}}_{(n_{\text{dof}}^s + n_{\text{dof}}^f + n_{\text{dof}}^{p_f}) \times 1}, \tag{4.524}$$

where

$$\begin{aligned}
\underbrace{\mathbf{K}_{u,u}}_{n_{\text{dof}}^s \times n_{\text{dof}}^s} &= \underbrace{\mathbf{A}_e}_{1 \times n_{\text{dof}}^{s,e}} \left\{ \mathbf{c}^{u,e} \right\}^T \cdot \sum_{i=1,2,5} \underbrace{\left[\mathbf{k}_{u,u}^{G_i^{\text{INT}},e} \right]}_{n_{\text{dof}}^{s,e} \times n_{\text{dof}}^{s,e}}, \\
\underbrace{\mathbf{K}_{u,u_f}}_{n_{\text{dof}}^s \times n_{\text{dof}}^f} &= \underbrace{\mathbf{A}_e}_{1 \times n_{\text{dof}}^{s,e}} \left\{ \mathbf{c}^{u,e} \right\}^T \cdot \sum_{i=1,5} \underbrace{\left[\mathbf{k}_{u,u_f}^{G_i^{\text{INT}},e} \right]}_{n_{\text{dof}}^{s,e} \times n_{\text{dof}}^{f,e}}, \\
\underbrace{\mathbf{K}_{u,p_f}}_{n_{\text{dof}}^s \times n_{\text{dof}}^{p_f}} &= \underbrace{\mathbf{A}_e}_{1 \times n_{\text{dof}}^{s,e}} \left\{ \mathbf{c}^{u,e} \right\}^T \cdot \sum_{i=1,3} \underbrace{\left[\mathbf{k}_{u,p_f}^{G_i^{\text{INT}},e} \right]}_{n_{\text{dof}}^{s,e} \times n_{\text{dof}}^{p_f,e}}, \\
\underbrace{\mathbf{K}_{u_f,u}}_{n_{\text{dof}}^f \times n_{\text{dof}}^s} &= \underbrace{\mathbf{A}_e}_{1 \times n_{\text{dof}}^{f,e}} \left\{ \mathbf{c}^{u_f,e} \right\}^T \cdot \sum_{i=1}^5 \underbrace{\left[\mathbf{k}_{u_f,u}^{T_i^{\text{INT}},e} \right]}_{n_{\text{dof}}^{f,e} \times n_{\text{dof}}^{s,e}}, \\
\underbrace{\mathbf{K}_{u_f,u_f}}_{n_{\text{dof}}^f \times n_{\text{dof}}^f} &= \underbrace{\mathbf{A}_e}_{1 \times n_{\text{dof}}^{f,e}} \left\{ \mathbf{c}^{u_f,e} \right\}^T \cdot \sum_{i=1,3,5} \underbrace{\left[\mathbf{k}_{u_f,u_f}^{T_i^{\text{INT}},e} \right]}_{n_{\text{dof}}^{f,e} \times n_{\text{dof}}^{f,e}}, \\
\underbrace{\mathbf{K}_{u_f,p_f}}_{n_{\text{dof}}^f \times n_{\text{dof}}^{p_f}} &= \underbrace{\mathbf{A}_e}_{1 \times n_{\text{dof}}^{f,e}} \left\{ \mathbf{c}^{u_f,e} \right\}^T \cdot \sum_{i=1,2,4} \underbrace{\left[\mathbf{k}_{u_f,p_f}^{T_i^{\text{INT}},e} \right]}_{n_{\text{dof}}^{f,e} \times n_{\text{dof}}^{p_f,e}}, \\
\underbrace{\mathbf{K}_{p_f,u}}_{n_{\text{dof}}^{p_f} \times n_{\text{dof}}^s} &= \underbrace{\mathbf{A}_e}_{1 \times n_{\text{dof}}^{f,e}} \left\{ \mathbf{c}^{p_f,e} \right\}^T \cdot \sum_{i=1}^5 \underbrace{\left[\mathbf{k}_{p_f,u}^{H_i^{\text{INT}},e} \right]}_{n_{\text{dof}}^{p_f,e} \times n_{\text{dof}}^{s,e}}, \\
\underbrace{\mathbf{K}_{p_f,u_f}}_{n_{\text{dof}}^{p_f} \times n_{\text{dof}}^f} &= \underbrace{\mathbf{A}_e}_{1 \times n_{\text{dof}}^{f,e}} \left\{ \mathbf{c}^{p_f,e} \right\}^T \cdot \sum_{i=2,4,5} \underbrace{\left[\mathbf{k}_{p_f,u_f}^{H_i^{\text{INT}},e} \right]}_{n_{\text{dof}}^{p_f,e} \times n_{\text{dof}}^{f,e}}, \\
\underbrace{\mathbf{K}_{p_f,p_f}}_{n_{\text{dof}}^{p_f} \times n_{\text{dof}}^{p_f}} &= \underbrace{\mathbf{A}_e}_{1 \times n_{\text{dof}}^{f,e}} \left\{ \mathbf{c}^{p_f,e} \right\}^T \cdot \sum_{i=1}^4 \underbrace{\left[\mathbf{k}_{p_f,p_f}^{H_i^{\text{INT}},e} \right]}_{n_{\text{dof}}^{p_f,e} \times n_{\text{dof}}^{f,e}}.
\end{aligned} \tag{4.525}$$

The solid skeleton displacement tangents are given as follows (where the definition for $\mathbf{k}_{u,u}^{G_2^{INT},e}$ remains unchanged from the (\mathbf{u}) and $(\mathbf{u}-p_f)$ formulations given by Equation (4.482)₂):

$$\begin{aligned} \underbrace{\left[\mathbf{k}_{u,u}^{G_1^{INT},e} \right]}_{n_{\text{dof}}^{s,e} \times n_{\text{dof}}^{s,e}} &= \int_{-1}^1 \underbrace{\left\{ \mathbf{N}^{e,u} \right\}^T}_{n_{\text{dof}}^{s,e} \times 1} \left(\underbrace{\rho_0^{s,h^e}}_{1 \times n_{\text{dof}}^{s,e}} \underbrace{\left\{ \mathbf{N}^{e,u} \right\}}_{1 \times n_{\text{dof}}^{s,e}} + a_f^{h^e} \rho^{\text{fR},h^e} (\beta \Delta t^2) \underbrace{\left\{ \mathbf{B}^{e,u} \right\}}_{1 \times n_{\text{dof}}^{s,e}} \right) A j^e d\xi, \\ \underbrace{\left[\mathbf{k}_{u,u}^{G_5^{INT},e} \right]}_{n_{\text{dof}}^{s,e} \times n_{\text{dof}}^{s,e}} &= \int_{-1}^1 \frac{\partial v_f^{h^e}}{\partial X} (n^{s,h^e} - n^{f,h^e}) (\kappa_f + 2\mu_f) (F_{11}^{h^e})^{-2} (\beta \Delta t^2) \underbrace{\left\{ \mathbf{B}^{e,u} \right\}}_{n_{\text{dof}}^{s,e} \times 1}^T \underbrace{\left\{ \mathbf{B}^{e,u} \right\}}_{1 \times n_{\text{dof}}^{s,e}} A j^e d\xi. \end{aligned} \quad (4.526)$$

For a nearly-inviscid pore fluid, Equation (4.526)₂ is zero. The solid skeleton displacement and pore fluid displacement coupling tangents are given as follows:

$$\begin{aligned} \underbrace{\left[\mathbf{k}_{u,u_f}^{G_1^{INT},e} \right]}_{n_{\text{dof}}^{s,e} \times n_{\text{dof}}^{f,e}} &= \int_{-1}^1 \rho_0^{f,h^e} \underbrace{\left\{ \mathbf{N}^{e,u} \right\}^T}_{n_{\text{dof}}^{s,e} \times 1} \underbrace{\left\{ \mathbf{N}^{e,u_f} \right\}}_{1 \times n_{\text{dof}}^{f,e}} A j^e d\xi, \\ \underbrace{\left[\mathbf{k}_{u,u_f}^{G_5^{INT},e} \right]}_{n_{\text{dof}}^{s,e} \times n_{\text{dof}}^{f,e}} &= \int_{-1}^1 \frac{n^{f,h^e}}{F_{11}^{h^e}} (\kappa_f + 2\mu_f) (\gamma \Delta t) \underbrace{\left\{ \mathbf{B}^{e,u} \right\}^T}_{n_{\text{dof}}^{s,e} \times 1} \underbrace{\left\{ \mathbf{B}^{e,u_f} \right\}}_{1 \times n_{\text{dof}}^{f,e}} A j^e d\xi. \end{aligned} \quad (4.527)$$

The solid skeleton displacement and pore fluid pressure coupling tangent is given as follows (where $\mathbf{k}_{u,p_f}^{G_3^{INT},e}$ remains unchanged from the $(\mathbf{u}-p_f)$ formulation given by Equation (4.500)):

$$\underbrace{\left[\mathbf{k}_{u,p_f}^{G_1^{INT},e} \right]}_{n_{\text{dof}}^{s,e} \times n_{\text{dof}}^{p_f,e}} = \int_{-1}^1 \frac{a_f^{h^e} J^{h^e} n^{f,h^e} \rho^{\text{fR},h^e}}{K_f^\eta} (\beta \Delta t^2) \underbrace{\left\{ \mathbf{N}^{e,u} \right\}^T}_{n_{\text{dof}}^{s,e} \times 1} \underbrace{\left\{ \mathbf{N}^{e,p_f} \right\}}_{1 \times n_{\text{dof}}^{p_f,e}} A j^e d\xi. \quad (4.528)$$

The pore fluid displacement and solid skeleton displacement coupling tangents are given as follows:

$$\begin{aligned}
\underbrace{\left[\mathbf{k}_{u_f, u}^{\mathcal{I}_1^{\text{INT}, e}} \right]}_{n_{\text{dof}}^{f, e} \times n_{\text{dof}}^{s, e}} &= \int_{-1}^1 \rho^{\text{fR}, h^e} a_f^{h^e} (\beta \Delta t^2) \underbrace{\left\{ \mathbf{N}^{e, u_f} \right\}^T}_{n_{\text{dof}}^{f, e} \times 1} \underbrace{\left\{ \mathbf{B}^{e, u} \right\}}_{1 \times n_{\text{dof}}^{s, e}} A_j^e d\xi, \\
\underbrace{\left[\mathbf{k}_{u_f, u}^{\mathcal{I}_2^{\text{INT}, e}} \right]}_{n_{\text{dof}}^{f, e} \times n_{\text{dof}}^{s, e}} &= \int_{-1}^1 \frac{n^{s, h^e}}{J^{h^e}} \frac{\partial p_f^{h^e}}{\partial X} (\beta \Delta t^2) \underbrace{\left\{ \mathbf{N}^{e, u_f} \right\}^T}_{n_{\text{dof}}^{f, e} \times 1} \underbrace{\left\{ \mathbf{B}^{e, u} \right\}}_{1 \times n_{\text{dof}}^{s, e}} A_j^e d\xi, \\
\underbrace{\left[\mathbf{k}_{u_f, u}^{\mathcal{I}_3^{\text{INT}, e}} \right]}_{n_{\text{dof}}^{f, e} \times n_{\text{dof}}^{s, e}} &= \int_{-1}^1 \underbrace{\left\{ \mathbf{N}^{e, u_f} \right\}^T}_{n_{\text{dof}}^{f, e} \times 1} \left(\left[1 + \frac{2n^{s, h^e}}{n^{f, h^e}} - \frac{J^{h^e} \delta_{\hat{k}}^{h^e}}{\hat{k}^{h^e}} \right] \frac{(n^{f, h^e})^2 \tilde{v}_f^{h^e}}{\hat{k}^{h^e}} (\beta \Delta t^2) \underbrace{\left\{ \mathbf{B}^{e, u} \right\}}_{1 \times n_{\text{dof}}^{s, e}} \right. \\
&\quad \left. - \frac{J^{h^e} (n^{f, h^e})^2}{\hat{k}^{h^e}} (\gamma \Delta t) \underbrace{\left\{ \mathbf{N}^{e, u} \right\}}_{1 \times n_{\text{dof}}^{s, e}} \right) A_j^e d\xi, \tag{4.529} \\
\underbrace{\left[\mathbf{k}_{u_f, u}^{\mathcal{I}_4^{\text{INT}, e}} \right]}_{n_{\text{dof}}^{f, e} \times n_{\text{dof}}^{s, e}} &= \int_{-1}^1 \rho^{\text{fR}, h^e} g (\beta \Delta t^2) \underbrace{\left\{ \mathbf{N}^{e, u_f} \right\}^T}_{n_{\text{dof}}^{f, e} \times 1} \underbrace{\left\{ \mathbf{B}^{e, u} \right\}}_{1 \times n_{\text{dof}}^{s, e}} A_j^e d\xi, \\
\underbrace{\left[\mathbf{k}_{u_f, u}^{\mathcal{I}_5^{\text{INT}, e}} \right]}_{n_{\text{dof}}^{f, e} \times n_{\text{dof}}^{s, e}} &= - \int_{-1}^1 \underbrace{\left\{ \mathbf{N}^{e, u_f} \right\}^T}_{n_{\text{dof}}^{f, e} \times 1} \left(\left[(n^{s, h^e} - n^{f, h^e}) \frac{\partial^2 v_f^{h^e}}{\partial X^2} - 4 \frac{\partial n^{f, h^e}}{\partial X} \frac{\partial n^{f, h^e}}{\partial X} \right] \underbrace{\left\{ \mathbf{B}^{e, u} \right\}}_{1 \times n_{\text{dof}}^{s, e}} \right. \\
&\quad \left. + \frac{n^{s, h^e}}{J^{h^e}} \frac{\partial v_f^{h^e}}{\partial X} \underbrace{\left\{ \mathbf{H}^{e, u} \right\}}_{1 \times n_{\text{dof}}^{s, e}} \right) (F_{11}^{h^e})^{-2} (\kappa_f + 2\mu_f) (\beta \Delta t^2) A_j^e d\xi.
\end{aligned}$$

For a nearly-inviscid pore fluid, Equation (4.529)₅ is zero. The pore fluid displacement tangents are given as follows:

$$\begin{aligned}
\underbrace{\left[\mathbf{k}_{u_f, u_f}^{\mathcal{I}_1^{\text{INT}, e}} \right]}_{n_{\text{dof}}^{f, e} \times n_{\text{dof}}^{f, e}} &= \int_{-1}^1 \rho_0^{f, h^e} \underbrace{\left\{ \mathbf{N}^{e, u_f} \right\}^T}_{n_{\text{dof}}^{f, e} \times 1} \underbrace{\left\{ \mathbf{N}^{e, u_f} \right\}}_{1 \times n_{\text{dof}}^{f, e}} A j^e d\xi, \\
\underbrace{\left[\mathbf{k}_{u_f, u_f}^{\mathcal{I}_3^{\text{INT}, e}} \right]}_{n_{\text{dof}}^{f, e} \times n_{\text{dof}}^{f, e}} &= \int_{-1}^1 \frac{J^{h^e} (n^{f, h^e})^2}{\hat{k}^{h^e}} (\gamma \Delta t) \underbrace{\left\{ \mathbf{N}^{e, u_f} \right\}^T}_{n_{\text{dof}}^{f, e} \times 1} \underbrace{\left\{ \mathbf{N}^{e, u_f} \right\}}_{1 \times n_{\text{dof}}^{f, e}} A j^e d\xi, \\
\underbrace{\left[\mathbf{k}_{u_f, u_f}^{\mathcal{I}_5^{\text{INT}, e}} \right]}_{n_{\text{dof}}^{f, e} \times n_{\text{dof}}^{f, e}} &= - \int_{-1}^1 \underbrace{\left\{ \mathbf{N}^{e, u_f} \right\}^T}_{n_{\text{dof}}^{f, e} \times 1} \left(\frac{\partial n^{f, h^e}}{\partial X} \underbrace{\left\{ \mathbf{B}^{e, u_f} \right\}}_{1 \times n_{\text{dof}}^{f, e}} + n^{f, h^e} \underbrace{\left\{ \mathbf{H}^{e, u_f} \right\}}_{1 \times n_{\text{dof}}^{f, e}} \right) (\kappa_f + 2\mu_f) (F_{11}^{h^e})^{-2} \times \\
&\quad (\gamma \Delta t) A j^e d\xi.
\end{aligned} \tag{4.530}$$

The pore fluid displacement and pore fluid pressure coupling tangents are given as follows:

$$\begin{aligned}
\underbrace{\left[\mathbf{k}_{u_f, p_f}^{\mathcal{I}_1^{\text{INT}, e}} \right]}_{n_{\text{dof}}^{f, e} \times n_{\text{dof}}^{p_f, e}} &= \int_{-1}^1 \frac{a_f^{h^e} \rho_0^{f, h^e}}{K_f^\eta} (\beta \Delta t^2) \underbrace{\left\{ \mathbf{N}^{e, u_f} \right\}^T}_{n_{\text{dof}}^{f, e} \times 1} \underbrace{\left\{ \mathbf{N}^{e, p_f} \right\}}_{1 \times n_{\text{dof}}^{p_f, e}} A j^e d\xi, \\
\underbrace{\left[\mathbf{k}_{u_f, p_f}^{\mathcal{I}_2^{\text{INT}, e}} \right]}_{n_{\text{dof}}^{f, e} \times n_{\text{dof}}^{p_f, e}} &= \int_{-1}^1 n^{f, h^e} (\beta \Delta t^2) \underbrace{\left\{ \mathbf{N}^{e, u_f} \right\}^T}_{n_{\text{dof}}^{f, e} \times 1} \underbrace{\left\{ \mathbf{B}^{e, p_f} \right\}}_{1 \times n_{\text{dof}}^{p_f, e}} A j^e d\xi, \\
\underbrace{\left[\mathbf{k}_{u_f, p_f}^{\mathcal{I}_4^{\text{INT}, e}} \right]}_{n_{\text{dof}}^{f, e} \times n_{\text{dof}}^{p_f, e}} &= \int_{-1}^1 \frac{J^{h^e} n^{f, h^e} \rho^{\text{fR}, h^e} g}{K_f^\eta} (\beta \Delta t^2) \underbrace{\left\{ \mathbf{N}^{e, u_f} \right\}^T}_{n_{\text{dof}}^{f, e} \times 1} \underbrace{\left\{ \mathbf{N}^{e, p_f} \right\}}_{1 \times n_{\text{dof}}^{p_f, e}} A j^e d\xi.
\end{aligned} \tag{4.531}$$

The pore fluid pressure and solid skeleton coupling tangents are given as follows, where $\mathbf{k}_{p_f, u}^{\mathcal{H}_1^{\text{INT}, e}}$ and $\mathbf{k}_{p_f, u}^{\mathcal{H}_3^{\text{INT}, e}}$ (and $\mathbf{k}_{p_f, u}^{\mathcal{H}^{\text{stab}, e}}$ when pressure stabilization is enabled), remain unchanged from the (\mathbf{u} - p_f) formulation given by Equation (4.501)_{1,3} (and Equation (4.502) when pressure stabilization is en-

abled):

$$\begin{aligned}
\underbrace{\left[\mathbf{k}_{p_f, u}^{\mathcal{H}_2^{\text{INT}, e}} \right]}_{n_{\text{dof}}^{p_f, e} \times n_{\text{dof}}^{s, e}} &= \int_{-1}^1 \underbrace{\left\{ \mathbf{N}^{e, p_f} \right\}^T}_{n_{\text{dof}}^{p_f, e} \times 1} \left(\left(\frac{\delta_k^{h^e}}{\hat{k}^{h^e}} (n^f \tilde{v}_f)^{h^e} + \hat{k}^{h^e} \frac{\partial p_f^{h^e}}{\partial X} [F_{11}^{h^e}]^{-2} \right. \right. \\
&+ \hat{k}^{h^e} (F_{11}^{h^e})^{-3} (\kappa_f + 2\mu_f) \left(\left[\frac{n^{s, h^e}}{(n^{f, h^e})^2} + \frac{5}{n^{f, h^e}} \right] \frac{\partial n^{f, h^e}}{\partial X} \frac{\partial v_f^{h^e}}{\partial X} + 2 \frac{\partial^2 v_f^{h^e}}{\partial X^2} \right) \left. \right) \underbrace{\left\{ \mathbf{B}^{e, u} \right\}}_{1 \times n_{\text{dof}}^{s, e}} \\
&- \hat{k}^{h^e} \frac{n^{s, h^e}}{n^{f, h^e}} (F_{11}^{h^e})^{-4} \frac{\partial v_f^{h^e}}{\partial X} (\kappa_f + 2\mu_f) \underbrace{\left\{ \mathbf{H}^{e, u} \right\}}_{1 \times n_{\text{dof}}^{s, e}} \left. \right) \frac{1}{K_f^\eta} \frac{\partial p_f^{h^e}}{\partial X} (\beta \Delta t^2) A_j^e d\xi, \\
\underbrace{\left[\mathbf{k}_{p_f, u}^{\mathcal{H}_4^{\text{INT}, e}} \right]}_{n_{\text{dof}}^{p_f, e} \times n_{\text{dof}}^{s, e}} &= \int_{-1}^1 \delta_k^{h^e} \rho^{\text{fR}, h^e} (a_f^{h^e} + g) (\beta \Delta t^2) \underbrace{\left\{ \mathbf{B}^{e, p_f} \right\}^T}_{n_{\text{dof}}^{p_f, e} \times 1} \underbrace{\left\{ \mathbf{B}^{e, u} \right\}}_{1 \times n_{\text{dof}}^{s, e}} A_j^e d\xi, \\
\underbrace{\left[\mathbf{k}_{p_f, u}^{\mathcal{H}_5^{\text{INT}, e}} \right]}_{n_{\text{dof}}^{p_f, e} \times n_{\text{dof}}^{s, e}} &= - \int_{-1}^1 \underbrace{\left\{ \mathbf{B}^{e, p_f} \right\}^T}_{n_{\text{dof}}^{p_f, e} \times 1} \hat{k}^{h^e} \left(\left[\frac{\delta_k^{h^e}}{n^{f, h^e} \hat{k}^{h^e}} \frac{\partial \sigma_{11(E)}^{f, h^e}}{\partial X} (F_{11}^{h^e})^2 \right. \right. \\
&- \left. \left(\frac{\partial n^{f, h^e}}{\partial X} \frac{\partial v_f^{h^e}}{\partial X} \left(\frac{n^{s, h^e}}{(n^{f, h^e})^2} + \frac{5}{n^{f, h^e}} \right) + 2 \frac{\partial^2 v_f^{h^e}}{\partial X^2} \right) (\kappa_f + 2\mu_f) \right] \underbrace{\left\{ \mathbf{B}^{e, u} \right\}}_{1 \times n_{\text{dof}}^{s, e}} \\
&+ \frac{n_0^s}{n^{f, h^e}} (F_{11}^{h^e})^{-2} \frac{\partial v_f^{h^e}}{\partial X} (\kappa_f + 2\mu_f) \underbrace{\left\{ \mathbf{H}^{e, u} \right\}}_{1 \times n_{\text{dof}}^{s, e}} \left. \right) (F_{11}^{h^e})^{-3} (\beta \Delta t^2) A_j^e d\xi,
\end{aligned} \tag{4.532}$$

For a nearly-inviscid pore fluid, the terms highlighted in red in Equation (4.532)₁ drop and Equation (4.532)₃ is zero. The pore fluid pressure and pore fluid displacement coupling tangents are

given as follows:

$$\begin{aligned}
\underbrace{\left[\mathbf{k}_{p_f, u_f}^{\mathcal{H}_2^{\text{INT}, e}} \right]}_{n_{\text{dof}}^{p_f, e} \times n_{\text{dof}}^{s, e}} &= - \int_{-1}^1 \underbrace{\left\{ \mathbf{N}^{e, p_f} \right\}^T}_{n_{\text{dof}}^{p_f, e} \times 1} \hat{k}^{h^e} \frac{\partial p_f^{h^e}}{\partial X} \frac{1}{K_f^\eta} \left(\rho^{\text{fR}, h^e} \underbrace{\left\{ \mathbf{N}^{e, u_f} \right\}}_{1 \times n_{\text{dof}}^{f, e}} + (\kappa_f + 2\mu_f) (F_{11}^{h^e})^{-2} (\gamma \Delta t) \times \right. \\
&\quad \left. \left[\frac{1}{n^{f, h^e}} \frac{\partial n^{f, h^e}}{\partial X} \underbrace{\left\{ \mathbf{B}^{e, u_f} \right\}}_{1 \times n_{\text{dof}}^{f, e}} + \underbrace{\left\{ \mathbf{H}^{e, u_f} \right\}}_{1 \times n_{\text{dof}}^{f, e}} \right] \right) A_j^e d\xi, \\
\underbrace{\left[\mathbf{k}_{p_f, u_f}^{\mathcal{H}_4^{\text{INT}, e}} \right]}_{n_{\text{dof}}^{p_f, e} \times n_{\text{dof}}^{f, e}} &= \int_{-1}^1 \hat{k}^{h^e} \rho^{\text{fR}, h^e} \underbrace{\left\{ \mathbf{B}^{e, p_f} \right\}^T}_{n_{\text{dof}}^{p_f, e} \times 1} \underbrace{\left\{ \mathbf{N}^{e, u_f} \right\}}_{1 \times n_{\text{dof}}^{f, e}} A_j^e d\xi, \\
\underbrace{\left[\mathbf{k}_{p_f, u_f}^{\mathcal{H}_5^{\text{INT}, e}} \right]}_{n_{\text{dof}}^{p_f, e} \times n_{\text{dof}}^{f, e}} &= - \int_{-1}^1 \underbrace{\left\{ \mathbf{B}^{e, p_f} \right\}^T}_{n_{\text{dof}}^{p_f, e} \times 1} \left(\frac{1}{n^{f, h^e}} \frac{\partial n^{f, h^e}}{\partial X} \underbrace{\left\{ \mathbf{B}^{e, u_f} \right\}}_{1 \times n_{\text{dof}}^{f, e}} + \underbrace{\left\{ \mathbf{H}^{e, u_f} \right\}}_{1 \times n_{\text{dof}}^{f, e}} \right) (\kappa_f + 2\mu_f) \frac{\hat{k}^{h^e}}{(F_{11}^{h^e})^2} \times \\
&\quad (\gamma \Delta t) A_j^e d\xi.
\end{aligned} \tag{4.533}$$

For a nearly-inviscid pore fluid, the terms marked in red of Equation (4.533)₁ are zero and Equation (4.533)₃ is zero. Lastly, the pore fluid pressure tangents are given as follows, where $\mathbf{k}_{p_f, p_f}^{\mathcal{H}_1^{\text{INT}, e}}$ and $\mathbf{k}_{p_f, p_f}^{\mathcal{H}_3^{\text{INT}, e}}$ (and $\mathbf{k}_{p_f, p_f}^{\mathcal{H}^{\text{stab}, e}}$ when pressure stabilization is enabled) remain unchanged from the $(\mathbf{u}-p_f)$ formulation given by Eqs. 4.503_{1,3} (and Equation (4.504) when pressure stabilization is enabled):

$$\begin{aligned}
\underbrace{\left[\mathbf{k}_{p_f, p_f}^{\mathcal{H}_2^{\text{INT}, e}} \right]}_{n_{\text{dof}}^{p_f, e} \times n_{\text{dof}}^{p_f, e}} &= \int_{-1}^1 \underbrace{\left\{ \mathbf{N}^{e, p_f} \right\}^T}_{n_{\text{dof}}^{p_f, e} \times 1} \left(\left[(n^f \tilde{v}_f)^{h^e} - \hat{k}^{h^e} \frac{\partial p_f^{h^e}}{\partial X} (F_{11}^{h^e})^{-1} \right] \underbrace{\left\{ \mathbf{B}^{e, p_f} \right\}}_{1 \times n_{\text{dof}}^{p_f, e}} \right. \\
&\quad \left. - \hat{k}^{h^e} \frac{\partial p_f^{h^e}}{\partial X} (a_f^{h^e} + g) \frac{\rho^{\text{fR}, h^e}}{K_f^\eta} \underbrace{\left\{ \mathbf{N}^{e, p_f} \right\}}_{1 \times n_{\text{dof}}^{p_f, e}} \right) \frac{1}{K_f^\eta} (\beta \Delta t^2) A_j^e d\xi, \\
\underbrace{\left[\mathbf{k}_{p_f, p_f}^{\mathcal{H}_4^{\text{INT}, e}} \right]}_{n_{\text{dof}}^{p_f, e} \times n_{\text{dof}}^{p_f, e}} &= \int_{-1}^1 \hat{k}^{h^e} (a_f^{h^e} + g) \frac{\rho^{\text{fR}, h^e}}{K_f^\eta} (\beta \Delta t^2) \underbrace{\left\{ \mathbf{B}^{e, p_f} \right\}^T}_{n_{\text{dof}}^{p_f, e} \times 1} \underbrace{\left\{ \mathbf{N}^{e, p_f} \right\}}_{1 \times n_{\text{dof}}^{p_f, e}} A_j^e d\xi.
\end{aligned} \tag{4.534}$$

4.3.3 Central-difference integration

For the central-difference (CD) in time integrator, the discretized balance equations take the similar general form as

$$\mathbf{M}\ddot{\mathbf{x}}_{n+1} + \mathbf{C}\dot{\mathbf{x}}_{n+1} + \mathbf{F}^{INT}(\ddot{\mathbf{x}}_{n+1}, \mathbf{x}_{n+1}) = \mathbf{F}_{n+1}^{EXT}, \quad (4.535)$$

where it is assumed that $\ddot{\mathbf{x}}_{n+1}$ is to be solved at time t_{n+1} , and \mathbf{M} , \mathbf{C} , \mathbf{F}^{INT} and \mathbf{F}^{EXT} are known at time t_{n+1} from values at t_n . For a CD scheme,

$$\begin{aligned} \mathbf{x}_{n+1} &= \mathbf{x}_n + \Delta t \dot{\mathbf{x}}_n + \frac{(\Delta t)^2}{2} \ddot{\mathbf{x}}_n, \\ \dot{\mathbf{x}}_{n+1} &= \dot{\mathbf{x}}_n + \frac{\Delta t}{2} (\ddot{\mathbf{x}}_n + \ddot{\mathbf{x}}_{n+1}). \end{aligned} \quad (4.536)$$

Next, we show how these are implemented for the (\mathbf{u}) and $(\mathbf{u}-p_f)$ formulations; as will be shown in Chapter 5, the CD integrator as applied to the $(\mathbf{u}-p_f)$ formulation is unstable for shock loading, thus, we did not formulate the integrator for the $(\mathbf{u}-\mathbf{u}_f-p_f)$ formulation which only adds more complexity and potential instability.

We also typically employ an adaptive time-stepping scheme for the central-difference time integrator that is loosely based on a localized Courant-Fredrichs-Lewy (CFL) condition. Recall for the critical time step

$$\Delta t_{cr}^e \leq \frac{\Delta x^e}{c^e}, \quad (4.537)$$

where $\Delta x^e = h^e$ is the shortest element length in the current configuration. The local P-wave speed c^e for uniaxial strain, assuming linear isotropic elasticity as an approximation, is usually determined as

$$c^e = \max \left\{ \begin{array}{l} \sqrt{\frac{K^{\text{skel}} + \frac{4}{3}G^{\text{skel}}}{\rho^e}} \\ \sqrt{\frac{n^{s,e}K_s + n^{f,e}K_f^\eta + \frac{4}{3}G^{\text{skel}}}{\rho^e}} \end{array} \right. . \quad (4.538)$$

For single-phase materials, the current total mass density is $\rho = J\rho_0$, and for multiphase materials $\rho = (n^s \rho^{sR} + n^f \rho^{fR})$. Then, the following time step is chosen:

$$\Delta t_{n+1} = \min_e \Delta t_{cr}^e, \quad (4.539)$$

where we can either manually constrain the time step to not exceed some global maximum should the CFL condition at time t_n produce a time step too large for calculations at time t_{n+1} , resulting in a greater likelihood of error buildup, or, more commonly, we multiply Equation (4.537) by a safety factor, $SF \in [0.2, 0.9]$.

4.3.3.1 (u) formulation

The FE formulation for the balance of momentum of the solid, variational Equation (4.18), is written in block-matrix form as

$$\underbrace{\left\{ \mathbf{R}_u \right\}}_{n_{\text{dof}}^s \times 1} = \mathbf{0}, \quad (4.540)$$

where this global residual for the solid displacement is given as

$$\mathbf{c}^{u,T} \cdot \mathbf{R}_u = \mathcal{G}^h = \mathcal{G}_1^{\text{INT},h} + \mathcal{G}_2^{\text{INT},h} + \mathcal{G}_4^{\text{INT},h} - \mathcal{G}^{\text{EXT},h} = 0, \quad (4.541)$$

where

$$\begin{aligned} \mathcal{G}_1^{\text{INT},h} &= \mathbf{A}_e^{n_e} \underbrace{\left\{ \mathbf{c}^{u,e} \right\}}_{1 \times n_{\text{dof}}^{s,e}} \cdot \underbrace{\left[\mathbf{m}_{u,u}^{\mathcal{G}_1^{\text{INT},e}} \right]}_{n_{\text{dof}}^{s,e} \times n_{\text{dof}}^{s,e}} \cdot \underbrace{\left\{ \ddot{\mathbf{d}}^e \right\}}_{n_{\text{dof}}^{s,e} \times 1}, \\ \mathcal{G}_2^{\text{INT},h} &= \mathbf{A}_e^{n_e} \underbrace{\left\{ \mathbf{c}^{u,e} \right\}}_{1 \times n_{\text{dof}}^{s,e}} \cdot \underbrace{\left\{ \mathbf{f}^{\mathcal{G}_2^{\text{INT},e}} \right\}}_{n_{\text{dof}}^{s,e} \times 1}, \\ \mathcal{G}_4^{\text{INT},h} &= \mathbf{A}_e^{n_e} \underbrace{\left\{ \mathbf{c}^{u,e} \right\}}_{1 \times n_{\text{dof}}^{s,e}} \cdot \underbrace{\left\{ \mathbf{f}^{\mathcal{G}_4^{\text{INT},e}} \right\}}_{n_{\text{dof}}^{s,e} \times 1}, \\ \mathcal{G}^{\text{EXT},h} &= \mathbf{A}_e^{n_e} \underbrace{\left\{ \mathbf{c}^{u,e} \right\}}_{1 \times n_{\text{dof}}^{s,e}} \cdot \underbrace{\left\{ \mathbf{f}^{\mathcal{G}^{\text{EXT},e}} \right\}}_{n_{\text{dof}}^{s,e} \times 1}, \end{aligned} \quad (4.542)$$

and

$$\begin{aligned}
\underbrace{\left\{ \mathbf{f}^{\mathcal{G}_2^{\text{INT}},e} \right\}}_{n_{\text{dof}}^{s,e} \times 1} &= \int_{-1}^1 \underbrace{\left\{ \mathbf{B}^{e,u} \right\}}_{n_{\text{dof}}^{s,e} \times 1}^T P_{11}^{h^e} A j^e d\xi, \\
\underbrace{\left\{ \mathbf{f}^{\mathcal{G}_4^{\text{INT}},e} \right\}}_{n_{\text{dof}}^{s,e} \times 1} &= \int_{-1}^1 \underbrace{\left\{ \mathbf{N}^{e,u} \right\}}_{n_{\text{dof}}^{s,e} \times 1}^T \rho_0^{h^e} g A j^e d\xi, \\
\underbrace{\left\{ \mathbf{f}^{\mathcal{G}^{\text{EXT}},e} \right\}}_{n_{\text{dof}}^{s,e} \times 1} &= \begin{cases} \underbrace{\left\{ \mathbf{N}^{e,u}(X=0, H) \right\}}_{n_{\text{dof}}^{s,e} \times 1}^T t^\sigma A & X=0, H \\ \mathbf{0} & 0 < X < H. \end{cases}
\end{aligned} \tag{4.543}$$

The mass matrix associated with the solid acceleration is given by

$$\underbrace{\left[\mathbf{m}_{u,u}^{\mathcal{G}_1^{\text{INT}},e} \right]}_{n_{\text{dof}}^{s,e} \times n_{\text{dof}}^{s,e}} = \int_{-1}^1 \rho_0^{h^e} \underbrace{\left\{ \mathbf{N}^{e,u} \right\}}_{n_{\text{dof}}^{s,e} \times 1}^T \underbrace{\left\{ \mathbf{N}^{e,u} \right\}}_{1 \times n_{\text{dof}}^{s,e}} A j^e d\xi. \tag{4.544}$$

Thus, the solution is given by

$$\underbrace{\left\{ \ddot{\mathbf{d}}_{n+1} \right\}}_{n_{\text{dof}}^s \times 1} = \underbrace{\left[\mathbf{M}_{u,u}^{\mathcal{G}_1^{\text{INT}}} \right]}_{n_{\text{dof}}^s \times n_{\text{dof}}^s}^{-1} \cdot \left(- \underbrace{\left\{ \mathbf{F}^{\mathcal{G}_2^{\text{INT}}} \right\}}_{n_{\text{dof}}^s \times 1} - \underbrace{\left\{ \mathbf{F}^{\mathcal{G}_4^{\text{INT}}} \right\}}_{n_{\text{dof}}^s \times 1} + \underbrace{\left\{ \mathbf{F}^{\mathcal{G}^{\text{EXT}}} \right\}}_{n_{\text{dof}}^s \times 1} \right), \tag{4.545}$$

where

$$\begin{aligned}
\underbrace{\left[\mathbf{M}_{u,u}^{\mathcal{G}_1^{\text{INT}}} \right]}_{n_{\text{dof}}^s \times n_{\text{dof}}^s} &= \mathbf{A}_e \underbrace{\left[\mathbf{m}_{u,u}^{\mathcal{G}_1^{\text{INT}},e} \right]}_{n_{\text{dof}}^{s,e} \times n_{\text{dof}}^{s,e}}, \\
\underbrace{\left\{ \mathbf{F}^{\mathcal{G}_2^{\text{INT}}} \right\}}_{n_{\text{dof}}^s \times 1} &= \mathbf{A}_e \underbrace{\left\{ \mathbf{f}^{\mathcal{G}_2^{\text{INT}},e} \right\}}_{n_{\text{dof}}^{s,e} \times 1}, \\
\underbrace{\left\{ \mathbf{F}^{\mathcal{G}_4^{\text{INT}}} \right\}}_{n_{\text{dof}}^s \times 1} &= \mathbf{A}_e \underbrace{\left\{ \mathbf{f}^{\mathcal{G}_4^{\text{INT}},e} \right\}}_{n_{\text{dof}}^{s,e} \times 1}, \\
\underbrace{\left\{ \mathbf{F}^{\mathcal{G}^{\text{EXT}}} \right\}}_{n_{\text{dof}}^s \times 1} &= \mathbf{A}_e \underbrace{\left\{ \mathbf{f}^{\mathcal{G}^{\text{EXT}},e} \right\}}_{n_{\text{dof}}^{s,e} \times 1}.
\end{aligned} \tag{4.546}$$

The solid velocity and solid displacement updates are recovered by

$$\begin{aligned} \underbrace{\left\{ \dot{\mathbf{d}}_{n+1} \right\}}_{n_{\text{dof}}^s \times 1} &= \underbrace{\left\{ \dot{\mathbf{d}}_n \right\}}_{n_{\text{dof}}^s \times 1} + \frac{\Delta t}{2} \left(\underbrace{\left\{ \ddot{\mathbf{d}}_n \right\}}_{n_{\text{dof}}^s \times 1} + \underbrace{\left\{ \ddot{\mathbf{d}}_{n+1} \right\}}_{n_{\text{dof}}^s \times 1} \right), \\ \underbrace{\left\{ \mathbf{d}_{n+1} \right\}}_{n_{\text{dof}}^s \times 1} &= \underbrace{\left\{ \mathbf{d}_n \right\}}_{n_{\text{dof}}^s \times 1} + \Delta t \underbrace{\left\{ \dot{\mathbf{d}}_n \right\}}_{n_{\text{dof}}^s \times 1} + \frac{\Delta t^2}{2} \underbrace{\left\{ \ddot{\mathbf{d}}_{n+1} \right\}}_{n_{\text{dof}}^s \times 1}. \end{aligned} \quad (4.547)$$

4.3.3.2 (\mathbf{u} - p_f) formulation

For the (\mathbf{u} - p_f) formulation, the variational equations are given by Equations (4.64) & Equation (4.66). The FE equations integrated in time using CD for the poroelastodynamic equations are solved in a staggered manner. A solid skeleton displacement update is computed first. There are no unknowns related to pore fluid pressure in the balance of linear momentum of the mixture. Then the solid displacements are substituted into the corresponding equations to compute a pore fluid pressure update; see Algorithm 1. The advantage of such a procedure is that there are no coupling matrices that would introduce off-diagonal entries in a block matrix of the system when trying to solve the solid skeleton acceleration and second time derivative on pore fluid pressure updates. This reduces computational cost at the expense of accuracy when compared to the explicit Runge-Kutta methods and the implicit Newmark-beta methods.

Algorithm 1 General concept of staggered solution process for (\mathbf{u} - p_f) formulation with CD time integration for a given time t_n

- 1: Update t_n
 - 2: Update external force vector(s)
 - 3: Compute deformations and stresses at time t_{n+1} from values at t_n
 - 4: Assemble internal force vector and mass matrix associated with \mathcal{G}^h from values at t_n
 - 5: Compute a^h at time t_{n+1}
 - 6: Assemble internal force vector and mass matrix associated with \mathcal{H}^h from values at t_n
 - 7: Compute \ddot{p}_f^h at time t_{n+1}
-

The FE formulation for the balance of momentum of the mixture variational equation is

written in block-matrix form as

$$\underbrace{\left\{ \mathbf{R}_u \right\}}_{n_{\text{dof}}^s \times 1} = \mathbf{0}. \quad (4.548)$$

This global residual for the solid skeleton displacement is given as

$$\mathbf{c}^{u,T} \cdot \mathbf{R}_u = \mathcal{G}^h = \mathcal{G}_1^{\text{INT},h} + \mathcal{G}_2^{\text{INT},h} + \mathcal{G}_3^{\text{INT},h} + \mathcal{G}_4^{\text{INT},h} - \mathcal{G}^{\text{EXT},h} = 0, \quad (4.549)$$

where

$$\begin{aligned} \mathcal{G}_1^{\text{INT},h} &= \mathbf{A}_e \underbrace{\left\{ \mathbf{c}^{u,e} \right\}^T}_{1 \times n_{\text{dof}}^{s,e}} \cdot \underbrace{\left[\mathbf{m}_{u,u}^{\mathcal{G}_1^{\text{INT},e}} \right]}_{n_{\text{dof}}^{s,e} \times n_{\text{dof}}^{s,e}} \cdot \underbrace{\left\{ \ddot{\mathbf{d}}^e \right\}}_{n_{\text{dof}}^{s,e} \times 1}, \\ \mathcal{G}_2^{\text{INT},h} &= \mathbf{A}_e \underbrace{\left\{ \mathbf{c}^{u,e} \right\}^T}_{1 \times n_{\text{dof}}^{s,e}} \cdot \underbrace{\left\{ \mathbf{f}^{\mathcal{G}_2^{\text{INT},e}} \right\}}_{n_{\text{dof}}^{s,e} \times 1}, \\ \mathcal{G}_3^{\text{INT},h} &= \mathbf{A}_e \underbrace{\left\{ \mathbf{c}^{u,e} \right\}^T}_{1 \times n_{\text{dof}}^{s,e}} \cdot \underbrace{\left\{ \mathbf{f}^{\mathcal{G}_3^{\text{INT},e}} \right\}}_{n_{\text{dof}}^{s,e} \times 1}, \\ \mathcal{G}_4^{\text{INT},h} &= \mathbf{A}_e \underbrace{\left\{ \mathbf{c}^{u,e} \right\}^T}_{1 \times n_{\text{dof}}^{s,e}} \cdot \underbrace{\left\{ \mathbf{f}^{\mathcal{G}_4^{\text{INT},e}} \right\}}_{n_{\text{dof}}^{s,e} \times 1}, \\ \mathcal{G}^{\text{EXT},h} &= \mathbf{A}_e \underbrace{\left\{ \mathbf{c}^{u,e} \right\}^T}_{1 \times n_{\text{dof}}^{s,e}} \cdot \underbrace{\left\{ \mathbf{f}^{\mathcal{G}^{\text{EXT},e}} \right\}}_{n_{\text{dof}}^{s,e} \times 1}, \end{aligned} \quad (4.550)$$

and

$$\begin{aligned}
\underbrace{\left\{ \mathbf{f}^{\mathcal{G}_2^{\text{INT},e}} \right\}}_{n_{\text{dof}}^{s,e} \times 1} &= \int_{-1}^1 \underbrace{\left\{ \mathbf{B}^{e,u} \right\}}_{n_{\text{dof}}^{s,e} \times 1}^T P_{11(E)}^{s,h^e} A j^e d\xi, \\
\underbrace{\left\{ \mathbf{f}^{\mathcal{G}_3^{\text{INT},e}} \right\}}_{n_{\text{dof}}^{s,e} \times 1} &= - \int_{-1}^1 \underbrace{\left\{ \mathbf{B}^{e,u} \right\}}_{n_{\text{dof}}^{s,e} \times 1}^T p_{f,n} A j^e d\xi, \\
\underbrace{\left\{ \mathbf{f}^{\mathcal{G}_4^{\text{INT},e}} \right\}}_{n_{\text{dof}}^{s,e} \times 1} &= \int_{-1}^1 \underbrace{\left\{ \mathbf{N}^{e,u} \right\}}_{n_{\text{dof}}^{s,e} \times 1}^T \rho_0^{h^e} g A j^e d\xi, \\
\underbrace{\left\{ \mathbf{f}^{\mathcal{G}^{\text{EXT},e}} \right\}}_{n_{\text{dof}}^{s,e} \times 1} &= \begin{cases} \underbrace{\left\{ \mathbf{N}^{e,u}(X=0, H) \right\}}_{n_{\text{dof}}^{s,e} \times 1}^T t^\sigma A & X=0, H \\ \mathbf{0} & 0 < X < H. \end{cases}
\end{aligned} \tag{4.551}$$

The mass matrix associated with the solid skeleton acceleration is given by

$$\underbrace{\left[\mathbf{m}_{u,u}^{\mathcal{G}_1^{\text{INT},e}} \right]}_{n_{\text{dof}}^{s,e} \times n_{\text{dof}}^{s,e}} = \int_{-1}^1 \rho_0^{h^e} \underbrace{\left\{ \mathbf{N}^{e,u} \right\}}_{n_{\text{dof}}^{s,e} \times 1}^T \underbrace{\left\{ \mathbf{N}^{e,u} \right\}}_{1 \times n_{\text{dof}}^{s,e}} A j^e d\xi. \tag{4.552}$$

The FE formulation for the balance of mass variational equation is written in block-matrix form as

$$\underbrace{\left\{ \mathbf{R}_{pf} \right\}}_{n_{\text{dof}}^{pf} \times 1} = \mathbf{0}, \tag{4.553}$$

where the global residual for the pore fluid pressure is given as

$$\mathbf{c}^{pf,T} \cdot \mathbf{R}_{pf} = \mathcal{H}^h = \mathcal{H}_1^{\text{INT},h} + \mathcal{H}_2^{\text{INT},h} + \mathcal{H}_3^{\text{INT},h} + \mathcal{H}_4^{\text{INT},h} - \mathcal{H}_1^{\text{EXT},h} = 0, \tag{4.554}$$

where

$$\begin{aligned}
\mathcal{H}_1^{\text{INT},h} &= \mathbf{A}_e^{n_e} \left\{ \mathbf{c}^{p_f,e} \right\}^T \cdot \left(\left[\mathbf{m}_{p_f,p_f}^{\mathcal{H}_1^{\text{INT},e}} \right] \cdot \left\{ \ddot{\pi}^e \right\} + \left[\mathbf{k}_{p_f,u}^{\mathcal{H}_1^{\text{INT},e}} \right] \cdot \left\{ \ddot{\mathbf{d}}^e \right\} + \left\{ \mathbf{f}^{\mathcal{H}_1^{\text{INT},e}} \right\} \right), \\
\mathcal{H}_2^{\text{INT},h} &= \mathbf{A}_e^{n_e} \left\{ \mathbf{c}^{p_f,e} \right\}^T \cdot \left(\left[\mathbf{k}_{p_f,u}^{\mathcal{H}_2^{\text{INT},e}} \right] \cdot \left\{ \ddot{\mathbf{d}}^e \right\} + \left\{ \mathbf{f}^{\mathcal{H}_2^{\text{INT},e}} \right\} \right), \\
\mathcal{H}_3^{\text{INT},h} &= \mathbf{A}_e^{n_e} \left\{ \mathbf{c}^{p_f,e} \right\}^T \cdot \left\{ \mathbf{f}^{\mathcal{H}_3^{\text{INT},e}} \right\}, \\
\mathcal{H}_4^{\text{INT},h} &= \mathbf{A}_e^{n_e} \left\{ \mathbf{c}^{p_f,e} \right\}^T \cdot \left(\left[\mathbf{k}_{p_f,u}^{\mathcal{H}_4^{\text{INT},e}} \right] \cdot \left\{ \ddot{\mathbf{d}}^e \right\} + \left\{ \mathbf{f}^{\mathcal{H}_4^{\text{INT},e}} \right\} \right), \\
\mathcal{H}^{\text{EXT},h} &= \mathbf{A}_e^{n_e} \left\{ \mathbf{c}^{p_f,e} \right\}^T \cdot \left\{ \mathbf{f}^{\mathcal{H}^{\text{EXT},e}} \right\},
\end{aligned} \tag{4.555}$$

with

$$\begin{aligned}
\left\{ \mathbf{f}^{\mathcal{H}_1^{\text{INT},e}} \right\}_{n_{\text{dof}}^{p_f,e} \times 1} &= \int_{-1}^1 \left\{ \mathbf{N}^{e,p_f} \right\}_{n_{\text{dof}}^{p_f,e} \times 1}^T \left[\frac{J^{h^e} n_f^{f,h^e}}{K_f^\eta} \left(\dot{p}_{f,n}^{h^e} + \frac{\Delta t}{2} \ddot{p}_{f,n}^{h^e} \right) + \left(\frac{\partial v_n^{h^e}}{\partial X} + \frac{\Delta t}{2} \frac{\partial a_n^{h^e}}{\partial X} \right) \right] A_j^e d\xi, \\
\left\{ \mathbf{f}^{\mathcal{H}_2^{\text{INT},e}} \right\}_{n_{\text{dof}}^{p_f,e} \times 1} &= - \int_{-1}^1 \left\{ \mathbf{N}^{e,p_f} \right\}_{n_{\text{dof}}^{p_f,e} \times 1}^T \frac{1}{K_f^\eta} \frac{\partial p_{f,n}}{\partial X} \hat{k}^{h^e} \left(\frac{\partial p_{f,n}^{h^e}}{\partial X} (F_{11}^{h^e})^{-1} - \rho^{\text{fR},h^e} g \right) A_j^e d\xi, \\
\left\{ \mathbf{f}^{\mathcal{H}_3^{\text{INT},e}} \right\}_{n_{\text{dof}}^{p_f,e} \times 1} &= \int_{-1}^1 \left\{ \mathbf{B}^{e,p_f} \right\}_{n_{\text{dof}}^{p_f,e} \times 1}^T \hat{k}^{h^e} \frac{\partial p_{f,n}^{h^e}}{\partial X} (F_{11}^{h^e})^{-1} A_j^e d\xi, \\
\left\{ \mathbf{f}^{\mathcal{H}_4^{\text{INT},e}} \right\}_{n_{\text{dof}}^{p_f,e} \times 1} &= \int_{-1}^1 \left\{ \mathbf{B}^{e,p_f} \right\}_{n_{\text{dof}}^{p_f,e} \times 1}^T \hat{k}^{h^e} \rho^{\text{fR},h^e} g A_j^e d\xi, \\
\left\{ \mathbf{f}^{\mathcal{H}^{\text{EXT},e}} \right\}_{n_{\text{dof}}^{p_f,e} \times 1} &= \begin{cases} \left\{ \mathbf{N}^{e,p_f}(X=H, X=0) \right\}_{n_{\text{dof}}^{p_f,e} \times 1}^T Q_f A & X=0, H \\ \mathbf{0} & 0 < X < H. \end{cases}
\end{aligned} \tag{4.556}$$

The coupling tangents that get multiplied by the updated solid skeleton acceleration at t_{n+1} are given by

$$\begin{aligned}
\underbrace{\left[\mathbf{k}_{p_f,u}^{\mathcal{H}_1^{\text{INT},e}} \right]}_{n_{\text{dof}}^{p_f,e} \times n_{\text{dof}}^{s,e}} &= \int_{-1}^1 \frac{\Delta t}{2} \underbrace{\left\{ \mathbf{N}^{e,p_f} \right\}^T}_{n_{\text{dof}}^{p_f,e} \times 1} \underbrace{\left\{ \mathbf{B}^{e,u} \right\}}_{1 \times n_{\text{dof}}^{s,e}} A_j^e d\xi, \\
\underbrace{\left[\mathbf{k}_{p_f,u}^{\mathcal{H}_2^{\text{INT},e}} \right]}_{n_{\text{dof}}^{p_f,e} \times n_{\text{dof}}^{s,e}} &= - \int_{-1}^1 \frac{1}{K_f^\eta} \frac{\partial p_{f,n}^{h^e}}{\partial X} \hat{k}^{h^e} \rho^{\text{fR},h^e} \underbrace{\left\{ \mathbf{N}^{e,p_f} \right\}^T}_{n_{\text{dof}}^{p_f,e} \times 1} \underbrace{\left\{ \mathbf{N}^{e,u} \right\}}_{1 \times n_{\text{dof}}^{s,e}} A_j^e d\xi, \\
\underbrace{\left[\mathbf{k}_{p_f,u}^{\mathcal{H}_4^{\text{INT},e}} \right]}_{n_{\text{dof}}^{p_f,e} \times n_{\text{dof}}^{s,e}} &= \int_{-1}^1 \hat{k}^{h^e} \rho^{\text{fR},h^e} \underbrace{\left\{ \mathbf{B}^{e,p_f} \right\}^T}_{n_{\text{dof}}^{p_f,e} \times 1} \underbrace{\left\{ \mathbf{N}^{e,u} \right\}}_{1 \times n_{\text{dof}}^{s,e}} A_j^e d\xi,
\end{aligned} \tag{4.557}$$

and the mass matrix associated with the pore fluid pressure is given by

$$\underbrace{\left[\mathbf{m}_{p_f,p_f}^{\mathcal{H}_1^{\text{INT},e}} \right]}_{n_{\text{dof}}^{p_f,e} \times n_{\text{dof}}^{p_f,e}} = \int_{-1}^1 \frac{J^{h^e} n^{f,h^e}}{K_f^\eta} \frac{\Delta t}{2} \underbrace{\left\{ \mathbf{N}^{e,p_f} \right\}^T}_{n_{\text{dof}}^{p_f,e} \times 1} \underbrace{\left\{ \mathbf{N}^{e,p_f} \right\}}_{1 \times n_{\text{dof}}^{p_f,e}} A_j^e d\xi. \tag{4.558}$$

When pressure stabilization is enabled, an additional term $\mathcal{H}^{\text{stab}}$ is added to the l.h.s. of Equation (4.554) and is defined as

$$\mathcal{H}^{\text{stab}} = \mathbf{A}_e^{n_e} \mathbf{c}^{p_f,e,T} \cdot \left(\underbrace{\left[\mathbf{m}_{p_f,p_f}^{\mathcal{H}^{\text{stab},e}} \right]}_{n_{\text{dof}}^{p_f,e} \times n_{\text{dof}}^{p_f,e}} \cdot \underbrace{\left\{ \ddot{\boldsymbol{\pi}}^e \right\}}_{n_{\text{dof}}^{p_f,e} \times 1} + \underbrace{\left\{ \mathbf{f}^{\mathcal{H}^{\text{stab},e}} \right\}}_{n_{\text{dof}}^{p_f,e} \times 1} \right), \tag{4.559}$$

where

$$\begin{aligned}
\underbrace{\left[\mathbf{m}_{p_f,p_f}^{\mathcal{H}^{\text{stab},e}} \right]}_{n_{\text{dof}}^{p_f,e} \times n_{\text{dof}}^{p_f,e}} &= \int_{-1}^1 \alpha^{\text{stab}} (F_{11}^{h^e})^{-1} \frac{\Delta t}{2} \underbrace{\left\{ \mathbf{B}^{e,p_f} \right\}^T}_{n_{\text{dof}}^{p_f,e} \times 1} \underbrace{\left\{ \mathbf{B}^{e,p_f} \right\}}_{1 \times n_{\text{dof}}^{p_f,e}} A_j^e d\xi, \\
\underbrace{\left\{ \mathbf{f}^{\mathcal{H}^{\text{stab},e}} \right\}}_{n_{\text{dof}}^{p_f,e} \times 1} &= \int_{-1}^1 \underbrace{\left\{ \mathbf{B}^{e,p_f} \right\}^T}_{n_{\text{dof}}^{p_f,e} \times 1} \alpha^{\text{stab}} (F_{11}^{h^e})^{-1} \left(\frac{\partial p_{f,n}^{h^e}}{\partial X} + \frac{\Delta t}{2} \frac{\partial \ddot{p}_{f,n}^{h^e}}{\partial X} \right) A_j^e d\xi.
\end{aligned} \tag{4.560}$$

Returning our attention to Equation (4.535), we see now that we can write it without introducing nonlinearity if we solve the equations in a staggered manner as described in Algorithm 1.

Therefore,

$$\underbrace{\left\{ \ddot{\mathbf{d}}_{n+1} \right\}}_{n_{\text{dof}}^s \times 1} = \underbrace{\left[\mathbf{M}_{u,u}^{\mathcal{G}_1^{\text{INT}}} \right]}_{n_{\text{dof}}^s \times n_{\text{dof}}^s}^{-1} \cdot \left(- \underbrace{\left\{ \mathbf{F}^{\mathcal{G}_2^{\text{INT}}} \right\}}_{n_{\text{dof}}^s \times 1} - \underbrace{\left\{ \mathbf{F}^{\mathcal{G}_3^{\text{INT}}} \right\}}_{n_{\text{dof}}^s \times 1} - \underbrace{\left\{ \mathbf{F}^{\mathcal{G}_4^{\text{INT}}} \right\}}_{n_{\text{dof}}^s \times 1} + \underbrace{\left\{ \mathbf{F}^{\mathcal{G}^{\text{EXT}}} \right\}}_{n_{\text{dof}}^s \times 1} \right), \tag{4.561}$$

where

$$\begin{aligned}
\underbrace{\left[\mathbf{M}_{u,u}^{\mathcal{G}_1^{\text{INT}}} \right]}_{n_{\text{dof}}^s \times n_{\text{dof}}^s} &= \mathbf{A}_e^{n_e} \underbrace{\left[\mathbf{m}_{u,u}^{\mathcal{G}_1^{\text{INT},e}} \right]}_{n_{\text{dof}}^{s,e} \times n_{\text{dof}}^{s,e}}, \\
\underbrace{\left\{ \mathbf{F}^{\mathcal{G}_2^{\text{INT}}} \right\}}_{n_{\text{dof}}^s \times 1} &= \mathbf{A}_e^{n_e} \underbrace{\left\{ \mathbf{f}^{\mathcal{G}_2^{\text{INT},e}} \right\}}_{n_{\text{dof}}^{s,e} \times 1}, \\
\underbrace{\left\{ \mathbf{F}^{\mathcal{G}_3^{\text{INT}}} \right\}}_{n_{\text{dof}}^s \times 1} &= \mathbf{A}_e^{n_e} \underbrace{\left\{ \mathbf{f}^{\mathcal{G}_3^{\text{INT},e}} \right\}}_{n_{\text{dof}}^{s,e} \times 1}, \\
\underbrace{\left\{ \mathbf{F}^{\mathcal{G}_4^{\text{INT}}} \right\}}_{n_{\text{dof}}^s \times 1} &= \mathbf{A}_e^{n_e} \underbrace{\left\{ \mathbf{f}^{\mathcal{G}_4^{\text{INT},e}} \right\}}_{n_{\text{dof}}^{s,e} \times 1}, \\
\underbrace{\left\{ \mathbf{F}^{\mathcal{G}^{\text{EXT}}} \right\}}_{n_{\text{dof}}^s \times 1} &= \mathbf{A}_e^{n_e} \underbrace{\left\{ \mathbf{f}^{\mathcal{G}^{\text{EXT},e}} \right\}}_{n_{\text{dof}}^{s,e} \times 1},
\end{aligned} \tag{4.562}$$

and the solid velocity and solid displacement updates are recovered by

$$\begin{aligned}
\underbrace{\left\{ \dot{\mathbf{d}}_{n+1} \right\}}_{n_{\text{dof}}^s \times 1} &= \underbrace{\left\{ \dot{\mathbf{d}}_n \right\}}_{n_{\text{dof}}^s \times 1} + \frac{\Delta t}{2} \left(\underbrace{\left\{ \ddot{\mathbf{d}}_n \right\}}_{n_{\text{dof}}^s \times 1} + \underbrace{\left\{ \ddot{\mathbf{d}}_{n+1} \right\}}_{n_{\text{dof}}^s \times 1} \right), \\
\underbrace{\left\{ \mathbf{d}_{n+1} \right\}}_{n_{\text{dof}}^s \times 1} &= \underbrace{\left\{ \mathbf{d}_n \right\}}_{n_{\text{dof}}^s \times 1} + \Delta t \underbrace{\left\{ \dot{\mathbf{d}}_n \right\}}_{n_{\text{dof}}^s \times 1} + \frac{\Delta t^2}{2} \underbrace{\left\{ \ddot{\mathbf{d}}_{n+1} \right\}}_{n_{\text{dof}}^s \times 1}.
\end{aligned} \tag{4.563}$$

Then, when solving for pore fluid pressure, we use the result given by Equation (4.561) for all values of $\ddot{\mathbf{d}}_{n+1}$ in Equations (4.555)₁₋₄. Therefore,

$$\begin{aligned}
\underbrace{\left\{ \ddot{\boldsymbol{\pi}}_{n+1} \right\}}_{n_{\text{dof}}^{p_f} \times 1} &= \underbrace{\left[\mathbf{M}_{p_f,p_f}^{\mathcal{H}_1^{\text{INT}}} \right]^{-1}}_{n_{\text{dof}}^{p_f} \times n_{\text{dof}}^{p_f}} \cdot \left(- \underbrace{\left\{ \mathbf{F}^{\mathcal{H}_1^{\text{INT}}} \right\}}_{n_{\text{dof}}^{p_f} \times 1} - \underbrace{\left\{ \mathbf{F}^{\mathcal{H}_2^{\text{INT}}} \right\}}_{n_{\text{dof}}^{p_f} \times 1} - \underbrace{\left\{ \mathbf{F}^{\mathcal{H}_3^{\text{INT}}} \right\}}_{n_{\text{dof}}^{p_f} \times 1} - \underbrace{\left\{ \mathbf{F}^{\mathcal{H}_4^{\text{INT}}} \right\}}_{n_{\text{dof}}^{p_f} \times 1} \right. \\
&\quad \left. + \left[\underbrace{\left[\mathbf{K}_{p_f,u}^{\mathcal{H}_1^{\text{INT}}} \right]}_{n_{\text{dof}}^{p_f} \times n_{\text{dof}}^s} + \underbrace{\left[\mathbf{K}_{p_f,u}^{\mathcal{H}_2^{\text{INT}}} \right]}_{n_{\text{dof}}^{p_f} \times n_{\text{dof}}^s} + \underbrace{\left[\mathbf{K}_{p_f,u}^{\mathcal{H}_4^{\text{INT}}} \right]}_{n_{\text{dof}}^{p_f} \times n_{\text{dof}}^s} \right] \cdot \underbrace{\left\{ \ddot{\mathbf{d}}_{n+1} \right\}}_{n_{\text{dof}}^s \times 1} + \underbrace{\left\{ \mathbf{F}^{\mathcal{H}^{\text{EXT}}} \right\}}_{n_{\text{dof}}^{p_f} \times 1} \right),
\end{aligned} \tag{4.564}$$

where

$$\begin{aligned}
\underbrace{\left[M_{p_f, p_f}^{\mathcal{H}_1^{\text{INT}}} \right]}_{n_{\text{dof}}^{p_f} \times n_{\text{dof}}^{p_f}} &= \mathbf{A}_e^{n_e} \underbrace{\left[m_{p_f, p_f}^{\mathcal{H}_1^{\text{INT}, e}} \right]}_{n_{\text{dof}}^{p_f, e} \times n_{\text{dof}}^{p_f, e}}, \\
\underbrace{\left[K_{p_f, u}^{\mathcal{H}_1^{\text{INT}}} \right]}_{n_{\text{dof}}^{p_f} \times n_{\text{dof}}^s} &= \mathbf{A}_e^{n_e} \underbrace{\left[m_{p_f, u}^{\mathcal{H}_1^{\text{INT}, e}} \right]}_{n_{\text{dof}}^{p_f, e} \times n_{\text{dof}}^{s, e}}, \\
\underbrace{\left[K_{p_f, u}^{\mathcal{H}_2^{\text{INT}}} \right]}_{n_{\text{dof}}^{p_f} \times n_{\text{dof}}^s} &= \mathbf{A}_e^{n_e} \underbrace{\left[m_{p_f, u}^{\mathcal{H}_2^{\text{INT}, e}} \right]}_{n_{\text{dof}}^{p_f, e} \times n_{\text{dof}}^{s, e}}, \\
\underbrace{\left[K_{p_f, u}^{\mathcal{H}_4^{\text{INT}}} \right]}_{n_{\text{dof}}^{p_f} \times n_{\text{dof}}^s} &= \mathbf{A}_e^{n_e} \underbrace{\left[m_{p_f, u}^{\mathcal{H}_4^{\text{INT}, e}} \right]}_{n_{\text{dof}}^{p_f, e} \times n_{\text{dof}}^{s, e}}, \\
\underbrace{\left\{ \mathbf{F}^{\mathcal{H}_1^{\text{INT}}} \right\}}_{n_{\text{dof}}^{p_f} \times 1} &= \mathbf{A}_e^{n_e} \underbrace{\left\{ \mathbf{f}^{\mathcal{H}_1^{\text{INT}, e}} \right\}}_{n_{\text{dof}}^{p_f, e} \times 1}, \\
\underbrace{\left\{ \mathbf{F}^{\mathcal{H}_2^{\text{INT}}} \right\}}_{n_{\text{dof}}^{p_f} \times 1} &= \mathbf{A}_e^{n_e} \underbrace{\left\{ \mathbf{f}^{\mathcal{H}_2^{\text{INT}, e}} \right\}}_{n_{\text{dof}}^{p_f, e} \times 1}, \\
\underbrace{\left\{ \mathbf{F}^{\mathcal{H}_3^{\text{INT}}} \right\}}_{n_{\text{dof}}^{p_f} \times 1} &= \mathbf{A}_e^{n_e} \underbrace{\left\{ \mathbf{f}^{\mathcal{H}_3^{\text{INT}, e}} \right\}}_{n_{\text{dof}}^{p_f, e} \times 1}, \\
\underbrace{\left\{ \mathbf{F}^{\mathcal{H}_4^{\text{INT}}} \right\}}_{n_{\text{dof}}^{p_f} \times 1} &= \mathbf{A}_e^{n_e} \underbrace{\left\{ \mathbf{f}^{\mathcal{H}_4^{\text{INT}, e}} \right\}}_{n_{\text{dof}}^{p_f, e} \times 1}, \\
\underbrace{\left\{ \mathbf{F}^{\mathcal{H}^{\text{EXT}}} \right\}}_{n_{\text{dof}}^{p_f} \times 1} &= \mathbf{A}_e^{n_e} \underbrace{\left\{ \mathbf{f}^{\mathcal{H}^{\text{EXT}, e}} \right\}}_{n_{\text{dof}}^{p_f, e} \times 1}.
\end{aligned} \tag{4.565}$$

The first time derivative on pore fluid pressure and the pore fluid pressure updates are recovered by

$$\begin{aligned}
\underbrace{\left\{ \dot{\boldsymbol{\pi}}_{n+1} \right\}}_{n_{\text{dof}}^{p_f} \times 1} &= \underbrace{\left\{ \dot{\boldsymbol{\pi}}_n \right\}}_{n_{\text{dof}}^{p_f} \times 1} + \frac{\Delta t}{2} \left(\underbrace{\left\{ \ddot{\boldsymbol{\pi}}_n \right\}}_{n_{\text{dof}}^{p_f} \times 1} + \underbrace{\left\{ \ddot{\boldsymbol{\pi}}_{n+1} \right\}}_{n_{\text{dof}}^{p_f} \times 1} \right), \\
\underbrace{\left\{ \boldsymbol{\pi}_{n+1} \right\}}_{n_{\text{dof}}^{p_f} \times 1} &= \underbrace{\left\{ \boldsymbol{\pi}_n \right\}}_{n_{\text{dof}}^{p_f} \times 1} + \Delta t \underbrace{\left\{ \dot{\boldsymbol{\pi}}_n \right\}}_{n_{\text{dof}}^{p_f} \times 1} + \frac{\Delta t^2}{2} \underbrace{\left\{ \ddot{\boldsymbol{\pi}}_{n+1} \right\}}_{n_{\text{dof}}^{p_f} \times 1}.
\end{aligned} \tag{4.566}$$

If pressure stabilization is enabled, then we invert a summation of matrices in Equation (4.564) and must subtract the force vector associated with pressure stabilization along with the other force vectors:

$$\begin{aligned}
\underbrace{\left\{ \ddot{\boldsymbol{\pi}}_{n+1} \right\}}_{n_{\text{dof}}^{p_f} \times 1} &= \left(\underbrace{\left[\mathbf{M}_{p_f, p_f}^{\mathcal{H}^{\text{INT}}} \right]}_{n_{\text{dof}}^{p_f} \times n_{\text{dof}}^{p_f}} + \underbrace{\left[\mathbf{M}_{p_f, p_f}^{\mathcal{H}^{\text{stab}}} \right]}_{n_{\text{dof}}^{p_f} \times n_{\text{dof}}^{p_f}} \right)^{-1} \cdot \left(- \underbrace{\left\{ \mathbf{F}^{\mathcal{H}_1^{\text{INT}}} \right\}}_{n_{\text{dof}}^{p_f} \times 1} - \underbrace{\left\{ \mathbf{F}^{\mathcal{H}_2^{\text{INT}}} \right\}}_{n_{\text{dof}}^{p_f} \times 1} - \underbrace{\left\{ \mathbf{F}^{\mathcal{H}_3^{\text{INT}}} \right\}}_{n_{\text{dof}}^{p_f} \times 1} \right. \\
&\quad - \underbrace{\left\{ \mathbf{F}^{\mathcal{H}_4^{\text{INT}}} \right\}}_{n_{\text{dof}}^{p_f} \times 1} - \underbrace{\left\{ \mathbf{F}^{\mathcal{H}^{\text{stab}}} \right\}}_{n_{\text{dof}}^{p_f} \times 1} + \left[\underbrace{\left[\mathbf{K}_{p_f, u}^{\mathcal{H}_1^{\text{INT}}} \right]}_{n_{\text{dof}}^{p_f} \times n_{\text{dof}}^s} + \underbrace{\left[\mathbf{K}_{p_f, u}^{\mathcal{H}_2^{\text{INT}}} \right]}_{n_{\text{dof}}^{p_f} \times n_{\text{dof}}^s} + \underbrace{\left[\mathbf{K}_{p_f, u}^{\mathcal{H}_4^{\text{INT}}} \right]}_{n_{\text{dof}}^{p_f} \times n_{\text{dof}}^s} \right] \cdot \underbrace{\left\{ \ddot{\mathbf{d}}_{n+1} \right\}}_{n_{\text{dof}}^s \times 1} \\
&\quad \left. + \underbrace{\left\{ \mathbf{F}^{\mathcal{H}^{\text{EXT}}} \right\}}_{n_{\text{dof}}^{p_f} \times 1} \right), \tag{4.567}
\end{aligned}$$

where,

$$\begin{aligned}
\underbrace{\left[\mathbf{M}_{p_f, p_f}^{\mathcal{H}^{\text{stab}}} \right]}_{n_{\text{dof}}^{p_f} \times n_{\text{dof}}^{p_f}} &= \mathbf{A}_e^{n_e} \underbrace{\left[\mathbf{m}_{p_f, p_f}^{\mathcal{H}^{\text{stab}, e}} \right]}_{n_{\text{dof}}^{p_f, e} \times n_{\text{dof}}^{p_f, e}}, \\
\underbrace{\left\{ \mathbf{F}^{\mathcal{H}^{\text{stab}}} \right\}}_{n_{\text{dof}}^{p_f} \times 1} &= \mathbf{A}_e^{n_e} \underbrace{\left\{ \mathbf{f}^{\mathcal{H}^{\text{stab}, e}} \right\}}_{n_{\text{dof}}^{p_f, e} \times 1}. \tag{4.568}
\end{aligned}$$

Owing to the gradient shape functions that appear in $\mathbf{m}_{p_f, p_f}^{\mathcal{H}^{\text{stab}, e}}$, pressure stabilization restricts one to use consistent mass matrices because typical row-sum mass lumping techniques are not possible with the gradient shape functions.

4.4 Stabilization techniques

Oftentimes for dynamical problems, particularly at high strain-rates, the stability of the numerical integration scheme is dependent on artificial damping introduced into the time-discretized balance equations. Of the integrators introduced above, only the Newmark-beta integration scheme with added dissipation, i.e., Newmark-beta method with the parameters $\beta = 0.3025$ and $\gamma = 0.6$, has some algorithmic damping. Therefore, whether or not the other numerical integration schemes remain stable is dependent upon tolerances (relative and/or absolute) and the length of the time steps. We have found that for shock-loading problems, tight tolerances and small time steps

(either fixed, or calculated through an adaptive time-stepping scheme with tight tolerance for truncation error, e.g., the Runge-Kutta methods discussed in Section 4.3.1) are not enough to control spurious pressure oscillations (or in some cases, negative Jacobians of deformation, i.e., an “inverted” element) that make the simulation go unstable. Furthermore, for consistent element types, at low-to-moderate permeabilities, we require element-stabilization techniques to satisfy the well known *inf-sup* condition. To address these issues, we have explored adding a canonical “shock viscosity” term to the solid skeleton stress, as well as a pressure stabilization term to the balance of mass of the mixture, both of which are discussed below. As will be shown in proceeding examples of shock-like loadings in Chapter 5, we have found that a combination of both shock viscosity and pressure stabilization allow us to obtain results for lung parenchyma deformations at higher overpressures, and with less computational expense given that we are able to take larger time-steps comparable to those suggested by a CFL condition. Additionally, when considering thermoporoelastodynamics, the pore fluid energy balance takes the form of an advection-diffusion equation, which may necessitate stabilization methods, such as streamline upwind Petrov-Galerkin (SUPG), to control spurious oscillations and overshoots in the pore fluid temperature solution.

4.4.1 Shock viscosity

The history of the artificial shock viscosity can be traced back to the seminal work by von Neumann and Richtmyer [1950] who proposed that a viscous term q be added to an otherwise inviscid fluid’s momentum equation for shocks propagating in one dimension, i.e.,

$$q := c_0^2 \rho (\Delta x)^2 \left(\frac{\partial \dot{x}}{\partial x} \right)^2, \quad (4.569)$$

where $q = 0$ for expanding motions ($\partial \dot{x} / \partial x \geq 0$), x is the coordinate in the direction of motion, Δx is the grid spacing, ρ is the material density and c_0 is a constant ≈ 2 . Landshoff [1955] introduced a q term that was linear in the velocity gradient, i.e.,

$$q := c_L \rho \Delta x c \left| \frac{\partial \dot{x}}{\partial x} \right|, \quad (4.570)$$

where c_L is a constant ≈ 1 and c is the local sound speed, i.e., the square root of the local P-wave modulus divided by the local density. For further reading on the subject, we refer the interested reader to reviews by Benson [2007] and Margolin and Lloyd-Ronning [2022], with details on thermodynamical validity discussed in Mattson and Rider [2014]. In this work, we use the artificial viscosity given by Wilkins [1980] (which is also used in LS-DYNA Dev. [2019]) which combines linear and quadratic terms into one form, i.e.,

$$q = \begin{cases} \rho l \left(C_0 l \dot{\epsilon}_{kk}^2 - C_1 c \dot{\epsilon}_{kk} \right) & \text{if } \dot{\epsilon}_{kk} < 0 \\ 0 & \text{if } \dot{\epsilon}_{kk} \geq 0, \end{cases} \quad (4.571)$$

where l is a characteristic length scale (in 1-D, this reduces to the local element length), C_0 and C_1 are constants typically taken to be 1.5 and 0.06, respectively, and $\dot{\epsilon}_{ij}$ is the strain-rate tensor,

$$\dot{\epsilon}_{ij} = l_{ij} := \frac{\partial v_i}{\partial x_j}. \quad (4.572)$$

The extent to which the shock viscosity effects the solution depends on the magnitude of the constants C_0 and C_1 . The latter is responsible for damping out oscillations behind the front (i.e., the weak waves produced by compression of the material, irrespective of the strength of the shock front) and the former is responsible for damping out oscillations near or ahead of the front. Large values of either constant tend to overly smooth out the shock over multiple elements; examples of shock-like loadings with varying ranges of the constants that demonstrate this phenomenon are shown in Section 5.3.1.

The shock viscosity is essentially an opposing pressure term added on to the solid skeleton stress, such that the augmented effective solid skeleton Cauchy stress is written as

$$\tilde{\boldsymbol{\sigma}}_E^s = \boldsymbol{\sigma}_E^{s,\text{dev}} - (P + q)\mathbf{1}, \quad (4.573)$$

which, using the common definitions for solid skeleton deviatoric stress $\boldsymbol{\sigma}_E^{s,\text{dev}}$ and solid skeleton

hydrostatic pressure P , we may also write as,

$$\tilde{\sigma}_{ij(E)}^s = \begin{cases} \sigma_{ij(E)}^s - \underbrace{\rho^s h [C_0 h l_{kk}^2 - C_1 c l_{kk}]}_{:=q} \delta_{ij} & \text{if } l_{kk} < 0 \text{ (in compression)} \\ \sigma_{ij(E)}^s & \text{if } l_{kk} \geq 0 \text{ (in tension),} \end{cases} \quad (4.574)$$

or, in the reference configuration,

$$\tilde{P}_{iI(E)}^s = \begin{cases} P_{iI(E)}^s - J \rho_0^s h_0 \underbrace{\left[C_0 J h_0 \left(\frac{\partial v_k}{\partial X_K} \right)^2 F_{Kk}^{-2} - C_1 c \frac{\partial v_k}{\partial X_K} F_{Kk}^{-1} \right]}_{:=Q} F_{Ii}^{-1} & \text{if } \frac{\partial v_k}{\partial X_K} < 0 \text{ (in compression)} \\ P_{iI(E)}^s & \text{if } \frac{\partial v_k}{\partial X_K} \geq 0 \text{ (in tension),} \end{cases} \quad (4.575)$$

where the F_{Kk}^{-1} scaling of the velocity gradient is omitted from the conditions because it does not affect the sign of the velocity gradient, which is what determines whether or not the shock viscosity is applied. In the 1-D uniaxial strain regime, Equation (4.575) reduces to, e.g., along the direction of motion,

$$\tilde{P}_{11(E)}^s = \begin{cases} P_{11(E)}^s - \rho^s h_0 \frac{\partial v}{\partial X} \underbrace{\left(C_0 h_0 \frac{\partial v}{\partial X} - C_1 c \right)}_{:=Q_{1-D}} & \text{if } \frac{\partial v}{\partial X} < 0 \\ P_{11(E)}^s & \text{if } \frac{\partial v}{\partial X} \geq 0, \end{cases} \quad (4.576)$$

where the F_{11}^{-1} scaling of the velocity gradient is omitted from the conditions for aforementioned reasons. For explicit and semi-implicit¹⁰ integration methods, the shock-viscosity terms are simply added to the stress (force residual) since we assume that solid skeleton stress is evaluated explicitly. For implicit integration methods, we require additional terms be added to the consistent tangent when shock-viscosity is enabled; refer to Appendix B.1 for the formulation of the linearized term and Appendix C.1.1 for the finite element formulation.¹¹

¹⁰ A semi-implicit predictor-corrector integration scheme was pursued at one point in this work. However, we found it to be computationally expensive when compared to the Runge-Kutta method, and, owing to its complexity (even for $(\mathbf{u}-p_f)$), it was abandoned. For details on implementation for simpler theory, the interested reader is referred to Markert et al. [2009].

¹¹ Note that the inverse deformation gradient which maps the solid skeleton velocity v from the current to the reference configuration has been omitted from the signage calculation of the strain-rate in Equation (4.576) given that for non-invertible elements it should be greater than zero and therefore play no role in the determination of whether or not the solid skeleton is undergoing expansion or compression.

Shock viscosity applied to the pore fluid. Suppose that an additional shock viscosity is applied to the pore fluid. Let

$$\boldsymbol{\sigma}^f = \boldsymbol{\sigma}_E^f - (n^f p_f + q^f) \mathbf{1}, \quad (4.577)$$

with

$$q^f := \rho^f h_f [C_0 h_f l_{kk(f)}^2 - C_1 c^f l_{kk(f)}]. \quad (4.578)$$

Therein, h_f represents the characteristic length scale of the pore fluid, such that

$$h_f = J_f h_{0(f)}. \quad (4.579)$$

Since the Lagrangian implementation at hand is defined with respect to the reference configuration of the solid skeleton (s) and not the reference configuration of the pore fluid (f), we will assume

$$h_f \approx h_s = J_s h_{0(s)}. \quad (4.580)$$

Thus, the pore fluid shock viscosity (dropping subscript (s) for notational convenience) is written as

$$q^f := \rho^f h [C_0 h l_{kk(f)}^2 - C_1 c^f l_{kk(f)}], \quad (4.581)$$

such that the augmented pore fluid stress is

$$\tilde{\sigma}_{ij}^f = \begin{cases} \sigma_{ij}^f - \rho^f h [C_0 h l_{kk(f)}^2 - C_1 c^f l_{kk(f)}] \delta_{ij} & \text{if } l_{kk(f)} < 0 \text{ (in compression)} \\ \sigma_{ij}^f & \text{if } l_{kk(f)} > 0 \text{ (in expansion)}. \end{cases} \quad (4.582)$$

This may be written in the reference configuration of the solid skeleton as

$$\tilde{P}_{iI}^f = \begin{cases} P_{iI}^f - \underbrace{J \rho_0^f h_0 [C_0 J h_0 \left(\frac{\partial v_{k(f)}}{\partial X_K} F_{Kk}^{-1} \right)^2 - C_1 c^f \frac{\partial v_{k(f)}}{\partial X_K} F_{Kk}^{-1}] F_{Ii}^{-1}}_{:=Q^f} & \text{if } \frac{\partial v_{k(f)}}{\partial X_K} < 0 \text{ (in compression)} \\ P_{iI}^f & \text{if } \frac{\partial v_{k(f)}}{\partial X_K} > 0 \text{ (in expansion)}. \end{cases} \quad (4.583)$$

In the 1-D uniaxial strain regime,

$$\tilde{P}_{11}^f = \begin{cases} \underbrace{P_{11}^f - \rho^f h_0 \frac{\partial v_f}{\partial X} \left(C_0 h_0 \frac{\partial v_f}{\partial X} - C_1 c^f \right)}_{:=Q_{1-D}^f} & \text{if } \frac{\partial v_f}{\partial X} < 0 \text{ (in compression)} \\ P_{11}^f & \text{if } \frac{\partial v_f}{\partial X} > 0 \text{ (in expansion)}. \end{cases} \quad (4.584)$$

Furthermore, the gas wave speed c^f will be assumed constant using the isentropic bulk modulus K_f^η . This assumption allows for an easier computation of $\text{div}(q^f)$ as it appears in the momentum balance:

$$\begin{aligned} \frac{\partial q^f}{\partial x_i} &= J \frac{\partial q^f}{\partial X_I} F_{Ii}^{-1} \\ \Rightarrow \frac{\partial q^f}{\partial X_I} &= \frac{\partial(n^f \rho^{\text{fR}})}{\partial X_I} J h_0 [C_0 J h_0 l_{kk(f)}^2 - C_1 K_f^\eta l_{kk(f)}] \\ &\quad + \rho^f h_0 [C_0 J h_0 l_{kk(f)}^2 - C_1 K_f^\eta l_{kk(f)}] \frac{\partial J}{\partial X_I} \\ &\quad + \rho^f J h_0 \left[C_0 h_0 \left(l_{kk(f)}^2 \frac{\partial J}{\partial X_I} + 2 J l_{mm(f)} \frac{\partial}{\partial X_I} \frac{\partial v_{k(f)}}{\partial x_k} \right) \right. \\ &\quad \left. + C_1 K_f^\eta \frac{\partial}{\partial X_I} \frac{\partial v_{k(f)}}{\partial x_k} \right]. \end{aligned} \quad (4.585)$$

Therein,

$$\begin{aligned} \frac{\partial n^f}{\partial X_I} &= \frac{n_0^s}{J} \frac{\partial^2 u_i}{\partial X_I \partial X_J}, \\ \frac{\partial \rho^{\text{fR}}}{\partial X_I} &= \begin{cases} \frac{\rho^{\text{fR}}}{K_f^\eta} \frac{\partial p_f}{\partial X_I} & p_f = p_f(\rho^{\text{fR}}) \text{ (loc. homogeneous temp. model)} \\ \frac{1}{\mathfrak{R}\theta^f} \frac{\partial p_f}{\partial X_I} - \frac{\rho^{\text{fR}}}{\theta^f} \frac{\partial \theta^f}{\partial X_I} & p_f = p_f(\rho^{\text{fR}}, \theta^f) \text{ (ideal gas model)}, \end{cases} \\ \frac{\partial J}{\partial X_I} &= J \frac{\partial^2 u_i}{\partial X_I \partial X_J}. \end{aligned} \quad (4.586)$$

Thus, divergence of the pore fluid shock viscosity is first written as

$$\begin{aligned} \frac{\partial q^f}{\partial x_i} &= J \left(n^s \rho^{\text{fR}} \frac{\partial^2 u_i}{\partial X_I \partial X_J} F_{Jj}^{-1} + n^f \frac{\partial \rho^{\text{fR}}}{\partial X_I} \right) J h_0 \left[C_0 J h_0 \left(\frac{\partial v_{k(f)}}{\partial X_K} F_{Kk}^{-1} \right)^2 - C_1 K_f^\eta \frac{\partial v_{k(f)}}{\partial X_K} F_{Kk}^{-1} \right] F_{Ii}^{-1} \\ &\quad + J \rho^f h_0 \left[C_0 J h_0 \left(\frac{\partial v_{k(f)}}{\partial X_K} F_{Kk}^{-1} \right)^2 - C_1 K_f^\eta \frac{\partial v_{k(f)}}{\partial X_K} F_{Kk}^{-1} \right] J \frac{\partial^2 u_i}{\partial X_I \partial X_J} F_{Jj}^{-1} F_{Ii}^{-1} \\ &\quad + J \rho^f J h_0 \left[C_0 h_0 \left(\frac{\partial v_{k(f)}}{\partial X_K} F_{Kk}^{-1} \right)^2 J \frac{\partial^2 u_i}{\partial X_I \partial X_J} F_{Jj}^{-1} + 2 C_0 J h_0 \frac{\partial v_{k(f)}}{\partial X_K} F_{Kk}^{-1} \frac{\partial^2 v_{m(f)}}{\partial X_I \partial X_M} F_{Mm}^{-1} \right. \\ &\quad \left. + C_1 K_f^\eta \frac{\partial^2 v_{k(f)}}{\partial X_I \partial X_K} F_{Kk}^{-1} \right] F_{Ii}^{-1}. \end{aligned} \quad (4.587)$$

The first two lines on the r.h.s. of Equation (4.587) can be simplified to

$$\frac{q^f}{\rho^f} \left(\rho^{\text{fR}} \frac{\partial^2 u_i}{\partial X_I \partial X_J} F_{Jj}^{-1} + n^f \frac{\partial \rho^{\text{fR}}}{\partial X_I} \right) J F_{Ii}^{-1}. \quad (4.588)$$

Thus, we may write

$$\begin{aligned} \frac{\partial q^f}{\partial x_i} &= \frac{q^f}{\rho^f} \left(\rho^{\text{fR}} \frac{\partial^2 u_i}{\partial X_I \partial X_J} F_{Jj}^{-1} + n^f \frac{\partial \rho^{\text{fR}}}{\partial X_I} \right) J F_{Ii}^{-1} \\ &+ J^2 \rho^f h_0 \left[C_0 J h_0 \frac{\partial v_{k(f)}}{\partial X_K} F_{Kk}^{-1} \left(\frac{\partial v_{m(f)}}{\partial X_M} F_{Mm}^{-1} \frac{\partial^2 u_i}{\partial X_I \partial X_J} F_{Jj}^{-1} + 2 \frac{\partial^2 v_{m(f)}}{\partial X_I \partial X_M} F_{Mm}^{-1} \right) \right. \\ &\quad \left. + C_1 K_f^\eta \frac{\partial^2 v_{k(f)}}{\partial X_I \partial X_K} F_{Kk}^{-1} \right] F_{Ii}^{-1}. \end{aligned} \quad (4.589)$$

Equation (4.589) may be added to the residual of the pore fluid momentum balance such that

$$\mathcal{I} = \begin{cases} \sum_{i=1}^5 \mathcal{I}_i^{\text{INT}} + \mathcal{I}_7 & (\mathbf{u} - \mathbf{u}_f - p_f) \\ \sum_{i=1}^6 \mathcal{I}_i^{\text{INT}} + \mathcal{I}_7 & (\mathbf{u} - \mathbf{u}_f - p_f - \theta^s - \theta^f), \end{cases} \quad (4.590)$$

with

$$\begin{aligned} \mathcal{I}_7^{\text{INT}} &= \int_{\mathcal{B}_0} w^{u_f} \left(\frac{q^f}{\rho^f} \left(\rho^{\text{fR}} \frac{\partial^2 u_i}{\partial X_I \partial X_J} F_{Jj}^{-1} + n^f \frac{\partial \rho^{\text{fR}}}{\partial X_I} \right) J F_{Ii}^{-1} \right. \\ &\quad \left. + J^2 \rho^f h_0 \left[C_0 J h_0 \frac{\partial v_{k(f)}}{\partial X_K} F_{Kk}^{-1} \left(\frac{\partial v_{m(f)}}{\partial X_M} F_{Mm}^{-1} \frac{\partial^2 u_i}{\partial X_I \partial X_J} F_{Jj}^{-1} + 2 \frac{\partial^2 v_{m(f)}}{\partial X_I \partial X_M} F_{Mm}^{-1} \right) \right. \right. \\ &\quad \left. \left. + C_1 K_f^\eta \frac{\partial^2 v_{k(f)}}{\partial X_I \partial X_K} F_{Kk}^{-1} \right] F_{Ii}^{-1} \right) dV. \end{aligned} \quad (4.591)$$

In the 1-D uniaxial strain approximation, Equation (4.589) simplifies to

$$\begin{aligned} \frac{\partial q^f}{\partial x} &= \frac{q^f}{\rho^f} \left(\rho^{\text{fR}} \frac{\partial^2 u}{\partial X^2} F_{11}^{-1} + n^f \frac{\partial \rho^{\text{fR}}}{\partial X} \right) \\ &+ \rho^f h_0 \left[C_0 h_0 \frac{\partial v_f}{\partial X} \left(\frac{\partial v_f}{\partial X} \frac{\partial^2 u}{\partial X^2} F_{11}^{-1} + 2 \frac{\partial^2 v_f}{\partial X^2} \right) + C_1 K_f^\eta \frac{\partial^2 v_f}{\partial X^2} \right], \end{aligned} \quad (4.592)$$

with

$$\frac{\partial \rho^{\text{fR}}}{\partial X} = \begin{cases} \frac{\rho^{\text{fR}}}{K_f^\eta} \frac{\partial p_f}{\partial X} & p_f = p_f(\rho^{\text{fR}}) \text{ (loc. homogeneous temp. model)} \\ \frac{1}{\mathfrak{R}\theta^f} \frac{\partial p_f}{\partial X} - \frac{\rho^{\text{fR}}}{\theta^f} \frac{\partial \theta^f}{\partial X} & p_f = p_f(\rho^{\text{fR}}, \theta^f) \text{ (ideal gas model)}. \end{cases} \quad (4.593)$$

$$(4.594)$$

Thus, Equation (4.591) simplifies to

$$\begin{aligned} \mathcal{I}_7^{\text{INT}} = & \int_0^{X=H} w^{u_f} \left(\frac{q^f}{\rho^f} \left(\rho^{\text{fR}} \frac{\partial^2 u}{\partial X^2} F_{11}^{-1} + n^f \frac{\partial \rho^{\text{fR}}}{\partial X} \right) \right. \\ & \left. + \rho^f h_0 \left[C_0 h_0 \frac{\partial v_f}{\partial X} \left(\frac{\partial v_f}{\partial X} \frac{\partial^2 u}{\partial X^2} F_{11}^{-1} + 2 \frac{\partial^2 v_f}{\partial X^2} \right) + C_1 K_f^\eta \frac{\partial^2 v_f}{\partial X^2} \right] \right) A dX . \end{aligned} \quad (4.595)$$

The additional terms that appear in the balance of momentum and balance of mass of the mixture, are, respectively,

$$\begin{aligned} \mathcal{G}_6^{\text{INT}} = & - \int_{\mathcal{B}_0} \frac{\partial w_i^u}{\partial X_I} Q^f dV , \\ \mathcal{H}_8^{\text{INT}} = & \int_{\mathcal{B}_0} \frac{\partial w^{p_f}}{\partial X_I} \frac{\hat{k}}{n^f} \left(\frac{q^f}{\rho^f} \left(\rho^{\text{fR}} \frac{\partial^2 u_i}{\partial X_I \partial X_J} F_{Jj}^{-1} + n^f \frac{\partial \rho^{\text{fR}}}{\partial X_I} \right) J F_{Ii}^{-1} \right. \\ & \left. + J^2 \rho^f h_0 \left[C_0 J h_0 \frac{\partial v_{k(f)}}{\partial X_K} F_{Kk}^{-1} \left(\frac{\partial v_{m(f)}}{\partial X_M} F_{Mm}^{-1} \frac{\partial^2 u_i}{\partial X_I \partial X_J} F_{Jj}^{-1} + 2 \frac{\partial^2 v_{m(f)}}{\partial X_I \partial X_M} F_{Mm}^{-1} \right) \right. \right. \\ & \left. \left. + C_1 K_f^\eta \frac{\partial^2 v_{k(f)}}{\partial X_I \partial X_K} F_{Kk}^{-1} \right] F_{Ii}^{-1} \right) dV , \end{aligned} \quad (4.596)$$

with 1-D counterparts

$$\begin{aligned} \mathcal{G}_6^{\text{INT}} = & - \int_0^{X=H} \frac{\partial w^u}{\partial X} Q^f A dX , \\ \mathcal{H}_8^{\text{INT}} = & \int_0^{X=H} \frac{\partial w^{p_f}}{\partial X} \frac{\hat{k}}{n^f} \left(\frac{q^f}{\rho^f} \left(\rho^{\text{fR}} \frac{\partial^2 u}{\partial X^2} F_{11}^{-1} + n^f \frac{\partial \rho^{\text{fR}}}{\partial X} \right) \right. \\ & \left. + \rho^f h_0 \left[C_0 h_0 \frac{\partial v_f}{\partial X} \left(\frac{\partial v_f}{\partial X} \frac{\partial^2 u}{\partial X^2} F_{11}^{-1} + 2 \frac{\partial^2 v_f}{\partial X^2} \right) + C_1 K_f^\eta \frac{\partial^2 v_f}{\partial X^2} \right] \right) A dX . \end{aligned} \quad (4.597)$$

A shock viscosity for the pore fluid is not pursued herein, but may be considered as part of future work.

4.4.2 Pressure stabilization

For stabilizing the linear Q2-Q1-P1, Q1-Q1-P1 and Q1-P1 elements¹², we follow the approach of Truty and Zimmerman [2006], which is based on the method of Brezzi and Pitkäranta [1984].

¹² In practice we found that using pressure stabilization on the Hermite cubic elements sped up computations and maintained accuracy, though strictly speaking this is not necessary given the higher-order continuity of the displacement variables in relation to pore fluid pressure.

The stabilization term acts like an opposing pore fluid pressure flux in the variational equation of the balance of mass, wherein

$$\mathcal{H} = \left(\sum_i^{n_{\text{INT}}} \mathcal{H}_i^{\text{INT}} \right) - \mathcal{H}^{\text{EXT}} + \mathcal{H}^{\text{stab}} = 0, \quad (4.598)$$

$$\mathcal{H}^{\text{stab}} := \int_{\mathcal{B}_0} \alpha^{\text{stab}} \frac{\partial w^{p_f}}{\partial X_I} F_{Ii}^{-1} \frac{\partial \dot{p}_f}{\partial X_K} F_{Ki}^{-1} J dV, \quad (4.599)$$

where the value of n_{INT} depends on the governing physics (refer to the variations of the variational forms of the balance of mass in Section 4.1). In the 1-D uniaxial strain regime, the stabilization term reduces to

$$\mathcal{H}^{\text{stab}} = \int_0^{X=H} \alpha^{\text{stab}} \frac{\partial w^{p_f}}{\partial X} F_{11}^{-1} \frac{\partial \dot{p}_f}{\partial X} A dX. \quad (4.600)$$

While Truty and Zimmerman [2006] have been able to relate the pressure stabilization parameter α^{stab} to material geometry and simulation time-step, such an approach would be difficult to derive for compressible pore fluid, large deformations and high strain-rate loadings. Therefore, we have chosen α^{stab} on an ad-hoc basis. Typically, the smaller the value of α^{stab} , the more stable the simulation and the closer the results become to the already stable (for low pressure amplitude loadings) Q2-Q2-P1 and Q2-P1 mixed elements. “Large” values of $\alpha^{\text{stab}} \geq 10^{-6}$ give rise to numerical instabilities or otherwise inaccurate results; $\alpha^{\text{stab}} = 10^{-10} \text{ m}^3\text{-s}^2/\text{kg}$ appears to give the best results. A detailed discussion on the effect of pressure stabilization as it applies to a numerical verification example is provided in Section 5.3.2.

For both explicit and implicit integration methods, the inclusion of the stabilization term requires an additional tangent matrix. For explicit methods, this is because of the inclusion of the time derivative on the pore fluid pressure gradient, which is unknown at solution time t_{n+1} . This tangent also limits us to use consistent “mass” matrices in the weak formulation of the balance of mass given that the gradient shape functions for linear-order interpolations produce constant off-diagonal terms that do not lead to cancellation at the Gauss points as they would for linear-order and quadratic-order interpolations (no gradients) using a row-sum lumping technique. This tangent is derived in Appendix B.3 and formulated for finite elements in Appendix C.1.2.

4.4.3 Streamline upwind Petrov-Galerkin

Recall from Section 4.1.5 that the strong formulation for pore fluid energy balance for an ideal gas with the assumptions $\boldsymbol{\sigma}_E^f \approx \mathbf{0}$, $\mathbf{a}_s \approx \mathbf{a}_f = \mathbf{a}$, i.e., $(\mathbf{u}-p_f-\theta^s-\theta^f)$ formulation, is written in the current configuration as

$$\begin{aligned} \rho^f(c_V^f + \mathfrak{R})D_t^s\theta^f + \rho^{\text{fR}}(c_V^f + \mathfrak{R})\text{grad}(\theta^f) \cdot (n^f\tilde{\mathbf{v}}_f) - \frac{n^s p_f}{J_s} D_t^s J_s - \frac{p_f}{n^f} \text{grad}(n^f) \cdot (n^f\tilde{\mathbf{v}}_f) \\ - n^f D_t^s p_f - \text{grad}(p_f) \cdot (n^f\tilde{\mathbf{v}}_f) + \text{div} \mathbf{q}^f - k_\theta^\varepsilon(\theta^s - \theta^f) = 0, \end{aligned} \quad (4.601)$$

which we may also write as [Koch, 2016]

$$\underbrace{\overset{*}{\mathbf{v}} \cdot \text{grad}(\theta^f)}_{\text{convective term}} - \underbrace{\overset{*}{d} \text{div} \text{grad}(\theta^f)}_{\text{diffusive term}} + \overset{*}{s} = 0, \quad (4.602)$$

such that

$$\begin{aligned} \overset{*}{\mathbf{v}} &:= \rho^{\text{fR}}(c_V^f + \mathfrak{R})(n^f\tilde{\mathbf{v}}_f), \\ \overset{*}{d} &:= n^f k^\theta, \\ \overset{*}{s} &:= \rho^f(c_V^f + \mathfrak{R})D_t^s\theta^f - \frac{n^s p_f}{J_s} D_t^s J_s - n^f D_t^s p_f - k_\theta^\varepsilon(\theta^s - \theta^f) - \left(\frac{p_f}{n^f} \text{grad}(n^f) + \text{grad} p_f \right) \cdot (n^f\tilde{\mathbf{v}}_f). \end{aligned} \quad (4.603)$$

Equation (4.602) resembles a convection-diffusion equation, which often require stabilization methods. A review of said methods is outlined in Donea and Huerta [2003]; herein, we turn our attention to the streamline upwind Petrov-Galerkin (SUPG) scheme.

Briefly, Equation (4.602) is stabilized by adding a stabilization term to the residual, such that

$$\underbrace{\int_{\mathcal{B}} (w^{\theta^f} [\overset{*}{\mathbf{v}} \cdot \text{grad}(\theta^f) - \overset{*}{s}] + \text{grad}(w^{\theta^f}) \cdot \text{grad}(\theta^f) \overset{*}{d}) dv - \int_{\Gamma} w^{\theta^f} \overset{*}{d} \text{grad}(\theta^f) \cdot \mathbf{n} da}_{\text{Standard Galerkin}} + \underbrace{\int_{\mathcal{B}} \tau [\overset{*}{\mathbf{v}} \cdot \text{grad}(w^{\theta^f})][\overset{*}{\mathbf{v}} \cdot \text{grad}(\theta^f) - \text{div}(\overset{*}{d} \text{grad}(\theta^f)) - \overset{*}{s}] dv}_{\text{SUPG stabilization}} = 0, \quad (4.604)$$

with

$$\begin{aligned} \tau^{\text{stab}} &:= \frac{\beta^{\text{stab}*} d \text{Pe}_{\theta^f}}{|\mathbf{v}^*|^2}, \\ \beta^{\text{stab}} &= \coth(\text{Pe}_{\theta^f}) - 1/\text{Pe}_{\theta^f} \approx \begin{cases} \text{Pe}_{\theta^f} & -3 \leq \text{Pe}_{\theta^f} \leq 3 \\ \text{sign}(\text{Pe}_{\theta^f}) & |\text{Pe}_{\theta^f}| \geq 3 \end{cases}, \\ \text{Pe}_{\theta^f} &:= \frac{\max\{v_1^* h_1, v_2^* h_2, v_3^* h_3\}}{2d}, \end{aligned} \quad (4.605)$$

where $\{v_1^*, v_2^*, v_3^*\}$ are the components of \mathbf{v}^* , and $\{h_1, h_2, h_3\}$ are the components of element expansion in 3-D.

Given the choice to interpolate θ^f using linear elements, the $d \text{div}(\text{grad}(\theta^f))$ term vanishes such that

$$\begin{aligned} \mathcal{K} &= \sum_{i=1}^8 \mathcal{K}_i^{\text{INT}} + \mathcal{K}^{\text{EXT}} + \mathcal{K}^{\text{stab}}, \\ \mathcal{K}^{\text{stab}} &:= \sum_{i=1}^6 \mathcal{K}_i^{\text{stab}}, \\ \mathcal{K}_1^{\text{stab}} &= - \int_{\mathcal{B}_0} J \frac{\partial w^{\theta^f}}{\partial X_I} F_{Ii}^{-1} \tau^{\text{stab}*} v_i D_t \theta^f dV, \\ \mathcal{K}_2^{\text{stab}} &= \int_{\mathcal{B}_0} J \frac{\partial w^{\theta^f}}{\partial X_I} F_{Ii}^{-1} \tau^{\text{stab}*} |v_i^*|^2 \frac{\partial \theta^f}{\partial X_K} F_{Kk}^{-1} dV, \\ \mathcal{K}_3^{\text{stab}} &= - \int_{\mathcal{B}_0} J \frac{\partial w^{\theta^f}}{\partial X_I} F_{Ii}^{-1} \tau^{\text{stab}*} v_i \frac{n^s p_f}{J} D_t J dV, \\ \mathcal{K}_4^{\text{stab}} &= - \int_{\mathcal{B}_0} J \frac{\partial w^{\theta^f}}{\partial X_I} F_{Ii}^{-1} \tau^{\text{stab}*} v_i n^f D_t p_f dV, \\ \mathcal{K}_5^{\text{stab}} &= - \int_{\mathcal{B}_0} J \frac{\partial w^{\theta^f}}{\partial X_I} F_{Ii}^{-1} \tau^{\text{stab}*} v_i k_{\theta}^{\varepsilon} (\theta^s - \theta^f) dV, \\ \mathcal{K}_6^{\text{stab}} &= - \int_{\mathcal{B}_0} J \frac{\partial w^{\theta^f}}{\partial X_I} F_{Ii}^{-1} \tau^{\text{stab}*} v_i \left(\frac{p_f}{n^f} \frac{\partial n^f}{\partial X_K} F_{Kk}^{-1} + \frac{\partial p_f}{\partial X_K} F_{Kk}^{-1} \right) (n^f \tilde{v}_{i(f)}) dV. \end{aligned} \quad (4.606)$$

Note the appearance of the additional pore fluid temperature rate term in Equation (4.606)₃. In

the 1-D uniaxial strain assumption, Equations (4.606)_{3–8} become

$$\begin{aligned}
\mathcal{K}_1^{\text{stab}} &= - \int_{\mathcal{B}_0} \frac{\partial w^{\theta^f}}{\partial X} \tau_{1-D}^{\text{stab}*} \dot{v} D_t \theta^f A dX, \\
\mathcal{K}_2^{\text{stab}} &= \int_{\mathcal{B}_0} \frac{\partial w^{\theta^f}}{\partial X_I} \tau_{1-D}^{\text{stab}*2} \frac{\partial \theta^f}{\partial X} F_{11}^{-1} A dX, \\
\mathcal{K}_3^{\text{stab}} &= - \int_{\mathcal{B}_0} \frac{\partial w^{\theta^f}}{\partial X} \tau_{1-D}^{\text{stab}*} \frac{n^s p_f}{J} D_t J A dX, \\
\mathcal{K}_4^{\text{stab}} &= - \int_{\mathcal{B}_0} \frac{\partial w^{\theta^f}}{\partial X} \tau_{1-D}^{\text{stab}*} n^f D_t p_f A dX, \\
\mathcal{K}_5^{\text{stab}} &= - \int_{\mathcal{B}_0} \frac{\partial w^{\theta^f}}{\partial X} \tau_{1-D}^{\text{stab}*} \dot{v} k_\theta^\varepsilon (\theta^s - \theta^f) A dX, \\
\mathcal{K}_6^{\text{stab}} &= - \int_{\mathcal{B}_0} \frac{\partial w^{\theta^f}}{\partial X} \tau_{1-D}^{\text{stab}*} \left(\frac{p_f}{n^f} \frac{\partial n^f}{\partial X} + \frac{\partial p_f}{\partial X} \right) (n^f \tilde{v}_f) F_{11}^{-1} A dX,
\end{aligned} \tag{4.607}$$

with

$$\begin{aligned}
\tau_{1-D}^{\text{stab}} &= \frac{J h_0 \beta_{1-D}^{\text{stab}}}{2 \dot{v}^{*2}} \\
\beta_{1-D}^{\text{stab}} &= \coth(\text{Pe}_{\theta^f, 1-D}) - 1/\text{Pe}_{\theta^f, 1-D} \approx \begin{cases} \text{Pe}_{\theta^f, 1-D} & -3 \leq \text{Pe}_{\theta^f, 1-D} \leq 3 \\ \text{sign}(\text{Pe}_{\theta^f, 1-D}) & |\text{Pe}_{\theta^f, 1-D}| \geq 3 \end{cases} \\
\text{Pe}_{\theta^f, 1-D} &= \frac{J h_0 \dot{v}^*}{2 n^f k^{\theta^f}}.
\end{aligned} \tag{4.608}$$

If instead we assume the $(\mathbf{u}-\mathbf{u}_f-p_f-\theta^s-\theta^f)$ formulation, such that $\boldsymbol{\sigma}_E^f \neq \mathbf{0}$ and $\mathbf{a}_f \neq \mathbf{a}_s$, pore fluid energy balance is written in the current configuration as

$$\rho^f c_V^f \left(D_t^s \theta^f + \text{grad}(\theta^f) \cdot \tilde{\mathbf{v}}_f \right) - \boldsymbol{\sigma}_E^f : \mathbf{d}_f + p_f n^f \text{div } \mathbf{v}_f + \text{div } \mathbf{q}^f - k_\theta^\varepsilon (\theta^s - \theta^f) = 0, \tag{4.609}$$

which we may also write as [Koch, 2016]

$$\underbrace{\dot{\mathbf{v}} \cdot \text{grad}(\theta^f)}_{\text{convective term}} - \underbrace{\dot{d} \text{div grad}(\theta^f)}_{\text{diffusive term}} + \dot{s} = 0, \tag{4.610}$$

such that

$$\begin{aligned}
 \mathbf{v}^* &:= \rho^f c_V^f \tilde{\mathbf{v}}_f, \\
 d^* &:= n^f k^{\theta^f}, \\
 \mathbf{s}^* &:= \rho^f c_V^f D_t^s \theta^f - \boldsymbol{\sigma}_E^f : \mathbf{d}_f + n^f p_f \operatorname{div} \mathbf{v}_f - k_\theta^\varepsilon (\theta^s - \theta^f).
 \end{aligned} \tag{4.611}$$

Thus,

$$\begin{aligned}
 \mathcal{K} &= \sum_{i=1,2,3,7,8} \mathcal{K}_i^{\text{INT}} + \mathcal{K}^{\text{EXT}} + \mathcal{K}^{\text{stab}}, \\
 \mathcal{K}^{\text{stab}} &:= \sum_{i=1}^5 \mathcal{K}_i^{\text{stab}}, \\
 \mathcal{K}_1^{\text{stab}} &= - \int_{\mathcal{B}_0} J \frac{\partial w^{\theta^f}}{\partial X_I} F_{Ii}^{-1} \tau^{\text{stab}*} v_i D_t \theta^f dV, \\
 \mathcal{K}_2^{\text{stab}} &= \int_{\mathcal{B}_0} J \frac{\partial w^{\theta^f}}{\partial X_I} F_{Ii}^{-1} \tau^{\text{stab}*} |v_i^*|^2 \frac{\partial \theta^f}{\partial X_K} F_{Kk}^{-1} dV, \\
 \mathcal{K}_3^{\text{stab}} &= - \int_{\mathcal{B}_0} J \frac{\partial w^{\theta^f}}{\partial X_I} F_{Ii}^{-1} \tau^{\text{stab}*} v_i \sigma_{kj(E)}^f d_{kj(f)} dV, \\
 \mathcal{K}_4^{\text{stab}} &= \int_{\mathcal{B}_0} J \frac{\partial w^{\theta^f}}{\partial X_I} F_{Ii}^{-1} \tau^{\text{stab}*} v_i n^f p_f \frac{\partial v_j}{\partial X_J} F_{Jj}^{-1} dV, \\
 \mathcal{K}_5^{\text{stab}} &= - \int_{\mathcal{B}_0} J \frac{\partial w^{\theta^f}}{\partial X_I} F_{Ii}^{-1} \tau^{\text{stab}*} v_i k_\theta^\varepsilon (\theta^s - \theta^f) dV.
 \end{aligned} \tag{4.612}$$

Note the appearance of the additional pore fluid temperature rate term in Equation (4.612)₃. In

the 1-D uniaxial strain assumption, Equations (4.612)₃₋₇ become

$$\begin{aligned}
\mathcal{K}_1^{\text{stab}} &= - \int_{\mathcal{B}_0} \frac{\partial w^{\theta^f}}{\partial X} \tau_{1-D}^{\text{stab}*} v D_t \theta^f A dX, \\
\mathcal{K}_2^{\text{stab}} &= \int_{\mathcal{B}_0} \frac{\partial w^{\theta^f}}{\partial X_I} \tau_{1-D}^{\text{stab}*} v^2 \frac{\partial \theta^f}{\partial X} F_{11}^{-1} A dX, \\
\mathcal{K}_3^{\text{stab}} &= - \int_{\mathcal{B}_0} \frac{\partial w^{\theta^f}}{\partial X} \tau_{1-D}^{\text{stab}*} v n^f \left[\frac{\partial v_f}{\partial X} F_{11}^{-1} \right]^2 (\kappa_f + 2\mu_f) A dX, \\
\mathcal{K}_4^{\text{stab}} &= - \int_{\mathcal{B}_0} \frac{\partial w^{\theta^f}}{\partial X} \tau_{1-D}^{\text{stab}*} v n^f p_f \frac{\partial v_f}{\partial X} F_{11}^{-1} A dX, \\
\mathcal{K}_5^{\text{stab}} &= - \int_{\mathcal{B}_0} \frac{\partial w^{\theta^f}}{\partial X} \tau_{1-D}^{\text{stab}*} v k_\theta^\varepsilon (\theta^s - \theta^f) A dX,
\end{aligned} \tag{4.613}$$

with

$$\begin{aligned}
\tau_{1-D}^{\text{stab}} &= \frac{J h_0 \beta_{1-D}^{\text{stab}}}{2v^{*2}} \\
\beta_{1-D}^{\text{stab}} &= \coth(\text{Pe}_{\theta^f, 1-D}) - 1/\text{Pe}_{\theta^f, 1-D} \approx \begin{cases} \text{Pe}_{\theta^f, 1-D} & -3 \leq \text{Pe}_{\theta^f, 1-D} \leq 3 \\ \text{sign}(\text{Pe}_{\theta^f, 1-D}) & |\text{Pe}_{\theta^f, 1-D}| \geq 3 \end{cases} \\
\text{Pe}_{\theta^f, 1-D} &= \frac{J h_0 v^*}{2n^f k^{\theta^f}}.
\end{aligned} \tag{4.614}$$

In practice we found that the SUPG stabilization has little-to-no effect on the overall stability of the pore fluid temperature's numerical solution (e.g., spurious oscillations are still observed, the mysterious “cooling effect,” discussed in Section 5.3.3.2, paragraph *Assessing numerical challenges at high strain-rate*, is not remediated, etc.). Therefore, the finite element forms of the above equations were omitted from Section 4.3.1.5 and Section 4.3.1.6, but have been implemented in SPONGE-1D nonetheless.

Chapter 5

Numerical Examples

This chapter provides an overview of the numerical results for applications of interest investigated in this thesis, ranging from extensive verification to shock loading of lung parenchyma. The numerical model, henceforth referred to as **SPONGE-1D**, has been implemented as a custom Python code, and has been made available for public use via GitHub. Therein, the reader may find detailed documentation for how to use this tool for themselves.

The **SPONGE-1D** simulations herein were conducted using the Blanca condo computing resource at the University of Colorado Boulder’s. Blanca is jointly funded by computing users and the University of Colorado Boulder. Simulations were conducted in serial (**SPONGE-1D** does not have parallel computing capability) using 2x Intel Xeon Gold 6230 processors with 192 GB of RAM.

5.1 Differences between LS-DYNA and SPONGE-1D models

Before presenting the numerical examples in this chapter, it would be prudent to highlight some key differences between the different numerical models. **LS-DYNA**, originally known as **DYNA3D**, was developed by John Hallquist at Lawrence Livermore National Laboratory in 1976. It is a “general-purpose finite element code for analyzing the large deformation static and dynamic response of structures including structures coupled to fluids” [Dev., 2019] written in **FORTRAN**, and has been highly optimized for massive multiparallel dynamic computations. The physical governing equation that **LS-DYNA** seeks to solve is the solid balance of linear momentum equation in the

current configuration, i.e.,

$$\rho \mathbf{a} = \operatorname{div} \boldsymbol{\sigma} + \rho \mathbf{b} \quad (5.1)$$

wherein the Cauchy stress $\boldsymbol{\sigma}$ is defined by a wide range of available constitutive models. In Section 5.3.1, the LS-DYNA material model we employed was a neo-Hookean material model (MAT 45), identical to the one we defined in Section 3.3.1 (refer to Equation (3.115)).

There also exists a poroelastodynamics framework in LS-DYNA, which is what we compare to in Section 5.2. However, its applications are limited. For starters, Darcy’s velocity in LS-DYNA does not account for inertial effects (refer to CONTROL_PORE_FLUID input card in the user’s manual [Dev., 2020]), i.e.,

$$(n^f \tilde{\mathbf{v}}_f) := -\hat{k} \left(\frac{\partial p_f}{\partial \mathbf{x}} - \rho^{\text{fr}} \mathbf{b} \right). \quad (5.2)$$

Note also that \hat{k} in Equation (5.2) is a *constant* hydraulic conductivity parameter, i.e., not a function of deformation (e.g., no dependence upon porosity change under large deformation). Furthermore, pore fluid pressure boundary conditions can only be specified at the top of the domain (in the z direction), which is limiting for modeling soft porous materials wherein one might want to apply pore fluid pressure boundary conditions at other surfaces on the domain. In our use of LS-DYNA’s poroelastodynamics model, we also found that we could only achieve accurate results for the verification problem in Section 5.2 by (1) using a linear isotropic elastic constitutive material model for the solid skeleton response, and (2) initializing the solid skeleton extra (effective) stress $\boldsymbol{\sigma}_E^s$ due to “geostatic” gravity. The result of (2) is that the solution for the solid skeleton extra (effective) stress $\boldsymbol{\sigma}_E^s$ does not match the analytical solution, because the analytical solution ignores body forces.

LS-DYNA also provides the user with the ability to write their own constitutive material model within the preexisting elastodynamics framework. This is what was accomplished for analysis of lung parenchyma tissue by Clayton and Freed [2019a] (for details on implementation, refer to Clayton [2020], Clayton et al. [2021]). This is the model we generally refer to as the “single-phase”

model (or “Clayton & Freed” in the figures), wherein pore air cannot move relative to the motion of the solid skeleton lung tissue. However, the constitutive model presented by Clayton and Freed [2019a] is based on the biological tissue constitutive theory, in contrast to our simpler neo-Hookean model. A viscoelastic response is also considered in the single-phase model, though more research is needed to determine whether or not lung tissue can be treated as a viscoelastic versus poroelastic material (or both) for high strain-rate loadings. A damage variable is also introduced in Clayton and Freed [2019a] to address local injury; when making comparisons to the single-phase model, we disable damage mechanics by adjusting the associated parameters appropriately. Enabling damage as part of the multiphase solid skeleton constitutive model is part of future work.

LS-DYNA provides the user with the ability to choose between several time integration schemes to find the solution of Equation (5.1); either an implicit Newmark-beta scheme (refer to Section 4.3.2) or a central-difference scheme (refer to Section 4.3.3). By default, LS-DYNA employs the central-difference time integration scheme with lumped mass matrices (row-sum lumping technique), where the time-step is limited by a local CFL condition (refer to Equation (4.537)). In our results of the LS-DYNA simulations, we use the default time integration scheme; for custom material models, it is not possible to choose from other time integration schemes. Lastly, for the linearly-interpolated hexahedral elements employed in the following LS-DYNA simulations, single-point quadrature rules are applied by default, i.e., properties such as stress are evaluated at the Gauss point (the centroid of the element), and shock viscosity (refer to the `CONTROL_BULK_VISCOSITY` input card in Dev. [2020]) is by default enabled to regularize shock front propagation, and in turn stabilize the numerical solution. Hourglass stabilization (refer to the `CONTROL_HOURLASS` input card in Dev. [2020]) is also added by default, but is inconsequential for the 1-D uniaxial strain simulations presented herein.

5.2 Verification

In the following sections we provide examples to verify the FE formulation of the various governing equations against either analytical solutions (if they exist), other published results, and

using the method of manufactured solutions. Validation of the model is beyond the scope of this thesis. For a limited discussion of the procedure of verification and validation (V&V), refer to Oberkampf et al. [2004], Babuska and Oden [2004], Schwer [2007], Sun [2019].

5.2.1 Method of manufactured solutions

The method of manufactured solutions (MMS) is a powerful tool to verify that implementation of the FE form of the governing equations of interest is correct. A detailed overview of the method is provided by Salari and Knupp [2000]. Briefly, MMS provides a way to verify that the numerical solver in question is solving the governing equations without any order of accuracy mistakes (OAM), e.g., the numerical error between an exact solution and the numerical solution should approach zero as the level of spatial or temporal discretization is increased ($h_0^e \rightarrow 0$, $\Delta t \rightarrow 0$, respectively).

The method by which this is accomplished is explained as follows. Suppose one wishes to solve Poisson's equation for some variable $\phi(x, y)$, i.e.,

$$\nabla^2 \phi = 0. \quad (5.3)$$

First, one proposes an arbitrary solution for $\phi(x, y)$. This solution need not satisfy Equation (5.3), nor need it be physically realistic in most cases.¹ E.g., suppose we choose

$$\phi(x, y) = x^4 y + 6xy^3. \quad (5.4)$$

Then, this solution is substituted into Equation (5.3), such that

$$\nabla^2 \phi(x, y) = 12x^2 y + 36xy = f(x, y). \quad (5.5)$$

The term $f(x, y)$ is known as the *forcing function*. It is named as such because when one substitutes

¹ As will be explained in the proceeding sections, some restrictions on the form of the pore fluid pressure solution $p_f(X, t)$ at finite strain are necessary to maintain stability of the coupled poroelastodynamic solutions. Furthermore, for resolving spatial or temporal accuracy, one must be careful in choosing solutions that use spatial and temporal terms with sufficient higher order terms for said resolution (e.g., choosing a solution that is linear in time t will not resolve acceleration terms).

it on the r.h.s. of Equation (5.3), i.e.,

$$\nabla^2 \phi(x, y) = f(x, y), \quad (5.6)$$

the solution of Equation (5.6) is “forced” to be Equation (5.4). Thus, inclusion of a forcing function gives rise to an additional term in the governing equation, which for the FE implementation herein, amounts to another term in the residual of the variational form of the governing equation. When included, one therefore obtains a numerical approximation of the known analytical solution, and a measurement of the error between the two may be made. In practice, one usually performs *convergence studies* to determine whether or not the source of the error is a numerical phenomenon (e.g., round-off error) or due to incorrect implementation of the governing equations (the variational form) in the numerical model. In subsequent subsections, we present results for temporal and spatial convergence studies of SPONGE-1D for the (\mathbf{u}) , $(\mathbf{u}-p_f)$, and $(\mathbf{u}-\mathbf{u}_f-p_f)$ formulations, with inertia terms.

5.2.1.1 (\mathbf{u}) formulation

Recall the strong form of elastodynamics given by Equation (4.3), such that for MMS

$$(\mathcal{S}) = \left\{ \begin{array}{l} \text{Choose } \mathbf{u}(\mathbf{X}, t) \in \mathcal{S}^u, \text{ with } t \in [0, T], \text{ such that:} \\ \text{DIV } \mathbf{P} + \rho_0 \mathbf{g} - \rho_0 \mathbf{a} = \mathbf{f}_{\text{mms}, u} \in \mathcal{B}_0, \\ \mathbf{g}^u(\mathbf{X}, t) = \mathbf{u}(\mathbf{X}, t) \text{ on } \Gamma_0^u, \\ \mathbf{t}^\sigma(\mathbf{X}, t) = \mathbf{P}(\mathbf{X}, t) \cdot \mathbf{N}(\mathbf{X}) \text{ on } \Gamma_0^t, \\ \mathbf{u}_0(\mathbf{X}) = \mathbf{u}(\mathbf{X}, t = 0) \in \mathcal{B}_0, \\ \mathbf{v}_0(\mathbf{X}) = \mathbf{v}(\mathbf{X}, t = 0) \in \mathcal{B}_0, \\ \mathbf{a}_0(\mathbf{X}) = \mathbf{a}(\mathbf{X}, t = 0) \in \mathcal{B}_0. \end{array} \right. \quad (5.7)$$

Note that in Equation (5.7), boundary and initial conditions have flipped equalities from their counterparts in Equation (4.3) such that they are prescribed not according to user inputs, but according to the chosen analytical solution.

For single-phase elastodynamics, we restrict the constitutive model for the solid skeleton to the neo-Hookean model (refer to Equation (3.106)) so that we may evaluate an analytical solution for $\text{DIV } \mathbf{P}$:

$$\begin{aligned} \text{DIV } \mathbf{P} &= \frac{\partial P_{iI}}{\partial X_I} = \frac{\partial}{\partial X_I} [\mu F_{iI} + (\lambda \ln(J) - \mu) F_{Ii}^{-1}] \\ &= \mu \frac{\partial F_{iI}}{\partial X_I} + \frac{\lambda}{J} F_{Ii}^{-1} \frac{\partial(\det(\mathbf{F}_{iI}))}{\partial X_I} + (\lambda \ln(J) - \mu) \frac{\partial F_{Ii}^{-1}}{\partial X_I} \\ &= \mu \frac{\partial^2 u_i}{\partial X_I^2} + \lambda F_{Ii}^{-2} \frac{\partial^2 u_i}{\partial X_I^2} - (\lambda \ln(J) - \mu) F_{Ii}^{-2} \frac{\partial^2 u_i}{\partial X_I^2} \end{aligned} \quad (5.8)$$

where we have used the identity

$$\frac{\partial \det(\mathbf{A}(t))}{\partial t} = \det(\mathbf{A}(t)) \text{tr} \left(\mathbf{A}(t)^{-1} \frac{\partial \mathbf{A}(t)}{\partial t} \right) \quad (5.9)$$

to evaluate the $\partial J / \partial X_I$ term. In the 1-D uniaxial strain implementation, Equation (5.8) reduces to

$$\frac{\partial P_{11}}{\partial X} = \frac{\partial^2 u}{\partial X^2} \left(\mu + \left[\lambda - \left(\lambda \ln \left(1 + \frac{\partial u}{\partial X} \right) - \mu \right) \right] \left[1 + \frac{\partial u}{\partial X} \right]^{-2} \right). \quad (5.10)$$

SPONGE-1D has been implemented with the following analytical solutions for $u(X, t)$ using $\lambda = \mu = 1 \text{ Pa}$, $\rho_0 = 2 \text{ kg/m}^3$:

$$\begin{aligned} u(X, t) &= X^2 t^2, \\ u(X, t) &= X^2 t^3, \\ u(X, t) &= -X^2 t^3, \\ u(X, t) &= X^3 t^2, \\ u(X, t) &= X^3 t^3, \\ u(X, t) &= -X^3 t^3, \\ u(X, t) &= X^4 t^3, \\ u(X, t) &= -X^4 t^3, \end{aligned} \quad (5.11)$$

with corresponding forcing functions (which were solved for with aid of `Mathematica`)

$$\begin{aligned}
f_{\text{mms},u} &= 2g + 4X^2 - 2t^2 \left(1 + \frac{2 - \ln(1 + 2Xt^2)}{(1 + 2Xt^2)^2} \right), \\
f_{\text{mms},u} &= 2g + 12X^2t - 2t^3 \left(1 + \frac{2 - \ln(1 + 2Xt^3)}{(1 + 2Xt^3)^2} \right), \\
f_{\text{mms},u} &= 2g - 12X^2t + 2t^3 \left(1 + \frac{2 - \ln(1 - 2Xt^3)}{(1 - 2Xt^3)^2} \right), \\
f_{\text{mms},u} &= 2g + 4X^3 - 6Xt^2 \left(1 + \frac{2 - \ln(1 + 3X^2t^2)}{(1 + 3X^2t^2)^2} \right), \\
f_{\text{mms},u} &= 2g + 12X^3t - 6Xt^3 \left(1 + \frac{2 - \ln(1 + 3X^2t^3)}{(1 + 3X^2t^3)^2} \right), \\
f_{\text{mms},u} &= 2g - 12X^3t + 6Xt^3 \left(1 + \frac{2 - \ln(1 - 3X^2t^3)}{(1 - 3X^2t^3)^2} \right), \\
f_{\text{mms},u} &= 2g + 12X^4t - 12X^2t^3 \left(1 + \frac{2 - \ln(1 + 4X^3t^2)}{(1 + 4X^3t^2)^2} \right), \\
f_{\text{mms},u} &= 2g - 12X^4t + 12X^2t^3 \left(1 + \frac{2 + \ln(1 - 4X^3t^2)}{(1 - 4X^3t^2)^2} \right).
\end{aligned} \tag{5.12}$$

The following convergence studies—here, and in the subsequent sections—were conducted using the Newmark-beta implicit integration scheme with constant acceleration Newmark parameters $\beta = 1/4, \gamma = 1/2$. The studies were run on a 1x1x1 meter unit cube (effectively a 1 m column for the 1-D uniaxial strain assumption). Simulations were run out to $t = 0.01$ seconds and data was saved at 0.001 second intervals. For the elastodynamics MMS, gravitational forces were disabled.

We see a good temporal convergence (variation of time step with fixed element length) profile for the two element types investigated in Figure 5.1. The trend is roughly quadratic, which is to be expected for a second-order-in-time numerical integration method [Hughes, 2000] and appears to level off, likely due to truncation error, at $\Delta t = 10^{-6}$ s. For this reason, the spatial convergence (variation of element length) studies used fixed time step $\Delta t = 10^{-6}$ s. Spatial convergence is excellent for both quadratic and Hermite cubic element types, as demonstrated in Figure 5.2.

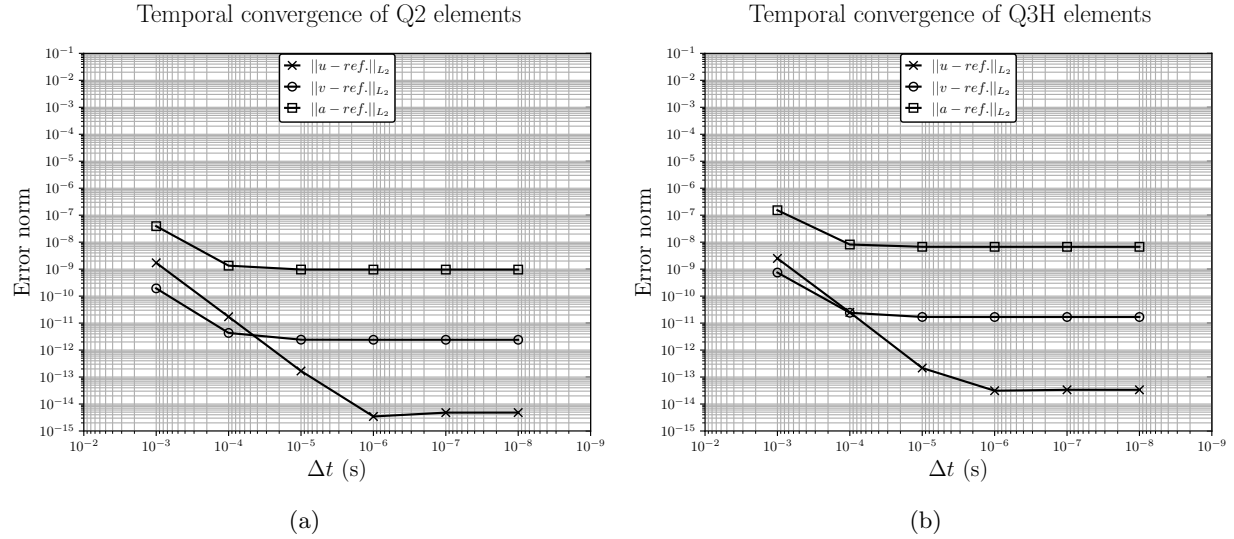


Figure 5.1: Temporal convergence of the elastodynamics MMS, using (a) quadratic elements with $u(X,t) := X^2t^3$, and (b) Hermite cubic elements with $u(X,t) := X^3t^3$, plotted at $t = 0.01$ s. A single element was used to minimize spatial discretization error.

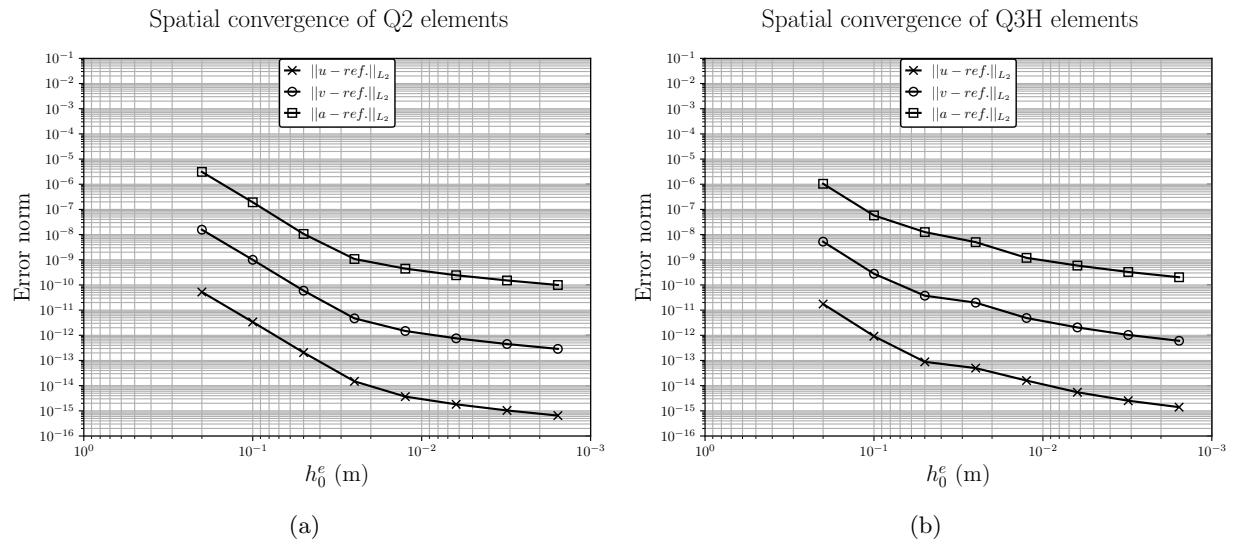


Figure 5.2: Spatial convergence of the elastodynamics MMS, using (a) quadratic elements with $u(X,t) := X^3t^3$, and (b) Hermite cubic elements with $u(X,t) := X^4t^3$, plotted at $t = 0.01$ s. The time step $\Delta t = 10^{-6}$ s was fixed to minimize temporal discretization error.

5.2.1.2 (\mathbf{u} - p_f) formulation

Recall the strong form of poroelastodynamics (\mathbf{u} - p_f) formulation given by Equation (4.44), such that for MMS

$$(\mathcal{S}) = \left\{ \begin{array}{l} \text{Choose } \mathbf{u}(\mathbf{X}, t) \in \mathcal{S}^u \text{ and } p_f(\mathbf{X}, t) \in \mathcal{S}^{p_f}, \\ \\ \text{with } t \in [0, T], \text{ such that:} \\ \\ \text{DIV } \mathbf{P} + \rho_0 \mathbf{g} - \rho_0 \mathbf{a} = \mathbf{f}_{\text{mms},u} \in \mathcal{B}_0, \\ \\ \mathbf{g}^u(\mathbf{X}, t) = \mathbf{u}(\mathbf{X}, t) \text{ on } \Gamma_0^u, \\ \\ \mathbf{t}^\sigma(\mathbf{X}, t) = \mathbf{P}(\mathbf{X}, t) \cdot \mathbf{N}(\mathbf{X}) \text{ on } \Gamma_0^t, \\ \\ \mathbf{u}_0(\mathbf{X}) = \mathbf{u}(\mathbf{X}, t=0) \in \mathcal{B}_0, \\ \\ \mathbf{v}_0(\mathbf{X}) = \mathbf{v}(\mathbf{X}, t=0) \in \mathcal{B}_0, \\ \\ \mathbf{a}_0(\mathbf{X}) = \mathbf{a}(\mathbf{X}, t=0) \in \mathcal{B}_0, \\ \\ \frac{J n^f}{K_f^{\zeta\eta}} D_t p_f + D_t J + \frac{J}{K_f^{\zeta\eta}} \text{GRAD}(p_f) \cdot \mathbf{F}^{-1} \cdot (n^f \tilde{\mathbf{v}}_f) \\ \\ + J \text{GRAD}(n^f \tilde{\mathbf{v}}_f) \cdot \mathbf{F}^{-T} = f_{\text{mms},p_f} \in \mathcal{B}_0, \\ \\ \mathbf{g}^p(\mathbf{X}, t) = p_f(\mathbf{X}, t) \text{ on } \Gamma_0^p, \\ \\ Q_f(\mathbf{X}, t) = -[J \mathbf{F}^{-1} \cdot (n^f \tilde{\mathbf{v}}_f)] \cdot \mathbf{N} \text{ on } \Gamma_0^{Q_f}, \\ \\ p_{f,0}(\mathbf{X}) = p_f(\mathbf{X}, t=0) \in \mathcal{B}_0, \\ \\ \dot{p}_{f,0}(\mathbf{X}) = \dot{p}_f(\mathbf{X}, t=0) \in \mathcal{B}_0. \end{array} \right. \quad (5.13)$$

Given that

$$\mathbf{P} := \mathbf{P}_E^s - J p_f \mathbf{F}^{-T} \quad (5.14)$$

the divergence of the mixture stress in the 1-D uniaxial regime has the analytical solution

$$\frac{\partial P_{11}}{\partial X} = \frac{\partial^2 u}{\partial X^2} \left(\mu + \left[\lambda - \left(\lambda \ln \left(1 + \frac{\partial u}{\partial X} \right) - \mu \right) \right] \left[1 + \frac{\partial u}{\partial X} \right]^{-2} \right) - \frac{\partial p_f(X, t)}{\partial X}. \quad (5.15)$$

For both $(\mathbf{u}-p_f)$ and $(\mathbf{u}-\mathbf{u}_f-p_f)$ formulations, we have found that the pore fluid pressure solution must be restricted to the form

$$p_f(X, t) = (aH - X)t^n, \quad (5.16)$$

where a and n are integers ≥ 1 . For $a < 1$, suction physics are introduced, and the numerical solution is unstable. Furthermore, we discovered that the exponential constitutive model for the real mass density of the pore fluid (refer to Equation (3.136)₁) introduces so much non-linearity within MMS that the solution cannot converge.² Therefore, we impose an additional constitutive model restriction, i.e., that the *linear* model for pore fluid real mass density be imposed (refer to Equation (3.140)₁). This changes the governing equation for balance of mass of the mixture for MMS to

$$\begin{aligned} \frac{J^2 n^f}{K_f^\eta} D_t p_f + D_t J + \frac{J^2}{K_f^\eta} \text{GRAD}(p_f) \cdot \mathbf{F}^{-1} \cdot (n^f \tilde{\mathbf{v}}_f) \\ + J \text{GRAD}(n^f \tilde{\mathbf{v}}_f) : \mathbf{F}^{-T} = f_{\text{mms}, p_f} \in \mathcal{B}_0, \end{aligned} \quad (5.17)$$

and the divergence of the solid skeleton extra stress has the analytical solution

$$\frac{\partial P_{11}}{\partial X} = \frac{\partial^2 u}{\partial X^2} \left(\mu(F_{11}^{-2} + 1) + \frac{\lambda(1 - n_0^s)^2}{(J - n_0^s)^2} \right) - \frac{\partial p_f(X, t)}{\partial X}. \quad (5.18)$$

For applications of an incompressible solid constituent at large strain, it is preferable to switch the standard neo-Hookean constitutive model (Equation (3.107)) to the Ehlers and Eipper [1999] neo-Hookean constitutive model (Equation (3.109)). Likewise, it is preferable to use the hyperbolic form for hydraulic conductivity (Equation (3.68)) rather than the Kozeny-Carman model (Equation (3.63)). Further discussion of these constitutive models is presented in Section 5.3.3.1, paragraph *Necessary constitutive adjustments for higher strain*. Parameter restrictions for SPONGE-1D are given in Table 5.1. SPONGE-1D has been implemented with the following coupled analytical

² With the exponential model, it can be shown that resulting forcing function for the balance of mass of the mixture, f_{mms, p_f} , contains spatial terms of $\mathcal{O}(12)$ or higher, and temporal terms of $\mathcal{O}(18)$ or higher. The former cannot be accurately captured by any Gauss quadrature rule, and the latter is unfit for the Newmark-beta temporal discretization schemes.

Table 5.1: Material parameters for the $(\mathbf{u}-p_f)$ and $(\mathbf{u}-\mathbf{u}_f-p_f)$ MMS convergence studies.

<i>Parameter</i>	<i>Value</i>
λ (Pa)	1
μ (Pa)	1
n_0^s	0.5
ρ_0^{sR} (m ³ /kg)	2
μ_f (Pa-s)	1
ρ_0^{fR} (m ³ /kg)	1

solutions for $u(X, t), p_f(X, t)$ for the $(\mathbf{u}-p_f)$ formulation:

$$\begin{aligned}
u(X, t) &= X^2 t^3; p_f(X, t) = (H - X)t^2, \\
u(X, t) &= X^3 t^3; p_f(X, t) = (H - X)t^2, \\
u(X, t) &= X^4 t^3; p_f(X, t) = (H - X)t^2,
\end{aligned} \tag{5.19}$$

with corresponding forcing functions for balance of linear momentum of the mixture

$$\begin{aligned}
f_{\text{mms},u} &= -t^2 - 2t^3 \left(1 + \frac{1/16}{(1/4 + Xt^3)^2} + \frac{1/4}{(1/2 + Xt^3)^2} \right) \\
&\quad + \frac{12X^2 t (K_f^\eta / 2 + t^2 (H - X) (1/4 + Xt^3))}{K_f^\eta} + g \left(\frac{t^2 (H - X) (1/2 + 2Xt^3)}{K_f^\eta} - 1 \right), \\
f_{\text{mms},u} &= -t^2 + 6X^3 t + \frac{18X^5 t^6 (H - X)}{K_f^\eta} - g \left(\frac{t^2 (1/2 + 3X^2 t^3) (H - X)}{K_f^\eta} - 1 \right) \\
&\quad + Xt^3 \left(\frac{3X^2 H - 3X^3}{K_f^\eta} - 6 - \frac{1/6}{(1/6 + X^2 t^3)^2} - \frac{2/3}{(1/3 + X^2 t^3)^2} \right), \\
f_{\text{mms},u} &= -t^2 + 6X^4 t + \frac{24X^7 t^6 (H - X)}{K_f^\eta} - g \left(\frac{t^2 (1/2 + 4X^3 t^3) (H - X)}{K_f^\eta} - 1 \right) \\
&\quad + X^2 t^3 \left(\frac{3X^2 H - 3X^3}{K_f^\eta} - 12 - \frac{3/16}{(1/8 + X^3 t^3)^2} - \frac{3/4}{(1/4 + X^3 t^3)^2} \right),
\end{aligned} \tag{5.20}$$

and corresponding forcing functions for balance of mass of the mixture

$$\begin{aligned}
f_{\text{mms},p_f} &= t \left(6Xt + \frac{8(H-X)(1/4 + Xt^3)(1/2 + Xt^3)}{K_f^\eta} \right. \\
&\quad - 2t^4(2^\kappa)\kappa\mathcal{Z}(1/2 + 2Xt^3)^{\kappa-1} \left(\frac{6(H-X)(X^2t + g/6)}{K_f^\eta} - \frac{1}{1 + 2Xt^3} \right) \\
&\quad + \frac{t^3\mathcal{Z}(1 + 2Xt^3)(1 + 4Xt^3)^\kappa \left(\frac{6(H-X)(X^2t + g/6)}{K_f^\eta} - \frac{1}{1 + 2Xt^3} \right)}{K_f^\eta} \\
&\quad \left. - t\mathcal{Z}(1 + 4Xt^3)^\kappa \left(X^2t \left[\frac{12XH - 18X^2}{K_f^\eta} + \frac{1t^2}{2(1/2 + Xt^3)^2} \right] - g/K_f^\eta \right) \right), \\
f_{\text{mms},p_f} &= t \left(9X^2t + \frac{18(H-X)(1/6 + X^2t^3)(1/3 + X^2t^3)}{K_f^\eta} \right. \\
&\quad - 6Xt^4(2^\kappa)\kappa\mathcal{Z}(1/2 + 3X^2t^3)^{\kappa-1} \left(\frac{6(H-X)(X^3t + g/6)}{K_f^\eta} - \frac{1}{1 + 3X^2t^3} \right) \\
&\quad + \frac{t^3\mathcal{Z}(1 + 3X^2t^3)(1 + 6X^2t^3)^\kappa \left(\frac{6(H-X)(X^3t + g/6)}{K_f^\eta} - \frac{1}{1 + 3X^2t^3} \right)}{K_f^\eta} \\
&\quad \left. - t\mathcal{Z}(1 + 6X^2t^3)^\kappa \left(Xt \left[\frac{28XH - 24X^2}{K_f^\eta} + \frac{2t^2}{3(1/3 + X^2t^3)^2} \right] - g/K_f^\eta \right) \right), \\
f_{\text{mms},p_f} &= t \left(12X^3t + \frac{32(H-X)(1/8 + X^3t^3)(1/4 + X^3t^3)}{K_f^\eta} \right. \\
&\quad - 12X^2t^4(2^\kappa)\kappa\mathcal{Z}(1/2 + 4X^3t^3)^{\kappa-1} \left(\frac{6(H-X)(X^4t + g/6)}{K_f^\eta} - \frac{1}{1 + 4X^3t^3} \right) \\
&\quad + \frac{t^3\mathcal{Z}(1 + 4X^3t^3)(1 + 8X^3t^3)^\kappa \left(\frac{6(H-X)(X^4t + g/6)}{K_f^\eta} - \frac{1}{1 + 4X^3t^3} \right)}{K_f^\eta} \\
&\quad \left. - t\mathcal{Z}(1 + 8X^3t^3)^\kappa \left(X^2t \left[\frac{24XH - 30X^2}{K_f^\eta} + \frac{3t^2}{4(1/4 + X^3t^3)^2} \right] - g/K_f^\eta \right) \right).
\end{aligned} \tag{5.21}$$

In the following convergence studies, we set $g = 10 \text{ m/s}^2$ (in the downward direction), $K_f^\eta = 1 \text{ Pa}$, and $\mathcal{Z} = 1 \text{ m}^2$.

We see a reasonable temporal convergence (variation of time step with fixed element length) profile for the two element types investigated in Figure 5.3. The trend continues to be roughly quadratic and appears to level off at $\Delta t = 10^{-4} \text{ s}$. Despite this, we have found that for finer meshes, fixed $\Delta t = 10^{-6} \text{ s}$ provides the most stability, and therefore this is the time-step that is used for the spatial convergence studies.

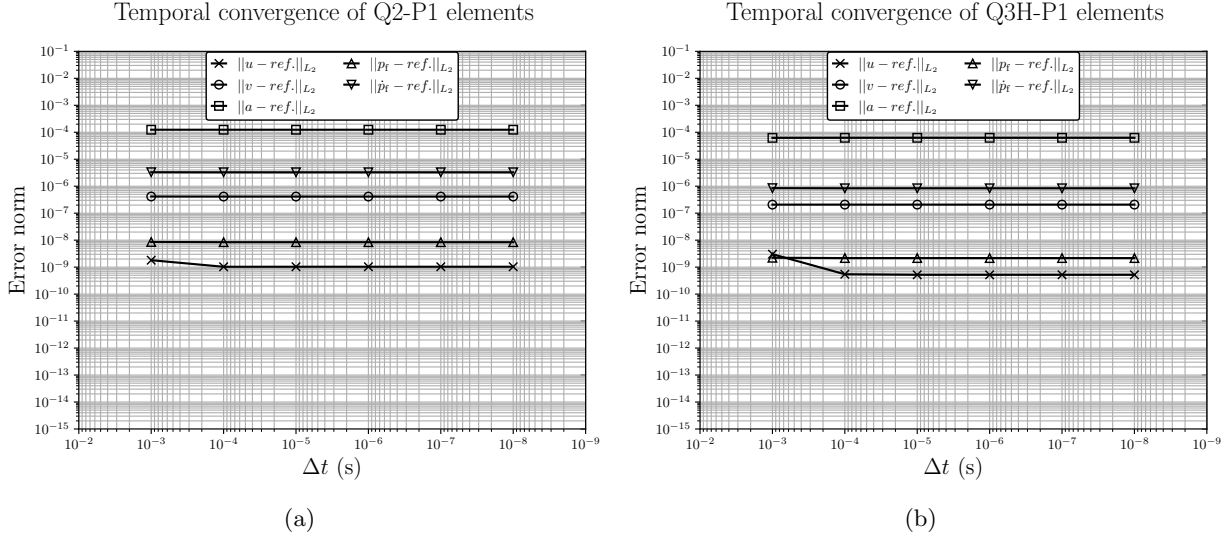


Figure 5.3: Temporal convergence of the poroelastodynamics ($\mathbf{u}\text{-}p_f$) formulation MMS, using (a) quadratic-linear displacement-pressure elements with $u(X, t) := X^2 t^3$, $p_f(X, t) := (H - X)t^2$, and (b) Hermite cubic-linear displacement-pressure elements with $u(X, t) := X^3 t^3$, $p_f(X, t) := (H - X)t^2$, plotted at $t = 0.01$ s. A single mixed-element was used to minimize spatial discretization error.

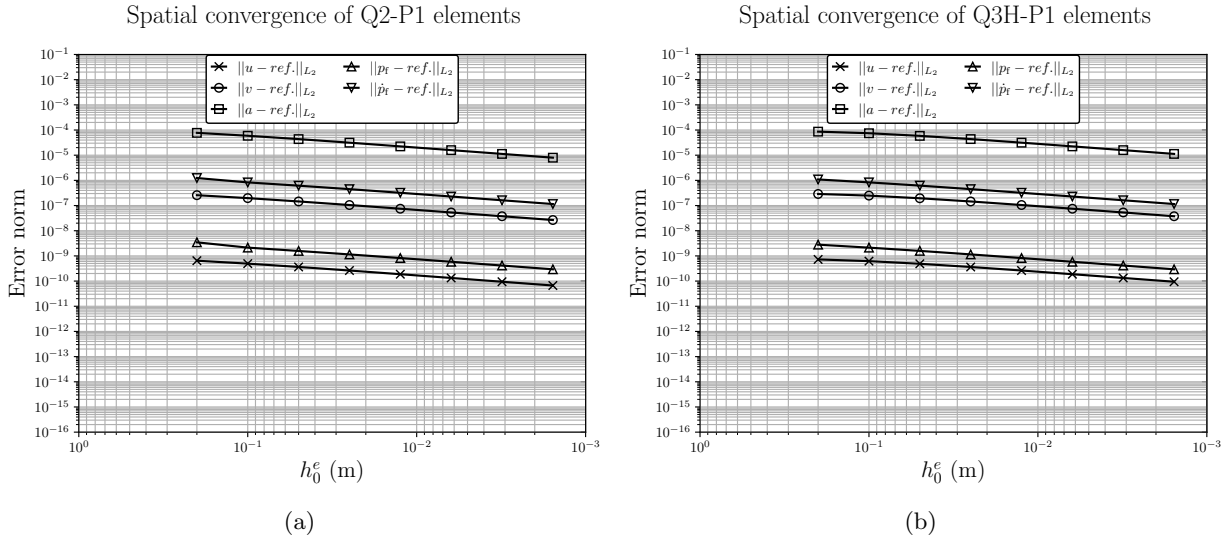


Figure 5.4: Spatial convergence of the poroelastodynamics ($\mathbf{u}\text{-}p_f$) formulation MMS, using (a) quadratic-linear displacement-pressure elements with $u(X, t) := X^3 t^3$, $p_f(X, t) := (H - X)t^2$, and (b) Hermite cubic-linear displacement-pressure elements with $u(X, t) := X^4 t^3$, $p_f(X, t) := (H - X)t^2$, plotted at $t = 0.01$ s. Time step is held fixed at $\Delta t = 10^{-6}$ s to minimize temporal discretization error.

The spatial convergence profiles for poroelastodynamics ($\mathbf{u}\text{-}p_f$) formulation are shown in

Figure 5.4. Both display good trends, with reduction in error between subsequent mesh refinements for all variables averaging a factor of 7.5, which is on par with Obaid et al. [2017].

5.2.1.3 $(\mathbf{u}-\mathbf{u}_f-p_f)$ formulation

Recall the strong form of poroelastodynamics $(\mathbf{u}-\mathbf{u}_f-p_f)$ formulation for nearly-inviscid pore fluid given by Equation (4.69), such that for MMS

$$(\mathcal{S}) = \left\{ \begin{array}{l} \text{Choose } \mathbf{u}(\mathbf{X}, t) \in \mathcal{S}^u, \mathbf{u}_f(\mathbf{X}, t) \in \mathcal{S}^{u_f}, \\ \text{and } p_f(\mathbf{X}, t) \in \mathcal{S}^{p_f}, \text{ with } t \in [0, T], \text{ such that:} \\ \\ \text{DIV } \mathbf{P} + \rho_0 \mathbf{g} - (\rho_0^s \mathbf{a} + \rho_0^f \mathbf{a}_f) = \mathbf{0} \in \mathcal{B}_0, \\ \\ \mathbf{g}^u(\mathbf{X}, t) = \mathbf{u}(\mathbf{X}, t) \text{ on } \Gamma_0^u, \\ \\ \mathbf{t}^\sigma(\mathbf{X}, t) = \mathbf{P}(\mathbf{X}, t) \cdot \mathbf{N}(\mathbf{X}) \text{ on } \Gamma_0^t, \\ \\ \mathbf{u}_0(\mathbf{X}) = \mathbf{u}(\mathbf{X}, t=0) \in \mathcal{B}_0, \\ \\ \mathbf{v}_0(\mathbf{X}) = \mathbf{v}(\mathbf{X}, t=0) \in \mathcal{B}_0, \\ \\ \mathbf{a}_0(\mathbf{X}) = \mathbf{a}(\mathbf{X}, t=0) \in \mathcal{B}_0, \\ \\ \rho_0^f \mathbf{a}_f + J n^f \text{GRAD}(p_f) \cdot \mathbf{F}^{-1} + J \frac{(n^f)^2}{\hat{k}} (\mathbf{v}_f - \mathbf{v}) - \rho_0^f \mathbf{g} = \mathbf{0} \in \mathcal{B}_0, \\ \\ \mathbf{g}_{u_f}(\mathbf{X}, t) = \mathbf{u}_f(\mathbf{X}, t) \text{ on } \Gamma_0^{u_f}, \\ \\ \mathbf{u}_{f,0}(\mathbf{X}) = \mathbf{u}_f(\mathbf{X}, t=0) \in \mathcal{B}_0, \\ \\ \mathbf{v}_{f,0}(\mathbf{X}) = \mathbf{v}_f(\mathbf{X}, t=0) \in \mathcal{B}_0, \\ \\ \mathbf{a}_{f,0}(\mathbf{X}) = \mathbf{a}_f(\mathbf{X}, t=0) \in \mathcal{B}_0, \\ \\ \frac{J^2 n^f}{K_f^\eta} D_t p_f + D_t J + \frac{J^2}{K_f^\eta} \text{GRAD}(p_f) \cdot \mathbf{F}^{-1} \cdot (n^f \tilde{\mathbf{v}}_f) \\ \quad + J \text{GRAD}(n^f \tilde{\mathbf{v}}_f) \cdot \mathbf{F}^{-T} = 0 \in \mathcal{B}_0, \\ \\ g^p(\mathbf{X}, t) = p_f(\mathbf{X}, t) \text{ on } \Gamma_0^p, \\ \\ Q_f(\mathbf{X}, t) = -[J \mathbf{F}^{-1} \cdot (n^f \tilde{\mathbf{v}}_f)] \cdot \mathbf{N} \text{ on } \Gamma_0^{Q_f}, \\ \\ p_{f,0}(\mathbf{X}) = p_f(\mathbf{X}, t=0) \in \mathcal{B}_0, \\ \\ \dot{p}_{f,0}(\mathbf{X}) = \dot{p}_f(\mathbf{X}, t=0) \in \mathcal{B}_0. \end{array} \right. \quad (5.22)$$

We enforce the same restrictions as those in Section 5.2.1.2. SPONGE-1D has been implemented with the following coupled analytical solutions for $u(X, t)$, $u_f(X, t)$, $p_f(X, t)$ for the $(\mathbf{u}-\mathbf{u}_f-p_f)$ formulation:

$$\begin{aligned} u(X, t) &= X^2 t^3; u_f(X, t) = \frac{1}{2} X^2 t^3; p_f(X, t) = (H - X)t^2, \\ u(X, t) &= X^3 t^3; u_f(X, t) = \frac{1}{2} X^3 t^3; p_f(X, t) = (H - X)t^2, \\ u(X, t) &= X^4 t^3; u_f(X, t) = \frac{1}{2} X^4 t^3; p_f(X, t) = (H - X)t^2, \end{aligned} \quad (5.23)$$

with corresponding forcing functions for balance of linear momentum of the mixture

$$\begin{aligned} f_{\text{mms},u} &= -t^2 + 6X^2 t + \frac{6X^2 t^3 (H - X)(1/4 + Xt^3)}{K_f^\eta} - 2t^3 \left(1 + \frac{1/16}{(1/4 + Xt^3)^2} + \frac{1/4}{(1/2 + Xt^3)^2} \right) \\ &\quad + g \left(\frac{t^2 (H - X)(1/2 + 2Xt^3)}{K_f^\eta} - 1 \right), \\ f_{\text{mms},u} &= -t^2 + 6X^3 t + \frac{9X^3 t^3 (H - X)(1/6 + X^2 t^3)}{K_f^\eta} - g \left(\frac{t^2 (1/2 + 3X^2 t^3)(H - X)}{K_f^\eta} - 1 \right) \\ &\quad + 6X t^3 \left(1 + \frac{1}{36(1/6 + X^2 t^3)^2} + \frac{1}{9(1/3 + X^2 t^3)^2} \right), \\ f_{\text{mms},u} &= -t^2 + 6X^4 t + \frac{12X^4 t^3 (H - X)(1/8 + X^3 t^3)}{K_f^\eta} - g \left(\frac{t^2 (1/2 + 4X^3 t^3)(H - X)}{K_f^\eta} - 1 \right) \\ &\quad + 12X^2 t^3 \left(1 + \frac{1}{64(1/8 + X^3 t^3)^2} + \frac{1}{16(1/4 + X^3 t^3)^2} \right), \end{aligned} \quad (5.24)$$

corresponding forcing functions for balance of linear momentum of the pore fluid

$$\begin{aligned} f_{\text{mms},u_f} &= t^2 \left(1 - \frac{1}{2 + 4Xt^3} \right) \left(\frac{(2g + 6X^2 t)(H - X)(1/2 + Xt^3)^2}{K_f^\eta} \right. \\ &\quad \left. - \frac{3X^2 (1/4 + Xt^3)(1 + 4Xt^3)^{\kappa-1}}{\varkappa} - 1 \right), \\ f_{\text{mms},u_f} &= t^2 \left(1 - \frac{1}{2 + 6X^2 t^3} \right) \left(\frac{(3g + 9X^3 t)(H - X)(1/3 + X^2 t^3)^2}{K_f^\eta} \right. \\ &\quad \left. - \frac{X^3 (3/4 + 4.5X^2 t^3)(1 + 6X^2 t^3)^{\kappa-1}}{\varkappa} - 1 \right), \\ f_{\text{mms},u_f} &= t^2 \left(1 - \frac{1}{2 + 8X^2 t^3} \right) \left(\frac{(4g + 12X^4 t)(H - X)(1/4 + X^3 t^3)^2}{K_f^\eta} \right. \\ &\quad \left. - \frac{X^4 (3/4 + 6X^3 t^3)(1 + 8X^3 t^3)^{\kappa-1}}{\varkappa} - 1 \right), \end{aligned} \quad (5.25)$$

and corresponding forcing functions for balance of the mass of the mixture

$$\begin{aligned}
f_{\text{mms},p_f} &= t \left(6Xt + \frac{8(H-X)(1/4 + Xt^3)(1/2 + Xt^3)}{K_f^\eta} \right. \\
&\quad - 2t^4(2^\kappa)\kappa\mathcal{Z}(1/2 + 2Xt^3)^{\kappa-1} \left(\frac{3(H-X)(X^2t + g/3)}{K_f^\eta} - \frac{1}{1 + 2Xt^3} \right) \\
&\quad + \frac{t^3\mathcal{Z}(1 + 2Xt^3)(1 + 4Xt^3)^\kappa \left(\frac{3(H-X)(X^2t + g/3)}{K_f^\eta} - \frac{1}{1 + 2Xt^3} \right)}{K_f^\eta} \\
&\quad \left. - t\mathcal{Z}(1 + 4Xt^3)^\kappa \left(\frac{6HXt - 9X^2t}{K_f^\eta} + \frac{t^3}{2(1/2 + Xt^3)^2} - g/K_f^\eta \right) \right), \\
f_{\text{mms},p_f} &= t \left(9X^2t + \frac{18(H-X)(1/6 + X^2t^3)(1/3 + X^2t^3)}{K_f^\eta} \right. \\
&\quad - 6Xt^4(2^\kappa)\kappa\mathcal{Z}(1/2 + 3X^2t^3)^{\kappa-1} \left(\frac{3(H-X)(X^3t + g/3)}{K_f^\eta} - \frac{1}{1 + 3X^2t^3} \right) \\
&\quad + \frac{t^3\mathcal{Z}(1 + 3X^2t^3)(1 + 6X^2t^3)^\kappa \left(\frac{3(H-X)(X^3t + g/3)}{K_f^\eta} - \frac{1}{1 + 3X^2t^3} \right)}{K_f^\eta} \\
&\quad \left. - t\mathcal{Z}(1 + 6X^2t^3)^\kappa \left(Xt \left[\frac{9HX - 12X^2}{K_f^\eta} + \frac{2t^2}{3(1/3 + X^2t^3)^2} \right] - g/K_f^\eta \right) \right), \\
f_{\text{mms},p_f} &= t \left(12X^3t + \frac{32(H-X)(1/8 + X^3t^3)(1/4 + X^3t^3)}{K_f^\eta} \right. \\
&\quad - 12X^2t^4(2^\kappa)\kappa\mathcal{Z}(1/2 + 4X^3t^3)^{\kappa-1} \left(\frac{3(H-X)(X^4t + g/3)}{K_f^\eta} - \frac{1}{1 + 4X^3t^3} \right) \\
&\quad + \frac{t^3\mathcal{Z}(1 + 4X^3t^3)(1 + 8X^3t^3)^\kappa \left(\frac{3(H-X)(X^4t + g/3)}{K_f^\eta} - \frac{1}{1 + 4X^3t^3} \right)}{K_f^\eta} \\
&\quad \left. - t\mathcal{Z}(1 + 8X^3t^3)^\kappa \left(X^2t \left[\frac{12HX - 15X^2}{K_f^\eta} + \frac{3t^2}{4(1/4 + X^3t^3)^2} \right] - g/K_f^\eta \right) \right).
\end{aligned} \tag{5.26}$$

In the following convergence studies, we set $g = 10 \text{ m/s}^2$ (in the downward direction), $K_f^\eta = 1 \text{ Pa}$, and $\mathcal{Z} = 1 \text{ m}^2$. The temporal convergence study (Figure 5.5) for the poroelastodynamics ($\mathbf{u}-\mathbf{u}_f-p_f$) formulation follows that of the poroelastodynamics ($\mathbf{u}-p_f$) formulation. Spatial convergence (Figure 5.6) also behaves as expected and is comparable to the ($\mathbf{u}-p_f$) spatial convergence study.

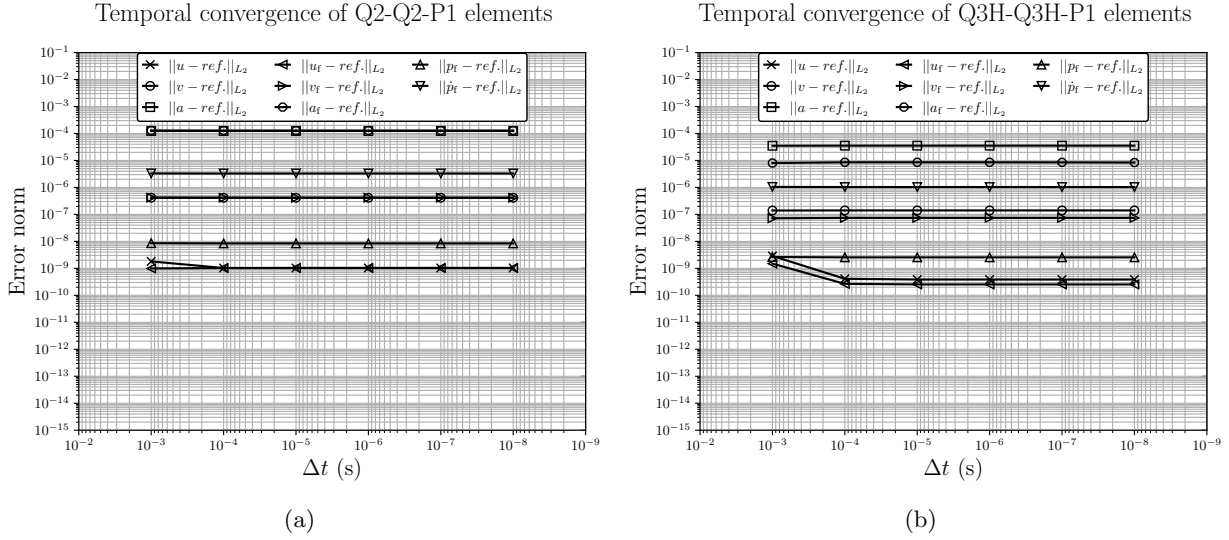


Figure 5.5: Temporal convergence of the poroelastodynamics ($\mathbf{u}\text{-}p_f$) formulation MMS, using (a) quadratic-quadratic-linear solid displacement-fluid displacement-pressure elements with $u(X, t) := X^2 t^3$, $u_f(X, t) := \frac{1}{2} X^2 t^3$, $p_f(X, t) := (H - X)t^2$, and (b) Hermite cubic-Hermite cubic-linear solid displacement-fluid displacement-pressure elements with $u(X, t) := X^3 t^3$, $u_f(X, t) := \frac{1}{2} X^3 t^3$, $p_f(X, t) := (H - X)t^2$, plotted at $t = 0.01$ s. A single element was used to minimize spatial discretization error.

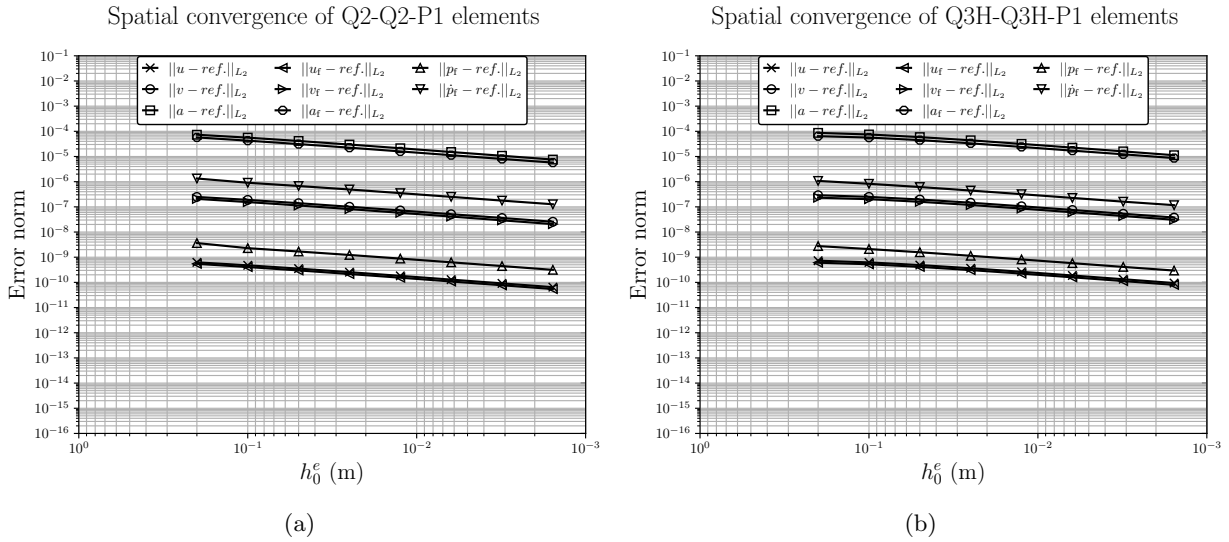


Figure 5.6: Spatial convergence of the poroelastodynamics ($\mathbf{u}\text{-}p_f$) formulation MMS, using (a) quadratic-quadratic-linear solid displacement-fluid displacement-pressure elements with $u(X, t) := X^3 t^3$, $u_f(X, t) := \frac{1}{2} X^3 t^3$, $p_f(X, t) := (H - X)t^2$, and (b) Hermite cubic-Hermite cubic-linear solid displacement-fluid displacement-pressure elements with $u(X, t) := X^4 t^3$, $u_f(X, t) := \frac{1}{2} X^4 t^3$, $p_f(X, t) := (H - X)t^2$, plotted at $t = 0.01$ s. The time step $\Delta t = 10^{-6}$ s was fixed to minimize temporal discretization error.

5.2.2 Elastodynamics

For this verification example, we employ the eigenfunction expansion technique used by Eringen and Suhubi [1975] (which is a modification of the technique proposed by Reismann [1967]) to solve the following differential equation:

$$c_1^2 \nabla^2 \mathbf{u} - c_2^2 \nabla \times \nabla \times \mathbf{u} + \mathbf{f} = \frac{\partial^2 \mathbf{u}}{\partial t^2} \quad \forall \mathbf{x} \in \Omega \times (0, T), \quad (5.27)$$

subjected to the boundary conditions

$$\begin{aligned} \mathbf{u}(\mathbf{x}, t) &= \mathbf{g}^u(\mathbf{x}, t) \quad \forall \mathbf{x} \in \Gamma^u, \\ \boldsymbol{\sigma}(\mathbf{x}, t) \cdot \mathbf{n}(\mathbf{x}) &= \mathbf{t}^\sigma(\mathbf{x}, t) \quad \forall \mathbf{x} \in \Gamma^t, \end{aligned} \quad (5.28)$$

and initial conditions

$$\begin{aligned} \mathbf{u}(\mathbf{x}, 0) &= \mathbf{u}_0(\mathbf{x}), \\ \mathbf{v}(\mathbf{x}, 0) &= \mathbf{v}_0(\mathbf{x}), \end{aligned} \quad (5.29)$$

where c_1 and c_2 are the irrotational and equivoluminal wave velocities, respectively. The solution $\mathbf{u}(\mathbf{x}, t)$ may also be expressed as a summation of an eigenfunction $\boldsymbol{\Psi}(\mathbf{x})$ subjected to homogeneous boundary conditions and a quasistatic displacement field $\boldsymbol{\Phi}(\mathbf{x}, t)$, i.e.,

$$\mathbf{u}(\mathbf{x}, t) = \boldsymbol{\Phi}(\mathbf{x}, t) + \sum_n \phi_n(t) \boldsymbol{\Psi}_n(\mathbf{x}), \quad (5.30)$$

wherein the strong formulation for the eigenfunction is given by

$$\begin{aligned} c_1^2 \nabla^2 \boldsymbol{\Psi} - c_2^2 \nabla \times \nabla \times \boldsymbol{\Psi} + \omega^2 \boldsymbol{\Psi} &= \mathbf{0} \quad \mathbf{x} \in \Omega \times (0, T), \\ \boldsymbol{\Psi}(\mathbf{x}, t) &= \mathbf{0} \quad \forall \mathbf{x} \in \Gamma^u, \\ \boldsymbol{\sigma}(\mathbf{x}, t) \cdot \mathbf{n}(\mathbf{x}) &= \mathbf{0} \quad \forall \mathbf{x} \in \Gamma^t, \end{aligned} \quad (5.31)$$

where ω is the natural frequency (i.e., the eigenvalue). The strong formulation for the quasi-static displacement field is given by

$$\begin{aligned} c_1^2 \nabla^2 \boldsymbol{\Phi} - c_2^2 \nabla \times \nabla \times \boldsymbol{\Phi} + \mathbf{f}(\mathbf{x}, t) &= \mathbf{0} \quad \mathbf{x} \in \Omega \times (0, T), \\ \boldsymbol{\Phi}(\mathbf{x}, t) &= \mathbf{g}^u(\mathbf{x}, t) \quad \forall \mathbf{x} \in \Gamma^u, \\ \boldsymbol{\sigma}(\mathbf{x}, t) \cdot \mathbf{n}(\mathbf{x}) &= \mathbf{t}^\sigma(\mathbf{x}, t) \quad \forall \mathbf{x} \in \Gamma^t. \end{aligned} \quad (5.32)$$

Substitution of Equation (5.30) into Equation (5.27) and making use of Equation (5.31) gives us

$$\sum_n \left(\ddot{\phi}_n + \omega_n^2 \phi_n \right) \Psi_n(\mathbf{x}) = -\ddot{\Psi}(\mathbf{x}, t). \quad (5.33)$$

Multiplying Equation (5.33) by $\Phi_m(\mathbf{x})$, integrating over Ω and invoking the orthogonality condition on Φ gives us

$$\ddot{\phi}_m + \omega_m^2 \phi_m = \ddot{\Phi}_m(t), \quad (5.34)$$

where

$$\Phi_m(t) = - \int_{\Omega} \phi(\mathbf{x}, t) \cdot \Psi(\mathbf{x}) d\Omega. \quad (5.35)$$

To solve Equation (5.34), we require initial conditions, which we can pull from Equation (5.29) and substitute into Equation (5.30) to find

$$\begin{aligned} \phi_m(0) &= \int_{\Omega} \mathbf{u}_0(\mathbf{x}) \cdot \Phi_m(\mathbf{x}) d\Omega + \Phi_m(0), \\ \dot{\phi}_m(0) &= \int_{\Omega} \mathbf{v}_0(\mathbf{x}) \cdot \Phi_m(\mathbf{x}) d\Omega + \dot{\Phi}_m(0). \end{aligned} \quad (5.36)$$

Then the solution to Equation (5.34) is

$$\begin{aligned} \phi_m(t) &= [\phi_m(0) - \Phi_m(0)] \cos(\omega_m t) + \frac{1}{\omega_m} [\dot{\phi}_m(0) - \dot{\Phi}_m(0)] \sin(\omega_m t) \\ &\quad + \Phi_m(t) - \omega_m \int_0^t \Phi_m(\tau) \sin(\omega_m(t - \tau)) d\tau. \end{aligned} \quad (5.37)$$

Then, Equation (5.30) may be rewritten as

$$\mathbf{u}(\mathbf{x}, t) = \sum_m \left[\alpha_m \cos(\omega_m t) + \frac{1}{\omega_m} \beta_m \sin(\omega_m t) - \omega_m \int_0^t \Phi_m(\tau) \sin(\omega_m(t - \tau)) d\tau \right] \Psi_m(\mathbf{x}), \quad (5.38)$$

wherein

$$\phi(\mathbf{x}, t) + \sum_m \Phi_m(t) \Psi_m(\mathbf{x}) \rightarrow 0, \quad (5.39)$$

and

$$\alpha_m = \int_{\Omega} \mathbf{u}_0(\mathbf{x}) \cdot \Phi(\mathbf{x}) d\Omega, \quad \beta_m = \int_{\Omega} \mathbf{v}_0(\mathbf{x}) \cdot \Phi(\mathbf{x}) d\Omega. \quad (5.40)$$

For this particular verification problem, we presuppose that our domain is 1-D, that it is fixed at its lower end & its sides, and that we apply a sinusoidal traction to the top surface, i.e.,

$$\begin{aligned} u(X, t) &= 0 \quad \forall X \in \Gamma^u, \\ \mathbf{t}^\sigma(t) &= \frac{t_0^\sigma}{2} [1 - \cos(\omega t)] \quad \forall X \in \Gamma^t, \end{aligned} \quad (5.41)$$

with initial conditions

$$\begin{aligned} u(X, 0) &= 0, \\ v(X, 0) &= 0. \end{aligned} \quad (5.42)$$

Then Equation (5.38) reduces to

$$u(X, t) = - \sum_m \omega_m \Psi_m(X) \int_0^t \Phi_m(\tau) \sin(\omega_m(t - \tau)) d\tau. \quad (5.43)$$

It can be shown that

$$\Phi_m(\tau) = \frac{2(2H)^{1/2} t^\sigma(X, t) (-1)^m}{\pi \rho_0 c_1 \omega_m (2m - 1)}, \quad (5.44)$$

where H is the initial height of the column, which allows us to rewrite Equation (5.43) as

$$u(X, t) = \frac{4}{\pi \rho_0 c_1} \sum_{m=1}^{\infty} \frac{(-1)^m}{2m - 1} \left[\int_0^t t^\sigma(\tau) \sin\left(\frac{(2m - 1)\pi c_1(t - \tau)}{2H}\right) d\tau \right] \sin\left(\frac{(2m - 1)\pi X}{2H}\right), \quad (5.45)$$

wherein

$$c_1 = \sqrt{\frac{E \left(\frac{1 - \nu}{(1 + \nu)(1 - 2\nu)} \right)}{\rho_0}} = \sqrt{\frac{M}{\rho_0}}, \quad (5.46)$$

and where E , ν and M are Young's modulus, the poisson ratio and the P-wave modulus for the material, respectively.

Geometrical and loading parameters are given in Table 5.3, with associated schematics in Figure 5.7; material parameters are given in Table 5.2. We see excellent agreement between the numerical and analytical solution, as shown in Figure 5.8.

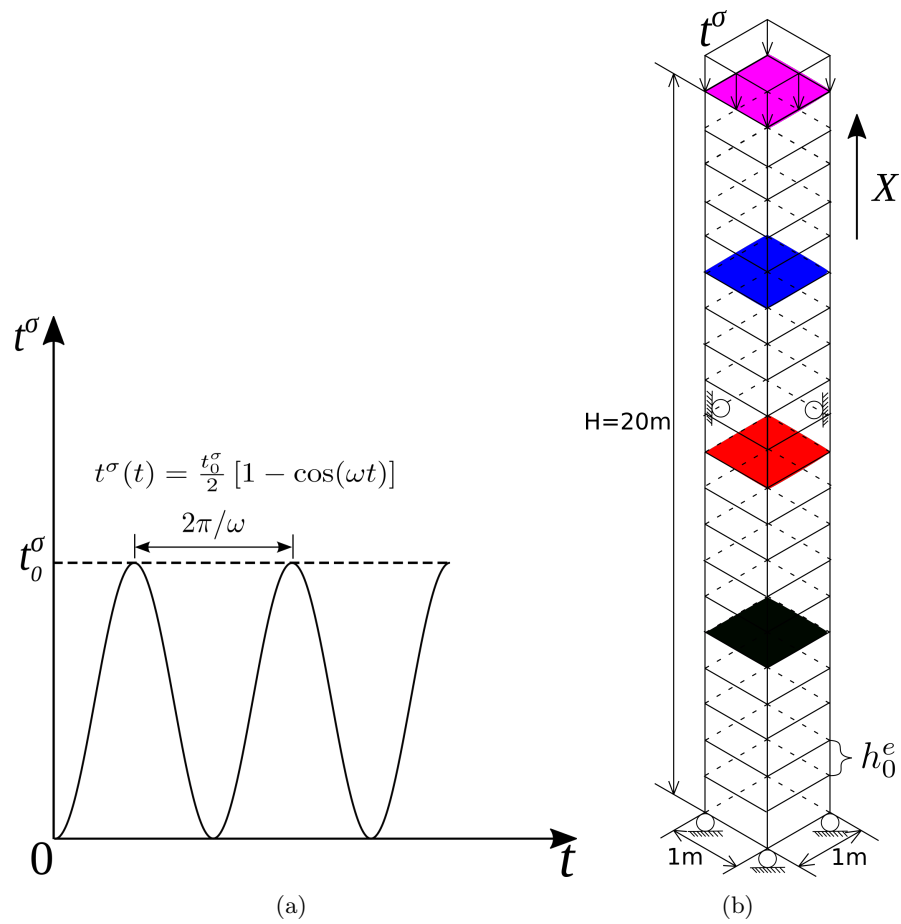


Figure 5.7: (a) Traction application and (b) schematic of column mesh for the elastodynamics verification example.

Table 5.2: Material parameters for elastodynamics verification example.

E (MPa)	ν	ρ_0 (kg/m ³)
50	0.3	1986

Table 5.3: Geometrical and loading parameters for elastodynamics verification example.

H (m)	A (m ²)	t_0^σ (kPa)	ω (rad/s)
20	1	40	50

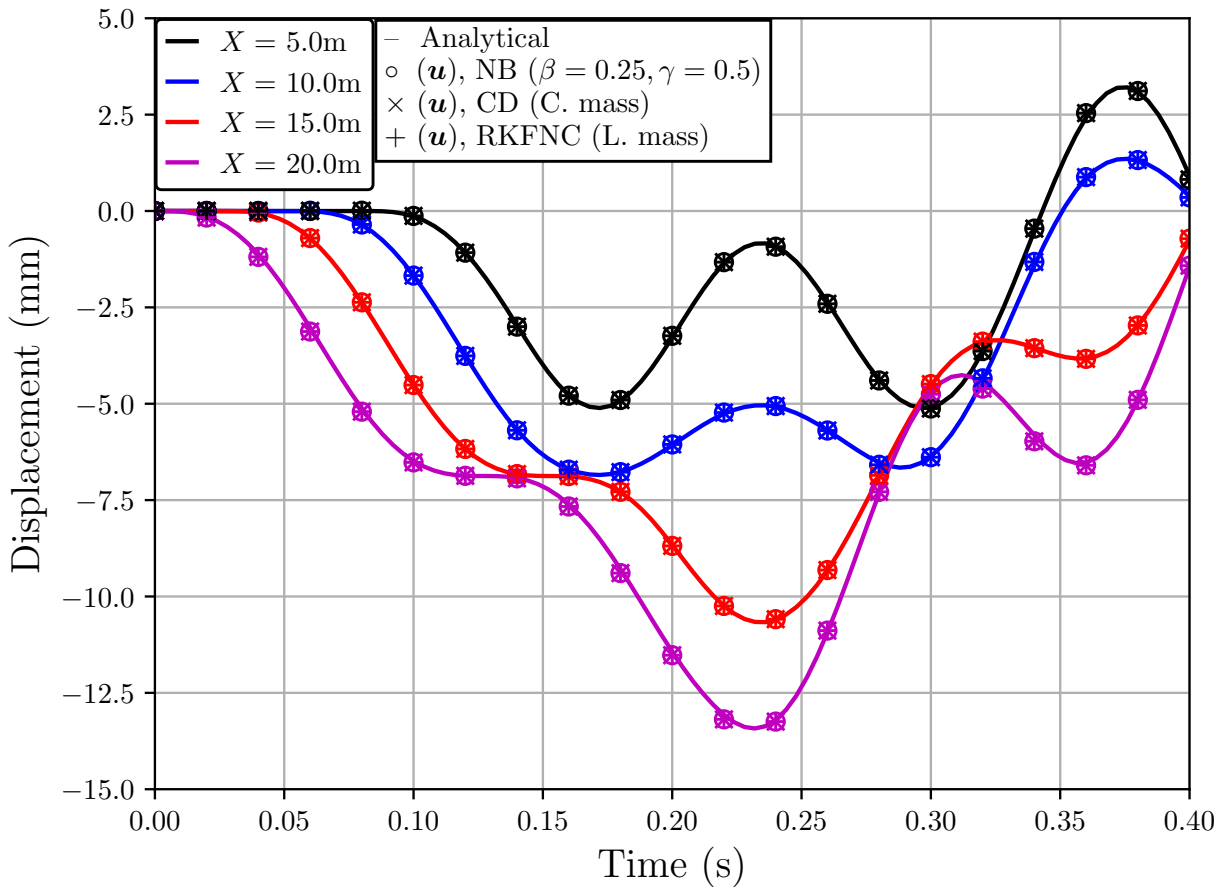


Figure 5.8: Results for the displacements for the elastodynamics verification. Here, Q1 elements were used in SPONGE-1D with mesh size $h_0^e = 1$ m.

5.2.3 Poroelasticity

Recall from Section 4.1.3 the formulation for poroelasticity, i.e., the $(\mathbf{u}-p_f)$ formulation *without* inertia terms. Here, we present results previously published in Li et al. [2004] that demonstrate the differences between small-strain theory and finite-strain theory (large deformation). Similar to the elastodynamics example in Section 5.2.2, a porous column is subjected to an external traction load while its base and sides remain fixed. The analytical solution in small-deformation theory is given by

$$\Delta H = \frac{t_0^\sigma H}{\lambda + 2\mu}, \quad (5.47)$$

where H is the initial height of the column and λ and μ are the first and second Lamé parameters of the solid skeleton, respectively. The upper boundary of the fully saturated column is perfectly drained with reference pressure $p_f(X = H, t) = 0$ atm and subjected to a uniform step load with finite rise time.

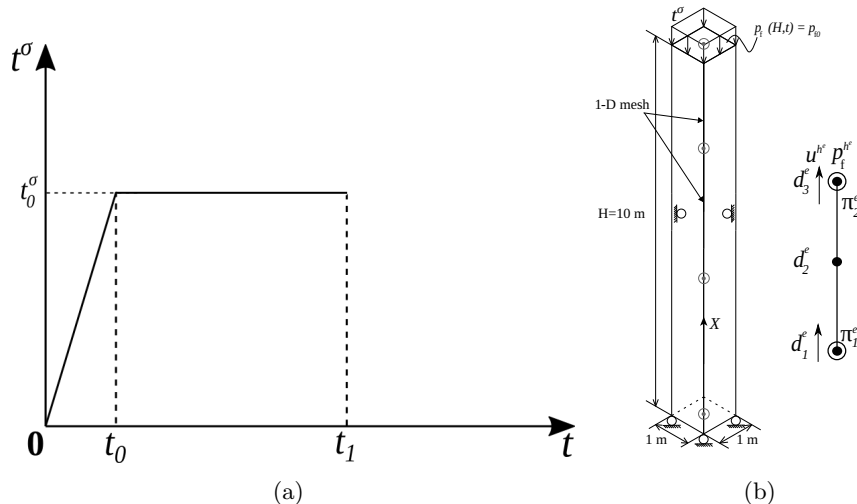


Figure 5.9: (a) Traction application and (b) schematic of column mesh for the poroelasticity verification example.

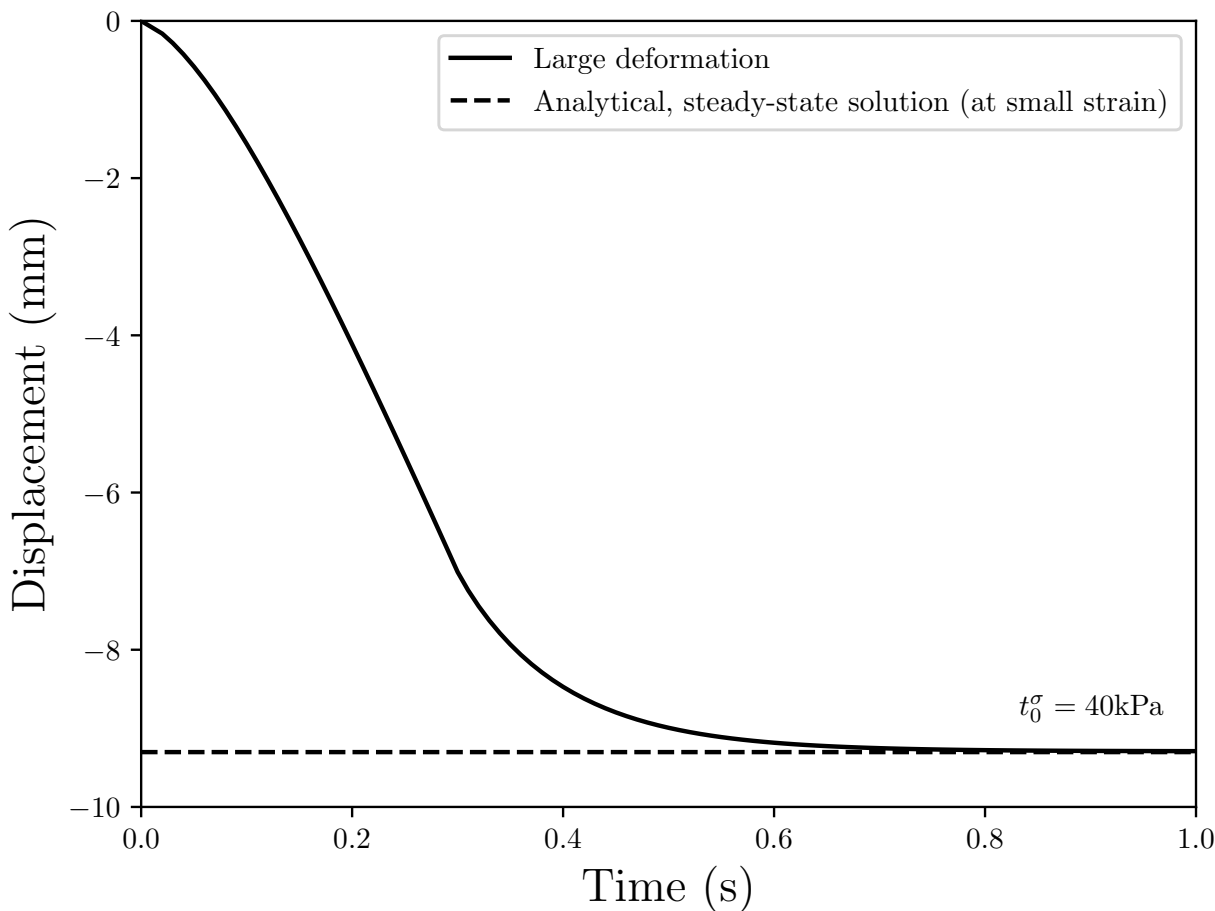
Geometrical and loading parameters are given in Table 5.5, with associated schematics in Figure 5.9; material parameters are given in Table 5.4. The displacement histories of the top of the column are plotted in Figure 5.10. Owing to the fact that the displacement for our large

Table 5.4: Material parameters for the poroelasticity verification example.

λ (MPa)	μ (MPa)	ρ_0^s (kg/m ³)	ρ_0^f (kg/m ³)	n^f	n^s
29	7	2700	1000	0.42	0.58

Table 5.5: Geometrical and loading parameters for the poroelasticity verification example.

H (m)	A (m ²)	h_0^e (m)	t_0^σ (MPa)	t_0	t_1
10	1	1	0.04; 2; 4; 8	0.3	1.0

Figure 5.10: Porous layer with uniform step load: vertical displacement-time history at topmost node for load $t_0^\sigma = 40\text{kPa}$.

deformation model is so small, the results line up well with the analytical solution for small-strain theory. However, when load is increased to the order of megapascals, the small-strain theory always predicts deformations well-exceeding that of finite-strain (large deformation).

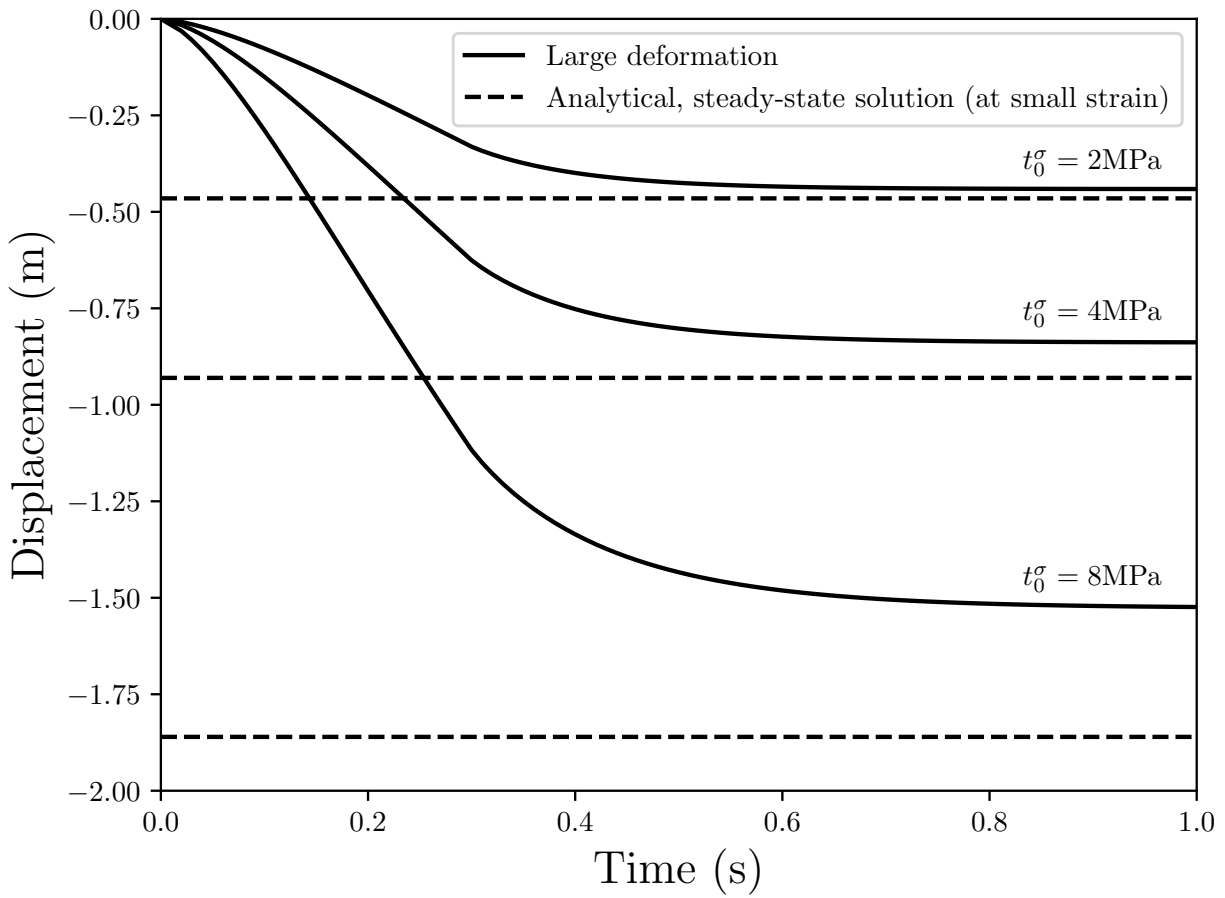


Figure 5.11: Porous layer with uniform step load: vertical displacement-time histories at topmost node for loads $t_0^\sigma = 2, 4$ and 8 MPa.

5.2.4 Poroelastodynamics

Recall from Sections 4.1.3 and 4.1.4 the formulation for poroelastodynamics, i.e., the $(\mathbf{u}-p_f)$ and $(\mathbf{u}-\mathbf{u}_f-p_f)$ formulations *with* inertia terms. Here, we present results comparing the numerical solution to an analytical solution developed by de Boer et al. [1993]. Similar to the previous examples, a porous column is subjected to an external traction load while its base and sides remain fixed. The top of the porous column is perfectly drained with reference pressure $p_f(X = H, t) = 0$ atm and subjected to a harmonic loading. The analytical solution for this problem is given as follows:

$$\begin{aligned}
u(X, t) &= -\frac{1}{\sqrt{a}(\lambda + 2\mu)} \int_0^t \left(t^\sigma(t - \tau) \exp\left[-\frac{b}{2a}\tau\right] I_0\left(\frac{b\sqrt{\tau^2 - aX^2}}{2a}\right) \mathbb{H}(\tau - \sqrt{a}X) \right) d\tau, \\
u_f(X, t) &= \frac{n^s}{n^f\sqrt{a}(\lambda + 2\mu)} \int_0^t \left(t^\sigma(t - \tau) \exp\left[-\frac{b}{2a}\tau\right] I_0\left(\frac{b\sqrt{\tau^2 - aX^2}}{2a}\right) \mathbb{H}(\tau - \sqrt{a}X) \right) d\tau, \\
p_f(X, t) &= \frac{1}{(n^f)^2(\lambda + 2\mu)} \left[n^f \rho^{fR} \frac{\partial^2 L(X, t)}{\partial t^2} + S_v \frac{\partial L(X, t)}{\partial t} \right], \\
\sigma_{11(E)}^s(X, t) &= \frac{b}{2\sqrt{a}} \int_0^t \left(t^\sigma(t - \tau) \exp\left[-\frac{b}{2a}\tau\right] I_1\left(\frac{b\sqrt{\tau^2 - aX^2}}{2a}\right) \frac{X}{\sqrt{\tau^2 - aX^2}} \mathbb{H}(\tau - \sqrt{a}X) \right) d\tau \\
&\quad + f(\tau - \sqrt{a}X) \exp\left[-\frac{b}{2\sqrt{a}}\right] X,
\end{aligned} \tag{5.48}$$

wherein

$$\begin{aligned}
L(X, t) &:= \int_0^t Q(t - \tau) G(X, \tau) d\tau, \\
Q(t) &:= \frac{1}{\sqrt{a}} \int_0^t t^\sigma(t - \tau) \exp\left[-\frac{b}{2a}\tau\right] I_0\left(\frac{b}{2a}\tau\right) d\tau, \\
G(X, t) &:= \frac{1}{\sqrt{a}} \exp\left[-\frac{b}{2a}t\right] I_0\left(\frac{b\sqrt{t^2 - aX^2}}{2a}\right) \mathbb{H}(t - \sqrt{a}X) - \frac{1}{\sqrt{a}} \exp\left[-\frac{b}{2a}t\right] I_0\left(\frac{b}{2a}t\right), \\
S_v &:= \frac{(n^f)^2 \rho^{fR} g}{\hat{k}}, \\
a &:= \frac{(n^s)^2 \rho^f + (n^f)^2 \rho^s}{(\lambda + 2\mu)(n^s)^2}, \\
b &:= \frac{S_v}{(\lambda + 2\mu)(n^f)^2},
\end{aligned} \tag{5.49}$$

and where I_m are the modified Bessel functions of order m , \mathbb{H} is the Heaviside function, $t^\sigma(t)$ is the harmonic loading function and λ and μ are the first and second Lamé parameters of the solid

skeleton, respectively.

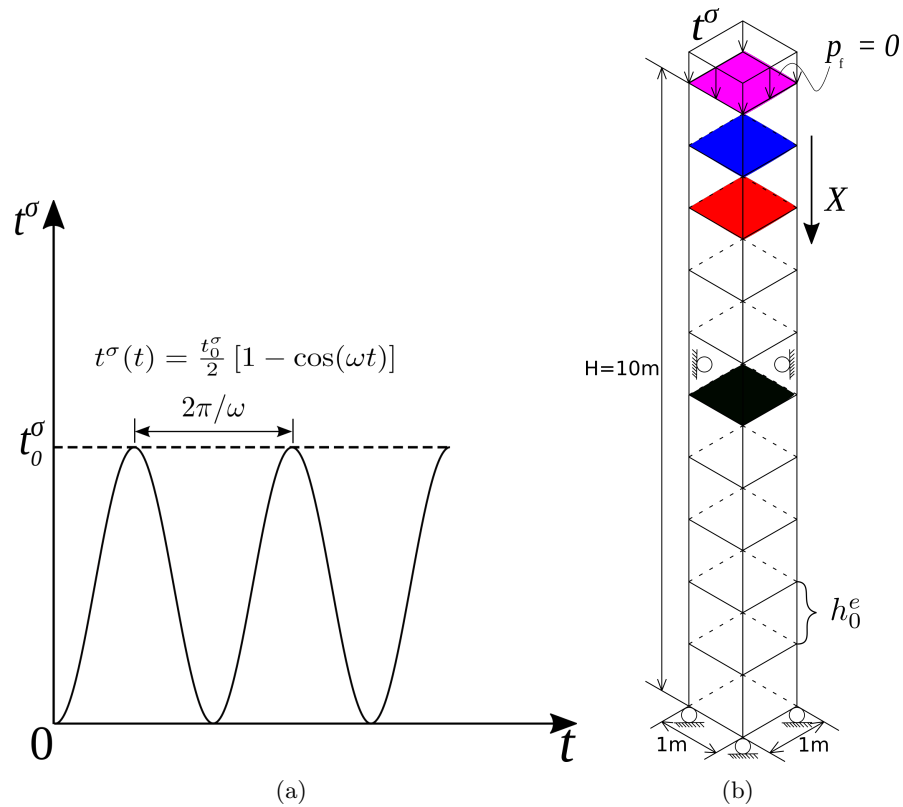


Figure 5.12: (a) Traction application and (b) schematic of column mesh for the poroelastodynamics verification example.

Table 5.6: Material parameters for the poroelastodynamics verification example.

λ (MPa)	μ (MPa)	ρ_0^s (kg/m ³)	ρ_0^f (kg/m ³)	n_0^f	n_0^s	k_0 (m/s)
5.6	8.4	2700	1000	0.42	0.58	10^{-2}

Table 5.7: Geometrical and loading parameters for the poroelastodynamics verification example.

H (m)	A (m ²)	h_0^e (m)	t_0^σ (kPa)	ω (rad/s)
10	1	1; 0.1	40	50

Geometrical and loading parameters are given in Table 5.7, with associated schematics in Figure 5.12; material parameters are given in Table 5.6. With SPONGE-1D, we see excellent agreement between numerical and analytical solutions (see Figure 5.13, Figure 5.14). However, there

are slight discrepancies in both solid skeleton displacement and pore fluid pressure in the LS-DYNA poroelastodynamics model. We suspect that this is caused by LS-DYNA ignoring the inertia term in the Darcy velocity constitutive equation, irrespective of whether or not the (\mathbf{u} - p_f) assumption is made. Furthermore, given that LS-DYNA assumes a (\mathbf{u} - p_f) formulation outright, its poroelastodynamics model cannot be used to verify the displacement of pore fluid because there is no governing equation for the third field variable, which the analytical solution includes (see Figure 5.13(b)). Lastly, we found that we were only able to obtain a close approximation with LS-DYNA by assuming a linear isotropic elastic material and initializing the geostatic stresses prior to starting the simulation. As a result, the resulting solid skeleton effective stress response σ_E^s in LS-DYNA does not match the analytical solution, and is not shown here for that reason.

We also observe poor agreement between the analytical solution and our FE solution for the pore fluid displacement (see Fig.5.13(b)). However, this is an entirely numerical phenomenon. The same discrepancies were observed by Heider [2012], who came to the conclusion that for coarse-mesh resolution, the pore fluid pressure gradient is numerically unstable at the drained surface. Given that the pressure there is set to 0 atm (reference pressure) and that a traction load is also applied there, this causes a large pore fluid pressure buildup at the surface, which must quickly dissipate to 0 atm. Thus, a large pore fluid pressure spatial gradient is created, and because of the coupling between pore fluid pressure and pore fluid displacement in the balance of momentum of the pore fluid, this leads to inaccuracy in the FE solution for the pore fluid displacement. Fortunately, this problem is easily remedied by using mesh refinement—see Figure 5.14 for a demonstration. Therefore, in addition to numerical issues with resolving the propagation of a shock wave with coarse meshes, as we shall see momentarily in Section 5.3.1, we elect to use finer meshes for the poroelastodynamics simulations of soft porous materials such as lung parenchyma.

The convergence profile for different element types with varying stabilization parameters is shown in Figure 5.15. Here we have used the implicit Newmark-beta integrator for constant acceleration, i.e., $\beta = 1/4, \gamma = 1/2$, at fixed time step for variable element lengths. The relative

displacement error

$$ERR_u[-] := \frac{|u_{\text{analytical}}(X = H, t = 0.2 \text{ s}) - u_{\text{numerical}}(X = H, t = 0.2 \text{ s})|}{|u_{\text{analytical}}(X = H, t = 0.2 \text{ s})|}. \quad (5.50)$$

It is apparent that the $(\mathbf{u}-p_f)$ formulation does not give as accurate of a result as the $(\mathbf{u}-\mathbf{u}_f-p_f)$ formulation, especially at the smaller element lengths. We do not observe a strong convergence profile, especially compared to the one obtained by Markert et al. [2009], Heider [2012]. We suspect that the poor convergence behavior is due to the abundance of nonlinearities in our model, whereas Markert et al. [2009], Heider [2012] assumed a linear, small strain theory. We have also considered

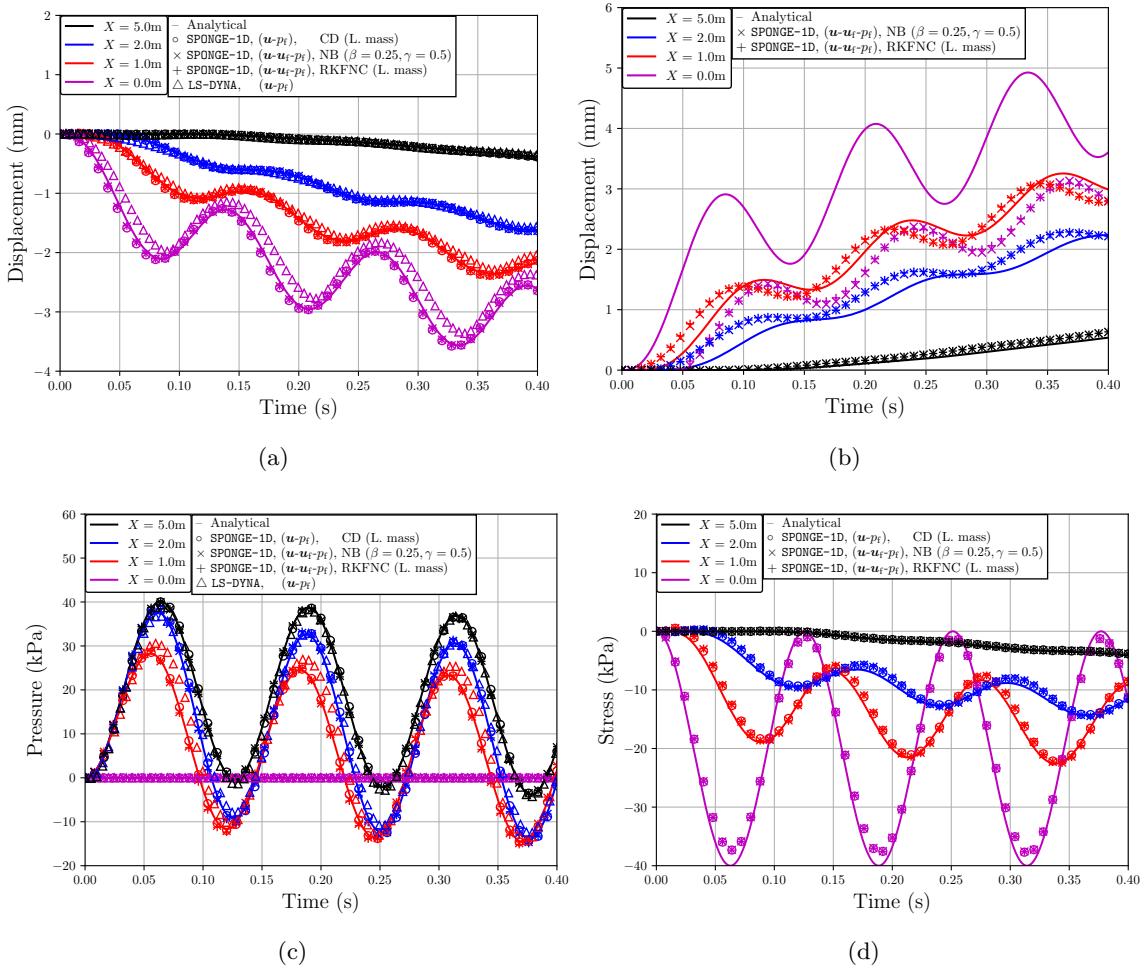


Figure 5.13: Verification results for the numerical approximation to the de Boer analytical solution, using $h_0^e = 1 \text{ m}$. All element types used in SPONGE-1D are stable, i.e., Q2-P1 or Q2-Q2-P1 depending on the formulation.

Pore fluid displacement

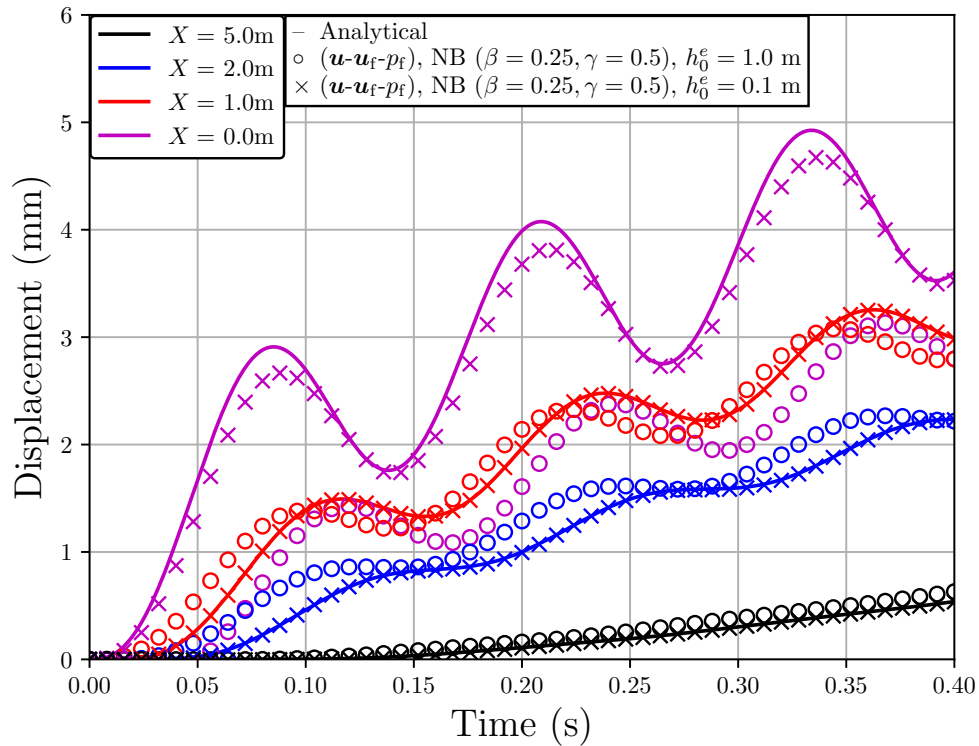


Figure 5.14: Comparison between two different mesh resolutions for multiple integrators demonstrating the importance of finer meshes in resolving the pore fluid displacement (using SPONGE-1D).

the viscous pore fluid stress for this problem; material parameters are unchanged with the addition of the pore fluid bulk viscosity $\kappa_f = 2.86$ mPa-s. Other than a bump in accuracy in the pore fluid displacements from the higher-order element (Figure 5.16), inclusion of the viscous pore fluid stress does not effect the solution, because for water, the viscous effects are essentially negligible (Figure 5.17).

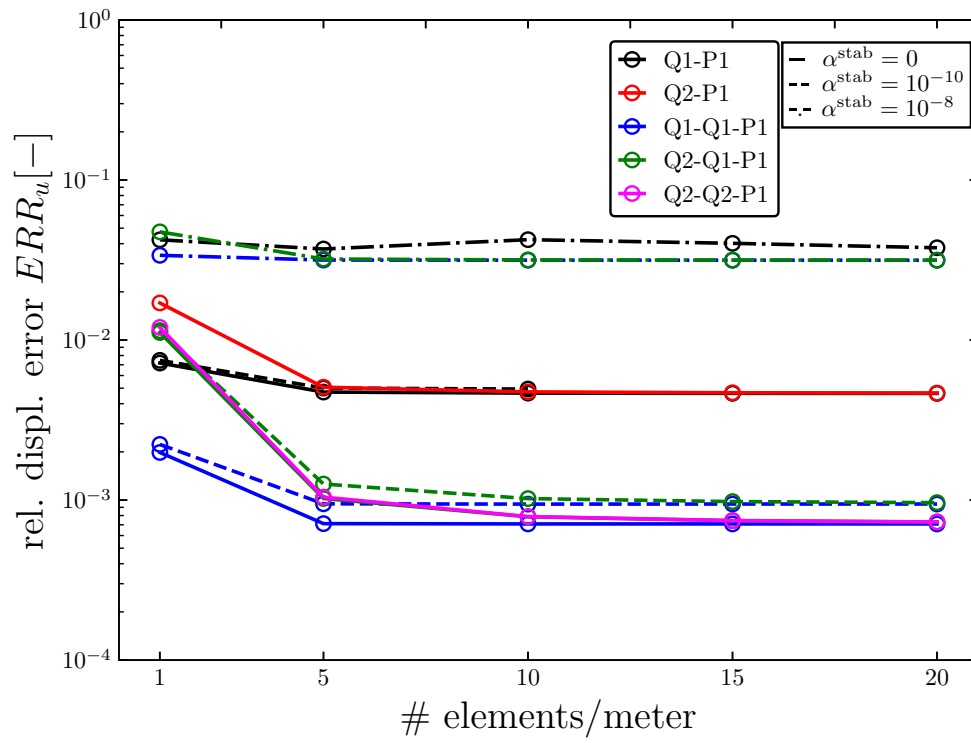


Figure 5.15: Relative solid skeleton displacement error (logarithmic scale) at $t = 0.2$ s for fixed $\Delta t = 10^{-6}$ s.

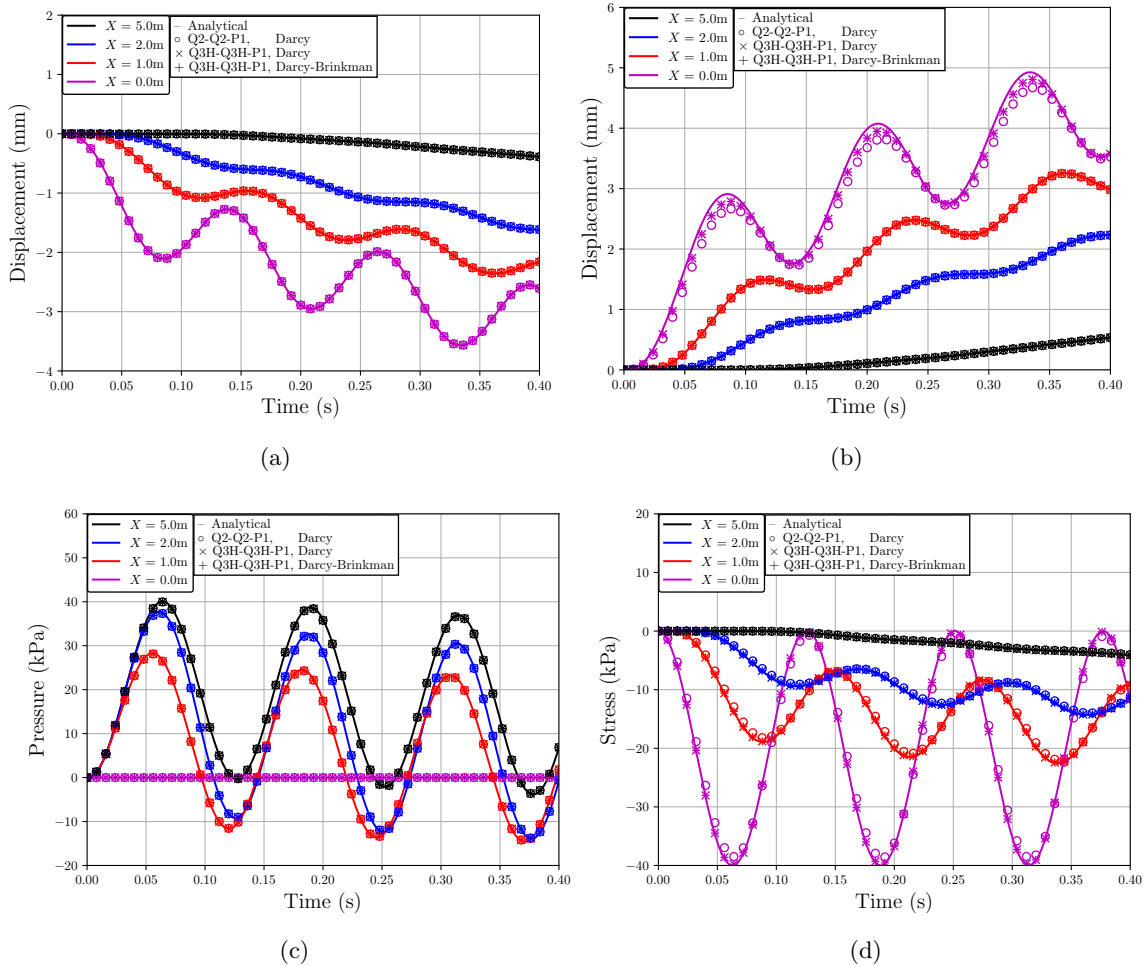


Figure 5.16: Verification results for the numerical approximation to the de Boer analytical solution, comparing the nearly inviscid (Darcy) to viscous (Darcy-Brinkman) formulations, using $h_0^e = 0.1$ m.

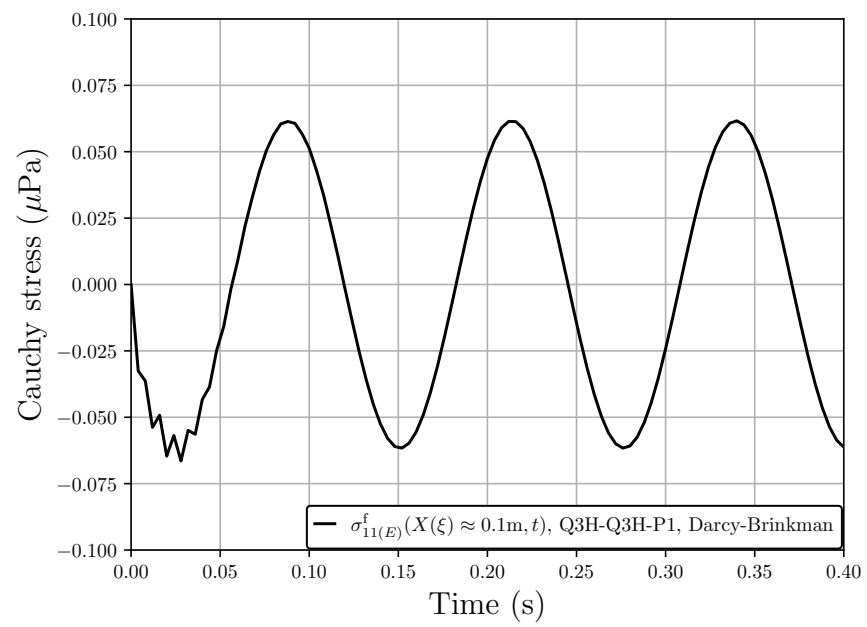


Figure 5.17: Viscous pore fluid stress for the de Boer verification problem.

5.3 High strain-rate loading

Of key importance for dynamic injury predictions of soft tissue (or dynamic damage predictions of another soft, porous material) is how lung tissue (or said material) deforms under shock loading. In the following sections, we present our findings for a column of lung parenchyma subjected to external traction loadings on the order of milliseconds or less. In all of the simulations, the lung parenchyma column is fixed on its sides and base. Furthermore, in many of the simulations, the sides and top are assumed to be an impermeable membrane (i.e., “undrained”, or, “no-flux”) such that the pore air is confined solely within the column.

While we do have full control over the boundary conditions at the ends of the column, we have chosen the impermeable boundary condition for comparative purposes to the model developed by Clayton and Freed [2019a,b], Clayton et al. [2020], Clayton [2020], Clayton and Freed [2020a], Clayton et al. [2021], in which they assume occluded pore air. One could imagine the experimental analog to this type of boundary condition wherein a small section of lung parenchyma is excised, placed in an impermeable sleeve and then uniaxially loaded. The advantage to our model over the one implemented by Clayton et al. [2021] is that we could allow for more realistic boundary conditions at the ends of the column of lung parenchyma in our simulations. For example, allowing an end to remain open to atmospheric pressure (i.e., “drained”; see, e.g., the section on viscous pore fluid stress in Chapter 5.3.3) such that experimentally the sleeve need not enclose this end of excised tissue, or specifying a mixed boundary condition wherein the pore fluid pressure gradient and pore fluid pressure at the end of the column are both free. This would enable experimentally that the sleeve need not enclose the end of excised tissue, and the impacting device would need only to maintain contact with a part of the tissue during loading.

5.3.1 Effects of shock viscosity for single-phase models

To begin with, we wish to demonstrate the effects that the shock viscosity imposes on the deformation of a single-phase material. For the single-phase model in LS-DYNA, we use the standard

neo-Hookean hyperelastic material model, MAT 45, so that we can make a one-to-one comparison with our neo-Hookean hyperelastic material model in SPONGE-1D. Material properties are given in Table 5.8. Geometrical and loading parameters are given in Table 5.9.

Table 5.8: Material parameters for an example on shock viscosity for a column of single-phase, elastodynamic lung parenchyma. Values taken from Clayton et al. [2021].

K (kPa)	G (kPa)	ρ_0 (kg/m ³)
213	3	337

Table 5.9: Geometrical and loading parameters for an example on shock viscosity for a column of single-phase, elastodynamic lung parenchyma.

Overpressure load type	H (cm)	A (cm ²)	h_0^c (cm)	t_0^σ (kPa)	t_0 (ms)	t_1 (ms)
Yen impulse	10	1	1, 0.1	50	0.17	0.34
Friedlander impulse	10	1	1, 0.1	25	10	N/A

The traction is applied to the top of the column in two forms. The first is a linear triangular impulse, hereafter referred to as the Yen impulse, shown in Figure 5.18, which rises to a maximum pressure $t_0^\sigma = 50$ kPa at time $t_0 = 170 \mu\text{s}$ relative to reference pressure, set to 0 atm for these single-phase simulations. It then decays to $t^\sigma = 0$ kPa at time $2t_0 = t_1 = 340 \mu\text{s}$. The time scales and pressure profile were chosen based on an experimental study of rabbit lung exposed to shock tubes by Yen et al. [1988]. Overpressure amplitude was chosen arbitrarily, though we note that Yen et al. [1988] observed that overpressures greater than 2 psi (≈ 14 kPa) resulted in edema of the exposed rabbit lung.

The second traction application is the Friedlander impulse [Friedlander, 1946], which is depicted in Figure 5.18(b). The profile is of an exponentially decaying function to 0 applied pressure at $t_0 = 10$ ms, whereby it then starts to act as a tensile force relative to atmospheric pressure. This profile is an analytical solution to sound waves diffracting off of a semi-infinite plate. Therefore, the Friedlander wave is more indicative of the overpressure profile of a blast wave [Dewey, 2018]

(e.g., one resulting from an explosion and impacting against a hard surface, such as body armor), than the Yen impulse, which is better suited to describe shock-tube-like experimental loading.

For both pressure profiles, we will vary the peak overpressure amplitude. As with the de Boer example in Section 5.2.4, the bottom and sides of the column remain fixed and rigid such that the motion is purely vertical in the X direction. The 1-D FE mesh is shown in Figure 5.18(c).

Different choices of element length h_0^e and different choices of shock viscosity (i.e., none or default values) are investigated in displacement predictions for the Yen loading protocol in Figure 5.19 and Figure 5.20. Similarly, predictions are compared for the Friedlander loading protocol in Figure 5.21 and Figure 5.22.

For both element lengths h_0^e , it is apparent that without shock viscosity, SPONGE-1D's integration schemes struggle to constrain the numerical overshoots. This is particularly noticeable for the coarser mesh with $h_0^e = 1$ cm in Figure 5.21(a) for the implicit solver which is taking constant time-steps $\Delta t = 10^{-6}$ s. When some shock viscosity is introduced, the “noise” from the shock is dampened significantly, and we see fairly good agreement with the results from LS-DYNA, which we note does not provide users the option to disable shock viscosity as is evident by the overlapping $C_0 = C_1 = 0.0$ (black) and $C_0 = 1.5, C_1 = 0.06$ (red) curves.

We show further comparisons for the Friedlander impulse with the fine mesh. In contrast to the results shown in Irwin et al. [2023c], here the central-difference scheme in Figure 5.22(a) looks nearly identical to Figure 5.22(b) and remains stable. This was due to imposing a severe restriction on the max allowable time step, reducing it from $\Delta t = 10^{-7}$ s to $\Delta t = 10^{-8}$ s. Without this restriction, the numerical solution went unstable.

In addition, care must be taken when choosing the coefficients C_0 and C_1 ; as the values of these coefficients increase, the shock is smeared across larger portions of the domain (i.e., over more elements). This can be seen in Figs. 5.23 and 5.24. Thus, if the constants are too large, we begin to eliminate physical effects that are important to measure. For that reason, we stick to the default values used by LS-DYNA in SPONGE-1D for shock loading.

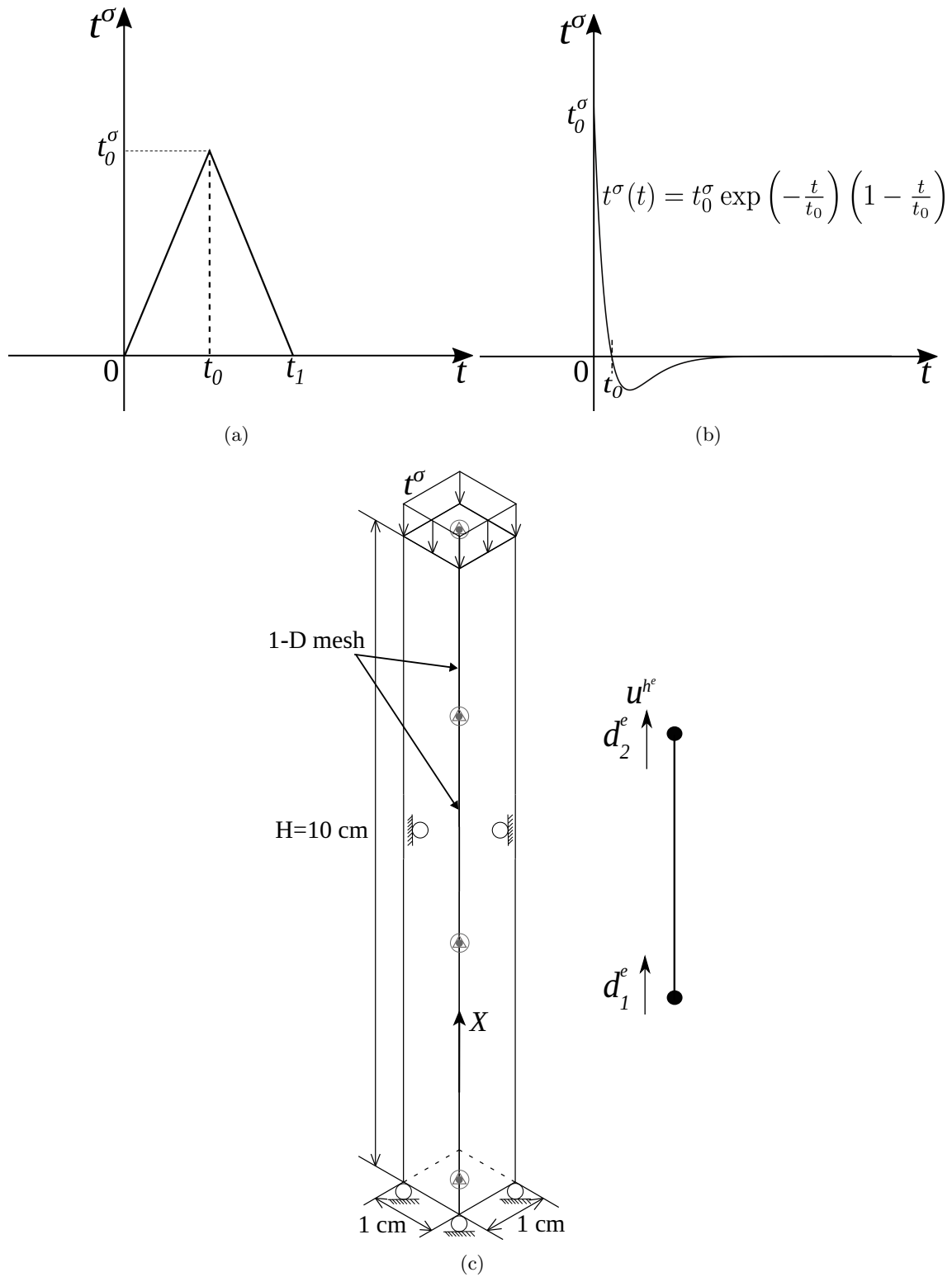


Figure 5.18: (a) Yen impulse traction application (b) Friedlander impulse traction application (c) schematic of column mesh for an example on shock viscosity for a column of single-phase/elastodynamic lung parenchyma, highlighting the Q1 element.

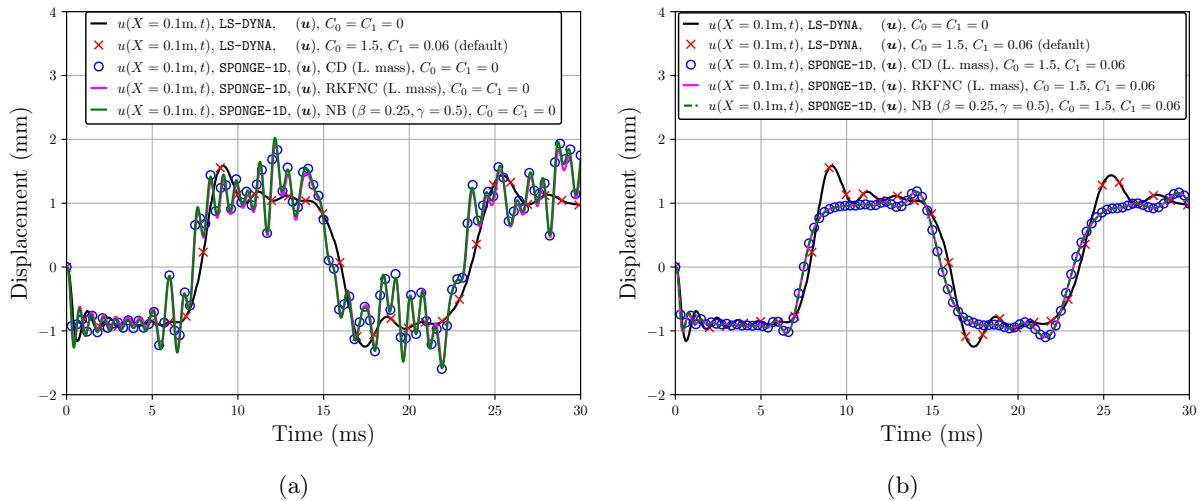


Figure 5.19: Comparison of elastodynamical response to Yen impulse loading for peak overpressure of 50 kPa with element size $h_0^e = 1$ cm for (a) simulations without shock viscosity enabled (b) shock viscosity set to default values.

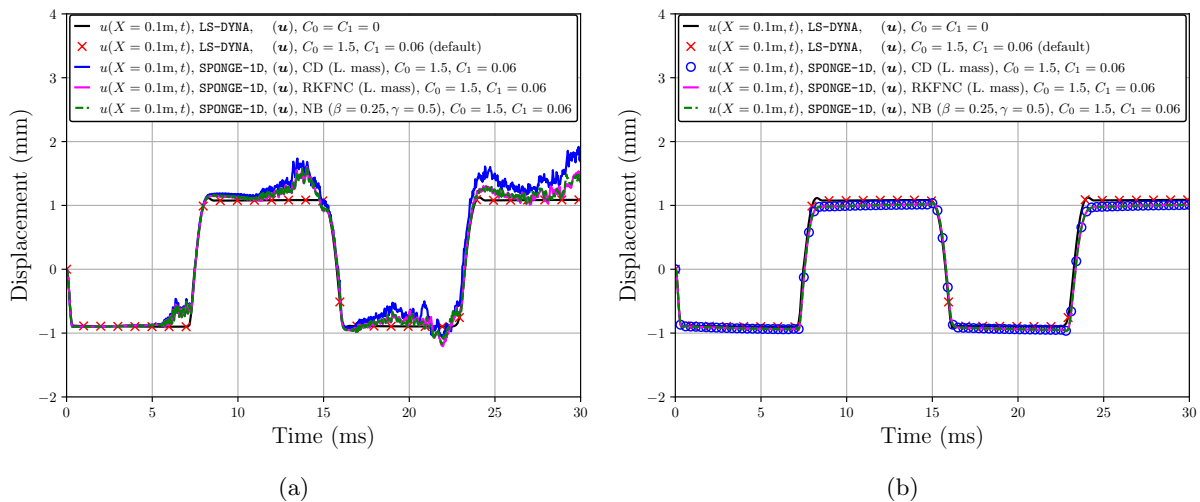


Figure 5.20: Comparison of elastodynamical response to Yen impulse loading for peak overpressure of 50 kPa with element size $h_0^e = 0.1$ cm for (a) simulations without shock viscosity enabled (b) shock viscosity set to default values.

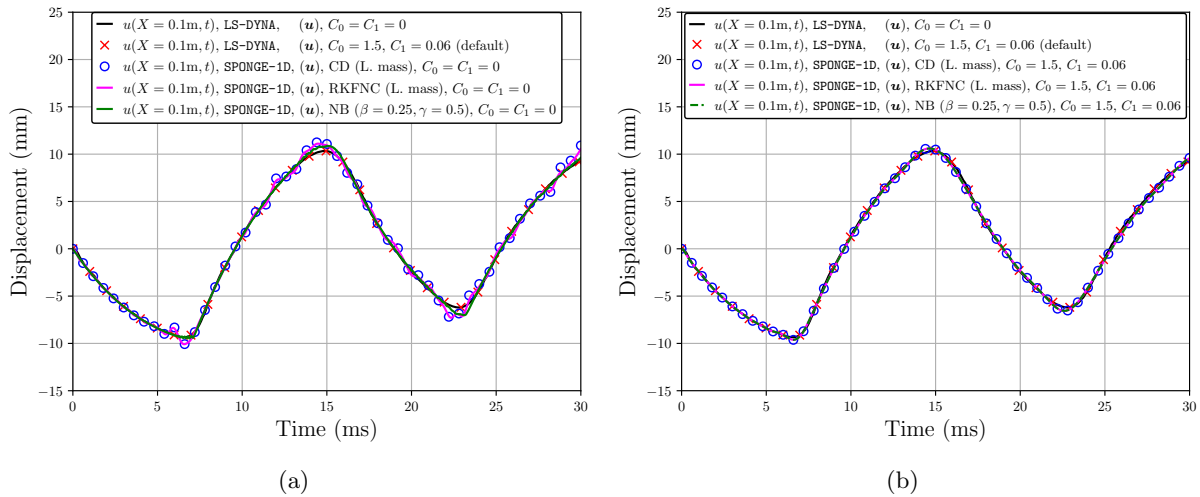


Figure 5.21: Comparison of elastodynamical response to Friedlander impulse loading for peak overpressure of 25kPa with element size $h_0^e = 1$ cm for (a) simulations without shock viscosity enabled (b) shock viscosity set to default values.

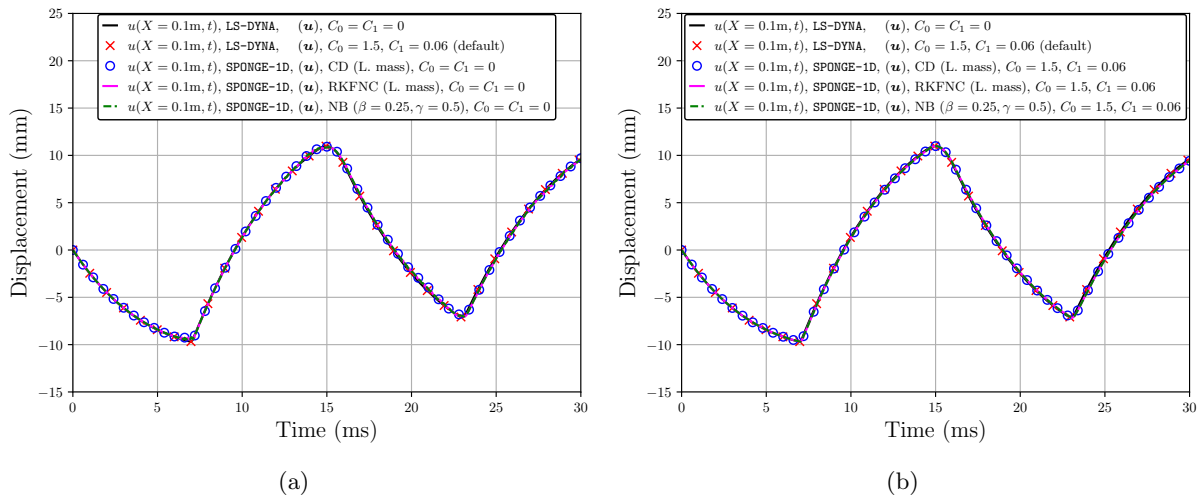


Figure 5.22: Comparison of elastodynamical response to Friedlander impulse loading for peak overpressure of 25kPa with element size $h_0^e = 0.1$ cm for (a) simulations without shock viscosity enabled (b) shock viscosity set to default values.

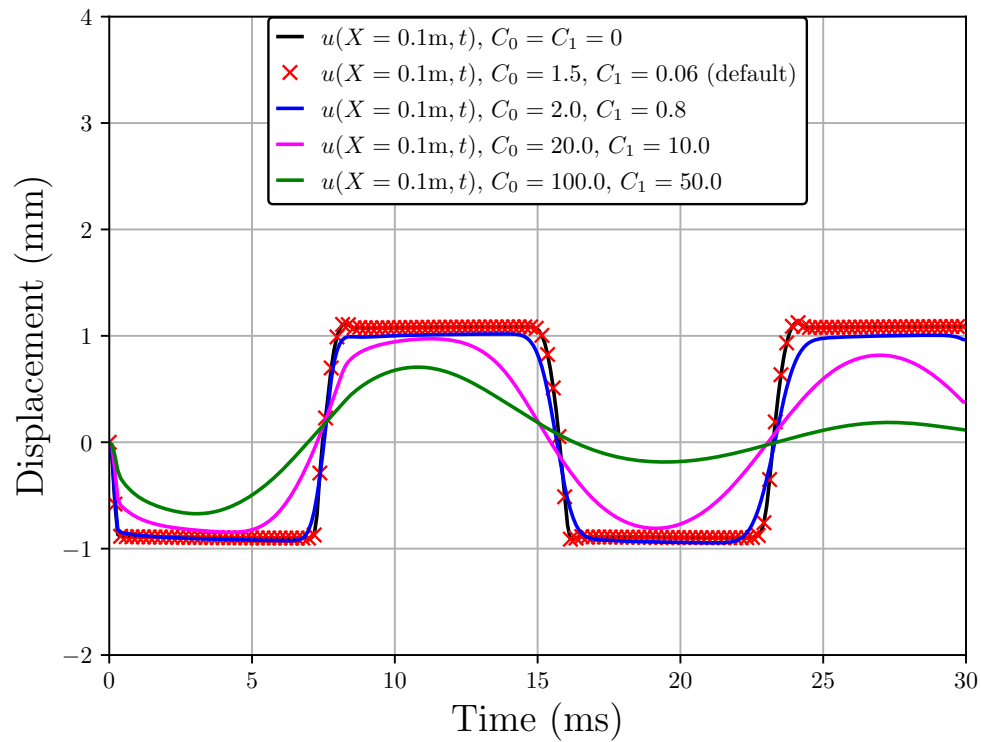


Figure 5.23: The effect of changing the shock viscosity coefficients C_0 and C_1 for the Yen impulse at peak overpressure of 50 kPa; here, all simulations were conducted using a neo-Hookean hyperelastic material (UMAT 45) in LS-DYNA with $h_0^c = 0.1$ cm.

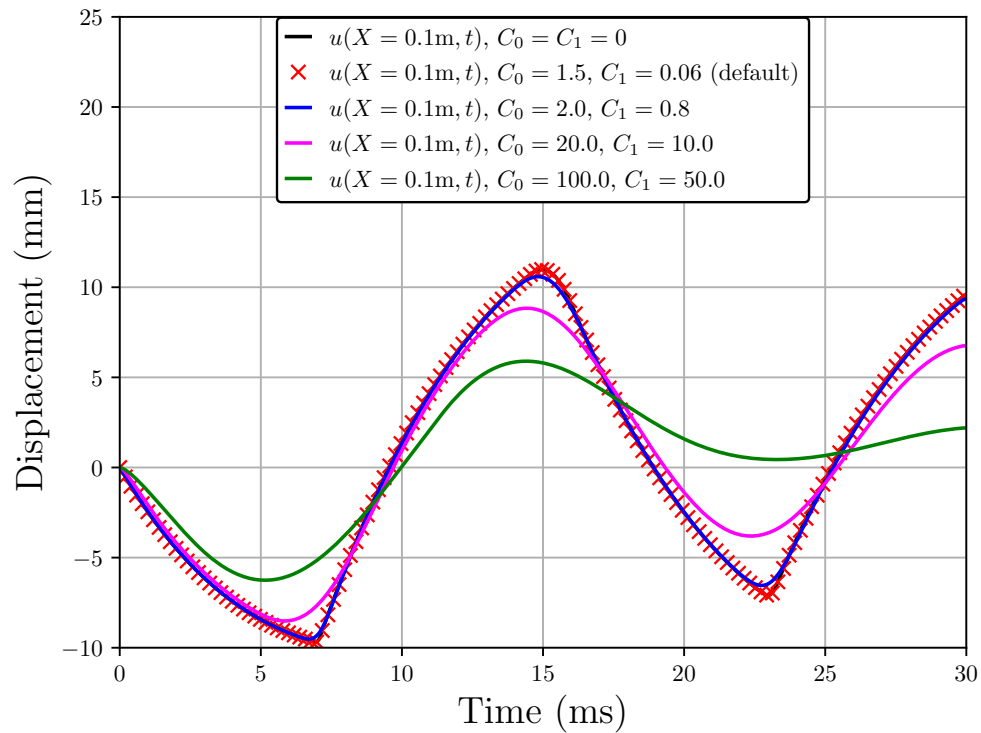


Figure 5.24: The effect of changing the shock viscosity coefficients C_0 and C_1 for the Friedlander impulse at peak overpressure of 25 kPa; here, all simulations were conducted using a neo-Hookean hyperelastic material (UMAT 45) in LS-DYNA with $h_0^e = 0.1$ cm

5.3.2 Effects of pore fluid pressure stabilization

As with our study of the shock viscosity and how varying the constants C_0 and C_1 can affect the solution, we shall do the same here for pressure stabilization by modifying the stabilizing parameter α^{stab} . In the following investigation, we use the $(\mathbf{u}-p_f)$ formulation and a Q1-P1 element with $h_0^e = 1$ cm. In contrast to the poroelastic and poroelastodynamic verification problems, here we set an impermeable boundary condition at the surface of the column of lung parenchyma: pore air is not allowed to escape the column at any position. Material parameters are listed in Table 5.10. Geometrical and loading parameters are given in Table 5.11.

As in previous examples, we apply a pressure load in the form of a traction at the top of the column. However, for the multiphase model, the applied overpressure is relative to 1 atm, as opposed to 0 atm for the single-phase model in Section 5.3.1.1. The two pressure profiles we explore are the Yen impulse and Friedlander impulse, as depicted by Figure 5.25(a) and Figure 5.25(b), respectively. For both pressure profiles, we choose a peak overpressure of 15 kPa.

Table 5.10: Material parameters for multiphase lung parenchyma simulations. Values taken from Clayton et al. [2021], Lande and Mitzner [2006].

K^{skel} (kPa)	G (kPa)	K_s (kPa)	K_f^η (kPa)	ρ_0^{sR} (kg/m ³)	ρ_0^{fR} (kg/m ³)	n_0^f	\hat{k}_0 (m ² /Pa-s)
7.5	3	2.2×10^6	140	1000	1.138	0.664	10^{-5}

Table 5.11: Geometrical and loading parameters for pressure stabilization study.

Overpressure load type	H (cm)	A (cm ²)	h_0^e (cm)	t_0^σ (kPa)	t_0 (ms)	t_1 (ms)
Yen impulse	10	1	0.1	15	0.17	0.34
Friedlander impulse	10	1	0.1	15	10	N/A

It is apparent from Figure 5.26 and Figure 5.27 that as we increase the value of α^{stab} , we introduce numerical error into the solution. We can see that this also results in oscillations in both the pore fluid and solid lung parenchyma pressure: refer to Figure 5.28 and Figure 5.29. Therefore, when enabling pressure stabilization, we choose a value of α^{stab} as close to 0 as possible, typically 10^{-10} m³s²/kg as this shows good overlap with the unstabilized formulation.

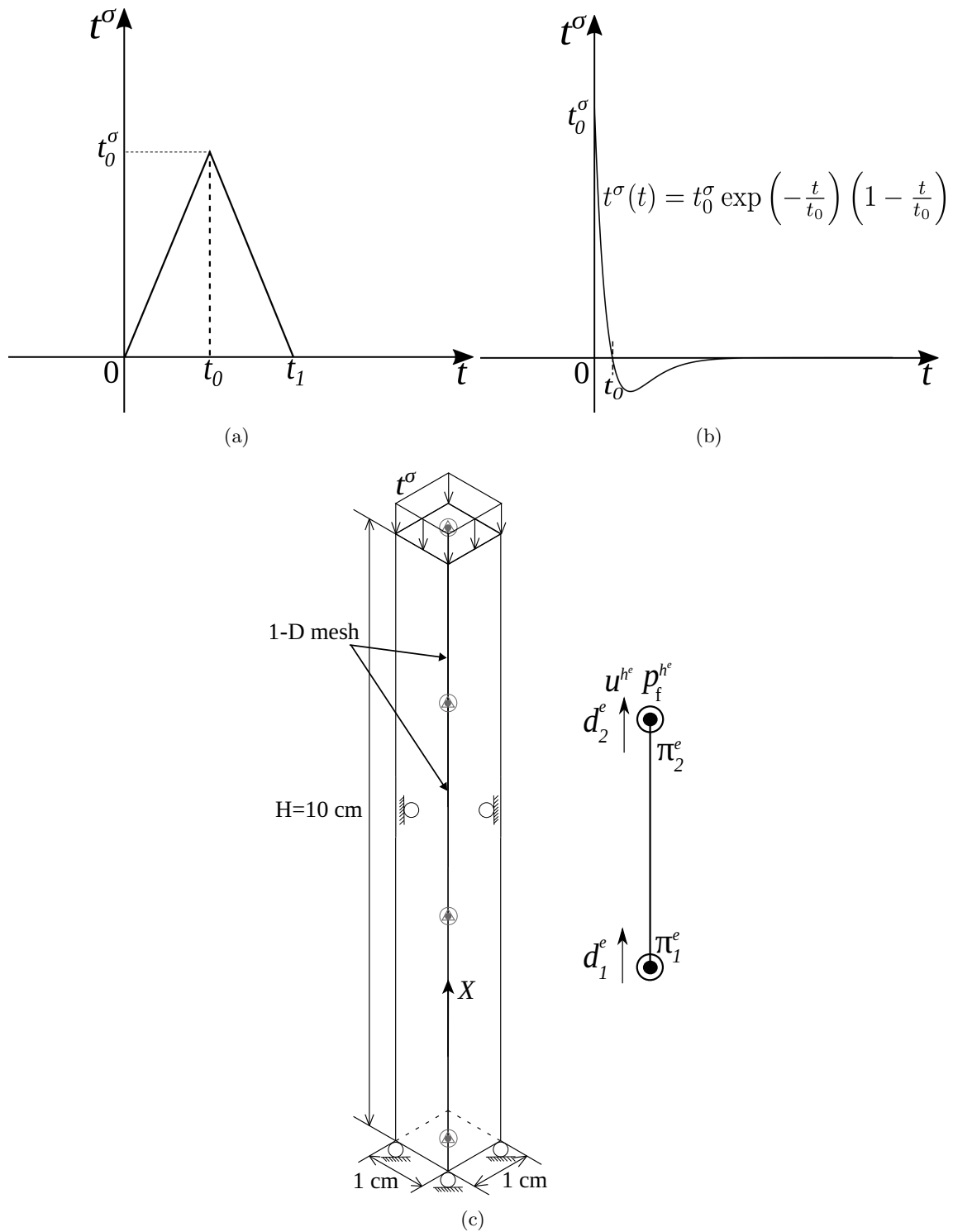


Figure 5.25: (a) Yen impulse traction application (b) Friedlander impulse traction application (c) schematic of multiphase column mesh for examples of lung parenchyma deformations, highlighting the Q1-P1 element type.

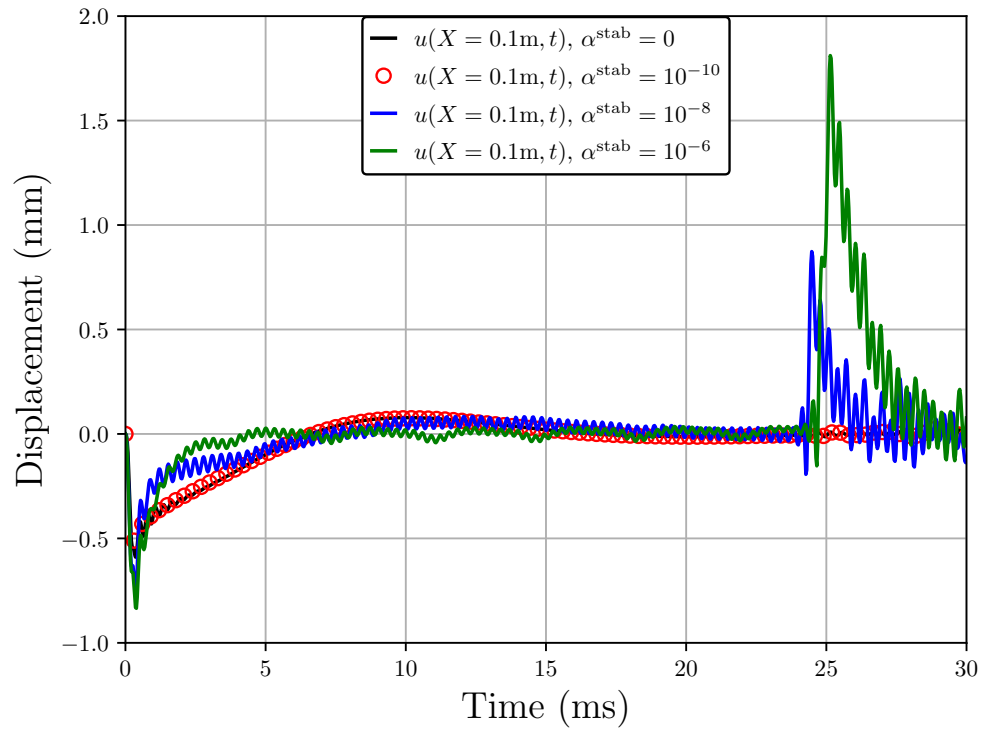


Figure 5.26: Comparison of lung parenchyma displacements undergoing overpressure loading from the Yen impulse at 15 kPa, using RKFNC numerical time integration with consistent mass matrices, tracking the nodes at the top of the column for varying values of α^{stab} . Here, we invoke a Q1-P1 element with $h_0^e = 1$ cm.

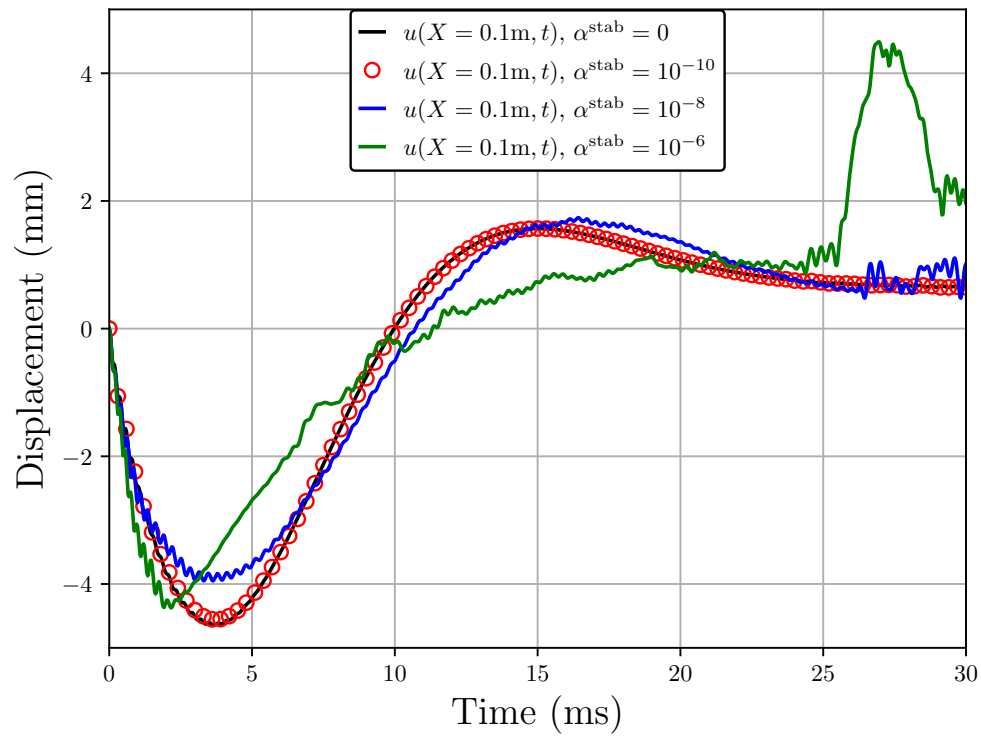


Figure 5.27: Comparison of lung parenchyma displacements undergoing overpressure loading from the Friedlander impulse at 15 kPa, using RKFNC numerical time integration with consistent mass matrices, tracking the nodes at the top of the column for varying values of α^{stab} . Here, we invoke a Q1-P1 element with $h_0^e = 1$ cm.

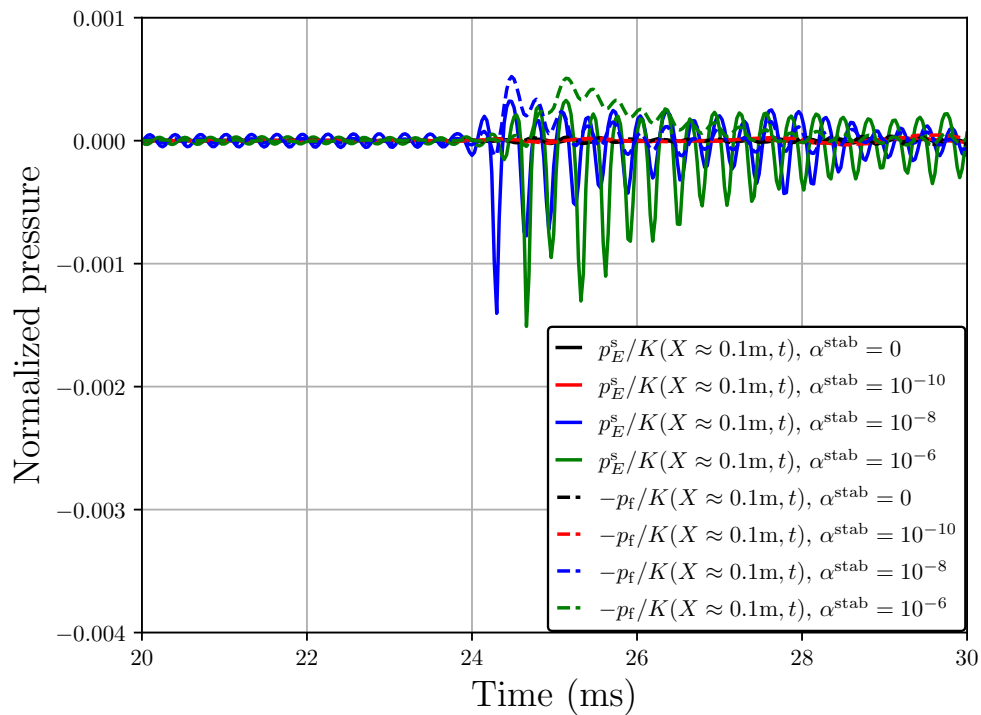


Figure 5.28: Comparison of lung parenchyma pressure p_E^s and pore fluid pressure p_f after over-pressure loading from the Yen impulse at 15 kPa, using RKFNC numerical time integration with consistent mass matrices, tracking the Gauss point closest to $X = H$ for varying values of α^{stab} . Here, we invoke a Q1-P1 element with $h_0^e = 1$ cm, and $K = 7.5$ kPa is the bulk modulus of the solid skeleton.

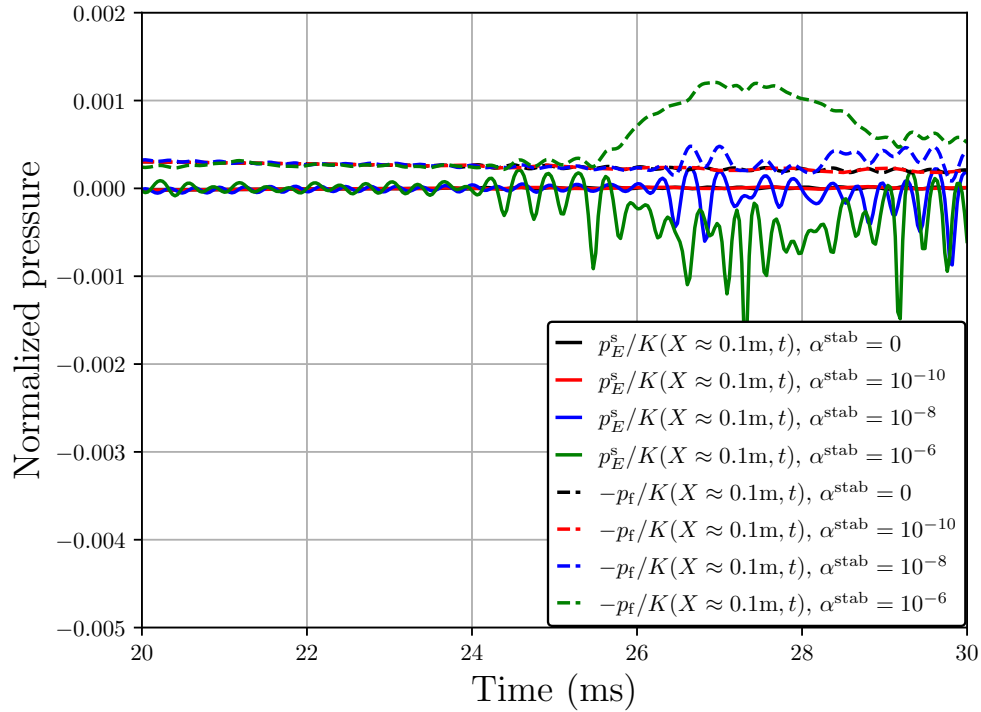


Figure 5.29: Comparison of lung parenchyma pressure p_E^s and pore fluid pressure p_f after overpressure loading from the Friedlander impulse at 15 kPa, using RKFNC numerical time integration with consistent mass matrices, tracking the Gauss points closest to $X = H$ for varying values of α^{stab} . Here, we invoke a Q1-P1 element with $h_0^c = 1$ cm, and $K = 7.5$ kPa is the bulk modulus of the solid skeleton.

5.3.3 Shock loading of lung parenchyma

5.3.3.1 Locally homogeneous temperature model

In the following sections we present our findings for a column of lung parenchyma subjected to external traction loading durations on the order of milliseconds or less. In all of the simulations, the column is fixed on its sides and base. Furthermore, when making comparisons to the single-phase model developed by Clayton and Freed [2019a], the sides and top are assumed to be impermeable (i.e., “undrained”) such that the pore fluid (air) is confined solely within the column. For the duration of this subsection (Section 5.3.3.1), we assume either the standard neo-Hookean model, or the Ehlers and Eipper [1999] neo-Hookean model, for the solid skeleton, devoid of thermomechanical coupling (refer to Equations (3.113) & (3.115) with $\alpha_V^s \rightarrow 0$). For the pore fluid, we assume a barotropic model, i.e., the exponential model assumed in the previous sections for poroelasticity and poroelastodynamics examples (refer to Equations (3.137) & (3.138); more details on these constitutive choices are discussed in subsequent sections).

This section is outlined as follows. In paragraph *Taylor-Hood mixed elements and shock loading* we discuss the shortcomings of the common Taylor-Hood element when applying shock loading. In paragraph *Necessary constitutive adjustments for higher strain* we discuss the inadequacy of the standard neo-Hookean model combined with the Kozeny-Carman model for high strains. In paragraph *Remarks on the impermeable boundary condition* we demonstrate findings regarding a no-flux (i.e., “impermeable”, “undrained”, “no-slip”) boundary condition applied to the pore fluid. In paragraph *A sensitivity study for \varkappa* we demonstrate findings from a sensitivity study on the intrinsic permeability; in paragraph *A sensitivity study for κ* we demonstrate findings from a sensitivity study on the hyperbolic hydraulic conductivity model. For paragraph *Investigation of the pore fluid viscous stress tensor*, we explore the impact of accounting for the pore fluid extra stress (viscous stress) as compared to the standard, nearly-inviscid pore fluid stress. Lastly, paragraph *Comparison between single-phase and multiphase models for shock loading* concludes with the comparison between single-phase and multiphase models for shock loading of lung parenchyma.

additional stabilization via shock viscosity or pressure stabilization is not necessary to obtain a stable solution. The standard neo-Hookean model (Equation (3.106)) is used for the solid skeleton response, the barotropic exponential model (Equation (3.137)) is used for the pore fluid response, and the Kozeny-Carman model (Equation (3.63)) is used for the functional form of the porosity-dependent hydraulic conductivity.

Figure 5.31 shows the displacement history of the top of the porous column over time after being subjected to the Yen impulse at 15 kPa overpressure. For the single-phase model (Clayton & Freed), the solution behaves elastodynamically, with little to no dissipation of the shock wave. For the multiphase model, we can directly observe the effect that the pore air has on the solid skeleton displacement, i.e., an “absorption” of the shock wave and eventual dissipation of that energy. Similar behavior is observed in the results for the Friedlander impulse, Figure 5.32.

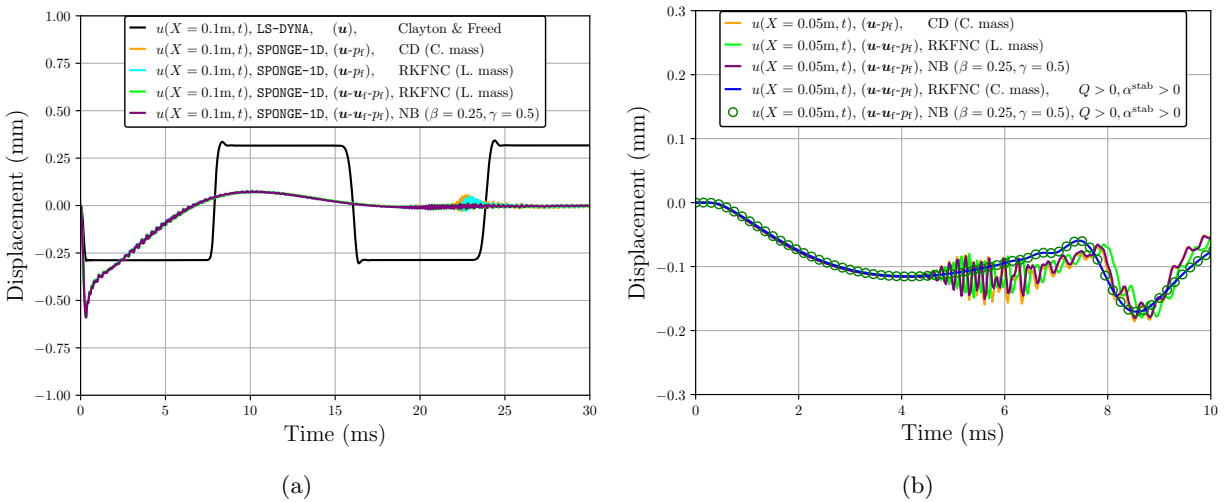


Figure 5.31: Comparison of solid skeleton displacements undergoing overpressure loading from the Yen impulse at 15 kPa between (a) the single-phase (Clayton & Freed) and multiphase models tracking the nodes at the top of the column, and (b) the multiphase models from SPONGE-1D tracking the nodes at the middle of the column with and without stabilization methods. Without shock viscosity Q and pressure stabilization α^{stab} , we invoke a Q2-P1 or Q2-Q2-P1 element; with shock viscosity Q (where $C_0 = 1.5, C_1 = 0.06$) and pressure stabilization (where $\alpha^{\text{stab}} = 10^{-10}$), we invoke a Q1-Q1-P1 element.

Notice that for the Taylor-Hood elements without any stabilization, numerical oscillations are present in the displacement solution, irrespective of the integration scheme. When shock vis-

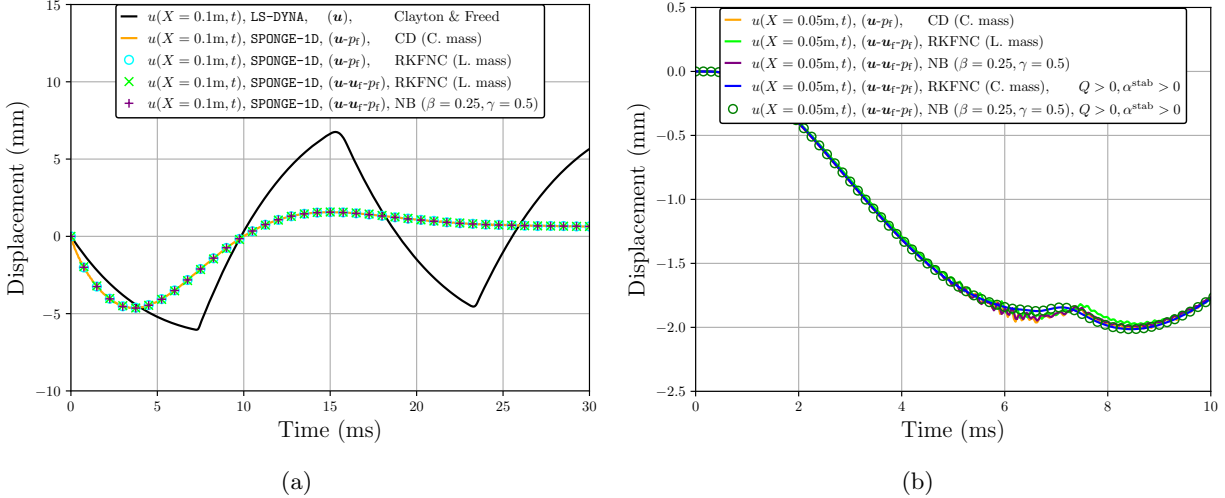


Figure 5.32: Comparison of solid skeleton displacements undergoing overpressure loading from the Friedlander impulse at 15 kPa between (a) the single-phase (Clayton & Freed) and multiphase models tracking the nodes at the top of the column, and (b) the multiphase models from SPONGE-1D tracking the nodes at the middle of the column with and without stabilization methods. Without shock viscosity Q and pressure stabilization α^{stab} , we invoke a Q2-P1 or Q2-Q2-P1 element; with shock viscosity Q (where $C_0 = 1.5, C_1 = 0.06$) and pressure stabilization (where $\alpha^{\text{stab}} = 10^{-10}$), we invoke a Q1-Q1-P1 element.

cosity and pressure stabilization are introduced, with a Q1-Q1-P1 element, as in Figure 5.31(b) and Figure 5.32(b), displacement solutions are smoother than their Taylor-Hood counterparts. Furthermore, we have found that *without* the shock viscosity and pressure stabilization techniques, we are unable to achieve greater magnitudes of peak overpressure loadings without one of the following numerical problems occurring: unstable pore fluid pressure (i.e., pore air pressure $\rightarrow \infty$), element e collapse ($J^e < 0$) or, for the implicit schemes, an inability to achieve convergence in the Newton-Raphson iterative solver; and for the adaptive time-stepping explicit schemes, e.g., Runge-Kutta Cash-Karp, the time-step goes to zero. Therefore, we choose to enable both stabilization techniques in our simulations of shock-like loadings of the lung parenchyma.³

³ In the absence of experimental data, or a known analytical solution to calibrate (or validate) or verify, respectively, the results for the high strain-rate examples, it cannot be said with absolute certainty whether or not the shock viscosity results are real or artificial. Future work must calibrate the present model to experimental data; see remarks in Chapter 6.

Necessary constitutive adjustments for higher strain. However, there is an overpressure limit even for the linear elements with shock viscosity and pressure stabilization enabled. Recall from the discussions in Section 3.1.4 and Section 3.3.1, paragraph *The neo-Hookean hyperelastic model*, that the Kozeny-Carman functional form of the hydraulic conductivity and the standard neo-Hookean model, respectively, are ill-suited for the finite-strain regime for an incompressible solid phase which bounds $n_0^s \leq J < \infty$.

At higher overpressures, it is possible, in the numerical sense, to have $J < n_0^s$, as demonstrated explicitly in Figure 5.33(b) & Figure 5.34(b) and implicitly (by way of simulation failure as $J \rightarrow n_0^s$) in Figure 5.33(a) & Figure 5.34(a). When this occurs, the deformation-dependent hydraulic conductivity goes unstable (e.g., the relative value of \hat{k} to \hat{k}_0 becomes negative; refer to Figure 3.1(a) for a qualitative example and Figure 5.33(b) or Figure 5.34(b) for a numerical example).

Such an instability does not necessarily arise with a combination of hyperbolic functional form of the hydraulic conductivity and the standard neo-Hookean model. However, for consistency's sake, it is better to use a free energy model for the solid skeleton that adheres to the same restrictions of skeleton deformation as the hydraulic conductivity model. As such, all subsequent multiphase results provided by SPONGE-1D in this work will use the additional penalty-like term proposed by Ehlers and Eipper [1999] (Equation (3.109)) for the neo-Hookean constitutive model and the hyperbolic form of the hydraulic conductivity proposed by Markert [2005] (Equation (3.68)).

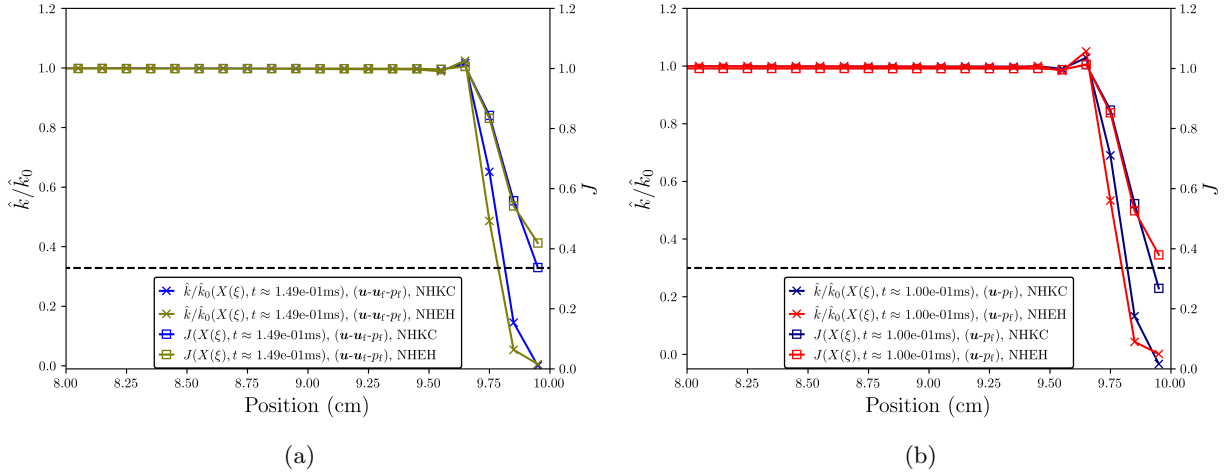


Figure 5.33: A demonstration of the instability of the neo-Hookean/Kozeny-Carman (NHKC) model versus the neo-Hookean-Eipper/hyperbolic (NHEH) model for (a) $(\mathbf{u}-\mathbf{u}_f-p_f)$ in response to Friedlander impulse loading at 50 kPa overpressure, and (b) $(\mathbf{u}-p_f)$ in response to Friedlander impulse loading at 100 kPa overpressure, both simulated using linear elements, with pressure and shock stabilization, for lung parenchyma with material parameters repeated from Table 5.10. The dashed black line is the initial solid volume fraction, n_0^s , relative to the secondary y -ordinate. In (a), the NHKC model J approaches its lower limit, n_0^s , and the NHKC model relative hydraulic conductivity approaches zero before simulation termination. In (b), the NHKC model values of J and relative hydraulic conductivity are non-physical well before simulation termination, demonstrating the issue with relying on results from the NHKC model combination at higher strain. In both (a) and (b), values for the NHEH model remain physical ($J > n_0^s$ and $\hat{k}/\hat{k}_0 > 0$), demonstrating its robustness at adhering to the incompressibility constraint on the solid phase. A value of $\kappa = 2.5$ was chosen for the NHEH simulations.

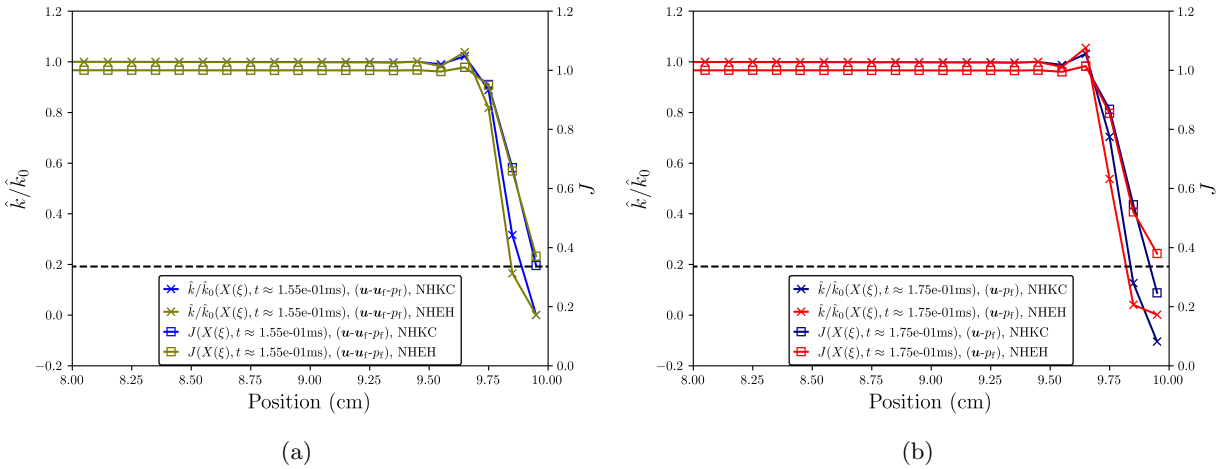


Figure 5.34: A demonstration of the instability of the neo-Hookean/Kozeny-Carman (NHKC) model versus the neo-Hookean-Eipper/hyperbolic (NHEH) model for (a) $(\mathbf{u}-\mathbf{u}_f-p_f)$ and (b) $(\mathbf{u}-p_f)$, both in response to Yen impulse loading at 100 kPa overpressure and simulated using linear elements, with pressure and shock stabilization, for lung parenchyma with material parameters repeated from Table 5.10. The dashed black line is the initial solid volume fraction, n_0^s , relative to the secondary y -ordinate. In (a), the NHKC model J approaches its lower limit, n_0^s , and the NHKC model relative hydraulic conductivity approaches zero before simulation termination. In (b), the NHKC model values of J and relative hydraulic conductivity are non-physical well before simulation termination, demonstrating the issue with relying on results from the NHKC model combination at higher strain. In both (a) and (b), values for the NHEH model remain physical ($J > n_0^s$ and $\hat{k}/\hat{k}_0 > 0$), demonstrating its robustness at adhering to the incompressibility constraint on the solid phase. A value of $\kappa = 2.5$ was chosen for the NHEH simulations.

Remarks on the impermeable boundary condition. While the no-flux Neumann boundary condition (Equations (4.43)₇, (4.44)₇, (4.69)₁₄, etc.) is mathematically sufficient to constrain the relative motion between solid and fluid at said boundary, the enforcement is only imposed weakly. As a consequence, the relative velocity between solid and fluid *approaches* zero as $h_0^\epsilon \rightarrow 0$, but is not guaranteed to be *exactly* zero. Two potential remedies to alleviate this issue have been explored as part of this work.

The first is an *ad-hoc* method, used in Irwin et al. [2023c,d, 2024], whereby the pore fluid degrees of freedom at the boundary (i.e., the topmost node in the 1-D mesh) are set equal to the solid skeleton degrees of freedom as a kind of “strong” enforcement of the no-flux boundary condition. This guarantees $u_f \leftarrow u, v_f \leftarrow v, a_f \leftarrow a$ at those degrees of freedom. Refer to Figure 5.35 for an example.

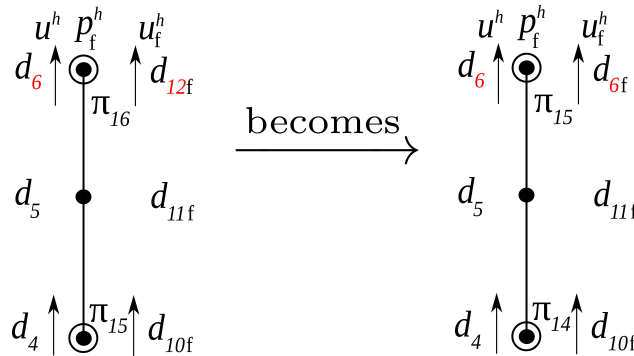


Figure 5.35: An example of the *ad-hoc* “strong” enforcement of the no-flux boundary condition applied to a 5-element Q2-Q2-P1 mesh. The leftmost element represents the “unperturbed” global DOFs where the pore fluid displacement global DOF, d_{12f} , is free, as it would be for a “weak” enforcement of the no-flux boundary condition alone. The rightmost element represents the assignment of the pore fluid displacement global DOF at the boundary to take on the value of the solid skeleton displacement global DOF at the boundary.

The other method was pursued first by Vuong [2016], Vuong et al. [2016] whereby a Lagrange multiplier method is constructed to weakly enforce no-flux or no-slip conditions.⁴ In essence, the Lagrange multiplier takes on the role of a *pseudo-traction* from the solid skeleton acting on the

⁴ For 3-D problems with viscous pore fluid flow, i.e., with $\sigma_E^f \neq 0$, a no-slip condition is preferred, i.e., $(\mathbf{v}_f - \mathbf{v}) = \mathbf{0}$ along the boundary, rather than the no-flux condition $n^f(\mathbf{v}_f - \mathbf{v}) \cdot \mathbf{n} = 0$, the latter of which restricts fluid flowing through open pores at the boundary but imposes no restriction on fluid-solid interfaces which is necessary when computing the macroscale viscous forces of the pore fluid.

pore fluid. While our attempt at implementation of this method in SPONGE-1D did not yield the desired effects, it is presented here in brief for the interested reader.

Begin by weakening the pressure gradient term in the pore fluid momentum balance, such that

$$\rho_0^f \mathbf{a}_f + J n^f \text{GRAD}(p_f) \cdot \mathbf{F}^{-1} + J \frac{(n^f)^2}{\hat{k}} (\mathbf{v}_f - \mathbf{v}) - \rho_0^f \mathbf{g} = \mathbf{0} \quad (5.51)$$

may be re-written as

$$\rho_0^f \mathbf{a}_f + J \text{GRAD}(p^f) \cdot \mathbf{F}^{-1} - J p_f \text{GRAD}(n^f) \cdot \mathbf{F}^{-T} + J \frac{(n^f)^2}{\hat{k}} (\mathbf{v}_f - \mathbf{v}) - \rho_0^f \mathbf{g} = \mathbf{0}. \quad (5.52)$$

Then, the variational form is written as follows:

$$\begin{aligned} \mathcal{I}(u_i, u_{i(f)}, p_f, w_i^{u_f}) &= \int_{\mathcal{B}_0} w_i^{u_f} \rho_0^f a_{i(f)} dV - \int_{\mathcal{B}_0} \frac{\partial w_i^{u_f}}{\partial X_I} J p^f F_{Ii}^{-1} dV \\ &\quad - \int_{\mathcal{B}_0} w_i^{u_f} \rho_0^f g_i dV + \int_{\mathcal{B}_0} w_i^{u_f} J \frac{(n^f)^2}{\hat{k}} (v_{i(f)} - v_i) dV \\ &\quad - \int_{\mathcal{B}_0} w_i^{u_f} J p_f \frac{\partial n^f}{\partial X_I} F_{Ii}^{-1} dV + \int_{\Gamma_0^{t_f}} w_i^{u_f} J p^f F_{Ii}^{-1} N_I dA = 0. \end{aligned} \quad (5.53)$$

Identifying the pore fluid traction as

$$\mathbf{t}^{\sigma^f} = J p^f \mathbf{F}^{-T} \cdot \mathbf{N}, \quad (5.54)$$

we may then postulate a strong formulation for the balance of linear momentum for the pore fluid

that includes the Neumann boundary condition as follows:

$$(\mathcal{S}) = \left\{ \begin{array}{l} \text{Find } \mathbf{u}_f(\mathbf{X}, t) \in \mathcal{S}^{u_f} \text{ with } t \in [0, T], \text{ such that:} \\ \rho_0^f \mathbf{a}_f + J \text{GRAD}(p^f) \cdot \mathbf{F}^{-1} - J p_f \text{GRAD}(n^f) \cdot \mathbf{F}^{-T} \\ \quad + J \frac{(n^f)^2}{\hat{k}} (\mathbf{v}_f - \mathbf{v}) - \rho_0^f \mathbf{g} = \mathbf{0} \in \mathcal{B}_0, \\ \mathbf{u}_f(\mathbf{X}, t) = \mathbf{g}_{u_f}(\mathbf{X}, t) \text{ on } \Gamma_0^{u_f}, \\ \mathbf{P}^f(\mathbf{X}, t) \cdot \mathbf{N}(\mathbf{X}) = \mathbf{t}^{\sigma^f}(\mathbf{X}, t) \text{ on } \Gamma_0^{t^f} \\ \mathbf{u}_f(\mathbf{X}, t = 0) = \mathbf{u}_{f,0}(\mathbf{X}) \in \mathcal{B}_0, \\ \mathbf{v}_f(\mathbf{X}, t = 0) = \mathbf{v}_{f,0}(\mathbf{X}) \in \mathcal{B}_0, \\ \mathbf{a}_f(\mathbf{X}, t = 0) = \mathbf{a}_{f,0}(\mathbf{X}) \in \mathcal{B}_0. \end{array} \right. \quad (5.55)$$

Note that this manipulation of the pore fluid linear momentum balance now introduces the porosity gradient, requiring resolution with C^1 -continuous finite elements for solid skeleton displacement (e.g., the Hermite cubic element).

The Lagrange multiplier method is chosen to weakly enforce the no-flux condition, such that

$$\begin{aligned} \int_{\Gamma_0^{t^f}} w_i^{u_f} t_i^{\sigma^f} dA &= \int_{\Gamma_0^{t^f}} w_i^{u_f} \lambda_{i(c)} dA, \quad \int_{\Gamma_0^I} w^{\lambda_\perp} J n^f (v_{i(f)} - v_i) F_{Ii}^{-1} N_I dA = 0, \\ \int_{\Gamma_0^I} w_i^{\lambda_\parallel} J \lambda_{i(c)} F_{Ii}^{-1} T_I dA &= 0, \end{aligned} \quad (5.56)$$

where $\Gamma_0^{t^f} \cup \Gamma_0^{Q^f} \in \Gamma_0^I$. Equation (5.56)₁ is an identification of the Lagrange multiplier as the “pseudo-traction” acting on the pore fluid (e.g., the force from the impermeable solid skeleton “membrane”). Equations (5.56)_{2,3} ensure the weak constraint of the no-flux condition normal to the surface, and that the Lagrange multiplier vanishes tangential to the surface, respectively.

The FE formulation for the $(\mathbf{u}-\mathbf{u}_f-p_f)$ formulation without the Lagrange multiplier is written

in block-matrix form as⁵

$$\underbrace{\begin{bmatrix} \mathbf{K}_{u,u} & \mathbf{K}_{u,u_f} & \mathbf{K}_{u,p_f} \\ \mathbf{K}_{u_f,u} & \mathbf{K}_{u_f,u_f} & \mathbf{K}_{u_f,p_f} \\ \mathbf{K}_{p_f,u} & \mathbf{K}_{p_f,u_f} & \mathbf{K}_{p_f,p_f} \end{bmatrix}}_{(n_{\text{dof}}^s+n_{\text{dof}}^f+n_{\text{dof}}^{p_f}) \times (n_{\text{dof}}^s+n_{\text{dof}}^f+n_{\text{dof}}^{p_f})} \cdot \underbrace{\begin{Bmatrix} \delta \ddot{\mathbf{d}} \\ \delta \ddot{\mathbf{d}}_f \\ \delta \ddot{\boldsymbol{\pi}} \end{Bmatrix}}_{(n_{\text{dof}}^s+n_{\text{dof}}^f+n_{\text{dof}}^{p_f}) \times 1} = \underbrace{\begin{Bmatrix} -\mathbf{R}_u \\ -\mathbf{R}_{u_f} \\ -\mathbf{R}_{p_f} \end{Bmatrix}}_{(n_{\text{dof}}^s+n_{\text{dof}}^f+n_{\text{dof}}^{p_f}) \times 1}. \quad (5.57)$$

Introduction of the Lagrange multiplier as a separate DOF yields

$$\underbrace{\begin{bmatrix} \mathbf{K}_{u,u} & \mathbf{K}_{u,u_f} & \mathbf{K}_{u,p_f} & \mathbf{K}_{u,\lambda_c} \\ \mathbf{K}_{u_f,u} & \mathbf{K}_{u_f,u_f} & \mathbf{K}_{u_f,p_f} & \mathbf{K}_{u_f,\lambda_c} \\ \mathbf{K}_{p_f,u} & \mathbf{K}_{p_f,u_f} & \mathbf{K}_{p_f,p_f} & \mathbf{K}_{p_f,\lambda_c} \\ \mathbf{K}_{\lambda_c,u} & \mathbf{K}_{\lambda_c,u_f} & \mathbf{K}_{\lambda_c,p_f} & \mathbf{K}_{\lambda_c,\lambda_c} \end{bmatrix}}_{(n_{\text{dof}}^s+n_{\text{dof}}^f+n_{\text{dof}}^{p_f}+n_{\text{dof}}^{\lambda_c}) \times (n_{\text{dof}}^s+n_{\text{dof}}^f+n_{\text{dof}}^{p_f}+n_{\text{dof}}^{\lambda_c})} \cdot \underbrace{\begin{Bmatrix} \delta \ddot{\mathbf{d}} \\ \delta \ddot{\mathbf{d}}_f \\ \delta \ddot{\boldsymbol{\pi}} \\ \delta \ddot{\Lambda} \end{Bmatrix}}_{(n_{\text{dof}}^s+n_{\text{dof}}^f+n_{\text{dof}}^{p_f}+n_{\text{dof}}^{\lambda_c}) \times 1} = \underbrace{\begin{Bmatrix} -\mathbf{R}_u \\ -\mathbf{R}_{u_f} - \mathbf{R}_{u_f}^c \\ -\mathbf{R}_{p_f} \\ -\mathbf{R}_{\lambda_c} \end{Bmatrix}}_{(n_{\text{dof}}^s+n_{\text{dof}}^f+n_{\text{dof}}^{p_f}+n_{\text{dof}}^{\lambda_c}) \times 1}, \quad (5.58)$$

where $\mathbf{R}_{u_f}^c$ is the finite element form of the pseudo-traction Neumann boundary condition, i.e., the contribution of the Lagrange multiplier to the pore fluid linear momentum balance given by Equation (5.56)₁.

Since the Lagrange multiplier appears only as a boundary condition in the pore fluid momentum balance via Equation (5.56)₁, and, by definition, as an enforcement of the no-flux boundary condition (dependent only upon the motion of the solid and fluid) via Equations (5.56)_{2,3}, the tangents

$$\mathbf{K}_{u,\lambda_c} = \mathbf{K}_{p_f,\lambda_c} = \mathbf{K}_{\lambda_c,p_f} = \mathbf{0}, \quad (5.59)$$

such that the block system may be written as

$$\underbrace{\begin{bmatrix} \mathbf{K}_{u,u} & \mathbf{K}_{u,u_f} & \mathbf{K}_{u,p_f} & \mathbf{0} \\ \mathbf{K}_{u_f,u} & \mathbf{K}_{u_f,u_f} & \mathbf{K}_{u_f,p_f} & \mathbf{K}_{u_f,\lambda_c} \\ \mathbf{K}_{p_f,u} & \mathbf{K}_{p_f,u_f} & \mathbf{K}_{p_f,p_f} & \mathbf{0} \\ \mathbf{K}_{\lambda_c,u} & \mathbf{K}_{\lambda_c,u_f} & \mathbf{0} & \mathbf{K}_{\lambda_c,\lambda_c} \end{bmatrix}}_{(n_{\text{dof}}^s+n_{\text{dof}}^f+n_{\text{dof}}^{p_f}+n_{\text{dof}}^{\lambda_c}) \times (n_{\text{dof}}^s+n_{\text{dof}}^f+n_{\text{dof}}^{p_f}+n_{\text{dof}}^{\lambda_c})} \cdot \underbrace{\begin{Bmatrix} \delta \ddot{\mathbf{d}} \\ \delta \ddot{\mathbf{d}}_f \\ \delta \ddot{\boldsymbol{\pi}} \\ \delta \ddot{\Lambda} \end{Bmatrix}}_{(n_{\text{dof}}^s+n_{\text{dof}}^f+n_{\text{dof}}^{p_f}+n_{\text{dof}}^{\lambda_c}) \times 1} = \underbrace{\begin{Bmatrix} -\mathbf{R}_u \\ -\mathbf{R}_{u_f} - \mathbf{R}_{u_f}^c \\ -\mathbf{R}_{p_f} \\ -\mathbf{R}_{\lambda_c} \end{Bmatrix}}_{(n_{\text{dof}}^s+n_{\text{dof}}^f+n_{\text{dof}}^{p_f}+n_{\text{dof}}^{\lambda_c}) \times 1}. \quad (5.60)$$

⁵ The Lagrange multiplier method necessitates an implicit time integration formulation; a penalty method appropriate for explicit time integration was not pursued in this work.

For 1-D uniaxial strain, unidirectional pore fluid flow with a fixed column base, the following must hold:

$$\begin{aligned}
n_{\text{dof}}^{\lambda_c} &= 1 \text{ (i.e., the no-flux BC is enforced at one DOF/boundary),} \\
\mathbf{K}_{\lambda_c, \lambda_c} &= \mathbf{0}, \\
\mathbf{R}_{\lambda_c} &= \int_{\Gamma_0^I} w^\lambda n^f (v_f - v) dA, \\
\mathbf{R}_{u_f}^c &= \int_{\Gamma_0^{f_f}} w^{u_f} \lambda_c dA.
\end{aligned} \tag{5.61}$$

The block system may thus be written as

$$\underbrace{\begin{bmatrix} \mathbf{K}_{u,u} & \mathbf{K}_{u,u_f} & \mathbf{K}_{u,p_f} & \mathbf{0} \\ \mathbf{K}_{u_f,u} & \mathbf{K}_{u_f,u_f} & \mathbf{K}_{u_f,p_f} & \mathbf{K}_{u_f,\lambda_c} \\ \mathbf{K}_{p_f,u} & \mathbf{K}_{p_f,u_f} & \mathbf{K}_{p_f,p_f} & \mathbf{0} \\ \mathbf{K}_{\lambda_c,u} & \mathbf{K}_{\lambda_c,u_f} & \mathbf{0} & \mathbf{0} \end{bmatrix}}_{(n_{\text{dof}}^s + n_{\text{dof}}^f + n_{\text{dof}}^{p_f} + 1) \times (n_{\text{dof}}^s + n_{\text{dof}}^f + n_{\text{dof}}^{p_f} + 1)} \cdot \underbrace{\begin{pmatrix} \delta \ddot{\mathbf{d}} \\ \delta \ddot{\mathbf{d}}_f \\ \delta \ddot{\boldsymbol{\pi}} \\ \delta \ddot{\boldsymbol{\Lambda}} \end{pmatrix}}_{(n_{\text{dof}}^s + n_{\text{dof}}^f + n_{\text{dof}}^{p_f} + 1) \times 1} = \underbrace{\begin{pmatrix} -\mathbf{R}_u \\ -\mathbf{R}_{u_f} - \mathbf{R}_{u_f}^c \\ -\mathbf{R}_{p_f} \\ -\mathbf{R}_{\lambda_c} \end{pmatrix}}_{(n_{\text{dof}}^s + n_{\text{dof}}^f + n_{\text{dof}}^{p_f} + 1) \times 1}. \tag{5.62}$$

If we do not wish to increment $\delta \ddot{\boldsymbol{\Lambda}}$ as part of the Newton-Raphson method, that is to say, assume $\delta \ddot{\boldsymbol{\Lambda}}_{n+1}^{i+1} = \delta \ddot{\boldsymbol{\Lambda}}_{n+1}^i$, a direct solve for the Lagrange multiplier would yield⁶

$$\ddot{\boldsymbol{\Lambda}}_{n+1} = -\mathbf{K}_{u_f, \lambda_c}^{-1} \cdot (\mathbf{R}_{u_f} + \mathbf{R}_{u_f}^c (\lambda_{n(c)}) + \mathbf{K}_{u_f, u} \cdot \delta \ddot{\mathbf{d}} + \mathbf{K}_{u_f, u_f} \cdot \delta \ddot{\mathbf{d}}_f + \mathbf{K}_{u_f, p_f} \cdot \delta \ddot{\boldsymbol{\pi}}). \tag{5.63}$$

Thus, the augmented block system is written as

$$\underbrace{\begin{bmatrix} \mathbf{K}_{u,u} & \mathbf{K}_{u,u_f} & \mathbf{K}_{u,p_f} \\ \mathbf{K}_{u_f,u} & \mathbf{K}_{u_f,u_f} & \mathbf{K}_{u_f,p_f} \\ \mathbf{K}_{p_f,u} & \mathbf{K}_{p_f,u_f} & \mathbf{K}_{p_f,p_f} \\ \mathbf{K}_{\lambda_c,u} & \mathbf{K}_{\lambda_c,u_f} & \mathbf{0} \end{bmatrix}}_{n+1}^i \cdot \underbrace{\begin{pmatrix} \delta \ddot{\mathbf{d}} \\ \delta \ddot{\mathbf{d}}_f \\ \delta \ddot{\boldsymbol{\pi}} \end{pmatrix}}_{n+1}^{i+1} = \underbrace{\begin{pmatrix} -\mathbf{R}_u \\ -\mathbf{R}_{u_f} - \mathbf{R}_{u_f}^c \\ -\mathbf{R}_{p_f} \\ -\mathbf{R}_{\lambda_c} \end{pmatrix}}_{n+1}^i + \underbrace{\begin{pmatrix} \mathbf{0} \\ \mathbf{0} \\ \mathbf{0} \\ \ddot{\boldsymbol{\Lambda}}_{n+1} \end{pmatrix}}_{n+1}. \tag{5.64}$$

For w^λ, w^{u_f} , we choose linear shape functions

$$\mathbf{N}^{e, \lambda} = \mathbf{N}^{e, u_f} = \left\{ \frac{1}{2}(1 - \xi), \frac{1}{2}(1 + \xi) \right\}. \tag{5.65}$$

⁶ SPONGE-1D does not use the direct solve method and increments the Lagrange multiplier DOF as part of the Newton-Raphson method.

For w^u , Hermite cubic shape functions are necessary to resolve a porosity gradient found elsewhere in the variational equations, i.e.,

$$\begin{aligned} \mathbf{N}^{e,u} &= \left\{ \frac{1}{4}(1-\xi)^2(2+\xi), \frac{j^e}{4}(1-\xi)^2(1+\xi), \frac{1}{4}(1+\xi)^2(2-\xi), \frac{j^e}{4}(1+\xi)^2(-1+\xi) \right\}, \\ \mathbf{B}^{e,u} &= \frac{1}{j^e} \left\{ \frac{3}{4}(\xi^2-1), \frac{j^e}{4}(3\xi^2-2\xi-1), -\frac{3}{4}(\xi^2-1), \frac{j^e}{4}(3\xi^2+2\xi-1) \right\}, \end{aligned} \quad (5.66)$$

In 1-D, we will assume the Lagrange multiplier is enforced at the topmost node $X = H$, i.e., for $e = n_e$ and $\xi = 1$. Thus, the residual and resulting stiffness matrices are independent of the area integral. Therefore, the stiffness matrix that couples the Lagrange multiplier and the solid skeleton displacement is written element-wise as

$$\mathbf{k}_{\lambda_c, u}^{e=n_e} := \left\{ \mathbf{N}^{e,\lambda} \right\}^T \Big|_{\xi=1} \left(\left[\frac{(n^s)^{h^e}}{J^{h^e}} \right] \Big|_{\xi=1} (d_t - d) \Big|_{n_{\text{node}}} (\beta \Delta t^2) \left\{ \mathbf{B}^{e,u} \right\} \Big|_{\xi=1} - (n^f)^{h^e} \Big|_{\xi=1} (\gamma \Delta t) \left\{ \mathbf{N}^{e,u} \right\} \Big|_{\xi=1} \right) A. \quad (5.67)$$

The stiffness matrix that couples the Lagrange multiplier and the pore fluid displacement is written element-wise as

$$\mathbf{k}_{\lambda_c, u_f}^{e=n_e} := \left\{ \mathbf{N}^{e,\lambda} \right\}^T \Big|_{\xi=1} (n^f)^{h^e} \Big|_{\xi=1} (\gamma \Delta t) \left\{ \mathbf{N}^{e, u_f} \right\} \Big|_{\xi=1} A. \quad (5.68)$$

The residual for the Lagrange multiplier's contribution to the pore fluid momentum balance is written as

$$\mathbf{R}_{u_f}^c = \int_{\Gamma_0^I} w^{u_f} \lambda_c dA, \quad (5.69)$$

or, for the 1-D problem, as

$$\mathbf{R}_{u_f}^c = A \mathbf{c}^{u_f, e} \Big|_{n_{\text{node}}} \lambda_c \Big|_{n_{\text{node}}}. \quad (5.70)$$

Linearization of the residual yields

$$\delta \mathbf{R}_{u_f}^c = \int_{\Gamma_0^I} w^{u_f} (\beta \Delta t^2) \delta \ddot{\lambda}_c dA. \quad (5.71)$$

Therefore, the stiffness matrix that couples the pore fluid displacement and the Lagrange multiplier is written element-wise as

$$\mathbf{k}_{u_f, \lambda_c}^{e=n_e} := \left\{ \mathbf{N}^{e, u_f} \right\}^T \Big|_{\xi=1} (\beta \Delta t^2) \left\{ \mathbf{N}^{e, \lambda} \right\} \Big|_{\xi=1} A. \quad (5.72)$$

Direct evaluation of the shape functions at $\xi = 1$ yields

$$\begin{aligned} \mathbf{N}^{e,\lambda} \Big|_{\xi=1} &= \mathbf{N}^{e,u_f} \Big|_{\xi=1} = \begin{Bmatrix} 0 & 1 \end{Bmatrix}, \\ \mathbf{N}^{e,u} \Big|_{\xi=1} &= \begin{Bmatrix} 0 & 0 & 1 & 0 \end{Bmatrix}, \\ \mathbf{B}^{e,u} \Big|_{\xi=1} &= \begin{Bmatrix} 0 & 0 & 0 & 1 \end{Bmatrix}. \end{aligned} \quad (5.73)$$

Therefore, the stiffness matrices are scalars function with the values

$$\begin{aligned} k_{\lambda_c, u}^{e=n_e} &= \left((\dot{d}_f - \dot{d}) \Big|_{n_{\text{node}}} \left[\frac{(n^s)^{h^e}}{J^{h^e}} \right] \Big|_{\xi=1} (\beta \Delta t^2) - (n^f)^{h^e} \Big|_{\xi=1} (\gamma \Delta t) \right) A, \\ k_{\lambda_c, u_f}^{e=n_e} &= (n^f)^{h^e} \Big|_{\xi=1} (\gamma \Delta t) A \\ k_{u_f, \lambda_c}^{e=n_e} &= (\beta \Delta t^2) A. \end{aligned} \quad (5.74)$$

For $k_{\lambda_c, u}^{e=n_e}$, care must be taken to insert the scalar functions at the appropriate DOFs. E.g., the linearization of the velocity component is inserted into the global stiffness matrix at the location $[n_{\text{dof}}, n_{\text{dof}}^s - 1]$ and the linearization of the gradient component (the porosity) is inserted at the location $[n_{\text{dof}}, n_{\text{dof}}^s]$, per the evaluation of the shape functions.

Lagrange cubic polynomials

$$\mathbf{N}^e := \frac{1}{16} \left\{ -9(\xi + 1/3)(\xi - 1/3)(\xi - 1), 27(\xi + 1)(\xi - 1/3)(\xi - 1), -27(\xi + 1)(\xi + 1/3)(\xi - 1), 9(\xi + 1/3)(\xi - 1/3)(\xi + 1) \right\} \quad (5.75)$$

are used to interpolate the Gauss point data for J^{h^e} , n^{s,h^e} , n^{f,h^e} at the nodes. E.g., assume J^{h^e} is known at the four Gauss points, such that

$$\begin{aligned} J^{h^e}(\xi = \tilde{\xi}_{\text{I}}, t) &= J_{\text{I}}(t), \\ J^{h^e}(\xi = \tilde{\xi}_{\text{II}}, t) &= J_{\text{II}}(t), \\ J^{h^e}(\xi = \tilde{\xi}_{\text{III}}, t) &= J_{\text{III}}(t), \\ J^{h^e}(\xi = \tilde{\xi}_{\text{IV}}, t) &= J_{\text{IV}}(t), \end{aligned} \quad (5.76)$$

with unknown nodal values J_1, J_2, J_3, J_4 . Therefore,

$$J^{h^e}(\xi = \tilde{\xi}_{\text{I}}, t) = N_1^e(\tilde{\xi}_{\text{I}})J_1(t) + N_2^e(\tilde{\xi}_{\text{II}})J_2(t) + N_3^e(\tilde{\xi}_{\text{III}})J_3(t) + N_4^e(\tilde{\xi}_{\text{IV}})J_4(t) = J_1(t), \quad (5.77)$$

such that

$$\begin{bmatrix} N_1^e(\tilde{\xi}_I) & N_2^e(\tilde{\xi}_I) & N_3^e(\tilde{\xi}_I) & N_4^e(\tilde{\xi}_I) \\ N_1^e(\tilde{\xi}_{II}) & N_2^e(\tilde{\xi}_{II}) & N_3^e(\tilde{\xi}_{II}) & N_4^e(\tilde{\xi}_{II}) \\ N_1^e(\tilde{\xi}_{III}) & N_2^e(\tilde{\xi}_{III}) & N_3^e(\tilde{\xi}_{III}) & N_4^e(\tilde{\xi}_{III}) \\ N_1^e(\tilde{\xi}_{IV}) & N_2^e(\tilde{\xi}_{IV}) & N_3^e(\tilde{\xi}_{IV}) & N_4^e(\tilde{\xi}_{IV}) \end{bmatrix} \begin{bmatrix} J_1(t) \\ J_2(t) \\ J_3(t) \\ J_4(t) \end{bmatrix} = \begin{bmatrix} J_I(t) \\ J_{II}(t) \\ J_{III}(t) \\ J_{IV}(t) \end{bmatrix}. \quad (5.78)$$

Then,

$$\begin{bmatrix} J_1(t) \\ J_2(t) \\ J_3(t) \\ J_4(t) \end{bmatrix} = \begin{bmatrix} N_1^e(\tilde{\xi}_I) & N_2^e(\tilde{\xi}_I) & N_3^e(\tilde{\xi}_I) & N_4^e(\tilde{\xi}_I) \\ N_1^e(\tilde{\xi}_{II}) & N_2^e(\tilde{\xi}_{II}) & N_3^e(\tilde{\xi}_{II}) & N_4^e(\tilde{\xi}_{II}) \\ N_1^e(\tilde{\xi}_{III}) & N_2^e(\tilde{\xi}_{III}) & N_3^e(\tilde{\xi}_{III}) & N_4^e(\tilde{\xi}_{III}) \\ N_1^e(\tilde{\xi}_{IV}) & N_2^e(\tilde{\xi}_{IV}) & N_3^e(\tilde{\xi}_{IV}) & N_4^e(\tilde{\xi}_{IV}) \end{bmatrix}^{-1} \begin{bmatrix} J_I(t) \\ J_{II}(t) \\ J_{III}(t) \\ J_{IV}(t) \end{bmatrix}. \quad (5.79)$$

We now demonstrate the three methods: weak enforcement of the no-flux condition via the no-flux Neumann boundary condition as it appears in the balance of mass, hereafter referred to as “weak”, weak enforcement and strong enforcement, hereafter referred to as “strong”, and weak enforcement with the Lagrange multiplier method, hereafter referred to as “Lagrange.” Material parameters are given by Table 5.13; geometrical and loading parameters are given in Table 5.14. Results for Yen impulse loading are very similar qualitatively to the results for Friedlander impulse loading, but are omitted for sake of brevity.

Table 5.13: Geometrical and loading parameters for the no-flux boundary condition study. Values taken from Clayton et al. [2021], Lande and Mitzner [2006].

K^{skel} (kPa)	G (kPa)	K_s (kPa)	K_f^η (kPa)	ρ_0^{sR} (kg/m ³)	ρ_0^{fR} (kg/m ³)	n_0^f	\hat{k}_0 (m ² /Pa-s)	κ
7.5	3	2.2×10^6	140	1000	1.138	0.664	10^{-5}	2.5

Table 5.14: Geometrical and loading parameters for the no-flux boundary condition study.

Overpressure load type	H (cm)	A (cm ²)	h_0^e (cm)	t_0^σ (kPa)	t_0 (ms)	t_1 (ms)
Friedlander impulse	10	1	0.1	25	10	N/A

For short-duration, shock-loading simulations, the negative effects from the Lagrange method are not observable on the typical time scales of interest; only for longer simulation times are these

effects noticeable. The fluid and solid displacements resulting from application of the Friedlander impulse at 25 kPa overpressure are plotted in Figure 5.36. We observe that the Lagrange method begins to go unstable around 40 ms, while both the weak and strong methods maintain a trend towards equilibrium. The strength of this instability is more apparent when observed as a contour plot of the displacements across the mesh at $t = 90$ ms (Figure 5.37). One positive of the Lagrange method is that the displacements at the no-flux boundary coincide with one another, even if they are wrong.

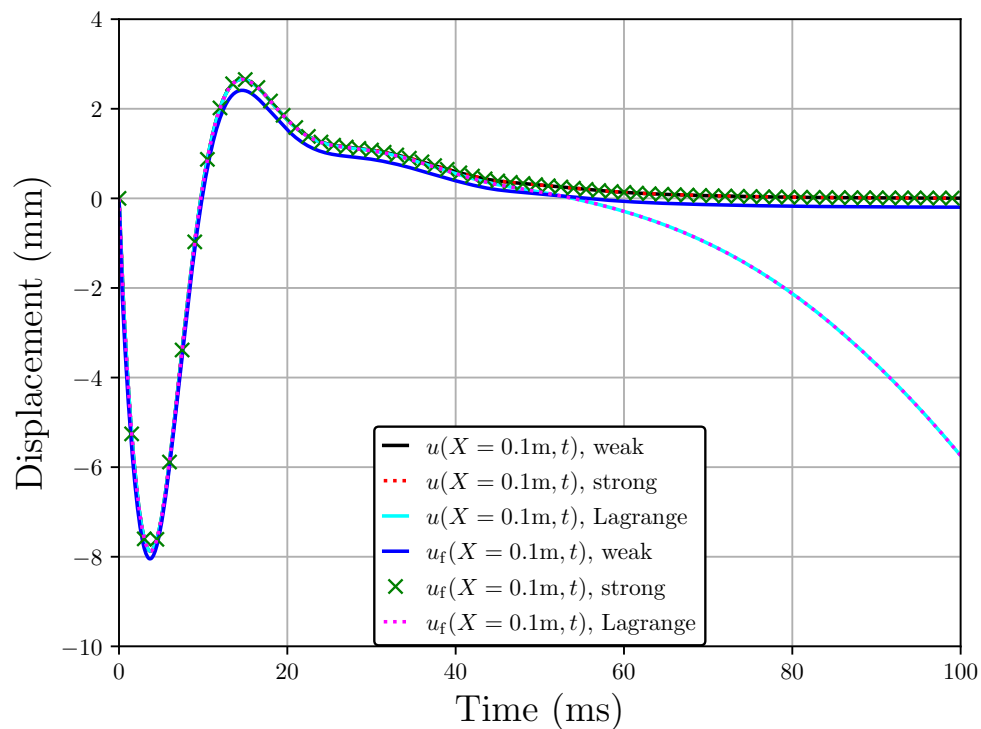


Figure 5.36: Solid and fluid displacements at $X = H$ of the various no-flux methods following application of the Friedlander impulse. Black, red, and green curves overlap throughout.

The instability likely arises from an unstable pore fluid pressure, shown in Figure 5.38. Whether or not this is a result of an overconstraint of the problem via two, essentially identical no-flux boundary conditions (one for the balance of mass of the mixture, the other for the pore fluid linear momentum balance), has yet to be determined.

Another positive of both the weak method and the Lagrange method is that the *actual* no-

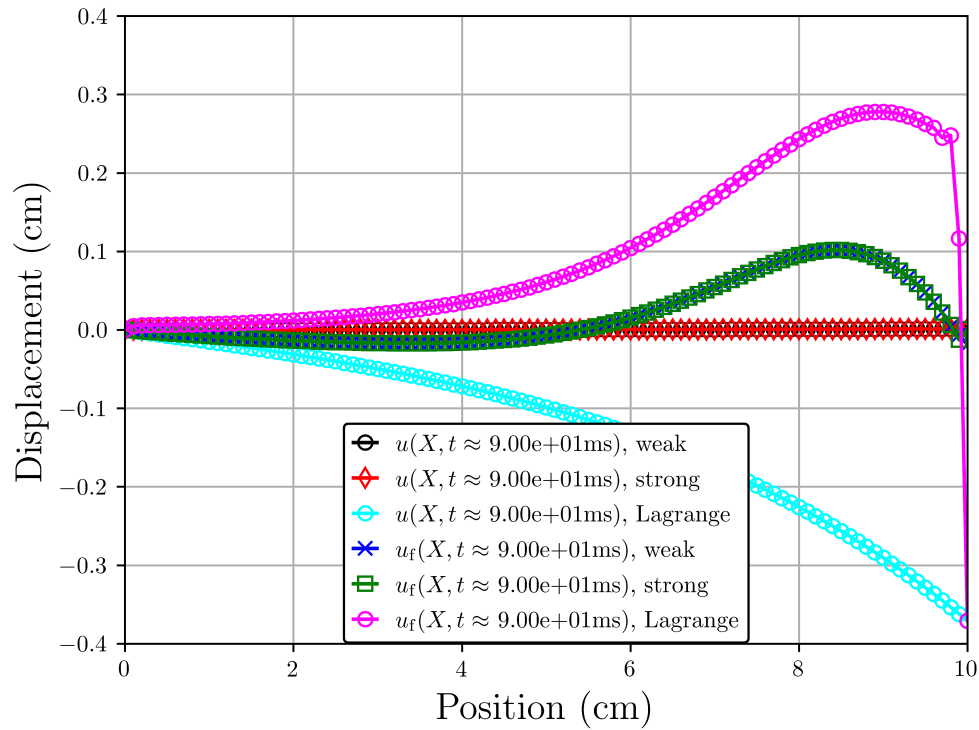


Figure 5.37: Solid and fluid displacements contours of the various no-flux methods following application of the Friedlander impulse at 25 kPa overpressure. Black and red curves, and green and blue curves overlap at this scale.

flux condition, that is, that the relative velocities should be equal at the boundary, is satisfied in the weak sense almost immediately for the Lagrange method and particularly for longer simulation times for the weak method. Absolute relative differences in phase velocities are smallest for the Lagrange method (Figure 5.39(a)); the weak method shows a convergence to zero difference in phase velocity as element size is decreased (Figure 5.39(b)). Thus, given that the strong method is *ad-hoc* and the Lagrange method presents an instability for longer simulation times, and given that the weak method is satisfied given enough simulation time, the simulations involving no-flux boundary conditions in the proceeding sections will use the weak method.

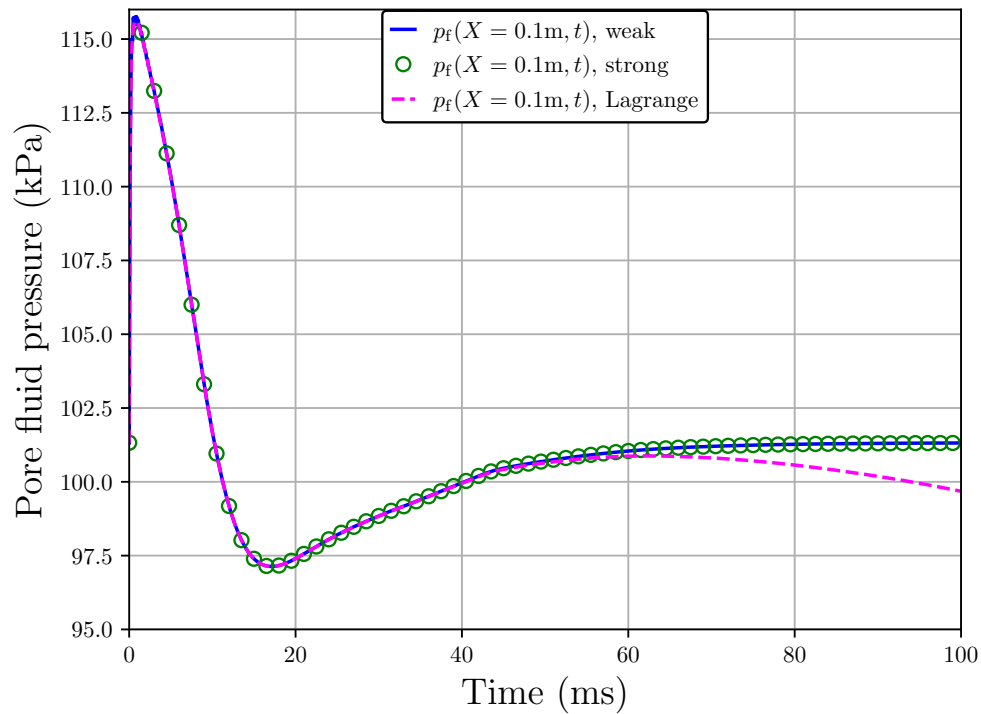


Figure 5.38: Pore fluid pressure at $X = H$ of the various no-flux methods following application of the Friedlander impulse at 25 kPa overpressure.

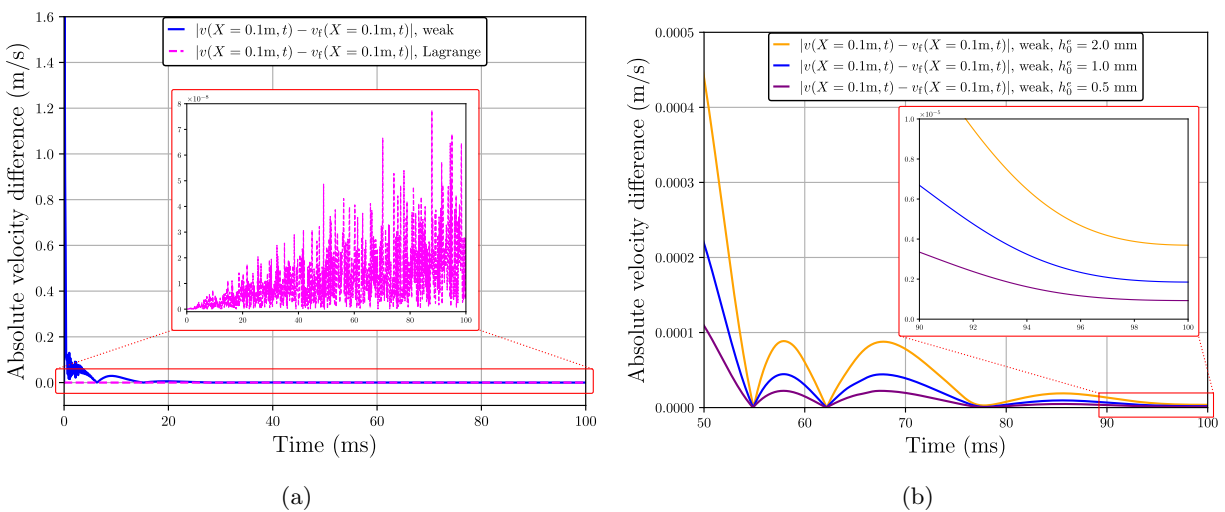


Figure 5.39: Absolute difference in relative velocities for (a) the weak and Lagrange method with element size $h_0^e = 1$ mm, and (b) the weak method for varying element sizes.

A sensitivity study for \varkappa . Perhaps one of the most important parameters for determining just how much fluid-structure interaction matters in a multiphase simulation is the intrinsic permeability of the porous solid skeleton, \varkappa . For lung parenchyma, there is high uncertainty regarding the magnitude of this parameter. Lande and Mitzner [2006] used a hydraulic conductivity $\hat{k} \sim \mathcal{O}(10^{-5})$ m²/Pa-s and initial porosity $n_0^f = 0.99$, which for pore air with $\mu_f \sim \mathcal{O}(10^{-5})$ Pa-s, necessitates $\varkappa \sim \mathcal{O}(10^{-10})$ m². In Dai et al. [2014], \varkappa was estimated $\mathcal{O}(10^{-11})$ m² based on an experiment in which air was passed through inflated, dry, swine lung parenchyma at a fixed flow rate. A pressure differential was recorded, thereby allowing them to calculate the permeability via the non-inertial form of Darcy’s law (refer to Equation (5.2)). Here, we simulate the lung parenchyma and pore air response to shock loading for various values of \varkappa . Material parameters are listed in Table 5.15; geometrical and loading parameters are listed in Table 5.16, with standard linear Q1-Q1-P1 or Q1-P1 elements, depending on the formulation. We note that initial porosity is held fixed $n_0^f = 0.664$ for comparative purposes. However, this is not realistic. For materials with smaller pore sizes, the initial porosity would be lower, and vice versa. A functional relationship between intrinsic permeability and initial porosity will be pursued as part of future work.

Table 5.15: Material parameters for sensitivity study of \varkappa . Known values taken from Clayton et al. [2021]. $\varkappa \in [1.89 \times 10^{-8}, 1.89 \times 10^{-12}]$ m².

K^{skel} (kPa)	G (kPa)	K_s (kPa)	K_f^η (kPa)	ρ_0^{sR} (kg/m ³)	ρ_0^{fR} (kg/m ³)	n_0^f	μ_f (Pa-s)	\varkappa
7.5	3	2.2×10^6	140	1000	1.138	0.664	1.89×10^{-5}	2.5

Table 5.16: Geometrical and loading parameters for sensitivity study on \varkappa .

Overpressure load type	H (cm)	A (cm ²)	h_0^e (cm)	t_0^σ (kPa)	t_0 (ms)	t_1 (ms)
Yen impulse	10	1	0.1	50	0.17	0.34
Friedlander impulse	10	1	0.1	50	10	N/A

Displacements for solid and fluid in response to Yen impulse loading are given in Figure 5.40(a) & Figure 5.40(b), respectively. For the lower permeabilities, the solution behaves as if it were elastodynamic, i.e., with little-to-no dissipation from the pore fluid (i.e., behaving as if it were “locally undrained”), suggesting a *lower* limit on permeability (or hydraulic conductivity) for

using TPM in this application space (high strain-rate loading of air-saturated porous materials).

Conversely, as permeability increases, dissipation becomes greater. We observe that for $\varkappa = 1.89 \times 10^{-8} \text{ m}^2$ (magenta curves), there is a bump in the solid displacement after the solution appears to have reached equilibrium; likewise, the solution for pore fluid displacement is not even remotely close to the solution for solid displacement (which it should be, for the no-flux boundary condition). This suggests an *upper* limit on the permeability (or hydraulic conductivity) for problems that use TPM. I.e., for finite strain applications with air as the pore fluid, one may be better off computing the dynamic response of the two phases using, e.g., a CFD-ALE approach when the pore sizes are this large.

When comparing displacements from $(\mathbf{u}-p_f)$ vs. $(\mathbf{u}-\mathbf{u}_f-p_f)$ formulations for the more moderate permeabilities, differences are minor (refer to Figure 5.41), particularly for the higher permeabilities. The same can be said for the total stress (Figure 5.42) and the solid extra stress (Figure 5.43). Of notable interest is how for the lower permeabilities, peak compressive solid extra stress is lower when compared to the higher permeabilities, demonstrating the importance of accounting for pore air (as compared to a single-phase model) for higher permeabilities when it can move more freely through the pore space. Yet, peak tensile solid extra stress is higher, demonstrating the role of the pore air in dissipating the stress wave when it (the air) can move more freely at higher permeabilities. This is corroborated by the pore fluid stress behaving in the opposite manner (i.e., higher pore fluid stress for more “immobile” pore fluid at the lower permeabilities, and vice versa), shown in Figure 5.44. Differences in total stress are negligible for all permeabilities, as one would expect.

Differences in the seepage velocity between formulations are negligible for lower permeabilities (Figure 5.45); at higher permeabilities, e.g., $\varkappa = 1.89 \times 10^{-9} \text{ m}^2$ (orange curves), choice of formulation becomes important. It was shown in Irwin et al. [2024] (and in paragraph *Comparison between single-phase and multiphase models for shock loading*) that pore air acceleration is not equivalent to the solid acceleration, nor mixture acceleration, for high strain-rate loadings. While choice of formulation appears to have little-to-no effect on important solid metrics, such as solid extra stress, there is a clear difference in the dynamics for larger pore sizes.

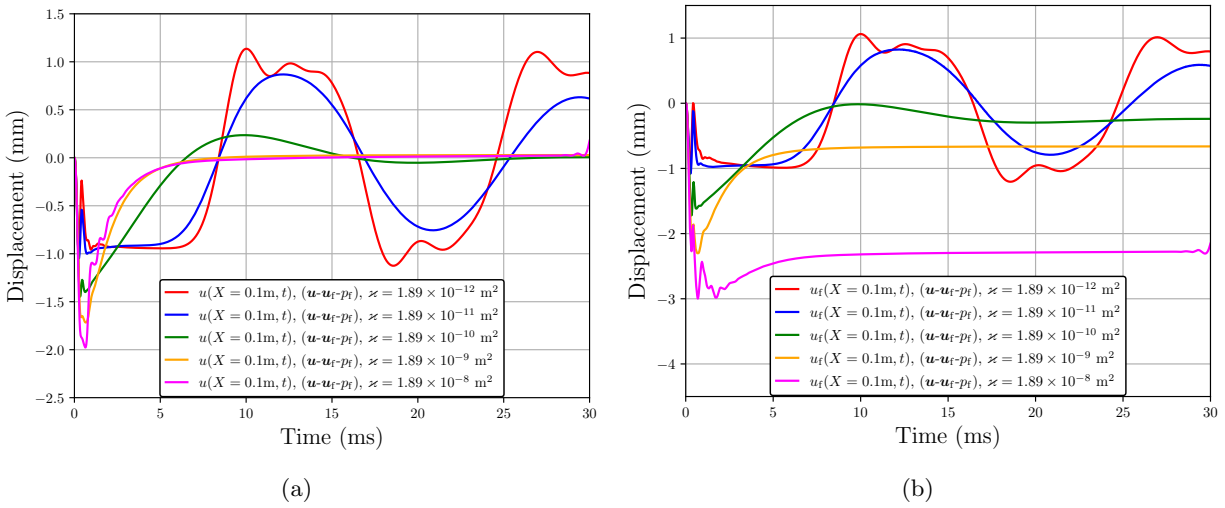


Figure 5.40: Displacements at $X = H$ for varying values of κ in response to the Yen impulse at 50 kPa overpressure for (a) the solid skeleton and (b) the pore fluid. Note the lower bound on the y -ordinate in (b) to account for irrecoverable pore fluid displacement when $\kappa = 1.89 \times 10^{-8} \text{ m}^2$ as compared to the lower permeabilities.

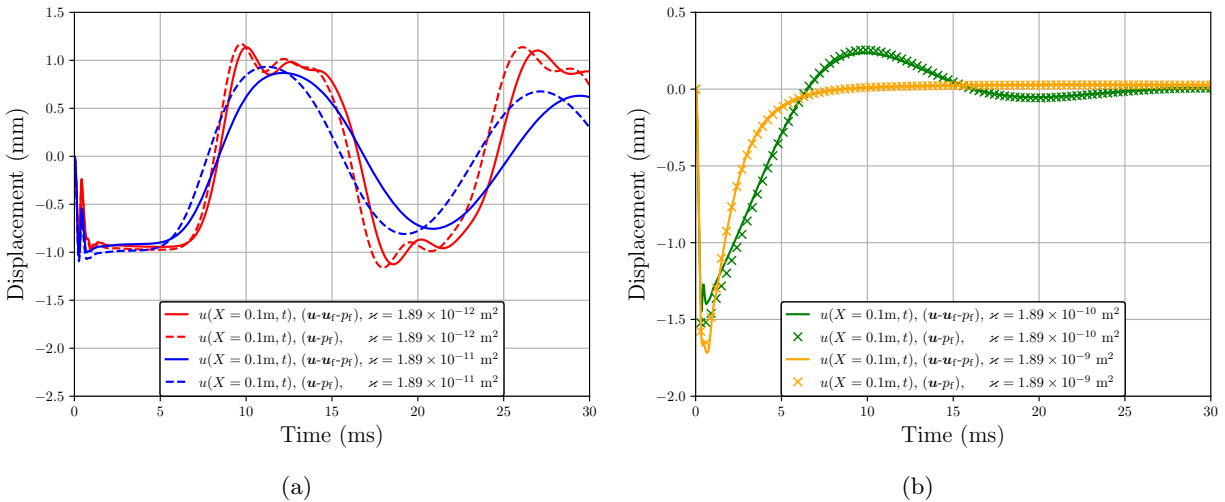


Figure 5.41: Comparing displacements at $X = H$ between $(\mathbf{u}-p_f)$ and $(\mathbf{u}-\mathbf{u}_f-p_f)$ formulations in response to the Yen impulse at 50 kPa overpressure for (a) lower permeabilities and (b) higher permeabilities.

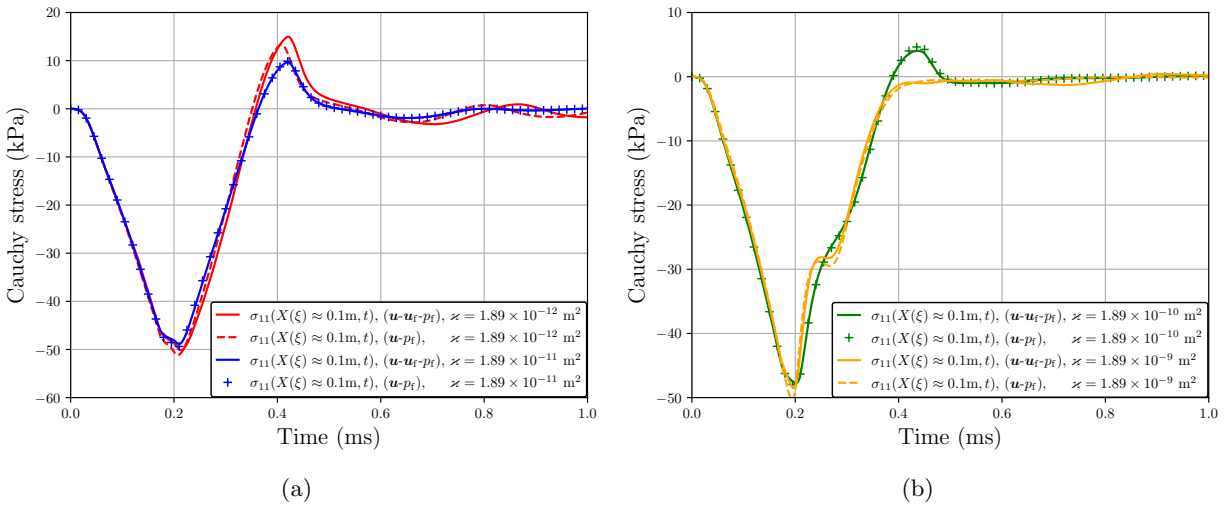


Figure 5.42: Comparing total stress at the Gauss point closest to $X = H$ between $(\mathbf{u}-p_f)$ and $(\mathbf{u}-\mathbf{u}_f-p_f)$ formulations in response to the Yen impulse at 50 kPa overpressure for (a) lower permeabilities and (b) higher permeabilities.

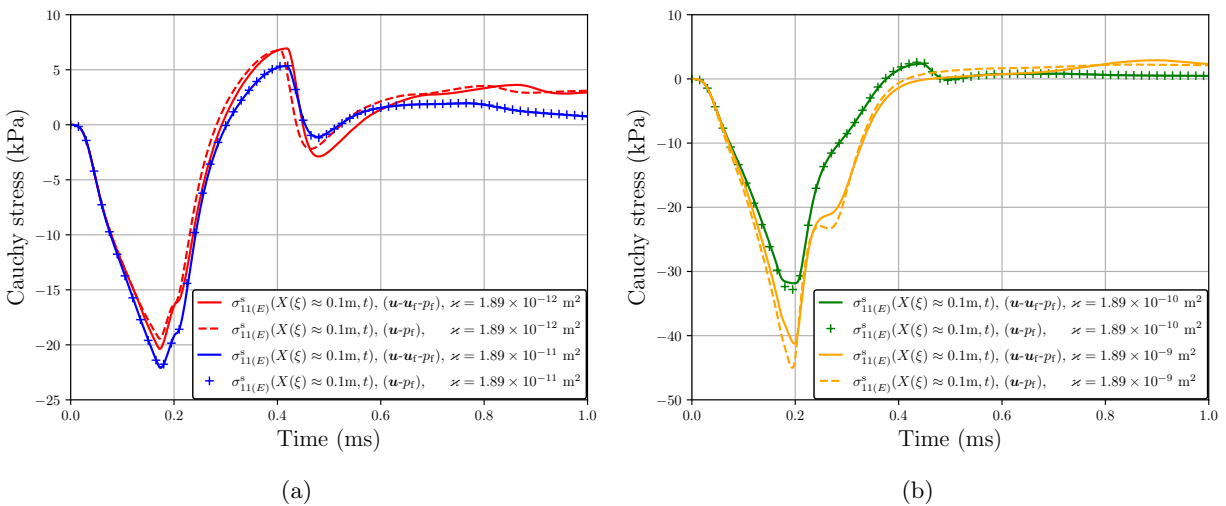


Figure 5.43: Comparing solid extra stress at $X = H$ between $(\mathbf{u}-p_f)$ and $(\mathbf{u}-\mathbf{u}_f-p_f)$ formulations in response to the Yen impulse at 50 kPa overpressure for (a) lower permeabilities and (b) higher permeabilities.

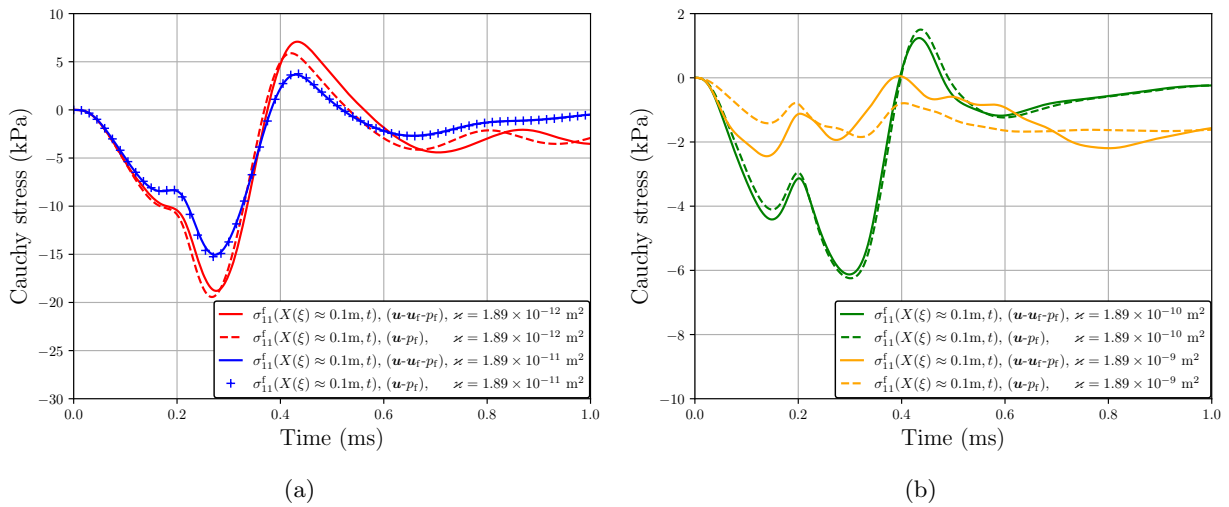


Figure 5.44: Comparing total pore fluid stress at the Gauss point closest to $X = H$ between $(\mathbf{u}-p_f)$ and $(\mathbf{u}-\mathbf{u}_f-p_f)$ formulations in response to the Yen impulse at 50 kPa overpressure for (a) lower permeabilities and (b) higher permeabilities.

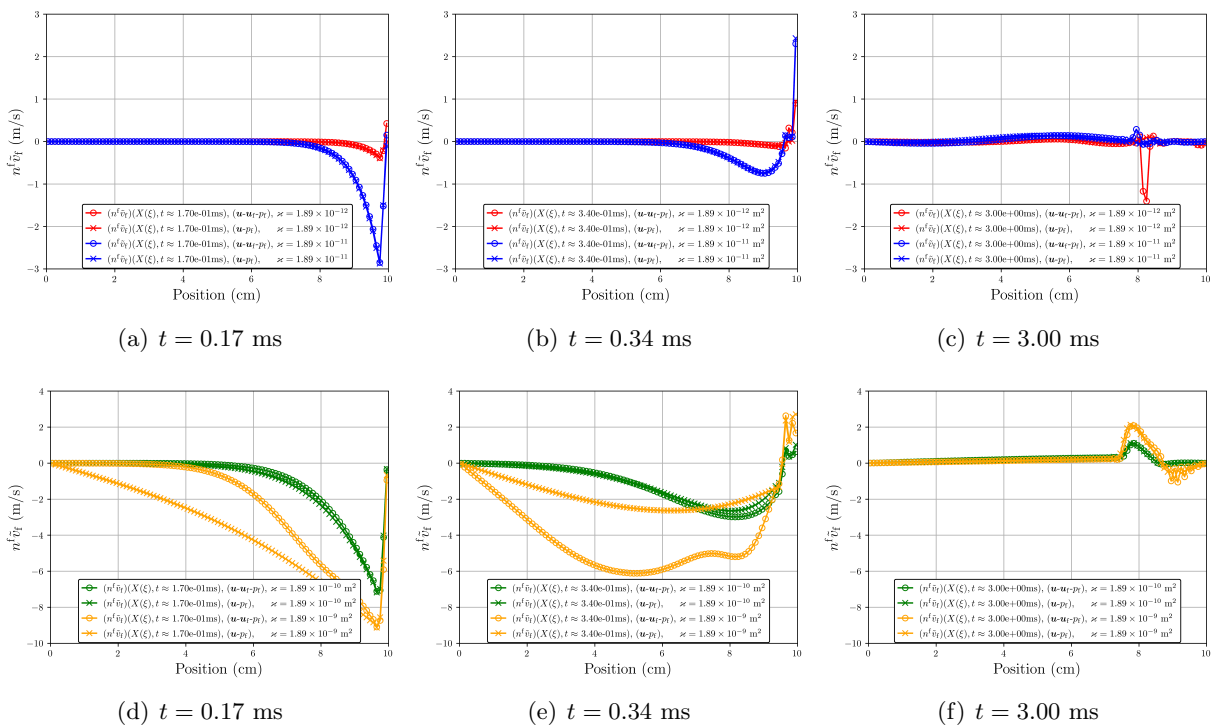


Figure 5.45: Contours along the length of the mesh for Darcy velocity ($n^f \tilde{v}_f$) for various permeabilities in response to the Yen impulse at 50 kPa overpressure. Note the change in y -ordinate for the bottom row.

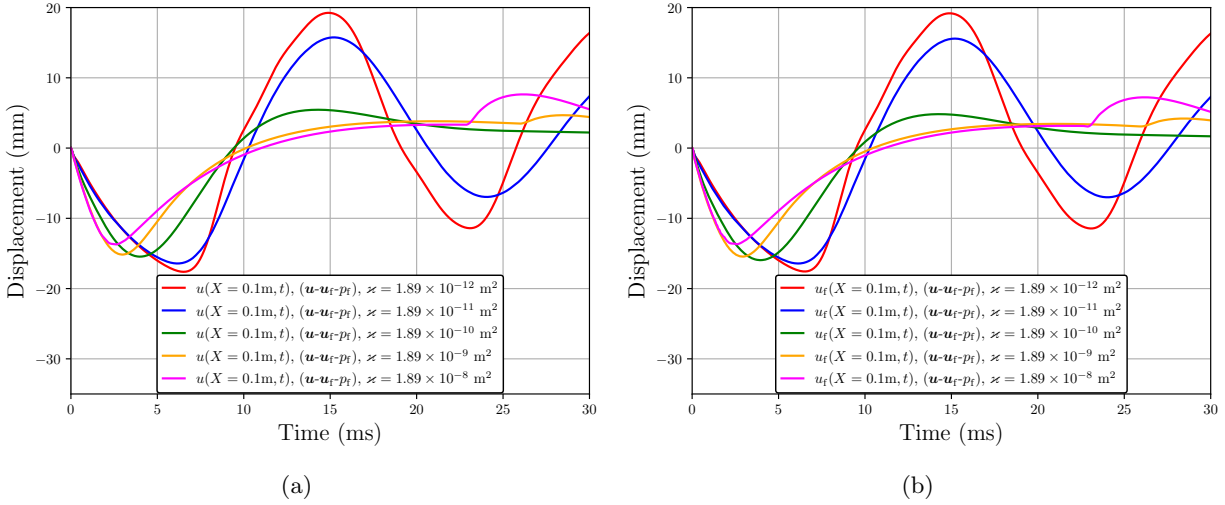


Figure 5.46: Displacements at $X = H$ for varying values of \varkappa in response to the Friedlander impulse at 50 kPa overpressure for (a) the solid skeleton and (b) the pore fluid.

Moving on to the Friedlander impulse, results show a similar trend compared to the Yen impulse. For lower permeabilities, the solution is nearly elastodynamic (i.e., “locally undrained”), and for higher permeabilities, pore fluid dissipation is dominant (refer to Figure 5.46). It also appears that results for $\varkappa = 1.89 \times 10^{-9}, 1.89 \times 10^{-8} \text{ m}^2$ (orange, magenta curves) have some numerical instability based on the bump in displacement that occurs after the solution appears to have reached equilibrium, though for long enough simulation time the solutions do trend towards zero displacement equilibrium (not shown). This bump is probably induced by the larger strain resulting from the longer duration loading, which is the only other qualitative change from the Yen impulse as far as displacements go. Nevertheless, the $\varkappa = 1.89 \times 10^{-9} \text{ m}^2$ (orange) curve is included in the subsequent analysis for completeness. Again we observe that there are more differences in the $(\mathbf{u}-p_f)$ vs. $(\mathbf{u}-\mathbf{u}_f-p_f)$ formulations for the lower permeabilities than for the higher permeabilities, where for the latter, the choice of formulation appears to be insignificant (refer to Figure 5.47) with the exception of the Darcy velocity. The story is the same regarding the analysis of the stresses (refer to Figure 5.48, Figure 5.49, and Figure 5.50)—for the Friedlander impulse, there are minute differences between formulations for the higher permeabilities just after shock

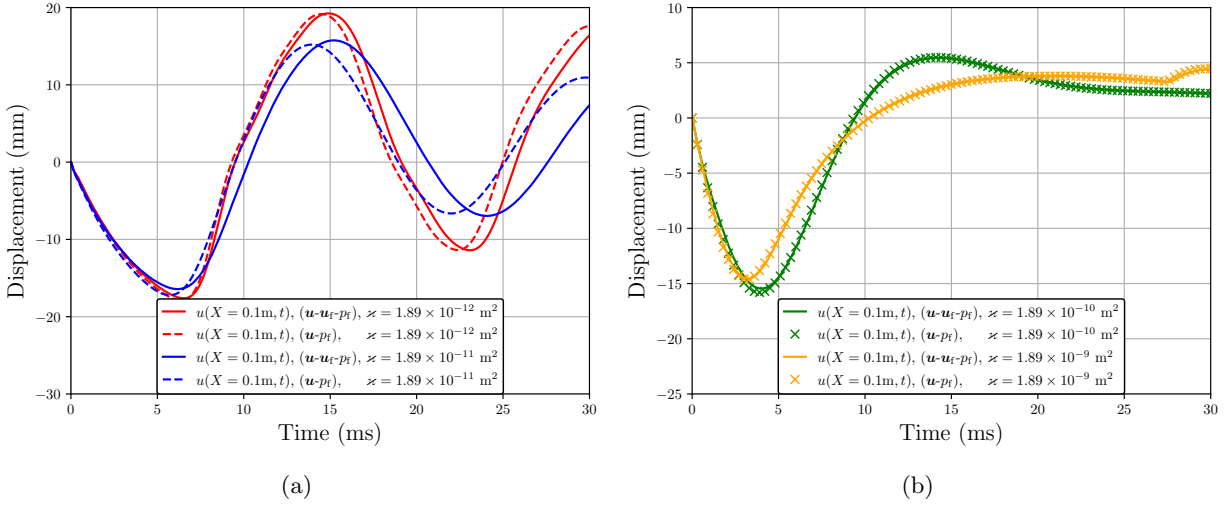


Figure 5.47: Comparing displacements at $X = H$ between $(\mathbf{u}-p_f)$ and $(\mathbf{u}-\mathbf{u}_f-p_f)$ formulations in response to the Friedlander impulse at 50 kPa overpressure for (a) lower permeabilities and (b) higher permeabilities.

loading (not shown for brevity), but after longer periods of time, the formulations converge to the same solution (Figure 5.49, Figure 5.50).

With regards to the seepage velocity, we again see no difference in formulations for the lower permeabilities (Figure 5.51(a)-Figure 5.51(c)), but at higher permeabilities (Figure 5.51(d)-Figure 5.51(f)), specifically for $\varkappa = 1.89 \times 10^{-9} \text{ m}^2$ (orange curves), the choice of formulation matters for reasons discussed above.

Given that the value of \varkappa is uncertain for lung parenchyma, and the promising results for $\varkappa \sim \mathcal{O}(10^{-10}) \text{ m}^2$, we choose to conduct simulations in the proceeding sections using $\varkappa = 1.89 \times 10^{-10} \text{ m}^2$. Future work must include calibration of this parameter to experimental data, as well as determining any potential functional relationship between intrinsic permeability and initial porosity.

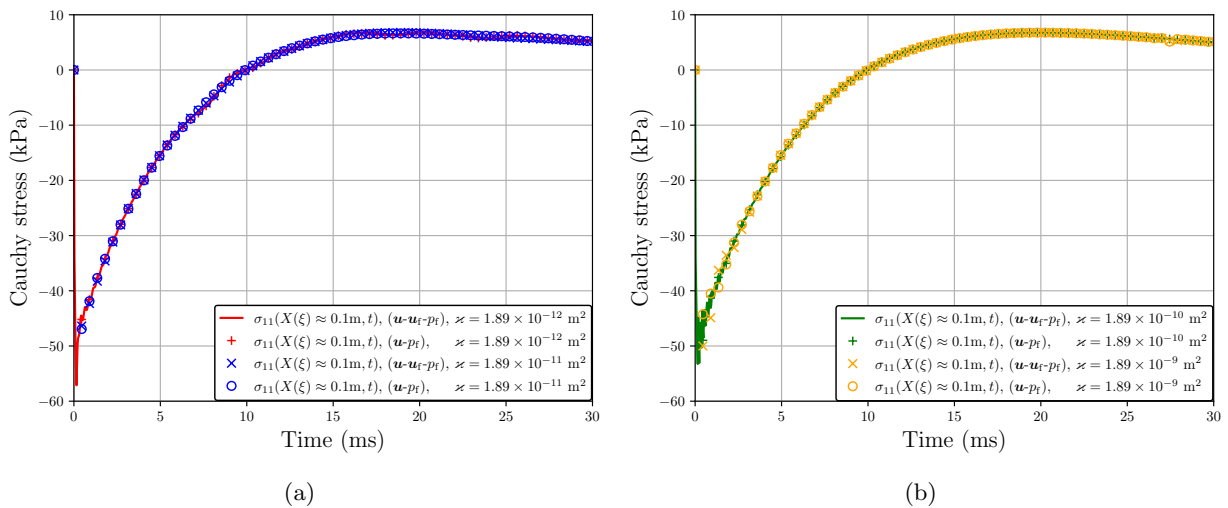


Figure 5.48: Comparing total stress at the Gauss point closest to $X = H$ between $(\mathbf{u}-p_f)$ and $(\mathbf{u}-\mathbf{u}_f-p_f)$ formulations in response to the Friedlander impulse at 50 kPa overpressure for (a) lower permeabilities and (b) higher permeabilities.

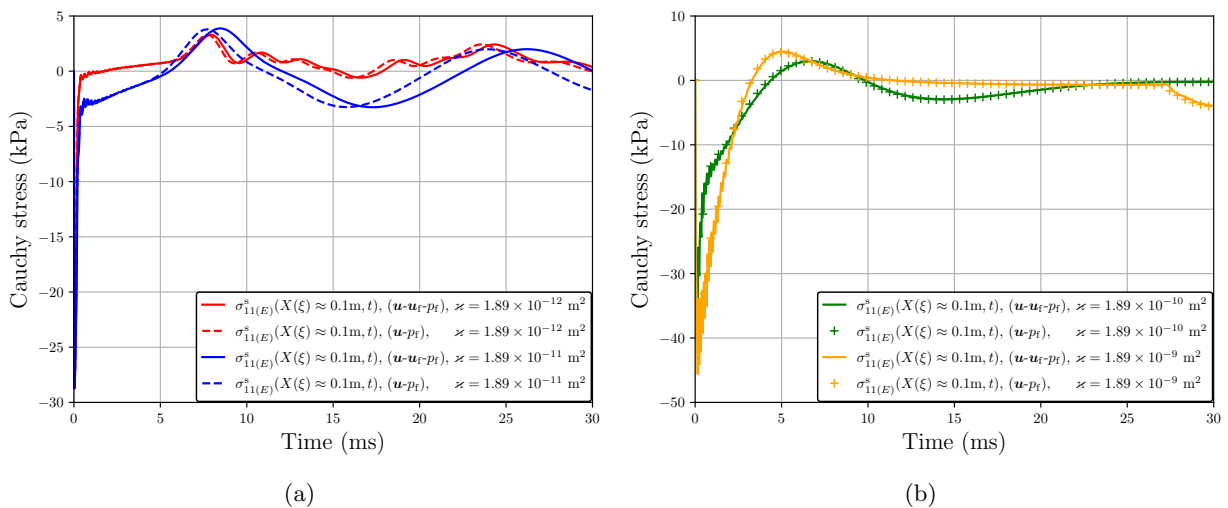


Figure 5.49: Comparing solid extra stress at the Gauss point closest to $X = H$ between $(\mathbf{u}-p_f)$ and $(\mathbf{u}-\mathbf{u}_f-p_f)$ formulations in response to the Friedlander impulse at 50 kPa overpressure for (a) lower permeabilities and (b) higher permeabilities.

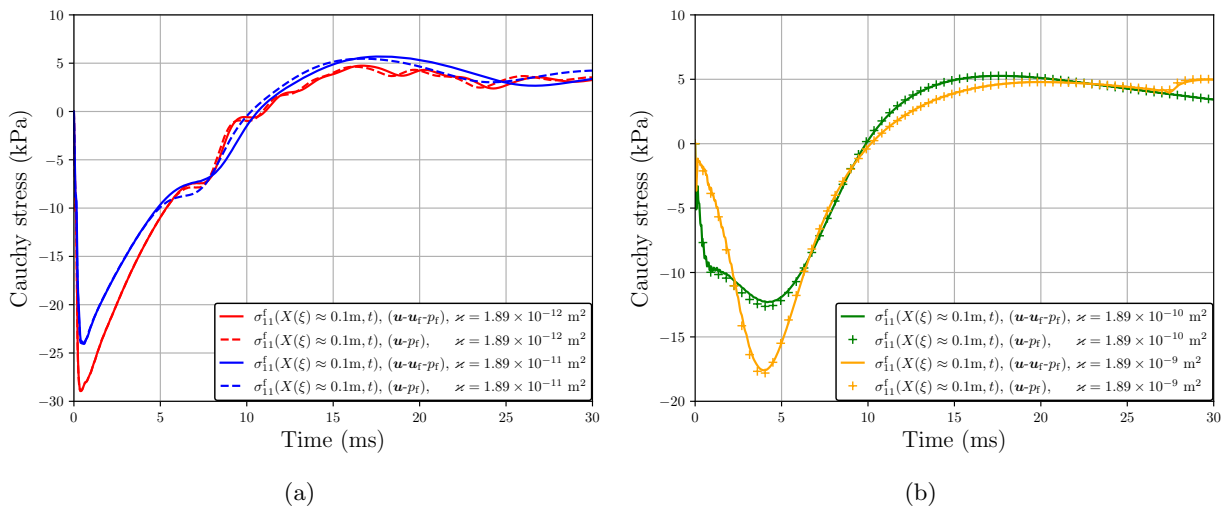


Figure 5.50: Comparing total pore fluid stress at $X = H$ between $(\mathbf{u}-p_f)$ and $(\mathbf{u}-\mathbf{u}_f-p_f)$ formulations in response to the Friedlander impulse at 50 kPa overpressure for (a) lower permeabilities and (b) higher permeabilities.

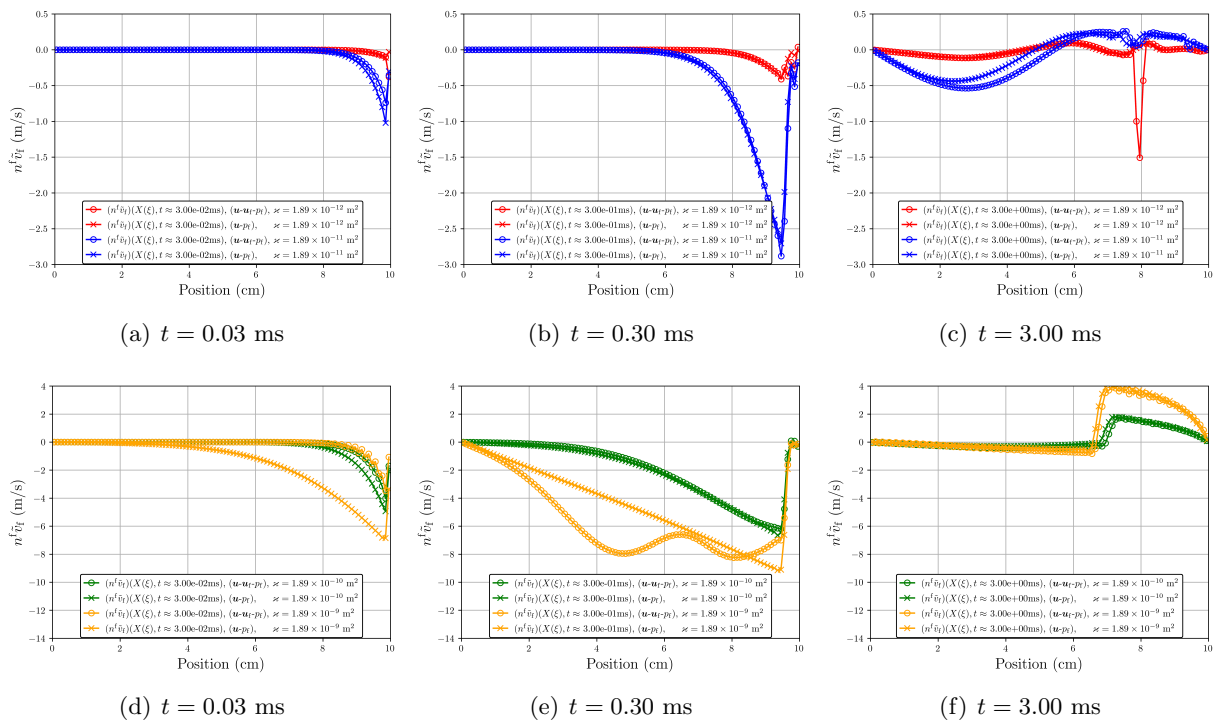


Figure 5.51: Contours along the length of the mesh for Darcy velocity ($n^f \tilde{v}_f$) for various permeabilities in response to the Friedlander impulse at 50 kPa overpressure. Note the change in y -ordinate for the bottom row. Time samples are shown in Figure 5.83.

A sensitivity study for κ . The parameter κ governs the rate of fluid flow through the porous medium; refer to Equation (3.68). Higher values of κ should, in theory, induce greater relative velocities between solid and fluid during expansion, and smaller relative velocities between solid and fluid during compression, since $\hat{k} \sim J^\kappa$ for this model.

The value of this parameter has not been measured for lung parenchyma. Markert [2005] deduced $\kappa \approx 2.65$ via calibration to experimental data for nearly quasi-static compression of PUR foam with intrinsic permeability $\varkappa = 1.69 \times 10^{-10} \text{ m}^2$ and initial porosity $n_0^f = 0.96$. Since we have chosen a value of the intrinsic permeability (which also governs rate of fluid flow through the porous medium) within an order of magnitude of that for PUR foam, it seems reasonable to keep the values of $\kappa \in [1.0, 5.0]$ in the following sensitivity study. Material parameters are listed in Table 5.17; geometrical and loading parameters are listed in Table 5.18, with standard linear Q1-Q1-P1 elements—differences in results between the $(\mathbf{u}-p_f)$ and $(\mathbf{u}-\mathbf{u}_f-p_f)$ formulaions are essentially negligible (with the exception of the Darcy velocity, where $(\mathbf{u}-p_f)$ shows slightly greater magnitudes in seepage velocity on $\mathcal{O}(10^{-1})$ m/s for just after shock loading onset for the Friedlander impulse across all κ , and some variation just after unloading for the Yen impulse for $\kappa = 5.0$), and are not included herein for brevity.

Table 5.17: Material parameters for sensitivity study of κ . Known values taken from Clayton et al. [2021]. $\kappa \in [1.0, 5.0]$.

K^{skel} (kPa)	G (kPa)	K_s (kPa)	K_f^η (kPa)	ρ_0^{sR} (kg/m ³)	ρ_0^{fR} (kg/m ³)	n_0^f	\hat{k} (m ² /Pa-s)
7.5	3	2.2×10^6	140	1000	1.138	0.664	1.89×10^{-10}

Table 5.18: Geometrical and loading parameters for sensitivity study on κ .

Overpressure load type	H (cm)	A (cm ²)	h_0^e (cm)	t_0^σ (kPa)	t_0 (ms)	t_1 (ms)
Yen impulse	10	1	0.1	50	0.17	0.34
Friedlander impulse	10	1	0.1	50	10	N/A

Beginning with the Yen impulse, solid displacements at the top of the mesh differ slightly from one another between the values of κ , but are otherwise in good agreement with one another (refer to Figure 5.52). At the middle of the mesh (Figure 5.53), differences in displacement are

apparent, particularly on the extreme ends of $\kappa = 1, 5$. Pore fluid displacements show greater variation at the top of the mesh, but less so at the middle of the mesh (refer to Figure 5.54 & Figure 5.55, respectively). Variations are minimal for all ranges of κ for the total and solid stress (Figure 5.56 & Figure 5.57, respectively), but not for the pore fluid stress (Figure 5.58) where there is greater variation between values of κ .

As the value of κ increases, the hydraulic conductivity is smaller during compression (near the onset of loading) than during expansion (well after loading). This inhibits the relative motion between solid and fluid, decreasing the amount of dissipation that occurs. As such, we see an increase in the amplitude of the pore fluid stress in both compressive and tensile states (see, e.g., the $\kappa = 5.0$ cyan curve, Figure 5.58(b)) when compared to lower values of κ (see, e.g., the $\kappa = 1.50$ green curve, Figure 5.58(b)). This is corroborated by smaller dissipation in the solid extra stress for higher values of κ than for lower values of κ (see, e.g., the cyan and green curves corresponding to $\kappa = 5.0, 1.50$, respectively, in Figure 5.57(a)). There is also a small phase shift in the Cauchy stresses for all three metrics (total, solid, fluid) between the Kozeny-Carman model and the the hyperbolic model.

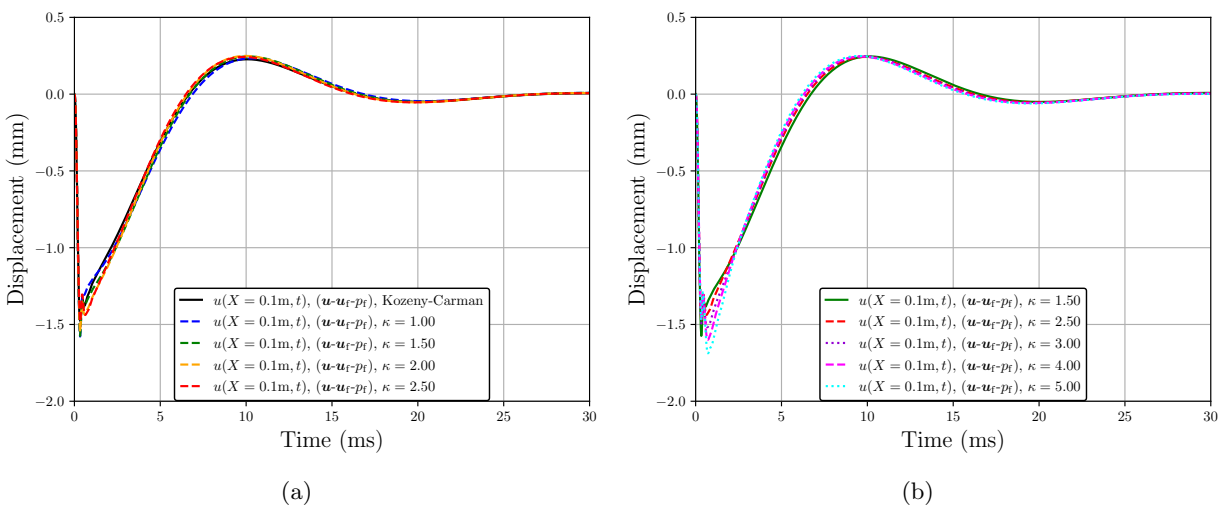


Figure 5.52: Solid skeleton displacements in response to the Yen impulse at 50 kPa overpressure at $X = H$ for (a) a moderate range of κ and (b) a greater range of κ .

Differences in relative motion between constituents are minor for changes in κ (refer to

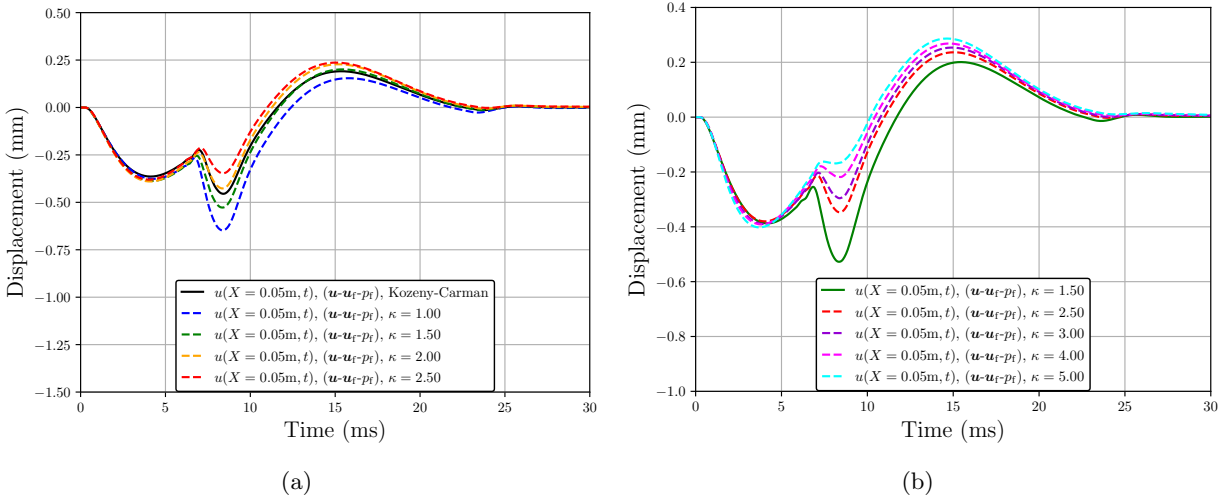


Figure 5.53: Solid skeleton displacements in response to the Yen impulse at 50 kPa overpressure at $X = H/2$ for (a) a moderate range of κ and (b) a greater range of κ .

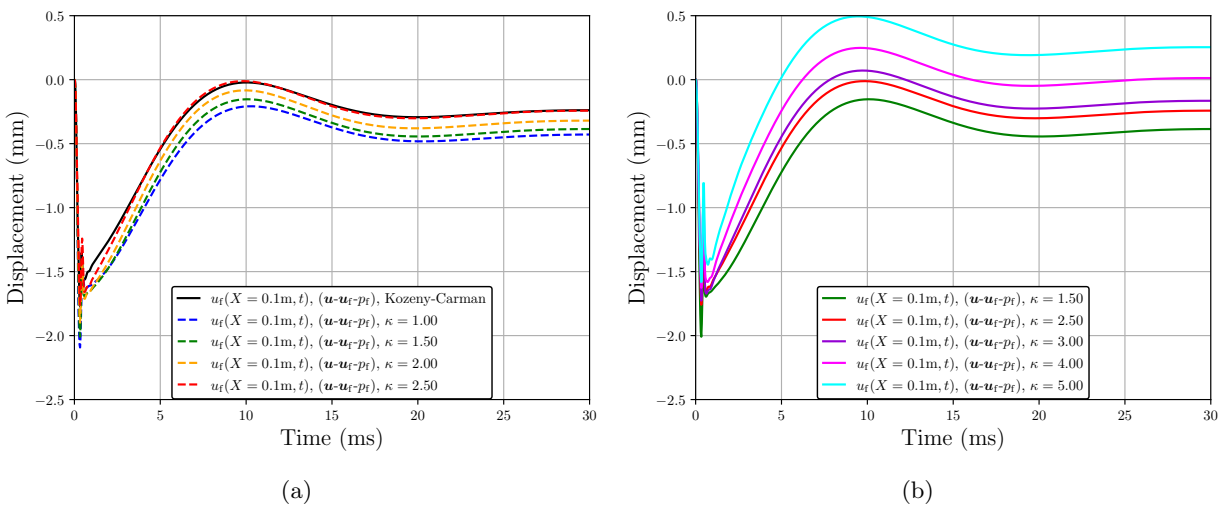


Figure 5.54: Pore fluid displacements in response to the Yen impulse at 50 kPa overpressure at $X = H$ for (a) a moderate range of κ and (b) a greater range of κ .

Figure 5.59). However, differences in relative values for hydraulic conductivity are not negligible, as shown in Figure 5.60. At peak loading (Figure 5.60(a), Figure 5.60(d)) and well after loading (Figure 5.60(c), Figure 5.60(f)) differences are fairly minor, but certainly apparent. At unloading (Figure 5.60(b), Figure 5.60(e)), differences are greatest, with smaller values of κ demonstrating decreased resistance (higher ratio of \hat{k}/\hat{k}_0) to relative motion, and vice versa. We note that for

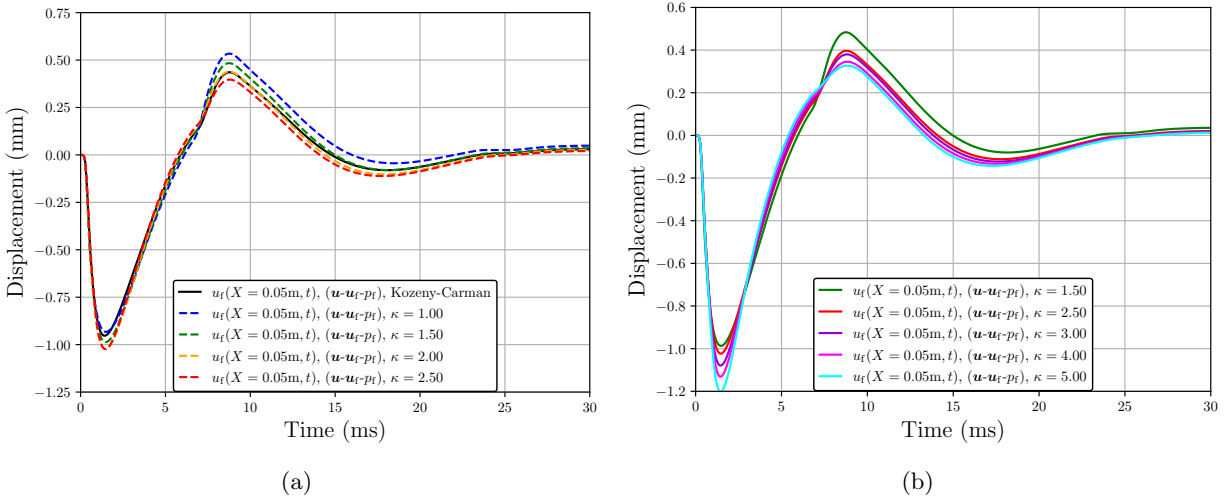


Figure 5.55: Pore fluid displacements in response to the Yen impulse at 50 kPa overpressure at $X = H/2$ for (a) a moderate range of κ and (b) a greater range of κ .

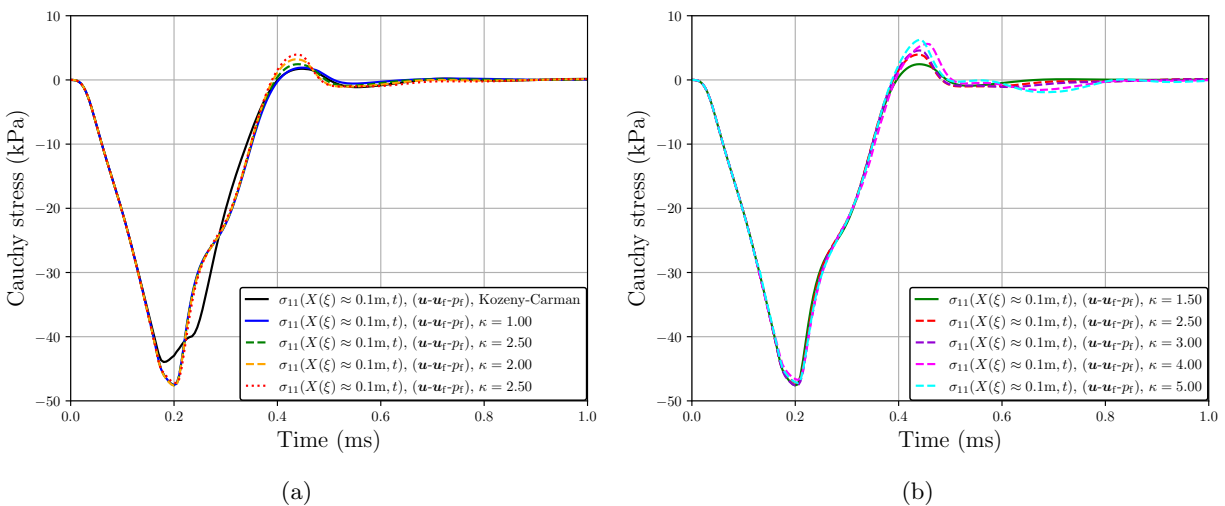


Figure 5.56: Total Cauchy stress in response to the Yen impulse at 50 kPa overpressure at the Gauss point closest to $X = H$ for (a) a moderate range of κ and (b) a greater range of κ .

all the results from the Yen impulse loading, a value of $2.0 \leq \kappa \leq 2.5$ (orange and red curves, respectively) seems to track best with the results from the Kozeny-Carman functional form (black curves).

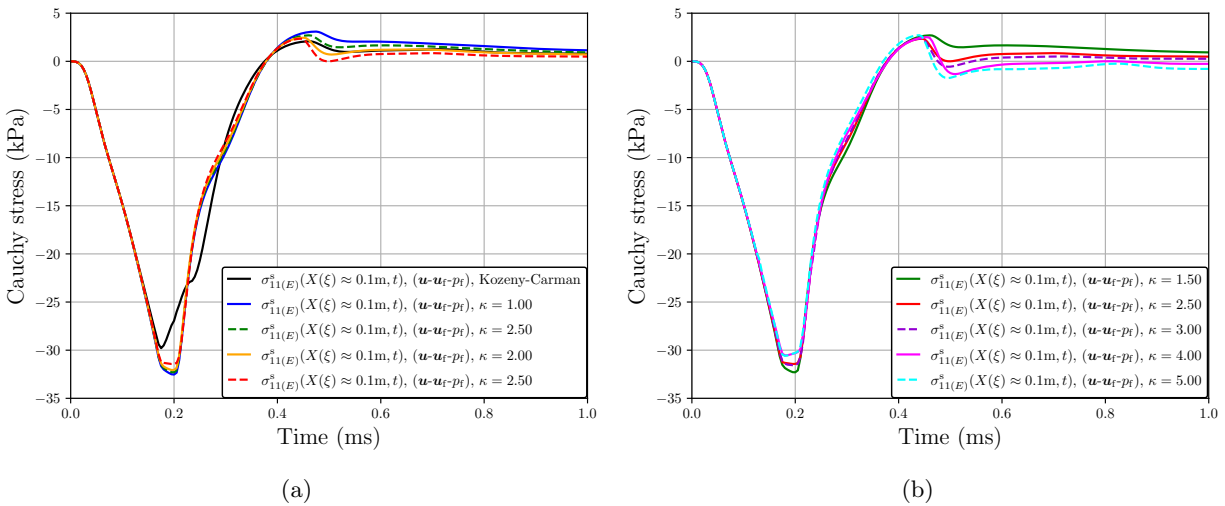


Figure 5.57: Solid extra stress in response to the Yen impulse at 50 kPa overpressure at the Gauss point closest to $X = H$ for (a) a moderate range of κ and (b) a greater range of κ .

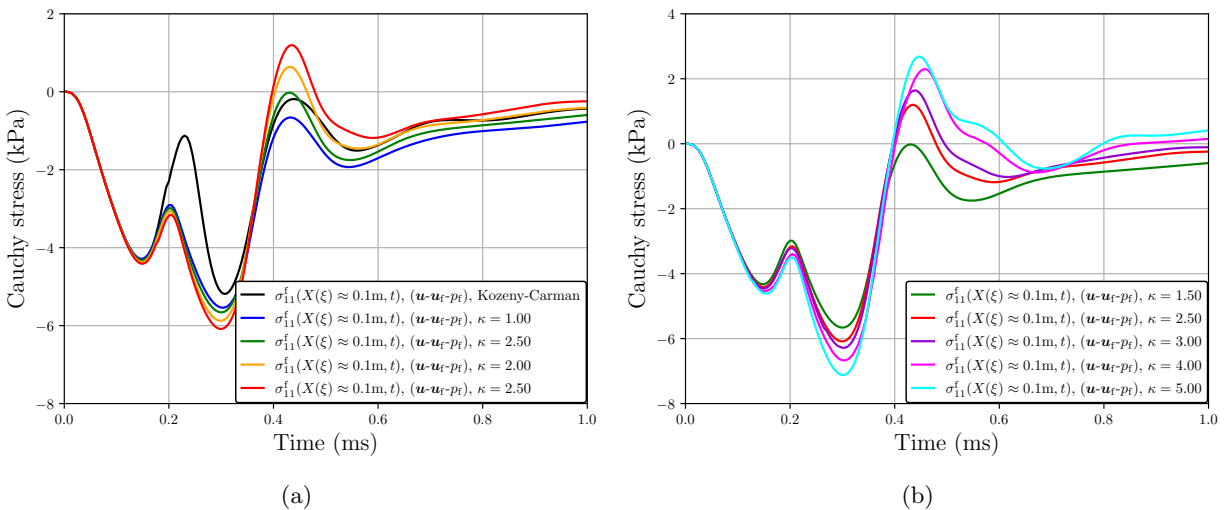


Figure 5.58: Total pore fluid stress in response to the Yen impulse at 50 kPa overpressure at the Gauss point closest to $X = H$ for (a) a moderate range of κ and (b) a greater range of κ .

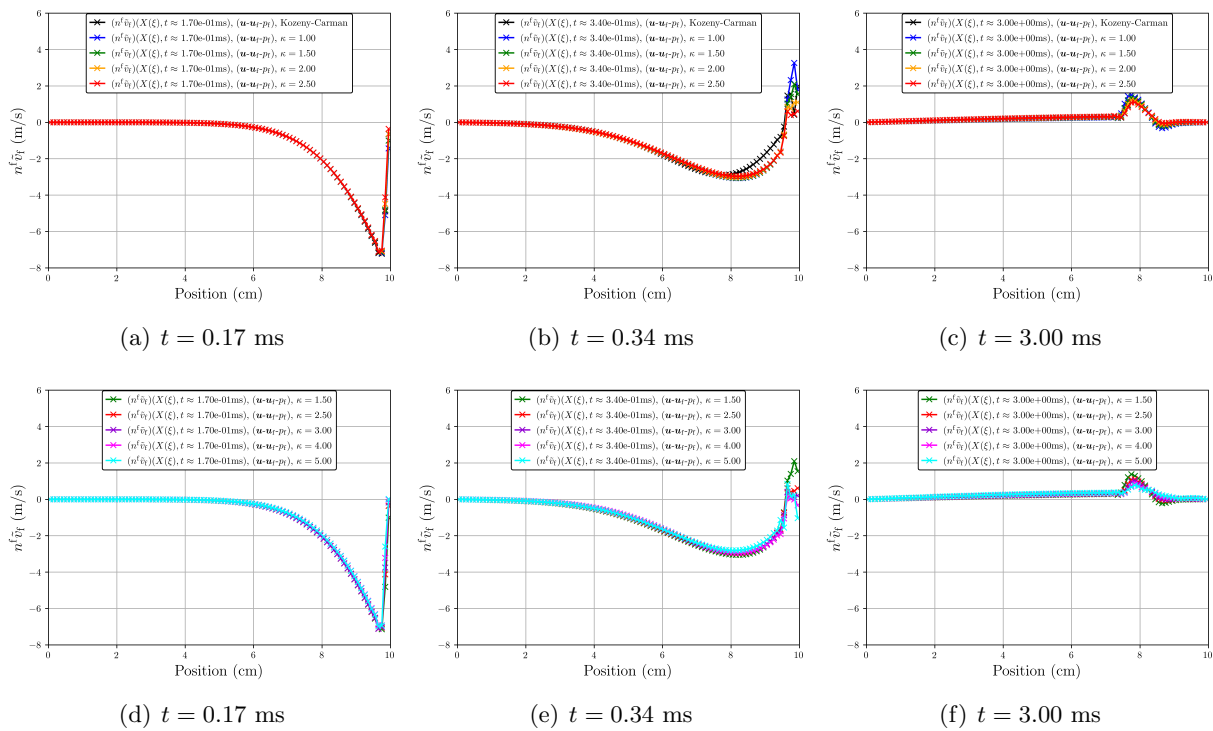


Figure 5.59: Darcy velocity contours in response to the Yen impulse at 50 kPa overpressure for (a)–(c) a moderate range of κ and (d)–(f) a greater range of κ .

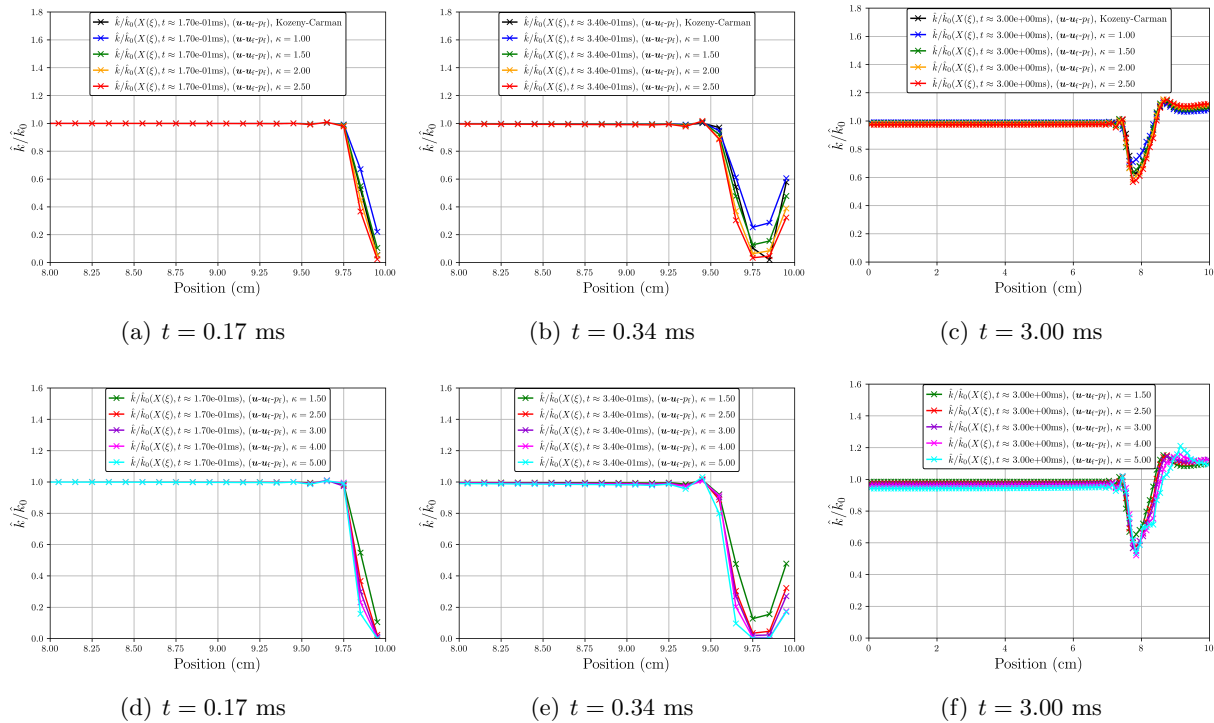


Figure 5.60: Relative hydraulic conductivity contours in response to the Yen impulse at 50 kPa overpressure for (a)–(c) a moderate range of κ and (d)–(f) a greater range of κ . Note that (a), (b), (d), and (e) all zoom in at the top of the mesh (where loading is applied) so as to better observe differences in relative hydraulic conductivity, differences which are non-existent further down the mesh for earlier simulation times.

Moving on to the Friedlander impulse, we see something slightly different from the Yen impulse results. For higher values of κ , there is greater variation in deformation of solid and fluid at the top of the mesh (Figure 5.61 & Figure 5.63), where amplitudes increase with increasing κ . Variation in displacements at the middle of the mesh (Figure 5.62 & Figure 5.64) is comparable to the Yen impulse loading, albeit at greater strains here (which is a result of the longer duration in shock loading).

In contrast to the Yen impulse, there is almost no discernable variation in total stress for the different values of κ (Figure 5.65). As for solid extra stress, for a moderate range of κ (Figure 5.66(a)), the differences are negligible. However, for a greater range of κ (Figure 5.66(b)), we observe that as κ increases, the propensity for the solid skeleton to go into tension (positive values of $\sigma_{11(E)}^s$) diminishes. This is in contrast to what we might expect physically (and from the Yen impulse results), where higher values of κ corresponded to a decrease in dissipation. Here we observe what appears to be an *increase* in dissipation. As stated previously, when the porous material is undergoing compression, larger values of κ decrease the hydraulic conductivity, which inhibits relative motion between solid and fluid (diminishing dissipation), as compared to when κ is small and the inverse occurs. We also note that pore fluid pressure peaks earlier, and higher, when κ increases as shown in Figure 5.67(b).

Again, the differences in relative motion between constituents are minor for changes in κ , particularly just after the onset of shock loading (Figure 5.68). Later in the simulation, we can observe that for greater values of κ , dissipative effects have already occurred (e.g., cyan curve in Figure 5.68(f)), whereas for smaller values of κ , dissipation is still occurring (e.g., green curve in Figure 5.68(f)). The trend in relative hydraulic conductivity follows that of the Yen impulse: greater values of κ induce smaller hydraulic conductivities during compression (Figure 5.69), and larger hydraulic conductivities during expansion (not shown). We note that for all the results from the Friedlander impulse loading, a value of $\kappa = 1.5$ (green curves) seems to track best with the results from the Kozeny-Carman functional form (black curves).

Having said that, for both the Yen and the Friedlander impulse, initial testing indicates that

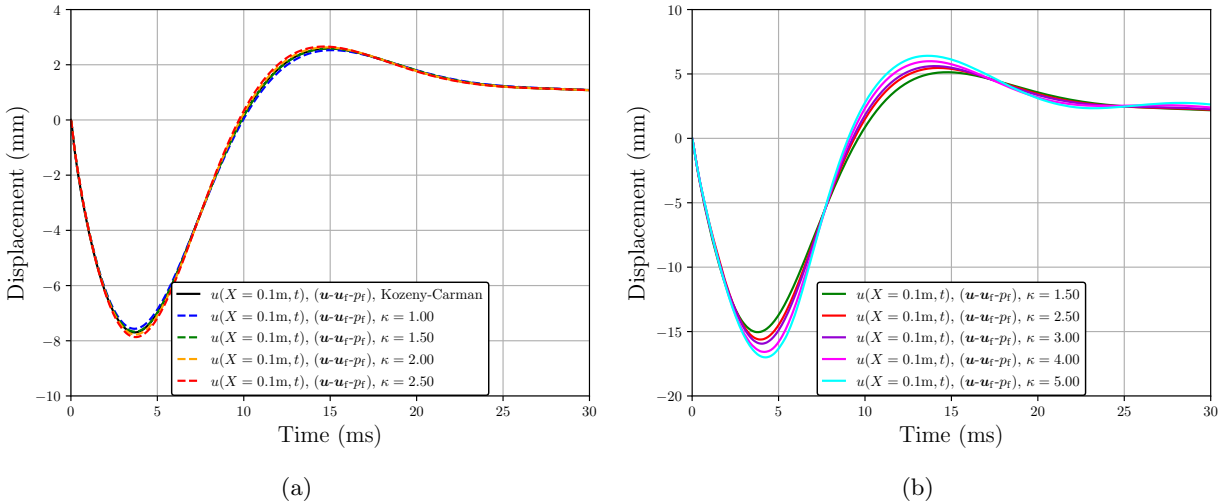


Figure 5.61: Solid skeleton displacements in response to the Friedlander impulse at $X = H$ for (a) 25 kPa overpressure and a moderate range of κ and (b) 50 kPa overpressure and a greater range of κ .

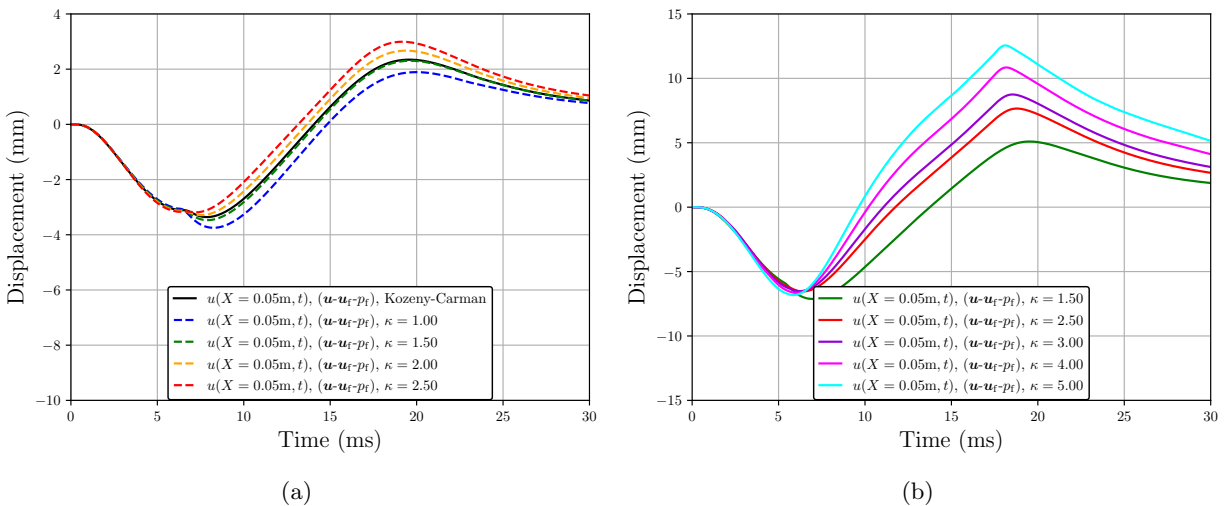


Figure 5.62: Solid skeleton displacements in response to the Friedlander impulse at $X = H/2$ for (a) 25 kPa overpressure and a moderate range of κ and (b) 50 kPa overpressure and a greater range of κ .

a higher value of κ is preferred for stability at even higher overpressures, as well as for the locally inhomogeneous temperature regime (Chapter 5.3.3.2). It appears from testing that $\kappa = 2.5$ is the “optimal” value, and is thus used throughout this work other than in this sensitivity study.

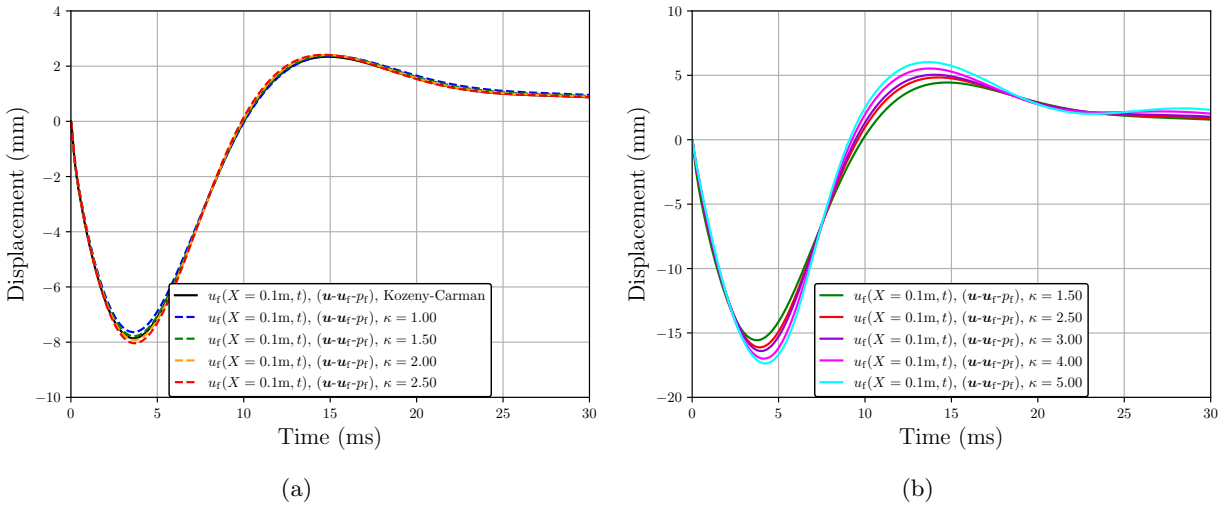


Figure 5.63: Pore fluid displacements in response to the Friedlander impulse at $X = H$ for (a) 25 kPa overpressure and a moderate range of κ and (b) 50 kPa overpressure and a greater range of κ .

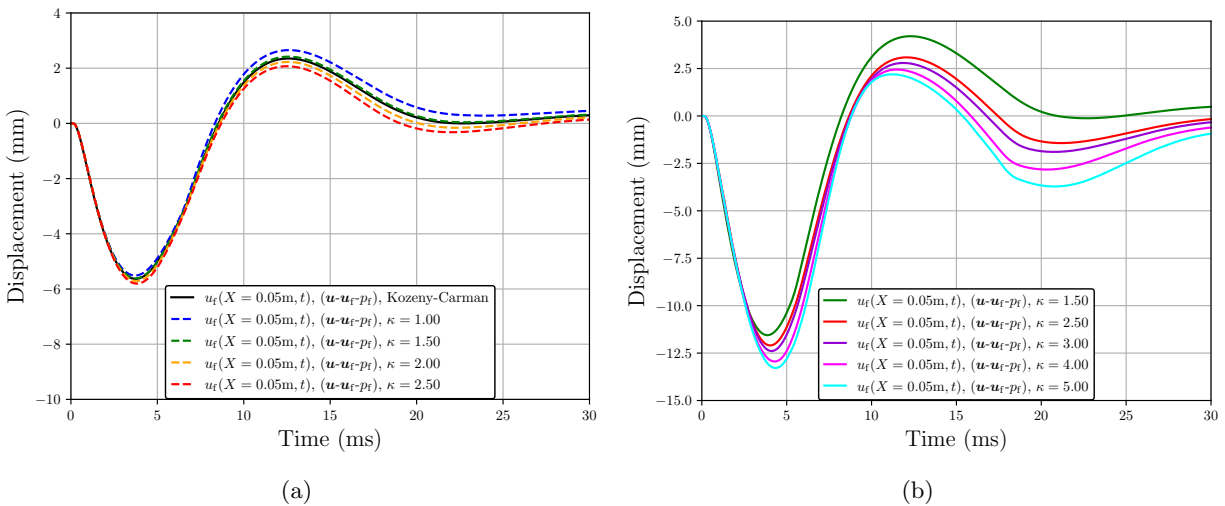


Figure 5.64: Pore fluid displacements in response to the Friedlander impulse at $X = H$ for (a) 25 kPa overpressure and a moderate range of κ and (b) 50 kPa overpressure and a greater range of κ .

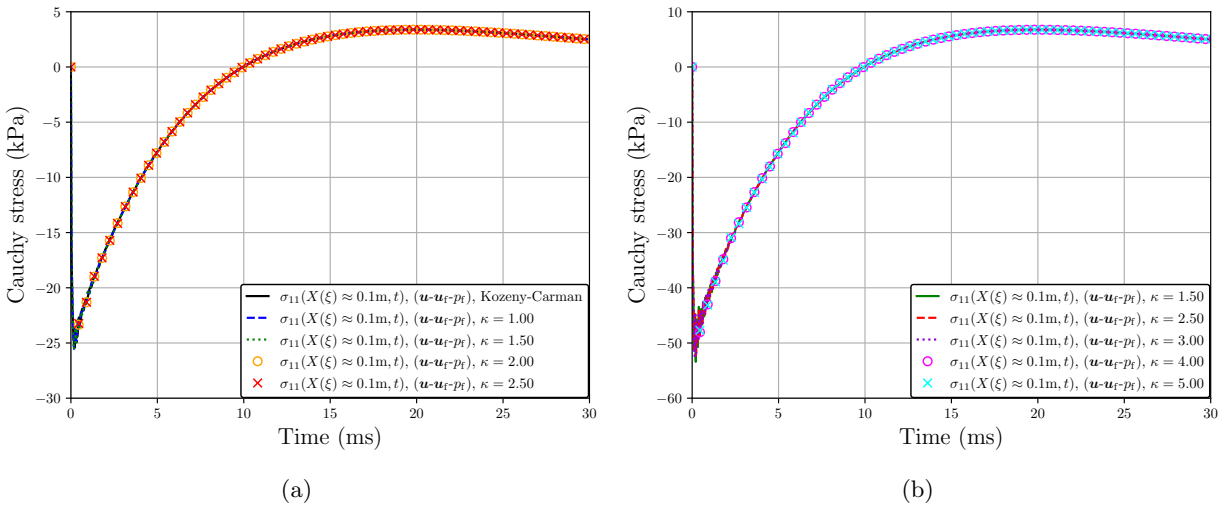


Figure 5.65: Total Cauchy stress in response to the Friedlander impulse at the Gauss point closest to $X = H$ for (a) 25 kPa overpressure and a moderate range of κ and (b) 50 kPa overpressure and a greater range of κ .

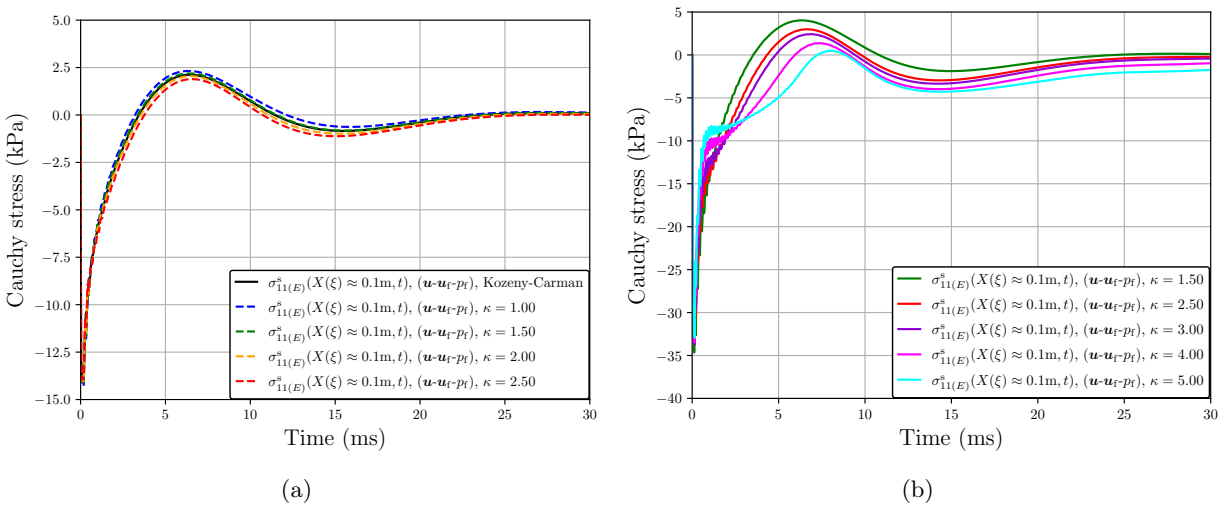


Figure 5.66: Solid extra stress in response to the Friedlander impulse at the Gauss point closest to $X = H$ for (a) 25 kPa overpressure and a moderate range of κ and (b) 50 kPa overpressure and a greater range of κ .

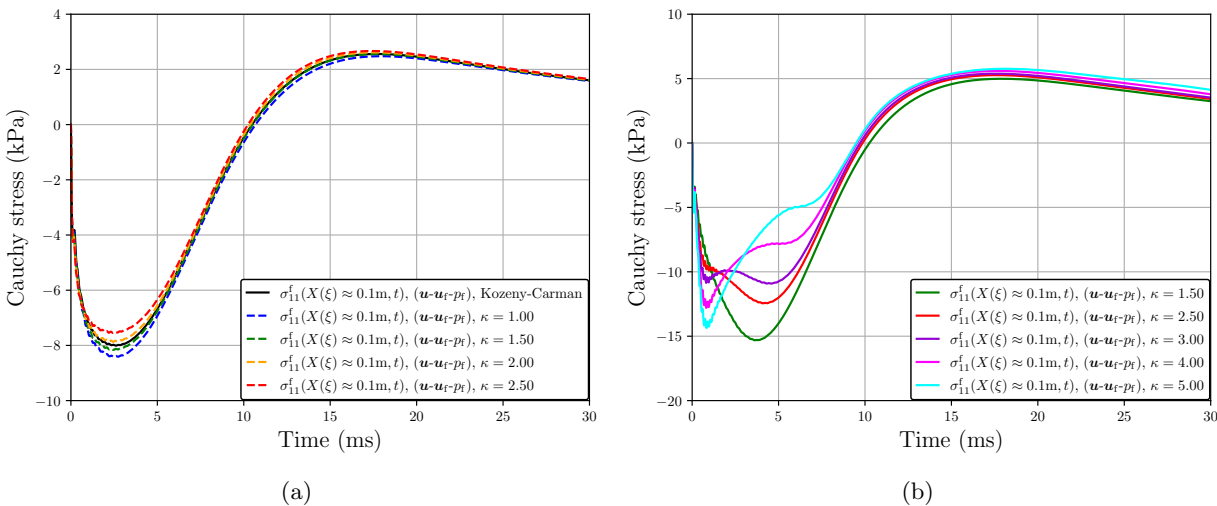


Figure 5.67: Total pore fluid stress in response to the Friedlander impulse at the Gauss point closest to $X = H$ for (a) 25 kPa overpressure and a moderate range of κ and (b) 50 kPa overpressure and a greater range of κ .

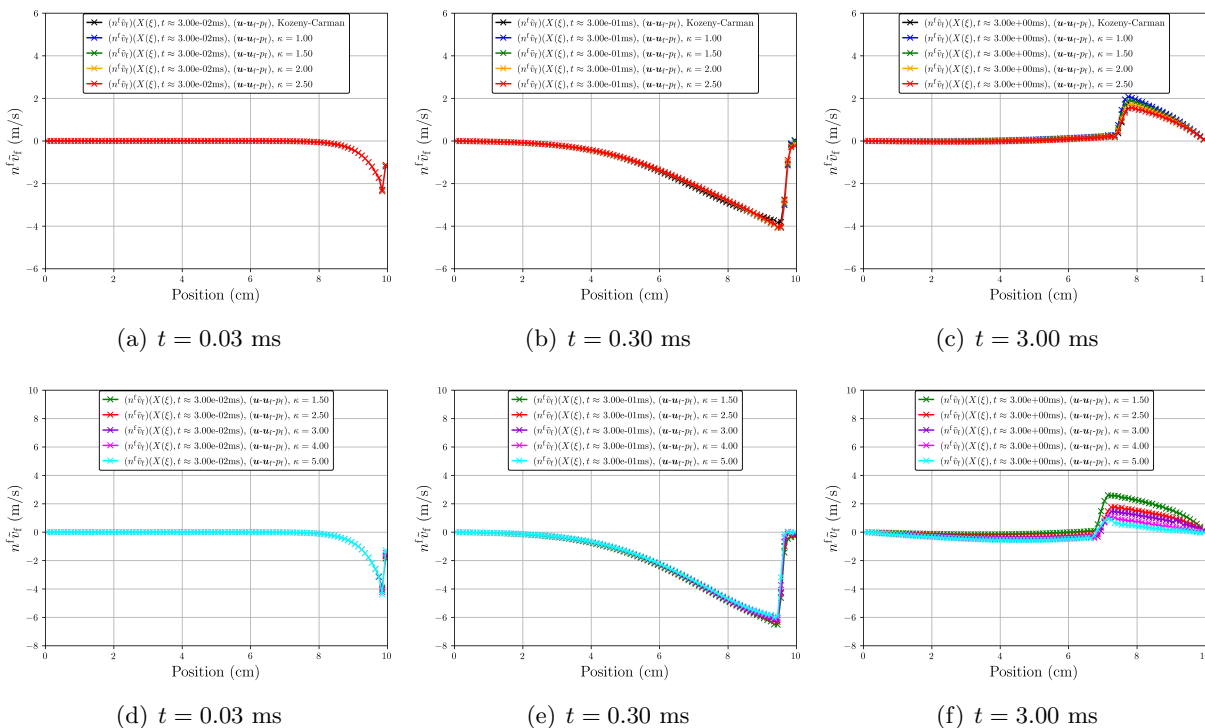


Figure 5.68: Darcy velocity contours in response to the Friedlander impulse (a)–(c) at 25 kPa overpressure for a moderate range of κ and (d)–(f) at 50 kPa overpressure for a greater range of κ . Time samples are shown in Figure 5.83.

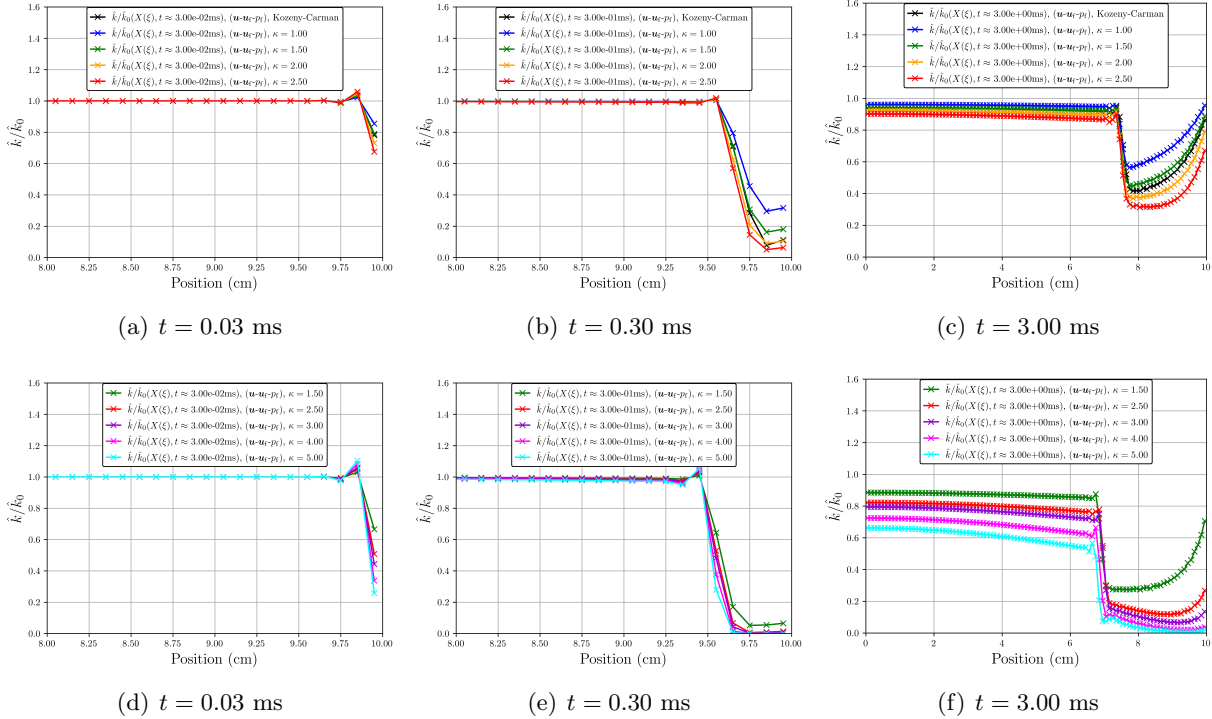


Figure 5.69: Relative hydraulic conductivity contours in response to the Friedlander impulse (a)–(c) at 25 kPa overpressure for a moderate range of κ and (d)–(f) at 50 kPa overpressure for a greater range of κ . Note that (a), (b), (d), and (e) all zoom in at the top of the mesh (where loading is applied) so as to better observe differences in relative hydraulic conductivity, differences which are non-existent further down the mesh for earlier simulation times. Time samples are shown in Figure 5.83.

Investigation of the pore fluid viscous stress tensor. In the preceding sections on shock loading of lung parenchyma, we have ignored the effects of the pore fluid extra stress $\boldsymbol{\sigma}_E^f$ on the poroelastodynamic response, i.e., we assumed $\boldsymbol{\sigma}_E^f \approx \mathbf{0}$. In the present section, this assumption is not made, and a Newtonian fluid law is assumed [Holzapfel, 2000], such that

$$\boldsymbol{\sigma}_E^f := n^f \kappa_f \text{tr}(\mathbf{d}_f) \mathbf{1} + 2\mu_f \mathbf{d}_f, \quad (5.80)$$

where κ_f denotes the constant bulk viscosity of the compressible pore fluid and

$$\mathbf{d}_f := \frac{1}{2}(\text{grad} \mathbf{v}_f + \text{grad}^T \mathbf{v}_f). \quad (5.81)$$

As noted in Section 4.1.4, paragraph *The need for higher-order elements in the case of viscous pore fluid flow*, as well as in Irwin et al. [2023d], introduction of the pore fluid extra stress requires resolution of the porosity gradient (appearing in Darcy’s law) and the Laplacian of the pore fluid velocity (appearing in the balance of linear momentum of the pore fluid). Both terms introduce C^1 -continuity requirements in the variational forms of the governing equations, thus, standard Lagrange elements are ill-suited to guarantee convergence, and the Hermite cubic elements are used in their stead (refer to Figure 4.1 and/or Figure 4.3(d)). Geometrical and material parameters for the following simulations are listed in Tables 5.19 & 5.20, respectively.

Table 5.19: Material parameters for pore fluid viscous stress tensor simulations. Values taken from Clayton et al. [2021], Lande and Mitzner [2006], Holmes et al. [2011], Rand et al. [1964], Shang et al. [2019]. Viscosity values for air are interpolated for resting body temperature 37° C; bulk modulus, density and bulk viscosity for blood are estimated using values for water at resting body temperature 37° C, while shear viscosity is estimated from Rand et al. [1964]. A value of $\kappa = 2.5$ was chosen for the hyperbolic hydraulic conductivity.

K^{skel} (kPa)	G (kPa)	K_s (kPa)	K_f^η (kPa)	ρ_0^{sR} (kg/m ³)
7.5	3	2.2×10^6	140; 2.2×10^6	1000
ρ_0^{fR} (kg/m ³)	n_0^f	\hat{k}_0 (m ² /Pa-s)	μ_f (mPa-s)	κ_f (mPa-s)
1.138; 1006	0.664; 0.99	10^{-5} ; 6.3×10^{-8}	1.89×10^{-2} ; 3	2.03×10^{-2} ; 1.93

To start, we assume an impermeable membrane of lung parenchyma, in other words, the pore air is allowed to move freely within the column of lung parenchyma, but cannot escape at either end.

Table 5.20: Geometrical and loading parameters for pore fluid viscous stress tensor simulations.

Overpressure load type	H (cm)	A (cm ²)	h_0^e (cm)	t_0^σ (kPa)	t_0 (ms)	t_1 (ms)
Yen impulse	10	1	0.1	50	0.17	0.34
Friedlander impulse	10	1	0.1	50	10	N/A

Displacement profiles between the nearly-inviscid (Darcy) and viscous (Darcy-Brinkman, inclusion of pore fluid extra stress) simulations subjected to the Yen impulse at 50 kPa overpressure are shown in Figure 5.70. It is evident that inclusion of the pore fluid extra stress for this example has a negligible effect on the motion of the lung parenchyma and pore fluid within. This is likely due to how small of a contribution the pore fluid extra stress, shown in Figure 5.71(a), has on the total fluid stress, shown in Figure 5.71(b). Pore fluid extra stress is three orders of magnitude smaller than the pore fluid pressure for this application.

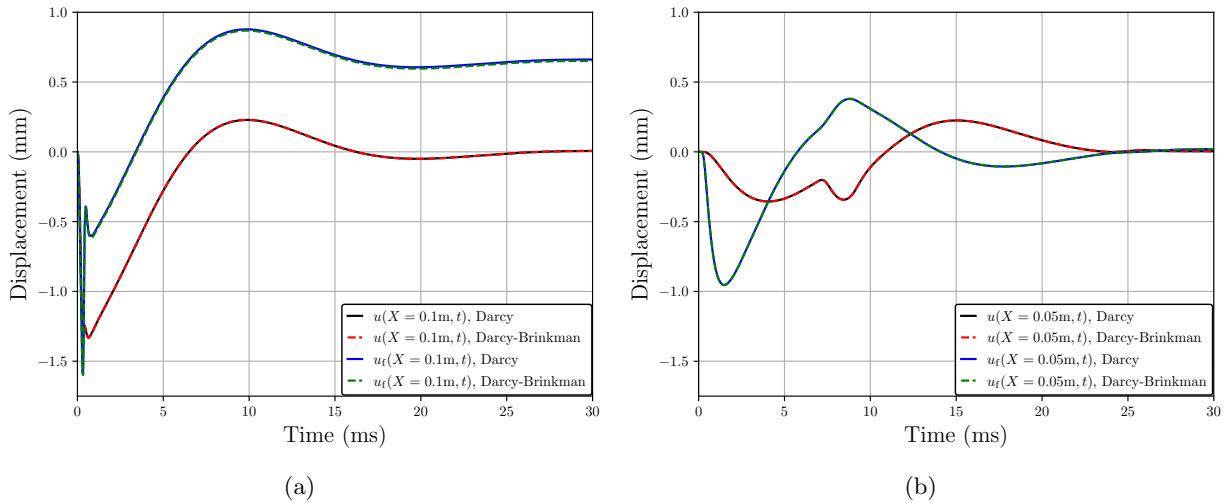


Figure 5.70: Displacement results from applying the Yen impulse (50 kPa) to the impermeable lung parenchyma for (a) solid skeleton displacement $u(X = H, t)$ and pore fluid displacement $u_f(X = H, t)$, and (b) solid skeleton displacement $u(X = H/2, t)$ and pore fluid displacement $u_f(X = H/2, t)$. Initial porosity is $n_0^f = 0.664$.

Next, we assume a permeable membrane, i.e., the pore air is allowed to escape from the top of the column. Again we see that the pore fluid extra stress has negligible effects on displacements (refer to Figure 5.72) and total fluid stress (refer to Figure 5.73). However, pore fluid extra stress is only one order of magnitude smaller than total pore fluid stress for the permeable membrane. In

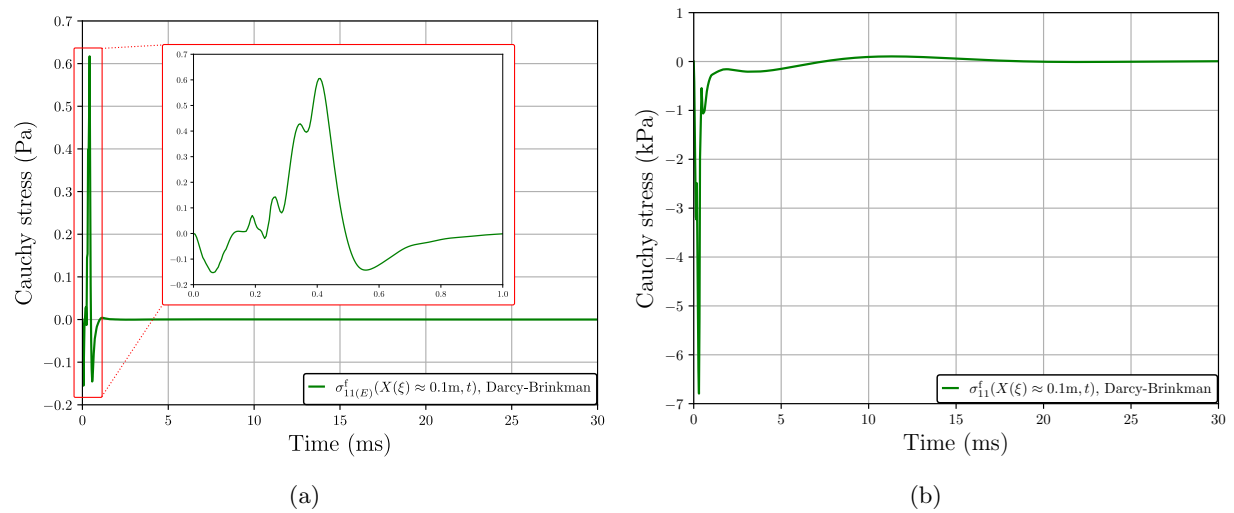


Figure 5.71: Pore fluid stress results from applying the Yen impulse (50 kPa) to the impermeable lung parenchyma for (a) pore fluid extra stress at the Gauss point closest to $X = H$, and (b) total pore fluid stress $\sigma_{11}^f := \sigma_{11(E)}^f - n^f p_f$ at the Gauss point closest to $X = H$. Initial porosity is $n_0^f = 0.664$.

Figure 5.74, we see how pore fluid extra stress “scales” with pore fluid velocity gradient—denoted by the slope of the velocity contour curve—and porosity, and how each evolve over time. Sampled times are (a) at maximum overpressure loading, (b) when overpressure loading stops, and (c) well after loading has ended. Peak overpressure loading occurs at $170 \mu\text{s}$, but the effects of the shock loading are not observed until later, see, for example, Figure 5.74(b) when the impulse ends. In Figure 5.74(c) we see that the magnitude of the pore fluid extra stress has greatly dissipated well after load is removed.

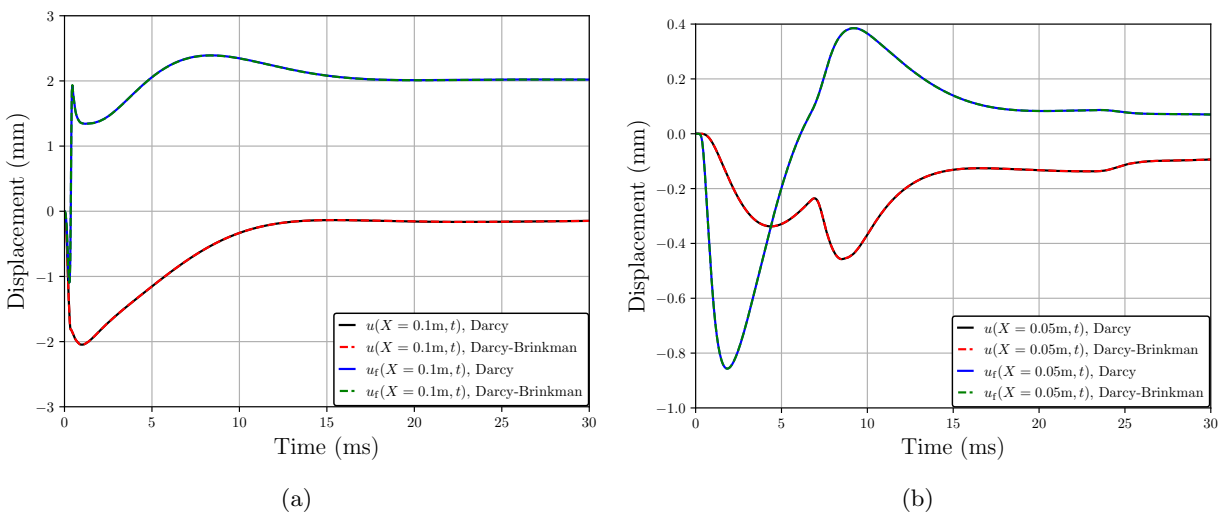


Figure 5.72: Displacement results from applying the Yen impulse (50 kPa) to the permeable lung parenchyma for (a) solid skeleton displacement $u(X = H, t)$ and pore fluid displacement $u_f(X = H, t)$, and (b) solid skeleton displacement $u(X = H/2, t)$ and pore fluid displacement $u_f(X = H/2, t)$. Initial porosity is $n_0^f = 0.664$.

Keeping the permeable boundary condition, we now swap the pore air for pore blood, in other words, we assume the lung is saturated with blood as the pore fluid, assuming blood can be modeled as a Newtonian fluid. We adjust the pore fluid density, bulk modulus, and viscosities appropriately (refer to Table 5.19). Initial porosity is also increased to $n_0^f = 0.99$ (from 0.664). While the high initial porosity is not a physically realistic scenario, the magnitude of the pore fluid extra stress should increase as pore fluid extra stress scales with porosity and viscosity. This is what is observed in Figure 5.76: the pore fluid extra stress accounts for some oscillations in the total

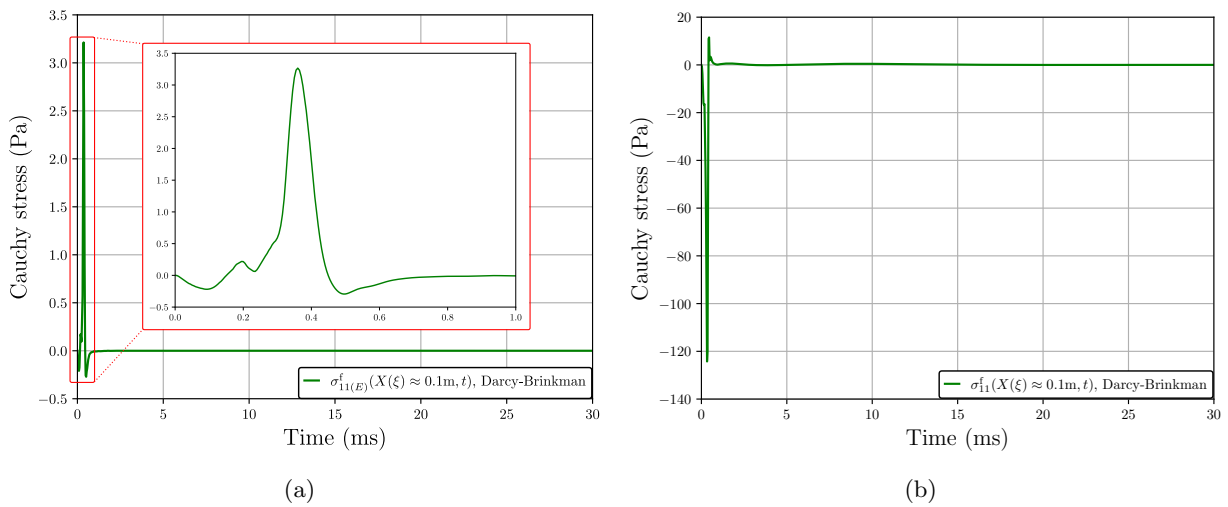


Figure 5.73: Pore fluid stress results from applying the Yen impulse (50 kPa) to the permeable lung parenchyma for (a) pore fluid extra stress at the Gauss point closest to $X = H$, and (b) total pore fluid stress $\sigma_{11}^f := \sigma_{11(E)}^f - n^f p_f$ at the Gauss point closest to $X = H$. Initial porosity is $n_0^f = 0.664$.

pore fluid stress at the onset of the shock load. However, the solid extra stress (i.e., the material stress of the lung parenchyma tissue itself) is not affected by the inclusion of the pore fluid extra stress (as shown in Figure 5.77). This may have to do with the fact that the motion of the lung parenchyma and the pore blood are not affected either (refer to Figure 5.75).

In contrast to the example with pore air (refer to Figure 5.72), pore fluid (blood) and solid skeleton (lung parenchyma) displacements are similar (Figure 5.75), owing to the similar densities of lung tissue and blood (i.e., the two phases behave similarly to a single-phase material because of the similarity in densities). Furthermore, when shear viscosity of the pore fluid is increased, the initial hydraulic conductivity \hat{k}_0 is reduced. Since seepage velocity ($n^f \tilde{\mathbf{v}}_f$) scales with hydraulic conductivity per Darcy's (and Darcy-Brinkman's) law, relative velocity between solid and fluid phases is reduced.

Comparing now the contours of pore fluid extra stress, pore fluid velocity, and porosity (Figure 5.78) for blood-saturated lung parenchyma to that of air-saturated lung parenchyma (Figure 5.74), we see that in the latter the shock wave percolates more quickly through the mixture than in the former. Velocity of pore air is also greater in magnitude than for pore blood. Furthermore, porosity gradients are small for high initial porosity in blood-saturated lung parenchyma compared to moderate initial porosity in air-saturated lung parenchyma. In fact, we see that porosity remains high for the duration of the simulation as compared to air-saturated lung parenchyma, where more fluctuations in porosity are observed.



(a) $t = 0.17$ ms

(b) $t = 0.34$ ms

(c) $t = 3.00$ ms

Figure 5.74: Contours along the length of the mesh for pore fluid extra stress $\sigma_{11(E)}^f$, pore fluid velocity v_f and porosity n^f for permeable lung parenchyma after applying the Yen impulse with 50 kPa maximum overpressure. Initial porosity is $n_0^f = 0.664$.

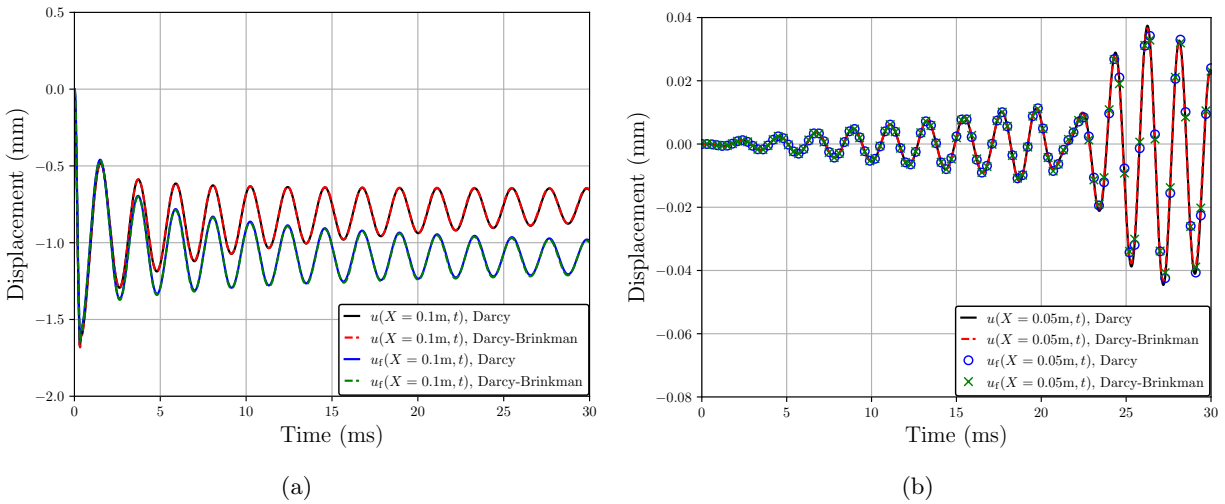


Figure 5.75: Displacement results from applying the Yen impulse (50 kPa) to the permeable, blood-saturated lung parenchyma for (a) solid skeleton displacement $u(X = H, t)$ and pore fluid displacement $u_f(X = H, t)$, and (b) solid skeleton displacement $u(X = H/2, t)$ and pore fluid displacement $u_f(X = H/2, t)$. Initial porosity is $n_0^f = 0.99$.

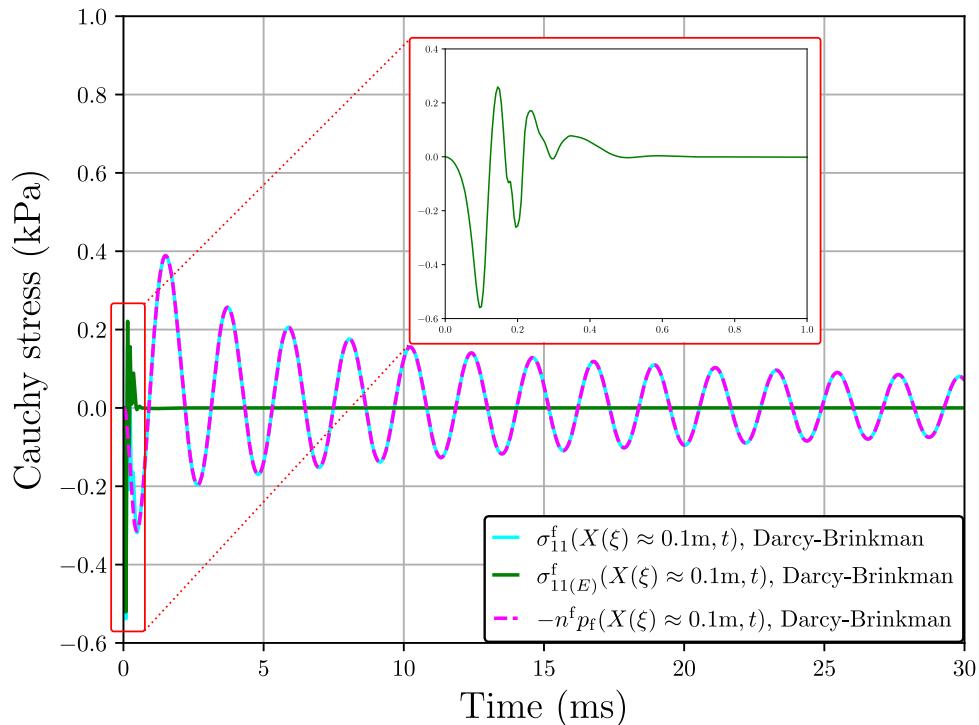


Figure 5.76: Pore fluid stress results from applying the Yen impulse (50 kPa) to the permeable, blood-saturated lung parenchyma for the Gauss point closest to $X = H$. Initial porosity is $n_0^f = 0.99$.

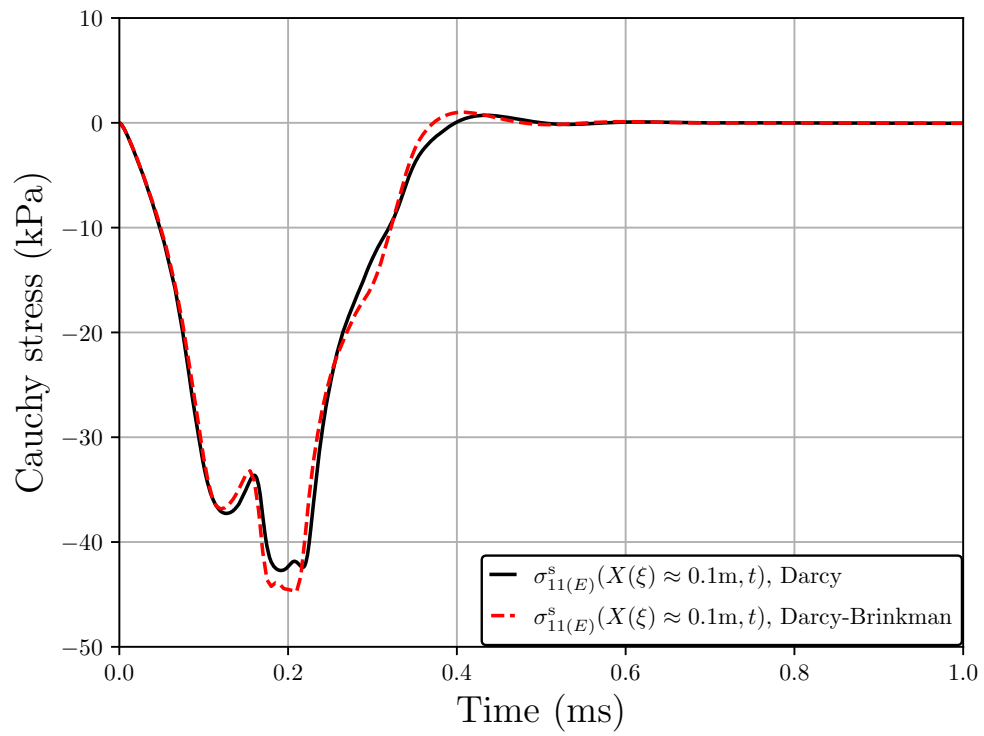


Figure 5.77: Solid extra stress results from applying the Yen impulse (50 kPa) to the permeable, blood-saturated lung parenchyma for the Gauss point closest to $X = H$. Initial porosity is $n_0^f = 0.99$.



(a) $t = 0.03$ ms

(b) $t = 0.30$ ms

(c) $t = 3.00$ ms

Figure 5.78: Contours along the length of the mesh for pore fluid extra stress $\sigma_{11(E)}^f$, pore fluid velocity v_f and porosity n^f for permeable, blood-saturated lung parenchyma after applying the Yen impulse with 50 kPa maximum overpressure.

We now present the results of the simulations using the Friedlander impulse loading at maximum overpressure $t_0^\sigma = 50$ kPa, which, again, is more applicable for free-field shock loading of the lung parenchyma. Proceeding as before, we first assume an impermeable membrane of air-saturated lung parenchyma with initial porosity $n_0^f = 0.664$. Looking at Figure 5.79 and Figure 5.80, we see a similar trend when comparing to the Yen impulse loading: the pore fluid extra stress is small and does not account for any discrepancy between motions of solid and fluid, and total fluid stress, between nearly-inviscid (Darcy) and viscous (Darcy-Brinkman) pore fluid flow.

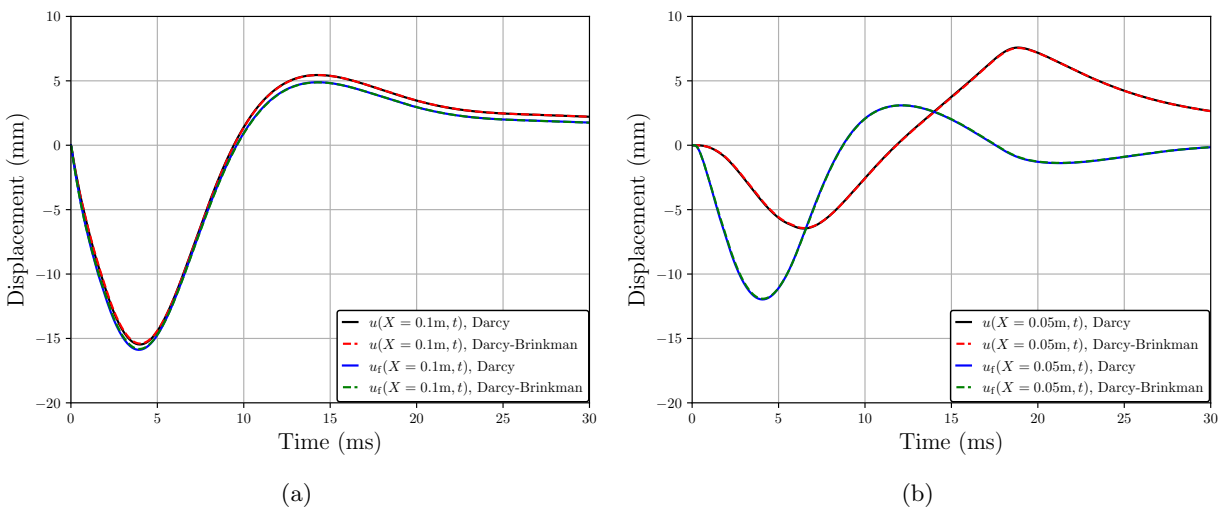


Figure 5.79: Displacement results from applying the Friedlander impulse (50 kPa) to the impermeable lung parenchyma for (a) solid skeleton displacement $u(X = H, t)$ and pore fluid displacement $u_f(X = H, t)$, and (b) solid skeleton displacement $u(X = H/2, t)$ and pore fluid displacement $u_f(X = H/2, t)$. Initial porosity is $n_0^f = 0.664$.

When the top of the column allows fluid to escape (i.e., when we use the permeable boundary condition), we again see no difference between the nearly-inviscid (Darcy) and viscous (Darcy-Brinkman) displacements (refer to Figure 5.81), though we note that strains are much larger here than for the impermeable boundary. Total pore fluid stress is unaffected by the pore fluid extra stress (refer to Figure 5.82). Furthermore, pore fluid extra stress begins to diminish as the shock wave moves along the mesh (where the time sampling locations used for the contour stills are shown by Figure 5.83), as shown in Figure 5.84. We again see how pore fluid extra stress is influenced by

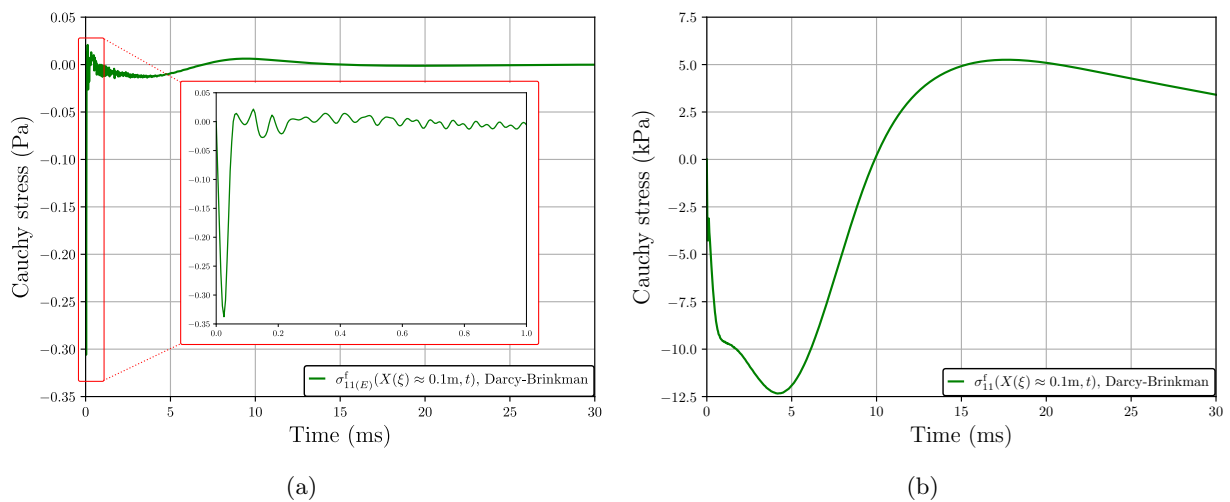


Figure 5.80: Pore fluid stress results from applying the Friedlander impulse (50 kPa) to the impermeable lung parenchyma for (a) pore fluid extra stress at the Gauss point closest to $X = H$, and (b) total pore fluid stress $\sigma_{11}^f := \sigma_{11(E)}^f - n^f p_f$ at the Gauss point closest to $X = H$. Initial porosity is $n_0^f = 0.664$.

large gradients in pore fluid velocity (Figure 5.84(a) and Figure 5.84(b)). In contrast to the Yen impulse (shock-tube loading), we also see larger porosity gradients (Figure 5.84(b)).

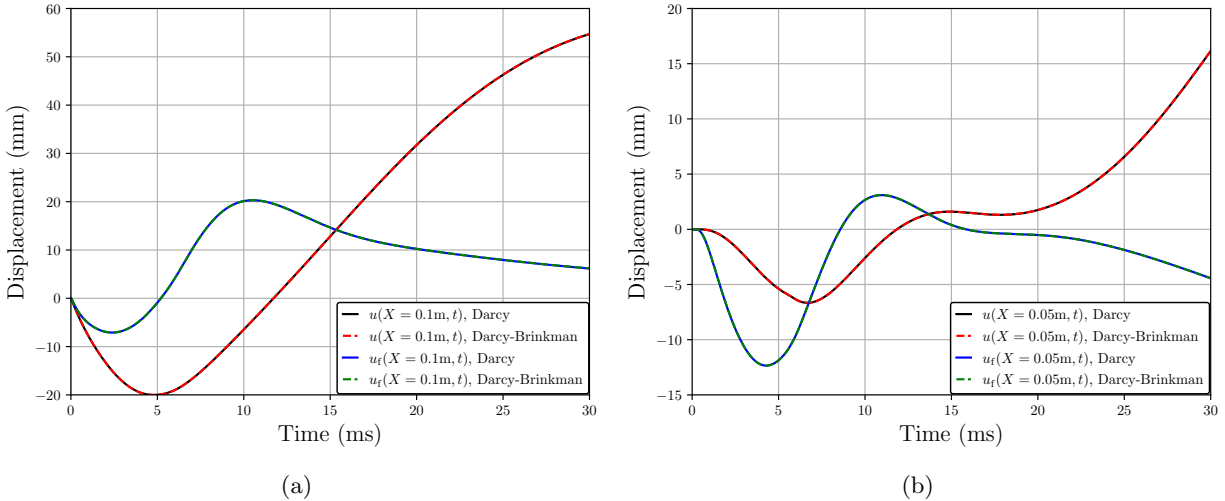


Figure 5.81: Displacement results from applying the Friedlander impulse (50 kPa) to the permeable lung parenchyma for (a) solid skeleton displacement $u(X = H, t)$ and pore fluid displacement $u_f(X = H, t)$, and (b) solid skeleton displacement $u(X = H/2, t)$ and pore fluid displacement $u_f(X = H/2, t)$. Initial porosity is $n_0^f = 0.664$.

Continuing, the pore air is now swapped for pore blood; pore fluid density, bulk modulus and viscosities are adjusted accordingly. Initial porosity is increased to 0.99. We observe that the pore fluid extra stress has no impact on displacement (refer to Figure 5.85), although its magnitude is on par with the total pore fluid stress, at least at the onset of the shock load before the pore fluid pressure response dominates (refer to Figure 5.86). However, the pore fluid extra stress does not affect the solid extra stress, that is, no additional tensile forces indicative of potential damage in the lung parenchyma [Fung, 1990] are observed as compared to the nearly-inviscid pore fluid (refer to Figure 5.87). Similarly to the Yen impulse for blood-saturated lung parenchyma, we see (refer to Figure 5.88) the shock wave percolating more slowly through the mixture than for air-saturated lung parenchyma, for either type of impulse loading.

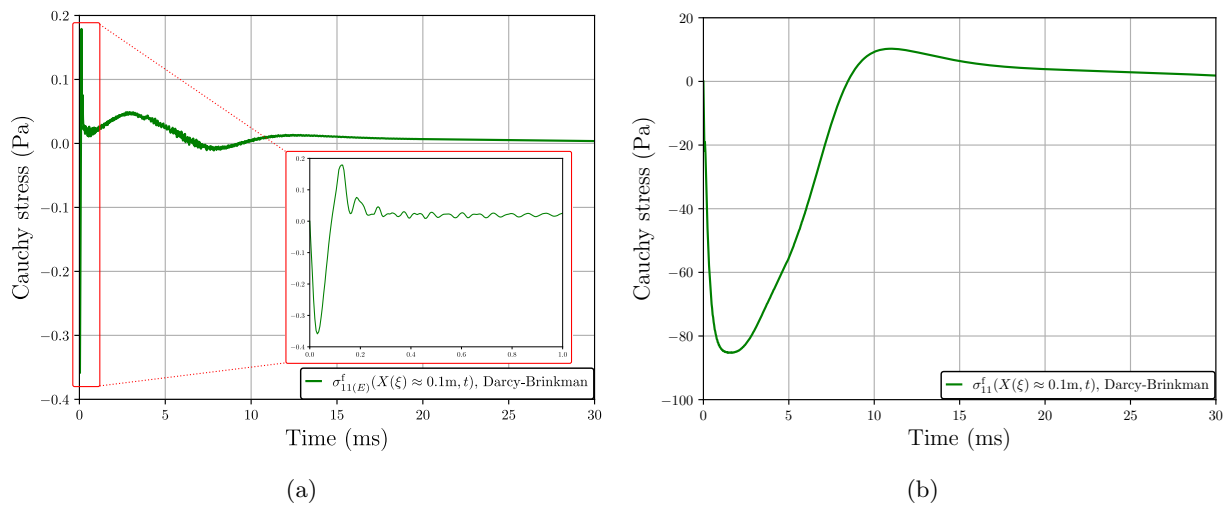


Figure 5.82: Pore fluid stress results from applying the Friedlander impulse (50 kPa) to the permeable lung parenchyma for (a) pore fluid extra stress at the Gauss point closest to $X = H$, and (b) total pore fluid stress $\sigma_{11}^f := \sigma_{11}^f(E) - n^f p_f$ at the Gauss point closest to $X = H$. Initial porosity is $n_0^f = 0.664$.

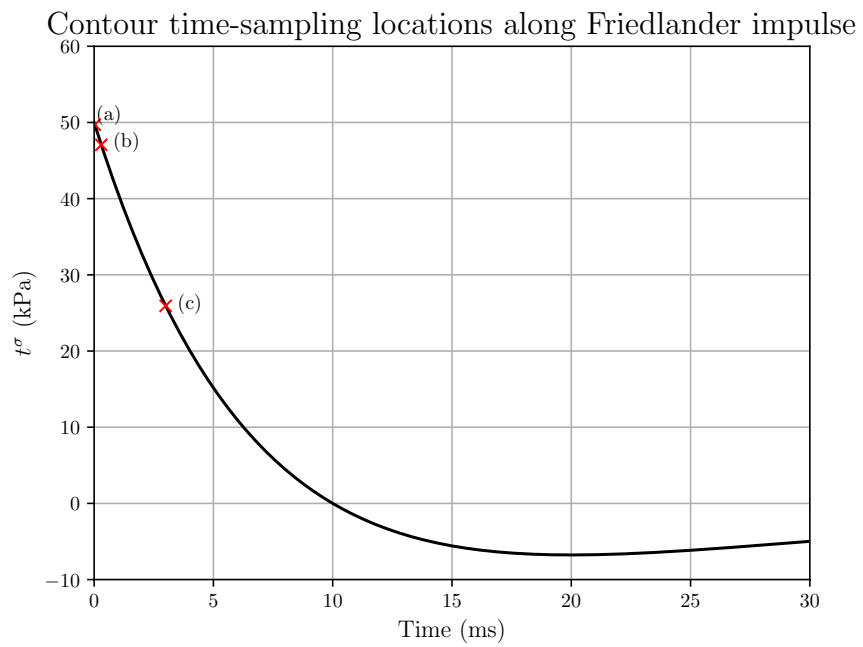
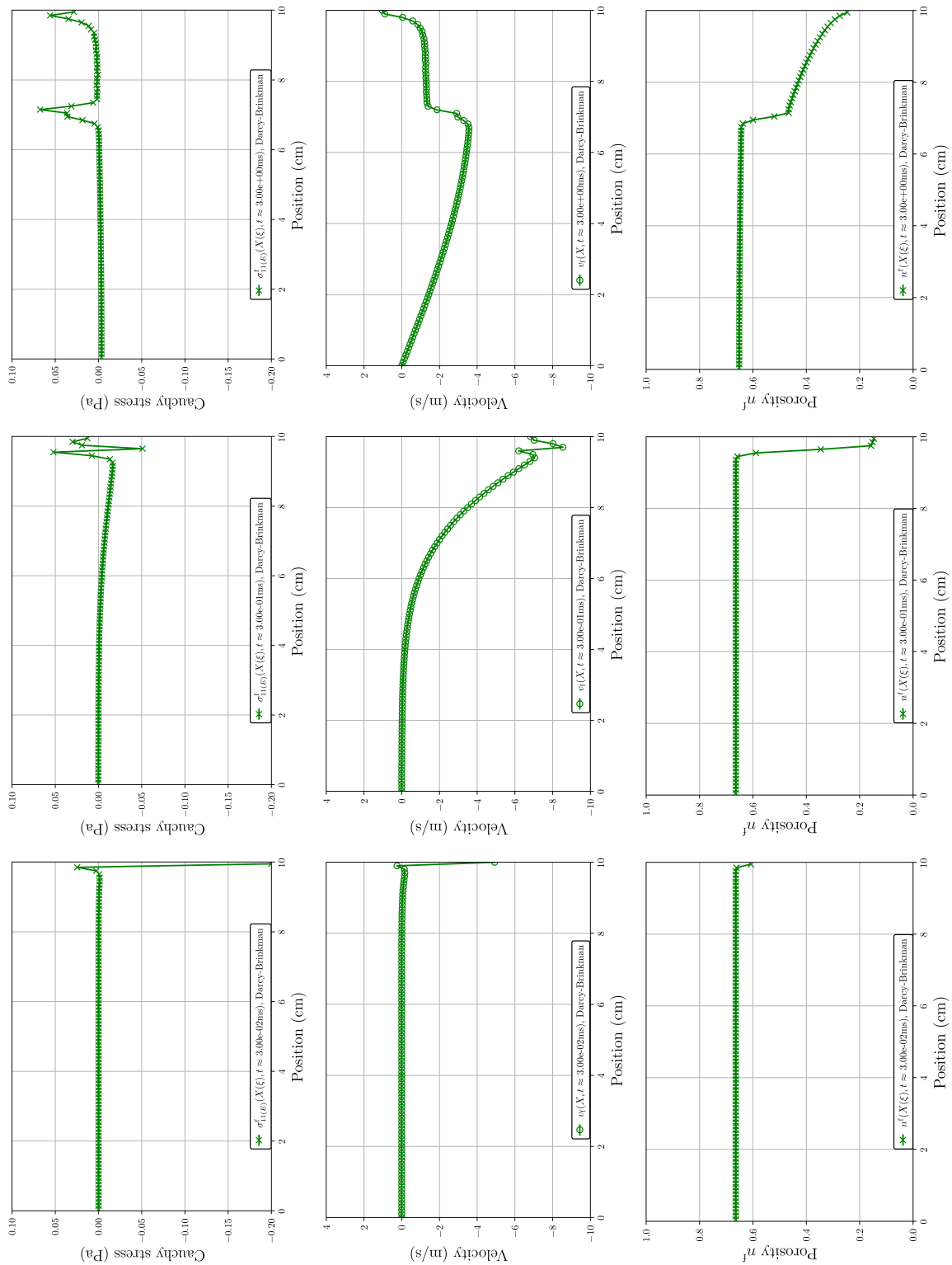


Figure 5.83: Sampling locations along the Friedlander impulse for 50 kPa maximum overpressure used in the contour plots



(a) $t = 0.03$ ms

(b) $t = 0.30$ ms

(c) $t = 3.00$ ms

Figure 5.84: Contours along the length of the mesh for pore fluid extra stress $\sigma_{11}^{(E)}$, pore fluid velocity v_f and porosity n^f for permeable lung parenchyma after applying the Friedlander impulse with 50 kPa maximum overpressure. Initial porosity is $n_0^f = 0.664$.

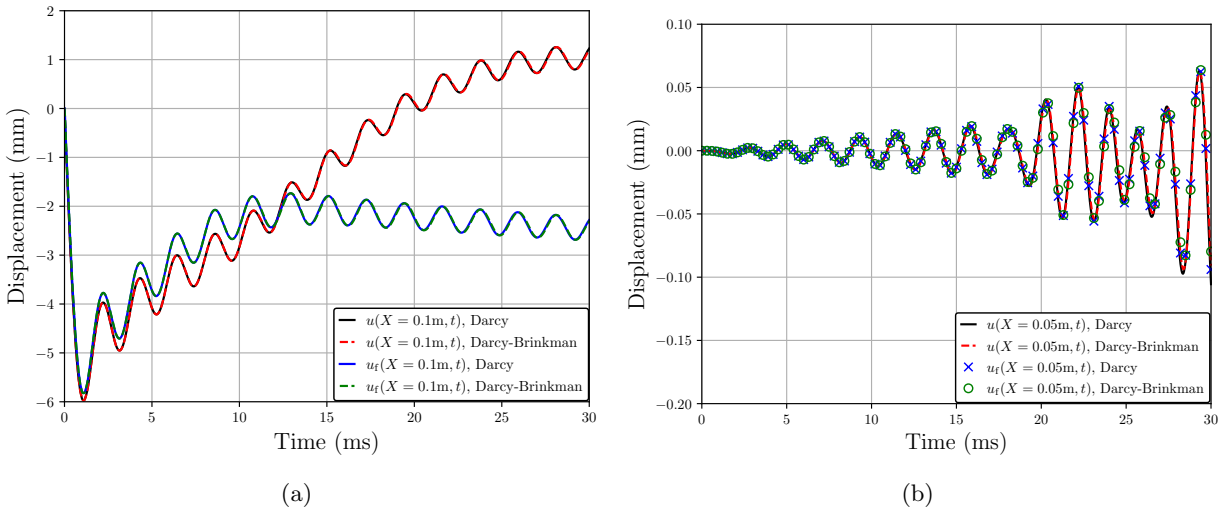


Figure 5.85: Displacement results from applying the Friedlander impulse (50 kPa) to the permeable, blood-saturated lung parenchyma for (a) solid skeleton displacement $u(X = H, t)$ and pore fluid displacement $u_f(X = H, t)$, and (b) solid skeleton displacement $u(X = H/2, t)$ and pore fluid displacement $u_f(X = H/2, t)$. Initial porosity is $n_0^f = 0.99$.

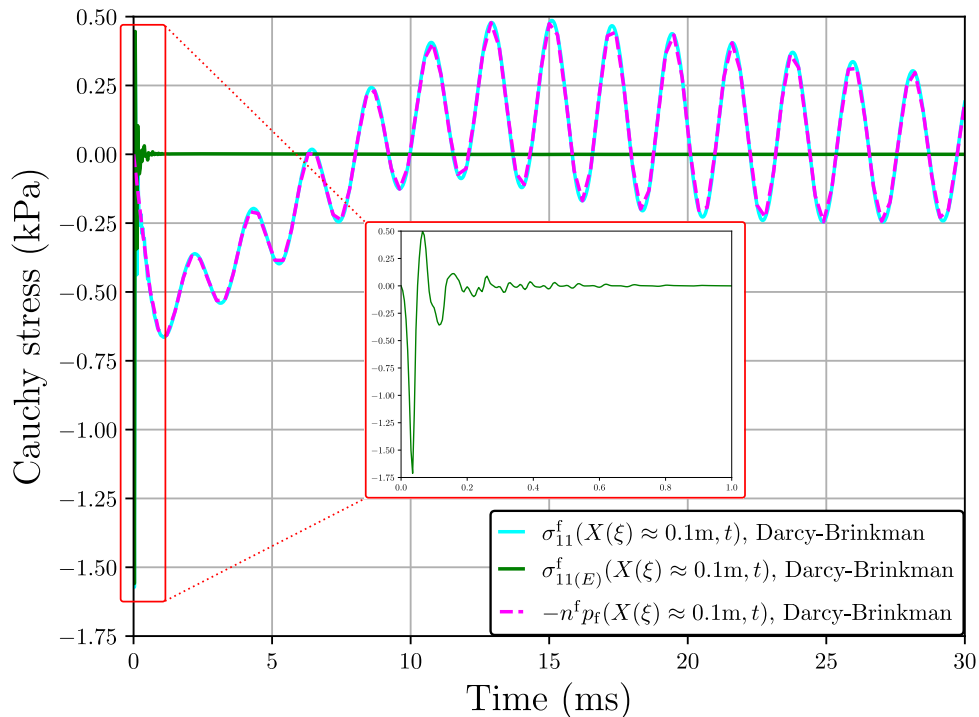


Figure 5.86: Pore fluid stress results from applying the Friedlander impulse (50 kPa) to the permeable, blood-saturated lung parenchyma for the Gauss point closest to $X = H$. Initial porosity is $n_0^f = 0.99$.

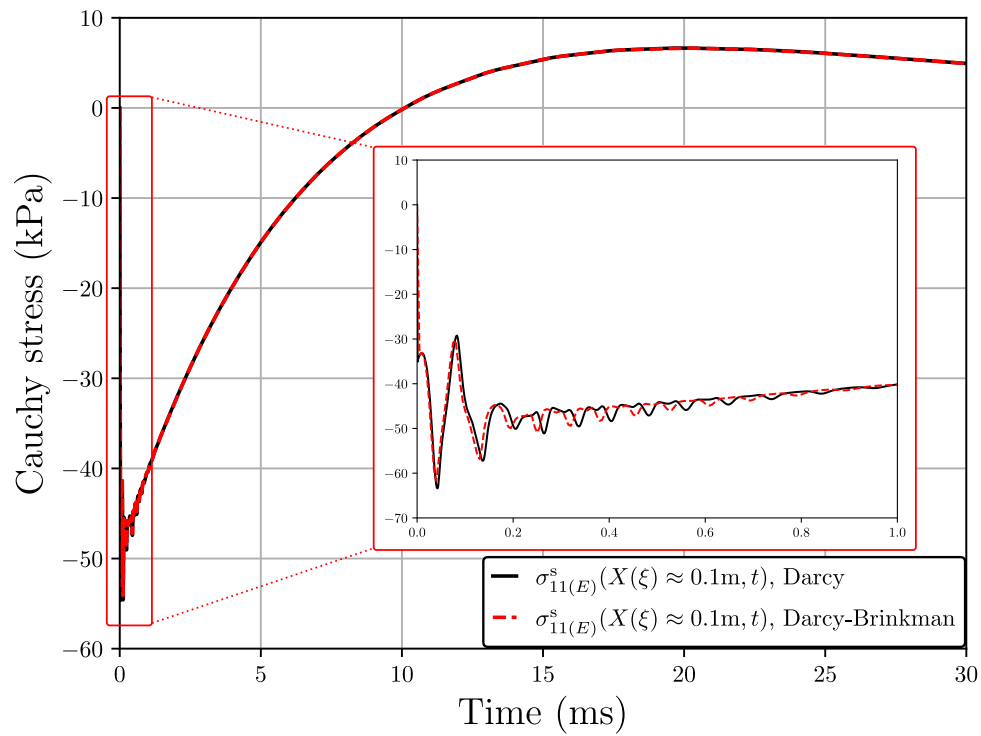


Figure 5.87: Solid extra stress results from applying the Friedlander impulse (50 kPa) to the permeable, blood-saturated lung parenchyma for the Gauss point closest to $X = H$. Slightly greater amplitude in the zoomed-in figure is due to higher time resolution for a second, shorter simulation. Initial porosity is $n_0^f = 0.99$.



(a) $t = 0.03$ ms

(b) $t = 0.30$ ms

(c) $t = 3.00$ ms

Figure 5.88: Contours along the length of the mesh for pore fluid extra stress $\sigma_{11}^f(E)$, pore fluid velocity v_f and porosity n^f for permeable, blood-saturated lung parenchyma after applying the Friedlander impulse with 50 kPa maximum overpressure.

Comparison between single-phase and multiphase models for shock loading. In this section, we present results that were published in Irwin et al. [2024], with the exception of the Taylor-Hood elements (discussed above in paragraph *Taylor-Hood mixed elements and shock loading*) and with higher overpressure from the Friedlander impulse. For brevity, we omit comparisons between the numerical time integration schemes implemented in SPONGE-1D, which have (nearly) overlapping results for all quantities of interest (refer to Irwin et al. [2023c, 2024]): only SPONGE-1D’s Runge-Kutta Cash-Karp integrator will be highlighted in this section.

Geometrical and loading parameters are given in Table 5.22. All LS-DYNA simulations from this point forward will assume the Clayton and Freed [2019a] model (with full non-linearity)⁷ for the bulk (single-phase) lung parenchyma response. Viscoelastic and damage effects are disabled for comparative purposes to the multiphase model developed in SPONGE-1D.⁸ Q8 hexahedral elements with reduced, single-point quadrature are used, and shock viscosity is turned on. Materials parameters are given in Table 5.21. Based on results presented in previous sections, for SPONGE-1D we have elected to:

- (1) disable the pore fluid viscous stress,
- (2) use the hyperbolic hydraulic conductivity model with $\kappa = 2.5$,
- (3) use $\varkappa = 1.89 \times 10^{-10} \text{ m}^2$,
- (4) use the weakly-enforced no-flux condition (again, the LS-DYNA single-phase Clayton and Freed [2019a] model cannot simulate permeable boundary conditions for the non-existent pore fluid),

⁷ In Clayton et al. [2021], the numerical implementation included a linearization of the shearing strains. In this work, that model was modified to use the exponential form of the shearing strains as originally presented in Clayton and Freed [2019a]. Differences in results are minor, but are not presented herein because that is out of scope of the present work.

⁸ Actually, the Clayton and Freed [2019a] hyperelastic solid skeleton model has been implemented in SPONGE-1D for both single-phase $((\mathbf{u}), (\mathbf{u}-\theta))$ and multiphase $((\mathbf{u}-p_f), (\mathbf{u}-\mathbf{u}_f-p_f), (\mathbf{u}-p_f-\theta^s-\theta^f), (\mathbf{u}-\mathbf{u}_f-p_f-\theta^s-\theta^f))$ formulations, with the viscoelastic relaxation. However, given that the Clayton and Freed [2019a] model does not necessarily obey the solid phase incompressibility assumption, we have elected to use the Ehlers and Eipper [1999] model, which does enforce the incompressibility constraint (in a weak sense) at the cost of a purely hyperelastic assumption. A damage model, as well as formulation of the incompressibility constraint on the solid phase for the Clayton and Freed [2019a] model, will be pursued as part of future work.

- (5) use the Ehlers and Eipper [1999] form of the strain-energy potential $U^s(J_s)$ as a means to enforce the nearly-incompressible solid phase assumption (i.e., enforce $n_{0(s)}^s \leq J_s < \infty$),
- (6) and use linearly-interpolated elements (with shock viscosity and pressure stabilization) given that they are low-cost (computationally speaking) and accurate, and higher-order spatial integration is not needed to resolve, e.g., a porosity gradient since such physics need not be considered for the locally homogeneous temperature regime and from points (1) and (4).

Table 5.21: Material parameters for single-phase vs. multiphase simulations. Values taken from Clayton et al. [2021], Lande and Mitzner [2006].

K, K^{skel} (kPa) ^a	G (kPa)	K_s (kPa)	$K_r^?$ (kPa)	ρ_0 (kg/m ³)	ρ_0^{sR} (kg/m ³)	ρ_0^{fR} (kg/m ³)	n_0^f	\hat{k}_0 (m ² /Pa-s)
213, 7.5	3	2.2×10^6	140	337	1000	1.138	0.664	10^{-5}

^a Here, K is used for the single-phase simulations and K^{skel} is used for the multiphase simulations.

Table 5.22: Geometrical and loading parameters for single-phase vs. multiphase simulations.

Overpressure load type	H (cm)	A (cm ²)	h_0^c (cm)	t_0^c (kPa)	t_0 (ms)	t_1 (ms)
Yen impulse	10	1	0.1	50	0.17	0.34
Friedlander impulse	10	1	0.1	50	10	N/A

As we saw in paragraph *Taylor-Hood mixed elements and shock loading*, the single-phase model behaves elastodynamically in response to shock loading via the Yen impulse, whereas the multiphase model shows the expected poroelastodynamic dissipation (Figure 5.89). Slight, but ultimately negligible, differences are observed in the solid displacements between $(\mathbf{u}-p_f)$ and $(\mathbf{u}-\mathbf{u}_f-p_f)$ formulations in Figure 5.89(a). Despite this, we see in Figure 5.90 that the pore fluid acceleration (dotted green curve) is several orders of magnitude larger than the solid acceleration—or mixture acceleration, as in the case of the $(\mathbf{u}-p_f)$ formulation—denoted by solid red and dashed green overlapping curves. I.e., the shock wave propagates more quickly through the air than it does the solid, which is also evident from the earlier displacement of air compared to the solid lung parenchyma at $X = H/2$ as shown in Figure 5.89(b). The multiphase model’s acceleration also shows dissipa-

tion over the simulation time, whereas the single-phase model's acceleration (solid black curve) has little-to-no dissipation.

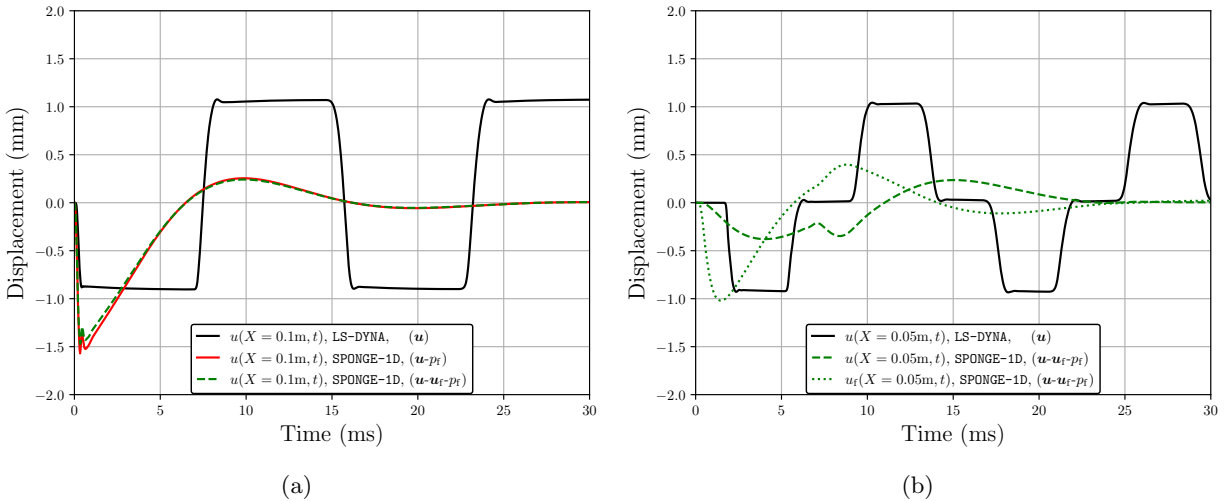


Figure 5.89: Overpressure loading from the Yen impulse at 50 kPa showing a comparison of (a) solid displacements between the single-phase LS-DYNA model developed by Clayton and Freed [2019a], Clayton et al. [2021] and the multiphase model developed in SPONGE-1D at $X = H$ and (b) solid and pore fluid displacements between aforementioned models at $X = H/2$.

Another advantage of the multiphase model over the single-phase model is that we can directly compute the solid skeleton and pore air pressures separate from one another, as well as separate computation of the solid skeleton extra stress and total stress; in the single-phase model, these metrics are lumped together. We see fairly good correlation between the total pressures and total stresses between the single-phase and multiphase model, shown in Figure 5.91. We believe that the slight discrepancies between the two models are due to the differences in Gaussian quadrature rules used. As mentioned previously, LS-DYNA (i.e., the single-phase model) assumes 1-point Gaussian quadrature, and here we use linear elements with 2-point quadrature for the multiphase model. Additionally, LS-DYNA seems to have an automatic, unchangeable lower limit on its adaptive time-step whereas in SPONGE-1D the user may set lower and upper limits themselves (at the risk of compromising speed and stability, respectively); here, SPONGE-1D has a finer time resolution for the data output.

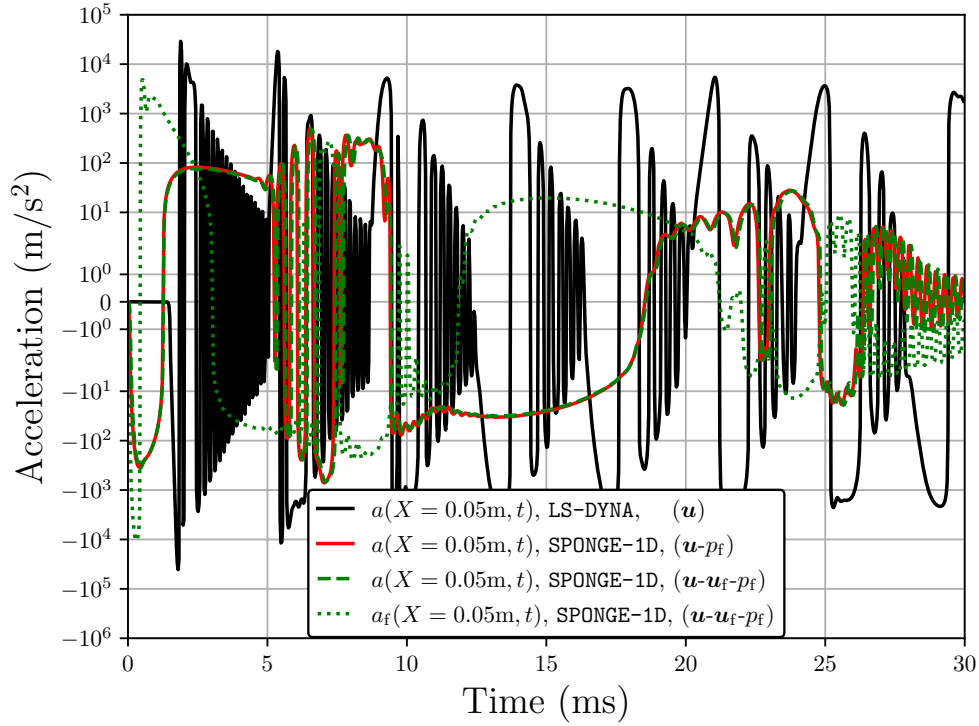


Figure 5.90: Overpressure loading from the Yen impulse at 50 kPa showing a comparison of accelerations at $X = H/2$ between the single-phase LS-DYNA model developed by Clayton and Freed [2019a], Clayton et al. [2021] and the multiphase model developed in SPONGE-1D.

Next, we present the results for the Friedlander impulse. As mentioned previously, strains are much higher for the Friedlander impulse's longer duration overpressure (10 ms Friedlander vs. 340 μ s Yen) followed by the tensile force relative to the reference pressure (i.e., atmospheric pressure), versus no force for the Yen impulse. This gives rise to strains on the order of 15-16% (nominal axial strain), i.e., 10x greater than those for the Yen impulse, as shown in Figure 5.92(a). As with the resulting deformations from the applied Yen impulse, we are also able to see the relative motion of the pore air to the solid skeleton, shown in Figure 5.92(b), and again we see the necessity of the full $(\mathbf{u}-\mathbf{u}_f-p_f)$ formulation in accounting for the differences in accelerations between the solid skeleton and pore air, shown in Figure 5.93.

In contrast to the Yen impulse, however, we see a better agreement between the total pressures and total stresses, shown in Figure 5.94. Of great interest is the solid skeleton stress going into tension sooner in the multiphase model than in the single-phase model. Fung [1990] has argued

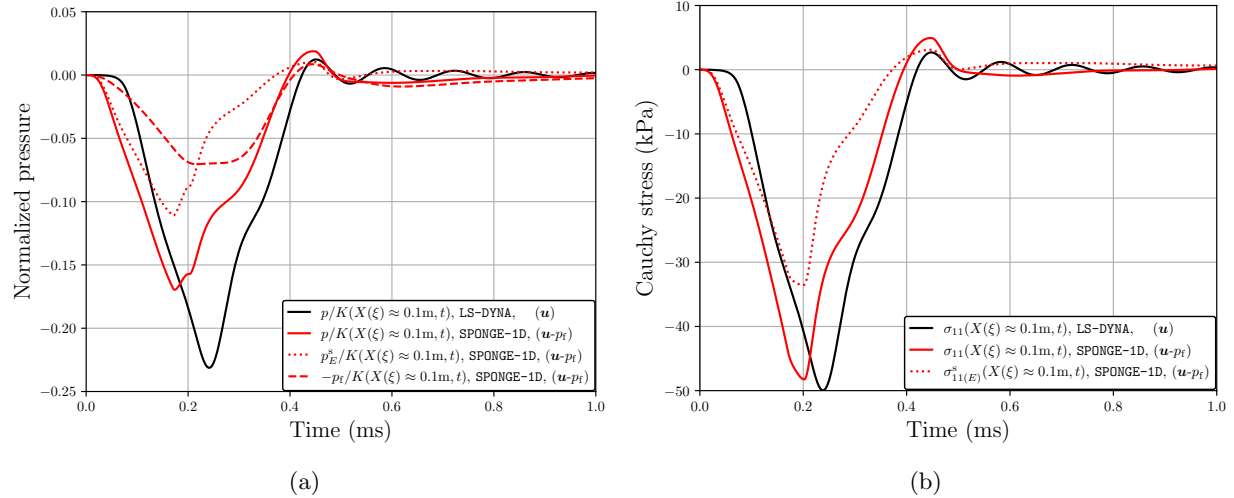


Figure 5.91: Overpressure loading from the Yen impulse at 50 kPa showing a comparison of (a) total pressures between the single-phase LS-DYNA model developed by Clayton and Freed [2019a], Clayton et al. [2021] and the multiphase model developed in SPONGE-1D at the Gauss point closest to $X = H$, as well as distinct solid skeleton extra pressure and pore air pressures, and (b) the total axial Cauchy stress between the single-phase and multiphase model, as well as the solid skeleton axial Cauchy stress for the multiphase model.

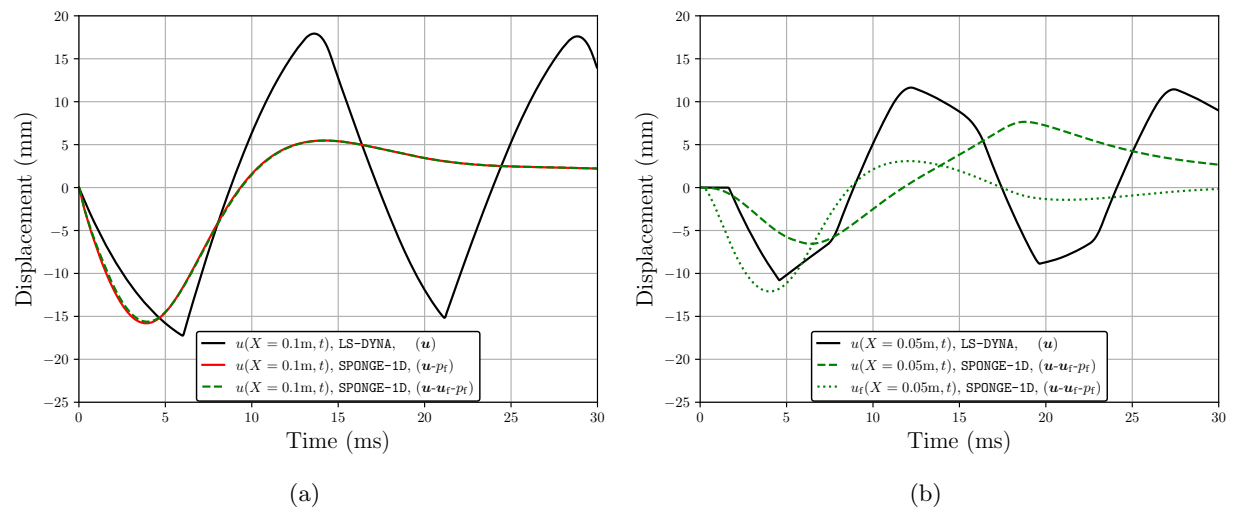


Figure 5.92: Overpressure loading from the Friedlander impulse at 50 kPa showing a comparison of (a) solid displacements between the single-phase LS-DYNA model developed by Clayton and Freed [2019a], Clayton et al. [2021] and the multiphase model developed in SPONGE-1D at $X = H$ and (b) solid and pore fluid displacements between aforementioned models at $X = H/2$.

that excessive tensile forces in the walls of the lung alveoli can lead to rupturing of the alveoli and

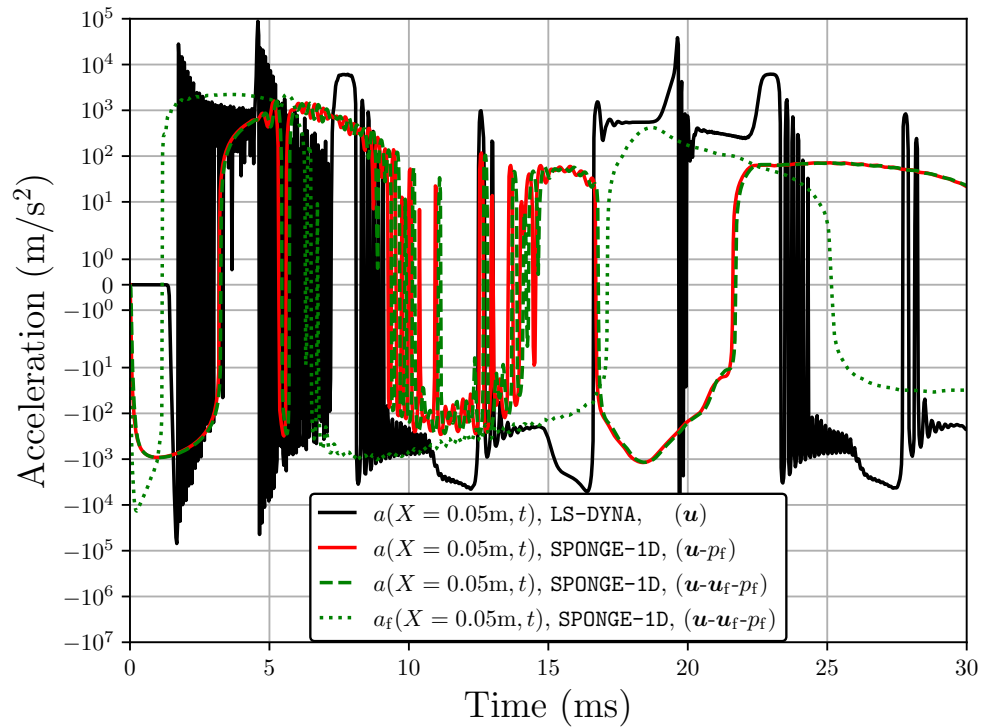


Figure 5.93: Overpressure loading from the Friedlander impulse at 50 kPa showing a comparison of accelerations at $X = H/2$ between the single-phase LS-DYNA model developed by Clayton and Freed [2019a], Clayton et al. [2021] and the multiphase model developed in SPONGE-1D.

local injury. Thus, we might be able to predict injury sooner by accounting for the relative motion of air to the lung parenchyma solid skeleton in the multiphase model. Future work is needed to quantify damage and local injury in the multiphase solid skeleton constitutive model to say for certain.

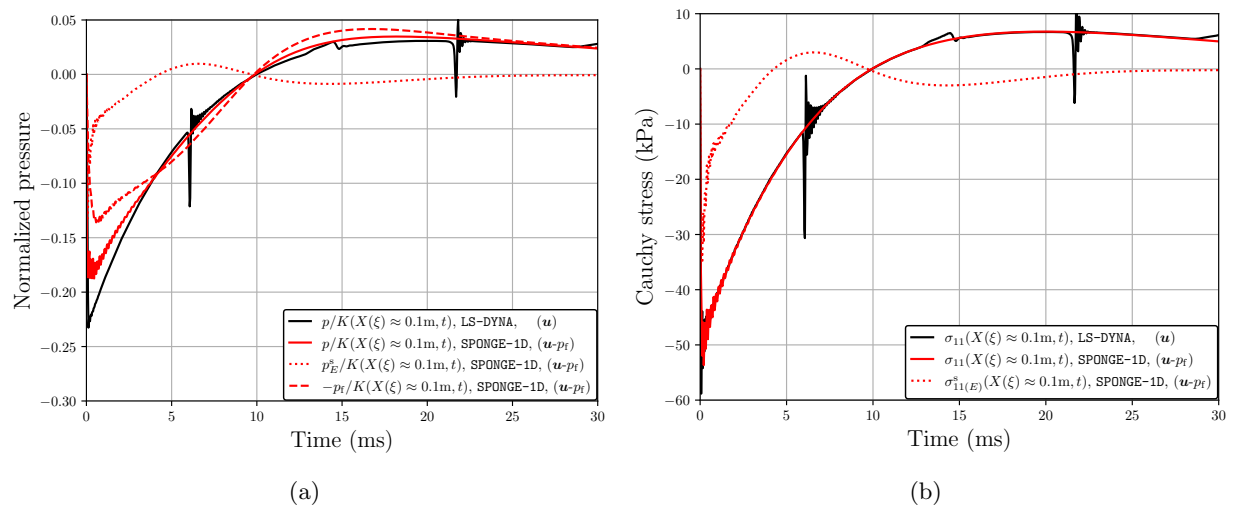


Figure 5.94: Overpressure loading from the Friedlander impulse at 50 kPa showing a comparison of (a) total pressures between the single-phase LS-DYNA model developed by Clayton and Freed [2019a], Clayton et al. [2021] and the multiphase model developed in SPONGE-1D at the Gauss point closest to $X = H$, as well as distinct solid skeleton extra pressure and pore air pressures, and (b) the total axial Cauchy stress between the single-phase and multiphase model, as well as the solid skeleton axial Cauchy stress for the multiphase model.

5.3.3.2 Locally inhomogeneous temperature model

As mentioned throughout this work, the assumption of locally homogeneous temperatures may perhaps be physically unrealistic, particularly when involving a gas undergoing shock loading. The thermal expansion coefficient for air is an order of magnitude larger than for the solid lung tissue, and given also the compressibility of the air, heating and cooling of the air will be more pronounced than it will for the solid lung tissue. Therefore, it would be pertinent to formulate equations which consider locally inhomogeneous temperatures. This formulation was pursued theoretically in Chapter 3, and numerically in Chapter 4.

Here we present preliminary results regarding the numerical implementation for an ideal gas pore fluid and thermoelastic solid. More constitutive models are implemented in SPONGE-1D (and discussed in Chapters 3 & 4), but the analysis thereof is omitted for the following reason: the current numerical implementation is incomplete from a physics standpoint, as we observe numerical oddities at the boundaries of the 1-D mesh for the temperature fields θ^s and θ^f . All simulations presented herein assume impermeable, zero heat flux boundary conditions since that seems to provide the most stability. Despite the numerical difficulties, results are still included as part of this work to demonstrate overall robustness of the formulation and resulting numerical implementation. Future work will seek to alleviate the numerical issues at the boundaries, either via reformulation of the governing and/or variational equations, use of a different numerical time integration scheme, or other unforeseen approaches.

Verification at low-to-moderate strain-rates. To begin with, we simulate 99% porosity, impermeable lung parenchyma undergoing dynamic impulse compression at low-to-moderate strain rate, and compare thermoporoelastodynamics results to the $(\mathbf{u}-p_f)$ formulation, the latter of which has been published in separate work [Regueiro et al., 2014]. Geometrical and loading parameters are given in Table 5.24 with examples of the $(\mathbf{u}-p_f-\theta^s-\theta^f)$ element and traction load type given in Figure 5.95 ($(\mathbf{u}-p_f)$, $(\mathbf{u}-p_f-\theta^s-\theta^f)$, $(\mathbf{u}-\mathbf{u}_f-p_f-\theta^s-\theta^f)$ results were generated using Q3H-P1, Q3H-P1-T1-T1 and Q3H-Q1-P1-T1-T1 element types, respectively); material parameters are given in Table 5.23.

Thermal convection between constituents is disabled for this example. (\mathbf{u} - p_f) examples assumed an isothermal ideal gas pore fluid (i.e., Equations (4.174)₁₋₄ with Equations (4.174)₅₋₆ set to zero), which is in contrast to prior (\mathbf{u} - p_f) formulation results presented thus far, where the mixture temperature was *not* held fixed even if it was not computed. Here we invoke the isothermal, ideal-gas model for comparative purposes only.

Table 5.23: Material parameters for thermoporoelastodynamic simulations at low-to-moderate strain rate. Values taken from Clayton et al. [2021], Lande and Mitzner [2006], Yang and Cao [2020]. Initial temperatures are $\theta_0^s = \theta_0^f = 310$ K. The hyperbolic hydraulic conductivity model is assumed with $\kappa = 2.5$.

E (kPa)	ν	K_s (kPa)	K_f^θ (kPa)	ρ_0^{sR} (kg/m ³)	ρ_0^{fR} (kg/m ³)	n_0^f
5	0.3	2.2×10^6	101.325	1000	1.138	0.99
\hat{k}_0 (m ² /Pa-s)	α_V^s (1/K)	c_V^s (kJ/kg-K)	c_V^f (kJ/kg-K)	k^{θ^s} (W/m-K)	k^{θ^f} (W/m-K)	k_θ^ε (W/m ³ -K)
10^{-5}	7.4×10^{-4}	2.2	0.717	0.509	0.026	0

Table 5.24: Geometrical and loading parameters for thermoporoelastodynamics simulations at low-to-moderate strain-rate.

Overpressure load type	H (cm)	A (cm ²)	h_0^ε (cm)	t_0^σ (kPa)	t_0 (s)	t_1 (s)
Triangular impulse	10	1	0.1	10	0.1	0.2

Solid skeleton displacements are provided in Figure 5.96. There is excellent agreement between the isothermal ideal gas (\mathbf{u} - p_f) and ideal gas (\mathbf{u} - p_f - θ^s - θ^f), (\mathbf{u} - \mathbf{u}_f - p_f - θ^s - θ^f) formulations. Total stress and solid stress also overlap (Figure 5.97) between the different formulations.

Pore fluid pressure and pore fluid temperature are shown in Figure 5.98; again, there is excellent agreement between the pore fluid pressure across formulations, but poor agreement for pore fluid temperatures between the thermoporoelastodynamic formulations. In addition, we note that there are some small oscillations in the temperature values nearly the boundaries, which are not negligible when zoomed in on, as shown in Figure 5.99. Such oscillations are certainly not a physical phenomena and may be the cause of issues observed for higher strain-rate loadings.

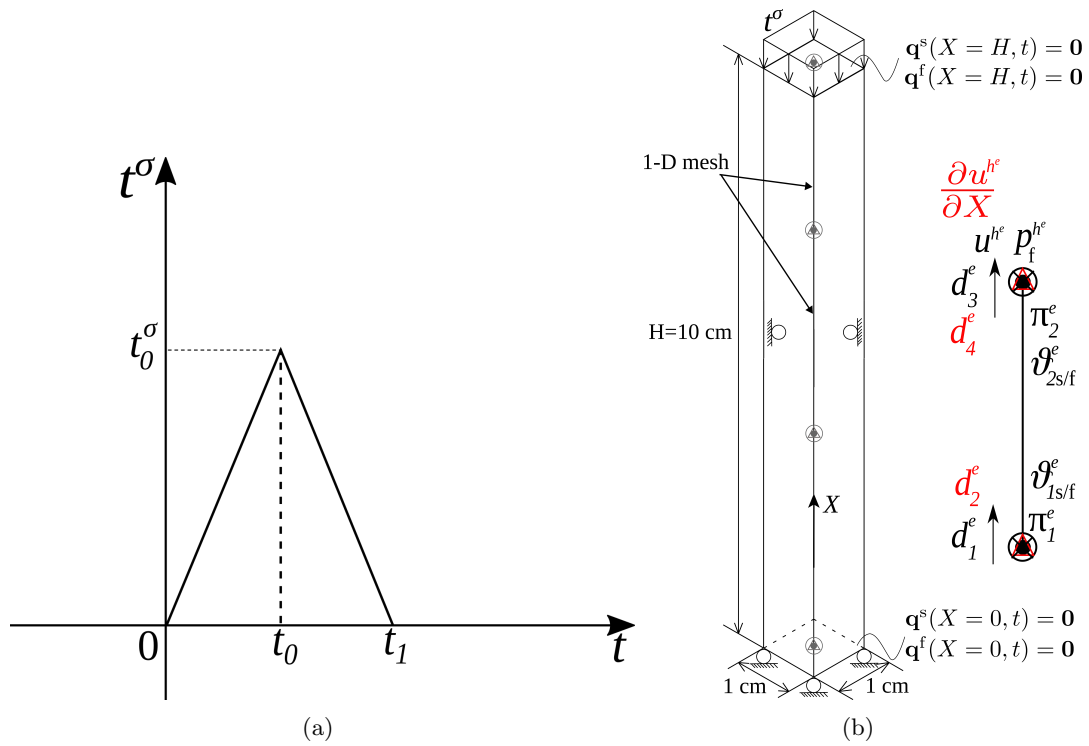


Figure 5.95: (a) Triangular impulse traction application (b) schematic of column mesh for the thermoporoelastodynamic simulations of lung parenchyma at low-to-moderate strain-rate, highlighting the Q3H-P1-T1-T1 element.

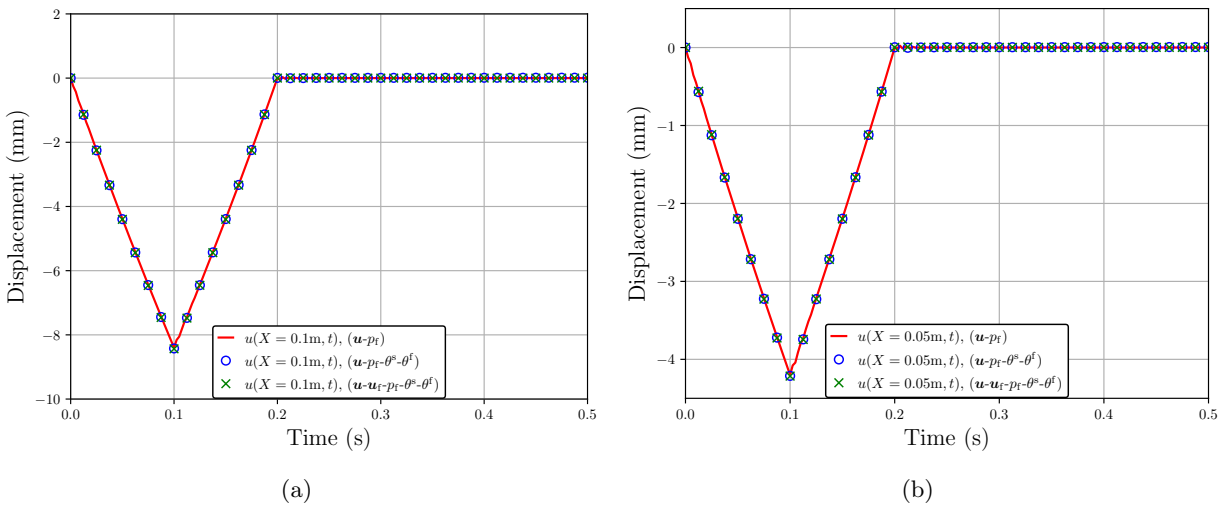


Figure 5.96: Solid skeleton displacements following slower, dynamic impulse loading at 10 kPa overpressure comparing the isothermal $(\mathbf{u}-p_f)$ formulation to the non-isothermal $(\mathbf{u}-p_f-\theta^s-\theta^f)$, $(\mathbf{u}-\mathbf{u}_f-p_f-\theta^s-\theta^f)$ formulations at (a) $X = H$ and (b) $X = H/2$.

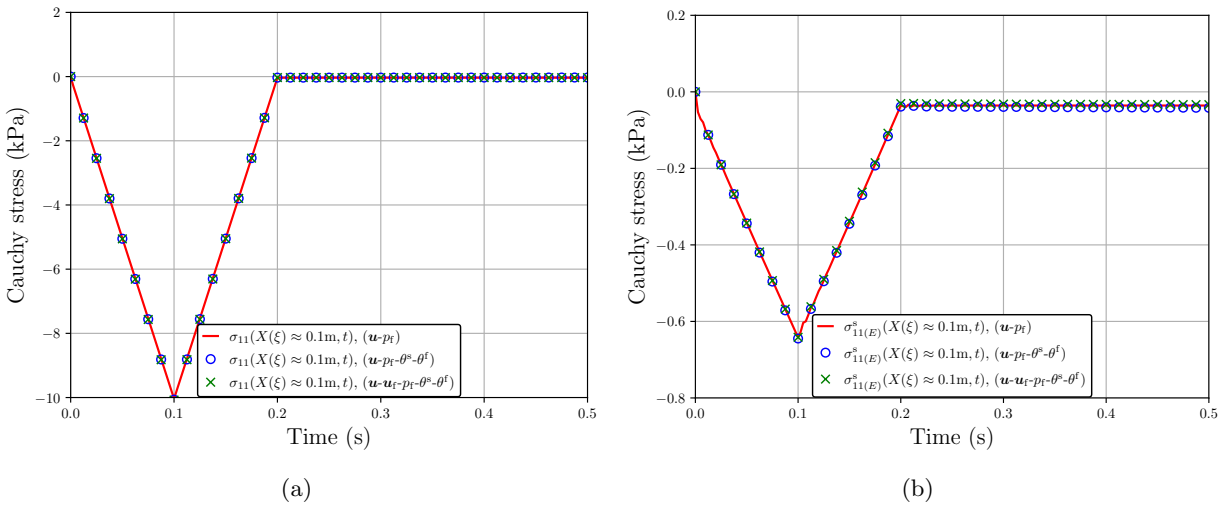


Figure 5.97: Slower, dynamic impulse loading at 10 kPa overpressure comparing the isothermal $(\mathbf{u}-p_f)$ formulation to the non-isothermal $(\mathbf{u}-p_f-\theta^s-\theta^f)$, $(\mathbf{u}-\mathbf{u}_f-p_f-\theta^s-\theta^f)$ formulations at the Gauss point closest to $X = H$ for (a) total axial Cauchy stress and (b) solid axial Cauchy stress (solid extra [effective] stress).

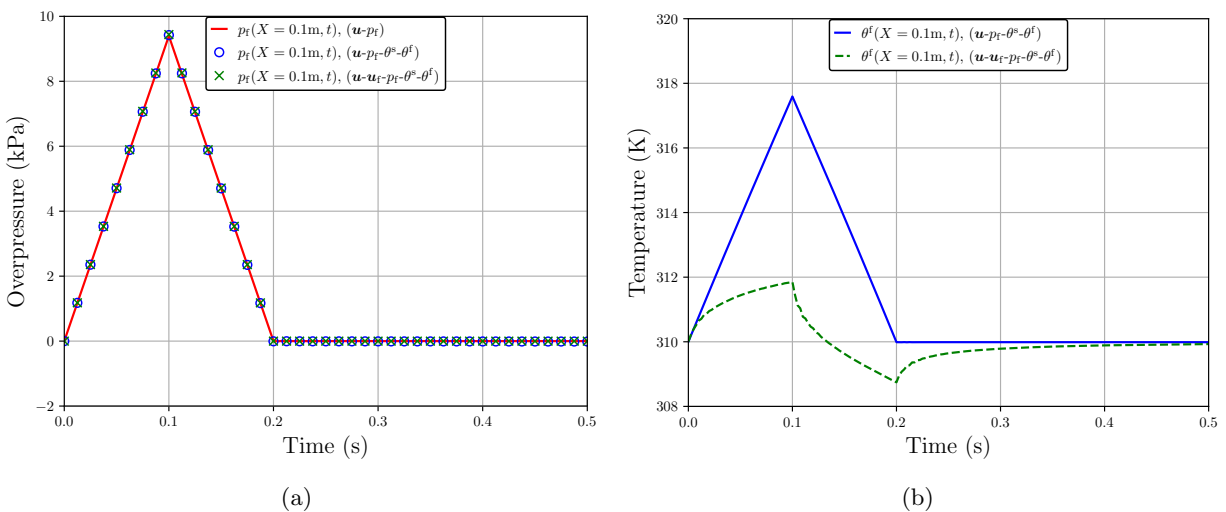
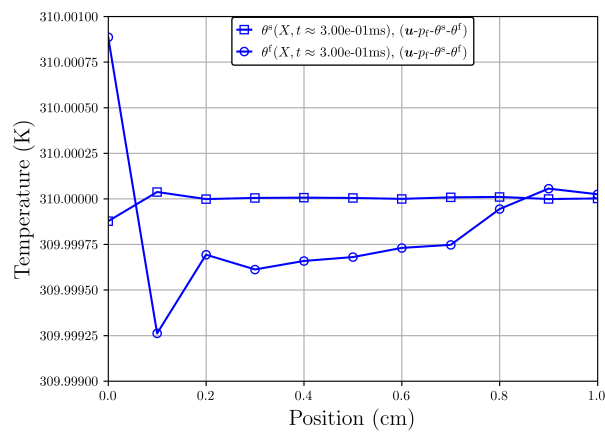
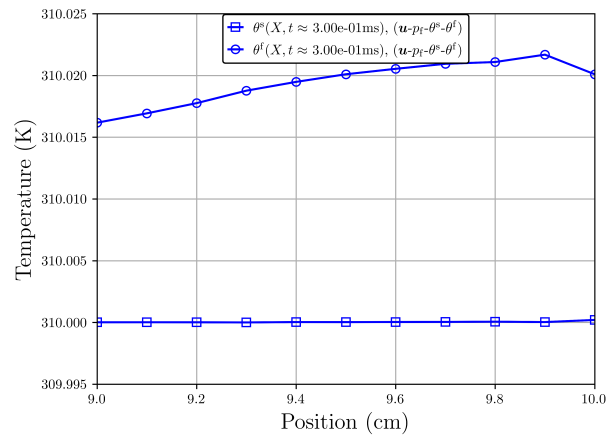


Figure 5.98: Slower, dynamic impulse loading at 10 kPa overpressure comparing the isothermal $(\mathbf{u}-p_f)$ formulation to the non-isothermal $(\mathbf{u}-p_f-\theta^s-\theta^f)$, $(\mathbf{u}-\mathbf{u}_f-p_f-\theta^s-\theta^f)$ formulations for (a) pore fluid pressure p_f and (b) comparing the pore fluid temperature θ^f for $(\mathbf{u}-p_f-\theta^s-\theta^f)$ and $(\mathbf{u}-\mathbf{u}_f-p_f-\theta^s-\theta^f)$ formulations.



(a)



(b)

Figure 5.99: Slower, dynamic impulse loading at 10 kPa overpressure comparing the temperatures near the (a) bottom of the mesh and (b) top of the mesh.

Assessing numerical challenges at high strain-rate. Returning our focus back to the high strain-rate regime, parameters from Clayton et al. [2021] are restored (listed in Table 5.25) and the impermeable lung parenchyma is loaded via Yen impulse (geometry and loading parameters listed in Table 5.26). For LS-DYNA, the Clayton et al. [2021] implementation has thermodynamics enabled (as it did in Section 5.3.3.1, even though temperature was not plotted), but thermodynamic variables are treated as internal state variables. Therefore, the plots still refer to this implementation as (\mathbf{u}) formulation even though temperature evolves. The $(\mathbf{u}-p_f)$ formulation presented herein assumes the barotropic exponential pore fluid model (Equation (3.138)), and uses the Q1-P1 element (refer to Figure 4.3(c)) with shock viscosity and pressure stabilization. The $(\mathbf{u}-p_f-\theta^s-\theta^f)$ and $(\mathbf{u}-\mathbf{u}_f-p_f-\theta^s-\theta^f)$ formulations assume the baroclinic, ideal gas model (Equations (3.141) & (3.152)), and use either the Q3H-P1-T1-T1 element (Figure 4.3(e)) or the Q3H-Q1-P1-T1-T1 element (Figure 4.3(f)). All three multiphase formulations assume the neo-Hookean Ehlers and Eipper [1999] model with hyperbolic hydraulic conductivity [Markert, 2005], but the thermodynamics models include the thermoelastic coupling (Equation (3.114)) whereas the $(\mathbf{u}-p_f)$ model does not (Equation (3.115), $\alpha_V^s \rightarrow 0$).

Solid displacements are shown in Figure 5.100. Again we see that the single-phase model (black curve) behaves elastodynamically, whereas the multiphase models (red, blue curves) show the expected poroelastodynamic dissipation. The thermoporoelastodynamics model (blue curve) also behaves more stiffly than the poroelastodynamics model. Good agreement exists between total stress and total pressure (Figure 5.101) across all models, with minor variations between the $(\mathbf{u}-p_f)$ and $(\mathbf{u}-p_f-\theta^s-\theta^f)$ formulations' solid metrics (dashed red and blue curves).

Comparing the pore fluid pressures between the $(\mathbf{u}-p_f)$ and $(\mathbf{u}-p_f-\theta^s-\theta^f)$ formulations, again we see the latter has the stiffer response, but is in otherwise good agreement (Figure 5.102). Moving our focus to the temperatures, it is apparent that there is strange behavior in both the $(\mathbf{u}-p_f-\theta^s-\theta^f)$ and $(\mathbf{u}-\mathbf{u}_f-p_f-\theta^s-\theta^f)$ models. Figure 5.104(a)–(c) shows a contour plot of pore fluid velocity plotted against pore fluid temperature. Initially (Figure 5.104(a)), the $(\mathbf{u}-p_f-\theta^s-\theta^f)$ model displays uncharacteristic cooling of the pore fluid—recall $D_t^f \theta^f \sim -\text{GRAD}_s(\mathbf{v}_f)$, i.e., compression of

Table 5.25: Material parameters for thermoporoelastodynamics simulations at high strain rates. Values taken from Clayton et al. [2021], Lande and Mitzner [2006], Yang and Cao [2020]. $(\cdot)^*$ indicates values used for single-phase formulation (some of which are also the initial mixture values).

K^* (kPa)	K^{skel} (kPa)	G (kPa)	K_s (kPa)	K_f^θ (kPa)
213	7.5	3	2.2×10^6	101.325
ρ_0^* (kg/m ³)	ρ_0^{sR} (kg/m ³)	ρ_0^{fR} (kg/m ³)	n_0^f	\hat{k}_0 (m ² /Pa-s)
337	1000	1.138	0.664	10^{-5}
α_V^* (1/K)	α_V^s (1/K)	c_V (kJ/kg-K)	c_V^s (kJ/kg-K)	c_V^f (kJ/kg-K)
2.39×10^{-3}	7.4×10^{-4}	1.2*	2.2	0.717
k^* (W/m-K)	k^{θ^s} (W/m-K)	k^{θ^f} (W/m-K)	k_θ^ε (W/m ³ -K)	
0.188	0.509	0.026	0	

Table 5.26: Geometrical and loading parameters for thermoporoelastodynamics simulations at high strain-rate.

Overpressure load type	H (cm)	A (cm ²)	h_0^ε (cm)	t_0^σ (kPa)	t_0 (ms)	t_1 (ms)
Yen impulse	10	1	0.1	50	0.17	0.34
Friedlander impulse	10	1	0.1	50	10	N/A

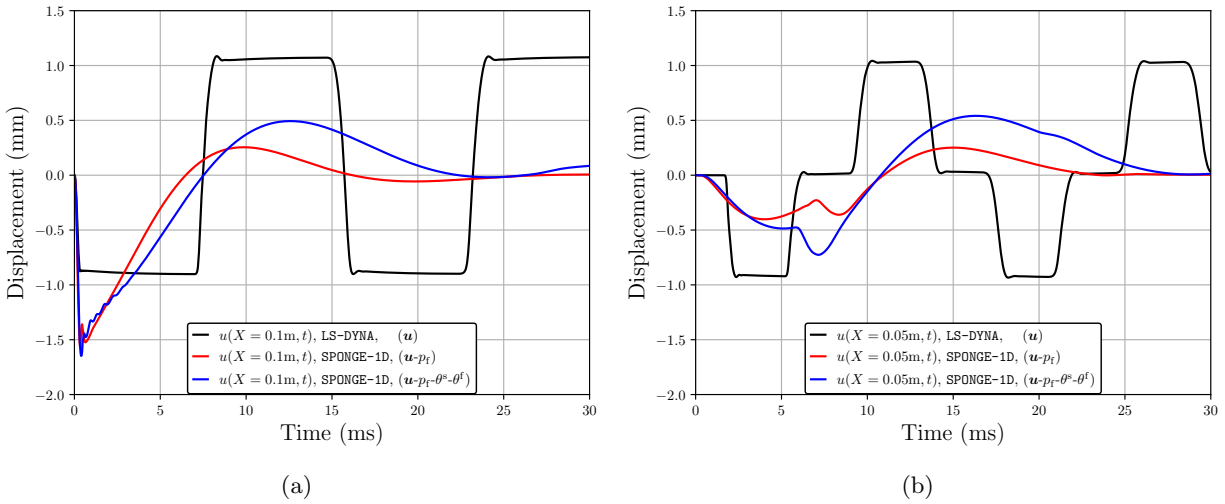


Figure 5.100: Overpressure loading from the Yen impulse at 50 kPa showing a comparison of (a) solid displacements between the single-phase LS-DYNA model developed by Clayton and Freed [2019a], Clayton et al. [2021] and the multiphase model developed in SPONGE-1D at $X = H$ and (b) solid displacements between aforementioned models at $X = H/2$.

the pore fluid (negative pore fluid strain-rate) should lead to an increase in pore fluid temperature— whereas the $(\mathbf{u}-\mathbf{u}_f-p_f-\theta^s-\theta^f)$ shows the expected temperature rise, which is correlated well with the numerical value of the pore fluid velocity gradient (i.e., the descending profile of the green circles).

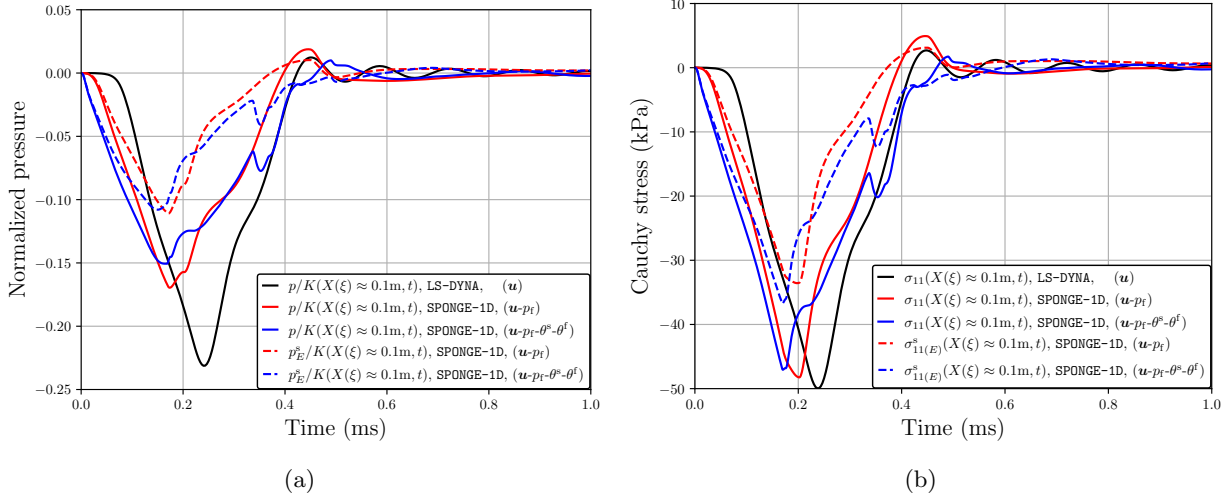


Figure 5.101: Overpressure loading from the Yen impulse at 50 kPa showing a comparison of (a) total pressures between the single-phase LS-DYNA model developed by Clayton and Freed [2019a], Clayton et al. [2021] and the multiphase model developed in SPONGE-1D at the Gauss point closest to $X = H$, as well as distinct solid skeleton extra pressure, and (b) the total axial Cauchy stress between the single-phase and multiphase model, as well as the solid skeleton axial Cauchy stress for the multiphase model.

About 0.1 ms later (Figure 5.104(b)), we observe cooling of the pore fluid in both formulations, which remains consistent with the pore fluid velocity gradient, though the $(\mathbf{u}-p_f-\theta^s-\theta^f)$ formulation has a larger dip in pore fluid temperature. Around 0.2 ms (Figure 5.104(c)), the $(\mathbf{u}-\mathbf{u}_f-p_f-\theta^s-\theta^f)$ formulation goes unstable, and the simulation terminates as $\Delta t \rightarrow 0$ when the RKFNC integrator tries to resolve the large gradients in both pore fluid velocity and pore fluid temperature.

The $(\mathbf{u}-p_f-\theta^s-\theta^f)$ simulation remains stable, however, and the mixture temperature, given by [Ruggeri and Simić, 2009],

$$\theta := \frac{\sum_{\alpha} c_V^{\alpha} \theta^{\alpha}}{\sum_{\alpha} c_V^{\alpha}}, \quad (5.82)$$

shows relatively good agreement with the single-phase temperature (Figure 5.105(a)–(c)). The rise in temperature near the boundary is due to the solid phase also displaying uncharacteristic heating behavior near the boundary (Figure 5.105(d)–(f)), which, unlike the pore fluid, does not decrease nor dissipate on a reasonable time scale.

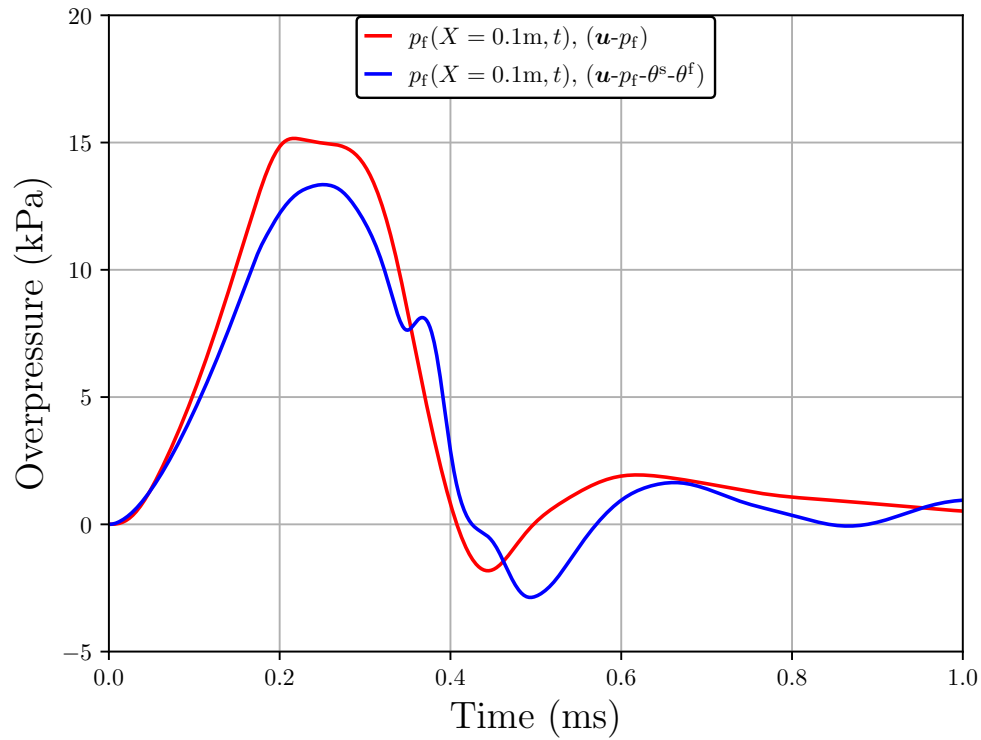


Figure 5.102: Overpressure loading from the Yen impulse at 50 kPa showing a comparison of $(\mathbf{u}-p_f)$ (barotropic exponential model) and $(\mathbf{u}-p_f-\theta^s-\theta^f)$ (baroclinic ideal gas model) formulations.

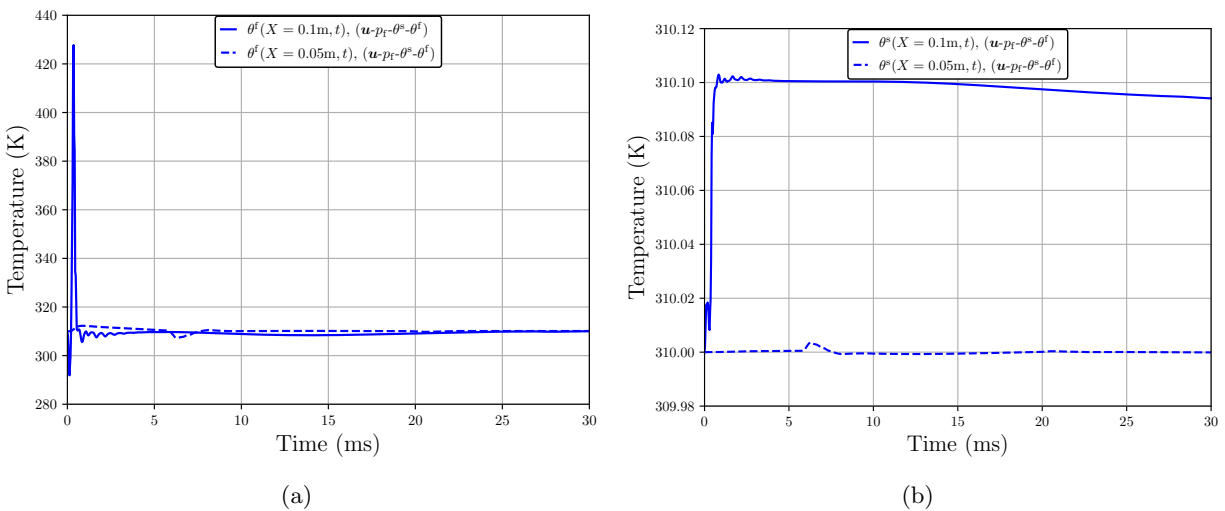


Figure 5.103: Overpressure loading from the Yen impulse at 50 kPa showing (a) pore fluid temperature θ^f and (b) solid lung tissue temperature θ^s for $(\mathbf{u}-p_f-\theta^s-\theta^f)$ plotted at the $X = H$ and $X = H/2$ nodes.

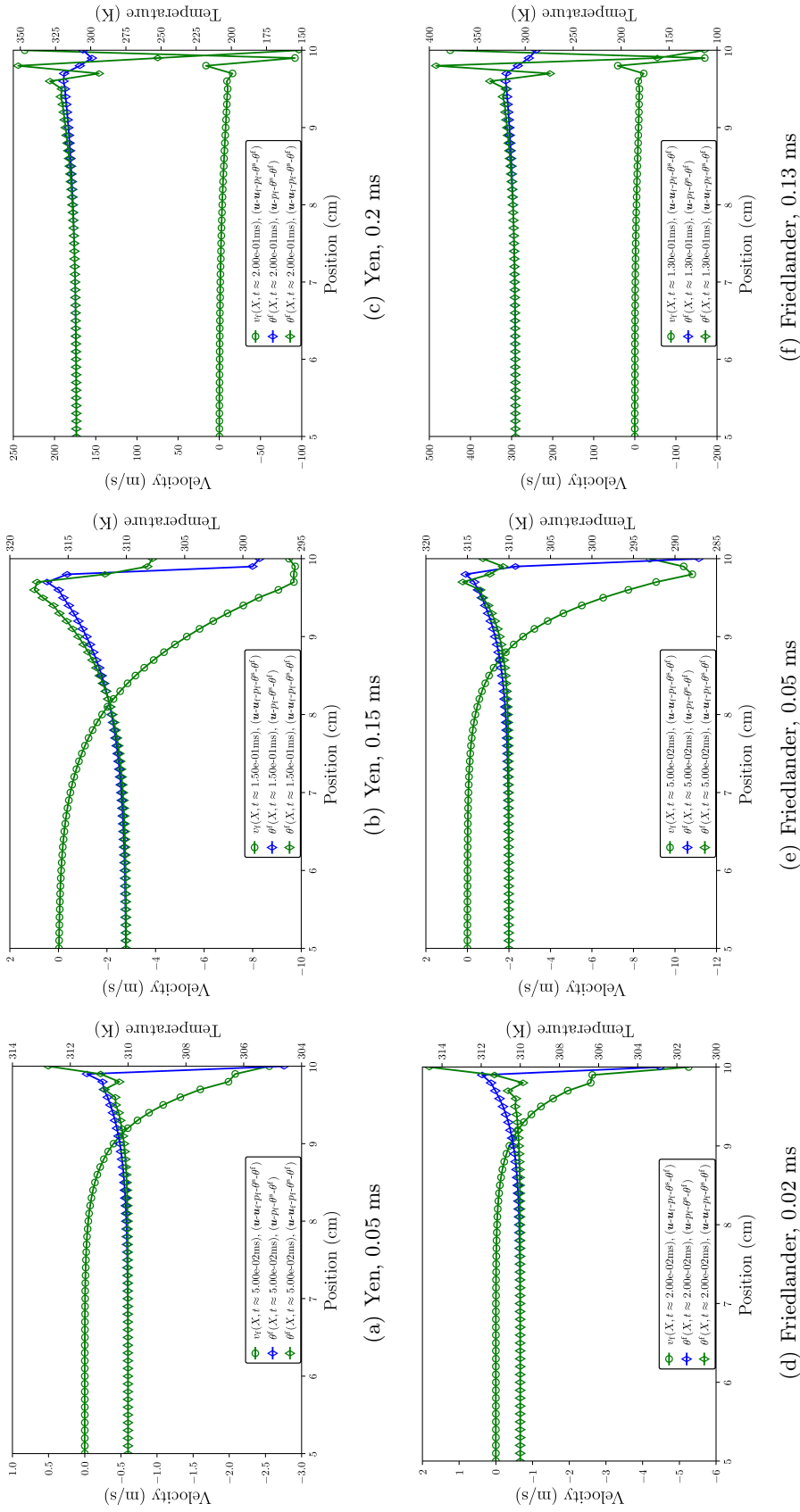
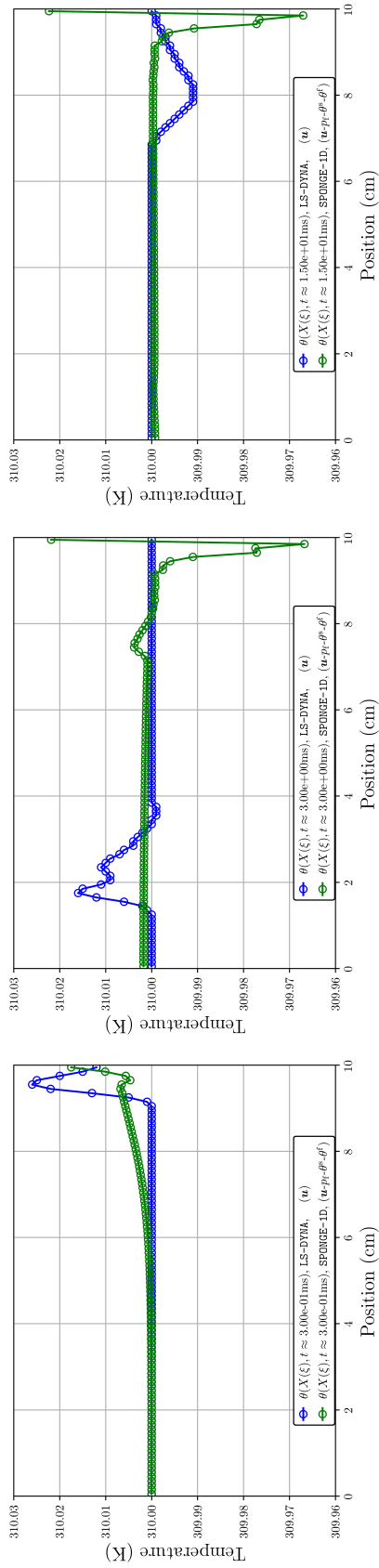
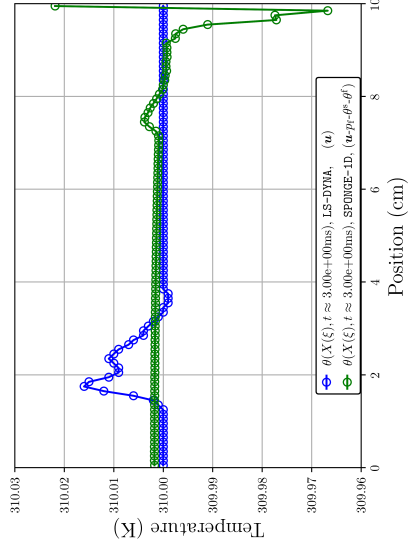


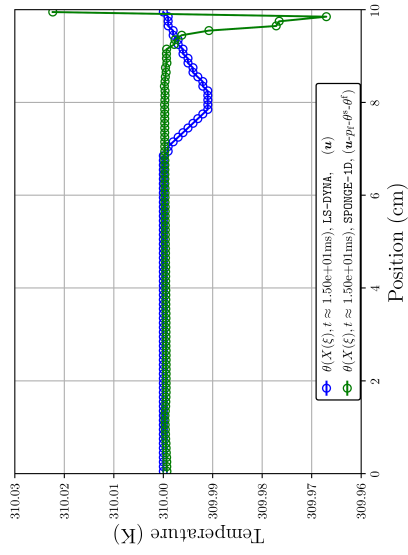
Figure 5.104: Overpressure loading at 50 kPa showing contour plots of pore fluid velocity v_f against pore fluid temperature θ^f for the $(\mathbf{u}-p_f-\theta^s-\theta^f)$ and $(\mathbf{u}-\mathbf{u}_f-p_f-\theta^s-\theta^f)$ formulations for (a)–(c) the Yen impulse and (d)–(f) the Friedlander impulse. Note the increasing range of y -ordinates as the simulation progresses.



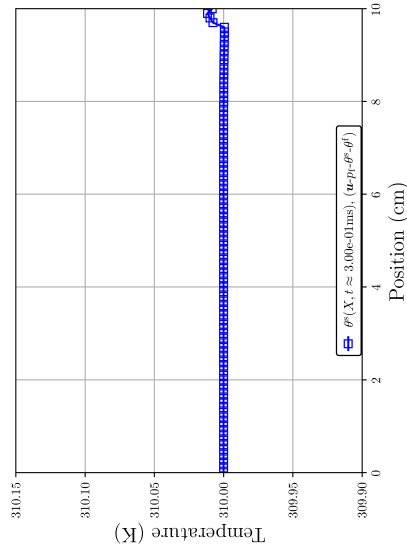
(a) θ , 0.30 ms



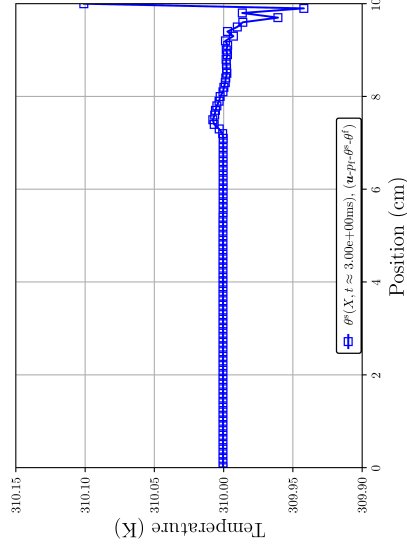
(b) θ , 3.00 ms



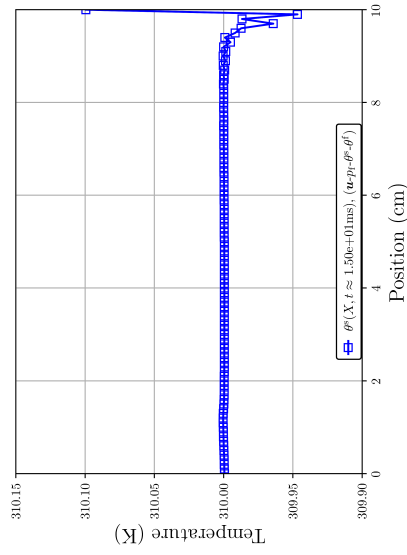
(c) θ , 15.0 ms



(d) θ^s , 0.30 ms



(e) θ^s , 3.00 ms



(f) θ^s , 15.0 ms

Figure 5.105: Overpressure loading from the Yen impulse at 50 kPa showing (a)–(c) contour plots of mixture temperature θ between the single-phase and multiphase models, and (d)–(f) contour plots of solid lung tissue temperature θ^s .

Moving onto discussion of the Friedlander impulse results, again we see the stiffer response from the $(\mathbf{u}-p_f-\theta^s-\theta^f)$ formulation's ideal gas model as compared to the $(\mathbf{u}-p_f)$ barotropic exponential model, with the LS-DYNA model behaving elastodynamically (Figure 5.106). In contrast to the Yen impulse, total pressure and total stress for the $(\mathbf{u}-p_f-\theta^s-\theta^f)$ simulation do not track as well with the $(\mathbf{u}-p_f)$ and single-phase simulations (Figure 5.107), though the discrepancy is not unreasonable, and solid metrics track fairly well between $(\mathbf{u}-p_f)$ and $(\mathbf{u}-p_f-\theta^s-\theta^f)$.

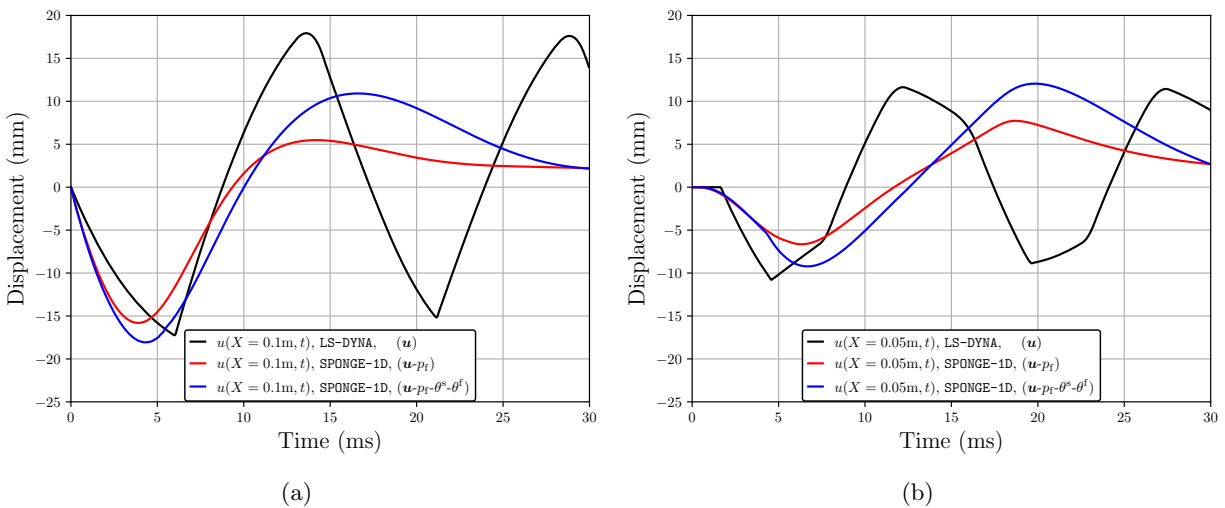


Figure 5.106: Overpressure loading from the Friedlander impulse at 50 kPa showing a comparison of (a) solid displacements between the single-phase LS-DYNA model developed by Clayton and Freed [2019a], Clayton et al. [2021] and the multiphase model developed in SPONGE-1D at $X = H$ and (b) solid displacements between aforementioned models at $X = H/2$.

Comparing the pore fluid pressures between the $(\mathbf{u}-p_f)$ and $(\mathbf{u}-p_f-\theta^s-\theta^f)$ formulations, again we see the latter has the stiffer response, but is in otherwise good agreement (Figure 5.108). Moving our focus to the temperatures, we see similar problems arise as we did with the Yen impulse. Figure 5.104(d)–(f) shows a contour plot of pore fluid velocity plotted against pore fluid temperature. Initially (Figure 5.104(d)), the $(\mathbf{u}-p_f-\theta^s-\theta^f)$ model displays the uncharacteristic cooling of the pore fluid, whereas, again, the $(\mathbf{u}-p_f)$ model shows the expected temperature rise, which is correlated well with the numerical value of the pore fluid velocity gradient. About 0.03 ms later (Figure 5.104(e)), we observe cooling of the pore fluid in both formulations, which remains

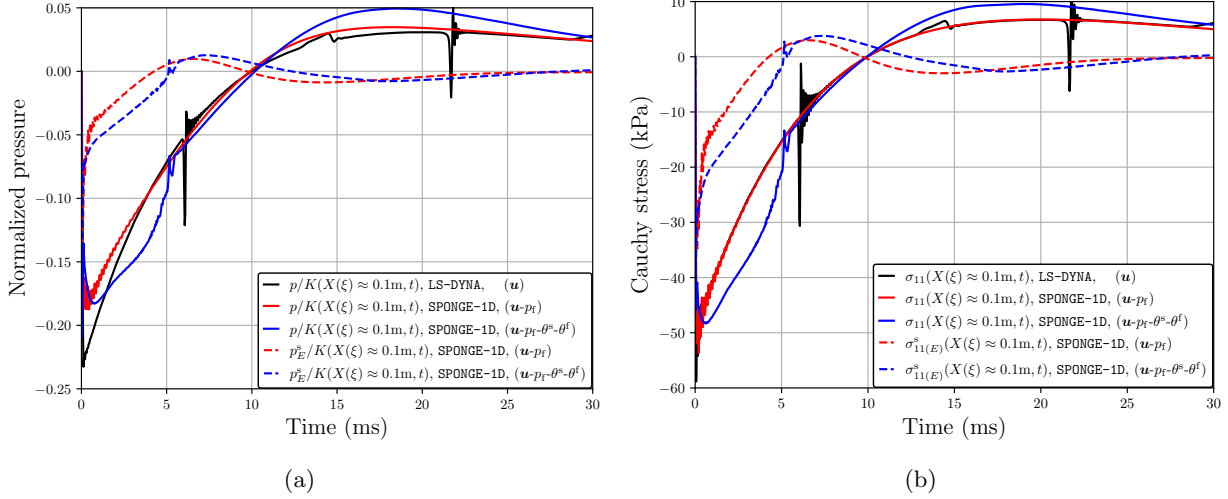


Figure 5.107: Overpressure loading from the Friedlander impulse at 50 kPa showing a comparison of (a) total pressures between the single-phase LS-DYNA model developed by Clayton and Freed [2019a], Clayton et al. [2021] and the multiphase model developed in SPONGE-1D at the Gauss point closest to $X = H$, as well as distinct solid skeleton extra pressure, and (b) the total axial Cauchy stress between the single-phase and multiphase model, as well as the solid skeleton axial Cauchy stress for the multiphase model.

consistent with the pore fluid velocity gradient, and again the $(\mathbf{u}-p_f-\theta^s-\theta^f)$ formulation has a larger dip in pore fluid temperature. Around 0.13 ms (Figure 5.104(f)), the $(\mathbf{u}-\mathbf{u}_f-p_f-\theta^s-\theta^f)$ formulation goes unstable, and the simulation terminates as $\Delta t \rightarrow 0$ when the RKFNC integrator tries to resolve the large gradients in both pore fluid velocity and pore fluid temperature.

As before, the $(\mathbf{u}-p_f-\theta^s-\theta^f)$ simulation remains stable, and the mixture temperature shows relatively good agreement with the single-phase temperature (Figure 5.110(a)–(c)). The rise in temperature near the loaded/topmost boundary is due to the solid phase also displaying uncharacteristic heating behavior near the boundary (Figure 5.110(d)–(f)), which, unlike the pore fluid, does not decrease nor dissipate on a reasonable time scale.

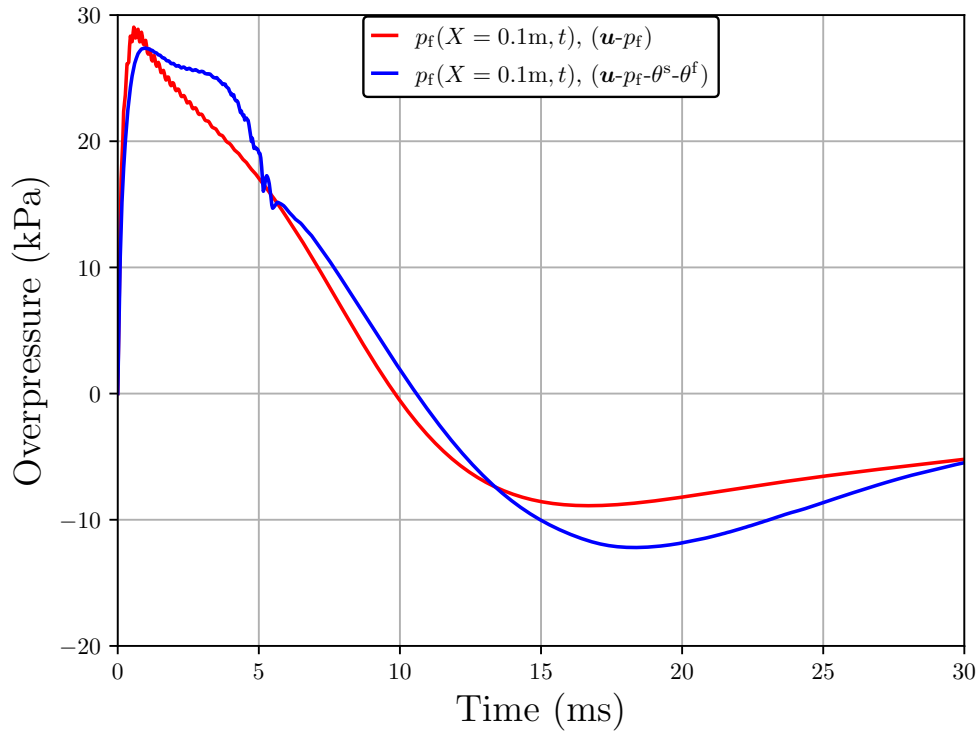


Figure 5.108: Overpressure loading from the Friedlander impulse at 50 kPa showing a comparison of $(\mathbf{u}-p_f)$ (barotropic exponential model) and $(\mathbf{u}-p_f-\theta^s-\theta^f)$ (baroclinic ideal gas model) formulations.

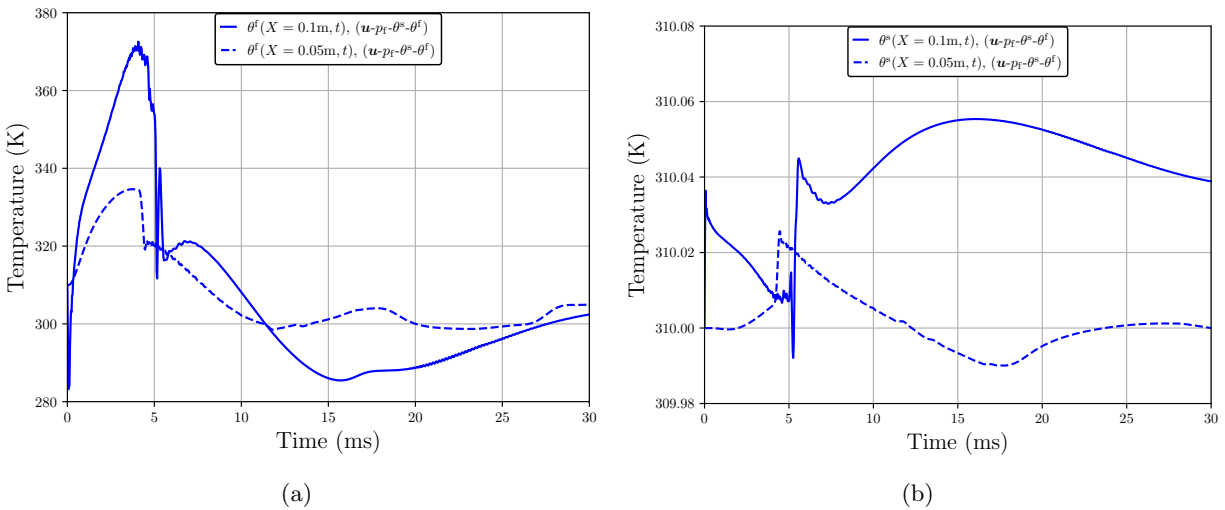


Figure 5.109: Overpressure loading from the Friedlander impulse at 50 kPa showing (a) pore fluid temperature θ^f and (b) solid lung tissue temperature θ^s for $(\mathbf{u}-p_f-\theta^s-\theta^f)$ plotted at the $X = H$ and $X = H/2$ nodes.

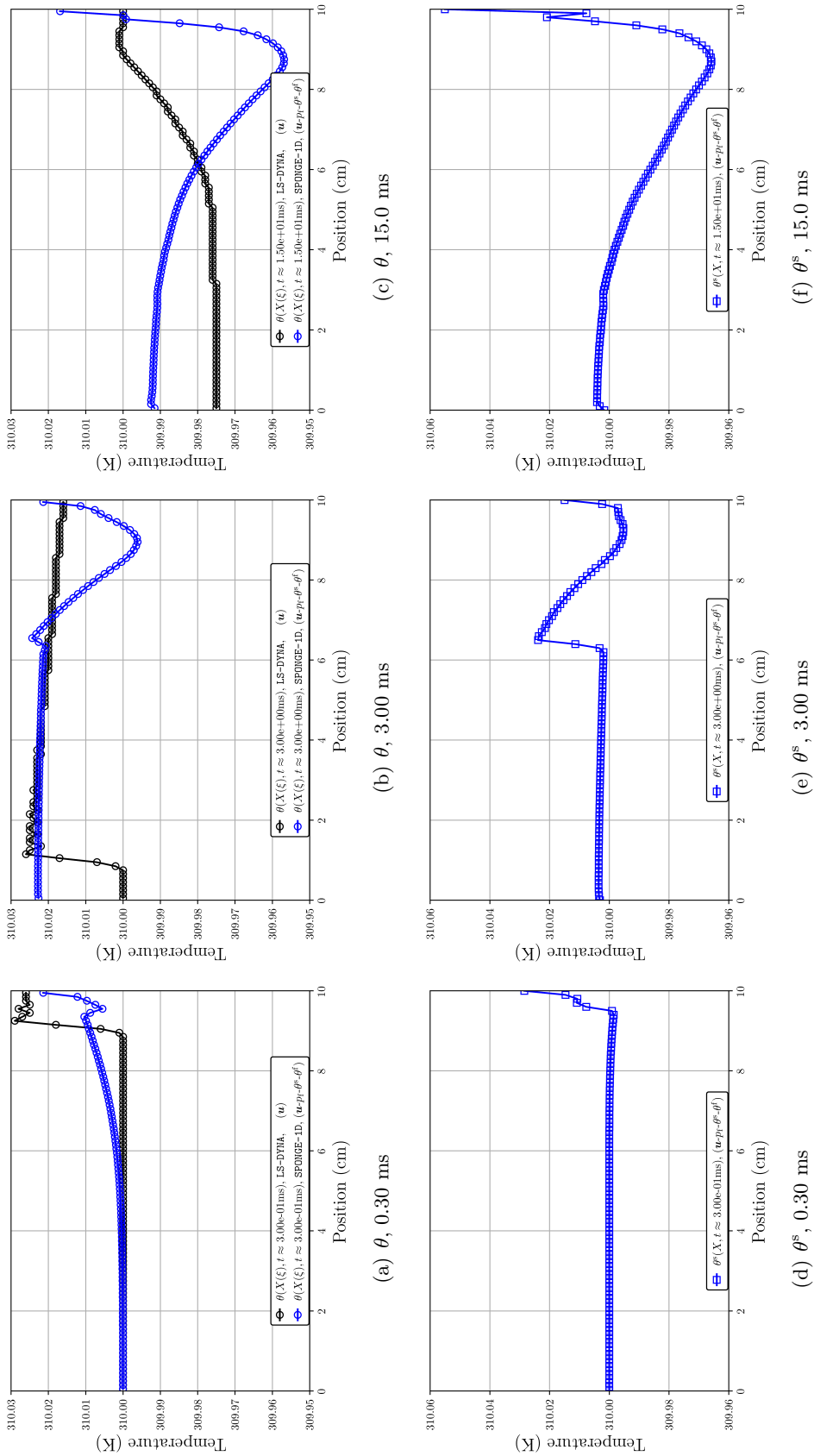


Figure 5.110: Overpressure loading from the Friedlander impulse at 50 kPa showing (a)–(c) contour plots of mixture temperature θ between the single-phase and multiphase models, and (d)–(f) contour plots of solid lung tissue temperature θ^s .

Chapter 6

Conclusion

6.1 Recapitulation of present work

In this work, we have developed a novel, thermodynamically consistent, multiphase, continuum mechanics model within the framework of the theory of porous media (TPM) to simulate soft porous materials subjected to shock loading. The underlying physical theory was presented in detail in Chapters 2 & 3. Therein we showed the complexity of accounting for two distinct phases in a biphasic medium, as compared to more traditional, single-phase models, particularly under the assumption of locally inhomogeneous phase temperatures. We dispelled with basic constitutive assumptions regarding the response of the solid skeleton that had been utilized in prior work [Regueiro and Ebrahimi, 2010, Regueiro et al., 2014, Irwin et al., 2023a,c,d, 2024] in favor of more rigorous constitutive models [Ehlers and Eipper, 1999, Markert, 2005]. The numerical implementation for all the various physical formulations explored in this work (including single-phase models) was presented in Chapter 4. We applied several numerical time integration schemes to each formulation, from the well-known implicit Newmark-beta [Newmark, 1959] and central-difference explicit schemes, to high order Runge-Kutta explicit schemes [Cash and Karp, 1990], the latter of which is preferable for high strain-rate loadings. The one-dimensional (1-D) model implementation is encapsulated in the custom Python code used in this work, `SPONGE-1D`.

In Chapter 5, we presented the results of the numerical simulations. Starting with verification examples, we showed, via use of the Method of Manufactured Solutions (MMS), positive convergence behavior as both temporal and spatial discretization is refined for various element

types applied to example problems. We continued the exercise in verification by showing how the implementation of: the single-phase elastodynamic model agrees with an analytical solution [Eringen and Suhubi, 1975], the multiphase poroelastic model compares to prior work [Li et al., 2004] and is necessary for finite strain, and the multiphase poroelastodynamic model agrees with an analytical solution [de Boer et al., 1993].

Following this, we presented a sensitivity study on the two numerical stabilization techniques used heavily for the multiphase model: shock viscosity and pressure stabilization. For the former, our analysis was constrained to single-phase modeling to isolate the behavior of the shock viscosity q , wherein we observed that the q term removes numerical oscillations (which are likely a result of Gibbs' phenomena) from the numerical solution. Care must be taken by appropriate adjustment of the associated parameters that govern the magnitude of this term so as not to “smooth out” the physical waves propagating through the geometry. Analysis for the pressure stabilization constant then followed, where we showed that smaller values of this constant allowed the solution to approach the unstabilized formulation solution.

Lastly, we simulated the multiphase model developed in `SPONGE-1D` to shock loading. We observed that the standard Taylor-Hood finite elements are objectively “worse” at producing stable solutions at higher overpressure and are much more costly than the linear finite elements (refer to Table 7 in Irwin et al. [2024]). We also showed that the neo-Hookean hyperelastic solid skeleton model with the standard logarithmic term combined with the widely-known Kozeny-Carman model was simply inadequate at enforcing the incompressibility assumption of the solid phase; in lieu of this, we used the Ehlers and Eipper [1999] hyperelastic solid skeleton model with the hyperbolic hydraulic conductivity model developed by Markert [2005] for the remainder of the multiphase analysis, since both models can weakly enforce the incompressibility assumption.

Following these examples, we conducted sensitivity studies on several key parameters that govern relative pore fluid flow through the porous material (lung parenchyma). Beginning with the intrinsic permeability of the solid skeleton, we showed how smaller values lead to almost non-existent relative motions akin to a “locally undrained” assumption, whereas larger values seem

to infer an upper limit on the applicability of TPM for high strain-rate loading with air as the pore fluid. Further investigation for other initial porosities and a different pore fluid is needed to say for certain. Next, we investigated a parameter governing the hyperbolic functional form of the hydraulic conductivity. Smaller values of this parameter were, generally speaking, correlated with larger relative velocities between the solid and fluid phases during compression of the porous material, and the opposite was observed for larger values. Given the uncertainty regarding the values of both the intrinsic permeability and the hyperbolic parameter for lung parenchyma, we chose moderate values that gave what we *believe*¹ would be physically realistic results and those which performed well numerically at higher overpressures.

Then, we investigated the role of the pore fluid viscous stress tensor on the kinematics of the porous medium when subjected to high strain-rate loadings, for both air and blood, and impermeable and permeable boundary conditions. We found that this term has little effect on the overall dynamics due to the difference in magnitude between the pore fluid pressure and the shear & bulk viscosities of the pore fluid. As discussed in Section 4.1.4, this is likely to do with the size of a boundary layer in a pore channel being insignificant compared to the scale of interest (several orders of magnitude difference). However, we note that in the 1-D uniaxial strain framework, it is unlikely that pore fluid shearing forces would have much of a role to play in the dynamics when compared to pore fluid pressure gradients, regardless of whether or not a TPM or traditional CFD framework is used. Future work on a 3-D model would be needed to investigate this further.

Finally, we showed the importance of using TPM to approximate the *pore-scale, smeared* FSI when compared to a simpler (kinematically speaking) single-phase model. The TPM model drastically altered the deformation response of the soft porous material (lung parenchyma). In particular, deformations of the solid skeleton are dampened out by the oscillating pore air, whereas the single-phase model behaves elastodynamically with minimal dissipation of the shock wave. It was also shown that accounting for differences in accelerations between the two constituents was

¹ As we have stated numerous times, calibration to or validation against experimental data is necessary to say for certain whether or not these parameter values are physically realistic.

effective in demonstrating the necessity for the more complex poroelastodynamics formulation for high strain-rate loading applications. Furthermore, by use of the solid extra stress [Ehlers, 2002], we are able to distinguish between solid skeleton, pore fluid (air) and total pressures, and stresses. Such metrics are important for understanding how damage from shock waves, or other impact events, that is, blunt trauma from sports injury or vehicular collisions, will propagate through the porous lung tissue. To this extent, it was shown that for a shock wave resulting from an explosion, the multiphase model can pick up tensile stresses in the solid skeleton sooner than in the single-phase model, which may be indicative of tissue rupture (and damage) [Fung, 1990].

6.2 Ongoing and future work

In Section 5.3.3.2 we presented preliminary results for the locally inhomogeneous temperature model. Therein it was shown that for moderate strain-rates, the resulting kinematics match the locally homogeneous temperature model. The thermodynamic response appears reasonable in the absence of experimental (or numerical) data, however, the response at the boundaries of the mesh displayed characteristics of numerical instability. This instability is more pronounced when the geometry is subjected to higher rates of strain, and causes the numerical solution to go unstable.

As such, there remains an ongoing effort to understand why this instability occurs. Approaches to resolution of this problem are not straightforward given the inherent novelty of this application space. One such remedy may be an approximation of a shock viscosity applied to the pore fluid rather than just the solid skeleton, as discussed in Section 4.4.1, paragraph *Shock viscosity applied to the pore fluid*. This may reduce instability in the pore fluid velocity gradient for the $(\mathbf{u}-\mathbf{u}_f-p_f-\theta^s-\theta^f)$ formulation, which, hopefully, should in turn reduce instability in the pore fluid temperature solution. Another strategy worth pursuing is further manipulation of the Dirichlet boundary conditions for the phase temperatures. While not shown, this was attempted to little avail, but perhaps there are approximations that can be made to recreate experimental conditions, or analytical solutions, by which to verify the present numerical implementation. It may also be worth investigating other numerical time integration schemes, such as those developed in LLNL's

ARKODE [Reynolds et al., 2022, Gardner et al., 2022, Hindmarsh et al., 2005], which combines explicit Runge-Kutta for “fast moving” components of a first order ODE with implicit Runge-Kutta for “slow-moving” components of a first order ODE.

Upon successful resolution of the thermal instabilities, work should proceed with implementation of a damage model for the solid material, as outlined in brief in Section 3.3.1, paragraph *A damage model for the solid constituent*. Quantification of damage is of utmost importance when studying soft porous materials subjected to impact or shock loading, particularly for soft biological tissues. Subsequent analysis can then follow to determine whether or not a multiphase model predicts “more” or “less” damage than a traditional single-phase model.

Further work necessitates validation of the present model, starting with calibration to experimental data. As mentioned, experimental data for lung parenchyma is limited (particularly thermal parameters) to three-dimensional (3-D) space. Therefore, in the absence of experimental data that recreates the uniaxial strain, unidirectional pore fluid flow constraints, it behooves us to extend the 1-D model presented herein to a full 3-D model. Said data could be obtained by enclosing the lung parenchyma in a (near-)frictionless sleeve, and subjecting it to uniaxial loading conditions.

In either case, there are unknown parameters that have discernable effects on the simulated deformation response of lung parenchyma, such as the intrinsic permeability and Grüneisen parameter of the solid skeleton, which would need to be calibrated against experimental data. Deeper investigation surrounding the constitutive models for seepage velocity could then follow. It may be that at higher rates of strain, the inertial Darcy’s law becomes invalid, and a Darcy-Forchheimer model is more appropriate (refer to discussion in Section 4.1.4, paragraph *The need for higher-order elements in the case of viscous pore fluid flow*). Said model also picks up the effects of tortuosity, a value of which is not presently known for lung parenchyma, and thus calibration of this parameter would be highly desirable for others simulating lung parenchyma. Furthermore, the constitutive law governing the hydraulic conductivity and associated parameters therein, and the effect of pore fluid viscosity, needs to be calibrated against experimental data, particularly 3-D data for the latter.

Bibliography

- S. Arezoo, V.L. Tagarielli, C.R. Siviour, and N. Petrinic. Compressive deformation of Rohacell foams: Effects of strain rate and temperature. International Journal of Impact Engineering, 51: 50–57, January 2013. ISSN 0734743X. doi: 10.1016/j.ijimpeng.2012.07.010.
- M. Ates, S. Karadag, A.A. Eker, and B. Eker. Polyurethane foam materials and their industrial applications. Polymer International, 71:1153–1252, October 2022.
- I. Babuska and J.T. Oden. Verification and validation in computational engineering and science: basic concepts. Computational Methods in Applied Mechanics and Engineering, 193:4057–4066, 2004.
- P. Basak. Non-Darcy flow and its implications to seepage problems. Journal of the Irrigation and Drainage Division, 103, 1977.
- J. Bear. Dynamics of Fluids in Porous Media. Dover Publications, Inc., New York, NY, USA, 1972.
- T. Belytschko, W.K. Liu, B. Moran, and K.I. Elkhodary. Nonlinear Finite Elements for Continua and Structures. Wiley, 2 edition, 2014.
- D.J. Benson. Chapter 25: Explicit Finite Element Methods for Large Deformation Problems in Solid Mechanics. In E. Stein, R. de Borst, and T.J.R. Hughes, editors, Encyclopedia of Computational Mechanics, volume 2, page 43. John Wiley & Sons, 2007.
- L. Berger. A Low Order Finite Element Method for Poroelasticity with Applications to Lung Modelling. PhD thesis, University of Oxford, Oxford, United Kingdom, 2015.
- K.B. Bhagavathula, J.S. Parcon, A. Azar, S. Ouellet, S. Satapathy, C.R. Dennison, and J.D. Hogan. Quasistatic response of a shear-thickening foam: Microstructure evolution and infrared thermography. Journal of Cellular Plastics, 57:863–892, November 2021. ISSN 0021-955X, 1530-7999. doi: 10.1177/0021955X20963989.
- J. Bhinder, S.K. Verma, and P.K. Agnihotri. Qualifying carbon nanotube reinforced polyurethane foam as helmet inner liner through in-situ, static and low velocity impact testing. Materials Science and Engineering B, 274:1155496, October 2021.
- L. Bianchi, F. Cavarzan, L. Ciampitti, M. Cremonesi, F. Grilli, and P. Saccomandi. Thermophysical and mechanical properties of biological tissues as a function of temperature: a systematic literature review. Journal of Hypothermia, 39:297–340, February 2022.

- M.A. Biot. General theory of three-dimensional consolidation. Journal of Applied Physics, 12: 155–164, 1941. doi: 10.1063/1.1712886.
- M.A. Biot and D.G. Wills. The elastic coefficients of the theory of consolidation. ASME Journal of Applied Mechanics, 24:594–601, 1957.
- P. Bogacki and L.F. Shampine. A 3(2) pair of runge - kutta formulas. Applied Mathematics Letters, 2:321–325, 1989. ISSN 0893-9659. doi: [https://doi.org/10.1016/0893-9659\(89\)90079-7](https://doi.org/10.1016/0893-9659(89)90079-7).
- R. Bowen. Incompressible porous media models by use of the theory of mixture. International Journal of Engineering Science, 18:1129–1148, 1980.
- R. Bowen. Compressible porous media models by use of the theory of mixtures. International Journal of Engineering Science, 20:697–735, 1982.
- R.M. Bowen. Continuum theory of mixtures. Technical Report CR-45, US Army Ballistic Research Laboratories, Aberdeen Proving Ground (MD), 1971.
- R.M. Bowen. Theory of Mixtures. In Continuum Physics, pages 1–127. Elsevier, 1976. ISBN 978-0-12-240803-8. doi: 10.1016/B978-0-12-240803-8.50017-7.
- R.M. Bowen and P.J. Chen. Shock waves in a mixture of linear elastic materials. Rendiconti del Circolo Matematico di Palermo, 21:267–283, 1972.
- R.M. Bowen and P.J. Chen. Shock waves in ideal fluid mixtures with several temperatures. Archive for Rational Mechanics and Analysis, 53:277–294, 1974.
- R.M. Bowen and M.L. Doria. Effect of diffusion on the growth and decay of acceleration waves in gases. Journal of the Acoustical Society of America, 53:75–82, 1973.
- R.M. Bowen and D.J. Garcia. On the thermodynamics of mixtures with several temperatures. International Journal of Engineering Science, 8:63–83, 1970.
- R.M. Bowen and R.L. Rankin. Acceleration waves in ideal fluid mixtures with several temperatures. Archive for Rational Mechanics and Analysis, 51:261–277, 1973.
- R.M. Bowen and T.W. Wright. On the growth and decay of wave fronts in a mixture of linearelastic materials. Rendiconti del Circolo Matematico di Palermo, 21:209–234, 1972a.
- R.M. Bowen and T.W. Wright. On wave propagation in a mixture of linear elastic materials. Technical Report 1581, US Army Ballistic Research Laboratories, Aberdeen Proving Ground (MD), 1972b.
- R.M. Bowen and T.W. Wright. On wave propagation in a mixture of linear elastic materials. Technical report, US Army Ballistic Research Laboratories, Aberdeen Proving Ground (MD), 1972c.
- R.M. Bowen, P.J. Chen, and J.W. Nunziato. Shock waves in a mixture of chemically reacting materials with memory. Acta Mechanica, 21:1–11, 1975.
- M. Brannen, G. Kang, S. Dutrisac, R. Banton, J.D. Clayton, and O.E. Petel. The influence of the tertiary bronchi on dynamic lung deformation. Journal of the Mechanical Behavior of Biomedical Materials, 130:105181, 2022.

- F. Brezzi and J. Pitkäranta. On the Stabilization of Finite Element Approximations of the Stokes Equations. In W. Hackbusch, editor, Efficient Solutions of Elliptic Systems: Proceedings of a GAMM-Seminar Kiel, January 27 to 29, 1984, pages 11–19. Vieweg+Teubner Verlag, Wiesbaden, 1984. ISBN 978-3-663-14169-3. doi: 10.1007/978-3-663-14169-3_2.
- R. Brun and L.Z. Dumitrescu, editors. On the Modelling of Wave Phenomena in Permeable Foam, Shock Waves @ Marseille III, Berlin, Heidelberg, 1995. Springer Berlin Heidelberg.
- T.H. Burford and B. Burbank. Traumatic wet lung. observations on certain physiologic fundamentals of thoracic trauma. Journal of Thoracic Surgery, 14:415–424, 1945.
- B. Burtschell, D. Chapelle, and P. Moireau. Effective and energy-preserving time discretization for a general nonlinear poromechanical formulation. Computers & Structures, 182:313–324, April 2017. ISSN 00457949. doi: 10.1016/j.compstruc.2016.10.022.
- I. Bush and S.A. Challener. Finite element modeling of non-penetrating thoracic impact. Proceedings of the International Research Council on Biokinetics Impacts, Bergisch Gladbach, Germany, 1988.
- T.D. Cao, L. Sanavia, and B.A. Schrefler. A thermo-hydro-mechanical model for multiphase geomaterials in dynamics with application to strain localization simulation. International Journal for Numerical Methods in Engineering, 107:312–337, July 2016. ISSN 00295981. doi: 10.1002/nme.5175.
- J. R. Cash and A.H. Karp. A variable order runge-kutta method for initial value problems with rapidly varying right-hand sides. ACM Transactions on Mathematical Software, 16:201–222, September 1990. ISSN 0098-3500. doi: 10.1145/79505.79507.
- Y. Chae, D. Protsenko, P.K. Holden, C. Chlebicki, and B.J.F. Wong. Thermoforming of tracheal cartilage: viability, shape change, and mechanical behavior. Lasers in Surgery and Medicine, 40: 550–561, June 2008.
- D. Chapelle and P. Moireau. General coupling of porous flows and hyperelastic formulations – From thermodynamics principles to energy balance and compatible time schemes. European Journal of Mechanics, 46:82–96, 2014.
- J. Chen, E. Li, W. Liu, Y. Mao, and S. Hou. Sustainable composites with ultrahigh energy absorption from beverage cans and polyurethane foam. Composites Science and Technology, 239:110047, 2023. ISSN 0266-3538. doi: <https://doi.org/10.1016/j.compscitech.2023.110047>.
- J. D. Clayton and A. D. Freed. A constitutive model for lung mechanics and injury applicable to static, dynamic, and shock loading. Mechanics of Soft Materials, 2, December 2020a. ISSN 2524-5600, 2524-5619. doi: 10.1007/s42558-020-0018-9.
- J.D. Clayton. Differential Geometry and Kinematics of Continua. World Scientific, Singapore, 2014.
- J.D. Clayton. Modeling lung tissue dynamics and injury under pressure and impact loading. Biomechanics and Modeling in Mechanobiology, 19:2603–2626, June 2020. doi: 10.1007/s10237-020-01358-9.

- J.D. Clayton. Analysis of shock waves in a mixture theory of a thermoelastic solid and fluid with distinct temperatures. International Journal of Engineering Science, 175:103675, May 2022. ISSN 00207225. doi: 10.1016/j.ijengsci.2022.103675.
- J.D. Clayton and A.D. Freed. A Continuum Mechanical Model of the Lung. Technical Report ARL-TR-8859, DEVCOM Army Research Laboratory, Aberdeen Proving Ground (MD), 2019a.
- J.D. Clayton and A.D. Freed. Viscoelastic-damage theory based on a QR decomposition of deformation gradient. Technical Report ARL-TR-8840, DEVCOM Army Research Laboratory, Aberdeen Proving Ground (MD), 2019b.
- J.D. Clayton and A.D. Freed. A constitutive framework for finite viscoelasticity and damage based on the Gram-Schmidt decomposition. Acta Mechanica, 231:3319–3362, 2020b.
- J.D. Clayton, R.J. Banton, and A.D. Freed. A nonlinear thermoelastic-viscoelastic continuum model of lung mechanics for shock wave analysis. In J.M.D. Lane, editor, Shock Compression of Condensed Matter, volume 2272, page 040001. AIP Conference Proceedings, Portland (OR), 2020.
- J.D. Clayton, R.J. Banton, and A.R. Goertz. A Continuum Model of the Human Lung: Implementation and Parameterization. Technical Report ARL-TR-9138, DEVCOM Army Research Laboratory, Aberdeen Proving Ground (MD), 2021.
- S.M. Cohn and J.J. DuBose. Pulmonary contusion: An update on recent advances in clinical management. World Journal of Surgery, 34:1959–1970, 2010. doi: 10.1007/s00268-010-0599-9.
- B.D. Coleman and W. Noll. The thermodynamics of elastic materials with heat conduction and viscosity. Archive for Rational Mechanics and Analysis, 13:167–178, 1963.
- F. Concha and D.E. Hurtado. Upscaling the poroelastic behavior of the lung parenchyma: A finite-deformation micromechanical model. Journal of the Mechanics and Physics of Solids, 145:104147, December 2020. ISSN 00225096. doi: 10.1016/j.jmps.2020.104147.
- F. Concha, S.-V. Mauricio, and H.D. Hurtado. Micromechanical model of lung parenchyma hyperelasticity. Journal of the Mechanics and Physics of Solids, 112:126–144, March 2018.
- D.M. Constantinescu and D.A. Apostol. Performance and Efficiency of Polyurethane Foams under the Influence of Temperature and Strain Rate Variation. Journal of Materials Engineering and Performance, 29:3016–3029, May 2020. ISSN 1059-9495, 1544-1024. doi: 10.1007/s11665-020-04860-4.
- G.J. Cooper. Protection of the lung from blast overpressure by thoracic stress wave decouplers. The Journal of Trauma: Injury, Infection, and Critical Care, 40:105S–110S, 1996. doi: 10.1097/00005373-199603001-00024.
- G.J. Cooper, D.J. Townend, S.R. Cater, and B.P. Pearce. The role of stress waves in thoracic visceral injury from blast loading: Modification of stress transmission by foams and high-density materials. Journal of Biomechanics, 24:273–285, 1991. doi: 10.1016/0021-9290(91)90346-O.
- O. Coussy. Poromechanics. John Wiley & Sons, 2004.

- D.S. Cronin. Model for Pulmonary Response Resulting from High Deformation Rate Loading. volume IRC-11-53, page 12. Ircobi Conference Proceedings, 2011.
- J.J. Cross. Mixtures of fluids and isotropic solids. Archive of Mechanics, 6:1025–1039, 1973.
- Z. Dai, Y. Peng, H.A. Mansy, R.H. Sandler, and T.J. Royston. Comparison of poroviscoelastic models for sound and vibration in the lungs. Journal of Vibration and Acoustics, 136:1–10, October 2014.
- L. Davison. Fundamentals of Shock Wave Propagation in Solids. Springer, 2008.
- R. de Boer. Trends in Continuum Mechanics of Porous Media: Theory and Applications of Transport in Porous Media. Springer, 2005.
- R. de Boer, W. Ehlers, and Z. Liu. One-dimensional transient wave propagation in fluid-saturated incompressible porous media. Archive of Applied Mechanics, 63:59–72, January 1993. ISSN 0939-1533, 1432-0681. doi: 10.1007/BF00787910.
- T. Decker and S. Kedziora. Optimizing the thickness of functionally graded lattice structures for high-performance energy absorption: A case study based on a bicycle helmet. Applied Sciences, 14:2788, March 2024.
- N. Dehghan, C. de Mestral, M.D. McKee, E.H. Schemitsch, and A. Nathens. Flail chest injuries: A review of outcomes and treatment practices from the national trauma data bank. Journal of Trauma and Acute Care Surgery, 76:462–468, February 2014.
- LS-DYNA Dev. LS-DYNA Theory Manual. Livermore Software Technology Corporation, Livermore, CA, USA, 2019.
- LS-DYNA Dev. LS-DYNA Keyword User’s Manual. Livermore Software Technology Corporation, Livermore, CA, USA, 2020.
- J.M. Dewey. The Friedlander Equations. In I. Sochet, editor, Blast Effects: Physical Properties of Shock Waves, pages 37–55. Springer International Publishing, 2018. ISBN 978-3-319-70831-7. doi: 10.1007/978-3-319-70831-7_3.
- S. Diebels and W. Ehlers. Dynamic analysis of a fully saturated porous medium accounting for geometrical and material non-linearities. International Journal for Numerical Methods in Engineering, 39:81–97, January 1996.
- J. Donea and A. Huerta. Finite Element Methods for Flow Problems. John Wiley & Sons, 2003. ISBN 0-471-49666-9.
- W. Ehlers. Foundations of multiphase and porous materials. In W. Ehlers and J. Bluhm, editors, Porous Media: Theory, Experiments and Numerical Applications, pages 3–86. Springer Berlin Heidelberg, Berlin, Heidelberg, 2002. ISBN 978-3-662-04999-0. doi: 10.1007/978-3-662-04999-0_1.
- W. Ehlers. Darcy, Forchheimer, Brinkman and Richards: classical hydromechanical equations and their significance in the light of the TPM. Archive of Applied Mechanics, 92:619–639, February 2022. ISSN 0939-1533, 1432-0681. doi: 10.1007/s00419-020-01802-3.

- W. Ehlers and G. Eipper. Finite elastic deformations in liquid-saturated and empty porous solids. Transport in Porous Media, 34:179–191, March 1999.
- W. Ehlers and K. Häberle. Interfacial mass transfer during gas–liquid phase change in deformable porous media with heat transfer. Transport in Porous Media, 114, March 2016. doi: 10.1007/s11242-016-0674-2.
- W. Ehlers, P. Ellsiepen, P. Blome, D. Mahnkopf, and B. Markert. Theoretische und numerische studien zur lösung von rand- und anfangswertproblemen in der theorie poröser medien, abschlußbericht zum dfg-forschungsvorhaben eh 107/6-2. [*Theoretical and numerical studies for the solution of boundary and initial value problems in the theory of porous media, final report on the DFG research project eh 107/6-2.*]. Technical Report 99-II-1, Institut für Mechanick, Unversität Stuttgart [*Institute for Mechanics, University of Stuttgart*], 1999.
- W. Ehlers, B. Markert, S. Diebels, and A. Nödling. Permeability studies on soft open-cell foams. PAMM, 2:162–163, March 2003. doi: <https://doi.org/10.1002/pamm.200310066>.
- G. Eipper. Theorie und Numerik finiter elastischer Deformationen in fluidgesättigten porösen Medien [*Theory and Numerical analysis of finite elastic Deformations in fluid-saturated porous Media*]. PhD thesis, Institut für Mechanik (Bauwesen) der Universität Stuttgart [*Institute for Mechanics (Civil Engineering), University of Stuttgart*], Stuttgart, Germany, 1998.
- A. C. Eringen and E. S. Suhubi. Elastodynamics. Vol. 2: Linear Theory. New York-London, Academic Press, 1975.
- D.P. Fankell. A Thermo-Poromechanics Finite Element Model for Predicting Arterial Tissue Fusion. PhD thesis, University of Colorado Boulder, Boulder, CO, USA, 2017.
- J.T. Fernandez. Natural Convection from Cylinders Buried in Porous Media. PhD thesis, University of California Berkeley, Berkeley, CA, USA, 1972.
- A.D. Freed and J.D. Clayton. Coordinate indexing strategies for the laplace stretch in two and three dimensions. Technical Report ARL-TR-9530, DEVCOM Army Research Laboratory, Aberdeen Proving Ground (MD), 2022.
- A.D. Freed, S. Zamana, S. Paul, and J.D. Clayton. A Dodecahedral Model for Alveoli. Part I. Theory and Numerical Methods. Technical Report ARL-TR-9148, DEVCOM Army Research Laboratory, Aberdeen Proving Ground (MD), 2021.
- F.G. Friedlander. The diffraction of sound pulses. I. Diffraction by a semi-infinite plane. The Royal Society, 186, September 1946.
- Y.C. Fung. Biomechanics. Motion, flow, stress, and growth. Springer, 1990.
- A. Gajo and R. Denzer. Finite element modelling of saturated porous media at finite strains under dynamic conditions with compressible constituents. International Journal for Numerical Methods in Engineering, 85:1705–1736, April 2011. doi: <https://doi.org/10.1002/nme.3051>.
- A. Gajo, A. Sietta, and R. Vitaliani. Evaluation of three- and two-field finite element methods for the dynamic response of saturated soil. International Journal for Numerical Methods in Engineering, 37:1231–1247, 1994. doi: <https://doi.org/10.1002/nme.1620370708>.

- D.J. Gardner, D.R. Reynolds, C.S. Woodward, and C.J. Balos. Enabling new flexibility in the SUNDIALS suite of nonlinear and differential/algebraic equation solvers. ACM Transactions on Mathematical Software (TOMS), 2022. doi: 10.1145/3539801.
- F.S. Gayzik, J.J. Hoth, and J.D. Stitzel. Finite element-based injury metrics for pulmonary contusion via concurrent model optimization. Biomechanics and Modeling in Mechanobiology, 10: 505–520, August 2010. doi: 10.1007/s10237-010-0251-5.
- S.R. Ghadiani. A Multiphasic Continuum Mechanical Model for Design Investigations of an Effusion-Cooled Rocket Thrust Chamber. PhD thesis, Institut für Mechanik (Bauwesen) Lehrstuhl für Kontinuumsmechanik der Univeät Stuttgart [*Institute for Mechanics (Civil Engineering), Chair of Continuum Mechanics, University of Stuttgart*], Stuttgart, Germany, 2005.
- J. Ghorbani, M. Nazem, and J.P. Carter. Numerical modelling of multiphase flow in unsaturated deforming porous media. Computers and Geotechnics, 71:195–206, January 2016. ISSN 0266352X. doi: 10.1016/j.compgeo.2015.09.011.
- H.W.J. Goossens, J.W. Cleijne, H.J. Smolders, and M.E.H. van Dongen. Shock wave induced evaporation of water droplets in a gas-droplet mixture. Experiments in Fluids, 6:561–568, February 1988.
- Q. Grimal, A. Watzky, and S. Naili. A one-dimensional model for the propagation of transient pressure waves through the lung. Journal of Biomechanics, 35:1081–1089, April 2002. doi: 10.1016/S0021-9290(02)00064-7.
- Y. Heider. Saturated Porous Media Dynamics with Application to Earthquake Engineering. PhD thesis, Institut für Mechanik (Bauwesen) Lehrstuhl für Kontinuumsmechanik der Univeät Stuttgart [*Institute for Mechanics (Civil Engineering), Chair of Continuum Mechanics, University of Stuttgart*], Stuttgart, Germany, 2012. OCLC: 824646288.
- A.C. Hindmarsh, P.N. Brown, K.E. Grant, S.L. Lee, R. Serban, D.E. Shumaker, and C.S. Woodward. SUNDIALS: Suite of nonlinear and differential/algebraic equation solvers. ACM Transactions on Mathematical Software (TOMS), 31(3):363–396, 2005. doi: 10.1145/1089014.1089020.
- M.J. Holmes, N.G. Parker, and M.J.W. Povey. Temperature dependence of bulk viscosity in water using acoustic spectroscopy. Journal of Physics: Conference Series, 269, January 2011.
- G.A. Holzapfel. Nonlinear Solid Mechanics: A Continuum Approach for Engineering. John Wiley & Sons, 2000.
- D.R. Hooker. Physiological effects of air concussion. American Journal of Physiology, 67:219–274, 1924.
- F. Hosseinejad, F. Kalateh, and A. Mojtahedi. Numerical Investigation of liquefaction in earth dams: A Comparison of Darcy and Non-Darcy flow models. Computers and Geotechnics, 116: 103182, December 2019. ISSN 0266352X. doi: 10.1016/j.compgeo.2019.103182.
- M. Huang, Z.Q. Yue, L.G. Tham, and O.C. Zienkiewicz. On the stable finite element procedures for dynamic problems of saturated porous media. International Journal for Numerical Methods in Engineering, 61:1421–1450, November 2004. ISSN 0029-5981, 1097-0207. doi: 10.1002/nme.1115.

- T.J.R. Hughes. The Finite Element Method: Linear Static and Dynamic Finite Element Analysis. Dover Publications, Inc., 2000. ISBN 978-0-486-41181-1.
- T.J.R. Hughes, J.A. Cottrell, and Y. Bazilevs. Isogeometric analysis: Cad, finite elements, nurbs, exact geometry and mesh refinement. Computer Methods in Applied Mechanics and Engineering, 194:4135–4195, October 2005.
- J.D. Humphrey. Review paper: Continuum biomechanics of soft biological tissues. Proceedings of the the Royal Society of London. Series A: Mathematical, Physical and Engineering Sciences, 459:3–46, 2003. doi: 10.1098/rspa.2002.1060.
- S. Idriz, A. Abbas, S. Sadigh, and S. Padley. Pulmonary laceration secondary to a traumatic soccer injury: A case report and review of the literature. American Journal of Emergency Medicine, 31:1625, November 2013. doi: 10.1016/j.ajem.2013.06.032.
- Z.T. Irwin, R.A. Regueiro, and J.D. Clayton. A Large Deformation Multiphase Continuum Mechanics Model for Shock Loading of Lung Parenchyma. Part I: Theory. Technical Report ARL-TR-9686, DEVCOM Army Research Laboratory, Aberdeen Proving Ground MD, 2023a. URL <https://apps.dtic.mil/sti/trecms/pdf/AD1201818.pdf>.
- Z.T. Irwin, R.A. Regueiro, and J.D. Clayton. A Large Deformation Multiphase Continuum Mechanics Model for Shock Loading of Lung Parenchyma. Part II: Numerical methods. Technical Report ARL-TR-9687, DEVCOM Army Research Laboratory, Aberdeen Proving Ground MD, 2023b. URL <https://apps.dtic.mil/sti/trecms/pdf/AD1201815.pdf>.
- Z.T. Irwin, R.A. Regueiro, and J.D. Clayton. A Large Deformation Multiphase Continuum Mechanics Model for Shock Loading of Lung Parenchyma. Part III: Numerical simulations. Technical Report ARL-TR-9688, US Army Research Laboratory, Aberdeen Proving Ground MD, 2023c. URL <https://apps.dtic.mil/sti/trecms/pdf/AD1201816.pdf>.
- Z.T. Irwin, R.A. Regueiro, and J.D. Clayton. A Large Deformation Multiphase Continuum Mechanics Model for Shock Loading of Lung Parenchyma: Investigating the Effects of Fluid Viscous Stress. Technical Report ARL-TR-9815, DEVCOM Army Research Laboratory, Aberdeen Proving Ground MD, 2023d. URL <https://apps.dtic.mil/sti/trecms/pdf/AD1214028.pdf>.
- Z.T. Irwin, J.D. Clayton, and R.A. Regueiro. A large deformation multiphase continuum mechanics model for shock loading of soft porous materials. International Journal for Numerical Methods in Engineering, 125:1–34, January 2024.
- H. Jain, D.P. Mondal, G. Gupta, A. Kothari, R. Kumar, A. Pandey, S. Shiva, and P. Agarwal. Microstructure and high temperature compressive deformation in lightweight open cell titanium foam. Manufacturing Letters, 27:67–71, January 2021. ISSN 22138463. doi: 10.1016/j.mfglet.2020.12.007.
- T.-R. Kim, J.K. Shin, T.S. Goh, H.-S. Kim, J.S. Lee, and C.-S. Lee. Modeling of elasto-viscoplastic behavior for polyurethane foam under various strain rates and temperatures. Composite Structures, 180:686–695, November 2017. ISSN 02638223. doi: 10.1016/j.compstruct.2017.08.032.
- B. Klahr, J.L. Medeiros Thiesen, O. Teixeira Pinto, T.A. Carniel, and E.A. Fancello. An investigation of coupled solution algorithms for finite-strain poroviscoelasticity applied to soft biological tissues. International Journal for Numerical Methods in Engineering, 123, May 2022. ISSN 0029-5981, 1097-0207. doi: 10.1002/nme.6928.

- D. Koch. Thermomechanical Modelling of Non-isothermal Porous Materials with Application to Enhanced Geothermal Systems. PhD thesis, Institut für Mechanik (Bauwesen) Lehrstuhl für Kontinuumsmechanik der Universität Stuttgart [*Institute for Mechanics (Civil Engineering), Chair of Continuum Mechanics, University of Stuttgart*], Stuttgart, Germany, 2016.
- A. Laadhari and G. Székely. Fully implicit finite element method for the modeling of free surface flows with surface tension effect. International Journal for Numerical Methods in Engineering, 111:1047–1074, September 2017. ISSN 00295981. doi: 10.1002/nme.5493.
- W. M. Lai, Van C. Mow, and V. Roth. Effects of Nonlinear Strain-Dependent Permeability and Rate of Compression on the Stress Behavior of Articular Cartilage. Journal of Biomechanical Engineering, 103:61–66, May 1981. ISSN 0148-0731, 1528-8951. doi: 10.1115/1.3138261.
- B. Lande and W. Mitzner. Analysis of lung parenchyma as a parametric porous medium. Journal of Applied Physiology, 101:926–933, September 2006. ISSN 8750-7587, 1522-1601. doi: 10.1152/jappphysiol.01548.2005.
- R. Landshoff. A numerical method for treating fluid flow in the presence of shocks. Technical Report 1930, Los Alamos Scientific Laboratory, 1955.
- M. E. Levenston, E. H. Frank, and A. J. Grodzinsky. Variationally derived 3-field finite element formulations for quasistatic poroelastic analysis of hydrated biological tissues. Computer Methods in Applied Mechanics and Engineering, 156:231–246, April 1998. ISSN 0045-7825. doi: [https://doi.org/10.1016/S0045-7825\(97\)00208-9](https://doi.org/10.1016/S0045-7825(97)00208-9).
- R.W. Lewis and B.A. Schrefler. The finite element method in the deformation and consolidation of porous media. John Wiley & Sons, Chichester, United Kingdom, 1987.
- R.W. Lewis and B.A. Schrefler. The Finite Element Method in the Static and Dynamic Deformation and Consolidation of Porous Media. John Wiley & Sons, Ltd., United Kingdom, 2 edition, 1998. ISBN 9780471928096.
- C. Li and R.I. Borja. Finite element formulation of poro-elasticity suitable for large deformation dynamic analysis. Technical report, John A. Blume Earthquake Engineering Center., 2005.
- C. Li, R.I. Borja, and R.A. Regueiro. Dynamics of porous media at finite strain. Computer Methods in Applied Mechanics and Engineering, 193:3837–3870, September 2004. ISSN 00457825. doi: 10.1016/j.cma.2004.02.014.
- L. Li, S. Zhou, X. Du, J. Song, and C. Gao. Numerical Study on the Seismic Response of Fluid-Saturated Porous Media Using the Precise Time Integration Method. Applied Sciences, 9:2037, May 2019. ISSN 2076-3417. doi: 10.3390/app9102037.
- X. Liang, H. Luo, Y. Mu, M. Chen, J. Ye, and D. Chi. Quasi-static and Dynamic Compression of Aluminum Foam at Different Temperatures. Journal of Materials Engineering and Performance, 28:4952–4963, August 2019. ISSN 1059-9495, 1544-1024. doi: 10.1007/s11665-019-04207-8.
- C.-H. Liu, M.N. Skryabina, M. Singh, J. Li, C. Wu, E. Sobol, and K.V. Larin. Elasticity measurement of nasal cartilage as a function of temperature using optical coherence elastography. volume 9327. SBIE, San Francisco, CA., March 2015.

- Y.-L. Liu, G.-Y. Li, H. Ping, Z.-Q. Mao, and Y. Cao. Temperature-dependent elastic properties of brain tissues measured with the shear wave elastography method. Journal of Mechanical Behavior of Biomedical Materials, 65:652–656, January 2017.
- Z. Lotfian and M.V. Sivaselvan. Mixed finite element formulation for dynamics of porous media: Dynamics of porous media. International Journal for Numerical Methods in Engineering, 115: 141–171, July 2018. ISSN 00295981. doi: 10.1002/nme.5799.
- S. C. H. Lu and K. S. Pister. Decomposition of deformation and representation of the free energy function for isotropic thermoelastic solids. International Journal of Solids and Structures, 11: 927–934, July 1975. ISSN 0020-7683. doi: [https://doi.org/10.1016/0020-7683\(75\)90015-3](https://doi.org/10.1016/0020-7683(75)90015-3).
- N.A. Lutsenko and V.A. Levin. Smoldering of porous media: numerical model and comparison of calculations with experiment. Journal of Physics: Conference Series. IOP Publishing Ltd, 2017.
- L.E. Malvern. Introduction to the Mechanics of a Continuous Medium. Prentice-Hall, Inc., 1969.
- L.G. Margolin and N.M. Lloyd-Ronning. Artificial Viscosity – Then and Now. [arXiv:2202.11084](https://arxiv.org/abs/2202.11084) [[astro-ph](https://arxiv.org/abs/2202.11084), [physics:math-ph](https://arxiv.org/abs/2202.11084), [physics:physics](https://arxiv.org/abs/2202.11084)], February 2022. arXiv: 2202.11084.
- B. Markert. Porous Media Viscoelasticity with Application to Polymeric Foams. PhD thesis, Institut für Mechanik (Bauwesen) Lehrstuhl für Kontinuumsmechanik der Universität Stuttgart [*Institute for Mechanics (Civil Engineering), Chair of Continuum Mechanics, University of Stuttgart*], 2005.
- B. Markert. A biphasic continuum approach for viscoelastic high-porosity foams: Comprehensive theory, numerics, and application. Archives of Computational Methods in Engineering, 15:371–446, August 2008.
- B. Markert, Y. Heider, and W. Ehlers. Comparison of monolithic and splitting solution schemes for dynamic porous media problems. International Journal for Numerical Methods in Engineering, 82:1341–1383, June 2009. ISSN 00295981, 10970207. doi: 10.1002/nme.2789.
- J.E. Marsden and T.J.R. Hughes. Mathematical Foundations of Elasticity. Dover Publications, Inc., 1983.
- L. Marshall. The Temperature-Dependent Mechanics of Human Articular Cartilage Under Large-Strain Shear. PhD thesis, University of Connecticut, 2019.
- L. Marshall, A. Tarakanova, P. Szarek, and D.M. Pierce. Cartilage and collagen mechanics under large-strain shear within *in vivo* and at supraphysiological temperatures. Journal of the Mechanical Behavior of Biomedical Materials, 103:103595, December 2019.
- A.E. Mattson and W.J. Rider. Artificial viscosity: back to the basics. International Journal for Numerical Methods in Fluid Mechanics, 77:400–417, November 2014.
- R.L. Maynard, G.J. Cooper, and R. Scott. Mechanisms of injury: bomb blast injuries and explosions. In Trauma, 1989.
- M.A. Mayorga. The pathology of primary blast overpressure injury. Toxicology, 121:17–28, 1997.

- C. Miehe, L.M. Schänzel, and H. Ulmer. Phase field modeling of fracture in multi-physics problems. part i. balance of crack surface and failure criteria for brittle crack propagation in thermo-elastic solids. Computer Methods in Applied Mechanics and Engineering, 294:449–485, December 2015.
- A. Mohammadi, L. Bianchi, S. Asadi, and P. Saccomandi. Measurement of Ex Vivo Liver, Brain and Pancreas Thermal Properties as Function of Temperature. Sensors, 21:4236, June 2021.
- A.A. Naderi, K. Imani, and H. Ahmadi. Crashworthiness study of an innovative helmet liner composed of an auxetic lattice structure and pu foam. Mechanics of Advanced Composite Structures, 9:25–35, January 2022.
- J. Naumann, N. Koppe, U.H. Thome, M. Laube, and M. Zink. Mechanical properties of the premature lung: From tissue deformation under load to mechanosensitivity of alveolar cells. Frontiers in Bioengineering and Biotechnology, 10:964318, September 2022.
- P. Navas, L. Sanavia, S. López-Querol, and R.C. Yu. Explicit meshfree solution for large deformation dynamic problems in saturated porous media. Acta Geotechnica, 13:227–242, December 2017. ISSN 1861-1125, 1861-1133. doi: 10.1007/s11440-017-0612-7.
- N.M. Newmark. A method of computation for structural dynamics. Journal of the Engineering Mechanics Divison, 85:67–94, July 1959.
- C. Nicholson. Diffusion and related transport mechanisms in brain tissue. Reports on Progress in Physics, 64:815–844, April 2001.
- D.A. Nield and A. Bejan. Convection in Porous Media. Springer New York, New York, NY, 2013. ISBN 978-1-4614-5540-0 978-1-4614-5541-7. doi: 10.1007/978-1-4614-5541-7.
- W.F. Noh. Errors for calculations of strong shocks using an artificial viscosity and an artificial heat flux. Journal of Computational Physics, 72:78–120, 1986.
- A. Obaid, S.T. Turek, Y. Heider, and B. Markert. A new monolithic Newton-multigrid-based FEM solution scheme for large strain dynamic poroelasticity problems: A new monolithic Newton-multigrid-based FEM solution scheme for large strain dynamic poroelasticity problems. International Journal for Numerical Methods in Engineering, 109:1103–1129, February 2017. ISSN 00295981. doi: 10.1002/nme.5315.
- W.L. Oberkampf, T.G. Trucano, and C. Hirsch. Verification, validation, and predictive capability in computational engineering and physics. Applied Mechanics Reviews, 57:345–384, December 2004.
- C. Patte, M. Genet, and D. Chapelle. A quasi-static poromechanical model of the lungs. Biomechanics and Modeling in Mechanobiology, 21:527–551, April 2022. ISSN 1617-7959, 1617-7940. doi: 10.1007/s10237-021-01547-0.
- D.R. Pauzé and D.K. Pauzé. Emergency management of blunt chest trauma in children: An evidence-based approach. Pediatric Emergency Medicine Practice, 10:1–22, November 2013.
- D.M. Pedroso. A consistent u-p formulation for porous media with hysteresis: A consistent u-p formulation for porous media with hysteresis. International Journal for Numerical Methods in Engineering, 101:606–634, February 2015. ISSN 00295981. doi: 10.1002/nme.4808.

- A. Popp, B. I. Wohlmuth, M. W. Gee, and W. A. Wall. Dual quadratic mortar finite element methods for 3d finite deformation contact. SIAM Journal on Scientific Computing, 34:B421–B446, 2012. doi: 10.1137/110848190.
- W.H. Press, S.A. Teukolsky, W.T. Vetterling, and B.P. Flannery. Numerical Recipes in C: The Art of Scientific Computing. Cambridge University Press, 2nd edition, 1992.
- D.E. Protsenko, A. Zemek, and B.J.F. Wong. Temperature dependent change in equilibrium elastic modulus after thermally induced stress relaxation in porcine septal cartilage. Lasers in Surgery and Medicine, 40:202–210, January 2008.
- Y.S. Pydi, A. Nath, A. Chawla, S. Mukherjee, S. Lalwani, and R. Malhotra. Strain-rate-dependent material properties of human lung parenchymal tissue using inverse finite element approach. Biomechanics and Modeling in Mechanobiology, 22:2083–2096, August 2023. doi: 10.1007/s10237-023-01751-0.
- P.W. Rand, E. Lacombe, H.E. Hunt, and W.H. Austin. Viscosity of normal human blood under normothermic and hypothermic conditions. Journal of Applied Physiology, 19:117–122, January 1964.
- R.A. Regueiro and D. Ebrahimi. Implicit dynamic three-dimensional finite element analysis of an inelastic biphasic mixture at finite strain. Computer Methods in Applied Mechanics and Engineering, 199:2024–2049, June 2010. ISSN 00457825. doi: 10.1016/j.cma.2010.03.003.
- R.A. Regueiro, B. Zhang, and S.L. Wozniak. Large Deformation Dynamic Three-Dimensional Coupled Finite Element Analysis of Soft Biological Tissues Treated as Biphasic Porous Media. Computer Modeling in Engineering and Sciences, 98:1–39, 2014.
- H. Reismann. On the forced motion of elastic solids. Applied Scientific Research, 18:156–165, 1967.
- D.R. Reynolds, D.J. Gardner, C.S. Woodward, and R. Chinomona. ARKODE: A flexible IVP solver infrastructure for one-step methods. arXiv preprint arXiv:2205.14077, 2022.
- M. Rodriguez-Millan, I. Rubio, F.J. Burpo, A. Olmedo, J.A. Loya, K.K. Parker, and M.H. Miguélez. Impact response of advance combat helmet pad systems. International Journal of Impact Engineering, 181:104757, August 2023.
- E. Rohan and Vladimír Lukeš. Modeling large-deforming fluid-saturated porous media using an Eulerian incremental formulation. Advances in Engineering Software, 113:84–95, November 2017. ISSN 09659978. doi: 10.1016/j.advensoft.2016.11.003.
- R. Rossio, M. Vecchio, and J. Abramczyk. Polyurethane energy absorbing foam for automotive applications. Technical Report 930433, SAE, 1993.
- E. Rostami-Tapeh-Esmaeil, S. Shojaei, and D. Rodrigue. Mechanical and Thermal Properties of Functionally Graded Polyolefin Elastomer Foams. Polymers, 14:4124, October 2022. ISSN 2073-4360. doi: 10.3390/polym14194124.
- Tommaso Ruggeri and Srboľjub Simić. Average temperature and maxwellian iteration in multi-temperature mixtures of fluids. Phys. Rev. E, 80:026317, August 2009. doi: 10.1103/PhysRevE.80.026317.

- K. Salari and P. Knupp. Code Verification by the Method of Manufactured Solutions. Technical Report SAND2000-1444, Sandia National Laboratories, Albuquerque, New Mexico, U.S.A., 2000. URL <https://osti.gov/servlets/purl/759450>.
- V.A. Salomoni and B.A. Schrefler. A CBS-type stabilizing algorithm for the consolidation of saturated porous media. International Journal for Numerical Methods in Engineering, 63:502–527, May 2005. ISSN 0029-5981, 1097-0207. doi: 10.1002/nme.1275.
- B. Sanborn, X. Nie, W. Chen, and T. Weerasooriya. High strain rate pure shear and axial compressive response of porcine lung tissue. Journal of Applied Mechanics, 80:011029–1–011029–6, January 2013.
- M. Schanz and S. Diebels. A comparative study of biot’s theory and the linear theory of porous media for wave propagation problems. Acta Mechanica, 161:213–235, April 2003. ISSN 0001-5970, 1619-6937. doi: 10.1007/s00707-002-0999-5.
- Martin Schanz. Poroelastodynamics: Linear Models, Analytical Solutions, and Numerical Methods. Applied Mechanics Reviews, 62:030803–1–030803–15, May 2009. ISSN 0003-6900, 2379-0407. doi: 10.1115/1.3090831.
- L.E. Schwer. An overview of ptc 60/v and v 10: Guide for verification and valid in computational solid mechanics. Engineering with Computers, 23:245–252, January 2007.
- T.A. Sebaey, D.K. Rajak, and H. Mehboob. Internally stiffened foam-filled carbon fiber reinforced composite tubes under impact loading for energy absorption applications. Composite Structures, 255, January 2021. ISSN 0263-8223. doi: <https://doi.org/10.1016/j.compstruct.2020.112910>.
- J. Shang, T. Wu, H. Wang, C. Yang, C. Ye, R. Hu, J. Tao, and X. He. Measurement of temperature-dependent bulk viscosities of nitrogen, oxygen and air from spontaneous rayleigh-brillouin scattering. IEEE Access, 7:136439–136451, September 2019. doi: 10.1109/ACCESS.2019.2942219.
- S.S. Shrestha, J. Tiwari, A. Rai, D.E. Hun, D. Howard, A.O. Desjarlais, M. Francoeur, and T. Feng. Solid and gas thermal conductivity models improvement and validation in various porous insulation materials. International Journal of Thermal Sciences, 187:108164, May 2023.
- J.C. Simo and T.R. Hughes. Computational Inelasticity. Springer, 1998.
- B. R. Simon, J. S.-S. Wu, and O. C. Zienkiewicz. Evaluation of higher order, mixed and hermitean finite element procedures for dynamic analysis of saturated porous media using one-dimensional models. International Journal for Numerical and Analytical Methods in Geomechanics, 10:483–499, 1986. doi: <https://doi.org/10.1002/nag.1610100503>.
- W. Sobieski and A. Trykozko. DARCY’S AND FORCHHEIMER’S LAWS IN PRACTICE. PART 1. THE EXPERIMENT. Technical Sciences, 17:321–355, 2014.
- S.S. Sobin, Y.C. Fung, and H.M. Tremer. Collagen and elastin fibers in human pulmonary alveolar walls. Journal of Applied Physiology, 64:1659–1675, 1988.
- B. Song, W.-Y. Lu, C.J. Syn, and W. Chen. The effects of strain rate, density, and temperature on the mechanical properties of polymethylene diisocyanate (PMDI)-based rigid polyurethane foams during compression. Journal of Materials Science, 44:351–357, January 2009. ISSN 0022-2461, 1573-4803. doi: 10.1007/s10853-008-3105-0.

- J.H. Stuhmiller. Blast Injury: Translating Research into Operational Medicine. Borden Institute Monograph Series. TMM Publications, May 2010.
- J.H. Stuhmiller, C.J. Chuong, Y.Y. Phillips, and K.T. Dodd. Computer modeling of thoracic response to blast. The Journal of Trauma, 28:S132–S139, 1988.
- B. Suki and J.H.T. Bates. Lung tissue mechanics as an emergent phenomenon. Journal of Applied Physiology, 110:1111–1118, 2011. doi: 10.1152/jappphysiol.01244.2010.
- B. Suki, S. Ito, D. Stamenović, K.R. Lutchen, and E.P. Ingenito. Biomechanics of the lung parenchyma: critical roles of collagen and mechanical forces. Journal of Applied Physiology, 98:1892–1899, 2005. doi: 10.1152/jappphysiol.01087.2004.
- W. Sun. Verification & Validation of Computational Models Associated with the Mechanics of Materials. The Minerals, Metals & Materials Society, 2019.
- WaiChing Sun, Jakob T. Ostien, and Andrew G. Salinger. A stabilized assumed deformation gradient finite element formulation for strongly coupled poromechanical simulations at finite strain. International Journal for Numerical and Analytical Methods in Geomechanics, 37, 2013.
- A.H. Sweidan, Y. Heider, and B. Markert. A unified water/ice kinematics approach for phase-field thermo-hydro-mechanical modeling of frost action in porous media. Computer Methods in Applied Mechanics and Engineering, 372:1–29, August 2020. ISSN 00457825. doi: 10.1016/j.cma.2020.113358.
- R.C. Tai and G.C. Lee. Isotropy and homogeneity of lung tissue deformation. Journal of Biomechanics, 14:243–252, 1981. doi: 0.1016/0021-9290(81)90069-5.
- C.S. Tan, J.A. Rongong, and E. Ghassemieh. Temperature and strain rate dependence of syntactic foam under tensile and shear loads. Proceedings of the Institution of Mechanical Engineers, Part L: Journal of Materials: Design and Applications, 227:26–37, January 2013. ISSN 1464-4207, 2041-3076. doi: 10.1177/1464420712451962.
- D.W. Taylor. Fundamentals of Soil Mechanics. John Wiley and Sons, 1948.
- K. Terzaghi. Theoretical Soil Mechanics. John Wiley and Sons, 1943.
- C. Truesdell. Rational Thermodynamics. Springer-Verlag, 2 edition, 1984.
- C. Truesdell and R. Toupin. The classical field theories. Handbuch der Physik, 1960.
- A. Truty and T. Zimmerman. Stabilized mixed finite element formulations for materially non-linear partially saturated two-phase media. Computational Methods in Applied Mechanical Engineering, 195:1517–1546, February 2006.
- M. Tsokos, F. Paulsen, S. Petri, B. Madea, K. Püschel, and E.E. Türk. Histologic, immunohistochemical, and ultrastructural findings in human blast lung injury. American Journal of Respiratory and Critical Care Medicine, 168:549–555, 2003. doi: 10.1164/rccm.200304-528OC. PMID: 12842857.
- V.R. Vedula, D.J. Green, and J.R. Hellmann. Thermal fatigue resistance of open cell ceramic foams. Journal of the European Ceramic Society, 18:2073–2080, December 1998. ISSN 09552219. doi: 10.1016/S0955-2219(98)00159-9.

- J. von Neumann and R.D. Richtmyer. A method for the numerical calculation of hydrodynamical shocks. Journal of Applied Physics, 21:232–237, September 1950.
- L. Vujosevic and V.A. Lubarda. Finite-strain thermoelasticity based on multiplicative decomposition of deformation gradient. Theoretical and Applied Mechanics, 28-29:379–399, 2002. ISSN 1450-5584, 2406-0925. doi: 10.2298/TAM0229379V.
- A.-T Vuong. A Computational Approach to Coupled Poroelastic Media Problems. PhD thesis, Technische Universität München, 2016.
- A.-T. Vuong, L. Yoshihara, and W.A. Wall. A general approach for modeling interacting flow through porous media under finite deformations. Computer Methods in Applied Mechanics and Engineering, 283:1240–1259, January 2015. ISSN 00457825. doi: 10.1016/j.cma.2014.08.018.
- A.-T Vuong, C. Ager, and W.A. Wall. Two finite element approaches for darcy and darcy–brinkman flow through deformable porous media—mixed method vs. nurbs based (isogeometric) continuity. Computer Methods in Applied Mechanics and Engineering, 305:634–657, June 2016.
- P. Wang, S. Xu, Z. Li, J. Yang, H. Zheng, and S. Hu. Temperature effects on the mechanical behavior of aluminum foam under dynamic loading. Materials Science and Engineering: A, 599: 174–179, April 2014. ISSN 09215093. doi: 10.1016/j.msea.2014.01.076.
- W. Wang. Coupled thermo-poro-mechanical axisymmetric finite element modeling of soil-structure interaction in partially saturated soils. PhD thesis, University of Colorado Boulder, 2014.
- B. Weed, S. Patnaik, M. Rougeau-Browning, B. Brazile, J. Liao, R. Prabhu, and L.N. Williams. Experimental evidence of mechanical isotropy in porcine lung parenchyma. Materials, 8:2454–2466, May 2015. doi: doi:10.3390/ma8052454.
- M.L. Wilkins. Use of artificial viscosity in multidimensional fluid dynamic calculations. Journal of Computational Physics, 36:281–303, July 1980. ISSN 00219991. doi: 10.1016/0021-9991(80)90161-8.
- R. Winter, A. Valsamidou, H. Class, and B. Flemisch. A Study on Darcy versus Forchheimer Models for Flow through Heterogeneous Landfills including Macropores. Water, 14:546, February 2022. ISSN 2073-4441. doi: 10.3390/w14040546.
- W. Wu, H. Zheng, and Y. Yang. Numerical manifold method for dynamic consolidation of saturated porous media with three-field formulation. International Journal for Numerical Methods in Engineering, 120:768–802, June 2019. doi: <https://doi.org/10.1002/nme.6157>.
- D. Yang and M. Cao. Effect of changes in lung physical properties on microwave ablation zone during respiration. Biomedical Engineering Letters, 10, January 2020. doi: 10.1007/s13534-019-00145-5.
- Z. Yang. Poroviscoelastic Dynamic Finite Element Model of Biological Tissue. PhD thesis, University of Pittsburgh, Pittsburgh, PA, USA, 2006.
- R.T. Yen, Y.C. Fung, and S.Q. Liu. Trauma of lung due to impact load. Journal of Biomechanics, 21:745–753, January 1988. ISSN 00219290. doi: 10.1016/0021-9290(88)90283-7.

- H.C. Yoon and J. Kim. Spatial stability for the monolithic and sequential methods with various space discretizations in poroelasticity. International Journal for Numerical Methods in Engineering, 114:694–718, May 2018. ISSN 0029-5981, 1097-0207. doi: 10.1002/nme.5762.
- W.-H. Yuan, J.-X. Zhu, K. Liu, W. Zhang, B.-B. Dai, and Y. Wang. Dynamic analysis of large deformation problems in saturated porous media by smoothed particle finite element method. Computer Methods in Applied Mechanics and Engineering, 392:114724, March 2022. ISSN 00457825. doi: 10.1016/j.cma.2022.114724.
- A. Zemek, D.E. Protsenko, and B.J.F. Wong. Mechanical properties of porcine cartilage after uniform RF heating. Lasers in Surgery and Medicine, 44:572–579, August 2012.
- Q. Zhang, X. Yu, F. Scarpa, D. Barton, Y. Zhu, Z.-Q. Lang, and D. Zhang. A dynamic poroelastic model for auxetic polyurethane foams involving viscoelasticity and pneumatic damping effects in the linear regime. Mechanic Systems and Signal Processing, 179:109375, November 2022.
- Y. Zhang, D.M. Pedroso, L. Li, A. Scheuermann, and W. Ehlers. Accurate and stabilised time integration strategy for saturated porous media dynamics. Acta Geotechnica, 15:1859–1879, December 2019. doi: <https://doi.org/10.1007/s11440-019-00879-7>.
- J. Zhao, W.G. Knauss, and G. Ravichandran. Applicability of the time–temperature superposition principle in modeling dynamic response of a polyurea. Mechanics of Time-Dependent Materials, 11:289–308, December 2007. ISSN 1385-2000, 1573-2738. doi: 10.1007/s11043-008-9048-7.
- O. C. Zienkiewicz and T. Shiomi. Dynamic behaviour of saturated porous media; the generalized biot formulation and its numerical solution. International Journal for Numerical and Analytical Methods in Geomechanics, 8:71–96, February 1984. doi: <https://doi.org/10.1002/nag.1610080106>.
- O.C. Zienkiewicz, A.H.C. Chan, M. Pastor, D.K. Paul, and T. Shiomi. Static and dynamic behaviour of soil: a rational approach to quantitative solutions. i. fully saturated problems. Proceedings of the Royal Society of London, 429:285–309, 1990.
- O.C. Zienkiewicz, M. Huang, J. Wu, and S. Wu. A new algorithm for the coupled soil–pore fluid problem. Shock and Vibration, 1:3–14, 1993. ISSN 1070-9622, 1875-9203. doi: 10.1155/1993/801536.
- O.C. Zienkiewicz, R.L. Taylor, and J.Z. Zhu. The Finite Element Method: Its Basis and Fundamentals. McGraw-Hill, 2 edition, 2005.
- S. Zinatbakhsh, D. Koch, K.C. Park, B. Markert, and W. Ehlers. Partitioned formulation and stability analysis of a fluid interacting with a saturated porous medium by localised lagrange multipliers. International Journal for Numerical Methods in Engineering, 106:1041–1130, June 2016.

Appendix A

Derivation of the Gateaux derivatives

Gateaux derivatives for linearization of the variational equations as presented in Chapter 4 are derived in this Appendix. Starting with the Gateaux derivative for the deformation gradient, we have

$$\delta(F_{11}) = \delta \left(1 + \frac{\partial u}{\partial X} \right) = \delta \left(\frac{\partial u}{\partial X} \right) = \frac{\partial(\delta u)}{\partial X} = \beta \Delta t^2 \frac{\partial(\delta a)}{\partial X} = \gamma \Delta t \frac{\partial(\delta v)}{\partial X}. \quad (\text{A.1})$$

The Gateaux derivative of the deformation gradient raised to any power n is thus

$$\begin{aligned} \delta(F_{11}^n) &= \delta \left(1 + \frac{\partial u}{\partial X} \right)^n = n F_{11}^{n-1} \delta(F_{11}) \\ &= n F_{11}^{n-1} \beta \Delta t^2 \frac{\partial(\delta a)}{\partial X} = n F_{11}^{n-1} \gamma \Delta t \frac{\partial(\delta v)}{\partial X}. \end{aligned} \quad (\text{A.2})$$

Recall that for 1-D uniaxial strain, $F_{11} = \det(F) = J$. Given that $\ln(J)$ appears throughout the constitutive equation for the single-phase/solid skeleton response, we find that

$$\delta(\ln(J)) = \frac{1}{J} \delta(J) = \frac{1}{J} \beta \Delta t^2 \frac{\partial(\delta a)}{\partial X} = \frac{1}{J} \gamma \Delta t \frac{\partial(\delta v)}{\partial X}. \quad (\text{A.3})$$

Gateaux derivative for inverse left Cauchy-Green tensor axial strain component is

$$\begin{aligned} \delta(C_{11}^{-1}) &= -C_{11}^{-2} \delta(C_{11}) = -C_{11}^{-2} \delta(F_{11}^2) = -2C_{11}^{-2} F_{11} \frac{\partial(\delta u)}{\partial X} \\ &= -2F_{11}^{-3} \beta \Delta t^2 \frac{\partial(\delta a)}{\partial X} = -2F_{11}^{-3} \gamma \Delta t \frac{\partial(\delta v)}{\partial X}. \end{aligned} \quad (\text{A.4})$$

Recall that for the implicit integrators, the solid skeleton stress model was that of a neo-Hookean hyperelastic material; thus, the following derivations of the variations of the solid skeleton extra

stresses are not generalizable to other material models. Starting with the second Piola-Kirchhoff solid extra stress, we have

$$\begin{aligned}
\delta(S_{11(E)}^s) &= \delta(\mu + [\lambda \ln(J) - \mu] C_{11}^{-1}) \\
&= \lambda \delta(\ln(J)) C_{11}^{-1} + [\lambda \ln(J) - \mu] \delta(C_{11}^{-1}) \\
&= (\lambda - 2[\lambda \ln(J) - \mu]) F_{11}^{-3} \beta \Delta t^2 \frac{\partial(\delta a)}{\partial X} \\
&= (\lambda - 2[\lambda \ln(J) - \mu]) F_{11}^{-3} \gamma \Delta t \frac{\partial(\delta v)}{\partial X}.
\end{aligned} \tag{A.5}$$

Thus the Gateaux derivative of the first Piola-Kirchhoff solid extra stress is

$$\begin{aligned}
\delta(P_{11(E)}^s) &= \delta(F_{11} S_{11(E)}^s) = \delta(F_{11}) S_{11(E)}^s + F_{11} \delta(S_{11(E)}^s) \\
&= (\mu + [\lambda \ln(J) - \mu] F_{11}^{-2}) \frac{\partial(\delta u)}{\partial X} \\
&\quad + (\lambda - 2[\lambda \ln(J) - \mu] F_{11}^{-2}) \frac{\partial(\delta u)}{\partial X} \\
&= (\mu + [\lambda - \lambda \ln(J) + \mu] F_{11}^{-2}) \beta \Delta t^2 \frac{\partial(\delta a)}{\partial X} \\
&= (\mu + [\lambda - \lambda \ln(J) + \mu] F_{11}^{-2}) \gamma \Delta t \frac{\partial(\delta v)}{\partial X}.
\end{aligned} \tag{A.6}$$

A Gateaux derivative of the viscous component to the second Piola-Kirchhoff solid extra stress is derived as follows:

$$\begin{aligned}
\delta(S_{11(E),vis}^s) &= \nu_0 [\lambda + 2(\mu - \ln F_{11})] \left(\delta(F_{11}^{-3}) \frac{\partial v}{\partial X} + F_{11}^{-3} \frac{\partial \delta(v)}{\partial X} \right) \\
&\quad + \nu_0 F_{11}^{-3} \frac{\partial v}{\partial X} (-2\delta(\ln F_{11})) \\
&= \nu_0 [\lambda + 2(\mu - \ln F_{11})] \left(-3F_{11}^{-4} \frac{\partial \delta(u)}{\partial X} \frac{\partial v}{\partial X} + F_{11}^{-3} \frac{\partial \delta(v)}{\partial X} \right) \\
&\quad + \nu_0 F_{11}^{-3} \frac{\partial v}{\partial X} \left(\frac{-2}{F_{11}} \frac{\partial \delta(u)}{\partial X} \right) \\
&= \nu_0 F_{11}^{-3} \left[(\lambda + 2(\mu - \ln F_{11})) \left(\gamma \Delta t - 3F_{11}^{-1} \frac{\partial v}{\partial X} \beta \Delta t^2 \right) \right. \\
&\quad \left. - 2F_{11}^{-1} \frac{\partial v}{\partial X} \beta \Delta t^2 \right] \frac{\partial(\delta a)}{\partial X} \\
&= \nu_0 F_{11}^{-3} \left[(\lambda + 2(\mu - \ln F_{11})) \left(1 - 3F_{11}^{-1} \frac{\partial v}{\partial X} \gamma \Delta t \right) \right. \\
&\quad \left. - 2F_{11}^{-1} \frac{\partial v}{\partial X} \gamma \Delta t \right] \frac{\partial(\delta v)}{\partial X}.
\end{aligned} \tag{A.7}$$

Thus, the Gateaux derivative of the viscous component of the first Piola-Kirchhoff solid extra stress is derived as follows:

$$\begin{aligned}
\delta(F_{11}S_{11(E),\text{vis}}^s) &= \nu_0 F_{11}^{-3} \frac{\partial v}{\partial X} [\lambda + 2(\mu - \ln F_{11})] \beta \Delta t^2 \frac{\partial(\delta a)}{\partial X} \\
&\quad + \nu_0 F_{11}^{-2} \left[(\lambda + 2(\mu - \ln F_{11})) \left(\gamma \Delta t - 3F_{11}^{-1} \frac{\partial v}{\partial X} \beta \Delta t^2 \right) \right. \\
&\quad \quad \left. - 2F_{11}^{-1} \frac{\partial v}{\partial X} \beta \Delta t^2 \right] \frac{\partial(\delta a)}{\partial X} \\
&= \nu_0 F_{11}^{-3} \frac{\partial v}{\partial X} [\lambda + 2(\mu - \ln F_{11})] \gamma \Delta t \frac{\partial(\delta v)}{\partial X} \\
&\quad + \nu_0 F_{11}^{-2} \left[(\lambda + 2(\mu - \ln F_{11})) \left(1 - 3F_{11}^{-1} \frac{\partial v}{\partial X} \gamma \Delta t \right) \right. \\
&\quad \quad \left. - 2F_{11}^{-1} \frac{\partial v}{\partial X} \gamma \Delta t \right] \frac{\partial(\delta v)}{\partial X}. \tag{A.8}
\end{aligned}$$

Together, Eq. (A.6) and Eq. (A.8) give the Gateaux derivative on the *total* first Piola-Kirchhoff solid extra stress (that is, the inviscid and viscous components sum to):

$$\begin{aligned}
\delta(P_{11(E)}^s) &= F_{11}^{-2} \left([\lambda + 2\mu] \left(\nu_0 \gamma \Delta t - 2\nu_0 F_{11}^{-1} \frac{\partial v}{\partial X} \beta \Delta t^2 \right) \right. \\
&\quad \left. - \ln F_{11} \left(2\nu_0 \gamma \Delta t - \left[4\nu_0 F_{11}^{-1} \frac{\partial v}{\partial X} - \lambda \right] \beta \Delta t^2 \right) \right. \\
&\quad \left. + \left([\lambda + \mu + \mu F_{11}^2] - 2\nu_0 F_{11}^{-1} \frac{\partial v}{\partial X} \right) \beta \Delta t^2 \right) \frac{\partial(\delta a)}{\partial X} \\
&= F_{11}^{-2} \left([\lambda + 2\mu] \left(\nu_0 - 2\nu_0 F_{11}^{-1} \frac{\partial v}{\partial X} \gamma \Delta t \right) \right. \\
&\quad \left. - \ln F_{11} \left(2\nu_0 - \left[4\nu_0 F_{11}^{-1} \frac{\partial v}{\partial X} - \lambda \right] \gamma \Delta t \right) \right. \\
&\quad \left. + \left([\lambda + \mu + \mu F_{11}^2] - 2\nu_0 F_{11}^{-1} \frac{\partial v}{\partial X} \right) \gamma \Delta t \right) \frac{\partial(\delta v)}{\partial X}. \tag{A.9}
\end{aligned}$$

The Gateaux derivative of the real mass density of the pore fluid, assuming no pressure-temperature coupling, is

$$\begin{aligned}
\delta(\rho^{\text{fR}}) &= \delta \left(\rho_0^{\text{fR}} \exp \left[\frac{p_{\text{f}} - p_{\text{f},0}}{K_{\text{f}}^{\eta}} \right] \right) = \rho_0^{\text{fR}} \exp \left[\frac{p_{\text{f}} - p_{\text{f},0}}{K_{\text{f}}^{\eta}} \right] \delta \left(\frac{p_{\text{f}}}{K_{\text{f}}^{\eta}} \right) \\
&= \frac{\rho^{\text{fR}}}{K_{\text{f}}^{\eta}} \delta(p_{\text{f}}) = \frac{\rho^{\text{fR}}}{K_{\text{f}}^{\eta}} \beta \Delta t^2 \delta \dot{p}_{\text{f}} = \frac{\rho^{\text{fR}}}{K_{\text{f}}^{\eta}} \gamma \Delta t \delta \dot{p}_{\text{f}}. \tag{A.10}
\end{aligned}$$

With pressure-temperature coupling, e.g., assuming an ideal gas law, we have

$$\begin{aligned}\delta(\rho^{\text{fR}}) &= \delta\left(\frac{p_{\text{f}}}{\mathfrak{R}\theta^{\text{f}}}\right) = \frac{1}{\mathfrak{R}}\delta\left(\frac{p_{\text{f}}}{\theta^{\text{f}}}\right) \\ &= \frac{1}{\mathfrak{R}}\left(\frac{1}{\theta^{\text{f}}}\delta(p_{\text{f}}) - \frac{p_{\text{f}}}{(\theta^{\text{f}})^2}\delta(\theta^{\text{f}})\right) = \frac{1}{\mathfrak{R}\theta^{\text{f}}}\beta\Delta t^2\left(\delta\ddot{p}_{\text{f}} - \frac{p_{\text{f}}}{\theta^{\text{f}}}\delta\ddot{\theta}^{\text{f}}\right) = \frac{1}{\mathfrak{R}\theta^{\text{f}}}\gamma\Delta t\left(\delta\dot{p}_{\text{f}} - \frac{p_{\text{f}}}{\theta^{\text{f}}}\delta\dot{\theta}^{\text{f}}\right),\end{aligned}\quad (\text{A.11})$$

and for a compressible liquid, we have

$$\begin{aligned}\delta(\rho^{\text{fR}}) &= \delta\left(\rho_0^{\text{fR}}\exp\left[\frac{p_{\text{f}} - p_{\text{f},0}}{K_{\text{f}}^{\theta}} - \alpha_{\text{V}}^{\text{f}}\theta^{\text{f}}\right]\right) = \rho^{\text{fR}}\delta\left(\frac{p_{\text{f}}}{K_{\text{f}}^{\theta}} - \alpha_{\text{V}}^{\text{f}}\theta^{\text{f}}\right) \\ &= \rho^{\text{fR}}(\beta\Delta t^2)\left(\frac{1}{K_{\text{f}}^{\theta}}\delta\ddot{p}_{\text{f}} - \alpha_{\text{V}}^{\text{f}}\delta\ddot{\theta}^{\text{f}}\right) = \rho^{\text{fR}}(\gamma\Delta t)\left(\frac{1}{K_{\text{f}}^{\theta}}\delta\dot{p}_{\text{f}} - \alpha_{\text{V}}^{\text{f}}\delta\dot{\theta}^{\text{f}}\right).\end{aligned}\quad (\text{A.12})$$

Gateaux derivative of the porosity is

$$\begin{aligned}\delta(n^{\text{f}}) &= \delta(1 - n^{\text{s}}) = -\delta(n^{\text{s}}) = -\delta\left(\frac{n_0^{\text{s}}}{J}\right) = \frac{n_0^{\text{s}}}{J^2}\delta(J) \\ &= \frac{n^{\text{s}}}{J}\beta\Delta t^2\frac{\partial(\delta a)}{\partial X} = \frac{n^{\text{s}}}{J}\gamma\Delta t\frac{\partial(\delta v)}{\partial X}.\end{aligned}\quad (\text{A.13})$$

Gateaux derivative of partial mass density of the pore fluid—in the absence of pressure-temperature coupling—in the reference configuration is thus

$$\begin{aligned}\delta(\rho_0^{\text{f}}) &= \delta(Jn^{\text{f}}\rho^{\text{fR}}) = n^{\text{f}}\rho^{\text{fR}}\delta(J) + J\rho^{\text{fR}}\delta(n^{\text{f}}) + Jn^{\text{f}}\delta(\rho^{\text{fR}}) \\ &= n^{\text{f}}\rho^{\text{fR}}\frac{\partial(\delta u)}{\partial X} + n^{\text{s}}\rho^{\text{fR}}\frac{\partial(\delta u)}{\partial X} + \frac{Jn^{\text{f}}\rho^{\text{fR}}}{K_{\text{f}}}\delta p_{\text{f}} \\ &= \beta\Delta t^2\left(\rho^{\text{fR}}\frac{\partial(\delta a)}{\partial X} + \frac{Jn^{\text{f}}\rho^{\text{fR}}}{K_{\text{f}}}\delta\ddot{p}_{\text{f}}\right) \\ &= \gamma\Delta t\left(\rho^{\text{fR}}\frac{\partial(\delta v)}{\partial X} + \frac{Jn^{\text{f}}\rho^{\text{fR}}}{K_{\text{f}}}\delta\dot{p}_{\text{f}}\right).\end{aligned}\quad (\text{A.14})$$

With pressure-temperature coupling, e.g., the ideal gas law, we have

$$\begin{aligned}\delta(\rho_0^{\text{f}}) &= \delta(Jn^{\text{f}}\rho^{\text{fR}}) = n^{\text{f}}\rho^{\text{fR}}\delta(J) + J\rho^{\text{fR}}\delta(n^{\text{f}}) + Jn^{\text{f}}\delta(\rho^{\text{fR}}) \\ &= n^{\text{f}}\rho^{\text{fR}}\frac{\partial(\delta u)}{\partial X} + n^{\text{s}}\rho^{\text{fR}}\frac{\partial(\delta u)}{\partial X} + \frac{Jn^{\text{f}}}{\mathfrak{R}\theta^{\text{f}}}\left(\delta p_{\text{f}} - \frac{p_{\text{f}}}{\theta^{\text{f}}}\delta\theta^{\text{f}}\right) \\ &= \beta\Delta t^2\left(\rho^{\text{fR}}\frac{\partial(\delta a)}{\partial X} + \frac{Jn^{\text{f}}}{\mathfrak{R}\theta^{\text{f}}}\left[\delta\ddot{p}_{\text{f}} - \frac{p_{\text{f}}}{\theta^{\text{f}}}\delta\ddot{\theta}^{\text{f}}\right]\right) \\ &= \gamma\Delta t\left(\rho^{\text{fR}}\frac{\partial(\delta v)}{\partial X} + \frac{Jn^{\text{f}}}{\mathfrak{R}\theta^{\text{f}}}\left[\delta\dot{p}_{\text{f}} - \frac{p_{\text{f}}}{\theta^{\text{f}}}\delta\dot{\theta}^{\text{f}}\right]\right)\end{aligned}\quad (\text{A.15})$$

and for a compressible pore liquid, we have

$$\begin{aligned}
\delta(\rho_0^f) &= \delta(Jn^f \rho^{\text{fR}}) = n^f \rho^{\text{fR}} \delta(J) + J \rho^{\text{fR}} \delta(n^f) + J n^f \delta(\rho^{\text{fR}}) \\
&= n^f \rho^{\text{fR}} \frac{\partial(\delta u)}{\partial X} + n^s \rho^{\text{fR}} \frac{\partial(\delta u)}{\partial X} + \rho_0^f \left(\frac{1}{K_f^\theta} \delta p_f - \alpha_V^f \delta \theta^f \right) \\
&= \beta \Delta t^2 \left(\rho^{\text{fR}} \frac{\partial(\delta a)}{\partial X} + \rho_0^f \left[\frac{1}{K_f^\theta} \delta \ddot{p}_f - \alpha_V^f \delta \ddot{\theta}^f \right] \right) \\
&= \gamma \Delta t \left(\rho^{\text{fR}} \frac{\partial(\delta v)}{\partial X} + \rho_0^f \left[\frac{1}{K_f^\theta} \delta \dot{p}_f - \alpha_V^f \delta \dot{\theta}^f \right] \right)
\end{aligned} \tag{A.16}$$

The Gateaux derivative of the hydraulic conductivity, assuming the Kozeny-Carman model for $\mathcal{F}(n^f)$, is derived as follows:

$$\begin{aligned}
\delta(\hat{k}) &= \delta \left(\frac{\varkappa \mathcal{F}(n^f)}{\eta_f \mathcal{F}(n_0^f)} \right) = \frac{\partial \hat{k}}{\partial n^f} \delta(n^f) = \frac{\partial \left(\frac{\varkappa}{\eta_f} \frac{1}{\mathcal{F}(n_0^f)} \frac{(n^f)^3}{(1-(n^f)^2)} \right)}{\partial n^f} \delta(n^f) \\
&= \frac{\varkappa \mathcal{F}(n^f)}{\eta_f \mathcal{F}(n_0^f)} \left[\frac{3}{n^f} + \frac{2n^f}{1-(n^f)^2} \right] \delta(n^f) = \hat{k} \left[\frac{3}{n^f} + \frac{2n^f}{1-(n^f)^2} \right] \delta(n^f) \\
&= \underbrace{\frac{\hat{k} n^s}{J} \left[\frac{3}{n^f} + \frac{2n^f}{1-(n^f)^2} \right]}_{\delta_{\hat{k}}} \beta \Delta t^2 \frac{\partial(\delta a)}{\partial X} = \delta_{\hat{k}} \gamma \Delta t \frac{\partial(\delta v)}{\partial X}.
\end{aligned} \tag{A.17}$$

The derivation for the hyperbolic model by Markert [2005] is shown as follows:

$$\begin{aligned}
\delta(\hat{k}) &= \delta \left(\frac{\varkappa \mathcal{F}(n^f)}{\eta_f \mathcal{F}(n_0^f)} \right) = \frac{\varkappa}{\eta_f} \delta \left(\left[\frac{J - n_0^s}{1 - n_0^s} \right]^\kappa \right) \\
&= \frac{\varkappa}{\eta_f} \left(\frac{J - n_0^s}{1 - n_0^s} \right)^{\kappa-1} \delta \left(\frac{J - n_0^s}{1 - n_0^s} \right) \\
&= \underbrace{\frac{\varkappa}{\eta_f} \frac{\kappa}{1 - n_0^s} \left(\frac{J - n_0^s}{1 - n_0^s} \right)^{\kappa-1}}_{\delta_{\hat{k}}} \beta \Delta t^2 \frac{\partial(\delta a)}{\partial X} = \delta_{\hat{k}} \gamma \Delta t \frac{\partial(\delta v)}{\partial X}
\end{aligned} \tag{A.18}$$

The derivation for the exponential model by Lai et al. [1981] is shown as follows:

$$\delta(\hat{k}) = \delta \left(\frac{\varkappa}{\eta_f} \exp \left[\kappa \frac{\partial u}{\partial X} \right] \right) = \underbrace{\varkappa \hat{k}}_{\delta_{\hat{k}}} \beta \Delta t^2 \frac{\partial(\delta a)}{\partial X} = \delta_{\hat{k}} \gamma \Delta t \frac{\partial(\delta v)}{\partial X}. \tag{A.19}$$

Divergence of the pore fluid extra stress tensor, as it appears in Eq. (4.93)₃, simplifies to the following with the 1-D uniaxial strain assumption:

$$\frac{\partial \sigma_{11(E)}^f}{\partial X} = \left[\frac{\partial n^f}{\partial X} \frac{\partial v_f}{\partial X} + n^f \frac{\partial^2 v_f}{\partial X^2} \right] (\kappa_f + 2\eta_f) F_{11}^{-2}. \tag{A.20}$$

The Gateaux derivatives of new variables are given as follows:

$$\begin{aligned}
\delta\left(\frac{\partial n^f}{\partial X}\right) &= \delta\left(n^s \frac{\partial^2 u}{\partial X^2} F_{11}^{-1}\right) \\
&= (\beta\Delta t^2) \left(-\frac{n^s}{J} \frac{\partial^2 u}{\partial X^2} F_{11}^{-1} \frac{\partial(\delta a)}{\partial X} + n^s F_{11}^{-1} \frac{\partial^2(\delta a)}{\partial X^2} - n^s F_{11}^{-2} \frac{\partial^2 u}{\partial X^2} \frac{\partial(\delta a)}{\partial X} \right) \\
&= (\beta\Delta t^2) \left(\frac{n^s}{J} \frac{\partial^2(\delta a)}{\partial X^2} - \frac{2n^s}{J^2} \frac{\partial^2 u}{\partial X^2} \frac{\partial(\delta a)}{\partial X} \right) = \frac{n^s}{J} \beta\Delta t^2 \left(\frac{\partial^2(\delta a)}{\partial X^2} - \frac{2}{J} \frac{\partial^2 u}{\partial X^2} \frac{\partial(\delta a)}{\partial X} \right), \quad (\text{A.21})
\end{aligned}$$

$$\begin{aligned}
\delta\left(\frac{\partial v_f}{\partial X}\right) &= (\gamma\Delta t) \frac{\partial(\delta a_f)}{\partial X}, \\
\delta\left(\frac{\partial^2 v_f}{\partial X^2}\right) &= (\gamma\Delta t) \frac{\partial^2(\delta a_f)}{\partial X^2}.
\end{aligned}$$

The variation of the divergence of the pore fluid extra stress term, which contributes to block matrices $\mathbf{K}_{u_f, u}$, \mathbf{K}_{u_f, u_f} , is

$$\begin{aligned}
\delta\left(\frac{\partial \sigma_{11(E)}^f}{\partial X}\right) &= (\kappa_f + 2\eta_f) F_{11}^{-2} \left((\gamma\Delta t) \left[\frac{\partial n^f}{\partial X} \frac{\partial(\delta a_f)}{\partial X} + n^f \frac{\partial^2(\delta a_f)}{\partial X^2} \right] + \frac{n^s}{J} \frac{\partial v_f}{\partial X} (\beta\Delta t^2) \frac{\partial^2(\delta a)}{\partial X^2} \right. \\
&\quad \left. + \frac{n^s}{J} (\beta\Delta t^2) \left[\frac{\partial^2 v_f}{\partial X^2} - \frac{2}{J} \frac{\partial v_f}{\partial X} \frac{\partial^2 u}{\partial X^2} \right] \frac{\partial(\delta a)}{\partial X} \right) - \frac{2}{J} \frac{\partial \sigma_{11(E)}^f}{\partial X} \partial X (\beta\Delta t^2) \frac{\partial(\delta a)}{\partial X}. \quad (\text{A.22})
\end{aligned}$$

Appendix B

Derivation of linearized equations

Linearizations for the implicit integrators discussed in Chapter 4.3.2 are derived in this Appendix.

B.1 (\mathbf{u}) formulation

The linearization of the variational equations given in Chapter 4.1.1 commences as follows:

$$\delta\mathcal{G}_1^{\text{INT}} = \int_0^{X=H} w^u \delta(\rho_0 a) A dX = \int_0^{X=H} w^u \rho_0 \delta a A dX . \quad (\text{B.1})$$

For quasi-static elasticity, (B.1) is zero. Next,

$$\begin{aligned} \delta\mathcal{G}_2^{\text{INT}} &= \int_0^{X=H} \frac{\partial w^u}{\partial X} \delta(P_{11}) A dX \\ &= \int_0^{X=H} \frac{\partial w^u}{\partial X} (\mu + [\lambda - \lambda \ln(J) + \mu] F_{11}^{-2}) (\beta \Delta t^2) \frac{\partial(\delta a)}{\partial X} A dX . \end{aligned} \quad (\text{B.2})$$

When viscous damping is considered, where ν_0 is the viscous dampening coefficient (unit (s)), (B.2) becomes

$$\begin{aligned} \delta\mathcal{G}_2^{\text{INT}} &= \int_0^{X=H} \frac{\partial w^u}{\partial X} F_{11}^{-2} \left([\lambda + 2\mu] \left[\nu_0 (\gamma \Delta t) - 2\nu_0 F_{11}^{-1} \frac{\partial v}{\partial X} (\beta \Delta t^2) \right] \right. \\ &\quad \left. - \ln(F_{11}) \left[2\nu_0 (\gamma \Delta t) - \left(4\nu_0 F_{11}^{-1} \frac{\partial v}{\partial X} - \lambda \right) (\beta \Delta t^2) \right] \right. \\ &\quad \left. + \left[(\lambda + \mu + \mu F_{11}^2) - 2\nu_0 F_{11}^{-1} \frac{\partial v}{\partial X} \right] (\beta \Delta t^2) \right) \frac{\partial(\delta a)}{\partial X} A dX . \end{aligned} \quad (\text{B.3})$$

For elasticity, (B.2) becomes

$$\delta\mathcal{G}_2^{\text{INT}} = \int_0^{X=H} \frac{\partial w^u}{\partial X} (\mu + [\lambda - \lambda \ln(J) + \mu] F_{11}^{-2}) (\gamma \Delta t) \frac{\partial(\delta v)}{\partial X} A dX. \quad (\text{B.4})$$

When viscous damping is considered, (B.4) becomes

$$\begin{aligned} \delta\mathcal{G}_2^{\text{INT}} = & \int_0^{X=H} \frac{\partial w^u}{\partial X} F_{11}^{-2} \left([\lambda + 2\mu] \left[\nu_0 - 2\nu_0 F_{11}^{-1} \frac{\partial v}{\partial X} (\gamma \Delta t) \right] \right. \\ & \left. - \ln(F_{11}) \left[2\nu_0 - \left(4\nu_0 F_{11}^{-1} \frac{\partial v}{\partial X} - \lambda \right) (\gamma \Delta t) \right] \right) \\ & + \left[(\lambda + \mu + \mu F_{11}^2) - 2\nu_0 F_{11}^{-1} \frac{\partial v}{\partial X} (\gamma \Delta t) \right] \frac{\partial(\delta v)}{\partial X} dX. \end{aligned} \quad (\text{B.5})$$

When shock viscosity is enabled, linearization with the additions given by Chapter 4.4.1 proceeds as follows:

$$\delta\mathcal{G}_2^{\text{INT}} = \int_0^{X=H} \frac{\partial w^u}{\partial X} (\delta(P_{11}) - \delta(Q)) A dX, \quad (\text{B.6})$$

where

$$\begin{aligned} \delta(Q) = & \rho_0 h_0 \left(C_0 h_0 \delta(J) F_{11}^{-2} \left[\frac{\partial v}{\partial X} \right]^2 + C_0 J h_0 \delta(F_{11}^{-2}) \left[\frac{\partial v}{\partial X} \right]^2 \right. \\ & + C_0 J h_0 F_{11}^{-2} \delta \left(\left[\frac{\partial v}{\partial X} \right]^2 \right) - C_1 \delta(c) F_{11}^{-2} \frac{\partial v}{\partial X} \\ & \left. - C_1 c \delta(F_{11}^{-1}) \frac{\partial v}{\partial X} - C_1 c F_{11}^{-1} \frac{\partial \delta v}{\partial X} \right), \end{aligned} \quad (\text{B.7})$$

with

$$\begin{aligned} \delta c = & \delta \sqrt{\frac{M}{\rho}} = -\frac{1}{2} M^{1/2} \rho^{-3/2} \delta \rho = -\frac{1}{2} M^{1/2} \rho^{-3/2} \delta \left(\frac{\rho_0}{J} \right) \\ = & \frac{1}{2} M^{1/2} \rho^{-3/2} \frac{\rho_0}{J^2} \delta J = \frac{1}{2} M^{1/2} \frac{\rho^{-1/2}}{J} \delta J = \frac{c}{2J} \delta J, \end{aligned} \quad (\text{B.8})$$

where M denotes the single-phase P-wave modulus. Thus, after some algebra,

$$\begin{aligned} \delta(Q) = & \rho_0 h_0 \left(C_0 h_0 F_{11}^{-2} \frac{\partial v}{\partial X} \left[(1 - 2F_{11}^{-1}) \frac{\partial v}{\partial X} (\beta \Delta t^2) + 2(\gamma \Delta t) \right] \right. \\ & \left. - C_1 F_{11}^{-1} c \left[\frac{3}{2} F_{11}^{-1} \frac{\partial v}{\partial X} (\beta \Delta t^2) - (\gamma \Delta t) \right] \right) \frac{\partial \delta a}{\partial X}. \end{aligned} \quad (\text{B.9})$$

Then, combining the results from Eqs. B.2 with B.9, (B.6) becomes

$$\begin{aligned} \delta\mathcal{G}_2^{\text{INT}} &= \int_0^{X=H} \frac{\partial w^u}{\partial X} \left([\mu + (\lambda - \lambda \ln(J) + \mu) F_{11}^{-2}] (\beta \Delta t^2) \right. \\ &\quad \left. - \rho_0 h_0 \left[C_0 h_0 F_{11}^{-2} \frac{\partial v}{\partial X} \left((1 - 2F_{11}^{-1}) \frac{\partial v}{\partial X} (\beta \Delta t^2) + 2(\gamma \Delta t) \right) \right. \right. \\ &\quad \left. \left. - C_1 F_{11}^{-1} c \left(\frac{3}{2} F_{11}^{-1} \frac{\partial v}{\partial X} (\beta \Delta t^2) - (\gamma \Delta t) \right) \right] \right) \frac{\partial(\delta a)}{\partial X} A dX . \end{aligned} \quad (\text{B.10})$$

Note that it would be unnecessary to derive the linearization of $\mathcal{G}_2^{\text{INT}}$ with shock viscosity and without inertia terms. We have found that for overall stability of the numerical solution, the shock viscosity is usually only necessary when the inertia terms are enabled, and so a quasi-static formulation of the linearization of $\mathcal{G}_2^{\text{INT}}$ with shock viscosity is omitted here.

B.2 (\mathbf{u} - θ) formulation

The linearization of the variational equations given in Chapter 4.1.2 commences as follows. Linearization of $\mathcal{G}_1^{\text{INT}}$ is unchanged from the (\mathbf{u}) formulation. Linearization of $\mathcal{G}_2^{\text{INT}}$ now includes the thermoelastic component:

$$\begin{aligned} \delta\mathcal{G}_2^{\text{INT}} &= \int_0^{X=H} \frac{\partial w^u}{\partial X} \delta(P_{11}) A dX \\ &= \int_0^{X=H} \frac{\partial w^u}{\partial X} \left([\mu + (\lambda - \lambda \ln(J) + \mu + K \alpha_V \Delta \theta) F_{11}^{-2}] (\beta \Delta t^2) \frac{\partial(\delta a)}{\partial X} - \frac{K \alpha_V}{J} (\beta \Delta t^2) \delta \ddot{\theta} \right) A dX . \end{aligned} \quad (\text{B.11})$$

With shock viscosity enabled,

$$\begin{aligned} \delta\mathcal{G}_2^{\text{INT}} &= \int_0^{X=H} \frac{\partial w^u}{\partial X} \left([\mu + (\lambda - \lambda \ln(J) + \mu + K \alpha_V \Delta \theta) F_{11}^{-2}] (\beta \Delta t^2) \right. \\ &\quad \left. - \rho_0 h_0 \left[C_0 h_0 F_{11}^{-2} \frac{\partial v}{\partial X} \left((1 - 2F_{11}^{-1}) \frac{\partial v}{\partial X} (\beta \Delta t^2) + 2(\gamma \Delta t) \right) \right. \right. \\ &\quad \left. \left. - C_1 F_{11}^{-1} c \left(\frac{3}{2} F_{11}^{-1} \frac{\partial v}{\partial X} (\beta \Delta t^2) - (\gamma \Delta t) \right) \right] \right) \frac{\partial(\delta a)}{\partial X} - \frac{K \alpha_V}{J} (\beta \Delta t^2) \delta \ddot{\theta} \Big) A dX . \end{aligned} \quad (\text{B.12})$$

For thermoelasticity,

$$\delta \mathcal{G}_2^{\text{INT}} = \int_0^{X=H} \frac{\partial w^u}{\partial X} \left([\mu + (\lambda - \lambda \ln(J) + \mu + K\alpha_V \Delta\theta) F_{11}^{-2}] (\gamma \Delta t) \frac{\partial(\delta v)}{\partial X} - \frac{K\alpha_V}{J} (\gamma \Delta t) \delta \dot{\theta} \right) A dX . \quad (\text{B.13})$$

Linearization of $\mathcal{J}_1^{\text{INT}}$ proceeds as follows:

$$\delta \mathcal{J}_1^{\text{INT}} = \int_0^{X=H} w^\theta \rho_0 c_V (\gamma \Delta t) \delta \ddot{\theta} A dX . \quad (\text{B.14})$$

For thermoelasticity,

$$\delta \mathcal{J}_1^{\text{INT}} = \int_0^{X=H} w^\theta \rho_0 c_V \delta \dot{\theta} A dX . \quad (\text{B.15})$$

Linearization of $\mathcal{J}_2^{\text{INT}}$ proceeds as follows:

$$\begin{aligned} \delta \mathcal{J}_2^{\text{INT}} &= \int_0^{X=H} w^\theta \left(\left[K\alpha_V \left(\frac{1}{J} \delta \theta + \theta \delta \left(\frac{1}{J} \right) + \delta(Q) \right) \right] j + \left[\frac{K\alpha_V \theta}{J} + Q \right] \delta(j) \right) A dX \\ &= \int_0^{X=H} w^\theta \left(\left[\frac{j}{J} \left(-(\beta \Delta t^2) \frac{K\alpha_V \theta}{J} + \rho_0 h_0 \left[\frac{c_0 h_0}{J} \frac{\partial v}{\partial X} \left([1 - 2F_{11}^{-1}] \frac{\partial v}{\partial X} (\beta \Delta t^2) + 2(\gamma \Delta t) \right) \right. \right. \right. \right. \\ &\quad \left. \left. \left. - c_1 c \left(\frac{3}{2J} \frac{\partial v}{\partial X} (\beta \Delta t^2) - (\gamma \Delta t) \right) \right] \right) \right. \right. \\ &\quad \left. \left. + (\gamma \Delta t) \left(\frac{K\alpha_V \theta}{J} + Q \right) \right] \frac{\partial(\delta a)}{\partial X} + \frac{K\alpha_V j}{J} (\beta \Delta t^2) \delta \ddot{\theta} \right) A dX . \end{aligned} \quad (\text{B.16})$$

In the absence of shock viscosity,

$$\delta \mathcal{J}_2^{\text{INT}} = \int_0^{X=H} w^\theta \frac{K\alpha_V \theta}{J} \left(\left[(\gamma \Delta t) - \frac{j}{J} (\beta \Delta t^2) \right] \frac{\partial(\delta a)}{\partial X} + j (\beta \Delta t^2) \delta \ddot{\theta} \right) A dX . \quad (\text{B.17})$$

For thermoelasticity,

$$\delta \mathcal{J}_2^{\text{INT}} = \int_0^{X=H} w^\theta \frac{K\alpha_V \theta}{J} \left(\left[1 - (\gamma \Delta t) \frac{j}{J} \right] \frac{\partial(\delta v)}{\partial X} + j (\gamma \Delta t) \delta \dot{\theta} \right) A dX . \quad (\text{B.18})$$

Linearization of $\mathcal{J}_3^{\text{INT}}$ proceeds as follows:

$$\begin{aligned}\delta\mathcal{J}_3^{\text{INT}} &= - \int_0^{X=H} \frac{\partial w^\theta}{\partial X} \delta(q) A dX = \int_0^{X=H} \frac{\partial w^\theta}{\partial X} k^\theta \left(\frac{1}{J} \delta \left(\frac{\partial \theta}{\partial X} \right) + \frac{\partial \theta}{\partial X} \delta \left(\frac{1}{J} \right) \right) A dX \\ &= \int_0^{X=H} \frac{\partial w^\theta}{\partial X} \frac{k^\theta}{J} (\beta \Delta t^2) \left(\frac{\partial(\delta \dot{\theta})}{\partial X} - \frac{1}{J} \frac{\partial \theta}{\partial X} \frac{\partial(\delta a)}{\partial X} \right) A dX .\end{aligned}\quad (\text{B.19})$$

For thermoelasticity,

$$\delta\mathcal{J}_3^{\text{INT}} = \int_0^{X=H} \frac{\partial w^\theta}{\partial X} \frac{k^\theta}{J} (\gamma \Delta t) \left(\frac{\partial(\delta \dot{\theta})}{\partial X} - \frac{1}{J} \frac{\partial \theta}{\partial X} \frac{\partial(\delta v)}{\partial X} \right) A dX .\quad (\text{B.20})$$

B.3 (\mathbf{u} - p_f) formulation

The linearization of the variational equations given in Chapter 4.1.3 commences as follows. The linearizations $\delta\mathcal{G}_1^{\text{INT}}$ and $\delta\mathcal{G}_2^{\text{INT}}$ remain unchanged from the (\mathbf{u}) formulation for this (\mathbf{u} - p_f) formulation, unless shock viscosity is added to the solid skeleton extra stress response. In such a case, $Q \neq Q(\rho)$ but rather $Q = Q(\rho^s)$. Incidentally, the variation of the wave speed is the same for an incompressible solid constituent:

$$\begin{aligned}\delta c^s &= \delta \sqrt{\frac{M^{\text{skel}}}{\rho^s}} = -\frac{1}{2} (M^{\text{skel}})^{1/2} (\rho^s)^{-3/2} \delta \rho^s = -\frac{1}{2} (M^{\text{skel}})^{1/2} (\rho^s)^{-3/2} \delta (n^s \rho^{\text{sR}}) \\ &= \frac{1}{2} (M^{\text{skel}})^{1/2} (\rho^s)^{-3/2} \rho_0^{\text{sR}} \frac{n_0^s}{J^2} \delta(J) = \frac{1}{2} (M^{\text{skel}})^{1/2} \frac{(\rho^s)^{-1/2}}{J} \delta(J) = \frac{c^s}{2J} \delta(J),\end{aligned}\quad (\text{B.21})$$

such that we recover (recalling $\delta(\rho_0^s) = \text{const.}$)

$$\begin{aligned}\delta\mathcal{G}_2^{\text{INT}} &= \int_0^{X=H} \frac{\partial w^u}{\partial X} \left([\mu + (\lambda - \lambda \ln(J) + \mu) F_{11}^{-2}] (\beta \Delta t^2) \right. \\ &\quad \left. - \rho_0^s h_0 \left[C_0 h_0 F_{11}^{-2} \frac{\partial v}{\partial X} \left((1 - 2F_{11}^{-1}) \frac{\partial v}{\partial X} (\beta \Delta t^2) + 2(\gamma \Delta t) \right) \right. \right. \\ &\quad \left. \left. - C_1 F_{11}^{-1} c^s \left(\frac{3}{2} F_{11}^{-1} \frac{\partial v}{\partial X} (\beta \Delta t^2) - (\gamma \Delta t) \right) \right] \right) \frac{\partial(\delta a)}{\partial X} A dX .\end{aligned}\quad (\text{B.22})$$

The first *required* linearization is given by

$$\delta\mathcal{G}_3^{\text{INT}} = - \int_0^{X=H} \frac{\partial w^u}{\partial X} \delta(p_f) A dX = - \int_0^{X=H} \frac{\partial w^u}{\partial X} (\beta \Delta t^2) \delta \ddot{p}_f A dX .\quad (\text{B.23})$$

For poroelasticity, (B.23) becomes

$$\delta\mathcal{G}_3^{\text{INT}} = - \int_0^{X=H} \frac{\partial w^u}{\partial X} (\gamma\Delta t) \delta\dot{p}_f A dX . \quad (\text{B.24})$$

The next linearization proceeds as follows:

$$\begin{aligned} \delta\mathcal{H}_1^{\text{INT}} &= \int_0^{X=H} w^{p_f} \delta \left(\frac{Jn^f}{K_f^\eta} \dot{p}_f + j \right) A dX \\ &= \int_0^{X=H} w^{p_f} \left(\frac{n^f \dot{p}_f}{K_f^\eta} \delta J + \frac{J \dot{p}_f}{K_f^\eta} \delta n^f + \frac{Jn^f}{K_f^\eta} \delta \dot{p}_f + \delta j \right) A dX \\ &= \int_0^{X=H} w^{p_f} \left(\left[\frac{n^f \dot{p}_f}{K_f^\eta} (\beta\Delta t^2) + \frac{J \dot{p}_f}{K_f^\eta} \frac{n^s}{J} (\beta\Delta t^2) + (\gamma\Delta t) \right] \frac{\partial(\delta a)}{\partial X} + \frac{Jn^f}{K_f^\eta} (\gamma\Delta t) \delta \dot{p}_f \right) A dX \\ &= \int_0^{X=H} w^{p_f} \left(\left[\frac{\dot{p}_f}{K_f^\eta} (\beta\Delta t^2) + (\gamma\Delta t) \right] \frac{\partial(\delta a)}{\partial X} + \frac{Jn^f}{K_f^\eta} (\gamma\Delta t) \delta \dot{p}_f \right) A dX . \end{aligned} \quad (\text{B.25})$$

For poroelasticity, (B.25) becomes

$$\delta\mathcal{H}_1^{\text{INT}} = \int_0^{X=H} w^{p_f} \left(\left[\frac{\dot{p}_f}{K_f^\eta} (\gamma\Delta t) + 1 \right] \frac{\partial(\delta v)}{\partial X} + \frac{Jn^f}{K_f^\eta} \delta \dot{p}_f \right) A dX . \quad (\text{B.26})$$

The next linearization proceeds as follows:

$$\begin{aligned} \delta\mathcal{H}_2^{\text{INT}} &= \int_0^{X=H} w^{p_f} \delta \left(\frac{1}{K_f^\eta} \frac{\partial p_f}{\partial X} n^f \tilde{v}_f \right) A dX \\ &= \int_0^{X=H} w^{p_f} \left(n^f \tilde{v}_f \frac{\partial(\delta p_f)}{\partial X} + \frac{\partial p_f}{\partial X} \delta(n^f \tilde{v}_f) \right) \frac{A}{K_f^\eta} dX \\ &= \int_0^{X=H} w^{p_f} \left(n^f \tilde{v}_f (\beta\Delta t^2) \frac{\partial(\delta \dot{p}_f)}{\partial X} + \frac{\partial p_f}{\partial X} \left[\underbrace{- \left(\frac{\partial p_f}{\partial X} F_{11}^{-1} + \rho^{\text{fR}}(a+g) \right) \delta \hat{k}}_{\text{Term 1}} \right. \right. \\ &\quad \left. \left. - \hat{k} \left(\frac{\partial(\delta p_f)}{\partial X} F_{11}^{-1} + \frac{\partial p_f}{\partial X} \delta F_{11}^{-1} + (a+g) \delta \rho^{\text{fR}} + \rho^{\text{fR}} \delta a \right) \right] \right) \frac{A}{K_f^\eta} dX \end{aligned} \quad (\text{B.27})$$

Term 2

$$\begin{aligned}
\mathbf{Term\ 1} &= -\delta_{\hat{k}} \left(\frac{\partial p_f}{\partial X} F_{11}^{-1} + \rho^{\text{fR}}(a+g) \right) (\beta \Delta t^2) \frac{\partial(\delta a)}{\partial X} \\
&= \frac{\delta_{\hat{k}}}{\hat{k}} (n^f \tilde{v}_f) (\beta \Delta t^2) \frac{\partial(\delta a)}{\partial X} , \\
\mathbf{Term\ 2} &= -\hat{k} \left(F_{11}^{-1} (\beta \Delta t^2) \frac{\partial(\delta \ddot{p}_f)}{\partial X} - \frac{\partial p_f}{\partial X} F_{11}^{-2} (\beta \Delta t^2) \frac{\partial \delta a}{\partial X} \right. \\
&\quad \left. + (a+g) \frac{\rho^{\text{fR}}}{K_f^\eta} (\beta \Delta t^2) \delta \ddot{p}_f + \rho^{\text{fR}} \delta a \right)
\end{aligned}$$

Combining terms leaves us with

$$\begin{aligned}
\delta \mathcal{H}_2^{\text{INT}} &= \int_0^{X=H} w^{p_f} \left(n^f \tilde{v}_f (\beta \Delta t^2) \frac{\partial(\delta \ddot{p}_f)}{\partial X} + \frac{\partial p_f}{\partial X} \left[\frac{\delta_{\hat{k}}}{\hat{k}} (n^f \tilde{v}_f) (\beta \Delta t^2) \frac{\partial(\delta a)}{\partial X} \right. \right. \\
&\quad \left. \left. - \hat{k} \left(F_{11}^{-1} (\beta \Delta t^2) \frac{\partial(\delta \ddot{p}_f)}{\partial X} - \frac{\partial p_f}{\partial X} F_{11}^{-2} (\beta \Delta t^2) \frac{\partial(\delta a)}{\partial X} \right) \right. \right. \\
&\quad \left. \left. + (a+g) \frac{\rho^{\text{fR}}}{K_f^\eta} (\beta \Delta t^2) \delta \ddot{p}_f + \rho^{\text{fR}} \delta a \right) \right] \frac{A}{K_f^\eta} dX . \tag{B.28}
\end{aligned}$$

Rearranging like terms, we arrive at

$$\begin{aligned}
\delta \mathcal{H}_2^{\text{INT}} &= \int_0^{X=H} w^{p_f} \left(\left[(n^f \tilde{v}_f) - \hat{k} \frac{\partial p_f}{\partial X} F_{11}^{-1} \right] (\beta \Delta t^2) \frac{\partial(\delta \ddot{p}_f)}{\partial X} - \hat{k} \frac{\partial p_f}{\partial X} (a+g) \times \right. \\
&\quad \left. \frac{\rho^{\text{fR}}}{K_f^\eta} (\beta \Delta t^2) \delta \ddot{p}_f + \frac{\partial p_f}{\partial X} \left[\frac{\delta_{\hat{k}}}{\hat{k}} (n^f \tilde{v}_f) + \hat{k} \frac{\partial p_f}{\partial X} F_{11}^{-2} \right] (\beta \Delta t^2) \frac{\partial(\delta a)}{\partial X} - \frac{\partial p_f}{\partial X} \hat{k} \rho^{\text{fR}} \delta a \right) \frac{A}{K_f^\eta} dX . \tag{B.29}
\end{aligned}$$

For poroelasticity, (B.29) becomes

$$\begin{aligned}
\delta \mathcal{H}_2^{\text{INT}} &= \int_0^{X=H} w^{p_f} \left(\left[(n^f \tilde{v}_f) - \hat{k} \frac{\partial p_f}{\partial X} F_{11}^{-1} \right] (\gamma \Delta t) \frac{\partial(\delta \dot{p}_f)}{\partial X} - \hat{k} \frac{\partial p_f}{\partial X} g \frac{\rho^{\text{fR}}}{K_f^\eta} (\gamma \Delta t) \delta \dot{p}_f \right. \\
&\quad \left. + \frac{\partial p_f}{\partial X} \left[\frac{\delta_{\hat{k}}}{\hat{k}} (n^f \tilde{v}_f) + \hat{k} \frac{\partial p_f}{\partial X} F_{11}^{-2} \right] (\gamma \Delta t) \frac{\partial(\delta v)}{\partial X} \right) \frac{A}{K_f^\eta} dX . \tag{B.30}
\end{aligned}$$

The next linearization proceeds as follows:

$$\begin{aligned}
\delta\mathcal{H}_3^{\text{INT}} &= \int_0^{X=H} \frac{\partial w^{\text{Pf}}}{\partial X} \delta \left(\hat{k} \frac{\partial p_{\text{f}}}{\partial X} F_{11}^{-1} \right) A dX \\
&= \int_0^{X=H} \frac{\partial w^{\text{Pf}}}{\partial X} \left(\frac{\partial p_{\text{f}}}{\partial X} F_{11}^{-1} \delta \hat{k} + \hat{k} F_{11}^{-1} \frac{\partial(\delta p_{\text{f}})}{\partial X} + \hat{k} \frac{\partial p_{\text{f}}}{\partial X} \delta F_{11}^{-1} \right) A dX \\
&= \int_0^{X=H} \frac{\partial w^{\text{Pf}}}{\partial X} \left(\frac{\partial p_{\text{f}}}{\partial X} F_{11}^{-1} \delta_{\hat{k}}(\beta \Delta t^2) \frac{\partial(\delta a)}{\partial X} \right. \\
&\quad \left. + \hat{k} F_{11}^{-1}(\beta \Delta t^2) \frac{\partial(\delta \ddot{p}_{\text{f}})}{\partial X} - \hat{k} \frac{\partial p_{\text{f}}}{\partial X} F_{11}^{-2}(\beta \Delta t^2) \frac{\partial(\delta a)}{\partial X} \right) A dX
\end{aligned} \tag{B.31}$$

Rearranging like terms, we arrive at

$$\delta\mathcal{H}_3^{\text{INT}} = \int_0^{X=H} \frac{\partial w^{\text{Pf}}}{\partial X} \left([\delta_{\hat{k}} - \hat{k} F_{11}^{-1}] \frac{\partial p_{\text{f}}}{\partial X} F_{11}^{-1}(\beta \Delta t^2) \frac{\partial(\delta a)}{\partial X} + \hat{k} F_{11}^{-1}(\beta \Delta t^2) \frac{\partial(\delta \ddot{p}_{\text{f}})}{\partial X} \right) A dX . \tag{B.32}$$

For poroelasticity, (B.32) becomes

$$\delta\mathcal{H}_3^{\text{INT}} = \int_0^{X=H} \frac{\partial w^{\text{Pf}}}{\partial X} \left([\delta_{\hat{k}} - \hat{k} F_{11}^{-1}] \frac{\partial p_{\text{f}}}{\partial X} F_{11}^{-1}(\gamma \Delta t) \frac{\partial(\delta v)}{\partial X} + \hat{k} F_{11}^{-1}(\gamma \Delta t) \frac{\partial(\delta \dot{p}_{\text{f}})}{\partial X} \right) A dX . \tag{B.33}$$

The next linearization proceeds as follows:

$$\begin{aligned}
\delta\mathcal{H}_4^{\text{INT}} &= \int_0^{X=H} \frac{\partial w^{\text{Pf}}}{\partial X} \delta(\hat{k} \rho^{\text{fR}}(a+g)) A dX \\
&= \int_0^{X=H} \frac{\partial w^{\text{Pf}}}{\partial X} \left(\rho^{\text{fR}}(a+g) \delta \hat{k} + \hat{k}(a+g) \delta \rho^{\text{fR}} + \hat{k} \rho^{\text{fR}} \delta a \right) A dX \\
&= \int_0^{X=H} \frac{\partial w^{\text{Pf}}}{\partial X} \rho^{\text{fR}} \left(\delta_{\hat{k}}(a+g)(\beta \Delta t^2) \frac{\partial(\delta a)}{\partial X} \right. \\
&\quad \left. + \hat{k}(a+g) \frac{1}{K_{\text{f}}^{\eta}}(\beta \Delta t^2) \delta \ddot{p}_{\text{f}} + \hat{k} \delta a \right) A dX .
\end{aligned} \tag{B.34}$$

For poroelasticity, (B.34) becomes

$$\delta\mathcal{H}_4^{\text{INT}} = \int_0^{X=H} \frac{\partial w^{\text{Pf}}}{\partial X} \rho^{\text{fR}} \left(\delta_{\hat{k}} g(\gamma \Delta t) \frac{\partial(\delta v)}{\partial X} + \hat{k} g \frac{1}{K_{\text{f}}^{\eta}}(\gamma \Delta t) \delta \dot{p}_{\text{f}} \right) A dX . \tag{B.35}$$

The next linearization is given by

$$\begin{aligned}
\delta\mathcal{H}^{\text{stab}} &= \int_0^{X=H} \frac{\partial w^{p_f}}{\partial X} \alpha^{\text{stab}} \delta \left(F_{11}^{-1} \frac{\partial \dot{p}_f}{\partial X} \right) A dX \\
&= \int_0^{X=H} \frac{\partial w^{p_f}}{\partial X} \alpha^{\text{stab}} \left(\frac{\partial \dot{p}_f}{\partial X} \delta(F_{11}^{-1}) + F_{11}^{-1} \frac{\partial \delta \dot{p}_f}{\partial X} \right) A dX \\
&= \int_0^{X=H} \frac{\partial w^{p_f}}{\partial X} \alpha^{\text{stab}} F_{11}^{-1} \left((\gamma \Delta t) \frac{\partial \delta \ddot{p}_f}{\partial X} - \frac{\partial \dot{p}_f}{\partial X} F_{11}^{-1} (\beta \Delta t^2) \frac{\partial \delta a}{\partial X} \right) A dX . \tag{B.36}
\end{aligned}$$

For poroelasticity, (B.36) becomes

$$\delta\mathcal{H}^{\text{stab}} = \int_0^{X=H} \frac{\partial w^{p_f}}{\partial X} \alpha^{\text{stab}} F_{11}^{-1} \left(\frac{\partial \delta \dot{p}_f}{\partial X} - \frac{\partial \dot{p}_f}{\partial X} F_{11}^{-1} (\gamma \Delta t) \frac{\partial \delta v}{\partial X} \right) A dX . \tag{B.37}$$

B.4 ($\mathbf{u}-\mathbf{u}_f-p_f$) formulation

The linearization of the variational equations given in Chapter 4.1.4 commences as follows:

$$\begin{aligned}
\delta\mathcal{G}_1^{\text{INT}} &= \int_0^{X=H} w^u \delta(\rho_0^s a + \rho_0^f a_f) A dX \\
&= \int_0^{X=H} w^u (\rho_0^s \delta a + a_f \delta \rho_0^f + \rho_0^f \delta a_f) A dX \\
&= \int_0^{X=H} w^u \left(\rho_0^s \delta a + a_f (\beta \Delta t^2) \left[\rho^{\text{fR}} \frac{\partial(\delta a)}{\partial X} + \frac{J n^f \rho^{\text{fR}}}{K_f^\eta} \delta \ddot{p}_f \right] + \rho_0^f \delta a_f \right) A dX \tag{B.38}
\end{aligned}$$

The linearizations $\delta\mathcal{G}_2^{\text{INT}}$, $\delta\mathcal{G}_3^{\text{INT}}$ remain unchanged from the $(\mathbf{u}-p_f)$ formulation for the $(\mathbf{u}-\mathbf{u}_f-p_f)$ formulation. The next linearization is obtained via

$$\begin{aligned}
\delta\mathcal{I}_1^{\text{INT}} &= \int_0^{X=H} w^{u_f} \delta(\rho_0^f a_f) A dX = \int_0^{X=H} q (a_f \delta \rho_0^f + \rho_0^f \delta a_f) A dX \\
&= \int_0^{X=H} w^{u_f} \left(a_f (\beta \Delta t^2) \left[\rho^{\text{fR}} \frac{\partial(\delta a)}{\partial X} + \frac{J n^f \rho^{\text{fR}}}{K_f^\eta} \delta \ddot{p}_f \right] + \rho_0^f \delta a_f \right) A dX . \tag{B.39}
\end{aligned}$$

The linearization of the next term proceeds as follows:

$$\begin{aligned}\delta\mathcal{I}_2^{\text{INT}} &= \int_0^{X=H} w^{u_f} \delta \left(n^f \frac{\partial p_f}{\partial X} \right) A dX = \int_0^{X=H} q \left(\frac{\partial p_f}{\partial X} \delta n^f + n^f \frac{\partial(\delta p_f)}{\partial X} \right) A dX \\ &= \int_0^{X=H} w^{u_f} \left(\frac{n^s}{J} \frac{\partial p_f}{\partial X} (\beta \Delta t^2) \frac{\partial(\delta a)}{\partial X} + n^f (\beta \Delta t^2) \frac{\partial(\delta \ddot{p}_f)}{\partial X} \right) A dX\end{aligned}\quad (\text{B.40})$$

The next linearization is then

$$\begin{aligned}\delta\mathcal{I}_3^{\text{INT}} &= \int_0^{X=H} w^{u_f} \delta \left(\frac{J(n^f)^2}{\hat{k}} \tilde{v}_f \right) A dX \\ &= \int_0^{X=H} w^{u_f} \left(\frac{(n^f)^2}{\hat{k}} \tilde{v}_f \delta(J) + \frac{2Jn^f}{\hat{k}} \tilde{v}_f \delta(n^f) + J(n^f)^2 \tilde{v}_f \delta(\hat{k}^{-1}) + \frac{J(n^f)^2}{\hat{k}} \delta(\tilde{v}_f) \right) A dX \\ &= \int_0^{X=H} w^{u_f} \left(\frac{(n^f)^2}{\hat{k}} \tilde{v}_f (\beta \Delta t^2) \frac{\partial(\delta a)}{\partial X} + \frac{2Jn^f \tilde{v}_f n^s}{\hat{k} J} (\beta \Delta t^2) \frac{\partial(\delta a)}{\partial X} \right. \\ &\quad \left. + J(n^f)^2 \tilde{v}_f (-\hat{k}^{-2}) \delta_{\hat{k}} (\beta \Delta t^2) \frac{\partial(\delta a)}{\partial X} + \frac{J(n^f)^2}{\hat{k}} (\gamma \Delta t) [\delta a_f - \delta a] \right) A dX .\end{aligned}\quad (\text{B.41})$$

Rearranging like terms,

$$\delta\mathcal{I}_3^{\text{INT}} = \int_0^{X=H} w^{u_f} \left(\left[1 + \frac{2n^s}{n^f} - \frac{J\delta_{\hat{k}}}{\hat{k}} \right] \frac{(n^f)^2 \tilde{v}_f}{\hat{k}} (\beta \Delta t^2) \frac{\partial \delta a}{\partial X} + \frac{J(n^f)^2}{\hat{k}} (\gamma \Delta t) (\delta a_f - \delta a) \right) A dX .\quad (\text{B.42})$$

The next requisite linearization proceeds as

$$\begin{aligned}\delta\mathcal{I}_4^{\text{INT}} &= \int_0^{X=H} w^{u_f} \delta \left(\rho_0^f g \right) A dX = \int_0^{X=H} q \delta(\rho_0^f) g A dX \\ &= \int_0^{X=H} w^{u_f} \left((\beta \Delta t^2) \left[\rho^{\text{fR}} \frac{\partial(\delta a)}{\partial X} + \frac{Jn^f \rho^{\text{fR}}}{K_f^\eta} \delta \ddot{p}_f \right] \right) g A dX .\end{aligned}\quad (\text{B.43})$$

The subsequent linearization for the $(\mathbf{u}-\mathbf{u}_f-p_f)$ formulation is similar to that derived in (B.29) for the $(\mathbf{u}-p_f)$ formulation, except that we now account for a variation on the pore fluid acceleration

rather than the mixture acceleration when the Darcy velocity is expanded.

$$\begin{aligned}
\delta\mathcal{H}_2^{\text{INT}} &= \int_0^{X=H} w^{p_f} \delta \left(\frac{1}{K_f^\eta} \frac{\partial p_f}{\partial X} n^f \tilde{v}_f \right) A dX \\
&= \int_0^{X=H} w^{p_f} \left(n^f \tilde{v}_f \frac{\partial(\delta p_f)}{\partial X} + \frac{\partial p_f}{\partial X} \delta(n^f \tilde{v}_f) \right) \frac{A}{K_f^\eta} dX \\
&= \int_0^{X=H} w^{p_f} \left(n^f \tilde{v}_f (\beta \Delta t^2) \frac{\partial(\delta \ddot{p}_f)}{\partial X} + \frac{\partial p_f}{\partial X} \left[\underbrace{- \left(\frac{\partial p_f}{\partial X} F_{11}^{-1} + \rho^{\text{fR}}(a_f + g) \right) \delta \hat{k}}_{\text{Term 1}} \right. \right. \\
&\quad \left. \left. - \hat{k} \left(\frac{\partial(\delta p_f)}{\partial X} \frac{\partial p_f}{\partial X} \delta(F_{11}^{-1}) + (a_f + g) \delta \rho^{\text{fR}} + \rho^{\text{fR}} \delta a_f \right) \right] \right) \frac{A}{K_f^\eta} dX \quad (\text{B.44})
\end{aligned}$$

$$\begin{aligned}
\text{Term 1} &= -\delta_{\hat{k}} \left(\frac{\partial p_f}{\partial X} + \rho^{\text{fR}}(a_f + g) \right) (\beta \Delta t^2) \frac{\partial(\delta a)}{\partial X} \\
&= \frac{\delta_{\hat{k}}}{\hat{k}} (n^f \tilde{v}_f) (\beta \Delta t^2) \frac{\partial(\delta a)}{\partial X}, \\
\text{Term 2} &= -\hat{k} \left((\beta \Delta t^2) \frac{\partial(\delta \ddot{p}_f)}{\partial X} - \frac{\partial p_f}{\partial X} F_{11}^{-2} (\beta \Delta t^2) \frac{\partial(\delta a)}{\partial X} + (a_f + g) \frac{\rho^{\text{fR}}}{K_f^\eta} (\beta \Delta t^2) \delta \ddot{p}_f + \rho^{\text{fR}} \delta a_f \right)
\end{aligned}$$

Combining terms leaves us with

$$\begin{aligned}
\delta\mathcal{H}_2^{\text{INT}} &= \int_0^{X=H} w^{p_f} \left(n^f \tilde{v}_f (\beta \Delta t^2) \frac{\partial(\delta \ddot{p}_f)}{\partial X} + \frac{\partial p_f}{\partial X} \left[\frac{\delta_{\hat{k}}}{\hat{k}} (n^f \tilde{v}_f) (\beta \Delta t^2) \frac{\partial(\delta a)}{\partial X} \right. \right. \\
&\quad \left. \left. - \hat{k} \left(F_{11}^{-1} (\beta \Delta t^2) \frac{\partial(\delta \ddot{p}_f)}{\partial X} - \frac{\partial p_f}{\partial X} F_{11}^{-2} (\beta \Delta t^2) \frac{\partial(\delta a)}{\partial X} + (a_f + g) \frac{\rho^{\text{fR}}}{K_f^\eta} \times \right. \right. \right. \\
&\quad \left. \left. \left. (\beta \Delta t^2) \delta \ddot{p}_f + \rho^{\text{fR}} \delta a_f \right) \right] \right) \frac{A}{K_f^\eta} dX. \quad (\text{B.45})
\end{aligned}$$

Rearranging like terms, we arrive at

$$\begin{aligned}
\delta\mathcal{H}_2^{\text{INT}} &= \int_0^{X=H} w^{p_f} \left(\left[(n^f \tilde{v}_f) - \hat{k} \frac{\partial p_f}{\partial X} \right] (\beta \Delta t^2) \frac{\partial(\delta \ddot{p}_f)}{\partial X} - \hat{k} \frac{\partial p_f}{\partial X} (a_f + g) \frac{\rho^{\text{fR}}}{K_f^\eta} \times \right. \\
&\quad \left. (\beta \Delta t^2) \delta \ddot{p}_f + \frac{\partial p_f}{\partial X} \left[\frac{\delta_{\hat{k}}}{\hat{k}} (n^f \tilde{v}_f) + \hat{k} \frac{\partial p_f}{\partial X} F_{11}^{-2} \right] (\beta \Delta t^2) \frac{\partial(\delta a)}{\partial X} - \frac{\partial p_f}{\partial X} \hat{k} \rho^{\text{fR}} \delta a_f \right) \frac{A}{K_f^\eta} dX. \quad (\text{B.46})
\end{aligned}$$

The final necessary linearization for the for the $(\mathbf{u}-\mathbf{u}_f-p_f)$ formulation proceeds as follows.

$$\begin{aligned}
\delta\mathcal{H}_4^{\text{INT}} &= \int_0^{X=H} \frac{\partial w^{p_f}}{\partial X} \delta(\hat{k}\rho^{\text{fR}}(a_f + g)) A dX \\
&= \int_0^{X=H} \frac{\partial w^{p_f}}{\partial X} (\rho^{\text{fR}}(a_f + g)\delta(\hat{k}) + \hat{k}(a_f + g)\delta(\rho^{\text{fR}}) + \hat{k}\rho^{\text{fR}}\delta(a_f)) A dX \\
&= \int_0^{X=H} \frac{\partial w^{p_f}}{\partial X} \rho^{\text{fR}} \left(\delta_{\hat{k}}(a_f + g)(\beta\Delta t^2) \frac{\partial(\delta a)}{\partial X} + \hat{k}(a_f + g) \frac{1}{K_f^\eta} (\beta\Delta t^2) \delta\ddot{p}_f + \hat{k}\delta a_f \right) A dX \quad (\text{B.47})
\end{aligned}$$

In the case that the pore fluid viscous stress tensor $\boldsymbol{\sigma}_E^f$ is assumed non-zero, recall that Darcy's law is

$$(n^f \tilde{\mathbf{v}}_f) = -\hat{k} \left(\rho^{\text{fR}}(\mathbf{a}_f - \mathbf{g}) + \text{grad} p_f - \frac{1}{n^f} \text{div} \boldsymbol{\sigma}_E^f \right). \quad (\text{B.48})$$

Thus, for the implicit formulation, additional terms are required in the variation of $\mathcal{H}_2^{\text{INT}}$, as well as a variation of $\mathcal{H}_5^{\text{INT}}$. Additionally, we require variations of $\mathcal{G}_5^{\text{INT}}$ and $\mathcal{I}_5^{\text{INT}}$, though these are simpler to formulate given that C^0 continuity can be maintained by weakening the terms. In the variations of the balance of mass terms, we seek to find the variation of the porosity-scaled divergence of the viscous stress term, which in 1-D reduces to the following from Eq. (4.97):

$$\frac{1}{n^f} \left[\frac{\partial n^f}{\partial X} \frac{\partial v_f}{\partial X} + n^f \frac{\partial^2 v_f}{\partial X^2} \right] (\kappa_f + 2\eta_f) F_{11}^{-2} \quad (\text{B.49})$$

This is identical to Eq. (A.20) except for the additional scaling of inverse porosity, whose variation is

$$\delta\left(\frac{1}{n^f}\right) = -\frac{1}{(n^f)^2} \delta(n^f) = -\frac{n^s}{J(n^f)^2} \beta\Delta t^2 \frac{\partial(\delta a)}{\partial X}. \quad (\text{B.50})$$

Thus the variation of Eq. (B.49) is

$$\begin{aligned}
&\frac{1}{n^f} (\kappa_f + 2\eta_f) F_{11}^{-2} \left((\gamma\Delta t) \left[\frac{\partial n^f}{\partial X} \frac{\partial(\delta a_f)}{\partial X} + n^f \frac{\partial^2(\delta a_f)}{\partial X^2} \right] + \frac{n^s}{J} \frac{\partial v_f}{\partial X} (\beta\Delta t^2) \frac{\partial^2(\delta a)}{\partial X^2} \right. \\
&\quad \left. + \frac{n^s}{J} (\beta\Delta t^2) \left[\frac{\partial^2 v_f}{\partial X^2} - \frac{2}{J} \frac{\partial v_f}{\partial X} \frac{\partial^2 u}{\partial X^2} \right] \frac{\partial(\delta a)}{\partial X} \right) \\
&- \frac{1}{J n^f} \left(2 + \frac{n^s}{n^f} \right) \frac{\partial \sigma_{11(E)}^f}{\partial X} (\beta\Delta t^2) \frac{\partial(\delta a)}{\partial X}. \quad (\text{B.51})
\end{aligned}$$

Thus, δH_2^{INT} becomes

$$\begin{aligned}
\delta \mathcal{H}_2^{\text{INT}} = & \int_0^{X=H} w^{p_f} \left(\left[(n^f \tilde{v}_f) - \hat{k} \frac{\partial p_f}{\partial X} \right] (\beta \Delta t^2) \frac{\partial(\delta \ddot{p}_f)}{\partial X} - \hat{k} \frac{\partial p_f}{\partial X} (a_f + g) \frac{\rho^{\text{fR}}}{K_f^\eta} \times \right. \\
& \left. (\beta \Delta t^2) \delta \ddot{p}_f + \frac{\partial p_f}{\partial X} \left[\frac{\delta \hat{k}}{\hat{k}} (n^f \tilde{v}_f) + \hat{k} \frac{\partial p_f}{\partial X} F_{11}^{-2} \right. \right. \\
& \left. \left. - \frac{\hat{k}}{J n^f} \left(\frac{n^s}{J^2} (\kappa_f + 2\eta_f) \left[\frac{\partial^2 v_f}{\partial X^2} - \frac{2}{J} \frac{\partial v_f}{\partial X} \frac{\partial u^2}{\partial X^2} \right] - \left[2 + \frac{n^s}{n^f} \right] \frac{\partial \sigma_{11(E)}^f}{\partial X} \right) \right] (\beta \Delta t^2) \frac{\partial(\delta a)}{\partial X} \right. \\
& \left. - \frac{\partial p_f}{\partial X} \hat{k} \frac{n^s}{J^3 n^f} \frac{\partial v_f}{\partial X} (\kappa_f + 2\eta_f) \beta \Delta t^2 \frac{\partial^2(\delta a)}{\partial X^2} - \frac{\partial p_f}{\partial X} \hat{k} \rho^{\text{fR}} \delta a_f \right. \\
& \left. - \frac{\partial p_f}{\partial X} \frac{\hat{k}}{J^2 n^f} \left[\frac{\partial n^f}{\partial X} \frac{\partial(\delta a_f)}{\partial X} + n^f \frac{\partial^2(\delta a_f)}{\partial X^2} \right] (\kappa_f + 2\eta_f) (\gamma \Delta t) \right) \frac{A}{K_f^\eta} dX . \tag{B.52}
\end{aligned}$$

Next, $\delta\mathcal{H}_5^{\text{INT}}$ is given as

$$\begin{aligned}
\delta\mathcal{H}_5^{\text{INT}} &= - \int_0^{X=H} \frac{\partial w^{pt}}{\partial X} \delta \left(\frac{\hat{k}}{n^f} \frac{\partial \sigma_{11(E)}^f}{\partial X} \right) A dX \\
&= - \int_0^{X=H} \frac{\partial w^{pt}}{\partial X} \left(\frac{1}{n^f} \frac{\partial \sigma_{11(E)}^f}{\partial X} \delta(\hat{k}) + \hat{k} \frac{\partial \sigma_{11(E)}^f}{\partial X} \delta \left(\frac{1}{n^f} \right) + \frac{\hat{k}}{n^f} \delta \left(\frac{\partial \sigma_{11(E)}^f}{\partial X} \right) \right) A dX \\
&= - \int_0^{X=H} \frac{\partial w^{pt}}{\partial X} \left(\frac{\delta_{\hat{k}}}{n^f} \frac{\partial \sigma_{11(E)}^f}{\partial X} (\beta \Delta t^2) \frac{\partial(\delta a)}{\partial X} \right. \\
&\quad \left. \frac{\hat{k}}{n^f} (\kappa_f + 2\eta_f) F_{11}^{-2} \left((\gamma \Delta t) \left[\frac{\partial n^f}{\partial X} \frac{\partial(\delta a_f)}{\partial X} + n^f \frac{\partial^2(\delta a_f)}{\partial X^2} \right] \right. \right. \\
&\quad \left. \left. + \frac{n^s}{J} \frac{\partial v_f}{\partial X} (\beta \Delta t^2) \frac{\partial^2(\delta a)}{\partial X^2} \right. \right. \\
&\quad \left. \left. + \frac{n^s}{J} (\beta \Delta t^2) \left[\frac{\partial^2 v_f}{\partial X^2} - \frac{2}{J} \frac{\partial v_f}{\partial X} \frac{\partial^2 u}{\partial X^2} \right] \frac{\partial(\delta a)}{\partial X} \right) \right. \\
&\quad \left. - \frac{\hat{k}}{J n^f} \left(2 + \frac{n^s}{n^f} \right) \frac{\partial \sigma_{11(E)}^f}{\partial X} (\beta \Delta t^2) \frac{\partial(\delta a)}{\partial X} \right) A dX \\
&= - \int_0^{X=H} \frac{\partial w^{pt}}{\partial X} \left(\frac{1}{n^f} (\beta \Delta t^2) \left[\frac{\partial \sigma_{11(E)}^f}{\partial X} \left(\delta_{\hat{k}} - \frac{1}{J} \left[2 + \frac{n^s}{n^f} \right] \right) \right. \right. \\
&\quad \left. \left. + \frac{\hat{k}}{J^3 n^s} (\kappa_f + 2\eta_f) \left(\frac{\partial^2 v_f}{\partial X^2} - \frac{2}{J} \frac{\partial v_f}{\partial X} \frac{\partial^2 u}{\partial X^2} \right) \right] \frac{\partial(\delta a)}{\partial X} \right. \\
&\quad \left. + \frac{\hat{k}}{J^2 n^f} (\kappa_f + 2\eta_f) (\gamma \Delta t) \left[\frac{\partial n^f}{\partial X} \frac{\partial(\delta a_f)}{\partial X} + n^f \frac{\partial^2(\delta a_f)}{\partial X^2} \right] \right) A dX . \tag{B.53}
\end{aligned}$$

For the variations of the momentum variational equation terms $\mathcal{G}_5^{\text{INT}}$ and $\mathcal{I}_5^{\text{INT}}$, we seek to find the variation of the viscous stress term

$$\delta(\sigma_{11(E)}^f) = \delta(P_{11(E)}^f) = \delta \left(n^f \frac{\partial v_f}{\partial X} F_{11}^{-1} \right) (\kappa_f + 2\mu_f), \tag{B.54}$$

which is simply

$$\frac{\partial v_f}{\partial X} F_{11}^{-2} (n^s - n^f) (\kappa_f + 2\mu_f) \beta \Delta t^2 \frac{\partial(\delta a)}{\partial X} + n^f F_{11}^{-1} (\kappa_f + 2\mu_f) \gamma \Delta t \frac{\partial(\delta a_f)}{\partial X}. \tag{B.55}$$

Thus, $\delta\mathcal{G}_5^{\text{INT}}$ is given as

$$\delta\mathcal{G}_5^{\text{INT}} = \int_0^{X=H} \frac{\partial w^u}{\partial X} (\kappa_f + 2\mu_f) \left(\frac{\partial v_f}{\partial X} F_{11}^{-2} (n^s - n^f) \beta \Delta t^2 \frac{\partial(\delta a)}{\partial X} + n^f F_{11}^{-1} \gamma \Delta t \frac{\partial(\delta a_f)}{\partial X} \right) A dX, \quad (\text{B.56})$$

and $\delta\mathcal{I}_5^{\text{INT}}$ is given as

$$\delta\mathcal{I}_5^{\text{INT}} = \int_0^{X=H} \frac{\partial w^{u_f}}{\partial X} (\kappa_f + 2\mu_f) \left(\frac{\partial v_f}{\partial X} F_{11}^{-2} (n^s - n^f) \beta \Delta t^2 \frac{\partial(\delta a)}{\partial X} + n^f F_{11}^{-1} \gamma \Delta t \frac{\partial(\delta a_f)}{\partial X} \right) A dX. \quad (\text{B.57})$$

B.5 (\mathbf{u} - p_f - θ^s - θ^f) formulation

The linearization of the variational equations given in Chapter 4.1.5 commences as follows. The linearizations $\delta\mathcal{G}_1^{\text{INT}}$ and $\delta\mathcal{G}_2^{\text{INT}}$ remain unchanged from the (\mathbf{u} - p_f) formulation for the (\mathbf{u} - p_f - θ^s - θ^f) formulation (save notation denoting a separate solid phase, i.e., $\theta \leftarrow \theta^s$, $A \leftarrow \alpha_V^s$, etc.).

Linearization of $\mathcal{G}_3^{\text{INT}}$ proceeds as follows:

$$\begin{aligned} \delta\mathcal{G}_3^{\text{INT}} &= - \int_0^{X=H} \frac{\partial w^u}{\partial X} \delta \left(p_f \left[\frac{\theta^s}{\theta^f} n^s + n^f \right] \right) A dX \\ &= - \int_0^{X=H} \frac{\partial w^u}{\partial X} \left(\delta(p_f) \left[\frac{\theta^s}{\theta^f} n^s + n^f \right] + p_f \frac{\theta^s}{\theta^f} \delta(n^s) + p_f \frac{n^s}{\theta^f} \delta(\theta^s) + p_f n^s \theta^s \delta \left(\frac{1}{\theta^f} \right) + p_f \delta(n^f) \right) A dX \\ &= - \int_0^{X=H} \frac{\partial w^u}{\partial X} (\beta \Delta t^2) \left(\delta \dot{p}_f + \frac{n^s p_f}{J} \left[1 - \frac{\theta^s}{\theta^f} \right] \frac{\partial(\delta a)}{\partial X} + \frac{n^s p_f}{\theta^f} \delta \dot{\theta}^s - \frac{n^s p_f \theta^s}{(\theta^f)^2} \delta \dot{\theta}^f \right) A dX. \end{aligned} \quad (\text{B.58})$$

For thermoporoelasticity,

$$\delta\mathcal{G}_3^{\text{INT}} = - \int_0^{X=H} \frac{\partial w^u}{\partial X} (\gamma \Delta t) \left(\delta \dot{p}_f + \frac{n^s p_f}{J} \left[1 - \frac{\theta^s}{\theta^f} \right] \frac{\partial(\delta v)}{\partial X} + \frac{n^s p_f}{\theta^f} \delta \dot{\theta}^s - \frac{n^s p_f \theta^s}{(\theta^f)^2} \delta \dot{\theta}^f \right) A dX. \quad (\text{B.59})$$

Recall that the constitutive relation between pore fluid real mass density and its pressure is related by the bulk modulus of the pore fluid (refer to Eq. (2.20)). For an ideal gas, the bulk modulus is the pore fluid pressure. Therefore, the scaling of the $\mathcal{H}_1^{\text{INT}}$ and $\mathcal{H}_2^{\text{INT}}$ terms by the pore fluid

isentropic bulk modulus must be replaced by the scaling of the pore fluid pressure. For $\mathcal{H}_1^{\text{INT}}$, the linearization is now

$$\begin{aligned}
\delta\mathcal{H}_1^{\text{INT}} &= \int_0^{X=H} w^{p_f} \delta \left(\frac{Jn^f}{p_f} \dot{p}_f + j \right) A dX \\
&= \int_0^{X=H} w^{p_f} \left(\frac{n^f \dot{p}_f}{p_f} \delta(J) + \frac{J \dot{p}_f}{p_f} \delta(n^f) + \frac{Jn^f}{p_f} \delta(\dot{p}_f) + Jn^f \dot{p}_f \delta \left(\frac{1}{p_f} \right) + \delta(j) \right) A dX \\
&= \int_0^{X=H} w^{p_f} \left(\left[\frac{\dot{p}_f}{p_f} (\beta \Delta t^2) + (\gamma \Delta t) \right] \frac{\partial(\delta a)}{\partial X} + \frac{Jn^f}{p_f} \left[(\gamma \Delta t) - \frac{\dot{p}_f}{p_f} (\beta \Delta t^2) \right] \delta \dot{p}_f \right) A dX . \quad (\text{B.60})
\end{aligned}$$

For thermoporoelasticity, (B.60) becomes

$$\delta\mathcal{H}_1^{\text{INT}} = \int_0^{X=H} w^{p_f} \left(\left[\frac{\dot{p}_f}{p_f} (\gamma \Delta t) + 1 \right] \frac{\partial(\delta v)}{\partial X} + \frac{Jn^f}{p_f} \left[1 - \frac{\dot{p}_f}{p_f} (\gamma \Delta t) \right] \delta \dot{p}_f \right) A dX , . \quad (\text{B.61})$$

For the compressible liquid model, the isentropic bulk modulus is replaced by the isothermal bulk modulus, such that,

$$\delta\mathcal{H}_1^{\text{INT}} = \int_0^{X=H} w^{p_f} \left(\left[\frac{\dot{p}_f}{K_f^\theta} (\beta \Delta t^2) + (\gamma \Delta t) \right] \frac{\partial(\delta a)}{\partial X} + \frac{Jn^f}{K_f^\theta} (\gamma \Delta t) \delta \dot{p}_f \right) A dX , \quad (\text{B.62})$$

which, for thermoporoelasticity, becomes

$$\delta\mathcal{H}_1^{\text{INT}} = \int_0^{X=H} w^{p_f} \left(\left[\frac{\dot{p}_f}{K_f^\theta} (\gamma \Delta t) + 1 \right] \frac{\partial(\delta v)}{\partial X} + \frac{Jn^f}{K_f^\theta} \delta \dot{p}_f \right) A dX . \quad (\text{B.63})$$

Recall that Darcy's law for thermoporoelastodynamics and thermoporoelasticity now includes the thermally-scaled porosity gradient term $(p_f/n^f)\text{grad}(n^f)[1 - \theta^s/\theta^f]$ in addition to the outer scaling by pore fluid pressure. The variation of the thermally-scaled porosity gradient term proceeds as

follows¹ :

$$\begin{aligned}
\delta \left(\frac{p_f}{n^f} \frac{\partial n^f}{\partial X} F_{11}^{-1} \left[1 - \frac{\theta^s}{\theta^f} \right] \right) &= \frac{1}{n^f} \frac{\partial n^f}{\partial X} F_{11}^{-1} \left[1 - \frac{\theta^s}{\theta^f} \right] \delta(p_f) - \frac{p_f}{(n^f)^2} \frac{\partial n^f}{\partial X} F_{11}^{-1} \left[1 - \frac{\theta^s}{\theta^f} \right] \delta(n^f) \\
&+ \frac{p_f}{n^f} \left[1 - \frac{\theta^s}{\theta^f} \right] \delta \left(\frac{\partial n^f}{\partial X} F_{11}^{-1} \right) - \frac{p_f}{n^f} \frac{\partial n^f}{\partial X} F_{11}^{-1} \frac{1}{\theta^f} \delta(\theta^s) \\
&+ \frac{p_f}{n^f} \frac{\partial n^f}{\partial X} F_{11}^{-1} \frac{\theta^s}{(\theta^f)^2} \delta(\theta^f) \\
&= \frac{1}{J n^f} \frac{\partial n^f}{\partial X} \left[1 - \frac{\theta^s}{\theta^f} \right] (\beta \Delta t^2) \delta \ddot{p}_f + \frac{n^s p_f}{J^2 n^f} \left[1 - \frac{\theta^s}{\theta^f} \right] (\beta \Delta t^2) \frac{\partial^2(\delta a)}{\partial X^2} \\
&- \frac{n^s p_f}{J^2 n^f} \left[1 - \frac{\theta^s}{\theta^f} \right] \left(\frac{1}{n^f} \frac{\partial n^f}{\partial X} + \frac{3}{J} \frac{\partial^2 u}{\partial X^2} \right) (\beta \Delta t^2) \frac{\partial(\delta a)}{\partial X} \\
&- \frac{p_f}{J n^f} \frac{\partial n^f}{\partial X} \frac{1}{\theta^f} (\beta \Delta t^2) \delta \ddot{\theta}^s + \frac{p_f}{J n^f} \frac{\partial n^f}{\partial X} \frac{\theta^s}{(\theta^f)^2} \delta \ddot{\theta}^f
\end{aligned} \tag{B.64}$$

Therefore, the variation of Darcy's law for the ideal gas pore fluid may be written as follows:

$$\begin{aligned}
\delta(n^f \tilde{v}_f) &= \left(\frac{\delta \hat{k}}{\hat{k}} (n^f \tilde{v}_f) + \frac{\hat{k}}{J^2} \left[\frac{\partial p_f}{\partial X} - \frac{n^s p_f}{n^f} \left(1 - \frac{\theta^s}{\theta^f} \right) \left(\frac{1}{n^f} \frac{\partial n^f}{\partial X} + \frac{3}{J} \frac{\partial^2 u}{\partial X^2} \right) \right] \right) (\beta \Delta t^2) \frac{\partial(\delta a)}{\partial X} \\
&- \frac{n^s p_f \hat{k}}{J^2 n^f} \left(1 - \frac{\theta^s}{\theta^f} \right) (\beta \Delta t^2) \frac{\partial^2(\delta a)}{\partial X^2} - \hat{k} \rho^{\text{fR}} \delta a - \frac{\hat{k}}{J} (\beta \Delta t^2) \frac{\partial(\delta \ddot{p}_f)}{\partial X} \\
&- \hat{k} \left(\frac{1}{J n^f} \frac{\partial n^f}{\partial X} \left[1 - \frac{\theta^s}{\theta^f} \right] + \frac{a+g}{\mathfrak{R} \theta^f} \right) (\beta \Delta t^2) \delta \ddot{p}_f + \frac{p_f \hat{k}}{J n^f \theta^f} \frac{\partial n^f}{\partial X} (\beta \Delta t^2) \delta \ddot{\theta}^s \\
&+ \hat{k} \frac{\rho^{\text{fR}}}{\theta^f} \left([a+g] - \frac{\mathfrak{R} \theta^s}{J n^f} \frac{\partial n^f}{\partial X} \right) (\beta \Delta t^2) \delta \ddot{\theta}^f.
\end{aligned} \tag{B.65}$$

For the compressible liquid pore fluid,

$$\begin{aligned}
\delta(n^f \tilde{v}_f) &= \left(\frac{\delta \hat{k}}{\hat{k}} (n^f \tilde{v}_f) + \frac{\hat{k}}{J^2} \left[\frac{\partial p_f}{\partial X} - \frac{n^s p_f}{n^f} \left(1 - \frac{\theta^s}{\theta^f} \right) \left(\frac{1}{n^f} \frac{\partial n^f}{\partial X} + \frac{3}{J} \frac{\partial^2 u}{\partial X^2} \right) \right] \right) (\beta \Delta t^2) \frac{\partial(\delta a)}{\partial X} \\
&- \frac{n^s p_f \hat{k}}{J^2 n^f} \left(1 - \frac{\theta^s}{\theta^f} \right) (\beta \Delta t^2) \frac{\partial^2(\delta a)}{\partial X^2} - \hat{k} \rho^{\text{fR}} \delta a - \frac{\hat{k}}{J} (\beta \Delta t^2) \frac{\partial(\delta \ddot{p}_f)}{\partial X} \\
&- \hat{k} \left(\frac{1}{J n^f} \frac{\partial n^f}{\partial X} \left[1 - \frac{\theta^s}{\theta^f} \right] + \frac{\rho^{\text{fR}}}{K_f \theta^f} [a+g] \right) (\beta \Delta t^2) \delta \ddot{p}_f + \frac{p_f \hat{k}}{J n^f \theta^f} \frac{\partial n^f}{\partial X} (\beta \Delta t^2) \delta \ddot{\theta}^s \\
&+ \hat{k} \left(\rho^{\text{fR}} \alpha_V^f [a+g] - \frac{p_f \theta^s}{J n^f (\theta^f)^2} \frac{\partial n^f}{\partial X} \right) (\beta \Delta t^2) \delta \ddot{\theta}^f.
\end{aligned} \tag{B.66}$$

¹ In the second equality of Eq. (B.64), we have used a variation of the form of the Gateaux derivative of the porosity gradient given by Eq. (A.21)₁.

Thus the derivation of the linearization for $\mathcal{H}_2^{\text{INT}}$ for the ideal gas pore fluid may proceed as follows:

$$\begin{aligned}
\delta\mathcal{H}_2^{\text{INT}} &= \int_0^{X=H} w^{p_f} \delta \left(\frac{1}{p_f} \frac{\partial p_f}{\partial X} n^f \tilde{v}_f \right) A dX \\
&= \int_0^{X=H} w^{p_f} \left(\frac{\partial p_f}{\partial X} (n^f \tilde{v}_f) \delta \left(\frac{1}{p_f} \right) + \frac{(n^f \tilde{v}_f)}{p_f} \delta \left(\frac{\partial p_f}{\partial X} \right) + \frac{1}{p_f} \frac{\partial p_f}{\partial X} \delta (n^f \tilde{v}_f) \right) A dX \\
&= \int_0^{X=H} w^{p_f} \left(\frac{1}{p_f} \frac{\partial p_f}{\partial X} \left[\frac{\delta \hat{k}}{\hat{k}} (n^f \tilde{v}_f) + \frac{\hat{k}}{J^2} \left(\frac{\partial p_f}{\partial X} - \frac{n^s p_f}{n^f} \left[1 - \frac{\theta^s}{\theta^f} \right] \left[\frac{1}{n^f} \frac{\partial n^f}{\partial X} + \frac{3}{J} \frac{\partial^2 u}{\partial X^2} \right] \right) \right] \times \right. \\
&\quad (\beta \Delta t^2) \frac{\partial(\delta a)}{\partial X} - \frac{\partial p_f}{\partial X} \frac{n^s \hat{k}}{J^2 n^f} \left[1 - \frac{\theta^s}{\theta^f} \right] (\beta \Delta t^2) \frac{\partial^2(\delta a)}{\partial X^2} - \frac{\partial p_f}{\partial X} \frac{\rho^{\text{FR}} \hat{k}}{p_f} \delta a \\
&\quad + \frac{1}{p_f} \left[(n^f \tilde{v}_f) - \frac{\hat{k}}{J} \frac{\partial p_f}{\partial X} \right] (\beta \Delta t^2) \frac{\partial(\delta \dot{p}_f)}{\partial X} \\
&\quad - \frac{1}{p_f} \frac{\partial p_f}{\partial X} \left[\frac{(n^f \tilde{v}_f)}{p_f} + \hat{k} \left(\frac{1}{J n^f} \frac{\partial n^f}{\partial X} \left[1 - \frac{\theta^s}{\theta^f} \right] + \frac{a+g}{\mathfrak{R} \theta^f} \right) \right] (\beta \Delta t^2) \delta \dot{p}_f \\
&\quad \left. + \frac{\hat{k}}{J n^f \theta^f} \frac{\partial p_f}{\partial X} \frac{\partial n^f}{\partial X} (\beta \Delta t^2) \delta \dot{\theta}^s + \frac{\partial p_f}{\partial X} \frac{\hat{k}}{(\theta^f)^2} \left(\frac{a+g}{\mathfrak{R}} - \frac{\theta^s}{J n^f} \frac{\partial n^f}{\partial X} \right) (\beta \Delta t^2) \delta \dot{\theta}^f \right) A dX. \quad (\text{B.67})
\end{aligned}$$

For thermoporoelasticity,

$$\begin{aligned}
\delta\mathcal{H}_2^{\text{INT}} &= \int_0^{X=H} w^{p_f} \left(\frac{1}{p_f} \frac{\partial p_f}{\partial X} \left[\frac{\delta \hat{k}}{\hat{k}} (n^f \tilde{v}_f) + \frac{\hat{k}}{J^2} \left(\frac{\partial p_f}{\partial X} - \frac{n^s p_f}{n^f} \left[1 - \frac{\theta^s}{\theta^f} \right] \left[\frac{1}{n^f} \frac{\partial n^f}{\partial X} + \frac{3}{J} \frac{\partial^2 u}{\partial X^2} \right] \right) \right] \times \right. \\
&\quad (\gamma \Delta t) \frac{\partial(\delta v)}{\partial X} - \frac{\partial p_f}{\partial X} \frac{n^s \hat{k}}{J^2 n^f} \left[1 - \frac{\theta^s}{\theta^f} \right] (\gamma \Delta t) \frac{\partial^2(\delta v)}{\partial X^2} \\
&\quad + \frac{1}{p_f} \left[(n^f \tilde{v}_f) - \frac{\hat{k}}{J} \frac{\partial p_f}{\partial X} \right] (\gamma \Delta t) \frac{\partial(\delta \dot{p}_f)}{\partial X} \\
&\quad - \frac{1}{p_f} \frac{\partial p_f}{\partial X} \left[\frac{(n^f \tilde{v}_f)}{p_f} + \hat{k} \left(\frac{1}{J n^f} \frac{\partial n^f}{\partial X} \left[1 - \frac{\theta^s}{\theta^f} \right] + \frac{g}{\mathfrak{R} \theta^f} \right) \right] (\gamma \Delta t) \delta \dot{p}_f \\
&\quad \left. + \frac{\hat{k}}{J n^f \theta^f} \frac{\partial p_f}{\partial X} \frac{\partial n^f}{\partial X} (\gamma \Delta t) \delta \dot{\theta}^s + \frac{\partial p_f}{\partial X} \frac{\hat{k}}{(\theta^f)^2} \left(\frac{g}{\mathfrak{R}} - \frac{\theta^s}{J n^f} \frac{\partial n^f}{\partial X} \right) (\gamma \Delta t) \delta \dot{\theta}^f \right) A dX. \quad (\text{B.68})
\end{aligned}$$

For the compressible liquid model,

$$\begin{aligned}
\delta\mathcal{H}_2^{\text{INT}} &= \int_0^{X=H} w^{p_f} \delta \left(\frac{1}{K_f^\theta} \frac{\partial p_f}{\partial X} n^f \tilde{v}_f \right) A dX \\
&= \int_0^{X=H} w^{p_f} \frac{1}{K_f^\theta} \left((n^f \tilde{v}_f) \delta \left(\frac{\partial p_f}{\partial X} \right) + \frac{\partial p_f}{\partial X} \delta(n^f \tilde{v}_f) \right) A dX \\
&= \int_0^{X=H} w^{p_f} \frac{1}{K_f^\theta} \left(\frac{\partial p_f}{\partial X} \left[\frac{\delta \hat{k}}{\hat{k}} (n^f \tilde{v}_f) + \frac{\hat{k}}{J^2} \left(\frac{\partial p_f}{\partial X} - \frac{n^s p_f}{n^f} \left[1 - \frac{\theta^s}{\theta^f} \right] \left[\frac{1}{n^f} \frac{\partial n^f}{\partial X} + \frac{3}{J} \frac{\partial^2 u}{\partial X^2} \right] \right) \right] \right) \times \\
&\quad (\beta \Delta t^2) \frac{\partial(\delta a)}{\partial X} - \frac{\partial p_f}{\partial X} \frac{n^s \hat{k}}{J^2 n^f} \left[1 - \frac{\theta^s}{\theta^f} \right] (\beta \Delta t^2) \frac{\partial^2(\delta a)}{\partial X^2} - \frac{\partial p_f}{\partial X} \rho^{\text{fR}} \hat{k} \delta a \\
&\quad + \left[(n^f \tilde{v}_f) - \frac{\hat{k}}{J} \frac{\partial p_f}{\partial X} \right] (\beta \Delta t^2) \frac{\partial(\delta \dot{p}_f)}{\partial X} \\
&\quad - \frac{\partial p_f}{\partial X} \left[(n^f \tilde{v}_f) + \hat{k} \left(\frac{1}{J n^f} \frac{\partial n^f}{\partial X} \left[1 - \frac{\theta^s}{\theta^f} \right] + \frac{\rho^{\text{fR}}}{K_f^\theta} [a + g] \right) \right] (\beta \Delta t^2) \delta \dot{p}_f \\
&\quad + \frac{\hat{k}}{J n^f \theta^f} \frac{\partial p_f}{\partial X} \frac{\partial n^f}{\partial X} (\beta \Delta t^2) \delta \dot{\theta}^s + \frac{\partial p_f}{\partial X} \hat{k} \left(\rho^{\text{fR}} \alpha_V^f [a + g] - \frac{p_f \theta^s}{J n^f (\theta^f)^2} \frac{\partial n^f}{\partial X} \right) \times \\
&\quad (\beta \Delta t^2) \delta \dot{\theta}^f \Big) A dX . \tag{B.69}
\end{aligned}$$

For thermoporoelasticity,

$$\begin{aligned}
\delta\mathcal{H}_2^{\text{INT}} &= \int_0^{X=H} w^{p_f} \frac{1}{K_f^\theta} \left(\frac{\partial p_f}{\partial X} \left[\frac{\delta \hat{k}}{\hat{k}} (n^f \tilde{v}_f) + \frac{\hat{k}}{J^2} \left(\frac{\partial p_f}{\partial X} - \frac{n^s p_f}{n^f} \left[1 - \frac{\theta^s}{\theta^f} \right] \left[\frac{1}{n^f} \frac{\partial n^f}{\partial X} + \frac{3}{J} \frac{\partial^2 u}{\partial X^2} \right] \right) \right] \right) \times \\
&\quad (\gamma \Delta t) \frac{\partial(\delta v)}{\partial X} - \frac{\partial p_f}{\partial X} \frac{n^s \hat{k}}{J^2 n^f} \left[1 - \frac{\theta^s}{\theta^f} \right] (\gamma \Delta t) \frac{\partial^2(\delta v)}{\partial X^2} \\
&\quad + \left[(n^f \tilde{v}_f) - \frac{\hat{k}}{J} \frac{\partial p_f}{\partial X} \right] (\gamma \Delta t) \frac{\partial(\delta \dot{p}_f)}{\partial X} \\
&\quad - \frac{\partial p_f}{\partial X} \left[(n^f \tilde{v}_f) + \hat{k} \left(\frac{1}{J n^f} \frac{\partial n^f}{\partial X} \left[1 - \frac{\theta^s}{\theta^f} \right] + \frac{\rho^{\text{fR}}}{K_f^\theta} [a + g] \right) \right] (\gamma \Delta t) \delta \dot{p}_f \\
&\quad + \frac{\hat{k}}{J n^f \theta^f} \frac{\partial p_f}{\partial X} \frac{\partial n^f}{\partial X} (\gamma \Delta t) \delta \dot{\theta}^s + \frac{\partial p_f}{\partial X} \hat{k} \left(\rho^{\text{fR}} \alpha_V^f g - \frac{p_f \theta^s}{J n^f (\theta^f)^2} \frac{\partial n^f}{\partial X} \right) \times \\
&\quad (\gamma \Delta t) \delta \dot{\theta}^f \Big) A dX . \tag{B.70}
\end{aligned}$$

The linearization of $\mathcal{H}_3^{\text{INT}}, \mathcal{H}_4^{\text{INT}}$ remain unchanged from the $(\mathbf{u}-p_f)$ formulation. The thermal contribution to Darcy's law comprises $\mathcal{H}_6^{\text{INT}}$, whose linearization proceeds as follows:

$$\begin{aligned}
\delta\mathcal{H}_6^{\text{INT}} &= \int_0^{X=H} \frac{\partial w^{p_f}}{\partial X} \delta \left(\hat{k} \frac{p_f}{n_f} \frac{\partial n^f}{\partial X} F_{11}^{-1} \left[1 - \frac{\theta^s}{\theta^f} \right] \right) A dX \\
&= \int_0^{X=H} \frac{\partial w^{p_f}}{\partial X} \left(\frac{p_f}{n_f} \frac{\partial n^f}{\partial X} F_{11}^{-1} \left[1 - \frac{\theta^s}{\theta^f} \right] \delta(\hat{k}) + \hat{k} \delta \left(\frac{p_f}{n_f} \frac{\partial n^f}{\partial X} F_{11}^{-1} \left[1 - \frac{\theta^s}{\theta^f} \right] \right) \right) A dX \\
&= \int_0^{X=H} \frac{\partial w^{p_f}}{\partial X} \left(\frac{p_f}{J n^f} \left[1 - \frac{\theta^s}{\theta^f} \right] \left[\delta_{\hat{k}} \frac{\partial n^f}{\partial X} - \frac{n^s \hat{k}}{J} \left(\frac{1}{n^f} \frac{\partial n^f}{\partial X} + \frac{3}{J} \frac{\partial^2 u}{\partial X^2} \right) \right] (\beta \Delta t^2) \frac{\partial(\delta a)}{\partial X} \right. \\
&\quad \left. + \frac{n^s p_f \hat{k}}{J^2 n^f} \left[1 - \frac{\theta^s}{\theta^f} \right] (\beta \Delta t^2) \frac{\partial^2(\delta a)}{\partial X^2} + \frac{\hat{k}}{J n^f} \frac{\partial n^f}{\partial X} \left[1 - \frac{\theta^s}{\theta^f} \right] (\beta \Delta t^2) \delta \ddot{p}_f \right. \\
&\quad \left. - \frac{\hat{k} p_f}{J n^f} \frac{\partial n^f}{\partial X} \frac{1}{\theta^f} (\beta \Delta t^2) \delta \ddot{\theta}^s + \frac{\hat{k} p_f}{J n^f} \frac{\partial n^f}{\partial X} \frac{\theta^s}{(\theta^f)^2} (\beta \Delta t^2) \delta \ddot{\theta}^f \right) A dX . \tag{B.71}
\end{aligned}$$

For thermoporoelasticity,

$$\begin{aligned}
\delta\mathcal{H}_6^{\text{INT}} &= \int_0^{X=H} \frac{\partial w^{p_f}}{\partial X} \left(\frac{p_f}{J n^f} \left[1 - \frac{\theta^s}{\theta^f} \right] \left[\delta_{\hat{k}} \frac{\partial n^f}{\partial X} - \frac{n^s \hat{k}}{J} \left(\frac{1}{n^f} \frac{\partial n^f}{\partial X} + \frac{3}{J} \frac{\partial^2 u}{\partial X^2} \right) \right] (\gamma \Delta t) \frac{\partial(\delta v)}{\partial X} \right. \\
&\quad \left. + \frac{n^s p_f \hat{k}}{J^2 n^f} \left[1 - \frac{\theta^s}{\theta^f} \right] (\gamma \Delta t) \frac{\partial^2(\delta v)}{\partial X^2} + \frac{\hat{k}}{J n^f} \frac{\partial n^f}{\partial X} \left[1 - \frac{\theta^s}{\theta^f} \right] (\gamma \Delta t) \delta \dot{p}_f \right. \\
&\quad \left. - \frac{\hat{k} p_f}{J n^f} \frac{\partial n^f}{\partial X} \frac{1}{\theta^f} (\gamma \Delta t) \delta \dot{\theta}^s + \frac{\hat{k} p_f}{J n^f} \frac{\partial n^f}{\partial X} \frac{\theta^s}{(\theta^f)^2} (\gamma \Delta t) \delta \dot{\theta}^f \right) A dX . \tag{B.72}
\end{aligned}$$

Linearization of $\mathcal{H}_7^{\text{INT}}$ for the ideal gas pore fluid proceeds as follows:

$$\begin{aligned}
\delta\mathcal{H}_7^{\text{INT}} &= - \int_0^{X=H} w^{p_f} \delta \left(\frac{Jn^f}{\theta^f} \dot{\theta}^f + \frac{\partial\theta^f}{\partial X} \frac{(n^f \tilde{v}_f)}{\theta^f} \right) A dX \\
&= - \int_0^{X=H} w^{p_f} \left(\frac{n^f}{\theta^f} \dot{\theta}^f \delta(J) + \frac{J}{\theta^f} \dot{\theta}^f \delta(n^f) - \frac{Jn^f}{(\theta^f)^2} \dot{\theta}^f \delta(\theta^f) + \frac{Jn^f}{\theta^f} \delta(\dot{\theta}^f) \right. \\
&\quad \left. + \frac{(n^f \tilde{v}_f)}{\theta^f} \frac{\partial(\delta\theta^f)}{\partial X} + \frac{1}{\theta^f} \frac{\partial\theta^f}{\partial X} \delta(n^f \tilde{v}_f) - \frac{(n^f \tilde{v}_f)}{(\theta^f)^2} \frac{\partial\theta^f}{\partial X} \delta(\theta^f) \right) A dX \\
&= - \int_0^{X=H} w^{p_f} \left(\frac{n^f}{\theta^f} \dot{\theta}^f (\beta\Delta t^2) \frac{\partial(\delta a)}{\partial X} + \frac{n^s}{\theta^f} \dot{\theta}^f (\beta\Delta t^2) \frac{\partial(\delta a)}{\partial X} - \frac{Jn^f}{(\theta^f)^2} \dot{\theta}^f (\beta\Delta t^2) \delta\ddot{\theta}^f \right. \\
&\quad \left. + \frac{Jn^f}{\theta^f} (\gamma\Delta t) \delta\ddot{\theta}^f + \frac{(n^f \tilde{v}_f)}{\theta^f} (\beta\Delta t^2) \frac{\partial(\delta\ddot{\theta}^f)}{\partial X} \right. \\
&\quad \left. + \frac{1}{\theta^f} \frac{\partial\theta^f}{\partial X} \left[\frac{\delta_{\hat{k}}}{\hat{k}} (n^f \tilde{v}_f) + \frac{\hat{k}}{J^2} \left(\frac{\partial p_f}{\partial X} - \frac{n^s p_f}{n^f} \left[1 - \frac{\theta^s}{\theta^f} \right] \left[\frac{1}{n^f} \frac{\partial n^f}{\partial X} + \frac{3}{J} \frac{\partial^2 u}{\partial X^2} \right] \right) \right] \times \right. \\
&\quad \left(\beta\Delta t^2 \right) \frac{\partial(\delta a)}{\partial X} - \frac{1}{\theta^f} \frac{\partial\theta^f}{\partial X} \frac{n^s p_f \hat{k}}{J^2 n^f} \left(1 - \frac{\theta^s}{\theta^f} \right) (\beta\Delta t^2) \frac{\partial^2(\delta a)}{\partial X^2} - \frac{\hat{k} \rho^{\text{fR}}}{\theta^f} \frac{\partial\theta^f}{\partial X} \delta a \\
&\quad - \frac{\hat{k}}{J\theta^f} \frac{\partial\theta^f}{\partial X} (\beta\Delta t^2) \frac{\partial(\delta\ddot{p}_f)}{\partial X} - \frac{\hat{k}}{\theta^f} \frac{\partial\theta^f}{\partial X} \left(\frac{1}{Jn^f} \frac{\partial n^f}{\partial X} \left[1 - \frac{\theta^s}{\theta^f} \right] + \frac{a+g}{\mathfrak{R}\theta^f} \right) (\beta\Delta t^2) \delta\ddot{p}_f \\
&\quad \left. + \frac{p_f \hat{k}}{Jn^f (\theta^f)^2} \frac{\partial\theta^f}{\partial X} \frac{\partial n^f}{\partial X} (\beta\Delta t^2) \delta\ddot{\theta}^s \right. \\
&\quad \left. + \hat{k} \frac{\rho^{\text{fR}}}{(\theta^f)^2} \frac{\partial\theta^f}{\partial X} \left([a+g] - \frac{\mathfrak{R}\theta^s}{Jn^f} \frac{\partial n^f}{\partial X} - \frac{(n^f \tilde{v}_f)}{\hat{k} \rho^{\text{fR}}} \right) (\beta\Delta t^2) \delta\ddot{\theta}^f \right) A dX . \tag{B.73}
\end{aligned}$$

Combining like terms,

$$\begin{aligned}
\delta\mathcal{H}_7^{\text{INT}} = & - \int_0^{X=H} w^{p_f} \left(\frac{1}{\theta^f} \left[\dot{\theta}^f + \frac{\partial\theta^f}{\partial X} \left(\frac{\delta\hat{k}}{\hat{k}} (n^f \tilde{v}_f) + \frac{\hat{k}}{J^2} \left[\frac{\partial p_f}{\partial X} - \frac{n^s p_f}{n^f} \left(1 - \frac{\theta^s}{\theta^f} \right) \left(\frac{1}{n^f} \frac{\partial n^f}{\partial X} + \frac{3}{J} \frac{\partial^2 u}{\partial X^2} \right) \right] \right] \right) \times \\
& (\beta\Delta t^2) \frac{\partial(\delta a)}{\partial X} - \frac{1}{\theta^f} \frac{\partial\theta^f}{\partial X} \frac{n^s p_f \hat{k}}{J^2 n^f} \left[1 - \frac{\theta^s}{\theta^f} \right] (\beta\Delta t^2) \frac{\partial^2(\delta a)}{\partial X^2} - \frac{\hat{k} \rho^{\text{fR}}}{\theta^f} \frac{\partial\theta^f}{\partial X} \delta a \\
& - \frac{\hat{k}}{J\theta^f} \frac{\partial\theta^f}{\partial X} (\beta\Delta t^2) \frac{\partial(\delta \dot{p}_f)}{\partial X} - \frac{\hat{k}}{\theta^f} \frac{\partial\theta^f}{\partial X} \left[\frac{1}{J n^f} \frac{\partial n^f}{\partial X} \left(1 - \frac{\theta^s}{\theta^f} \right) + \frac{a+g}{\mathfrak{R}\theta^f} \right] (\beta\Delta t^2) \delta \dot{p}_f \\
& + \frac{p_f \hat{k}}{J n^f (\theta^f)^2} \frac{\partial\theta^f}{\partial X} \frac{\partial n^f}{\partial X} (\beta\Delta t^2) \delta \dot{\theta}^s + \frac{(n^f \tilde{v}_f)}{\theta^f} (\beta\Delta t^2) \frac{\partial(\delta \ddot{\theta}^f)}{\partial X} \\
& + \frac{1}{(\theta^f)^2} \left[J n^f \theta^f (\gamma\Delta t) + \left(\hat{k} \rho^{\text{fR}} \frac{\partial\theta^f}{\partial X} \left[(a+g) - \frac{\mathfrak{R}\theta^s}{J n^f} \frac{\partial n^f}{\partial X} - \frac{(n^f \tilde{v}_f)}{\hat{k} \rho^{\text{fR}}} \right] - J n^f \dot{\theta}^f \right) \times \right. \\
& \left. (\beta\Delta t^2) \right] \delta \ddot{\theta}^f \Big) A dX . \tag{B.74}
\end{aligned}$$

For thermoporoelasticity,

$$\begin{aligned}
\delta\mathcal{H}_7^{\text{INT}} = & - \int_0^{X=H} w^{p_f} \left(\frac{1}{\theta^f} \left[\dot{\theta}^f + \frac{\partial\theta^f}{\partial X} \left(\frac{\delta\hat{k}}{\hat{k}} (n^f \tilde{v}_f) + \frac{\hat{k}}{J^2} \left[\frac{\partial p_f}{\partial X} - \frac{n^s p_f}{n^f} \left(1 - \frac{\theta^s}{\theta^f} \right) \left(\frac{1}{n^f} \frac{\partial n^f}{\partial X} + \frac{3}{J} \frac{\partial^2 u}{\partial X^2} \right) \right] \right) \right) \times \\
& (\gamma\Delta t) \frac{\partial(\delta v)}{\partial X} - \frac{1}{\theta^f} \frac{\partial\theta^f}{\partial X} \frac{n^s p_f \hat{k}}{J^2 n^f} \left[1 - \frac{\theta^s}{\theta^f} \right] (\gamma\Delta t) \frac{\partial^2(\delta v)}{\partial X^2} \\
& - \frac{\hat{k}}{J\theta^f} \frac{\partial\theta^f}{\partial X} (\gamma\Delta t) \frac{\partial(\delta \dot{p}_f)}{\partial X} - \frac{\hat{k}}{\theta^f} \frac{\partial\theta^f}{\partial X} \left[\frac{1}{J n^f} \frac{\partial n^f}{\partial X} \left(1 - \frac{\theta^s}{\theta^f} \right) + \frac{g}{\mathfrak{R}\theta^f} \right] (\gamma\Delta t) \delta \dot{p}_f \\
& + \frac{p_f \hat{k}}{J n^f (\theta^f)^2} \frac{\partial\theta^f}{\partial X} \frac{\partial n^f}{\partial X} (\gamma\Delta t) \delta \dot{\theta}^s + \frac{(n^f \tilde{v}_f)}{\theta^f} (\gamma\Delta t) \frac{\partial(\delta \dot{\theta}^f)}{\partial X} \\
& + \frac{1}{(\theta^f)^2} \left[J n^f \theta^f + \left(\hat{k} \rho^{\text{fR}} \frac{\partial\theta^f}{\partial X} \left[g - \frac{\mathfrak{R}\theta^s}{J n^f} \frac{\partial n^f}{\partial X} - \frac{(n^f \tilde{v}_f)}{\hat{k} \rho^{\text{fR}}} \right] - J n^f \dot{\theta}^f \right) (\gamma\Delta t) \right] \delta \dot{\theta}^f \Big) \times \\
& A dX . \tag{B.75}
\end{aligned}$$

For the compressible liquid model,

$$\begin{aligned}
\delta\mathcal{H}_7^{\text{INT}} &= - \int_0^{X=H} w^{p_f} \alpha_V^f \delta \left(J n^f \dot{\theta}^f + \frac{\partial \theta^f}{\partial X} (n^f \tilde{v}_f) \right) A dX \\
&= - \int_0^{X=H} w^{p_f} \alpha_V^f \left(n^f \dot{\theta}^f \delta(J) + J \dot{\theta}^f \delta(n^f) + J n^f \delta(\dot{\theta}^f) \right. \\
&\quad \left. + (n^f \tilde{v}_f) \frac{\partial(\delta\theta^f)}{\partial X} + \frac{\partial\theta^f}{\partial X} \delta(n^f \tilde{v}_f) \right) A dX \\
&= - \int_0^{X=H} w^{p_f} \alpha_V^f \left(n^f \dot{\theta}^f (\beta\Delta t^2) \frac{\partial(\delta a)}{\partial X} + n^s \dot{\theta}^f (\beta\Delta t^2) \frac{\partial(\delta a)}{\partial X} \right. \\
&\quad \left. + J n^f (\gamma\Delta t) \delta\ddot{\theta}^f + (n^f \tilde{v}_f) (\beta\Delta t^2) \frac{\partial(\delta\ddot{\theta}^f)}{\partial X} \right. \\
&\quad \left. + \frac{\partial\theta^f}{\partial X} \left[\frac{\delta\hat{k}}{\hat{k}} (n^f \tilde{v}_f) + \frac{\hat{k}}{J^2} \left(\frac{\partial p_f}{\partial X} - \frac{n^s p_f}{n^f} \left[1 - \frac{\theta^s}{\theta^f} \right] \left[\frac{1}{n^f} \frac{\partial n^f}{\partial X} + \frac{3}{J} \frac{\partial^2 u}{\partial X^2} \right] \right) \right] \right) \times \\
&\quad (\beta\Delta t^2) \frac{\partial(\delta a)}{\partial X} - \frac{\partial\theta^f}{\partial X} \frac{n^s p_f \hat{k}}{J^2 n^f} \left(1 - \frac{\theta^s}{\theta^f} \right) (\beta\Delta t^2) \frac{\partial^2(\delta a)}{\partial X^2} - \hat{k} \rho^{\text{fR}} \frac{\partial\theta^f}{\partial X} \delta a \\
&\quad - \frac{\hat{k}}{J} \frac{\partial\theta^f}{\partial X} (\beta\Delta t^2) \frac{\partial(\delta\ddot{p}_f)}{\partial X} - \hat{k} \frac{\partial\theta^f}{\partial X} \left(\frac{1}{J n^f} \frac{\partial n^f}{\partial X} \left[1 - \frac{\theta^s}{\theta^f} \right] + \frac{\rho^{\text{fR}}}{K_\theta^{\text{f}}} [a + g] \right) (\beta\Delta t^2) \times \\
&\quad \delta\ddot{p}_f + \frac{p_f \hat{k}}{J n^f \theta^f} \frac{\partial\theta^f}{\partial X} \frac{\partial n^f}{\partial X} (\beta\Delta t^2) \delta\ddot{\theta}^s \\
&\quad \left. + \hat{k} \frac{\partial\theta^f}{\partial X} \left(\rho^{\text{fR}} \alpha_V^f [a + g] - \frac{p_f \theta^s}{J n^f (\theta^f)^2} \frac{\partial n^f}{\partial X} \right) (\beta\Delta t^2) \delta\ddot{\theta}^f \right) A dX . \tag{B.76}
\end{aligned}$$

Combining like terms,

$$\begin{aligned}
\delta\mathcal{H}_7^{\text{INT}} = & - \int_0^{X=H} w^{p_f} \alpha_V^f \left(\left[\dot{\theta}^f + \frac{\partial\theta^f}{\partial X} \left(\frac{\delta\hat{k}}{\hat{k}} (n^f \tilde{v}_f) + \frac{\hat{k}}{J^2} \left[\frac{\partial p_f}{\partial X} - \frac{n^s p_f}{n^f} \left(1 - \frac{\theta^s}{\theta^f} \right) \left(\frac{1}{n^f} \frac{\partial n^f}{\partial X} + \frac{3}{J} \frac{\partial^2 u}{\partial X^2} \right) \right] \right] \right) \times \\
& (\beta\Delta t^2) \frac{\partial(\delta a)}{\partial X} - \frac{\partial\theta^f}{\partial X} \frac{n^s p_f \hat{k}}{J^2 n^f} \left[1 - \frac{\theta^s}{\theta^f} \right] (\beta\Delta t^2) \frac{\partial^2(\delta a)}{\partial X^2} - \hat{k} \rho^{\text{fR}} \frac{\partial\theta^f}{\partial X} \delta a \\
& - \frac{\hat{k}}{J} \frac{\partial\theta^f}{\partial X} (\beta\Delta t^2) \frac{\partial(\delta\dot{p}_f)}{\partial X} - \hat{k} \frac{\partial\theta^f}{\partial X} \left[\frac{1}{J n^f} \frac{\partial n^f}{\partial X} \left(1 - \frac{\theta^s}{\theta^f} \right) + \frac{\rho^{\text{fR}}}{K_f^\theta} (a + g) \right] (\beta\Delta t^2) \times \\
& \delta\dot{p}_f + \frac{p_f \hat{k}}{J n^f \theta^f} \frac{\partial\theta^f}{\partial X} \frac{\partial n^f}{\partial X} (\beta\Delta t^2) \delta\dot{\theta}^s + (n^f \tilde{v}_f) (\beta\Delta t^2) \frac{\partial(\delta\dot{\theta}^f)}{\partial X} \\
& + \left[J n^f (\gamma\Delta t) + \left(\hat{k} \frac{\partial\theta^f}{\partial X} \left[\rho^{\text{fR}} \alpha_V^f (a + g) - \frac{p_f \theta^s}{J n^f (\theta^f)^2} \frac{\partial n^f}{\partial X} \right] \right) (\beta\Delta t^2) \right] \delta\dot{\theta}^f \Big) \times \\
& A dX . \tag{B.77}
\end{aligned}$$

For thermoporoelasticity,

$$\begin{aligned}
\delta\mathcal{H}_7^{\text{INT}} = & - \int_0^{X=H} w^{p_f} \alpha_V^f \left(\left[\dot{\theta}^f + \frac{\partial\theta^f}{\partial X} \left(\frac{\delta\hat{k}}{\hat{k}} (n^f \tilde{v}_f) + \frac{\hat{k}}{J^2} \left[\frac{\partial p_f}{\partial X} - \frac{n^s p_f}{n^f} \left(1 - \frac{\theta^s}{\theta^f} \right) \left(\frac{1}{n^f} \frac{\partial n^f}{\partial X} + \frac{3}{J} \frac{\partial^2 u}{\partial X^2} \right) \right] \right] \right) \times \\
& (\gamma\Delta t) \frac{\partial(\delta v)}{\partial X} - \frac{\partial\theta^f}{\partial X} \frac{n^s p_f \hat{k}}{J^2 n^f} \left[1 - \frac{\theta^s}{\theta^f} \right] (\gamma\Delta t) \frac{\partial^2(\delta v)}{\partial X^2} \\
& - \frac{\hat{k}}{J} \frac{\partial\theta^f}{\partial X} (\gamma\Delta t) \frac{\partial(\delta\dot{p}_f)}{\partial X} - \hat{k} \frac{\partial\theta^f}{\partial X} \left[\frac{1}{J n^f} \frac{\partial n^f}{\partial X} \left(1 - \frac{\theta^s}{\theta^f} \right) + \frac{\rho^{\text{fR}}}{K_f^\theta} g \right] (\gamma\Delta t) \delta\dot{p}_f \\
& + \frac{p_f \hat{k}}{J n^f \theta^f} \frac{\partial\theta^f}{\partial X} \frac{\partial n^f}{\partial X} (\gamma\Delta t) \delta\dot{\theta}^s + (n^f \tilde{v}_f) (\gamma\Delta t) \frac{\partial(\delta\dot{\theta}^f)}{\partial X} \\
& + \left[J n^f + \left(\hat{k} \frac{\partial\theta^f}{\partial X} \left[\rho^{\text{fR}} \alpha_V^f g - \frac{p_f \theta^s}{J n^f (\theta^f)^2} \frac{\partial n^f}{\partial X} \right] \right) (\gamma\Delta t) \right] \delta\dot{\theta}^f \Big) A dX . \tag{B.78}
\end{aligned}$$

$\mathcal{J}_1^{\text{INT}}$ now includes a dependence on porosity, which it did not have in the $(\mathbf{u}-\theta)$ formulation, such that its linearization in the $(\mathbf{u}-p_f-\theta^s-\theta^f)$ formulation is

$$\begin{aligned}
\delta\mathcal{J}_1^{\text{INT}} = & \int_0^{X=H} w^{\theta^s} c_V^s \delta(\rho_0^s \dot{\theta}^s) A dX = \int_0^{X=H} w^{\theta^s} c_V^s (\rho_0^{\text{sR}} \dot{\theta}^s \delta(n^s) + \rho_0^s \delta(\dot{\theta}^s)) A dX \\
= & \int_0^{X=H} w^{\theta^s} c_V^s \left(\rho_0^s (\gamma\Delta t) \delta\dot{\theta}^s - \frac{\rho_0^s}{J} \dot{\theta}^s (\beta\Delta t^2) \frac{\partial(\delta a)}{\partial X} \right) A dX . \tag{B.79}
\end{aligned}$$

For thermoporoelasticity,

$$\delta \mathcal{J}_1^{\text{INT}} = \int_0^{X=H} w^{\theta^s} c_V^s \left(\rho_0^s \delta \dot{\theta}^s - \frac{\rho_0^s}{J} \dot{\theta}^s (\gamma \Delta t) \frac{\partial(\delta v)}{\partial X} \right) A dX . \quad (\text{B.80})$$

$\mathcal{J}_2^{\text{INT}}$ now includes a pore fluid pressure coupling term,

$$\begin{aligned} n^s p_f \frac{\theta^s}{\theta^f} \rightarrow \delta \left(n^s p_f \frac{\theta^s}{\theta^f} \right) &= - \frac{n^s p_f}{J} \frac{\theta^s}{\theta^f} (\beta \Delta t^2) \frac{\partial(\delta a)}{\partial X} + n^s \frac{\theta^s}{\theta^f} (\beta \Delta t^2) \delta \ddot{p}_f \\ &+ \frac{n^s p_f}{\theta^f} (\beta \Delta t^2) \delta \ddot{\theta}^s - n^s p_f \frac{\theta^s}{(\theta^f)^2} (\beta \Delta t^2) \delta \ddot{\theta}^f . \end{aligned} \quad (\text{B.81})$$

Therefore, there are additional components for $\partial(\delta a)/\partial X$ and $\delta \ddot{\theta}^s$, such that the linearization of $\mathcal{J}_2^{\text{INT}}$ is written as

$$\begin{aligned} \delta \mathcal{J}_2^{\text{INT}} &= \int_0^{X=H} w^{\theta^s} \left(\left[\frac{j}{J} \left(- (\beta \Delta t^2) \left[\frac{K^{\text{skel}} \alpha_V^s \theta^s}{J} + n^s p_f \frac{\theta^s}{\theta^s} \right] \right. \right. \right. \\ &\quad \left. \left. \left. + \rho_0^s h_0 \left[\frac{c_0 h_0}{J} \frac{\partial v}{\partial X} \left([1 - 2F_{11}^{-1}] \frac{\partial v}{\partial X} (\beta \Delta t^2) + 2(\gamma \Delta t) \right) \right. \right. \right. \right. \\ &\quad \left. \left. \left. - c_1 c \left(\frac{3}{2J} \frac{\partial v}{\partial X} (\beta \Delta t^2) - (\gamma \Delta t) \right) \right] \right) \right. \\ &\quad \left. + (\gamma \Delta t) \left(\frac{K^{\text{skel}} \alpha_V^s \theta^s}{J} + n^s p_f \frac{\theta^s}{\theta^f} + Q \right) \right] \frac{\partial(\delta a)}{\partial X} \\ &\quad \left. + j \left[\frac{K^{\text{skel}} \alpha_V^s}{J} + \frac{n^s p_f}{\theta^f} \right] (\beta \Delta t^2) \delta \ddot{\theta}^s + n^s j \frac{\theta^s}{\theta^f} (\beta \Delta t^2) \delta \ddot{p}_f - n^s p_f j \frac{\theta^s}{(\theta^f)^2} (\beta \Delta t^2) \delta \ddot{\theta}^f \right) A dX . \end{aligned} \quad (\text{B.82})$$

Without shock viscosity,

$$\begin{aligned} \delta \mathcal{J}_2^{\text{INT}} &= \int_0^{X=H} w^{\theta^s} \left(\left[\frac{j}{J} \left(- (\beta \Delta t^2) \left[\frac{K^{\text{skel}} \alpha_V^s \theta^s}{J} + n^s p_f \frac{\theta^s}{\theta^s} \right] \right) \right. \right. \\ &\quad \left. \left. + (\gamma \Delta t) \left(\frac{K^{\text{skel}} \alpha_V^s \theta^s}{J} + n^s p_f \frac{\theta^s}{\theta^f} \right) \right] \frac{\partial(\delta a)}{\partial X} \right. \\ &\quad \left. + j \left[\frac{K^{\text{skel}} \alpha_V^s}{J} + \frac{n^s p_f}{\theta^f} \right] (\beta \Delta t^2) \delta \ddot{\theta}^s + n^s j \frac{\theta^s}{\theta^f} (\beta \Delta t^2) \delta \ddot{p}_f - n^s p_f j \frac{\theta^s}{(\theta^f)^2} (\beta \Delta t^2) \delta \ddot{\theta}^f \right) \\ &\quad \times A dX . \end{aligned} \quad (\text{B.83})$$

For thermoporoelasticity,

$$\begin{aligned} \delta \mathcal{J}_2^{\text{INT}} = & \int_0^{X=H} w^{\theta^s} \left(\left[\frac{j}{J} \left(-(\gamma \Delta t) \left[\frac{K^{\text{skel}} \alpha_V^s \theta^s}{J} + n^s p_f \frac{\theta^s}{\theta^f} \right] \right) + \left(\frac{K^{\text{skel}} \alpha_V^s \theta^s}{J} + n^s p_f \frac{\theta^s}{\theta^f} \right) \right] \frac{\partial(\delta v)}{\partial X} \right. \\ & \left. + j \left[\frac{K^{\text{skel}} \alpha_V^s}{J} + \frac{n^s p_f}{\theta^f} \right] (\gamma \Delta t) \delta \dot{\theta}^s + n^s j \frac{\theta^s}{\theta^f} (\gamma \Delta t) \delta \dot{p}_f - n^s p_f j \frac{\theta^s}{(\theta^f)^2} (\gamma \Delta t) \delta \dot{\theta}^f \right) A dX . \end{aligned} \quad (\text{B.84})$$

Linearization of $\mathcal{J}_3^{\text{INT}}$ now includes dependence on porosity, such that its derivation proceeds as follows:

$$\begin{aligned} \delta \mathcal{J}_3^{\text{INT}} = & - \int_0^{X=H} \frac{\partial w^{\theta^s}}{\partial X} \delta(q^s) A dX \\ = & \int_0^{X=H} \frac{\partial w^{\theta^s}}{\partial X} k^{\theta^s} \left(\frac{n^s}{J} \delta \left(\frac{\partial \theta^s}{\partial X} \right) + n^s \frac{\partial \theta^s}{\partial X} \delta \left(\frac{1}{J} \right) + \frac{1}{J} \frac{\partial \theta^s}{\partial X} \delta(n^s) \right) A dX \\ = & \int_0^{X=H} \frac{\partial w^{\theta}}{\partial X} \frac{n^s k^{\theta^s}}{J} (\beta \Delta t^2) \left(\frac{\partial(\delta \ddot{\theta})}{\partial X} - \frac{2n^s}{J} \frac{\partial \theta}{\partial X} \frac{\partial(\delta a)}{\partial X} \right) A dX . \end{aligned} \quad (\text{B.85})$$

For thermoelasticity

$$\delta \mathcal{J}_3^{\text{INT}} = \int_0^{X=H} \frac{\partial w^{\theta}}{\partial X} \frac{n^s k^{\theta^s}}{J} (\gamma \Delta t) \left(\frac{\partial(\delta \dot{\theta})}{\partial X} - \frac{2n^s}{J} \frac{\partial \theta}{\partial X} \frac{\partial(\delta v)}{\partial X} \right) A dX . \quad (\text{B.86})$$

Linearization of $\mathcal{J}_4^{\text{INT}}$ proceeds as follows:

$$\begin{aligned} \delta \mathcal{J}_4^{\text{INT}} = & \int_0^{X=H} w^{\theta^s} k_{\theta}^{\varepsilon} \delta(J[\theta^s - \theta^f]) A dX = \int_0^{X=H} w^{\theta^s} k_{\theta}^{\varepsilon} ([\theta^s - \theta^f] \delta(J) + J \delta(\theta^s) - J \delta(\theta^f)) A dX \\ = & \int_0^{X=H} w^{\theta^s} k_{\theta}^{\varepsilon} (\beta \Delta t^2) \left([\theta^s - \theta^f] \frac{\partial(\delta a)}{\partial X} + J \delta \ddot{\theta}^s - J \delta \ddot{\theta}^f \right) A dX . \end{aligned} \quad (\text{B.87})$$

For thermoporoelasticity,

$$\delta \mathcal{J}_4^{\text{INT}} = \int_0^{X=H} w^{\theta^s} k_{\theta}^{\varepsilon} (\gamma \Delta t) \left([\theta^s - \theta^f] \frac{\partial(\delta v)}{\partial X} + J \delta \dot{\theta}^s - J \delta \dot{\theta}^f \right) A dX . \quad (\text{B.88})$$

Linearization of $\mathcal{J}_5^{\text{INT}}$ for the ideal gas pore fluid proceeds as follows:

$$\begin{aligned}
\delta\mathcal{J}_5^{\text{INT}} &= - \int_0^{X=H} w^{\theta^s} \delta\left(\frac{J(n^f \tilde{v}_f)^2}{\hat{k}}\right) A dX \\
&= - \int_0^{X=H} w^{\theta^s} \left(\frac{(n^f \tilde{v}_f)^2}{\hat{k}} \delta(J) + \frac{2J(n^f \tilde{v}_f)}{\hat{k}} \delta(n^f \tilde{v}_f) - \frac{J(n^f \tilde{v}_f)^2}{(\hat{k})^2} \delta(\hat{k}) \right) A dX \\
&= - \int_0^{X=H} w^{\theta^s} \left(\left[\frac{(n^f \tilde{v}_f)^2}{\hat{k}} - \frac{J(n^f \tilde{v}_f)^2}{(\hat{k})^2} \delta_{\hat{k}} \right] (\beta \Delta t^2) \frac{\partial(\delta a)}{\partial X} \right. \\
&\quad + \frac{2J(n^f \tilde{v}_f)}{\hat{k}} \left[\left(\frac{\delta_{\hat{k}}}{\hat{k}} (n^f \tilde{v}_f) + \frac{\hat{k}}{J^2} \left[\frac{\partial p_f}{\partial X} - \frac{n^s p_f}{n^f} \left(1 - \frac{\theta^s}{\theta^f} \right) \left(\frac{1}{n^f} \frac{\partial n^f}{\partial X} + \frac{3}{J} \frac{\partial^2 u}{\partial X^2} \right) \right] \right) (\beta \Delta t^2) \frac{\partial(\delta a)}{\partial X} \right. \\
&\quad - \frac{n^s p_f \hat{k}}{J^2 n^f} \left(1 - \frac{\theta^s}{\theta^f} \right) (\beta \Delta t^2) \frac{\partial^2(\delta a)}{\partial X^2} - \hat{k} \rho^{\text{fR}} \delta a - \frac{\hat{k}}{J} (\beta \Delta t^2) \frac{\partial(\delta \dot{p}_f)}{\partial X} \\
&\quad - \hat{k} \left(\frac{1}{J n^f} \frac{\partial n^f}{\partial X} \left[1 - \frac{\theta^s}{\theta^f} \right] + \frac{a+g}{\mathfrak{R} \theta^f} \right) (\beta \Delta t^2) \delta \dot{p}_f + \frac{p_f \hat{k}}{J n^f \theta^f} \frac{\partial n^f}{\partial X} (\beta \Delta t^2) \delta \ddot{\theta}^s \\
&\quad \left. + \hat{k} \frac{\rho^{\text{fR}}}{\theta^f} \left([a+g] - \frac{\mathfrak{R} \theta^s}{J n^f} \frac{\partial n^f}{\partial X} \right) (\beta \Delta t^2) \delta \dot{\theta}^f \right] A dX \\
&= \int_0^{X=H} w^{\theta^s} \left((n^f \tilde{v}_f) \left[\frac{(n^f \tilde{v}_f)}{\hat{k}} \left(1 + \frac{J}{\hat{k}} \delta_{\hat{k}} \right) + \frac{2}{J} \left(\frac{\partial p_f}{\partial X} - \frac{n^s p_f}{n^f} \left[1 - \frac{\theta^s}{\theta^f} \right] \left[\frac{1}{n^f} \frac{\partial n^f}{\partial X} + \frac{3}{J} \frac{\partial^2 u}{\partial X^2} \right] \right) \right] (\beta \Delta t^2) \frac{\partial(\delta a)}{\partial X} \right. \\
&\quad - \frac{2n^s p_f (n^f \tilde{v}_f)}{J n^f} \left(1 - \frac{\theta^s}{\theta^f} \right) (\beta \Delta t^2) \frac{\partial^2(\delta a)}{\partial X^2} - 2J(n^f \tilde{v}_f) \rho^{\text{fR}} \delta a - 2(n^f \tilde{v}_f) (\beta \Delta t^2) \frac{\partial(\delta \dot{p}_f)}{\partial X} \\
&\quad - 2J(n^f \tilde{v}_f) \left(\frac{1}{J n^f} \frac{\partial n^f}{\partial X} \left[1 - \frac{\theta^s}{\theta^f} \right] + \frac{a+g}{\mathfrak{R} \theta^f} \right) (\beta \Delta t^2) \delta \dot{p}_f + \frac{2p_f (n^f \tilde{v}_f)}{n^f \theta^f} \frac{\partial n^f}{\partial X} (\beta \Delta t^2) \delta \ddot{\theta}^s \\
&\quad \left. + 2J(n^f \tilde{v}_f) \frac{\rho^{\text{fR}}}{\theta^f} \left([a+g] - \frac{\mathfrak{R} \theta^s}{J n^f} \frac{\partial n^f}{\partial X} \right) (\beta \Delta t^2) \delta \dot{\theta}^f \right) A dX . \tag{B.89}
\end{aligned}$$

For thermoporoelasticity,

$$\begin{aligned}
\delta\mathcal{J}_5^{\text{INT}} &= \int_0^{X=H} w^{\theta^s} \left((n^f \tilde{v}_f) \left[\frac{(n^f \tilde{v}_f)}{\hat{k}} \left(1 + \frac{J}{\hat{k}} \delta_{\hat{k}} \right) + \frac{2}{J} \left(\frac{\partial p_f}{\partial X} - \frac{n^s p_f}{n^f} \left[1 - \frac{\theta^s}{\theta^f} \right] \left[\frac{1}{n^f} \frac{\partial n^f}{\partial X} + \frac{3}{J} \frac{\partial^2 u}{\partial X^2} \right] \right) \right] (\gamma \Delta t) \frac{\partial(\delta v)}{\partial X} \right. \\
&\quad - \frac{2n^s p_f (n^f \tilde{v}_f)}{J n^f} \left(1 - \frac{\theta^s}{\theta^f} \right) (\gamma \Delta t) \frac{\partial^2(\delta v)}{\partial X^2} - 2(n^f \tilde{v}_f) (\gamma \Delta t) \frac{\partial(\delta \dot{p}_f)}{\partial X} \\
&\quad - 2J(n^f \tilde{v}_f) \left(\frac{1}{J n^f} \frac{\partial n^f}{\partial X} \left[1 - \frac{\theta^s}{\theta^f} \right] + \frac{g}{\mathfrak{R} \theta^f} \right) (\gamma \Delta t) \delta \dot{p}_f + \frac{2p_f (n^f \tilde{v}_f)}{n^f \theta^f} \frac{\partial n^f}{\partial X} (\gamma \Delta t) \delta \dot{\theta}^s \\
&\quad \left. + 2J(n^f \tilde{v}_f) \frac{\rho^{\text{fR}}}{\theta^f} \left(g - \frac{\mathfrak{R} \theta^s}{J n^f} \frac{\partial n^f}{\partial X} \right) (\gamma \Delta t) \delta \dot{\theta}^f \right) A dX . \tag{B.90}
\end{aligned}$$

For the compressible liquid pore fluid,

$$\begin{aligned}
\delta \mathcal{J}_5^{\text{INT}} = & \int_0^{X=H} w^{\theta^s} \left((n^f \tilde{v}_f) \left[\frac{(n^f \tilde{v}_f)}{\hat{k}} \left(1 + \frac{J}{\hat{k}} \delta_{\hat{k}} \right) + \frac{2}{J} \left(\frac{\partial p_f}{\partial X} - \frac{n^s p_f}{n^f} \left[1 - \frac{\theta^s}{\theta^f} \right] \left[\frac{1}{n^f} \frac{\partial n^f}{\partial X} + \frac{3}{J} \frac{\partial^2 u}{\partial X^2} \right] \right) \right] (\beta \Delta t^2) \frac{\partial(\delta a)}{\partial X} \right. \\
& - \frac{2n^s p_f (n^f \tilde{v}_f)}{J n^f} \left(1 - \frac{\theta^s}{\theta^f} \right) (\beta \Delta t^2) \frac{\partial^2(\delta a)}{\partial X^2} - 2J (n^f \tilde{v}_f) \rho^{\text{fR}} \delta a - 2(n^f \tilde{v}_f) (\beta \Delta t^2) \frac{\partial(\delta \dot{p}_f)}{\partial X} \\
& - 2J (n^f \tilde{v}_f) \left(\frac{1}{J n^f} \frac{\partial n^f}{\partial X} \left[1 - \frac{\theta^s}{\theta^f} \right] + \frac{\rho^{\text{fR}}}{K_f^\theta} [a + g] \right) (\beta \Delta t^2) \delta \dot{p}_f + \frac{2p_f (n^f \tilde{v}_f)}{n^f \theta^f} \frac{\partial n^f}{\partial X} (\beta \Delta t^2) \delta \dot{\theta}^s \\
& \left. + 2J (n^f \tilde{v}_f) \left(\rho^{\text{fR}} \alpha_V^f [a + g] - \frac{p_f \theta^s}{J n^f (\theta^f)^2} \right) (\beta \Delta t^2) \delta \dot{\theta}^f \right) A dX . \tag{B.91}
\end{aligned}$$

For thermoporoelasticity,

$$\begin{aligned}
\delta \mathcal{J}_5^{\text{INT}} = & \int_0^{X=H} w^{\theta^s} \left((n^f \tilde{v}_f) \left[\frac{(n^f \tilde{v}_f)}{\hat{k}} \left(1 + \frac{J}{\hat{k}} \delta_{\hat{k}} \right) + \frac{2}{J} \left(\frac{\partial p_f}{\partial X} - \frac{n^s p_f}{n^f} \left[1 - \frac{\theta^s}{\theta^f} \right] \left[\frac{1}{n^f} \frac{\partial n^f}{\partial X} + \frac{3}{J} \frac{\partial^2 u}{\partial X^2} \right] \right) \right] (\gamma \Delta t) \frac{\partial(\delta v)}{\partial X} \right. \\
& - \frac{2n^s p_f (n^f \tilde{v}_f)}{J n^f} \left(1 - \frac{\theta^s}{\theta^f} \right) (\gamma \Delta t) \frac{\partial^2(\delta v)}{\partial X^2} - 2(n^f \tilde{v}_f) (\gamma \Delta t) \frac{\partial(\delta \dot{p}_f)}{\partial X} \\
& - 2J (n^f \tilde{v}_f) \left(\frac{1}{J n^f} \frac{\partial n^f}{\partial X} \left[1 - \frac{\theta^s}{\theta^f} \right] + \frac{\rho^{\text{fR}} g}{K_f^\theta} \right) (\gamma \Delta t) \delta \dot{p}_f + \frac{2p_f (n^f \tilde{v}_f)}{n^f \theta^f} \frac{\partial n^f}{\partial X} (\gamma \Delta t) \delta \dot{\theta}^s \\
& \left. + 2J (n^f \tilde{v}_f) \left(\rho^{\text{fR}} \alpha_V^f g - \frac{p_f \theta^s}{J n^f (\theta^f)^2} \right) (\gamma \Delta t) \delta \dot{\theta}^f \right) A dX . \tag{B.92}
\end{aligned}$$

Linearization of $\mathcal{J}_6^{\text{INT}}$ for the ideal gas pore fluid proceeds as follows:

$$\begin{aligned}
\delta\mathcal{J}_6^{\text{INT}} &= \int_0^{X=H} w^{\theta^s} \delta\left(\frac{\theta^s p_f}{\theta^f n^f} \frac{\partial n^f}{\partial X}(n^f \tilde{v}_f)\right) A dX \\
&= \int_0^{X=H} w^{\theta^s} \left(\frac{1}{\theta^f} \frac{p_f}{n^f} \frac{\partial n^f}{\partial X}(n^f \tilde{v}_f) \delta(\theta^s) - \frac{\theta^s}{(\theta^f)^2} \frac{p_f}{n^f} \frac{\partial n^f}{\partial X}(n^f \tilde{v}_f) \delta(\theta^f) + \frac{\theta^s}{\theta^f} \frac{1}{n^f} \frac{\partial n^f}{\partial X}(n^f \tilde{v}_f) \delta(p_f) \right. \\
&\quad \left. - \frac{\theta^s}{\theta^f} \frac{p_f}{(n^f)^2} \frac{\partial n^f}{\partial X}(n^f \tilde{v}_f) \delta(n^f) + \frac{\theta^s p_f}{\theta^f n^f} (n^f \tilde{v}_f) \delta\left(\frac{\partial n^f}{\partial X}\right) + \frac{\theta^s p_f}{\theta^f n^f} \frac{\partial n^f}{\partial X} \delta(n^f \tilde{v}_f)\right) A dX \\
&= \int_0^{X=H} w^{\theta^s} \left(\frac{1}{\theta^f} \frac{p_f}{n^f} \frac{\partial n^f}{\partial X}(n^f \tilde{v}_f) (\beta \Delta t^2) \delta\ddot{\theta}^s - \frac{\theta^s}{(\theta^f)^2} \frac{p_f}{n^f} \frac{\partial n^f}{\partial X}(n^f \tilde{v}_f) (\beta \Delta t^2) \delta\ddot{\theta}^f \right. \\
&\quad \left. + \frac{\theta^s}{\theta^f} \frac{1}{n^f} \frac{\partial n^f}{\partial X}(n^f \tilde{v}_f) (\beta \Delta t^2) \delta\ddot{p}_f - \frac{\theta^s}{\theta^f} \frac{p_f}{(n^f)^2} \frac{n^s}{J} \frac{\partial n^f}{\partial X}(n^f \tilde{v}_f) (\beta \Delta t^2) \frac{\partial(\delta a)}{\partial X} \right. \\
&\quad \left. + \frac{\theta^s p_f n^s}{\theta^f n^f J} (n^f \tilde{v}_f) (\beta \Delta t^2) \left[\frac{\partial^2(\delta a)}{\partial X^2} - \frac{2}{J} \frac{\partial^2 u}{\partial X^2} \frac{\partial(\delta a)}{\partial X}\right] \right. \\
&\quad \left. + \frac{\theta^s p_f}{\theta^f n^f} \frac{\partial n^f}{\partial X} \left[\left(\frac{\delta \hat{k}}{\hat{k}} (n^f \tilde{v}_f) + \frac{\hat{k}}{J^2} \left[\frac{\partial p_f}{\partial X} - \frac{n^s p_f}{n^f} \left(1 - \frac{\theta^s}{\theta^f}\right) \left(\frac{1}{n^f} \frac{\partial n^f}{\partial X} + \frac{3}{J} \frac{\partial^2 u}{\partial X^2}\right)\right]\right)\right] \times \right. \\
&\quad \left. (\beta \Delta t^2) \frac{\partial(\delta a)}{\partial X} - \frac{n^s p_f \hat{k}}{J^2 n^f} \left(1 - \frac{\theta^s}{\theta^f}\right) (\beta \Delta t^2) \frac{\partial^2(\delta a)}{\partial X^2} - \hat{k} \rho^{\text{fR}} \delta a \right. \\
&\quad \left. - \frac{\hat{k}}{J} (\beta \Delta t^2) \frac{\partial(\delta \ddot{p}_f)}{\partial X} - \hat{k} \left(\frac{1}{J n^f} \frac{\partial n^f}{\partial X} \left[1 - \frac{\theta^s}{\theta^f}\right] + \frac{a+g}{\mathfrak{R} \theta^f}\right) (\beta \Delta t^2) \delta \ddot{p}_f \right. \\
&\quad \left. + \frac{p_f \hat{k}}{J n^f \theta^f} \frac{\partial n^f}{\partial X} (\beta \Delta t^2) \delta \ddot{\theta}^s + \hat{k} \frac{\rho^{\text{fR}}}{\theta^f} \left([a+g] - \frac{\mathfrak{R} \theta^s}{J n^f} \frac{\partial n^f}{\partial X}\right) (\beta \Delta t^2) \delta \ddot{\theta}^f\right] \times \\
&\quad A dX
\end{aligned} \tag{B.93}$$

Combining like terms,

$$\begin{aligned}
\delta \mathcal{J}_6^{\text{INT}} = & \int_0^{X=H} w^{\theta^s} \left(\left[\frac{\theta^s p_f}{\theta^f n^f} \left(\frac{\partial n^f}{\partial X} \left[\frac{\delta_{\hat{k}}}{\hat{k}} (n^f \tilde{v}_f) + \frac{\hat{k}}{J^2} \left(\frac{\partial p_f}{\partial X} - \frac{n^s p_f}{n^f} \left[1 - \frac{\theta^s}{\theta^f} \right] \left[\frac{1}{n^f} \frac{\partial n^f}{\partial X} + \frac{3}{J} \frac{\partial^2 u}{\partial X^2} \right] \right) \right. \right. \right. \\
& \left. \left. \left. - (n^f \tilde{v}_f) \frac{n^s}{J} \left[\frac{1}{n^f} \frac{\partial n^f}{\partial X} + \frac{2}{J} \frac{\partial^2 u}{\partial X^2} \right] \right] \right) (\beta \Delta t^2) \frac{\partial(\delta a)}{\partial X} \right. \\
& + \frac{\theta^s p_f n^s}{\theta^f n^f J} \left[(n^f \tilde{v}_f) - \frac{p_f \hat{k}}{J n^f} \left(1 - \frac{\theta^s}{\theta^f} \right) \right] (\beta \Delta t^2) \frac{\partial^2(\delta a)}{\partial X^2} - \frac{\theta^s (\rho^{\text{fR}})^2}{n^f \mathfrak{R}} \frac{\partial n^f}{\partial X} \hat{k} \delta a \\
& + \frac{\theta^s}{\theta^f} \frac{1}{n^f} \frac{\partial n^f}{\partial X} \left[(n^f \tilde{v}_f) - \hat{k} p_f \left(\frac{1}{J n^f} \frac{\partial n^f}{\partial X} \left[1 - \frac{\theta^s}{\theta^f} \right] + \frac{a+g}{\mathfrak{R} \theta^f} \right) \right] (\beta \Delta t^2) \delta \dot{p}_f \\
& - \frac{\theta^s p_f}{\theta^f n^f} \frac{\partial n^f}{\partial X} \frac{\hat{k}}{J} (\beta \Delta t^2) \frac{\partial(\delta \dot{p}_f)}{\partial X} + \frac{p_f}{n^f \theta^f} \frac{\partial n^f}{\partial X} \left[(n^f \tilde{v}_f) + \frac{\theta^s p_f}{\theta^f n^f} \frac{\partial n^f}{\partial X} \frac{\hat{k}}{J} \right] (\beta \Delta t^2) \delta \dot{\theta}^s \\
& + \frac{\theta^s}{(\theta^f)^2} \frac{p_f}{n^f} \frac{\partial n^f}{\partial X} \left[\hat{k} \rho^{\text{fR}} \left([a+g] - \frac{\mathfrak{R} \theta^s}{J n^f} \frac{\partial n^f}{\partial X} \right) - (n^f \tilde{v}_f) \right] (\beta \Delta t^2) \delta \dot{\theta}^f \Big] A dX . \tag{B.94}
\end{aligned}$$

For thermoporoelasticity

$$\begin{aligned}
\delta \mathcal{J}_6^{\text{INT}} = & \int_0^{X=H} w^{\theta^s} \left(\left[\frac{\theta^s p_f}{\theta^f n^f} \left(\frac{\partial n^f}{\partial X} \left[\frac{\delta_{\hat{k}}}{\hat{k}} (n^f \tilde{v}_f) + \frac{\hat{k}}{J^2} \left(\frac{\partial p_f}{\partial X} - \frac{n^s p_f}{n^f} \left[1 - \frac{\theta^s}{\theta^f} \right] \left[\frac{1}{n^f} \frac{\partial n^f}{\partial X} + \frac{3}{J} \frac{\partial^2 u}{\partial X^2} \right] \right) \right. \right. \right. \\
& \left. \left. \left. - (n^f \tilde{v}_f) \frac{n^s}{J} \left[\frac{1}{n^f} \frac{\partial n^f}{\partial X} + \frac{2}{J} \frac{\partial^2 u}{\partial X^2} \right] \right] \right) (\gamma \Delta t) \frac{\partial(\delta v)}{\partial X} \right. \\
& + \frac{\theta^s p_f n^s}{\theta^f n^f J} \left[(n^f \tilde{v}_f) - \frac{p_f \hat{k}}{J n^f} \left(1 - \frac{\theta^s}{\theta^f} \right) \right] (\gamma \Delta t) \frac{\partial^2(\delta v)}{\partial X^2} \\
& + \frac{\theta^s}{\theta^f} \frac{1}{n^f} \frac{\partial n^f}{\partial X} \left[(n^f \tilde{v}_f) - \hat{k} p_f \left(\frac{1}{J n^f} \frac{\partial n^f}{\partial X} \left[1 - \frac{\theta^s}{\theta^f} \right] + \frac{g}{\mathfrak{R} \theta^f} \right) \right] (\gamma \Delta t) \delta \dot{p}_f \\
& - \frac{\theta^s p_f}{\theta^f n^f} \frac{\partial n^f}{\partial X} \frac{\hat{k}}{J} (\gamma \Delta t^2) \frac{\partial(\delta \dot{p}_f)}{\partial X} + \frac{p_f}{n^f \theta^f} \frac{\partial n^f}{\partial X} \left[(n^f \tilde{v}_f) + \frac{\theta^s p_f}{\theta^f n^f} \frac{\partial n^f}{\partial X} \frac{\hat{k}}{J} \right] (\gamma \Delta t) \delta \dot{\theta}^s \\
& + \frac{\theta^s}{(\theta^f)^2} \frac{p_f}{n^f} \frac{\partial n^f}{\partial X} \left[\hat{k} \rho^{\text{fR}} \left(g - \frac{\mathfrak{R} \theta^s}{J n^f} \frac{\partial n^f}{\partial X} \right) - 1 \right] (\gamma \Delta t) \delta \dot{\theta}^f \Big] A dX . \tag{B.95}
\end{aligned}$$

For the compressible liquid pore fluid model,

$$\begin{aligned}
\delta \mathcal{J}_6^{\text{INT}} = & \int_0^{X=H} w^{\theta^s} \left(\left[\frac{\theta^s p_f}{\theta^f n^f} \left(\frac{\partial n^f}{\partial X} \left[\frac{\delta \hat{k}}{\hat{k}} (n^f \tilde{v}_f) + \frac{\hat{k}}{J^2} \left(\frac{\partial p_f}{\partial X} - \frac{n^s p_f}{n^f} \left[1 - \frac{\theta^s}{\theta^f} \right] \left[\frac{1}{n^f} \frac{\partial n^f}{\partial X} + \frac{3}{J} \frac{\partial^2 u}{\partial X^2} \right] \right) \right] \right. \right. \\
& \left. \left. - (n^f \tilde{v}_f) \frac{n^s}{J} \left[\frac{1}{n^f} \frac{\partial n^f}{\partial X} + \frac{2}{J} \frac{\partial^2 u}{\partial X^2} \right] \right] \right) (\beta \Delta t^2) \frac{\partial(\delta a)}{\partial X} \\
& + \frac{\theta^s p_f n^s}{\theta^f n^f J} \left[(n^f \tilde{v}_f) - \frac{p_f \hat{k}}{J n^f} \left(1 - \frac{\theta^s}{\theta^f} \right) \right] (\beta \Delta t^2) \frac{\partial^2(\delta a)}{\partial X^2} - \frac{\theta^s p_f}{\theta^f n^f} \frac{\partial n^f}{\partial X} \hat{k} \delta a \\
& + \frac{\theta^s}{\theta^f} \frac{1}{n^f} \frac{\partial n^f}{\partial X} \left[(n^f \tilde{v}_f) - \hat{k} p_f \left(\frac{1}{J n^f} \frac{\partial n^f}{\partial X} \left[1 - \frac{\theta^s}{\theta^f} \right] + \frac{\rho^{\text{fR}}}{K_f^\theta} [a + g] \right) \right] (\beta \Delta t^2) \delta \dot{p}_f \\
& - \frac{\theta^s p_f}{\theta^f n^f} \frac{\partial n^f}{\partial X} \frac{\hat{k}}{J} (\beta \Delta t^2) \frac{\partial(\delta \dot{p}_f)}{\partial X} + \frac{p_f}{n^f \theta^f} \frac{\partial n^f}{\partial X} \left[(n^f \tilde{v}_f) + \frac{\theta^s p_f}{\theta^f n^f} \frac{\partial n^f}{\partial X} \frac{\hat{k}}{J} \right] (\beta \Delta t^2) \delta \dot{\theta}^s \\
& + \frac{\theta^s p_f}{\theta^f n^f} \frac{\partial n^f}{\partial X} \left[\hat{k} \left(\rho^{\text{fR}} \alpha_V^f [a + g] - \frac{p_f \theta^s}{J n^f (\theta^f)^2} \frac{\partial n^f}{\partial X} \right) - (n^f \tilde{v}_f) \right] (\beta \Delta t^2) \delta \dot{\theta}^f \Big] A dX . \quad (\text{B.96})
\end{aligned}$$

For thermoporoelasticity,

$$\begin{aligned}
\delta \mathcal{J}_6^{\text{INT}} = & \int_0^{X=H} w^{\theta^s} \left(\left[\frac{\theta^s p_f}{\theta^f n^f} \left(\frac{\partial n^f}{\partial X} \left[\frac{\delta \hat{k}}{\hat{k}} (n^f \tilde{v}_f) + \frac{\hat{k}}{J^2} \left(\frac{\partial p_f}{\partial X} - \frac{n^s p_f}{n^f} \left[1 - \frac{\theta^s}{\theta^f} \right] \left[\frac{1}{n^f} \frac{\partial n^f}{\partial X} + \frac{3}{J} \frac{\partial^2 u}{\partial X^2} \right] \right) \right] \right. \right. \\
& \left. \left. - (n^f \tilde{v}_f) \frac{n^s}{J} \left[\frac{1}{n^f} \frac{\partial n^f}{\partial X} + \frac{2}{J} \frac{\partial^2 u}{\partial X^2} \right] \right] \right) (\gamma \Delta t) \frac{\partial(\delta v)}{\partial X} \\
& + \frac{\theta^s p_f n^s}{\theta^f n^f J} \left[(n^f \tilde{v}_f) - \frac{p_f \hat{k}}{J n^f} \left(1 - \frac{\theta^s}{\theta^f} \right) \right] (\gamma \Delta t) \frac{\partial^2(\delta v)}{\partial X^2} \\
& + \frac{\theta^s}{\theta^f} \frac{1}{n^f} \frac{\partial n^f}{\partial X} \left[(n^f \tilde{v}_f) - \hat{k} p_f \left(\frac{1}{J n^f} \frac{\partial n^f}{\partial X} \left[1 - \frac{\theta^s}{\theta^f} \right] + \frac{\rho^{\text{fR}}}{K_f^\theta} g \right) \right] (\gamma \Delta t) \delta \dot{p}_f \\
& - \frac{\theta^s p_f}{\theta^f n^f} \frac{\partial n^f}{\partial X} \frac{\hat{k}}{J} (\gamma \Delta t^2) \frac{\partial(\delta \dot{p}_f)}{\partial X} + \frac{p_f}{n^f \theta^f} \frac{\partial n^f}{\partial X} \left[(n^f \tilde{v}_f) + \frac{\theta^s p_f}{\theta^f n^f} \frac{\partial n^f}{\partial X} \frac{\hat{k}}{J} \right] (\gamma \Delta t) \delta \dot{\theta}^s \\
& + \frac{\theta^s p_f}{\theta^f n^f} \frac{\partial n^f}{\partial X} \left[\hat{k} \left(\rho^{\text{fR}} \alpha_V^f g - \frac{p_f \theta^s}{J n^f (\theta^f)^2} \frac{\partial n^f}{\partial X} \right) - 1 \right] (\gamma \Delta t) \delta \dot{\theta}^f \Big] A dX . \quad (\text{B.97})
\end{aligned}$$

Linearization of $\mathcal{K}_1^{\text{INT}}$ for the ideal gas pore fluid proceeds as follows:

$$\begin{aligned}
\delta\mathcal{K}_1^{\text{INT}} &= \int_0^{X=H} w^{\theta^f} (c_V^f + \mathfrak{R}) \delta(\rho_0^f \dot{\theta}^f) A dX = \int_0^{X=H} w^{\theta^f} (c_V^f + \mathfrak{R}) (\dot{\theta}^f \delta(\rho_0^f) + \rho_0^f \delta(\dot{\theta}^f)) A dX \\
&= \int_0^{X=H} w^{\theta^f} (c_V^f + \mathfrak{R}) \left(\rho^{\text{fR}} \dot{\theta}^f (\beta \Delta t^2) \frac{\partial(\delta a)}{\partial X} + \frac{J n^f}{\mathfrak{R} \theta^f} \dot{\theta}^f (\beta \Delta t^2) \delta \ddot{p}_f \right. \\
&\quad \left. + \rho_0^f \left[(\gamma \Delta t) - \frac{(\beta \Delta t^2)}{\theta^f} \dot{\theta}^f \right] \delta \ddot{\theta}^f \right) A dX .
\end{aligned} \tag{B.98}$$

For thermoporoelasticity,

$$\begin{aligned}
\delta\mathcal{K}_1^{\text{INT}} &= \int_0^{X=H} w^{\theta^f} (c_V^f + \mathfrak{R}) \left(\rho^{\text{fR}} \dot{\theta}^f (\gamma \Delta t^t) \frac{\partial(\delta v)}{\partial X} + \frac{J n^f}{\mathfrak{R} \theta^f} \dot{\theta}^f (\gamma \Delta t) \delta \ddot{p}_f \right. \\
&\quad \left. + \rho_0^f \left[1 - \frac{(\gamma \Delta t)}{\theta^f} \dot{\theta}^f \right] \delta \ddot{\theta}^f \right) A dX .
\end{aligned} \tag{B.99}$$

For the compressible liquid pore fluid,

$$\begin{aligned}
\delta\mathcal{K}_1^{\text{INT}} &= \int_0^{X=H} w^{\theta^f} (c_V^f \delta(\rho_0^f \dot{\theta}^f) + K_f^\theta [\alpha_V^f]^2 \delta(J n^f \theta^f \dot{\theta}^f)) A dX \\
&= \int_0^{X=H} w^{\theta^f} (c_V^f [\dot{\theta}^f \delta(\rho_0^f) + \rho_0^f \delta(\dot{\theta}^f)] + K_f^\theta [\alpha_V^f]^2 [n^f \theta^f \dot{\theta}^f \delta(J) + J \theta^f \dot{\theta}^f \delta(n^f) \\
&\quad + J n^f \dot{\theta}^f \delta(\theta^f) + J n^f \theta^f \delta(\dot{\theta}^f)]) A dX \\
&= \int_0^{X=H} w^{\theta^f} \left(c_V^f \dot{\theta}^f (\beta \Delta t^2) \left[\rho^{\text{fR}} \frac{\partial(\delta a)}{\partial X} + \rho_0^f \left(\frac{1}{K_f^\theta} \delta \ddot{p}_f - \alpha_V^f \delta \ddot{\theta}^f \right) \right] + c_V^f \rho_0^f (\gamma \Delta t) \delta \ddot{\theta}^f \right. \\
&\quad \left. + K_f^\theta [\alpha_V^f]^2 \left[n^f \theta^f \dot{\theta}^f (\beta \Delta t^2) \frac{\partial(\delta a)}{\partial X} + n^s \theta^f \dot{\theta}^f (\beta \Delta t^2) \frac{\partial(\delta a)}{\partial X} \right. \right. \\
&\quad \left. \left. + J n^f \dot{\theta}^f (\beta \Delta t^2) \delta \ddot{\theta}^f + J n^f \theta^f (\gamma \Delta t) \delta \ddot{\theta}^f \right] \right) A dX .
\end{aligned} \tag{B.100}$$

Combining like terms,

$$\begin{aligned} \delta\mathcal{K}_1^{\text{INT}} = & \int_0^{X=H} w^{\theta^f} \left(\dot{\theta}^f \left[\rho^{\text{fR}} c_V^f + K_f^\theta [\alpha_V^f]^2 \theta^f \right] (\beta \Delta t^2) \frac{\partial(\delta a)}{\partial X} + \rho_0^f c_V^f \frac{\dot{\theta}^f}{K_f^\theta} (\beta \Delta t^2) \delta \ddot{p}_f \right. \\ & \left. + [(\rho_0^f c_V^f + K_f^\theta [\alpha_V^f]^2 J n^f \theta^f) (\gamma \Delta t) + K_f^\theta [\alpha_V^f]^2 J n^f \dot{\theta}^f (\beta \Delta t^2)] \delta \ddot{\theta}^f \right) A dX . \quad (\text{B.101}) \end{aligned}$$

For thermoporoelasticity,

$$\begin{aligned} \delta\mathcal{K}_1^{\text{INT}} = & \int_0^{X=H} w^{\theta^f} \left(\dot{\theta}^f \left[\rho^{\text{fR}} c_V^f + K_f^\theta [\alpha_V^f]^2 \theta^f \right] (\gamma \Delta t) \frac{\partial(\delta v)}{\partial X} + \rho_0^f c_V^f \frac{\dot{\theta}^f}{K_f^\theta} (\gamma \Delta t) \delta \dot{p}_f \right. \\ & \left. + [(\rho_0^f c_V^f + K_f^\theta [\alpha_V^f]^2 J n^f \theta^f) + K_f^\theta [\alpha_V^f]^2 J n^f \dot{\theta}^f (\gamma \Delta t)] \delta \dot{\theta}^f \right) A dX . \quad (\text{B.102}) \end{aligned}$$

Linearization of $\mathcal{K}_2^{\text{INT}}$ for the ideal gas pore fluid proceeds as follows:

$$\begin{aligned} \delta\mathcal{K}_2^{\text{INT}} = & \int_0^{X=H} w^{\theta^f} (c_V^f + \mathfrak{R}) \delta \left(\rho^{\text{fR}} \frac{\partial \theta^f}{\partial X} (n^f \tilde{v}_f) \right) A dX \\ = & \int_0^{X=H} w^{\theta^f} (c_V^f + \mathfrak{R}) \left(\frac{\partial \theta^f}{\partial X} (n^f \tilde{v}_f) \delta(\rho^{\text{fR}}) + \rho^{\text{fR}} (n^f \tilde{v}_f) \frac{\partial(\delta \theta^f)}{\partial X} + \rho^{\text{fR}} \frac{\partial \theta^f}{\partial X} \delta(n^f \tilde{v}_f) \right) A dX \\ = & \int_0^{X=H} w^{\theta^f} (c_V^f + \mathfrak{R}) \left(\frac{\partial \theta^f}{\partial X} \frac{(n^f \tilde{v}_f)}{\mathfrak{R} \theta^f} (\beta \Delta t^2) \left[\delta \ddot{p}_f - \frac{p_f}{\theta^f} \delta \ddot{\theta}^f \right] + \rho^{\text{fR}} (n^f \tilde{v}_f) (\beta \Delta t^2) \frac{\partial(\delta \ddot{\theta}^f)}{\partial X} \right. \\ & \left. + \rho^{\text{fR}} \frac{\partial \theta^f}{\partial X} \left[\left(\frac{\delta \hat{k}}{\hat{k}} (n^f \tilde{v}_f) + \frac{\hat{k}}{J^2} \left[\frac{\partial p_f}{\partial X} - \frac{n^s p_f}{n^f} \left(1 - \frac{\theta^s}{\theta^f} \right) \left(\frac{1}{n^f} \frac{\partial n^f}{\partial X} + \frac{3}{J} \frac{\partial^2 u}{\partial X^2} \right) \right] \right) \times \right. \\ & \left. (\beta \Delta t^2) \frac{\partial(\delta a)}{\partial X} - \frac{n^s p_f \hat{k}}{J^2 n^f} \left(1 - \frac{\theta^s}{\theta^f} \right) (\beta \Delta t^2) \frac{\partial^2(\delta a)}{\partial X^2} - \hat{k} \rho^{\text{fR}} \delta a \right. \\ & \left. - \frac{\hat{k}}{J} (\beta \Delta t^2) \frac{\partial(\delta \ddot{p}_f)}{\partial X} - \hat{k} \left(\frac{1}{J n^f} \frac{\partial n^f}{\partial X} \left[1 - \frac{\theta^s}{\theta^f} \right] + \frac{a+g}{\mathfrak{R} \theta^f} \right) (\beta \Delta t^2) \delta \ddot{p}_f \right. \\ & \left. + \frac{p_f \hat{k}}{J n^f \theta^f} \frac{\partial n^f}{\partial X} (\beta \Delta t^2) \delta \ddot{\theta}^s + \hat{k} \frac{\rho^{\text{fR}}}{\theta^f} \left([a+g] - \frac{\mathfrak{R} \theta^s}{J n^f} \frac{\partial n^f}{\partial X} \right) (\beta \Delta t^2) \delta \ddot{\theta}^f \right) \end{aligned} \quad (\text{B.103})$$

Combining like terms,

$$\begin{aligned}
\delta\mathcal{K}_2^{\text{INT}} = & \int_0^{X=H} w^{\theta^f} (c_V^f + \mathfrak{R}) \left(\rho^{\text{fR}} \frac{\partial\theta^f}{\partial X} \left(\frac{\delta_{\hat{k}}}{\hat{k}} (n^f \tilde{v}_f) + \frac{\hat{k}}{J^2} \left[\frac{\partial p_f}{\partial X} - \frac{n^s p_f}{n^f} \left(1 - \frac{\theta^s}{\theta^f} \right) \left(\frac{1}{n^f} \frac{\partial n^f}{\partial X} + \frac{3}{J} \frac{\partial^2 u}{\partial X^2} \right) \right] \right) \right) \times \\
& (\beta \Delta t^2) \frac{\partial(\delta a)}{\partial X} - \frac{n^s \rho^{\text{fR}} p_f \hat{k}}{J^2 n^f} \frac{\partial\theta^f}{\partial X} \left(1 - \frac{\theta^s}{\theta^f} \right) (\beta \Delta t^2) \frac{\partial^2(\delta a)}{\partial X^2} - \hat{k} (\rho^{\text{fR}})^2 \frac{\partial\theta^f}{\partial X} \delta a \\
& + \frac{\partial\theta^f}{\partial X} \left[\frac{(n^f \tilde{v}_f)}{\mathfrak{R}\theta^f} - \rho^{\text{fR}} \hat{k} \left(\frac{1}{J n^f} \frac{\partial n^f}{\partial X} \left[1 - \frac{\theta^s}{\theta^f} \right] + \frac{a+g}{\mathfrak{R}\theta^f} \right) \right] (\beta \Delta t^2) \delta \dot{p}_f \\
& - \rho^{\text{fR}} \frac{\hat{k}}{J} \frac{\partial\theta^f}{\partial X} (\beta \Delta t^2) \frac{\partial(\delta \dot{p}_f)}{\partial X} + \frac{\hat{k} (p_f)^2}{J n^f \mathfrak{R} (\theta^f)^2} \frac{\partial\theta^f}{\partial X} \frac{\partial n^f}{\partial X} (\beta \Delta t^2) \delta \dot{\theta}^s \\
& + \rho^{\text{fR}} (n^f \tilde{v}_f) (\beta \Delta t^2) \frac{\partial(\delta \dot{\theta}^f)}{\partial X} \\
& + \frac{1}{\theta^f} \frac{\partial\theta^f}{\partial X} \left[\hat{k} (\rho^{\text{fR}})^2 \left([a+g] - \frac{\mathfrak{R}\theta^s}{J n^f} \frac{\partial n^f}{\partial X} \right) - \frac{(n^f \tilde{v}_f)}{\mathfrak{R}\theta^f} p_f \right] (\beta \Delta t^2) \delta \dot{\theta}^f \Big] A dX . \tag{B.104}
\end{aligned}$$

For thermoporoelasticity,

$$\begin{aligned}
\delta\mathcal{K}_2^{\text{INT}} = & \int_0^{X=H} w^{\theta^f} (c_V^f + \mathfrak{R}) \left(\rho^{\text{fR}} \frac{\partial\theta^f}{\partial X} \left(\frac{\delta_{\hat{k}}}{\hat{k}} (n^f \tilde{v}_f) + \frac{\hat{k}}{J^2} \left[\frac{\partial p_f}{\partial X} - \frac{n^s p_f}{n^f} \left(1 - \frac{\theta^s}{\theta^f} \right) \left(\frac{1}{n^f} \frac{\partial n^f}{\partial X} + \frac{3}{J} \frac{\partial^2 u}{\partial X^2} \right) \right] \right) \right) \times \\
& (\gamma \Delta t) \frac{\partial(\delta v)}{\partial X} - \frac{n^s \rho^{\text{fR}} p_f \hat{k}}{J^2 n^f} \frac{\partial\theta^f}{\partial X} \left(1 - \frac{\theta^s}{\theta^f} \right) (\gamma \Delta t) \frac{\partial^2(\delta v)}{\partial X^2} \\
& + \frac{\partial\theta^f}{\partial X} \left[\frac{(n^f \tilde{v}_f)}{\mathfrak{R}\theta^f} - \rho^{\text{fR}} \hat{k} \left(\frac{1}{J n^f} \frac{\partial n^f}{\partial X} \left[1 - \frac{\theta^s}{\theta^f} \right] + \frac{g}{\mathfrak{R}\theta^f} \right) \right] (\gamma \Delta t) \delta \dot{p}_f \\
& - \rho^{\text{fR}} \frac{\hat{k}}{J} \frac{\partial\theta^f}{\partial X} (\gamma \Delta t) \frac{\partial(\delta \dot{p}_f)}{\partial X} + \frac{\hat{k} (p_f)^2 \mathfrak{R}}{J n^f} \frac{\partial\theta^f}{\partial X} \frac{\partial n^f}{\partial X} (\gamma \Delta t) \delta \dot{\theta}^s \\
& + \rho^{\text{fR}} (n^f \tilde{v}_f) (\gamma \Delta t) \frac{\partial(\delta \dot{\theta}^f)}{\partial X} \\
& + \frac{1}{\theta^f} \frac{\partial\theta^f}{\partial X} \left[\hat{k} (\rho^{\text{fR}})^2 \left(g - \frac{\mathfrak{R}\theta^s}{J n^f} \frac{\partial n^f}{\partial X} \right) - \frac{(n^f \tilde{v}_f)}{\mathfrak{R}\theta^f} p_f \right] (\gamma \Delta t) \delta \dot{\theta}^f \Big] A dX . \tag{B.105}
\end{aligned}$$

For the compressible liquid,

$$\begin{aligned}
\delta\mathcal{K}_2^{\text{INT}} &= \int_0^{X=H} w^{\theta^f} \delta \left([\rho^{\text{fR}} c_V^f + \theta^f K_f^\theta [\alpha_V^f]^2] \right) \frac{\partial \theta^f}{\partial X} (n^f \tilde{v}_f) A dX \\
&= \int_0^{X=H} w^{\theta^f} \left([c_V^f \delta(\rho^{\text{fR}}) + K_f^\theta [\alpha_V^f]^2 \delta(\theta^f)] \frac{\partial \theta^f}{\partial X} (n^f \tilde{v}_f) + [\rho^{\text{fR}} c_V^f + K_f^\theta [\alpha_V^f]^2 \theta^f] \times \right. \\
&\quad \left. \left[(n^f \tilde{v}_f) \frac{\partial(\delta\theta^f)}{\partial X} + \frac{\partial\theta^f}{\partial X} \delta(n^f \tilde{v}_f) \right] \right) A dX \\
&= \int_0^{X=H} w^{\theta^f} \left([\rho^{\text{fR}} c_V^f (\beta\Delta t^2) \left(\frac{1}{K_f^\theta} \delta\ddot{p}_f - \alpha_V^f \delta\ddot{\theta}^f \right) + K_f^\theta [\alpha_V^f]^2 (\beta\Delta t^2) \delta\ddot{\theta}^f] \frac{\partial \theta^f}{\partial X} (n^f \tilde{v}_f) \right. \\
&\quad + [\rho^{\text{fR}} c_V^f + K_f^\theta [\alpha_V^f]^2 \theta^f] \left[(n^f \tilde{v}_f) (\beta\Delta t^2) \frac{\partial(\delta\ddot{\theta}^f)}{\partial X} \right. \\
&\quad \left. \left. + \frac{\partial\theta^f}{\partial X} \left(\frac{\delta\hat{k}}{\hat{k}} (n^f \tilde{v}_f) + \frac{\hat{k}}{J^2} \left[\frac{\partial p_f}{\partial X} - \frac{n^s p_f}{n^f} \left(1 - \frac{\theta^s}{\theta^f} \right) \left(\frac{1}{n^f} \frac{\partial n^f}{\partial X} + \frac{3}{J} \frac{\partial^2 u}{\partial X^2} \right) \right] \right) \right] \times \right. \\
&\quad \left(\beta\Delta t^2 \right) \frac{\partial(\delta a)}{\partial X} - \frac{n^s p_f \hat{k}}{J^2 n^f} \left(1 - \frac{\theta^s}{\theta^f} \right) (\beta\Delta t^2) \frac{\partial^2(\delta a)}{\partial X^2} - \hat{k} \rho^{\text{fR}} \delta a - \frac{\hat{k}}{J} (\beta\Delta t^2) \frac{\partial(\delta\ddot{p}_f)}{\partial X} \\
&\quad - \hat{k} \left(\frac{1}{J n^f} \frac{\partial n^f}{\partial X} \left[1 - \frac{\theta^s}{\theta^f} \right] + \frac{\rho^{\text{fR}}}{K_f^\theta} [a + g] \right) (\beta\Delta t^2) \delta\ddot{p}_f + \frac{p_f \hat{k}}{J n^f \theta^f} \frac{\partial n^f}{\partial X} (\beta\Delta t^2) \delta\ddot{\theta}^s \\
&\quad \left. \left. + \hat{k} \left(\rho^{\text{fR}} \alpha_V^f [a + g] - \frac{p_f \theta^s}{J n^f (\theta^f)^2} \frac{\partial n^f}{\partial X} \right) (\beta\Delta t^2) \delta\ddot{\theta}^f \right] \right) A dX . \tag{B.106}
\end{aligned}$$

Combining like terms,

$$\begin{aligned}
\delta\mathcal{K}_2^{\text{INT}} = & \int_0^{X=H} w^{\theta^f} \left([\rho^{\text{fR}} c_V^f + K_f^\theta (\alpha_V^f)^2 \theta^f] \frac{\partial \theta^f}{\partial X} \left[\left(\frac{\delta \hat{k}}{\hat{k}} (n^f \tilde{v}_f) \right. \right. \right. \\
& + \frac{\hat{k}}{J^2} \left[\frac{\partial p_f}{\partial X} - \frac{n^s p_f}{n^f} \left(1 - \frac{\theta^s}{\theta^f} \right) \left(\frac{1}{n^f} \frac{\partial n^f}{\partial X} + \frac{3}{J} \frac{\partial^2 u}{\partial X^2} \right) \right] \right) (\beta \Delta t^2) \frac{\partial(\delta a)}{\partial X} \\
& - \frac{n^s p_f \hat{k}}{J^2 n^f} \left(1 - \frac{\theta^s}{\theta^f} \right) (\beta \Delta t^2) \frac{\partial^2(\delta a)}{\partial X^2} - \hat{k} \rho^{\text{fR}} \delta a - \frac{\hat{k}}{J} (\beta \Delta t^2) \frac{\partial(\delta \ddot{p}_f)}{\partial X} \\
& + \frac{p_f \hat{k}}{J n^f \theta^f} \frac{\partial n^f}{\partial X} (\beta \Delta t^2) \delta \dot{\theta}^s + [\rho^{\text{fR}} c_V^f + K_f^\theta (\alpha_V^f)^2 \theta^f] (n^f \tilde{v}_f) (\beta \Delta t^2) \frac{\partial(\delta \dot{\theta}^f)}{\partial X} \\
& + \frac{\partial \theta^f}{\partial X} \left[\frac{\rho^{\text{fR}} c_V^f}{K_f^\theta} (n^f \tilde{v}_f) - (\rho^{\text{fR}} c_V^f + K_f^\theta [\alpha_V^f]^2 \theta^f) \left(\frac{1}{J n^f} \frac{\partial n^f}{\partial X} \left[1 - \frac{\theta^s}{\theta^f} \right] + \frac{\rho^{\text{fR}}}{K_f^\theta} [a + g] \right) \right] \times \\
& (\beta \Delta t^2) \delta \ddot{p}_f + \frac{\partial \theta^f}{\partial X} (\beta \Delta t^2) \left[\alpha_V^f (K_f^\theta [\alpha_V^f] - \rho^{\text{fR}} c_V^f) (n^f \tilde{v}_f) \right. \\
& \left. + (\rho^{\text{fR}} c_V^f + K_f^\theta [\alpha_V^f]^2 \theta^f) \hat{k} \left(\rho^{\text{fR}} \alpha_V^f [a + g] - \frac{p_f \theta^s}{J n^f (\theta^f)^2} \frac{\partial n^f}{\partial X} \right) \right] \delta \dot{\theta}^f \Big) A dX .
\end{aligned} \tag{B.107}$$

For thermoporoelasticity,

$$\begin{aligned}
\delta\mathcal{K}_2^{\text{INT}} = & \int_0^{X=H} w^{\theta^f} \left([\rho^{\text{fR}} c_V^f + K_f^\theta (\alpha_V^f)^2 \theta^f] \frac{\partial \theta^f}{\partial X} \left[\left(\frac{\delta \hat{k}}{\hat{k}} (n^f \tilde{v}_f) \right. \right. \right. \\
& + \frac{\hat{k}}{J^2} \left[\frac{\partial p_f}{\partial X} - \frac{n^s p_f}{n^f} \left(1 - \frac{\theta^s}{\theta^f} \right) \left(\frac{1}{n^f} \frac{\partial n^f}{\partial X} + \frac{3}{J} \frac{\partial^2 u}{\partial X^2} \right) \right] \right) (\gamma \Delta t) \frac{\partial(\delta v)}{\partial X} \\
& - \frac{n^s p_f \hat{k}}{J^2 n^f} \left(1 - \frac{\theta^s}{\theta^f} \right) (\gamma \Delta t) \frac{\partial^2(\delta v)}{\partial X^2} - \frac{\hat{k}}{J} (\gamma \Delta t) \frac{\partial(\delta \dot{p}_f)}{\partial X} \\
& + \frac{p_f \hat{k}}{J n^f \theta^f} \frac{\partial n^f}{\partial X} (\gamma \Delta t) \delta \dot{\theta}^s + [\rho^{\text{fR}} c_V^f + K_f^\theta (\alpha_V^f)^2 \theta^f] (n^f \tilde{v}_f) (\gamma \Delta t) \frac{\partial(\delta \dot{\theta}^f)}{\partial X} \\
& + \frac{\partial \theta^f}{\partial X} \left[\frac{\rho^{\text{fR}} c_V^f}{K_f^\theta} (n^f \tilde{v}_f) - (\rho^{\text{fR}} c_V^f + K_f^\theta [\alpha_V^f]^2 \theta^f) \left(\frac{1}{J n^f} \frac{\partial n^f}{\partial X} \left[1 - \frac{\theta^s}{\theta^f} \right] + \frac{\rho^{\text{fR}}}{K_f^\theta} g \right) \right] \times \\
& (\gamma \Delta t) \delta \dot{p}_f + \frac{\partial \theta^f}{\partial X} (\gamma \Delta t) \left[\alpha_V^f (K_f^\theta [\alpha_V^f] - \rho^{\text{fR}} c_V^f) (n^f \tilde{v}_f) \right. \\
& \left. + (\rho^{\text{fR}} c_V^f + K_f^\theta [\alpha_V^f]^2 \theta^f) \hat{k} \left(\rho^{\text{fR}} \alpha_V^f g - \frac{p_f \theta^s}{J n^f (\theta^f)^2} \frac{\partial n^f}{\partial X} \right) \right] \delta \dot{\theta}^f \Big) A dX .
\end{aligned} \tag{B.108}$$

Linearization of $\mathcal{K}_3^{\text{INT}}$ proceeds as follows:

$$\begin{aligned}
\delta\mathcal{K}_3^{\text{INT}} &= - \int_0^{X=H} w^{\theta^f} \delta(n^s p_f \dot{J}) A dX = - \int_0^{X=H} w^{\theta^f} (p_f \dot{J} \delta(n^s) + n^s \dot{J} \delta(p_f) + n^s p_f \delta(\dot{J})) A dX \\
&= - \int_0^{X=H} w^{\theta^f} \left(- \frac{n^s p_f}{J} \dot{J} (\beta \Delta t^2) \frac{\partial(\delta a)}{\partial X} + n^s \dot{J} (\beta \Delta t^2) \delta \ddot{p}_f + n^s p_f (\gamma \Delta t) \frac{\partial(\delta a)}{\partial X} \right) A dX \\
&= \int_0^{X=H} w^{\theta^f} n^s \left(p_f \left[\frac{\dot{J}}{J} (\beta \Delta t^2) - (\gamma \Delta t) \right] \frac{\partial(\delta a)}{\partial X} - \dot{J} (\beta \Delta t^2) \delta \ddot{p}_f \right) A dX .
\end{aligned} \tag{B.109}$$

For thermoporoelasticity,

$$\delta\mathcal{K}_3^{\text{INT}} = \int_0^{X=H} w^{\theta^f} n^s \left(p_f \left[\frac{\dot{J}}{J} (\gamma \Delta t) - 1 \right] \frac{\partial(\delta v)}{\partial X} - \dot{J} (\gamma \Delta t) \delta \dot{p}_f \right) A dX . \tag{B.110}$$

Linearization of $\mathcal{K}_4^{\text{INT}}$ for the ideal gas pore fluid proceeds as follows:

$$\begin{aligned}
\delta\mathcal{K}_4^{\text{INT}} &= - \int_0^{X=H} w^{\theta^f} \delta \left(\frac{p_f}{n^f} \frac{\partial n^f}{\partial X} (n^f \tilde{v}_f) \right) A dX \\
&= - \int_0^{X=H} w^{\theta^f} \left(\frac{1}{n^f} \frac{\partial n^f}{\partial X} (n^f \tilde{v}_f) \delta(p_f) - \frac{p_f}{(n^f)^2} \frac{\partial n^f}{\partial X} (n^f \tilde{v}_f) \delta(n^f) + \frac{p_f}{n^f} (n^f \tilde{v}_f) \delta \left(\frac{\partial n^f}{\partial X} \right) + \frac{p_f}{n^f} \frac{\partial n^f}{\partial X} \delta(n^f \tilde{v}_f) \right) A dX \\
&= - \int_0^{X=H} w^{\theta^f} \left(\frac{1}{n^f} \frac{\partial n^f}{\partial X} (n^f \tilde{v}_f) (\beta \Delta t^2) \delta \ddot{p}_f - \frac{n^s p_f}{J (n^f)^2} \frac{\partial n^f}{\partial X} (n^f \tilde{v}_f) (\beta \Delta t^2) \frac{\partial(\delta a)}{\partial X} \right. \\
&\quad \left. + \frac{n^s p_f}{J n^f} (n^f \tilde{v}_f) (\beta \Delta t^2) \left[\frac{\partial^2(\delta a)}{\partial X} - \frac{2}{J} \frac{\partial^2 u}{\partial X^2} \frac{\partial(\delta a)}{\partial X} \right] \right. \\
&\quad \left. + \frac{p_f}{n^f} \frac{\partial n^f}{\partial X} \left[\left(\frac{\delta \hat{k}}{\hat{k}} (n^f \tilde{v}_f) + \frac{\hat{k}}{J^2} \left[\frac{\partial p_f}{\partial X} - \frac{n^s p_f}{n^f} \left(1 - \frac{\theta^s}{\theta^f} \right) \left(\frac{1}{n^f} \frac{\partial n^f}{\partial X} + \frac{3}{J} \frac{\partial^2 u}{\partial X^2} \right) \right] \right) \times \right. \right. \\
&\quad \left. \left(\beta \Delta t^2 \right) \frac{\partial(\delta a)}{\partial X} - \frac{n^s p_f \hat{k}}{J^2 n^f} \left(1 - \frac{\theta^s}{\theta^f} \right) (\beta \Delta t^2) \frac{\partial^2(\delta a)}{\partial X^2} - \hat{k} \rho^{\text{fR}} \delta a \right. \\
&\quad \left. - \frac{\hat{k}}{J} (\beta \Delta t^2) \frac{\partial(\delta \ddot{p}_f)}{\partial X} - \hat{k} \left(\frac{1}{J n^f} \frac{\partial n^f}{\partial X} \left[1 - \frac{\theta^s}{\theta^f} \right] + \frac{a+g}{\mathfrak{R} \theta^f} \right) (\beta \Delta t^2) \delta \ddot{p}_f \right. \\
&\quad \left. + \frac{p_f \hat{k}}{J n^f \theta^f} \frac{\partial n^f}{\partial X} (\beta \Delta t^2) \delta \ddot{\theta}^s + \hat{k} \frac{\rho^{\text{fR}}}{\theta^f} \left([a+g] - \frac{\mathfrak{R} \theta^s}{J n^f} \frac{\partial n^f}{\partial X} \right) (\beta \Delta t^2) \delta \ddot{\theta}^f \right) A dX
\end{aligned} \tag{B.111}$$

Combining like terms,

$$\begin{aligned}
\delta\mathcal{K}_4^{\text{INT}} = & \int_0^{X=H} w^{\theta^f} \left(\frac{p_f}{n^f} \left[\frac{\partial n^f}{\partial X} \left(\frac{n^s}{J n^f} (n^f \tilde{v}_f) - \frac{\delta_{\hat{k}}}{\hat{k}} (n^f \tilde{v}_f) \right) \right. \right. \\
& - \frac{\hat{k}}{J^2} \left[\frac{\partial p_f}{\partial X} - \frac{n^s p_f}{n^f} \left(1 - \frac{\theta^s}{\theta^f} \right) \left(\frac{1}{n^f} \frac{\partial n^f}{\partial X} + \frac{3}{J} \frac{\partial^2 u}{\partial X^2} \right) \right] \left. \right) + \frac{2n^s}{J^2} \frac{\partial^2 u}{\partial X^2} (n^f \tilde{v}_f) \Big] \times \\
& (\beta \Delta t^2) \frac{\partial(\delta a)}{\partial X} + \frac{n^s p_f}{J n^f} \left[\frac{p_f \hat{k}}{J} \frac{\partial n^f}{\partial X} \left(1 - \frac{\theta^s}{\theta^f} \right) - (n^f \tilde{v}_f) \right] (\beta \Delta t^2) \frac{\partial^2(\delta a)}{\partial X^2} + \frac{p_f}{n^f} \hat{k} \rho^{\text{fR}} \frac{\partial n^f}{\partial X} \delta a \\
& + \frac{1}{n^f} \frac{\partial n^f}{\partial X} \left[p_f \hat{k} \left(\frac{1}{J n^f} \frac{\partial n^f}{\partial X} \left[1 - \frac{\theta^s}{\theta^f} \right] + \frac{a+g}{\mathfrak{R} \theta^f} \right) - (n^f \tilde{v}_f) \right] (\beta \Delta t^2) \delta \dot{p}_f \\
& + \frac{p_f}{n^f} \frac{\hat{k}}{J} \frac{\partial n^f}{\partial X} (\beta \Delta t^2) \frac{\partial(\delta \dot{p}_f)}{\partial X} \\
& - \frac{\hat{k}}{J \theta^f} \left[\frac{p_f}{n^f} \frac{\partial n^f}{\partial X} \right]^2 (\beta \Delta t^2) \delta \dot{\theta}^s - \frac{\hat{k} (\rho^{\text{fR}})^2 \mathfrak{R}}{n^f} \frac{\partial n^f}{\partial X} \left([a+g] - \frac{\mathfrak{R} \theta^s}{J n^f} \frac{\partial n^f}{\partial X} \right) (\beta \Delta t^2) \delta \dot{\theta}^f \Big] A dX . \quad (\text{B.112})
\end{aligned}$$

For thermoporoelasticity,

$$\begin{aligned}
\delta\mathcal{K}_4^{\text{INT}} = & \int_0^{X=H} w^{\theta^f} \left(\frac{p_f}{n^f} \left[\frac{\partial n^f}{\partial X} \left(\frac{n^s}{J n^f} (n^f \tilde{v}_f) - \frac{\delta_{\hat{k}}}{\hat{k}} (n^f \tilde{v}_f) \right) \right. \right. \\
& - \frac{\hat{k}}{J^2} \left[\frac{\partial p_f}{\partial X} - \frac{n^s p_f}{n^f} \left(1 - \frac{\theta^s}{\theta^f} \right) \left(\frac{1}{n^f} \frac{\partial n^f}{\partial X} + \frac{3}{J} \frac{\partial^2 u}{\partial X^2} \right) \right] \left. \right) + \frac{2n^s}{J^2} \frac{\partial^2 u}{\partial X^2} (n^f \tilde{v}_f) \Big] \times \\
& (\gamma \Delta t) \frac{\partial(\delta v)}{\partial X} + \frac{n^s p_f}{J n^f} \left[\frac{p_f \hat{k}}{J} \frac{\partial n^f}{\partial X} \left(1 - \frac{\theta^s}{\theta^f} \right) - (n^f \tilde{v}_f) \right] (\gamma \Delta t) \frac{\partial^2(\delta v)}{\partial X^2} \\
& + \frac{1}{n^f} \frac{\partial n^f}{\partial X} \left[p_f \hat{k} \left(\frac{1}{J n^f} \frac{\partial n^f}{\partial X} \left[1 - \frac{\theta^s}{\theta^f} \right] + \frac{g}{\mathfrak{R} \theta^f} \right) - (n^f \tilde{v}_f) \right] (\gamma \Delta t) \delta \dot{p}_f \\
& + \frac{p_f}{n^f} \frac{\hat{k}}{J} \frac{\partial n^f}{\partial X} (\gamma \Delta t) \frac{\partial(\delta \dot{p}_f)}{\partial X} \\
& - \frac{\hat{k}}{J \theta^f} \left[\frac{p_f}{n^f} \frac{\partial n^f}{\partial X} \right]^2 (\gamma \Delta t) \delta \dot{\theta}^s - \frac{\hat{k} (p_f)^2}{n^f} \frac{\partial n^f}{\partial X} \left(g - \frac{\mathfrak{R} \theta^s}{J n^f} \frac{\partial n^f}{\partial X} \right) (\gamma \Delta t) \delta \dot{\theta}^f \Big] A dX . \quad (\text{B.113})
\end{aligned}$$

For the compressible liquid,

$$\begin{aligned}
\delta\mathcal{K}_4^{\text{INT}} = & \int_0^{X=H} w^{\theta^f} \left(\frac{p_f}{n^f} \left[\frac{\partial n^f}{\partial X} \left(\frac{n^s}{J n^f} (n^f \tilde{v}_f) - \frac{\delta_{\hat{k}}}{\hat{k}} (n^f \tilde{v}_f) \right) \right. \right. \\
& - \frac{\hat{k}}{J^2} \left[\frac{\partial p_f}{\partial X} - \frac{n^s p_f}{n^f} \left(1 - \frac{\theta^s}{\theta^f} \right) \left(\frac{1}{n^f} \frac{\partial n^f}{\partial X} + \frac{3}{J} \frac{\partial^2 u}{\partial X^2} \right) \right] \left. \right) + \frac{2n^s}{J^2} \frac{\partial^2 u}{\partial X^2} (n^f \tilde{v}_f) \Big] \times \\
& (\beta \Delta t^2) \frac{\partial(\delta a)}{\partial X} + \frac{n^s p_f}{J n^f} \left[\frac{p_f \hat{k}}{J} \frac{\partial n^f}{\partial X} \left(1 - \frac{\theta^s}{\theta^f} \right) - (n^f \tilde{v}_f) \right] (\beta \Delta t^2) \frac{\partial^2(\delta a)}{\partial X^2} + \frac{p_f}{n^f} \hat{k} \rho^{\text{fR}} \frac{\partial n^f}{\partial X} \delta a \\
& + \frac{1}{n^f} \frac{\partial n^f}{\partial X} \left[p_f \hat{k} \left(\frac{1}{J n^f} \frac{\partial n^f}{\partial X} \left[1 - \frac{\theta^s}{\theta^f} \right] + \frac{\rho^{\text{fR}}}{K_f^\theta} [a + g] \right) - (n^f \tilde{v}_f) \right] (\beta \Delta t^2) \delta \dot{p}_f \\
& + \frac{p_f}{n^f} \frac{\hat{k}}{J} \frac{\partial n^f}{\partial X} (\beta \Delta t^2) \frac{\partial(\delta \dot{p}_f)}{\partial X} \\
& - \frac{\hat{k}}{J \theta^f} \left[\frac{p_f}{n^f} \frac{\partial n^f}{\partial X} \right]^2 (\beta \Delta t^2) \delta \dot{\theta}^s - \frac{\hat{k}}{n^f} \frac{\partial n^f}{\partial X} \left(\rho^{\text{fR}} \alpha_V [a + g] - \frac{p_f \theta^s}{J n^f (\theta^f)^2} \frac{\partial n^f}{\partial X} \right) (\beta \Delta t^2) \delta \dot{\theta}^f \Big] A dX . \quad (\text{B.114})
\end{aligned}$$

For thermoporoelasticity,

$$\begin{aligned}
\delta\mathcal{K}_4^{\text{INT}} = & \int_0^{X=H} w^{\theta^f} \left(\frac{p_f}{n^f} \left[\frac{\partial n^f}{\partial X} \left(\frac{n^s}{J n^f} (n^f \tilde{v}_f) - \frac{\delta_{\hat{k}}}{\hat{k}} (n^f \tilde{v}_f) \right) \right. \right. \\
& - \frac{\hat{k}}{J^2} \left[\frac{\partial p_f}{\partial X} - \frac{n^s p_f}{n^f} \left(1 - \frac{\theta^s}{\theta^f} \right) \left(\frac{1}{n^f} \frac{\partial n^f}{\partial X} + \frac{3}{J} \frac{\partial^2 u}{\partial X^2} \right) \right] \left. \right) + \frac{2n^s}{J^2} \frac{\partial^2 u}{\partial X^2} (n^f \tilde{v}_f) \Big] \times \\
& (\gamma \Delta t) \frac{\partial(\delta v)}{\partial X} + \frac{n^s p_f}{J n^f} \left[\frac{p_f \hat{k}}{J} \frac{\partial n^f}{\partial X} \left(1 - \frac{\theta^s}{\theta^f} \right) - (n^f \tilde{v}_f) \right] (\gamma \Delta t) \frac{\partial^2(\delta v)}{\partial X^2} \\
& + \frac{1}{n^f} \frac{\partial n^f}{\partial X} \left[p_f \hat{k} \left(\frac{1}{J n^f} \frac{\partial n^f}{\partial X} \left[1 - \frac{\theta^s}{\theta^f} \right] + \frac{\rho^{\text{fR}}}{K_f^\theta} g \right) - (n^f \tilde{v}_f) \right] (\gamma \Delta t) \delta \dot{p}_f \\
& + \frac{p_f}{n^f} \frac{\hat{k}}{J} \frac{\partial n^f}{\partial X} (\gamma \Delta t) \frac{\partial(\delta \dot{p}_f)}{\partial X} \\
& - \frac{\hat{k}}{J \theta^f} \left[\frac{p_f}{n^f} \frac{\partial n^f}{\partial X} \right]^2 (\gamma \Delta t) \delta \dot{\theta}^s - \frac{\hat{k} p_f}{n^f} \frac{\partial n^f}{\partial X} \left(\frac{\rho^{\text{fR}}}{K_f^\theta} g - \frac{p_f \theta^s}{J n^f (\theta^f)^2} \frac{\partial n^f}{\partial X} \right) (\gamma \Delta t) \delta \dot{\theta}^f \Big] A dX . \quad (\text{B.115})
\end{aligned}$$

Linearization of $\mathcal{K}_5^{\text{INT}}$ proceeds as follows:

$$\begin{aligned}
\delta\mathcal{K}_5^{\text{INT}} &= - \int_0^{X=H} w^{\theta^f} \delta(Jn^f \dot{p}_f) A dX = - \int_0^{X=H} w^{\theta^f} (n^f \dot{p}_f \delta(J) + J \dot{p}_f \delta(n^f) + Jn^f \delta(\dot{p}_f)) A dX \\
&= - \int_0^{X=H} w^{\theta^f} \left(n^f \dot{p}_f (\beta \Delta t^2) \frac{\partial(\delta a)}{\partial X} + n^s \dot{p}_f (\beta \Delta t^2) \frac{\partial(\delta a)}{\partial X} + Jn^f (\gamma \Delta t) \delta \dot{p}_f \right) A dX \\
&= - \int_0^{X=H} w^{\theta^f} \left(\dot{p}_f (\beta \Delta t^2) \frac{\partial(\delta a)}{\partial X} + Jn^f (\gamma \Delta t) \delta \dot{p}_f \right) A dX .
\end{aligned} \tag{B.116}$$

For thermoporoelasticity,

$$\delta\mathcal{K}_5^{\text{INT}} = - \int_0^{X=H} w^{\theta^f} \left(\dot{p}_f (\gamma \Delta t) \frac{\partial(\delta v)}{\partial X} + Jn^f \delta \dot{p}_f \right) A dX . \tag{B.117}$$

Linearization of $\mathcal{K}_6^{\text{INT}}$ for the ideal gas pore fluid proceeds as follows:

$$\begin{aligned}
\delta\mathcal{K}_6^{\text{INT}} &= - \int_0^{X=H} w^{\theta^f} \delta \left(\frac{\partial p_f}{\partial X} (n^f \tilde{v}_f) \right) A dX = - \int_0^{X=H} w^{\theta^f} \left((n^f \tilde{v}_f) (\beta \Delta t^2) \frac{\partial(\delta \dot{p}_f)}{\partial X} + \frac{\partial p_f}{\partial X} \delta(n^f \tilde{v}_f) \right) A dX \\
&= \int_0^{X=H} w^{\theta^f} \left(- \frac{\partial p_f}{\partial X} \left[\frac{\delta \hat{k}}{\hat{k}} (n^f \tilde{v}_f) + \frac{\hat{k}}{J^2} \left(\frac{\partial p_f}{\partial X} - \frac{n^s p_f}{n^f} \left[1 - \frac{\theta^s}{\theta^f} \right] \left[\frac{1}{n^f} \frac{\partial n^f}{\partial X} + \frac{3}{J} \frac{\partial^2 u}{\partial X^2} \right] \right) \right] \times \right. \\
&\quad \left. (\beta \Delta t^2) \frac{\partial(\delta a)}{\partial X} + \frac{n^s p_f \hat{k}}{J^2 n^f} \frac{\partial p_f}{\partial X} \left(1 - \frac{\theta^s}{\theta^f} \right) (\beta \Delta t^2) \frac{\partial^2(\delta a)}{\partial X^2} + \hat{k} \rho^{\text{fR}} \frac{\partial p_f}{\partial X} \delta a \right. \\
&\quad \left. + \left[\frac{\hat{k}}{J} \frac{\partial p_f}{\partial X} - (n^f \tilde{v}_f) \right] (\beta \Delta t^2) \frac{\partial(\delta \dot{p}_f)}{\partial X} + \hat{k} \frac{\partial p_f}{\partial X} \left(\frac{1}{Jn^f} \frac{\partial n^f}{\partial X} \left[1 - \frac{\theta^s}{\theta^f} \right] + \frac{a+g}{\mathfrak{R}\theta^f} \right) (\beta \Delta t^2) \delta \dot{p}_f \right. \\
&\quad \left. - \frac{p_f \hat{k}}{Jn^f \theta^f} \frac{\partial p_f}{\partial X} \frac{\partial n^f}{\partial X} (\beta \Delta t^2) \delta \theta^s - \hat{k} \frac{\rho^{\text{fR}}}{\theta^f} \frac{\partial p_f}{\partial X} \left([a+g] - \frac{\mathfrak{R}\theta^s}{Jn^f} \frac{\partial n^f}{\partial X} \right) (\beta \Delta t^2) \delta \theta^f \right) A dX .
\end{aligned} \tag{B.118}$$

For thermoporoelasticity,

$$\begin{aligned}
\delta\mathcal{K}_6^{\text{INT}} &= \int_0^{X=H} w^{\theta^f} \left(- \frac{\partial p_f}{\partial X} \left[\frac{\delta \hat{k}}{\hat{k}} (n^f \tilde{v}_f) + \frac{\hat{k}}{J^2} \left(\frac{\partial p_f}{\partial X} - \frac{n^s p_f}{n^f} \left[1 - \frac{\theta^s}{\theta^f} \right] \left[\frac{1}{n^f} \frac{\partial n^f}{\partial X} + \frac{3}{J} \frac{\partial^2 u}{\partial X^2} \right] \right) \right] \right) \times \\
&\quad \left(\gamma \Delta t \right) \frac{\partial(\delta v)}{\partial X} + \frac{n^s p_f \hat{k}}{J^2 n^f} \frac{\partial p_f}{\partial X} \left(1 - \frac{\theta^s}{\theta^f} \right) (\gamma \Delta t) \frac{\partial^2(\delta v)}{\partial X^2} \\
&\quad + \left[\frac{\hat{k}}{J} \frac{\partial p_f}{\partial X} - (n^f \tilde{v}_f) \right] (\gamma \Delta t) \frac{\partial(\delta \dot{p}_f)}{\partial X} + \hat{k} \frac{\partial p_f}{\partial X} \left(\frac{1}{Jn^f} \frac{\partial n^f}{\partial X} \left[1 - \frac{\theta^s}{\theta^f} \right] + \frac{g}{\mathfrak{R}\theta^f} \right) (\gamma \Delta t) \delta \dot{p}_f \\
&\quad - \frac{p_f \hat{k}}{Jn^f \theta^f} \frac{\partial p_f}{\partial X} \frac{\partial n^f}{\partial X} (\gamma \Delta t) \delta \theta^s - \hat{k} \frac{\rho^{\text{fR}}}{\theta^f} \frac{\partial p_f}{\partial X} \left(g - \frac{\mathfrak{R}\theta^s}{Jn^f} \frac{\partial n^f}{\partial X} \right) (\gamma \Delta t) \delta \theta^f \right) A dX .
\end{aligned} \tag{B.119}$$

For a compressible liquid,

$$\begin{aligned}
\delta\mathcal{K}_6^{\text{INT}} = & \int_0^{X=H} w^{\theta^f} \left(-\frac{\partial p_f}{\partial X} \left[\frac{\delta \hat{k}}{\hat{k}} (n^f \tilde{v}_f) + \frac{\hat{k}}{J^2} \left(\frac{\partial p_f}{\partial X} - \frac{n^s p_f}{n^f} \left[1 - \frac{\theta^s}{\theta^f} \right] \left[\frac{1}{n^f} \frac{\partial n^f}{\partial X} + \frac{3}{J} \frac{\partial^2 u}{\partial X^2} \right] \right) \right] \right) \times \\
& (\beta \Delta t^2) \frac{\partial(\delta a)}{\partial X} + \frac{n^s p_f \hat{k}}{J^2 n^f} \frac{\partial p_f}{\partial X} \left(1 - \frac{\theta^s}{\theta^f} \right) (\beta \Delta t^2) \frac{\partial^2(\delta a)}{\partial X^2} + \hat{k} \rho^{\text{fR}} \frac{\partial p_f}{\partial X} \delta a \\
& + \left[\frac{\hat{k}}{J} \frac{\partial p_f}{\partial X} - (n^f \tilde{v}_f) \right] (\beta \Delta t^2) \frac{\partial(\delta \dot{p}_f)}{\partial X} + \hat{k} \frac{\partial p_f}{\partial X} \left(\frac{1}{J n^f} \frac{\partial n^f}{\partial X} \left[1 - \frac{\theta^s}{\theta^f} \right] + \frac{\rho^{\text{fR}}}{K_f^{\theta}} [a + g] \right) (\beta \Delta t^2) \delta \dot{p}_f \\
& - \frac{p_f \hat{k}}{J n^f \theta^f} \frac{\partial p_f}{\partial X} \frac{\partial n^f}{\partial X} (\beta \Delta t^2) \delta \dot{\theta}^s - \hat{k} \frac{\partial p_f}{\partial X} \left(\rho^{\text{fR}} \alpha_V^f [a + g] - \frac{p_f \theta^s}{J n^f (\theta^f)^2} \frac{\partial n^f}{\partial X} \right) (\beta \Delta t^2) \delta \dot{\theta}^f \Big) A dX . \quad (\text{B.120})
\end{aligned}$$

For thermoporoelasticity,

$$\begin{aligned}
\delta\mathcal{K}_6^{\text{INT}} = & \int_0^{X=H} w^{\theta^f} \left(-\frac{\partial p_f}{\partial X} \left[\frac{\delta \hat{k}}{\hat{k}} (n^f \tilde{v}_f) + \frac{\hat{k}}{J^2} \left(\frac{\partial p_f}{\partial X} - \frac{n^s p_f}{n^f} \left[1 - \frac{\theta^s}{\theta^f} \right] \left[\frac{1}{n^f} \frac{\partial n^f}{\partial X} + \frac{3}{J} \frac{\partial^2 u}{\partial X^2} \right] \right) \right] \right) \times \\
& (\gamma \Delta t) \frac{\partial(\delta v)}{\partial X} + \frac{n^s p_f \hat{k}}{J^2 n^f} \frac{\partial p_f}{\partial X} \left(1 - \frac{\theta^s}{\theta^f} \right) (\gamma \Delta t) \frac{\partial^2(\delta v)}{\partial X^2} \\
& + \left[\frac{\hat{k}}{J} \frac{\partial p_f}{\partial X} - (n^f \tilde{v}_f) \right] (\gamma \Delta t) \frac{\partial(\delta \dot{p}_f)}{\partial X} + \hat{k} \frac{\partial p_f}{\partial X} \left(\frac{1}{J n^f} \frac{\partial n^f}{\partial X} \left[1 - \frac{\theta^s}{\theta^f} \right] + \frac{\rho^{\text{fR}}}{K_f^{\theta}} g \right) (\gamma \Delta t) \delta \dot{p}_f \\
& - \frac{p_f \hat{k}}{J n^f \theta^f} \frac{\partial p_f}{\partial X} \frac{\partial n^f}{\partial X} (\gamma \Delta t) \delta \dot{\theta}^s - \hat{k} \frac{\partial p_f}{\partial X} \left(\rho^{\text{fR}} \alpha_V^f g - \frac{p_f \theta^s}{J n^f (\theta^f)^2} \frac{\partial n^f}{\partial X} \right) (\gamma \Delta t) \delta \dot{\theta}^f \Big) A dX . \quad (\text{B.121})
\end{aligned}$$

Linearization of $\mathcal{K}_7^{\text{INT}}$ proceeds as follows:

$$\begin{aligned}
\delta\mathcal{K}_7^{\text{INT}} = & - \int_0^{X=H} \frac{\partial w^{\theta^f}}{\partial X} \delta(q^f) A dX = \int_0^{X=H} \frac{\partial w^{\theta^f}}{\partial X} k^{\theta^f} \delta \left(\frac{n^f}{J} \frac{\partial \theta^f}{\partial X} \right) A dX \\
= & \int_0^{X=H} \frac{\partial w^{\theta^f}}{\partial X} k^{\theta^f} \left(\frac{n^s}{J^2} \frac{\partial \theta^f}{\partial X} (\beta \Delta t^2) \frac{\partial(\delta a)}{\partial X} - \frac{n^f}{J^2} \frac{\partial \theta^f}{\partial X} (\beta \Delta t^2) \frac{\partial(\delta a)}{\partial X} \right. \\
& \left. + \frac{n^f}{J} (\beta \Delta t^2) \frac{\partial(\delta \dot{\theta}^f)}{\partial X} \right) A dX \\
= & \int_0^{X=H} \frac{\partial w^{\theta^f}}{\partial X} \frac{k^{\theta^f}}{J} (\beta \Delta t^2) \left(\frac{n^s - n^f}{J} \frac{\partial(\delta a)}{\partial X} + n^f \frac{\partial(\delta \dot{\theta}^f)}{\partial X} \right) A dX . \quad (\text{B.122})
\end{aligned}$$

For thermoporoelasticity,

$$\delta\mathcal{K}_7^{\text{INT}} = \int_0^{X=H} \frac{\partial w^{\theta^f}}{\partial X} \frac{k^{\theta^f}}{J} (\gamma \Delta t) \left(\frac{n^s - n^f}{J} \frac{\partial(\delta v)}{\partial X} + n^f \frac{\partial(\delta \dot{\theta}^f)}{\partial X} \right) A dX . \quad (\text{B.123})$$

Linearization of $\mathcal{K}_8^{\text{INT}}$ proceeds as follows:

$$\begin{aligned}
\delta\mathcal{K}_8^{\text{INT}} &= - \int_0^{X=H} w^{\theta^f} k_\theta^\varepsilon \delta(J[\theta^s - \theta^f]) A dX \\
&= - \int_0^{X=H} w^{\theta^f} k_\theta^\varepsilon ([\theta^s - \theta^f] \delta(J) + J \delta(\theta^s) - J \delta(\theta^f)) A dX \\
&= \int_0^{X=H} w^{\theta^f} k_\theta^\varepsilon (\beta \Delta t^2) \left(J \delta \ddot{\theta}^f - J \delta \ddot{\theta}^s - [\theta^s - \theta^f] \frac{\partial(\delta a)}{\partial X} \right) A dX . \tag{B.124}
\end{aligned}$$

For thermoporoelasticity,

$$\delta\mathcal{K}_8^{\text{INT}} = \int_0^{X=H} w^{\theta^f} k_\theta^\varepsilon (\gamma \Delta t) \left(J \delta \dot{\theta}^f - J \delta \dot{\theta}^s - [\theta^s - \theta^f] \frac{\partial(\delta v)}{\partial X} \right) A dX . \tag{B.125}$$

Appendix C

Derivation of the FE equations

Numerical ingredients such as consistent tangents for the implicit and explicit central-difference FE formulations Chapter 4 are derived in this Appendix.

C.1 Implicit integration

C.1.1 (\mathbf{u}) formulation

For elastodynamics ((\mathbf{u}) formulation), we first apply the FE discretization as follows:

$$\delta \mathcal{G}_1^{\text{INT}} = \underbrace{\mathbf{A}_e}_{1 \times n_{\text{dof}}^{s,e}} \underbrace{\left\{ \mathbf{c}^{u,e} \right\}^T}_{1 \times n_{\text{dof}}^{s,e}} \cdot \left(\int_{-1}^1 \underbrace{\left\{ \mathbf{N}^{e,u} \right\}^T}_{n_{\text{dof}}^{s,e} \times 1} \rho_0^{h^e} \underbrace{\left\{ \mathbf{N}^{e,u} \right\}}_{1 \times n_{\text{dof}}^{s,e}} \underbrace{\left\{ \delta \ddot{\mathbf{d}}^e \right\}}_{n_{\text{dof}}^{s,e} \times 1} A_j^e d\xi \right). \quad (\text{C.1})$$

Then, pulling out the variation $\delta \ddot{\mathbf{d}}^e$ leaves us with

$$\delta \mathcal{G}_1^{\text{INT}} = \underbrace{\mathbf{A}_e}_{1 \times n_{\text{dof}}^{s,e}} \underbrace{\left\{ \mathbf{c}^{u,e} \right\}^T}_{1 \times n_{\text{dof}}^{s,e}} \cdot \underbrace{\left[\mathbf{k}_{u,u}^{\mathcal{G}_1^{\text{INT}},e} \right]}_{n_{\text{dof}}^{s,e} \times n_{\text{dof}}^{s,e}} \cdot \underbrace{\left\{ \delta \ddot{\mathbf{d}}^e \right\}}_{n_{\text{dof}}^{s,e} \times 1}, \quad (\text{C.2})$$

where we recover

$$\underbrace{\left[\mathbf{k}_{u,u}^{\mathcal{G}_1^{\text{INT}},e} \right]}_{n_{\text{dof}}^{s,e} \times n_{\text{dof}}^{s,e}} = \int_{-1}^1 \rho_0^{h^e} \underbrace{\left\{ \mathbf{N}^{e,u} \right\}^T}_{n_{\text{dof}}^{s,e} \times 1} \underbrace{\left\{ \mathbf{N}^{e,u} \right\}}_{1 \times n_{\text{dof}}^{s,e}} A_j^e d\xi. \quad (\text{C.3})$$

Next we apply the FE discretization as

$$\delta\mathcal{G}_2^{\text{INT}} = \mathbf{A}_e^{n_e} \underbrace{\left\{ \mathbf{c}^{u,e} \right\}^T}_{1 \times n_{\text{dof}}^{s,e}} \cdot \left(\int_{-1}^1 \underbrace{\left\{ \mathbf{B}^{e,u} \right\}^T}_{n_{\text{dof}}^{s,e} \times 1} \left[\mu + (\lambda - \lambda \ln [J^{h^e}] + \mu) (F_{11}^{h^e})^{-2} \right] \times \right. \\ \left. [\beta \Delta t^2] \underbrace{\left\{ \mathbf{B}^{e,u} \right\}}_{1 \times n_{\text{dof}}^{s,e}} \underbrace{\left\{ \delta \ddot{\mathbf{d}}^e \right\}}_{n_{\text{dof}}^{s,e} \times 1} A_j^e d\xi \right). \quad (\text{C.4})$$

Then, pulling out the variation $\delta \ddot{\mathbf{d}}^e$ leaves us with

$$\delta\mathcal{G}_1^{\text{INT}} = \mathbf{A}_e^{n_e} \underbrace{\left\{ \mathbf{c}^{u,e} \right\}^T}_{1 \times n_{\text{dof}}^{s,e}} \cdot \underbrace{\left[\mathbf{k}_{u,u}^{\mathcal{G}_2^{\text{INT}},e} \right]}_{n_{\text{dof}}^{s,e} \times n_{\text{dof}}^{s,e}} \cdot \underbrace{\left\{ \delta \ddot{\mathbf{d}}^e \right\}}_{n_{\text{dof}}^{s,e} \times 1}, \quad (\text{C.5})$$

where we recover

$$\underbrace{\left[\mathbf{k}_{u,u}^{\mathcal{G}_2^{\text{INT}},e} \right]}_{n_{\text{dof}}^{s,e} \times n_{\text{dof}}^{s,e}} = \int_{-1}^1 (\mu + [\lambda - \lambda \ln (J^{h^e}) + \mu] (F_{11}^{h^e})^{-2} (\beta \Delta t^2)) \underbrace{\left\{ \mathbf{B}^{e,u} \right\}^T}_{n_{\text{dof}}^{s,e} \times 1} \underbrace{\left\{ \mathbf{B}^{e,u} \right\}}_{1 \times n_{\text{dof}}^{s,e}} A_j^e d\xi. \quad (\text{C.6})$$

Now, to derive the tangent for $\delta\mathcal{G}_2^{\text{INT}}$ for elasticity, apply the FE discretization as follows:

$$\delta\mathcal{G}_2^{\text{INT}} = \mathbf{A}_e^{n_e} \underbrace{\left\{ \mathbf{c}^{u,e} \right\}^T}_{1 \times n_{\text{dof}}^{s,e}} \cdot \left(\int_{-1}^1 \underbrace{\left\{ \mathbf{B}^{e,u} \right\}^T}_{n_{\text{dof}}^{s,e} \times 1} \left[\mu + (\lambda - \lambda \ln [J^{h^e}] + \mu) (F_{11}^{h^e})^{-2} \right] \times \right. \\ \left. [\gamma \Delta t] \underbrace{\left\{ \mathbf{B}^{e,u} \right\}}_{1 \times n_{\text{dof}}^{s,e}} \underbrace{\left\{ \delta \dot{\mathbf{d}}^e \right\}}_{n_{\text{dof}}^{s,e} \times 1} A_j^e d\xi \right). \quad (\text{C.7})$$

Then, pulling out the variation $\delta \dot{\mathbf{d}}^e$ leaves us with

$$\delta\mathcal{G}_2^{\text{INT}} = \mathbf{A}_e^{n_e} \underbrace{\left\{ \mathbf{c}^{u,e} \right\}^T}_{1 \times n_{\text{dof}}^{s,e}} \cdot \underbrace{\left[\mathbf{k}_{u,u}^{\mathcal{G}_2^{\text{INT}},e} \right]}_{n_{\text{dof}}^{s,e} \times n_{\text{dof}}^{s,e}} \cdot \underbrace{\left\{ \delta \dot{\mathbf{d}}^e \right\}}_{n_{\text{dof}}^{s,e} \times 1}, \quad (\text{C.8})$$

where

$$\underbrace{\left[\mathbf{k}_{u,u}^{\mathcal{G}_2^{\text{INT}},e} \right]}_{n_{\text{dof}}^{s,e} \times n_{\text{dof}}^{s,e}} = \int_{-1}^1 (\mu + [\lambda - \lambda \ln (J^{h^e}) + \mu] (F_{11}^{h^e})^{-2} (\gamma \Delta t)) \underbrace{\left\{ \mathbf{B}^{e,u} \right\}^T}_{n_{\text{dof}}^{s,e} \times 1} \underbrace{\left\{ \mathbf{B}^{e,u} \right\}}_{1 \times n_{\text{dof}}^{s,e}} A_j^e d\xi. \quad (\text{C.9})$$

To derive the tangent for $\delta\mathcal{G}_2^{\text{INT}}$ when viscous damping is considered, we start from (B.3), and we then apply the FE discretization as follows.

$$\begin{aligned}
\delta\mathcal{G}_2^{\text{INT}} = & \underbrace{\mathbf{A}_e}_{1 \times n_{\text{dof}}^{s,e}} \underbrace{\left\{ \mathbf{c}^{u,e} \right\}^T}_{1 \times n_{\text{dof}}^{s,e}} \cdot \left(\int_{-1}^1 [F_{11}^{h^e}]^{-2} \left[(\lambda + 2\mu) \left(\nu_0 [\gamma \Delta t] - 2\nu_0 [F_{11}^{h^e}]^{-1} \frac{\partial v^{h^e}}{\partial X} [\beta \Delta t^2] \right) \right. \right. \\
& - \ln(F_{11}^{h^e}) \left(2\nu_0 [\gamma \Delta t] - \left[4\nu_0 (F_{11}^{h^e})^{-1} \frac{\partial v^{h^e}}{\partial X} - \lambda \right] [\beta \Delta t^2] \right) \\
& \left. \left. + \left([\lambda + \mu + \mu (F_{11}^{h^e})^2] - 2\nu_0 (F_{11}^{h^e})^{-1} \frac{\partial v^{h^e}}{\partial X} \right) (\beta \Delta t^2) \right] \right. \\
& \left. \underbrace{\left\{ \mathbf{B}^{e,u} \right\}^T}_{n_{\text{dof}}^{s,e} \times 1} \underbrace{\left\{ \mathbf{B}^{e,u} \right\}}_{1 \times n_{\text{dof}}^{s,e}} \cdot \underbrace{\left\{ \delta \ddot{\mathbf{d}}^e \right\}}_{n_{\text{dof}}^{s,e} \times 1} A_j^e d\xi \right)
\end{aligned} \tag{C.10}$$

Then, pulling out the variation $\delta \ddot{\mathbf{d}}^e$ leaves us with

$$\delta\mathcal{G}_2^{\text{INT}} = \underbrace{\mathbf{A}_e}_{1 \times n_{\text{dof}}^{s,e}} \underbrace{\left\{ \mathbf{c}^{u,e} \right\}^T}_{1 \times n_{\text{dof}}^{s,e}} \cdot \underbrace{\left[\mathbf{k}_{u,u}^{\mathcal{G}_2^{\text{INT}},e} \right]}_{n_{\text{dof}}^{s,e} \times n_{\text{dof}}^{s,e}} \cdot \underbrace{\left\{ \delta \ddot{\mathbf{d}}^e \right\}}_{n_{\text{dof}}^{s,e} \times 1}, \tag{C.11}$$

where

$$\begin{aligned}
\underbrace{\left[\mathbf{k}_{u,u}^{\mathcal{G}_2^{\text{INT}},e} \right]}_{n_{\text{dof}}^{s,e} \times n_{\text{dof}}^{s,e}} = & \int_{-1}^1 (F_{11}^{h^e})^{-2} \left([\lambda + 2\mu] \left[\nu_0 (\gamma \Delta t) - 2\nu_0 (F_{11}^{h^e})^{-1} \frac{\partial v^{h^e}}{\partial X} (\beta \Delta t^2) \right] \right. \\
& - \ln(F_{11}^{h^e}) \left[2\nu_0 (\gamma \Delta t) - \left(4\nu_0 (F_{11}^{h^e})^{-1} \frac{\partial v^{h^e}}{\partial X} - \lambda \right) (\beta \Delta t^2) \right] \\
& \left. + \left[(\lambda + \mu + \mu (F_{11}^{h^e})^2) - 2\nu_0 (F_{11}^{h^e})^{-1} \frac{\partial v^{h^e}}{\partial X} \right] (\beta \Delta t^2) \right) \times \\
& \underbrace{\left\{ \mathbf{B}^{e,u} \right\}^T}_{n_{\text{dof}}^{s,e} \times 1} \underbrace{\left\{ \mathbf{B}^{e,u} \right\}}_{1 \times n_{\text{dof}}^{s,e}} A_j^e d\xi.
\end{aligned} \tag{C.12}$$

To derive the tangent for $\delta\mathcal{G}_2^{\text{INT}}$ when viscous damping and elasticity are considered, start

from (B.5) and apply the FE discretization as follows:

$$\begin{aligned}
\delta \mathcal{G}_2^{\text{INT}} = & \underbrace{\mathbf{A}_e}_{1 \times n_{\text{dof}}^{s,e}} \underbrace{\left\{ \mathbf{c}^{u,e} \right\}^T}_{1 \times n_{\text{dof}}^{s,e}} \cdot \left(\int_{-1}^1 [F_{11}^{h^e}]^{-2} \left[(\lambda + 2\mu) \left(\nu_0 - 2\nu_0 [F_{11}^{h^e}]^{-1} \frac{\partial v^{h^e}}{\partial X} [\gamma \Delta t] \right) \right. \right. \\
& - \ln(F_{11}^{h^e}) \left(2\nu_0 - \left[4\nu_0 (F_{11}^{h^e})^{-1} \frac{\partial v^{h^e}}{\partial X} - \lambda \right] [\gamma \Delta t] \right) \\
& \left. \left. + \left([\lambda + \mu + \mu (F_{11}^{h^e})^2] - 2\nu_0 (F_{11}^{h^e})^{-1} \frac{\partial v^{h^e}}{\partial X} \right) (\gamma \Delta t) \right] \right. \\
& \left. \underbrace{\left\{ \mathbf{B}^{e,u} \right\}^T}_{n_{\text{dof}}^{s,e} \times 1} \underbrace{\left\{ \mathbf{B}^{e,u} \right\}}_{1 \times n_{\text{dof}}^{s,e}} \cdot \underbrace{\left\{ \delta \dot{\mathbf{d}}^e \right\}}_{n_{\text{dof}}^{s,e} \times 1} A j^e d\xi \right). \tag{C.13}
\end{aligned}$$

Then, pulling out the variation $\delta \dot{\mathbf{d}}^e$ leaves us with

$$\delta \mathcal{G}_2^{\text{INT}} = \underbrace{\mathbf{A}_e}_{1 \times n_{\text{dof}}^{s,e}} \underbrace{\left\{ \mathbf{c}^{u,e} \right\}^T}_{1 \times n_{\text{dof}}^{s,e}} \cdot \underbrace{\left[\mathbf{k}_{u,u}^{s,e} \right]}_{n_{\text{dof}}^{s,e} \times n_{\text{dof}}^{s,e}} \cdot \underbrace{\left\{ \delta \dot{\mathbf{d}}^e \right\}}_{n_{\text{dof}}^{s,e} \times 1}, \tag{C.14}$$

where

$$\begin{aligned}
\underbrace{\left[\mathbf{k}_{u,u}^{s,e} \right]}_{n_{\text{dof}}^{s,e} \times n_{\text{dof}}^{s,e}} = & \int_{-1}^1 (F_{11}^{h^e})^{-2} \left([\lambda + 2\mu] \left[\nu_0 - 2\nu_0 (F_{11}^{h^e})^{-1} \frac{\partial v^{h^e}}{\partial X} (\gamma \Delta t) \right] \right. \\
& - \ln(F_{11}^{h^e}) \left[2\nu_0 - \left(4\nu_0 (F_{11}^{h^e})^{-1} \frac{\partial v^{h^e}}{\partial X} - \lambda \right) (\gamma \Delta t) \right] \\
& \left. + \left[(\lambda + \mu + \mu (F_{11}^{h^e})^2) - 2\nu_0 (F_{11}^{h^e})^{-1} \frac{\partial v^{h^e}}{\partial X} \right] (\gamma \Delta t) \right) \times \\
& \underbrace{\left\{ \mathbf{B}^{e,u} \right\}^T}_{n_{\text{dof}}^{s,e} \times 1} \underbrace{\left\{ \mathbf{B}^{e,u} \right\}}_{1 \times n_{\text{dof}}^{s,e}} A j^e d\xi. \tag{C.15}
\end{aligned}$$

To derive the tangent for $\delta \mathcal{G}_2^{\text{INT}}$ when shock viscosity is considered, start from (B.10), and

apply the FE discretization as follows:

$$\begin{aligned}
\delta\mathcal{G}_2^{\text{INT}} = & \mathbf{A}_e^{n_e} \underbrace{\left\{ \mathbf{c}^{u,e} \right\}^T}_{1 \times n_{\text{dof}}^{s,e}} \cdot \left(\int_{-1}^1 \left[(\mu + [\lambda - \lambda \ln(J^{h^e}) + \mu] (F_{11}^{h^e})^{-2}) (\beta \Delta t^2) \right. \right. \\
& - \rho_0^{h^e} h_0 \left(C_0 h_0 (F_{11}^{h^e})^{-2} \frac{\partial v^{h^e}}{\partial X} \left[(1 - 2(F_{11}^{h^e})^{-1}) \frac{\partial v^{h^e}}{\partial X} (\beta \Delta t^2) + 2(\gamma \Delta t) \right] \right. \\
& \left. \left. - C_1 (F_{11}^{h^e})^{-1} c^{h^e} \left[\frac{3}{2} (F_{11}^{h^e})^{-1} \frac{\partial v^{h^e}}{\partial X} (\beta \Delta t^2) - (\gamma \Delta t) \right] \right] \right) \\
& \underbrace{\left\{ \mathbf{B}^{e,u} \right\}^T}_{n_{\text{dof}}^{s,e} \times 1} \underbrace{\left\{ \mathbf{B}^{e,u} \right\}}_{1 \times n_{\text{dof}}^{s,e}} \cdot \underbrace{\left\{ \delta \ddot{\mathbf{d}}^e \right\}}_{n_{\text{dof}}^{s,e} \times 1} A_j^e d\xi \Bigg). \tag{C.16}
\end{aligned}$$

Then, pulling out the variation $\delta \ddot{\mathbf{d}}^e$ leaves us with

$$\delta\mathcal{G}_2^{\text{INT}} = \mathbf{A}_e^{n_e} \underbrace{\left\{ \mathbf{c}^{u,e} \right\}^T}_{1 \times n_{\text{dof}}^{s,e}} \cdot \underbrace{\left[\mathbf{k}_{u,u}^{\mathcal{G}_2^{\text{INT}},e} \right]}_{n_{\text{dof}}^{s,e} \times n_{\text{dof}}^{s,e}} \cdot \underbrace{\left\{ \delta \ddot{\mathbf{d}}^e \right\}}_{n_{\text{dof}}^{s,e} \times 1}, \tag{C.17}$$

where

$$\begin{aligned}
\underbrace{\left[\mathbf{k}_{u,u}^{\mathcal{G}_2^{\text{INT}},e} \right]}_{n_{\text{dof}}^{s,e} \times n_{\text{dof}}^{s,e}} = & \int_{-1}^1 \left([\mu + (\lambda - \lambda \ln(J^{h^e}) + \mu) (F_{11}^{h^e})^{-2}] (\beta \Delta t^2) \right. \\
& - \rho_0^{h^e} h_0 \left[C_0 h_0 (F_{11}^{h^e})^{-2} \frac{\partial v^{h^e}}{\partial X} \left[(1 - 2(F_{11}^{h^e})^{-1}) \frac{\partial v^{h^e}}{\partial X} (\beta \Delta t^2) + 2(\gamma \Delta t) \right] \right. \\
& \left. \left. - C_1 (F_{11}^{h^e})^{-1} c^{h^e} \left(\frac{3}{2} (F_{11}^{h^e})^{-1} \frac{\partial v^{h^e}}{\partial X} (\beta \Delta t^2) - (\gamma \Delta t) \right) \right] \right) \underbrace{\left\{ \mathbf{B}^{e,u} \right\}^T}_{n_{\text{dof}}^{s,e} \times 1} \underbrace{\left\{ \mathbf{B}^{e,u} \right\}}_{1 \times n_{\text{dof}}^{s,e}} A_j^e d\xi. \tag{C.18}
\end{aligned}$$

C.1.2 (\mathbf{u} - p_f) formulation

The FE formulations for the tangents relating to the linearized terms $\delta\mathcal{G}_1^{\text{INT}}$ and $\delta\mathcal{G}_2^{\text{INT}}$ remain unchanged from the (\mathbf{u}) formulation; refer to the equations in the preceding section. To derive the tangent for $\delta\mathcal{G}_3^{\text{INT}}$, we start by applying the FE discretization as follows:

$$\delta\mathcal{G}_3^{\text{INT}} = \mathbf{A}_e^{n_e} \underbrace{\left\{ \mathbf{c}^{u,e} \right\}^T}_{1 \times n_{\text{dof}}^{s,e}} \cdot \left(- \int_{-1}^1 \underbrace{\left\{ \mathbf{B}^{e,u} \right\}^T}_{n_{\text{dof}}^{s,e} \times 1} [\beta \Delta t^2] \underbrace{\left\{ \mathbf{N}^{e,p_f} \right\}}_{1 \times n_{\text{dof}}^{p_f,e}} \underbrace{\left\{ \delta \ddot{\boldsymbol{\pi}}^e \right\}}_{n_{\text{dof}}^{p_f,e} \times 1} A_j^e d\xi \right). \tag{C.19}$$

Then, pulling out the variation $\delta\dot{\boldsymbol{\pi}}^e$ leaves us with

$$\delta\mathcal{G}_3^{\text{INT}} = \mathbf{A}_e^{n_e} \underbrace{\left\{ \mathbf{c}^{u,e} \right\}^T}_{1 \times n_{\text{dof}}^{s,e}} \cdot \underbrace{\left[\mathbf{k}_{u,p_f}^{\mathcal{G}_3^{\text{INT}},e} \right]}_{n_{\text{dof}}^{s,e} \times n_{\text{dof}}^{p_f,e}} \cdot \underbrace{\left\{ \delta\dot{\boldsymbol{\pi}}^e \right\}}_{n_{\text{dof}}^{p_f,e} \times 1}, \quad (\text{C.20})$$

where we recover

$$\underbrace{\left[\mathbf{k}_{u,p_f}^{\mathcal{G}_3^{\text{INT}},e} \right]}_{n_{\text{dof}}^{s,e} \times n_{\text{dof}}^{p_f,e}} = - \int_{-1}^1 (\beta \Delta t^2) \underbrace{\left\{ \mathbf{B}^{e,u} \right\}^T}_{n_{\text{dof}}^{s,e} \times 1} \underbrace{\left\{ \mathbf{N}^{e,p_f} \right\}}_{1 \times n_{\text{dof}}^{p_f,e}} A_j^e d\xi. \quad (\text{C.21})$$

To derive the tangent for $\delta\mathcal{G}_3^{\text{INT}}$ when poroelasticity is considered, we start from (B.24) and apply the FE discretization as follows:

$$\delta\mathcal{G}_3^{\text{INT}} = \mathbf{A}_e^{n_e} \underbrace{\left\{ \mathbf{c}^{u,e} \right\}^T}_{1 \times n_{\text{dof}}^{s,e}} \cdot \left(- \int_{-1}^1 \underbrace{\left\{ \mathbf{B}^{e,u} \right\}^T}_{n_{\text{dof}}^{s,e} \times 1} [\gamma \Delta t] \underbrace{\left\{ \mathbf{N}^{e,p_f} \right\}}_{1 \times n_{\text{dof}}^{p_f,e}} \underbrace{\left\{ \delta\dot{\boldsymbol{\pi}}^e \right\}}_{n_{\text{dof}}^{p_f,e} \times 1} A_j^e d\xi \right). \quad (\text{C.22})$$

Then, pulling out the variation $\delta\dot{\boldsymbol{\pi}}^e$ leaves us with

$$\delta\mathcal{G}_3^{\text{INT}} = \mathbf{A}_e^{n_e} \underbrace{\left\{ \mathbf{c}^{u,e} \right\}^T}_{1 \times n_{\text{dof}}^{s,e}} \cdot \underbrace{\left[\mathbf{k}_{u,p_f}^{\mathcal{G}_3^{\text{INT}},e} \right]}_{n_{\text{dof}}^{s,e} \times n_{\text{dof}}^{p_f,e}} \cdot \underbrace{\left\{ \delta\dot{\boldsymbol{\pi}}^e \right\}}_{n_{\text{dof}}^{p_f,e} \times 1}, \quad (\text{C.23})$$

where

$$\underbrace{\left[\mathbf{k}_{u,p_f}^{\mathcal{G}_3^{\text{INT}},e} \right]}_{n_{\text{dof}}^{s,e} \times n_{\text{dof}}^{p_f,e}} = - \int_{-1}^1 (\gamma \Delta t) \underbrace{\left\{ \mathbf{B}^{e,u} \right\}^T}_{n_{\text{dof}}^{s,e} \times 1} \underbrace{\left\{ \mathbf{N}^{e,p_f} \right\}}_{1 \times n_{\text{dof}}^{p_f,e}} A_j^e d\xi. \quad (\text{C.24})$$

To derive the tangents for $\delta\mathcal{H}_1^{\text{INT}}$, apply the FE discretization as follows:

$$\begin{aligned} \delta\mathcal{H}_1^{\text{INT}} &= \mathbf{A}_e^{n_e} \underbrace{\left\{ \mathbf{c}^{p_f,e} \right\}^T}_{1 \times n_{\text{dof}}^{p_f,e}} \cdot \left(\int_{-1}^1 \underbrace{\left\{ \mathbf{N}^{e,p_f} \right\}^T}_{n_{\text{dof}}^{p_f,e} \times 1} \left[\left(\frac{\dot{p}_f^h}{K_f^\eta} [\beta \Delta t^2] + [\gamma \Delta t] \right) \times \right. \right. \\ &\quad \left. \left. \underbrace{\left\{ \mathbf{B}^{e,u} \right\}}_{1 \times n_{\text{dof}}^{s,e}} \underbrace{\left\{ \delta\ddot{\mathbf{d}}^e \right\}}_{n_{\text{dof}}^{s,e} \times 1} + \frac{J^{h,e} n^{f,h,e}}{K_f^\eta} [\gamma \Delta t] \underbrace{\left\{ \mathbf{N}^{e,p_f} \right\}}_{1 \times n_{\text{dof}}^{p_f,e}} \underbrace{\left\{ \delta\dot{\boldsymbol{\pi}}^e \right\}}_{n_{\text{dof}}^{p_f,e} \times 1} \right] A_j^e d\xi \right). \end{aligned} \quad (\text{C.25})$$

Then, pulling out the variations $\delta\ddot{\mathbf{d}}^e$ and $\delta\dot{\boldsymbol{\pi}}^e$ leaves us with

$$\delta\mathcal{H}_1^{\text{INT}} = \mathbf{A}_e^{n_e} \underbrace{\left\{ \mathbf{c}^{p_f,e} \right\}^T}_{1 \times n_{\text{dof}}^{p_f,e}} \cdot \left(\underbrace{\left[\mathbf{k}_{p_f,u}^{\mathcal{H}_1^{\text{INT}},e} \right]}_{n_{\text{dof}}^{p_f,e} \times n_{\text{dof}}^{s,e}} \cdot \underbrace{\left\{ \delta\ddot{\mathbf{d}}^e \right\}}_{n_{\text{dof}}^{s,e} \times 1} + \underbrace{\left[\mathbf{k}_{p_f,p_f}^{\mathcal{H}_1^{\text{INT}},e} \right]}_{n_{\text{dof}}^{p_f,e} \times n_{\text{dof}}^{p_f,e}} \cdot \underbrace{\left\{ \delta\dot{\boldsymbol{\pi}}^e \right\}}_{n_{\text{dof}}^{p_f,e} \times 1} \right), \quad (\text{C.26})$$

where we recover

$$\underbrace{\left[\mathbf{k}_{p_f, u}^{\mathcal{H}_1^{\text{INT}}, e} \right]}_{n_{\text{dof}}^{p_f, e} \times n_{\text{dof}}^{s, e}} = \int_{-1}^1 \left(\frac{\dot{p}_f^{h^e}}{K_f^\eta} (\beta \Delta t^2) + (\gamma \Delta t) \right) \underbrace{\left\{ \mathbf{N}^{e, p_f} \right\}^T}_{n_{\text{dof}}^{p_f, e} \times 1} \underbrace{\left\{ \mathbf{B}^{e, u} \right\}}_{1 \times n_{\text{dof}}^{s, e}} A_j^e d\xi, \quad (\text{C.27})$$

$$\underbrace{\left[\mathbf{k}_{p_f, p_f}^{\mathcal{H}_1^{\text{INT}}, e} \right]}_{n_{\text{dof}}^{p_f, e} \times n_{\text{dof}}^{p_f, e}} = \int_{-1}^1 \frac{J^{h^e} n^{f, h^e}}{K_f^\eta} (\gamma \Delta t) \underbrace{\left\{ \mathbf{N}^{e, p_f} \right\}^T}_{n_{\text{dof}}^{p_f, e} \times 1} \underbrace{\left\{ \mathbf{N}^{e, p_f} \right\}}_{1 \times n_{\text{dof}}^{p_f, e}} A_j^e d\xi. \quad (\text{C.28})$$

To derive the tangents for $\delta \mathcal{H}_1^{\text{INT}}$ when poroelasticity is considered, start from (B.26) and apply the FE discretization as follows:

$$\delta \mathcal{H}_1^{\text{INT}} = \underbrace{\mathbf{A}_e}_{n_e} \underbrace{\left\{ \mathbf{c}^{p_f, e} \right\}^T}_{1 \times n_{\text{dof}}^{p_f, e}} \cdot \left(\int_{-1}^1 \underbrace{\left\{ \mathbf{N}^{e, p_f} \right\}^T}_{n_{\text{dof}}^{p_f, e} \times 1} \left[\left(\frac{\dot{p}_f^{h^e}}{K_f^\eta} [\gamma \Delta t] + 1 \right) \underbrace{\left\{ \mathbf{B}^{e, u} \right\}}_{1 \times n_{\text{dof}}^{s, e}} \underbrace{\left\{ \delta \dot{\mathbf{d}}^e \right\}}_{n_{\text{dof}}^{s, e} \times 1} \right. \right. \\ \left. \left. + \frac{J^{h^e} n^{f, h^e}}{K_f^\eta} \underbrace{\left\{ \mathbf{N}^{e, p_f} \right\}}_{1 \times n_{\text{dof}}^{p_f, e}} \underbrace{\left\{ \delta \dot{\boldsymbol{\pi}}^e \right\}}_{n_{\text{dof}}^{p_f, e} \times 1} \right] A_j^e d\xi \right). \quad (\text{C.29})$$

Then, pulling out the variations $\delta \dot{\mathbf{d}}^e$ & $\delta \dot{\boldsymbol{\pi}}^e$ leaves us with

$$\delta \mathcal{H}_1^{\text{INT}} = \underbrace{\mathbf{A}_e}_{n_e} \underbrace{\left\{ \mathbf{c}^{p_f, e} \right\}^T}_{1 \times n_{\text{dof}}^{p_f, e}} \cdot \left(\underbrace{\left[\mathbf{k}_{p_f, u}^{\mathcal{H}_1^{\text{INT}}, e} \right]}_{n_{\text{dof}}^{p_f, e} \times n_{\text{dof}}^{s, e}} \cdot \underbrace{\left\{ \delta \dot{\mathbf{d}}^e \right\}}_{n_{\text{dof}}^{s, e} \times 1} + \underbrace{\left[\mathbf{k}_{p_f, p_f}^{\mathcal{H}_1^{\text{INT}}, e} \right]}_{n_{\text{dof}}^{p_f, e} \times n_{\text{dof}}^{p_f, e}} \cdot \underbrace{\left\{ \delta \dot{\boldsymbol{\pi}}^e \right\}}_{n_{\text{dof}}^{p_f, e} \times 1} \right), \quad (\text{C.30})$$

where

$$\underbrace{\left[\mathbf{k}_{p_f, u}^{\mathcal{H}_1^{\text{INT}}, e} \right]}_{n_{\text{dof}}^{p_f, e} \times n_{\text{dof}}^{s, e}} = \int_{-1}^1 \left(\frac{\dot{p}_f^{h^e}}{K_f^\eta} (\gamma \Delta t) + 1 \right) \underbrace{\left\{ \mathbf{N}^{e, p_f} \right\}^T}_{n_{\text{dof}}^{p_f, e} \times 1} \underbrace{\left\{ \mathbf{B}^{e, u} \right\}}_{1 \times n_{\text{dof}}^{s, e}} A_j^e d\xi, \quad (\text{C.31})$$

$$\underbrace{\left[\mathbf{k}_{p_f, p_f}^{\mathcal{H}_1^{\text{INT}}, e} \right]}_{n_{\text{dof}}^{p_f, e} \times n_{\text{dof}}^{p_f, e}} = \int_{-1}^1 \frac{J^{h^e} n^{f, h^e}}{K_f^\eta} \underbrace{\left\{ \mathbf{N}^{e, p_f} \right\}^T}_{n_{\text{dof}}^{p_f, e} \times 1} \underbrace{\left\{ \mathbf{N}^{e, p_f} \right\}}_{1 \times n_{\text{dof}}^{p_f, e}} A_j^e d\xi. \quad (\text{C.32})$$

To derive the tangents for $\delta\mathcal{H}_2^{\text{INT}}$, we apply the FE discretization as follows:

$$\begin{aligned}
\delta\mathcal{H}_2^{\text{INT}} = & \mathbf{A}_e^{n_e} \underbrace{\left\{ \mathbf{c}^{p_f, e} \right\}^T}_{1 \times n_{\text{dof}}^{p_f, e}} \cdot \left(\int_{-1}^1 \underbrace{\left\{ \mathbf{N}^{e, p_f} \right\}^T}_{n_{\text{dof}}^{p_f, e} \times 1} \left[\left([n^f \tilde{v}_f]^{h^e} - \hat{k}^{h^e} \frac{\partial p_f^{h^e}}{\partial X} (F_{11}^{h^e})^{-1} \right) \right. \right. \\
& \times (\beta \Delta t^2) \underbrace{\left\{ \mathbf{B}^{e, p_f} \right\}}_{1 \times n_{\text{dof}}^{p_f, e}} \underbrace{\left\{ \delta \ddot{\boldsymbol{\pi}}^e \right\}}_{1 \times n_{\text{dof}}^{p_f, e}} - \hat{k}^{h^e} \frac{\partial p_f^{h^e}}{\partial X} (a^{h^e} + g) \frac{\rho^{\text{fR}, h^e}}{K_f^\eta} (\beta \Delta t^2) \underbrace{\left\{ \mathbf{N}^{e, p_f} \right\}}_{1 \times n_{\text{dof}}^{p_f, e}} \underbrace{\left\{ \delta \ddot{\boldsymbol{\pi}}^e \right\}}_{n_{\text{dof}}^{p_f, e} \times 1} \\
& + \frac{\partial p_f^{h^e}}{\partial X} \left(\frac{\delta \hat{k}^{h^e}}{\hat{k}^{h^e}} (n^f \tilde{v}_f)^{h^e} + \hat{k}^{h^e} \frac{\partial p_f^{h^e}}{\partial X} (F_{11}^{h^e})^{-2} \right) (\beta \Delta t^2) \underbrace{\left\{ \mathbf{B}^{e, u} \right\}}_{1 \times n_{\text{dof}}^{s, e}} \underbrace{\left\{ \dot{\mathbf{d}}^e \right\}}_{n_{\text{dof}}^{s, e} \times 1} \\
& \left. - \frac{\partial p_f^{h^e}}{\partial X} \hat{k}^{h^e} \rho^{\text{fR}, h^e} \underbrace{\left\{ \mathbf{N}^{e, u} \right\}}_{1 \times n_{\text{dof}}^{s, e}} \underbrace{\left\{ \delta \ddot{\mathbf{d}}^e \right\}}_{n_{\text{dof}}^{s, e} \times 1} \right] \frac{A}{K_f^\eta} j^e d\xi \Bigg). \tag{C.33}
\end{aligned}$$

Then, pulling out the variations $\delta \ddot{\mathbf{d}}^e$ and $\delta \ddot{\boldsymbol{\pi}}^e$ leaves us with

$$\delta\mathcal{H}_2^{\text{INT}} = \mathbf{A}_e^{n_e} \underbrace{\left\{ \mathbf{c}^{p_f, e} \right\}^T}_{1 \times n_{\text{dof}}^{p_f, e}} \cdot \left(\underbrace{\left[\mathbf{k}_{p_f, u}^{\mathcal{H}_2^{\text{INT}, e}} \right]}_{n_{\text{dof}}^{p_f, e} \times n_{\text{dof}}^{s, e}} \cdot \underbrace{\left\{ \delta \ddot{\mathbf{d}}^e \right\}}_{n_{\text{dof}}^{s, e} \times 1} + \underbrace{\left[\mathbf{k}_{p_f, p_f}^{\mathcal{H}_2^{\text{INT}, e}} \right]}_{n_{\text{dof}}^{p_f, e} \times n_{\text{dof}}^{p_f, e}} \cdot \underbrace{\left\{ \delta \ddot{\boldsymbol{\pi}}^e \right\}}_{n_{\text{dof}}^{p_f, e} \times 1} \right), \tag{C.34}$$

whereby we recover the following tangents:

$$\begin{aligned}
\underbrace{\left[\mathbf{k}_{p_f, u}^{\mathcal{H}_2^{\text{INT}, e}} \right]}_{n_{\text{dof}}^{p_f, e} \times n_{\text{dof}}^{s, e}} = & \int_{-1}^1 \underbrace{\left\{ \mathbf{N}^{e, p_f} \right\}^T}_{n_{\text{dof}}^{p_f, e} \times 1} \left(\left[\frac{\delta \hat{k}^{h^e}}{\hat{k}^{h^e}} (n^f \tilde{v}_f)^{h^e} + \hat{k}^{h^e} \frac{\partial p_f^{h^e}}{\partial X} (F_{11}^{h^e})^{-2} \right] (\beta \Delta t^2) \underbrace{\left\{ \mathbf{B}^{e, u} \right\}}_{1 \times n_{\text{dof}}^{s, e}} \right. \\
& \left. - \hat{k}^{h^e} \rho^{\text{fR}, h^e} \underbrace{\left\{ \mathbf{N}^{e, u} \right\}}_{1 \times n_{\text{dof}}^{s, e}} \right) \frac{\partial p_f^{h^e}}{\partial X} \frac{1}{K_f^\eta} A j^e d\xi, \tag{C.35}
\end{aligned}$$

$$\begin{aligned}
\underbrace{\left[\mathbf{k}_{p_f, p_f}^{\mathcal{H}_2^{\text{INT}, e}} \right]}_{n_{\text{dof}}^{p_f, e} \times n_{\text{dof}}^{p_f, e}} = & \int_{-1}^1 \underbrace{\left\{ \mathbf{N}^{e, p_f} \right\}^T}_{n_{\text{dof}}^{p_f, e} \times 1} \left(\left[(n^f \tilde{v}_f)^{h^e} - \hat{k}^{h^e} \frac{\partial p_f^{h^e}}{\partial X} (F_{11}^{h^e})^{-1} \right] \underbrace{\left\{ \mathbf{B}^{e, p_f} \right\}}_{1 \times n_{\text{dof}}^{p_f, e}} \right. \\
& \left. - \hat{k}^{h^e} \frac{\partial p_f^{h^e}}{\partial X} (a^{h^e} + g) \frac{\rho^{\text{fR}, h^e}}{K_f^\eta} \underbrace{\left\{ \mathbf{N}^{e, p_f} \right\}}_{1 \times n_{\text{dof}}^{p_f, e}} \right) \frac{1}{K_f^\eta} (\beta \Delta t^2) A j^e d\xi. \tag{C.36}
\end{aligned}$$

To derive the tangents for $\delta\mathcal{H}_2^{\text{INT}}$ when poroelasticity is considered, start from (B.30), and

apply the FE discretization as follows:

$$\begin{aligned}
\delta\mathcal{H}_2^{\text{INT}} &= \mathbf{A}_e^{n_e} \underbrace{\left\{ \mathbf{c}^{p_f, e} \right\}^T}_{1 \times n_{\text{dof}}^{p_f, e}} \cdot \left(\int_{-1}^1 \underbrace{\left\{ \mathbf{N}^{e, p_f} \right\}^T}_{n_{\text{dof}}^{p_f, e} \times 1} \left[\left([n^f \tilde{v}_f]^{h^e} - \hat{k}^{h^e} \frac{\partial p_f^{h^e}}{\partial X} (F_{11}^{h^e})^{-1} \right) \right. \right. \\
&\quad \times (\gamma \Delta t) \underbrace{\left\{ \mathbf{B}^{e, p_f} \right\}}_{1 \times n_{\text{dof}}^{p_f, e}} \underbrace{\left\{ \delta \dot{\boldsymbol{\pi}}^e \right\}}_{n_{\text{dof}}^{p_f, e} \times 1} - \hat{k}^{h^e} \frac{\partial p_f^{h^e}}{\partial X} g \frac{\rho^{\text{fR}, h^e}}{K_f^\eta} (\gamma \Delta t) \underbrace{\left\{ \mathbf{N}^{e, p_f} \right\}}_{1 \times n_{\text{dof}}^{p_f, e}} \underbrace{\left\{ \delta \dot{\boldsymbol{\pi}}^e \right\}}_{n_{\text{dof}}^{p_f, e} \times 1} \\
&\quad \left. \left. + \frac{\partial p_f^{h^e}}{\partial X} \left(\frac{\delta \hat{k}^{h^e}}{\hat{k}^{h^e}} (n^f \tilde{v}_f)^{h^e} + \hat{k}^{h^e} \frac{\partial p_f^{h^e}}{\partial X} (F_{11}^{h^e})^{-2} \right) \right. \right. \\
&\quad \left. \left. \times (\gamma \Delta t) \underbrace{\left\{ \mathbf{B}^{e, u} \right\}}_{1 \times n_{\text{dof}}^{s, e}} \underbrace{\left\{ \delta \dot{\mathbf{d}}^e \right\}}_{n_{\text{dof}}^{s, e} \times 1} \right] \frac{A}{K_f^\eta} j^e d\xi \right). \tag{C.37}
\end{aligned}$$

Then, pulling out the variations $\delta \dot{\mathbf{d}}^e$ & $\delta \dot{\boldsymbol{\pi}}^e$ leaves us with

$$\delta\mathcal{H}_2^{\text{INT}} = \mathbf{A}_e^{n_e} \underbrace{\left\{ \mathbf{c}^{p_f, e} \right\}^T}_{1 \times n_{\text{dof}}^{p_f, e}} \cdot \left(\underbrace{\left[\mathbf{k}_{p_f, u}^{\mathcal{H}_2^{\text{INT}, e}} \right]}_{n_{\text{dof}}^{p_f, e} \times n_{\text{dof}}^{s, e}} \cdot \underbrace{\left\{ \delta \dot{\mathbf{d}}^e \right\}}_{n_{\text{dof}}^{s, e} \times 1} + \underbrace{\left[\mathbf{k}_{p_f, p_f}^{\mathcal{H}_2^{\text{INT}, e}} \right]}_{n_{\text{dof}}^{p_f, e} \times n_{\text{dof}}^{p_f, e}} \cdot \underbrace{\left\{ \delta \dot{\boldsymbol{\pi}}^e \right\}}_{n_{\text{dof}}^{p_f, e} \times 1} \right), \tag{C.38}$$

whereby we recover the following tangents:

$$\underbrace{\left[\mathbf{k}_{p_f, u}^{\mathcal{H}_2^{\text{INT}, e}} \right]}_{n_{\text{dof}}^{p_f, e} \times n_{\text{dof}}^{s, e}} = \int_{-1}^1 \underbrace{\left\{ \mathbf{N}^{e, p_f} \right\}^T}_{n_{\text{dof}}^{p_f, e} \times 1} \left(\left[\frac{\delta \hat{k}^{h^e}}{\hat{k}^{h^e}} (n^f \tilde{v}_f)^{h^e} + \hat{k}^{h^e} \frac{\partial p_f^{h^e}}{\partial X} (F_{11}^{h^e})^{-2} \right] (\gamma \Delta t) \underbrace{\left\{ \mathbf{B}^{e, u} \right\}}_{1 \times n_{\text{dof}}^{s, e}} \right) \frac{\partial p_f^{h^e}}{\partial X} \frac{1}{K_f^\eta} A j^e d\xi, \tag{C.39}$$

$$\begin{aligned}
\underbrace{\left[\mathbf{k}_{p_f, p_f}^{\mathcal{H}_2^{\text{INT}, e}} \right]}_{n_{\text{dof}}^{p_f, e} \times n_{\text{dof}}^{p_f, e}} &= \int_{-1}^1 \underbrace{\left\{ \mathbf{N}^{e, p_f} \right\}^T}_{n_{\text{dof}}^{p_f, e} \times 1} \left(\left[(n^f \tilde{v}_f)^{h^e} - \hat{k}^{h^e} \frac{\partial p_f^{h^e}}{\partial X} (F_{11}^{h^e})^{-1} \right] \underbrace{\left\{ \mathbf{B}^{e, p_f} \right\}}_{1 \times n_{\text{dof}}^{p_f, e}} \right. \\
&\quad \left. - \hat{k}^{h^e} \frac{\partial p_f^{h^e}}{\partial X} g \frac{\rho^{\text{fR}, h^e}}{K_f^\eta} \underbrace{\left\{ \mathbf{N}^{e, p_f} \right\}}_{1 \times n_{\text{dof}}^{p_f, e}} \right) \frac{1}{K_f^\eta} (\gamma \Delta t) A j^e d\xi. \tag{C.40}
\end{aligned}$$

To derive the tangents for $\delta\mathcal{H}_3^{\text{INT}}$, we apply the FE discretization as follows:

$$\begin{aligned}
\delta\mathcal{H}_3^{\text{INT}} &= \mathbf{A}_e^{n_e} \underbrace{\left\{ \mathbf{c}^{p_f, e} \right\}^T}_{1 \times n_{\text{dof}}^{p_f, e}} \cdot \left(\int_{-1}^1 \underbrace{\left\{ \mathbf{B}^{e, p_f} \right\}^T}_{n_{\text{dof}}^{p_f, e} \times 1} \left[\left(\delta \hat{k}_k^{h^e} - \hat{k}^{h^e} (F_{11}^{h^e})^{-1} \right) \frac{\partial p_f^{h^e}}{\partial X} (F_{11}^{h^e})^{-1} (\beta \Delta t^2) \times \right. \right. \\
&\quad \left. \left. \underbrace{\left\{ \mathbf{B}^{e, u} \right\}}_{1 \times n_{\text{dof}}^{s, e}} \underbrace{\left\{ \delta \dot{\mathbf{d}}^e \right\}}_{n_{\text{dof}}^{s, e} \times 1} + \hat{k}^{h^e} (F_{11}^{h^e})^{-1} (\beta \Delta t^2) \underbrace{\left\{ \mathbf{B}^{e, p_f} \right\}}_{1 \times n_{\text{dof}}^{p_f, e}} \underbrace{\left\{ \delta \dot{\boldsymbol{\pi}}^e \right\}}_{n_{\text{dof}}^{p_f, e} \times 1} \right] A j^e d\xi \right). \tag{C.41}
\end{aligned}$$

Then, pulling out the variations $\delta\ddot{\mathbf{d}}^e$ and $\delta\ddot{\boldsymbol{\pi}}^e$ leaves us with

$$\delta\mathcal{H}_3^{\text{INT}} = \mathbf{A}_e \underbrace{\left\{ \mathbf{c}^{p_f, e} \right\}^T}_{1 \times n_{\text{dof}}^{p_f, e}} \cdot \left(\underbrace{\left[\mathbf{k}_{p_f, u}^{\mathcal{H}_3^{\text{INT}}, e} \right]}_{n_{\text{dof}}^{p_f, e} \times n_{\text{dof}}^{s, e}} \cdot \underbrace{\left\{ \delta\ddot{\mathbf{d}}^e \right\}}_{n_{\text{dof}}^{s, e} \times 1} + \underbrace{\left[\mathbf{k}_{p_f, p_f}^{\mathcal{H}_3^{\text{INT}}, e} \right]}_{n_{\text{dof}}^{p_f, e} \times n_{\text{dof}}^{p_f, e}} \cdot \underbrace{\left\{ \delta\ddot{\boldsymbol{\pi}}^e \right\}}_{n_{\text{dof}}^{p_f, e} \times 1} \right), \quad (\text{C.42})$$

whereby we recover

$$\underbrace{\left[\mathbf{k}_{p_f, u}^{\mathcal{H}_3^{\text{INT}}, e} \right]}_{n_{\text{dof}}^{p_f, e} \times n_{\text{dof}}^{s, e}} = \int_{-1}^1 \frac{\partial p_f^{h^e}}{\partial X} (F_{11}^{h^e})^{-1} (\delta_k^{h^e} - \hat{k}^{h^e} (F_{11}^{h^e})^{-1}) (\beta \Delta t^2) \underbrace{\left\{ \mathbf{B}^{e, p_f} \right\}^T}_{n_{\text{dof}}^{p_f, e} \times 1} \underbrace{\left\{ \mathbf{B}^{e, u} \right\}}_{1 \times n_{\text{dof}}^{s, e}} A_j^e d\xi, \quad (\text{C.43})$$

$$\underbrace{\left[\mathbf{k}_{p_f, p_f}^{\mathcal{H}_3^{\text{INT}}, e} \right]}_{n_{\text{dof}}^{p_f, e} \times n_{\text{dof}}^{p_f, e}} = \int_{-1}^1 \hat{k}^{h^e} (F_{11}^{h^e})^{-1} (\beta \Delta t^2) \underbrace{\left\{ \mathbf{B}^{e, p_f} \right\}^T}_{n_{\text{dof}}^{p_f, e} \times 1} \underbrace{\left\{ \mathbf{B}^{e, p_f} \right\}}_{1 \times n_{\text{dof}}^{p_f, e}} A_j^e d\xi. \quad (\text{C.44})$$

To derive the tangents for $\delta\mathcal{H}_3^{\text{INT}}$ when poroelasticity is considered, start from Eq. (B.33), and apply the FE discretization as follows:

$$\delta\mathcal{H}_3^{\text{INT}} = \mathbf{A}_e \underbrace{\left\{ \mathbf{c}^{p_f, e} \right\}^T}_{1 \times n_{\text{dof}}^{p_f, e}} \cdot \left(\underbrace{\int_{-1}^1 \left\{ \mathbf{B}^{e, p_f} \right\}^T}_{n_{\text{dof}}^{p_f, e} \times 1} \left[\left(\delta_k^{h^e} - \hat{k}^{h^e} (F_{11}^{h^e})^{-1} \right) \frac{\partial p_f^{h^e}}{\partial X} (F_{11}^{h^e})^{-1} (\gamma \Delta t) \times \right. \right. \\ \left. \left. \underbrace{\left\{ \mathbf{B}^{e, u} \right\}}_{1 \times n_{\text{dof}}^{s, e}} \underbrace{\left\{ \delta\dot{\mathbf{d}}^e \right\}}_{n_{\text{dof}}^{s, e} \times 1} + \hat{k}^{h^e} (F_{11}^{h^e})^{-1} (\gamma \Delta t) \underbrace{\left\{ \mathbf{B}^{e, p_f} \right\}}_{1 \times n_{\text{dof}}^{p_f, e}} \underbrace{\left\{ \delta\dot{\boldsymbol{\pi}}^e \right\}}_{n_{\text{dof}}^{p_f, e} \times 1} \right] A_j^e d\xi \right). \quad (\text{C.45})$$

Then, pulling out the variations $\delta\dot{\mathbf{d}}^e$ and $\delta\dot{\boldsymbol{\pi}}^e$ leaves us with

$$\delta\mathcal{H}_3^{\text{INT}} = \mathbf{A}_e \underbrace{\left\{ \mathbf{c}^{p_f, e} \right\}^T}_{1 \times n_{\text{dof}}^{p_f, e}} \cdot \left(\underbrace{\left[\mathbf{k}_{p_f, u}^{\mathcal{H}_3^{\text{INT}}, e} \right]}_{n_{\text{dof}}^{p_f, e} \times n_{\text{dof}}^{s, e}} \cdot \underbrace{\left\{ \delta\dot{\mathbf{d}}^e \right\}}_{n_{\text{dof}}^{s, e} \times 1} + \underbrace{\left[\mathbf{k}_{p_f, p_f}^{\mathcal{H}_3^{\text{INT}}, e} \right]}_{n_{\text{dof}}^{p_f, e} \times n_{\text{dof}}^{p_f, e}} \cdot \underbrace{\left\{ \delta\dot{\boldsymbol{\pi}}^e \right\}}_{n_{\text{dof}}^{p_f, e} \times 1} \right), \quad (\text{C.46})$$

where

$$\underbrace{\left[\mathbf{k}_{p_f, u}^{\mathcal{H}_3^{\text{INT}}, e} \right]}_{n_{\text{dof}}^{p_f, e} \times n_{\text{dof}}^{s, e}} = \int_{-1}^1 \frac{\partial p_f^{h^e}}{\partial X} (F_{11}^{h^e})^{-1} (\delta_k^{h^e} - \hat{k}^{h^e} (F_{11}^{h^e})^{-1}) (\gamma \Delta t) \underbrace{\left\{ \mathbf{B}^{e, p_f} \right\}^T}_{n_{\text{dof}}^{p_f, e} \times 1} \underbrace{\left\{ \mathbf{B}^{e, u} \right\}}_{1 \times n_{\text{dof}}^{s, e}} A_j^e d\xi, \quad (\text{C.47})$$

$$\underbrace{\left[\mathbf{k}_{p_f, p_f}^{\mathcal{H}_3^{\text{INT}}, e} \right]}_{n_{\text{dof}}^{p_f, e} \times n_{\text{dof}}^{p_f, e}} = \int_{-1}^1 \hat{k}^{h^e} (F_{11}^{h^e})^{-1} (\gamma \Delta t) \underbrace{\left\{ \mathbf{B}^{e, p_f} \right\}^T}_{n_{\text{dof}}^{p_f, e} \times 1} \underbrace{\left\{ \mathbf{B}^{e, p_f} \right\}}_{1 \times n_{\text{dof}}^{p_f, e}} A_j^e d\xi. \quad (\text{C.48})$$

To derive the tangents for $\delta\mathcal{H}_4^{\text{INT}}$, we start by applying the FE discretization as follows:

$$\begin{aligned} \delta\mathcal{H}_4^{\text{INT}} = & \mathbf{A}_e^{n_e} \underbrace{\left\{ \mathbf{c}^{p_f, e} \right\}^T}_{1 \times n_{\text{dof}}^{p_f, e}} \cdot \left(\int_{-1}^1 \underbrace{\left\{ \mathbf{B}^{e, p_f} \right\}^T}_{n_{\text{dof}}^{p_f, e} \times 1} \rho^{\text{fR}, h^e} \left[\delta_k^{h^e} (a^{h^e} + g) (\beta \Delta t^2) \underbrace{\left\{ \mathbf{B}^{e, u} \right\}}_{1 \times n_{\text{dof}}^{s, e}} \underbrace{\left\{ \delta \ddot{\mathbf{d}}^e \right\}}_{n_{\text{dof}}^{s, e} \times 1} \right. \right. \\ & + \hat{k}^{h^e} (a^{h^e} + g) \frac{1}{K_f^\eta} (\beta \Delta t^2) \underbrace{\left\{ \mathbf{N}^{e, p_f} \right\}}_{1 \times n_{\text{dof}}^{p_f, e}} \underbrace{\left\{ \delta \ddot{\boldsymbol{\pi}}^e \right\}}_{n_{\text{dof}}^{p_f, e} \times 1} \\ & \left. \left. + \hat{k}^{h^e} \underbrace{\left\{ \mathbf{N}^{e, u} \right\}}_{1 \times n_{\text{dof}}^{s, e}} \underbrace{\left\{ \delta \ddot{\mathbf{d}}^e \right\}}_{n_{\text{dof}}^{s, e} \times 1} \right] A_j^e d\xi \right). \end{aligned} \quad (\text{C.49})$$

Then, pulling out the variations $\delta \ddot{\mathbf{d}}^e$ and $\delta \ddot{\boldsymbol{\pi}}^e$ leaves us with

$$\delta\mathcal{H}_4^{\text{INT}} = \mathbf{A}_e^{n_e} \underbrace{\left\{ \mathbf{c}^{p_f, e} \right\}^T}_{1 \times n_{\text{dof}}^{p_f, e}} \cdot \left(\underbrace{\left[\mathbf{k}_{p_f, u}^{\mathcal{H}_4^{\text{INT}}, e} \right]}_{n_{\text{dof}}^{p_f, e} \times n_{\text{dof}}^{s, e}} \cdot \underbrace{\left\{ \delta \ddot{\mathbf{d}}^e \right\}}_{n_{\text{dof}}^{s, e} \times 1} + \underbrace{\left[\mathbf{k}_{p_f, p_f}^{\mathcal{H}_4^{\text{INT}}, e} \right]}_{n_{\text{dof}}^{p_f, e} \times n_{\text{dof}}^{p_f, e}} \cdot \underbrace{\left\{ \delta \ddot{\boldsymbol{\pi}}^e \right\}}_{n_{\text{dof}}^{p_f, e} \times 1} \right), \quad (\text{C.50})$$

where we recover

$$\underbrace{\left[\mathbf{k}_{p_f, u}^{\mathcal{H}_4^{\text{INT}}, e} \right]}_{n_{\text{dof}}^{p_f, e} \times n_{\text{dof}}^{s, e}} = \int_{-1}^1 \underbrace{\left\{ \mathbf{B}^{e, p_f} \right\}^T}_{n_{\text{dof}}^{p_f, e} \times 1} \left(\delta_k^{h^e} (a^{h^e} + g) (\beta \Delta t^2) \underbrace{\left\{ \mathbf{B}^{e, u} \right\}}_{1 \times n_{\text{dof}}^{s, e}} + \hat{k}^{h^e} \underbrace{\left\{ \mathbf{N}^{e, u} \right\}}_{1 \times n_{\text{dof}}^{s, e}} \right) \rho^{\text{fR}, h^e} A_j^e d\xi, \quad (\text{C.51})$$

$$\underbrace{\left[\mathbf{k}_{p_f, p_f}^{\mathcal{H}_4^{\text{INT}}, e} \right]}_{n_{\text{dof}}^{p_f, e} \times n_{\text{dof}}^{p_f, e}} = \int_{-1}^1 \hat{k}^{h^e} (a^{h^e} + g) \frac{\rho^{\text{fR}, h^e}}{K_f^\eta} (\beta \Delta t^2) \underbrace{\left\{ \mathbf{B}^{e, p_f} \right\}^T}_{n_{\text{dof}}^{p_f, e} \times 1} \underbrace{\left\{ \mathbf{N}^{e, p_f} \right\}}_{1 \times n_{\text{dof}}^{p_f, e}} A_j^e d\xi. \quad (\text{C.52})$$

To derive the tangents for $\delta\mathcal{H}_4^{\text{INT}}$ when poroelasticity is considered, start from (B.35), and apply the FE discretization as follows:

$$\begin{aligned} \delta\mathcal{H}_4^{\text{INT}} = & \mathbf{A}_e^{n_e} \underbrace{\left\{ \mathbf{c}^{p_f, e} \right\}^T}_{1 \times n_{\text{dof}}^{p_f, e}} \cdot \left(\int_{-1}^1 \underbrace{\left\{ \mathbf{B}^{e, p_f} \right\}^T}_{n_{\text{dof}}^{p_f, e} \times 1} \rho^{\text{fR}, h^e} \left[\delta_k^{h^e} g (\gamma \Delta t) \underbrace{\left\{ \mathbf{B}^{e, u} \right\}}_{1 \times n_{\text{dof}}^{s, e}} \underbrace{\left\{ \delta \dot{\mathbf{d}}^e \right\}}_{n_{\text{dof}}^{s, e} \times 1} \right. \right. \\ & \left. \left. + \hat{k}^{h^e} g \frac{1}{K_f^\eta} (\gamma \Delta t) \underbrace{\left\{ \mathbf{N}^{e, p_f} \right\}}_{1 \times n_{\text{dof}}^{p_f, e}} \underbrace{\left\{ \delta \dot{\boldsymbol{\pi}}^e \right\}}_{n_{\text{dof}}^{p_f, e} \times 1} \right] A_j^e d\xi \right). \end{aligned} \quad (\text{C.53})$$

Then, pulling out the variations $\delta \dot{\mathbf{d}}^e$ and $\delta \dot{\boldsymbol{\pi}}^e$ leaves us with

$$\delta\mathcal{H}_4^{\text{INT}} = \mathbf{A}_e^{n_e} \underbrace{\left\{ \mathbf{c}^{p_f, e} \right\}^T}_{1 \times n_{\text{dof}}^{p_f, e}} \cdot \left(\underbrace{\left[\mathbf{k}_{p_f, u}^{\mathcal{H}_4^{\text{INT}}, e} \right]}_{n_{\text{dof}}^{p_f, e} \times n_{\text{dof}}^{s, e}} \cdot \underbrace{\left\{ \delta \dot{\mathbf{d}}^e \right\}}_{n_{\text{dof}}^{s, e} \times 1} + \underbrace{\left[\mathbf{k}_{p_f, p_f}^{\mathcal{H}_4^{\text{INT}}, e} \right]}_{n_{\text{dof}}^{p_f, e} \times n_{\text{dof}}^{p_f, e}} \cdot \underbrace{\left\{ \delta \dot{\boldsymbol{\pi}}^e \right\}}_{n_{\text{dof}}^{p_f, e} \times 1} \right), \quad (\text{C.54})$$

where

$$\underbrace{\left[\mathbf{k}_{p_f, u}^{\mathcal{H}_4^{\text{INT}}, e} \right]}_{n_{\text{dof}}^{p_f, e} \times n_{\text{dof}}^{s, e}} = \int_{-1}^1 \underbrace{\left\{ \mathbf{B}^{e, p_f} \right\}^T}_{n_{\text{dof}}^{p_f, e} \times 1} \left(\delta_k^{h^e} g(\gamma \Delta t) \underbrace{\left\{ \mathbf{B}^{e, u} \right\}}_{1 \times n_{\text{dof}}^{s, e}} \right) \rho^{\text{fR}, h^e} A_j^e d\xi, \quad (\text{C.55})$$

$$\underbrace{\left[\mathbf{k}_{p_f, p_f}^{\mathcal{H}_4^{\text{INT}}, e} \right]}_{n_{\text{dof}}^{p_f, e} \times n_{\text{dof}}^{p_f, e}} = \int_{-1}^1 \hat{k}^{h^e} g \frac{\rho^{\text{fR}, h^e}}{K_f^\eta} (\gamma \Delta t) \underbrace{\left\{ \mathbf{B}^{e, p_f} \right\}^T}_{n_{\text{dof}}^{p_f, e} \times 1} \underbrace{\left\{ \mathbf{N}^{e, p_f} \right\}}_{1 \times n_{\text{dof}}^{p_f, e}} A_j^e d\xi. \quad (\text{C.56})$$

To derive the tangents for $\delta \mathcal{H}^{\text{stab}}$, start from (B.36), and apply the FE discretization as follows:

$$\begin{aligned} \delta \mathcal{H}^{\text{stab}} = & \mathbf{A}_e^{n_e} \underbrace{\left\{ \mathbf{c}^{p_f, e} \right\}^T}_{1 \times n_{\text{dof}}^{p_f, e}} \cdot \left(\int_{-1}^1 \underbrace{\left\{ \mathbf{B}^{e, p_f} \right\}^T}_{n_{\text{dof}}^{p_f, e} \times 1} \alpha^{\text{stab}} (F_{11}^{h^e})^{-1} \left[(\gamma \Delta t) \underbrace{\left\{ \mathbf{B}^{e, p_f} \right\}}_{1 \times n_{\text{dof}}^{p_f, e}} \cdot \underbrace{\left\{ \delta \bar{\boldsymbol{\pi}}^e \right\}}_{n_{\text{dof}}^{p_f, e} \times 1} \right. \right. \\ & \left. \left. - \frac{\partial \dot{p}_f^{h^e}}{\partial X} (F_{11}^{h^e})^{-1} (\beta \Delta t^2) \underbrace{\left\{ \mathbf{B}^{e, u} \right\}}_{1 \times n_{\text{dof}}^{s, e}} \cdot \underbrace{\left\{ \delta \ddot{\mathbf{d}}^e \right\}}_{n_{\text{dof}}^{s, e} \times 1} \right] A_j^e d\xi \right). \quad (\text{C.57}) \end{aligned}$$

Then, pulling out the variations $\delta \ddot{\mathbf{d}}^e$ and $\delta \bar{\boldsymbol{\pi}}^e$ leaves us with

$$\delta \mathcal{H}^{\text{stab}} = \mathbf{A}_e^{n_e} \underbrace{\left\{ \mathbf{c}^{p_f, e} \right\}^T}_{1 \times n_{\text{dof}}^{p_f, e}} \cdot \left(\underbrace{\left[\mathbf{k}_{p_f, u}^{\mathcal{H}^{\text{stab}, e}} \right]}_{n_{\text{dof}}^{p_f, e} \times n_{\text{dof}}^{s, e}} \cdot \underbrace{\left\{ \delta \ddot{\mathbf{d}}^e \right\}}_{n_{\text{dof}}^{s, e} \times 1} + \underbrace{\left[\mathbf{k}_{p_f, p_f}^{\mathcal{H}^{\text{stab}, e}} \right]}_{n_{\text{dof}}^{p_f, e} \times n_{\text{dof}}^{p_f, e}} \cdot \underbrace{\left\{ \delta \bar{\boldsymbol{\pi}}^e \right\}}_{n_{\text{dof}}^{p_f, e} \times 1} \right), \quad (\text{C.58})$$

where we recover

$$\underbrace{\left[\mathbf{k}_{p_f, u}^{\mathcal{H}^{\text{stab}, e}} \right]}_{n_{\text{dof}}^{p_f, e} \times n_{\text{dof}}^{s, e}} = - \int_{-1}^1 \alpha^{\text{stab}} (F_{11}^{h^e})^{-2} \frac{\partial \dot{p}_f^{h^e}}{\partial X} (\beta \Delta t^2) \underbrace{\left\{ \mathbf{B}^{e, p_f} \right\}^T}_{n_{\text{dof}}^{p_f, e} \times 1} \underbrace{\left\{ \mathbf{B}^{e, u} \right\}}_{1 \times n_{\text{dof}}^{s, e}} A_j^e d\xi, \quad (\text{C.59})$$

$$\underbrace{\left[\mathbf{k}_{p_f, p_f}^{\mathcal{H}^{\text{stab}, e}} \right]}_{n_{\text{dof}}^{p_f, e} \times n_{\text{dof}}^{p_f, e}} = \int_{-1}^1 \alpha^{\text{stab}} (F_{11}^{h^e})^{-1} (\gamma \Delta t) \underbrace{\left\{ \mathbf{B}^{e, p_f} \right\}^T}_{n_{\text{dof}}^{p_f, e} \times 1} \underbrace{\left\{ \mathbf{B}^{e, p_f} \right\}}_{1 \times n_{\text{dof}}^{p_f, e}} A_j^e d\xi. \quad (\text{C.60})$$

To derive the tangents for $\delta \mathcal{H}^{\text{stab}}$ when poroelasticity is considered, start from (B.37) and

apply the FE discretization as follows:

$$\begin{aligned} \delta \mathcal{H}^{\text{stab}} = & \mathbf{A}_e^{n_e} \underbrace{\left\{ \mathbf{c}^{p_f, e} \right\}^T}_{1 \times n_{\text{dof}}^{p_f, e}} \cdot \left(\int_{-1}^1 \underbrace{\left\{ \mathbf{B}^{e, p_f} \right\}^T}_{n_{\text{dof}}^{p_f, e} \times 1} \alpha^{\text{stab}} (F_{11}^{h^e})^{-1} \left[\underbrace{\left\{ \mathbf{B}^{e, p_f} \right\}}_{1 \times n_{\text{dof}}^{p_f, e}} \cdot \underbrace{\left\{ \delta \dot{\boldsymbol{\pi}}^e \right\}}_{n_{\text{dof}}^{p_f, e} \times 1} \right. \right. \\ & \left. \left. - \frac{\partial \dot{p}_f^h}{\partial X} (F_{11}^{h^e})^{-1} (\gamma \Delta t) \underbrace{\left\{ \mathbf{B}^{e, u} \right\}}_{1 \times n_{\text{dof}}^{s, e}} \cdot \underbrace{\left\{ \delta \dot{\mathbf{d}}^e \right\}}_{n_{\text{dof}}^{s, e} \times 1} \right] A_j^e d\xi \right). \end{aligned} \quad (\text{C.61})$$

Then, pulling out the variations $\delta \dot{\mathbf{d}}^e$ and $\delta \dot{\boldsymbol{\pi}}^e$ leaves us with

$$\delta \mathcal{H}^{\text{stab}} = \mathbf{A}_e^{n_e} \underbrace{\left\{ \mathbf{c}^{p_f, e} \right\}^T}_{1 \times n_{\text{dof}}^{p_f, e}} \cdot \left(\underbrace{\left[\mathbf{k}_{p_f, u}^{\mathcal{H}^{\text{stab}, e}} \right]}_{n_{\text{dof}}^{p_f, e} \times n_{\text{dof}}^{s, e}} \cdot \underbrace{\left\{ \delta \dot{\mathbf{d}}^e \right\}}_{n_{\text{dof}}^{s, e} \times 1} + \underbrace{\left[\mathbf{k}_{p_f, p_f}^{\mathcal{H}^{\text{stab}, e}} \right]}_{n_{\text{dof}}^{p_f, e} \times n_{\text{dof}}^{p_f, e}} \cdot \underbrace{\left\{ \delta \dot{\boldsymbol{\pi}}^e \right\}}_{n_{\text{dof}}^{p_f, e} \times 1} \right), \quad (\text{C.62})$$

where

$$\underbrace{\left[\mathbf{k}_{p_f, u}^{\mathcal{H}^{\text{stab}, e}} \right]}_{n_{\text{dof}}^{p_f, e} \times n_{\text{dof}}^{s, e}} = - \int_{-1}^1 \alpha^{\text{stab}} (F_{11}^{h^e})^{-2} \frac{\partial \dot{p}_f^h}{\partial X} (\gamma \Delta t) \underbrace{\left\{ \mathbf{B}^{e, p_f} \right\}^T}_{n_{\text{dof}}^{p_f, e} \times 1} \underbrace{\left\{ \mathbf{B}^{e, u} \right\}}_{1 \times n_{\text{dof}}^{s, e}} A_j^e d\xi, \quad (\text{C.63})$$

$$\underbrace{\left[\mathbf{k}_{p_f, p_f}^{\mathcal{H}^{\text{stab}, e}} \right]}_{n_{\text{dof}}^{p_f, e} \times n_{\text{dof}}^{p_f, e}} = \int_{-1}^1 \alpha^{\text{stab}} (F_{11}^{h^e})^{-1} \underbrace{\left\{ \mathbf{B}^{e, p_f} \right\}^T}_{n_{\text{dof}}^{p_f, e} \times 1} \underbrace{\left\{ \mathbf{B}^{e, p_f} \right\}}_{1 \times n_{\text{dof}}^{p_f, e}} A_j^e d\xi. \quad (\text{C.64})$$

C.1.3 ($\mathbf{u}-\mathbf{u}_f-p_f$) formulation

To derive the tangents for $\delta \mathcal{G}_1^{\text{INT}}$, we start by applying the FE discretization as follows:

$$\begin{aligned} \delta \mathcal{G}_1^{\text{INT}} = & \mathbf{A}_e^{n_e} \underbrace{\left\{ \mathbf{c}^{u, e} \right\}^T}_{1 \times n_{\text{dof}}^{s, e}} \cdot \left(\int_{-1}^1 \underbrace{\left\{ \mathbf{N}^{e, u} \right\}^T}_{n_{\text{dof}}^{s, e} \times 1} \left[\rho_0^{s, h^e} \underbrace{\left\{ \mathbf{N}^{e, u} \right\}}_{1 \times n_{\text{dof}}^{s, e}} \underbrace{\left\{ \delta \ddot{\mathbf{d}}^e \right\}}_{n_{\text{dof}}^{s, e} \times 1} \right. \right. \\ & + a_f^{h^e} (\beta \Delta t^2) \left(\underbrace{\left\{ \mathbf{B}^{e, u} \right\}}_{1 \times n_{\text{dof}}^{s, e}} \underbrace{\left\{ \ddot{\mathbf{d}}^e \right\}}_{n_{\text{dof}}^{s, e} \times 1} + \frac{J^{h^e} n^{f, h^e} \rho^{\text{fR}, h^e}}{K_f^\eta} \underbrace{\left\{ \mathbf{N}^{e, p_f} \right\}}_{1 \times n_{\text{dof}}^{p_f, e}} \underbrace{\left\{ \ddot{\boldsymbol{\pi}}^e \right\}}_{n_{\text{dof}}^{p_f, e} \times 1} \right) \\ & \left. \left. + \rho_0^{f, h^e} \underbrace{\left\{ \mathbf{N}^{e, u_f} \right\}}_{1 \times n_{\text{dof}}^{f, e}} \underbrace{\left\{ \ddot{\mathbf{d}}_f^e \right\}}_{n_{\text{dof}}^{f, e} \times 1} \right] A_j^e d\xi \right). \end{aligned} \quad (\text{C.65})$$

Then, pulling out the variations $\delta \ddot{\mathbf{d}}^e$, $\delta \ddot{\mathbf{d}}_f^e$, and $\delta \ddot{\boldsymbol{\pi}}^e$ leaves us with

$$\delta \mathcal{G}_1^{\text{INT}} = \mathbf{A}_e^{n_e} \underbrace{\left\{ \mathbf{c}^{u, e} \right\}^T}_{1 \times n_{\text{dof}}^{s, e}} \cdot \left(\underbrace{\left[\mathbf{k}_{u, u}^{\mathcal{G}_1^{\text{INT}, e}} \right]}_{n_{\text{dof}}^{s, e} \times n_{\text{dof}}^{s, e}} \cdot \underbrace{\left\{ \delta \ddot{\mathbf{d}}^e \right\}}_{n_{\text{dof}}^{s, e} \times 1} + \underbrace{\left[\mathbf{k}_{u, u_f}^{\mathcal{G}_1^{\text{INT}, e}} \right]}_{n_{\text{dof}}^{s, e} \times n_{\text{dof}}^{f, e}} \cdot \underbrace{\left\{ \delta \ddot{\mathbf{d}}_f^e \right\}}_{n_{\text{dof}}^{f, e} \times 1} + \underbrace{\left[\mathbf{k}_{u, p_f}^{\mathcal{G}_1^{\text{INT}, e}} \right]}_{n_{\text{dof}}^{s, e} \times n_{\text{dof}}^{p_f, e}} \cdot \underbrace{\left\{ \delta \ddot{\boldsymbol{\pi}}^e \right\}}_{n_{\text{dof}}^{p_f, e} \times 1} \right), \quad (\text{C.66})$$

where we recover the following tangent matrices:

$$\underbrace{\left[\mathbf{k}_{u,u}^{\mathcal{G}_1^{\text{INT}},e} \right]}_{n_{\text{dof}}^{s,e} \times n_{\text{dof}}^{s,e}} = \int_{-1}^1 \underbrace{\left\{ \mathbf{N}^{e,u} \right\}^T}_{n_{\text{dof}}^{s,e} \times 1} \left(\underbrace{\rho_0^{s,h^e}}_{1 \times n_{\text{dof}}^{s,e}} \underbrace{\left\{ \mathbf{N}^{e,u} \right\}}_{1 \times n_{\text{dof}}^{s,e}} + a_f^{h^e} \rho^{\text{fR},h^e} (\beta \Delta t^2) \underbrace{\left\{ \mathbf{B}^{e,u} \right\}}_{1 \times n_{\text{dof}}^{s,e}} \right) A_j^e d\xi, \quad (\text{C.67})$$

$$\underbrace{\left[\mathbf{k}_{u,u_f}^{\mathcal{G}_1^{\text{INT}},e} \right]}_{n_{\text{dof}}^{s,e} \times n_{\text{dof}}^{f,e}} = \int_{-1}^1 \rho_0^{f,h^e} \underbrace{\left\{ \mathbf{N}^{e,u} \right\}^T}_{n_{\text{dof}}^{s,e} \times 1} \underbrace{\left\{ \mathbf{N}^{e,u_f} \right\}}_{1 \times n_{\text{dof}}^{f,e}} A_j^e d\xi, \quad (\text{C.68})$$

$$\underbrace{\left[\mathbf{k}_{u,p_f}^{\mathcal{G}_1^{\text{INT}},e} \right]}_{n_{\text{dof}}^{s,e} \times n_{\text{dof}}^{p_f,e}} = \int_{-1}^1 \frac{a_f^{h^e} J^{h^e} n^{f,h^e} \rho^{\text{fR},h^e}}{K_f^\eta} (\beta \Delta t^2) \underbrace{\left\{ \mathbf{N}^{e,u} \right\}^T}_{n_{\text{dof}}^{s,e} \times 1} \underbrace{\left\{ \mathbf{N}^{e,p_f} \right\}}_{1 \times n_{\text{dof}}^{p_f,e}} A_j^e d\xi. \quad (\text{C.69})$$

The tangents for $\delta \mathcal{G}_2^{\text{INT}}$ and $\delta \mathcal{G}_3^{\text{INT}}$ remain unchanged from (\mathbf{u}) and $(\mathbf{u}-p_f)$ formulations, respectively. Refer to Eqs. C.6, C.12 and C.21. When the pore fluid viscous stress tensor is considered, we start by applying the FE discretization to $\delta \mathcal{G}_5^{\text{INT}}$ as follows:

$$\delta \mathcal{G}_5^{\text{INT}} = \underbrace{\mathbf{A}_e}_{1 \times n_{\text{dof}}^{s,e}} \underbrace{\left\{ \mathbf{c}^{u,e} \right\}^T}_{1 \times n_{\text{dof}}^{s,e}} \cdot \left(\int_{-1}^1 \underbrace{\left\{ \mathbf{B}^{e,u} \right\}^T}_{n_{\text{dof}}^{s,e} \times 1} (\kappa_f + 2\mu_f) \left[\frac{\partial v_f}{\partial X} F_{11}^{-2} (n^s - n^f) \beta \Delta t^2 \underbrace{\left\{ \mathbf{B}^{e,u} \right\}}_{1 \times n_{\text{dof}}^{s,e}} \underbrace{\left\{ \delta \ddot{\mathbf{d}}^e \right\}}_{n_{\text{dof}}^{s,e} \times 1} \right. \right. \\ \left. \left. + n^f F_{11}^{-1} \gamma \Delta t \underbrace{\left\{ \mathbf{B}^{e,u_f} \right\}^T}_{1 \times n_{\text{dof}}^{f,e}} \underbrace{\left\{ \delta \ddot{\mathbf{d}}_f^e \right\}}_{n_{\text{dof}}^{f,e} \times 1} \right] A_j^e \right). \quad (\text{C.70})$$

Then, pulling out the variations $\delta \ddot{\mathbf{d}}^e$ and $\delta \ddot{\mathbf{d}}_f^e$ leaves us with

$$\delta \mathcal{G}_5^{\text{INT}} = \underbrace{\mathbf{A}_e}_{1 \times n_{\text{dof}}^{s,e}} \underbrace{\left\{ \mathbf{c}^{u,e} \right\}^T}_{1 \times n_{\text{dof}}^{s,e}} \cdot \left(\underbrace{\left[\mathbf{k}_{u,u}^{\mathcal{G}_5^{\text{INT}},e} \right]}_{n_{\text{dof}}^{s,e} \times n_{\text{dof}}^{s,e}} \cdot \underbrace{\left\{ \delta \ddot{\mathbf{d}}^e \right\}}_{n_{\text{dof}}^{s,e} \times 1} + \underbrace{\left[\mathbf{k}_{u,u_f}^{\mathcal{G}_5^{\text{INT}},e} \right]}_{n_{\text{dof}}^{s,e} \times n_{\text{dof}}^{f,e}} \cdot \underbrace{\left\{ \delta \ddot{\mathbf{d}}_f^e \right\}}_{n_{\text{dof}}^{f,e} \times 1} \right), \quad (\text{C.71})$$

where we recover the following tangent matrices:

$$\underbrace{\left[\mathbf{k}_{u,u}^{\mathcal{G}_5^{\text{INT}},e} \right]}_{n_{\text{dof}}^{s,e} \times n_{\text{dof}}^{s,e}} = \int_{-1}^1 (\kappa + 2\mu_f) \left(\frac{\partial v_f^{h^e}}{\partial X} (F_{11}^{h^e})^{-2} (n^{s,h^e} - n^{f,h^e}) \beta \Delta t^2 \right) \underbrace{\left\{ \mathbf{B}^{e,u} \right\}^T}_{n_{\text{dof}}^{s,e} \times 1} \underbrace{\left\{ \mathbf{B}^{e,u} \right\}}_{1 \times n_{\text{dof}}^{s,e}} A_j^e d\xi, \quad (\text{C.72})$$

$$\underbrace{\left[\mathbf{k}_{u,u_f}^{\mathcal{G}_5^{\text{INT}},e} \right]}_{n_{\text{dof}}^{s,e} \times n_{\text{dof}}^{f,e}} = \int_{-1}^1 (\kappa_f + 2\mu_f) n^{f,h^e} (F_{11}^{h^e})^{-1} \gamma \Delta t \underbrace{\left\{ \mathbf{B}^{e,u} \right\}^T}_{n_{\text{dof}}^{s,e} \times 1} \underbrace{\left\{ \mathbf{B}^{e,u_f} \right\}}_{1 \times n_{\text{dof}}^{f,e}} A_j^e d\xi. \quad (\text{C.73})$$

To derive the tangents for $\delta\mathcal{I}_1^{\text{INT}}$, we apply the FE discretization as follows:

$$\begin{aligned} \delta\mathcal{I}_1^{\text{INT}} = & \mathbf{A}_e^{n_e} \left\{ \mathbf{c}^{u_f, e} \right\}^T \cdot \left(\int_{-1}^1 \underbrace{\left\{ \mathbf{N}^{e, u_f} \right\}}_{n_{\text{dof}}^{f, e} \times 1}^T \left[a_f^{h^e} (\beta \Delta t^2) \left(\underbrace{\rho^{\text{fR}, h^e}}_{1 \times n_{\text{dof}}^{s, e}} \underbrace{\left\{ \mathbf{N}^{e, u} \right\}}_{n_{\text{dof}}^{s, e} \times 1} \left\{ \delta \ddot{\mathbf{d}}^e \right\} \right. \right. \\ & \left. \left. + \frac{J^{h^e} n_f^{f, h^e} \rho^{\text{fR}, h^e}}{K_f^\eta} \underbrace{\left\{ \mathbf{N}^{e, p_f} \right\}}_{1 \times n_{\text{dof}}^{p_f, e}} \underbrace{\left\{ \ddot{\boldsymbol{\pi}}^e \right\}}_{n_{\text{dof}}^{p_f, e} \times 1} \right) + \rho_0^{f, h^e} \underbrace{\left\{ \mathbf{N}^{e, u_f} \right\}}_{1 \times n_{\text{dof}}^{f, e}} \underbrace{\left\{ \ddot{\mathbf{d}}_f^e \right\}}_{n_{\text{dof}}^{f, e} \times 1} \right] A_j^e d\xi \right). \end{aligned} \quad (\text{C.74})$$

Then, pulling out the variations $\delta \ddot{\mathbf{d}}^e$, $\delta \ddot{\mathbf{d}}_f^e$, and $\delta \ddot{\boldsymbol{\pi}}^e$ leaves us with

$$\delta\mathcal{I}_1^{\text{INT}} = \mathbf{A}_e^{n_e} \left\{ \mathbf{c}^{u_f, e} \right\}^T \cdot \left(\underbrace{\left[\mathbf{k}_{u_f, u}^{\mathcal{I}_1^{\text{INT}}, e} \right]}_{n_{\text{dof}}^{f, e} \times n_{\text{dof}}^{s, e}} \cdot \underbrace{\left\{ \delta \ddot{\mathbf{d}}^e \right\}}_{n_{\text{dof}}^{s, e} \times 1} + \underbrace{\left[\mathbf{k}_{u_f, u_f}^{\mathcal{I}_1^{\text{INT}}, e} \right]}_{n_{\text{dof}}^{f, e} \times n_{\text{dof}}^{f, e}} \cdot \underbrace{\left\{ \delta \ddot{\mathbf{d}}_f^e \right\}}_{n_{\text{dof}}^{f, e} \times 1} + \underbrace{\left[\mathbf{k}_{u_f, p_f}^{\mathcal{I}_1^{\text{INT}}, e} \right]}_{n_{\text{dof}}^{f, e} \times n_{\text{dof}}^{p_f, e}} \cdot \underbrace{\left\{ \delta \ddot{\boldsymbol{\pi}}^e \right\}}_{n_{\text{dof}}^{p_f, e} \times 1} \right), \quad (\text{C.75})$$

where we recover

$$\underbrace{\left[\mathbf{k}_{u_f, u}^{\mathcal{I}_1^{\text{INT}}, e} \right]}_{n_{\text{dof}}^{f, e} \times n_{\text{dof}}^{s, e}} = \int_{-1}^1 \rho^{\text{fR}, h^e} a_f^{h^e} (\beta \Delta t^2) \underbrace{\left\{ \mathbf{N}^{e, u_f} \right\}}_{n_{\text{dof}}^{f, e} \times 1}^T \underbrace{\left\{ \mathbf{B}^{e, u} \right\}}_{1 \times n_{\text{dof}}^{s, e}} A_j^e d\xi, \quad (\text{C.76})$$

$$\underbrace{\left[\mathbf{k}_{u_f, u_f}^{\mathcal{I}_1^{\text{INT}}, e} \right]}_{n_{\text{dof}}^{f, e} \times n_{\text{dof}}^{f, e}} = \int_{-1}^1 \rho_0^{f, h^e} \underbrace{\left\{ \mathbf{N}^{e, u_f} \right\}}_{n_{\text{dof}}^{f, e} \times 1}^T \underbrace{\left\{ \mathbf{N}^{e, u_f} \right\}}_{1 \times n_{\text{dof}}^{f, e}} A_j^e d\xi, \quad (\text{C.77})$$

$$\underbrace{\left[\mathbf{k}_{u_f, p_f}^{\mathcal{I}_1^{\text{INT}}, e} \right]}_{n_{\text{dof}}^{f, e} \times n_{\text{dof}}^{p_f, e}} = \int_{-1}^1 a_f^{h^e} \frac{\rho_0^{f, h^e}}{K_f^\eta} (\beta \Delta t^2) \underbrace{\left\{ \mathbf{N}^{e, u_f} \right\}}_{n_{\text{dof}}^{f, e} \times 1}^T \underbrace{\left\{ \mathbf{N}^{e, p_f} \right\}}_{1 \times n_{\text{dof}}^{p_f, e}} A_j^e d\xi. \quad (\text{C.78})$$

To derive the tangents for $\delta\mathcal{I}_2^{\text{INT}}$, we start by applying the FE discretization as follows:

$$\begin{aligned} \delta\mathcal{I}_2^{\text{INT}} = & \mathbf{A}_e^{n_e} \left\{ \mathbf{c}^{u_f, e} \right\}^T \cdot \left(\int_{-1}^1 \underbrace{\left\{ \mathbf{N}^{e, u_f} \right\}}_{n_{\text{dof}}^{f, e} \times 1}^T \left[\frac{n^{s, h^e}}{J^{h^e}} \frac{\partial p_f^{h^e}}{\partial X} \underbrace{\left\{ \mathbf{B}^{e, u} \right\}}_{1 \times n_{\text{dof}}^{s, e}} \underbrace{\left\{ \delta \ddot{\mathbf{d}}^e \right\}}_{n_{\text{dof}}^{s, e} \times 1} \right. \right. \\ & \left. \left. + n^{f, h^e} \underbrace{\left\{ \mathbf{B}^{e, p_f} \right\}}_{1 \times n_{\text{dof}}^{p_f, e}} \underbrace{\left\{ \delta \ddot{\boldsymbol{\pi}}^e \right\}}_{n_{\text{dof}}^{p_f, e} \times 1} \right] (\beta \Delta t^2) A_j^e d\xi \right). \end{aligned} \quad (\text{C.79})$$

Then, pulling out the variations $\delta \ddot{\mathbf{d}}^e$ & $\delta \ddot{\boldsymbol{\pi}}^e$ leaves us with

$$\delta\mathcal{I}_2^{\text{INT}} = \mathbf{A}_e^{n_e} \left\{ \mathbf{c}^{u_f, e} \right\}^T \cdot \left(\underbrace{\left[\mathbf{k}_{u_f, u}^{\mathcal{I}_2^{\text{INT}}, e} \right]}_{n_{\text{dof}}^{f, e} \times n_{\text{dof}}^{s, e}} \cdot \underbrace{\left\{ \delta \ddot{\mathbf{d}}^e \right\}}_{n_{\text{dof}}^{s, e} \times 1} + \underbrace{\left[\mathbf{k}_{u_f, p_f}^{\mathcal{I}_2^{\text{INT}}, e} \right]}_{n_{\text{dof}}^{f, e} \times n_{\text{dof}}^{p_f, e}} \cdot \underbrace{\left\{ \delta \ddot{\boldsymbol{\pi}}^e \right\}}_{n_{\text{dof}}^{p_f, e} \times 1} \right), \quad (\text{C.80})$$

where we recover the following tangents:

$$\underbrace{\left[\mathbf{k}_{u_f, u}^{\mathcal{I}_2^{\text{INT}, e}} \right]}_{n_{\text{dof}}^{f, e} \times n_{\text{dof}}^{s, e}} = \int_{-1}^1 \frac{n^{s, h^e}}{J^{h^e}} \frac{\partial p_f^{h^e}}{\partial X} (\beta \Delta t^2) \underbrace{\left\{ \mathbf{N}^{e, u_f} \right\}^T}_{n_{\text{dof}}^{f, e} \times 1} \underbrace{\left\{ \mathbf{B}^{e, u} \right\}}_{1 \times n_{\text{dof}}^{s, e}} A_j^e d\xi, \quad (\text{C.81})$$

$$\underbrace{\left[\mathbf{k}_{u_f, p_f}^{\mathcal{I}_2^{\text{INT}, e}} \right]}_{n_{\text{dof}}^{f, e} \times n_{\text{dof}}^{p_f, e}} = \int_{-1}^1 n^{f, h^e} (\beta \Delta t^2) \underbrace{\left\{ \mathbf{N}^{e, u_f} \right\}^T}_{n_{\text{dof}}^{f, e} \times 1} \underbrace{\left\{ \mathbf{B}^{e, p_f} \right\}}_{1 \times n_{\text{dof}}^{p_f, e}} A_j^e d\xi. \quad (\text{C.82})$$

To derive the tangents for $\delta \mathcal{I}_3^{\text{INT}}$, we start by applying the FE discretization as follows:

$$\begin{aligned} \delta \mathcal{I}_3^{\text{INT}} &= \mathbf{A}_e^{n_e} \underbrace{\left\{ \mathbf{c}^{u_f, e} \right\}^T}_{1 \times n_{\text{dof}}^{f, e}} \left(\int_{-1}^1 \underbrace{\left\{ \mathbf{N}^{e, u_f} \right\}^T}_{n_{\text{dof}}^{f, e} \times 1} \left[\left(\left[1 + \frac{2n^{s, h^e}}{n^{f, h^e}} - \frac{J^{h^e} \delta_k^{h^e}}{\hat{k}^{h^e}} \right] \right. \right. \right. \\ &\quad \times \left. \left. \frac{(n^{f, h^e})^2 \tilde{v}_f^{h^e}}{\hat{k}^{h^e}} (\beta \Delta t^2) - \frac{J^{h^e} (n^{f, h^e})^2}{\hat{k}^{h^e}} (\gamma \Delta t) \right) \right\} \underbrace{\left\{ \mathbf{N}^{e, u} \right\}}_{1 \times n_{\text{dof}}^{s, e}} \underbrace{\left\{ \delta \ddot{\mathbf{d}}^e \right\}}_{n_{\text{dof}}^{s, e} \times 1} \\ &\quad \left. + \frac{J^{h^e} (n^{f, h^e})^2}{\hat{k}^{h^e}} (\gamma \Delta t) \underbrace{\left\{ \mathbf{N}^{e, u_f} \right\}}_{1 \times n_{\text{dof}}^{f, e}} \underbrace{\left\{ \delta \ddot{\mathbf{d}}_f^e \right\}}_{n_{\text{dof}}^{f, e} \times 1} \right] A_j^e d\xi \Big). \end{aligned} \quad (\text{C.83})$$

Then, pulling out the variations $\delta \ddot{\mathbf{d}}^e$ and $\delta \ddot{\mathbf{d}}_f^e$ leaves us with

$$\delta \mathcal{I}_3^{\text{INT}} = \mathbf{A}_e^{n_e} \underbrace{\left\{ \mathbf{c}^{u_f, e} \right\}^T}_{1 \times n_{\text{dof}}^{f, e}} \cdot \left(\underbrace{\left[\mathbf{k}_{u_f, u}^{\mathcal{I}_1^{\text{INT}, e}} \right]}_{n_{\text{dof}}^{f, e} \times n_{\text{dof}}^{s, e}} \cdot \underbrace{\left\{ \delta \ddot{\mathbf{d}}^e \right\}}_{n_{\text{dof}}^{s, e} \times 1} + \underbrace{\left[\mathbf{k}_{u_f, u_f}^{\mathcal{I}_1^{\text{INT}, e}} \right]}_{n_{\text{dof}}^{f, e} \times n_{\text{dof}}^{f, e}} \cdot \underbrace{\left\{ \delta \ddot{\mathbf{d}}_f^e \right\}}_{n_{\text{dof}}^{f, e} \times 1} \right), \quad (\text{C.84})$$

whereby we recover the tangents

$$\underbrace{\left[\mathbf{k}_{u_f, u}^{\mathcal{I}_3^{\text{INT}, e}} \right]}_{n_{\text{dof}}^{f, e} \times n_{\text{dof}}^{s, e}} = \int_{-1}^1 \underbrace{\left\{ \mathbf{N}^{e, u_f} \right\}^T}_{n_{\text{dof}}^{f, e} \times 1} \left(\left[1 + \frac{2n^{s, h^e}}{n^{f, h^e}} - \frac{J^{h^e} \delta_k^{h^e}}{\hat{k}^{h^e}} \right] \frac{(n^{f, h^e})^2 \tilde{v}_f^{h^e}}{\hat{k}^{h^e}} (\beta \Delta t^2) \underbrace{\left\{ \mathbf{B}^{e, u} \right\}}_{1 \times n_{\text{dof}}^{s, e}} \right. \\ \left. - \frac{J^{h^e} (n^{f, h^e})^2}{\hat{k}^{h^e}} (\gamma \Delta t) \underbrace{\left\{ \mathbf{N}^{e, u} \right\}}_{1 \times n_{\text{dof}}^{s, e}} \right) A_j^e d\xi, \quad (\text{C.85})$$

$$\underbrace{\left[\mathbf{k}_{u_f, u_f}^{\mathcal{I}_3^{\text{INT}, e}} \right]}_{n_{\text{dof}}^{f, e} \times n_{\text{dof}}^{f, e}} = \int_{-1}^1 \frac{J^{h^e} (n^{f, h^e})^2}{\hat{k}^{h^e}} (\gamma \Delta t) \underbrace{\left\{ \mathbf{N}^{e, u_f} \right\}^T}_{n_{\text{dof}}^{f, e} \times 1} \underbrace{\left\{ \mathbf{N}^{e, u_f} \right\}}_{1 \times n_{\text{dof}}^{f, e}} A_j^e d\xi. \quad (\text{C.86})$$

To derive the tangents for $\delta\mathcal{I}_4^{\text{INT}}$, start by applying the FE discretization as follows:

$$\begin{aligned} \delta\mathcal{I}_4^{\text{INT}} = & \mathbf{A}_e^{n_e} \left\{ \mathbf{c}^{u_f, e} \right\}^T \cdot \left(\int_{-1}^1 \underbrace{\left\{ \mathbf{N}^{e, u_f} \right\}}_{n_{\text{dof}}^{f, e} \times 1}^T \left[\underbrace{\rho^{\text{fR}, h^e}}_{1 \times n_{\text{dof}}^{s, e}} \underbrace{\left\{ \mathbf{B}^{e, u} \right\}}_{n_{\text{dof}}^{s, e} \times 1} \underbrace{\left\{ \delta \ddot{\mathbf{d}}^e \right\}}_{n_{\text{dof}}^{s, e} \times 1} \right. \right. \\ & \left. \left. + \frac{Jh^e n^{f, h^e} \rho^{\text{fR}, h^e}}{K_f^\eta} \underbrace{\left\{ \mathbf{N}^{e, p_f} \right\}}_{1 \times n_{\text{dof}}^{p_f, e}} \underbrace{\left\{ \delta \ddot{\boldsymbol{\pi}}^e \right\}}_{n_{\text{dof}}^{p_f, e} \times 1} \right] (\beta \Delta t^2) g A j^e d\xi \right). \end{aligned} \quad (\text{C.87})$$

Then, pulling out the variations $\delta \ddot{\mathbf{d}}^e$ and $\delta \ddot{\boldsymbol{\pi}}^e$ leaves us with

$$\delta\mathcal{I}_4^{\text{INT}} = \mathbf{A}_e^{n_e} \left\{ \mathbf{c}^{u_f, e} \right\}^T \cdot \left(\underbrace{\left[\mathbf{k}_{u_f, u}^{\mathcal{I}_4^{\text{INT}}, e} \right]}_{n_{\text{dof}}^{f, e} \times n_{\text{dof}}^{s, e}} \cdot \underbrace{\left\{ \delta \ddot{\mathbf{d}}^e \right\}}_{n_{\text{dof}}^{s, e} \times 1} + \underbrace{\left[\mathbf{k}_{u_f, p_f}^{\mathcal{I}_4^{\text{INT}}, e} \right]}_{n_{\text{dof}}^{f, e} \times n_{\text{dof}}^{p_f, e}} \cdot \underbrace{\left\{ \delta \ddot{\boldsymbol{\pi}}^e \right\}}_{n_{\text{dof}}^{p_f, e} \times 1} \right), \quad (\text{C.88})$$

where we recover

$$\underbrace{\left[\mathbf{k}_{u_f, u}^{\mathcal{I}_4^{\text{INT}}, e} \right]}_{n_{\text{dof}}^{f, e} \times n_{\text{dof}}^{s, e}} = \int_{-1}^1 \rho^{\text{fR}, h^e} g (\beta \Delta t^2) \underbrace{\left\{ \mathbf{N}^{e, u_f} \right\}}_{n_{\text{dof}}^{f, e} \times 1}^T \underbrace{\left\{ \mathbf{B}^{e, u} \right\}}_{1 \times n_{\text{dof}}^{s, e}} A j^e d\xi, \quad (\text{C.89})$$

$$\underbrace{\left[\mathbf{k}_{u_f, p_f}^{\mathcal{I}_4^{\text{INT}}, e} \right]}_{n_{\text{dof}}^{f, e} \times n_{\text{dof}}^{p_f, e}} = \int_{-1}^1 \frac{Jh^e n^{f, h^e} \rho^{\text{fR}, h^e}}{K_f^\eta} g (\beta \Delta t^2) \underbrace{\left\{ \mathbf{N}^{e, u_f} \right\}}_{n_{\text{dof}}^{f, e} \times 1}^T \underbrace{\left\{ \mathbf{N}^{e, p_f} \right\}}_{1 \times n_{\text{dof}}^{p_f, e}} A j^e d\xi. \quad (\text{C.90})$$

When the pore fluid viscous stress tensor is considered, we start by applying the FE discretization to $\delta\mathcal{I}_5^{\text{INT}}$ as follows.

$$\begin{aligned} \delta\mathcal{I}_5^{\text{INT}} = & \mathbf{A}_e^{n_e} \left\{ \mathbf{c}^{u_f, e} \right\}^T \cdot \left(\int_{-1}^1 \underbrace{\left\{ \mathbf{B}^{e, u_f} \right\}}_{n_{\text{dof}}^{f, e} \times 1}^T (\kappa_f + 2\mu_f) \left[\frac{\partial v_f}{\partial X} F_{11}^{-2} (n^s - n^f) \beta \Delta t^2 \underbrace{\left\{ \mathbf{B}^{e, u} \right\}}_{1 \times n_{\text{dof}}^{s, e}}^T \underbrace{\left\{ \delta \ddot{\mathbf{d}}^e \right\}}_{n_{\text{dof}}^{s, e} \times 1} \right. \right. \\ & \left. \left. + n^f F_{11}^{-1} \gamma \Delta t \underbrace{\left\{ \mathbf{B}^{e, u_f} \right\}}_{1 \times n_{\text{dof}}^{f, e}}^T \underbrace{\left\{ \delta \ddot{\mathbf{d}}_f^e \right\}}_{n_{\text{dof}}^{f, e} \times 1} \right] A j^e \right). \end{aligned} \quad (\text{C.91})$$

Then, pulling out the variations $\delta \ddot{\mathbf{d}}^e$ and $\delta \ddot{\mathbf{d}}_f^e$ leaves us with

$$\delta\mathcal{I}_5^{\text{INT}} = \mathbf{A}_e^{n_e} \left\{ \mathbf{c}^{u_f, e} \right\}^T \cdot \left(\underbrace{\left[\mathbf{k}_{u_f, u}^{\mathcal{I}_5^{\text{INT}}, e} \right]}_{n_{\text{dof}}^{f, e} \times n_{\text{dof}}^{s, e}} \cdot \underbrace{\left\{ \delta \ddot{\mathbf{d}}^e \right\}}_{n_{\text{dof}}^{s, e} \times 1} + \underbrace{\left[\mathbf{k}_{u_f, u_f}^{\mathcal{I}_5^{\text{INT}}, e} \right]}_{n_{\text{dof}}^{f, e} \times n_{\text{dof}}^{f, e}} \cdot \underbrace{\left\{ \delta \ddot{\mathbf{d}}_f^e \right\}}_{n_{\text{dof}}^{f, e} \times 1} \right), \quad (\text{C.92})$$

where we recover the following tangent matrices:

$$\underbrace{\left[\mathbf{k}_{u_f, u}^{\mathcal{I}_5^{\text{INT}}, e} \right]}_{n_{\text{dof}}^{f, e} \times n_{\text{dof}}^{s, e}} = \int_{-1}^1 (\kappa + 2\mu_f) \left(\frac{\partial v_f^{h^e}}{\partial X} (F_{11}^{h^e})^{-2} (n^{s, h^e} - n^{f, h^e}) \beta \Delta t^2 \right) \underbrace{\left\{ \mathbf{B}^{e, u_f} \right\}^T}_{n_{\text{dof}}^{f, e} \times 1} \underbrace{\left\{ \mathbf{B}^{e, u} \right\}}_{1 \times n_{\text{dof}}^{s, e}} A_j^e d\xi, \quad (\text{C.93})$$

$$\underbrace{\left[\mathbf{k}_{u_f, u_f}^{\mathcal{I}_5^{\text{INT}}, e} \right]}_{n_{\text{dof}}^{f, e} \times n_{\text{dof}}^{f, e}} = \int_{-1}^1 (\kappa_f + 2\mu_f) n^{f, h^e} (F_{11}^{h^e})^{-1} \gamma \Delta t \underbrace{\left\{ \mathbf{B}^{e, u_f} \right\}^T}_{n_{\text{dof}}^{f, e} \times 1} \underbrace{\left\{ \mathbf{B}^{e, u_f} \right\}}_{1 \times n_{\text{dof}}^{f, e}} A_j^e d\xi. \quad (\text{C.94})$$

The tangent for $\delta \mathcal{H}_1^{\text{INT}}$ remains unchanged from (\mathbf{u} - p_f) formulation: refer to (C.28).

To derive the tangents for $\delta \mathcal{H}_2^{\text{INT}}$, we start by applying the FE discretization as follows:

$$\begin{aligned} \delta \mathcal{H}_2^{\text{INT}} &= \mathbf{A}_e^{n_e} \underbrace{\left\{ \mathbf{c}^{p_f, e} \right\}^T}_{1 \times n_{\text{dof}}^{p_f, e}} \cdot \left(\int_{-1}^1 \underbrace{\left\{ \mathbf{N}^{e, p_f} \right\}^T}_{n_{\text{dof}}^{p_f, e} \times 1} \left[\left([n^f \tilde{v}_f]^{h^e} - \hat{k}^{h^e} \frac{\partial p_f^{h^e}}{\partial X} (F_{11}^{h^e})^{-1} \right) (\beta \Delta t^2) \right. \right. \\ &\quad \times \underbrace{\left\{ \mathbf{B}^{e, p_f} \right\}}_{1 \times n_{\text{dof}}^{p_f, e}} \underbrace{\left\{ \delta \tilde{\boldsymbol{\pi}}^e \right\}}_{n_{\text{dof}}^{p_f, e} \times 1} - \hat{k}^{h^e} \frac{\partial p_f^{h^e}}{\partial X} (a_f^{h^e} + g) \frac{\rho^{\text{fR}, h^e}}{K_f^\eta} (\beta \Delta t^2) \underbrace{\left\{ \mathbf{N}^{e, p_f} \right\}}_{1 \times n_{\text{dof}}^{p_f, e}} \underbrace{\left\{ \delta \tilde{\boldsymbol{\pi}}^e \right\}}_{n_{\text{dof}}^{p_f, e} \times 1} \\ &\quad \left. \left. + \frac{\partial p_f^{h^e}}{\partial X} \left(\frac{\delta \hat{k}^{h^e}}{\hat{k}^{h^e}} (n^f \tilde{v}_f)^{h^e} + \hat{k}^{h^e} \frac{\partial p_f^{h^e}}{\partial X} (F_{11}^{h^e})^{-2} \right) (\beta \Delta t^2) \right. \right. \\ &\quad \left. \left. \times \underbrace{\left\{ \mathbf{B}^{e, u} \right\}}_{1 \times n_{\text{dof}}^{s, e}} \underbrace{\left\{ \delta \ddot{\mathbf{d}}^e \right\}}_{n_{\text{dof}}^{d, e} \times 1} - \frac{\partial p_f^{h^e}}{\partial X} \hat{k}^{h^e} \rho^{\text{fR}, h^e} \underbrace{\left\{ \mathbf{N}^{e, u_f} \right\}}_{1 \times n_{\text{dof}}^{f, e}} \underbrace{\left\{ \delta \ddot{\mathbf{d}}_f^e \right\}}_{n_{\text{dof}}^{f, e} \times 1} \right] \frac{A}{K_f^\eta} j^e d\xi \right). \end{aligned} \quad (\text{C.95})$$

Then, pulling out the variations $\delta \ddot{\mathbf{d}}^e$, $\delta \ddot{\mathbf{d}}_f^e$, and $\delta \tilde{\boldsymbol{\pi}}^e$ leaves us with

$$\delta \mathcal{H}_2^{\text{INT}} = \mathbf{A}_e^{n_e} \underbrace{\left\{ \mathbf{c}^{p_f, e} \right\}^T}_{1 \times n_{\text{dof}}^{p_f, e}} \cdot \left(\underbrace{\left[\mathbf{k}_{p_f, u}^{\mathcal{H}_2^{\text{INT}}, e} \right]}_{n_{\text{dof}}^{p_f, e} \times n_{\text{dof}}^{s, e}} \cdot \underbrace{\left\{ \delta \ddot{\mathbf{d}}^e \right\}}_{n_{\text{dof}}^{s, e} \times 1} + \underbrace{\left[\mathbf{k}_{p_f, u}^{\mathcal{H}_2^{\text{INT}}, e} \right]}_{n_{\text{dof}}^{p_f, e} \times n_{\text{dof}}^{f, e}} \cdot \underbrace{\left\{ \delta \ddot{\mathbf{d}}_f^e \right\}}_{n_{\text{dof}}^{f, e} \times 1} + \underbrace{\left[\mathbf{k}_{p_f, p_f}^{\mathcal{H}_2^{\text{INT}}, e} \right]}_{n_{\text{dof}}^{p_f, e} \times n_{\text{dof}}^{p_f, e}} \cdot \underbrace{\left\{ \delta \tilde{\boldsymbol{\pi}}^e \right\}}_{n_{\text{dof}}^{p_f, e} \times 1} \right), \quad (\text{C.96})$$

whereby we recover

$$\underbrace{\left[\mathbf{k}_{p_f, u}^{\mathcal{H}_2^{\text{INT}, e}} \right]}_{n_{\text{dof}}^{p_f, e} \times n_{\text{dof}}^{s, e}} = \int_{-1}^1 \frac{\partial p_f^{h^e}}{\partial X} \left(\frac{\delta \hat{k}^{h^e}}{\hat{k}^{h^e}} (n^f \tilde{v}_f)^{h^e} + \hat{k}^{h^e} \frac{\partial p_f^{h^e}}{\partial X} (F_{11}^{h^e})^{-2} \right) (\beta \Delta t^2) \underbrace{\left\{ \mathbf{N}^{e, p_f} \right\}^T}_{n_{\text{dof}}^{p_f, e} \times 1} \underbrace{\left\{ \mathbf{B}^{e, u} \right\}}_{1 \times n_{\text{dof}}^{s, e}} \frac{1}{K_f^\eta} A j^e d\xi, \quad (\text{C.97})$$

$$\underbrace{\left[\mathbf{k}_{p_f, u_f}^{\mathcal{H}_2^{\text{INT}, e}} \right]}_{n_{\text{dof}}^{p_f, e} \times n_{\text{dof}}^{s, e}} = - \int_{-1}^1 \hat{k}^{h^e} \rho^{\text{fR}, h^e} \frac{\partial p_f^{h^e}}{\partial X} \frac{1}{K_f^\eta} \underbrace{\left\{ \mathbf{N}^{e, p_f} \right\}^T}_{n_{\text{dof}}^{p_f, e} \times 1} \underbrace{\left\{ \mathbf{N}^{e, u_f} \right\}}_{1 \times n_{\text{dof}}^{f, e}} A j^e d\xi, \quad (\text{C.98})$$

$$\begin{aligned} \underbrace{\left[\mathbf{k}_{p_f, p_f}^{\mathcal{H}_2^{\text{INT}, e}} \right]}_{n_{\text{dof}}^{p_f, e} \times n_{\text{dof}}^{p_f, e}} &= \int_{-1}^1 \underbrace{\left\{ \mathbf{N}^{e, p_f} \right\}^T}_{n_{\text{dof}}^{p_f, e} \times 1} \left(\left[(n^f \tilde{v}_f)^{h^e} - \hat{k}^{h^e} \frac{\partial p_f^{h^e}}{\partial X} (F_{11}^{h^e})^{-1} \right] \underbrace{\left\{ \mathbf{B}^{e, p_f} \right\}}_{1 \times n_{\text{dof}}^{p_f, e}} \right. \\ &\quad \left. - \hat{k}^{h^e} \frac{\partial p_f^{h^e}}{\partial X} (a_f^{h^e} + g) \frac{\rho^{\text{fR}, h^e}}{K_f^\eta} \underbrace{\left\{ \mathbf{N}^{e, p_f} \right\}}_{1 \times n_{\text{dof}}^{p_f, e}} \right) \frac{1}{K_f^\eta} (\beta \Delta t^2) A j^e d\xi. \end{aligned} \quad (\text{C.99})$$

When the pore fluid viscous stress tensor is considered, we start by applying the FE discretization

to $\delta\mathcal{H}_2^{\text{INT}}$ as follows:

$$\begin{aligned}
\delta\mathcal{H}_2^{\text{INT}} = & \underbrace{\mathbf{A}_e^{n_e}}_{1 \times n_{\text{dof}}^{p_f, e}} \left\{ \mathbf{c}^{p_f, e} \right\}^T \cdot \left(\int_{-1}^1 \underbrace{\left\{ \mathbf{N}^{e, p_f} \right\}^T}_{n_{\text{dof}}^{p_f, e} \times 1} \left[\left([n^f \tilde{v}_f]^{h^e} - \hat{k}^{h^e} \frac{\partial p_f^{h^e}}{\partial X} (F_{11}^{h^e})^{-1} \right) (\beta \Delta t^2) \right. \right. \\
& \times \underbrace{\left\{ \mathbf{B}^{e, p_f} \right\}}_{1 \times n_{\text{dof}}^{p_f, e}} \underbrace{\left\{ \delta \ddot{\boldsymbol{\pi}}^e \right\}}_{n_{\text{dof}}^{p_f, e} \times 1} - \hat{k}^{h^e} \frac{\partial p_f^{h^e}}{\partial X} (a_f^{h^e} + g) \frac{\rho^{\text{fR}, h^e}}{K_f^\eta} (\beta \Delta t^2) \underbrace{\left\{ \mathbf{N}^{e, p_f} \right\}}_{1 \times n_{\text{dof}}^{p_f, e}} \underbrace{\left\{ \delta \ddot{\boldsymbol{\pi}}^e \right\}}_{n_{\text{dof}}^{p_f, e} \times 1} \\
& + \frac{\partial p_f^{h^e}}{\partial X} \left(\frac{\delta \hat{k}^{h^e}}{\hat{k}^{h^e}} (n^f \tilde{v}_f)^{h^e} + \hat{k}^{h^e} \frac{\partial p_f^{h^e}}{\partial X} (F_{11}^{h^e})^{-2} \right. \\
& + \hat{k}^{h^e} (F_{11}^{h^e})^{-3} (\kappa_f + 2\mu_f) \left[\frac{\partial n^{f, h^e}}{\partial X} \frac{\partial v_f^{h^e}}{\partial X} \left(\frac{n^{s, h^e}}{(n^{f, h^e})^2} + \frac{5}{n^{f, h^e}} \right) + 2 \frac{\partial^2 v_f^{h^e}}{\partial X^2} \right] \left. \right) (\beta \Delta t^2) \times \\
& \underbrace{\left\{ \mathbf{B}^{e, u} \right\}}_{1 \times n_{\text{dof}}^{s, e}} \underbrace{\left\{ \delta \ddot{\mathbf{d}}^e \right\}}_{n_{\text{dof}}^{s, e} \times 1} - \frac{\partial p_f^{h^e}}{\partial X} \hat{k}^{h^e} \rho^{\text{fR}, h^e} \underbrace{\left\{ \mathbf{N}^{e, u_f} \right\}}_{1 \times n_{\text{dof}}^{f, e}} \underbrace{\left\{ \delta \ddot{\mathbf{d}}_f^e \right\}}_{n_{\text{dof}}^{f, e} \times 1} \\
& - \hat{k}^{h^e} \frac{\partial p_f^{h^e}}{\partial X} \frac{n^{s, h^e}}{n^{f, h^e} (F_{11}^{h^e})^{-4}} \frac{\partial v_f^{h^e}}{\partial X} (\kappa_f + 2\mu_f) (\beta \Delta t^2) \underbrace{\left\{ \mathbf{H}^{e, u} \right\}}_{1 \times n_{\text{dof}}^{s, e}} \underbrace{\left\{ \delta \ddot{\mathbf{d}}^e \right\}}_{n_{\text{dof}}^{s, e} \times 1} \\
& - \frac{\partial p_f^{h^e}}{\partial X} \hat{k}^{h^e} (\kappa_f + 2\mu_f) (F_{11}^{h^e})^{-2} (\gamma \Delta t) \left(\frac{1}{n^{f, h^e}} \frac{\partial n^{f, h^e}}{\partial X} \underbrace{\left\{ \mathbf{B}^{e, u_f} \right\}}_{1 \times n_{\text{dof}}^{f, e}} + \underbrace{\left\{ \mathbf{H}^{e, u_f} \right\}}_{1 \times n_{\text{dof}}^{f, e}} \right) \underbrace{\left\{ \delta \ddot{\mathbf{d}}_f^e \right\}}_{n_{\text{dof}}^{f, e} \times 1} \left. \right] \frac{A}{K_f^\eta} j^e d\xi \Bigg). \tag{C.100}
\end{aligned}$$

Then, pulling out the variations $\delta \ddot{\mathbf{d}}^e$, $\delta \ddot{\mathbf{d}}_f^e$, and $\delta \ddot{\boldsymbol{\pi}}^e$ leaves us with

$$\delta\mathcal{H}_2^{\text{INT}} = \underbrace{\mathbf{A}_e^{n_e}}_{1 \times n_{\text{dof}}^{p_f, e}} \left\{ \mathbf{c}^{p_f, e} \right\}^T \cdot \left(\underbrace{\left[\mathbf{k}_{p_f, u}^{\mathcal{H}_2^{\text{INT}, e}} \right]}_{n_{\text{dof}}^{p_f, e} \times n_{\text{dof}}^{s, e}} \cdot \underbrace{\left\{ \delta \ddot{\mathbf{d}}^e \right\}}_{n_{\text{dof}}^{s, e} \times 1} + \underbrace{\left[\mathbf{k}_{p_f, u}^{\mathcal{H}_2^{\text{INT}, e}} \right]}_{n_{\text{dof}}^{p_f, e} \times n_{\text{dof}}^{f, e}} \cdot \underbrace{\left\{ \delta \ddot{\mathbf{d}}_f^e \right\}}_{n_{\text{dof}}^{f, e} \times 1} + \underbrace{\left[\mathbf{k}_{p_f, p_f}^{\mathcal{H}_2^{\text{INT}, e}} \right]}_{n_{\text{dof}}^{p_f, e} \times n_{\text{dof}}^{p_f, e}} \cdot \underbrace{\left\{ \delta \ddot{\boldsymbol{\pi}}^e \right\}}_{n_{\text{dof}}^{p_f, e} \times 1} \right), \tag{C.101}$$

whereby we recover Eq. (C.99), with new additions

$$\begin{aligned} \underbrace{\left[\mathbf{k}_{p_f, u}^{\mathcal{H}_2^{\text{INT}, e}} \right]}_{n_{\text{dof}}^{p_f, e} \times n_{\text{dof}}^{s, e}} &= \int_{-1}^1 \underbrace{\left\{ \mathbf{N}^{e, p_f} \right\}^T}_{n_{\text{dof}}^{p_f, e} \times 1} \frac{\partial p_f^{h^e}}{\partial X} \left(\left[\frac{\delta_{\hat{k}}^{h^e}}{\hat{k}^{h^e}} (n^f \tilde{v}_f)^{h^e} + \hat{k}^{h^e} \frac{\partial p_f^{h^e}}{\partial X} (F_{11}^{h^e})^{-2} \right. \right. \\ &+ \hat{k}^{h^e} (F_{11}^{h^e})^{-3} (\kappa_f + 2\mu_f) \left(\left[\frac{n^{s, h^e}}{(n^{f, h^e})^2} + \frac{5}{n^{f, h^e}} \right] \frac{\partial n^{f, h^e}}{\partial X} \frac{\partial v_f^{h^e}}{\partial X} + 2 \frac{\partial^2 v_f^{h^e}}{\partial X^2} \right) \underbrace{\left\{ \mathbf{B}^{e, u} \right\}}_{1 \times n_{\text{dof}}^{s, e}} \\ &\left. \left. - \hat{k}^{h^e} \frac{n^{s, h^e}}{n^{f, h^e}} (F_{11}^{h^e})^{-4} \frac{\partial v_f^{h^e}}{\partial X} (\kappa + 2\mu_f) \underbrace{\left\{ \mathbf{H}^{e, u} \right\}}_{1 \times n_{\text{dof}}^{s, e}} \right) (\beta \Delta t^2) \frac{1}{K_f^\eta} A_j^e d\xi, \end{aligned} \quad (\text{C.102})$$

$$\begin{aligned} \underbrace{\left[\mathbf{k}_{p_f, u_f}^{\mathcal{H}_2^{\text{INT}, e}} \right]}_{n_{\text{dof}}^{p_f, e} \times n_{\text{dof}}^{s, e}} &= - \int_{-1}^1 \underbrace{\left\{ \mathbf{N}^{e, p_f} \right\}^T}_{n_{\text{dof}}^{p_f, e} \times 1} \hat{k}^{h^e} \frac{\partial p_f^{h^e}}{\partial X} \frac{1}{K_f^\eta} \left(\rho^{\text{fR}, h^e} \underbrace{\left\{ \mathbf{N}^{e, u_f} \right\}}_{1 \times n_{\text{dof}}^{f, e}} + (\kappa_f + 2\mu_f) (F_{11}^{h^e})^{-2} (\gamma \Delta t) \times \right. \\ &\left. \left[\frac{1}{n^{f, h^e}} \frac{\partial n^{f, h^e}}{\partial X} \underbrace{\left\{ \mathbf{B}^{e, u_f} \right\}}_{1 \times n_{\text{dof}}^{f, e}} + \underbrace{\left\{ \mathbf{H}^{e, u_f} \right\}}_{1 \times n_{\text{dof}}^{f, e}} \right] \right) A_j^e d\xi. \end{aligned} \quad (\text{C.103})$$

To derive the tangents for $\delta \mathcal{H}_4^{\text{INT}}$, we start by applying the FE discretization as follows:

$$\begin{aligned} \delta \mathcal{H}_4^{\text{INT}} &= \mathbf{A}_e^{n_e} \underbrace{\left\{ \mathbf{c}^{p_f, e} \right\}^T}_{1 \times n_{\text{dof}}^{p_f, e}} \cdot \left(\int_{-1}^1 \underbrace{\left\{ \mathbf{B}^{e, p_f} \right\}^T}_{n_{\text{dof}}^{p_f, e} \times 1} \rho^{\text{fR}, h^e} \left[\delta_{\hat{k}}^{h^e} (a_f^{h^e} + g) (\beta \Delta t^2) \underbrace{\left\{ \mathbf{B}^{e, u} \right\}}_{1 \times n_{\text{dof}}^{s, e}} \underbrace{\left\{ \delta \ddot{\mathbf{d}}^e \right\}}_{n_{\text{dof}}^{s, e} \times 1} \right. \right. \\ &\left. \left. + \hat{k}^{h^e} (a_f^{h^e} + g) \frac{1}{K_f^\eta} (\beta \Delta t^2) \underbrace{\left\{ \mathbf{N}^{e, p_f} \right\}}_{1 \times n_{\text{dof}}^{p_f, e}} \underbrace{\left\{ \delta \ddot{\boldsymbol{\pi}}^e \right\}}_{n_{\text{dof}}^{p_f, e} \times 1} + \hat{k}^{h^e} \underbrace{\left\{ \mathbf{N}^{e, u_f} \right\}}_{1 \times n_{\text{dof}}^{f, e}} \underbrace{\left\{ \delta \ddot{\mathbf{d}}_f^e \right\}}_{n_{\text{dof}}^{f, e} \times 1} \right] A_j^e d\xi \right). \end{aligned} \quad (\text{C.104})$$

Then, pulling out the variations $\delta \ddot{\mathbf{d}}^e$, $\delta \ddot{\mathbf{d}}_f^e$, and $\delta \ddot{\boldsymbol{\pi}}^e$ leaves us with

$$\delta \mathcal{H}_4^{\text{INT}} = \mathbf{A}_e^{n_e} \underbrace{\left\{ \mathbf{c}^{p_f, e} \right\}^T}_{1 \times n_{\text{dof}}^{p_f, e}} \cdot \left(\underbrace{\left[\mathbf{k}_{p_f, u}^{\mathcal{H}_4^{\text{INT}, e}} \right]}_{n_{\text{dof}}^{p_f, e} \times n_{\text{dof}}^{s, e}} \cdot \underbrace{\left\{ \delta \ddot{\mathbf{d}}^e \right\}}_{n_{\text{dof}}^{s, e} \times 1} + \underbrace{\left[\mathbf{k}_{p_f, u_f}^{\mathcal{H}_4^{\text{INT}, e}} \right]}_{n_{\text{dof}}^{p_f, e} \times n_{\text{dof}}^{f, e}} \cdot \underbrace{\left\{ \delta \ddot{\mathbf{d}}_f^e \right\}}_{n_{\text{dof}}^{f, e} \times 1} + \underbrace{\left[\mathbf{k}_{p_f, p_f}^{\mathcal{H}_4^{\text{INT}, e}} \right]}_{n_{\text{dof}}^{p_f, e} \times n_{\text{dof}}^{p_f, e}} \cdot \underbrace{\left\{ \delta \ddot{\boldsymbol{\pi}}^e \right\}}_{n_{\text{dof}}^{p_f, e} \times 1} \right), \quad (\text{C.105})$$

whereby we recover the tangents

$$\underbrace{\left[\mathbf{k}_{p_f, u}^{\mathcal{H}_4^{\text{INT}, e}} \right]}_{n_{\text{dof}}^{p_f, e} \times n_{\text{dof}}^{s, e}} = \int_{-1}^1 \delta_{\hat{k}}^{h^e} (a_f^{h^e} + g) \rho^{\text{fR}, h^e} (\beta \Delta t^2) \underbrace{\left\{ \mathbf{B}^{e, p_f} \right\}^T}_{n_{\text{dof}}^{p_f, e} \times 1} \underbrace{\left\{ \mathbf{B}^{e, u} \right\}}_{1 \times n_{\text{dof}}^{s, e}} A_j^e d\xi, \quad (\text{C.106})$$

$$\underbrace{\left[\mathbf{k}_{p_f, u_f}^{\mathcal{H}_4^{\text{INT}, e}} \right]}_{n_{\text{dof}}^{p_f, e} \times n_{\text{dof}}^{f, e}} = \int_{-1}^1 \hat{k}^{h^e} \rho^{\text{fR}, h^e} \underbrace{\left\{ \mathbf{B}^{e, p_f} \right\}^T}_{n_{\text{dof}}^{p_f, e} \times 1} \underbrace{\left\{ \mathbf{N}^{e, u} \right\}}_{1 \times n_{\text{dof}}^{s, e}} A_j^e d\xi, \quad (\text{C.107})$$

$$\underbrace{\left[\mathbf{k}_{p_f, p_f}^{\mathcal{H}_4^{\text{INT}, e}} \right]}_{n_{\text{dof}}^{p_f, e} \times n_{\text{dof}}^{p_f, e}} = \int_{-1}^1 \hat{k}^{h^e} (a_f^{h^e} + g) \frac{\rho^{\text{fR}, h^e}}{K_f \eta} (\beta \Delta t^2) \underbrace{\left\{ \mathbf{B}^{e, p_f} \right\}^T}_{n_{\text{dof}}^{p_f, e} \times 1} \underbrace{\left\{ \mathbf{N}^{e, p_f} \right\}}_{1 \times n_{\text{dof}}^{p_f, e}} A_j^e d\xi \quad (\text{C.108})$$

To derive the tangents for $\delta \mathcal{H}_5^{\text{INT}}$, when the pore fluid viscous stress tensor is considered, we start by applying the FE discretization as follows.

$$\begin{aligned} \delta \mathcal{H}_5^{\text{INT}} = & - \mathbf{A}_e^{n_e} \underbrace{\left\{ \mathbf{c}^{p_f, e} \right\}^T}_{1 \times n_{\text{dof}}^{p_f, e}} \cdot \left(\int_{-1}^1 \underbrace{\left\{ \mathbf{B}^{e, p_f} \right\}^T}_{n_{\text{dof}}^{p_f, e} \times 1} \hat{k}^{h^e} \left(\left[\frac{\delta_{\hat{k}}^{h^e}}{n^{f, h^e} \hat{k}^{h^e}} \frac{\partial \sigma_{11}^{f, h^e}}{\partial X} (F_{11}^{h^e})^2 \right. \right. \right. \\ & - \left. \left. \left[\frac{\partial n^{f, h^e}}{\partial X} \frac{\partial v_f^{h^e}}{\partial X} \left(\frac{n^{s, h^e}}{(n^{f, h^e})^2} + \frac{5}{n^{f, h^e}} \right) + 2 \frac{\partial^2 v_f^{h^e}}{\partial X^2} \right] (\kappa_f + 2\mu_f) \right\} \mathbf{B}^{e, u} \right)_{1 \times n_{\text{dof}}^{s, e}} \\ & + \frac{n_0^s}{n^{f, h^e}} (F_{11}^{h^e})^{-2} \frac{\partial v_f^{h^e}}{\partial X} (\kappa_f + 2\mu_f) \underbrace{\left\{ \mathbf{H}^{e, u} \right\}}_{1 \times n_{\text{dof}}^{s, e}} \left. \right) (F_{11}^{h^e})^{-3} (\beta \Delta t^2) \underbrace{\left\{ \delta \ddot{\mathbf{d}}^e \right\}}_{n_{\text{dof}}^{s, e} \times 1} \\ & + \left[\frac{1}{n^{f, h^e}} \frac{\partial n^{f, h^e}}{\partial X} \underbrace{\left\{ \mathbf{B}^{e, u_f} \right\}}_{1 \times n_{\text{dof}}^{f, e}} + \underbrace{\left\{ \mathbf{H}^{e, u_f} \right\}}_{1 \times n_{\text{dof}}^{f, e}} \right] (\kappa_f + 2\mu_f) (F_{11}^{h^e})^{-2} (\gamma \Delta t) \underbrace{\left\{ \delta \ddot{\mathbf{d}}_f^e \right\}}_{n_{\text{dof}}^{f, e} \times 1} A_j^e d\xi \right). \quad (\text{C.109}) \end{aligned}$$

Then, pulling out the variations $\delta \ddot{\mathbf{d}}^e$ and $\delta \ddot{\mathbf{d}}_f^e$ leaves us with

$$\delta \mathcal{H}_5^{\text{INT}} = \mathbf{A}_e^{n_e} \underbrace{\left\{ \mathbf{c}^{p_f, e} \right\}^T}_{1 \times n_{\text{dof}}^{p_f, e}} \cdot \left(\underbrace{\left[\mathbf{k}_{p_f, u}^{\mathcal{H}_4^{\text{INT}, e}} \right]}_{n_{\text{dof}}^{p_f, e} \times n_{\text{dof}}^{s, e}} \cdot \underbrace{\left\{ \delta \ddot{\mathbf{d}}^e \right\}}_{n_{\text{dof}}^{s, e} \times 1} + \underbrace{\left[\mathbf{k}_{p_f, u_f}^{\mathcal{H}_5^{\text{INT}, e}} \right]}_{n_{\text{dof}}^{p_f, e} \times n_{\text{dof}}^{f, e}} \cdot \underbrace{\left\{ \delta \ddot{\mathbf{d}}_f^e \right\}}_{n_{\text{dof}}^{f, e} \times 1} \right), \quad (\text{C.110})$$

whereby we recover the tangents

$$\begin{aligned}
\underbrace{\left[\mathbf{k}_{p_f, u}^{\mathcal{H}_5^{\text{INT}, e}} \right]}_{n_{\text{dof}}^{p_f, e} \times n_{\text{dof}}^{s, e}} &= - \int_{-1}^1 \underbrace{\left\{ \mathbf{B}^{e, p_f} \right\}^T}_{n_{\text{dof}}^{p_f, e} \times 1} \hat{\mathbf{k}}^{h^e} \left(\left[\frac{\delta_k^{h^e}}{n^{f, h^e} \hat{k}^{h^e}} \frac{\partial \sigma_{11}^{f, h^e}}{\partial X} (F_{11}^{h^e})^2 \right. \right. \\
&\quad \left. \left. - \left(\frac{\partial n^{f, h^e}}{\partial X} \frac{\partial v_f^{h^e}}{\partial X} \left(\frac{n^{s, h^e}}{(n^{f, h^e})^2} + \frac{5}{n^{f, h^e}} \right) + 2 \frac{\partial^2 v_f^{h^e}}{\partial X^2} \right) (\kappa_f + 2\mu_f) \right] \underbrace{\left\{ \mathbf{B}^{e, u} \right\}}_{1 \times n_{\text{dof}}^{s, e}} \right. \\
&\quad \left. + \frac{n_0^s}{n^{f, h^e}} (F_{11}^{h^e})^{-2} \frac{\partial v_f^{h^e}}{\partial X} (\kappa_f + 2\mu_f) \underbrace{\left\{ \mathbf{H}^{e, u} \right\}}_{1 \times n_{\text{dof}}^{s, e}} \right) (F_{11}^{h^e})^{-3} (\beta \Delta t^2) A j^e d\xi, \tag{C.111}
\end{aligned}$$

$$\begin{aligned}
\underbrace{\left[\mathbf{k}_{p_f, u_f}^{\mathcal{H}_5^{\text{INT}, e}} \right]}_{n_{\text{dof}}^{p_f, e} \times n_{\text{dof}}^{f, e}} &= - \int_{-1}^1 \underbrace{\left\{ \mathbf{B}^{e, p_f} \right\}^T}_{n_{\text{dof}}^{p_f, e} \times 1} \hat{\mathbf{k}}^{h^e} \left[\frac{1}{n^{f, h^e}} \frac{\partial n^{f, h^e}}{\partial X} \underbrace{\left\{ \mathbf{B}^{e, u_f} \right\}}_{1 \times n_{\text{dof}}^{f, e}} + \underbrace{\left\{ \mathbf{H}^{e, u_f} \right\}}_{1 \times n_{\text{dof}}^{f, e}} \right] (\kappa_f + 2\mu_f) (F_{11}^{h^e})^{-2} (\gamma \Delta t) A j^e d\xi. \tag{C.112}
\end{aligned}$$

C.2 Explicit integration

C.2.1 CD scheme

In this final section, we show the derivation of the FE formulation for the $(\mathbf{u}-p_f)$ formulation using central-difference (CD) integration. Time-dependent variables that are zeroeth-order in time are evaluated at t_n ; those that are first or second order in time (i.e., \dot{x}, \ddot{x}) are evaluated at t_{n+1} . Therefore, this derivation requires some manipulation of variables that have explicit dependence on solution variables.

The balance of momentum of the mixture is trivial to adapt to the CD scheme from the variational form of the equation. The acceleration update of the solid skeleton is readily separable from the variational equation, and the stress update does not explicitly depend the solution variable at t_{n+1} .

Here, we begin with the balance of mass of the mixture, from which

$$\mathcal{H}_1^{\text{INT}, h} = \int_0^{X=H} w^{p_f} \left(\frac{J^h n^{f, h}}{K_f^\eta} \dot{p}_f^h + j^h \right) A dX. \tag{C.113}$$

We may rewrite the above as

$$\mathcal{H}_1^{\text{INT},h} = \int_0^{X=H} w^{p_f} \left(\frac{J^h n^{f,h}}{K_f^\eta} \left[\dot{p}_{f,n}^h + \frac{\Delta t}{2} \ddot{p}_{f,n}^h + \frac{\Delta t}{2} \ddot{p}_f^h \right] + \frac{\partial v_n^h}{\partial X} + \frac{\Delta t}{2} \frac{\partial a_n^h}{\partial X} + \frac{\Delta t}{2} \frac{\partial a^h}{\partial X} \right) A dX, \quad (\text{C.114})$$

which we can write element-wise as

$$\mathcal{H}_1^{\text{INT},h} = \mathbf{A}_e^{n_e} \underbrace{\left\{ \mathbf{c}^{p_f,e} \right\}^T}_{n_{\text{dof}}^{p_f,e} \times 1} \cdot \left(\int_{-1}^1 \underbrace{\left\{ \mathbf{N}^{e,p_f} \right\}^T}_{n_{\text{dof}}^{p_f,e} \times 1} \left(\frac{J^{h^e} n^{f,h}}{K_f^\eta} \left[\dot{p}_{f,n}^{h^e} + \frac{\Delta t}{2} \ddot{p}_{f,n}^{h^e} + \frac{\Delta t}{2} \underbrace{\left\{ \mathbf{N}^{e,p_f} \right\}}_{1 \times n_{\text{dof}}^{p_f,e}} \underbrace{\left\{ \ddot{\boldsymbol{\pi}}^e \right\}}_{n_{\text{dof}}^{p_f,e} \times 1} \right] \right. \right. \\ \left. \left. + \frac{\partial v_n^{h^e}}{\partial X} + \frac{\Delta t}{2} \frac{\partial a_n^{h^e}}{\partial X} + \frac{\Delta t}{2} \underbrace{\left\{ \mathbf{B}^{e,u} \right\}}_{1 \times n_{\text{dof}}^{s,e}} \underbrace{\left\{ \ddot{\mathbf{d}}^e \right\}}_{n_{\text{dof}}^{s,e} \times 1} \right) A_j^e d\xi. \quad (\text{C.115})$$

(C.115) can be split into a force vector, a mass matrix and a tangent coupling matrix written as follows:

$$\mathbf{f}^{\mathcal{H}_1^{\text{INT},e}} = \int_{-1}^1 \underbrace{\left\{ \mathbf{N}^{e,p_f} \right\}^T}_{n_{\text{dof}}^{p_f,e} \times 1} \left(\frac{J^{h^e} n^{f,h^e}}{K_f^\eta} \left[\dot{p}_{f,n}^{h^e} + \frac{\Delta t}{2} \ddot{p}_{f,n}^{h^e} \right] + \frac{\partial v_n^{h^e}}{\partial X} + \frac{\Delta t}{2} \frac{\partial a_n^{h^e}}{\partial X} \right) A_j^e d\xi, \quad (\text{C.116})$$

$$\underbrace{\mathbf{m}_{p_f,p_f}^{\mathcal{H}_1^{\text{INT},e}}}_{n_{\text{dof}}^{p_f,e} \times n_{\text{dof}}^{p_f,e}} = \int_{-1}^1 \frac{J^{h^e} n^{f,h^e}}{K_f^\eta} \frac{\Delta t}{2} \underbrace{\left\{ \mathbf{N}^{e,p_f} \right\}^T}_{n_{\text{dof}}^{p_f,e} \times 1} \underbrace{\left\{ \mathbf{N}^{e,p_f} \right\}}_{1 \times n_{\text{dof}}^{p_f,e}} A_j^e d\xi, \quad (\text{C.117})$$

$$\underbrace{\mathbf{k}_{p_f,u}^{\mathcal{H}_1^{\text{INT},e}}}_{n_{\text{dof}}^{p_f,e} \times n_{\text{dof}}^{s,e}} = \int_{-1}^1 \frac{\Delta t}{2} \underbrace{\left\{ \mathbf{N}^{e,p_f} \right\}^T}_{n_{\text{dof}}^{p_f,e} \times 1} \underbrace{\left\{ \mathbf{B}^{e,u} \right\}}_{1 \times n_{\text{dof}}^{s,e}} A_j^e d\xi. \quad (\text{C.118})$$

Next,

$$\mathcal{H}_2^{\text{INT},h} = \int_0^{X=H} w^{p_f} \frac{1}{K_f^\eta} \frac{\partial p_{f,n}^h}{\partial X} (n^{f,h} \hat{v}_f^h) A dX \\ = - \int_0^{X=H} w^{p_f} \frac{1}{K_f^\eta} \frac{\partial p_{f,n}^h}{\partial X} \hat{k}^h \left[\frac{\partial p_{f,n}^h}{\partial X} F_{11}^h + \rho^{\text{fR},h} (a_{n+1}^h + g) \right] A dX, \quad (\text{C.119})$$

which we can write element-wise as

$$\mathcal{H}_2^{\text{INT},h} = \mathbf{A}_e^{n_e} \underbrace{\left\{ \mathbf{c}^{p_f,e} \right\}^T}_{n_{\text{dof}}^{p_f,e} \times 1} \cdot \left(- \int_{-1}^1 \underbrace{\left\{ \mathbf{N}^{e,p_f} \right\}^T}_{n_{\text{dof}}^{p_f,e} \times 1} \left[\frac{1}{K_f^\eta} \frac{\partial p_{f,n}^{h^e}}{\partial X} \hat{k}^{h^e} \left(\frac{\partial p_{f,n}^{h^e}}{\partial X} (F_{11}^{h^e})^{-1} \right. \right. \right. \\ \left. \left. \left. + \rho^{\text{fR},h^e} \left[\underbrace{\left\{ \mathbf{N}^{e,u} \right\}}_{1 \times n_{\text{dof}}^{s,e}} \underbrace{\left\{ \ddot{\mathbf{d}}^e \right\}}_{n_{\text{dof}}^{s,e} \times 1} + g \right] \right) \right] \right) A_j^e d\xi \quad (\text{C.120})$$

(C.120) can be split into a force vector and a tangent coupling matrix written as follows:

$$\mathbf{f}^{\mathcal{H}_2^{\text{INT},e}} = - \int_{-1}^1 \underbrace{\left\{ \mathbf{N}^{e,p_f} \right\}^T}_{n_{\text{dof}}^{p_f,e} \times 1} \frac{1}{K_f^\eta} \frac{\partial p_{f,n}}{\partial X} \hat{k}^{he} \left(\frac{\partial p_{f,n}^{he}}{\partial X} (F_{11}^{he})^{-1} + \rho^{\text{fR},he} g \right) A j^e d\xi, \quad (\text{C.121})$$

$$\underbrace{\mathbf{k}_{p_{f,u}}^{\mathcal{H}_2^{\text{INT},e}}}_{n_{\text{dof}}^{p_f,e} \times n_{\text{dof}}^{s,e}} = - \int_{-1}^1 \frac{1}{K_f^\eta} \frac{\partial p_{f,n}^{he}}{\partial X} \hat{k}^{he} \rho^{\text{fR},he} \underbrace{\left\{ \mathbf{N}^{e,p_f} \right\}^T}_{n_{\text{dof}}^{p_f,e} \times 1} \underbrace{\left\{ \mathbf{N}^{e,u} \right\}}_{1 \times n_{\text{dof}}^{s,e}} A j^e d\xi. \quad (\text{C.122})$$

Given that $\mathcal{H}_3^{\text{INT}}$ has no explicit dependence on solution variables at t_{n+1} , we omit the trivial derivation herein. Next,

$$\mathcal{H}_4^{\text{INT},h} = \int_0^{X=H} \frac{\partial w^{p_f}}{\partial X} \hat{k}^{h} \rho^{\text{fR},h} (a_{n+1}^h + g) A dX, \quad (\text{C.123})$$

which we can write element-wise as

$$\mathcal{H}_4^{\text{INT},h} = \mathbf{A}_e^{n_e} \underbrace{\left\{ \mathbf{c}^{p_f,e} \right\}^T}_{n_{\text{dof}}^{p_f,e} \times 1} \cdot \left(\int_{-1}^1 \underbrace{\left\{ \mathbf{B}^{e,p_f} \right\}^T}_{n_{\text{dof}}^{p_f,e} \times 1} \hat{k}^{he} \rho^{\text{fR},he} \left[\underbrace{\left\{ \mathbf{N}^{e,u} \right\}}_{1 \times n_{\text{dof}}^{s,e}} \underbrace{\left\{ \ddot{\mathbf{d}}^e \right\}}_{n_{\text{dof}}^{s,e} \times 1} + g \right] A j^e d\xi \right). \quad (\text{C.124})$$

(C.124) can be split into a force vector and a tangent coupling matrix written as follows:

$$\mathbf{f}^{\mathcal{H}_4^{\text{INT},e}} = \int_{-1}^1 \underbrace{\left\{ \mathbf{B}^{e,p_f} \right\}^T}_{n_{\text{dof}}^{p_f,e} \times 1} \hat{k}^{he} \rho^{\text{fR},he} g A j^e d\xi, \quad (\text{C.125})$$

$$\underbrace{\mathbf{k}_{p_{f,u}}^{\mathcal{H}_4^{\text{INT},e}}}_{n_{\text{dof}}^{p_f,e} \times n_{\text{dof}}^{s,e}} = \int_{-1}^1 \hat{k}^{he} \rho^{\text{fR},he} \underbrace{\left\{ \mathbf{B}^{e,p_f} \right\}^T}_{n_{\text{dof}}^{p_f,e} \times 1} \underbrace{\left\{ \mathbf{N}^{e,u} \right\}}_{1 \times n_{\text{dof}}^{s,e}} A j^e d\xi. \quad (\text{C.126})$$

When pressure stabilization is enabled, we must apply the time discretization update to the $\partial p_f / \partial X$ term:

$$\mathcal{H}^{\text{stab},h} = \int_0^{X=H} \frac{\partial w^{p_f}}{\partial X} \alpha^{\text{stab}} (F_{11}^h)^{-1} \frac{\partial \dot{p}_f^h}{\partial X} A dX. \quad (\text{C.127})$$

In the CD scheme, we may rewrite the above as

$$\mathcal{H}^{\text{stab},h} = \int_0^{X=H} \frac{\partial w^{p_f}}{\partial X} \alpha^{\text{stab}} (F_{11}^h)^{-1} \frac{\partial (\dot{p}_{f,n}^h + \frac{\Delta t}{2} [\ddot{p}_{f,n}^h + \ddot{p}_f^h])}{\partial X} A dX, \quad (\text{C.128})$$

which we can formulate element-wise as

$$\mathcal{H}^{\text{stab},h} = \mathbf{A}_e^{n_e} \underbrace{\left\{ \mathbf{c}^{p_f,e} \right\}^T}_{n_{\text{dof}}^{p_f,e} \times 1} \cdot \left(\int_{-1}^1 \underbrace{\left\{ \mathbf{B}^{e,p_f} \right\}^T}_{n_{\text{dof}}^{p_f,e} \times 1} \alpha^{\text{stab}} (F_{11}^{h^e})^{-1} \left[\frac{\partial \dot{p}_{f,n}^h}{\partial X} + \frac{\Delta t}{2} \frac{\partial \ddot{p}_{f,n}^h}{\partial X} \right. \right. \\ \left. \left. + \frac{\Delta t}{2} \underbrace{\left\{ \mathbf{B}^{e,p_f} \right\}}_{1 \times n_{\text{dof}}^{p_f,e}} \cdot \underbrace{\left\{ \ddot{\boldsymbol{\pi}}^e \right\}}_{n_{\text{dof}}^{p_f,e}} \right] A_j^e d\xi \right) \quad (\text{C.129})$$

Lastly, (C.129) can be split into a force vector and a mass matrix as follows:

$$\underbrace{\left\{ \mathbf{f}^{\mathcal{H}^{\text{stab},e}} \right\}}_{n_{\text{dof}}^{p_f,e} \times 1} = \int_{-1}^1 \underbrace{\left\{ \mathbf{B}^{e,p_f} \right\}^T}_{n_{\text{dof}}^{p_f,e} \times 1} \alpha^{\text{stab}} (F_{11}^{h^e})^{-1} \left(\frac{\partial \dot{p}_{f,n}^e}{\partial X} + \frac{\Delta t}{2} \frac{\partial \ddot{p}_{f,n}^e}{\partial X} \right) A_j^e d\xi, \quad (\text{C.130})$$

$$\underbrace{\left[\mathbf{m}_{p_f,p_f}^{\mathcal{H}^{\text{stab},e}} \right]}_{n_{\text{dof}}^{p_f,e} \times n_{\text{dof}}^{p_f,e}} = \int_{-1}^1 \alpha^{\text{stab}} (F_{11}^{h^e})^{-1} \frac{\Delta t}{2} \underbrace{\left\{ \mathbf{B}^{e,p_f} \right\}^T}_{n_{\text{dof}}^{p_f,e} \times 1} \underbrace{\left\{ \mathbf{B}^{e,p_f} \right\}}_{1 \times n_{\text{dof}}^{p_f,e}} A_j^e d\xi. \quad (\text{C.131})$$